DOE Symposium Series 51

LA-1876

NATURAL RADIATION ENVIRONMENT III

Volume 2

Technical Information Center
U.S. DEPARTMENT OF ENERGY

DISTRIBUTION OF THIS DOCUMENT IS UNLIMITED

DISCLAIMER

This report was prepared as an account of work sponsored by an agency of the United States Government. Neither the United States Government nor any agency Thereof, nor any of their employees, makes any warranty, express or implied, or assumes any legal liability or responsibility for the accuracy, completeness, or usefulness of any information, apparatus, product, or process disclosed, or represents that its use would not infringe privately owned rights. Reference herein to any specific commercial product, process, or service by trade name, trademark, manufacturer, or otherwise does not necessarily constitute or imply its endorsement, recommendation, or favoring by the United States Government or any agency thereof. The views and opinions of authors expressed herein do not necessarily state or reflect those of the United States Government or any agency thereof.

DISCLAIMER

Portions of this document may be illegible in electronic image products. Images are produced from the best available original document.

CONF-780422 (Vol.2)

NATURAL RADIATION ENVIRONMENT III

Volume 2

Proceedings of a symposium held at
Houston, Texas, April 23–28, 1978

Sponsored by
U.S. Department of Energy
Assistant Secretary for Environment
Office of Health and Environmental Research
and
The University of Texas
School of Public Health

Editors
Thomas F. Gesell, The University of Texas
Wayne M. Lowder, U.S. Department of Energy

1980

Published by
Technical Information Center/U.S. Department of Energy

DISTRIBUTION OF THIS DOCUMENT IS UNLIMITED

NOTICE

International Copyright, © U. S. Department of Energy, 1978, under the provisions of the Universal Copyright Convention. United States copyright is not asserted under the United States Copyright Law, Title 17, United States Code.

Library of Congress Cataloging in Publication Data

International Symposium on the Natural Radiation Environment, 3d, Houston, Tex., 1978.
Natural radiation environment III.

(DOE symposium series ; 51)
"CONF-780422."
Bibliography: p.
Includes indexes.
1. Radiation, Background—Congresses. 2. Radon—Measurement—Congresses. 3. Radioisotopes—Congresses. 4. Atmospheric radioactivity—Congresses. I. Gesell, Thomas G. II. Lowder, Wayne M. III. United States. Dept. of Energy. Office of the Assistant Secretary for the Environment. IV. University of Texas Health Science Center at Houston. School of Public Health. V. Title. VI. Series: United States. Dept. of Energy. DOE symposium series ; 51.
QC809.R3I5 1978 539.2 80-607130
ISBN 0-87079-129-X

The set of two volumes is available as CONF-780422 (Vols. 1 and 2) for $39.50 from

National Technical Information Service
U. S. Department of Commerce
Springfield, Virginia 22161

DOE Distribution Category UC-11

Printed in the United States of America
April 1980

CONTENTS

VOLUME 2
(Pages 855 to 1738)

Penetrating Radiation Measurements

Exposure to Cosmic-Ray Neutrons at Commercial Jet Aircraft Altitudes 855
J. E. Hewitt, L. Hughes, J. B. McCaslin, A. R. Smith, L. D. Stephens, C. A. Syvertson, R. H. Thomas, and A. B. Tucker

Anomalous Atmospheric Attenuation of Cosmic-Ray-Produced Neutrons near the Earth's Surface 882
Masahiro Kodama, Shinkichi Kawasaki, Takashi Imai, Kazuyoshi Takahashi, and Masani Wada

Measurement of Environmental Radiations with a Scintillation Spectrometer Equipped with a Spherical NaI(Tl) Scintillator 896
Masaharu Okano, Koichi Izumo, Hidekazu Kumagai, Takeo Katou, Masami Nisida, Tatsuiji Hamada, and Masahiro Kodama

Gamma-Ray Measurements in an Area of High Natural Radioactivity 912
L. Løvborg, L. Bøtter-Jensen, E. Mose Christiansen, and B. Leth Nielsen

Environmental Radiation Studies Relevant to Thermoluminescence Dating 927
A. S. Murray, S. G. E. Bowman, and M. J. Aitken

Analysis of Error in Measuring the Environmental Radiation Background Using Thermoluminescence Dosimetry 950
J. H. White, C. W. Sunbeck, and C. L. Lindeken

Energy Dependence of Thermoluminescent Dosimetry in Environmental Monitoring . . . 965
Eric Vold

TLD Measurements and Model Calculations of Environmental Radiation Exposure Rates . . 987
Gail de Planque

Studies of the Absolute Measurement of Low-Level Natural Environmental Radiation Using the Normal Pressure Ionization Chamber 1004
Hisao Kobayashi, Masahiro Tsukuda, and Akira Sasaki

Radiation Surveys and Population Exposure

Methods and Results of Measurements of the Environmental Radiation in Bavaria . . .1022
F. Wachsmann and D. F. Regulla.

Natural Radiation in Japan 1034
Siro Abe, Kazunobu Fujitaka, and Kenzo Fujimoto

Natural Radiation Measurements and Interpretation of Their Results in Terms of Dose to Population 1049
T. Niewiadomski, J. Koperski, and E. Ryba

Measurement Program of Natural Radiation in France: Description and Preliminary Results . .1059
Jean-Marie Guezengar, Claude Madelmont, and André Bouville

Study of Genetic Effects in Plants Induced by Natural Radioactivity in Southwest France 1072
M. Delpoux, M. Fabries, F. Faure, H. Dulieu, A. Leonard, and M. Dalebroux

Measurements of Gamma Radiation in Swedish Houses by Means of Mailed $CaSO_4$/Dy Dosimeters 1077
Lars Mjönes

Sources of Natural Radiation Exposure in a Low-Monazite Environment 1090
M. A. R. Iyengar, M. P. Rajan, S. Ganapathy, and P. R. Kamath

Results of a National Survey on Natural Radioactivity in Italy 1107
G. Sciocchetti and F. Scacco

Age-, Sex-, and Weight-Dependent Dose Patterns Due to Inhaled Natural Radionuclides 1116
W. Hofmann, F. Steinhäusler, and E. Pohl

Local and Temporal Distribution Pattern of Radon and Daughters in an Urban Environment and Determination of Organ-Dose Frequency Distributions with Demoscopical Methods 1145
F. Steinhäusler, W. Hofmann, E. Pohl, and J. Pohl-Rüling

Human Dose from Radiation of Terrestrial Origin 1163
Keran O'Brien

Radioactivity in the Indoor Environment

Exhalation of Radon-222 from Building Materials and Walls 1211
Niels Jonassen and J. P. McLaughlin

The Effect of Pressure Drops on Radon Exhalation from Walls 1225
J. P. McLaughlin and Niels Jonassen

Radon in Dwellings in Sweden 1237
Gun Astri Swedjemark

Measurements of Radon-222 Concentrations in Dwellings in Great Britain 1260
K. D. Cliff

The Distribution of Ambient Radon and Radon Daughters in Residential Buildings in the New Jersey—New York Area 1272
A. C. George and A. J. Breslin

Methods for a Continuous Registration of Radon, Thoron, and Their Decay Products Indoors and Outdoors 1293
J. Porstendörfer, A. Wicke, and A. Schraub

Diurnal Variation of Radon Measured Indoors and Outdoors in Grand Junction, Colorado, and Teaneck, New Jersey, and the Influence That Ventilation Has on the Buildup of Radon Indoors 1308
Henry B. Spitz, McDonald E. Wrenn, and Norman Cohen

Radiation Exposure from Building Materials 1331
G. C. Eichholz, F. J. Clarke, and B. Kahn

The Contribution of Radon in Tap Water to Indoor Radon Concentrations 1347
Thomas F. Gesell and Howard M. Prichard

The Contribution of Bored Wells to Respiratory Radon Daughter Exposure in Finland 1364
O. Castrén

Radon- and Thoron-Produced Radiation in National Park Service Caves 1371
Keith A. Yarborough

Distribution of Natural Radioactive Isotope Concentrations and Emanation Factors Measured on Concrete and Brick Samples Produced in Hungary 1396
A. Tóth, I. Fehér, S. Novotny Lakatos, L. Koszorus, and B. Keszthelyi

Emanating Power of Radon-222 Measured in Building Materials 1407
J. Peńsko, Z. Stpiczyńska, and K. Blaton-Albicka

Outdoor and Indoor Radon Concentrations in Air in the Territory of Slovenia, Yugoslavia . .1415
I. Kobal, M. Škofljanec, and J. Kristan

Population Dose Equivalent from Naturally Occurring Radionuclides in Building Materials 1424
Dade W. Moeller, Dwight W. Underhill, and Gary V. Gulezian

Summary of an Informal Meeting on Radon in Buildings 1444

Technologically Enhanced Natural Radioactivity

Population Doses from Natural Radionuclides Due to Certain Aspects of Human Activity 1446
L. A. Ilyin, V. A. Knizhnikov, R. M. Barkhudarov, R. M. Alexakhin, B. K. Borisov, and N. Ja. Novikova

Radiological Evaluation of Structures Constructed on Phosphate-Related Land . . .1457
Richard Guimond and Samuel T. Windham

The Effect of Mining and Land Reclamation on the Radiological Characteristics of the Terrestrial Environment of Florida's Phosphate Regions 1476
C. E. Roessler, R. Kautz, W. E. Bolch, Jr., and J. A. Wethington, Jr.

Modification of the Natural Radionuclide Distribution by Some Human Activities in Canada 1494
G. B. Knight and C. E. Makepeace

An Assessment of Natural Radionuclides in the Coal Fuel Cycle 1511
Clarence E. Styron

Perturbations on the Natural Radiation Environment Due to the Utilization of Coal as an Energy Source 1521
Harold L. Beck, Carl V. Gogolak, Kevin M. Miller, and Wayne M. Lowder

Uranium Mill Tailings Piles as Sources of Atmospheric Radon-222 1559
William E. Clements, Sumner Barr, and M. Lynn Marple

Transport of Radon Which Diffuses from Uranium Mill Tailings 1584
W. A. Goldsmith, F. F. Haywood, and R. W. Leggett

The Uranium District of the Texas Gulf Coastal Plain 1602
Lewis M. Cook

Radon and Radon Daughters Due to Natural Uranium Occurrences in a Rural Ontario Community 1623
H. Taniguchi and P. Vasudev

Radium-228 and Radium-226 Levels in a River Environment and Its Modification by Human Activities 1633
A. C. Paul, V. S. Londhe, and K. C. Pillai

Distribution of Radium and Chemical Toxins in the Environment of a Uranium Complex 1655
P. M. Markose, K. P. Eappen, S. Venkataraman, and P. R. Kamath

Accumulation of Radium-226 from Phosphate Fertilizers in Cultivated Soils and Transfer to Crops 1667
R. Kirchmann, M. Darcheville, and G. Koch

Determinants of Radon Flux from Complex Media: Virgin and Reclaimed Lands in Florida Phosphate Region 1673
W. Emmett Bolch, Nayan Desai, Charles E. Roessler, and Randy S. Kautz

Ecological Considerations of Natural and Depleted Uranium 1682
Wayne C. Hanson

Intercomparison Experiment at NRE III . . .1698

List of Attendees 1714

Author Index 1724

Subject Index 1727

CONTENTS

VOLUME 1
(Pages 1 to 854)

Preface iii

Introduction iv

The Natural Radiation Environment Symposiums 1
John A. S. Adams

Radon in the Ground

Radon Migration in the Ground: A Supplementary Review 5
Allan B. Tanner

Techniques and Principles for Mapping of Integrated Radon Emanation Within the Earth 57
Robert L. Fleischer and Antonio Mogro-Campero

Search for Long-Distance Migration of Subsurface Radon 72
Antonio Mogro-Campero and Robert L. Fleischer

Track Etch Radon Ratios to Soil Uranium and a New Uranium Abundance Estimate . . .84
H. Ward Alter

Radon Transport Processes Below the Earth's Surface 90
Marvin Wilkening

Radon-222 Exhalation and Its Variation in Soil Air 105
Sadamu Mochizuki and Toshio Sekikawa

Reconnaissance of Radon Emanation Power of Poços de Caldas, Brazil, Uranium Ore and Associated Rocks 117
Enio B. Pereira

Statistical Analysis of Radon Flux Measurements 124
M. A. Haghi, N. K. Savani, P. V. Rao, and J. A. Wethington, Jr.

Seismicity and Radioactivity

Automated Radon—Thoron Monitoring for Earthquake Prediction Research 137
M. H. Shapiro, J. D. Melvin, N. A. Copping, T. A. Tombrello, and J. H. Whitcomb

Roles of Radon-222 and Other Natural Radionuclides in Earthquake Prediction . . . 154
Alan R. Smith, Harold A. Wollenberg, and Duane F. Mosier

Radioactivity in the Atmosphere

Role of Natural Radiation Environment in Earth Sciences 184
K. G. Vohra

Radon Emanation in Tectonically Active Areas 175
Chi-Yu King

Effect of Increased Ionization on the Atmospheric Electric Field 201
William L. Boeck

Meteorological Influences on Atmospheric Radioactivity and Its Effects on the Electrical Environment 210
Sven Israelsson

Use of Natural Radioactive Tracers for the Determination of Vertical Exchanges in the Planetary Boundary Layer 226
Aimé Druilhet, Daniel Guedalia, and Jacques Fontan

Variation of Vertical Atmospheric Stability by Means of Radon Measurements and of Sodar Monitoring 242
Daniel Guedalia, Aimé Druilhet, Jacques Fontan, and André N'Tsila

Experimental Tests of Turbulent Diffusion Models by High-Resolution Gamma-Ray Spectroscopy of Radon Daughters (summary only) 256
Mark H. Shapiro

Diurnal Variations of Radon Daughter Concentrations in the Lower Atmosphere . . 259
Carl V. Gogolak and Harold L. Beck

Diffusion Coefficient of Radon Decay Products and Their Attachment Rate to the Atmospheric Aerosol 281
J. Porstendörfer and T. T. Mercer

The Mean Size Among the Particles of Short-Lived Radon Daughter Products in the Atmosphere 294
S. Nakatani

Radon-222 as an Indicator of Continental Air Masses and Air Mass Boundaries over Ocean Areas 308
R. E. Larson and D. J. Bressan

Natural Radioactivity of the Atmosphere over the Indian Land Mass, Inside Deep Mines, and over Adjoining Oceans 327
U. C. Mishra, C. Rangarajan, and C. D. Eapen

A Technique for Evaluating Airborne Concentrations of Daughters of Radon Isotopes 347
P. T. Perdue, R. W. Leggett, and F. F. Haywood

In Situ Ge(Li)-Spectrometric Measurements of Gamma Radiation from Radon Daughters Under Different Weather Conditions 357
Robert R. Finck and Bertil R. R. Persson

Some Observations of the Variations in Natural Gamma Radiation Due to Rainfall . . 370
Susumu Minato

Global Distribution and Sources of Uranium, Radium-226, and Lead-210 383
Z. Jaworowski, L. Kownacka, and M. Bysiek

Use of Lead-210 and Polonium-210 as Tracers of Atmospheric Processes 405
A. Nevissi and W. R. Schell

Size Distribution and Origin of Lead-210, Bismuth-210, and Polonium-210 on Airborne Particles in the Troposphere 415
Howard E. Moore, Stewart E. Poet, and Edward A. Martell

Trends in the Chemical State of Polonium-210 in the Atmosphere 430
Michiko Abe and Siro Abe

Contamination of Air by Lead-210 and Polonium-210 in Territories with High Natural Radioactivity 440
O. N. Popova and A. I. Taskaev

Lead-210 in the Atmosphere 445
J. Sanak, G. Lambert, and B. Ardouin

Radionuclides in Marine Systems

The Distribution of Radon and Radium in the Ocean and Its Bearing on Some Oceanographic Problems 458
Yasuo Miyake, Yukio Sugimura, and Katsuko Saruhashi

Lead-210 and Polonium-210 as Marine Geochemical Tracers: Review and Discussion of Results from the Labrador Sea 473
Michael P. Bacon, Derek W. Spencer, and Peter G. Brewer

Vertical Oceanic Transport of Alpha-Radioactive Nuclides by Zooplankton Fecal Pellets 502
J. J. W. Higgo, R. D. Cherry, M. Heyraud, S. W. Fowler, and T. M. Beasley

Radioactive and Stable Trace Metals in Narragansett Bay, Rhode Island 514
P. H. Santschi, W. S. Broecker, Y.-H. Li, J. Bell, S. Carson, G. Morrison, and E. Davie

Radionuclides in Aquatic and Terrestrial Systems

Investigations of Natural Levels of Radon-222 in Groundwater in Maine for Assessment of Related Health Effects 529
C. T. Hess, R. E. Casparius, S. A. Norton, and W. F. Brutsaert

Lead-210 and Radon-222 Contents of Rainwater in Tokyo 547
Y. Miyake, K. Saruhashi, Y. Sugimura, T. Kanazawa, Y. Katsuragi, and H. Uemura

Radiochemical and Radioecological Studies of Natural and Artificial Alpha-Emitting Radionuclides 560
Elis Holm and Bertil Persson

Applications of Environmental Radon-222 to Some Cases of Water Circulation 581
S. Kimura and T. Komae

Transfer of Radium from Soil to Plants in an Area of High Natural Radioactivity in Ramsar, Iran 600
B. Khademi, A. A. Alemi, and A. Nasseri

Distribution of Lead-210 in Japanese Soils and Its Relation to the Distributions of Strontium-90, Cesium-137, and Stable Lead 611
K. Kodaira, M. Kato, M. Komamura, A. Kawamura, A. Yamototo, R. Ebisawa, M. Sakanoue, and K. Komura

Measurements of Radium in Water Using Impregnated Fibers 633
C. J. Bland

Determination of Radium-226 in Environmental Samples 640
Robert P. Powers, Neill E. Turnage, and Larry G. Kanipe

Radioactive Contamination of Natural and Artificial Materials 661
E. L. Kovalchuk, A. A. Pomansky, A. A. Smolnikov, and A. H. Temmoev

Surface Alpha Activity of Different Materials 673
E. L. Kovalchuk, V. V. Kuzminov, and A. A. Pomansky

Mobility of Elevated Levels of Uranium in the Environment 681
F. R. Miera, Jr., W. C. Hanson, E. S. Gladney, and P. Jose

Scintillation Detectors for Radon-222 in Air and Water 700
Giovanni G. Mastinu

Variation of Uranium Isotopes in Some Carbonate Aquifers 711
J. B. Cowart

Migration of Heavy Natural Radionuclides in a Humid Climatic Zone 734
N. A. Titaeva, R. M. Alexakhin, A. I. Taskaev, and V. I. Maslov

Redistribution of Natural Radioactive Elements Resulting from Animal and Plant Life Activity in Regions with High Radioactivity 738
V. I. Maslov, K. I. Maslova, and R. M. Alexakhin

Radionuclides in Food and Tissue

Normal Dietary Levels of Radium-226, Radium-228, Lead-210, and Polonium-210 for Men 755
Richard Holtzman

Thorium in Human Tissues 783
M. E. Wrenn, N. P. Singh, S. A. Ibrahim, N. Cohen, and G. Saccomanno

Natural Radioactivity in Indian Foodstuffs . . 800
B. Y. Lalit and T. V. Ramachandran

Radium-226 Levels in Italian Drinking Waters and Foods 810
G. G. Mastinu and G. P. Santaroni

Lognormal Analysis of Naturally Occurring Radionuclides in Soil and Vegetation of the Hanford Area 826
M. L. Miller, J. J. Fix, and P. E. Bramson

Radium and Thorium with Barium in Micronodules of Cattle Thyroids 832
L. Van Middlesworth

Radiation Exposure for Radium-226 Ingestion 839
D. H. Keefer and E. J. Fenyves

Author Index I-1

Subject Index I-4

Exposure to Cosmic-Ray Neutrons at Commercial Jet Aircraft Altitudes

J. E. HEWITT,* L. HUGHES,* J. B. McCASLIN,† A. R. SMITH,†
L. D. STEPHENS,† C. A. SYVERTSON,* R. H. THOMAS,† and
A. B. TUCKER‡
*Ames Research Center, National Aeronautics and Space Administration, Moffett Field, California, †Lawrence Berkeley Laboratory, University of California, Berkeley, California, ‡San Jose State University, San Jose, California

ABSTRACT

The growth of commercial jet aviation has increased the exposure of passengers and crews to secondary cosmic-ray radiation at high altitudes. Starting in 1974 the National Aeronautics and Space Administration—Ames Research Center has sponsored a program to measure, with several types of detectors, the flux, absorbed dose, and energy spectrum of the neutron component of this radiation field.

The neutron energy spectrum has been measured with a complete set of Bonner spheres as well as with other energy-sensitive threshold detectors. Flights at an altitude of 12.5 km at 20°N and 40°N latitudes show the derived energy spectra to be in general agreement with previous work. Comparison of measured and theoretical energy spectra is presented in this paper.

We continue to improve our neutron detector systems and the computational procedures that must be used to convert the measurements into neutron spectral shapes and intensities. Constraints on spectral shape are provided by inclusion of a $^{27}Al \rightarrow {}^{24}Na$ threshold detector as well as a bismuth fission counter, with energy thresholds of 6.5 MeV and 50 MeV, respectively. For us to resolve the region near the evaporation peak at approximately 1 MeV, we must have measurements with a statistical precision of the order of 1%. Equipment now being prepared will allow us this order of precision.

The fast neutron contribution to the absorbed dose has been determined by a scintillation detector. Pulse-shape discrimination separated the recoil proton pulses from gamma-ray and external proton signals. The instrument has been flown in a C-141 aircraft at 12.5 km. At 40°N the energy deposition rate in a hydrogenous scintillator by 2- to 10-MeV recoil protons was 5.2 μrads/hr, which would convert to 0.034 mrem/hr dose equivalent if the same dose rate were measured in tissue.

A latitude survey mission was flown in a CV-990 aircraft in November 1976 from 70°N to 70°S at an altitude of 10.1 km. A moderated BF_3 counter measured the fast neutron flux, and an argon-filled ionization chamber monitored the ionizing component. In addition, altitude attenuation profiles were measured at several latitudes.

AMES COLLABORATIVE STUDIES OF COSMIC RADIATION (ACSCR)

A principal goal of the Ames Collaborative Study of Cosmic Radiation (ACSCR), a program initiated in 1974, was an experimental determination of the cosmic-ray neutron spectrum through use of improved techniques now available. When this goal is achieved, it will be possible to systematically study the variation of the neutron spectrum with respect to altitude and geomagnetic latitude during various phases of the solar cycle. Details of this collaboration and its purpose have been given by Hewitt et al. (1976). To summarize, precise and accurate measurement of cosmic radiation is obtained during the many flights of National Aeronautics and Space Administration (NASA) aircraft that are devoted primarily to astronomical observations, and the accumulation of these cosmic-ray data over many years will provide an extensive data base which may be used to map the radiation field in both space and time.

Although there is a variety of reasons for such studies, we are specifically interested in one practical reason. Interest has increased in the exposure of large populations to low levels of ionizing radiation owing to man's activities. The growth of commercial aviation, for example, has increased the exposure of passengers and crews to secondary cosmic radiation at high altitudes (Upton et al., 1966; Rossi et al., 1975). Recently this interest has been heightened by two factors: first, supersonic aircraft are now in regular commercial service; second, it has been suggested that the risk of leukemia from small absorbed doses due to neutrons is considerably higher than previously thought (Rossi and Kellerer, 1974; Rossi, 1977).

Primary cosmic rays, predominantly very high energy protons, interact with atomic nuclei near the top of the atmosphere to produce a complex field of secondary radiation. Multiplication and eventual absorption in reactions with atmospheric nuclei produce a vertical intensity variation that peaks near a 20-km altitude. Deflection of low-energy primaries by the Earth's magnetic field leads to strong latitude dependence wherein the intensity increases at higher latitudes. The radiation field comprises both low and high linear energy transfer (LET) components of roughly comparable

magnitude at commercial flight altitudes, the latter component contributed principally by neutrons.

The ionizing radiation (low LET) environment produced by the interaction of the primary galactic cosmic radiation has been studied for more than 50 years; consequently the literature is voluminous. As a convenience, several recent reviews are cited here: Adams and Lowder, 1964; Sandstrom, 1965; UNSCEAR Report, 1966; Hayakawa, 1969; Adams, Lowder, and Gesell, 1975; UNSCEAR, 1972; NCRP Report, 1975. This component of the radiation field is relatively easy to measure and produces a dose equivalent rate of a few tenths mrem/hr (NCRP Report, 1975).

The contribution of the neutron (high LET) component is more difficult to measure. Pioneering neutron surveys were made in the 1950s by Simpson (1951) and Hess et al. (1959), and in the next decade worldwide measurements of high-energy neutrons were made with liquid scintillation detector systems (Mendel and Korff, 1963; Haymes, 1964; Merker et al., 1973; Merker, 1973). More recent measurements have concentrated on the neutron energy spectrum at high altitudes (Preszler, Sinnett, and White, 1974, Klumpar et al., 1973). Estimates of population exposures resulting from both subsonic and supersonic flight depend not only on a knowledge of radiation intensity but also on a knowledge of radiation quality.

Stimulated by increased interest, by availability of improved instrumentation, and by development of models for calculating radiation transport through the atmosphere (O'Brien, 1971; Armstrong, Chandler, and Barish, 1973; Merker et al., 1973), the NASA—Ames Research Center is sponsoring a program of new measurements. In this paper we report preliminary results of this study of the neutron energy spectrum, total flux, and absorbed dose as functions of latitude, altitude, and time.

DETECTORS AND INSTRUMENTATION

Hewitt et al. (1976) described our instrumentation in detail, therefore only a brief summary is included here.

Ionization Measurements

A commercial environmental radiation monitor (Type RSS-111) providing a continuous record of this radiation component has been aboard all flights. This is a sensitive, high-pressure, argon-filled ionization chamber designed to measure low-level exposure rates. The instrument was modified by the manufacturer to extend its range to 1000 μR/hr.

Neutron Measurements

In their 1959 measurement of the cosmic-ray neutron spectrum, Hess et al. (1959) used BF_3 counters surrounded by varying thicknesses of cylindrical paraffin moderator to study the energy region from thermal to about 50 MeV, while neutrons greater than about 50 MeV were measured with a bismuth fission counter.

Significant improvements have occurred in these detector systems since 1959. Bonner and his colleagues (Bramblett, Erving, and Bonner, 1960) developed spherical moderators, resulting in improved angular response. Sanna (1973) has extended the response function calculations upwards to 400-MeV neutron energy for both polyethylene and water moderators. He has also included the perturbation of thermal neutron flux caused by presence of the thermal neutron detector. The use of LiI(Eu) crystal neutron detectors in the moderators has simplified the calculations in providing both geometric symmetry and a closer approximation to a "point" detector. Furthermore, the introduction of solid-state technology in electronics has resulted in equipment that is more reliable, more compact, and lighter in weight than was available previously (e.g., light-weight multichannel pulse height analyzers).

At high-energy accelerator laboratories, activation detectors have been developed to determine neutron spectra (Smith, 1965; McCaslin et al., 1968; Thomas, 1973). Activation detectors have step-like response functions in contrast to Bonner spheres which have slowly varying response functions. Thus addition of activation detectors to the Bonner spectrometer will greatly improve the precision with which the neutron spectrum can be determined at energies close to activation reaction thresholds. Two such detectors have been incorporated into the present program.

The aluminum detector, using the $^{27}Al(n,\alpha)^{24}Na$ reaction with a 6-MeV threshold, is most useful to spectral determination in the energy range of 3 to 30 MeV; it was shown to be adequately sensitive during Flight Series I and III (*see* "Determination of Cosmic-Ray Neutron Spectrum," this paper).

The bismuth fission counter, using the $^{209}Bi(n,f)$ reaction with a 50-MeV threshold, is most useful in the energy range of 30 to 500 MeV. McCaslin et al. (1968) significantly improved the operating characteristics of this detector in comparison to its use in previous cosmic-ray work (Hess et al., 1959). The counter, which is very sensitive to microphonics, underwent successful tests during Flight Series II (*see* "Determination of Cosmic-Ray Neutron Spectrum," this paper). These flights also provided enough data for estimating

the flight time required to obtain data of acceptable statistical quality for inclusion in the spectral analysis program.

During all flights a moderated BF_3 counter was used to monitor neutrons in the energy range from epithermal up to about 20 MeV. Data (Kodama et al., this symposium) from this counter were subsequently used to normalize data taken with other neutron detectors at different altitudes, latitudes, and times. Neutron data recorded during this experimental program were also correlated with the appropriate cosmic-ray neutron monitor station; e.g., the Deep River Station (Ontario, Canada) was used for midlatitude flights (Hatton, 1971; Wilson and Bercovitch, 1975).

Recoil Proton Detector

The fast neutron contribution to the absorbed dose has been measured with the "phoswich" scintillator shown in Fig. 1. The basic detector is a 5-cm x 5-cm cylinder of organic scintillator. Recoil protons, produced by neutron—hydrogen elastic scattering, deposit their kinetic energy in the detector. This is the primary mechanism for neutron energy deposition in tissue. The light output of the resulting scintillation is approximately proportional to the energy absorbed.

Recoil protons can be distinguished from gamma rays and external charged particles by their characteristic pulse shape. In NE 213 the scintillation decay time, and hence the rise time of the electrical pulse from the phototube, is measurably slower for protons than for electrons generated by photon interactions. To screen out signals from the external proton flux, we enclosed the NE 213 in a 7.5-mm shield of NE 102 in which scintillations produced by all charged particles have approximately the same pulse shape as photons in NE 213. Thus signals proportional to recoil proton energies from neutron interactions inside the volume of NE 213 can be distinguished from those of gamma rays or other charged particles, including externally produced protons, making this detector a useful neutron dosimeter in mixed radiation fields.

Pulses from the scintillator are recorded in a two-parameter multichannel analyzer, with rise-time information displayed on one axis and pulse height on the other. Calibration of the energy axis was accomplished using the Compton edges of the 0.511-MeV and 1.27-MeV gamma rays of ^{22}Na and the 0.66-MeV gamma ray of ^{137}Cs. The light output of NE 213 is linear for this range of electron energies. Conversion to proton energies, for which the light output is not linear, was accomplished using the published tables of Verbinski

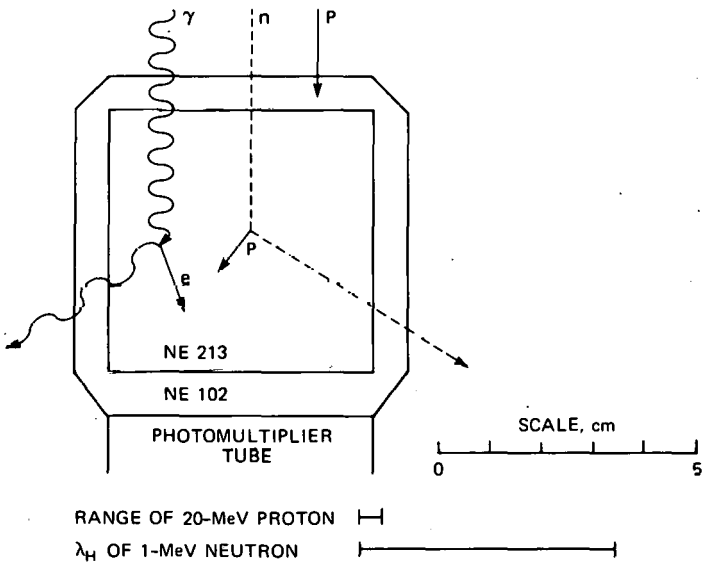


Fig. 1 Diagram of a phoswich scintillator.

et al. (1968). Data from this detector will be incorporated with data from all the neutron detectors in future spectral analyses.

Brookhaven National Laboratory Dose Equivalent Meter

The Brookhaven dose equivalent meter (Kuehner, Chester, and Baum, 1973), a Rossi-type LET spectrometer (Rossi and Rosenzweig, 1955), with a modified electrode system is used as a portable, mixed-radiation dose equivalent meter. The detector consists of a 0.6-cm-thick spherical shell approximately 20 cm in diameter constructed of A-150 Shonka conducting plastic. The spectrometer gas filling consists of the usual "tissue equivalent" mixture of 66% methane, 3% nitrogen, and 31% carbon dioxide at a pressure of 10 torr. Under these conditions the detector simulates a tissue sphere approximately 3 μm in diameter.

An ionizing event in the detector produces a current pulse that is converted to a voltage pulse proportional to the initial event and then is modified by two special biased amplifier systems to produce an output proportional to the dose equivalent rate. Because both the observed dose rate and the dose equivalent rate are presented, the average quality factor may also be determined.

The instrument flown was equipped with mechanical registers that printed accumulated microrads and microrems every 2 min. The

detector was calibrated about an hour before and immediately following each flight with an internal alpha source that had been previously calibrated against a radium standard. Small changes (<10%) in sensitivity due to temperature variations during the flight were corrected by using the preflight and postflight calibration data and assuming a linear variation between the two.

EXPERIMENTAL DATA

Summary of ACSCR Flights

Over the past 4 years experimental data have been obtained aboard a total of 24 flights in four series.

For the first three series of flights, data were taken aboard the NASA C-141 Airborne Observatory. The first series consisted of three flights from Moffett Field between May and October of 1974. Hewitt et al. (1976, 1978) have described the flight paths and the experimental data obtained. The second series consisted of four flights from Hickam Field, Hawaii, during August 1975, while the third series consisted of two flights from Moffett Field in October 1975. Stephens et al. (1978) have described the flight paths and data taken aboard these two series of flights.

For the fourth series of flights, data were taken aboard a CV-990 aircraft during the NASA latitude survey mission in October and November of 1976 (Gauntner and Haughney, 1977). The aircraft made 15 flights over a latitude range from 75°N to 61.5°S. Flight routes are shown in Fig. 2. The aircraft usually flew at an altitude of 10.1 to 12.2 km (33,000 to 40,000 ft) except where altitude profiles were taken in cooperation with ground stations.

Variation of Ionization and Neutron Intensity with Altitude and Geomagnetic Latitude

Figure 3 summarizes the accumulated measurements of exposure rates made with the ionization chamber, as a function of both altitude and geomagnetic latitude, during each series of flights. For all altitudes the exposure rate is less at lower latitudes. A series of measurements at 44°N geomagnetic latitude gave a relaxation length of 140 g/cm^2 using the data between 3.1 and 7.6 km (10,000 and 25,000 ft), where the curve is exponential.

Simpson (1951) showed that the relaxation length of the neutrons produced by the interaction of cosmic rays varies with geomagnetic latitude. The variation is such that the attenuation length increases with decreasing geomagnetic latitude, particularly in

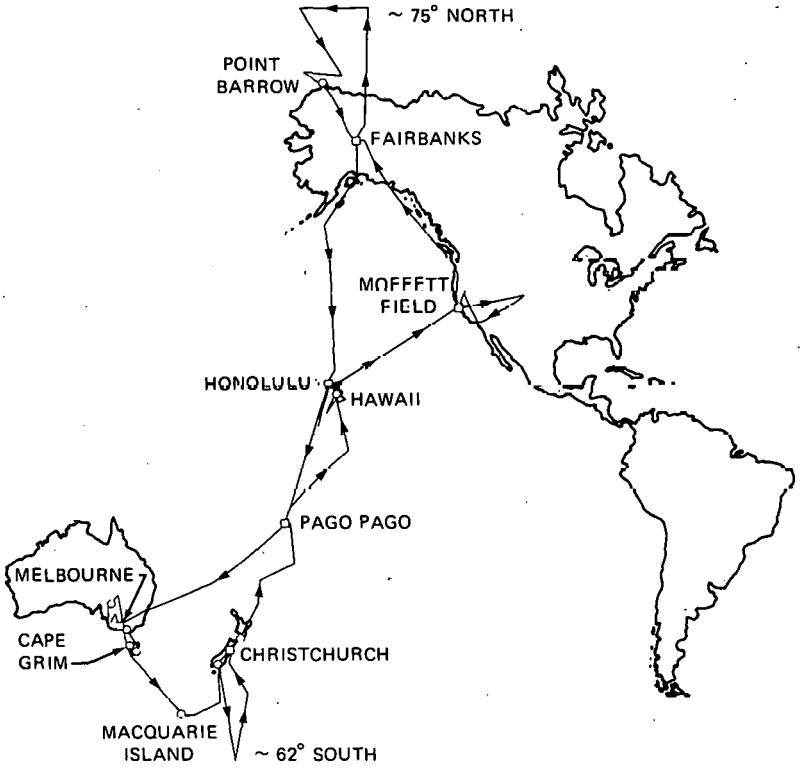


Fig. 2 Diagram showing the routes flown by the NASA CV-990 aircraft during the 1976 latitude survey.

the latitude range of 50 to 20°. This effect is interpreted in terms of the magnetic cutoff energy for primary cosmic-ray protons; longer attenuation lengths are observed for latitudes at which the magnetic cutoff energy is higher. Simpson also concluded that the shape of the neutron spectrum from thermal energy up to the range of 30 to 40 MeV is relatively independent of geomagnetic latitude.

Figure 4 summarizes data taken with the moderated BF_3 counter during the 1976 latitude survey (Hewitt et al., 1977). As shown in Table 1, these results agree with the earlier data of Simpson (1951).

A greater value for attenuation length implies higher energies for source particles and, therefore, higher energies for some neutrons. Thus we might expect to see differences in the shape of the neutron spectrum as a function of geomagnetic latitude in the energy region above ~40 MeV. As we shall discuss later (*see* "Determination of the

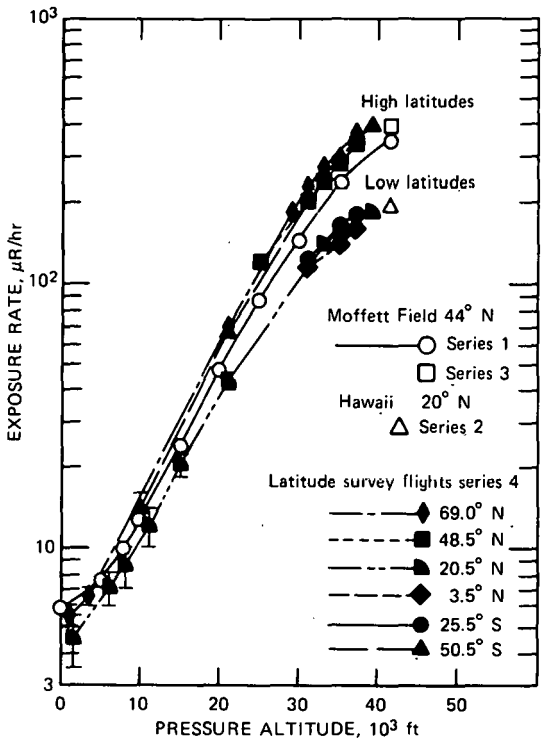


Fig. 3 Exposure rate measured with the RS 111 ionization chamber as a function of altitude and geomagnetic latitude.

Cosmic-Ray Neutron Spectrum," this paper), our determination of the cosmic-ray-produced spectrum is not yet sufficiently advanced to have observed these differences. It is clear that use of the bismuth fission chamber (energy threshold ~50 MeV) will be crucial in this investigation. The bismuth fission counter gives its principal response in the energy region of interest (~40 MeV) and is the only detector that gives spectral shape information above ~100 MeV.

The earlier work of Simpson (1951) showed that there is approximate symmetry of both ionization and neutron intensity about the geomagnetic equator. These findings are confirmed by our data obtained during the 1976 latitude survey. Figure 5 shows the variation of both the neutron and ionizing dose equivalents at all latitudes at 10.1 km (33,000 ft). Using a quality factor of 6.5 for cosmic-ray neutrons (Patterson, Routti, and Thomas, 1971) gives 0.12 mrem/hr for neutrons and 0.27 mrem/hr for the ionizing component for a total of 0.39 mrem/hr at high latitudes.

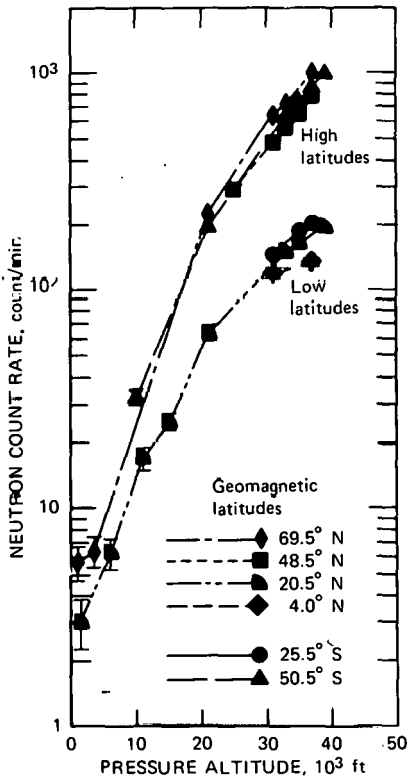


Fig. 4 Counting rate of moderated BF_3 counter as a function of pressure altitude.

TABLE 1

Summary of Measured Values of Relaxation Length of Cosmic-Ray Produced Neutrons in the Atmosphere

Geomagnetic latitude, deg	Attenuation length, g/cm^2	Reference
0	212 ± 4	Simpson, 1951
19	206 ± 4	Simpson, 1951
20	190 ± 4	Hewitt et al., 1977
40	181 ± 3	Simpson, 1951
50	155 ± 4	Hewitt et al., 1977
53	157 ± 2	Simpson, 1951
65	157 ± 3	Simpson, 1951

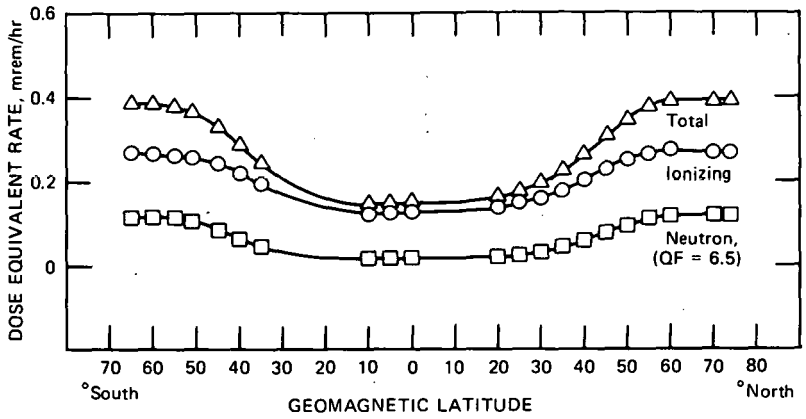


Fig. 5 Dose equivalent rate due to the low LET component (ionizing) and high LET component (neutrons) of the cosmic radiation as a function of geomagnetic latitude [altitude 10.1 km (33,000 ft)].

Figure 6 shows an example of the altitude dependence of the ionizing and neutron components at a geomagnetic latitude of 20°N. The relaxation lengths obtained are 167 g/cm^{-2} and 190 g/cm^{-2} for ionization and neutrons, respectively.

The intensity of primary cosmic-ray protons reaching the top of the atmosphere increases at higher latitudes because the shielding effect of the Earth's magnetic field is least at the magnetic poles (where the field is parallel to the velocity of the incoming particles). The increase is greater for primaries of low energy, whose interactions with the atmosphere result mostly in nucleons (neutrons and protons) as disintegrated products (Pomerantz, 1974). Hence the composition of secondary radiation in the atmosphere changes with latitude. The neutron component increases much more than the ionizing component and represents a larger percentage of the total radiation at high latitudes than at the equator. This effect is shown in Fig. 7, where the data are normalized to unity at the equator. The neutron dose equivalent rate at 60° is 6 times its value at the equator, whereas the ionizing component increases by a factor of only 2.2.

Determination of the Cosmic-Ray Neutron Spectrum

Although the first reported measurements of the neutron spectrum produced by cosmic-ray interactions with the Earth's atmosphere were made 20 years ago (Hess et al., 1959), there are still

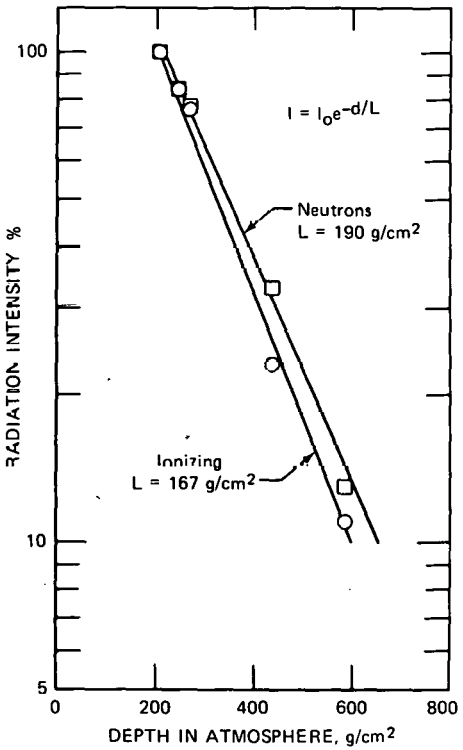


Fig. 6 Altitude dependence of radiation intensity at 20° N geomagnetic latitude.

questions concerning both the absolute intensity and the energy spectrum.

Published estimates of the cosmic-ray neutron flux density at midlatitudes and at sea-level range from 6.5×10^{-3} neutron cm^{-2} sec^{-1} to 1.8×10^{-2} neutron cm^{-2} sec^{-1} (Boella et al., 1963; Kent, 1963; Boella et al., 1965; Watt, Clare, and Gordon, 1965; Hajnal et al., 1971). Hajnal et al. (1971) have summarized these estimates and show that they are basically of two types: measurements made at or near sea level, and measurements made at altitudes of 10 km or greater that have been extrapolated to sea level through application of attenuation coefficients for air. In the same work, Hajnal et al. (1971) reported measurement of the cosmic-ray neutron spectrum at sea level using a Bonner sphere spectrometer.

Measurements made at high altitude have the advantage of being performed at neutron flux densities that are much greater than those

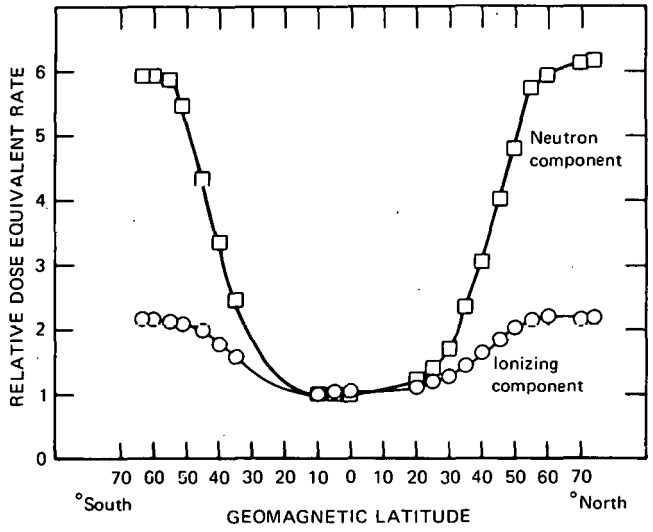


Fig. 7 Dependence of relative dose-equivalent rates on geomagnetic latitude [altitude 10.1 km (33,000 ft)].

at sea level. Estimating the sea-level flux density from such data, however, introduces an element of uncertainty because we do not yet have sufficiently accurate knowledge of the transport of cosmic-ray-produced neutrons through the atmosphere. For example, by assuming an attenuation length of 145 g/cm^{-2} through the atmosphere, Watt, Clare, and Gordon (1965) averaged results of several investigators to estimate a value of 1.8×10^{-2} neutron cm^{-2} sec^{-1} for the sea-level flux density at midlatitudes. This value is considerably higher than the recent measurements made at sea level (Table 2).

The cosmic-ray neutron flux density at sea level is small and difficult to measure. In particular, the spectrum in the thermal and near-thermal energy region may be perturbed by features of the local terrain (Yamashita, Stephens, and Patterson, 1966). Such difficulties may explain the 30% spread in the data of Table 2. Note that variations in solar activity have been estimated to account for fluctuations in neutron flux density of no more than 5% at a given location (Simpson, 1951; O'Brien and Burke, 1973).

In view of these uncertainties in the absolute value of neutron flux density integrated over the entire energy spectrum, it is not surprising that there is no general agreement as to the detailed shape of the neutron differential energy spectrum. One of the major problems in the experimental determination of the cosmic-ray

TABLE 2

Summary of Measured Values of Cosmic-Ray Neutron Flux Density at Mid-Latitudes and at Sea Level

Latitude, deg N	Neutron flux density, neutrons cm^{-2} sec^{-1}	Reference
46	0.0065	Boella et al., 1963
46	0.0084	Kent, 1963
44	0.0071	Yamashita, Stephens, and Patterson, 1966
41	0.0082	Hajnal et al., 1971

neutron spectrum is that it extends over a wide energy range, from ~0.01 eV to at least several 10s of GeV. The spectral intensity is also relatively low even at high altitudes, and the flux lacks strong directional characteristics. For determining the entire cosmic-ray neutron spectrum, the practical consequence of these constraints is to require use of a spectrometer system that has relatively low resolution (Routti, 1969).

The general approach has been to use a limited number of high-sensitivity neutron detectors, each of which responds over a fairly wide segment of the total energy range. Detector response functions must overlap on the energy scale so that no energy region is omitted. Response functions with contrasting shapes are selected so that, although they overlap on the energy scale, the energy regions for maximum response of individual detectors are distributed across the total energy domain.

The work carried out to date has been directed primarily toward establishing good experimental technique and toward ensuring that the neutron detectors (*see* "Detectors and Instrumentation," this paper) operate reliably in flight. Nevertheless, enough data have been obtained to make possible the three separate estimates of the neutron energy spectrum described in the following paragraphs.

Moffett I Spectrum. During the first series of three flights described by Hewitt et al. (1978), neutron measurements were made with a set of polyethylene moderators. The accuracy of the data acquired was limited by the use of only one lithium iodide detector (i.e., measurements were not made simultaneously in each moderator). Data were normalized using the moderated BF_3 counter monitor, a technique which may introduce errors in data taken during flights in which there are large changes in geomagnetic latitude. During the third flight, however, the aircraft flew at an altitude of 12.5 km

(41,000 ft) and at constant geomagnetic latitude for a period of time long enough to obtain data from a complete set of moderators. The statistical accuracy ranged from ±3% to ±10% and was judged good enough to obtain a preliminary estimate of the neutron spectrum in the energy region from thermal to a few 10s of MeV.

Table 3 shows the values for detector response calculated from the differential neutron spectrum unfolded from the experimental data using the computer program LOUHI (Routti, 1969). Quite good agreement between the measured and calculated response is obtained as is true for the two spectra discussed later. Figure 8 shows the neutron spectrum unfolded from these data; for comparison, the measured spectrum of Hess, Canfield, and Lingenfelter (1961) and the spectra calculated by Merker et al. (1973) and Armstrong, Chandler, and Barish (1973) are also shown. In the light of subsequent work, however, it is premature to draw any detailed conclusions from this preliminary spectrum.

TABLE 3

Bonner Sphere Measurements: Moffett I

Detector	Measured responses*	Calculated responses†
1.3 cm (0.5 in.)—LiI bare	51	51
Cadmium covered	34	34
5.1 cm (2 in.)—PE‡	119	119
7.6 cm (3 in.)—PE	198	199
12.7 cm (5 in.)—PE	271	268
20.3 cm (8 in.)—PE	186	192
25.4 cm (10 in.)—PE	145	137
30.5 cm (12 in.)—PE	98	101
45.7 cm (18 in.)—PE	56	56

*Measured responses: counting rates normalized to 1000 cpm of BF_3 neutron monitor.

†Calculated responses: counting rates to be expected for each detector from the assumed spectrum and known response functions.

‡Polyethylene.

Hawaii Spectrum. The second spectrum (Fig. 9) is obtained from data taken during the series of flights from Hawaii (Stephens et al., 1978) in the range of geomagnetic latitude $17°N \leqslant \lambda \leqslant 21°N$ at an altitude of 12.5 km (41,000 ft). Interpretation of the data taken during these flights is made difficult by two factors:

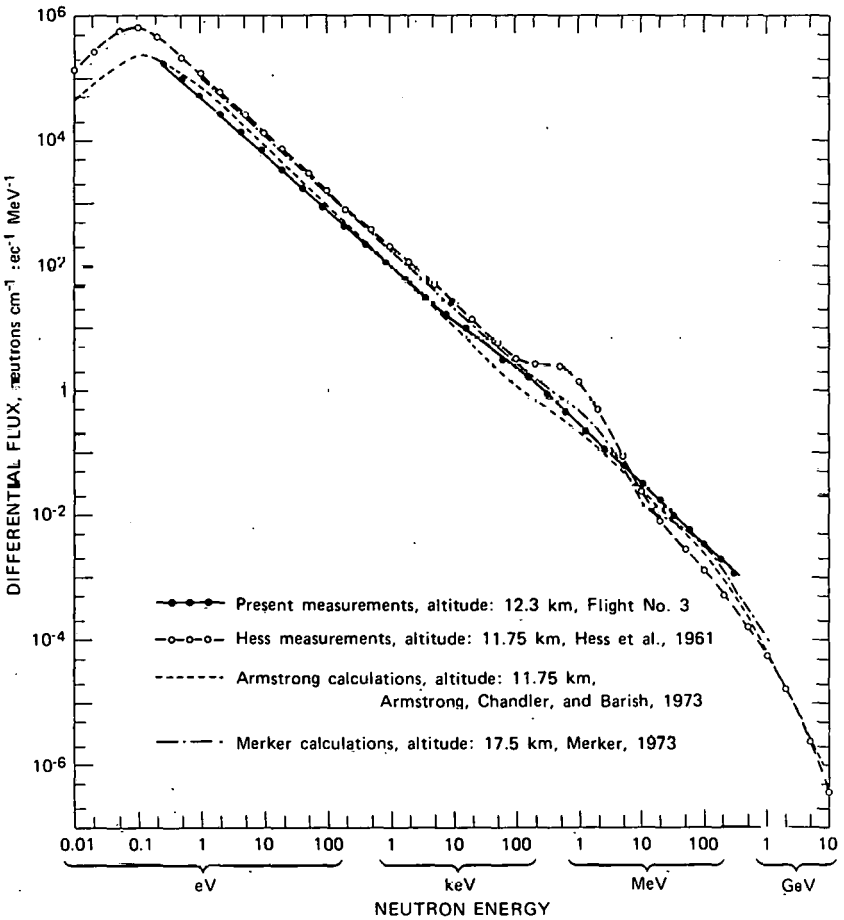


Fig. 8 A comparison of the cosmic-ray neutron spectrum obtained from the Bonner sphere neutron spectrometer on flight 3 with the spectrum measured by Hess et al. (1959) and calculated by Armstrong, Chandler, and Barish (1973) and by Merker et al. (1973).

1. A LiI crystal 8 mm diameter x 4 mm high was used rather than the standard 12.7-mm diameter x 12.7-mm high (0.5 in. x 0.5 in.) crystal for which response functions have been calculated.

2. A mixed set of moderators was used—the smaller moderators, 12.7 cm diameter (5 in. diameter) and less, being of polyethylene and the larger moderators consisting of water-filled aluminum shells.

The experimental data taken with the smaller crystal were later normalized to that which would have been observed if a standard-size crystal detector had been used. These normalization factors were

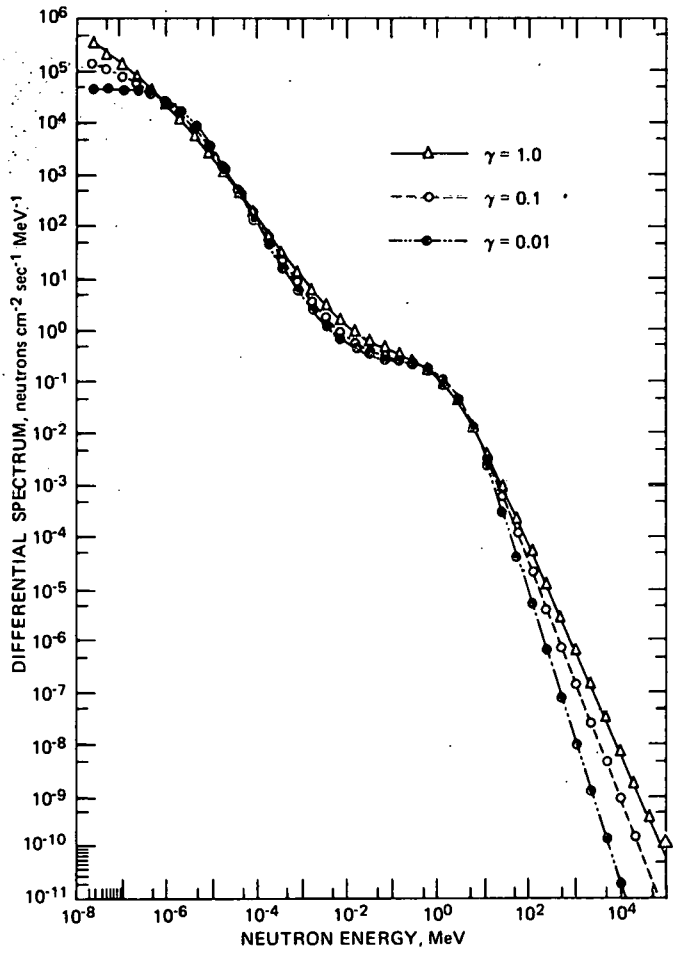


Fig. 9 Neutron differential energy spectra unfolded from Hawaii data (12.4 km) for different values of smoothing parameter γ.

obtained during Flight Series III, which was done at higher geomagnetic latitudes (44°N to 56°N). They are, therefore, uncertain to the extent that they vary with the neutron spectrum and that the cosmic-ray neutron spectrum varies with geomagnetic latitude. At present, errors introduced by this normalization are judged to be smaller than errors due to other sources.

The experimental data obtained with the Bonner sphere spectrometer at an altitude of 12.5 km (41,000 ft) have been used to estimate the neutron differential energy spectrum with the computer program LOUHI (Routti, 1969). The results are shown in Fig. 9.

The LOUHI unfolding routine permits varying constraints to be placed on the rapidity and magnitude of fluctuations in the solutions it generates. This is achieved by the use of a smoothing parameter, γ, which normally is given values between 0 and 1.0. The higher the value of γ, the more constrained are fluctuations in the solution generated and the lower the ability to resolve sharp structure in the spectrum. Figure 9 shows solutions for values of $\gamma = 1.0$ (heavily damped), $\gamma = 0.1$ (moderately damped), and $\gamma = 0.01$ (lightly damped). Significant differences in the calculated spectra are evident, but it is not entirely clear whether these differences are due to fluctuations of statistical origin or to systematic errors introduced by the use of two detectors of different size and a mixed set of moderators.

Moffett II Spectrum. The third spectrum (Fig. 10) is calculated from data obtained during flight 9 on Oct. 30, 1974. The data were normalized to an altitude of 12.5 km (41,000 ft) and a geomagnetic latitude of 45°N. During this flight, measurements were made of the production of ^{24}Na by the ^{27}Al(n,α)^{24}Na reaction. Sufficient activity was produced during the flight to permit its determination to a precision of ±3% at the Lawrence Berkeley Laboratory low-background facility (Wollenberg and Smith, 1966). This reaction, with a threshold of 6 MeV, provides constraints on the allowed spectral shape, particularly from threshold energy up to about 30 MeV. Preliminary studies with computer code LOUHI (Routti, 1960) show that the resolution in this energy interval improves by inclusion of the aluminum detector with the Bonner spectrometer detectors. Results from this flight show that, at the level of precision we have achieved in data acquisition, the presently used response functions of the Bonner spectrometer and the aluminum detector represent an internally consistent set according to the criteria used to evaluate computer-calculated spectra. The experimentally observed and computer-calculated detector counting rates are closely matched from a spectral distribution of reasonable shape. This constitutes an important step forward toward our goal of obtaining an improved determination of the cosmic-ray neutron spectrum.

Recoil Proton Detector Data

Figure 11 shows typical data collected during a flight in July 1977 at 12.8 km (42,000 ft) at about 40°N latitude. This representation shows the number of pulses as a function of their rise time for five different recoil proton energies. On the rise-time axis, one channel represents about 10 nsec. The first peak represents the

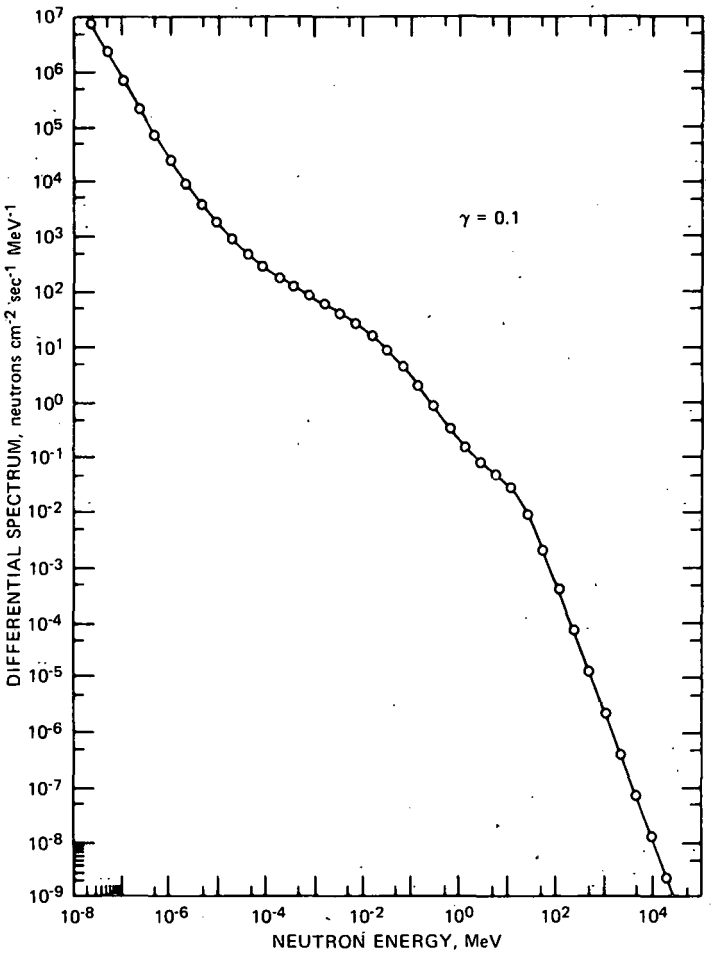


Fig. 10 Neutron differential energy spectra unfolded from data obtained during flight 9 originating from Moffett Field. [Altitude 12.5 km (41,000 ft); geomagnetic latitude, 45°N; $\gamma = 0.1$.]

fast rise-time component of the radiation (the gamma, electron, and external proton radiation), and the second peak contains those pulses generated by neutron interactions. A significant feature of these data is that the rise time of the proton peak shifts with amplitude, hence, no single rise time discriminator setting would effectively resolve the recoil protons of different energies from the mixed background radiation. The use of the two-parameter analyzer was therefore crucial to our calculation of neutron dose.

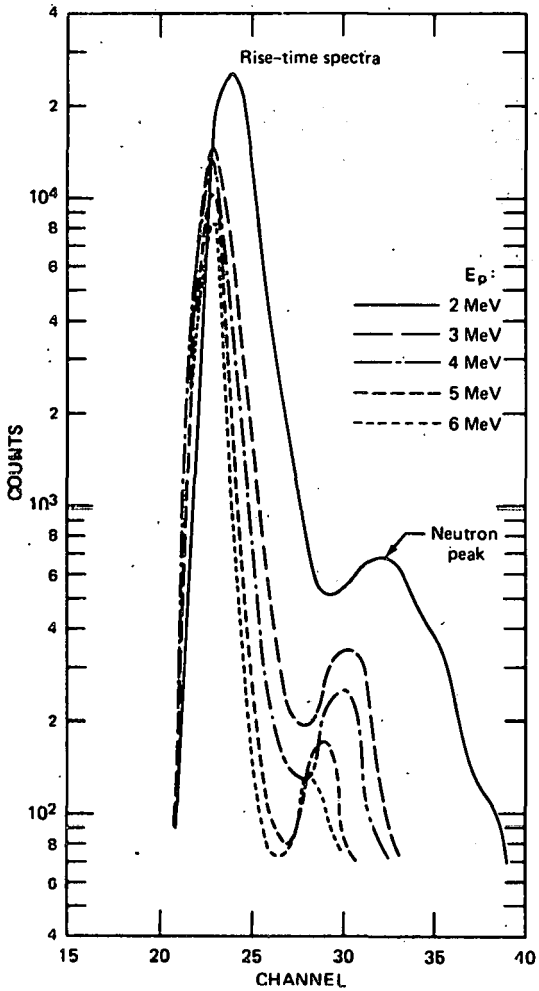


Fig. 11 Typical recoil proton detector data.

Having isolated the neutron signals from those of the background radiation, we evaluated the neutron dose by separating the recoil protons into a number of energy bands and summing the total number of pulses in each band. The result of this calculation is that, at 12.8 km (42,000 ft) and 40°N latitude, the neutron dose rate from 2- to 10-MeV recoil protons was 5.2 μrads/hr. Accepting the literature value of 6.5 for the quality factor for cosmic-ray neutrons (Patterson, Routti, and Thomas, 1971) would give a dose equivalent rate of 0.034 mrem/hr, if the same dose rate were measured in tissue.

Dose Equivalent Meter Data

Hewitt et al. (1976) reported the experimental data obtained using the Brookhaven National Laboratory (BNL) dose equivalent meter during the first three flights of this collaboration. The instrument gives readings for the absorbed dose rate, $\dot{D}$, and dose equivalent rate, $\dot{H}$, in the mixed radiation field. If it is assumed that this radiation field consists of two components—the first lightly ionizing, consisting of electrons, muons, and photons (denoted by the suffix L) and the second due to neutrons (denoted by the suffix N)—it is easily shown that

$$\frac{\dot{D}_L}{\dot{D}_N} = \frac{Q_N - Q}{Q - 1} \tag{1}$$

$$\frac{\dot{H}_L}{\dot{H}_N} = \frac{1}{Q_N} \frac{Q_N - Q}{Q - 1} \tag{2}$$

Q is the quality factor for the mixed radiation field (given by $\dot{H}/\dot{D}$).

The values of Q obtained during flights 1 and 2 were 1.70 and 1.85, respectively. If we assume a value of $Q_N = 6.5$ for cosmic-ray neutrons (Patterson, Routti, and Thomas, 1971) and substitute into Eqs. 1 and 2, we obtain

$$\frac{\dot{H}_L}{\dot{H}_N} = 1.1 \text{ (flight 1) and } 0.85 \text{ (flight 2)}$$

Thus, for these two flights, neutrons contributed from 13 to 15% of the total absorbed dose rate and from 48 to 54% of the total dose equivalent rate. These results are very similar to values calculated by O'Brien and McLaughlin (1972), who estimated the neutron contribution to be 11% to the absorbed dose rate and 45% to the dose equivalent rate at middle latitudes. Furthermore, the neutron dose equivalent rate, $\dot{H}_N$, deduced from the measured values $\dot{H}$ and $\dot{D}$ and an assumed value of $Q_N = 6.5$, was in fair agreement with estimates obtained from other neutron detectors (Hewitt et al., 1976).

SUMMARY AND CONCLUSIONS

Since the beginning of this collaboration in 1974, we have obtained preliminary neutron intensity and spectral data at commercial jet aircraft altitudes over a wide range of latitudes. We have been able to demonstrate the successful operation under high-altitude flight conditions of the RSS-111 ionization chamber, the

BNL dose equivalent meter, the moderated BF_3 counter, the Bonner spectrometer, aluminum activation detectors, and a recoil proton detector.

In a latitude survey mission during November of 1976, we determined the dose equivalent rates of both the neutron and the ionizing components of the atmospheric radiation from latitudes of 75°N to 62°S. On these and other flights we recorded intensity data up to 13.7 km (45,000 ft).

The fast neutron contribution to the absorbed dose has been evaluated from the recoil proton spectrum in an organic scintillator.

Data were obtained with the RSS-111 ionization chamber and moderated BF_3 counter in all flights, and these instruments have been consistently reliable. These data are in essential agreement with previously published data.

The BNL dose equivalent meter was used to obtain values of an average quality factor of the cosmic-radiation environment at these altitudes. Values of dose equivalent measured with this instrument were in fair agreement with estimates obtained from our other instruments (Hewitt et al., 1976).

Our experience with the neutron spectrometer shows:

1. Data obtained with the Bonner spheres must have a statistical accuracy of about ±1% if the neutron spectrum in the region 0.1 to 10 MeV is to be well-defined. (At the present time our data contain statistical errors ranging from ±3% to ±10%.) By accumulating data simultaneously on all moderators, statistical precision of ±1% or better can be obtained during a single flight, and, furthermore, any systematic uncertainties due to the present normalizing technique will be eliminated.

2. It will be desirable to obtain a complete set of experimental data with a moderator made of one material.

3. Data should be taken with LiI detectors of the standard dimensions (0.5 in. diameter × 0.5 in. high).

4. We have been able to determine the quantity of ^{24}Na produced in our aluminum activation detectors during a 6-hr flight to an accuracy of about ±3%.

5. We have been able to combine Bonner sphere data with aluminum activation detector data, with an important improvement in the resolution of the spectrometer system in the energy region of ~10 MeV. The addition of data from the bismuth fission counter, which has been shown to be stable and reliable in operation during flight at high altitudes, is most important to the determination of the high energy flux density.

Data obtained with the neutron spectrometer system have enabled three estimates of the cosmic-ray spectrum to be evaluated.

These spectra, although preliminary, are in essential agreement with the previously published experimental and theoretical data.

ACKNOWLEDGMENTS

The authors express their gratitude to Hans Mark, former Director, Ames Research Center, for his interest and assistance. They also wish to thank A. Henson and A. Rindi, Lawrence Berkeley Laboratory, University of California, who played an important role in using the LOUHI program to determine the neutron spectra, and R. V. Griffith of the Lawerence Livermore Laboratory, who obtained preliminary data with the Bonner spectrometer system.

Thanks are also due J. McLaughlin and F. Hajnal, Environmental Measurements Laboratory, for their useful information and encouragement. J. W. Baum and A. V. Kuehner, Brookhaven National Laboratory, loaned us the Brookhaven Dose Equivalent Meter and helped in data analysis. R. Mendell, New York University, provided the initial liquid scintillation detector.

Special thanks are also due to R. Kirby, A. B. Buckner, W. Buckley and A. S. Bunker, students at San Jose State University, who participated in data acquisition and analysis. R. M. Cameron, C. M. Gillespie, Jr., and L. C. Haughney, Ames Research Center, were extremely helpful in arranging for flight time and locating the experimental equipment on the C-141 and CV-990 aircraft. G. K. Kojima and A. L. Campbell, Ames Research Center, aided by modifying the electronic circuitry of this system and interfacing all the experimental packages with the aircraft environment.

This work was supported in part by the USDOE.

REFERENCES

Adams, J. A. S., and W. M. Lowder (Eds.), 1964, *The Natural Radiation Environment*, University of Chicago Press, Chicago.

——, W. M. Lowder, and T. F. Gesell (Eds.), 1975, in *The Natural Radiation Environment II*, Symposium Proceedings, Houston, Tex., Aug. 7—11, 1972, ERDA Report CONF-720805-P1 (2 Vols.), Rice University and the University of Texas, Houston, Tex., NTIS.

Armstrong, T. W., K. C. Chandler, and J. Barish, 1973, Calculations of Neutron Flux Spectra Induced in the Earth's Atmosphere by Galactic Cosmic Rays, *J. Geophys. Res.*, 78: 2715-2726.

Boella, G., et al., 1963, Measurements of the Cosmic-Ray Neutron Flux in the Atmosphere, *Nuovo Cim.*, 29: 103-117.

——, G. D. Antoni, C. Dilworth, M. Panetti, and L. Scarsi, 1965, Measurement of the Cosmic Ray Neutron Flux at 4.6 Billion Volts Geomagnetic Cutoff Rigidity, *J. Geophys. Res.*, 70: 1019-1030.

Bramblett, R. L., R. I. Erving, and T. W. Bonner, 1960, A New Type of Neutron Spectrometer, *Nucl. Instrum. Methods*, 2: 1-12.

Gauntner, D. J., and L. C. Haughney (Eds.), 1977, *Interhemispheric Survey of Minor Upper Atmospheric Constituents During October—November 1976*, Report NASA-TM-X-73630, National Aeronautics and Space Administration.

Hajnal, F., J. E. McLaughlin, M. S. Weinstein, and K. O'Brien, 1971, *1970 Sea-Level Cosmic Ray Neutron Measurements*, USAEC Report HASL-241, Health and Safety Laboratory.

Hatton, C., 1971, The Neutron Monitor, in *Progress in Elementary Particles and Cosmic Ray Physics*, Vol. XVI, pp. 1-100, J. G. Wilson and S. A. Wouthuysen (Eds.), Interscience Publishers, New York.

Hayakawa, S., 1969, *Cosmic Ray Physics*, Wiley-Interscience, New York.

Haymes, R. C., 1964, Fast Neutrons in the Earth's Atmosphere, *J. Geophys. Res.*, 69: 841-852.

Hess, W. N., H. W. Patterson, R. W. Wallace, and E. L. Chupp, 1959, Cosmic-Ray Neutron Energy Spectrum, *Phys. Rev.*, 116. 445-457.

——, E. H. Canfield, and R. E. Lingenfelter, 1961, Cosmic-Ray Neutron Demography, *J. Geophys. Res.*, 6: 665-677.

Hewitt, J. E., et al., 1976, *Ames Collaborative Study of Cosmic-Ray Neutrons*, Report NASA-TM-X-3329, National Aeronautics and Space Administration.

——, et al., 1977, *Brief Report on Radiation Dose Rate Measurements During the 1976 Latitude Survey Mission*, Report NASA-TM-X-73630, National Aeronautics and Space Administration.

——, et al., 1978, Ames Collaborative Study of Cosmic-Ray Neutrons: Mid-Latitude Flights, *Health Phys.*, 34: 375-384.

Kent, R. A. R., 1963, *Cosmic-Ray Neutron Measurements*, USAEC Report HW-SA-2870, Hanford Atomic Products Operation.

Klumpar, D. M., J. A. Lockwood, R. N. St. Onge, and L. A. Friling, 1973, Energy Spectrum and Flux of 3- to 20-MeV Neutrons and 1- to 10-MeV Gamma Rays in the Atmosphere, *J. Geophys. Res.*, 78: 7954-7967.

Kuehner, A. V., J. D. Chester, and J. W. Baum, 1973, Portable Mixed Radiation Dose Equivalent Meter, in *Neutron Monitoring for Radiation Protection Purposes*, Symposium Proceedings, Vienna, 1972, pp. 233-246, STI/PUB/318, Vol. 1, International Atomic Energy Agency, Vienna.

McCaslin, J. B., H. W. Patterson, A. R. Smith, and L. D. Stephens, 1968, Some Recent Developments in Technique for Monitoring High-Energy Radiation, in *Proceedings of the First International Congress of Radiation Protection*, Rome, 1966, pp. 1131-1137, Pergamon Press, Oxford.

Mendel, R. B., and S. A. Korff, 1963, Fast-Neutron Flux in the Atmosphere, *J. Geophys. Res.*, 68: 5487-5495.

Merker, M., 1973, Contribution of Galactic Cosmic Rays to the Atmospheric Neutron Maximum Dose Equivalent as a Function of Neutron Energy and Altitude, *Health Phys.*, 25: 524-527.

——, E. S. Light, H. J. Verschell, R. B. Mendell, and S. A. Korff, 1973, Time Dependent Worldwide Distribution of Atmospheric Neutrons and of Their Products. Part I. Fast Neutron Observations, *J. Geophys. Res.*, 78: 2727-2740.

NCRP Report 45, 1975, *Natural Background Radiation in the United States*, National Council on Radiation Protection and Measurements, Washington, D. C.

O'Brien, K., 1971, Cosmic Ray Propagation in the Atmosphere, *Nuovo Cim.*, 3A: 521-547.

——, and J. E. McLaughlin, 1972, The Radiation Dose to Man from Galactic Cosmic Rays, *Health Phys.*, 22: 225-232.

——, and G. de Planque Burke, 1973, Calculated Cosmic-Ray Neutron Monitor Response to Solar Modulation of Galactic Cosmic Rays, *J. Geophys. Res.*, 78: 3013-3019.

Patterson, H. W., J. T. Routti, and R. H. Thomas, 1971, What Quality Factor? *Health Phys.*, 20: 517-527.

Pomerantz, M. A., 1974, Relativistic Solar Cosmic Rays, *J. Franklin Inst.*, 298: 363-383.

Preszler, A. M., G. M. Sinnett, and R. S. White, 1974, Angular Distribution and Altitude Dependence of Atmospheric Neutrons from 10 to 100 MeV, *J. Geophys. Res.*, 79: 17-22.

Rossi, H. H., 1977, The Effects of Small Doses of Ionizing Radiation: Fundamental Biophysical Characteristics, *Radiat. Res.*, 71: 1-8. (Presented in San Francisco in June 1976 as part of a Symposium on The Radiological Response Relationships at Low Doses at the 24th Annual Meeting of the Radiation Research Society.)

——, and A. M. Kellerer, 1974, The Validity of Risk Estimates of Leukemia Incidence Based on Japanese Data, *Radiat. Res.*, 58: 131-140.

——, and W. Rosenzweig, 1955, Measurements of Neutron Dose as a Function of Linear Energy Transfer, *Radiat. Res.*, 2: 417-425.

——, et al., 1975, Final Report of the Advisory Committee for Radiation Biology Aspects of the SST: Cosmic Radiation Exposure in Supersonic and Subsonic Flight, *Aviat., Space Environ. Med.*, 46: 1170-1185.

Routti, J. T., 1969, *High-Energy Neutron Spectroscopy with Activation Detectors Incorporating New Methods for the Analysis of Ge(Li) Gamma-Ray Spectra and the Solution of Fredholm Integral Equations*, USAEC Report UCRL-18514, Lawrence Radiation Laboratory.

Sandstrom, A. E., 1965, *Cosmic Ray Physics*, North-Holland Publishing Company, Amsterdam.

Sanna, R. S., 1973, *Thirty-One Group Response Matrices for the Multisphere Neutron Spectrometer over the Range Thermal to 400 MeV*, USAEC Report HASL-267, Health and Safety Laboratory.

Simpson, J. A., 1951, Neutrons Produced in the Atmosphere by the Cosmic Radiations, *Phys. Rev.*, 83: 1175-1188.

Smith, A. R., 1965, Threshold Detector Applications to Neutron Spectroscopy at the Berkeley Accelerators, in *Proceedings of the First Symposium on Accelerator Radiation and Dosimetry and Experience, Brookhaven National Laboratory, Upton, New York, Nov. 3—5, 1965*, USAEC Report CONF-651109, p. 224, Division of Operational Safety, Division of Research, and Division of Biology and Medicine.

Stephens, L. D., J. B. McCaslin, A. R. Smith, R. H. Thomas, J. E. Hewitt, and L. Hughes, 1978, *Ames Collaborative Study of Cosmic Ray Neutrons, II: Southern and Mid-Latitude Flights*, Report LBL-6738, Lawrence Berkeley Laboratory.

Thomas, R. H., 1973, Neutron Dosimetry at High-Energy Particle Accelerators, in *Neutron Monitoring for Radiation Protection Purposes*, Symposium Proceedings, Vienna, 1972, pp. 327-353, STI/PUB/318, Vol. 1, International Atomic Energy Agency, Vienna.

UNSCEAR Report of the United Nations Scientific Committee on the Effects of Atomic Radiation, General Assembly, Official Records, 21st Session, Supplement 14 (A/6314), New York, 1966.

UNSCEAR, *Ionizing Radiation: Levels and Effects*, Vol. I, United Nations, 1972.

Upton, A. C., et al., 1966, Radiobiological Aspects of the Supersonic Transport, *Health Phys.*, 12: 209-226.

Verbinski, V. V., W. R. Burrus, T. A. Love, W. Zobel, and N. W. Hill, 1968, Calibration of an Organic Scintillator for Neutron Spectrometry, *Nucl. Instrum. Methods*, 65: 8-25.

Watt, D. E., D. M. Clare, and A. R. B. Gordon, 1965, *Tissue Dose-Equivalent Rates. I. From Cosmic Ray Neutrons. II. In the Low Level Environment of Chapelcross Nuclear Power Station*, UKAEA Report PG-Report-734.

Wilson, M. D., and M. Bercovitch, 1975, *Cosmic Ray NM-64 Neutron Monitor Data 28 and 29*, National Research Council of Canada Report, April and December 1975.

Wollenberg, H. A., and A. R. Smith, 1966, A Concrete Low Background Counting Enclosure, *Health Phys.*, 12: 53-60.

Yamashita, M., L. D. Stephens, and H. W. Patterson, 1966, Cosmic Ray Produced Neutrons at Ground Level: Neutron Production Rate and Flux Distribution, *J. Geophys. Res.*, 71: 3817-3834.

DISCUSSION

Koperski: What ionization chamber did you use? What sources were used for chamber calibration? What was the ionization chamber's measurement error?

Tucker: The ionization chamber was a commercially available high-pressure oxygen-filled spherical chamber, based on the design of the U. S. Department of Energy Environmental Measurements Laboratory in New York. The basic calibration is with National Bureau of Standards traceable ^{226}Ra sources; additional calibrations were done with ^{22}Na and ^{137}Cs sources. The intensity of ionizing radiation at flight altitudes is >100 μrads/hr—a high level for this instrument, so the measurement errors are only a few percent.

de Ras: Did you use TLD in the Bonner spheres, and how did you discriminate against other ionizing radiation? In calibrating did you have measuring points between thermal and 100 keV for neutron response?

Tucker: A LiF (Eu) scintillation crystal was used in all Bonner spheres measurements. Data from each sphere were accumulated in a multichannel pulse height analyzer, so that events belonging to the thermal neutron capture peak (desired events) could be correctly separated from the underlying continuum that was produced by passage of charged particles through the detector. Use of the multichannel analyser was important because the height of this continuum relative to the capture peak was different for each size sphere. The response functions used for Bonner spheres are those

calculated by Sanna (1973), the reference given in the text. We have not done experimental measurements to verify these calculations.

McLaughlin: Do you use a single value or a spectrally dependent set of values for Q. F., and in comparing the present Neutron Spectrum Data with Hess, was any account taken of the different solar cycles or points in the cycle?

Tucker: A spectrally dependent set of Q. F. values was used; however, at this stage of the measurement program, the calculation of dose equivalent is rather in the nature of an exercise than as a result. The present effort is concentrated toward acquisition of more precise data for determination of neutron spectral shape and intensity. When this has been achieved, we will then apply whatever Q. F. values are currently accepted to generate an estimate of dose equivalent. We have not attempted to take into account solar cycle differences when making comparisons of these results with those of Hess et al. I don't know what adjustment could be made beyond a simple intensity normalization based on data from cosmic-ray monitor stations located at appropriate geomagnetic latitudes.

McLaughlin: (Comment) The calculated low-energy response of Bonner spheres is not well known, and in connection with investigations of neutron exposure at nuclear power reactors, Livermore is investigating the responses experimentally.

Riel: What is the energy threshold of the proton recoil spectrometer? Data for the Bonner system on the National Bureau of Standards 144 keV n beams will be available soon.

Tucker: It is 1 MeV; we hope to lower it by better time resolutions.

Okano: How did you transfer the reading of altitude to atmospheric depth?

Tucker: The aircraft carried both atmospheric pressure and radar altimeters. In the work reported here, we have used atmospheric pressure data and converted to atmospheric depth (g/cm^2) through the use of tables of standard atmosphere parameters: *U. S. Standard Atmosphere, 1976*, published by the National Oceanic and Atmospheric Administration, National Aeronautics and Space Administration, and the U. S. Air Force, Washington, D. C., 1976.

Kodama: (Comment) In Japan we have a regular airborne survey for cosmic-ray measurements approximately once a year, and similar altitude and latitudinal data of ionizing and neutron components to be compared with your data are obtained by various types of detectors.

Anomalous Atmospheric Attenuation of Cosmic-Ray-Produced Neutrons near the Earth's Surface

MASAHIRO KODAMA, SHINKICHI KAWASAKI, TAKASHI IMAI, KAZUYOSHI TAKAHASHI, and MASAMI WADA
Cosmic Ray Laboratory, Institute of Physical and Chemical Research, Tokyo, Japan

ABSTRACT

The altitude distributions of cosmic-ray-produced neutron fluxes were measured in the lower atmosphere near the air—ground boundary at a geomagnetic latitude of 25°N. A pair of large BP-28 BF_3 proportional counters, each enclosed in a 2-cm polyethylene tube, were hung down out of a helicopter. One counter was covered by a cadmium sheet to separate the contributions from thermal and fast neutrons. Flights were carried out over land at two different altitudes and over seawater at various levels up to 1000 m above the surface. At high altitudes the attenuation length is 145 g/cm^2; this indicates an equilibrium condition for the neutrons at this latitude. Abrupt reductions of the attenuation length of fast neutrons exist at the same height (~50 g/cm^2 at ~400 m) above the land or water surface regardless of altitude. Because of the difference in the surface counting rates, the attenuation lengths are ~70 and ~50 g/cm^2 over land and water, respectively. Further altitude variations were obtained by a mobile survey along a mountain road. The counting rates vary in parallel with those in free air, being higher in free air for fast neutrons and higher on land for thermal neutrons. These results can be interpreted in terms of the air—ground boundary effects on the cosmic-ray neutron-flux distribution.

The diffusion of cosmic-ray neutrons in the atmosphere has been fairly well solved both experimentally and theoretically, from the standpoint of an equilibrium condition between the absorption and production rates as a function of neutron energy (Bethe, Korff, and Placzek, 1940; Light et al., 1973).

In the course of regular airborne surveys organized by our institute, atmospheric neutrons were measured repeatedly with

various types of moderated BF_3 counters (Kawasaki and Wada, 1974). Results for the attenuation length are in accord with other experiments and calculations (Raubenheimer and Stoker, 1971; Merker et al., 1973). In addition the neutron flux at the ground surface was found to be always below the smooth extension of the altitude curve. This tendency suggests that the air—ground boundary effect is being detected; i.e., in the lower atmosphere near the earth's surface, the equilibrium condition is broken because of discontinuity in the decelerating power and the production rate caused by the presence of a different medium, soil or water. Hence, the altitude dependence of neutrons near the ground is expected to be quite different from that in the upper atmosphere and is energy dependent (Yamashita, Stephens, and Patterson, 1966; O'Brien et al., 1978). Hendrick and Edge (1966) pointed out experimentally a peculiar transition behavior of neutrons at the air—ground boundary.

Despite its importance in environmental radiation studies, there are insufficient experimental data in this field. The airplane experiment is unsuitable to measure the altitude dependence of atmospheric neutrons near soil and water surfaces because of rapid altitude changes in flight. Moreover, the body materials of a jet plane may possibly modulate the energy spectrum of neutrons from that in free air. The helicopter experiment is free from these defects.

Helicopter surveys were carried out at heights of 0 to 1000 m at three different environmental sites: (1) sea-level land, (2) mountain land, and (3) seawater. Some additional surveys on land and water were performed from an automobile and a boat, respectively. In most of these surveys, we used a pair of large BP-28 BF_3 counters, 180 cm long, 15 cm in diameter, at 20 cm Hg gas pressure, and with 2-cm-thick polyethylene moderators (generally used for the cosmic-ray neutron monitor). One counter was covered with a cadmium sheet at the outer surface of the moderator to discriminate between thermal and fast neutrons. In this paper we describe the experiments, summarize the observations and results, and discuss the atmospheric attenuation of neutrons in connections with various air—ground boundary effects.

EXPERIMENTAL DETAILS

The first helicopter experiment was performed over sea-level land in 1976. A polyethylene-moderated BP-28 counter and a cadmium-shielded International Geophysical Year (IGY) type BF_3 counter, 90 cm long, 3.8 cm in diameter, and surrounded by 2.5-cm-thick paraffin, were used. The energy response of this kind of moderated neutron counter is almost flat over the energy range from

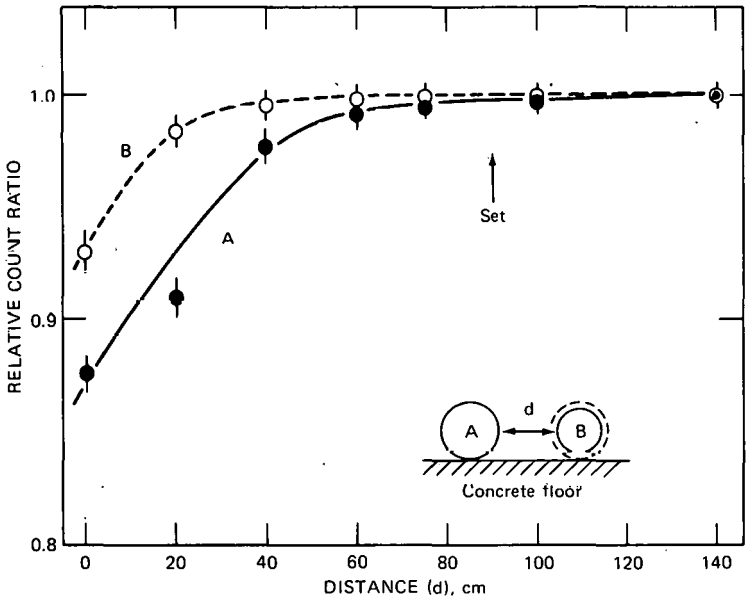


Fig. 1 Counting rates of two moderated BF_3 counters (— —○— —, counter A; ——●——, counter B, which is cadmium covered) as functions of the distance between the two, in relation to counting rates obtained when the distance is infinite.

25 keV to about 1 MeV (Yamashita et al., 1966). These counter assemblies were hung in the air by steel wires 5 m beneath the helicopter cabin so that a free-air condition was approximated throughout the flight. Two additional helicopter experiments were carried out in 1977 over the mountain region (900 m above sea level) and the Sagami ocean bay with a pair of BP-28 counters, one of which was cadmium covered. For the sake of comparison, a mobile survey was made on land at various elevations in parallel with the helicopter altitudes.

Before the flights in 1977, the effect of mutual interference of the double-counter array was investigated since counting rates may be influenced by a nearby counter acting as a neutron absorber. Figure 1 gives the counting rates relative to the value obtained by a single counter as functions of distance between the two. It is evident from the figure that the counters must be separated by at least 80 cm to avoid the interference effect. In our experiment two BP-28 counters were arranged with a spacing of 90 cm.

Details of the helicopter-loaded equipment are indicated in Fig. 2. Particular attention was paid in construction to eliminating

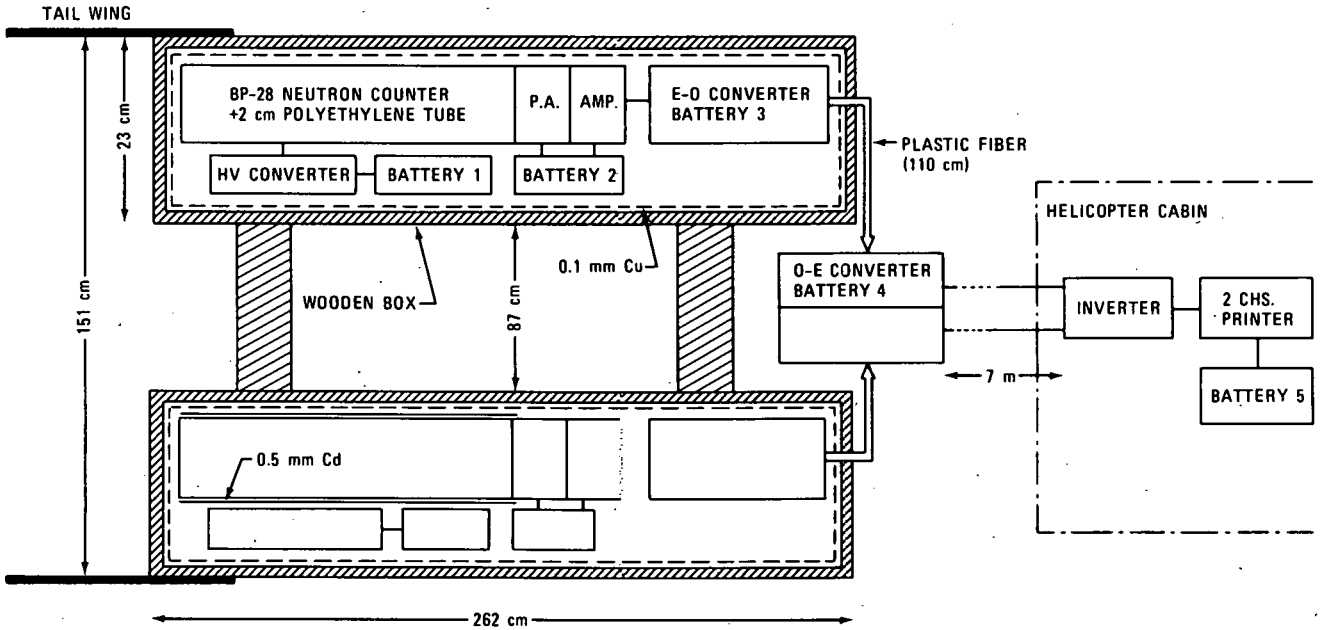


Fig. 2 Arrangement of the neutron detector used in our experiments.

electromagnetic noise from outside the equipment. First, each counter assembly, including the amplifier and power supply, was shielded completely by a 0.1-mm copper sheet. Then the optical coupling system was applied; a part of the cable between the counter assembly and the recorder installed in the helicopter cabin was replaced by a plastic optical fiber. A diagram of the electronic coupling circuit is shown in Fig. 3. With these two devices, we ensured satisfactory operation of the equipment in any flight.

The mobile survey was made with the same equipment on the Mount Fuji highway at ground-level heights equivalent to the helicopter flight levels. Water-surface measurements were made from a small motor boat on Yamanaka Lake at the foot of Mount Fuji. The observation site (a 6.4-km^2 area 980 m above sea level) was 500 m or more offshore.

RESULTS

Our first indication of the anomalous attenuation property of atmospheric neutrons came from the results of airborne experiments in 1973 and 1974, shown in Fig. 4. The black circles represent the altitude variation measured by the BP-28 counter and the open circles that for the IGY type counter. Four IGY counters were used, each surrounded by a different thickness of paraffin (0, 1, 2.5, and 5 cm). All observed data were averaged, however, because differences among the counters were insignificant. Although the counting statistics are not excellent, even in the BP-28, an apparent steepening of the attenuation is recognizable at a height of around 950 to 1000 g/cm^2.

Results of the helicopter experiments over land and ocean are summarized in Fig. 5. The figure clearly shows an abrupt change of the attenuation length at ~980 g/cm^2 over sea-level land and ocean and at ~865 g/cm^2 over the mountain of 918 g/cm^2. In other words, the attenuation length clearly changes at a residual mass of ~50 g/cm^2, regardless of the altitude of surface land or of the medium (soil or water). The separation of the altitude variations over land and ocean is apparent. The counting rate over water is lower than that over soil (Wada and Kawasaki, 1975; O'Brien et al., 1978), but the two essentially coincide at high altitudes. The counting rate above the mountain lake does not display this behavior because of the small size of the lake relative to the total area affecting the helicopter measurements.

Results from the mobile survey conducted using the same equipment used in the helicopter experiment are shown in Fig. 6.

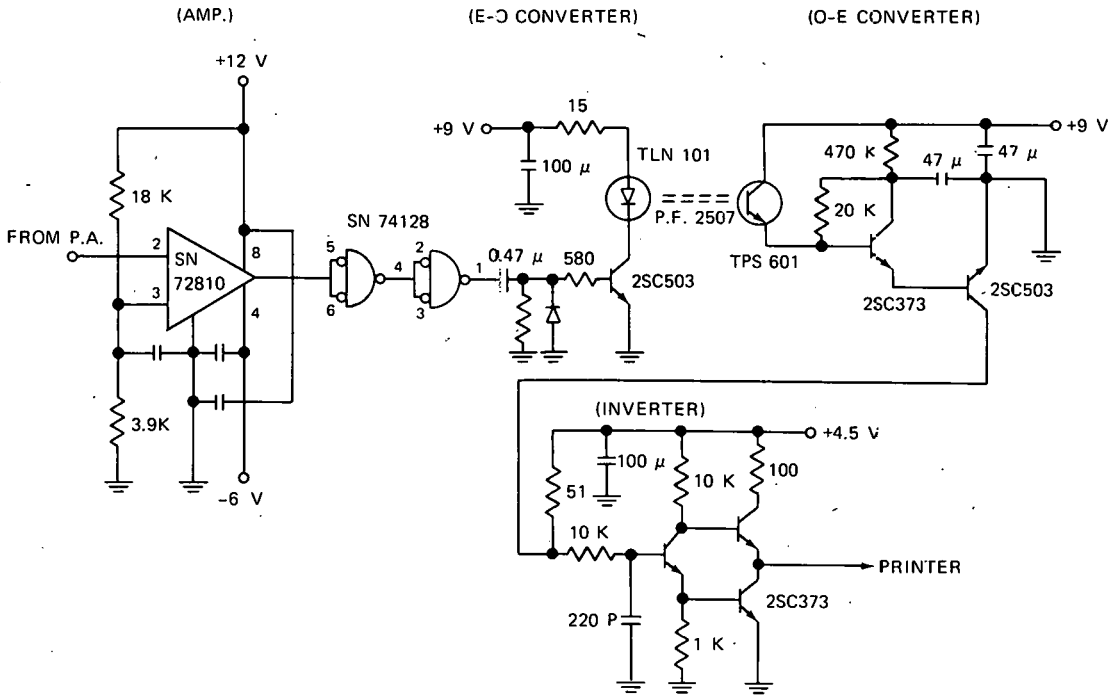


Fig. 3 Electronic circuits of the electric-optical signal converters.

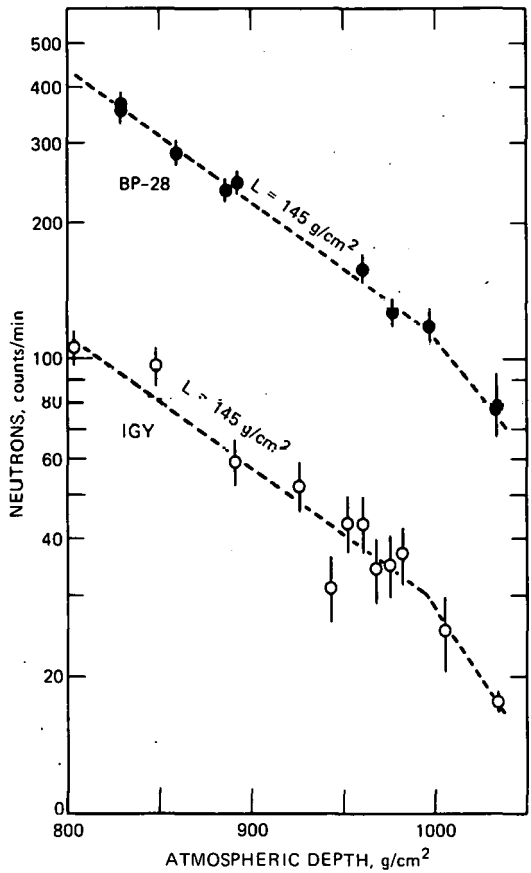


Fig. 4 Cosmic-ray-produced neutron flux measured by BP-28 (●) and IGY (○) counters aboard the aircraft as a function of atmospheric depth.

The spaces marked with letters (A, B, C, etc.) indicate the sites where measurements were made while parked; other measurements were made while moving. There is significant scatter in the counting rates over the statistical limits; this may reveal the effects of the varying composition of soil and other circumstances. The altitude variations are plotted in Fig. 7. Though the scatter of the points is large, as mentioned earlier, the slope does not differ from the value of 145 g/cm^2 observed in air. Also plotted are the counting rates on the lake, which are substantially below the land values.

Figure 8 shows the attenuation character of the thermal neutrons as defined by the cadmium difference, where two groups of data (for

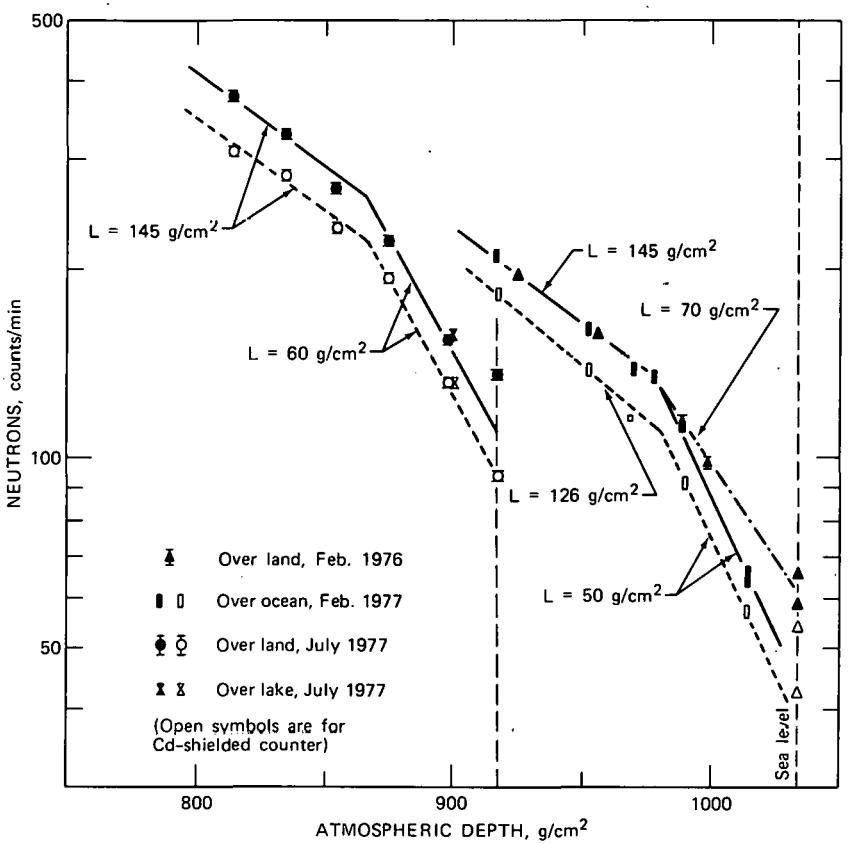


Fig. 5 Altitude variations of neutron fluxes measured in three helicopter surveys, two over land and one over seawater, and one lake survey from a boat.

land and free air) are plotted. They vary in parallel with each other and show the same attenuation length as fast neutrons. The thermal neutron flux on land is higher than that in free air, with a ratio 1 : 0.6. Observed values over the lake at 170 and 370 m are also shown, together with the value on lake surface. All three points coincide with the values in air within the experimental accuracy.

DISCUSSION AND SUMMARY

The atmospheric neutrons produced by cosmic rays are in equilibrium with the parent nucleonic component, and the energy

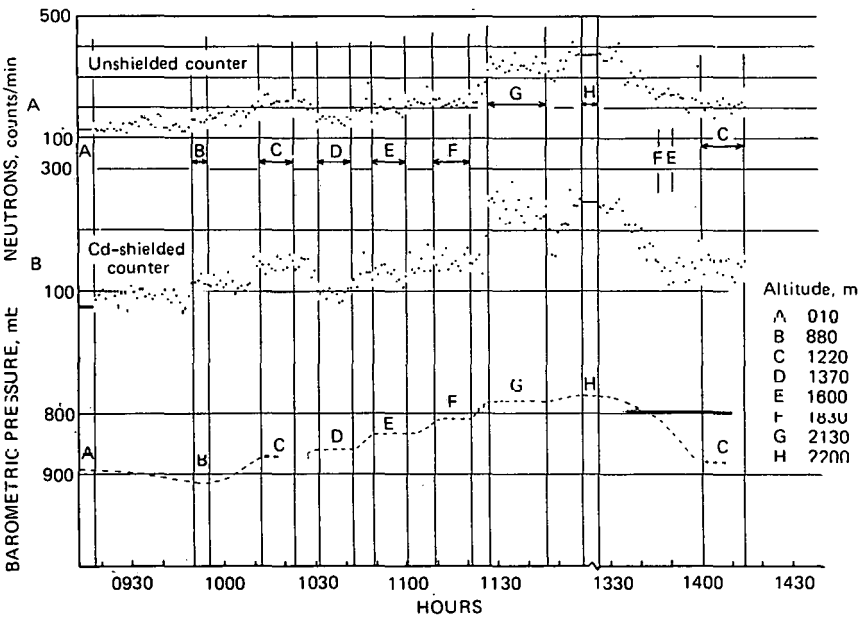


Fig. 6 Time profiles of 1-min counts of neutrons and barometric pressure in the mobile survey on Mount Fuji, July 26, 1977. The altitudes of the parking sites are denoted by the letters (values are given on the figure).

spectrum maintains a nearly constant functional form throughout the whole atmosphere. This situation causes a nearly constant attenuation length over wide ranges of energies and altitudes. At altitudes near the ground, however, the equilibrium condition no longer holds, and some change in the attenuation length is expected because the production, moderation, and absorption of neutrons differ between air and soil or water. A theoretical estimation by Yamashita, Stephens, and Patterson (1966) indicates that such a change for the thermal neutrons occurs at about 100 m above the ground, where the flux increases rapidly toward the surface. At about 750 m (residual mass of ~90 g/cm^2), the fast neutron flux gradually decreases. According to a similar estimation by O'Brien et al. (1978), 1-MeV neutrons exhibit the variational points at about 20 g/cm^2 (~170 m) over land and at about 50 g/cm^2 (~420 m) over seawater, but the variation is not so abrupt. For the thermal neutrons the flux has its minimum at about 20 g/cm^2 over land or seawater and then shows a marked rise near the interface.

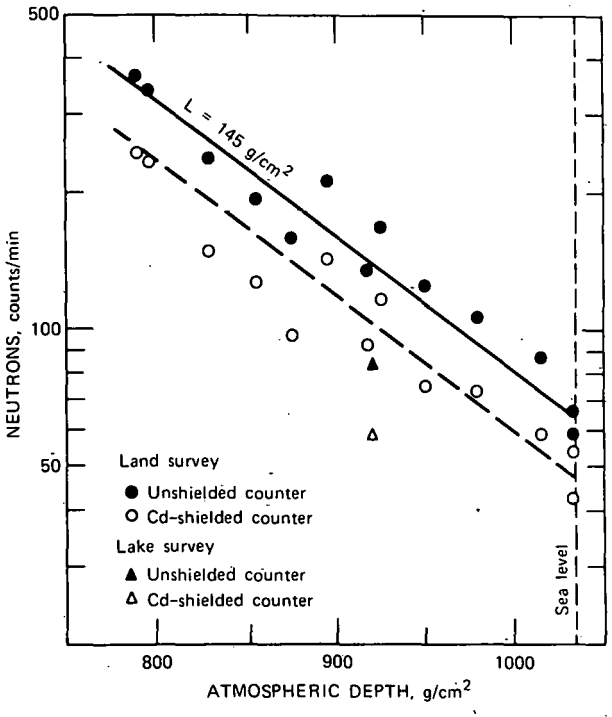


Fig. 7 Altitude variations of neutron fluxes measured in the mobile survey covering the altitude range from sea level to 2200 m. Also shown is the counting rate over the lake, which is 981 m above sea level.

For the sake of thorough comparison of experimental results, the representative lines in Figs. 4 to 7 are combined in Fig. 9. The following points are summarized from the figure.

Fast Neutrons (Cadmium Shielded)

1. All the attenuation lengths just above the transition region near the surface are 145 g/cm^2 independent of the measuring conditions.

2. The altitude variation obtained by the mobile survey shows the same attenuation as that in free air, but the absolute counting rates are lower than those in air.

3. The free-air counting rates decrease suddenly near the ground. The break occurs at ~50 g/cm^2, 420 m above the ground, and the slope of the decrease is around 60 to 70 g/cm^2, which may be independent of the atmospheric depth of the ground level. The break

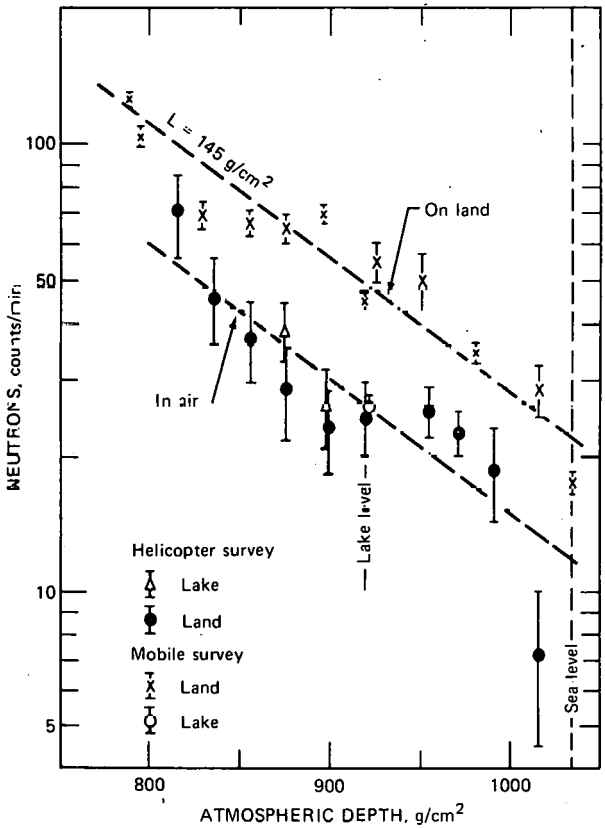


Fig. 8 Altitude variations of the count difference between the cadmium-shielded and unshielded counters, measured from the helicopter over land and lake and mobile surveys on the land and lake surfaces.

position was found to be between the theoretical estimations of Yamashita, Stephens, and Patterson (1966) and O'Brien et al. (1978).

4. The conclusions in item 3 mean that the free air and the ground counting rates, which are parallel to each other, as shown in Fig. 9, can be connected everywhere by the pattern described here regardless of the atmospheric depth.

5. The free-air counting rates over seawater reveal the same height for the break, but the slope below it is slightly steeper (50 g/cm^2) than over land. This arises from different counting rates on land and on seawater. The break position does not contradict the estimation by O'Brien et al. (1978).

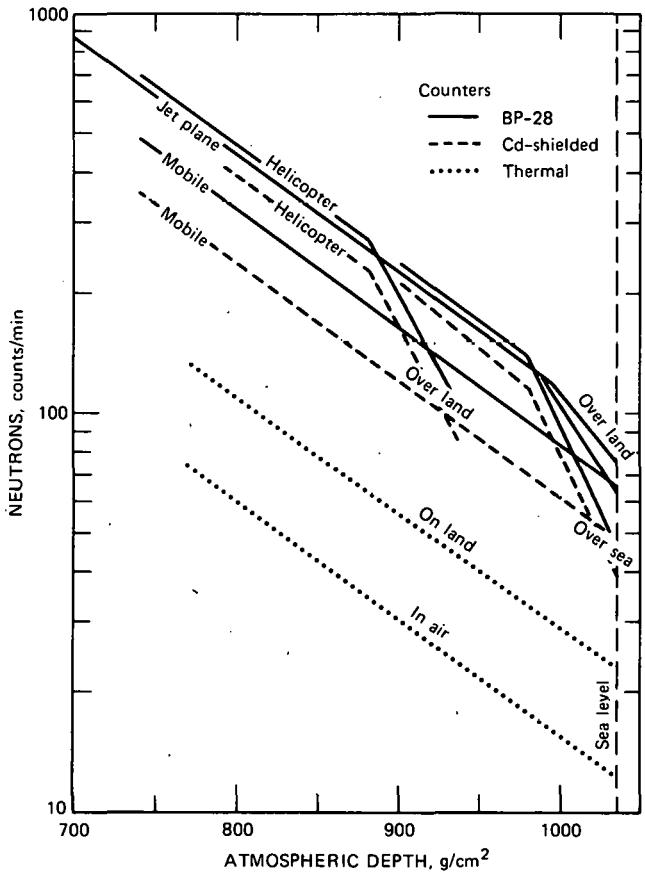


Fig. 9 Collected plots of altitude variations of neutron fluxes measured in aircraft, helicopter, and automobile surveys, showing only the lines that best fit observed values. Dashed line (— — —) is for the cadmium-shielded counter, the solid line (——), for the BP-28 counter, and two dotted lines (· · ·), for the cadmium difference, i.e., thermal neutrons.

Thermal Neutrons

1. Despite the scatter in the counting rates, we can say that both air and ground measurements give the same attenuation length, which also is the same as that for the fast neutrons.

2. Unlike fast neutrons, the counting rates on the ground are higher than those in air, with a ratio 1 : 0.6.

3. Item 2 suggests that the transition behavior between air and ground is opposite to that of fast neutrons. This is in accord with the theoretical view.

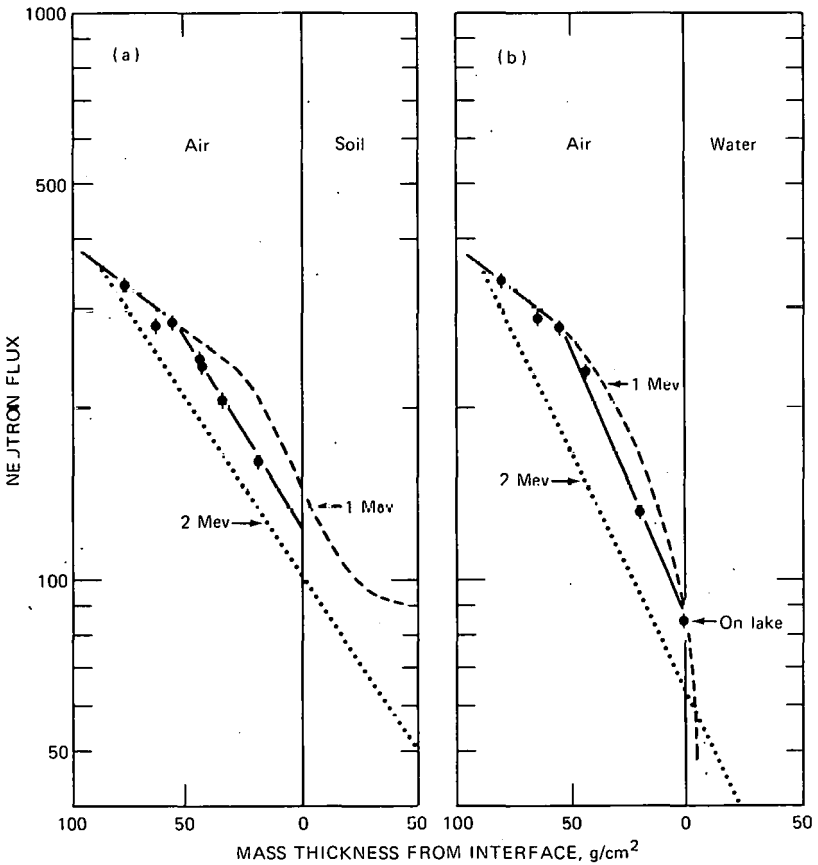


Fig. 10 Fast neutron flux as a function of depth at (a) the air–ground interface and (b) the air–water interface, shown as a solid line (——). Also shown are two theoretical curves for different neutron energies estimated by O'Brien et al., 1978 (— — —) and by Yamashita, Stephens and Patterson, 1966 (• • •).

4. As seen in Fig. 8, the free-air counting rate at the point nearest sea-level ground is very low in comparison with the extension of the altitude curve. This suggests the existence of a fine structure at the region very near the boundary, which should be investigated further.

In Fig. 10 the anomalous attenuations of the fast neutrons near the earth's surface are compared with theoretical estimations for the (a) air–ground and (b) air–water interfaces. The estimation by Yamashita, Stephens and Patterson (1966) is an empirical one based on some experimental data. O'Brien et al. (1978) performed the

basic neutron transport calculations. Taking into account the energy response of the detector, it seems reasonable that the theoretical estimations for 1- to 2-MeV neutrons are comparable with the present experimental results. Since the attenuation of the neutron flux very near the air—ground interface and underground is sensitive to the character of the soil (e.g., the water content and the elemental composition), we concluded that the qualitative consistency between experiment and calculation is satisfactory. The better agreement shown in Fig. 10, part b, may result from the fact that the air—water interface effect is rather simple.

ACKNOWLEDGMENT

We thank H. Kumagai for his help in constructing the optical coupling circuits.

REFERENCES

Bethe, H. A., S. A. Korff, and G. Placzek, 1940, On Interpretation of Neutron Measurements in Cosmic Radiation, *Phys. Rev.*, 57: 573-587.

Hendrick, L. D., and R. D. Edge, 1966, Cosmic-Ray Neutrons Near the Earth, *Phys. Rev.*, 145: 1023-1025.

Kawasaki, S., and M. Wada, 1974, Measurements of Altitude and Latitude Variations of Neutron Intensity by a Large BF_3 Counter Aboard an Aircraft, *Sci. Pap. Inst. Phys. Chem. Res. (Jpn.)*, 68:31-37.

Light, E. S., M. Merker, H. J. Verschell, R. B. Mendel, and S. A. Korff, 1973, Time Dependent Worldwide Distribution of Atmospheric Neutrons and of Their Products. 2. Calculations, *J. Geophys. Res.*, 78: 2741-2762.

Merker, M., E. S. Light, H. J. Verschell, R. B. Mendel, and S. A. Korff, 1973, Time Dependent Worldwide Distribution of Atmospheric Neutrons and of Their Products. 1. Fast Neutron Observations, *J. Geophys. Res.*, 78: 2727-2740.

O'Brien, K., H. A. Sandmeier, G. E. Hansen, and J. E. Campbell, 1978, Cosmic Ray Induced Neutron Background Sources and Fluxes for Geometries of Air Over Water, Ground, Iron and Aluminum, *J. Geophys. Res.*, 83: 114-120.

Raubenheimer, B. C., and P. H. Stoker, 1971, Attenuation Coefficients of Various Cosmic Ray Components in the Lower Atmosphere, in *Proceedings of the Twelfth International Conference on Cosmic Rays*, Hobart, Australia, Aug. 16–25, 1971, pp. 893-896.

Wada, M. and S. Kawasaki, 1975, Measurements of Sea-Level Counting Rates of a Large BF_3 Neutron Counter, *Sci. Pap. Inst. Phys. Chem. Res. (Jpn.)*, 69: 29-36.

Yamashita, M., L. D. Stephens, and H. W. Patterson, 1966, Cosmic-Ray-Produced Neutrons at Ground Level: Neutron Production Rate and Flux Distribution, *J. Geophys. Res.*, 71: 3817-3834.

——, L. D. Stephens, A. R. Smith, and H. W. Patterson, 1966, Detection Efficiency of Bare and Moderated BF_3-Gas-Filled Proportional Counters for Isotropic Neutron Fluxes, *J. Nucl. Sci. Technol. (Tokyo)*, 3: 343-353.

Measurement of Environmental Radiations with a Scintillation Spectrometer Equipped with a Spherical NaI(Tl) Scintillator

MASAHARU OKANO, KOICHI IZUMO, HIDEKAZU KUMAGAI, TAKEO KATOU, MASAMI NISHIDA, TATSUJI HAMADA, and MASAHIRO KODAMA
Institute of Physical and Chemical Research, Saitama Prefecture, Japan

ABSTRACT

Scintillation spectroscopy, in which a 3-in. spherical NaI(Tl) scintillator was used as a detector, was applied to a study of environmental radiations.

Below 3 MeV the total energy absorption of photons in the scintillator was obtained by the peeling-off method. As a result of this study, relative values of photon flux and exposure of seven energy groups of environmental gamma rays were compared with the theoretical values given by Beck (1972). The exposure rate contribution of various radionuclides estimated from a Ge(Li) spectrum is also given.

Analysis was made for cosmic rays above 3 MeV of energy absorption. The photon component in the NaI(Tl) spectrum was subtracted referring to the spectrum obtained with a plastic scintillator. Altitude dependence of the intensity of cosmic-ray charged particles was then obtained, where the conversion into the vertical intensity was made by taking into consideration the incident angle distribution of cosmic rays.

The construction and performance of a portable scintillation spectrometer that weighs about 10 kg are presented.

The NaI(Tl) scintillation counter is a useful tool and is widely used for environmental radiation measurements. The NaI(Tl) scintillation spectrometer is used to obtain information on radionuclides in the environment and on the radiation dose due to environmental gamma radiations.

Identification of the environmental radionuclides and determination of their contributions to the total exposure rate are done by means of in situ gamma-ray spectrometry developed and examined by Beck, DeCampo, and Gogolak (1972). They applied the technique

to the evaluation of exposure above a flat and infinite ground containing gamma-ray sources with assumed uniform of exponential distributions.

The photon-energy spectrum of environmental gamma rays was calculated by Minato and Kawano (1970) using a response matrix method. This method has the disadvantages that a number of response functions must be determined under each environmental condition to be studied and that the solution of simultaneous equations would introduce an appreciable error in the high energy region. Moreover, the work of both Beck and Minato was confined only to the analysis of gamma rays and did not extend to that of cosmic rays.

In our work a scintillation gamma-ray spectrometer equipped with a spherical NaI(Tl) scintillator was constructed and used to determine the incident photon-energy spectrums and the exposure of the environmental gamma rays. Information on cosmic rays has also been obtained from higher energy regions of the scintillation spectra.

SPHERICAL NaI(Tl) SCINTILLATOR

The use of a spherical NaI(Tl) scintillator in studying environmental radiations has two great advantages over other detectors: (1) the scintillator has almost no directional dependence of sensitivity, i.e., it gives the total amount of incoming radiations integrated with respect to their directions (Fig. 1), and (2) the spectrum of the absorbed energy of the incident charged-particle radiations with energy high enough to penetrate the scintillator should be simply represented as a triangle if the broadening in the detector system is neglected. Figure 2 is an example of the absorbed energy spectrums produced by the scintillator on Mt. Norikura (2770 m) with and without a lead shield. The spectrum with the lead shield represents a typical triangle profile in higher energy part. This simplicity promises an easy analysis of the scintillation spectrum. The excess in the spectrum over the triangle is attributed to the contributions from the lower energy particles that cannot penetrate the scintillator.

The construction of the spherical scintillation detector used in this study is shown in Fig. 3.

The detection efficiencies of gamma rays necessary for gamma-ray spectroscopy were determined by calculations and measurements. The total counting efficiency of the spherical NaI(Tl) scintillator can be calculated by an analytical integration to obtain

$$1 - 2/(\mu d)^2 + 2 \exp [-\mu d] [1/(\mu d)^2 + 1/(\mu d)]$$

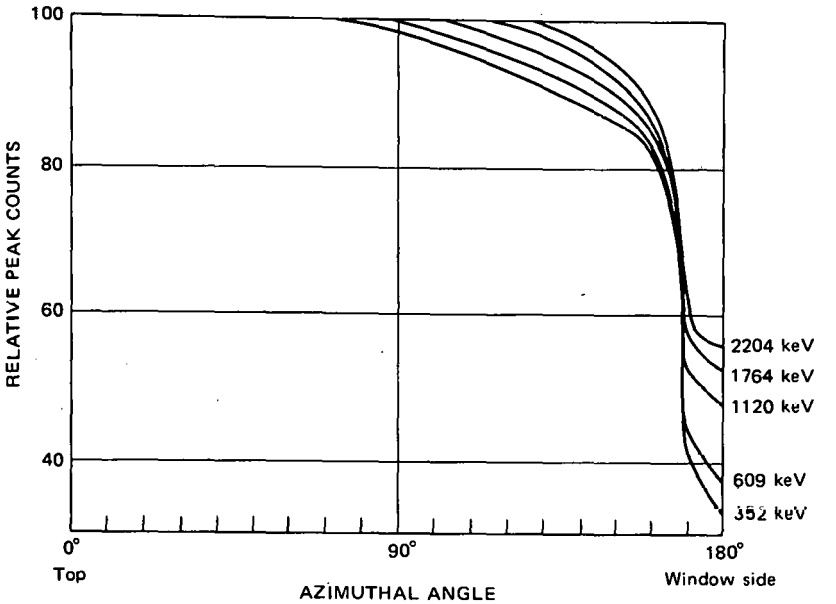


Fig. 1 Directional dependence of peak counts for a point radium source at about 1 m.

The counting efficiency of the spherical scintillator is only slightly smaller than that of the 3-in. ϕ by 3-in. NaI(Tl) cylindrical scintillator (Fig. 4).

The photopeak counting efficiencies were determined by measuring the peak-to-total ratios of the spectrums of monochromatic gamma-ray point sources. Figure 5 shows the peak-to-total ratios in comparison with the values of a 3-in. ϕ by 3-in. NaI(Tl) scintillator given by Heath (1957).

Gamma rays from potassium included in the window material of the photomultiplier tube could be reduced to a negligible level by an appropriate choice of the tube.

The absorbed energy spectrum of cosmic-ray charged particles with energy high enough to penetrate the scintillator should be a triangle, as mentioned above. The maximum absorbed energy in the present case is 47 MeV. The observed spectrum of cosmic rays is constructed by adding to the ideal spectrum the contributions from photon component, electron cascade showers, neutron-capture gamma rays, charged particles that cannot penetrate the scintillator, and the background from the detector itself. The neutron-capture gamma rays contribute to the spectrum in the energy region of 3 to 10 MeV. Under these circumstances it is preferable in analysis to divide the spectrum into the following three parts:

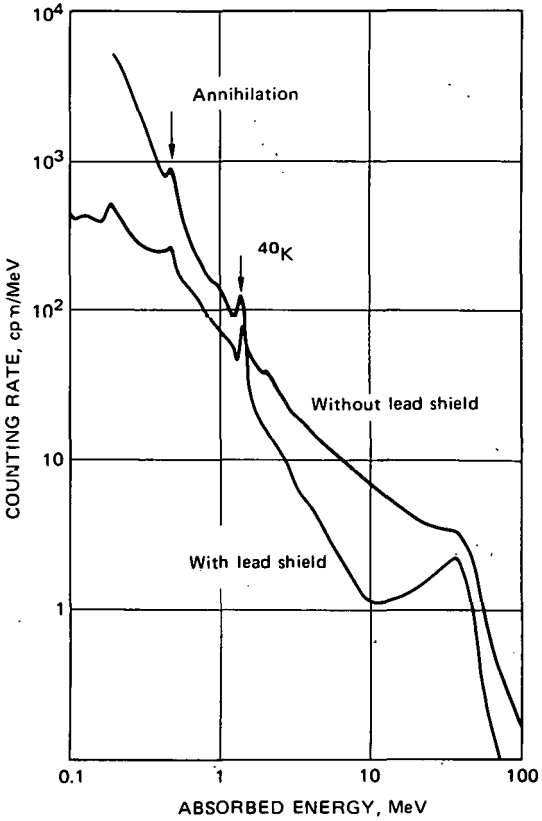


Fig. 2 Absorbed energy spectrums taken by the spherical NaI(Tl) scintillator on Mt. Norikura (2770 m).

1. *Environmental gamma-ray region (up to 3 MeV).* Included in this region are almost all radiations due to environmental radioactive materials and a negligibly small part (less than 1%) of the contribution to the spectrum from cosmic-ray charged particles.

2. *Middle energy region (over 3 to 10 MeV).* The spectrum in this region consists of the contributions from slow charged particles that cannot penetrate the scintillator, from neutron-capture gamma rays, and a fraction (4%) of the triangle mentioned above.

3. *Cosmic-ray region (above 10 MeV).*

OBSERVATION OF ENVIRONMENTAL GAMMA RAYS

Figure 6 is a block diagram of the detection system for environmental gamma rays. The Ge(Li) spectrometer in the diagram

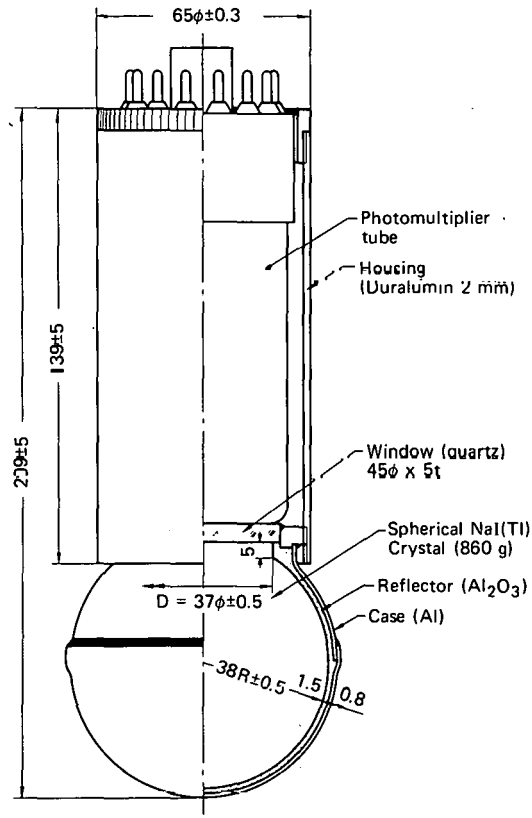


Fig. 3 Construction of the spherical scintillation detector.

was adopted for measuring uncollided gamma rays. Four-thousand channels of the dual–single multichannel pulse height analyzer were divided into two groups, one group of 3000 channels for the Ge(Li) detector and the other group of 1000 channels for the NaI(Tl) detector. An example of the observed spectrums is shown in Fig. 7.

In analyzing the absorbed energy spectrums in the region up to 3 MeV, we omitted the effects from high-energy cosmic rays and the background from the detector itself because of their small contributions.

The spectrums were analyzed as a composition of the photopeaks and their corresponding Compton continuums. The Compton continuum was assumed to have a flat distribution, i.e., the counting contribution from the Compton continuum to each channel below the channel corresponding to the so-called Compton edge, E_c, is assumed to be n_c with

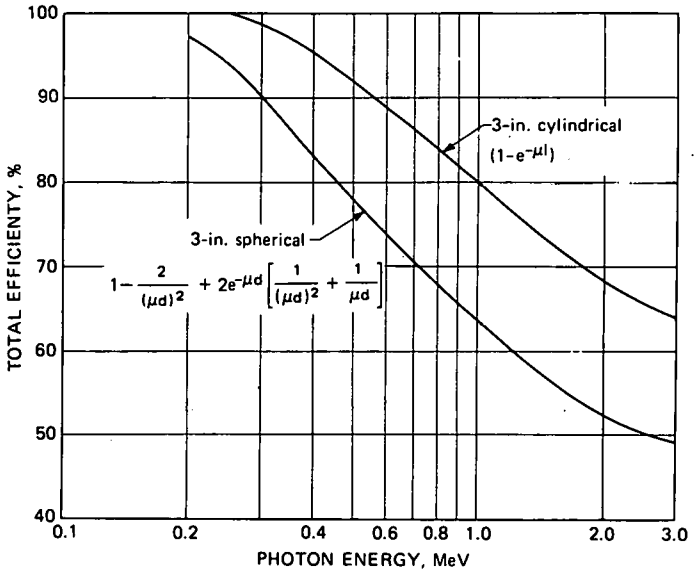


Fig. 4 Intrinsic efficiency of spherical and cylindrical NaI(Tl) scintillators for a beam parallel to cylinder axis.

$$n_c = n_p\,(1/R - 1) \cdot W/E_c$$

and

$$E_c = E_\gamma/(1 + mc^2/2E_\gamma)$$

where n_p = peak count
R = peak-to-total ratio
E = peak energy
W = energy width corresponding to one 10-keV channel
mc^2 = rest energy of an electron

After correction to the relation between energy and channel number is made by third-order polynomials, these Compton continuums are subtracted by the peeling-off method to obtain the total energy-absorption spectrum.

The spectrum thus obtained is then converted into gamma-ray flux density by taking into consideration the intrinsic peak efficiency and the cross section of the scintillator. The flux density of each channel can be easily converted into the absorbed dose by using energy absorption coefficient of the material concerned. Figure 8 shows every step of the conversion calculation from an observed

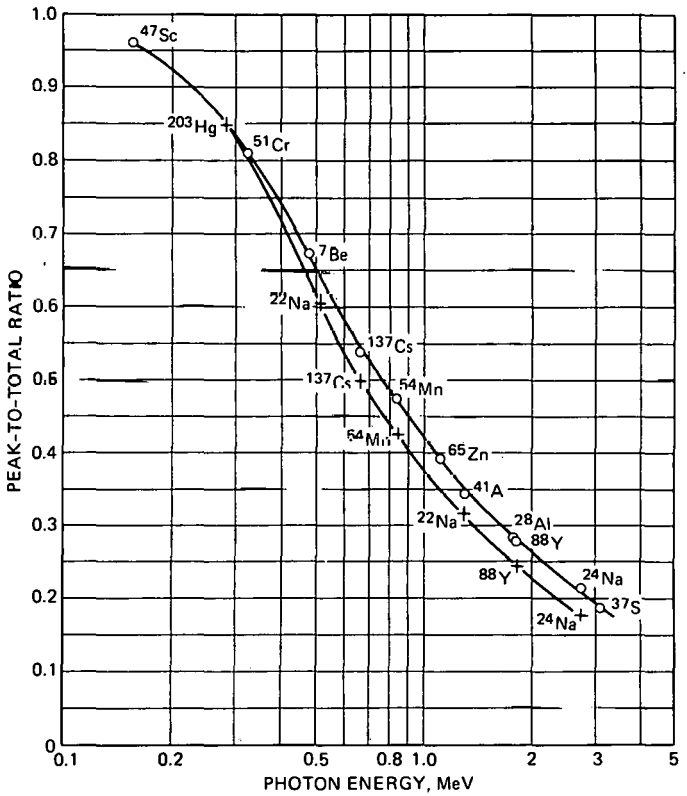


Fig. 5 Comparison of experimental results of the peak-to-total ratios: +, 3-in. ϕ spherical NaI(Tl) scintillator 30 cm from source; ○, 3-in. ϕ by 3-in. cylindrical scintillator 10 cm from source.

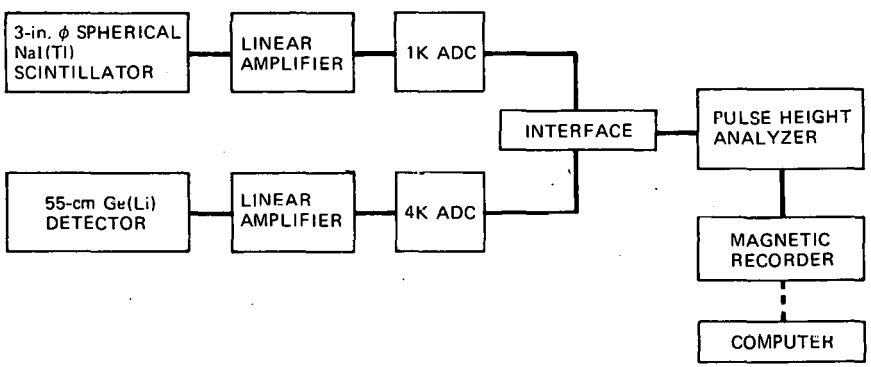


Fig. 6 Block diagram of the in situ radiation spectrometer.

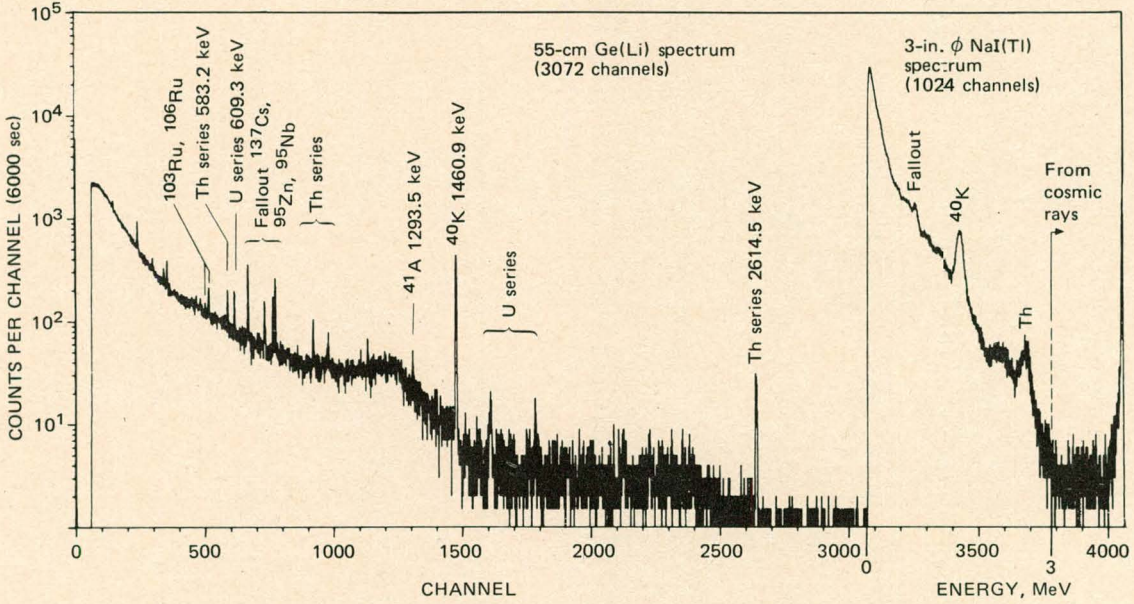


Fig. 7 In situ spectrums with the Ge(Li) and NaI(Tl) detectors.

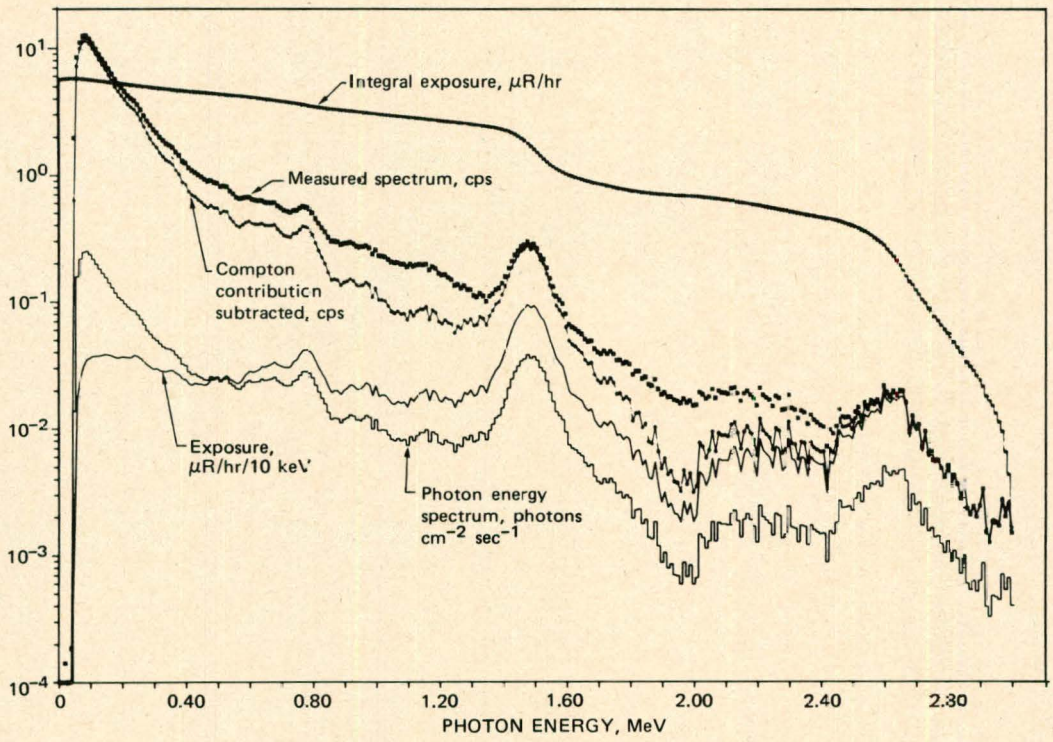


Fig. 8 Steps in the conversion calculation of the observed scintillation spectrum.

spectrum into exposure. These analyses are usually made by a minicomputer in that physical constants necessary for the analysis are given in numerical characters or in functional relations.

The total absorbed dose rate is obtained by integrating the contributions from all channels. The dose rate integrated above an energy up to 3 MeV is also shown in Fig. 8.

In Table 1 the gamma-ray flux density and the exposure rate obtained by measurements in an open place are compared with the calculation by Beck (1972) for a typical composition of natural radionuclides in the soil. Table 2 gives the exposure rates due to

TABLE 1

Comparison of Total Flux and Total Exposure Rate with Calculations by Beck (1972)

Energy range, keV	Flux, %		Exposure, %	
	Experimental	Calculated	Experimental	Calculated
Less than 50		4		1
50—100	18.3	23	2.5	3
100—250	31.3	30	9.7	10
250—500	15.7	16	11.6	11
500—1000	15.8	13	23.6	23
1000—2000	15.6	11	40.7	41
Above 2000	2.9	3	11.8	12

TABLE 2

Exposure Rate Contributions of Radionuclides Estimated from a 55-cm Ge(Li) Spectrum*

Nuclide	Exposure, μR/hr
Th series	1.48 ± 0.11
U series	0.753 ± 0.05
^{40}K	2.59 ± 0.15
^{95}Zr	0.147 ± 0.01
^{95}Nb	0.16 ± 0.02
^{137}Cs	0.21 ± 0.01
^{103}Ru	0.01 ± 0.003
^{106}Ru	0.08 ± 0.01
^{41}Ar†	0.085 ± 0.02
Total	5.52 ± 0.17

*Exposure rates as determined by Beck (1972).

†Uncollided photons only.

radionuclides in the ground as determined by Beck using the in situ Ge(Li) spectrometer. The sum of the exposure rates, 5.52 μR/hr, is in good agreement with the exposure rate value of 5.57 μR/hr obtained from the simultaneous measurement with the scintillation spectrometer. The latter was corrected for the contributions of cosmic rays up to 3 MeV and of potassium included in the detector which adds up to 0.26 μR/hr.

OBSERVATION OF COSMIC RAYS

Cosmic rays near the earth's surface mainly consist of charged particles, i.e., electrons and charged mesons. In addition, they have photons, which are as abundant as electrons, and a small amount of neutrons. In the region above 3 MeV in the scintillation spectrum, the number of counts above E (MeV), N(E), is therefore expressed by a sum of the counts due to penetrating charged particles, N_H; stopped charged particles, N_s; photons, N_p; and neutrons, N_n.

$$N(E) = N_H(E) + N_s(E) + N_p(E) + N_n(E)$$

As mentioned above, if the statistical fluctuation of counting is neglected, we have

$$\frac{N_H(E)}{N_H(0)} = 1 - (E/E_{max.})^2$$

where $E_{max.}$ is the maximum energy loss of particles in a scintillator, being 47 MeV for a 3-in. ϕ NaI(Tl). Then the value of $N_H(E)/N_H(0)$ becomes 99.6% above 3 MeV and 95.5% above 10 MeV.

The separate measurement of stopped charged particles and photons is normally done by using a detector surrounded by another detector connected in coincidence with the former detector. In our study we have made the separate assessment of those components by comparing the two spectrums obtained by a 3-in. ϕ NaI(Tl) and a 95-mm ϕ spherical plastic scintillator, respectively. Figure 9 shows altitude profiles observed during balloon flights. The results obtained by the NaI(Tl) scintillator are expressed with flux densities corresponding to energy loss above 3 MeV and above 10 MeV, whereas results from the 95-mm plastic scintillator are total flux density of penetrating charged particles calculated from counts above 14 MeV. For the plastic scintillator, $E_{max.}$ is 19 MeV. The difference of intensities observed with both scintillators is due to photon components of cosmic rays. From these data we find

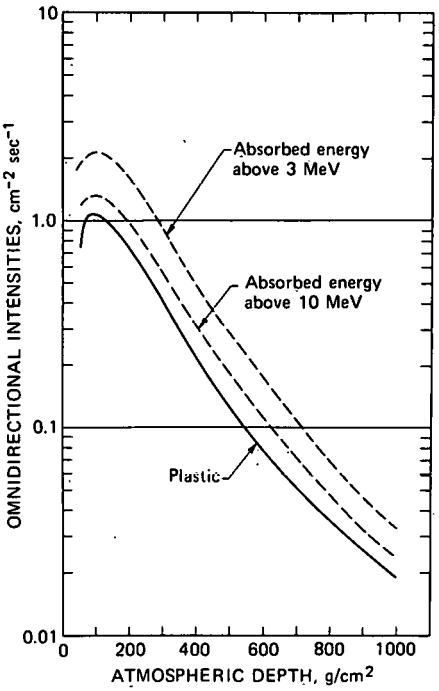


Fig. 9 Altitude dependence of the omnidirectional intensity of cosmic rays measured with a spherical (95-mm ϕ) plastic and a spherical (3-in. ϕ) NaI(Tl) scintillator (see text).

$$k = \frac{N_p(10) + N_s(10)}{N_p(3) + N_s(3)} = 0.45$$

which was almost constant at every altitude. If we neglect the neutron contribution N_n, $N_H(3)$ and $N_p(3) + N_s(3)$ can then be obtained from N(3) and N(10) by solving the equations

$$N(3) = N_H(3) + N_s(3) + N_p(3)$$

$$N(10) = N_H(3) \times 0.955/0.996 + [N_s(3) + N_p(3)] \times 0.45$$

If the neutron contribution is to be taken into consideration, one more equation of N(E) for higher energy, for example, 30 MeV, should be added.

The results obtained by the plastic scintillator represent omnidirectional intensities of charged particles. To convert them into vertical intensities, we measured the directional distribution of

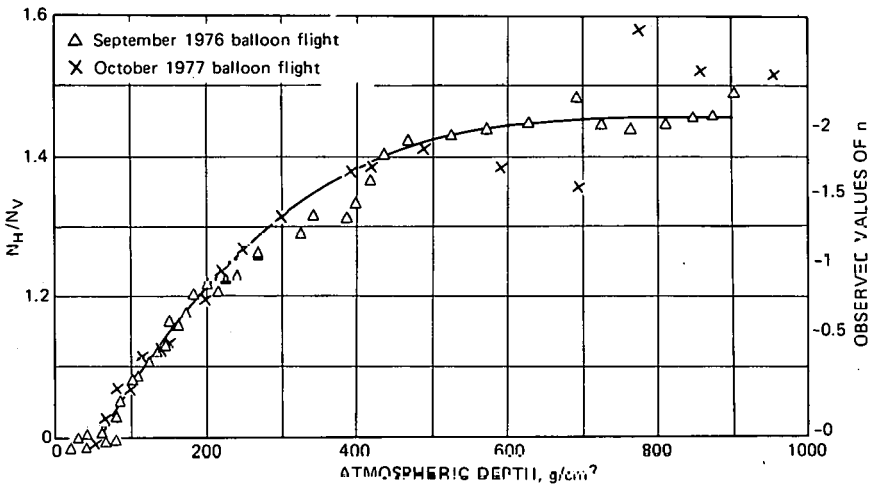


Fig. 10 Altitude variation of the directional parameter n of cosmic rays.

charged particles with two, perpendicularly crossing, long Geiger–Mueller counters (22.5 mm ϕ by 650 mm). From the count ratio of the two counters, the exponent n in the equation

$$I_\theta = I_v \cos^n\theta \qquad (\theta = \text{zenith angle})$$

was calculated. Figure 10 shows the altitude variation of observed values of n. Then we have the vertical intensity, I_v, from the equation

$$I_{total} = \frac{I_v \pi^2 d^2}{2(n+1)}$$

The altitude profile of the vertical intensity thus obtained is in fair agreement with the data of Rossi (1948), as shown in Fig. 11.

PORTABLE SCINTILLATION SPECTROMETER FOR FIELD USE EQUIPPED WITH A SPHERICAL NaI(Tl) SCINTILLATOR

A portable scintillation spectrometer for field use, applicable to the in situ measurement of environmental radiations, has been developed. The spectrometer consists of a spherical NaI(Tl) scintillation detector, an interface, and a commercial stereo tape recorder. The detector output is recorded on magnetic tape by converting the

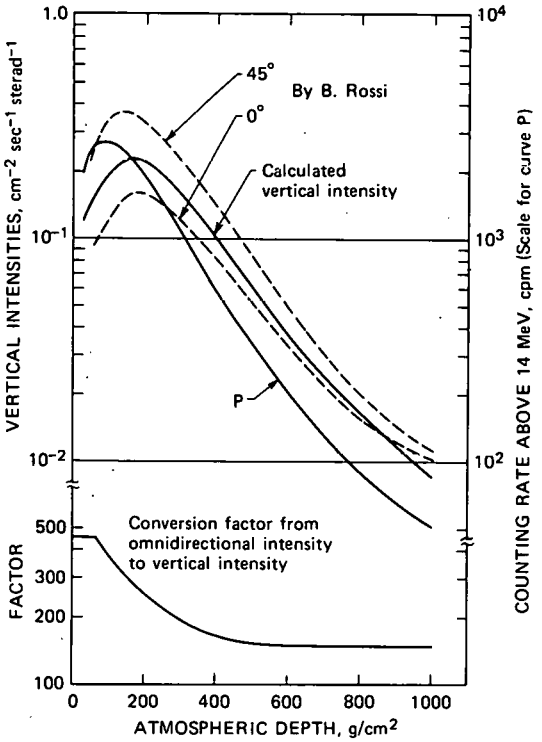


Fig. 11 Altitude dependence of the vertical intensity of cosmic rays derived from the data of plastic scintillation counter (curve P). Rossi's curves for geomagnetic latitudes of 0 and 45° are also shown.

pulse height into serial bit code by the interface. The interface, operated by a direct-current source of 7 to 30 V, consists of an amplifier, an analog-to-digital converter (ADC) and a parallel-to-serial converter (PSC) that converts the parallel output signals from the ADC into serial. The interface also incorporates a direct-current/direct-current (dc—dc) converter and functions as a low voltage (±15 V) source for other electronic circuits and as a high voltage source for a photomultiplier tube (PMT). The serial signals from the PSC are recorded in a two-channel tape, "0" bit in the first channel and "1" bit in the second channel. The dead time for successive counts is reduced by a buffer memory having a capacity of 13 bits x 16 words. The clock frequency of the output of the interface is changeable to either 7.5 or 15 kHz and enables the maximum counting rate of 500 or 1000 cps, respectively, which is sufficient for the measurements of environmental radiations.

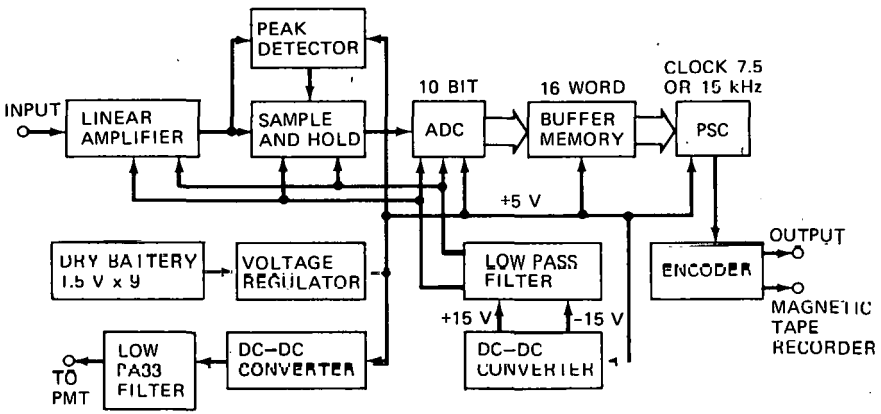


Fig. 12 Block diagram of the portable spectrometer.

The whole system of the spectrometer weighs about 10 kg. The recorded detector output is reproduced by the pulse height analyzer via a readout interface. Figure 12 is a block diagram of the spectrometer.

The scintillation spectrometer equipped with a spherical NaI(Tl) scintillator is thus a useful tool for measuring environmental radiations since it permits us to obtain parameters required for the dose calculation, i.e., energy and flux of direct and scattered gamma rays, and also some information on cosmic rays.

ACKNOWLEDGMENTS

This work was sponsored by our Science and Technology Agency. The authors express thanks to the staffs of Norikura Cosmic Ray Observatory of the Institute for Cosmic Ray Research and to the staffs of the Sanriku Balloon Center of the Institute of Space and Aeronautical Science.

REFERENCES

Beck, H. L., 1972, The Physics of Environmental Radiation Fields, in *The Natural Radiation Environment II*, Symposium Proceedings, Houston, Tex., Aug. 7—11, 1972, J. A. S. Adams, W. M. Lowder, and T. F. Gesell (Eds.), ERDA Report CONF-720805, pp. 101-133, Rice University and the University of Texas School of Public Health, NTIS.

——, J. DeCampo, and C. Gogolak, 1972, *In Situ Ge(Li) and NaI(Tl) Gamma-Ray Spectrometry*, USAEC Report HASL-258, USAEC Health and Safety Laboratory, NTIS.

Heath, R. L., 1975, *Scintillation Spectrometry—Gamma-Ray Spectrum Catalogue*, USAEC Report IDO-16408, Phillips Petroleum Co., Atomic Energy Division, NTIS.

Minato, S., and M. Kawano, 1970, Evaluation of Exposure Due To Terrestrial Gamma Radiation by Response Matrix Method, *J. Nucl. Sci. Technol.*, 7: 401-406.

Rossi, B., 1948, Interpretation of Cosmic-Ray Phenomena, *Rev. Mod. Phys.*, 20: 537-583.

Gamma-Ray Measurements in an Area of High Natural Radioactivity

L. LØVBORG,* L. BØTTER-JENSEN,* E. MOSE CHRISTIANSEN,* and B. LETH NIELSEN†
*Risø National Laboratory, DK-4000 Roskilde, Denmark, and †The Geological Survey of Greenland, Østervoldgade 10, DK-1350 Copenhagen K, Denmark

ABSTRACT

Natural radiation levels of several hundred microroentgens per hour are typically observed on the 2.5 km^2 Kvanefjeld plateau in South Greenland. The outcropping Th—U mineralized rocks continue at depth and represent a major low-grade uranium resource. About 5000 determinations of the radioelement concentrations in the terrain surface are available from exploration surveys with portable gamma-ray spectrometers, and it is of interest to interpret these data in radiological terms. A number of field locations were monitored with LiF thermoluminescence dosimeters, a high-pressure ionization chamber, and a portable gamma-ray spectrometer to study the relation between exposure rate and Th—U—K surface concentrations. These measurements were accompanied by carefully designed calibration experiments and a two-media gamma-ray transport calculation. Reliable factors for the conversion of a set of surface concentration values into a gamma-ray exposure rate were established. These factors are: 0.25 μR/hr per parts per million thorium; 0.50 μR/hr per parts per million uranium; 1.25 μR/hr per percent potassium. An additional contribution of 20 μR/hr from gamma-ray "skyshine" and cosmic rays was also deduced.

Extensive outcrops of peralkaline nepheline syenite and metasomatically altered gabbro are found on the Kvanefjeld plateau near the town of Narssaq, South Greenland. These rocks contain from 100 to 3000 ppm thorium and from 50 to 1000 ppm uranium and are therefore much more radioactive than ordinary igneous rocks. Many thousand square meters of the terrain surface have gamma-ray exposure rates of several hundred microroentgens per hour, and in places more than 1000 μR/hr can be observed.

The area is uninhabited and fairly inaccessible, and very few people stay in it for extended periods. Therefore the high natural radiation levels have not given rise to concern up to now. However, the body of radioactive rock represents a major low-grade uranium resource that may become exploitable in the future (Sørensen et al., 1974). Prolonged human activity in this anomalous radiation environment can thus be foreseen. Because of this aspect, the radiation levels in the potential mining area and its surroundings are being studied rather closely.

One source of information is a comprehensive set of data on the detailed surface distribution of thorium, uranium, and potassium. These data have been compiled in exploration surveys with portable gamma-ray spectrometers. The survey work was commenced several years ago (Løvborg et al., 1971), and today more than 5000 individual measurements have been completed.

This paper describes the evaluation of numerical constants that make it possible to convert the surface concentrations determined by in situ gamma-ray spectrometry into exposure rates near ground level. The experimental basis of the evaluation is an initial radiological survey reported by Bøtter-Jensen, Christensen, and Nielsen (1978). In that survey the exposure rates at selected field sites were monitored by thermoluminescence dosimeters (TLD's) and a high-pressure ionization chamber. Along with these measurements the radioelement concentrations in the ground below each monitoring point were determined using a portable spectrometer. The combined use of these data was supported by a gamma-ray transport calculation in plane, semi-infinite geometry.

RADIOACTIVE AREA

Kvanefjeld is a minor mountainous area situated at 60°58′N and 46°00′W. The plateau hosting the radioactive mineralization has an area of 2.5 km^2 and elevations varying from 500 to 685 m. Between 5 and 50% of the terrain surface is outcropping rock; the rest consists of in situ boulders and soil covered by low arctic vegetation.

Figure 1 shows a geological map of the area, which forms the northernmost part of the Ilímaussaq alkaline intrusion (1168 ± 21 x 10^6 years) (Blaxland, van Breemen, and Steenfelt, 1976). This intrusion belongs to the suite of Gardar igneous complexes in South Greenland (Emeleus and Upton, 1976), and it is composed of an early series of syenites and alkali granite and a later series of peralkaline nepheline syenites (kakortokite, foyaite, naujaite, and lujavrite). The latest differentiation product, lujavrite, consists of microcline, albite,

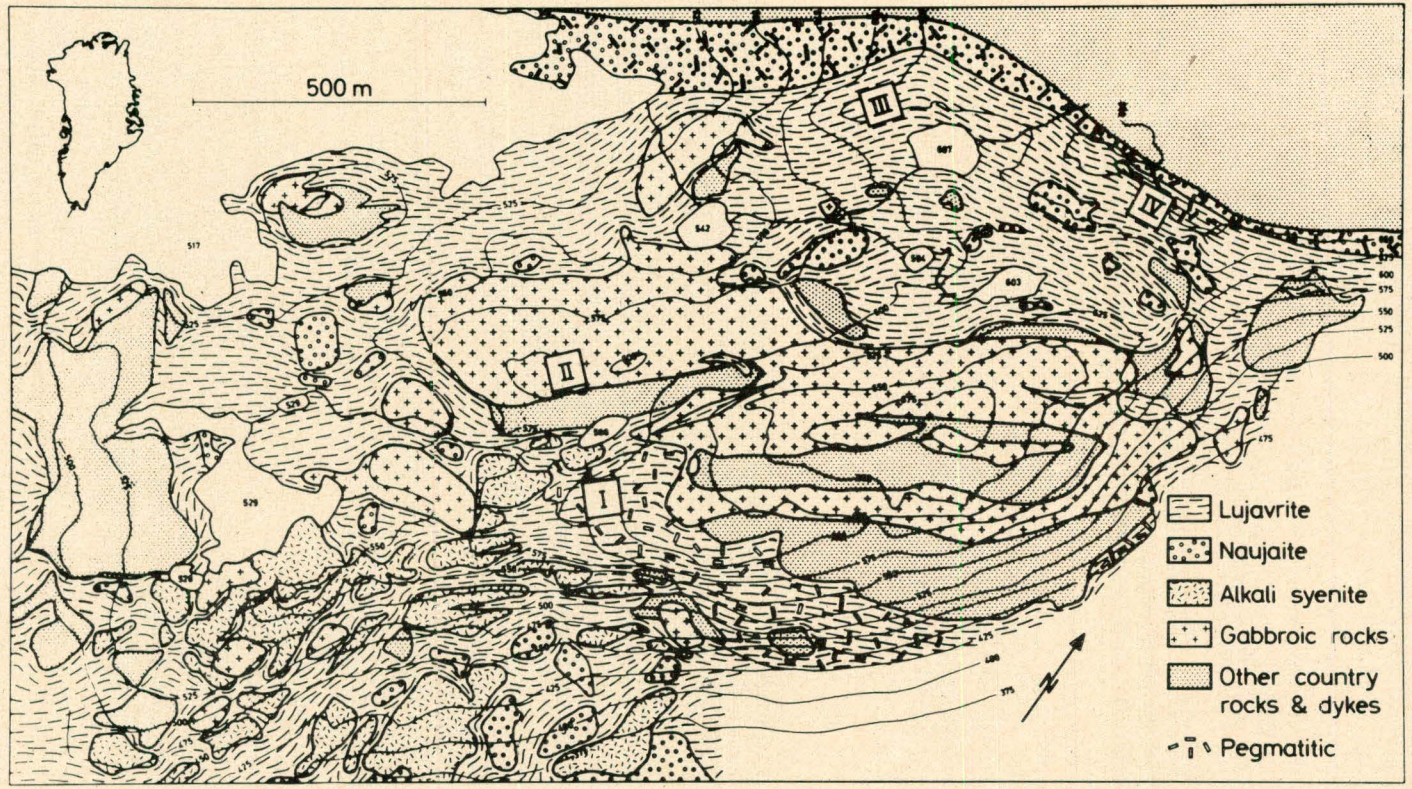


Fig. 1 Simplified geological map of the Kvanefjeld plateau, the Ilímaussaq intrusion, South Greenland. Monitored areas are marked with Roman numbers. [From Sørensen, Hansen, and Bondesen (1969).]

nepheline, arfvedsonite, and aegirine, plus a number of rare accessory minerals. Some of these carry thorium and uranium.

At Kvanefjeld, lujavrite was emplaced at a high level in the intrusion below a cover series of sandstone and lavas (Sørensen, Hansen, and Bondesen, 1969). The average concentration of uranium in this lujavrite is in the range 300 to 350 ppm; the concentration of thorium is two to three times greater. The area has been diamond-drilled to depths of several hundred meters, and a deposit of 27,000 metric tons of uranium metal in the class of "reasonably assured resources" has been established. There is no evidence of radioactive disequilibrium in the deposit. Gamma-ray spectrometry has accordingly been widely used to determine uranium concentrations in drill core and rock outcrops (Løvborg, Wollenberg, Rose-Hansen, and Nielsen, 1972; Løvborg, 1972).

The Kvanefjeld plateau forms a complicated intrusive megabreccia (Fig. 1). The lujavrite represents the youngest intrusive pulses and forms the matrix in the breccia. The xenoliths are up to 100 m across, and there are areas of preserved gabbro sills and volcanic roof rocks. The surface radioactivity consequently exhibits abrupt changes over short lateral distances. Line spacings of 10 m or less have been used in the spectrometric exploration surveys carried out on the plateau. The most comprehensive surface concentration map compiled up to now covers the entire area northeast of lake 542.

Average surface concentrations of uranium and thorium, calculated from many hundred field-spectrometric measurements, are listed in Table 1. The result given for fine-grained lujavrite dates from 1977; the other results are from the work of Løvborg et al. (1971).

TABLE 1

Average Concentrations of Uranium and Thorium in the Surface of the Kvanefjeld Plateau

Rock type	Number of field-spectrometric measurements	ppm U	ppm Th
Fine-grained lujavrite	1567	245	597
Pegmatitic lujavrite with hydrothermal veins	616	538	1064
Metasomatically altered gabbroic rocks	433	435	1402
Naujaite } Xenoliths }	298	88	255

FIELD MEASUREMENTS

The program reported by Bøtter-Jensen, Christensen, and Nielsen (1978) included radiation monitoring of four representative small areas. The locations of these, I to IV, are shown in Fig. 1. Information on the geology and topography of the areas is given in Table 2. Each area was covered by nine monitoring points placed 10 m from each other on a square grid. Four additional monitoring points were established over the most radioactive part of the plateau surface, roughly 150 m to the east of area I. A point covering a drilling site southwest of lake 607 was also monitored.

TABLE 2

Characteristics of the Areas Monitored in the Present Investigation

Area	Prevailing rock type	Outcropping rock, %	Surface relief, m
I	Pegmatitic lujavrite	100	1
II	Gabbro	50	2
III	Fine-grained arfvedsonite lujavrite	50	4
IV	Fine-grained arfvedsonite lujavrite and aegirine lujavrite	50	3

On each of these monitoring locations, 41 in total, a wooden post was erected to support a TLD package at an elevation of 1 m. The experimental setup is shown in Fig. 2, which also gives an impression of the terrain.

All TLD packages contained a set of three hot-pressed solid TLD's made of lithium fluoride (LiF, Harshaw TLD-700). The latter is a suitable phosphor for environmental monitoring purposes because of its excellent sensitivity and low fading and because the low atomic number provides a flat energy response (Cox, 1968). The TLD package used incorporates a dosimeter holder moulded from plastic and equipped with a binary identification hole code. A sandwich shielding of 1 mm of aluminum is provided to obtain electron equilibrium (Bøtter-Jensen, Christensen, and Majborn, 1974).

The TLD's were annealed and the TLD packages were assembled at Risø National Laboratory. Since the dosimeters received radiation exposure during their transport (by air) to and from Greenland, they were accompanied by control dosimeters which made it possible to

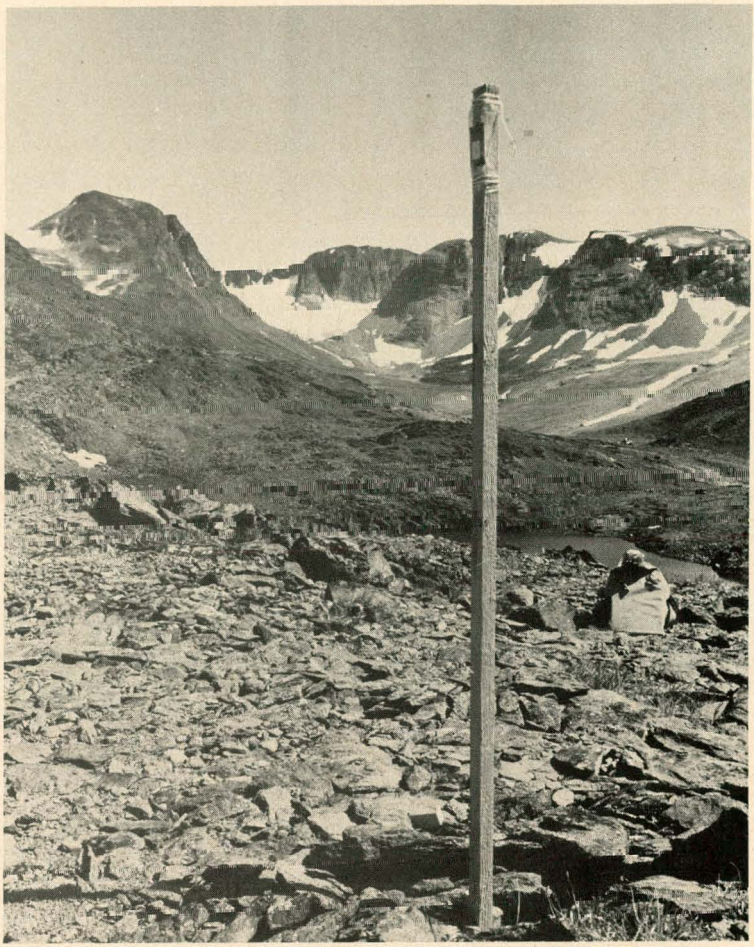


Fig. 2 TLD package on the Kvanefjeld plateau.

letermine the transit exposure. While the field dosimeters were in heir terrain positions for almost 3 months, the control dosimeters were kept on a low-background storage location in the town of Narssaq, 8 km away from Kvanefjeld.

Direct exposure-rate readings were taken with a high-pressure argon ionization chamber. This instrument (Reuter—Stokes Environmental Monitoring System RS 111) is of a design described by DeCampo, Beck, and Raft (1972). The pressurized chamber unit is protected by a carrying case with three telescopic legs. With these extracted, it was possible to position the unit adjacent to the field

dosimeters. A second carrying case contains a digital voltmeter for repetitive sampling of the ionization current and conversion of the latter into units of microroentgens per hour. A built-in tape deck has been added so that the recorded exposure rates can be stored in a computer-compatible form. At each field location the fluctuating exposure-rate signal was recorded every fifth second for about 10 min. Locations with more than ~500 μR/hr could not be monitored because of saturation effects. The ionization chamber was further used to determine the exposure rate (8.8 μR/hr) at the place in Narssaq where the control dosimeters were stored.

The radioelement concentration measurements at the field locations were carried out by a Geometrics/Exploranium Model GR-410 portable gamma-ray spectrometer. With this instrument, the pulses from a NaI(Tl) scintillation detector can be counted for a preselected time in three narrow energy windows. These have center positions of 2.62, 1.76, and 1.46 MeV, which are the energies of penetrating primary gamma radiation produced by thorium, uranium, and potassium, respectively. The detector unit is provided with an attached ^{133}Ba source, and the 356-keV gamma rays from this source can be used to display the gain drift of the photomultiplier on a front-panel meter in the control unit. A fine-gain potentiometer makes it possible to maintain a stable counting performance in the field.

We used a detector unit equipped with a NaI(Tl) crystal of dimensions 76 by 76 mm. Counts were accumulated for several minutes with the crystal placed at a field dosimeter position. The measurements in area II, where the ground is formed by gabbro of low radioactivity, were repeated for nearly 30 days to detect fluctuations introduced by radon in the air. None of the window count rates fluctuated significantly during this period. Constant background count rates could therefore be assumed. Background counts were accumulated at sea, on a 2-km wide fjord east of Narssaq, and the result is presented in Table 3.

CALIBRATION AND DATA REDUCTION

Exposed TLD's are processed in the laboratory using a hot-gas readout system (Bøtter-Jensen, 1971), and the evaluation of the radiation exposures is fully automated (Bøtter-Jensen, Christensen, and Majborn, 1974). Calibration is accomplished by determining the response of dosimeters that have been irradiated in a beam of ^{60}Co gamma radiation. The exposure rates along this beam are accurately known from intercomparisons with radiation standards available

TABLE 3

Window Settings and Background Count Rates of the Portable Gamma-Ray Spectrometer

Counting window	Window setting, MeV	Background, cps
Thorium	2.46—2.78	0.2
Uranium	1.66—1.87	0.5
Potassium	1.37—1.55	1.0

within the European Community. The calibration procedure is quite elaborate (Bøtter-Jensen, to be published).

The control dosimeters received a total exposure of 22.1 mR. They were kept at the storage location with 8.8 μR/hr for 1946 hr, and the transit exposure common to all dosimeters thus amounted to 22.1 mR $-$ 0.0088 mR/hr x 1946 hr = 4.98 mR. The evaluation of exposure rates for the individual field locations is illustrated by the following example: A dosimeter was in the field position (area I) for 1898 hr and showed a total exposure of 506.5 mR. The dosimeter was kept at the storage location for a time of roughly 1946 $-$ 1898 = 48 hr, corresponding to an extraneous exposure of 0.0088 mR/hr x 48 hr = 0.42 mR. The field exposure rate is accordingly calculated as (506.5 $-$ 4.98 $-$ 0.42) mR/1898 hr = 0.264 mR/hr (264 μR/hr).

The calibration of the ionization chamber was checked by an Amersham ^{226}Ra source certified to contain 0.959 mg of radium (±1%) at the time of purchase. This source is screened with 0.5 mm of platinum and thus has a specific gamma-ray constant of 8.25 R cm^2 hr^{-1} mg^{-1} (Beck, 1972; Payne and Waggener, 1974). A flat ground at Risø National Laboratory was selected for a calibration experiment in which the source was mounted on a 3-m-high post. The chamber unit and a standard LiF TLD package were successively attached to an identical post in a similar elevated position, 3 m away from the source. The ionization-chamber measurement was repeated 1 year later, just before the program in Greenland was started, using another outdoor locality and a measuring height of only 1 m. The gamma-ray albedo presented by the ground in the two cases was calculated according to the model of Chilton and Huddleston (1963). A correction for absorption and buildup in the air was not included as it was determined to be negligible over a distance of 3 m. In both

TABLE 4
Results of Calibration Experiments with a 1 mCi ^{226}Ra Standard Source

Source-detector configuration		Calculated gamma-ray albedo, %	μR/hr		
Elevation, m	Distance, m		Calculated	Ionization chamber	TLD (^{60}Co calibration)
3	3.00	8.0	90.7	91.2	91.0
1	2.80	6.8	106.9	106.6	

experiments ionization-chamber readings were taken with the source removed, and the measured background values (11.39 and 9.68 μR/hr, respectively) were subtracted.

The results presented in Table 4 show that the ionization chamber responded in almost perfect agreement with the exposure rates predicted from the source activity (corrected for decay) and the geometries of the experiments. Table 4 also shows that ^{226}Ra gamma radiation produces the same TLD response as that obtained with the ^{60}Co calibration facility.

Counts recorded with the portable spectrometer were processed from the conversion equations

$$\text{ppm Th} = n_T/s_T$$

$$\text{ppm U} = n'_U/s_U; \qquad n'_U = n_U - \alpha\, n_T$$

$$\%\,\text{K} = n'_K/s_K; \qquad n'_K = n_K - \beta\, n_T - \gamma\, n'_U$$

where n_T, n_U, and n_K denote the background-corrected count rates in the thorium window, the uranium window, and the potassium window. The sensitivity constants (s_T, s_U, and s_K) and the stripping ratios (α, β, and γ) were evaluated from calibration measurements on large radioactive concrete pads available at Risø National Laboratory. These pads have known concentrations of thorium, uranium, and potassium and make it possible to calibrate in a source-detector geometry of nearly 2π. Radioactive disequilibrium caused by migrating radon in the uranium-doped pad was taken into consideration (Løvborg, Bøtter-Jensen, and Kirkegaard, 1978), and the measured sensitivity constants were corrected to match the detector elevation of 1 m used in the field (Løvborg, Kirkegaard, and Rose-Hansen, 1975). The following values were determined:

$$s_T = 0.125 \text{ cps/ppm Th}$$

$$s_U = 0.270 \text{ cps/ppm U}$$

$$s_K = 3.05 \text{ cps/\% K}$$

$$\alpha = 0.615$$

$$\beta = 0.565$$

$$\gamma = 0.773$$

The radioelement concentrations measured at the field locations were converted into a set of gamma-ray exposure rates. The preliminary conversion factors used for this purpose were derived from a gamma-ray transport calculation in which the ground was represented by a plane, homogeneous, and infinite source. Information on the energies and the intensities of the gamma rays from decaying ^{232}Th and ^{238}U was obtained from Beck (1972); the intensity of the 1.46-MeV emission from ^{40}K (3.30 γ/sec per gram K) was taken from Martin and Blichert-Toft (1970). A double P_L polynomial expansion technique with L = 1 was used to solve the scattered part of the one-dimensional transport equation, and evenly spaced wavelengths in the energy interval from 100 keV to 3 MeV were used in the numerical evaluation (Kirkegaard and Løvborg, 1974). The small exposure-rate contribution below 100 keV was obtained by extrapolation.

Table 5 shows the exposure rates calculated for a reference point 1 m above a solid rock medium with unit concentrations of thorium, uranium, and potassium. The values representing the combined effect of uncollided and all scattered radiation are in good agreement with the values for soil reported by Beck, DeCampo, and Gogolak (1972). More than 85% of the exposure rate is contributed by uncollided and ground-scattered gamma radiation. This contribution is upward-directed, and 90% of it can be estimated to come from a circular area with a diameter of roughly 15 m. About 13% of the exposure rate from these ground sources can be ascribed to air-scattered gamma rays directed toward the ground. Over a heterogeneous source (Kvanefjeld) this skyshine contribution does not show the same significant variation from place to place as the upward-directed radiation component, and it cannot be reliably predicted from a local set of radioelement concentrations. For this reason the values in the first row of Table 5 were used to convert the experimental Th—U—K concentrations into gamma-ray exposure rates.

TABLE 5

Gamma-Ray Exposure Rates Calculated for a Reference Point 1 m Above a Plane, Homogeneous, and Infinite Rock Medium

Radiation contribution	μR/hr		
	1 ppm Th	1 ppm U	1% K
Uncollided and ground-scattered	0.27	0.55	1.37
Air-scattered (skyshine)	0.04	0.09	0.18
Total	0.31	0.64	1.55

RESULTS AND DISCUSSION

Average results obtained for areas I to IV are presented in Table 6. The individual radioelement concentrations and exposure rates measured within these small areas varied characteristically from 10 to 25%. The variability observed within area I could be ascribed to a heterogeneous radioelement distribution in the outcropping rock (pegmatitic lujavrite). On each of the other sites, the detected signals mainly varied because of the uneven terrain (Table 2) and a debris of weathering products.

All radioelement concentrations stated in Table 6 are apparent concentrations. These would have been true concentrations if the plateau surface had been plane and uniformly radioactive. The gabbro monitored in area II really contains 2.0 ppm thorium and 1.4 ppm uranium; this result was obtained from a gamma-spectrometric analysis, in the laboratory, of 49 rock samples collected from this

TABLE 6

Average Radioelement Concentrations and Exposure Rates Determined for the Four Monitored Areas

Area	ppm Th	ppm U	% K	μR/hr		
				Calculated	TLD	Ionization chamber
I	476	223	3.1	254	255	251
II	20.6	7.1	1.4	30.5	25.3	23.0
III	418	248	1.7	251	253	240
IV	1314	454	1.7	578	575	

area. Figure 1 shows that area II was situated only 150 m away from the massive outcrops of strongly radioactive pegmatitic lujavrite southeast of lake 588. A significant amount of extraneous Th—U gamma radiation was consequently detected by the portable spectrometer, and apparent concentrations of 20.6 ppm thorium and 7.1 ppm uranium were measured.

Table 6 shows that the ionization chamber measured from 2 to 9% less exposure rate than the TLD's, and this observation indicates that the chamber has a slightly inaccurate response when exposed to a natural radiation field. Such a field is characterized by a high abundancy of low-energy, scattered gamma rays and is therefore quite different from the field produced by a ^{226}Ra point source.

The final data evaluation was based on the TLD exposure rates and the apparent radioelement concentrations determined for the individual measuring locations, including the five locations monitored outside the four main areas. Figure 3 plots about half of the experimental exposure rates against their calculated counterparts. The undisplayed data points all belong to the lower left corner of the diagram and do not change the general picture of a close linear relation. The regression line shown was calculated from all 41 sets of results. The small dispersion of the data points around the line indicates that the total gamma radiation detected by a TLD essentially had the same origin as the uncollided high-energy gamma rays counted with the portable spectrometer.

The slope of the line, 0.916 ± 0.005 μR/hr per microroentgen per hour, is significantly smaller than unity, and it must be concluded that the preliminary conversion factors in the first row of Table 5 are approximately 9% too large. This inaccuracy can possibly be ascribed to the fact that the terrain roughness was disregarded in the gamma-ray transport calculation. An empirical correction of −9% makes it possible to establish the following set of final conversion factors:

0.25 μR/hr per ppm Th
0.50 μR/hr per ppm U
1.25 μR/hr per % K

and these values represent the main result of the present investigation.

The line in Fig. 3 has a zero intercept of 20 ± 3 μR/hr which may be interpreted as an almost constant exposure rate detected anywhere on the plateau. This exposure rate should, naturally, be added to any gamma-ray exposure rate calculated from a set of Th—U—K concentrations. About 4 μR/hr is produced by cosmic

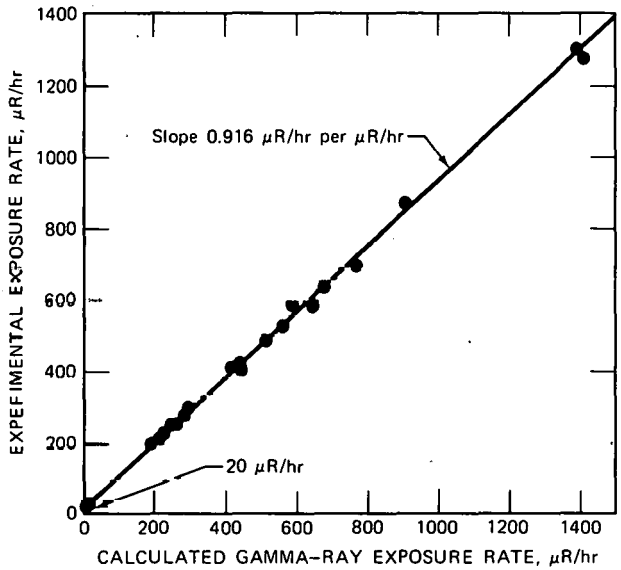


Fig. 3 Experimental exposure rates (TLD) and gamma-ray exposure rates calculated from field gamma-spectrometric Th—U—K concentrations.

rays, whereas no more than 1 μR/hr is probably contributed by airborne radon daughters and fallout. The remaining ~15 μR/hr may be ascribed to gamma-ray skyshine from the radioactive mineralization.

The calculated exposure rates shown in Table 6 are based on the conversion procedure just outlined. They agree very well with the TLD results. It should therefore be possible to make reliable estimates of the exposure rates in the large areas covered by field-spectrometric exploration surveys.

The large area (0.2 km^2) surveyed northeast of lake 542 was covered by 3000 evenly spaced spectrometer measurements. Average surface concentrations of 430 ppm thorium, 170 ppm uranium, and ~2% potassium were determined, corresponding to a calculated average exposure rate of 215 μR/hr.

ACKNOWLEDGMENTS

We wish to thank our colleagues P. Christensen and P. Sørensen for their assistance with the field measurements. Thanks are also due to P. Hedemann Jensen who calculated the gamma-ray albedo in the calibration experiments with ^{226}Ra. This paper is published with permission from the Director of the Geological Survey of Greenland.

REFERENCES

Beck, H. L., 1972, *The Absolute Intensities of Gamma Rays from the Decay of ^{238}U and ^{232}Th*, USAEC Report HASL-262, Health and Safety Laboratory, New York.

——, J. DeCampo, and C. Gogolak, 1972, *In Situ Ge(Li) and NaI(Tl) Gamma-Ray Spectrometry*, USAEC Report HASL-258, Health and Safety Laboratory, New York.

Blaxland, A. B., O. van Breemen, and A. Steenfelt, 1976, Age and Origin of Agpaitic Magmatism at Ilímaussaq, South Greenland: Rb—Sr Study, *Lithos*, 9: 31-38.

Bøtter-Jensen, L., 1971, Read-Out Instruments for Solid Thermoluminescence Dosimeters, Using Hot Nitrogen Gas as the Heating Medium, in *Advances in Physical and Biological Radiation Detectors*, Symposium Proceedings, Vienna, 1970, pp. 113-124, STI/PUB/269, International Atomic Energy Agency, Vienna.

——, P. Christensen, and B. Majborn, 1974, A TLD Personnel Monitoring System with Automatic Processing, in *Proceedings of the Third International Congress of the International Radiation Protection Association*, Washington, D. C., Sept. 9—14, 1973, USAEC Report CONF-730907-P1, pp. 572-577, NTIS.

——, P. Christensen, and B. L. Nielsen, 1978, *External Radiation Exposure Associated with Uranium—Thorium Mineralization on the Kvanefjeld Plateau, Greenland*, Report Risø-M-1989, Risø National Laboratory, Roskilde, Denmark.

Chilton, A. B., and C. M. Huddleston, 1963, A Semi-Empirical Formula for Differential Dose Albedo for Gamma Rays on Concrete, *Nucl. Sci. Eng.*, 17: 419-424.

Cox, F. M., 1968, New Solid Lithium Fluoride Thermoluminescent Dosimeters, in *Proceedings of the Second International Conference on Luminescence Dosimetry*, Gatlinburg, Tenn., Sept. 23—26, 1968, J. A. Auxier, K. Becker, and E. M. Robinson (Eds.), USAEC Report CONF-680920, pp. 60-67, Oak Ridge National Laboratory, NTIS.

DeCampo, J. A., H. L. Beck, and P. D. Raft, 1972, *High Pressure Ionization Chamber Systems for the Measurement of Environmental Radiation Exposure Rates*, USAEC Report HASL-260, Health and Safety Laboratory, New York.

Emeleus, C. H., and B. G. J. Upton, 1976, The Gardar Period in Southern Greenland, in *Geology of Greenland*, A. Escher and W. S. Watt (Eds.), pp. 153-181, Grønlands Geologiske Undersøgelse, Copenhagen, Denmark.

Kirkegaard, P., and L. Løvborg, 1974, *Computer Modelling of Terrestrial Gamma-Radiation Fields*, Risø Report No. 303, Danish Atomic Energy Commission, Research Establishment Risø, Roskilde, Denmark.

Løvborg, L., 1972, Assessment of Uranium by Gamma-Ray Spectrometry, in *Uranium Prospecting Handbook*, S. H. U. Bowie, M. Davis, and D. Ostle (Eds.), pp. 157-173, Institution of Mining and Metallurgy, London.

——, L. Bøtter-Jensen, and P. Kirkegaard, 1978, Experiences with Concrete Calibration Sources for Radiometric Field Instruments, *Geophysics*, 43: 543-549.

——, P. Kirkegaard, and J. Rose-Hansen, 1975, Quantitative Interpretation of the Gamma-Ray Spectra from Geological Formations, in *The Natural Radiation Environment II*, Vol. 1, Symposium Proceedings, Houston, Tex., Aug. 7—11,

1972, J. A. S. Adams, W. M. Lowder, and T. F. Gesell (Eds.), ERDA Report CONF-720805-P1, pp. 155-180, Rice University and the University of Texas, Houston, NTIS.

——, H. Wollenberg, J. Rose-Hansen, and B. L. Nielsen, 1972, Drill-Core Scanning for Radioelements by Gamma-Ray Spectrometry, *Geophysics*, 37: 675-693.

——, H. Wollenberg, P. Sørensen, and J. Hansen, 1971, Field Determination of Uranium and Thorium by Gamma-Ray Spectrometry, Exemplified by Measurements in the Ilímaussaq Alkaline Intrusion, South Greenland, *Econ. Geol.*, 66: 368-384.

Martin, M. J., and P. H. Blichert-Toft, 1970, *Radioactive Atoms, Nuclear Data Tables*, A8, 1-196.

Payne, W. H., and R. G. Waggener, 1974, A Theoretical Calculation of the Exposure Rate Constant for Radium-226, *Med. Phys.*, 1: 210-214.

Sørensen, H., J. Hansen, and E. Bondesen, 1969, *Preliminary Account of the Geology of the Kvanefjeld Area of the Ilímaussaq Intrusion, South Greenland*, Grønlands Geologiske Undersøgelse Rapport, 18, Copenhagen, Denmark.

——, J. Rose-Hansen, B. L. Nielsen, L. Løvborg, E. Sørensen, and T. Lundgaard, 1974, *The Uranium Deposit at Kvanefjeld, The Ilímaussaq Intrusion, South Greenland*, Grønlands Geologiske Undersøgelse Rapport, 50, Copenhagen, Denmark.

Environmental Radiation Studies Relevant to Thermoluminescence Dating

A. S. MURRAY, S. G. E. BOWMAN, and M. J. AITKEN
Research Laboratory for Archaeology, Oxford University, England

ABSTRACT

To determine the age of a potsherd by the thermoluminescence (TL) technique, one must have an accurate knowledge of the cosmic and environmental gamma dose rate in quartz. This is obtained by leaving a sensitive TL dosimeter, e.g., CaF_2 (MBLE type S), buried as near as possible to the position from which the sherd was removed. Quartz cannot be used directly because it is not sufficiently sensitive. The ratios of the response of a quartz-like dosimeter to those of CaF_2 and LiF, when the dosimeters are exposed to an infinite-matrix natural gamma spectrum, have been measured. This experiment used a 1-m cube of concrete containing 3000 ppm of uranium and its daughters. Smaller, less active matrixes of ^{40}K and thorium and its daughters have also been constructed. A means of making direct dose-rate determinations when the site context remains but burial of a dosimeter is impractical was developed using a NaI(Tl) system. It was possible to choose a threshold value (0.45 MeV) above which the number of gamma counts is directly proportional to the dose rate in CaF_2 irrespective of the relative concentrations of the natural emitters present. The equipment was field tested on ~40 Peruvian archaeological sites, and results are compared with CaF_2 measurements.

The basic notion of thermoluminescence (TL) dating of archaeological ceramics is expressed in the simplified age relation:

$$\text{Age} = \frac{\text{TL accumulated since firing by ancient man}}{(\text{TL/rad}) \times (\text{rads/year})}$$

The TL is carried by mineral inclusions in the clay fabric of the pottery (e.g., quartz and feldspar), and the radiation dose rate is provided by radioelements in the clay and in the surrounding burial

soil. Cosmic radiation contributes a few percent also. It is convenient for discussion to take the following levels as typical:

Uranium, 2.8 ppm
Thorium, 10 ppm
K_2O, 2%

Obviously these levels vary widely depending on the geology of the region concerned. There is also a contribution of $< 2\%$ from rubidium, typically present at a level of 100 ppm (Warren, 1978).

Although for such levels the dose rate from alpha particles is 80% of the whole—with the external gamma dose rate from the soil amounting to only 7%—when account is taken of the much lower effectiveness of alpha particles in producing thermoluminescence (typically a factor of 7) (Zimmerman, 1972), the dominance by this type of radiation is removed. In terms of effective dose rates, the contributions are as follows:

Alpha, 40%
Beta, 36%
Gamma, 22%
Cosmic, 3%

The importance of the gamma contribution is further enhanced in the quartz-inclusion technique, which is one of the two main methods routinely used for TL dating today, the other being the fine-grain technique. In the inclusion technique quartz grains $\sim 100\ \mu m$ in diameter are extracted from the pottery, and the TL measurements are made on these. Because the average range of alpha particles from the uranium and thorium series is only $25\ \mu m$, the inner cores of such grains receive dosages only from beta and gamma radiation. Thus, if the outer layers of the grains are etched away with hydrofluoric acid, the alpha particle contribution can be reduced to negligible proportions. The effective dose rates, again for the typical levels of radioactivity, are then:

Beta, 206 mrads/year
Gamma, 125 mrads/year
Cosmic, 15 mrads/year

Thus gamma radiation contributes 36% of the whole, and the accuracy of the TL data obtained is highly dependent on its reliable evaluation. This greater dependence on environmental dose rate is of course a drawback. The quartz inclusion technique is, nevertheless, preferred because, unlike the fine-grain technique, it is not prone to the malign phenomena of anomalous fading (Wintle, 1973).

The breakdown of the gamma dose rate is given in Table 1 on the basis of data obtained by Bell (1976, 1977) by equating energy

absorbed to energy released—the latter being derived from relevant nuclear data tables. The X-ray contribution is included in the gamma dose rate, but the internal conversion electron contribution is excluded.

Often the radioactivity of the pottery is different from that of the burial soil. To avoid sample material from the region in which the

TABLE 1

Gamma and X-Ray Dose Rates for an Infinite Medium of Soil*

^{238}U series	
Radioisotopes before ^{222}Rn	1.1
^{222}Rn and later	30.6
^{235}U series	0.5
^{232}Th series	
Radioisotopes before ^{220}Rn	20.8
^{220}Rn and later	30.6
^{40}K	41.0
Total	124.6

*The soil contains 2.8 ppm of uranium, 10 ppm of thorium, and 2% K_2O (in mrads/year). The principal gamma emissions above 1 MeV are 1.76 MeV from ^{214}Bi (post ^{222}Rn), 2.65 MeV from ^{208}Tl (post ^{220}Rn), and 1.46 MeV from ^{40}K; these carry 4, 15, and 33%, respectively, of the total gamma dose rate.

beta dose rate is transitional between the two levels, we discarded the outer 2-mm layer of each specimen. Because the thickness of the pottery fragment is not usually more than 20 mm, it is assumed that the internal contribution to the gamma dose rate is negligible and that the external contribution is not significantly attenuated.

In the following sections we describe two methods currently used for on-site measurement of the environmental dose rate. In the first, a small capsule of highly sensitive TL dosimeter powder is buried in the same surroundings or in surroundings as similar as possible to those from which the pottery fragments were removed. In the second, a sodium iodide scintillator is used; its electronic threshold is chosen so that the conversion factor from count rate to dose rate is independent of whether the predominant radioisotope is uranium,

thorium, or potassium. The first method is the preferred technique because the capsule can be inserted into position with less disturbance than can the scintillator. It also has the advantage that, site permitting, it can be left in position for a year to average out seasonal variations in water content (Mejdahl, 1970, 1972).

For sites on which it is not possible even to make scintillator measurements, radioactive analyses of soil samples are made in the laboratory. Currently this is done with a NaI gamma spectrometer, for which the minimum sample size is 100 g. An intrinsic germanium well-type detector with a sample size of 10 g is shortly to be commissioned. Thick-source alpha counting with a zinc sulfide screen, combined with flame photometry for potassium determination, is an alternative. The disadvantage of alpha counting is that an average thorium-to-uranium ratio must be assumed in deducing the gamma dose rate, and the ratio of gamma dose rate to alpha count rate differs strongly between the two series (it is higher by a factor of 1.5 in the thorium series). Another disadvantage of both methods of laboratory analysis is that for some soils there is substantial escape of radon and the degree of escape may be different when the sample is being counted in the laboratory from what it was when in the ground. The level of 21-year ^{210}Pb can be used to measure the in situ radon retention, however. At present this is measured by alpha spectrometry of deposited ^{210}Po, but with the germanium detector the 46-keV gamma emission from ^{210}Pb itself will be used. Besides radon escape, there are other forms of decay-chain disequilibriums that may upset laboratory evaluation, particularly the alpha counting method.

Whether on-site or laboratory measurements are used, a strong consideration in the selection of samples for TL dating is the homogeneity of the immediate surroundings (to a distance of 0.3 m). This is more acute in the case of laboratory measurement, but it is also a limitation of on-site measurements because of the practical difficulty of positioning even a small capsule so that it receives the same gamma flux as the pottery fragment removed for dating. Another factor to be considered is the rapidity with which the pottery became buried.

For an account of the other aspects of archaeological TL dating, see Aitken, Zimmerman, and Fleming (1968), Zimmerman (1971), Aitken and Fleming (1972), Aitken (1975), and Fleming (1977). Currently it is practical to think in terms of a dating uncertainty of 5 to 10% of the age. Thus it is reasonable to set an uncertainty of 5% as the objective for accuracy of assessment of the environmental dose rate.

SIMULATION OF SOIL SPECTRA

Whether we are considering the use of a thermoluminescence dosimeter or a scintillator to evaluate gamma dose rate in the ground, we are faced with the problem that, although the primary spectrum may be well-known, the secondary spectrum resulting from photon degradation through Compton interactions is not. Since a thermoluminescence dosimeter measures absorbed dose, knowledge of the spectrum is needed only to correct for any differences in mass absorption coefficients between dosimeter material and the relevant mineral in the pottery, i.e., quartz (SiO_2)—and perhaps for attenuation effects in the capsule wall. From Fig. 1, we see that, as

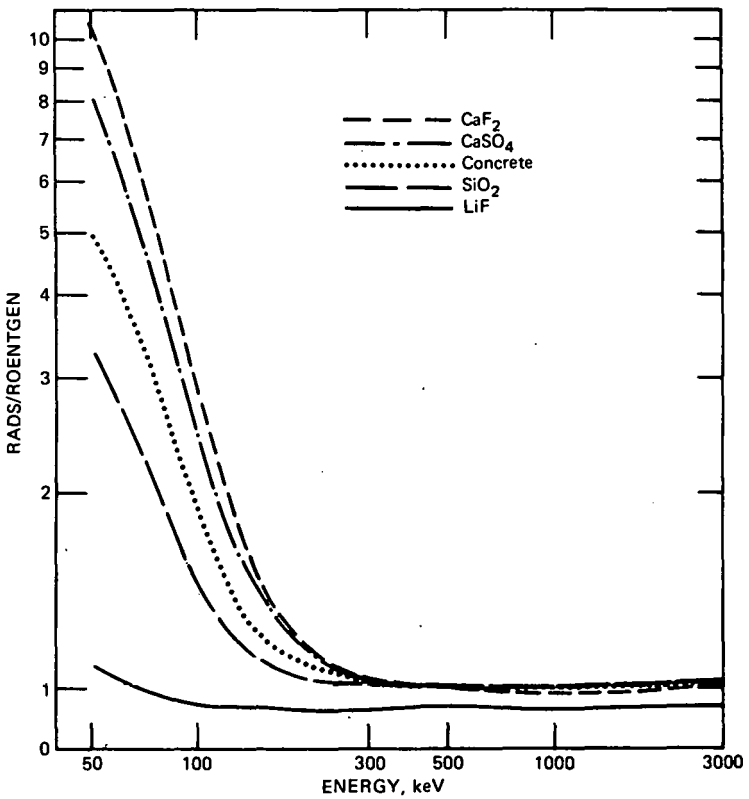


Fig. 1 Energy absorption characteristics of various materials, calculated from Storm and Israel (1970) and Evans (1968b): $(\mu/\rho) = \Sigma_i (\mu_i/\rho_i)w_i$, where μ_i/ρ_i is the mass absorption coefficient of the element concerned and w_i is the fraction by weight (Evans, 1968b).

long as the major part of the absorbed dose comes from photons above 0.2 MeV, the correction for differences in mass absorption coefficients is unlikely to be a strong one. On the other hand, the factor for converting scintillator count rate to soil dose rate depends strongly on the size of the scintillation crystal and its absorption characteristics and on the gamma spectrum being measured.

As an alternative to dealing with this problem by computation, we built three concrete blocks, 51 by 51 by 51 cm, one each doped with uranium, thorium, and potassium and each having a pluggable access channel to its center to permit insertion of a capsule or scintillator. A fourth undoped block of the same size was built as a background monitor. The uranium and thorium additives were chemically analyzed New Brunswick sands from the U. S. Department of Energy, pitchblende (sand 6) and monazite (sand 7A), respectively. Agricultural potassium sulfate was used for the third block.

For the expected concrete density, 2.35 g/cm^3, we calculated that the dose rate at the center of a block should be within 5% of the dose rate for an infinite matrix of the same radioactive concentration. Unfortunately the density turned out to be 1.93 g/cm^3, and it was calculated that the central dose rate would be ~7% below the infinite-matrix dose rate for the uranium block and ~11% below that for the thorium and potassium blocks. Nevertheless, we assumed that the spectral shape, especially at the lower energy end, would be indistinguishable from that for a true infinite matrix.

As an additional facility to make short-term experiments feasible with relatively insensitive TL phosphors, we later constructed a large (1 m^3) concrete block (U3) doped with 15 kg of uranium ore, which was part of a sample from Katanga that had been left in the university museum. A chemical analysis of unknown origin specified a uranium content of 53.1%. The block is made up of 125 20-cm cubes with a nominal uranium concentration of 3000 ppm. These can be assembled with other subunits (10 by 10 by 20 cm) to give a matrix variable in size from (20 cm)^3 to (1 m)^3. There is also a range of undoped subunits to permit investigation of inhomogeneous situations such as might be encountered on an archaeological site. Access to the center is by an 8-cm diameter hole that can be filled with plugs of the same material. Each subunit was given two coats of emulsion paint. The average density was 2.27 g/cm^3.

Table 2 gives the results of analyses of U3 components using a NaI(Tl) system calibrated against sealed concrete masters made from New Brunswick sands and potassium chloride. The large error limit in item 2 arises from uncertainty as to the amount of water added (and

TABLE 2

Apparent Uranium Concentrations in Block U3 Determined by Gamma Spectrometry*

Condition	Before sealing	After sealing	Implied radon escape
1. Ore concentration evaluated from measurement on accurately weighed mix into concrete	49.4%	53.6%	8%
2. Calculated concentration in U3 from item 1 and weights of ingredients		3010 ± 100 ppm	
3. U3 concentration according to samples abstracted from concrete mix	2625 ± 25 ppm	2835 ± 35 ppm	7.5%

*Radiochemical measurement of the ^{210}Po activity in the ore gave a value corresponding to 53 ± 3% that of the parent.

the exact water content at present). We took 2835 ± 35 ppm as the preferred value. Using data from Table 1 and an assumed figure of 4 ± 2% for the radon escape from the actual subunits, we predicted the dose rate at the center of U3 to be 31.4 ± 0.8 rads/year. Note that, although the data for the 1.76-MeV emission from ^{214}Bi is well-established, this is not the case for the myriad other emissions from ^{214}Bi. Table 1 is based on the findings of Bell (1977), which made a downward revision of 10% in this earlier value for the uranium series gamma energy release (Bell, 1976).

The characteristics of all blocks used are summarized in Table 3.

EVALUATION OF DOSE RATE BY THERMOLUMINESCENCE CAPSULE

The thermoluminescent powder used in this work was natural CaF_2 (Super S fluorite kindly supplied by Manufacture Belge de Lampes et de Material Electronique S/A, Brussels). This powder can be used down to dose levels of a fraction of a millirad if appropriate precautions are taken (Aitken, 1968). Unfortunately it is not available commercially. Its other disadvantages are that it has some sensitivity to light, particularly sunlight or fluorescent light and it has a significant self-dose, estimated at 11 mrads/year for Super S fluorite. A commercial alternative is $CaSO_4$ doped with dysprosium or thallium, which has an insignificant sensitivity to light. There are conflicting reports as to whether it exhibits fading, however; possibly

TABLE 3

Summary of Data for Radioactive Concrete Blocks

Characteristic	Block*			
	K	Th	U1	U3
1. Concentration† of parent	6.5% of K_2O	191 ppm (plus 7 ppm U)	170 ppm	2835 ppm
2. Calculated dose rate (assuming no gas loss), rads/year	0.133	1.02	1.97	32.7
3. Predicted loss from gas escape‡		0.04 ± 0.04	0.2 ± 0.05	1.3 ± 0.7
4. Measured dose rate§ after subtracting background, rads/year	0.12 ± 0.01	0.62 ± 0.03	1.22 ± 0.05	34.6 ± 1.5
5. Ratio of Item 4 to Item 2 — Item 3, with allowance for noninfinite size	1.03 ± 0.1	0.73 ± 0.07	0.78 ± 0.06	1.10 ± 0.05
6. Size (side of cube)	51 cm	51 cm	51 cm	1 m

*For K, Th, and U1, the measured dose rates are averages of all types of capsules used. For a discussion of the discrepancy between predicted and measured dose rates, see Bowman, 1976.

†Concentrations for Th and U1 are calculated from weights of ore (sands 7A and 6, respectively) and concrete constituents used. For K and U3 concentrations were determined by flame photometry and gamma spectrometry, respectively.

‡Loss from gas escape was estimated by gamma spectrometry of laboratory samples.

§Measured dose rate in the undoped 51-cm concrete block was 63 mrads/year; that in U3 was derived as described in text.

this depends on the method of preparation. For peak III of Super S fluorite, the fading measured over a 5-year period was equivalent to less than 1%/year.

In use, ~50 mg of powder are sealed in a capsule and buried in an auger hole at the relevant position on the site for a period upwards of several weeks. As mentioned earlier, the optimum burial time is a year but, as in the application described later in this paper, this is not always practical. The powder is drained of previous TL as late as possible before burial and is measured as soon as possible after retrieval. If the powder is carried in a lead container with 1-in. walls, the dose rate is typically about 0.1 mrad/day, but, in the application

described here, circumstances permitted a container of only 0.25-in. wall thickness. Measurement consists of comparing the height of the TL glow peak (III) with that induced by subsequent irradiation with a laboratory ^{90}Sr—^{90}Y beta source calibrated against a ^{137}Cs gamma source standardized by the National Radiological Protection Board, Harwell (Wintle and Murray, 1977).

Initially aluminum-alloy capsules were used. These were chosen because the average atomic number of both soil and CaF_2 is close to that of aluminum. A significant alpha activity was found in all types of aluminum tested, however, even in super-pure aluminum. Next, capsules of black nylon with wall thicknesses of 4 mm to shield off beta particles were used. At present copper capsules with walls 0.7 mm thick, an internal diameter of 3 mm, and a length of 15 mm are being used. They are sealed by hard soldering and, hence, can be conveniently annealed (at 500°C) in a portable oven designed to run from an electric-light socket.

Now let us consider, first, the validity of using CaF_2 as a dosimeter for evaluating the dose rate to quartz and, second, the effect of different wall materials. The TL response of CaF_2 cannot be compared with that of quartz directly, even in the more active U3 block, because quartz is too insensitive.

As can be seen from Fig. 1, CaF_2 has a strong overresponse relative to quartz at low energies; at high energies the value of rads per roentgen drops to about 0.98 that of quartz. Hence the two materials have the same response to the gamma flux in the ground only if low-energy photons deposit an insignificant portion of the absorbed energy. The question of spectral distribution of energy flux was considered by Mejdahl (1970) with respect to the TL dosimeter material $CaSO_4$—Dy. He used polyethylene capsules in a 1.5-mm-thick steel tube. Besides being convenient for driving the dosimeter into the ground, the steel modifies the incident spectrum so that the overall response is similar to that of quartz grains embedded in a baked-clay tablet. Observing a ratio of 1.12 between the soil dose rate measured by $CaSO_4$—Dy in a polyethylene capsule and that measured when the capsule is inside the steel tube, he suggested that the low-energy region may carry about 4% of the total exposure. We see from Fig. 1 that overresponse is likely to be more serious with CaF_2 than with $CaSO_4$.

The wall material can modify response in two ways. First, there is selective attenuation of the spectrum, as just mentioned. Second, the TL phosphor may receive a significant dosage from the secondary electrons generated in the wall, depending on the relative absorption characteristics and the ranges of the electrons in the two media.

When relating observed dose rates to the energy-release predictions of Table 1, in addition to the relative response of the dosimeter material with respect to quartz, there is also the question of the absorption characteristics of the matrix—concrete in our experiments, soil or rock in the actual archaeological application. For dating, we used 100 μm quartz grains that received their dosage when embedded in a baked-clay matrix 1 or 2 cm across which, in turn, was surrounded by soil or rock. For the moment we are assuming that the absorption characteristics of quartz, soil, and rock are not significantly different. The small size of the quartz grains is also relevant here.

Some types of obsidian are much more TL sensitive than quartz, and, since obsidian is predominantly SiO_2, it can be used as a substitute for quartz. Assuming a typical obsidian composition of 10% Al_2O_3 and 84% SiO_2, with the remainder Na, K, and Ca (Taylor, 1977), we calculated absorption characteristics on the same basis as the other materials shown in Fig. 1. They were found to be indistinguishable from quartz between 50 keV and 3 MeV. Obsidian from a particular source in British Columbia (Obsidian Creek) was used because of its exceptional sensitivity; it permitted dose measurement down to 750 mrads at an uncertainty level of 3%, making it possible to work with a 9-day exposure in U3.

Lithium fluoride (Harshaw TLD-100) was also used; its rads-per-roentgen value is effectively constant in the energy region mentioned. This value is about 0.92 times that of concrete at high energies, falling to 0.2 at 50 keV. Thus LiF, if appropriately encapsulated in a material of similar average atomic number, can be expected to give a lower limit to the true infinite-matrix dose rate ("true" meaning the dose rate to the matrix itself).

The three phosphors were variously exposed in nylon, glass, aluminum, and copper, with wall thicknesses sufficient for effective removal of any beta contribution. An aluminum thickness of 1.5 mm was calculated to attenuate the total beta flux from the ^{238}U series by 97% (Evans, 1968a). The other walls are all more effective than this.

The observed dose rates at the center of U3 are given in Table 4. We can see that the obsidian-in-glass result is very near the matrix dose rate of 31.4 ± 0.8 rads/year derived from the concentration measurements.

In drawing conclusions from these data, it is useful to consider the attenuation caused by various types of capsule walls. Table 5 gives the value of $\exp(-\mu t)$ for various wall materials, where μ is the linear absorption coefficient (derived from Evans, 1968b) and t is the wall thickness.

TABLE 4

Observed Dose Rates (rads/year) in Block U3 with Various Dosimeter Materials*

Wall material and thickness	Natural CaF_2	Obsidian	LiF
Nylon, 4 mm	34.7 ± 0.3		30.7 ± 0.7
Glass, 3 mm		31.1 ± 0.9	
Aluminum, 1.5 mm	31.8 ± 0.1		
Copper, 0.7 mm	29.5 ± 0.1	40.0 ± 0.3	36.8 ± 0.8
	29.0 ± 0.2	38.7 ± 0.6	
	29.5 ± 0.3		

*Errors shown are standard errors on at least four measurements from each capsule.

TABLE 5

Effective Attenuation by Various Wall Materials*

Energy, MeV	Nylon, 4 mm	Glass, 3 mm	Aluminum, 1.5 mm	Copper, 1.5 mm
0.05	0.99	0.91	0.93	0.05
0.10	0.99	0.98	0.98	0.07
0.3	0.99	0.98	0.99	0.95
1.0	0.99	0.98	0.99	0.97
3.0	0.99	0.98	0.99	0.97

*The values are exp $(-\mu t)$, where μ is the linear absorption coefficient and t is the wall thickness (see discussion in text).

As mentioned earlier, LiF should absorb at least 8% less energy than a "concrete" dosimeter. Thus the LiF-in-nylon result (Table 4) defines a lower limit for the dose rate in concrete of 30.7 x 1.09 = 33.5 rads/year, including a 1% correction for wall attenuation.

Similarly, the CaF_2-in-nylon result can be used to define an upper limit. In the high-energy region, CaF_2 underresponds by 2% compared with concrete; including the low-energy region can only reduce this figure. Thus the dose rate in concrete must be less than 34.7 x 1.03 = 35.7 rads/year. We, therefore, took 34.6 ± 1.5 rads/year as the best estimate of the dose rate to concrete. This is about 10% more than the predicted dose rate of 31.4 ± 0.8 rads/year; this implies that the measured uranium concentration is too low—

leaving aside the possibility that Bell's downward revision of his dose-rate data was incorrect. The discrepancy is barely outside experimental error, however. Also, the predicted dose rate assumes a rather arbitrary 4% escape of radon, and perhaps the actual escape was less.

Following an argument similar to that in the preceding paragraphs, we expect the obsidian dose rate to be slightly less than 3% below the concrete dose rate (including the 2% glass capsule attenuation). In fact, this is within the measurement error.

Although calcium fluoride in aluminum gives the best match to the quartz dose rate, as recorded by obsidian in the glass capsule, it is not good practice to use aluminum routinely because of its significant level of radioactive impurity. Despite the need for a correction factor of 1.06, we prefer to use a copper capsule. In addition to the convenience of "near site" annealing, the activity in copper is negligible, and it is more resistant to corrosion. The correction factor will be a little smaller for the thorium and potassium spectra because of their smaller low-energy contribution; this is in the process of evaluation.

DIRECT MEASUREMENT OF GAMMA DOSE RATES WITH A NaI(Tl) DETECTOR

A NaI(Tl) crystal is a suitable detector for making an estimate of the intensity of a low-activity gamma flux. Converting this to a measure of energy absorbed by another medium (in this case CaF_2) independent of the energy of the gamma ray, however, requires that the ratio of the detection efficiency of NaI(Tl) to the mass absorption coefficient of CaF_2 be constant over the energy range of interest. As we see from Fig. 2, there is a gross overresponse of NaI with respect to CaF_2 below ~0.3 MeV; above this the response is virtually flat. There is a further effect caused by the relative sizes of the NaI detector and the phosphor used (typically 50 mg). The relative response shown in Fig. 2 is valid only if the mean free path through the detector and the phosphor are the same. As the NaI crystal size increases, the relative efficiency of detection of low-energy gammas decreases, compared with that of high-energy gammas, because the low energies are effectively stopped by the crystal. Thus there is a maximum size beyond which there can be no further increase in detection efficiency.

Unfortunately we are not dealing with a spectrum from a single parent. There are at least three independent contributors to the total gamma spectrum, the uranium and thorium chains and ^{40}K. Only if

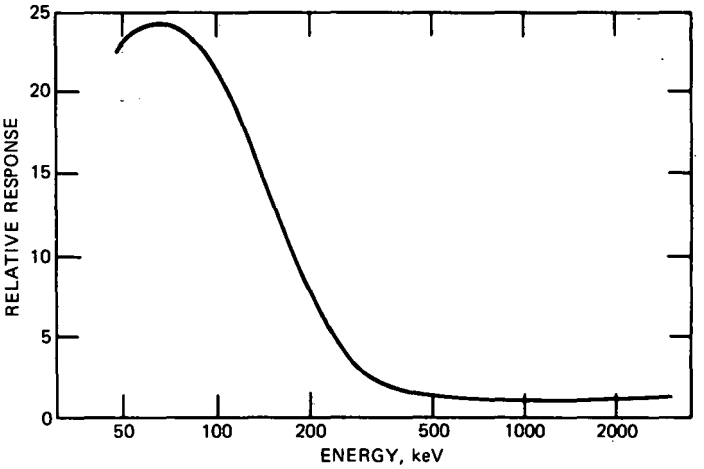


Fig. 2 Ratio of mass absorption characteristics of NaI to CaF_2. (See Fig. 1 for details of calculations.)

each of these deliver a similar proportion of energy to CaF_2 from the energy region of interest, as compared with the total energy delivered by the complete spectrum, will there be a single conversion ratio applicable to all three and independent of relative concentrations. At first glance this seems unlikely, especially since there is no low-energy contribution from ^{40}K; all absorbed low-energy gammas in the potassium spectrum are derived from Compton scattering in the medium and in the detector. In practice this absence is not important, however, as will be shown.

Experimental Procedures

The instrument used for our measurements was developed for the purpose. It consists of a NaI(Tl) crystal 1.75 in. in diameter and 2 in. high, with a photomultiplier tube (Centronic type P4231BA) in a watertight tubular aluminum housing connected to a self-contained high voltage generator and amplifier—discriminator with a scalar—timer. The instrument is powered by nickel—cadmium rechargeable batteries and weighs 4.5 kg to allow for field use. Gain stability is assisted by spectrum stabilization, with an ^{241}Am source mounted next to the detector in the aluminum housing. This source is held against the end of the crystal by a lead—cadmium—copper laminate designed to reduce the intensity of the low-energy gammas, which would otherwise interfere with the 60-keV stabilizing peak. This is important because it will further reduce the overresponse of

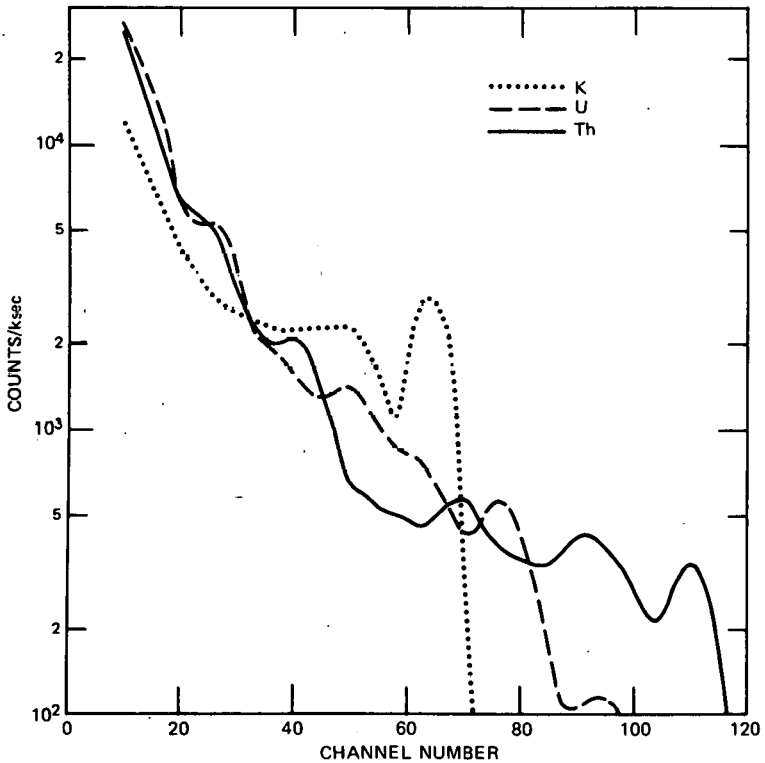


Fig. 3 Block spectra, normalized to a dose rate of 1 mrad/day in CaF_2 and a count time of 1 ksec.

the NaI crystal compared with CaF_2. A pulse-height analyzer was also used to obtain spectral information.

As a calibration facility we have available the four 51-cm concrete matrixes discussed earlier. We assume that they are sufficiently large to give a good approximation to the appropriate infinite-matrix spectral shape at the centers.

To determine the position of a suitable threshold, we recorded the gamma spectra above 0.1 MeV, using the pulse-height analyzer. These were then normalized to unit time, and the background spectrum was subtracted. The resulting spectra were divided by the appropriate dose rate (Table 3, item 4) to produce spectra seen by the NaI(Tl) crystal in 1 ksec, corresponding to a CaF_2 dose rate of 1 mrad/day. These are shown in Fig. 3. To determine the position of a suitable threshold, we then plotted the total counts recorded above a given energy in 1 ksec against energy as shown in Fig. 4.

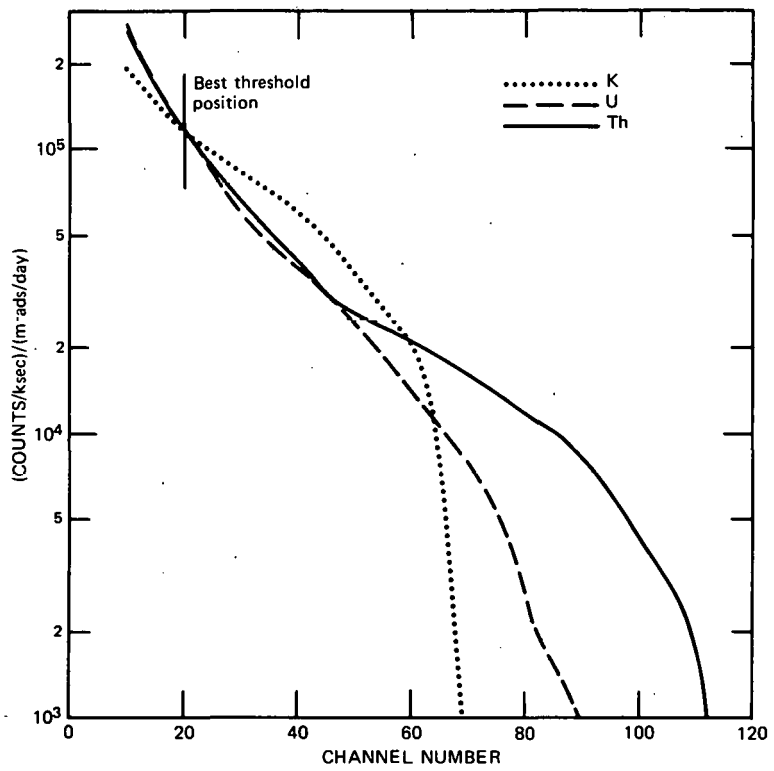


Fig. 4 Integral block spectra (calculated from Fig. 3).

Calibration and Errors

The original calibration used in the Peruvian results presented in the next section was at a threshold of about 0.6 MeV. The average count rate, assuming equal contributions from the uranium and thorium chains and from ^{40}K, was 12.9 cpm, for a dose rate in calcium fluoride of .1 mrad/year. If the site being measured was abnormally high in the concentration of any individual parent, the maximum error was calculated as:

U chain only, +0.05%
Th chain only, −5.5%
^{40}K only, +5.5%

The calibration from Fig. 4 suggests a revised threshold position at channel 20, corresponding to an energy of 0.45 MeV. This position gives an average count of 117 cps, for a dose rate in CaF_2 of

1 mrad/day; this is equivalent to 19.2 cpm; for a dose rate of 1 mrad/year. The maximum deviation from this figure because of variation in the relative concentrations of the uranium and thorium chains or ^{40}K can be calculated as:

U chain only, −0.5%
Th chain only, +0.7%
^{40}K only, −0.1%

Thus the conversion figure is nearly independent of the relative contribution of uranium, thorium, and ^{40}K.

Unfortunately this threshold occurs at a fast change of count rate with energy (a 1% change in count rate for 1% change in gain); hence the stability of the system is of considerable importance. Considering the reproducibility of threshold position, with temperature and after switch-on, suggests that this will usually give rise to an error of 3% on the calculated dose rates for temperatures between 5 and 20°C. This is acceptably low since the typical operating temperatures are in this range. At higher temperatures, however, up to 35°C, the error may increase to −10%.

Finally, the reproducibility of the dose-rate measurements for CaF_2 in the blocks gives an uncertainty of 5%, for a total calibration uncertainty of 6%. The corresponding uncertainty for the original calibration used in Peru is estimated at 7%.

Cosmic Contribution to Dose Rate

In the preceding discussion we assumed that the cosmic contribution had been removed from both the dose-rate measurements and the spectral measurements by subtracting the total background obtained from the background block. When counting on site, however, there will be some count rate from cosmic rays. This was estimated by submerging the detector in water with at least 1.5 m between the detector and the ground in all directions; this is sufficient to shield it from terrestrial radiation. The count rate observed, 65 cpm, is made up of a contribution from cosmic radiation, the activity in the crystal itself, and the activity in the photomultiplier tube.

The cosmic dose rate at a depth of about 50 cm in chalk was estimated by TL measurements to be 15 ± 0.15 mrads/year at sea level in Britain (latitude 51° N) by Aitken (1968). This depth corresponds to the likely burial depth of the detector on site. The count rate of 65 cpm will be observed when making site measurements near this latitude and altitude, whether it is of cosmic or scintillator origin. It must be subtracted from the observed count

rate, and the cosmic dose-rate correction of 15 mrads/year is added on. Typically this is ~10% of the total dose rate.

It is interesting to note that Løvborg and Kirkegaard (1974) adopted a similar approach in calibrating a 3- by 3-in. crystal to determine the surface dose rate in air above geological formations with a threshold value of 0.37 MeV.

FIELD COMPARISON OF SCINTILLATOR AND CAPSULE MEASUREMENTS ON PERUVIAN ARCHAEOLOGICAL SITES

Some 46 different sites were visited between June and September 1975; half were near sea level (at altitudes less than 250 m), and half were at altitudes between 3000 and 4500 m. At all sites several measurements of the dose rates were made at a depth of not less than 30 cm in soil (usually about 50 cm), with both a 1.75-in.-diameter by 2-in. and a 1-in.-diameter by 2-in. crystal. At 19 of the sites, it was possible to bury capsules for eventual recovery, usually in the borehole made for the detector. Both crystals were calibrated as previously discussed, and the results agree well. Further discussion is restricted to the results from the 1.75-in.-diameter detector.

All the coastal sites were dry (water contents were less than 10% of dry weight). Some of the highland sites were very wet (water contents were 60% of dry weight).

Capsule Dose Rates

Although it was possible to anneal the capsules a few hours before burial, readout was a minimum of 10 days after recovery—in some cases 50 days. This included an air flight of 18 hr. During this time the capsules were stored in lead pots with 0.25-in. wall thicknesses, selected for low radioactive contamination. Since the maximum burial time was 72 days, it is obviously important to make an accurate estimate of the "carriage" dose rate; i.e., the dose rate from terrestrial and cosmic radiation and internal activity of the CaF_2 (termed "self dose") while the capsule was being returned to the laboratory. This was done by retaining one capsule from every batch annealed for burial and storing this directly in the lead pots so that the capsules would record only the carriage dose. These dose rates are listed in Table 6.

Since the spread in the average dose rate is unusually large if all the capsules are indeed measuring the same quantity, it was decided to assess two distinct dose rates, one at sea level and one in the

TABLE 6

Carriage Dose Rates Recorded by CaF_2 in Copper in 0.25-in. Lead Pots

Capsule number	Recorded dose, mrads	Days at sea level	Days in highlands	Dose rate, mrads/year
III	25.4	57	40	96
VIII	23.6	47	40	99
XII	23.5	39	40	109
XVIII	19.4	31	38	103
LXVI	14.5	51	9	88
XXIII	33.3	43	66	112
LVIII	24.2	17	58	118
			Average	104
			Sigma	10%

Linear regression analysis, assuming two distinct dose rates:

Sea-level dose rate	Highland dose rate
76.3 mrads/year	130.7 mrads/year
Sigma 6%	Sigma 3%

highlands. Two rates could be expected because of the higher level of cosmic radiation at higher altitudes.

The better fit of the results obtained by least-squares regression on the data (Table 6) confirms that there are in fact two distinct dose rates. Using these figures, we calculated the site dose rates listed in Table 7. A self dose in CaF_2 of 11 mrads/year, which had been previously assessed for the type of CaF_2 used (Aitken, 1968), was assumed during burial. During transport this is included in the carriage dose rate.

Scintillator Dose Rates

Before comparing scintillator and capsule results directly, further thought must be given to the cosmic-ray correction for two reasons, latitude and altitude effects.

Latitude Effect

Peru is at a latitude of 12° S; Oxford is about 51.5° N. Assuming the cosmic dose at a depth of 50 cm to be from only the hard component, the intensity at sea level in Peru is likely to be about 0.91 of that at sea level in the United Kingdom (NCRP, 1976); i.e., a

TABLE 7

CaF_2 and Scintillator Dose Rates

Site number	Water, %	Total dose, mrads,	Burial time, days	Carriage		Dose rate, mrads/year	Scintillator dose rate (+ corrections), mrads/year	
				Sea level, days	Highland, days		cosmic	water (%)
Sea-Level Sites								
P02K	1.6	41.9	70	16	0	190	155	147
P04J	4.6	28.1	72	14	0	117	128	125
P06N	8.7	31.2	71	14	0	135	151	153
P10K	3.2	32.0	68	15	0	144	138	133
P12Q	8.1	25.8	67	14	0	113	121	122
P17L	1.8	24.3	62	17	0	111	129	123
P23	1.9	28.1	59	17	0	141	151	143
P34	3.1	20.9	51	17	0	113	120	115
P35I/J	0.6	28.5	54	14	0	162	152	143
P35K	0.6	22.8	54	12	0	126	137	129
P36A	1.2	16.0	53	14	0	78	97	91
Highland Sites								
P37J	25	35.4	60	42	6	139	109	126
P37L	24	37.6	60	42	6	152	120	137
$P37Q_1$	30	28.5	60	42	6	97	87	103
$P37Q_2$	30	39.2	60	42	6	161	114	133
P39J	36	37.9	58	42	4	162	121	151
P40	63	26.7	58	42	4	93	71	112
$P44_1$	12	64.5	51	18	26	358	211	219
$P44_2$	12	47.2	51	18	26	234	211	219
$P44_3$	12	47.4	51	18	26	235	211	219
P45	11	34.0	56	18	21	137	104	107
$P46J_1$		48.9	51	17	7	296	187	
$P46J_2$		36.9	51	17	7	210	187	

dose rate of about 13 ± 2 mrads/year. The scintillator count rate when surrounded by 1.5 m of water was measured near sea level in Peru as 65 ± 3 cpm; this was subtracted from the observed-site count rates before converting to dose rates. The cosmic dose rate of 13 mrads/year was then added to give the total dose rate determined by the scintillator.

Altitude Effect

At an altitude of 4 km the intensity of the hard component will be between two and three times that at sea level (Lowder, 1978; derived from data in NCRP, 1975; O'Brien, 1975). At a level of 30 ± 4 mrads/year, this provides an important fraction of the total dose rate and must be added to the dose rate predicted by the scintillator count rate obtained after subtracting the count rate submerged in water, which was measured at an altitude of 3.5 km as 121 ± 5 cpm.

It is interesting to note that, if the increase in count rate when submerged in water is attributed solely to the increase by a factor of 2.3 in the cosmic-ray intensity, a "true" sea-level cosmic count rate of 24 cpm is predicted. Thus it seems likely that impurities in the detector head contribute about 40 cpm.

Capsule and scintillator results are listed in columns 7 and 8 of Table 7, with the appropriate cosmic correction included in the scintillator data.

We suggest that the results from sites $P44_1$, $P46J_1$, and $P46J_2$ be disregarded. The $P44_1$ result is not consistent with $P44_2$ and $P44_3$. Since all three capsules were in the same borehole, this suggests a local inhomogeneity to which the capsule would be much more sensitive than the scintillator. Site P46 was very poor from the point of view of dosimetry; the detector and capsules were placed at the boundary of a soil layer with loose slate and vegetation.

A brief examination of the cosmic-corrected scintillator and capsule results shows that, although the lowland sites give moderate agreement, the scintillator gives consistently low readings compared with the capsules in the highland sites. Assuming the amount added for the cosmic contribution at a high altitude to be correct (it would need to be doubled to remove the discrepancy), a possible reason for the difference is the change in radon retention when the soil is disturbed to insert the scintillator and capsule—especially on wet sites. It is well known that water plays an important part in radon emanation and transport (see, e.g., Tanner, 1964). Most of the gamma dose rate and scintillator count rate from the uranium chain is derived from radon daughters, and the scintillator measures the

count rate from these daughters with the soil in a recently disturbed state, partially dried out after excavation. The capsule is buried, however, and measures the dose rate with the surrounding soil close to its original condition over a long period of time compared with the radon half-life. Although this change in emanation is likely to be variable, some correlation between water content and the fractional difference of the capsule and scintillator dose rates can be seen.

The last column in Table 7 lists the scintillator results after a water-content correction is applied:

$$\text{Corrected scintillator dose rate} = \text{Scintillator dose rate} \times \left[1 + \frac{1}{100}(0.85 \times W - 6.4)\right]$$

where W is the percentage water content of the soil. This equation was empirically derived from the capsule and cosmic-corrected scintillator data in Table 7. (Of course, such a water-content correction should be applied only to the portion of the gamma dose that is derived from radon daughters). It is worth noting that the intercept term, implying that no correction is necessary if the water content is ~7.5%, is consistent with the measured water content of the calibration blocks, ~8%.

This correction formula almost completely removed the systematic difference in the highland results (less than 5 ± 5% to one sigma) and further reduced any average difference in the sea-level data (less than 2 ± 4% to one sigma), without increasing the spread of the differences, ~12% to one sigma.

This comparison of capsule and scintillator results cannot be considered conclusive because of the relatively large corrections to both sets of results. For those sites where it was impossible to use a capsule, however, it does show that the measurements taken with the scintillator are meaningful if the appropriate cosmic and water-content corrections are applied.

ACKNOWLEDGMENTS

We are grateful to D. A. Morris for designing the spectrum stabilization for the scintillator; to M. Marshall, United Kingdom Atomic Energy Research Establishment, Harwell, for gamma spectrometry of the U. S. Department of Energy ore; and to Erle Nelson, Simon Fraser University, for providing the obsidian.

S. G. E. Bowman and A. S. Murray gratefully acknowledge financial support from Natural Environment Research Council

(NERC) studentships. The Peruvian data came from work undertaken by the Oxford and Liverpool Universities Archaeomagnetic Expedition 1975, also financed by the NERC.

Finally, we are indebted to Wayne M. Lowder for his helpful comments and advice.

REFERENCES

Aitken, M. J., 1968, Low-Level Environmental Radiation Measurements Using Natural Calcium Fluoride, in *Proceedings of the Second International Conference on Luminescence Dosimetry*, Gatlinburg, Tenn., Sept. 23—26, 1968, J. A. Auxier, K. Becker, and E. M. Robinson (Eds.), USAEC Report CONF-680920, pp. 281-290, Oak Ridge National Laboratory, NTIS.

——, 1975, *Physics and Archaeology*, 2nd Ed., Chap. 3, Clarendon Press, Oxford University.

——, and S. J. Fleming, 1972, Thermoluminescence Dosimetry in Archaeological Dating, in *Radiation Dosimetry*, Supplement 1, *Topics in Radiation Dosimetry*, F. H. Attix and W. Roesch (Eds.), Academic Press, Inc., New York.

——, D. W. Zimmerman, and S. J. Fleming, 1968, Thermoluminescent Dating of Ancient Pottery, *Nature*, 219: 442-444.

Bell, W. T., 1976, The Assessment of the Radiation Dose Rate for Thermoluminescence Dating, *Archaeometry*, 18(1): 107-111.

——, 1977, Thermoluminescent Dating: Revision of Dose Rate Data, *Archaeometry*, 19(1): 100.

Bowman, S. G. E., 1976, Ph.D. Thesis, App. A5, Oxford University, Oxford, England.

Evans, R. D., 1968a, *The Atomic Nucleus*, p. 627, McGraw-Hill Book Company, London.

——, 1968b, X-Ray and Gamma Interactions, in *Radiation Dosimetry*, Vol. 1, *Fundamentals*, 2nd ed., F. H. Attix and W. C. Roesch (Eds.), pp. 94-144, Academic Press, Inc., New York.

Fleming, S. J., 1977, *Dating in Archaeology*, Chap. 5, J. M. Dent & Sons, Ltd., London.

Løvborg, L., and P. Kirkegaard, 1974, Response of 3″ x 3″ NaI(Tl) Detectors to Terrestrial Gamma Radiation, *Nucl. Instrum. Methods*, 121: 239-251.

Lowder, W. M., 1978, U. S. Department of Energy, Environmental Measurements Laboratory, New York, personal communication.

Mejdahl, V., 1970, Measurement of Environmental Radiation at Archaeological Excavation Sites, *Archaeometry*, 12(2): 147-159.

——, 1972, *Dosimetry Technique in Thermoluminescent Dating*, Risø Report No. 261, Research Establishment Risø, Danish Atomic Energy Commission.

NCRP, 1975, *Natural Background Radiation in the United States*, NCRP Report 45, p. 12, National Council on Radiation Protection and Measurements, Washington, D. C.

——, 1976, *Environmental Radiation Measurements*, NCRP Report 50, p. 31, National Council on Radiation Protection and Measurements, Washington, D. C.

O'Brien, K., 1975, The Cosmic Ray Field at Ground Level, in *The Natural Radiation Environment II*, Symposium Proceedings, Houston, Tex., Aug. 7—11, 1972, J. A. S. Adams, W. M. Lowder, and T. F. Gesell (Eds.),

ERDA Report CONF-720805, Rice University and the University of Texas, Houston, NTIS.

Storm, E., and H. I. Israel, 1970, *Nuclear Data Tables, A7*, p. 565, Academic Press, Inc., New York.

Tanner, A. B., 1964, Radon Migration in the Ground-A Review, in *The Natural Radiation Environment*, J. A. S. Adams and W. M. Lowder (Eds.), University of Chicago Press, Chicago.

Taylor, R. E. (Ed.), 1977, Advances in Obsidian Glass Studies: Archaeological and Geochemical Perspectives, Noyes Data Corp., Park Ridge, N. J.

Warren, S. E., 1978, Rubidium—A Potential Source of Systematic Error in Thermoluminescence Dating of Pottery, *Archaeometry*, 20: 66-70.

Wintle, A. G., 1973, Anomalous Fading of Thermoluminescence in Mineral Samples, *Nature*, 245. 143-144.

——, and A. S. Murray, 1977, Thermoluminescence Dating: Reassessment of the Fine Grain Dose Rate, *Archaeometry*, 19(1): 97.

Zimmerman, D. W., 1971, Thermoluminescent Dating Using Fine Grains from Pottery, *Archaeometry*, 13(1): 29-52.

——, 1972, Relative Thermoluminescence Effects of Alpha and Beta Radiation, *Radiat. Eff.*, 14: 81-92.

Analysis of Error in Measuring the Environmental Radiation Background Using Thermoluminescence Dosimetry

J. H. WHITE, C. W. SUNDBECK, and C. L. LINDEKEN
Lawrence Livermore Laboratory, Livermore, California

ABSTRACT

Thermoluminescence dosimetry (TLD) is now widely used for monitoring the environmental radiation background in the vicinity of nuclear facilities. The performance of the Lawrence Livermore Laboratory TLD system has been evaluated with respect to errors associated with phosphor characteristics, precision, calibration, and curve fitting. The errors for LiF (TLD-700) and CaF_2 : Dy (TLD-200) have been determined to be in the range of 10 to 20% and 20 to 30%, respectively. Analysis of variance techniques was used on the CaF_2 : Dy data to determine the effect of temporal and spatial biases on the measurement of the environmental radiation background. These analyses indicates that there is a significant added variance component due to each bias. Although there is significant variation in the data, small differences (10 to 20%) can be detected in the environmental radiation background using log normal statistical techniques.

Thermoluminescence dosimetry (TLD) is now widely used in the measurement of the environmental radiation background in the vicinity of nuclear facilities. Evaluation of the data from these measurements is facilitated as understanding is improved of such parameters as dosimetric material characteristics and spatial and temporal variations of the natural radiation background. In this paper we will discuss four main topics concerned with error analysis and data interpretation:

- Errors due to dosimetric material characteristics.
- Reproducibility and uniformity.
- Analysis of variance for spatial and temporal effects.
- Log-normal statistical treatment of the data.

At the Lawrence Livermore Laboratory (LLL) there has been an ongoing routine environmental radiation background monitoring program since 1972. We obtained the measurements using a procedure described in a previously published report (Lindeken et al., 1976). The environmental TLD package consists of two types of phosphors: CaF_2 : Dy (TLD-200) and ^7LiF (TLD-700). At quarterly intervals, dosimeter packages are exchanged at 41 off-site locations. After waiting for the low-temperature traps to decay, the TLD's are loaded into a reader designed at LLL and calibration dosimeters are interspersed within each group. The output is then analyzed by a computer program, and the results are evaluated using previous knowledge of exposure patterns and by statistical methods.

The following discussions are concerned with two questions:

1. How well can the TLD system measure the environmental radiation background?

2. What can be learned from these measurements that can be applied to environmental monitoring around nuclear facilities?

ERROR ANALYSIS

Assessment of the total error in making TLD measurements is complex due to the interaction of many factors, such as the thermoluminescent (TL) material properties, mechanical operations of equipment, natural fluctuations of the background radiation, and climatology. This analysis attempts to evaluate the major components of the total error and considers the error associated with the minor components to be included in all error values. The major components include the type of TL material used, the precision of the TLD reader (the parameters of mechanical operation are assumed to be constant), the calibration curve fitting, and operation of the calibration facility. Also, multiple dosimeter packages have been placed in the same location over the last several years to study the precision of the TL material in measuring the same radiation field and the reproducibility of the TLD reader.

Characteristics of Dosimeter Material

The environmental TLD package at LLL contains two phosphors: CaF_2 : Dy (TLD-200) and ^7LiF (TLD-700). The use of two different phosphors is beneficial for determining a more precise exposure and for indicating low-energy radiation. However, each phosphor has different characteristics that must be considered when analyzing errors for overall performance. Dose and energy responses

for the TL materials are very well documented in the literature. The most significant component of the material properties is stability, or as it is more commonly known, fading. Over the 3-month field exposure cycle used at LLL, the TL signal fading of LiF is quite insignificant; however, the signal loss associated with CaF_2 : Dy is not only significant but also complex. Generally, the CaF_2 : Dy phosphor will lose approximately 20% of the TL signal within the first 24 hr after irradiation and a total of 30% over the 3-month period (Jones, Lindeken, and McMillen, 1971).

To determine the effect of these material characteristic properties, the model developed by Burke and Gesell (1976a) has been used to estimate the error for dose assessment. This model includes such factors as the energy response and directional dependence, as well as fading of signal during storage, transit, and exposure, and errors in time of placement. Table 1 summarizes some of the parameters and values used to analyze the errors of the LLL dosimeters. As is shown in the table the errors associated with directional dependence, energy response, and timing are relatively small, whereas the errors in the fading values have much more uncertainty. Also the values for the fading of the CaF_2 : Dy signal include some interpretations based on the work of Jones, Lindeken, and McMillen (1974). Following the mathematical techniques of the Burke—Gesell method, the LiF values are associated with an error of 12% at the 2σ confidence level and CaF_2 : Dy value are associated with an error of 25% at the 2σ confidence level. Allowing for some adjustment in the parameters of Table 1, the error values for the LiF and CaF_2 : Dy phosphors can be considered in the range of 10 to 15% and 20 to 25%, respectively, as shown in Table 2.

Readout Equipment

During 1972 and 1973 the TLD packages were read out on a semiautomatic hot gas reader designed at LLL (Petrock and Jones, 1968). An LLL designed automatic hot gas reader (Samardzich et al., 1974) developed for the personnel dosimetry program has been used for TLD readout during 1974 to 1976. Recently there has been a return to the semiautomatic reader for the environmental monitoring dosimeters. Both readout units operate using the same principle; however, the operating voltage on the automatic system could not be increased sufficiently to provide the desired sensitivity. The errors associated with the mechanical operation of the readout equipment have been assumed to be constant, and the only errors evaluated are those associated with Poisson counting statistics. The standard deviation of the light output readings was calculated using estimates

TABLE 1

Parameters Used in Burke—Gesell Calculations

Parameter	^{7}LiF, %	CaF_2 : Dy, %
Energy response	1.00 ± 2	1.00 ± 2
Directional dependence	1.00 ± 2	1.00 ± 2
Preexposure storage time	48 hr ± 0	48 hr ± 0
Preexposure transit time	8 hr ± 0	8 hr ± 0
Exposure time	2400 hr ± 0.4	2400 hr ± 0.4
Postexposure transit time	8 hr ± 0	8 hr ± 0
Postexposure storage time	48 hr ± 0	48 hr ± 0
Preexposure storage fading	1.000 ± 0.5	0.8 ± 5
Preexposure transit fading	1.000 ± 0.5	0.9 ± 5
Exposure fading	0.970 ± 5.0	0.7 ± 10
Postexposure transit fading	1.000 ± 0.5	0.8 ± 5
Postexposure storage fading	1.000 ± 0.5	0.8 ± 5

TABLE 2

Error Values* for TLD Measurements

Source of error	LiF, %	CaF_2 : Dy, %
Phosphor	10—15	20—25
Precision	2—8	2—10
Curve fit	3—10	2—8
Calibration	2—4	2—4
Total	11—20	20—28

*All values are at the 95% confidence level.

$$(2\sigma)_{total} = [(2\sigma)^2_{phosphor} + (2\sigma)^2_{precision} + (2\sigma)^2_{curve\ fit} + (2\sigma)^2_{calibration}]^{1/2}$$

$(2\sigma)_{phosphor}$—derived from Burke—Gesell model

$(2\sigma)_{precision}$—[(highest value—lowest value) X 0.591] X 2, from Dixon and Massey

$(2\sigma)_{curve\ fit}$—linear least squares regression confidence interval, from Sokal and Rohlf

$(2\sigma)_{calibration}$—LLL operational experience of the calibration facility

of dispersion for small samples (Dixon and Massey, 1957), and the standard error of the mean was derived by dividing the standard deviation by the square root of the number of samples. In general, the 2σ error of the light output readings ranges from 2 to 8% for the LiF phosphor and 2 to 10% for the CaF_2 : Dy phosphor.

Calibration Curve Fit

During the readout procedures, calibration dosimeters are interspersed with those dosimeters from the field. The readout data are then used as the input to a computer program, which calculates exposure doses and confidence limits for all dosimeters. The confidence limits represent the propagation of the precision of the light output readings (as discussed in the preceding paragraph) and the error calculated from the linear least square regression fit of the calibration dosimeters. The confidence limits on the regression fit have been calculated under the condition of more than one Y value for each X (Sokal and Rohlf, 1969) since each calibration dose is represented by three TL chips. The calibration curve fitting errors for LiF are 3 to 10% and for CaF_2 : Dy are 2 to 8%.

Calibration Facility

At LLL the calibration facility consists of a room 9- by 9- by 7-m with an aluminum grid floor suspended midway between the bottom floor and ceiling to provide minimum scattering. The TLD calibrations have been made with a ^{60}Co source encapsuled in a small aluminum cylinder using a pneumatic transfer system. A ^{137}Cs source is currently used for calibration to reduce any error associated with an over response from electrons produced in the TLD packet and the surrounding air, as described by Graham and Homann (1978). The parameters that affect the error involved with delivering a calibrating dose to a TLD are the accuracy of the source strength, the timing of the pneumatic transfer system, and the placement of the TL dosimeter at the desired distance from the source. The major component of the error associated with calibrating the TLD's is the certainty with which the calibration source strength is known. The calibration sources are generally within ±5% of the stated value; however, further measurements are made with ionization chambers at the time of calibration and the 2σ error then associated with the procedure is in the range of 2 to 4%. The placement of the dosimeter is made using solid rods of 1, 2, and 3 m, and the 2σ error is approximately 0.5%. Since the automatic timer for the pneumatic transfer system is accurate to milliseconds and the exposures are for

several minutes, the error associated with this parameter is considered to be negligible. Thus the total error for calibrating the TL dosimeter is 2 to 4% at the 95% confidence level.

Precision and Reproducibility

To study the variability of TLD measurements of the same radiation field, we monitored three locations on the LLL perimeter by three replicate dosimeters at each location (see Fig. 1). The three TL chips in each dosimeter are from a batch that has been matched

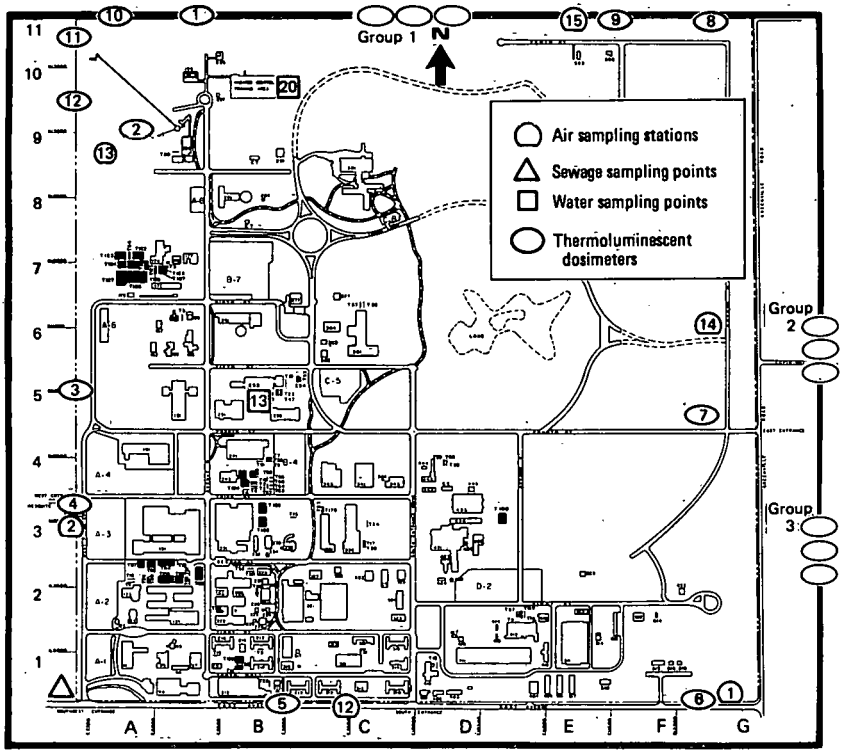


Fig. 1 Location of replicate dosimeters on LLL perimeter.

to ±4% at the 95% confidence level. The data for 10 quarters have been accumulated, and the results of these measurements are shown in Table 3. The individual dosimeter measurements have been adjusted using both Chauvenet's Criterion (Chase and Rabinowitz,

1967) and a range/ratio method described by Dixon and Massey (1957) to reject extreme values (outliers). The precision at the 95% confidence level for the data for each quarter ranges from 4 to 30%. These errors include not only those from the readout but also those associated with the matching and the mechanical operation of the readout equipment. The latter errors have not been quantified and have also been assumed to be constant for all quarters. However, this component of error may result in some of the larger values in Table 3. In general, over a period of 10 quarters, the measurements in each group are reproducible within a 2σ error of 20%.

TABLE 3

Results of Replicate Dosimeter Measurements

	mR ± 2σ, %		
Quarter	Group 1	Group 2	Group 3
1	20.05 ± 4.9	18.21 ± 6.8	19.26 ± 7.4
2	19.20 ± 8.3	16.57 ± 11.5	17.13 ± 11.9
3	18.24 ± 13.0	16.60 ± 13.9	16.59 ± 8.8
4	19.34 ± 28.9		19.60 ± 21.5
5	21.04 ± 10.3	18.79 ± 20.0	20.63 ± 11.7
6	20.20 ± 12.7	17.60 ± 25.6	19.23 ± 12.4
7	20.36 ± 11.0	18.28 ± 26.8	19.46 ± 19.6
8	18.67 ± 11.8	17.18 ± 7.2	18.30 ± 7.0
9	19.09 ± 12.9	18.42 ± 9.8	19.30 ± 5.9
10	19.01 ± 3.7	17.23 ± 9.1	17.63 ± 6.2
Total	19.50 ± 15.7	17.67 ± 17.8	18.70 ± 17.1

DATA INTERPRETATION

A 5-year data base for TLD measurements of the environmental radiation background has been analyzed using the techniques of analysis of variance (Sokal and Rohlf, 1969). Table 4 shows the data in milliroentgens as measured with CaF_2 : Dy dosimeters by quarters and by location; the 5-year period is from 1972 to 1976, and the 41 locations are shown in Fig. 2. A two-way analysis of variance (ANOVA) was made to examine any major trending in either the

TABLE 4

The CaF_2 : Dy Measurements of the Environmental Radiation Background (mR)

	Quarters, 1972—1976																			
Location*	1	2	3	4	5	6	7	8	9	10	11	12	13	14	15	16	17	18	19	20
1	19	21	21	21	—	—	—	20	12	15	16	17	21	19	19	21	22	21	—	19
2	†	15	14	20	19	—	—	—	11	13	15	15	20	17	17	22	19	20	19	19
3	17	13	15	22	16	—	12	18	12	—	—	16	21	19	16	20	—	19	20	13
4	16	—	—	21	16	15	—	—	12	13	16	15	21	18	17	—	19	18	21	19
5	15	14	14	20	16	17	17	18	12	—	15	15	—	—	18	19	20	18	20	18
6	13	16	16	21	18	—	14	20	13	14	17	16	19	21	23	21	21	19	20	18
7	10	15	14	24	15	17	15	—	13	15	19	17	23	20	20	22	22	23	23	21
8	16	18	19	21	19	19	17	—	12	14	15	15	20	19	18	17	21	20	20	17
9	15	15	14	21	20	15	15	19	12	15	16	15	22	19	15	24	—	20	19	20
10	15	16	14	19	—	15	—	19	12	14	16	—	—	18	18	19	20	20	20	19
11	18	—	17	—	14	17	12	—	13	15	16	16	21	19	18	22	21	18	21	20
12	14	17	15	20	17	15	17	—	11	13	15	14	25	19	17	18	19	19	19	18
13	—	14	14	—	16	15	19	—	11	—	14	15	19	17	14	20	—	18	17	18
14	16	14	14	15	—	15	12	—	11	13	15	14	18	18	15	19	18	18	—	18
15	18	14	16	20	18	14	13	—	11	13	17	15	—	18	17	17	19	19	20	18
16	17	15	15	18	18	13	14	—	14	13	15	16	19	—	18	21	21	19	20	19
17	16	—	—	20	21	19	13	19	13	16	17	17	20	20	19	21	22	20	23	21
19	18	14	13	23	21	20	19	19	13	14	17	17	25	23	24	21	25	21	22	21
20	20	14	16	14	14	15	15	—	12	14	15	13	18	18	16	17	19	19	19	16
21	13	17	14	20	18	15	14	—	12	15	15	15	28	18	18	22	21	19	21	18
22	16	15	14	19	13	15	13	17	12	13	14	15	19	16	15	17	19	17	19	18
23	16	17	16	—	19	16	11	—	12	14	17	16	20	18	19	—	21	19	16	18
24	18	—	—	—	—	13	15	—	12	14	16	13	20	19	—	18	19	20	19	13
25	12	—	—	14	14	13	—	—	11	—	13	12	17	—	15	15	15	16	16	16
26	14	13	13	—	—	13	17	17	11	13	—	13	18	17	14	19	—	18	15	17
27	14	13	14	14	15	15	11	—	11	—	16	14	18	17	16	19	20	18	19	17
28	17	19	—	21	18	18	16	19	12	15	17	15	21	19	17	21	22	22	21	19
29	18	14	14	20	20	19	13	—	12	13	17	16	21	19	19	21	22	—	21	—
30	—	15	13	17	14	—	—	—	12	14	—	14	20	20	17	22	—	—	19	19
31	14	14	—	19	17	—	12	—	11	13	13	13	17	16	16	17	16	18	19	17
32	16	16	12	—	18	16	—	—	13	15	15	14	19	19	17	17	21	20	18	17
33	16	18	17	14	19	17	12	—	12	16	16	16	22	20	19	21	21	21	22	20
34	—	17	—	15	13	15	11	—	12	14	15	15	20	18	17	19	20	20	20	19
35	19	—	16	18	14	16	13	—	11	14	15	14	19	—	17	19	20	20	20	17
36	15	14	15	17	19	15	—	17	12	14	16	16	19	18	18	21	22	21	20	20
37	17	16	17	21	18	—	17	17	12	14	15	14	20	19	18	18	20	20	21	—
38	19	12	17	15	19	18	12	18	12	13	16	14	20	18	17	20	20	20	20	21
39	16	17	16	19	—	17	19	18	13	13	16	16	20	18	18	21	21	20	21	18
40	18	19	18	21	16	—	15	17	11	16	—	16	21	20	16	18	20	20	21	20
41	18	12	15	15	17	18	16	17	17	13	16	15	20	18	20	19	21	20	20	17

*See Fig. 2 for sample location.
†Indicates TL dosimeter was lost in the field.

temporal (quarters) or spatial (location) parameter. The results of this analysis show that there are highly significant variations in the TLD measurements in both the temporal and spatial dimensions, with the greater variation being reflected in the temporal data. This general analysis leads into a more detailed examination of each dimension; the temporal variations are analyzed by quarters and by years and the spatial variations by geographical and geological bias.

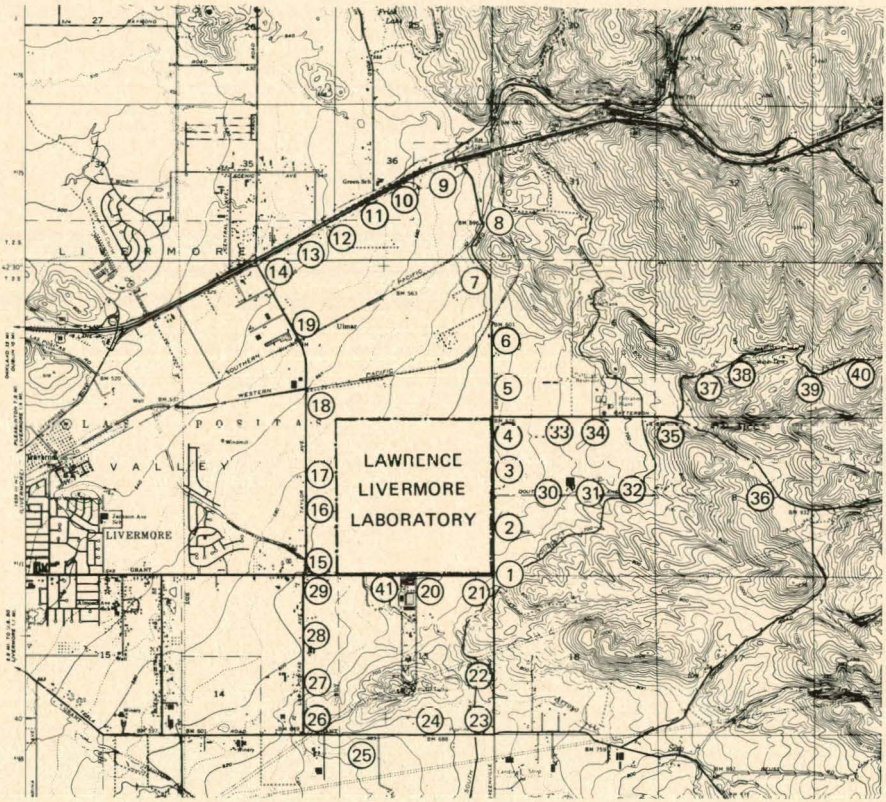


Fig. 2 Location of TL dosimeters in the vicinity of LLL.

Temporal Variations

The highly significant variation among the whole quarterly data set was tested using a one-way analysis of variance (ANOVA), and the added variance component contributed 62% of the total variance. To isolate this component, we divided the data into groupings of all first, second, third, and fourth quarters for all years, and individual one-way analyses of variance were performed. All these quarter groupings exhibited highly significant ($P \ll 0.001$) variations. To further study which quarter grouping contributed the largest share of the added variance component, each quarter grouping was subtracted from the total of all quarter groupings and a one-way ANOVA was performed. The results of all the quarterly tests are shown in Table 5. The first-quarter grouping exhibits the most added variation, and this is confirmed by examining the effect of subtracting the first-quarter

TABLE 5

Summary of Analyses of Variance on the Quarterly Groupings

Grouping	Number of quarters	Number of measurements	Variance components,* %	
			Expected	Added
1st	5	182	25.5	74.5
2nd	5	175	31.1	68.9
3rd	5	178	44.2	55.8
4th	5	166	48.6	51.4
All	20	701	37.6	62.4
All, 1st	15	519	42.9	57.1
All, 2nd	15	526	38.0	62.0
All, 3rd	15	523	34.6	65.4
All, 4th	15	535	35.2	64.8

*The expected variance component is the variance in a group of data due to sampling from a normal population, and the added variance component is due to any bias that may be present in the sampled pattern.

grouping data from the total. The highly variable weather associated with a change from winter to spring may be partially responsible for the large added variance of the first-quarter data. However, there may be other unknown biases over the 5-year period.

During this time period some of the procedures for handling the TLD's were modified, and a change to the use of the automated personnel dosimetry TLD reader was made in 1974. The data for each year have been analyzed by the one-way ANOVA and are summarized in Table 6. Even though each year exhibits a highly significant ($P < 0.001$) variation among the quarters of that year, it appears that the data from 1974 have been biased by changing readers. As experience was gained in using the automated reader, the added variance component decreased, also indicating that this bias may have been due to the readout equipment.

Spatial Variations

The variation of the data due to spatial distribution has been analyzed using all the data for 40 locations in the vicinity of LLL (see Fig. 2). The one-way ANOVA shows a significant variation ($P < 0.001$) among these locations, even though the added variance component is only 8% of the total. The locations were then divided

TABLE 6

Summary of Analyses of Variance for the Data by Year

Year	Number of quarters	Number of measurements	Variance components, %	
			Expected	Added
1972	4	137	65.9	34.1
1973	4	115	67.0	33.0
1974	4	150	34.3	65.7
1975	4	150	77.0	23.0
1976	4	149	83.7	16.3

into major geographical regions; locations 5 to 14 and 16 to 19 are designated as North, locations 1 to 4 and 30 to 40 as East, and locations 20 to 29, 15, and 41 as South. The data for location 18 reflect the operation of a nearby industrial radiography unit and have been excluded from the calculations. The results of the one-way ANOVA for each region are summarized in Table 7. Although there is no strong bias in the spatial distribution, those measurements made in the South region have the greatest added variance component, followed by the North and East regions. One of the reasons for this bias is the geologic properties of the soils in these regions. The soil matrix consists primarily of gravelly soils in the South region, progresses through loamy sands to the East, and is predominantly clay soil in the North. The natural radioactivity in these regions also

TABLE 7

Summary of Analyses of Variance for Spatial Distribution

Region	Number of locations	Number of measurements	Variance components, %	
			Expected	Added
North	13	233	92.1	7.9
East	15	257	97.6	2.4
South	12	211	88.9	11.1
All	40	701	91.7	8.3

contributes to the bias, as the ^{40}K content will decrease from North to South (Lindeken et al., 1973). Other parameters, such as the soil-water balance as described by Burke and Gesell (1976b), may be responsible for these variations.

Log-Normal Distributions

Up to this point all the calculations and ANOVA's have been performed, assuming that the TLD measurements are from a normal population. The distribution of environmental radioactivity has also been shown to follow a log-normal statistical distribution (Denham and Waite, 1975). Applying the log-normal assumption allows a graphical representation of the data from Table 4 as shown in Fig. 3. Although the analyses of variance indicate significant added variation due to temporal variations, all the individual yearly data exhibit single populations with small geometric standard deviations. The data for 1974 had the largest added variance component, and the log-normal analysis showed the same data to have the smallest geometric mean. The data for 1972 and 1973 showed similar distributions, as did the data for 1975 and 1976. Thus the change to the automated readout system in 1974 did bias the environmental

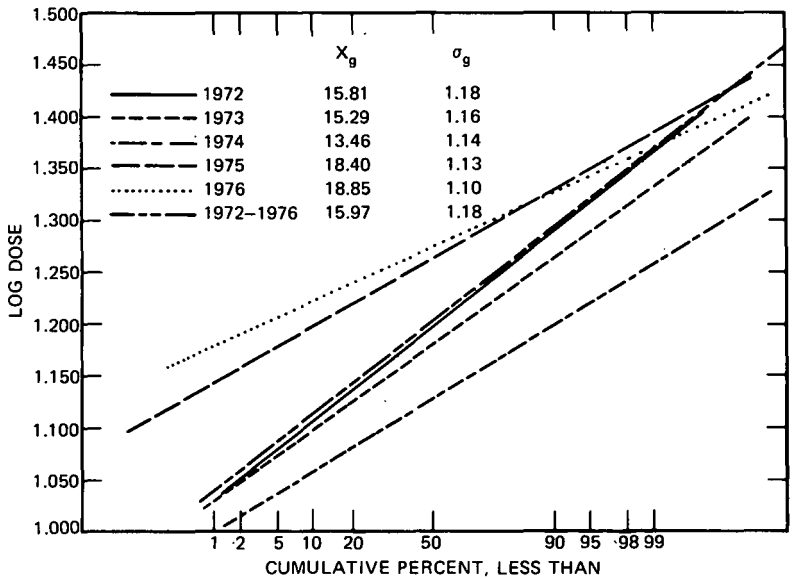


Fig. 3 Regression fit of log-normal distributions.

radiation background data. The small geometric standard deviations imply that, although there is significant variation within each population, small differences (10 to 20%) may be detected in the environmental radiation background using CaF_2 : Dy thermoluminescence dosimeters.

CONCLUSIONS

Several parameters have been analyzed to evaluate the accuracy with which thermoluminescence dosimetry can measure the environmental radiation background. Errors associated with the phosphor characteristics, precision of the readout, calibration, and curve fitting have been quantified using various models and assumptions. The largest parametric contributors to the error are the fading properties of the phosphor, and the 2σ error due to the phosphor characteristics is approximately 10 to 15% for LiF and 20 to 25% for CaF_2 : Dy. The overall performance for individual measurements generally has associated 2σ errors within 20% for LiF and within 30% for CaF_2 : Dy; these errors are within the criteria specified by the ANSI Standard (American National Standards Institute, 1975) for thermoluminescence dosimetry (environmental applications). Groups of data for replicate dosimeters at the same location have been analyzed to determine the precision of the TLD measurement system. In general, over a period of 10 quarters the measurements are reproducible within a 2σ error of 20%.

In assessing TLD measurements for an environmental monitoring program, these errors will remain constant each quarter if the phosphors and/or the handling procedures are not modified. However, the environmental radiation background may fluctuate due to temporal (time or seasonal) or spatial (location) bias. Analyses of variance techniques are useful in isolating these biases, and results of these analyses indicate that measurements in the first quarters are the most variable and those in the fourth are the least. Interpretation of elevated measurements during the first quarter require some knowledge of this variability for assessment of the possible impact of the facility operations. With respect to spatial bias, the analysis indicates more variability in the region to the South, followed by that for the North region, and the least variability is in the East region. The soil structure and natural radioactivity content of the soil are possible sources for the differences and must be considered when assessing the possible impact of the facility operations. Even though these biases are part of the environmental monitoring measurements, small differences on the order of 10 to 20% may still be detected when the data are analyzed using log-normal statistical techniques.

In this study we have evaluated the sources of error that accompany measurements of the environmental radiation background when using thermoluminescence dosimetry. Application of analysis of variance techniques to TLD data obtained from measurements within the Livermore Valley has indicated anomalies requiring

investigation. These analyses of error and of variance have led to a better understanding of the results of the environmental monitoring program in measuring the natural radiation background.

ACKNOWLEDGMENT

Work performed under the auspices of the U. S. Department of Energy by the Lawrence Livermore Laboratory under contract No. W-7405-Eng-48.

REFERENCES

American National Standards Institute, 1975, *Performance, Testing, and Procedural Specifications for Thermoluminescence Dosimetry (Environmental Applications)*, Report N545, 1975.

Burke, Gail de P., and T. F. Gesell, 1976a, Error Analysis of Environmental Radiation Measurements Made with Integrating Detectors, in *Measurements for the Safe Use of Radiation*, NBS 75th Anniversary Symposium Proceedings, Gaithersburg, Md., March 1—4, 1976, Report NBS-SP-456, pp. 187-195, National Bureau of Standards.

——, 1976b, Thermoluminescence Dosimetry: Environmental Monitoring Near Nuclear Reactor Sites, *IEEE Trans. Nucl. Sci.*, NS-23: 1224-1236 (1976).

Chase, Grafton D., and J. L. Rabinowitz, 1967, *Principles of Radioisotope Methodology*, 3rd ed., pp. 104-107, Burgess Publishing Co., Minneapolis.

Denham, Dale H., and D. A. Waite, 1975, Some Practical Applications of the Log-Normal Distribution for Integrating Environmental Data, *Health Phys. Soc.*, 29: 303.

Dixon, Wilfred J., and F. J. Massey, Jr., 1957, *Introduction to Statistical Analysis*, 2nd ed., pp. 273-274, McGraw-Hill Book Co., New York.

——, and F. J. Massey, Jr., 1957, op. cit., pp. 275-277.

Graham, C. L., and S. G. Homann, 1977, Gamma-Ray Dosimetry, Errors with TLDs, in *National and International Standardization in Radiation Dosimetry*, Symposium Proceedings, Atlanta, Ga., 1977, pp. 335-348, STI/PUB/471, International Atomic Energy Agency, Vienna, 1978.

Jones, D. E., C. L. Lindeken, and R. E. McMillen, 1974, Natural Radiation Background Dose Measurements with CaF_2 : Dy TLD, in *The Third International Conference on Luminescence Dosimetry*, Symposium Proceedings, Riso, Denmark, Oct. 11—14, 1974, Part III, pp. 985-993.

Lindeken, Carl L., J. H. White, A. J. Toy, and C. W. Sundbeck, 1976, Ambient Environmental Radiation Monitoring at the Lawrence Livermore Laboratory, in *Ninth Midyear Topical Symposium on Operational Health Physics*, Symposium Proceedings, Denver, Colo., Feb. 9—12, 1976, pp. 716-721, USAEC Report CONF-760202-2, NTIS.

——, P. H. Gudiksen, J. W. Meadows, K. O. Hanby, and L. R. Anspaugh, 1973, *Environmental Levels of Radioactivity in Livermore Valley Soils*, USAEC Report UCRL-74424, Lawrence Livermore Laboratory, NTIS.

Petrock, K. F., and D. E. Jones, 1968, Hot Nitrogen Gas for Heating Thermoluminescent Dosimeters, in *Second International Conference on Luminescence Dosimetry*, Symposium Proceedings, Gatlinburg, Tenn., Sept. 23—26, 1968, J. A. Auxier, K. Becker, and E. M. Robinson (Eds.), USAEC Report CONF-680920, p. 652, Oak Ridge National Laboratory, NTIS, 1969.

Samardzich, B. G., D. E. Jones, K. F. Petrock, and E. G. Shapiro, 1971, *Thermoluminescent Dosimeter System for Personnel Monitoring*, Report UCRL-73084, Lawrence Livermore Laboratory.

Sokal, Robert R., and F. James Rohlf, 1969, *Biometry*, pp. 420-430, W. H Freeman and Company, San Francisco.

——, and F. James Rohlf, 1969, op. cit., Chaps 8-11.

DISCUSSION

Koperski: (Comment) I'm surprised by the large error of your reported LiF measurements. In my laboratory we have produced our LiF detectors for many years, and measurements with those we used for monitoring of gamma radiation from natural environments exhibit overall statistical error, as well as the precision, equal to ±6% at the 2σ level of confidence. These values were established on the basis of the identical procedure that you applied. Maybe the reason for the occurrence of this difference is that our dosimeters used for measuring the natural gamma background in the environment were carefully selected from our production batches, containing also dosimeters with a sensitivity spread of about ±20%, which may cause overall measurement error of ±30% at the 2σ confidence level. This is admissible in routine dosimetry monitoring but not in the environmental case where the levels of, and differences in the natural gamma exposures to be detected, are generally small. Therefore only high quality detectors, those exhibiting a small sensitivity spread as well as overall measuring system, should be applied. In any case, measurement errors ought to be at least two times lower than those you observed.

Murray: (Comment) We use natural CaF_2 and estimate the fading of the high temperature peak at about 1% per year. This can give reproducibility to 1σ of 2 to 3%, although we do use a different measurement regime.

Energy Dependence of Thermoluminescent Dosimetry in Environmental Monitoring

ERIK VOLD
Argonne National Laboratory, Argonne, Illinois*

ABSTRACT

The dose response for several thermoluminescent dosimeters (TLDs) and tissue to radiation from environmental terrestrial, cosmic, and ^{226}Ra calibration sources is calculated. Calculations are applied to TLD field data to quantify environmental radiation quality and a tissue dose.

In field experiments the increased dose near a research reactor was not associated with an energy spectrum significantly different from natural background, but the radiation quality near low energy shielded sources in the environment was characterized by the relative response of tandem TLD's.

The unattenuated tissue-equivalent dose (mrad) conversion from a ^{226}Ra calibration exposure (mR) at a natural radiation field of 60% terrestrial air dose is determined to be 0.96 for LiF or CaF_2 in cadmium, 0.75 for CaF_2 unshielded, and about 0.3 for BaF_2 unshielded. The terrestrial source contribution to total environmental radiation dose in the United States ranges from 25 to 66%. Over this range the tissue-equivalent (TE) correction factors to maximum tissue dose for LiF, CaF_2 in cadmium, CaF_2, and BaF_2 vary by 2, 7, 17, and about 100%, respectively.

Thermoluminescent dosimetry (TLD) is gaining in use as an environmental radiation surveillance technique since it offers a relatively simple, inexpensive and reliable means of assessing dose due to direct penetrating radiation. An important application of TLD is the evaluation of nuclear power plant site boundary and off-site doses to determine compliance with the design criteria of 10 C.F.R. Part 50, Appendix I (Burke, 1976; de Planque, 1979; ANSI N545,

*Present address: Radiologic Health, California Department of Health Services, Sacramento, Calif.

1975). It is now in widespread use at commercial nuclear power facilities. Of 26 ERDA (now Department of Energy) contractor sites required to submit an environmental surveillance report, approximately 50% report TLD results (ERDA, 1976, 1977).

It is the intent in this paper to develop TLD response calculations, compare them to field results for several types of TLD, and use the derived information to calculate tissue doses from the TLD responses. Appropriate calibration will vary with the relative contributions of the terrestrial gamma- and cosmic-ray source terms. The fraction of air dose due to the terrestrial gamma radiation can be quantified by the relative responses of the appropriate TLD's at a given location. This quantification is possible by the rough generalization that TLD response due to cosmic radiation varies only slightly among materials, but TLD response to the terrestrial gamma radiation increases dramatically with the effective atomic number, Z, of the TLD material.

ENVIRONMENTAL RADIATION

The environmental radiation is modeled with two components, the terrestrial gamma and the cosmic radiation. Only the penetrating radiations are considered, i.e., those that contribute to gonadal dose or the dose to TLD encased in 3-mm thick plastic. The alpha radiation from radon and the terrestrial beta radiation are thus excluded from consideration and from detection. This leaves a terrestrial source term which can be represented with a fluence distribution of photons and a cosmic source term which is approximated by a fluence distribution of fast charged particles and photons.

Response to Cosmic Radiation

The environmental radiation from cosmic rays is complex, with several components making significant contributions to tissue dose or detector response. The relevant data are summarized in several sources (UNSCEAR, 1972, 1977; EPA, 1977; NCRP, 1975, 1976; Lowder, 1976). Cosmic-ray muons, which together with the associated collision electrons produce more than 70% of the free air absorbed dose from cosmic radiation at sea level, are not significantly attenuated in the human body and thus contribute directly to the tissue penetrating dose. Cosmic-ray electrons from muon and pion decay, which contribute the bulk of the remaining dose, are somewhat attenuated by the body. Cosmic-ray neutrons and protons contribute only slightly to the air and tissue doses. The TLD

response to the neutrons and protons is considered to be negligible in the response calculations.

The cosmic-ray response calculation is to a first approximation the response to the cosmic-ray muons. The muon energy distribution can be approximated by assigning the muons to four energy groups at 0.5, 2, 8, and 20 GeV with fractional fluences of 0.313, 0.364, 0.149 and 0.174, respectively (Lowder and Burke, 1977). The collisional mass stopping powers, ${}_m\bar{S}$, in MeV-cm^2 · g^{-1} for muons at these energies on various detector materials are taken from the calculations of Bertel et al. (1971). The stopping powers are then averaged over the preceding fractional fluences in the environmental spectrum and yield a value proportional to the cosmic muon response as

$$(\text{Dose rate})_{TLD} \propto {}_m\bar{S}\,(\text{muons on TLD}) = \frac{\Sigma\,[{}_m\bar{S}(E_i)\,\phi_i]}{\Sigma\,\phi_i} \qquad (1)$$

where i is incremented over each energy group of average particle energy, E_i, and particle flux density, ϕ_i, within the group. This average response is then taken relative to that for air so that air dose may be considered as a common denominator between the terrestrial, cosmic, and calibration source terms. This is shown in Table 1. Similar values are obtained for cosmic-ray electrons from muon and pion decay so that the relative responses given in the table can be applied to the entire cosmic-ray component (Lowder and Burke, 1977).

Corrections for the cosmic-ray photon dose contribution are too complicated to proceed completely from calculations (O'Brien, 1975). The photons arise primarily from electron bremsstrahlung and annihilation processes and subsequent Compton scattering (Lowder, 1969). Experimental data from atmospheric radiation studies by Peterson (1963) and Brini et al. (1967) indicate that there are approximately 10 low energy photons (~20 to 200 keV) for every charged particle incident on our detector. Using this value and assuming an average absorption coefficient for each TLD to the low energy photon flux, and with the fluence-averaged charged particle stopping power, we can calculate the expected TLD dose due to charged particles relative to dose due to the cosmic-ray photons. Our calculated results indicate the cosmic-ray dose response for BaF_2 relative to air, as determined by relative charged particle stopping powers, must be increased 30% to account for the effect of the dose due to these low energy photons. For CaF_2 the response factor is increased 5%, and there is no significant response increase due to cosmic-ray photons for CaF_2 in cadmium, LiF, or tissue.

TABLE 1

Collisional Mass Stopping Power ($_mS$)* for Environmental Cosmic Muon Spectrum on Several Detector Materials

E(MeV)	ϕ†	Air	Tissue	LiF	BeO	$CaSO_4$	NaI	Anthracene	CaF_2	BaF_2
500	0.313	1.837	1.977	1.628	1.685	1.692	1.312	1.888	1.624	1.5
2,000	0.364	2.127	2.178	1.789	1.857	1.897	1.517	2.087	1.836	1.7
8,000	0.149	2.466	2.407	1.973	2.042	2.111	1.721	2.303	2.049	2.0
20,000	0.174	2.657	2.529	2.072	2.142	2.221	1.828	2.415	2.157	2.1
Fluence weighted average	$_m\bar{S}$:‡	2.18	2.22	1.83	1.90	1.94	1.55	2.14	1.87	1.7
$(_m\bar{S})_i/(_m\bar{S})_{air}$:		1.00	1.02	0.84	0.87	0.89	0.71	0.98	0.86	0.8

*$_mS$ is in units of MeV cm^2 g^{-1}.

† ϕ is the fraction of muon fluence grouped at energy, E.

‡ $_m\bar{S}$ is the fluence weighted average (see text).

Response to Terrestrial Radiation

The penetrating component of terrestrial radiation consists of photons originating in the decay series of uranium and thorium and also from potassium, with lesser contributions from the atmospheric radon and fallout (mostly ^{137}Cs) in the soil. The photon radiation field has been measured and characterized by calculations in several works (Beck, 1975; Beck, DeCampo, and Gogolak, 1972; Minato, 1977). There is good agreement between the studies' measurements and calculations (see also Okano et al., this volume). The typical environmental photon fluence spectrum is broken into seven energy groups with their respective fractions of the total fluence as given in NCRP (1976; from Beck, 1975). The energy-dependent response of a TLD to this photon spectrum is assumed proportional to the dose rate to the detector, $\dot{D}$, given as

$$\dot{D} \propto \frac{1}{\rho} \int \mu_{en}(E) \frac{d\phi}{dE} dE \cong \sum (\mu_{en}/\rho)_i \, \phi_i E_i \qquad (2)$$

In a similar manner, the response of the TLD to the photon calibration source is determined. The fractional photon fluences in the spectrum for the ^{226}Ra source are also taken from NCRP (1976).

The absorption coefficients were taken from Attix, Roesch, and Tochelin (1968) and Hubbell (1969). Some interpolation was necessary for barium, leaving the greatest uncertainty (~5%) in the values for BaF_2. The absorption coefficients for the lower energies were corrected to effective absorption coefficients, μ^*_{en}, derived from experimental data obtained on the low energy roll-off insensitivity of the actual dosimeters used in this study. The experimentally determined energy-dependent response curves are presented in Fig. 1. These curves represent the dose response to broad-energy spectrum (filtered X-ray beam) photons relative to air dose, with the response to ^{226}Ra (essentially no low energy photons) normalized to one for each type of TLD.

In the final analysis, this low energy correction based on the experimental data was significantly corrected against monoenergetic response calculations. The experimental and calculated response curves are compared for CaF_2 in Fig. 2, where it is seen that the experimental points tend to undershoot the calculated data peak (at about 50 to 60 keV) and overshoot the calculated points at higher energies (75 to 200 keV).

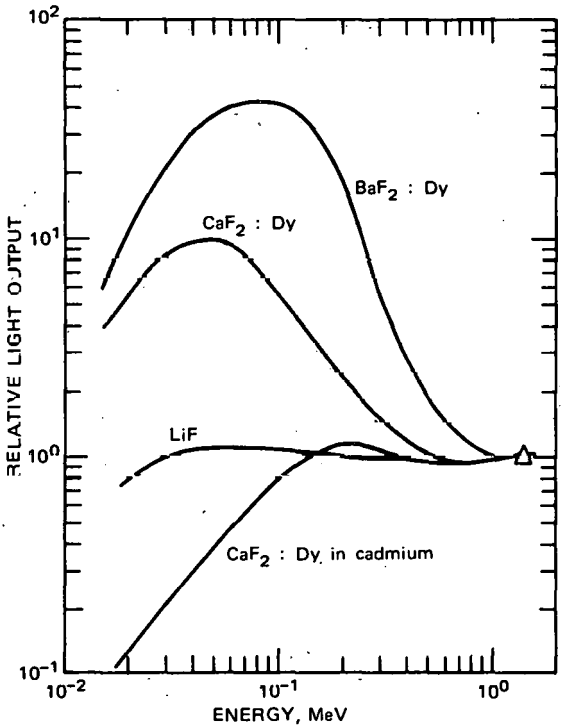


Fig. 1 Experimentally determined dosimeter energy response relative to air, normalized to that for a ^{226}Ra source.

In the first set of calculations, the integration in Eq. 2 is carried out for the primary source (environmental or ^{226}Ra) fluences only. In subsequent calculations, the photon build-up was included, introduced by Compton scatter in the TLD itself and more significantly in the plastic case. The build-up was calculated at the average energy of the Compton scattered photon for each initial energy assigned in the primary photon distributions. The primary and secondary photon energy groups, primary photon fluence fractions, and the effective absorption coefficients for the materials considered are compiled in Table 2.

For the present purpose, in the case of tissue, we assume the photons are neither attenuated nor significantly built up in the tissue. This will yield a maximum expected tissue dose. The effects of self-shielding by the body will be considered in the section on deriving a tissue-equivalent dose from the TLD field readings.

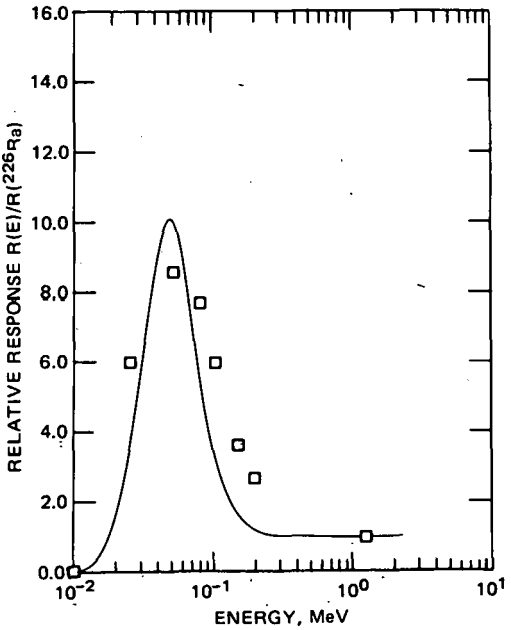


Fig. 2 Energy response of CaF_2, normalized to that for a ^{226}Ra source. ——, calculation; □, experiment.

ENERGY-DEPENDENCE CORRECTION

In this section the dose response calculations are summarized for application to a field monitoring situation. Where the response calculations were integrated over appropriate fluence spectrums, we simplify the expressions by assuming an average absorption coefficient, $\overline{\mu}_{en}/\rho$, and an average stopping power, $_m\overline{S}$, appropriate for the response to the sources considered.

The dose in air at a field location, D_f, can be related to TLD field readings derived using a calibration source calibrated in mR, with the expression

$$D_f = 0.869 \times K_{calib} \times K_E \times R_{TLD} \qquad (3)$$

where the factor 0.869 converts exposure (mR) to dose (mrad) in air, and R_{TLD} is the net TLD reading for the field dose (i.e., total reading less transit and storage contributions). The factor K_{calib} is the calibration conversion factor in units of "(mR of the calibration source) per net TLD reading." It is assumed to include effects of the

TABLE 2

Input Data for TLD Response to Photon Source Calculations

Energy group	Energy, MeV	Fraction of primary source—photon fluence		Effective* absorption coefficients, cm^2/g					
		Terrestrial gamma	^{226}Ra	Air	Tissue	LiF	CaF_2	CaF_2 in Cd	BaF_2
1	0.024			0.032	0.035	0.037	0.2	0 01	0.5
2	0.025	0.04	0.02	0.032	0.035	0.037	0.2	0 01	0.5
3	0.066			0.027	0.030	0.028	0.3	0 015	0.8
4	0.075	0.23	0.01	0.026	0.028	0.026	0.2	0.02	1.4
5	0.140			0.026	0.0283	0.025	0.1	0.03	0.6
6	0.175	0.30	0.05	0.0259	0.0285	0.024	0.035	0.035	0.25
7	0.263			0.0275	0.030	0.0255	0.032	0.032	0.15
8	0.375	0.16	0.285	0.0293	0.0323	0.0272	0.0295	0.0295	0.069
9	0.470			0.0292	0.0322	0.0271	0.0293	0.0293	0.058
10	0.750	0.125	0.29	0.0290	0.0320	0.0269	0.0284	0.0284	0.030
11	0.859			0.0280	0.032	0.026	0.0275	0.0275	0.028
12	1.5	0.115	0.305	0.0254	0.028	0.0236	0.0250	0.025	0.023
13	1.3			0.0260	0.029	0.024	0.026	0.026	0.023
14	2.3	0.03	0.04	0.0225	0.0245	0.021	0.022	0.022	0.021

*Low energy values for μ_{en}/ρ were corrected as described in the text. The even-numbered energy groups represent the primary spectra for the sources, and the odd-numbered energy groups are the average secondary photon energies resulting from the Compton-scattered primaries in the succeeding energy group.

reader, fading, and angular dependence of the system. The factor K_E is the correction for energy dependence.

When considering the environmental terrestrial gamma source, labeled EG below, which is for our purposes only photons, the energy dependent correction factor would be

$$K_E(EG) = \frac{(\mu_{en}/\rho)_{air,EG}}{(\mu_{en}/\rho)_{air,Ra}} \frac{(\mu_{en}/\rho)_{TLD,Ra}}{(\mu_{en}/\rho)_{TLD,EG}} \tag{4a}$$

where the first subscript refers to the dose medium and the second to the energy spectrum over which the absorption coefficient, μ_{en}/ρ, is averaged.

A basic dosimetric consideration is that the absorption coefficient is the appropriate weighting factor for dose in a detector made larger than the range of the secondary recoil electrons. This condition is maintained experimentally by encasing the TLD in a sufficient build-up layer of plastic casing. In air, charged particle equilibrium is closely approximated, and thus the ratio given in the first term of Eq. 4a is justifiable regardless of the volume of air considered.

The cosmic source correction factor used to convert from TLD dose due to cosmic rays to dose in air is approximated as $_mS_{air,\mu}/{}_mS_{TLD,\mu}$, where μ is the symbol for muons. Introducing the variable, T, to represent the fraction of the penetrating radiations' air dose due to the terrestrial source, then 1 — T represents that fraction due to the cosmic source. Combining terms, we obtain the following expression for the net energy correction for air dose in an environmental field monitored with a TLD and using ^{226}Ra as the calibration source

$$K_E(\text{Environ}) = \frac{(\mu_{en}/\rho)_{TLD,Ra}}{(\mu_{en}/\rho)_{air,Ra}} \times \left[\frac{(\mu_{en}/\rho)_{TLD,EG}}{(\mu_{en}/\rho)_{air,EG}} T + \frac{{}_mS_{TLD,\mu}}{{}_mS_{air,\mu}}(1-T)\right]^{-1} \tag{4b}$$

The dose in a small mass of tissue can be obtained by multiplying both sides of Eq. 3 by the term

$$\left[\frac{{}_mS_{tis,\mu}}{{}_mS_{air,\mu}}(1-T) + \frac{(\mu/\rho)_{tis,EG}}{(\mu/\rho)_{air,EG}} T\right]$$

Then, for tissue dose, retaining the form of Eq. 3,

$$K_E(\text{Environ}) = \frac{(\mu/\rho)_{TLD,Ra}}{(\mu/\rho)_{air,Ra}} \times \left\{ \frac{[(\mu/\rho)_{tis,EG}/(\mu/\rho)_{air,EG}]\,T + [{}_mS_{tis,\mu}/{}_mS_{air,\mu}]\,(1-T)}{[(\mu/\rho)_{TLD,EG}/(\mu/\rho)_{air,EG}]\,T + [{}_mS_{TLD,\mu}/{}_mS_{air,\mu}]\,(1-T)} \right\} \quad (4c)$$

Values of K_E (Eq. 4c) have been calculated for the various TLD's as a function of T and the resultant values used to correct TLD field results to a tissue dose. The values of K_E are graphed as a function of T in Figs. 3 to 6.

The integral response factors generated for each of the TLD's and tissues to each of the sources, terrestrial, cosmic, and radium calibration, are taken relative to the response factors generated for air, as summarized in Table 3. Graphs depicting relative TLD dose response in Figs. 7 and 8 show BaF_2 and CaF_2 relative to LiF with each TLD response normalized to that for the ^{226}Ra source.

EXPERIMENTAL

Experimental data were obtained from two pilot field studies, denoted BAF II and BAF III. The field dosimeters contained the four TLD's of LiF, CaF_2 : Dy, CaF_2 : Dy in a 1-mm cadmium filter, and BaF_2 : Dy, all 0.9 by 3.2 by 3.2 mm. All TLD's were contained within a minimum of 400 mg/cm^2 of plastic tubing (Table 4), to provide electronic equilibrium and to eliminate most of the terrestrial beta radiation. Two to four chips of each detector type were included per dosimeter in a staggered spatial orientation to minimize errors due to angular dependence. These plastic tubes are wrapped in aluminum foil to provide a light shield and to maintain consistency in the thermal equilibrium between the field dosimeters.

The field studies included dosimeter placement in the environs of Argonne National Laboratory (ANL). The radiation field is considered to be natural at locations designated W, NW, and M, which are, respectively, an ANL west gate boundary, a northwest boundary, and a suburban backyard in Madison, Wis. The locations labeled CP + 200 and CP + 20 are at distances of about 200 and 20 m downwind from CP-5, an operating research reactor at ANL. The locations labeled lead are inside a lead pig with 7 cm of lead surrounding a ¼-in. steel annulus. The dosimeter labeled as being inside copper was further wrapped in about 1 mm of copper. The locations, G and Co, are near significant sources of radioactive waste and ^{60}Co, respectively. Both sources are shielded in the direction toward the dosimeter locations.

(Text continues on page 978)

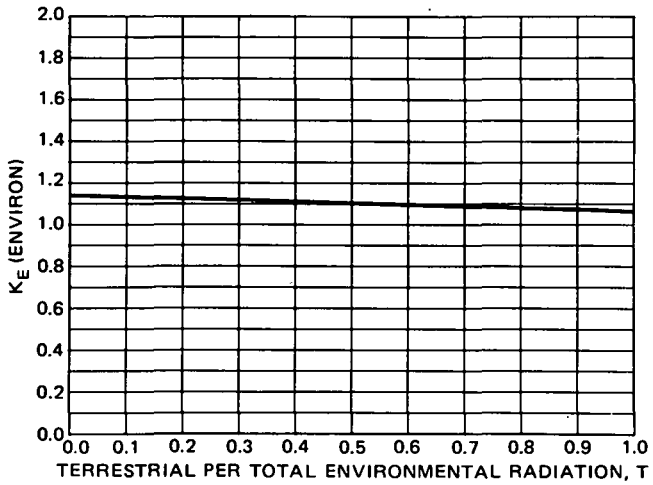


Fig. 3 Tissue-dose energy correction, K_E(ENVIRON), for LiF calibrated against ^{226}Ra, as a function of environmental gamma fraction of total natural background (gamma and cosmic) air dose.

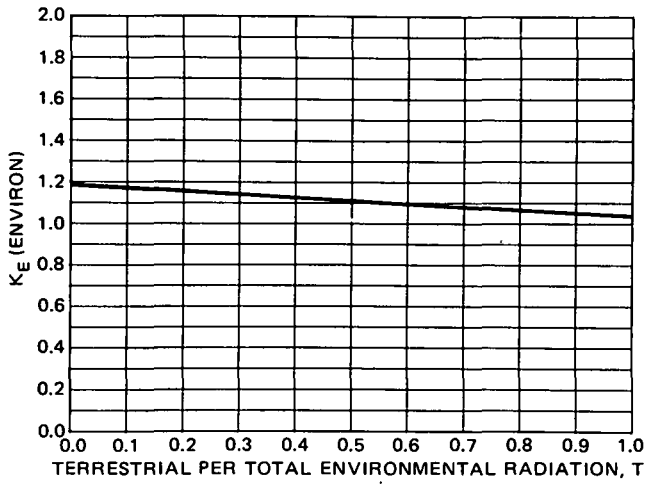


Fig. 4 Tissue-dose energy correction, K_E(ENVIRON), for CaF_2 in cadmium calibrated against ^{226}Ra, as a function of environmental gamma fraction of total natural background (gamma and cosmic) air dose.

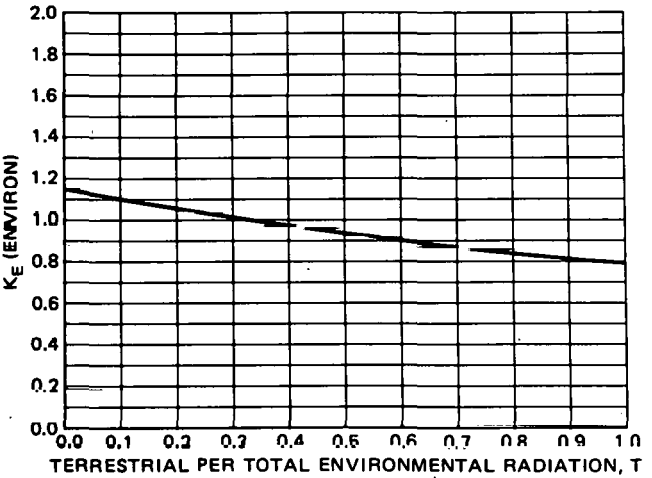


Fig. 5 Tissue-dose energy correction, K_E(ENVIRON), for CaF_2 calibrated against ^{226}Ra, as a function of environmental gamma fraction of total natural background (gamma and cosmic) air dose.

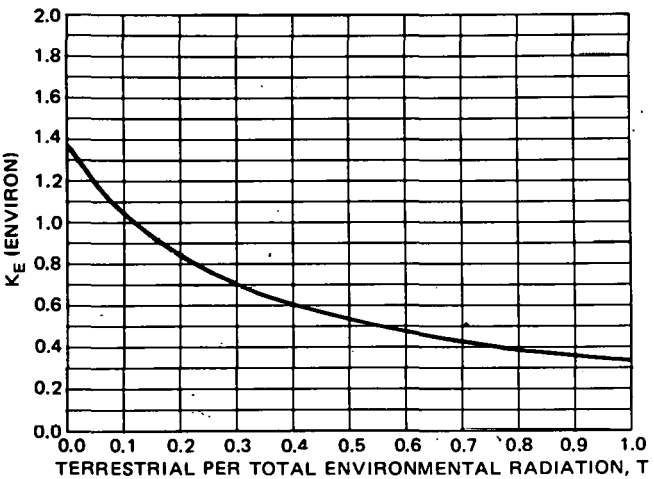


Fig. 6 Tissue-dose energy correction, K_E(ENVIRON), for BaF_2 calibrated against ^{226}Ra, as a function of environmental gamma fraction of total natural background (gamma and cosmic) air dose.

TABLE 3

Calculated Integral TLD Response Factors*

Material	Source		
	Environmental terrestrial	Environmental cosmic	^{226}Ra
LiF (no buildup)	0.93	0.84	0.93
(With buildup)	0.95		0.94
CaF_2 (no buildup)	1.29	0.90	1.00
(With buildup)	1.38		1.02
CaF_2 in cadmium (no buildup)	1.02	0.86	0.99
(With buildup)	1.03		1.00
BaF_2 (no buildup)	3.8	1.0	1.2
(With buildup)	4.3		1.35
Tissue (no buildup)	1.08	1.02	1.08

*The response factors to these sources are on a dose basis for the material relative to that for air. Buildup for the photon sources is considered in the plastic case and the TLD standard chip.

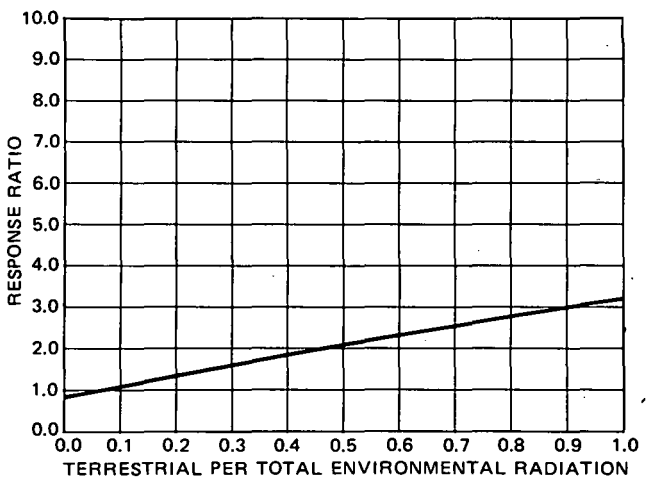


Fig. 7 Ratio of BaF_2 to LiF responses, each normalized to that for ^{226}Ra, as a function of the environmental gamma fraction of the natural background (gamma and cosmic) air dose.

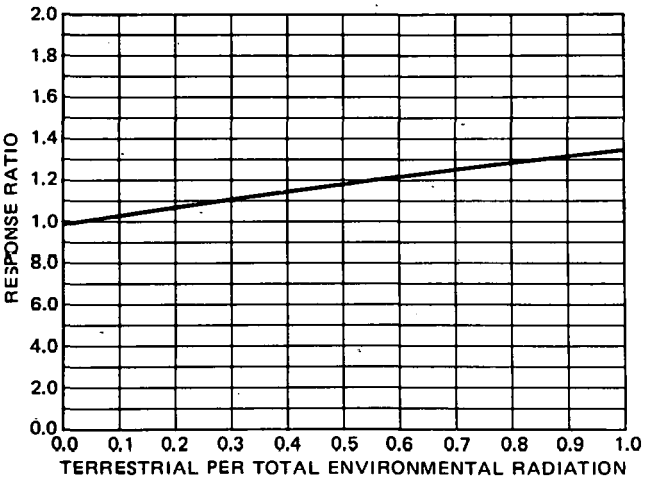


Fig. 8 Ratio of CaF_2 to LiF responses, each normalized to that for ^{226}Ra, as a function of the environmental gamma fraction of the natural background (gamma and cosmic) air dose.

TABLE 4

Summary for TLD Phosphors Used in This Study

Property	TLD		
	LiF	CaF_2 : Dy	BaF_2 : Dy
Specific gravity	2.7	3.12	4.7
Effective Z	8.1	16.4	51.6
Peak low energy response per response to ^{226}Ra	1.2	10	40
Main glow peak temperatures, °C	190	110, 180	110, 200
Dosimeter efficiency for ^{226}Ra exposure relative to LiF	1	17	5

Calibration dosing for the field studies was performed using a ^{226}Ra source. Each study involved two calibration dosings. The first dosing was for dosimeters that were placed in the field alongside undosed field dosimeters to determine the location-dependent fading of the TLD signal due to the calibration dose. Two dosimeters, identical to the field dosimeters but which had been retained in the laboratory during the field interval, were annealed and one was dosed

with the calibration source at a time 1 day before the field dosimeters were read out. These two dosimeters were carried to the field while collecting the field dosimeters and read out with the field dosimeters. Their readings yield the transit dose correction and the calibration factor for an unfaded TLD. "No fading" is defined as the read-out 24-hr postcalibration exposure, for practical convenience.

Several field fade studies, using LiF and CaF_2 : Dy, show that signal fading for a calibration-dosed TLD follows a nearly logarithmic decay with time. Assuming an ln(t) fit for the fading, it can be shown that the calibration factor appropriate for the average fade of the continuous field dosing over the field study interval is given by

$$K_{TLD,FIELD} = K(t_i) + \frac{[K(t_f) - K(t_i)]}{\ln(t_f)} \times \ln(t_m) \qquad (5)$$

where K = calibration factors in reader units per milliroentgens of ^{226}Ra

$K(t_i)$ = unfaded calibration factor (read-out at 24-hr postexposure)

$K(t_f)$ = read-out of the calibration-dosed TLD's that were in the field

t_f = total time of the field interval (in days)

t_m = half the total time = $t_f/2$ (in days)

Because the fading is very temperature dependent, the field sites were chosen in expectation of a nearly identical average temperature at each site over the field interval.

RESULTS

The results of the two field studies are presented in Tables 5 and 6 by TLD type and dosimeter location. The field values reported are in milliroentgens of ^{226}Ra per year. In Tables 7 and 8, the relative response of the TLD's at each location is presented for the two studies. As covered in the following discussion, the field data and TE correction are then combined to a tissue equivalent dose and normalized to an annual dose rate in Table 9.

DISCUSSION

Precision Considerations

The field results for LiF are precise (1σ) to about ±8%, limited in our reader by its relatively low light output. The results for CaF_2 and

TABLE 5

Field Results for "BAF II," In-field: Sept. 30, 1977 to Dec. 2, 1977*

Location†	TLD			
	LiF	CaF_2 : Dy in cadmium	CaF_2 : Dy	BaF_2 : Dy
W	62	69.2	86.9	276
NW	93	97.4	120	362
CP + 200	160	153	208	576
CP + 20	400	378	494	1390
G	640	640	1330	5620
Cobalt	280	260	502	1900
Lead	21	24.6	21.2	47
Lead (inside 1-mm copper)	21	23.1	19.4	43

*All results are fade corrected and normalized to a 1-year interval tabulated in units of milliroentgens of ^{226}Ra per year.

†The locations are described in the text.

TABLE 6

Field Results* for "BAF III," Infield: Dec. 3, 1977 to Jan. 21, 1978

Location†	TLD			
	LiF	CaF_2 : Dy in cadmium	CaF_2 : Dy	BaF_2 : Dy
W	59	59.8	81.9	204
NW	85	75.7	118	287
M	65	69.5	89.7	223
CP + 200	110	107	164	437
CP + 20	290	208	428	975
Lead	20	25.0	22.7	54.4

*Results are fade corrected and normalized to a 1-year interval tabulated in units of milliroentgens of ^{226}Ra per year.

†The locations are described in the text.

TABLE 7

Relative TLD Response in "BAF II"*

Location†	BaF_2/LiF	BaF_2/CaF_2(Cd)	CaF_2/LiF	CaF_2(Cd)/LiF
W	4.4	4.0	1.39	1.10
NW	3.9	3.7	1.35	1.04
CP + 200	3.8	3.75	1.36	1.00
CP + 20	3.5	3.7	1.23	0.94
G	8.75	8.8	2.07	1.00
Cobalt	6.8	7.3	1.8	0.94
Lead	2.3	1.9	1.02	1.18
Lead (inside 1-mm copper)	2.3	2.1	0.93	1.11

*Tabulated as ratios of the field results taken from Table 5.
†The locations are described in the text.

TABLE 8

Relative TLD Response in "BAF III"*

Location†	BaF_2/LiF	BaF_2/CaF_2(Cd)	CaF_2/LiF	CaF_2(Cd)/LiF
W	3.5	3.45	1.33	1.01
NW	3.4	3.7	1.34	0.89
M	3.4	3.2	1.38	1.07
CP + 200	3.9	4.1	1.5	0.96
CP + 20	3.35	3.5	1.5	0.96
Lead	2.7	2.2	1.15	1.27

*Tabulated as ratios of the field results taken from Table 6.
†The locations are described in the text.

TABLE 9

Tissue Dose Determined Using the Energy Correction to Different TLD's

Study, location	Tissue dose rate (mrads/year) determined with TLD				Mean ± 1σ(% σ/mean)
	LiF	CaF_2 in cadmium	CaF_2	BaF_2	
BAF II, W	57	62	57	72	62 ± 7(11%)
BAF II, NW	85	87	82	94	87 ± 5(6%)
BAF III, W	54	54	54	53	54 ± 0.5(1%)
BAF III, NW	78	68	77	75	75 ± 5(6%)
BAF III, M	59	63	59	58	60 ± 2(4%)

BaF_2 are limited only by the precision to which the chips have been sorted, about 3 to 4% in these cases. The fade correction is, however, more extensive for these TLD's and so their net field responses are precise to 5 to 6%.

Natural Radiation Environments

The locations that represent natural radiation environments, W, NW, and M, reflect the expected response trends between the TLD's. The readings of the CaF_2 in cadmium are comparable to those of the LiF dosimeters. The relative response of CaF_2/LiF is approximately constant (5% variation) with an average value of 1.35. The relative responses of BaF_2/LiF and BaF_2/(CaF_2 in cadmium) have mean values with a 5% uncertainty within either field study.

At these locations we expect that about 60 to 65% of the radiation field is due to the terrestrial source term (EPA, 1977). The calculated value for the relative response of two TLD's in that radiation field (Figs. 7 and 8) consistently underestimated the observed field values of relative response (Tables 7 and 8). Comparing these field values to Figs. 7 or 8, we expect a value for T in the range 1.0 to 1.1. Although inaccurate as the actual terrestrial component, this value of T is used to obtain a TE dose factor from Figs. 3 to 6. In this way the discrepancy between the dose model and observed values approximately cancel in the final dose determination.

A tentative explanation for the observed discrepancy is that the dose model cannot be accurately applied to the TLD in a radiation field when the TLD size is comparable to the range of the secondary electrons. In this case the TLD reading may be more directly related to the incident photon number fluence than to the dose rate. A preliminary examination has shown that calculations for tandem TLD response based on number fluence rather than dose are in good agreement with the field observations and that a reasonably accurate value of T is obtained.

The total field values reported in a location in BAF III (Table 6) are systematically lower than in a location in BAF II (Table 5). On a rough average, there was no snow cover during BAF II and about 10 to 12 in. of snow during BAF III. This latter cover could be 2 to 3 in. of water equivalent, depending on the average compaction of the fallen snow. A dose reduction would be expected owing to attenuation of primary terrestrial photons by the snow, as well as reducing radon release from the soil. The dose reduction should be larger for a high Z dosimeter responding preferentially to the lower energy photons. This is consistent with the relative responses and the

field data, where the BaF_2/LiF decreases about 20% and the BaF_2/(CaF_2 in cadmium) decreases about 8% from BAF II to BAF III, at the locations of natural radiation, W and NW.

Near Man-Made Sources

The field results taken near the ANL research reactor, CP-5, at locations CP + 200 and CP + 20 show penetrating radiation dose increased above the natural background. The relative readings for BaF_2/LiF and BaF_2/(CaF_2 in cadmium) are fairly constant between field studies, indicating a constant radiation quality. The relative response values near the reactor are not unusual enough to distinguish an energy spectrum different from that of the natural radiation locations. The dosimeters in BAF II, used near the heavily shielded radioactive sources (G and Co), show a response pattern that reflects lower energy photons introduced by Compton interactions in the shielding material and produces a dramatic overresponse in both the CaF_2 and the BaF_2.

In the Lead Shield

The response within the lead shield of BaF_2 relative to CaF_2 in cadmium or to LiF is larger than expected, and this fact and the attenuation of dose in the dosimeters inside copper foil (400 mg/cm^2) indicate a substantial low energy photon component in the lead shield. The increase in CaF_2 response behind the cadmium may be due to bremsstrahlung production in the high Z element, cadmium. The average reading of the low Z dosimeters, about 22 mR of ^{226}Ra per year, requires a correction factor of 1.4 to obtain the ionizing component of the cosmic tissue dose rate, 30 mrems/year, expected in this region (NCRP, 1975).

Tissue Dose Correction

Table 9 gives the tissue dose after the TE energy correction is applied to each of the TLD's field responses. The mean tissue dose between the detectors per location has one sigma deviation from 1% to 11%.

If we consider a human phantom represented by a 30-cm-thick slab of tissue, after O'Brien (1972), the path length through the material is large enough to significantly attenuate the incident photons as well as to introduce a large dose contribution due to scatter. The calculations for tissue response from the literature include calculations of tissue dose due to terrestrial gamma photons (Spiers and Overton, 1962; Jones, 1966; Bennett, 1970; O'Brien and Sanna,

1976, 1978) and application to TLD monitoring (Kramer, Regulla, and Drexler, 1977). The studies yield a value for the average depth dose in tissue per exposure to terrestrial radiation ranging from 0.6 (O'Brien and Sanna, 1976) to 0.8 (Bennett, 1970). Our own simplified calculations in a 30-cm tissue slab yield the factor 0.81 as the average tissue depth dose per air dose. This is consistent with the fraction 0.71 for average tissue depth dose per exposure. With the consideration for self-shielding of the terrestrial radiation, the final values obtained are in close agreement with expectations from the recent calculations of tissue dose due to the natural terrestrial radiation (O'Brien and Sanna, 1978).

APPLICATION

A tandem TLD dosimeter can be used with the flat energy response TLD to approximate the tissue dose, and the high Z unfiltered TLD can be used to improve statistical reliability in detecting small changes in exposure in the environment. It can easily be shown that for BaF_2, which is four times more sensitive to the terrestrial source than LiF, the response increase provides a dramatic improvement in the confidence level for detection of a statistically significant dose increment. This issue will be investigated in future studies for possible application to nuclear facility monitoring by the Radiologic Health Section of the California Department of Health Services.

SUMMARY

Dose response for several TLD's and tissue was calculated to the environmental, terrestrial, cosmic, and ^{226}Ra calibration source terms. Calculations were applied to TLD field data to quantify a measure of environmental radiation quality and a tissue dose. The simple dose response model underestimated the observed relative response for two tandem TLD's.

The unattenuated tissue equivalent dose (mrad) conversion from a ^{226}Ra calibration exposure (mR) at a natural radiation field of 60% terrestrial air dose is about 0.96 for LiF or CaF_2 in cadmium, 0.75 for CaF_2, and about 0.3 for BaF_2. The terrestrial source contribution to total environmental radiation dose in the United States ranges from 25 to 66%. Over this range the TE correction factors to maximum tissue dose for LiF, CaF_2 in cadmium, CaF_2, and BaF_2 vary by 2, 7, 17, and about 100%, respectively. Several man-made radiation fields were identified by unique ratios of the relative response of tandem TLD's.

ACKNOWLEDGMENTS

I thank Jacob Sedlet at Argonne for his helpful and encouraging discussions and for making this study possible through the Argonne Center for Educational Affairs. At the Medical Physics Division, University of Wisconsin, my thanks to Paul DeLuca, Jr., for his helpful criticism of the manuscript and to J. R. Cameron and F. H. Attix for their continual support and helpful discussions.

REFERENCES

Adams, J. A. S., W. M. Lowder, and T. F. Gesell (Eds.), 1975, *The Natural Radiation Environment II*, Vols. 1 and 2, Symposium Proceedings, Houston, Tex., Aug. 7—11, 1972, ERDA Report CONF-720805-P1,P2, Rice University and the University of Texas, Houston, NTIS.

ANSI N545, 1975, *Performance, Testing, and Procedural Specifications for Thermoluminescent Dosimetry (Environmental Applications)*, American National Standards Institute, Inc., New York.

Attix, F. H., W. C. Roesch, and E. Tochelin, 1968, *Radiation Dosimetry*, Vols. I and III, Academic Press, New York.

Beck, H. L., 1975, The Physics of Environmental Radiation Fields, in *The Natural Radiation Environment II*, Vol. 1, Symposium Proceedings, Houston, Tex., Aug. 7—11, 1972, J. A. S. Adams, W. M. Lowder, and T. F. Gesell (Eds.), ERDA Report CONF-720805-P1, pp. 101-133, Rice University and the University of Texas, Houston, NTIS.

——, J. A. DeCampo, C. V. Gogolak, 1972, *In Situ Ge(Li) and NaI(Tl) Gamma-Ray Spectroscopy*, USAEC Report HASL-258, Health and Safety Laboratory.

Bennett, Burton G., 1970, Estimation of Gonadal Absorbed Dose Due to Environmental Gamma Radiation, *Health Phys.*, 19: 757-767.

Bertel, E., and L. Pages, 1971, *Evaluation of Stopping Power and Range of Charged Particles of 10 MeV to 30 GeV in Matter*, Report CEA-R-4198, Commissariat à l'Énergie Atomique, Fontenay-aux-Roses, France.

Brini, D., V. Ciriegi, F. Fuligni, and E. Moretti, 1967, Low Energy Cosmic-Ray Photons in Atmosphere, *J. Geophys. Res.*, 72(3): 903-913.

Burke, G. deP., 1976, Thermoluminescent Dosimetry: Environmental Monitoring Near Nuclear Reactor Sites, *IEEE Trans. Nucl. Sci.*, NS-23(3): 1224-1226.

De Planque, G., 1979, Evaluation of Methods for the Determination of X- and Gamma-Ray Exposure Attributable to a Nuclear Facility Using Environmental TLD Measurements, USDOE Report EML-355 (NUREG/CR-0711), Environmental Measurements Laboratory.

EPA, 1977, *Radiological Quality of the Environment in the United States, 1977*, Report EPA 520/1-77-009, Environmental Protection Agency, Washington, D. C.

ERDA, 1976, 1977, *Environmental Monitoring at Major U. S. Energy Research and Development Administration Contractor Sites: Calendar Year 1975*, ERDA Report ERDA-76-104 (2 vols.); *Calendar Year 1976*, ERDA Report ERDA-77-104 (2 vols.), Energy Research and Development Administration.

Hubbell, J. H., 1969, *Photon Cross Sections, Attenuation Coefficients and Energy Absorption Coefficients from 10 keV to 100 GeV*, Report NSRDS-NBS 29, U. S. National Bureau of Standards, Washington, D. C., GPO.

Jones, A. R., 1966, Proposed Calibration Factors for Various Dosimeters at Different Energies, *Health Phys.*, 12: 663-671.

Kramer, R., D. F. Regulla, and G. Drexler, 1977, Thermoluminescent Dosimetry Radiation Monitoring: Processing Experiences and Data Interpretation, in *Proceedings of the Fifth International Conference on Thermoluminescent Dosimetry*, São Paulo, Brazil, Feb. 14—17, 1977, pp. 298-312, Justus-Liebig Universität, Giessen, Germany (BRD)

Lowder, W. M., 1969, *Low-Energy Atmospheric Gamma Radiation as a Measure of Cosmic-Ray Secondary Flux*, USAEC Report HASL-209, Health and Safety Laboratory.

——, 1976, Basic Aspects of Environmental Radiation Measurement, in *Proceedings of the Health Physics Society 10th Midyear Topical Symposium on Natural Radioactivity in Man's Environment*, Oct. 11—13, 1976, Saratoga Springs, N. Y., Rensselaer Polytechnic Institute, Troy, N. Y.

——, and G. deP. Burke, 1977, *The Response of LiF TLD to Natural Environmental Radiation*, ERDA Report HASL-313, Health and Safety Laboratory.

Minato, S., 1977, A Simple Analytical Approximation for the Spectral Distribution of Natural Gamma Radiation Flux, *Health Phys.*, 33: 205-211.

NCRP, 1975, *Natural Background Radiation in the United States*, NCRP Report No. 45, National Council on Radiation Protection and Measurements, Washington, D. C.

NCRP, 1976, *Environmental Radiation Measurements*, NCRP Report No. 50, National Council on Radiation Protection and Measurements, Washington, D. C.

O'Brien, K., 1975, The Cosmic-Ray Field at Ground Level, in *The Natural Radiation Environment II*, Vol. 1, Symposium Proceedings, Houston, Tex., Aug. 7—11, 1972, J. A. S. Adams, W. M. Lowder, and T. F. Gesell (Eds.), ERDA Report CONF-720805-P1, pp. 15-54, Rice University and the University of Texas, Houston, NTIS.

——, and R. Sanna, 1976, The Distribution of Absorbed Dose Rates in Humans from Exposure to Environmental Gamma Rays, *Health Phys.*, 30(1): 71-78.

——, and R. Sanna, 1978, The Effect of the Male—Female Body Size Difference on Absorbed Dose-Rate Distributions in Humans from Natural Gamma Rays, *Health Phys.*, 34(1): 107-109.

Peterson, L. E., 1963, The 0.5 MeV Gamma Ray and the Low Energy Gamma-Ray Spectrum to 6 g/cm^2 over Minneapolis, *J. Geophys. Res.*, 68(4): 979-987.

Spiers, F. W., and T. R. Overton, 1962, Attenuation Factors for Certain Tissues When the Body Is Exposed to Nearly Omni-Directional Gamma Radiation, *Phys. Med. Biol*, 7: 35-43.

UNSCEAR, 1972, Ionizing Radiation: Levels and Effects, Report of the United Nations Scientific Committee on the Effects of Atomic Radiation, United Nations, New York.

——, 1977, Sources and Effects of Ionizing Radiation, Report to the General Assembly of the United Nations Scientific Committee on the Effects of Atomic Radiation, United Nations, New York.

TLD Measurements and Model Calculations of Environmental Radiation Exposure Rates

GAIL de PLANQUE
Environmental Measurements Laboratory, U. S. Department of Energy,
New York, New York

ABSTRACT

Measurements of mean monthly outdoor exposure rates from gamma and cosmic radiation are given for a 5-year period, October 1971 through September 1976, at five residential sites within 50 km of New York City. The measurements were made with thermoluminescence dosimeters, LiF (TLD-700) chips, 3.2 X 3.2 X 0.9 mm. Average monthly exposure rates at these sites range from 6.8 to 8.2 μR/hr, with a mean of 7.5 μR/hr. Monthly variations are about 0.5 μR/hr (root mean square deviation). The average annual exposure for the five sites was 66 mR, with a range over the 5 years of 3 to 5 mR.

Most of the observed monthly variations are attributable to fluctuations in that part of the exposure rate due to gamma radiation (naturally occurring radionuclides as well as fallout) from the ground. Variations occur because changes in the soil-moisture balance affect the density of the soil-water medium and because the variable amounts of water on the surface act as a shield with respect to radiation originating in the ground. The results of a model designed to reflect the monthly exposure rate variations due to changes in the soil-moisture balance are compared with the measurements.

Studies of the composition of the environmental radiation field and of its geographical variations have been described in the symposiums on natural radiation environment (Adams and Lowder, 1964; Adams, Lowder, and Gesell, 1975). However, not as much work has been done on the variation of environmental radiation exposure rates over long periods of time. Yet studies, such as that reported by Burch et al. (1964), contribute to verifying the physical factors affecting

these variations and establishing baseline data from which human disturbances of the radiation environment may be assessed. A practical example of the need for such studies arises from the growth of the nuclear power industry. In this case, methods must be developed for isolating any perturbations of the radiation environment imposed by the operation of the facility.

In response to these needs, a project was initiated in 1971 with LiF thermoluminescence dosimeters to measure mean outdoor natural environmental radiation exposure rates on a monthly basis at several homes within 50 km of New York City. These sites are unaffected by man-made radiation sources except for global fallout from atmospheric nuclear testing. The goals of this project were to accumulate data and evaluate the performance of TLDs for studying the long-term variations of natural environmental radiation levels. Preliminary results of this study have been reported (Burke, 1975; 1975). In this paper we describe the time variations over a 5-year period and a model for estimating these variations.

TLD MEASUREMENTS

The TLD System used for the study consists of a reader designed and constructed at the Environmental Measurements Laboratory and dosimeters composed of five LiF chips (TLD-700), 0.32 by 0.32 by 0.09 cm, encased in a light-tight Lucite holder providing a thickness of about 370 mg/cm^2 surrounding the chips. The system itself and the procedures followed are described in detail in the laboratory's procedures manual (Harley, 1972).

Histories are maintained on every chip, and a batch calibration is performed with every readout. This system has been tested for compliance with the ANSI Standard (American National Standards Institute, 1975) for environmental applications of TLDs and has performed well in the two International Intercomparisons for environmental integrating dosimeters (Gesell, Burke, and Becker, 1976, and Burke, Gesell, and Becker, 1976).

The uncertainty of a single measurement, estimated using the scheme delineated by Burke and Gesell (1976) varies somewhat with each measurement but should be less than 7%. The precision of a single measurement (the average exposure determined from five chips) is estimated to be within ±3%. This factor is of primary concern for measurements of time variations made with a single system since systematic biases have no influence.

The average monthly exposure rates* measured at five homes from October 1971 through September 1976 are shown in Fig. 1. To simplify the figure an average error bar, representing the 3% precision uncertainty, is shown only once in the legend. The data suggest seasonal trends, the rates being high in the summer and low in the winter, with obvious decreases in exposure rate in the midwinter months due to snow cover.

The average annual exposure rates (average of the 12 monthly exposure rates) are designated by the solid lines in Fig. 2. In this case, assuming each measurement is independent, the precision of the yearly averages should be within ±1%. The yearly averages of monthly LiF measurements made in the TLD lead (9.5 cm thick) storage facility are shown for comparison.

Table 1 shows the variations observed over different time periods. The root mean square (rms) deviations for the monthly measurements in a single year range from about 0.3 to 0.6 μR/hr. For the entire 5-year period, the rms deviations for the monthly measurements are about 0.45 μR/hr for all five sites. The yearly exposure rates show smaller variations over the 5-year period with rms deviations of 0.11 to 0.22 μR/hr. The ranges of the yearly values run from 0.33 to 0.59 μR/hr. This represents a range in the total (gamma plus cosmic) average yearly exposures of approximately 4 to 7%, roughly 3 to 5 mR at a site with a yearly exposure of 66 mR (i.e., an average hourly rate of 7.5 μR/hr), and corresponds to a range in the yearly gamma exposures of about 7 to 14%. The expected standard deviation due to precision of measurement at a site with an average hourly rate of 7.5 μR/hr is about 0.2 μR/hr for the monthly values and that for the yearly values is less than 0.1 μR/hr. The standard deviation of the yearly averages for TLDs in the storage shield is 1.7%, somewhat larger than that expected from just measurement error. However, each of these measurements is made at the 1-mR level at which precision is not quite as good as at 5 mR, the approximate monthly exposure level at the residential sites.

FACTORS CONTRIBUTING TO THE MONTHLY EXPOSURE RATE VARIATIONS

To evaluate the observed exposure rate variations, we must take into account the composition of the radiation field incident upon the

*Exposure (rate) is used because the TLDs were calibrated using a ^{137}Cs source. The results are expressed in terms of the ^{137}Cs exposure required to produce an identical response from the TLD. The problems associated with applying a ^{137}Cs calibration to cosmic-ray and terrestrial gamma-ray exposures are discussed by Lowder and de Planque (1977).

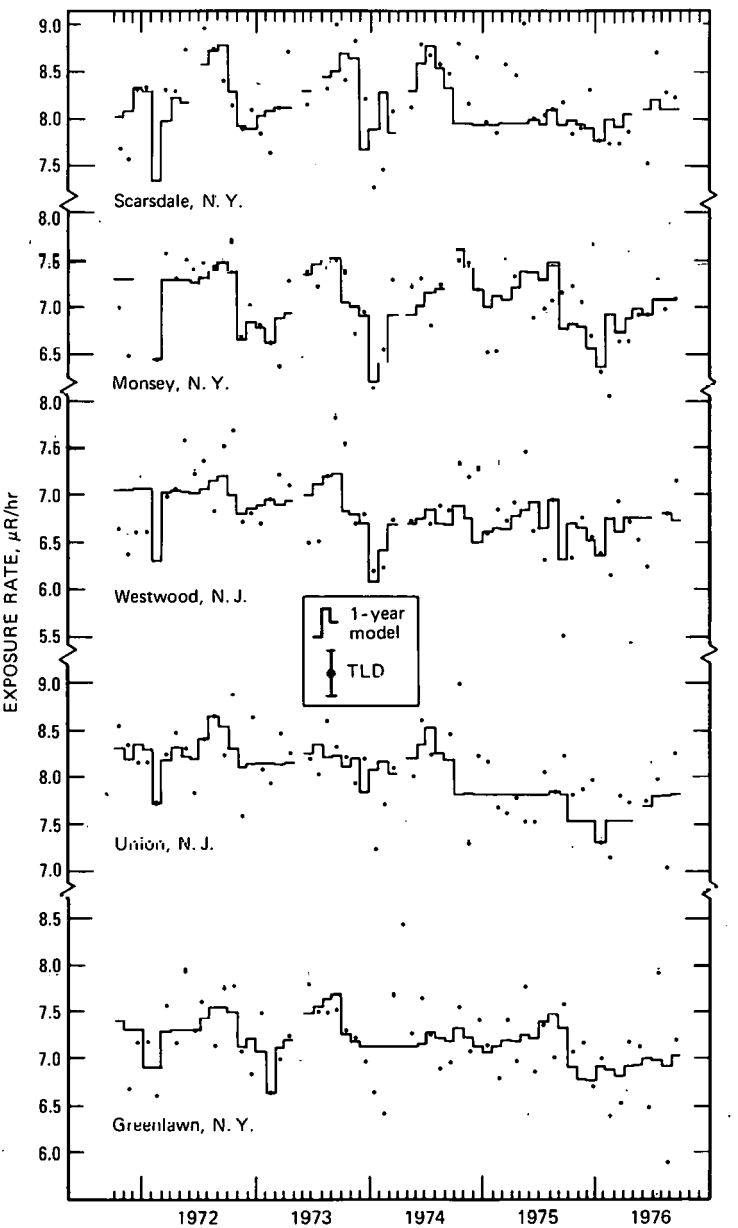


Fig. 1 Comparison of mean monthly outdoor exposure rates determined via the model (Eq. 1) with LiF TLD measurements at homes near New York City. ⎍, 1-year model; ⎀, TLD.

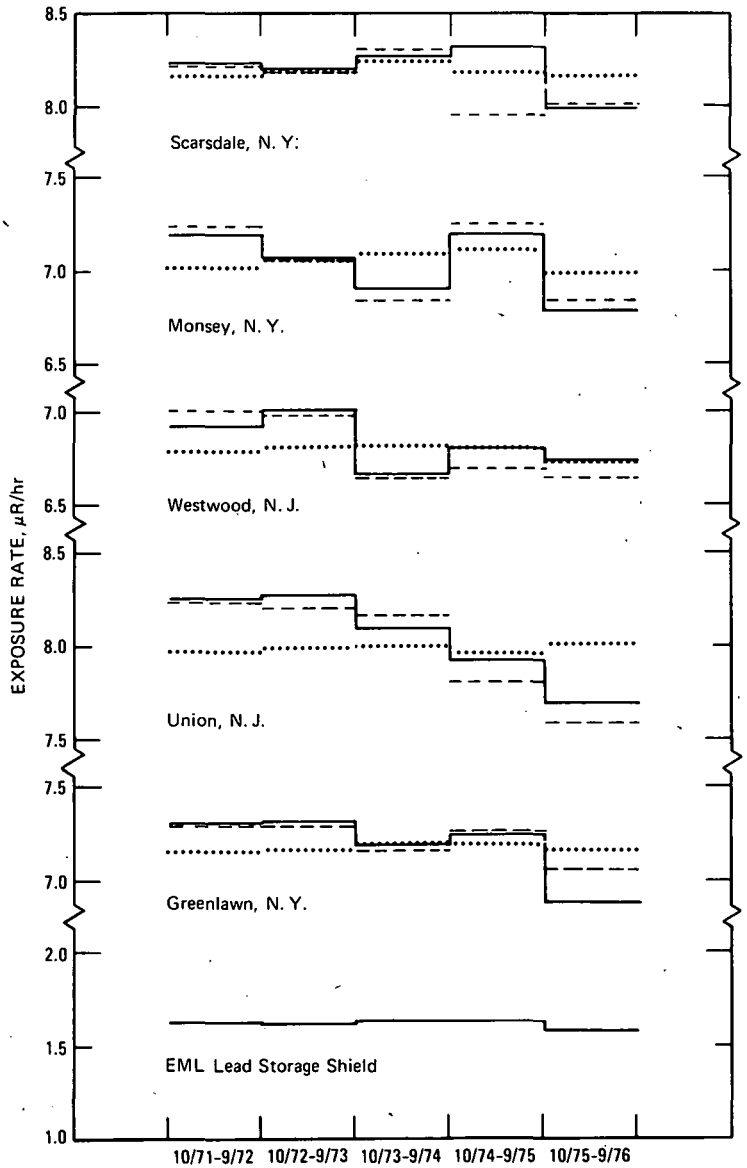


Fig. 2 Comparison of mean annual outdoor exposure rates determined via the model (Eq. 1) applied to the 5-year period and to individual yearly segments with LiF TLD measurements at homes near New York City. ——, TLD; · · ·, 5-year model: — — —, 1-year model.

TABLE 1

Variations in Measured (TLD) Monthly Exposure Rates

Location	Average monthly exposure rates, μR/hr	Root mean square deviation* of monthly exposure rates, μR/hr						Root mean square deviation of yearly exposure rates μR/hr	Range of average yearly exposure rates, μR/hr
	10/71—9/76	10/71—9/72	10/72—9/73	10/73—9/74	10/74—9/75	10/75—9/76	10/71—9/76		
Scarsdale, N. Y.	8.19	0.52	0.41	0.51	0.37	0.35	0.44	0.11	0.33
Monsey, N. Y.	7.04	0.43	0.42	0.47	0.44	0.37	0.44	0.16	0.39
Westwood, N. J.	6.80	0.44	0.45	0.58	0.55	0.31	0.49	0.16	0.43
Union, N. J.	8.05	0.28	0.35	0.37	0.46	0.38	0.43	0.22	0.59
Greenlawn, N. Y.	7.18	0.39	0.38	0.61	0.31	0.53	0.47	0.16	0.42

*Root mean square deviation = $\left[\frac{\sum_{i=1}^{n} (x_i - \bar{x})^2}{n}\right]^{1/2}$

detector. At these residential sites the radiation field interacting with the TLD arises from cosmic radiation, terrestrial gamma radiation from naturally occurring radionuclides in the ground and air, and gamma radiation from fallout.

Terrestrial gamma radiation in the ground arises from the naturally occurring isotopes of uranium, potassium, and thorium as well as from fallout already distributed in the ground. The former can generally be considered to be uniformly distributed with depth, whereas the latter more closely approximates an exponential distribution. Spectrometer measurements made at one of the sites indicates that the exposure rate from fallout already distributed in the ground is less than 0.5 μR/hr, a value that agrees with what is considered to be typical for the continental United States (NCRP, 1976).

The component of the total exposure rate due to gamma radiation in the ground varies with time mainly because of seasonal variations in the soil-moisture balance. Calculations by Beck and de Planque (1968) show that one of the largest factors affecting fluctuations of exposure rate due to distributed gamma-ray sources in the ground is the variation in the density of the soil-water medium, which depends on the amount of water present. For a uniformly distributed source, which the naturally occurring radionuclides closely approximate, a percentage increase in density results in the same percentage decrease in the exposure in air and vice versa since changing the density by some factor is equivalent to changing the source intensity in the mean free path interval by this same factor. In addition, the exposure rate is affected by water (or snow) standing on the top of the ground and acting as a shield with respect to the radiation originating in the ground.

Concentrations of radon in the air, emanating from the natural sources in the ground, have been shown by Cox, Blanchard, and Kahn (1970) to vary directly with atmospheric stability and inversely with soil moisture. However, the effect of changes in both atmospheric and ground radon concentrations on actual exposure rate is complicated (Beck et al., 1966; NCRP, 1976). Migration of radon from the ground to the atmosphere redistributes the source, and any change in the exposure rate from radon and radon daughters depends on meteorological factors (Beck, 1974). However, the variations in exposure rates from radon and radon daughters, particularly when averaged over monthly periods, are most likely significantly less than the variations due to the effects of soil-moisture fluctuations on the terrestrial gamma-ray component.

Nevertheless, further study of long-term exposure-rate fluctuations attributable to radon variations is needed.

Cosmic-ray levels vary with time according to atmospheric temperature, pressure, and the 11-year solar cycle, however, the variations during the 5-year period studied are considered minimal (O'Brien, 1978). This is substantiated by the TLD measurements in the lead storage shield shown in Fig. 2 since these measurements reflect only radioactivity in the shield itself and the hard component of cosmic radiation. The monthly variations are consistent, within the expected precision, with a constant exposure rate from the cosmic-ray component and indicate that this component is probably not a major contributor to the observed variations.

Some fallout, mainly from atmospheric nuclear tests in China, has occurred during the 5-year measurement period. The amounts have been relatively small and probably can be neglected, at least to a first approximation, as a source of monthly exposure-rate variations. However, this perturbation will be discussed later. A more detailed discussion of all these time variations is given in NCRP No. 50 (1976).

Thus it appears that the monthly variations observed at the residential sites are likely to be due mainly to changes in the exposure-rate contributions of gamma radiation from radionuclides in the ground as affected by seasonal fluctuations in the soil-moisture balance.

MODEL

On the basis of the above assumption, a model was developed to reflect the measured variations (Burke and O'Brien, 1974). The measured exposure rates, after the subtraction of 3.7 μR/hr attributable to the cosmic-ray component of the field, were assumed to depend primarily on the density changes of the soil-water medium and the shielding effects of surface water (rain or snow) according to the following equation:

$$\dot{X}(t) = \frac{E}{2\rho(t)} \exp - \left\{ \frac{[h_w(t)d_w + h_s(t)d_s]}{\lambda} \right\} \qquad (1)$$

where $\dot{X}(t)$ = average gamma exposure rate in μR/hr for time t

E = effective source term and equals the gamma-ray energy emitted per cubic centimeter of soil per second multiplied by a conversion factor (1.6×10^{-6} ergs/MeV) x (R g/86.9 ergs) x (3600 sec/hr) x ($10^6 \mu$R/R)

$\rho(t)$ = density of the soil-water medium in grams/cubic centi-

meter for time t and is dependent on the average amount of water stored in the soil during time t

h_w = height of surplus water in centimeters available as standing water above the soil for time t

h_s = height of snow, expressed in equivalent centimeters of water, available as standing water above the soil for time t

d_w = factor that modifies $h_w(t)$ to yield that part of the surplus water which can be considered to be the average amount of water actually remaining on the surface during time t

d_s = factor that modifies $h_s(t)$ to yield that part of snow in equivalent centimeters of water which can be considered to be the average amount actually remaining on the surface during time t

λ = relaxation length in water, determined to be 13 cm from transport calculations by Beck, DeCampo, and Gogolak (1972)

Three of the parameters, ρ, h_w, and h_s, depend on the climate and the soil-moisture balance at each site as a function of time. The density of the soil-water medium, ρ, is determined from the component densities: the density of the dry soil itself, which is assumed to be constant with time, and the mass of the water in the soil per unit volume (down to the bottom of the root depth zone) which varies with time. The amount of water stored within the soil-water medium as well as the amount of surplus water (h_w or h_s), i.e., that on the surface available for evaporation, runoff or penetration below the root depth zone, are determined by the balance between precipitation and evapotranspiration. This balance is affected primarily by the type of soil and vegetation, the water-holding capacity of the soil, the number of hours of sunlight, and the temperature. Thornthwaite and Mather (1957) developed a model based on these parameters for calculating water storage and surplus-water values. A computer code was written to calculate these quantities by the method of Thornthwaite and Mather. The operation of this code for a particular site requires the determination of the soil-water holding capacity and the input of monthly temperature, precipitation, and solar radiation data. This is discussed in detail by Burke and Marcin (1974).

After computing ρ, h_w, and h_s for the time periods of interest, Eq. 1 was used to determine E, d_w, and d_s for a particular site by correlating the density and surplus-water values with the exposure-rate data by an iterative process. The fitting process exploits the fact

that there are three different regimes. When the stored water is less than the water-holding capacity there is no surplus, in which case

$$\dot{X}(t) = \frac{E}{2\rho(t)} \tag{1a}$$

and E can be determined. This generally occurs in the summer when the soil tends to dry out due to lack of rain, enhanced evapotranspiration, and increased demand for water by vegetation. When there is surplus in the form of snow, the assumption is made that the water-holding capacity has been reached (a reasonable assumption for the New York area) and that there is no surplus in the form of water. Then

$$\dot{X}(t) = \frac{E}{2\rho(t)} \exp -\left[\frac{d_s h_s(t)}{\lambda}\right] \tag{1b}$$

and d_s can be determined. Analogously, when there is surplus water

$$\dot{X}(t) = \frac{E}{2\rho(t)} \exp -\left[\frac{d_w h_w(t)}{\lambda}\right] \tag{1c}$$

The data are divided into three groups corresponding to the three parts of Eq. 1. First, those data for which there is no surplus are collected and E is calculated for each of these periods using Eq. 1a and then averaged. Next, the data for which there is surplus in the form of snow are collected. The value of d_s is determined by stepping d_s from 0 in increments of 0.001 to the possible maximum of unity. Corresponding to each trial d_s, trial values of $\dot{X}$ are calculated and compared with the experimental values of $\dot{X}$. That value of d_s is chosen which yields the minimum variance.

Last, the value of d_w is stepped from 0 in increments of 0.001 to the possible maximum of 1. The variance is calculated as before, except that it is not restricted to cases of surplus water only. All measured and calculated exposures are used in forming the variance from which the minimum variance is determined, and from which the value of d_w is chosen.

DISCUSSION

The model was applied at each site in two ways. It was first tested against the data for each of the 5 separate yearly intervals (October through September), and then against the data for the entire 5-year period. The histograms in Fig. 1 show the monthly values generated by the model as applied to yearly segments of the

data. As shown in Table 2, the fit is reasonably good. These rms deviations can be directly compared with those in Table 1 in the sense that the values in Table 1 represent an analogous evaluation assuming the average yearly exposure rates are used for comparison with each monthly exposure rate instead of the values determined via the model. In most cases the fit is better using the model, although the differences are small especially when the 5-year period is considered. This difference will be discussed again in the following paragraphs.

One difficulty of the model is that of correctly accounting for snow cover. The problem arises in the handling of the climatic data rather than in the radiological model itself. In its present form the climatic portion of the model determines whether surplus water is really water as opposed to snow simply from the mean temperature of the period. Although this is a highly practical method, it does not account for a situation wherein snow cover exists for most of a period but the average temperature is raised above 0°C by a brief hot spell during the period. In this case the surplus is erroneously considered to be water by the model and the average amount on the surface for the month is governed by d_w rather than d_s, the two usually being quite different since the runoff properties tend to differ. An example of this can be seen in January and February of 1974. At Monsey, N. Y., and Westwood, N. J., where the mean monthly temperature was less than 0°C, the water surplus was regarded as snow. In fact there was extensive snow cover at all sites throughout much of the 2 months. However, at Scarsdale, N. Y., Union, N. J., and Greenlawn, N. Y., the monthly temperatures were just over 0°C and the surplus was considered to be water. Yet the measurements at these locations are quite low, reflecting the effects of the snow cover. To improve the situation, either a more sophisticated model is required for determining the nature of the surplus, e.g., analysis of climatic data on a daily basis, or more accurate input, actual snow depths in water equivalent, could be used. Unfortunately this parameter is not usually available. However, such a refinement might be advisable where monthly estimates rather than yearly averages are desired, e.g., if such a model were to be used in the interpretation of monthly TLD data at a nuclear facility (Burke, 1976).

A second difficulty is that of having a sufficiently long dry period to determine the source term, E, with good precision. This is shown by the model values during the fourth yearly period at Union and Scarsdale for which only 1 and 2 months of data, respectively, were available for determining E. One of the assumptions of the

TABLE 2

Comparison of Estimated (Model) and Measured (TLD) Monthly Exposure Rates

	Root mean square deviation* of the fit, μR/hr					
	1-year model					5-year model
Location	10/71—9/72	10/72—9/73	10/73—9/74	10/74—9/75	10/75—9/76	10/71—9/76
Scarsdale, N. Y.	0.33	0.33	0.41	0.54	0.31	0.38
Monsey, N. Y.	0.33	0.24	0.26	0.39	0.32	0.37
Westwood, N. J.	0.39	0.41	0.56	0.47	0.33	0.46
Union, N. J.	0.18	0.36	0.38	0.48	0.39	0.43
Greenlawn, N. Y.	0.35	0.24	0.62	0.31	0.52	0.46

*Root mean square deviation = $\left[\frac{\sum_{i=1}^{n} (x_{i\,calc.} - x_{i\,meas.})^2}{n}\right]^{1/2}$

model is that the exposure rates during these dry months will be higher than during the months with surplus water or snow. If this is not the case, as might happen due to the combination of measurement fluctuations and a small number of measurements, then any higher exposure rate can never be matched with the model. By the same token, when this situation forces the choice of the minimum value for d_w (maximum runoff), smaller values will not be calculated during periods of surplus water and the result is a relatively constant exposure rate value for the entire period. This difficulty can be avoided by obtaining measurements with higher precision or more frequent measurements during these periods.

Figure 2 shows the yearly averages determined from the monthly values obtained with the model analyzed for each year as well as for the entire 5-year period. A striking difference can be seen between the two sets of results. The 5-year model shows very little structure, whereas the yearly models indicate a structure that corresponds to the changes in the measured values. The 5-year-model values are close to the mean measured exposure rates and hence the rms deviations for this comparison (Table 2) are similar to those for the monthly measurements over the 5-year period (Table 1). This is not the case for individual years where the model values provide a slightly better fit to the monthly measurements than does the mean measured exposure rate, as evaluated by the rms deviation. An examination of the model parameters revealed that the values of d_w and d_s differed very little from year to year at each site, yet there were differences in rain and snowfall (h_w and h_s). The trends exhibited in the annual exposure rates generally tend to reflect these gross climatic variations to a certain extent. The third and fifth yearly segments were characterized by significantly more snow cover than were the other 3 years. As a result, the lower exposure rates for the winter months influence the overall yearly averages. However, when the yearly averages of the measured values are recalculated excluding the months December through March, a slight trend toward gradually decreasing exposure rates becomes evident, with the range being about 0.5 μR/hr.

The model does show significant differences in the annual values of the source term, E, with the pattern tracking the trends indicated by the measurements. Since climatic variations should not affect the source term per se, the other possible time variations discussed earlier must be reconsidered, either individually or in combination, in looking for the cause.

On the basis of the available data, it still seems unlikely that variations in cosmic radiation are responsible for more than a small

part of the observed annual variations. Also, as indicated earlier, annual changes due to variations in the exposure rate from radon and radon daughters are probably negligible, but further information is needed. Another possibility is the influence of the maturation of vegetation as well as man-made changes in the soil (addition of topsoil, etc.). These effects are difficult to determine and are not decipherable from the data at hand. Finally, variations in the fallout component should be considered. A gradual decline in this component is expected as the fallout that has been present for some time, mainly ^{137}Cs, slowly decays, erodes, and leaches further into the ground. Since the total exposure rate from deposited ^{137}Cs is less than 0.5 μR/hr in the area of the residences, this decline appears to be small and the component can increase as new fallout occurs. The deposition patterns (Environmental Quarterly, 1977) during the 5-year period show that additional ^{137}Cs has provided a negligible contribution, but a variation in shorter-lived ^{95}Zr—^{95}Nb depositions was such that a variation on the order of 0.2 μR/hr in annual average exposure rate is possible. The observed gradual decline in the annual residential exposure rates over the 5 years and an increase in those rates following the Sept. 26, 1976, Chinese nuclear test, from which measurable fallout resulted, suggest the possible effects of this component. Field spectrometry (Beck, DeCampo, and Gogolak, 1972; Harley, 1976) indicated that the exposure rate varied from less than 0.1 μR/hr to almost 0.4 μR/hr in the New York vicinity, depending on the time of the measurements. These data are not inconsistent with the TLD trends. However, the levels involved are too small to permit any definitive conclusions regarding the role of ^{95}Zr—^{95}Nb in total exposure rate variations.

The measured annual variations are small with an average exposure rate range of about 0.5 μR/hr. Although the differences exceed only slightly those expected from measurement error considerations, the consistency of the pattern at all locations argues against completely ascribing them to measurement imprecision. The model results suggest that the variations are primarily in the source term, and the trends observed are not inconsistent with what is known about the variations in the components comprising the total exposure rates. Additional data and spectrometric information would be required to permit more definitive conclusions.

SUMMARY AND CONCLUSIONS

A TLD system with good precision can be used effectively to obtain monthly measurements of environmental radiation exposure

rates and to study relatively long-term variations. Annual variations exceeding 1 mR are detectable with the system used.

Measurements made at five homes in the vicinity of New York City over a 5-year period showed typical monthly variations of about 6% (rms deviation) in the total exposure rate, corresponding to about 0.5 μR/hr for a location with an average rate of 7.5 μR/hr (66 mR/year). Typical annual variations were found to be about 1 to 2 mR (rms deviation) with a range of 4 mR. The observed annual trends are not inconsistent with what is known about fluctuations in the contributing components.

A model designed to account for variations in exposure rate from the gamma sources in the ground as a function of changes in the soil-moisture balance was found to account fairly well for monthly variations. The model was not designed to account for long-term changes in the source term and would have to be expanded to do so. However, it does provide a tool for investigating these changes. The applicability of the model for other geographical areas has not been tested, but it could be expected to work optimally where the exposure rate for terrestrial gamma radiation is a significant portion of the total exposure rate and where the climate results in considerable variability in the soil-moisture balance.

ACKNOWLEDGMENTS

The author is grateful to numerous students engaged in the EML Drexel University work-study program for their assistance in carrying out the measurements and the computer analysis and to Michael Boyle who assisted in the fieldwork.

REFERENCES

American National Standards Institute, 1975, American National Standard Performance, Testing, and Procedural Specifications for Thermoluminescence Dosimetry (Environmental Applications), ANSI N545-1975.

Beck, H. L., 1974, Gamma Radiation from Radon Daughters in the Atmosphere, *J. Geophys. Res.*, 79: 2215-2221.

——, J. DeCampo, and C. Gogolak, 1972, *In Situ Ge(Li) and NaI(Tl) Gamma-Ray Spectrometry*, USAEC Report HASL-258, Health and Safety Laboratory.

——, W. M. Lowder, B. G. Bennett, and W. J. Condon, 1966, *Further Studies of External Environmental Radiation*, USAEC Report HASL-170, Health and Safety Laboratory.

——, and G. de Planque, 1968, *The Radiation Field in Air Due to Distributed Gamma-Ray Sources in the Ground*, USAEC Report HASL-195, Health and Safety Laboratory.

Burch, P. R. J., J. C. Duggleby, B. Oldroyd, and F. W. Spires, 1964, Studies of Environmental Radiation at a Particular Site with a Static γ-Ray Monitor, in *The Natural Radiation Environment*, International Symposium, J. A. S. Adams and W. M. Lowder (Eds.), pp. 767-779, The University of Chicago Press, Chicago.

Burke, G. de P., 1975, Thermoluminescent Dosimeter Measurements of Perturbations of the Natural Radiation Environment, in *The Natural Radiation Environment II*, Vol. 1, Symposium Proceedings, Houston, Texas, Aug. 7—11, 1972, J. A. S. Adams, W. M. Lowder, and T. F. Gesell (Eds.), ERDA Report CONF-720805-P-1, pp. 305-315, Rice University and the University of Texas, Houston, NTIS.

——, 1975, *Variations in Natural Environmental Gamma Radiation and Its Effect on the Interpretability of TLD Measurements Made Near Nuclear Facilities*, ERDA Report HASL-289, Health and Safety Laboratory.

——, 1976, Thermoluminescence Dosimetry: Environmental Monitoring Near Nuclear Reactor Sites, *IEEE Trans. Nucl. Sci.*, NS-23: 1224-1236.

——, and T. F. Gesell, 1976, Error Analysis of Environmental Radiation Measurements Made with Integrating Detectors, in *Measurements for the Safe Use of Radiation*, Symposium Proceedings, Gaithersburg, Md., Mar. 1—4, 1976, S. P. Fivozinsky (Ed.), pp. 187-198, U. S. Department of Commerce, NBS Special Publication 456.

——, T. F. Gesell, and K. Becker, 1976, Second International Intercomparison of Environmental Dosimeters Under Field and Laboratory Conditions, in *Tenth Midyear Topical Symposium of the Health Physics Society*, Symposium Proceedings, Saratoga Springs, New York, Oct. 11—13, 1976, pp. 555-563, Rensselaer Polytechnic Institute, Troy, N. Y.

——, and D. G. Marcin, 1974, *Computer Program for Calculating Various Parameters Related to Soil-Water Balance*, USAEC Report HASL-282, Health and Safety Laboratory.

——, and K. O'Brien, 1974, *Operating Manual for GRANIA, a Code for the Analysis of Climatic Effects on Natural Environmental Gamma-Ray Exposure Rates*, USAEC Report HASL-283, Health and Safety Laboratory.

Cox, W. M., R. L. Blanchard, and B. Kahn, 1970, Relation of Radon Concentration in the Atmosphere to Total Moisture Detention in Soil and Atmospheric Thermal Stability, *Adv. Chem. Ser.*, 93: 436-446.

Environmental Quarterly, Appendix, 1977, USDOE Report EML-334.

Gesell, T. F., G. de P. Burke, and K. Becker, 1976, An International Intercomparison of Environmental Dosimeters Under Field and Laboratory Conditions, *Health Phys.*, 30: 125-133.

Harley, J. H. (Ed.), 1972, *HASL Procedures Manual*, USAEC Report HASL-300, pp. C-04-01—C-04-11, Health and Safety Laboratory (this report is updated annually).

——, 1976, *HASL Measurements of Fallout Following the September 26, 1976 Chinese Nuclear Test*, ERDA Report HASL-314, Health and Safety Laboratory.

Lowder, W. M., and G. de Planque, 1977, *Response of LiF Thermoluminescence Dosimeters to Natural Environmental Radiation*, ERDA Report HASL-313, Health and Safety Laboratory.

National Council on Radiation Protection and Measurements, 1976, *Environmental Radiation Measurements*, NCRP Report No. 50, Washington, D. C.

O'Brien, K., 1978, *LUIN, A Code for the Calculation of Cosmic Ray Propagation in the Atmosphere* (update of HASL-275), USDOE Report EML-338, Environmental Measurements Laboratory.

Thornthwaite, C. W., and J. R. Mather, 1957, Instructions and Tables for Computing Potential Evapotranspiration and the Water Balance, *Publ. Clim.*, 10.

Studies of the Absolute Measurement of Low-Level Natural Environmental Radiation Using the Normal-Pressure Ionization Chamber

HISAO KOBAYASHI,* MASAHIRO TSUKUDA,† and AKIRA SASAKI‡
*Institute for Atomic Energy, Rikkyo University, Nagasaka, Yokosuka, Japan;
†Department of Physics, Rikkyo University, Toshima-ku, Tokyo, Japan;
‡Nesco Co. Ltd., Yuigahama, Kamakura, Japan

ABSTRACT

The characteristics and the measurement results of a normal-pressure dry-air ionization chamber of 21-liter cylindrical type with 0.5-cm-thick walls are given. A specially designed electrometer is capable of measuring 1×10^{-14} A current to within ±0.5% accuracy. Alpha contamination, which is an important factor affecting the accuracy of the environmental measurements, is precisely evaluated. The estimated alpha contamination for the four ionization chambers of the same design has been evaluated to contribute a signal equivalent to 0.12 to 0.22 μrad/hr. The uncertainty of the absolute measurement of the environmental radiation dose in free air is found to be ±5.2%, of which ±2.2% is from *inherent factors* and ±3.0% is from *common factors*. The fluctuation of the ionization current, which determines the precision of the measurement, is also quantitatively evaluated as a function of the charge integration time. The precision for 10-min integration time is estimated to be ±2.4% (2σ) at 6 μrads/hr.

The technique for the measurement of the penetrating component of the environmental radiation field using a pressurized argon-filled ionization chamber has been well established (DeCampo, Beck, and Raft, 1972). Use of a normal pressure air-filled ionization chamber has been considered to be difficult because of its low-level ionization current and alpha (and beta) activity contaminations. In this paper the results of the absolute measurement of low-level natural environmental radiation are presented using large-volume normal-pressure air equivalent ionization chambers with phenolic resin airlike walls. Development of a novel MOSFET electrometer of extremely low leakage current and the minimization of alpha

contaminations as well as the precise evaluation of their contributions are given.

ABSOLUTE MEASUREMENT TECHNIQUE

In usual ionization chamber measurements, a calibration constant of dose rate vs. output current is obtained using known radiation sources. The uncertainty of the intensity of calibration sources, however, is rarely below 3%. In addition, the deviation from the inverse-square law (Kondo and Randolph, 1960) and the amount of the scattered gamma rays cannot be neglected.

We, therefore, have decided to use the method of absolute measurement under the conditions that the necessary physical quantities (length, time, temperature, air pressure, capacitance, and voltage) are obtainable within an accuracy that can readily be reached in general laboratory conditions. In the following section the accuracy or uncertainty of the various physical quantities are generally given as 95% confidence interval (Kreyszig, 1970; Dunn and Clark, 1974), except as noted.

NATURE OF THE ENVIRONMENTAL RADIATIONS

The penetrating component of the environmental radiation field consists of X and gamma rays (photons) of terrestrial origin and muons and high-energy electrons of cosmic-ray origin. In this paper the environmental radiation dose is expressed by absorbed dose in air. The environmental radiation includes beta particles originating from ^{40}K, ^{87}Rb, and the natural uranium and thorium decay series, but their contribution to the ionization current is estimated to be negligibly small for 0.7 g/cm^2 phenolic resin walls. Cosmic rays are in general high-energy particles corresponding to near-minimum specific ionization; thus their energy distribution can be considered unchanged by the presence of thin phenolic resin walls. The probability of forming electromagnetic cascades by the low-Z walls is so small that a significant enhancement of secondary electrons and photons is unlikely to occur. Therefore the absorbed dose in air due to the cosmic rays could be measured without any corrections for the energy and the directional response of the chamber.

DESIGN CONSIDERATIONS OF THE IONIZATION CHAMBER

A large-volume normal-pressure air ionization chamber with phenolic resin walls has been selected for the following several

reasons. The natural radiation field consists of many kinds of sources which are widely spread in the environment. For the dosimetry of the environmental radiation, it is desirable that the ratio of the dose to the chamber output current is independent of the incident photon energy. The effective atomic number of the phenolic resin ($\bar{Z} \simeq 6.1$, $\rho = 1.38$ g/cm^3) slightly differs from that of air ($\bar{Z} \simeq 7.4$). Therefore considerable inhomogeneous effects should occur for the dose measurements by a small-volume chamber in the low-energy region ($E_\gamma < 0.1$ MeV). Making the gas volume large is effective in obtaining a flat energy response. This situation is discussed later in the section on Energy Response. In addition to the improvement of the response in the low-energy region, the large gas volume is also advantageous for the enhancement of the amount of produced charge and for the reduction of the statistical fluctuations of the produced current.

The chamber is of a cylindrical type (30 cm ϕ x 30.3 cm height), and the central electrode (0.4 cm ϕ) and the walls (0.5-cm-thick phenolic resin) are covered with conductive colloidal graphite film of $\sim$1.6 mg/cm^2 mean thickness. Figure 1 gives the construction details of the chamber. The volume of the chamber is calculated by measuring the dimensions of each part. The hatched part of Fig. 1 is a dead space governed by the guard ring, and its volume is estimated to be 21 cm^3 which is only 0.1% of the total volume. The effective volume excluding the dead space is calculated as 21217 $\pm$ 83 cm^3 ($\pm$0.39%) for the case of the NS-551 chamber. The uncertainty does not indicate the statistical deviation of directly measured volume but the maximally estimated difference between the calculated volume and the unknown true volume. Four chambers of the same dimensions were constructed in order to confirm the reliability of the measurements comparing the dispersions of measured dose with the estimated uncertainty.

The chamber is sealed to eliminate alpha contamination due to radon and thoron in the air and uses normal-pressure dry air after lengthy storage (3 months or more). The quantity of the ionizing gas is determined from the physical dimensions, the temperature, and the air pressure. The quantity variation is regularly checked through the output current of the chamber using a check source and is less than $\pm$0.1% precision under the normal outdoor temperature range. The output current variation for the check source has always been smaller than $\pm$0.1% over a period of 1 year.

THE ELECTROMETER

The electrometer for measuring the ionization current is housed in a small airtight brass box. Figure 2 shows the circuit details of the

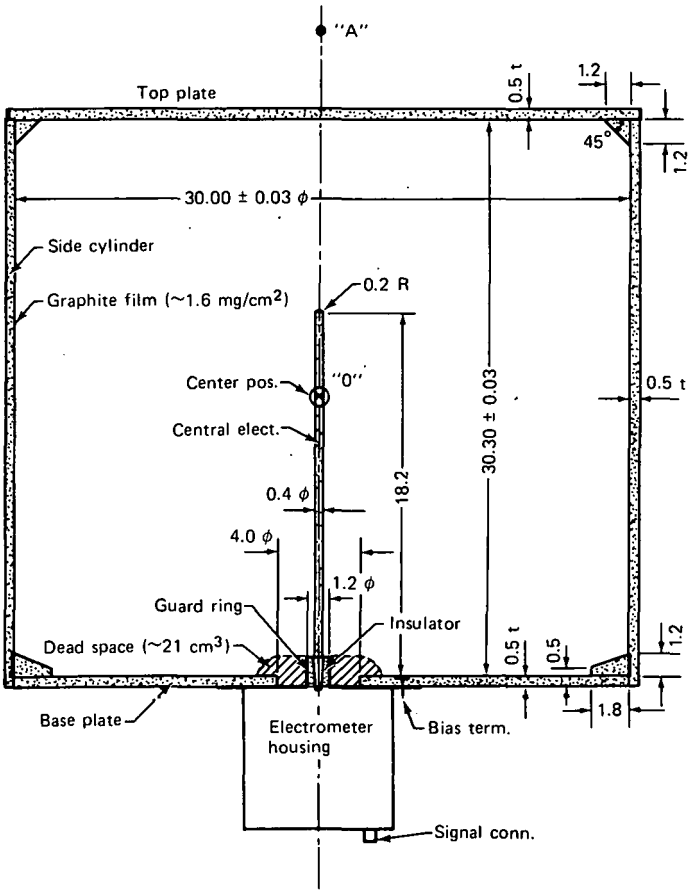


Fig. 1 Cross-sectional view of the 21.2-liter dry-air filled cylindrical ionization chamber.

electrometer, and Fig. 3 gives the block diagram of the measurement system. The input stage is a matched pair differential-type MOSFET operational amplifier, directly connected to the central electrode. The current measurement is done either by a direct reading of potential difference using a 4.7×10^{12} ohm feedback resistor (direct reading method) or by a time integration of the current on a capacitor (500 to 550 pF) resulting from the voltage output (charge integration method).

The value of the d-c capacitance is determined from extrapolating the relation between observed capacitance and measuring frequency to zero frequency using second-order regression (Draper and Smith, 1966; Dunn and Clark, 1974). An example of the

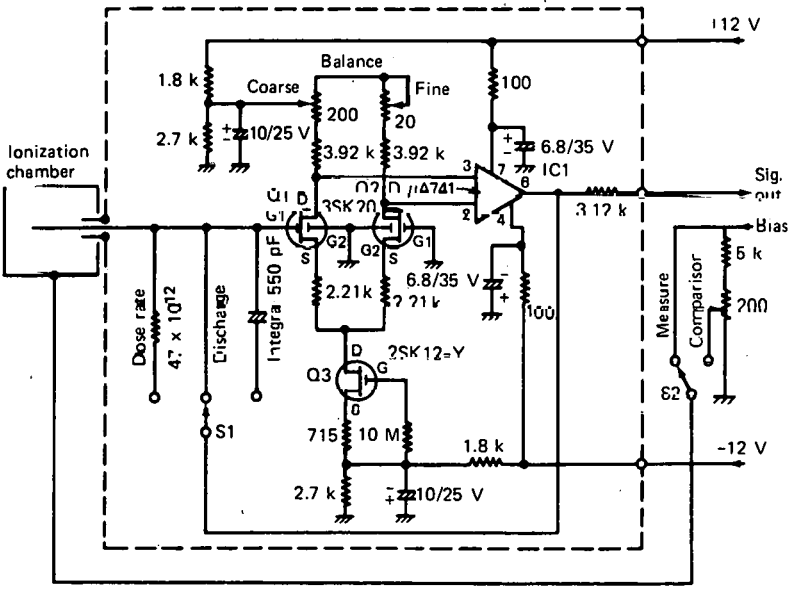


Fig. 2 Circuit diagram of the electrometer.

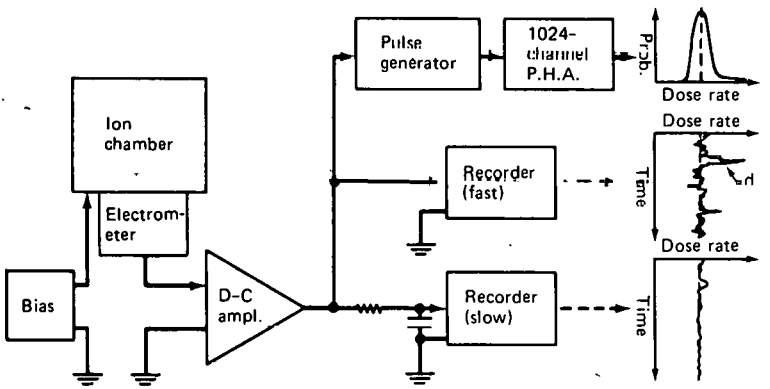


Fig. 3 Block diagram of the environmental radiation dose measuring system to record the probability distributions of the dose rate as well as the instantaneous dose rate.

measured value on a stylor resin capacitor of $< 10^{-16}$ A leakage current is 537.50 ± 0.02 pF at 23°C. The temperature coefficient of the capacitor is -2.0×10^{-2}%/°C, and the systematic uncertainty of the capacitance value is estimated to be ±0.2% under the ±10°C temperature change usually encountered in the field experiments.

The zero point and the amount of drift of the electrometer are determined by determining the null value of the current from the chamber to the input MOSFET gate after necessary compensation of the contact potential difference using a comparison bias (see Fig. 2). The amount of the equivalent input leakage current (MOSFET gate current plus capacitor leakage current) of the four electrometers are $< 2 \times 10^{-16}$ A, which is to be compared with the ionization current of 1.2×10^{-14} A at 6 μrads/hr.

Considering that the uncertainties of the measurements of capacitance, voltage, time, and leakage current are ±0.2, ±0.1, ±0.01, and ±0.2%, respectively, the overall uncertainty of the measured charge is estimated to be ±0.5% in the temperature range of 23 ± 10°C. For the most precise absolute measurements of environmental radiation, special precaution has been taken to keep the temperature change of the electrometer within ±3°C/hr.

CHARGE COLLECTION EFFICIENCY

The collected ionization current i has been found to vary with the inverse electric field 1/E of the chamber, which agrees well with the initial recombination law (Niatel, 1967). As an example, for the chamber NS-551, the correlation coefficient of the i vs. $1/\bar{E}$ ($\propto 1/V$) regression line is −0.9994 for the range of applied voltage V of 10 to 200 V. The 95% confidence interval of the collected current is ±0.28% and ±0.30% of the most probable current for V = 50 V and V = ∞, respectively. The resultant collection efficiency η is estimated to be 0.976 ± 0.003 at 6 μrads/hr for V = 50 V. The value η, of course, depends on the dose rate and the applied voltage. For example, η = 0.972 ± 0.003 at 80 μrads/hr for V = 50 V.

ALPHA-PARTICLE CONTRIBUTIONS

As indicated previously, the alpha-particle contamination of the filled air itself has been kept to a minimum. The contributions from alpha emitters adsorbed in a colloidal graphite film on the walls, however, cannot be neglected. The specific activity and the energy spectrum in the graphite film was measured by a gridded ionization chamber (Kikuchi and Doke, 1972). Figure 4 gives the energy

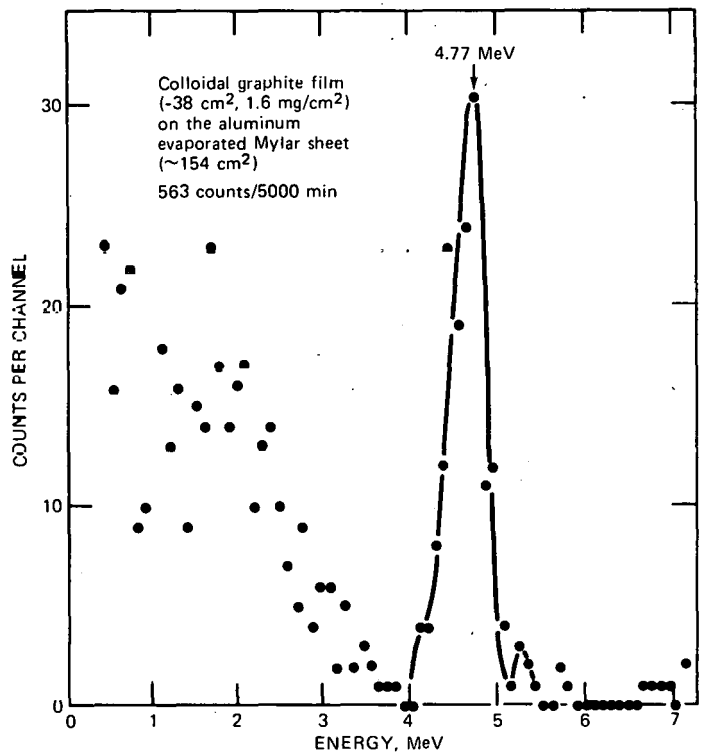


Fig. 4 Alpha-ray energy spectrum of the colloidal graphite film of 1.6 mg/cm^2 thickness on the aluminum evaporated Mylar (polyethylene terephthalate) sheet using the gridded ionization chamber.

spectrum of the graphite film, which is the same material as painted on the inside walls of the chamber. The main peak energy of 4.8 MeV is observed in the spectrum and is probably due to ^{210}Po alpha particles (5.3 MeV). The specific alpha activity of the graphite film is determined to be 0.039 α/hr-cm^2. Considering the total inside area of 4300 cm^2 of the chamber, the total alpha-particle frequency, the mean energy, and the equivalent mean dose rate for $E_\alpha > 0.47$ MeV are estimated to be 169 α/hr, 3.2 MeV, and 0.31 μrad/hr, respectively, and for $E_\alpha > 4$ MeV to be 51.0 α/hr, 4.8 MeV, and 0.15 μrad/hr, respectively. The results may be compared with those obtained by the following direct estimation using the chamber itself.

Large current spikes produced by alpha particles in the chamber are clearly recognizable by the direct reading method on a strip chart recorder with fast response (see Fig. 3). There are, however, low-energy alpha particles, as shown in Fig. 4. Some of the current

spikes produced by these low-energy particles are weak and may be hidden in the photon current fluctuations. Therefore such spikes cannot be distinguished from the current fluctuations by their amplitude. Further, individual countings of many spikes appearing on the long-term chart record are tedious and time-consuming. We have developed a simpler method for estimating the alpha contamination in the chamber.

The instantaneous values of the fluctuating output current including the alpha spikes are sampled regularly at 20-msec intervals, and their probability distributions are analyzed and accumulated for 10 to 18 hr on a commercial 1024-channel pulse height analyzer (P.H.A.), as shown in Fig. 3. One of the measured probability distributions is shown in Fig. 5 for the chamber NS-551. In the probability distribution curves, we can define the value ΔD which corresponds to twice the standard deviation. From Fig. 5 ΔD is estimated to be 1.2 ± 0.2 μrad/hr. We can safely say that the current spikes whose amplitudes exceed the mean value $\bar{D}$ by at least ΔD are almost definitely from alpha particles. The adequacy of this criterion of alpha discrimination is confirmed by the analysis of alpha spikes on the strip chart. The right side of the vertical dashed line denoted as $\bar{D} + \Delta D$ in Fig. 5 (> 7.45 μrads/hr, the hatched area C) should be a probability distribution due to alpha contamination, and the hatched area C gives a lower limit for such contamination. The buried probability distribution due to low-energy alpha particles is assumed to be the long dashed curve in Fig. 5. For simplicity of calculation, an approximation is made to this curve, given by the solid straight line A. Two extreme cases are also assumed by hatched areas B and C, which give an uncertainty of the curve A. Table 1 shows the estimated alpha contaminations for the four chambers. Column 2 indicates the mean alpha dose rate $\bar{D}_\alpha$ estimated from the most probable curve A in Fig. 5. Columns 3 to 5 also indicate the lowest mean dose rate $\bar{D}'_\alpha$, the lowest counting rate $\bar{n}'_\alpha$, and the corresponding mean energy $\bar{E}'_\alpha$ estimated from curve C. The values for $\bar{D}_\alpha$ given in Table 1 are considerably smaller than the measurement results on the graphite film. The difference may be explained as a consequence of the minimum contamination of the filled air itself.

Up to this point, the factors and their uncertainties which must be determined for each chamber individually have been discussed. These factors are called the *inherent factors*, and their uncertainties are summarized in Table 2. The uncertainties are defined as the residual of the systematic errors. It is debatable how these systematic uncertainties should be combined. According to the recommendation of ICRU (1968), the positive and negative systematic uncertainties

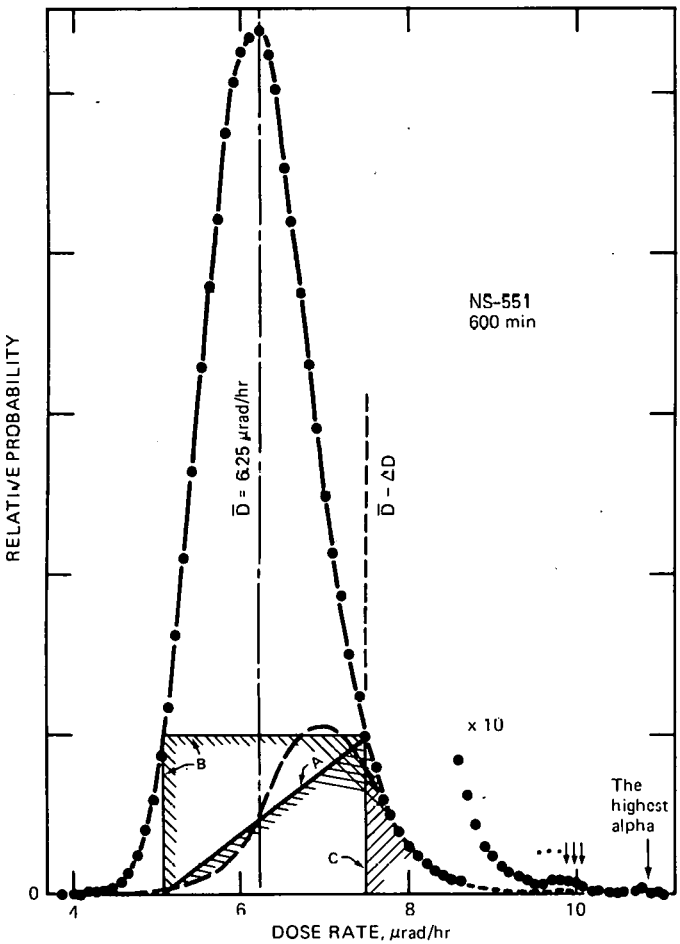


Fig. 5 Observed probability distribution of dose rate measured by the system.

should be arithmetically summed separately to provide the limits of maximum uncertainty. Therefore the subtotal in Table 2 is simply taken as the arithmetic sum of the uncertainties. Table 2 also shows twice the standard deviation (95% confidence) of measured environmental radiation dose by the four chambers. The value 2σ coincides with the subtotal ±2.2% of the *inherent factors.*

ENERGY RESPONSE

We may call the ratio of the current produced by the ionization chamber to the current in free air of the same volume as the

TABLE 1

Estimated Alpha Contamination of the Ionization Chambers

Name of chamber	$\bar{D}_\alpha$,* μrad/hr	$\bar{D}'_\alpha$,† μrad/hr	$\bar{n}'_\alpha$,† cph	$\bar{E}'_\alpha$,† MeV
NS-551	0.160 ± 0.049	0.111	33.8 ± 5.8	5.6 ± 1.0
NS-539	0.219 ± 0.050	0.169	40.1 ± 6.3	7.2 ± 1.1
NS-551	0.161 ± 0.041	0.122	35.1 ± 5.9	6.0 ± 1.0
NS-558	0.118 ± 0.043	0.082	31.5 ± 5.6	4.5 ± 0.8

*Estimated from curve A in Fig. 5.
†Estimated from curve C in Fig. 5.

TABLE 2

Uncertainties for Various Factors in an Absolute Measurement of Natural Environmental Radiation with the Air Equivalent Chamber

Accuracy or Uncorrected Systematic Uncertainties	Estimated uncertainty, %
Inherent factors for the individual chambers	
Twice the standard deviation of observed dose for four chambers	±2.2
Example of the factors for chamber No. NS-551	
Air volume (21217 ± 83 cm^3)	±0.4
Air density (temperature and pressure)	±0.2
Charge (voltage, capacitance, leakage current, and drift)	±0.5
Ion collection efficiency (η = 0.976 ± 0.003 at 6 μrads/hr)	±0.3
Alpha contamination (0.160 ± 0.049 μrad/hr)	±0.8
Subtotal	±2.2
Common factors for our 21.2-liter chambers	
W-value (33.73 ± 0.30 eV/ion pair)	±0.9
Energy dependence for unspecified environment ($\bar{S}_{ER}$ = 0.943 ± 0.017)	±1.8
Angular dependence for unspecified source spread ($\bar{S}_\theta$ /S(0) = 0.986 ± 0.003, S(0) = $\bar{S}_{ER}$)	±0.3
Subtotal	±3.0

Precision (Standard Deviation for Various Integration Times)

Integration time, min	0.17	1.0	5.0	10.	30.	60.
Standard deviation, %	7.0	3.9	1.7	1.2	0.7	0.6

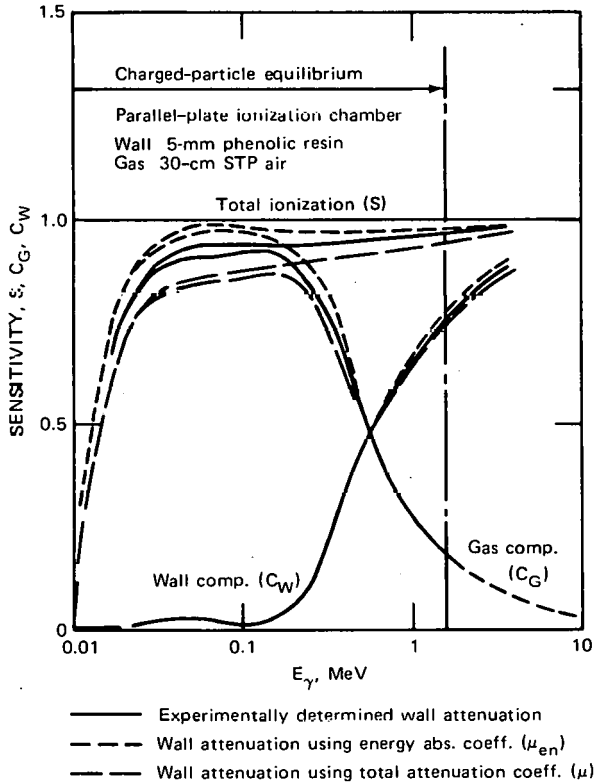


Fig. 6 Energy dependence of the sensitivity $S(E_\gamma)$, $C_G(E_\gamma)$, and $C_W(E_\gamma)$ of the parallel ionization chamber.

sensitivity S of the chamber. The sensitivity as a function of the photon energy $S(E_\gamma)$ is in general called *energy response.* Since it is rather difficult to experimentally determine the energy response, the results of the approximate calculations on a one-dimensional parallel-plate ionization chamber (Kobayashi, 1977) have been slightly modified for our chamber. The modified results are shown in Fig. 6. In Fig. 6 the chamber walls were phenolic resin of 0.5-cm thickness, and incoming photons were assumed to enter perpendicular to the walls. Two sets of numerical values as a function of photon energy were used in the modifications, i.e., the mean stopping power ratios of the phenolic resin to the air (White, 1959) including the density effect corrections (Sternheimer, 1952, 1954; White, 1954) and experimentally determined values of attenuation of the photon energy flux by the phenolic resin wall.

In the low-energy region ($E_\gamma < 0.1$ MeV), the ionization current due to the secondary electrons from the air in the chamber—we may call this gas component C_G current—plays the main role, thus enabling measurement of the true absorbed dose in the air itself. However, the attenuation effect by walls becomes increasingly important as the photon energy is lowered. As an example, $S(E_\gamma = 30$ keV) = 0.87 (see Fig. 6). In the high-energy region ($E_\gamma > 0.5$ MeV), the ionization current due to the secondary electrons produced in the walls—we may call this wall component C_W current—plays the main role. Inhomogeneous effects between the phenolic resin wall and dry air should be considered as well as the attenuation effect. Thus the large volume (21.2 liters) assures a nearly flat response of the chamber. For example, the sensitivity $S(E_\gamma = 60$ keV) is equal to 0.916 and increases gradually with increasing energy to $S(E_\gamma = 1.5$ MeV) = 0.953.

In the environmental radiation measurements, the sensitivity must be modified by the actual energy distribution $P(E_\gamma)$ defining the mean sensitivity $\bar{S}_{ER}$ as follows:

$$\bar{S}_{ER} = \frac{\int_0^{E_{max.}} P(E_\gamma)\, S(E_\gamma)\, dE_\gamma}{\int_0^{E_{max.}} P(E_\gamma)\, dE_\gamma} \tag{1}$$

The environmental radiation sources considered in this paper consist of ^{40}K and thorium and uranium series as the natural radiation sources; ^{137}Cs, ^{54}Mn, $^{95}Zr/^{95}Nb$, and ^{106}Rh as the fallout gamma-ray sources; and ^{41}Ar as the artificial source. Also considered are scattered photons amounting to about 10 to 30% of the total dose rate. For the sources mentioned above, $\bar{S}_{ER}$ is individually calculated by using $S(E_\gamma)$ of Fig. 6. For thorium and uranium series, a typical source composition $P(E_\gamma)$ can be obtained from Sakai, Terada, and Katagiri (1976) and the energy flux spectrum of scattered photons from Beck and de Planque (1968). An uncertainty of $\bar{S}_{ER}$ is evaluated from the maximum and the minimum values of the calculated $\bar{S}_{ER}$ for the individual sources, with 10 to 30% scatter. In this manner, $\bar{S}_{ER}$ is estimated to be 0.943 ± 0.017 for undefined environmental radiation sources under the condition that the radiation come from the normal direction ($\theta = 0$; see next section) to the top plate shown in Fig. 1. The estimated uncertainty consists of the uncertainties due to the source difference, to experimentally determined attenuation data, and to flux and energy spectrum of the scattered radiation. Not included are uncertainties from parallel plate approximations, from the mass

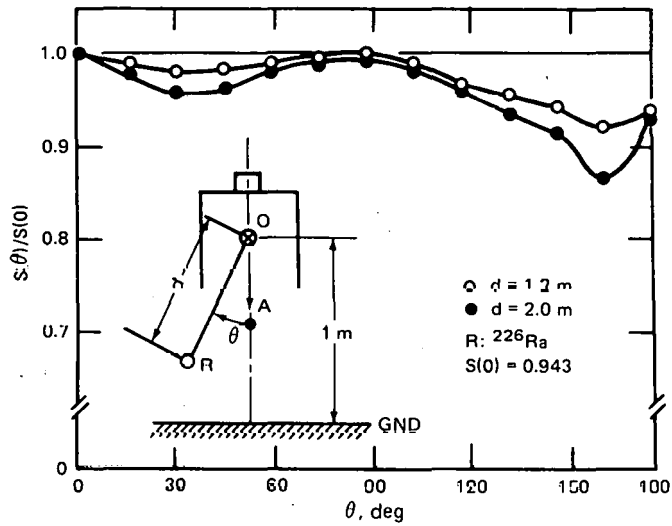


Fig. 7 Angular dependence of the chamber sensitivity $S(\theta)$ relative to the $\bar{S}$ at $\theta = 0^{\circ}$. For the environmental radiation field, S(0) is equal to $\bar{S}_{ER} = 0.943 \pm 0.017$.

energy absorption coefficient (ICRU, 1962), and from the mean stopping power ratios (White, 1959).

Environmental radiation sources include photon sources of energy greater than 1.5 MeV such as ^{208}Tl (2.615 MeV) and ^{214}Bi (1.73 to 2.448 MeV). These photons are measured under the condition that charged particle equilibrium does not exist in a strict sense. Secondary electrons with energies above 1.5 MeV, which originate not from the air or the chamber walls but from the other places such as the ground or nearby structures, will be detected. The uncertainty introduced by this factor, however, is estimated to be less than ±1% of the dose rate due to the dominant high-energy photons.

DIRECTIONAL RESPONSE

The ionization yield of the chamber depends on the direction of the incident photons because of the change of the effective wall thickness and the change of the energy response. Figure 7 shows the measurement results of the directional response of the relative sensitivity $S(\theta)/S(0)$ using a ^{226}Ra source for distances d ($\overline{OR}$ in Fig. 7) of 1.2 and 2 m. The source is rotated on a circular orbit in a plane including the central axis, starting from the direction O → A

($\theta = 0$; see Fig. 7) opposite to the electrometer casing on the central axis. The minimum value occurs at $\theta = 165°$ because of the maximum volume of the chamber shadowed by the electronic apparatus. The directional dependence decreases as d increases.

The theoretical directional dependence $P_{E_\gamma}(\theta)$ of the photon flux (with scattered rays) for a uniformly distributed plane source of ^{40}K and thorium and uranium series at 1 m height above the plane is given by Beck and de Planque (1968). The mean sensitivity $\bar{S}_\theta$ is defined as

$$\bar{S}_\theta = 2\pi \int_0^\pi P_{E_\gamma}(\theta)\, S(\theta) \sin\theta \, d\theta \qquad (2)$$

where the integral of $P_{E_\gamma}(\theta)$ overall angles is assumed to be normalized to 1. The values $\bar{S}_\theta$ for the three sources using the $S(\theta)$ in Fig. 7 and using the $P(\theta)$ from Beck and de Planque (1968) are all within the value $\bar{S}_\theta/S(0) = 0.986 \pm 0.003$ under the condition of the line $\overline{OA}$ directed vertically downward. The result for the case when the line $\overline{OA}$ is directed vertically upward is $\bar{S}_\theta/S(0) = 0.954 \pm 0.003$. The ratio of the $\bar{S}_\theta$ for the two cases above is 0.968, which is consistent with the experimentally obtained ratio of 0.958 ± 0.018 from the actual chamber measurements in its normal position and upside-down position.

The factors discussed in the last two sections depend only on the chamber construction and are called the *common factors*. The common factors together with the W-value (ICRU, 1962) are summarized in Table 2. Uncertainties of $\bar{S}_{ER}$ and $\bar{S}_\theta/S(0)$ arise from the variation of spatial distribution and the quality of environmental radiation sources. The subtotal is also taken as the arithmetic sum of the individual uncertainties.

STATISTICAL FACTORS

The fluctuation of ionization current is caused by the statistics related to the number and energy distribution of secondary electrons generated in the chamber. The time variation of the current waveform on the electrodes also causes a current fluctuation. The measured fluctuation of the current may depend on the intensity and energy of the photons, the applied voltage, and the integration time of the current.

Figure 8 shows an example of the dependence of the current fluctuation (given as a variance) on the integration time at the environmental radiation level. The environmental radiation level itself is continuously monitored by recording the current variation of

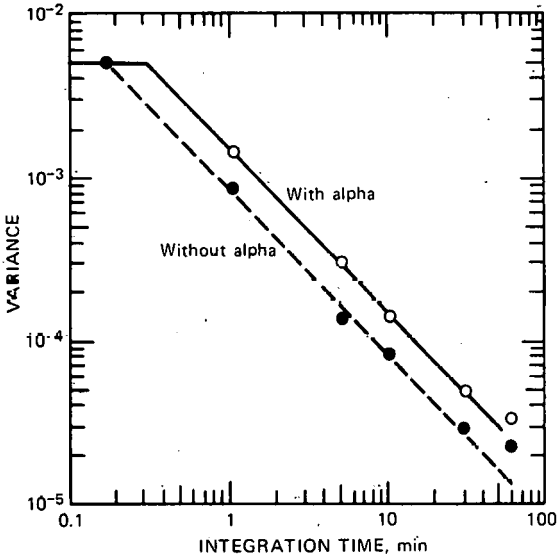


Fig. 8 Variance of integrated charge vs. integration time.

a second chamber using the direct reading method with slow time response (see Fig. 3). The closed circles and the dashed line having a slope of −1 in Fig. 8 show the variance without the effects of alpha particles and are obtained from the records of the integrated current values for every 1 min, excluding those values of alpha origin. When the integration time is less than 10 sec, the variance becomes time-independent and is determined by the ion collection time, which can be estimated to be about 10 sec. The horizontal line in Fig. 8 is drawn on that basis.

Table 2 shows the standard deviation for 10-sec integration time excluding alpha events and for the longer integration time including alpha events.

ABSOLUTE MEASUREMENT OF PHOTON FIELDS BY A RADIATION SOURCE

Since we are doing an absolute measurement, it is not necessary to calibrate the chamber using known sources. However, the results using a calibrated ^{226}Ra source (±3%: 99.7% confidence) are given for comparison purposes.

To calibrate a chamber using a known source, it is necessary to measure the dose D_{direct} caused by the direct fluxes from the source. To separate the dose D_{scatt} of scattered rays and D_{direct}

from the observed dose D_{obs}, a shadowing experiment is useful. A lead shield block of 30-cm thickness and 20- by 20-cm area is used in this experiment. With the shadowing method, results of absolute measurements of the radium gamma-ray field are summarized in Table 3. The necessary corrections for estimating the D_{direct} such as ion collection efficiency η (see row 7 in Table 3) and the direct beam attenuation factor, $\xi = \exp[-(\mu/\rho)_{air} \times (\rho/d')]$ (see row 8), by the air thickness d' between the source and the chamber wall are all considered. In row 2, D_{cal} is calculated using the inverse-square law and does not contain the uncertainty in the specific gamma-ray constant Γ [0.825 mR/mg-hr at 1 m (ICRU, 1961)]. The uncertainty of values D_{direct} and D_{scatt} are obtained using the ±1.4% accuracy of Table 2 excluding the uncertainty of alpha contamination and including the statistical uncertainties and the source-to-chamber distance uncertainties. The value of D_{direct} does not contain the

TABLE 3

Summary of Absolute Measurements of ^{226}Ra* Gamma-Ray Field with Shadowing Experiments

Source to chamber distance d, m	1	2	3
Calculated photon dose D_{cal}, μR/hr	89.2 ± 2.7	22.30 ± 0.67	9.91 ± 0.30
Measured direct beam D_{direct},† μR/hr	93.0 ± 1.7	22.67 ± 0.52	9.95 ± 0.30
Measured scattered ray D_{scatt},‡ μR/hr	4.7 ± 0.3	3.26 ± 0.21	2.38 ± 0.17
Ratio D_{direct}/D_{cal}	1.042	1.017	1.004
Yield of scattered photons, %	5	14	24
Ion collection efficiency η	0.972	0.975	0.976
Attenuation by the air gap ξ	0.991	0.982	0.973
Sensitivity for Ra source $\bar{S}_{Ra}$		0.950	
Angular dependence S(90°)/S(0°)		1.000	

*The ^{226}Ra source is 108.1 ± 3.2 μg in weight with 0.5-mm thick Ir(10%)—Pt screenage.

†D_{direct} = (total dose rate without the shadow block) — (dose rate with the shadow block).

‡D_{scatt} = (dose rate with the shadow block) — (dose rate of environment).

correction for the inhomogeneous effect of incident primaries (Kondo and Randolph, 1960). We can see that the ratio D_{direct}/D_{cal} in row 5 of Table 3 slightly depends on the distance d. However, the dependence is small and within the estimated uncertainty, and the agreement between the measured D_{direct} and the calculated D_{cal} is fairly good.

CONCLUSION

In environmental radiation measurements, the use of a large-volume ionization chamber is effective from the standpoint of uniform sensitivity over a wide energy range (> 30 keV) as well as the large ionization currents. From the results given in Table 2, the 95% confidence interval for the absolute measurement method using our 21-liter chambers is ±2.2% for the inherent factors and ±5.2% including common factors. It is to be noted that these figures can be obtained in the laboratory without special experimental techniques. The key factors for the realization of ±5% accuracy are the high reliability of the specially designed electrometer and accurate dosimetry of the alpha particles.

Another achievement in this study is the analysis of the statistical character of the ion current fluctuations. For example, to be able to detect a change in the environmental radiation dose rate, the estimation of the precision is inevitable, as shown in Fig. 8 or Table 2. It should be pointed out that by using these results we can set the measurement condition, such as the charge integration time, in advance, when we expect results of given precision for an arbitrary confidence interval. For example, when we expect a result of ±6% precision for a 95% confidence interval (2σ), the necessary charge integration time is estimated to be 100 sec and for ±1.2% precision to be 60 min.

Finally, in field measurements, it is important that the ionization chamber is rugged enough to withstand the severe environment while retaining simplicity of operation. Our chambers have remained in good condition and operated stably during continuous measurements near the seashore since February 1977 in the temperature range of 0 to 35°C and while exposed to strong wind and rain. They are also insensitive to shock such as vibrations, can be operated on batteries, and are well suited for measurements on the sea.

ACKNOWLEDGMENTS

We gratefully acknowledge E. Tajima, T. Doke, and A. Kato for many valuable discussions. We would like to thank J. Kikuchi of

Science and Engineering Research Laboratory, Waseda University, for performing the alpha spectra measurements with the gridded chamber. For high precision capacitance measurements, we are also indebted to A. Igarashi of Japan Electric Meters Inspection Co.

REFERENCES

Beck, H. L., and G. de Planque, 1968, *The Radiation Field in Air Due to Distributed Gamma-Ray Sources in the Ground*, USAEC Report HASL-195, Health and Safety Laboratory, New York.

DeCampo, J. A., H. L. Beck, and P. D. Raft, 1972, *High Pressure Argon Ionization Chamber Systems for the Measurement of Environmental Radiation Exposure Rates*, USAEC Report HASL-260, Health and Safety Laboratory, New York.

Draper, N. R., and H. Smith, 1966, *Applied Regression Analysis*, John Wiley & Sons, New York.

Dunn, O. J., and V. A. Clark, 1974, *Applied Statistics: Analysis of Variance and Regression*, John Wiley & Sons, New York.

ICRU, 1961, *Report of the International Commission on Radiological Units and Measurements (ICRU)*, NBS Handbook 78, GPO, Washington.

——, 1962, *Physical Aspects of Irradiation* (ICRU Report 10b), NBS Handbook 85, GPO, Washington.

——, 1968, *Certification of Standardized Radioactive Sources* (ICRU Report 12), International Commission on Radiation Units and Measurements, Washington.

Kikuchi, J., and T. Doke, 1972, Reduction of Alpha Ray Background in a Cylindrical Gridded Ionization Chamber by the Cathode Pulse Method, *Nucl. Instrum. Methods*, 99: 469-475.

Kobayashi, H., 1977, Studies for Absolute Dose Measurements of Low Level Environmental Radiation (in Japanese), in *Report of the Expert Committee of Low Level Dose Measurements*, pp. 101-105, The Japan Society of Applied Physics, Tokyo.

Kondo, S., and M. L. Randolph, 1960, Effect of Finite Size of Ionization Chambers on Measurements of Small Photon Sources, *Radiat. Res.*, 13: 37-60.

Kreyszig, E., 1970, *Introductory Mathematical Statistics—Principles and Methods*, John Wiley & Sons, New York.

Niatel, M. T., 1967, An Experimental Study of Ion Recombination in Parallel-Plate Free-Air Ionization Chambers, *Phys. Med. Biol.*, 12(4): 555-563.

Sakai, E., H. Terada, and M. Katagiri, 1976, *In-Situ Measurement of the Environmental Gamma-Rays by Portable Ge(Li) Detectors* (in Japanese), Report JAERI-M 6498, Japan Atomic Energy Research Institute.

Sternheimer, R. M., 1952, The Density Effect for the Ionization Loss in Various Materials, *Phys. Rev.*, 88: 851-859.

——, 1954, The Density Effect for the Ionization Loss at Low Energies, *Phys. Rev.*, 93: 351.

White, G. N., 1954, Density Effect in Gamma-Ray Measurements, *Nucleonics*, 12(2): 18-21.

——, 1959, *Principles of Radiation Dosimetry*, John Wiley & Sons, New York.

Methods and Results of Measurements of the Environmental Radiation in Bavaria

F. WACHSMANN and D. F. REGULLA
Gesellschaft für Strahlen- und Umweltforschung, Neuherberg,
Federal Republic of Germany

ABSTRACT

The terrestrial component of the radiation environment in Bavaria was found to vary within a wide range and that outdoors between 1 and 25 μR/hr, depending on the geological composition of the ground. Indoor measurements yielded, on the average, an increased dose level with remarkable variations due to the building material. In one case the exposure rate reached approximately 100 μR/hr. On the basis of measurements in and around more than 4000 dwellings, average values for the outdoor and indoor exposure rates were determined to be 5.7 and 7.6 μR/hr, respectively, i.e., the indoor exposure is a factor 1.33 higher than outdoors. This result could be correlated with the radiation source effect of the predominant solid stone construction mode in Germany. Further, an increased source effect was found for houses constructed before 1900 and after 1948. Relative results of the radioactivity concentrations are given for different building materials revealing materials with obvious shielding or source effect.

In 1973 the Ministry of the Interior of the Federal Republic of Germany initiated a research program with the aim of determining the exposure of the population to natural sources of radiation. Eleven institutions were designated to perform the necessary measurements; the task was to investigate at least about 1 per 1000 houses or apartments in villages and about 1 per 5000 dwellings in larger towns.

For each house or apartment, at least three measurements were carried out indoors, at the most frequented places, and additionally one or two measurements outdoors, each measurement at 1 m aboveground. From the measurements, average values were calcu-

lated from which the amount of exposure due to cosmic radiation was subtracted. The exposure rate from cosmic radiation was found by measurements on lakes, resulting in about 2.5 μR/hr on the average, which is in reasonable agreement with other authors (National Council on Radiation Protection and Measurements, 1975, 1976).

By this procedure, more than 30,000 dwellings were surveyed in all Germany during 1973 and 1974 (Kolb, 1974). Overall results will be published by the German Ministry of the Interior after careful evaluation by the Physikalisch-Technische Bundesanstalt (PTB), Braunschweig. In this paper we report on a limited number of results obtained by our own measurements in the federal state of Bavaria. The results may, however, be considered typical for all the Federal Republic of Germany.

METHODOLOGY

The measurements were performed with a dose rate meter based on a scintillation counter with a 3- by 3-in. organic crystal (Fig. 1). For improvement of the energy dependence of response in the low energy range, the crystal is covered with a thin layer of fluorescent zinc sulfide (Lauterbach, Kolb, and Seyfried, 1970) providing approximate energy independence above 20 keV (Fig. 2). With this instrument, full-scale exposure rates from 3 up to 300 μR/hr can be measured.

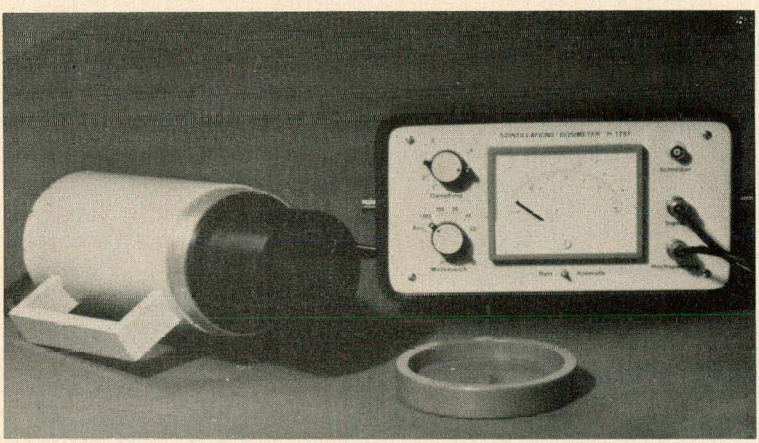


Fig. 1 Dose rate meter based on a scintillation counter.

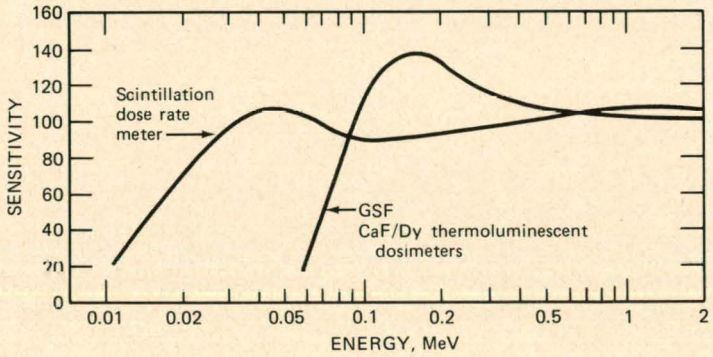


Fig. 2 Energy dependence of response of the scintillation dose rate meter and the GSF environmental thermoluminescent dosimeters.

In addition to the scintillation dose rate meter, thermoluminescent dosimeters (TLDs) with dysprosium doped calcium fluoride crystals (CaF_2/Dy) were used (only for the Bavarian measurements) (Fig. 3). For flattening the pronounced oversensitivity of response for photon energies below 300 keV, the 3- by 3- by 0.9-mm crystals are covered with a 3-mm-thick copper filter (Kramer, Regulla, and Drexler, 1977) (Fig. 2). A plastic capsule provides protection against dust and moisture, and two thermomarkers (50 and 70°C) indicate

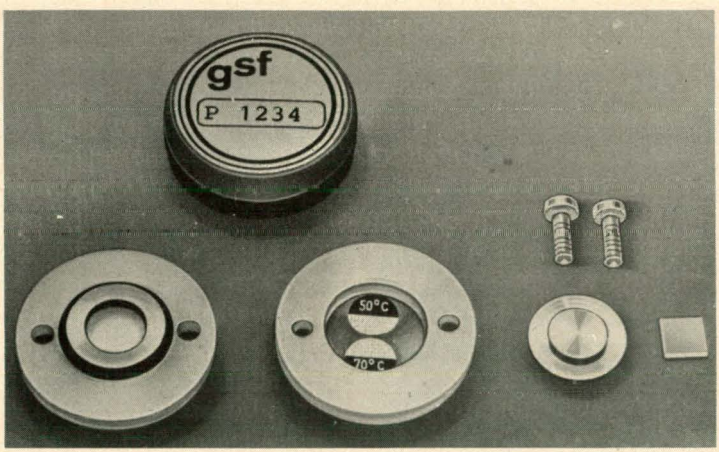


Fig. 3 GSF environmental dosimeter with thermoluminescent CaF_2/Dy chips, copper filter, and plastic capsule containing two thermomarkers.

the occurrence of an unusually high temperature during irradiation or transport allowing for the application of a special annealing program prior to readout to avoid fading errors.

The lower limit of detection of the dosimeter is about 1 mR with the readout system used. The precision depends on the magnitude of exposure and is characterized by a coefficient of variation of $\sigma_r \leqslant 5\%$ for an exposure $\geqslant 10$ mR on a 95% confidence level (Fig. 4). The figures on uniformity also given in Fig. 4 are very good but of limited significance since they may change from batch to batch or can be improved by selection. Except for energy dependence, these dosimetric properties correspond well with the recommendations of the American National Standards Institute (ANSI) for TLDs in environmental application (ANSI-N545-1975).

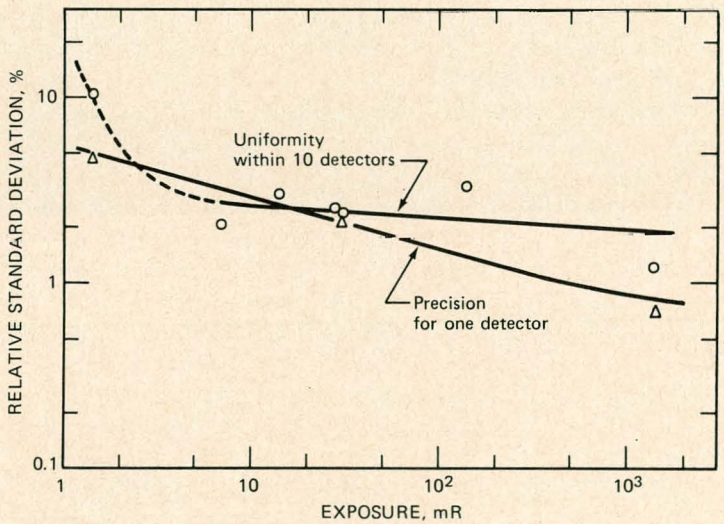


Fig. 4 Precision and uniformity of the CaF_2/Dy thermoluminescent dosimeters as a function of exposure.

The environmental dosimeter and readout procedure used by Gesellschaft für Strahlen- und Umweltforschung (GSF) have achieved good reliability in different intercomparisons (Table 1). For irradiation under calibration conditions at the German primary standard laboratory (PTB, 1976, Table 1) and for advanced laboratory or 1- to 3-month field conditions [Energy Research and Development Administration's Health and Safety Laboratory (ERDA/HASL), 1976; Oak Ridge National Laboratory (ORNL), 1977], the reported

TABLE 1

Intercomparison Results with GSF Environmental Dosimeters

Irradiation by	Radiation	Actual exposure, mR	Reported exposure, mR	Difference, %
PTB, 1976	^{60}Co	19.0	19.7	+3.7
	^{60}Co	19.0	18.2	+4.2
ERDA/HASL, 1976	^{137}Co	21.3	23.8	+7.0
	Field	17.1	17.1	0
ORNL, 1977	Laboratory	91.7	92.7	+1.0
	Field	34.9	33.7	−3.0

exposure values approach the given exposure within quite acceptable error limits of only a few percent. In particular, the results from field irradiation appear to be remarkable since, because of the filter design of the dosimeter, there is a cutoff for photon energies below about 70 keV. This result may be of interest for consideration of the low energy limit to be recommended in guidelines for environmental dosimetry.

For surveying the radiation environment, the TLDs were mailed and distributed to selected houses by the administrative authorities, particularly in smaller villages or villages with difficult access. There they were exposed both indoors and outdoors for at least 4 weeks, according to the accompanying instructions, and were then collected and sent back to Munich for readout. For the determination of the local exposure rate, a transfer exposure rate of the cosmic and terrestrial radiation of normally 6 μrads/hr was taken into consideration.

With the two types of dosimeters, the exposure rate of 4689 dwellings has been investigated, i.e., 1894 dwellings using the scintillation dose rate meter and 2795 dwellings with the TLDs. The dwellings selected are distributed uniformly over the area of Bavaria, as shown in Fig. 5. The agreement between the results achieved with both the scintillation dose rate meter and the TLD at the same locality is reasonably good, i.e., normally within ±10%.

RESULTS

The distribution of exposure rates for indoor and outdoor measurements in air is shown in Fig. 6. Obviously the exposure outdoors and also the exposure inside of the houses varies in a wide range from about 1 to 20 μR/hr or more. The average value of the

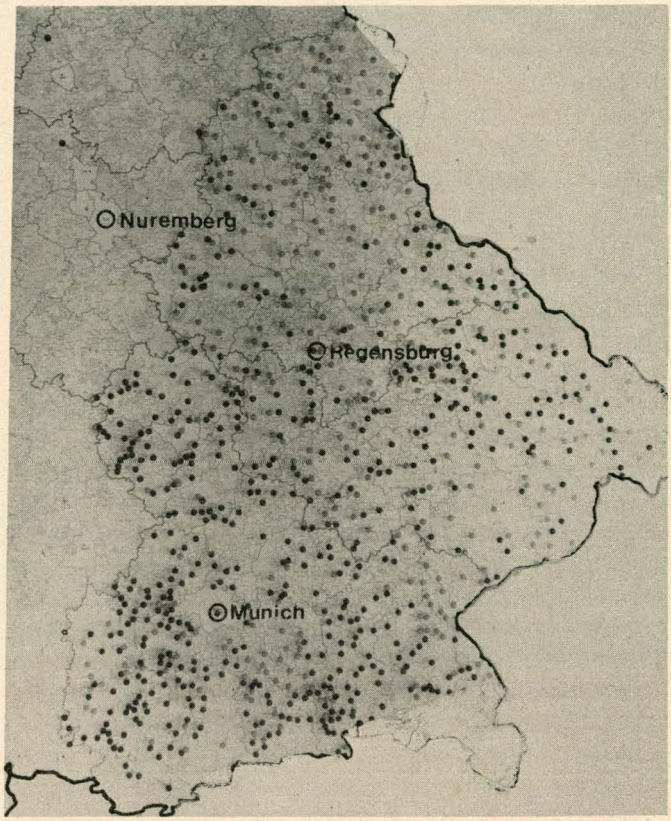


Fig. 5 Map of Bavaria with the measuring places marked. ●, TLD; ○, scintillation dose rate meter.

exposure rate in air was found to be 5.7 μR/hr outdoors and 7.6 μR/hr indoors. The average ratio of the indoor-to-outdoor exposure rate in air is 1.33. This means that in Bavaria the exposure in houses is normally higher than outdoors, which is in contrast to findings of similar surveys in the United States (National Council on Radiation Protection and Measurements, 1975, 1976).

The discrepancy between these results may be explained by different construction methods in the two countries. Construction materials, on the average, contain more radioactive components in Germany than those in the United States. For clarification, we separately plotted the relative number of houses of different construction modes vs. the indoor-minus-outdoor exposure rate (Fig. 7). By this procedure, we indeed found that the exposure in

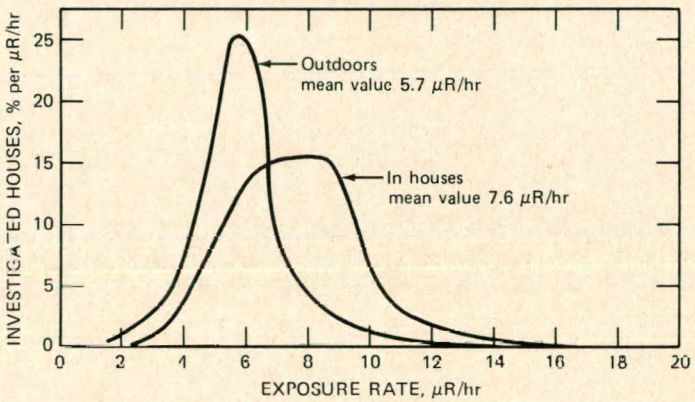


Fig. 6 Frequency distribution of the measured indoor and outdoor exposure rates.

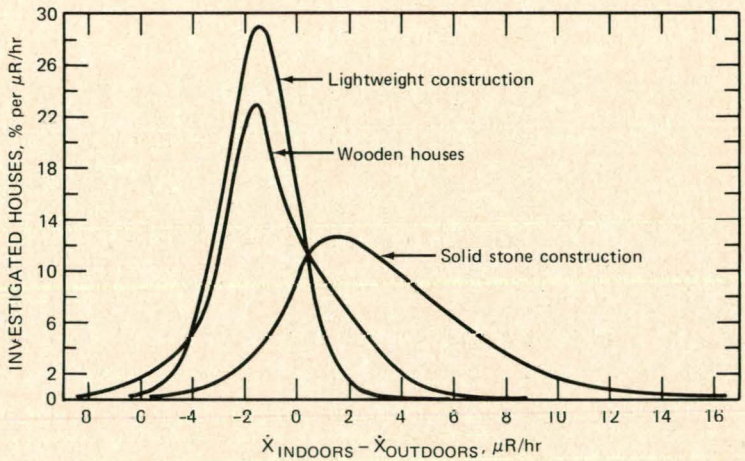


Fig. 7 Frequency distribution of houses of different construction styles vs. indoor-minus-outdoor exposure rates.

wooden houses and in houses built of lightweight construction, the styles favored in the United States, is normally lower than outdoors. Only in houses with a solid stone construction, as is usual in Germany, does the contribution of radiation from the walls regularly dominate their shielding effect.

A further elaboration of the results concerned the question of whether the exposure is higher or lower in new houses as compared

to old houses, since the construction style has changed over the years. Figure 8 shows the relative number of houses of different age vs. the indoor-minus-outdoor exposure rate. As a result it becomes obvious that the attenuation effect of the walls regularly dominates the source effect, especially for houses built between 1900 and 1948, which, however, is not the case for the older and newer houses.

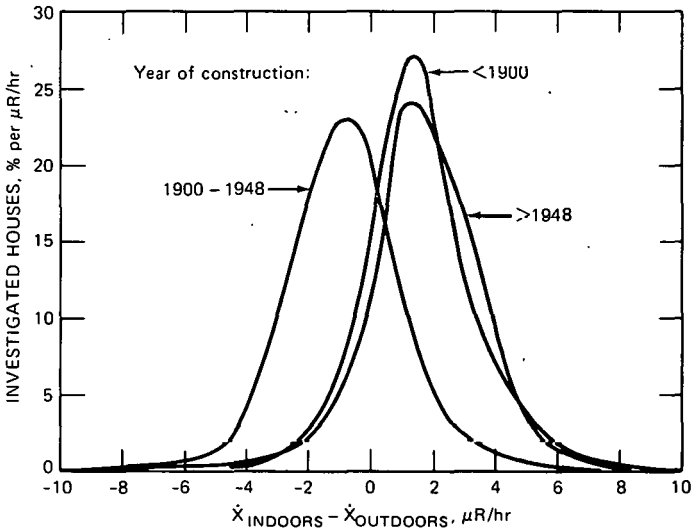


Fig. 8 Frequency distribution of houses of different building periods vs. indoor-minus-outdoor exposure rates.

Apparently the two effects of building materials, i.e., attenuation of and contribution to the ambient exposure rate, are acting in a rather complex manner according to their shielding properties and radioactivity content. This is clearly shown when measurements of the exposure rate of different building materials are compared, as shown in Fig. 9. The measurements were performed with the scintillation dose rate meter introduced into a pile of each material. The data given in Fig. 9 include the environmental radiation, i.e., both the terrestrial and cosmic component, which was found to be 6 μR/hr on the average. Obviously there are remarkable differences in the radiation level up to a factor of approximately 10, e.g., bitumen plates or pumice stones. Of course, these data allow only a comparison between the different building materials but do not represent a direct estimate of the exposure that would be received in dwellings constructed with these materials. However, when the

environmental exposure level is considered, one can conclude that such materials as gas concrete or chalk stone predominantly attenuate the environmental radiation, whereas such building materials as flagstones, bricks, and pumice stones mainly contribute additional radiation.

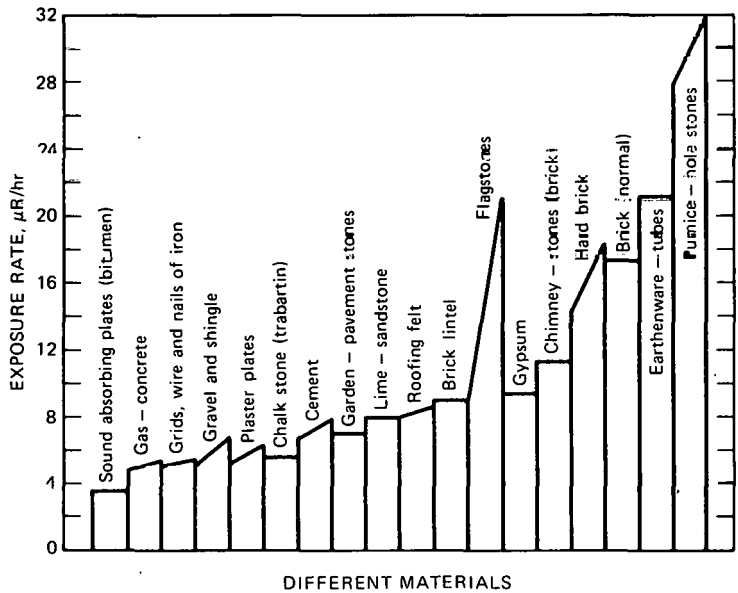


Fig. 9 Exposure rates measured in piles of different building materials. The local environmental (terrestrial and cosmic) radiation level of 6 μR/hr is not subtracted.

The effect of a building material with increased radioactivity concentration on the indoor exposure level can be demonstrated at a house with the highest exposure rate found in Germany, which is situated in Bavaria. The structure, built in 1948, is a normal one-family house with two floors constructed of brick. The owner, who worked in a chemical factory that prepared artificial fertilizers among other products, used scoria from the factory as a filling material for the ceilings. The scoria contains an unusually high activity concentration, probably from radium. This explains the high exposure rates up to about 100 μR/hr, shown in Fig. 10, which reach the maximum values where two ceilings contribute to the radiation level, i.e., on the ground floor. It is remarkable that the annual site exposure reaches an amount of about 1 R for a private dwelling.

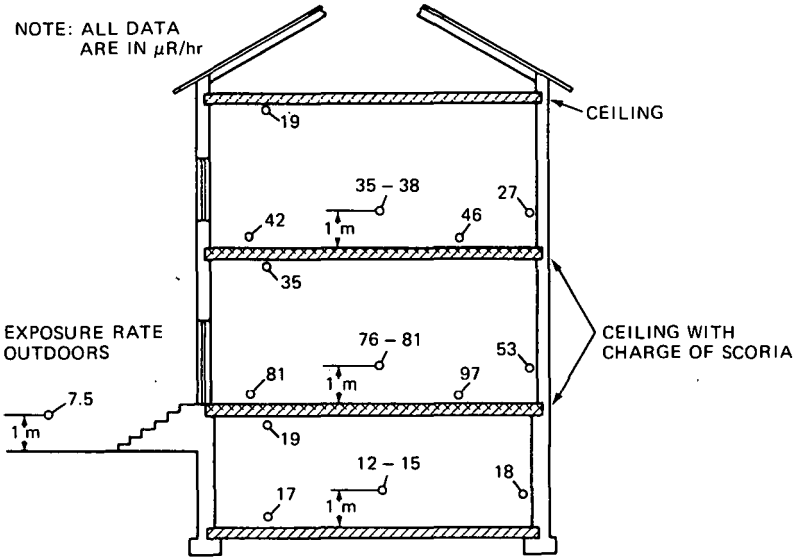


Fig. 10 Exposure rates measured in a private house with unusually high radiation levels.

Figure 11 shows the results of exposure rate measurements carried out with the scintillation dose rate meter in connection with a strip chart recorder while travelling by car on highways in Bavaria. Obviously the registered exposure rates vary within a wide range. The reason for the variation is, however, due more to differences in the radioactivity concentration of the covering material of the highway than to differences in the radiation emitted from soil. This conclusion is trivial since, even with high exposure rates measured on the highway, the exposure rates on both sides of the road in a distance of only a few meters were low again and typical for the local terrestrial radiation level. This explains the fact that the more significant changes in the exposure rate on highways always occur suddenly and in an unpredictable way.

REFERENCES

American National Standards Institute, 1975, *Performance, Testing and Procedural Specifications for Thermoluminescence Dosimetry in Environmental Applications,* ANSI-N545-1975, Washington.

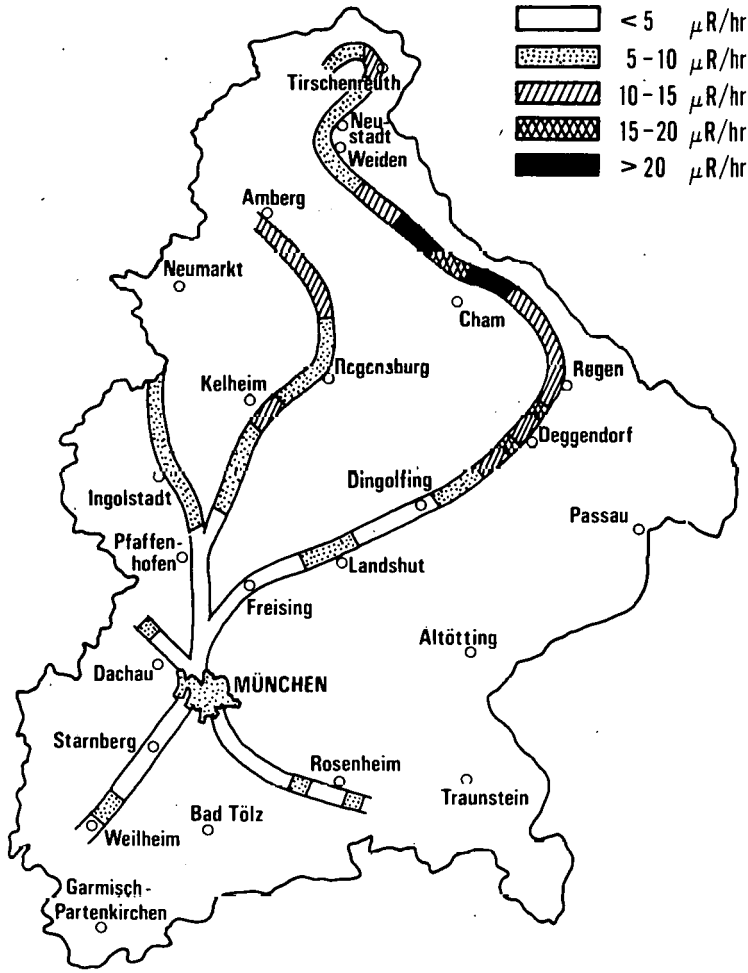


Fig. 11 Changes in exposure rate measured on highways in Bavaria.

Kolb, W., 1974, Die Strahlenbelastung der Bevölkerung in Wohnhäusern, *Jahrestagung des Fachverbandes für Strahlenschutz, Helgoland.*

Kramer, R., D. F. Regulla, and G. Drexler, 1977, TLD Environmental Radiation Monitoring: Processing, Experiences and Data Interpretation, in *Proceedings of the Fifth International Conference on Luminescence Dosimetry,* São Paulo, Brazil, Feb. 14—17, 1977, A. Scharmann (Ed.), Gießen, 1977.

Lauterbach, U., W. Kolb, P. Seyfried, 1970, Ein empfindlicher Dosisleistungsmesser mit Szintillationsdetektor für Strahlenschutzzwecke, *Bull. ASE,* 61: 24.

National Council on Radiation Protection and Measurements, 1975, *Natural Background Radiation in the United States,* Report 45, Washington.

——, 1976, *Environmental Radiation Measurements,* Report 50, Washington.

DISCUSSION

Cook: Have you done ^{222}Rn measurements in the one case with high levels?

Wachsman: We have made some measurements only for orientation. More exact measurements are provided in connection with a program started just recently.

Mjones: Could you comment on the accuracy of your measurements, especially for the mailed thermoluminescent dosimeters (TLDs)?

Wachsman: The overall accuracy of the used TLD was about ±10% maximum and the median error 6%.

Roessler: I have two questions: (1) what is the source of "chemical gypsum" and (2) to what extent is by-product gypsum from phosphoric acid production used in building materials in Europe?

Muth: (1) The so-called "chemical gypsum" is a by-product of phosphate production. Because it is cheaper than material gypsum, it is used more and more for house construction. (2) Professor Wachsmann has pointed out in his paper that the indoor gamma-ray dose rate in houses of the Saerland is the highest in the Federal Republic of Germany. The reason for these findings is that people used stones and bricks from blast-furnace cinder or slags with relatively high ^{226}Ra and thorium concentrations in constructing houses. The Saerland is a small but important coal and steel region of the Federal Republic of Germany, and these stones and bricks are relatively cheap.

Smith: It may be misleading to characterize the radioactive content of a particular class of building material as a single quantity since members in any class will usually show a wide range of variability. For example, you have listed gypsum as having relatively high radioactivity, whereas we have often found this material to be among the lowest in radioactivity when it is a natural mineral material; only the manufactured gypsum contained significant radioactivity. Listing the range of radioelement content is more useful, but, whenever particular cases are studied, the materials actually used in building construction must be measured if any expressed relationship between the construction materials and radiation levels is to have physical significance.

Wachsmann: I agree! The figures given in this paper are only to show what differences occur and their relative values. More exact measurements on radioactivity in building materials are made in Germany by Schmier at the Bundes Gesundheits in Berlin.

Natural Radiation in Japan

SIRO ABE, KAZUNOBU FUJITAKA, and KENZO FUJIMOTO
Environmental Health Division, National Institute of Radiological Sciences, Chiba, Japan

ABSTRACT

In situ measurements of natural terrestrial radiation were conducted during the 11 years from 1967 to 1977 over Japan. An ionization chamber and scintillation survey meters were used. From the data obtained at 1127 sites, the distribution of the level was obtained within a satisfactory accuracy. The average level in Japan was found to be 9.0 μR/hr. Because the mean contribution from cosmic rays was considered to be 3.4 μR/hr, the average level of the terrestrial radiation turned out to be 5.6 μR/hr in Japan.

The results were also interpreted from geological points of view. Rough estimation of the average radiation level in each geological area was made by comparing the survey data with the geological maps. Although the direct effect comes from the surface soil, the gross features of the distribution reflect the characters of the underlying rocks.

Radiation of natural origin at the earth's surface consists of two components, cosmic rays and radiation from the radioactive nuclides in the earth's crust. The latter component, the terrestrial radiation, mainly comes from the so-called primordial radioactive nuclides that were made in the early stage of the formation of the solar system. Nuclides of relatively short half-lives, however, have already decreased sufficiently in intensity that we can ignore them at present. There are fewer than 20 nuclides remaining at present. The ^{238}U series, the ^{232}Th series, and ^{40}K are the main sources. These are liable to be combined with oxygen and are classified into the lithophile elements. Because such components have lower densities, they concentrate in the surface region of the earth. Thus the concentration of the radioactive nuclides in rocks can be estimated by analogy by the amount of silicates, the main component of the crust.

The silicate content of rocks varies considerably according to the type of rock. Generally, igneous rocks contain more silicates than sedimentary rocks, although some sedimentary rocks have a high concentration of silicates, reflecting their formation mechanism. Among the igneous rocks, the highest content can be found in the acidic rocks (SiO_2, more than 66%) and lowest in the ultrabasic rocks (SiO_2, less than 45%). Basic rocks contain an intermediate content (Shibata, 1968).

Granite is a representative acidic rock and is considered to have come from the continental crust. Basalt, a representative basic rock, comes from the crust that formed the bottom of the ocean (Shimazu, 1966). In the general case, basalt on the land surface is brought out as volcanic rocks.

It is well known that almost all the volcanoes in Japan are composed of basalt. Thus the volcanic region in Japan is expected to be basically covered with the rocks that contain less radioactive materials. However, metamorphism and weathering have changed the structure considerably. The pile of volcanic ash and the humus that contains little radioactive material cover the activity of the underlying rocks.

However, the situation may be different for volcanoes that effuse highly viscous lava. Viscosity of lava depends on the concentration of silica in it. Silica-rich lava is viscous and the effusion occurs violently with black smoke. This used to be called Vulcano-type effusion after Mt. Vulcano in Italy; Mt. Usu in Hokkaido Island in Japan belongs to this category.

SURVEY OF THE EXTERNAL RADIATION

A series of field surveys of outdoor exposure rates due to natural radiation throughout Japan was started in 1967 and completed in 1977.

Measurements were carried out at 778 locations, which covers almost all the cities in Japan. Each location involves 1 to 32 observation sites according to the number of inhabitants there. Generally one site was allotted to every 100,000 inhabitants. That is because our ultimate purpose was reduction of population dose due to natural radiation at the domestic level. A total of 1127 sites were involved.

In every site, data were taken at several points (five, in general) which made a figure of a cross. After the extraordinary values were removed carefully, data were averaged to give a representative value of the site. This procedure would decrease the effect of varied

surface conditions in a small plot. Almost all the data were obtained in the daytime.

A plastic ionization chamber and a survey meter were used as the main equipment in this survey. The former is spherical with an inner diameter and wall thickness of 200 mm and 3 mm, respectively. It contains air at 1 atm and is closed.

With regard to energy response, ionization chambers are usually recognized as the most appropriate apparatus for measurement of the external radiation. The drawback is that it requires great care, which restricts the conditions of use. The survey meter, however, can be used under more difficult conditions. To save the excessive time that would be required to use the ion chamber in every case, the survey meter with a 1-in. by 1-in. NaI(Tl) scintillator was used for practical measurements. At 137 sites measurements were made using the chamber and the survey meter simultaneously. Then a collective relation between them was obtained and was applied to every survey meter result, and the corresponding chamber value was calculated. This conversion might have introduced an uncertainty of 5% in standard deviation.

Two additional survey meters, one with a 2-in. by 2-in. NaI(Tl) scintillator and the other with a 3-in. by 3-in. NaI(Tl) scintillator, were used as complementary devices.

Measurements were done in open bare fields of more than 1000 m^2 to avoid the influence of neighboring buildings. The ionization chamber and the smallest meter were set at 1 m above the ground, and the latter was always set horizontally. The survey meter with the 2-in. by 2-in. NaI(Tl) scintillator was set horizontally 30 cm above the ground, and the 3-in. by 3-in. NaI(Tl) scintillator was set horizontally 50 cm above the ground.

To avoid the influence of transient increases of exposure rate due to radon daughters, results obtained in initial periods of rainfall were carefully excluded from the data.

Calibration of the instruments was always carried out in the most neighboring period. The induced uncertainty of the measurements was revealed to be less than 7% as a whole in standard deviation.

Data were classified into four groups and are plotted in Fig. 1. The cumulative frequency distribution of the exposure rates is shown in Fig. 2. The average value was 9.0 μR/hr. The exposure rate in every local administrative area is shown in Fig. 3.

Obtained gamma-ray exposure rates reflect both cosmic rays and terrestrial radiation with a slight contribution from fallout due to nuclear testing. Fallout in Japan was estimated to be 0.2 μR/hr (Okano, 1974) from the data obtained in 1969, 1970, and 1971.

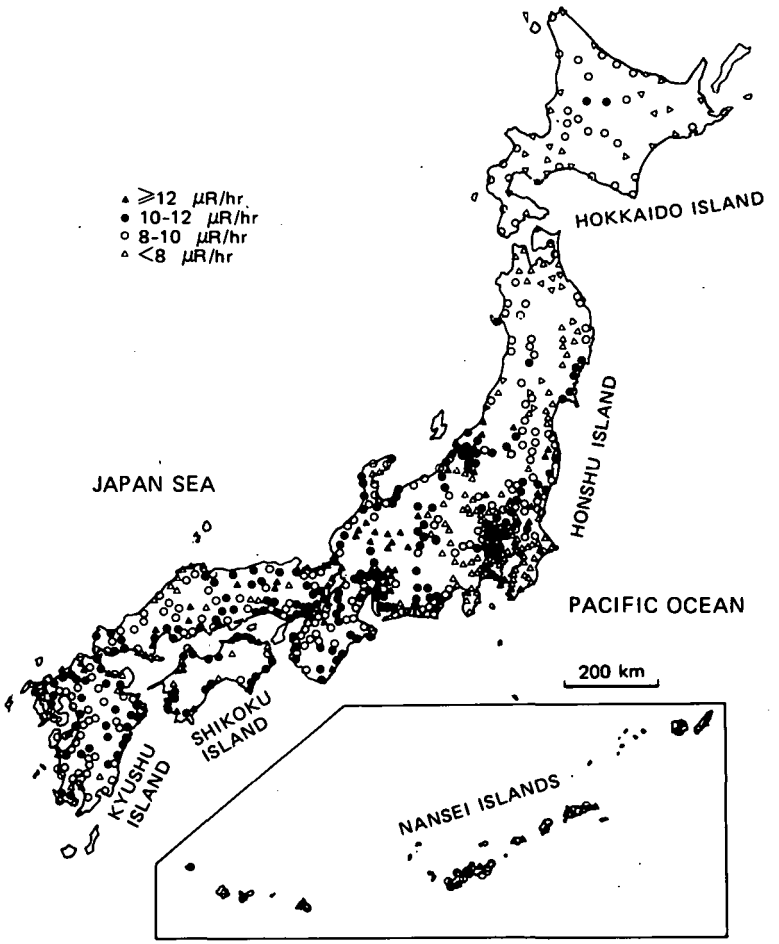


Fig. 1 Distribution of measured exposure rates due to natural external radiation including both terrestrial radiation and cosmic rays in Japan, with values classified into four ranges.

Because the periods of our measurements were chosen to avoid the influence of Chinese nuclear tests, the contribution from fallout to our data seemed to be less than 0.2 μR/hr and was considered negligible in this work.

The intensity of cosmic rays varies temporally according to the variation of the geomagnetic field strength and configuration. Since this series of surveys was conducted during 11 years, it covers almost a whole stage of a solar activity cycle. The contribution from the

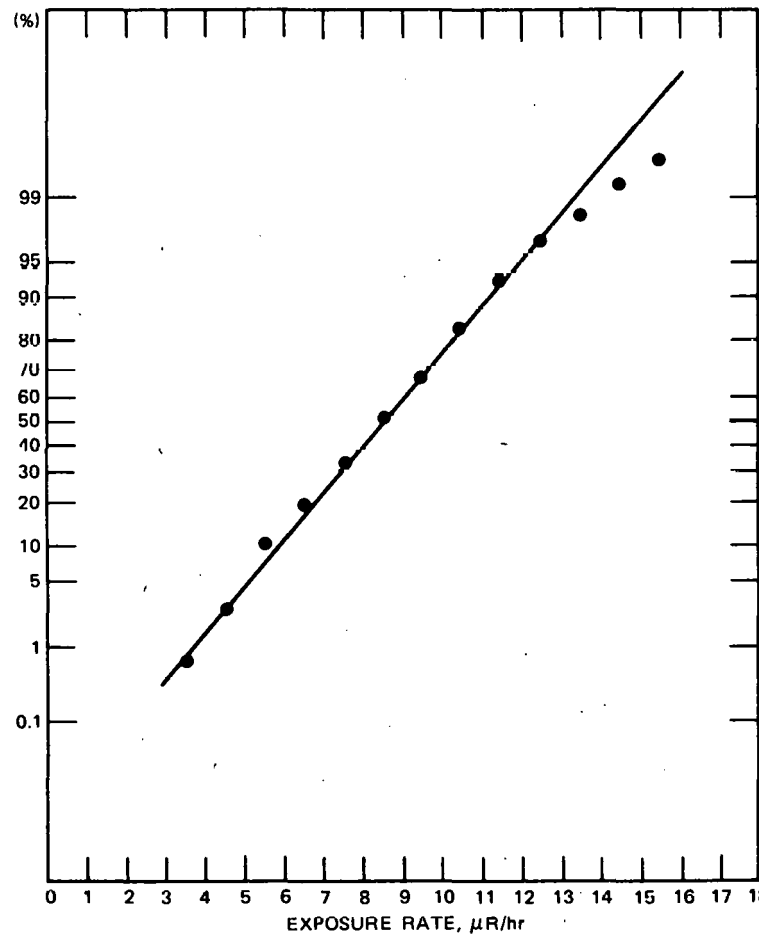


Fig. 2 Cumulative frequency distribution of the exposure rates due to natural external radiation in Japan. Each value plotted in the intermediate point between the exposure rates, a and b, represents the proportion of the data less than b.

solar variation depends greatly on the altitude and is estimated to be less than 20%, a few percent in the usual case, on the ground level. Since Japan is at lower geomagnetic latitudes compared with the United States and European countries, a smaller contribution from cosmic rays is expected. According to the United Nations Scientific Committee on the Effect of Atomic Radiation (1966, 1977) [hereafter referred to as UNSCEAR (1966, 1977)], the exposure rate due to cosmic rays in Japan is about 3.4 μR/hr, which is in good

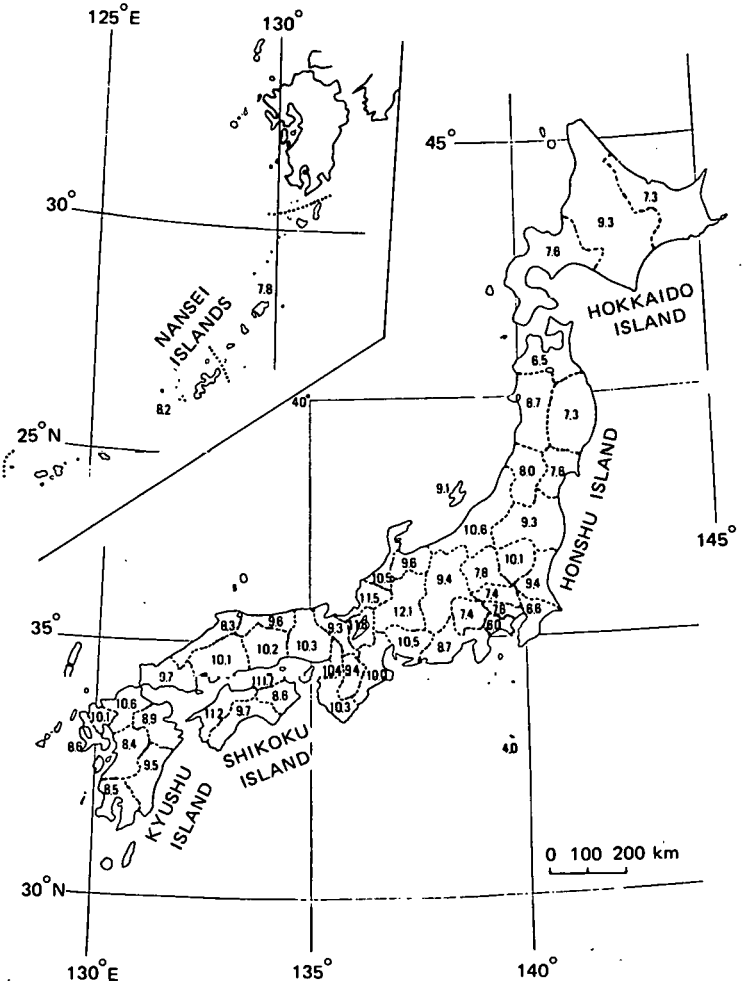


Fig. 3 Distribution of the exposure rates due to natural external radiation in Japan. The average value (in microroentgens per hour) is given in each administrative area except Hokkaido Island and the Nansei Islands where borders are drawn only for convenience.

agreement with the recent study (Nakajima et al., 1978). The strength of the geomagnetic field varies according to the geomagnetic latitude. The total strength of the geomagnetic field varies nearly 10% over the main part of Japan, which results in a difference of only a few percent of the cosmic-ray flux on the surface.

Because the purpose is to know the gross feature of spatial distribution of natural terrestrial radiation in Japan, such a slight difference can be ignored; cosmic-ray intensity was regarded to have a constant value of 3.4 μR/hr over Japan, and the contribution from fallout was neglected. Thus the exposure rate due to terrestrial radiation averaged over Japan was 5.6 μR/hr, which implies an average absorbed dose rate in air of 4.87 μrads/hr.

DISCUSSION

Measurements of the external radiation have been made in many countries by various methods. Estimates of the exposure levels have been done by two different ways, the direct measurement of the field strength and the estimation by analysis of local soil samples. The results and the methods are summarized in UNSCEAR (1977).

Figure 4 shows the frequency distribution of the absorbed dose rate in air. Figure 4(a) indicates the distribution as given in Fig. IV of UNSCEAR (1977), with the extraordinary high-level regions in Italy removed. Figure 4(b) indicates our new result in Japan. UNSCEAR (1977) suggests 4.5 μrads/hr as an average exposure rate all over the world, and this value comes to the annual absorbed dose of 39 mrads. However, our new data imply 42.7 mrads. Such difference will be explained by the condition whether it is a continent or an island, old or new.

Japan was divided into several hundred 30-km meshes, and all the data were averaged in every mesh to give a representative value for each of them (Fig. 5). But, the region of the Nansei Islands was excluded because of the small size of the islands. In Fig. 5 the representative values are classified into two groups, one for the values which equal or exceed the averaged abosorbed dose rate and the other for the values below it. In the blank meshes, measurement has not been done because of traffic difficulties.

As a general tendency, Southwest Japan has larger values compared with Northeast Japan. These two regions seem to be divided by the major tectonic line, Itoigawa-Shizuoka Line (discussed later). However, it is not clear whether the other major tectonic line, Central Tectonic Line (discussed later), divides eastern Japan into two parts because of the lack of data.

It is well known that the terrestrial radiation originates mostly in the surface soil. The thickness of the soil layer which contributes to the external radiation is estimated to be about 30 cm. Because most surface soil in Japan is considered to have come from the weathering of the rocks, the nature of the rocks seems to be the basic factor that determined the terrestrial radiation strength.

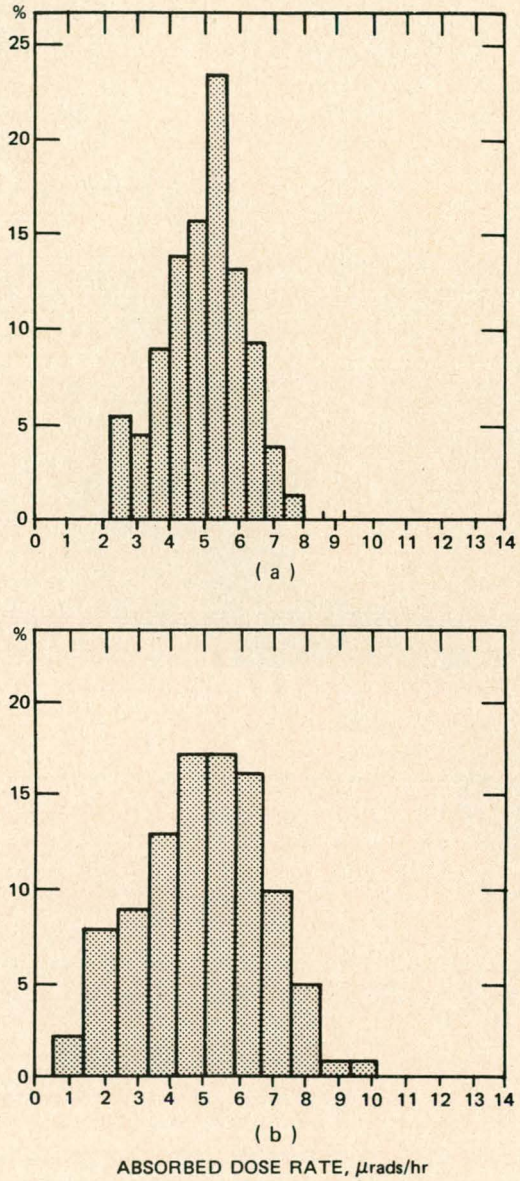


Fig. 4 Frequency distribution of the absorbed dose rate in air. Figure 4(a) indicates the population-weighted average of four countries: the Federal Republic of Germany, Italy, Japan, and the United States (UNSCEAR, 1977). Figure 4(b) indicates the newly obtained distribution in Japan.

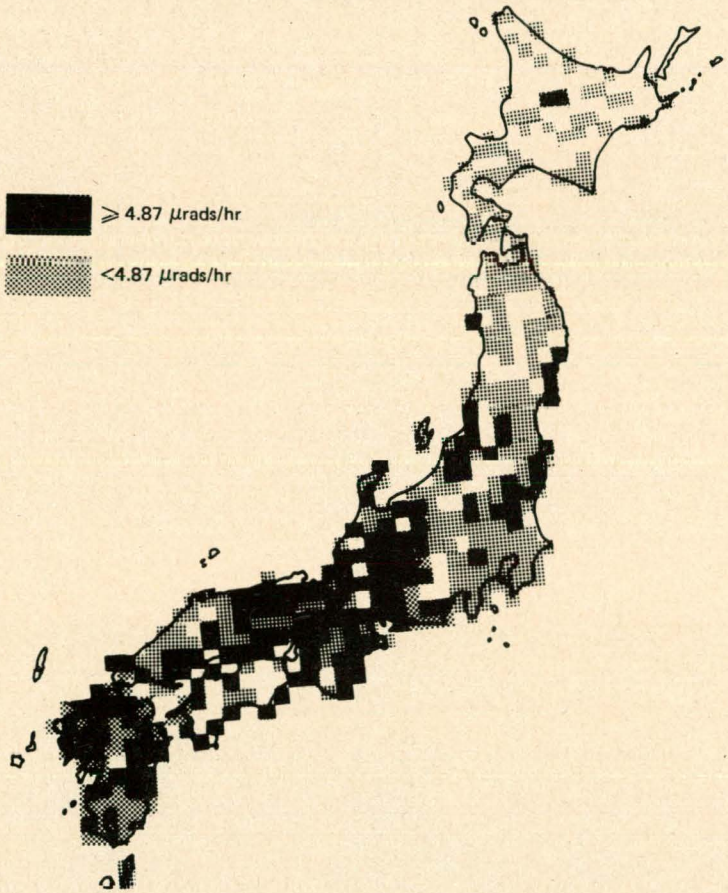


Fig. 5 Distribution of the absorbed dose rate due to terrestrial radiation in Japan. The average level in each 30-km mesh area is shown by shading.

The distribution of the various kinds of rocks is characterized by the metamorphic zone. In each metamorphic zone, rocks have a common feature in the components and the structure. Thus the systematic correlation can be anticipated between the distribution of the terrestrial radiation strength and that of the metamorphic zones. The metamorphism accompanied the tectonic movement which transported and redistributed the rocks on the surface of the earth. This means that the distribution of the metamorphic zones in Japan reflects the geological history of the islands of Japan.

In each of the representative metamorphic zones in Japan (The National Atlas of Japan, 1977), the average terrestrial radiation level was obtained as is shown in Fig. 6. The exposure rates in the region vary from 3 to 7 μR/hr, and the higher values were obtained in the Tamba-Mino Belt, Ashio Belt, and Ryoke Belt, for example, which are in Southwest Japan. The lower values were obtained in Green-Tuff Belt and Kurile-Islands Arc which are the volcanic regions in Japan.

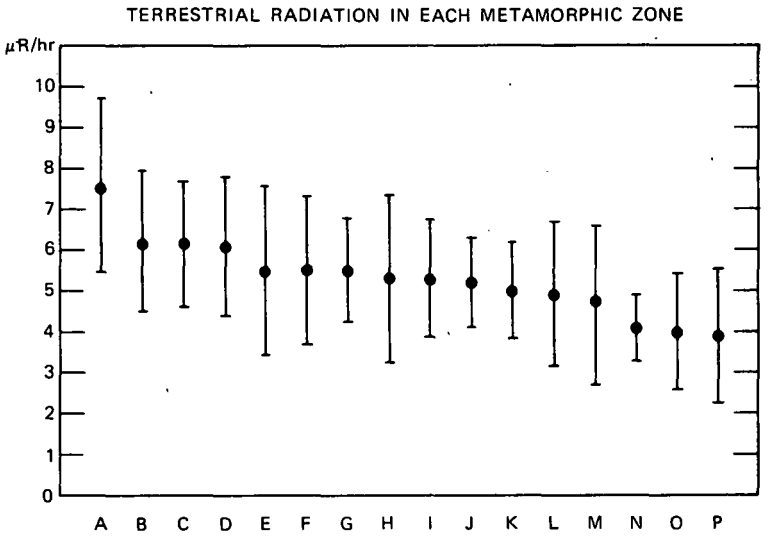


Fig. 6 Average level of terrestrial radiation in each metamorphic zone in Japan. Dots indicate the means, and the bars indicate the standard deviations. A,Tamba-Mino Belt and Ashio Belt. B, Ryoke Belt. C, Sangun Belt and Jyoetsu Belt. D, Uetsu Folded Belt. E, Southern Shimanto Belt. F, Northern Shimanto Belt. G, Abukuma Belt. H, Southern Kitakami Belt. I, Chichibu Belt. J, Hidaka Unmetamorphosed Belt. K, Hidaka Front Belt. L, Green-Tuff Belt. M, Sanbagawa Belt. N, Kurile-Islands Arc. O, Kitakami Eastern Front Belt. P, Northern Kitakami Belt.

The gross feature can be seen clearly when the zones are classified into two groups according to whether the average strength in a zone is greater than 5.6 μR/hr, which is the average value of all Japan (Fig. 7). The backbone area of Southwest Japan can be seen to have higher values and is surrounded by the regions of lower values. The region of such a structure is discussed below.

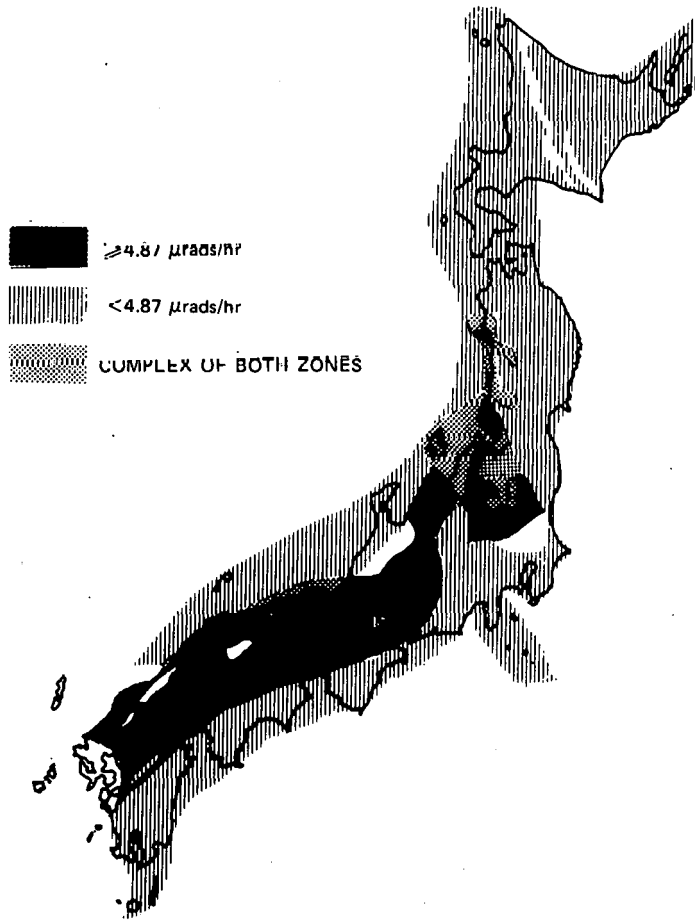


Fig. 7 Distribution of the absorbed dose rate in air due to natural terrestrial radiation in Japan. The average level in each metamorphic zone is shown by shading.

The Region of Higher Radiation Level

Figure 8 indicates the distribution of granitic rocks in Japan (The National Atlas of Japan, 1977). Both of the great tectonic lines are also shown. The granitic rocks in Southwest Japan are distributed as if they are bounded by the tectonic lines. The exposure to the surface of the granitic rocks, which were originally plutonic rocks, is considered to be brought about by the folding motion due to the pressure of the northern continent and the following erosion of the

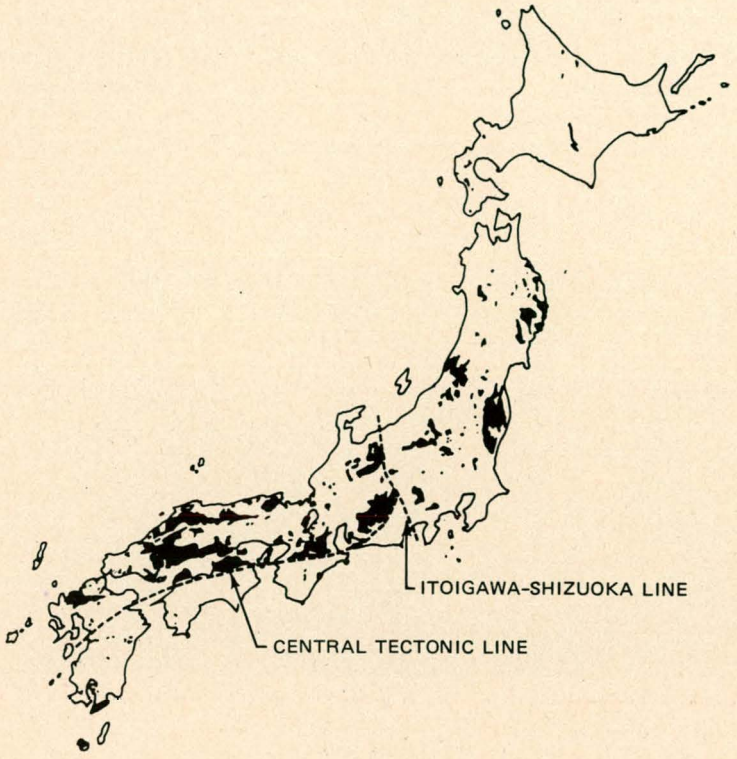


Fig. 8 Distribution of granitic rocks in Japan. Two major tectonic lines are also shown.

upper layer. As the expansion coefficients of the mineral contents in granite are widely different, granitic rocks can be easily weathered to form soil, and this results in the higher radiation level on the surface.

Comparison of Figs. 7 and 8 shows a good coincidence as to the higher exposure rate region in Southwest Japan. However, the regions in Northeast Japan, on the Pacific Ocean side, show rather a low radiation level. This can be explained as follows. The metamorphic zones that covered such northeast granitic regions stretched from the coast of the Pacific Ocean to the coast of Japan Sea across Honshu Island. And the western part of the granitic regions were covered with the Cenozoic volcanic deposit which shielded the terrestrial radiation; this should have reduced the average value of the field strength in such zones. In addition, the coarseness of the observational mesh might have missed the character there.

The Region of Lower Radiation Level

The region that indicates a lower radiation level than the average can be divided into two different areas: the volcanic area and the alluvium or diluvium area.

Volcanoes in Japan are distributed along the whole coast of Japan Sea; in addition a belt extends toward the Izu Islands from the coast of Japan Sea across central Japan (Fig. 9). In Japan effusive

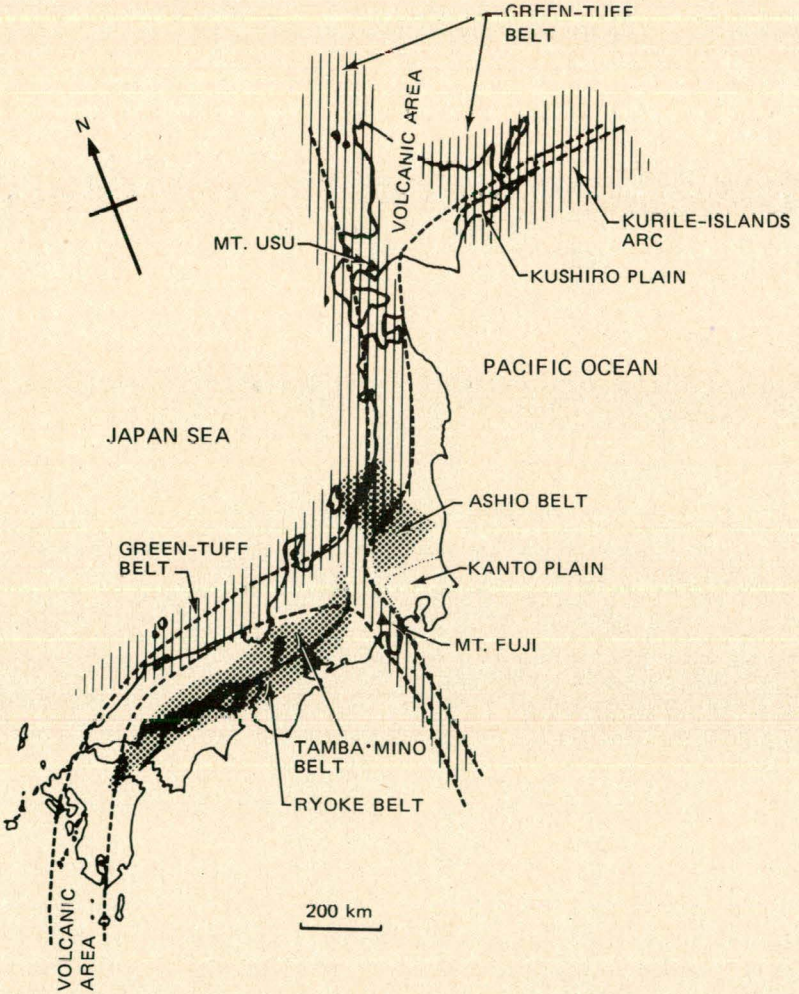


Fig. 9 Map of the volcanic area and the major metamorphic zones. The representative metamorphic zones which indicate the higher natural terrestrial radiation level are shown with dots. The representative zones which indicate the lower level are shown with stripes.

rocks from the earth's interior are essentially basaltic, which should give the low-level terrestrial radiation. Although the data were obtained at only one island among the Izu Islands, the distribution of the low-level terrestrial radiation corresponds well to that of volcanoes as a whole.

The other low-level area seems to extend along the Pacific Ocean. Actually, Kanto Plain and Kushiro Plain, for example, are the alluviums made in the Quaternary Period. These are covered with the thick layer of volcanic ash origin (the thickness came to several tens of meters) and have a little radioactive material. The southernmost area of Kyushu Island and other Pacific Ocean coast areas also have similar volcanic effusion materials.

CONCLUSION

The basic feature of the terrestrial external radiation is determined by the nature of the underlying rocks. But the direct effect is brought about from the soil which came from the weathering of the rocks. In Japan the average radiation level in the region of the soil (The National Atlas of Japan, 1977) which came from the granitic rocks indicated 6.5 μR/hr, and t at of the soil which came from the volcanic effusion indicated 4.2 μR/hr. Comparison of the average radiation level in the volcanic rock regions of the Tertiary Period and the Quaternary Period (The National Atlas of Japan, 1977) has revealed that the former has an average of 8.2 μR/hr and the latter has an average of 5.5 μR/hr. It may be a result of the fact that the degree of weathering depends on the length of the term. But it should be mentioned that the values given above are quite rough estimates and should be used only in the relative comparison.

Detailed discussion of the real environment, however, requires consideration of the land surface, knowledge about the actual composition of the soil, and the effects of artificial environments. Soil samples were collected from all the locations of our measurements, which are now being prepared for analysis. As to the influence from artificial environments, a study of building materials (including roads) will be the urgent problem.

In addition to these, the time variation of the exposure rate due to the change of meteorological conditions had to be considered. In this case the local time of the observation is an important problem. Analysis of the correlation among the external radiation level and meteorological factors has been done by us. However, it seems that the above results will not require a great change so far as the gross feature is concerned because most of our measurements were made only in the daytime.

Geological and geophysical considerations will be a great aid in estimating the background radiation level before the actual measurement.

ACKNOWLEDGMENTS

We thank Dr. Ryushi Ichikawa, Head of the Environmental Health Division, National Institute of Radiological Sciences, for his continuous encouragement on the survey and his useful discussions and suggestions and other members of the Institute for their support in many fields. We also thank people outside the Institute who offered access and assistance.

REFERENCES

Nakajima, T., and Environmental Radiation Study Group, 1978, *Measurement of Ionizing Component Due to Cosmic Rays at Wakasa Area*, Preprint for Japan Health Physics Society, 13th Scientific Meeting, Tohkai, Ibaragi.

Okano, M., 1974, Variation of External Radiation, in *Methods and Techniques for Measurement of Environmental Radiation*, Symposium Proceedings, National Institute of Radiological Sciences, Chiba.

Shibata, H., 1968, *Magazine of Rocks in Japan* (in Japanese), 1st ed., separate volume, page 4, Asakura-Shoten, Tokyo.

Shimazu, Y., 1966, *Physics of the Earth's Interior* (in Japanese), 2nd ed., Shoka-Bo, Tokyo.

The National Atlas of Japan, 1st ed., 1977, Geographical Survey Institute, Ministry of Construction, Tokyo.

United Nations Scientific Committee on the Effect of Atomic Radiation, *A Report of the United Nations Scientific Committee on the Effect of Atomic Radiation*, 1966, United Nations, New York.

——, 1977, United Nations, New York.

Natural Radiation Measurements and Interpretation of Their Results in Terms of Dose to Population

T. NIEWIADOMSKI, J. KOPERSKI, and E. RYBA
Institute of Nuclear Physics, Kraków, Poland

ABSTRACT

Doses to populations calculated on the basis of experimental natural radiation data can differ substantially if measurements are made using different methods. To investigate this problem, we measured personal, indoor, and outdoor exposures at 22 locations (weather stations) by means of thermoluminescent cards during four 3-month periods and checked them several times using a pressurized ionization chamber. The personal doses were found to be closer to indoor than to outdoor exposures. Indoor exposures were highly influenced by building materials (wood, red bricks, prefabricated elements and slag). The fluctuations with time were higher in open air than indoors, whereas the differences between the local average exposures were lower outdoors than within the buildings. It was concluded that the results of measurements in the open air cannot be used for estimating actual doses to population and that the results of momentary dose rate measurements are less reliable for this purpose than the results of long-term integrating methods.

Doses received by individuals and populations from natural ionizing radiation sources can hardly ever be measured directly, e.g., by personal dosimeters. The doses are usually estimated on the basis of measurements carried out using different methods and the measurements usually differ, depending on the method applied and on season and place of measurement.

Three principal techniques have been used for this purpose up till now:

1. Momentary dose rate measurements.
2. Integrating measurements.
3. Calculations based on the spectrometric soil analyses.

Momentary dose rates are measured by means of pressurized ionization chambers, scintillation counters, and, in some cases, by Geiger-Müller counters. This technique is sometimes used in combination with portable recorders mounted on aircraft or cars, which enables us to perform continuous recording of dose rates over large areas.

Integrating measurements are now becoming popular because recently new sensitive and stable detectors have been developed. Here thermoluminescent (TL) detectors have demonstrated their particular usefulness. The integration can also be made mathematically using dose rate curves registered over prolonged time periods.

The data for calculation of dose rates outdoors and indoors are taken from spectrometric analysis of natural and artificial radionuclide contents in the upper layer of soil or in construction materials. Several equations and calibration factors have been derived and computer programs developed, which enable us to obtain dose rates in 2π or 4π geometries.

It is a trivial statement that results of any technique or method should give comparable results. Comparability is at present an important requirement because environmental radiation studies are carried out on an ever increasing scale in several countries. Recent international comparisons of dosimeters used for this purpose (Gesell, Burke, and Becker, 1976; Burke, Gesell, and Becker, 1976) can be of use only for checking integrating dosimeters. Other methods must be compared in a different way, e.g., by measuring doses or dose rates simultaneously using different methods and by studying differences between respective values. Results of an investigation, which may be considered to be the first step in this direction, are given in the following sections.

EXPERIMENTAL PROCEDURE

The following measurements were undertaken in a rural region at 22 different points (based on the weather station network) in southern Poland to study particular attributes of the techniques used most frequently for population-exposure estimates. At every measuring point the following types of measurements were performed throughout 1 year:

1. Three months' exposure, by means of TL cards worn by one or two inhabitants living in the monitored house next to the meteorological instrument shelter. These measurements are labeled PERS in this paper.

2. Three months' exposure by means of three separate TL cards located in the dwelling houses, IND; outdoors, OUT; and in the meteorological instrument shelter, SH.

3. Momentary exposure rates, every 6 weeks, in the dwelling houses, in the open air, and at the shelter, by means of a high-pressure ionization chamber. The measurements are denoted similarly, i.e., IND, OUT, SH.

The TL measurements were based on the Automated TL System Model 748 described by Daszkiewicz and Niewiadomski (1974). The system consists of a reader and KD-75 type dosimetric cards. Each card is provided with an identification number and contains three LiF detectors regarded as a single dosimeter since the reader calculates the mean value for three detector readings. For the exposures the cards were placed in two types of badges: personal badges, which protect the cards against harmful environmental factors, assure secondary electron equilibrium, and can be easily fastened to clothing; and field badges, made of 2-mm-thick, hard polyvinyl chloride (PVC) welded tightly into 0.1-mm hard plastic foil. The badges of the latter type were used in both outdoor and indoor TL measurements.

The ionization chamber was a portable steel bottle, of 5-liter volume, filled with argon at 35 atm. The bottle, a duplicate of the one developed by Pernsko, Mamont-Cieślak, and Wardaszko (1969), is placed in a 1.5-mm-thick aluminium shield. The shield is isolated with respect to the bottle, which in turn constitutes an external electrode operating at +85 V. The internal electrode mounted in a Teflon insulator is at ground potential. The leakage current is about 10^{-14} A, and the signal at 5 μR/hr exposure rate is about 10^{-13} A. The signal, i.e., the charge collected on the input capacity, was measured by a Vakutronik VAJ-51 type electrometer. Both the electrometer and the chamber can be powered from the mains or from a 12-V battery.

The chamber was calibrated with a ^{226}Ra source in the Dosimetry Department of the Central Laboratory for Radiological Protection (Gwiazdowski et al., 1974).

Every 6 weeks the measuring team made a 5-day tour to measure exposure rates with the ionization chamber. On every other tour the TL cards were replaced. The measuring team that distributed the cards also noted relevant information on exposure conditions, especially those which could affect the results. Two batches of dosimetric cards, each containing 120 cards, have been applied alternately. Before use, each batch was cycled through the

reader,* annealed at 80°C for 17 hr, and then divided into two parts. One hundred cards intended for measurements were inserted into badges, while the rest, assigned for calibration, were stored for three months in a lead shield where the average exposure rate is 2.5 ± 0.3 μR/hr.

All measurement points at every station were selected very carefully. Each indoor thermoluminescent dosimeter (TLD) was located in the middle of a living room just below the table top. The outdoor TL badges were attached to tree trunks 10 to 30 m from the dwelling house and 2.5 m above the ground. The in-shelter badges were placed horizontally near the rear wall, in a manner similar to that used in a parallel program (Niewiadomski and Ryba, 1977). The distances between outdoor and shelter locations were 150 to 250 m, but in one case, 1500 m. The ionization chamber measurements were made as close as possible to TLD locations. The personal badges were worn on a belt and kept in the users' bedrooms at night. We must note with approval that the monitored people treated their obligations very seriously.

The cards were evaluated immediately on return. The calibration method and calculations relating dosimeter responses to exposure rate units with all correction factors have been described by Niewiadomski and Ryba (1977). We decided to express the results in μR/hr, although the genetically significant or somatic dose should be given in absorbed dose or dose equivalent units. We think the exposure units are easily comparable and can form a basis for further calculations of the desired units by applying simple and familiar calculation factors.

It was quite clear even before measurements were commenced that differences in doses to be detected were to be small, therefore measurement accuracy has had to be high. An assessment of TLD measurement errors was made (Niewiadomski and Ryba, 1977), and measures were undertaken to keep the errors as low as possible. It was found that the overall statistical errors, sensitivity spread of the cards, reader instability, background fluctuation of the cards, and fading of response are ±6% at 95% confidence level and that the systematic errors due to the uncertainty of calibration exposure and differences in calibration and field exposures were of the same order, i.e., also ±6%.

*The final readout temperature of 300°C removes almost all residual electrons from the traps, whereas natural cooling assures reproducible sensitivity.

As far as the ionization chamber errors are concerned, it is assumed that the following groups of error sources influence the accuracy and precision.

1. Physical and dosimetric properties of the chamber.
2. Stability of the electrometer.
3. Scrupulousness of the measurement team.

To the first group of error sources belong anisotropy of chamber sensitivity, energy dependence of its response, leakage current, and its susceptibility to environmental agents. Among the environmental agents, humidity has the strongest influence on the chamber signal. If relative humidity does not exceed 80%, errors in the chamber current are less than ±10% on the 300 mV electrometer range. During rainfall the errors are usually considerably higher. Temperature and atmospheric pressure variation affect the useful signal very little.

The stability of the electronic device has been rated by the electrometer producer at ±2% of the range of interest. Owing to a built-in voltage stabilizer, the output signal error was contained within the ±2%.

The errors committed by the operator do not exceed ±1% and are only time measurement errors.

Finally, the errors of chamber measurements can be estimated to be no higher than ±12% at the 2σ confidence level.

RESULTS AND DISCUSSION

Data were collected in the course of 1 year, therefore we can discuss differences between results obtained by two techniques as well as time fluctuations of exposure rates at every location.

The basic results of measurements are collected in Fig. 1, where fluctuations with time and location as well as differences between IND, OUT, SH, and PERS exposures are shown. The ends of vertical bars represent maximum and minimum quarterly data for any particular type of measurement.

All the data are horizontally divided in accordance with the type of construction material used in the monitored dwelling and are divided vertically according to the type of measurement made at every location. We had encountered four kinds of building materials, i.e., wood (W), prefabricated elements (P), red brick (B), and slag (S).

We can see in Fig. 1 that the highest seasonal fluctuations appeared outdoors (OUT and SH points), and the lowest ones

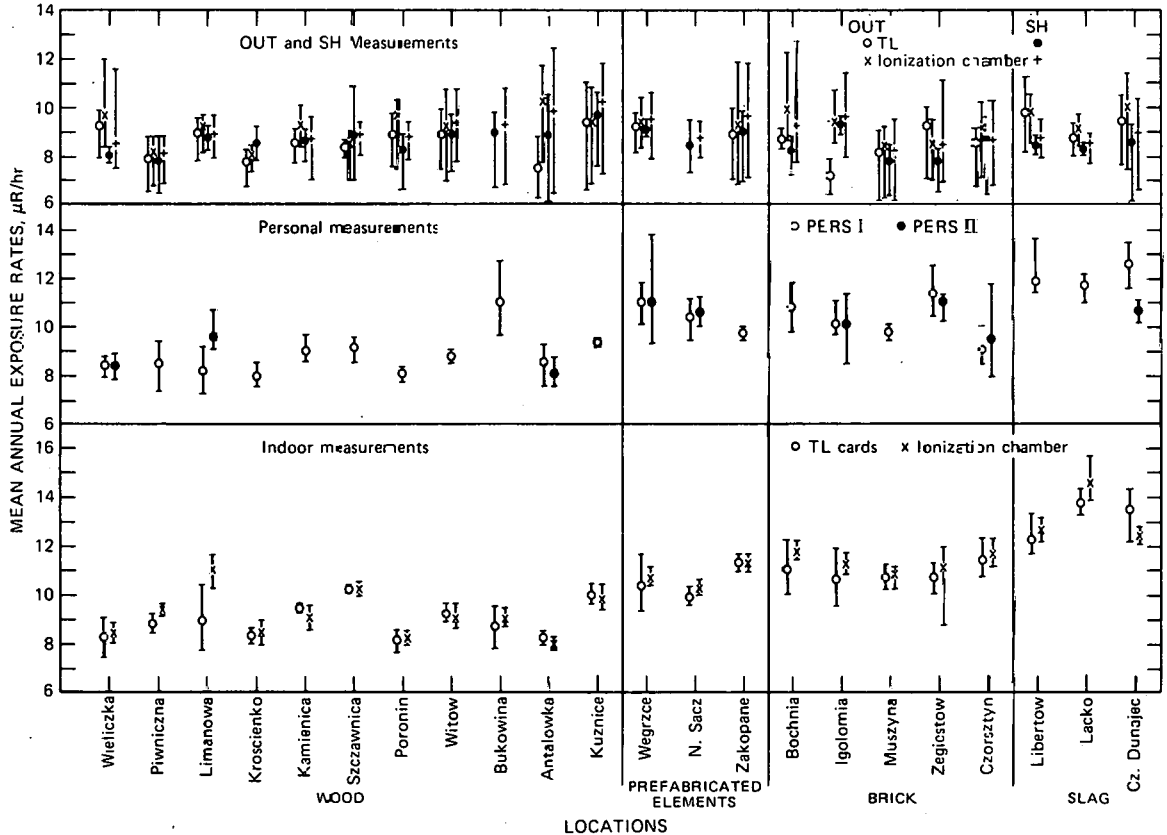


Fig. 1 Fluctuations with time and location of mean annual exposure rates.

appeared indoors (IND). This could be expected since the indoor exposure rates are due to radiation from building materials to a higher degree than to soil radiation that is strongly influenced by soil water. The values of personal exposures followed the indoor exposure rates rather than those measured in the open air.

There were also differences between chamber and TL measurements. The differences are more pronounced outdoors than indoors. Chamber OUT data exceed TL data by about 5%, whereas IND data from both devices are nearly equal (a difference of only 1%). These differences were due to a susceptibility of the chamber to environmental conditions, such as higher humidity and temperature variations outdoors, and to time fluctuations of the exposure rate, higher in the open air than indoors. Chamber outdoor measurements exhibit a higher dispersion in comparison with TL outdoor data. Compared with outdoor doses, both chamber and TL doses are evidently less scattered.

In Fig. 2 we see that indoor exposures in houses made of slag, red brick, prefabricated elements, and wood exceeded outdoor exposures by 55, 30, 20, and 3% respectively. Thus in wooden houses the exposures were nearly equal to those outdoors.

Personal doses, PERS, of people living in houses made of slag, red brick, and prefabricated elements exceeded outdoor exposures by 40, 20, and 20%, respectively. This difference was about 1% for people living in wooden houses.

CONCLUSIONS

The following conclusions can be drawn from this research:

1. Results of measurements in the open air cannot be used for estimating actual doses to population. Errors in this estimation are especially high for people living in modern, multifloor apartment houses.

2. Although in most cases the indoor doses are somewhat higher than the personal ones, they approximate well the doses to individuals and, consequently, to the population. The indoor measurements seem to be very fruitful in performing large-scale monitoring of population doses in chosen locations. Here the TL dosimeters seem to be especially useful.

3. Dosimetric devices must be carefully calibrated (an important but difficult enough procedure). If indeed they are, the results obtained using either method were satisfactorily comparable in indoor measurements, whereas open-air measurements gave, as a rule, different results.

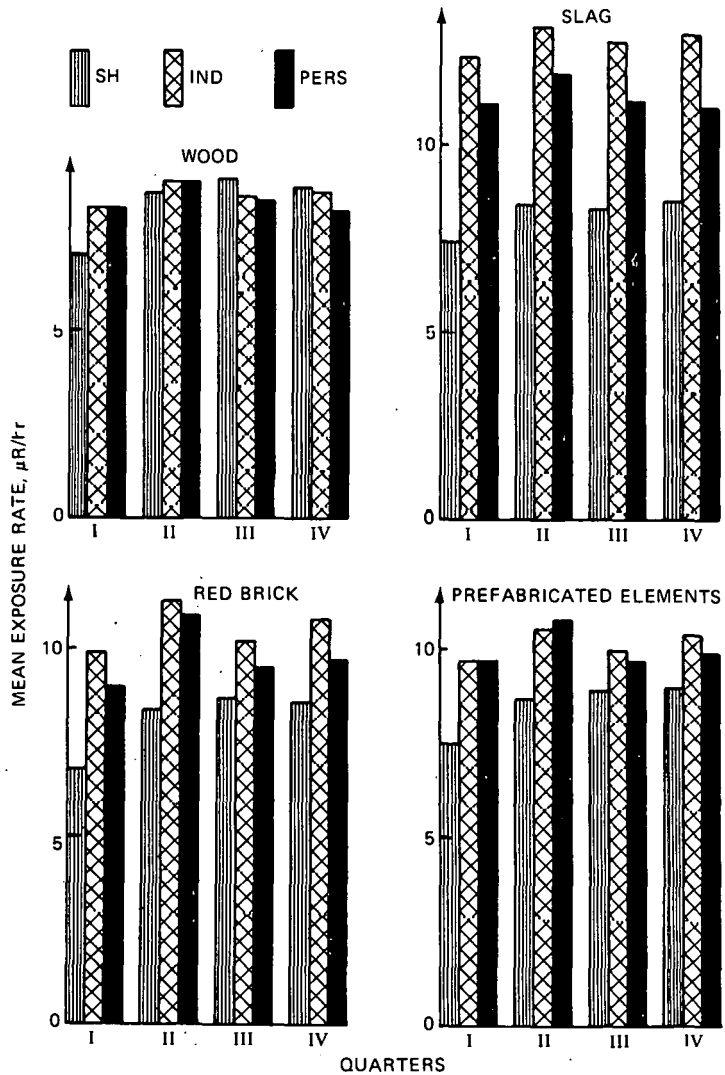


Fig. 2 Differences in results obtained from various types of measurements (TL measurements only).

4. The TL dosimeters are easier to distribute indoors than in the open air where they have to be protected against theft.

5. Organization and psychological obstacles may severely limit large-scale measurements.

6. Using an ionization chamber, it is possible to perform measurements fairly quickly at a large number of sites. But it is

necessary to repeat them several times in each point to average the dose rate fluctuations, especially as far as open-air measurements are concerned. Due to the good stability of the indoor radiation field, chamber results obtained indoors by a skilled operating team can be extrapolated without significant errors to doses to the population.

The preceding conclusions have been drawn on the basis of measurements performed in a rural region, where people spend comparatively more time outdoors than people in town and where the open-air radiation fields are more natural, i.e., not disturbed by pavements or closely located buildings. We may argue that the reservations found occur even to a higher degree in towns; even more if we consider some of the new materials used by the building industry, which contain more radioactivity than traditional materials. Therefore application of the best measuring methods for estimating population doses from the environment in towns, and their correct interpretation, are indeed very important problems.

ACKNOWLEDGMENT

Research sponsored by the International Atomic Energy Agency under contract No. 1767/RB.

REFERENCES

Burke, G. de Planque, T. F. Gesell, and K. Becker, 1976, Second International Intercomparison of Environmental Dosimeters Under Field and Laboratory Conditions, in *Natural Radioactivity in Man's Environment*, Symposium Proceedings, Saratoga Springs, N.Y., Oct. 11, 1976, pp. 554-575; also in *Health Phys.* (in press).

Daszkiewicz, O. K., and T. Niewiadomski, 1974, Programme of an Environmental Dose Survey in Poland Utilizing the Automated TL System, in *Fourth International Conference on Luminescence Dosimetry*, Conference Proceedings, Kraków, Poland, Aug. 27—31, 1974, T. Niewiadomski (Ed.), Report CONF-740833-P2, pp. 713-725, Institute of Nuclear Physics.

Gesell, T. F., G. de Planque Burke, and K. Becker, 1976, An International Intercomparison of Environmental Dosimeters, *Health Phys.* 30: 125-133.

Gwiazdowski, B., J. Pełsko, J. Jagielak, M. Biernacka, and K. Mamont-Cieślak, 1974, Environmental Gamma Radiation Measurements in Nuclear Power Station Siting Studies in Poland, in *Environmental Surveillance Around Nuclear Installations*, Symposium Proceedings, Warsaw, 1973, pp. 89-105, STI/PUB/353, International Atomic Energy Agency, Vienna.

Niewiadomski, T., and E. Ryba, 1977, Rozkład Mocy Dawek Promieniowania Naturalnego w Polsce, INP Raport 960/D, Institute of Nuclear Physics, Kraków, Poland (in Polish).

Pełsko, J., K. Mamont, and T. Wardaszko, 1969, Pomiary Promieniowania Jonizującego, w Niektórych Budynkach Mieszkalnych w Polsce, CLRP Report CLOR-73/D, Central Laboratory for Radiological Protection, Warsaw Poland (in Polish).

DISCUSSION

Tanner: Did you compare data for persons living in multifloor houses with those living in single-floor houses of the same type, particularly wooden houses? Would you expect persons spending more time on upper floors to receive somewhat less radiation exposure than those in single-floor houses?

Koperski: No, I didn't, because all houses monitored were single-floor ones. Concerning the second question: Yes, I would, but this difference, if it exists, is very small, especially in wooden houses. In case of houses made of other materials, the difference might be more distinct because of a stronger screening capacity of the gamma radiation from the soil.

Measurement Program of Natural Radiation in France: Description and Preliminary Results

JEAN-MARIE GUEZENGAR, CLAUDE MADELMONT,
and ANDRÉ BOUVILLE
Commissariat à l'Energie Atomique, Fontenay Aux Roses, France

ABSTRACT

The Commissariat à l'Énergie Atomique has undertaken a program for measuring natural radiation levels which is expected to gradually cover the territory of metropolitan France. The measurements have thus far dealt essentially with external irradiation. A preliminary experiment was conducted to determine the type of dosimeter to be used in the national survey and to study the influence of the seasonal variations, the duration of exposure, and the sampling height. On the basis of the results obtained, it was decided to use $CaSO_4$/Dy dosimeters that would be exposed for 2 to 6 months at a height of about 1 m above the ground level.

During another experiment, about 300 dosimeters were placed for 3 months in various locations in the Paris area. The arithmetic averages of the terrestrial absorbed doses were found to have the same value both outdoors and indoors (43 mrads/year), but, owing to the influence of building materials, there is a greater variability inside dwellings than outside. The measurement program proceeded with the setting up, in the Yonne department, of about 500 dosimeters distributed half indoors and half outdoors. The arithmetic averages of the terrestrial absorbed doses indoors and outdoors were 61 and 51 mrads/year, respectively. The highest doses were measured in the southeast areas of the department, which lies next to an important granitic formation.

With regard to internal irradiation, analyses of natural radionuclides in flour samples originating from 10 regions have been carried out since 1973. The ^{226}Ra concentrations were found to vary from 0.3 to 4.5 pCi/kg. It is intended to complement the survey with measurements of short-lived ^{222}Rn decay products in dwellings.

A measurement program of natural radiation in France was undertaken by the Commissariat à l'Energie Atomique (CEA) in 1975.

The measurements have thus far dealt essentially with external irradiation. During a preliminary experiment the material expected

to be used in the national survey was tested. The experiment, which lasted 1 year, enabled us to compare the results of two types of thermoluminescent dosimeters, $CaSO_4$/Dy and LiF, and also to give an estimate of the uncertainties that result from climatic variations, from the duration of exposure, and from differences in the sampling height. During another experiment, about 300 $CaSO_4$/Dy dosimeters were exposed for 3 months in a number of locations in the Paris area. The Yonne department was then surveyed during 1977 by means of 510 dosimeters equally distributed indoors and outdoors.

The program of measurement of external radiation is complemented by analyses of ^{226}Ra and other natural radionuclides in samples of flour originating from various areas in France. Finally the short-lived decay products of ^{222}Rn will be measured in dwellings with a device that is being developed at CEA.

MEASUREMENT PROGRAM OF EXTERNAL IRRADIATION

Comparative Study and Reliability Tests

A preliminary experiment consisted in exposing 40 LiF and 240 $CaSO_4$ dosimeters in 11 locations for 2, 4, and 6 months. The dosimeters were in the shape of small cylinders about 2 cm long and 0.5 cm in diameter and were enclosed in a plastic container. The response of the dosimeters includes:

1. Cosmic radiation, which varies very little from one location to another at the 11 locations selected and was assumed to be equal to 30 mrads/year.

2. Terrestrial radiation, which, among other factors, depends on the geological nature of the soil and on the activities contained in the building materials.

3. Contamination of the soil by fallout products and other radionuclides and the activity contained in the air. Those sources were neglected in the calculation of the doses.

The aims of the preliminary experiment were to determine the type of dosimeter to be used in the national survey and to study the influence of the seasonal variations, the duration of exposure, and the sampling height. A discussion of the results follows.

Comparison Between Two Dosimeter Types

In each location a LiF and a $CaSO_4$ dosimeter were exposed for two 6-month periods; a comparison of the results shows that there is no statistically significant difference between the values obtained.

The arithmetic averages of the doses were 66 and 67 mrads/year for the $CaSO_4$ and the LiF dosimeters, respectively. For practical purposes the two types of dosimeter therefore yield the same results. The $CaSO_4$ dosimeter was preferred for the following surveys because it is more sensitive than the LiF dosimeter and thus allows the exposure time to be shorter.

Climatic Variations

To assess the uncertainties resulting from the climatic variations, we compared the results of six successive 2-month exposures (Fig. 1). A statistically significant difference of about 10% was observed only for the June—July and October—November exposures; the values obtained during those months were less than those during the rest of the year.

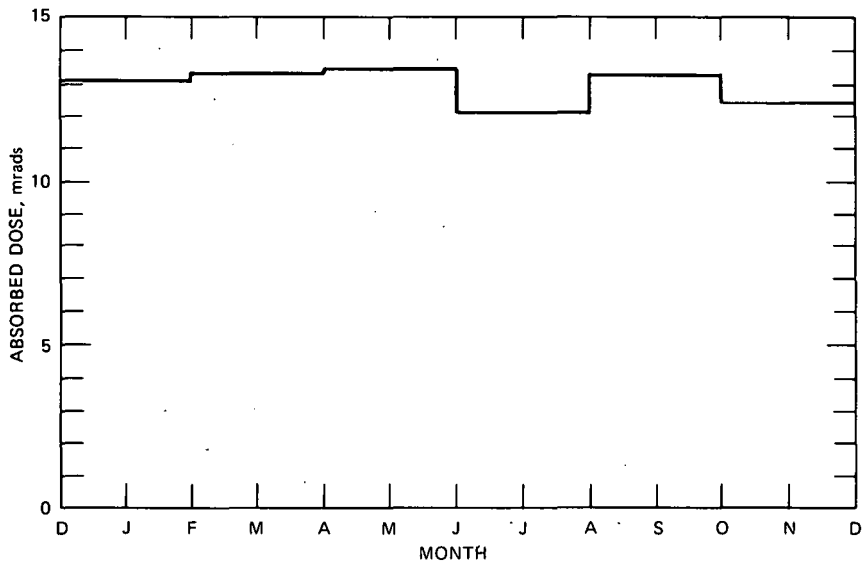


Fig. 1 Variation of the absorbed dose according to the time of exposure during the year.

During June and July the weather conditions were exceptional in that the temperature and the total duration of sunlight were very high. A temperature effect could explain the difference observed. However, another factor cannot be ruled out: the processing of the dosimeters was performed by persons who were not specialists in the field.

During October and November the number of rainy days was large; a greater water content in the soil could account for the lower observed doses.

Duration of Exposure

The influence of the duration of exposure (in the range of 2 to 6 months) was also studied. The biggest difference is between the dosimeters exposed for 6 months at a time and the dosimeters exposed for 2 months each during the same 6-month period: the difference is 5% on the average, the lower value being obtained for the dosimeters exposed during 6 months at a time. The mean deviation between the results obtained for the dosimeters exposed during 4 months at a time and the addition of the two results obtained for the dosimeters exposed during 2 months each is 3%. Those differences may be due to the background noise of the processing device which is relatively more important for the smaller doses, i.e., for the shorter exposure periods.

Sampling Height

The dosimeters were set up at 0.5, 1, 1.5, and 2 m at three locations to study the influence of the sampling height. The arithmetic average of the doses obtained at the four sampling heights were 61, 71, and 93 mrads/year for locations 1, 2, and 3, respectively (Fig. 2). For locations 1 and 2, the differences observed between the results obtained at the four sampling heights are not statistically significant, whereas they are statistically significant at location 3, where the doses are higher. The deviation, which is about 10% between the results obtained at 0.5 and 2 m, might result from a heterogeneity of the radioactive content of the soil at that location.

On the basis of the results obtained in the preliminary experiment, it was decided that the $CaSO_4$/Dy dosimeters would be used in the national survey. The dosimeters would be exposed for 2 to 6 months at a height of about 1 m above the ground level.

Results of the Survey in the Paris Area

A survey in Paris and in the surrounding departments (population 9,122,803; area 6082 km^2) was carried out with the help of the Météorologie Nationale. Calcium sulfate dosimeters were distributed to members of the Météorologie Nationale and to a number of CEA personnel; a form requesting information on the sampling location and its environment was attached to each dosimeter. The dosimeters

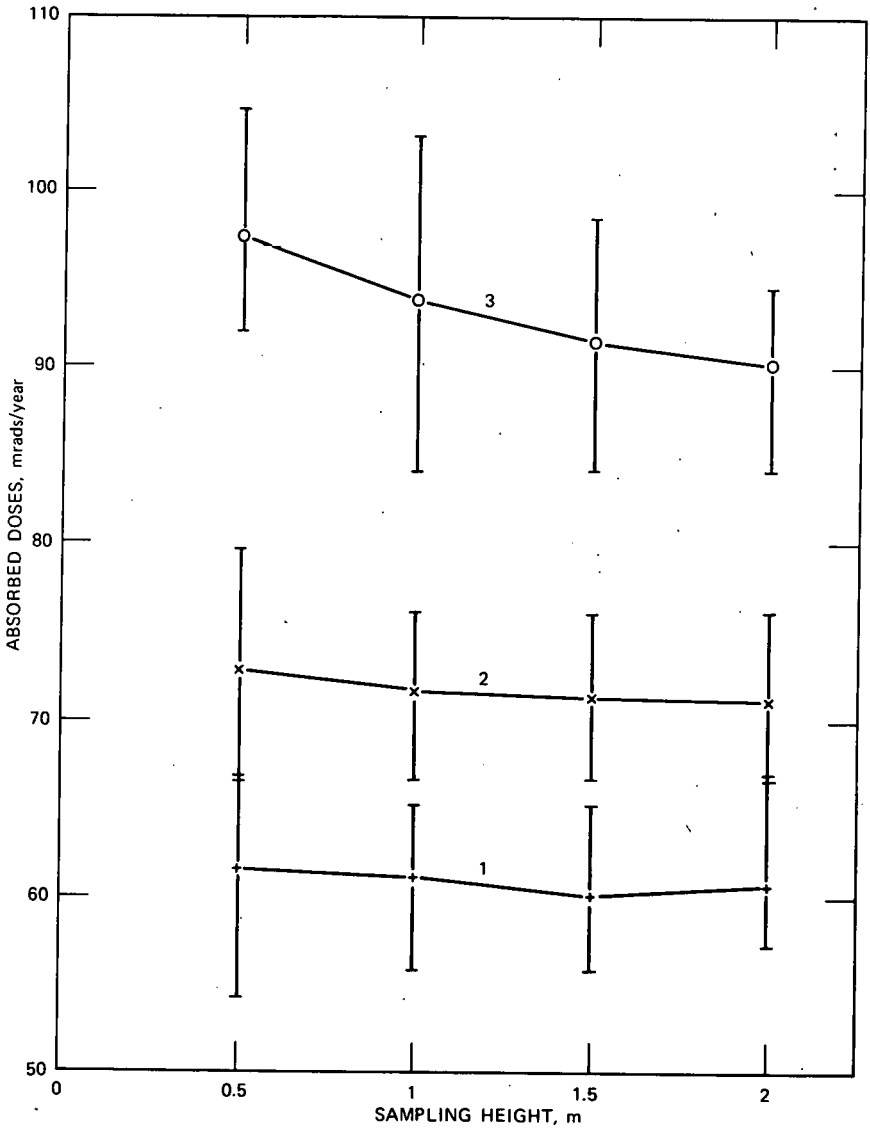


Fig. 2 Variation of the absorbed dose as a function of sampling height for three locations.

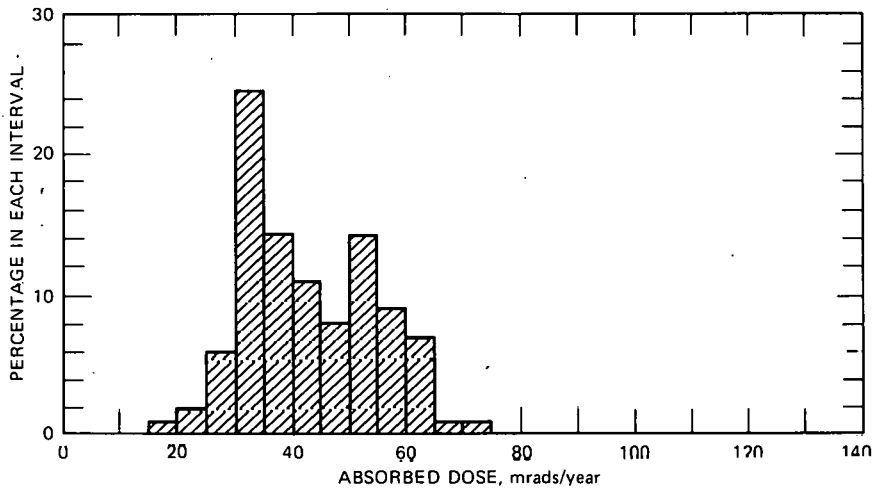


Fig. 3 Distribution of the outdoor terrestrial doses in the Paris area.

were exposed for 3 months. Of the 300 dosimeters distributed, 283 were recovered; 98 of the dosimeters had been set up outdoors and 185 indoors.

The terrestrial absorbed doses outdoors ranged from 16 to 72 mrads/year, with an arithmetic mean of 43 mrads/year. The distribution of the results obtained is shown in Fig. 3; the histogram is similar to a normal curve, with a standard deviation of 11 mrads/year.

In the indoor doses the influence of the building materials brings about a greater variability in the results. The absorbed doses arising from the terrestrial radiation ranged from 14 to 134 mrads/year, with an arithmetic mean of 43 mrads/year. The histogram of the results (Fig. 4) is better fitted with a lognormal curve than with a normal curve.

Results of the Survey in the Yonne Department

During 1977, in collaboration with the Service Central de Protection contre les Rayonnements Ionisants and under the administrative authority of the Direction de la Sécurité Civile, 510 dosimeters were installed in the Yonne department (population of 300,000; area of 7425 km^2). The number of dosimeters set up indoors and outdoors was about equal. A form requesting information on the sampling location and its environment was attached to each dosimeter. A total of 472 dosimeters were recovered; this corresponds to an average loss of 7.5%. As expected, the loss was

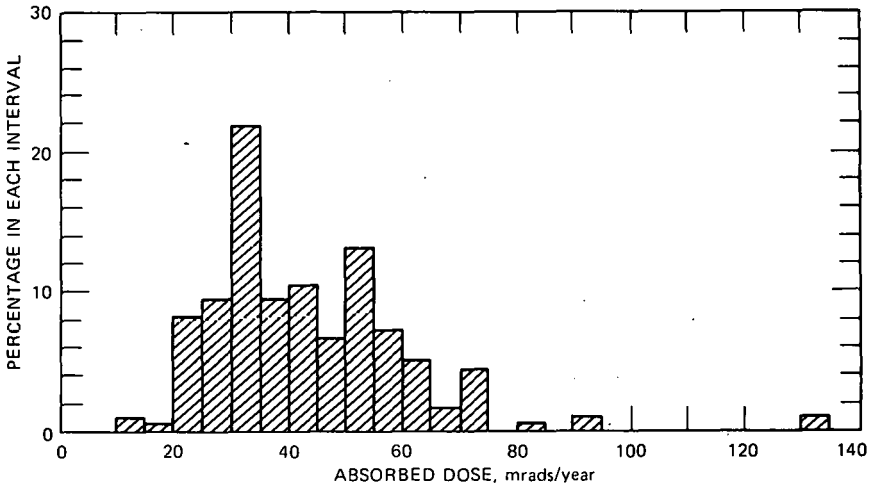


Fig. 4 Distribution of the indoor terrestrial doses in the Paris area.

greater for the dosimeters installed outdoors (10%) than for those indoors (5%). The major reason for loss indoors was because the people who provided the location for the dosimeter were absent from home at retrieval time.

The terrestrial absorbed doses outdoors ranged from 21 to 138 mrads/year, with an arithmetic mean of 51 mrads/year. The dose distribution is shown in Fig. 5. Of the 13 highest doses, 12 were observed in the southeast area of the department which lies next to the important granitic formation of the Morvan massif. In that department the influence of the geological nature of the soil is thus clearly revealed.

The indoor terrestrial doses ranged from 21 to 151 mrads/year, with an arithmetic mean of 61 mrads/year. The dose distribution (Figs. 6 and 7) can be assimilated to a lognormal curve. As in the outdoor doses, the highest doses were observed in the southeast area of the department.

Current Program

About 400 dosimeters were installed in each of the following departments:

Department	Population	Area, km^2
Haute-Vienne	359,000	5555
Corrèze	251,000	5888
Creuse	151,000	5605

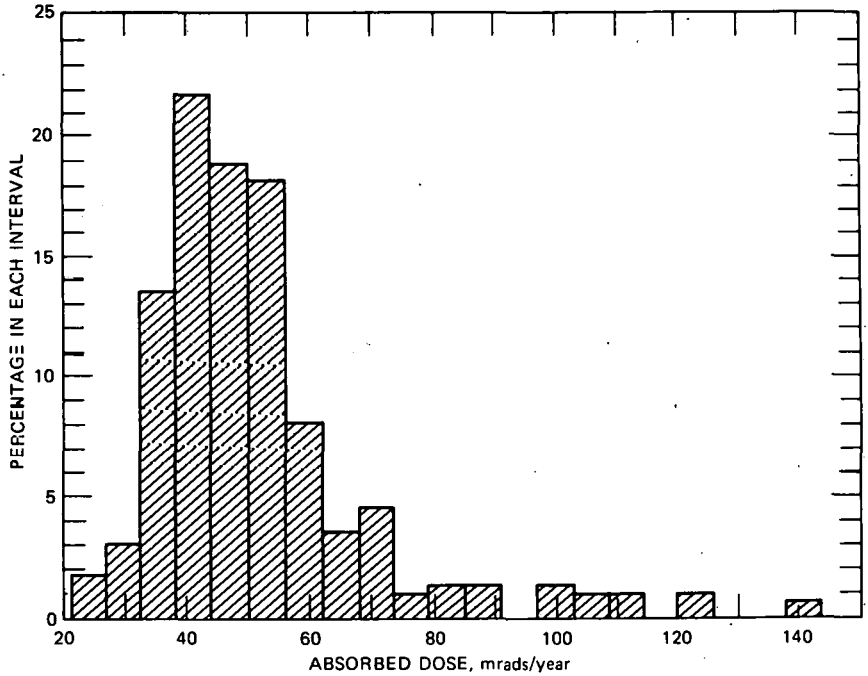


Fig. 5 Distribution of the outdoor terrestrial doses in the Yonne department.

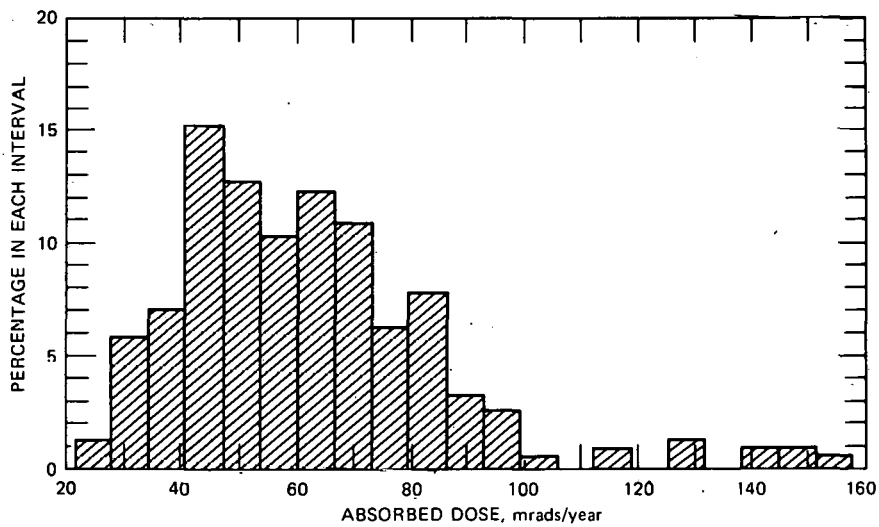


Fig. 6 Distribution of the indoor terrestrial doses in the Yonne department.

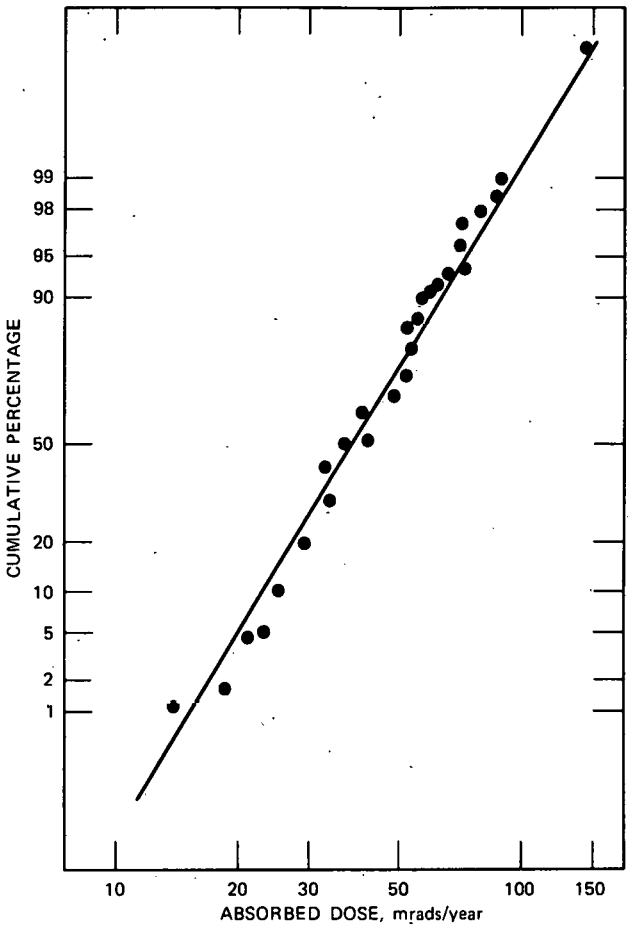


Fig. 7 Cumulative distribution of the indoor terrestrial doses in the Yonne department.

The setting-up operation was carried out by the Inspection Départementale des Services d'Incendie et de Secours, and we provided a list of the communes where one or several pairs of dosimeters were to be placed. The dosimeters will be retrieved by September 1978.

For a few other departments, the first contacts have been taken with the authorities. It is planned to accelerate the program to cover the whole country within 5 years.

As soon as sufficient results are available, we will undertake a statistical study on the influence of various parameters, such as the

geological nature of the soil, the type of building, and the age of the dwelling.

MEASUREMENTS CONNECTED TO INTERNAL IRRADIATION

The surveys of external irradiation are or will be complemented by measurements connected to internal irradiation.

^{226}Ra Concentrations in Flour

Analyses of several natural radionuclides (^{226}Ra, ^{228}Ra, ^{210}Bi, and ^{210}Po) have been carried out on flour samples of a few kilograms originating from 10 French regions. The ^{226}Ra concentrations obtained are given in Table 1.

TABLE 1

^{226}Ra Concentrations in Flour

Region	Concentration, pCi/kg fresh weight		
	1973	1974	1976
Normandie	1.2	0.6	0.5
Nord	0.9	0.9	0.5
Ile de France	1.0	0.3	0.6
Champagne	0.8	0.8	0.6
Bretagne	2.2	0.3	1.3
Maine—Vendée	1.0	0.8	4.5
Centre	1.1	1.4	0.5
Charente	1.1	0.6	0.5
Causses—Aquitaine	0.7	1.1	0.9
Saône Rhône	0.7	0.8	0.7

Even though the samples are expected to be representative of the situation on the regional scale, large differences are observed from one year to the next. Those variations could arise from the fact that it is not the same fields which are used year after year for the production of wheat.

^{222}Rn Measurements in Dwellings

Since the short-lived decay products of ^{222}Rn are the main contributors to the lung dose equivalent arising from natural irradiation, it is important to measure those radionuclides in the places where people spend most of their time, that is, in dwellings.

We intend to carry out 1-month samplings in houses with the help of a device developed within the CEA which allows a discrimination between the activities of ^{218}Po and ^{214}Po to be made.

CONCLUSIONS

A national survey of the exposure of the French population to external radiation was undertaken by CEA. In that survey, which is carried out on a departmental basis, $CaSO_4$/Dy dosimeters are installed indoors and outdoors in about the same proportion and are exposed for a duration of a few months. The results obtained thus far with respect to the terrestrial doses are given in Table 2.

TABLE 2

Measurement of Terrestrial Radiation with $CaSO_4$/Dy Dosimeters

Region		Dose, mrads/year	
		Outdoors	Indoors
Paris area	Average	43	43
	Range	16—72	14—134
Yonne	Average	51	61
	Range	21—138	21—151

At the present time, dosimeters have been installed in three departments, and contacts have been made in a few others. The whole survey is planned to be completed within 5 years.

With regard to internal irradiation, analyses of natural radionuclides in flour samples originating from 10 regions have been carried out since 1973. The ^{226}Ra concentrations were found to vary from 0.3 to 4.5 pCi/kg. Measurements of short-lived ^{222}Rn daughters in dwellings will complement the survey.

DISCUSSION

Van Middlesworth: When we measure 2 to 3 μrems/hr, we should consider the dose in the context of the irreducible minimum dose of radiation from the body itself.

Bouville: According to the 1977 UNSCEAR report, the absorbed dose rates from internal irradiation from natural sources in "normal" areas vary from 18 to 50 mrads/year, depending on the tissue

considered. To this must be added the absorbed dose rate from cosmic rays, which is equal to 28 mrads/year at sea level and can be taken to be irreducible under normal conditions of exposure. The total irreducible absorbed dose thus amounts to 46 to 78 mrads/year. However, the external absorbed dose from terrestrial radiation has a wide range of variation and can be, as Dr. Van Middlesworth indicates, as low as 2 to 3 μrads/hr, which corresponds to 17 to 26 mrads/year. Even at that low level, the dose from terrestrial radiation is not insignificant when it is compared to the total irreducible absorbed dose.

Uzzan: I would like to make some comment about this paper. The French Atomic Energy Commission and Euratom have a contract concerning epidemiologic studies about the problem of the hypothetical relationship between stochastic effects on populations and high natural radioactivity. In the contract, we are working specially in Brittany with the public health school and in Ireland with the University of Dublin. The work consists in (1) determining a time scale in which the data are available, that means descriptive data concerning the doses, (2) determining data on epidemiologic factors, such as mortality and morbidity, and (3) comparing the data with a population control living near the areas studied. It is a very difficult problem.

I would like to know if teams in other parts of the world are working in this field; also, if epidemiological studies are being made of populations living in naturally high radioactive areas (such as Kerala, India; Brazil; Nigeria; and France) or living in areas where the natural dose is ±300 mrems/year.

Bouville: Epidemiological studies designed to determine if populations living in areas where the external radiation dose equivalent is about 300 mrads/year exhibit any biological effects at a rate higher than similar populations living in normal background areas are likely to be very difficult to carry out. To my knowledge, no study of this kind has ever been performed.

Piesch: I would like to comment briefly on the use of TLD systems in environmental monitoring and the activities of the European community in this field. As was discussed during the conference, the overall error or the precision of dose measurement can vary significantly, depending on the properties of the thermoluminescent material, the quality of the individual thermoluminescent reader, and the annealing and postirradiation treatment applied in the laboratory. In addition to recommendations and intercomparison experiments conducted by the University of Texas and the U. S. Department of Energy, there is a need for further detailed performance criteria. A workshop of the Fachverband für

Strahlenschutz and Euratom organized an interlaboratory-type test program in which each laboratory must perform the same kinds of calibration exposures and procedures. The main parameters investigated are the lower detection limit, the zero dose reading, batch uniformity, reproducibility or gamma value as a function of dose, and long-term sterility of the TLD system. Laboratories interested in the intercomparison program are invited to participate. To date, 43 different TLD and RPL systems are available.

Study of Genetic Effects in Plants Induced by Natural Radioactivity in Southwest France

M. DELPOUX, M. FABRIES, F. FAURE,* H. DULIEU,† A. LEONARD,‡ and M. DALEBROUX§

*Service de Botanique et Biogéographie, Université Paul Sabatier, Toulouse, France; †C.N.R.S., Station d'Amélioration des Plantes de l'I.N.R.A., Dijon, France; ‡Laboratoire de Cytogénétique du Centre d'Etude de l'Energie Nucléaire, Mol, Belgium; and §Services de Biologie de la Commission des Communautés Européennes, Belgium.

ABSTRACT

Southwest France has a number of radioactive areas with an average background rate ranging between 1 and 30 μrads/hr. However, "hot" sites that yield rates up to 1 mrad/hr are not uncommon. Even some small outcrops as high as 10 mrads/hr were recorded. Reference response curves were established for the a_1^+/a_1 a_2^+/a_2 system of tobacco in the artificially radioactive site of the French Atomic Energy Commission at Cadarache (^{137}Cs); the response was found to be linear between 10 μrads/hr (background) and 1 rad/hr. The response of the system, together with that of the *waxy* system in Barley, was then studied over natural uranous sites in the Permian Basin of Lodève (Hérault) and the area of Lagravette (Aude).

PROSPECTED AREA

Several years of prospecting were necessary to make a gross survey of gamma radioactivity at the ground level in the eastern half of the Pyrenees, involving Languedoc-Roussillon and the area bordering the southern edge of the "Massif Central" (Central Mountain Mass). The prospected area is about one-twentieth of the total French territory. The survey, made by means of a portable scintillation counter, stresses the existence of a conspicuous variability of the background. Five classes of radioactivity were made for dose rates ranging between 0.001 and 0.030 mrad/hr. However, there are areas with

higher radioactivity; Delpoux has personally discovered some of these sites, especially in the Pyrenees. Information and authorizations delivered by the French Atomic Energy Commission made possible the exploration of zones of abnormally high radioactivity, where dose rates ranging between 0.030 and 1 mrad/hr are not uncommon. This was the case in the area discovered by the Hérault Mission of the French Atomic Energy Commission in the Permian Basin of Lodève. Dose rates up to 10 mrads/hr were recorded at some points. It was thus possible to choose adequate areas in order to perform accurate dosimetry together with biological experiments.

ABNORMAL DOSE LEVELS OF NATURAL RADIOACTIVITY IN THE PERMIAN BASIN OF LODÈVE (FRANCE)

With the permission of, and on the basis of information from, the French Atomic Energy Commission, two main areas with abnormal radioactivity were studied using thermoluminescent dosimeters. Over the first area, near the locality called Mas d'Alary, rates ranging between 0.02 and 10 mrads/hr were found. Over the second area, located near Saint Martin du Bosc, the dose rates range between 0.02 and 10 mrads/hr. At both places the highest values are observed on very small areas (just a few square meters); nevertheless, they are, as far as we know, the highest naturally occurring dose levels actually observed anywhere in the world. Ionizing radiations are emitted by uranous rocks containing mainly ^{238}U and the products of its radioactive family. Around both points, there is a decreasing radioactivity gradient progressively dropping to the background level. The size of each area is about 2 acres. This accurate dosimetry is a prerequisite to the design of experiments planned to evaluate in situ the effects of natural radioactivity on living organisms.

GENETIC EFFECTS OF LOW AND VERY LOW CHRONIC DOSES OF IONIZING RADIATIONS ON THE a_1^+/a_1 a_2^+/a_2 SYSTEM OF TOBACCO*

An experiment was designed with this genetic system to obtain reference response curves to well-controlled chronic doses of gamma

*_Mutat. Res._, 25: 289-304 (1974); 28: 69-77 (1975); and 30: 63-70 (1975); _Ann. Amélior. Plantes_, 26(4): 569-577 (1976). The system is involved in chloroplast differentiation in _Nicotiana tabacum_ var. _Xanthi_ n.c. A carrier plant has greenish-yellow leaves; either spontaneously or under the action of mutagens, a given cell can revert to a green phenotype. This kind of event can be easily detected in the palisade tissue.

rays. With this object, two radioactivity gradients were chosen in the artificially radioactive natural site of the French Atomic Energy Commission at Cadarache, where a 1200-Ci source of ^{137}Cs has been installed. The dose rates were as follows:

Control: 10 μrads/hr (≃ 0)

Very low, mrads/hr	Low, rad/hr
0.5	0.25
3.5	0.50
6.5	0.75
9.5	1.00

The total exposure time was 1273 hr. However, the total doses have no real meaning on the genetic effects observed. Since continuously dividing material is involved, the reversion of a given cell takes place during cell division, so that the effective irradiation period is at most equal to the duration of a cell cycle, which lasts approximately 24 hr. Under these conditions the effective doses delivered were 0.24 (control), 12, 84, 156, and 228 mrads at very low dose rates. They amounted to 0.24 mrad (control), 6, 12, 18, and 24 rads at low dose rates. At each location chosen for a given dose rate, two-leaf plants were placed in individual pots over the ground on a small platform in a shelter that protected them from climatic variations (especially temperature) and strong daylight. In all cases the experimental units were placed under similar environmental conditions.

The plants grew several leaves during the total exposure period. The observations were made on the pooled fifth, sixth, and seventh leaves, entirely developed during the exposure.

If (1) leaf growth was of monolayer type, (2) both original and reverted cells divided at the same rate, and (3) there was no selection against either cell type, then the number of cell cycles, t, necessary to yield the total number of cells observed, N (i.e., the number of cells constituting the palisade tissue of leaves five, six, and seven), can be readily determined on the basis of the total leaf area S (5, 6, and 7) and the cell density d. Finally, assuming a constant reversion rate p, this rate can be calculated as follows:

$$p = 1 - \left(\frac{S - S_g}{S}\right)^{1/t}$$

where S_g is the value of the reverted leaf area.

The analysis of variance was performed on the p values. The response was found to be linear in both dose ranges; there was no

difference between the two slopes and no plateau was statistically detectable.

GENETIC EFFECTS OF CHRONIC IONIZING RADIATIONS FROM NATURAL URANOUS SITES ON THE a_1^+/a_1 a_2^+/a_2 SYSTEM OF TOBACCO

Permian Basin of Lodève (Hérault)

The reversion rate per cell cycle was studied on the basis of the following experimental design:

1. One hundred plants were sown in two subsets of 50 pots in a greenhouse on the university campus in Toulouse and allowed to grow four to five leaves.

2. Then the set of 100 plants (in their pots) was taken to Lodève. One subset of 50 pots (subset Nr. 1) was placed over a uranous site yielding a dose rate ranging between 3 and 10 mrads/hr. The second subset (subset Nr. 2) was placed in the vicinity over a substrate yielding the very low dose rate of 30 μrads/hr considered as a control. Both subsets were allowed to grow from nine to ten leaves.

3. Finally the whole set was taken back to Toulouse and placed under the same conditions as before its transfer to Lodève. The plants were then allowed to grow a few more leaves.

The reversion rates were calculated and found to be as follows:

	Toulouse	Lodève	Toulouse
Subset Nr. 1	2.59×10^{-5}	12.68×10^{-5}	2.17×10^{-5}
Subset Nr. 2	2.55×10^{-5}	2.09×10^{-5}	3.65×10^{-5}

It clearly appears from these data that the reversion rate over the uranous site, which delivered a maximum efficient 24-hr dose ranging between 72 and 240 mrads, was about five times larger than that of the average control.

Uranous Site of Lagravette near Castelnaudary (Aude)

This experiment was undertaken with dose rates that were much smaller than the very small dose rates used in the reference experiment above, in which the very small dose rates amounted to the following 24-hr doses: 0.24, 12, 84, 156, and 228 mrads. The dose rates delivered in this new experiment were 0.043, 0.080, 0.179, 0.292, 0.449, and 0.686 mrad/hr, which amounted to 1.03, 1.92, 4.30, 7.01, 10.78, and 16.46 mrads in 24 hr. As for the Permian Basin of Lodève, the doses were measured with thermo-

luminescent dosimeters by the Dosimetry Department of the French Atomic Energy Commission. All these doses but the highest range within the first interval of the very small doses chosen in the site of Cadarache. This allowed finer investigation of the beginning of the response curve. The first dose of 1.03 mrads in 24 hr is very close to the background level; in fact, no dose lower than that could be found in the "nonradioactive" neighborhood in the same environment. The first four treatments were found to produce the same effect in terms of reversion rate per cell cycle, i.e., $p = 0.74 \times 10^{-5}$. The last two treatments had the same effect, i.e., $p = 1.61 \times 10^{-5}$, which was significantly higher than that of the first four treatments.

FREQUENCY OF *WAXY* MUTANTS IN POLLEN POPULATIONS OF BARLEY (*Hordeum vulgare* var. Monlon)

The material was sown over the uranous site of Mas d'Alary in the Permian basin of Lodève. Three controls were sown in the neighborhood over nonradioactive sites with dose rates equal to 0.020, 0.019, and 0.019 mrad/hr, respectively. The dose rate over the radioactive site was 1.81 mrads/hr. After a total exposure of 1680 hr, the frequencies of *waxy* mutants were as follows:

Uranous site, 6.69×10^{-4}
Average control, 2.12×10^{-4}

The difference between these frequencies was found to be highly significant.

ACKNOWLEDGMENT

This research program was performed under Contracts No. 239 and 240-76-1 BIO F of the Commission of the European Communities.

Measurements of Gamma Radiation in Swedish Houses by Means of Mailed $CaSO_4$/Dy Dosimeters

LARS MJÖNES
National Institute of Radiation Protection, Stockholm, Sweden

ABSTRACT

A nationwide investigation of gamma radiation in Swedish houses has been made. The occupants of 2000 apartments and houses were picked at random and asked to participate. The measurements were made with $CaSO_4$/Dy thermoluminescence dosimeters. Three such detectors were sent to each of the selected dwellings by mail. The participants put the detectors in the apartment in the three different places carefully specified in the accompanying instructions. After a period of 4 weeks the detectors were returned for evaluation.

Desirable detector qualities for this kind of investigation are discussed, and some measurements to check the qualities of $CaSO_4$/Dy dosimeters are described, including energy dependence, fading, annealing, sensitivity to light, and response to cosmic radiation. The problem of determining the transit dose during mail transport is also discussed.

Some preliminary results are shown for four different types of building materials. The preliminary mean annual absorbed tissue dose in Sweden is 0.58 mGy (58 mrads) when the contribution from cosmic radiation has been subtracted.

The gamma radiation in houses originates mainly from the building materials. Naturally occurring radioactive nuclides are present in substances in the ground in varying amounts. These nuclides in the clay, gravel, and rock used to produce building materials result in small amounts of ionizing radiation in buildings. In addition, there are contributions from cosmic radiation and radiation from the ground. The main gamma radiation in building materials, as well as the ground, originates from the daughter products of ^{226}Ra and ^{232}Th and from ^{40}K.

The absorbed dose rates in air found in Swedish houses in earlier investigations were usually less than 2.5 mGy/year (250 mrads/year). The lowest values were found in wooden houses and in houses built from sand-based aerated concrete. Wood contains hardly any radioactive nuclides. The gamma radiation measured in a wooden house is the sum of radiation from the ground and cosmic radiation. Wooden houses often have foundations made from stone or concrete, and, in that case, there is a contribution from the foundation too. The highest values were found in houses built from aerated concrete containing alum shale (Hultqvist, 1956).

INVESTIGATION PROCEDURES

The National Institute of Radiation Protection in Stockholm, Sweden, has made a nationwide investigation of gamma radiation in Swedish houses. The occupants of 2000 apartments and houses were picked at random and asked to participate in the investigation. The selection was intended to cover all types of dwellings and building materials.

An introductory letter was sent to the selected participants in which the investigation was presented, and some background information regarding ionizing radiation in buildings and radioactive nuclides in building materials was given. The letter also included a reply card on which the participant indicated if he was willing to participate and when it would suit him best. He could also indicate if he wanted to know the result of the measurements in his own apartment and if he wanted further information about radiation in dwellings.

We had a special brochure prepared, aimed at the general public about gamma radiation and radon in dwellings, which has proved very useful. The reply card was returned to us in a postage-paid envelope.

The measurements were made with thermoluminescence dosimeters, $CaSO_4$/Dy in teflon. Each dosimeter was surrounded by an energy compensation filter and a cover made from polystyrene. The dosimeter and cover were placed in a polyvinylchloride (PVC) bag. Three such detectors were sent to each of the selected dwellings by mail. The detectors were accompanied by instructions in which three different places in the apartment were carefully specified, and the participants put the detectors in these places themselves. The chosen places were: (1) under a sofa or armchair in the living room, (2) under a table or chair in the kitchen or dining room, and (3) under a bed in the bedroom. After a period of 4 weeks the

participants were requested to send the detectors back for evaluation. They also got a questionnaire including questions about the house they live in, such as type of house, number of stories, and building materials. The 24 counties of Sweden were included. The measurements were made at a rate of 70 to 80 dwellings per month.

DESIRABLE DETECTOR QUALITIES

Since the absorbed dose rate in air in a normal building is relatively low, down to approximately 0.03 mGy/month (3 mrads/month), the chosen detector must have a high sensitivity. Since it will remain in the house for a period of about 4 weeks, it must also have a low fading rate. Other desirable detector qualities are good linearity, a simple annealing procedure, low energy dependence, low sensitivity to light, and a good reuse capability.

The best compromise we could find among these desirable qualities was $CaSO_4$/Dy thermoluminescence dosimeters (TLD). The diameter of the dosimeters was 12.7 mm, and the thickness was 0.4 mm. The $CaSO_4$/Dy in teflon has a high sensitivity, it is capable of routine measurements down to less than 1 mrad, the linearity is good up to at least 1 Gy (100 rads), and the reuse capability is good up to at least 20 reuse cycles (Webb, Dauch, and Bodin, 1972).

The $CaSO_4$/Dy was a new material to us, so before the investigation started we made rather extensive measurements to check the qualities of the dosimeters. We checked linearity, energy dependence, fading, annealing, and sensitivity to light.

Energy Dependence

One disadvantage with $CaSO_4$/Dy is its energy dependence. At 30 keV the response per roentgen is a factor of 11 greater than the response at 1.25 MeV. To compensate for this, we designed an energy compensation filter made from 1.0 mm of aluminum, 0.7 mm of copper, and a cover made from 3.0 mm of polystyrene, Fig. 1.

Fading

Various fading rates for $CaSO_4$/Dy can be found in the literature: 1 to 2% per month for $CaSO_4$/Dy powder (Becker, 1973). For $CaSO_4$/Dy in teflon the fading rates are considerably higher: 10% fading for the first 24 hr and 20% for the first week (Becker, 1973); 11% for the first 24 hr and 17% for the first week (Webb,

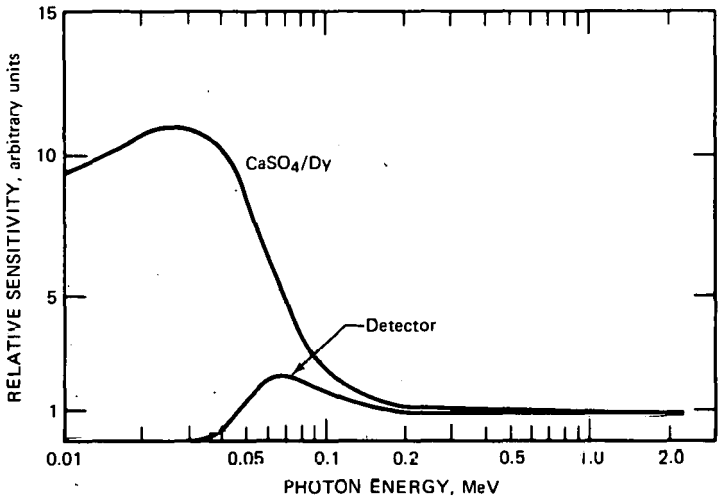


Fig. 1 Energy dependence for $CaSO_4$/Dy and for the detector with energy compensation filter. The curve for $CaSO_4$/Dy is normalized to 1.0 for the photon energy 1.25 MeV.

Dauch, and Bodin, 1972). Our own measurements indicated a fading rate of 4% for the first 24 hr and 10% for the first month (Mjönes, 1976).

When the dosimeters are exposed for long periods, in our case several weeks, we must correct for the fading taking place continuously while the dose is being absorbed in the detector. Assuming that the fading is exponential with a half-life $T_{½}$ days and that the absorbed dose rate is a linear function of time, the following equation will describe the fading:

$$\frac{dE}{dt} = K - \lambda E \tag{1}$$

where E = energy absorbed in the traps of the detector
K = rate of absorbed energy in the traps
λ = transformation constant
t = time

The solution is

$$E = \frac{K}{\lambda}(1 - e^{-\lambda t}) \tag{2}$$

If the fading rate is 10% per month, the correction for fading will be 1.04 for 4 weeks (Fig. 2).

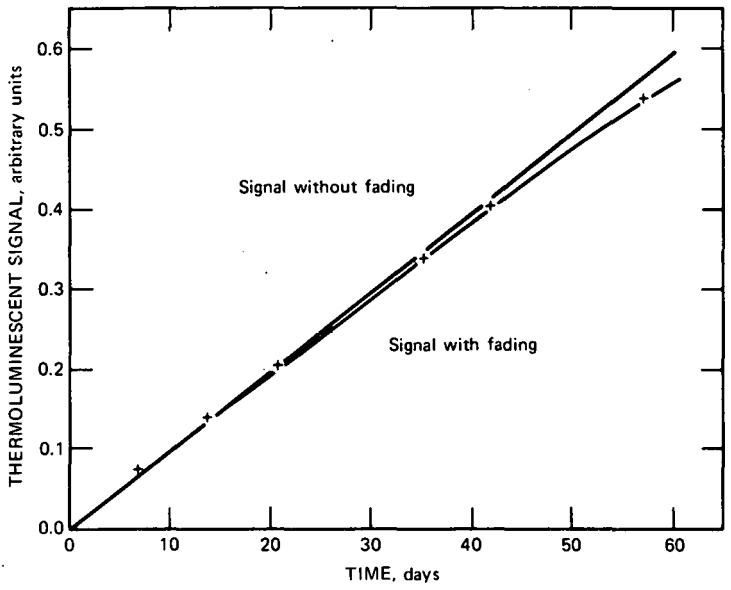


Fig. 2 Fading taking place continuously while the dose is being absorbed in the detector.

Annealing

We found that a simple annealing for 1 hr at 300°C plus 8 sec preannealing at 135°C in the TLD reader (Teledyne TLD-7300B) gives a low and stable background signal from unirradiated dosimeters.

Sensitivity to Light

The $CaSO_4$/Dy dosimeters are sensitive to light. Unirradiated dosimeters showed a response equivalent to a 0.007 mGy (0.7 mrad), air absorbed dose, signal after 5-min exposure to sunlight, and a 0.034-mGy (3.4 mrads) signal after 1 hr in sunlight, and a 0.003-mGy (0.3 mrad) signal after exposure to the normal laboratory illumination for 1 hr. Webb, Dauch, and Bodin (1972) have found that this signal was almost entirely removed by using a preheat procedure. In our measurements we found the above-mentioned signals after preheat to 135°C for 8 sec.

Another well-known effect is optical fading. Irradiated dosimeters show an increased fading rate if they are exposed to light. After

a 5-min exposure to sunlight, the signal had faded to 90%, and after 1 hr the signal had faded to 50% of the original. Irradiated dosimeters exposed to the normal laboratory illumination showed no increased fading. The sensitivity to light means that the dosimeters must be packed in lightproof covers and that work with uncovered dosimeters should be carried out in subdued illumination.

RESPONSE TO COSMIC RADIATION

Cosmic radiation constitutes a relatively large fraction of the natural penetrating background radiation. At sea level the annual absorbed dose in air from the ionizing component of cosmic radiation is 0.28 mGy (28 mrads), according to UNSCEAR (1977). In the lower atmosphere the absorbed dose rate varies, depending on several different factors including altitude, geomagnetic latitude, atmospheric pressure, and time.

Near sea-level altitude is an important factor. Values for the galactic cosmic-ray dosimetric profile in the lower atmosphere have been calculated by O'Brien and McLaughlin (1972) for latitudes 43°N and 55°N, for both solar minimum and maximum periods.

Our measurements were made during a solar minimum period. The latitude dependence is small between 55°N and 70°N where Sweden is situated so the calculated values for 55°N and solar minimum will approximate the conditions for our investigation. The dwellings included in the investigation are situated at altitudes between sea level and 600 m.

The contribution from cosmic radiation will be corrected for altitude according to the O'Brien and McLaughlin (1972) calculations normalized to the UNSCEAR value at sea level.

Variations in atmospheric pressure give relatively small variations in the absorbed dose rate, and we have made no corrections for such variations. Time variations for the period of our measurements are also relatively small. Seasonal and shorter term changes are on the order of ±1% (Lowder and Beck, 1966). The change over the 11-year solar cycle at sea level, at 55°N geomagnetic latitude, is approximately 10% (O'Brien and McLaughlin, 1972). The variation during the 2 years of our investigation is of the magnitude of 2%.

Near sea level the cosmic radiation consists of 80 to 90% muons (O'Brien and McLaughlin, 1970). This means that the usual gamma calibration cannot be used without modifying factors to infer the total absorbed dose. Lowder and de Planque Burke (1975) have exposed LiF dosimeters to 8-GeV muons from a synchrotron. They found a reduced response of 0.90 ± 0.04 to muons.

We have made measurements at sea outside Stockholm to check the cosmic-radiation calibration factor for $CaSO_4$/Dy. Dosimeters were placed on spar buoys and kept there for about 4 weeks. These buoys were situated about 1 km from land.

One problem in interpreting the results from these measurements is to assess the gamma contribution from radon daughters in the air. According to Lowder and Beck (1966) this contribution may amount to 10 to 20% of the total ionization, and it varies significantly with time and location. We must make further investigations of this matter before we can make the correct subtraction for the contribution from cosmic radiation.

CALIBRATION

The detector is shown in Fig. 3. The energy-compensation filter plates and the polystyrene cover were glued together in two parts, and the $CaSO_4$/Dy dosimeter was placed between them. The two

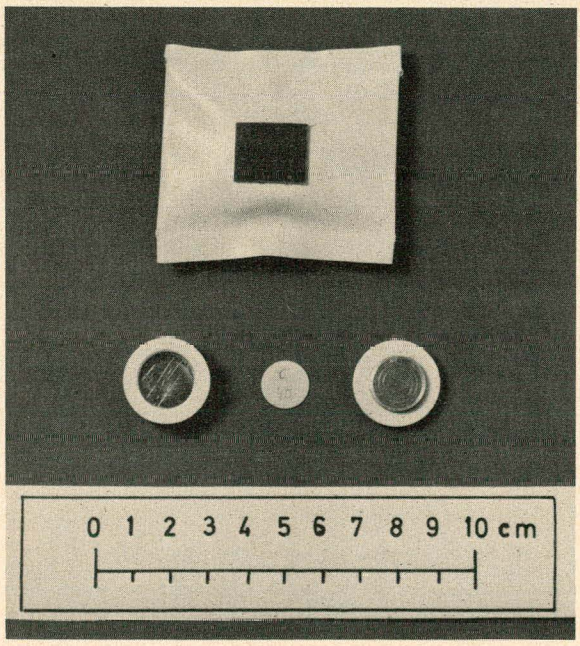


Fig. 3 At top: detector packed in PVC bag with double-sided adhesive tape applied. At bottom: energy compensation filter plates and polystyrene cover glued together in two parts. $CaSO_4$/Dy dosimeter is shown in between.

parts were secured together with paper adhesive tape. The unit was then placed in a 0.05-mm PVC bag that was welded to keep out light and moisture. To facilitate attachment by the participants, a double-sided adhesive tape was attached to the PVC bag (Fig. 3).

The dosimeters were treated in groups of 50. Each dosimeter was individually calibrated within the group. Five dosimeters per group were control dosimeters and were used exclusively for calibration purposes. If possible, all the dosimeters in a group were read out at the same time. Before readout the control dosimeters were exposed to a carefully determined absorbed dose in air of the magnitude 0.15 to 0.20 mGy (15 to 20 mrads) from a ^{226}Ra source to determine a calibration constant for the group. The magnitude of the dose was about the same as that received by the dosimeters during a normal exposure period in an apartment. Although we used ^{226}Ra as a calibration source, building materials usually also contain ^{40}K and ^{232}Th and daughters. However, the differences in gamma energies are relatively small and have been neglected.

STORING THE DETECTORS

When the detectors arrived by mail, after the exposure period, they were stored in a lead container with 3-cm thick walls. The air absorbed dose rate in the container was 0.04 μGy/hr (4 μrads/hr).

TRANSIT DOSE

One problem in our investigation was the transit dose. For the evaluation of the results for the detectors sent by mail we must determine the dose absorbed in the detector during the transport. This is a rather tricky subject. Gesell, de Planque Burke, and Becker (1976) have found that the correlation between transport dose and round-trip distance is very poor. The high transit doses they found in some cases could not be attributed solely to the increased cosmic-radiation exposure in high-flying aircraft. They imply that, at least in the cases of some unusually high values, the detectors may have been transported or stored together with radioisotope shipments. At first sight there is one obvious solution to this problem, i.e., to send a transit detector in the letter to the participants containing the regular detectors. The transit detector should then be returned immediately. This procedure could be repeated when the detectors are returned for evaluation. This would give a good estimate of the transit dose and it would be possible to find out if the letter has received

additional radiation from some other source. In practice, however, there are several disadvantages with a system using transit detectors. First, it means almost a double amount of work with readout, annealing, and calibration. The administrative work increases and, what is very important, it means more work for the participants. Even if transit detectors are used when the detectors are sent out and when they are returned, the transit detector must be sent alone in one direction so that an accurate determination of the transit dose for the regular detectors is still not obtained.

We chose not to use transit detectors. We have checked with the Swedish Post Office Administration and the department responsible for transport of radioactive goods at the National Institute of Radiation Protection and found that the risk of a letter being transported or stored with radioactive material is very small in the domestic Swedish mail. Most radioactive goods are transported separately by other means.

We have determined a typical value for the transit dose rate during mail transport. We sent out transit detectors to 36 people living in different parts of the country and asked them to return the detectors immediately. The mean absorbed dose rate in air was 0.15 ± 0.04 μGy/hr ($1\ \sigma$) (15 ± 4 μrads/hr). The dose rates ranged from 9 to 29 μrads/hr. The mean mail transport time was about 3 days, that means about 0.01 mGy (1 mrad) in transit dose.

ACCURACY

The accuracy in the final result depends on the magnitude of the dose absorbed in the detector. The contributions from transport and storing were subtracted and so was the contribution from cosmic radiation. The relative accuracy increases rapidly with increasing dose. The absorbed dose in the detector depends in turn on the dose rate in the house and on the length of the exposure period. The dose rates can differ very much among houses built from different kinds of building materials.

We have tried to adjust the exposure period so that the absorbed dose in the detector would be about 0.10 to 0.15 mGy (10 to 15 mrads). To avoid an unreasonably long exposure period, absorbed doses of 0.05 mGy (5 mrads), and in exceptional cases even less than that, have had to be accepted. An exposure period of 4 weeks was chosen. In most cases the period was longer in practice, about 5 to 6 weeks, because the participants did not return the detectors immediately. The total uncertainty in the final result ranged from about 20 to 60%. In most cases the uncertainty is about 25%.

TABLE 1

Absorbed Dose Rates from Gamma Radiation in Swedish Houses

(Preliminary values averaged over all the 24 counties)*

Building material in outer walls	Number of houses measured	Tissue absorbed dose rate† mean, mGy/year‡
Wood	405	0.32
Brick	382	0.56
Concrete	221	0.70
Aerated concrete§	181	1.01
Overall average	1189	0.58

*The mean value of the three measurements made in each apartment has been used for the evaluation of the values in the table. The estimated contribution from cosmic radiation has been subtracted.

†These values can be converted to absorbed dose rate in air (μrad/hr) by multiplying by the conversion factor 16.5 given by UNSCEAR.

‡Can be converted to mrads/year by multiplying by the factor 100.

§Mostly containing alum shale.

PRELIMINARY RESULTS

The preliminary results are presented in Table 1. The tissue absorbed dose rate for a person remaining 24 hr a day all the year in the apartment is given in milligrays per year. The estimated contribution from cosmic radiation has been subtracted.

It is difficult to classify dwellings according to the building materials. Several building materials are used in each house, and it is virtually impossible to find a simple and at the same time useful classification. We have not yet made the final evaluation of our data, and until then we can only give preliminary results. The houses are classified into four groups according to the main building material in the outer walls: wood, brick, concrete, and aerated concrete (including aerated concrete containing alum shale). The mean value for all measured houses is given at the end of Table 1.

The investigation shows that there are substantial variations in the absorbed dose rates among dwellings in different parts of the country (see Fig. 4). The lowest values have been found in the county of Gotland where the mean annual tissue dose was 0.15 mGy

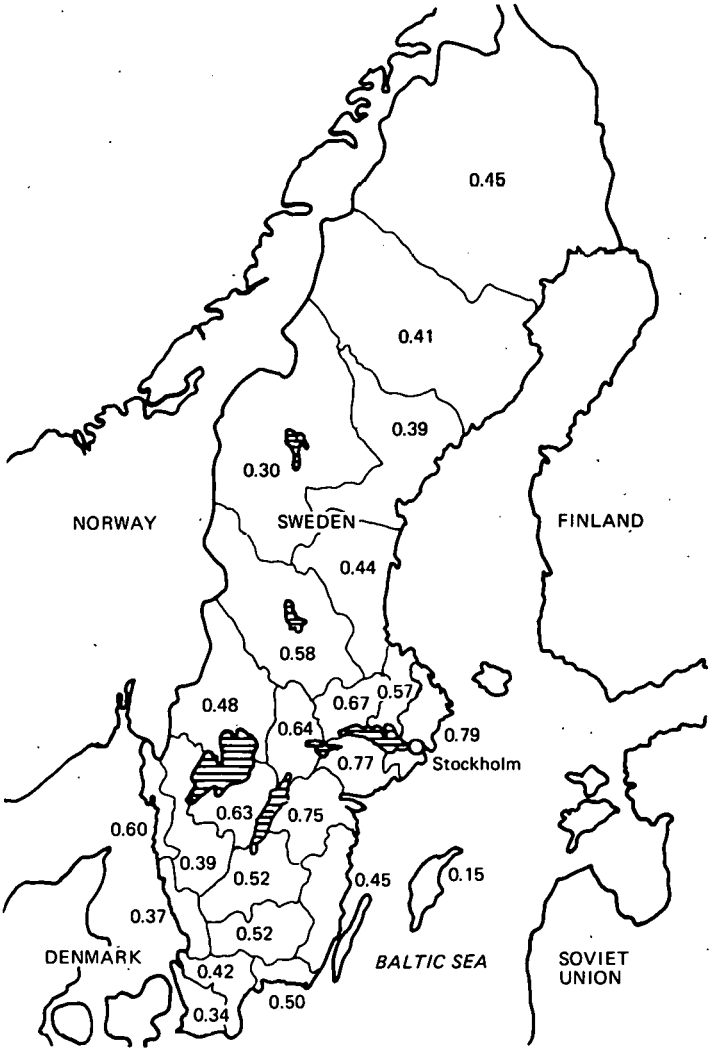


Fig. 4 Map of Sweden. The mean absorbed tissue dose rates from gamma radiation in the 24 counties of Sweden are shown in milligrays per year. The estimated contribution from cosmic radiation has been subtracted (preliminary values).

(15 mrads). Gotland is an island with a limestone bedrock in the Baltic Sea, and only small amounts of building materials are imported from the mainland.

The highest mean values are found in central Sweden, with Stockholm in the lead with 0.79 mGy (79 mrads) per year. In this part of the country the specific activity of ^{226}Ra in the soil tends to be higher than the national average, and the proportion of houses built from aerated concrete containing alum shale is high. In Stockholm it is about 30%. In addition, the proportion of apartment houses is higher than the national average.

In the northern parts of Sweden the mean values are lower. In Jämtland, for instance, it is 0.30 mGy (30 mrads) per year. These parts of Sweden have a high percentage of wooden houses. In Jämtland as much as 75% are wooden. In other northern counties the proportion of wooden houses is about 50%.

REFERENCES

Becker, K., 1973, *Solid State Dosimetry*, CRC Press, Cleveland, Ohio.

Gesell, T. F., G. de Planque Burke, and K. Becker, 1976, An International Intercomparison of Environmental Dosimeters, *Health Phys.*, 30: 125-133.

Hultqvist, B., 1956, Studies of Naturally Occurring Ionizing Radiations, *K. sven. VetenskAkad. Handl.*, Fjärde serien, Band 6, Nr 3.

Lowder, W. M., and H. L. Beck, 1966, Cosmic-Ray Ionization in the Lower Atmosphere, *J. Geophys. Res.*, 71: 4661-4668.

——, and G. de Planque Burke, 1975, The Cosmic-Ray Response of LiF TL-Dosimeters, Abstract P 42, in *20th Annual Meeting of the Health Physics Society*, Feb. 24, 1975, Richland, Wash.

Mjönes, L., 1976, *A Method for Measurements of Gamma Radiation in Dwellings by $CaSO_4$-Dy TL-Dosimeters* (in Swedish), Report SSI:1976-039, National Institute of Radiation Protection, Stockholm, Sweden, NTIS.

O'Brien, K., and J. E. McLaughlin, 1970, *Calculation of Dose and Dose-Equivalent Rates to Man in the Atmosphere from Galactic Rays*, USAEC Report HASL-228, Health and Safety Laboratory, NTIS.

——, and J. E. McLaughlin, 1972, The Radiation Dose to Man from Galactic Cosmic Rays, *Health Phys.*, 22: 225-232.

UNSCEAR, 1977, *Sources and Effects of Ionizing Radiation*, pp. 39-40, United Nations, New York.

Webb, G. A. M., J. E. Dauch, and B. Bodin, 1972, Operational Evaluation of a New High Sensitivity Thermoluminescent Dosimeter, *Health Phys.*, 23: 89-94.

DISCUSSION

Lowe: You said you subtract the cosmic-ray component of the population dose. Why do you do this since it is the total dose that is

important when considering the effects of natural radiation on populations?

Mjones: Not only are we interested in the total population dose, but we are also interested in how much the gamma radiation in a building contributes to the population dose. That is why we try to determine and subtract the cosmic-ray component.

Vold: (Comment) After hearing several studies this morning in which TLD measurements were used for large-scale population-dose determinations, I would like to comment that, for an accurate comparison between the doses reported in these studies, it is important to be consistent in referencing the medium in which the dose is reported. Our results indicate that the environmental tissue dose on a per rad basis is 10% greater than the environmental dose to the common dosimeter types of lithium fluoride, or calcium fluoride in an "energy filter," or calcium sulphate in the energy filter. This does not consider cosmic neutron dose or self-shielding by the human body, which can also change the average human-organ dose by more than 10%.

Sources of Natural Radiation Exposure in a Low-Monazite Environment

M. A. R. IYENGAR, M. P. RAJAN, S. GANAPATHY, and P. R. KAMATH
Environmental Survey Laboratory, Health Physics Division, Bhabha Atomic Research Center, Kalpakkam, Tamilnadu, India

ABSTRACT

Kalpakkam, 75 km south of Madras, on the east coast of India, is developing into a major nuclear center. On site under construction are two 215-MW(e) units of the Madras Atomic Power Project, a fast breeder test reactor, and a number of supporting research and development laboratories. Preoperational environmental surveys revealed significant radiation levels, particularly in the beach areas, which could be traced to the presence of monazite in the beach sands. Detailed radiological surveys were carried out in this low-monazite environment to investigate the population exposure levels.

Demographic surveys identified the existence of two main occupational groups: (1) fishermen residing on beaches and (2) farmers living inland. Dietary information demonstrated the essential dependence of fishermen on seafood and of farmers on land crops, thus clearly demarcating the dietary routes to be investigated under the study. Presented is the natural radioactivity distribution in the local environment, in the beach sands, marine matrices, and land crops. The samples were subjected to gamma spectroscopy and analyses of ^{226}Ra, ^{228}Ra, ^{210}Pb, and ^{210}Po. The marine food sources have been investigated in considerable detail, and the activity distribution is reported with reference to different species and, further, in different tissues of the same species. The marine organisms demonstrated significant uptake of the radionuclides, with ^{210}Po showing some of the highest accumulation. The ^{210}Po/^{210}Pb ratios were also measured in the marine samples, and they were found to be always higher than unity and usually above 10, which indicated the unsupported nature of ^{210}Po. The data were used in arriving at concentration factors in the marine environment, and these concentration factors demonstrated a preferential uptake of ^{210}Po and a lower tendency to uptake of ^{226}Ra, ^{228}Ra, and ^{210}Pb. In the land-crops category, only spinach appears to concentrate significant radionuclide levels, with ^{210}Pb at the maximum.

The study has also shown that the leaves of casuarina trees [*Casuarina equisetifolia*] contain appreciable amounts of radioactivity, depending upon the

growth site, i.e., whether in the region of a hot spot or away from it. A segment of the local population uses the dry casuarina foliage as a source of fuel for their domestic energy needs. This practice could contribute to significant exposure.

Finally, the fishing community appears to be subject to a relatively higher exposure than the farmers living inland, from the twin exposure sources: (1) higher radiation exposure rates from residing on the beach and (2) higher radioactivity appearing in marine food sources than from the land sources.

Kalpakkam (12°33′N and 80°11′E), situated 75 km south of Madras, on the east coast of India, is developing into a major nuclear center. Two CANDU type nuclear power stations of 215 MW(e) each, a fast breeder test reactor, a number of supporting research and development laboratories, and a centralized waste treatment facility are under construction.

Preoperational baseline radiation surveys in the environment are in progress at Kalpakkam. Figure 1 describes the Kalpakkam environment and shows the site location and radial zones at distances of 8, 18, 24, and 32 km. Since it is a coastal site, Kalpakkam is influenced by the strong winds from the Bay of Bengal. The area receives rain mainly from the northeast and, to a minor extent, southwest monsoons. The annual rainfall is around 1340 mm. The major water source for agricultural and domestic requirements in this rural area is the Palar, a subterranean river. Another important water course is the man-made Buckingham Canal that runs along the coast close to the sea.

PREOPERATIONAL SURVEYS

During the preoperational surveys the local beach sands at some places showed radiation levels of 200 to 300 μR/hr, which were far higher than the normal background of 20 μR/hr observed in the interior. When the presence of natural radioactivity from monazite in the beach sands was suspected, gamma spectra were taken and compared with the radioactivity of the Kerala monazite sand. Figure 2 presents a typical gamma spectrum of the Kalpakkam beach sand obtained with a 2-in. NaI(Tl) well-type detector along with the spectrum of the Kerala monazite sample. The close identity of the two spectra confirmed the presence of monazite in the beach sands of Kalpakkam. On analysis of the spectra, the monazite content of Kalpakkam beach sand was found to be 0.5%, whereas the Kerala sands contained 5 to 9% monazite (Iyer, Iyengar, and Ganapathy, 1974). In establishing a baseline exposure evaluation, the existence of monazite in the local beach sands and the resultant exposure of

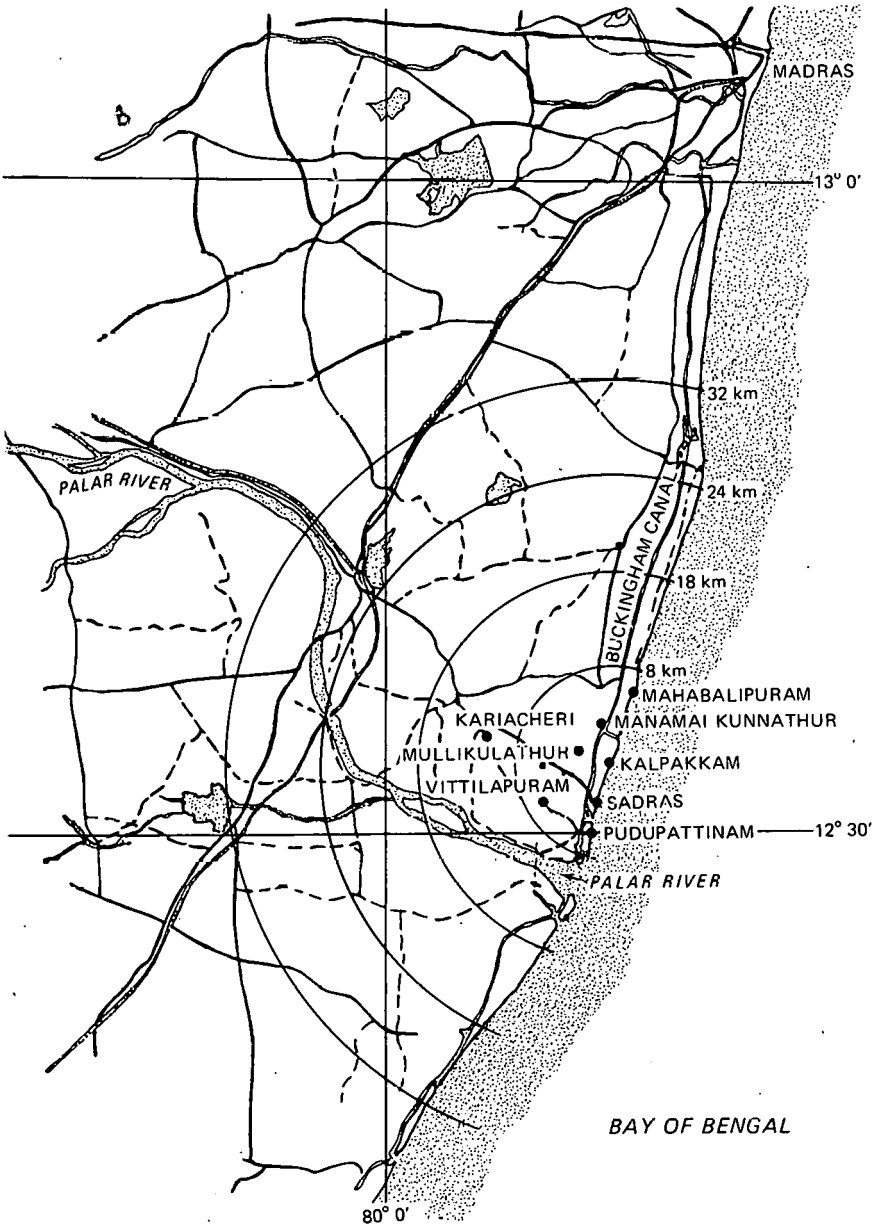


Fig. 1 Kalpakkam site and environment.

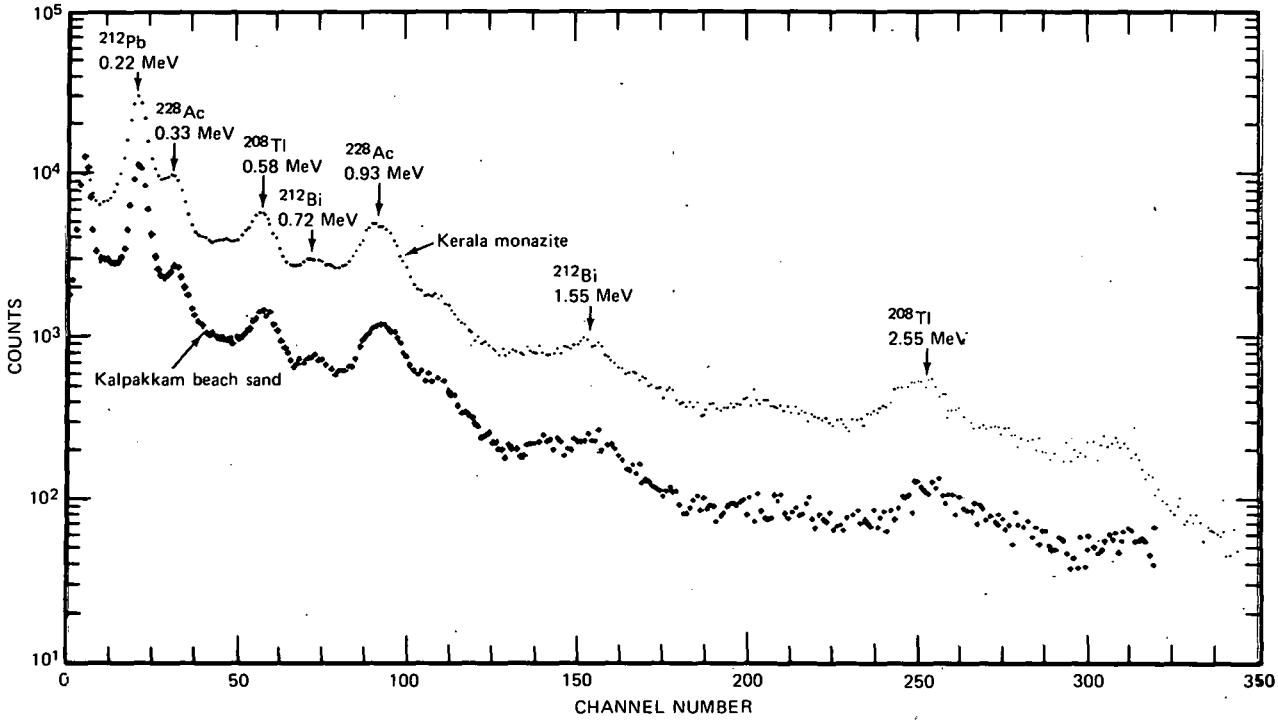


Fig. 2 Gamma spectrum of Kalpakkam beach sand.

the local population are of considerable significance. This paper presents results of the background survey in the low-monazite region of Kalpakkam and estimates its impact on the public.

Radiation Surveys

The ambient gamma-radiation levels were measured with a scintillometer [NaI(Tl) crystal, 1.75 by 2 in., with a reading range of 0 to 2000 μR/hr in three operating ranges]. Beach surveys revealed a rapidly changing nonuniform radiation profile with the readings ranging from 20 to 400 μR/hr. The higher radiation levels were usually traceable to patches of dispersed monazite in the vicinity. These hot spots were found to be limited to surface sands and confined to small pockets, since depth samples taken $\leq$1 m showed a negligible presence of monazite. Table 1 summarizes the observed radiation levels on the beach and in adjoining areas. The discontinuous nature of monazite occurrence and distribution is evident from the varying radiation levels observed in the coastal beaches.

TABLE 1

Terrestrial Gamma-Radiation Levels

Description	Exposure rate, μR/hr
On the Beach	
Sadras beach	
Opposite quarter No. 28, 70 m from sea (G)*	200 to 400
Meyyur Kuppam	
Fishermen's village (G)	50 to 150
Fishermen's huts (D)†	30 to 45
Pudupattinam beach	
Between hospital and security camp (G)	120 to 250
Adjoining the Beach	
Department of Atomic Energy housing colony	
Residential premises (D)	15 to 135
Residential interiors (D)	15 to 40
Reactor site neighborhood	
Contractor's residential premises (G)	50 to 350
Contractor's residential interiors (D)	40 to 120
Villages in 5-mile radial zone (G)	8 to 20

*G, general ambient.
†D, dwelling ambient.

As one moves away from the shore toward the mainland, the radiation levels rapidly fall close to the background of 10 to 20 μR/hr. This background value is nearly twice that appearing in other areas of the country (Bhat et al., 1972). The higher radiation levels in the beach areas compared with those of the mainland lead to the conclusion that its occurrence is of marine origin. The eastern seacoast of India is reported to be subject to extensive littoral transport, which reverses with currents seasonally and results in the movement of large quantities of shore sand (Tata Consultants Report, 1972). It is of interest that similar but more extensive monazite deposits occur both on the northeast and on the southwest coasts of India. Therefore the population residing on the coast is exposed to a higher radiation level than the population living in the interior. Data collected from a demographic survey carried out in the 8-km radial zone have brought out the existence of three occupational categories of population: fishermen living on the coastal beaches, farmers living inland, and a miscellaneous trades group residing inland. Diet data demonstrated the essential dependence of fishermen on seafood (about 120 g/day) and of farmers on land-grown crops. Food habits lead to the identification of pathways of exposure for detailed evaluation.

MATERIALS AND METHODS

The potential degree of internal exposure to the local population as a result of natural radioactivity in air, water, and diet media was investigated. Air samples were counted for gross alpha and beta activity. Detailed analyses for some of the key radionuclides of the thorium and the uranium series were performed for water and diet components. The analysis of marine food sources such as Mollusca, Crustacea, and fishes included study of tissue concentration of radionuclides. Many of the samples were analyzed for ^{226}Ra, ^{228}Ra, and ^{210}Po content. Lead-210 was determined in samples where it was of interest to establish the equilibrium status of ^{210}Po with ^{210}Pb. Details of the analytical methods used are given in the appendix to this paper. In brief, the estimations were carried out as follows: (1) ^{226}Ra by emanometry; (2) ^{228}Ra by allowing equilibrium growth of its daughter ^{228}Ac ($T_{½}$, 6.1 hr) and separation of the latter on LaF_3 and counting in a low-beta counter; (3) ^{210}Po by electrodeposition on a silver planchet and subsequent alpha counting; (4) ^{210}Pb by allowing equilibrium growth of ^{210}Bi ($T_{½}$, 5 days) and separation on $BiPO_4$ and counting in a low-beta counter.

The counting instruments used were (1) an alpha counter with ZnS (Ag) detector with a background of 0.03 cpm and efficiency of

25%, and (2) a gas-flow type (argon) low-beta counter with a background of 1.2 cpm and efficiency of 40%.

RESULTS AND DISCUSSION

Air Monitoring

The average ambient air concentrations of long-lived alpha and beta activity were found to range from 0.89 ± 0.68 to 1.75 ± 0.9 pCi/m^3 and from 40.6 ± 11.0 to 135.3 ± 18.0 pCi/m^3, respectively. These activities are comparable to the levels reported from other sites, i.e., Tarapur and Rajasthan (Bhat et al., 1972; Gurg, Bhat, and Kamath, 1975). No unusual buildup of activity due to radon emanation was seen at Kalpakkam.

Water Monitoring

The main source of water supply in the region comes from the Palar River (Fig. 1). The additional required water supply is obtained from a number of borewells and community groundwater wells scattered in the area. Radium-226 content of the well waters is presented in Table 2. The ^{226}Ra data demonstrate the activity to be of a low order (0.03 ± 0.01 to 2.1 ± 0.07 pCi/liter), well within the permissible limits. Radium-228 values in well waters from the beach area were also below permissible levels. These data indicate the absence of leaching of radium from the beach monazite to the water body.

TABLE 2

Radium Content* of Drinking Water

Location of wells	^{226}Ra, pCi/liter	^{228}Ra, pCi/liter
Pudupattinam	2.1 ± 0.07	
Mahabalipuram	1.3 ± 0.07	
Sadras	0.39 ± 0.02	
Kokilimedu Kuppam	0.03 ± 0.01	
Meyyur Kuppam	0.03 ± 0.02	0.56 ± 0.18
Sadras Kuppam	0.03 ± 0.01	0.63 ± 0.12
Palar River water	0.2 ± 0.03	

*Maximum permissible concentration $(MPC)_w$ limits for members of public: for ^{226}Ra, 12.5 pCi/liter; for ^{228}Ra, 27.5 pCi/liter (International Atomic Energy Agency, 1967).

Marine Source Monitoring

The Kalpakkam beach sands have varying monazite activity levels in different locations; therefore there is a direct interest in monitoring exposure sources in the coastal marine environment. A number of samples of beach sand, seawater, suspended silt, marine organisms, of the pelagic and demersal types, were analyzed for ^{226}Ra, ^{228}Ra, ^{210}Pb, and ^{210}Po. The results are shown in Tables 3 and 4.

In Table 3 good correlations are shown between the radiation levels and the observed radium concentrations in beach sands. The dissolved radionuclide concentrations in seawater are in broad agreement with those reported by Cherry and Shannon (1974). Sea-silt analysis showed significant enrichment with respect to ^{228}Ra, ^{210}Pb, and ^{210}Po. Data in Table 4 demonstrate radioactivity concentrations in the three groups of marine organisms examined, i.e., Mollusca, Crustacea, and fishes. Gamma spectra for prawn and barnacle samples (Figs. 3 and 4) clearly show the influence of monazite activity in the samples. Careful scrutiny of the data, however, reveals varying degrees of concentration for the four nuclides, with ^{210}Po showing the maximum.

On the basis of the data in Tables 3 and 4, concentration factors (CF) were calculated for the organisms and their individual tissues. The CF values are given in Table 5. An examination of CF's and their magnitude shows the radionuclides falling into two groups: (1) ^{210}Po and (2) ^{226}Ra, ^{228}Ra, and ^{210}Pb.

For ^{210}Po, the CF's observed are as follows: for Crustacea, 10^3 to 10^4; for Mollusca, 10^4; and for fishes, 10^2 to 10^4. The CF data

TABLE 3

Activity in Marine Matrices

Sample and exposure rate	Location	Radioactivity, pCi/g			
		^{226}Ra	^{228}Ra	^{210}Pb*	^{210}Po
Beach sand from hot-spot regions (110 to 300 μR/hr)	Kalpakkam Coast	4.6 to 9.4	27.7 to 95.3		
Beach sand from normal low background region (30 μR/hr)	Mahabalipuram	0.13 ± 0.05	2.72 ± 1.3		
Beach sand from moderate background region (50 μR/hr)	Sadras	0.44 ± 0.04	19.8 ± 1.0	10.4 ± 0.5	1.2 ± 0.08
Seawater	Kalpakkam Coast	0.04 ± 0.02†	0.32 ± 0.12†	0.18 ± 0.02†	0.09 ± 0.01†
Suspended sea silt	Kalpakkam Coast	BDL‡	0.14 ± 0.05	0.68 ± 0.04	0.95 ± 0.09

*Lead-210 concentration in seawater is derived from ^{210}Po from the reported ratio of 1 : 2 for $^{210}Po/^{210}Pb$ (Cherry and Shannon, 1974; Nevissi and Schell, 1975).

†Picocuries per liter.

‡Below detection limit.

TABLE 4

Radioactivity Content of Local Seafoods*

Sample	Location	Radioactivity content, pCi/kg			
		^{226}Ra	^{228}Ra	^{210}Pb	^{210}Po
		Mollusca			
Clam (soft parts)	Buckingham Canal	5.7 ± 3.0	53.5 ± 11.1	36.5 ± 8.2	1982.2 ± 48.7
Oyster	Mahabalipuram				
Soft parts		2.9 ± 1.5	41.3 ± 9.0	21.2 ± 3.6	729.5 ± 45.0
Shell		BDL†	31.6 ± 11.8	168.0 ± 46.7	BDL†
		Crustacea			
Prawn (muscle)	Sadras backwaters	3.2 ± 2.6	113.5 ± 10.6	8.9 ± 4.1	121.4 ± 4.6
Crab (*Scylla serrata* sp.)	Buckingham Canal				
Muscle		4.4 ± 1.2	37.0 ± 8.4	21.3 ± 4.0	107.5 ± 7.0
Gills, liver		13.6 ± 5.4	52.1 ± 25.0	104.7 ± 15.4	5063.2 ± 66.4
Crab (*Neptunus* sp.)	Kalpakkam				
Muscle	Coast	BDL†	11.2 ± 4.7	11.4 ± 1.7	2364.4 ± 56.6
Gills		437.9 ± 12.8	3662.9 ± 73.9	1472.8 ± 36.1	1480.9 ± 43.0
Shell		33.1 ± 8.2	256.0 ± 39.5	58.4 ± 19.5	3471.9 ± 153.0
Mole crab	Kalpakkam				
Muscle	Coast	8.2 ± 1.2	21.9 ± 4.3	31.9 ± 3.2	339.6 ± 10.5
Shell		8.8 ± 2.9	74.0 ± 18.7	64.8 ± 2.8	1833.3 ± 38.3
Prawn	Kalpakkam				
Muscle	Coast	BDL†	18.0 ± 3.5	6.1 ± 1.3	334.7 ± 17.3
Shell		14.4 ± 2.0	94.6 ± 12.4	21.2 ± 3.1	827.4 ± 30.6
		Fishes			
Sole	Kalpakkam				
Muscle	Coast	2.2 ± 0.5	6.6 ± 2.9	8.8 ± 1.6	173.7 ± 14.8
Bone		14.9 ± 4.3	51.2 ± 12.7	37.6 ± 9.8	1576.8 ± 46.3
Mackerel sp.	Kalpakkam				
Muscle	Coast	4.7 ± 0.8	20.2 ± 4.7	15.9 ± 2.4	25.0 ± 3.7
Bone			223.3 ± 19.9	167.2 ± 12.2	414.2 ± 18.0
Ray	Kalpakkam				
Muscle	Coast	2.4 ± 1.4	BDL†		17.8 ± 8.1
Cartilage		2.6 ± 1.6	31.5 ± 7.5	28.5 ± 5.6	31.4 ± 3.8
Liver			23.4 ± 3.9	20.3 ± 4.5	1424.8 ± 36.0
Oil sardine	Kalpakkam				
Muscle	Coast	5.3 ± 0.7	14.2 ± 3.9	7.6 ± 1.4	55.6 ± 4.4
Bone		24.5 ± 3.5	56.1 ± 12.0	48.8 ± 8.0	238.4 ± 16.2

*Data reported on wet-weight basis.
†Below detection limit.

apparently do not show any exclusive preference among the organisms, although a lower figure is indicated for fishes. Even among the fishes, sole, a demersal fish, has shown a relatively high ^{210}Po value in muscle (173.7 pCi/kg) and bone (1576.8 pCi/kg). CF distribution in tissue in the organisms are in the following order: for fish, liver (10^4) > bone (10^3) > muscle (10^2); and for Crustacea, shell (10^4) > soft parts (10^3).

As for the equilibrium relationship between ^{210}Po and ^{210}Pb, the calculated ^{210}Po/^{210}Pb ratios are always above 1 and usually exceed 10. This is clear evidence that ^{210}Po is not supported by ^{210}Pb in the organisms. The organisms appear to accumulate ^{210}Po in preference to ^{210}Pb from the environment, either directly or

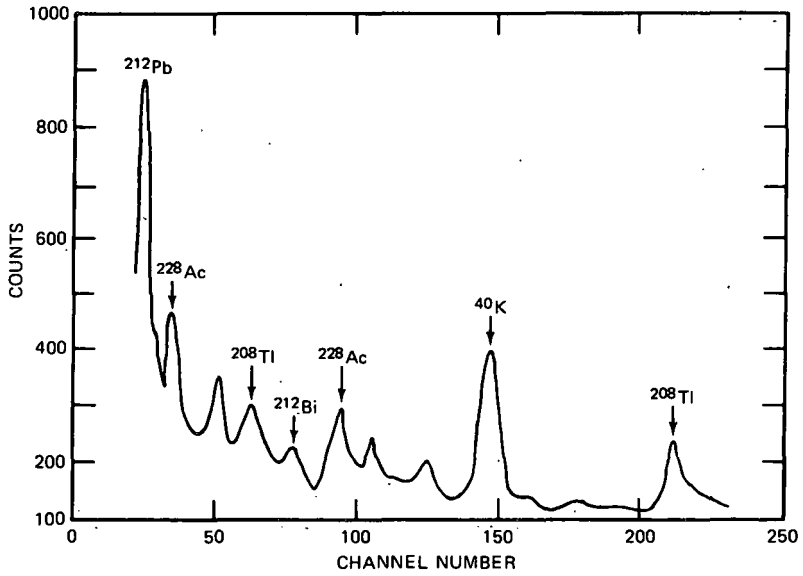


Fig. 3 Gamma spectrum of sample of prawn flesh.

through their food chain which contains higher concentrations of ^{210}Po. Similar ^{210}Po/^{210}Pb ratios have been reported by Schell, Jokela, and Eagle (1973) and Folsom and Beasley (1973).

For the second group of nuclides, i.e., ^{226}Ra, ^{228}Ra, and ^{210}Pb, their CF's in comparison to that of ^{210}Po in the same organism are generally less by a factor of 10 or even of 100 in some cases. The CF's generally display the following range: for Crustacea, 10 to 10^2; for Mollusca, 10^2; and for fishes, 10^2.

For crab, a high value [(8.2 to 12.0) x 10^3] is observed for the gill tissue. Generally, higher concentrations are seen for Mollusca and Crustacea as compared with fish tissue. The CF's in tissues in fishes would be greater in bone than in soft parts. The order of concentration levels and the CF's reported here appear to agree well with the data of other investigators (Kauranen and Miettinen, 1970; Beasley, 1968; Mauchline and Templeton, 1964).

Terrestrial Monitoring

The radioactivity intake through terrestrial sources was measured by analyses of samples of grass, milk, vegetables, cereals, fruits, and local soil for ^{226}Ra content. Some samples were also analyzed for their ^{228}Ra, ^{210}Pb, and ^{210}Po content. Results are

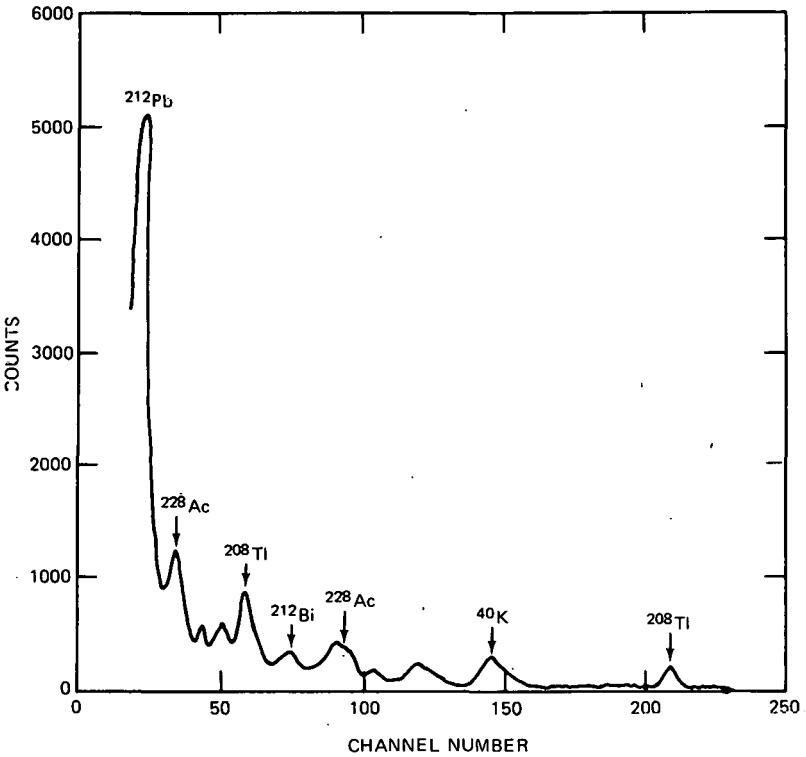


Fig. 4 Gamma spectrum of barnacle sample.

summarized in Table 6. The samples are mainly from areas with radiation levels of 10 to 20 μR/hr. The root-vegetable sample analysis suggests equilibrium between ^{210}Pb and ^{210}Po. The succulent vegetables show a conspicuous lack of ^{210}Po uptake. In spinach leaves there is high uptake of all the radioelements, with ^{210}Pb (44.5 pCi/kg) the highest.

Other Sources

During the survey it was observed that the rural population uses as fuel dry leaves of the casuarina tree (*Casuarina equisetifolia*) which grows abundantly in the region. A study of the radioactivity distribution in the dry leaves showed significant concentrations of ^{226}Ra, ^{228}Ra, and ^{210}Po (see Table 7). The level of radionuclide concentrations in the foliage appeared to vary with the radiation level at the sampling site.

TABLE 5

Concentration Factors for Marine Organisms

Sample	Location	^{226}Ra	^{228}Ra	^{210}Pb	^{210}Po
		Mollusca			
Clam (soft parts)	Buckingham Canal	1.4×10^2	1.7×10^2	2×10^2	2.2×10^4
Oyster	Mahabalipuram				
Soft parts		7.3 X 10	1.3×10^2	1.2×10^2	8.1×10^3
Shell			1×10^2	9.3×10^2	
		Crustacea			
Prawn (muscle)	Sadras back-waters	8 X 10	3.6×10^2	4.9 X 10	1.4×10^3
Crab (*Scylla serrata*)	Buckingham				
Muscle	Canal	1.1×10^2	1.8×10^2	1.2×10^2	1.2×10^3
Gills and liver		3.4×10^2	1.6×10^2	5.8×10^2	5.6×10^4
Crab (*Neptunus* sp.)	Kalpakkam				
Muscle	Coast		3.5 X 10	6.3 X 10	2.6×10^4
Gills		1.1×10^4	1.2×10^4	8.2×10^3	1.7×10^4
Shell		8.3×10^2	8×10^2	3.2×10^2	3.9×10^4
Mole crab	Kalpakkam				
Muscle	Coast	2.1×10^2	6.8 X 10	1.8×10^2	3.8×10^3
Shell		2.2×10^2	2.3×10^2	3.6×10^2	2×10^4
Prawn	Kalpakkam				
Muscle	Coast		5.6 X 10	3.4 X 10	3.7×10^3
Shell		3.6×10^2	3×10^2	1.2×10^2	9.2×10^3
		Fishes			
Sole	Kalpakkam				
Muscle	Coast	5.5 X 10	2.1 X 10	4.9 X 10	1.9×10^3
Bone		3.7×10^2	1.6×10^2	2.1×10^2	1.8×10^4
Mackerel	Kalpakkam				
Muscle	Coast	1.2×10^2	6.3 X 10	8.8 X 10	2.8×10^2
Bone			7×10^2	9.3×10^2	4.6×10^3
Ray	Kalpakkam				
Muscle	Coast	6 X 10			2×10^2
Cartilage		6.5 X 10	9.8 X 10	1.6×10^2	3.5×10^2
Liver			7.2 X 10	1.1×10^2	1.6×10^4
Oil sardine	Kalpakkam				
Muscle	Coast	1.3×10^2	4.4 X 10	4.2 X 10	6.2×10^2
Bone		6.1×10^2	1.8×10^2	2.7×10^2	2.6×10^3

The dwellings in the huts where the casuarina foliage is used as fuel are usually small and poorly ventilated. There is thus an exposure potential through smoke inhalation. The casuarina samples were investigated for their ^{210}Po content in the dry leaf and in the ash after combustion. Before ashing, dry casuarina leaves had a ^{210}Po content of 398.0 pCi/kg. After ashing, the residue from the leaves showed a ^{210}Po content of 50.6 pCi/kg. It will be observed that ~347 pCi/kg of ^{210}Po would have escaped to the ambient atmosphere during combustion. Polonium-210 is a considerably

TABLE 6

Radioactivity Content of Land Produce

Sample	Location	^{226}Ra	^{228}Ra	^{210}Pb	^{210}Po
Soil*	Project site	0.25 ± 0.02	0.78 ± 0.07		1.2 ± 0.18
Grass	Laboratory premises	6.1 ± 0.2			
Milk†	Township milk society	0.13 ± 0.02			
Vegetables‡					
Sweet potato	Kariacheri	0.53 ± 0.13	4.3 ± 0.5	3.86 ± 0.56	3.15 ± 1.6
Suran (Amorpho-phallus)	Kunnathur	0.5 ± 0.16	2.0 ± 0.9	3.4 ± 0.62	4.45 ± 2.39
Brinjal	Manamai	0.58 ± 0.23	6.0 ± 1.6	3.1 ± 0.68	BDL§
Bottle gourd	Voyalur	1.0 ± 0.66	10.0 ± 3.6		BDL§
Spinach leaves	Manamai	8.4 ± 0.66	21.8 ± 3.6	44.5 ± 2.5	6.3 ± 1.5
Cereals					
Rice	Manamai	BDL§	2.2 ± 0.46	3.7 ± 0.5	14.6 ± 6.1
Ragi (*Eleusine coracana*)	Kunnathur	2.4 ± 0.8	14.3 ± 1.8	8.9 ± 1.3	3.5 ± 3.0
Other cereals (black gram, etc.)	Sadras	1.51 ± 0.21 to 4.4 ± 0.4			

*Soil samples are reported as picocuries per gram.
†Milk samples are reported as picocuries per gram of ash.
‡Vegetable samples are reported on wet-weight basis in picocuries per kilogram.
§Below detection limit.

TABLE 7

Radioactivity in Casuarina Foliage

Location and radiation level	Radioactivity, pCi/kg		
	^{226}Ra	^{228}Ra	^{210}Po
Near Environmental Survey Laboratory (30 to 40 μR/hr)	0.37 ± 0.04	22.6 ± 1.55	
Near Madras Atomic Power Project site (160 to 200 μR/hr)	54.8 ± 5.5	930.0 ± 35.8	398.0 ± 19.00*

*Duplicate sample from the same region.

volatile element at the combustion temperature, and hence it was chosen for studying the significance of the domestic use of casuarina foliage. The results demonstrate considerable inhalation exposure potential for the rural population from such a practice.

CONCLUSION

External exposure level in dwellings in the beach and adjoining areas containing pockets of monazite, vary widely in the range of 15

to 120 μR/hr. The population of fishermen who live permanently on the beaches is placed at a higher exposure level (0.26 to 0.4 R/year) as compared with farmers and others living inland (0.07 to 0.17 R/year). Among the various dietary items examined, the marine sources stand out from the terrestrial sources as contributing to a higher input of radioactivity to the population. Again, the fishermen are significant as the critical group since marine food items form major components of their daily diet. The survey also points out the significance of exposure potential to the local population who use casuarina foliage as fuel since it contains an appreciable amount of radioactivity. Further studies may clarify the actual status of this exposure and its contribution to the overall exposure of the local population.

ACKNOWLEDGMENTS

We are indebted to Dr. A. K. Ganguly and Shri. S. D. Soman for their constant guidance and encouragement. Thanks also are due to our colleagues in the Environmental Survey Laboratory for their cooperation, discussions, and support in analyses.

This work was carried out under International Atomic Energy Research Agency research contract No. 1788/RB.

REFERENCES

Beasley, T. M., 1968, Pb-210 in Selected Marine Organisms, Ph.D. Dissertation, Oregon State University, Corvallis, Oregon.

Bhat, I. S., et al., 1972, Environmental Radioactivity at Tarapur Atomic Power Station Site, Report BARC-I/161 [1972], Bhabha Atomic Research Centre.

Cherry, R. D., and L. V. Shannon, 1974, The Alpha Radioactivity of Marine Organisms, *At. Energy Rev.*, 12(1): 1-45.

Folsom, T. R., and T. M. Beasley, 1973, Contribution from the Alpha Emitter ^{210}Po to the Natural Radiation Environment of Marine Organisms, in *Radioactive Contamination of the Marine Environment*, Symposium Proceedings, Seattle, 1972, 625-632, STI/PUB/313, International Atomic Energy Agency, Vienna.

Gurg, R. P., I. S. Bhat, and P. R. Kamath, 1975, *Progress Report of Environmental Survey Laboratory, Rajasthan Atomic Power Station*, Report BARC-I/369, Bhabha Atomic Research Centre.

International Atomic Energy Agency, 1967, *Basic Safety Standards for Radiation Protection*, 1967, STI/PUB/147, International Atomic Energy Agency, Vienna.

Iyer, M. R., M. A. R. Iyengar, and S. Ganapathy, 1974, Radiation Survey of the Monazite Areas at Kalpakkam, Report BARC-I/315 [1974], Bhabha Atomic Research Centre.

Kauranen, P., and J. K. Miettinen, 1970, Helsinki University Department of Radiochemistry Annual Report, August 1969—August 1970, NYO-3466-14, paper 27.

Mauchline, J., and W. L. Templeton, 1964, *Oceanogr. Mar. Biol. Ann. Rev.*, 2: 229.

Nevissi, A., and W. R. Schell, 1975, ^{210}Po, ^{239}Pu, ^{240}Pu in Biological and Water Samples from the Bikini and Eniwetok Atolls, *Nature*, 255(5506): 321-323.

Schell, W. R., T. Jokela, and R. Eagle, 1973, Natural ^{210}Pb and ^{210}Po in the Marine Environment, in *Radioactive Contamination of the Marine Environment*, pp. 701-723, Symposium Proceedings, Seattle, 1972, STI/PUB/313, International Atomic Energy Agency, Vienna.

Tata Consultants Report, 1972, for Madras Atomic Power Project, Department of Atomic Energy, Bombay.

APPENDIX

Sample Preparation

Soil and Sand. The soil and sand samples (5 to 10 g) are ground to pass 100 mesh and heated to 450°C for 5 to 6 hr to remove organic matter. These samples are then heated three times with concentrated HNO_3, evaporating to dryness each time. The residue is extracted with 4*N* HNO_3, filtered, and made up to a known volume.

Water. Samples of well water (3 to 5 liters) and seawater (40 liters) are taken after filtration through Whatman 40 paper.

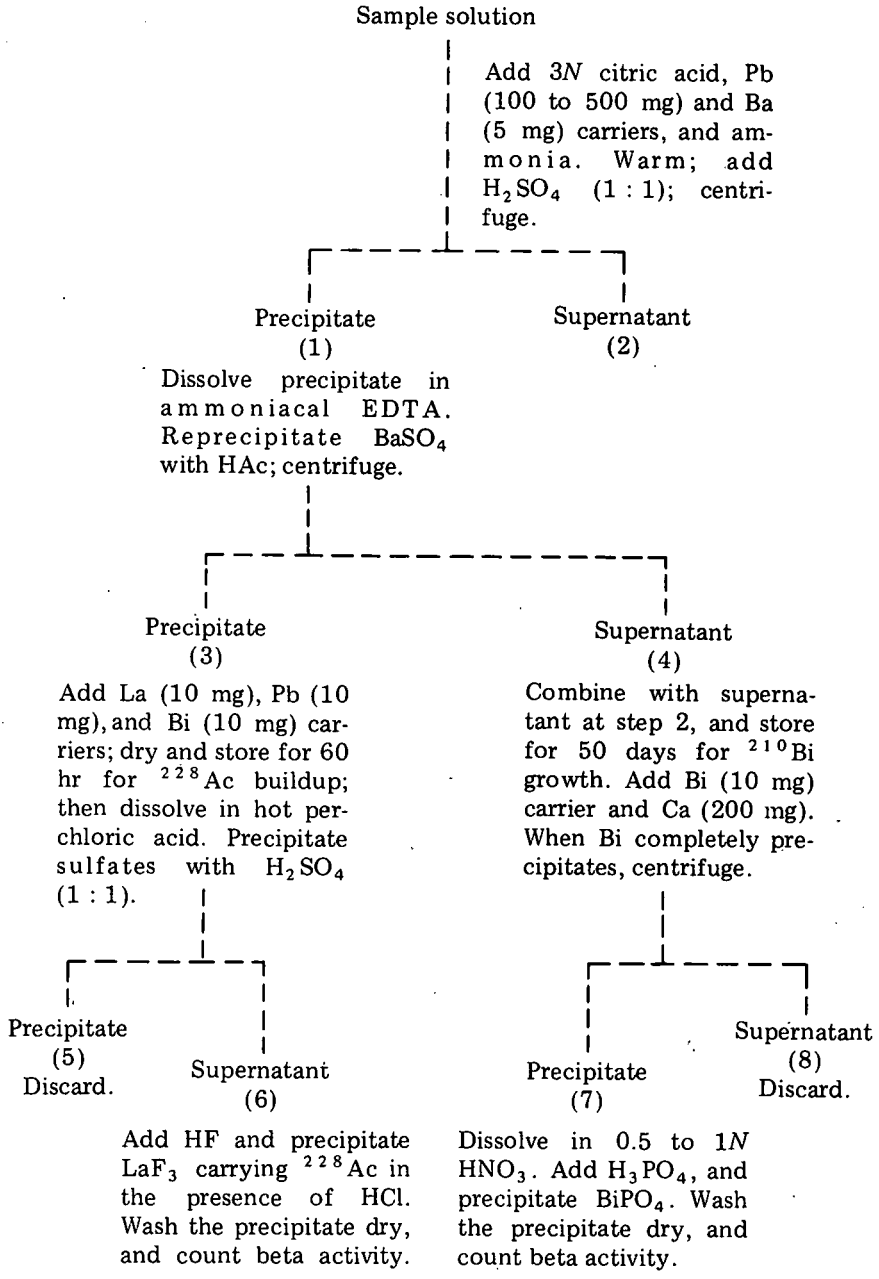
Seafood and Vegetation. Seafood and vegetation samples are ashed at 450°C to obtain a white ash, which is taken up for analysis after it is leached with HNO_3 and processed as given for soil samples.

Sample Preparation for ^{210}Po. Because of the volatile nature of polonium in dry-ashing conditions, the biological samples for ^{210}Po estimations are wet processed with $HNO_3 : H_2O_2$ (1 : 1) oxidizing mixture. The resulting clear solution is evaporated with HCl and processed for polonium estimation. (See details under ^{210}Po estimation.)

Estimations

Radium-226 by Emanometry. The method consists of storing the solution containing ^{226}Ra in dissolved form in a bubbler for a known period (2 to 4 weeks, depending upon the concentration of ^{226}Ra) to allow buildup of the gaseous daughter ^{222}Rn ($T_{1/2}$ = 3.8 days). At the end of the buildup period, an evacuated scintillation cell made of aluminum and coated with ZnS (Ag) is coupled directly to the bubbler, and the radon gas is collected in the cell. The cell is now stored for 180 min to reach equilibrium of ^{222}Rn with its

^{228}Ra and ^{210}Pb Analysis*



*Based on Kamath et al., 1964.

daughter products (RaA, RaB, RaC, and RaC'). It is then coupled to a photomultiplier and counter assembly and counted. Radium-226 content in the solution is calculated as follows:

$$^{226}\text{Ra (in picocuries per milliliter)} = \left[\frac{1.883 \times 10^{-3}\ C}{V\ E e^{-\lambda t}(1 - e^{-\lambda T})}\right]\left(\frac{1}{F}\right)$$

where C = total counts in T min
E = efficiency (average, 70%)
t = counting delay (> 180 min. The counting delay adopted is generally between 200 and 300 min.)
T = counting period (min)
F = buildup factor for ^{222}Rn from ^{226}Ra
V = volume of sample in bubbler
λ = decay constant of ^{222}Rn = 1.258×10^{-4} (min^{-1})

Polonium-210 by Electrodeposition. Soil, seafood, and vegetation samples are wet ashed with $HNO_3 : H_2O_2$ mixture (1 : 1) to bring ^{210}Po into solution. After several additions of HCl and digestion, the solution is made up to 0.5 to 1*N* HCl. The solution is kept on a water bath and ^{210}Po is plated (for 5 to 6 hr) on a silver disk by the electrochemical displacement method, and the activity is alpha counted (Holtzmann, 1967).

For seawater samples ^{210}Po is carried on $AlPO_4$ precipitate (Koide and Bruland, 1975). The collected $AlPO_4$ is dissolved in 0.5*M* HCl, and polonium is plated as above and alpha counted.

Radium-228 and Lead-210. These isotopes are treated according to the flow chart on the preceding page.

REFERENCES

Holtzmann, R. B., 1967, Concentrations of the Naturally Occurring Radionuclides ^{226}Ra, ^{210}Pb, and ^{210}Po in Aquatic Fauna, in *Symposium on Radioecology*, Proceedings of the Second National Symposium on Radioecology, Ann Arbor, Mich., May 15—17, 1967, D. J. Nelson and F. C. Evans (Eds.), pp. 535-546, USAEC CONF-670503, Ecological Society of America, NTIS.

Kamath, P. R., et al., 1964, Recent Radiochemical Procedures for Bioassay Studies at Trombay, in *Assessment of Radioactive Body Burden in Man*, STI/PUB/84, p. 203, International Atomic Energy Agency, Vienna.

Koide, Minoru, and K. W. Bruland, 1975, The Electrodeposition and Determination of Radium by Isotopic Dilution in Sea Water and in Sediments Simultaneously with Other Natural Radionuclides, *Anal. Chim. Acta*, 75: 1-19.

Results of a National Survey on Natural Radioactivity in Italy

G. SCIOCCHETTI and F. SCACCO
Comitato Nazionale per l'Energia Nucleare, Rome, Italy

ABSTRACT

In this paper data are reported on the natural radiation environments in Italian mines and spas. The survey and relevant internal exposure assessment indicated that large groups of persons are chronically exposed to nonnegligible levels of radon and daughter products, which are always present in variable concentrations.

Since the radiological environment of the spa is similar (in some respects) to that of mine one, there is the possibility of comparing two population groups living in different conditions, but similarly exposed, to evaluate the synergistic factors, if any.

There is a growing worldwide interest in collection of experimental data concerning natural radioactivity and associated special groups of exposed persons (Snihs, 1974; Pohl and Scheminzky, 1973). As a consequence of peculiar geological characteristics of Italy, it was possible to identify some slightly high natural radiation environments. In this paper extensive data are reported relating to underground nonuranium mines, selected on a geographical and geological basis, and to radon spas, located at the two largest hydrothermal spa areas in Italy. The purpose of this study was the evaluation of the contribution to population dose of inhaled radon daughter products, the only natural radionuclides giving rise to nonnegligible internal exposure.

Previous surveys in mines (Bottino et al., 1973) indicated the radiological situation of a large group of persons chronically exposed to nonnegligible levels of radon daughter products always present in variable concentrations in underground galleries. Preliminary results,

valuable for collective dose assessment and as data for planning monitoring programs, lead to survey programs including radon spas, preliminary to comparing, from an epidemiological point of view, population groups living in different environmental conditions but similarly exposed. For collecting data, Italy is in a very propitious situation. The country has both numerous mines and radioactive hydrothermal springs. Spa areas, as mines, are located in almost all Italian territory, over about 400 areas, particularly in the Piemonte, Veneto, and Campania districts. In almost all spas are treatment facilities with mineral and hot springs and baths, where high levels of radon and daughter products are inhaled by workers and patients.

MONITORING PROCEDURES

All measurements were made with the technical assistance of our Radiometric Unit. Standardized dosimetric techniques and specific instrumentation were developed for the survey.

Preliminary assessments of air quality in mine and spa environments were accomplished by a radon-concentration survey. Measurements were made with scintillation chambers and the double-filter technique. Radiation exposures of miners and spa workers were estimated from environmental data, gathered by repetitive sampling of radon daughter concentrations.

Routine measurements for determining equilibrium equivalent radon were carried out by the Markov (Markov, Ryabov, and Stas, 1962) method. Accuracy and precision tests against Tsivoglou and spectrometric methods confirmed reliability of method selected for routine monitoring (Scacco and Sciocchetti, 1977). Some physical characteristics of inhaled atmospheres were also investigated, including the unattached fraction of ^{218}Po (RaA) determined by a special spectrometric technique (Sciocchetti, 1977).

RESULTS

Table 1 gives results of a survey made in 17 Italian underground mines with values of maximum radon concentrations found in each mine and the relevant estimated annual occupational exposures. Mines were divided into three groups according to geological and geographical characteristics of Italian territory. Setting up some simple relationship between airborne radioactivity and geological characteristics is very arduous, even if some correlation between radon concentration and the orogenetic belt was observed

TABLE 1

Annual Occupational Exposures in Mines

Mine	Maximum radon concentration, pCi/liter	Annual exposure, WLM/year*
Group I		
Alps		
A	800	1.24
B	500	6.0
C	370	4.8
D	300	3.6
G	120	2.76
H	100	1.2
Sardinia		
E	200	2.4
F	200	0.24
Q	20	0.02
Group II		
Apennines		
I	60	0.09
L	35	1.35
M	30	0.05
N	30	0.28
O	20	0.66
P	20	0.05
R	20	0.09
Group III		
Uranium prospecting areas		
S	700	15.9

*Annual occupational exposure, 2000 hr/year.

(Sciocchetti, 1977). Analogously, Table 2 gives results of a survey made in 20 Italian radon spas.

In surveyed nonuranium mines, radon concentrations ranged from about 800 to 10 pCi/liter, potential alpha energy concentrations from 0.60 to 0.01 working levels (WL), and equilibrium factors from 0.5 to 0.01. In spas the ranges were from 14,000 to 10 pCi/liter, from 2 to 0.001 WL, and from 0.05 to 0.001.

Figure 1 gives equilibrium factor* distributions in surveyed mines and spas. Diagrams show that radon was never found in equilibrium

*Equilibrium factor is: $100 \times \frac{\text{Daughter concentration (WL)}}{\text{Radon concentration (pCi/liter)}}$

TABLE 2

Annual Occupational Exposures in Spas

Spa	Maximum radon concentration, pCi/liter	Annual exposure, WLM/year*
South Italy		
Ischia		
TRI	13,900	23.6
TC	420	0.37
TDP	170	0.06
TVS	170	0.87
TA	140	0.07
TSM	120	0.22
TLP	99	0.08
TM	88	0.02
TMI	59	0.22
TVT	40	0.04
TS	40	0.02
TF	40	0.16
TB	20	0.13
TI	20	0.03
TS	15	0.06
TCP	15	0.02
TCL	12	0.03
North Italy		
Abano Terme		
TTM	180	0.94
TGT	110	0.46
Lurisia		
TL	8,520	1.92

*Annual occupational exposure, 2000 hr/year.

conditions with its daughters. The F values cover a wide range but are always lower than 0.5 in mines and 0.05 in spas, respectively. Partial accumulation of equilibrium factors near origin of coordinate axes seems to confirm the practical possibility of measuring radon concentrations for extensive surveys and routine monitoring. Consequently exposure assessment might be performed by an estimated equilibrium factor F.

Figure 2 gives distributions of persons grouped in four exposed ranges in surveyed mines and spas. The mine diagram is related to about 2500 underground miners, a sample of the worker population engaged in extractive industry which is estimated in the thousands. The spa diagram is related to a group of about 500 workers out of

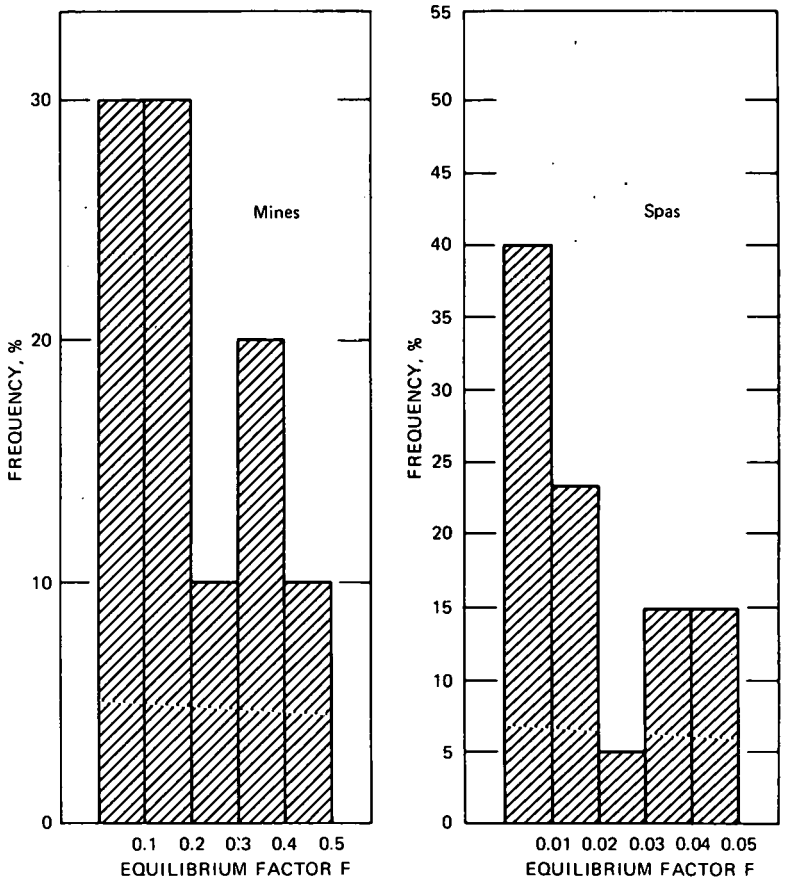


Fig. 1 Distribution of equilibrium factor F in surveyed mines and spas.

the whole population engaged in the many Italian hydrothermal baths. The diagrams, as comparative risk patterns, show significant analogies concerning both exposures, even though mines and spas are two very different living environments.

From the data we found several spa radon concentrations remarkably higher than in mines; the relevant occupational exposure distributions were substantially similar because the equilibrium factor distribution for spas is an order of magnitude lower than for mines.

Table 3 gives preliminary data obtained in a research program designed to assess ^{210}Pb and ^{210}Po burdens for subjects exposed in radioactive spas and underground mines (Breuer et al., 1977). As a consequence of results, the distribution in spa workers seems to be

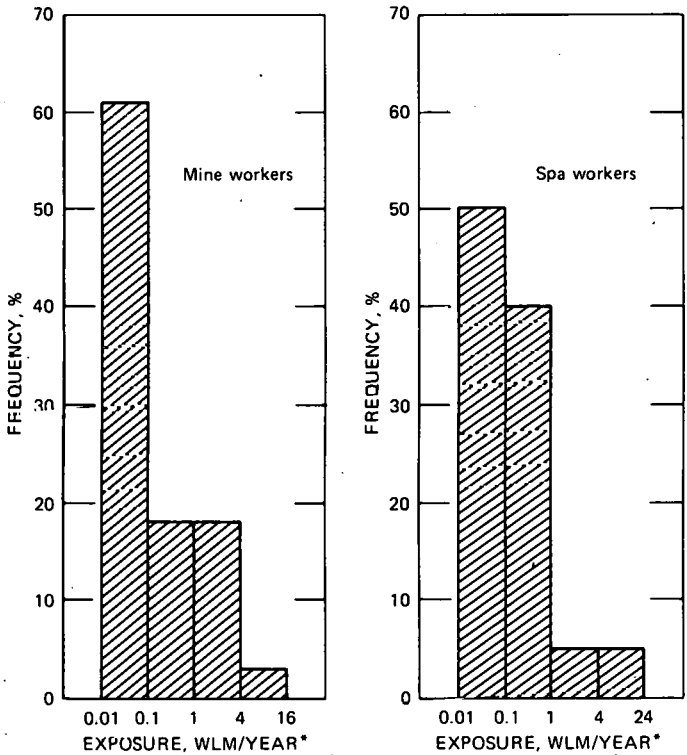


Fig. 2 Distribution of mine and spa workers grouped in four exposure ranges. (*Occupational annual exposure, 2000 hr/year.)

completely different from the distribution obtained in uranium miners. The table gives skeletal burdens and exposures. Lung dose was not evaluated because of uncertainties regarding relationship between exposure and dose. The WLM (working level month) cumulative exposure for each spa worker was evaluated on the basis of both measurements performed in the spa atmosphere and the working history of the subjects.

CONCLUSIONS

Collected data gave a national pattern of a preliminary dose assessment on internal exposure to naturally occurring radionuclides for two large population groups. The screening of mines revealed that risk to radiation exposure is not restricted to uranium mines but is also present in nonuranium mines. Analogously, the spa survey

TABLE 3

Burden and Exposure for Some of the Spa Workers Sampled*

Subject No.	Skeletal burden, nCi		Exposure, WLM	Working period, years
	^{210}Po	^{210}Pb		
1	30	40	348	26
2	25	33	†	†
3	11	14.7	200	15
4	15	20	12	25
5	7	9.3	3.7	32
6	7	9.3	270	20

*From F. Breuer, G. F. Clemente, A. Renzetti, and G. Santori, 1977, *Proceedings of the Fourth International Congress of the International Radiation Protection Association*, Vol. 3, p. 757, International Radiation Protection Association, Washington, D. C.

†Unclear working history.

indicated that a large group of persons are exposed to nonnegligible levels of radon and daughter products.

It is remarkable that, in this type of mine and in radon spas, physical and medical surveillance is not being exercised; as a consequence the exposure limits that should be considered are population and not occupational ones. Particularly, exposures to spa patients should not be considered as medical exposures because of uncertain and/or limited therapeutical effects of these medical practices.

Because spa radiological environment presents strict analogies with mine one, results might at last permit epidemiological studies on internal exposure of large groups of exposed persons, on the basis of complementary physical and biomedical data. The possibility of comparing lung disease induction in two population groups living in different environmental conditions, but exposed to similar radon daughter concentrations, might be a remarkable opportunity to evaluate effects of synergistic factors, if any.

REFERENCES

Bottino, A., G. Lembo, F. Scacco, G. Sciocchetti, and S. Tagliati, 1973, Results of a Survey of Airborne Radioactivity in Italian Mines, in *Proceedings of the Regional Conference on Radiation Protection*, Jerusalem, Mar. 5—8, 1973,

Y. Feige and T. Schlesinger (Eds.), Report CONF-730345-P1, pp. 217-223, Israel Atomic Energy Commission, Soreq Nuclear Research Centre, Yavne, Israel.

Breuer, F., G. F. Clemente, A. Renzetti, and G. Santori, 1977, 210 Pb and 210 Po Urine Concentration in Subjects Working in Radon Spa, in *Proceedings of the Fourth International Congress of the International Radiation Protection Association*, Paris, April 24—30, 1977, Vol. 3, p. 757, International Radiation Protection Association.

Markov, K. P., N. V. Ryabov, and K. N. Stas, 1962, A Rapid Method for Estimating the Hazard Associated with the Presence of Radon Daughter Products in Air, *At. Energ.*, 12: 315.

Pohl, J., and F. Scheminzky, 1973, The Natural Radiation Environment of Badgastein, Austria and Its Biological Effects, in *The Natural Radiation Environment II*, Symposium Proceedings, Houston, Tex., Aug. 7—11, 1972, J. A. S. Adams, W. M. Lowder, and T. F. Gesell (Eds.), ERDA Report CONF-720805, p 393, Rice University and the University of Texas, Houston, NTIS.

Scacco, F., e G. Sciocchetti, 1977, Indagine sulla radioattività dell'aria in miniere e terme italiane, in *XX Congresso Nazionale AIFSPR Bologna*, 26—28 ott. 1977 (in press).

Sciocchetti, G., 1977, Assessment of Airborne Radioactivity in Italian Mines, in *Specialist Meeting on Personal Dosimetry and Area Monitoring Suitable for Radon and Daughter Products*, Proceedings of the Nuclear Energy Agency Meeting, Elliot Lake, Canada, Oct. 4—8, 1976, p. 259. Available from the Director of Information, Organization for Economic Cooperation and Development, Paris, France.

Snihs, J. O., 1974, The Approach to Radon Problems in Nonuranium Mines in Sweden, in *Proceedings of the Third International Congress of the International Radiation Protection Association*, Washington, D. C., Sept. 9—14, 1973, USAEC Report CONF-730907-P2, pp. 900-911, NTIS.

DISCUSSION

Holtzman: The body contents of ^{210}Pb and ^{210}Po for the spa workers appear to be very high compared to estimates we might make for working levels (very low equilibrium values for radon daughters). Have working levels been made from the estimated body burdens in comparison to those of uranium miners?

Sciocchetti: The exposure in each spa, recorded in WLM, was obtained from measurements made in spas by our radiometric unit. The WLM cumulative exposure for each spa worker was obtained by multiplying the measured WL units, as estimates of an average annual value for each spa, by the number of months the men worked in it, and adding these products for the whole working experience.

Wrenn: How was ^{210}Pb measured in the skeleton?

Sciocchetti: It wasn't measured in the skeleton, only in the urine.

Wrenn: Then this may be the reason for seeing high ^{210}Pb, namely, that the ^{210}Pb reflects current exposure rather than

cumulative exposure. Cumulative exposure (in WLM) is related to ^{210}Pb in bone, which can be determined by dual thin crystal counting over the skull which can be sensitive for roughly several hundred working levels or greater. Details have been published recently in *Health Physics* by Cohen et al.

Ellett: Are you planning epidemiological studies, and when might these start?

Sciocchetti: The described survey has identified two large population groups exposed to significant levels of internal dose of natural origin. The program is in progress, and, if future results will confirm actual findings, an epidemiological survey might be carried out through a joint work with Comisión Nacional de Energía Nuclear biomedical laboratories in the next few years.

Age-, Sex-, and Weight-Dependent Dose Patterns Due to Inhaled Natural Radionuclides

W. HOFMANN, F. STEINHÄUSLER, and E. POHL
Institute of Physics, University of Salzburg, Salzburg, Austria

ABSTRACT

Calculations of doses due to inhaled radionuclides are in general based on the lung model of the International Commission on Radiological Protection (ICRP) Task Group on Lung Dynamics. All its parameters, including the pathways to other organs, refer to an adult reference man and are also averaged for the differences in sex and weight. At first we developed age-dependent lung models by using feasible theoretical considerations as well as experimental data for the postnatal growth of the respiratory tract. On the basis of these age-dependent models, we then calculated the regional particle deposition for the short-lived decay products of ^{222}Rn and ^{220}Rn since these radionuclides occur everywhere in our environment, outdoors as well as indoors.

Dose calculations were carried out for defined reference atmospheres and living activities, the latter being responsible for the respiratory minute volume. The mean doses for the various parts of the respiratory tract and for other organs show a maximum at the age of about six years. These doses are more than twice as high as for an adult for most of the organs and tissues. We found the half-life of the clearance time for the absorption of decay products from the alveolar region into the blood to be about 1 hr, which is in contradiction to the ICRP retention model. Furthermore, it was shown that for precise dose calculations the differences in sex and weight have to be considered as well.

The physiological data used for all dose calculations were compiled by the International Commission on Radiological Protection (hereafter referred to as ICRP) Task Group on Reference Man (1975). This reference man is defined as being between 20 and 30 years old, weighing 70 kg, and standing 170 cm high. As the report points out, only a few individuals of any population will have characteristics similar to those of the reference man. This is true particularly for all

age-dependent, changing physiological properties of infants and youths. Since the growing organism is in general more radiation sensitive than the adult, children are of particular importance with respect to radiation protection when nonoccupational exposures are considered.

In this study we investigated the doses to human organs and tissues from the inhalation of radon and its daughters as functions of age, sex, and weight. Radon and its decay products in the atmosphere of workplaces and living rooms in a normal environment are the main contributors to the natural radiation burden. In parts of the respiratory tract, they often cause the highest doses due to all natural radiation sources (Pohl et al., 1976; Steinhäusler et al., 1976; Steinhäusler et al., this volume). The bases for the present lung-dose calculations are the deposition and retention models of the earlier ICRP Task Group on Lung Dynamics (1966). The compartment model of the respiratory tract is still widely used for radiation protection study purposes because of its simplicity (Dyson and Beach, 1968; Kotrappa, 1969; Voillequé, 1970; Morrow, 1970; Jacobi, 1972; Jacobi and Schraub, 1974; Brain and Valberg, 1974; Snyder, Ford, and Watson, 1975). Since this model does not account for the inhomogeneity within the compartments, various other authors (Thomas, 1964; Jacobi, 1964, 1965; Altshuler, Nelson, and Kuschner, 1964; Haque and Collinson, 1967; Bykhovskii et al., 1972; Harley and Pasternack, 1972, 1973; Parthasarathy and Unnikrishnan, 1977) studied the dose distribution according to the anatomical–physiological models of Landahl (1950) and Weibel (1963). They found that the highest doses are received by the basal cells of the segmental and subsegmental bronchial epithelium which are therefore considered to be the critical target for the induction of lung cancer. All these models and calculations refer only to the adult reference man and to a mean respiratory minute volume (RMV). The various parameters of the respiratory tract, however, are highly dependent on age and, furthermore, on sex and weight. The amount of radon decay products accumulated in the individual regions of the respiratory tract is also determined by the RMV which is influenced not only by age and sex but also strongly by the actual physical activities of a person.

For continuous inhalation about 30% of ^{222}Rn-decay products and 50% of ^{220}Rn decay products deposited in the respiratory tract are distributed, mainly by the bloodstream, to the various organs and tissues (Pohl, 1965; Pohl and Pohl-Rüling, 1967, 1977). Therefore the changes in this deposit, which depend on age and sex, determine also the amount of the nuclides accumulated in the

individual organs other than the respiratory tract. Dose calculations for these organs and tissues, moreover, must consider their masses according to age, sex, and weight.

For the dose calculations in our study of the influence of age, sex, and weight, we developed an age-dependent lung model and modified the calculations of Pohl and Pohl-Rüling (1977) for the other organs.

AGE-DEPENDENT LUNG MODELS

The respiratory tract of a child differs greatly from that of an adult. The main age-dependent parameters are geometry of respiratory tract as to length, diameter, and number of airways; airflow conditions; velocity and Reynolds' number; respiratory minute volume; and tidal volume and respiratory frequency. These age-dependent data are necessary for calculating deposition probabilities in individual parts of the respiratory tract. Only few data can be found in the literature on the variation of the above parameters with age. These data, furthermore, are incomplete and/or inconsistent and show large differences for the same parameter. To overcome these difficulties, we made the following assumptions: (1) the infant lung represents and remains a miniature version of an adult lung during postnatal growth (Hislop et al., 1972) and (2) the regional number of airways remains constant for the upper airways but changes with age for the lower airways (Geigy, 1969; ICRP, 1975; Hötter, 1975).

In general, the curves of most lung parameters showed the same tendency, i.e., a steep increase during the first 10 years of life, gradually continuing into a saturation value, which is the one given for the reference man. In this way age-dependent lung models, based on the models for an adult lung by Landahl (1950) and Weibel (1963), were developed. In both models the airways are represented as cylindrical tubes which divide into further tubes, with the diameters getting smaller and smaller. In the Landahl model the respiratory tract is divided into nine regions, six of which belong to the tracheobronchial compartment and three to the alveolar area. In Table 1 the number of airways are given together with their dimensions during inspiration. Weibel was able to determine the geometry of the lung regions much more precisely according to late morphological investigations. The respiratory tract was divided into 24 generations with all tubes of each generation of equal length and diameter and at the same distance from their origin. Table 2 gives the various parameters for the generations of this model.

TABLE 1
Lung Model of Landahl

Region	Number of airways	Radius, cm	Length, cm	Surface area, cm^2	Mucus transit time, min
Trachea	1	0.8	12	60	8
Main bronchi	2	0.5	6	40	8
Lobar bronchi	12	0.2	3	45	10
Segmental bronchi	100	0.1	1.5	100	15
Subsegmental bronchi	800	0.075	0.5	200	25
Terminal bronchi	6×10^4	0.03	0.3	3,400	70
Respiratory bronchi	2×10^5	0.025	0.15	4,700	
Alveolar ducts	2×10^6	0.02	0.05	30,000	
Alveolar sacs	5×10^7	0.02		250,000	

Age-Dependent Landahl Model

For the calculation of the deposition values in the rather simple ICRP compartment model of the respiratory tract, the model by Landahl was felt to be satisfactory. The regional number of airways N(a) was assumed to be independent of age for the regions from the trachea to the subsegmental bronchioles, therefore the adult values from Landahl were used. However, age-dependent functions of N(a) were calculated for all other lung regions. Figure 1 represents the flow diagram for the calculation of the age-dependent regional geometry of the respiratory tract.

N(a) = constant

The age dependence of the regional lung volume V(a) can be calculated from data on the total lung volume V′(a) for a given age (ICRP, 1975) and from the ratio of regional lung volume to total lung volume for an adult (Landahl, 1950). A function was defined for the age dependence of the mean length of the main bronchioles from published data (ICRP, 1975). The data from this curve were normalized for the adult value from Landahl (1950), and normalization factors were calculated for every age. The airway diameters d(a) can be calculated as a function of age by using these values of l(a) and assuming a cylindrical shape for V(a). For example, Fig. 2 shows the airway diameters for the trachea to the subsegmental bronchioles as a function of age. For comparison experimental data have been included.

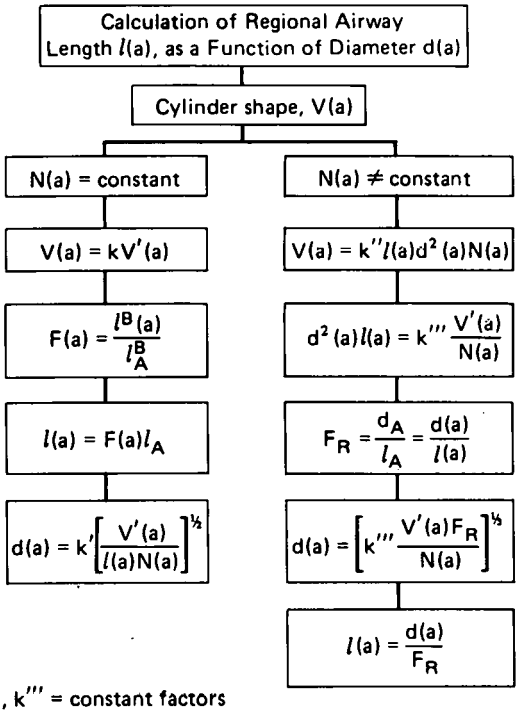
TABLE 2

Lung Model A of Weibel

Region	Generation	Number	Radius, cm	Length, cm	Surface area, cm^2	Mucus transit time, min
Trachea	0	1	0.9000	12.0	67.8	8
Bronchi						
Main	1	2	0.6100	4.76	36.5	6
Secondary	2	4	0.4150	1.90	19.8	8
	3	8	0.2800	0.76	10.7	3
Tertiary	4	16	0.2250	1.27	28.7	14
	5	32	0.1750	1.07	37.6	12
	6	64	0.1400	0.90	50.7	10
Quaternary	7	128	0.1150	0.76	70.0	32
	8	256	0.0930	0.64	95.7	27
	9	512	0.0770	0.54	134	23
Terminal	10	1.02×10^3	0.0650	0.46	192	445
	11	2.05×10^3	0.0545	0.39	274	378
	12	4.09×10^3	0.0475	0.33	403	320
	13	8.19×10^3	0.0410	0.27	570	261
	14	1.63×10^4	0.0370	0.23	876	223
	15	3.27×10^4	0.0330	0.20	1360	194
	16	6.55×10^4	0.0300	0.165	2040	160
Respiratory	17	1.31×10^5	0.0270	0.141		
	18	2.62×10^5	0.0250	0.117		
	19	5.24×10^5	0.0235	0.099		
Alveolar ducts	20	1.05×10^6	0.0225	0.083		
	21	2.09×10^6	0.0215	0.070		
	22	4.19×10^6	0.0205	0.059		
Alveolar sacs	23	8.39×10^6	0.0205	0.050		
Alveoli	24		~0.02			

$N(a) \neq$ constant

The age dependence of the regional number of airways N(a) was determined by interpolating published data (ICRP, 1975). Furthermore, a cylindrical shape for the regional lung volume V(a) and a constant ratio of airway diameter d(a) to length l(a) for each region, by the use of data from Landahl (1950), were assumed. In this manner age-dependent functions for d(a) and l(a) were derived for each of these regions (Fig. 3). Again, our results are in satisfactory agreement with experimentally derived data that are also contained in this figure.



k, k', k'', k''' = constant factors
V(a), V'(a) = regional, as a function of total lung volume
$l^B(a), l^B_A$ = age-dependent, as a function of adult mean length of main bronchioles
d_A, l_A = regional adult airway diameter, as a function of length
N(a) = regional number of airways

Fig. 1 Flow diagram for the calculation of the age-dependent regional geometry of the Landahl lung model. +, adult diameter (Landahl, 1950). ●, experimentally derived data for trachea (Hislop et al., 1972).

Age-Dependent Weibel Model

For the calculation of a more detailed distribution of doses to the basal cells within the tracheobronchial region, a refined version of an age-dependent respiratory tract was established according to the model A of Weibel (1963). The basic idea of this model was to represent the age dependence of each parameter by a simple analytical expression and to fit the various available data to appropriate functions. Therefore if improved experimental data are available, only the respective functions need to be exchanged. Since the data on adults of the Weibel model are represented by functions,

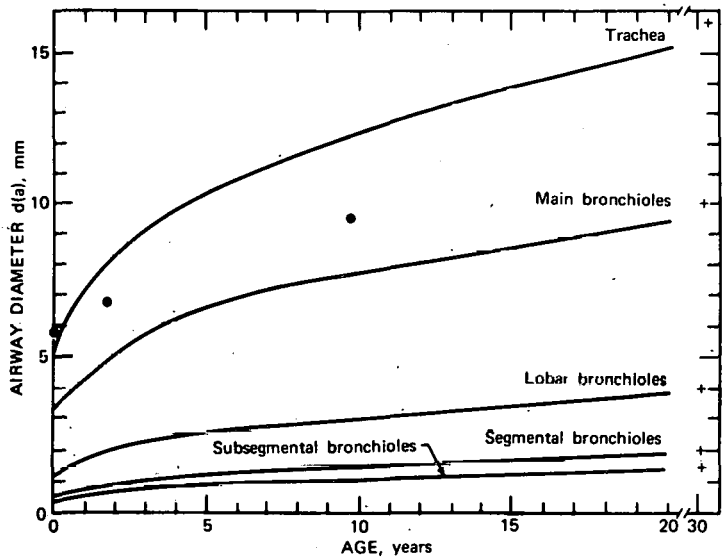


Fig. 2 Airway diameter d(a) as a function of age for the lung-region trachea to the subsegmental bronchioles of the Landahl lung model. +, adult diameter (Landahl, 1950). ●, experimentally derived data for trachea (Hislop et al., 1972).

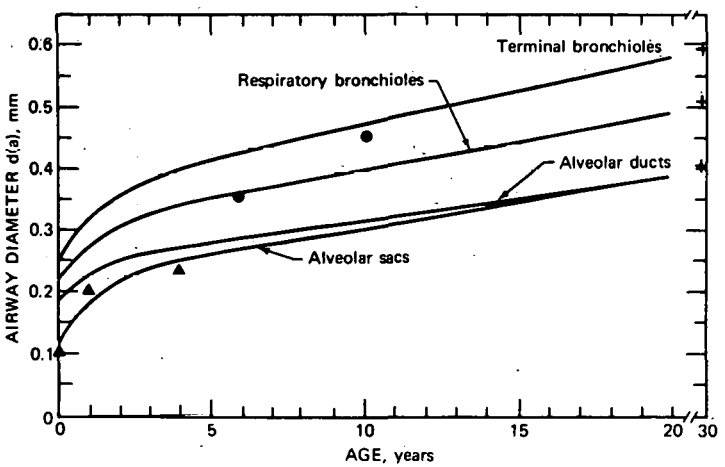


Fig. 3 Airway diameter d(a) as a function of age for the terminal bronchioles to the alveolar sacs of the Landahl lung model. +, adult diameter (Landahl, 1950). ●, experimentally derived data for terminal bronchioles and for ▲, respiratory alveoli (Dunnill, 1962; Hislop et al., 1972; Charnock and Doershuk, 1973).

small differences sometimes occur when they are compared with the original data. The following assumptions were made:

1. As a first approximation, the volumes of the individual generations grow in proportion to the total lung volume (Hislop et al., 1972); for calculating the growth of the latter, the ICRP data from reference man (1975) were used. However, according to the ICRP findings, the portion of the alveolar volume in the total lung volume is about 25% smaller in infants than it is in adults. Therefore the proportionality with regard to the growth of the individual generations assumed before was modified, by introducing a correction factor dependent on age and generation.

2. The age-dependent alteration of the lung volume is divided equally for each age group into the linear dimensions total radius, R(g,a), and total length, L(g,A), of one generation (Yu and Taulbee, 1977; Hughes, Hoppin, and Mead, 1972) as shown by

$$R(g,a) = \left(\frac{V(a)}{V}\right)^{1/3} R(g) \tag{1}$$

where R(g) = total airway radius of a generation for an adult (Weibel, 1963)
V(a) = total lung volume as a function of age (ICRP, 1975)
V = total lung volume for an adult (Hötter, 1975)

3. For the age dependence of the airway radius of a generation, the following apply:

$$r(g,a) = \left(\frac{V(a)}{V}\right)^{1/3} \left\{\frac{R(g)}{[N(g,a)]^{1/3}}\right\} \tag{2}$$

where N(g,a) is the number of airways of a generation as a function of age. Analogous considerations are applied to the determination of the lengths of the individual generations.

4. N(g,a) is calculated in the following equation:

$$N(g,a) = N(g)\,[1 - k(a)\,l(g)\,m(g)] \tag{3}$$

where N(g) = number of airways of a generation for an adult (Weibel, 1963)
k(a) = number of respiratory airways in generations 20 to 23 as a function of age
$l(g)$ = ratio of the number of airways in the newborn to the number of airways in the adult in generations 20 to 23
m(g) = ratio of the number of airways in the newborn to the number of airways in the adult for a particular age as a function of the generation number

The exact calculation of this geometry will be described in more detail in a separate publication. Figure 4 shows an example of the airway radius r(a) in generations 0, 1, 3, 6, and 15 as a function of age.

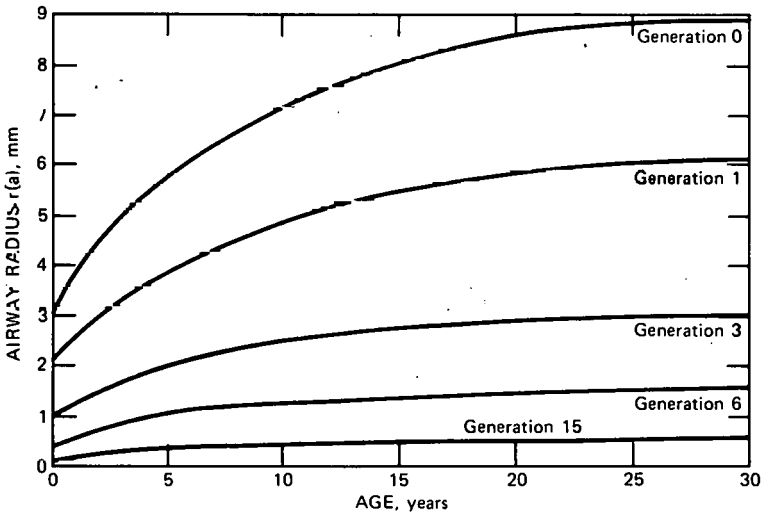


Fig. 4 Airway radius r(a) as a function of age for different generations of the Weibel model A.

PARAMETERS INFLUENCING PARTICLE DEPOSITION AND INHALED RADIOACTIVITY

The amount of radioactive nuclides inhaled depends on the atmospheric nuclide concentration as well as on the respiratory minute volume (RMV). The RMV influences also the deposition of radionuclides in the individual regions of the respiratory tract. It is strongly dependent not only on age but also on the physical activity (PA) of a person.

For practical purposes mean dose values covering a longer period, e.g., 1 year, are often required. For one certain individual it is therefore necessary to know the amount of time this person spent at each of several locations, the mean nuclide concentration at these locations, and the various RMV's due to different physical activities. To demonstrate the results of our calculations, we chose the following two examples. In long-term investigations of a normal urban natural radioactive environment in the town of Salzburg, Austria (Pohl et al., 1976; Steinhäusler et al., 1976; this volume),

TABLE 3

Definition of Reference Atmospheres for an Urban Environment Under Various Conditions

Condition	Indoors		Outdoors	
	^{222}Rn, pCi/liter	^{222}Rn : ^{218}Po : ^{214}Pb : ^{214}Bi	^{222}Rn, pCi/liter	^{222}Rn : ^{218}Po : ^{214}Pb : ^{214}Bi
Favorable	0.1	1 : 0.9 : 0.6 : 0.4	0.1	1 : 0.9 : 0.5 : 0.4
Disadvantageous	2.0	1 : 1 : 0.7 : 0.5	0.5	1 : 1 : 0.6: 0.5
	^{220}Rn, pCi/liter	^{220}Rn : ^{216}Po : ^{212}Pb : ^{212}Bi	^{220}Rn, pCi/liter	^{220}Rn : ^{216}Po : ^{212}Pb : ^{212}Bi
Disadvantageous	0.4	1 : 1 : 0.13 : 0.08	0.4	1 : 1 : 0.013 : 0.008

mean ^{222}Rn decay product and short-lived decay product concentrations were determined indoors as well as outdoors. Reference atmospheres were defined (Table 3) from these values. Low concentrations of radionuclides near the lower end of the ranges are called favorable conditions, and relatively high concentrations (near the upper end of the ranges) are called disadvantageous conditions. For calculating doses resulting from inhalation of ^{220}Rn and its decay products, we used only one reference atmosphere, which had a high ^{212}Pb content indoors and is also called disadvantageous conditions (Table 3).

Furthermore, the amount of time spent indoors and outdoors was considered to be age dependent, i.e., that the ratio of time outdoors to time indoors increases during childhood and youth and starts decreasing after the age of 15 years. The data for the age dependence of the RMV were partly derived from reference man (ICRP, 1975) and partly from Hötter (1975). For the deposition calculations the RMV data were subdivided into age-dependent values for tidal volume and respiratory frequency (ICRP, 1975). Typical age-dependent PA functions were defined for such daily activities as resting, light activity, and heavy work.

According to the ICRP (1975), the tidal volume for light work and heavy work is increased by a factor of 2 and 3, respectively, as compared with resting. The corresponding respiratory frequency for light work and heavy work is also higher by a factor of 1.5 and 2, respectively.

Up to the age of 15 years, individual PA was assumed to be the same for all children of a particular age. From the age of 15 years on (in most European countries basic schooling is finished at about that age), the physical activities are categorized for two extreme cases:

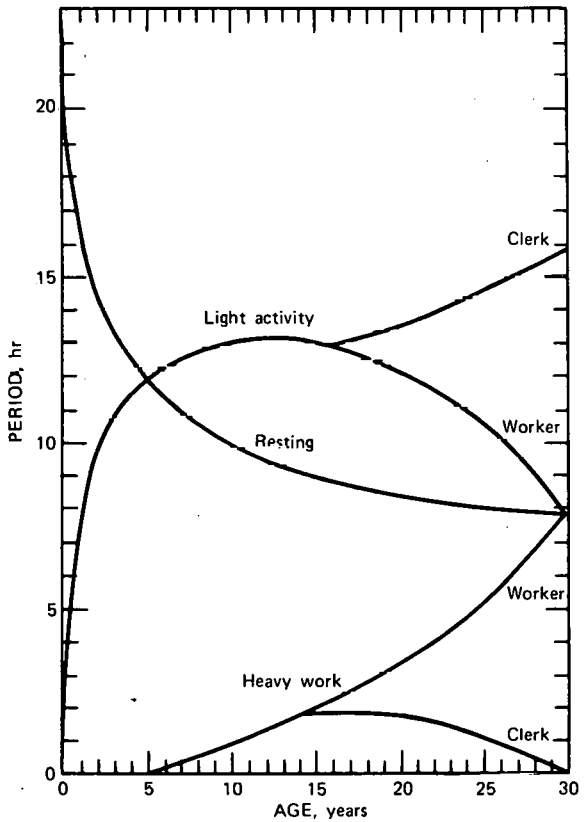


Fig. 5 Amount of time spent daily in resting, light activity, and heavy work as a function of age.

(1) predominantly working light activity and little nonoccupational heavy work, denoted as "clerk"; and (2) mainly occupational heavy work and nonoccupational light activity, defined as "worker". For our calculations only male individuals were considered. Functions for the daily life patterns, representing the daily amount of time spent during different periods of activity, were defined as age dependent, and they were fitted to simple analytical expressions represented by the curves of Fig. 5.

CALCULATION OF PARTICLE DEPOSITION

The flow of particles in the respiratory tract changes with age since the geometrical dimensions of the respiratory tract as well as

the velocity of the airstream—because of changing tidal volume and respiratory frequency—are different for a child as compared with an adult. This requires the calculation of deposition probabilities for inhaled particles as a function of age. These probabilities were calculated for deposition due to diffusion, sedimentation, and impaction. Deposition by diffusion was evaluated by applying the equation of Gormley and Kennedy (1949), whereas impaction and sedimentation were determined after the methods of Landahl (1950) and Beeckmans (1965). Total deposition is determined by combining the probabilities of the individual deposition mechanisms and by using the successive method of Landahl (1950).

For the reference atmospheres (Table 3), the following assumptions were made: (1) particle size-distribution of the decay products attached to the natural aerosol according to Jacobi (1965), and (2) uncombined fractions of the short-lived decay products as given by Jacobi and Schraub (1974); e.g., for ^{216}Po, 100%; for ^{218}Po, 20%; for ^{214}Pb, ^{212}Pb, 2%; and for ^{218}Bi, ^{212}Bi, all attached.

On the basis of the age-dependent Landahl model, regional deposition values were calculated for each year of age. The results show that, in general, the compartmental deposition values for the tracheobronchial and the pulmonary regions do not change significantly within the first 30 years of life, although there are some differences in the particle distribution within the regions. The changes in the deposition values because of the smaller geometrical dimensions of a child seem to be partly compensated for by smaller respiratory parameters such as tidal volume and cycle time. This can be demonstrated by combining adult geometrical dimensions with infant respiratory parameters or vice versa, which leads to large differences in the deposition values. The deposition is also dependent on the RMV with respect to the physical activities. Therefore age-dependent deposition values were calculated for three activities, i.e., resting, light work, and heavy work, in accordance with the PA functions for each age (Hofmann and Steinhäusler, 1977; Hofmann, Steinhäusler, and Daschil, 1977). For example, the results of calculations of the compartmental deposition values for the tracheobronchial and the pulmonary compartments as functions of PA are given in Table 4 for a 6-year-old child.

DETERMINATION OF MEAN ABSORBED DOSES IN COMPARTMENTS OF THE RESPIRATORY TRACT

The clearance model for class D aerosols as proposed by the ICRP Task Group on Lung Dynamics (ICRP, 1966) was the basis for

TABLE 4.

Compartmental Deposition Values in Tracheobronchial (TB) and Pulmonary (P) Compartments as Functions of Physical Activity for the Age of 6 Years

	Compartmental deposition values, %							
	^{216}Po		^{218}Po		^{214}Pb, ^{212}Pb		^{214}Bi, ^{212}Bi	
Physical activity	TB	P	TB	P	TB	P	TB	P
Resting	75.7	≈0	26.0	21.8	14.8	26.8	13.5	27.3
Light activity	87.0	1.9	23.2	29.7	8.8	36.4	7.2	37.2
Heavy work	91.4	3.4	22.3	29.3	6.8	35.9	5.0	36.6

the calculation of the mean absorbed dose due to radon and its decay products. For class D aerosol, the ICRP model assumes a half-life of 0.5 day for transport from the pulmonary region to the blood. This value is in contradiction to experimental results on guinea pigs with continuous natural aerosol inhalation as obtained by Pohl and co-workers (1965, 1967, 1968). When the physiological differences between man and guinea pig were considered, it was assessed that for man about 30% of ^{218}Bi and 50% of ^{212}Bi, respectively, are transported to the blood. On the basis of these percentages, the half-life for the pathway in the ICRP model was calculated to be about 1 hr instead of 0.5 day. The results presented here use both values so as to show the influence of the half-lives on the pulmonary dose.

In the case of inhalation of radon and its decay products, it is necessary to consider radioactive decay in addition to deposition and clearance. Contrary to the ICRP model, the deposition values and the amount of inhaled radionuclides change with age for each compartment. A possible age dependence of clearance parameters was disregarded since the data published represent mean values derived from different investigations. Furthermore, simulations of possible variations of these parameters showed no significant influence on the resulting activities.

Temporal changes in the compartmental activities can be described by a set of linear differential equations. The ICRP compartments were divided into subcompartments corresponding to the various clearance pathways (Voillequé, 1970). Since the equations for the temporal changes in the activities in the individual subcompartments differ only in the values for the various parame-

ters, they can be represented by the following equation (Hofmann, Steinhäusler, and Daschil, 1977):

$$\frac{dA_l^n}{dt} = -A_l^n\,(\lambda_l + \lambda_r^n) + f_l\,(A_l^{n-1} + A_m^{n-1})\,\lambda_r^n + f_l \sum_{ijk} D_{ki}^n\, Q_{ij}^n \qquad (4)$$

where Q_{ij}^n = RMV k_i T_{ij} C_j^n

$A_k^n = A_l^n + A_m^n$

A_l^n, A_m^n = activity of nuclide n in subcompartments l and m of compartment k according to clearance pathways l and m

λ_l = clearance rate for pathway l

λ_r^n = radioactive decay constant of nuclide n

f_l = clearance fraction for pathway l

D_{ki}^n = compartmental deposition value (%) of nuclide n for compartment k and physical activity i

Q_{ij}^n = annual inhaled activity of nuclide n for physical activity i at site j

RMV = respiratory minute volume for resting

k_i = scaling factor of the RMV for different physical activities i

T_{ij} = time spent at site j for physical activity i

C_j^n = atmospheric concentration of nuclide n at site j

where (1) for nuclide n,
n = 0 for ^{222}Rn, ^{220}Rn
n = 1 for ^{218}Po, ^{216}Po
n = 2 for ^{214}Pb, ^{212}Pb
n = 3 for ^{214}Po, ^{212}Bi—^{212}Po
(for $n \leqslant 0$, all A_l^n, $Q_{ij}^n = 0$)

and (2) for physical activity i,
i = 1 for resting
i = 2 for light activity
i = 3 for heavy work
(for scaling factors $k_1 = 1$, $k_2 = 3$, $k_3 = 6$)

and (3) for site of inhalation j,
j = 1 indoors
j = 2 outdoors

For each age a mean compartmental dose was calculated from the steady-state solutions for the A_l^n (Eq. 4) and the age-dependent

mass m_k of each compartment. Under the assumption of homogeneous irradiation, the mean alpha dose $\overline{D}_k$ for a given compartment k can be calculated in the following way:

$$\overline{D}_k \text{ (mrads/year)} = 18.69 \sum_n \frac{A_k^n \text{ (pCi) } E_\alpha^n \text{ (MeV)}}{m_k \text{ (g)}} \qquad (5)$$

where E_α^n is the energy of alpha rays from radon decay products.

Equation 5 is valid only for n = 1 (for ^{218}Ra and ^{216}Po) and n = 3 (for ^{214}Po and ^{212}Bi—^{212}Po) and not for the beta-decaying ^{214}Pb and ^{212}Pb. The dose resulting from the latter as well as the gamma dose was considered to be negligible as compared with the alpha dose.

Since diameter and wall thickness of blood capillaries are small as compared with the range of alpha rays, the nuclides deposited irradiate the lung tissue as well as the blood contained in the capillaries (Pohl, 1965; Pohl and Pohl-Rüling, 1968). The mean pulmonary compartment dose calculated according to Eq. 5 is equivalent to the mean pulmonary tissue dose since m_k represents the total compartment mass (tissue plus blood). Assuming for an adult 500 g of tissue and 480 g of pulmonary blood (ICRP, 1975), about 49% of the total emitted radioactive energy is absorbed by the pulmonary blood. Because of this irradiation the blood receives about $\frac{1}{10}$ of the pulmonary tissue dose, considering that about 10% of the total blood volume is contained in the lung (ICRP, 1975). In this value the dose due to radioactive nuclides in the blood itself is not included. The contribution of ^{222}Rn and ^{220}Rn to the dose in the alveolar tissue amounts to about 2% and was therefore considered negligible.

For these calculations a hybrid computer was used, since it offers the advantages of generating solutions of differential equations and variations of the single parameters in a quick and easy way (Hofmann and Steinhäusler, 1977; Hofmann, Steinhäusler, and Daschil, 1977). Figures 6a to 6c present the mean annual alpha doses for the tracheobronchial (TB) and pulmonary (P) compartments as functions of age. For showing the wide range of dose values, the doses represented in these figures were calculated for (1) light activity under favorable conditions as for the clerk and (2) for heavy work under disadvantageous conditions as for the worker (Table 3, Fig. 5).

It can be seen that the alpha dose to the respiratory tract is strongly age dependent. At the age of about 6 years, a maximum dose is reached in both compartments for ^{222}Rn- and ^{220}Rn-decay

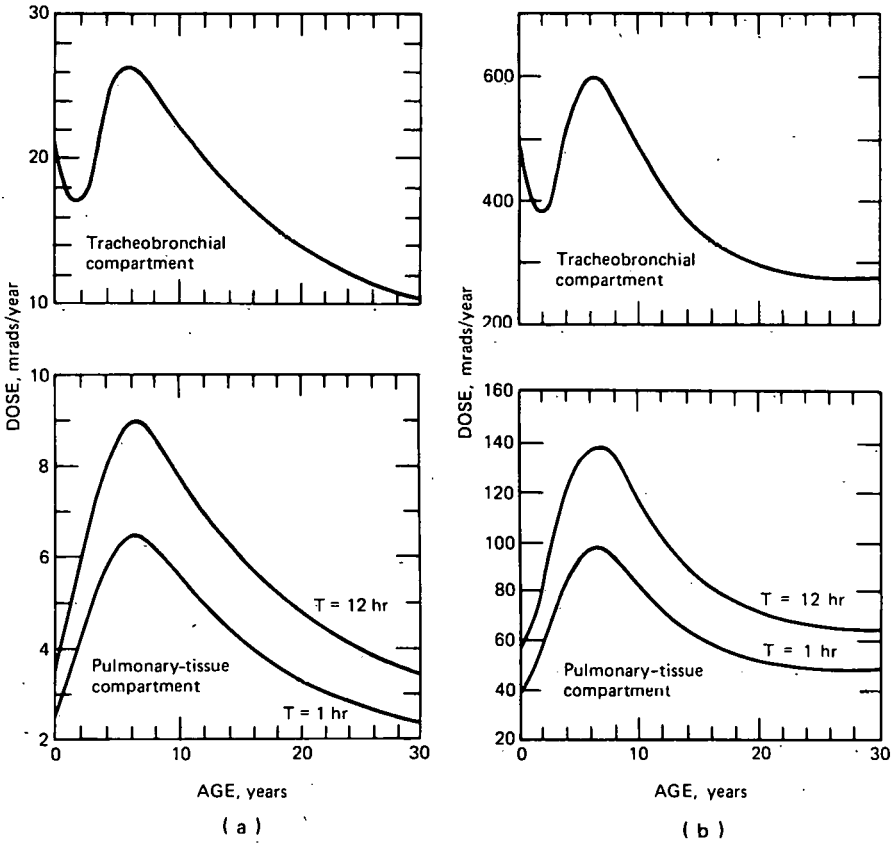


Fig. 6 Mean annual alpha-doses from ^{222}Rn-decay products for the tracheobronchial (TB) compartment and pulmonary-tissue (P) compartment as functions of age. (a) Under favorable conditions and for adult light activity (as for a clerk). (b) Under disadvantageous conditions and for adult heavy work (worker). (Figure 6 continues on next page.)

products. With increasing age the dose decreases again and approaches the adult dose value, depending on the assumed adult physical activity and the defined atmospheric conditions.

The minimum for the annual dose in the tracheobronchial compartment at the age of 2 years is determined by the following two factors:

1. The growth of the respiratory airways of the bronchial tree between birth and 2 years of age is slower than the increase of the respiratory minute volume, which results in smaller deposition probabilities.

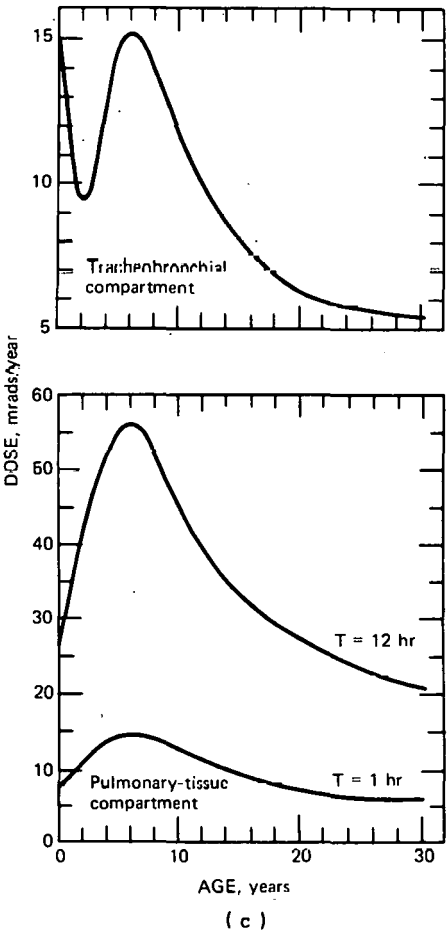


Fig. 6 (Continued) (c) Mean annual alpha-doses from ^{220}Rn-decay products for the tracheobronchial (TB) compartment and pulmonary-tissue (P) compartment as functions of age for adult light activity (clerk).

2. The living pattern of the first years of life is characterized by a marked increase in light activity with a simultaneous decrease of resting. For light activity, however, the deposition probabilities are smaller than for resting as a result of higher air velocities.

The maximum dose value, representing the dose for a 6-year-old, is about a factor of 2 higher than the corresponding dose for an adult living in the same radioactive environment. The influence of the half-life of 1 hr instead of 0.5 day results in a reduction of the mean pulmonary compartment dose by 30% for radon daughters and 75% for thoron daughters. Variations in the nuclide concentrations and in the half-life of clearance processes do not alter the shape of the age-dependent dose curves but only the absolute dose values.

DOSE TO THE BASAL CELLS OF SEGMENTAL BRONCHIOLES

For the calculation of the mean dose for the tracheobronchial region, the inhomogeneous dose distribution within this region (Figs. 6a to 6c) is not considered. Dose calculations for adults have indicated that the basal cells of the segmental bronchioles receive the highest radiation doses in the respiratory system (Altshuler, Nelson, and Kuschner, 1964; Jacobi, 1964, 1965; Jacobi and Schraub, 1974; Haque and Collinson, 1967) and are therefore regarded as the critical target for the induction of lung cancer. On the basis of the age-dependent Landahl model, the doses to the basal cells were investigated for their dependence on age. A dynamic equilibrium results from the activity deposited, radioactive decay, mucus transport, and clearance into the blood. The surface activity a_k^n in each region k of the compartmental model of the respiratory tract (k = 1 to 6) can be described by the following differential equation:

$$\frac{da_k^n}{dt} = \sum_{ijk} \frac{D_{ki}^n \, Q_{ij}^n}{S_k} + \lambda_{k+1} \, a_{k+1}^n \, \frac{S_{k+1}}{S_k} + \lambda_r^n \, a_k^{n-1} - (\lambda_k + \lambda_r^n + \lambda_b) \, a_k^n \qquad (6)$$

where a_k^n = surface activity of nuclide n in region k (for $n \leqslant 0$, all $a_k^n = 0$)

S_k = surface area of region k

λ_k = elimination rate by mucus transport in region k ($\lambda_k = 1/T_k$, where T_k is mucus transit time)

λ_b = biological clearance rate from bronchial epithelium to blood

All other parameters were already defined in Eq. 4. The data on age dependence of the mucus transit times were calculated, assuming that the thickness of the mucus layer grows proportionally to the airway diameter of a region, whereas the mucus production per unit of area remains independent of age (Altshuler, Nelson, and Kuschner, 1964). The alteration assumed in the thickness of the mucus layer has almost no influence on the surface activities, because the maximum reduction of the transit times is only about one-third. For λ_b we used recent experimental results of James, Greenhalgh, and Smith (1977), who found a fast phase with a half-life of 4 min (20%) and a slower phase with a half-life of about 9 hr (80%) for the clearance of decay products from bronchial epithelium to blood. These half-lives were assumed to be the same for all regions.

No published data were found regarding age dependence of the thickness of the mucus layer and of the depth of the basal cells. Since the data show large discrepancies, the thickness of the mucus layer d_m and the depth of the shallowest basal-cell nuclei d_b in adults were assumed, according to Harley and Pasternack (1972), to be 15 and 22 μm, respectively. For their age dependence two extreme cases were discussed in which (1) both distances do not change with age, and (2) both grow proportionally to the airway diameters.

Assuming a homogeneously distributed alpha activity within the mucus layer, we calculated the doses for both cases according to Harley and Pasternack (1972). Figures 7a and 7b show the results of the inhalation of ^{222}Rn decay products for the two cases, i.e., those engaged in light activity (clerk) under favorable conditions and those occupied in heavy work (worker) under disadvantageous conditions (Table 3, Fig. 5). An apparent age dependence can be seen with a maximum at about 6 years as well. For an adult of 30 years, we calculated values that are about one-half the values calculated by Jacobi (1964, 1965). Preliminary results of dose calculations on the basis of the more detailed age-dependent Weibel model show decreased dose values. This seems to agree with the estimations of Harley and Pasternack (1972) who also used the Weibel model (Table 5). The choice of the appropriate lung model seems to play a deciding part in lung dose calculations, beside the uncertainty in the depth of the basal cells.

DOSE CALCULATIONS FOR HUMAN ORGANS AS FUNCTIONS OF AGE, SEX, AND WEIGHT

Inhalation of ^{222}Rn itself and of those daughters produced by its decay in the body results in a more or less uniformly distributed dose in organs and tissues except in fat, the adrenal glands, and bones. Inhalation of ^{220}Rn, however, results in a nonuniform dose distribution because of its much shorter half-life (Pohl, 1965). The dose rates at continuous inhalation depend only on the radon concentration in the air but not on the respiratory minute volume (see column A in Table 5).

Airborne decay products are first deposited throughout the respiratory tract. About 30% of the ^{222}Rn decay products and 50% of the ^{220}Rn decay products deposited in the respiratory tract pass into the blood and are transported to the various organs and tissues, where the nuclides are accumulated according to their metabolism.

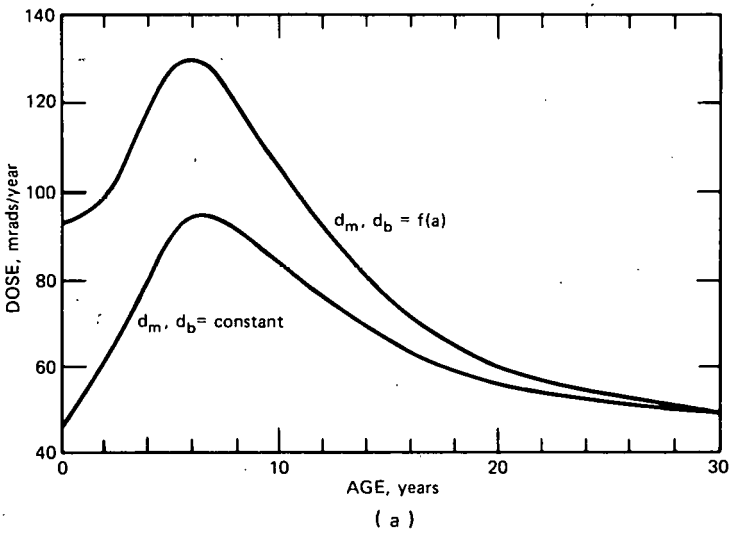


Fig. 7a Dose to the basal cells of the segmental bronchioles as a function of age under favorable conditions (clerk).

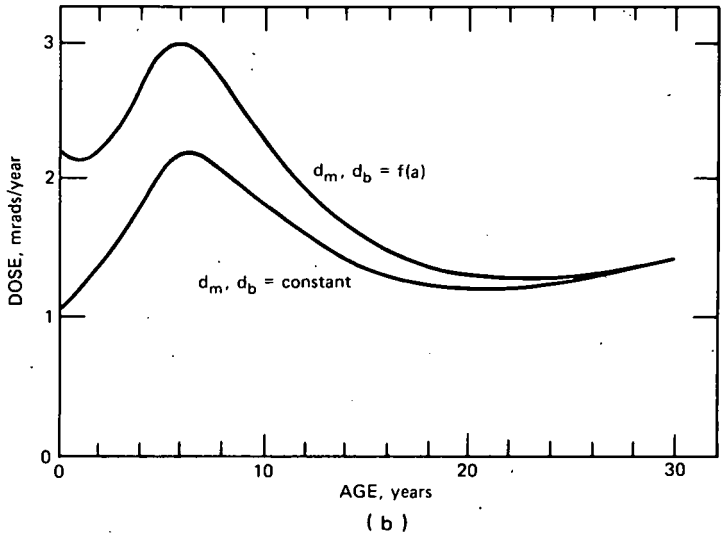


Fig. 7b Dose to the basal cells of the segmental bronchioles as a function of age under disadvantageous conditions (worker).

TABLE 5

Dose Rate (μrads/hr) in Some Organs and Tissues for Continuous Inhalation at the Respiratory Minute Volume (ϕ_n = 13.8 liters/min)

Organ or tissue	Air containing 1 pCi/liter of			
	^{222}Rn (A)	^{218}Po—^{214}Po (B)	^{220}Rn—^{216}Po (A)	^{212}Pb—^{208}Tl (B)
Basal cells of bronchioepithelium (4th to 9th generation)		60.5* 34.3† 8.0§	Unknown	470‡
Lungs (alveolar tissue)	0.023	3.77¶	0.057	22.8
Blood	0.015	0.157	0.0078	4.00
Liver	0.013	0.090	0.0015	2.51
Kidneys	0.015	0.380	0.0029	6.06
Adrenal glands	0.034	0.040	0.0013	0.61
Muscles	0.013	0.013	0.00014	0.11
Bones	0.0034	0.034	0.00089	0.75
Bone marrow	0.015	0.035	0.0013	1.75
Gonads	0.021	0.008	0.00023	0.10

*Altshuler, Nelson, and Kuschner, 1964.
†Jacobi, 1964.
‡Harley and Pasternack, 1973.
§Harley and Pasternack, 1972.
¶Jacobi, 1964, modified to investigations of Pohl and Pohl-Rüling (1968), considering that about one-third of the deposited activity is resorbed into the bloodstream.

For continuous inhalation of airborne decay products, the dose rate to an organ not only depends on their concentrations but also is proportional to the respiratory minute volume (see column B in Table 5). The results presented in Table 5 are based on extensive experiments with different kinds of animals and additional investigations on man (Pohl, 1965; Pohl and Pohl-Rüling, 1967, 1968; Plattner, 1967, 1968).

On the basis of dose calculations for adults (Pohl and Pohl-Rüling, 1977), the mean annual dose in microrads for a certain organ or tissue as a function of age (a), sex (s), and weight (w) can be calculated by the following equation:

$$D(a,s,w) = A \sum Rn_i t_i + B(a,s,w) \sum Rn_i\, z_i\, t_i \frac{\phi_i(a)}{\phi_n} d_{rel}\left(\frac{\phi_i}{\phi_n}\right)$$

$$(\Sigma t_i = 8760 \text{ hr}) \qquad (7)$$

where A = dose conversion factor taken from Table 5
B = dose conversion factor taken from Table 5, modified for dependence of age, sex, and weight
Rn_i = radon concentration at site i (pCi/liter)
t_i = time (hr) spent at site i
ϕ_n = annual mean respiratory minute volume for reference man (13.8 liters/min)
$\phi_i(a)$ = actual respiratory minute volume for a given age according to the physical activity at site i
ϕ_i = actual respiratory minute volume for an adult according to his physical activity
z_i = factor calculated from decay product ratio at site i
d_{rel} = mean relative deposition value (for $\phi_i = \phi_n : d_{rel} = 1$)

The z_i are factors depending on the decay product concentrations in air. From measurements one obtains the radon concentration Rn_i in air and the ratio $^{222}Rn : {}^{218}Po : {}^{214}Pb : {}^{214}Bi = 1 : a : b : c$. As in Table 5 the dose rates are given for equilibrium of the decay products, the z becomes for any values of a, b, and c (Pohl and Pohl-Rüling, 1977),

$$z = \frac{765a + 4640b + 1706c}{7141} \qquad (8)$$

For ^{212}Pb—^{208}Tl, z is always almost 1. For ϕ_i/ϕ_n we used the values given in Table 6 which are based on data from the reference man

TABLE 6

Ratio of Actual Respiratory Minute Volume ϕ_i to Mean Respiratory Minute Volume ϕ_n (13.8 liters/min)

Adult	Resting	Light activity	Heavy work	Maximum work
Male	0.54	1.45	3.12	8.04
Female	0.43	1.38	1.81	6.52

(ICRP, 1975) which are different for both sexes. The distribution of ϕ_i/ϕ_n within 1 year as a function of age is shown in Fig. 5 for our two examples assumed, i.e., clerk and worker. Furthermore, the amount of time spent indoors and outdoors was considered to be age dependent.

The mean relative deposition value d_{rel} is defined as the mean relative deviation of the regional deposition values for the mean

RMV ($\phi_i/\phi_n = 1$) caused by different physical activities. Figure 8 shows these values for ^{218}Po, ^{214}Pb, and ^{214}Bi for the alveolar tissue and segmental and subsegmental bronchioles. The differences between the curves for the individual decay products occur owing to different fractions of unattached nuclides as defined in our reference atmospheres. Since the amount of nuclides transported to other organs depends mainly on the activities deposited in the alveolar region, the value of d_{rel} for this compartment can be used for all other organs as well.

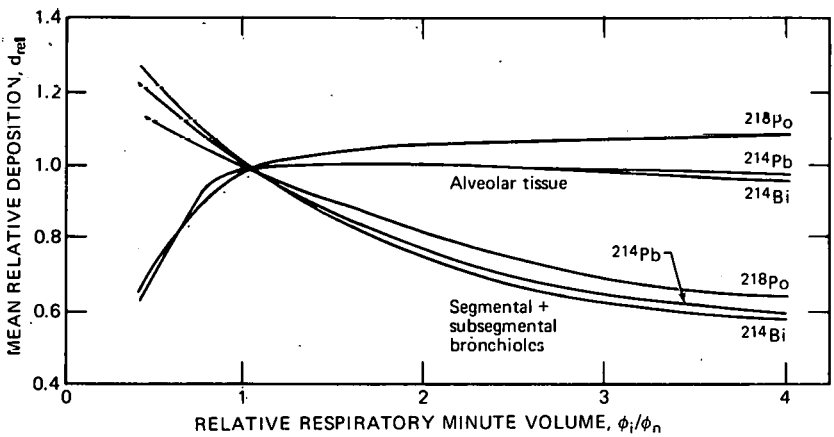


Fig. 8 Mean relative deposition value d_{rel} for ^{218}Po, ^{214}Pb, and ^{214}Bi as functions of the relative respiratory minute volume.

The factors A and B, which are different for each organ and tissue and, of course, are different for ^{222}Rn and ^{220}Rn, are compiled in Table 5 (values for adults only). Because of a constant solubility coefficient in the individual organs for radon, the activity per unit mass remains unchanged. Therefore factor A is independent of age, sex, and weight. Factor B, however, is dependent on age, sex, and weight because the organ-mass ratios of a child are different from those of an adult.

The $\phi_i(a)$ depends not only on the person's physical activity but also, of course, on age, sex, and weight. The ϕ_n in Eq. 7 is not the mean RMV for a certain age, but in any case it is the standard value of 13.8 liters/min. Therefore $\phi_i(a)/\phi_n$ depends on age, sex, and weight as well.

The superposition of all age-dependent parameters on dose calculations for ^{222}Rn—^{214}Po is shown in Fig. 9 for some selected

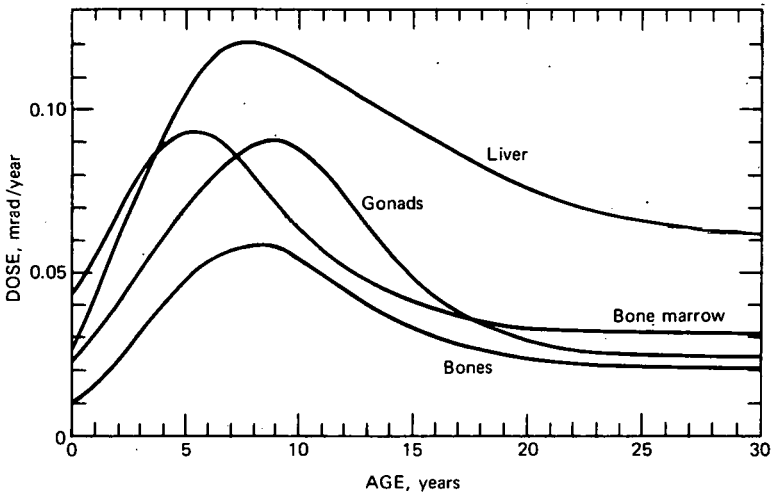


Fig. 9 Dose to some organs as a function of age under favorable conditions (clerk).

organs of a clerk, under favorable conditions, as defined above. The shape of the individual curves is again similar to the previous ones. Differences in the growth of the masses and in the influence of factors A and B result, however, in different positions of the maximum values, ranging from 5 to 9 years. In our calculations of the age-dependent organ masses, we hitherto started from the reference man representing a mean value between male and female. The dependence on sex only occurred in the RMV (ϕ_i), and Figs. 6a, 6b, 6c, 7, and 9 refer to male individuals. In arriving at an entire sex dependence of dose, one should consider not only the changes in RMV but also those caused by sex in the organ masses. Their influences are represented for dose to the bones in Fig. 10. When the changing in RMV only is considered, a high difference in dose results (curves 1 and 2), whereas when the different mass ratios of organs and tissues for male and female also are taken into account, the deviation according to sex becomes smaller (curves 3 and 4). These calculations were based on a male and female reference man with adult body masses of 75 and 65 kg, respectively (ICRP, 1975).

For the simultaneous influence of age, sex, and weight on organ doses, the following results can be derived from Fig. 10. The shape of the dose curve is determined by the age dependence of the single parameters, whereas the absolute dose values depend on the respiratory minute volume and the ratio of the masses of the various

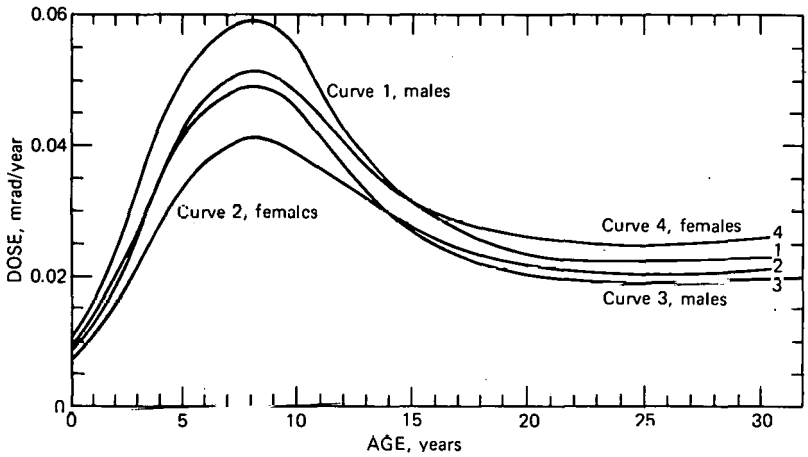


Fig. 10 Dose to the bones as a function of age, sex, and weight under favorable conditions (clerk).

organs. For increasing RMV and decreasing the relative mass for a certain organ, the dose curves are shifted to higher doses.

CONCLUSIONS

Our investigations show that the dose due to the inhalation of soluble radionuclides is strongly influenced by age, by physical activity, and, slightly, by sex and weight. This is valid not only for the respiratory tract but also for all other organs and tissues of the body. All organ doses show a maximum for children between 5 and 9 years, many of the values being more than twice the values for an adult. Whenever the individual doses from inhalation of radionuclides are to be calculated or the doses for epidemiological studies are to be estimated, their dependence on age, sex, and weight must be taken into consideration.

An example of such a study is given by Steinhäusler et al. in this volume.

ACKNOWLEDGMENTS

We wish to thank H. Hummer at the Hybrid Computer Center of the Technical University of Vienna as well as F. Daschil and P. Pfligersdorffer of the Institute of Physics, University of Salzburg, for their assistance in computer calculations. Experimental investiga-

tions for this work were supported by the Fonds zur Förderung der wissenschaftlichen Forschung, Vienna (Project No. 928), the International Atomic Energy Agency (under contract No. 1493/RB), and Stiftungs- und Förderungsgesellschaft der Paris-Lodron-Universität Salzburg.

REFERENCES

Altshuler, B., N. Nelson, and M. Kuschner, 1964, Estimation of Lung Tissue Dose from the Inhalation of Radon and Daughters, *Health Phys.*, 10: 1137-1161.

Beeckmans, J. M., 1965, The Deposition of Aerosols in the Respiratory Tract. I. Mathematical Analysis and Comparison with Experimental Data, *Can. J. Physiol. Pharmacol.*, 43: 157-172.

Brain, J. D., and P. A. Valberg, 1974, Models of Lung Retention Based on ICRP Task Group Report, *Arch. Environ. Health*, 28: 1-11.

Bykhovskii, A. V., D. G. Khachirov, N. G. Shishkanov, S. A. Dubrovin, and V. E. Klyuch, 1972, Dose to the Epithelium of the Upper Respiratory Tract from Radon and Its Daughter Products, *Health Phys.*, 23: 13-22.

Charnock, E. L., and C. F. Doershuk, 1973, Developmental Aspects of the Human Lung, *Pediatr. Clin. North Am.*, 20: 275-292.

Dunnill, M. S., 1962, Postnatal Growth of the Lung, *Thorax*, 17: 329-333.

Dyson, E. D., and S. A. Beach, 1968, The Movement of Inhaled Material from the Respiratory Tract to Blood: An Analogue Investigation of the New Lung Model, *Health Phys.*, 15: 385-397.

Geigy, J. R., 1969, *Wissenschaftliche Tabellen*, J. R. Geigy A.G., Pharma, Basel.

Gormley, P. G., and M. Kennedy, 1949, Diffusion from a Stream Flowing Through a Cylindrical Tube, *Proc. R. Irish Acad.*, Sect. A, 52: 163.

Haque, A. K. M. M., and A. J. L. Collinson, 1967, Radiation Dose to the Respiratory System Due to Radon and Its Daughter Products, *Health Phys.*, 13: 431-443.

Harley, N. H., and B. S. Pasternack, 1972, Alpha Absorption Measurements Applied to Lung Dose from Radon Daughters, *Health Phys.*, 23: 771-782.

——, and B. S. Pasternack, 1973, Experimental Absorption Applied to Lung Dose from Thoron Daughters, *Health Phys.*, 24: 379-386.

Hislop, A., D. C. F. Muir, M. Jacobsen, G. Simon, and L. Reid, 1972, Postnatal Growth and Function of the Pre-Acinar Airways, *Thorax*, 27: 265-274.

Hofmann, W., and F. Steinhäusler, 1977, Dose Calculations for Infants and Youths Due to the Inhalation of Radon and Its Decay Products, in *Fourth International Congress of the International Radiation Protection Association*, Symposium Proceedings, Paris, Apr. 24—30, 1977, pp. 479-500, International Radiation Protection Association, Paris.

——, F. Steinhäusler, and F. Daschil, 1977, LUMO—A Simulation Study of Age Dependent Lung Dosimetry for Inhaled Radioactivity, in *1977 Decus (Digital Equipment Users Society) Europe Symposium*, Symposium Proceedings, London, Sept. 6—8, 1977, pp. 315-320, Decus Europe, Geneva.

Hötter, G. J., 1975, *Die Lungenfunktion unter besonderer Berücksichtigung des wachsenden Organismus*, Steinkopff-Verlag, Darmstadt.

Hughes, J. M. B., F. G. Hoppin, and J. Mead, 1972, Effect of Lung Inflation on Bronchial Length and Diameter in Excised Lungs, *J. Appl. Physiol.*, 32: 25-35.

International Commission on Radiological Protection Task Group on Lung Dynamics, 1966, Deposition and Retention Models for Internal Dosimetry of the Human Respiratory Tract, *Health Phys.*, 12: 173-207.

International Commission on Radiological Protection Task Group on Reference Man, 1975, *Report of the Task Group on Reference Man*, 1st ed., ICRP Publication No. 23, Pergamon Press, New York.

Jacobi, W., 1964, The Dose to the Human Respiratory Tract by Inhalation of Short-Lived ^{222}Rn- and ^{220}Rn-Decay Products, *Health Phys.*, 10: 1163-1174.

——, 1965, Die natürliche Strahleneinwirkung auf den Atemtrakt, *Biophysik*, 2: 282-300.

——, 1972, Relations Between the Inhaled Potential α-Energy of ^{222}Rn- and ^{220}Rn-Daughters and the Absorbed α-Energy in the Bronchial and Pulmonary Region, *Health Phys.*, 23: 3-11.

——, and A. Schraub, 1974, Interne Strahlenexposition durch ^{222}Rn, ^{220}Rn und ihre kurzlebigen Zerfallsprodukte, in *Die natürliche Strahlenexposition des Menschen*, Symposium Proceedings, Frankfurt/Main, Sept. 18, 1973, pp. 118-128, Georg Thieme Verlag, Stuttgart.

James, A. C., J. R. Greenhalgh, and H. Smith, 1977, Clearance of Lead-212 Ions from Rabbit Bronchial Epithelium to Blood, *Phys. Med. Biol.*, 22: 932-948.

Kotrappa, P., 1969, Calculation of the Burden and Dose to the Respiratory Tract from Continuous Inhalation of a Radioactive Aerosol, *Health Phys.*, 17: 429-432.

Landahl, H. D., 1950, On the Removal of Air-Borne Droplets by the Human Respiratory Tract: I. The Lung, *Bull. Math. Biophys.*, 12: 43-56.

Morrow, P. E., 1970, Models for the Study of Particle Retention and Elimination in the Lung, in *Inhalation Carcinogenesis*, AEC Symposium Series, Gatlinburg, Tennessee, Oct. 8—11, 1969, M. G. Hanna, Jr., P. Nettesheim, J. R. Gilbert, pp. 103-122, CONF-691001, NTIS.

Parthasarathy, K. S., and K. Unnikrishnan, 1977, Bronchial Dose Due to Decay Products of ^{222}Rn in the Living Environment, *Chemosphere*, 5: 279-284.

Plattner, H., 1967, Die Strahlendosisverteilung im Säugetierorganismus bei der Inhalation von Thoron (Em220), *Oesterr. Akad. Wiss., Math. Naturwiss. Kl., Sitzungsber., Abt. IIa, Wien*, 176: 381-437.

——, 1968, Tierexperimentelle Untersuchungen zum Problem der Strahlenbelastung durch den Thorongehalt der Luft, *Strahlentherapie*, 136: 750-757.

Pohl, E., 1965, Biophysikalische Untersuchungen über die Inkorporation der natürlich radioaktiven Emanationen und deren Zerfallsprodukte, *Oesterr. Akad. Wiss., Math. Naturwiss. Kl., Sitzungsber., Abt. IIa, Wien*, 174: 309-442.

——, and J. Pohl-Rüling, 1967, The Radiation Dose Received by Inhalation of Air Containing Rn 222, Rn 220, Pb 212 (ThB) and Their Decay Products, *An. Acad. Bras. Cienc.*, 39: 393-404.

——, and J. Pohl-Rüling, 1968, Die Strahlenbelastung bei der Inhalation von Radon, Thoron und deren Zerfallsprodukte, *Strahlentherapie*, 136: 738-749.

——, and J. Pohl-Rüling, 1977, Dose Calculations Due to the Inhalation of ^{222}Rn, ^{220}Rn, and Their Daughters, *Health Phys.*, 32: 552-555.

——, F. Steinhäusler, W. Hofmann, and J. Pohl-Rüling, 1976, Methodology of Measurement and Statistical Evaluation of Radiation Burden to Various

Population Groups from All Internal and External Natural Sources, in *Biological and Environmental Effects of Low-Level Radiation*, Symposium Proceedings, Chicago, Nov. 3—7, 1975, pp. 305-315, STI/PUB/409, International Atomic Energy Agency, Vienna.

Snyder, W. S., M. R. Ford, and S. B. Watson, 1975, *A Computer Program for Estimating Microcurie-Days of a Radionuclide in the Organs of the Human Body*, USAEC Report ORNL-5046, Oak Ridge National Laboratory, NTIS.

Steinhäusler, F., W. Hofmann, E. Pohl, and J. Pohl-Rüling, 1976, Natural Radioactivity in an Urban Environment and the Resulting Dose Frequency Distributions of the Population for the Most Important Organs, in *Tenth Midyear Topical Symposium of the Health Physics Society*, Symposium Proceedings, Saratoga Springs, N. Y., Oct. 11—13, 1976, pp. 167-181, Rensselaer Polytechnic Institute, Troy, N. Y.

Thomas, J., 1964, A Method for Calculation of the Absorbed Dose to the Epithelium of the Respiratory Tract After Inhalation of Daughter Products of Radon, *Ann. Occup. Hyg.*, 7: 271-284.

Voillequé, P. G., 1970, AERIN, A Code for Acute Aerosol Inhalation Exposure Calculations, *Health Phys.*, 19: 427-432.

Weibel, E. R., 1963, *Morphometry of the Human Lung*, Springer Verlag, West Berlin.

Yu, C. P., and D. B. Taulbee, 1977, A Theory of Predicting Respiratory Tract Deposition of Inhaled Particles in Man, in *Proceedings of the Fourth International Symposium on Inhaled Particles and Vapours*, Edinburgh, Sept. 22—26, 1975, Pergamon Press, New York.

DISCUSSION

Wrenn: How does the time-integrated average dose rate to the lung over the first 20 years of life compare with the adult dose rate? A quick scan of your graphs would seem to indicate that the values might be quite close.

Steinhäusler: The mean dose integrated from age 0 to 4 years of age differs greatly from that of from age four to 20 years (Figs. 6a, 6b, 6c, or 7a and 7b).

Middleworth: When you consider particulate transport from the respiratory tract to the organ, do you consider that the particle is deposited on mucus and moved by cilia to the glottis and swallowed, and then the isotope is absorbed from the intestine? Is it valid to use data from the guinea pig and apply them to the human being?

Steinhäusler: In the series of experiments with guinea pigs by Pohl and Pohl-Rüling in various inhalation rooms with "natural" aerosols, the results showed that in all cases a large portion of the total amount of accumulated decay products was found in organs other than the respiratory and gastrointestinal tracts. Numerous experiments with man in different atmospheres, also with varying temperature and relative humidity, showed about the same excess of decay products in blood samples taken after inhalation as for guinea

pigs. When we considered the physiological differences between man and guinea pigs, it was assessed that for man out of the total accumulated decay products about 30% of RaC and 50% of ThC are transported to organs other than the respiratory and the gastrointestinal tracts.

Bouville: Could you explain how you obtained the value of 1 hr for the mean residence time of radon decay products in the lung?

Steinhäusler: This value is based on experimental results obtained with guinea pigs and continuous inhalation of natural aerosol, by Steinhäusler, Hofmann, Pohl, and Pohl-Rüling (paper in this volume). Physiological differences between man and guinea pig were taken into consideration. The results of these experiments showed that about one-third of the decay products, deposited in the alveolar region, were transported to other organs outside the respiratory tract. This mechanism cannot be explained with a half-life of 12 hr. With the analog computer it was simplified by changing the half-life value until there was satisfactory agreement with experimental data. By assuming 1 hr for ^{222}Rn and ^{220}Rn products, we found good agreement.

Lowe: The ICRP (MPC_a) for radon is dependent on the unattached fraction of its daughters. Did you consider this and, also, the size of the attached particles?

Steinhäusler: Yes, we did. We used the following data: (a) particle size distribution of the decay products attached to the natural aerosol according to Jacobi (1965) and (b) uncombined fractions of the short-lived decay products as given by Jacobi and Schraub (1974): ThA, 100%; RaA, 20%; RaB and ThB, 2%; and RaC and ThC, all attached.

Nelson: Was mouth breathing, nose breathing, or a combination of both used in the calculations?

Steinhäusler: A combination of both.

Nelson: What depth was used for basal cells in the model?

Steinhäusler: The depth of the shallowest basal cell nuclei in adults was assumed to be 22 μm, according to Harley and Pasternack (1973). For all other ages we calculated two extreme cases: that depth changes with age and that depth stays constant with age.

Local and Temporal Distribution Pattern of Radon and Daughters in an Urban Environment and Determination of Organ-Dose Frequency Distributions with Demoscopical Methods

F. STEINHÄUSLER,* W. HOFMANN,* E. POHL,* and J. POHL-RÜLING†
*Institute of Physics, University of Salzburg, and †Research Institute Gastein of the Austrian Academy of Sciences, Salzburg, Austria

ABSTRACT

In a normal urban environment, inhaled radon and its decay products cause an important part of the human radiation burden not only for the respiratory tract but also for several other organs. Measurements of air activity are, however, complicated by the fact that large local and temporal fluctuations occur outdoors and even more indoors where an urban population mainly lives. For proper information concerning the dose distribution within an urban population, it is necessary to use demoscopical methods, which means selecting test persons and determining their individual mean annual doses for the most important organs and tissues. We made such a study with 729 test persons in Salzburg, Austria (150,000 inhabitants). Each person was questioned regarding his living activity, i.e., the mean times he spent in individual sleeping, living, and working places and the corresponding physical activities that strongly influence the respiratory minute volume and consequently the inhaled radioactivity. At all these places and also inside other buildings and outdoors, the annual means of the external gamma radiation as well as of the air content of ^{222}Rn and its short-lived decay products were determined. Because of the great short- and long-term fluctuations of air activity, we developed a special method for obtaining significant annual mean values with a limited number of measurements, i.e., at five control stations (in different buildings), measurements were made once or twice a day to obtain information on the temporal variations. This supplies correction factors for all the other sites where only grab sampling (four times a year) was done. Lead-210, ^{220}Rn, and ^{212}Pb were determined only at the control stations and outdoors.

From all these measurements (more than 8000) and the information obtained, we calculated mean annual organ doses for each test person. The doses due to cosmic radiation, ^{40}K, and other radionuclides incorporated were totaled. Dose frequency distributions for eight organs and tissues are given in this paper. The range of the mean annual doses in millirems is only from 73 to

126 for gonads and 70 to 336 for the kidneys and finally reaches from 117 to 10,700 for the basal cells of the bronchial epithelium.

During the past years extensive investigations have been published concerning the assessment of the radiation burden of man living in a normal environment. Most of these studies were incomplete for the following reasons:

1. The contribution of radon and daughters has mostly been underestimated. The inhalation of these radionuclides often causes nonnegligible doses for several organs and tissues of the human organism. In parts of the respiratory tract, these are mostly higher than all the doses due to the other sources of natural radiation.

2. Many papers either report mean values for certain areas or deal with differences such as, for example, those resulting from building material. These data are insufficient for calculations of individual doses, since each person spends his time at various locations.

3. As a result of many investigations, only "whole body" doses are presented. All natural sources of ionizing radiation, however, cause an inhomogeneous dose distribution within the human body. This is valid for external irradiation, which is absorbed and which produces secondary radiation, and even more for all kinds of incorporated radionuclides. Therefore only a determination of dose distribution patterns in the organism supplies satisfactory data.

To obtain complete information on dose frequency distribution for the most important organs and tissues in a population living in a normal environment, we started investigations in the town of Salzburg, Austria, some years ago. Salzburg (150,000 inhabitants) is situated 420 m above sea level on the northern slope of the Alps. The natural radioactivity of the geological subsoil is low, the mean gamma dose rate above ground lies below the mean value for Austria. There are no other special sources of natural radioactivity such as thermal springs. The materials of the houses cover a wide range from prefabricated concrete parts to many kinds of bricks and natural stone. The different architectural types of the buildings that are inhabited comprise modern multistoried buildings as well as medieval houses. All these features are typical for a European town.

For our investigations we used a demoscopical method. Inquiries of selected test persons were made about their living pattern; then all components of their individual radiation environment (living and working sites) were measured. On the basis of these data, individual mean annual organ doses were determined. From those we calculated frequency histograms for the organ doses representative for the entire population.

CHOICE OF TEST PERSONS AND SITES FOR MEASUREMENTS

The town of Salzburg has been divided into 31 districts by the local municipal department of statistics. According to the population density, we chose a number of test families and test persons from each district, a total of 729 individuals. Inquiries of these test persons were made about age, sex, kind of work and living activities, all of which strongly influence the respiratory minute volume, average times spent on the single sites, e.g., sleeping, reposing, and working places, indoors as well as outdoors. Measurements of the test persons were carried out in all these places. Additional measurements were made in other buildings of different construction, mainly in the staircase areas since it can be rather difficult at times to obtain permission of the owners to perform measurements inside their flats. We did not find big differences in the results between the flats and the staircases in front of them. We also investigated sites outdoors over different subsoils such as asphalt and stone pavements, grass plots, etc.

The concentration of radionuclides in the room air showed large temporal fluctuations (up to a factor of 10) at the same site, mainly caused by meteorological parameters and by local ventilation conditions (Steinhäusler, 1975). For calculation of a significant annual mean value, it would be necessary to carry out hundreds of measurements on each single site. Therefore a suitable sampling method was developed. This method combined grab sampling with long-term series of measurements. Five so-called control stations were established; they were selected according to the construction materials of the houses and had defined ventilation conditions. In these control stations long-term measurements of radon and decay products were carried out once or twice daily (Pohl et al., 1976).

EXPERIMENTAL METHODS

External Gamma Radiation

For measuring external gamma radiation, we used the low-level scintillation dosimeter developed by Kolb and Lauterbach (1972) with a highest sensitivity of 3 μR/hr, full scale. The response to cosmic rays of this instrument was 2.2 μR/hr at the altitude above sea level of Salzburg. This value was subtracted from all measurements before displaying them in Fig. 1.

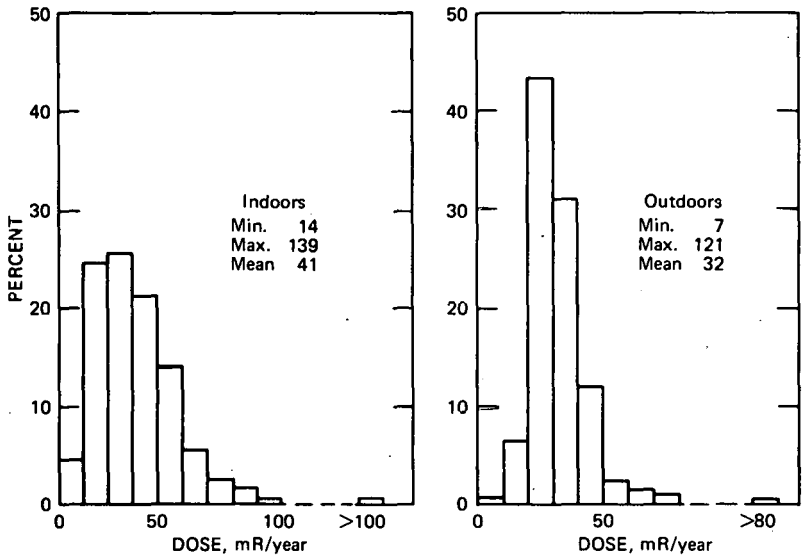


Fig. 1 Frequency distribution in percent of the terrestrial gamma-dose rate (without cosmic rays) indoors (1102 measurements) and outdoors (545 measurements).

^{222}Rn, ^{220}Rn, and Decay Products

For the determination of ^{222}Rn itself, we used the sensitive and rapid method of sampling and measurement developed by Pohl and Pohl-Rüling (1976); i.e., in special 30-liter containers of flexible foil, air samples were taken either with a simple hand pump (spot sampling) or with an electric aquarium pump that collects the air into the container over several hours (integral sampling). The samples were then measured in the laboratory with a 10- to 20-liter ionization chamber. Though the main radiation load from air activity is caused by the short-lived decay products, it is reasonable to measure the ^{222}Rn content itself in many samples, since temporal fluctuations of radon are much more pronounced than those of the decay-product portions. Moreover, this costs less and takes less time.

We have measured the ^{222}Rn and ^{220}Rn daughters by using normal filter devices equipped with membrane filters. In some cases we also determined the ^{210}Pb content of the air from the decay curves of these filters. For ^{220}Rn, however, double-filter equipment was necessary. These apparatuses supply simultaneously the content of ^{222}Rn and also of the short- and long-lived decay products of ^{222}Rn and ^{220}Rn. But the taking as well as the measuring of a single

sample requires several hours. The membrane filters used for our measurements have a retention of more than 99.99% for natural aerosols (Pohl, 1962; Märk, 1969), but they permit only a relatively small airflow. This requires sampling times of several hours with small air activities. In these cases only the total amount of the ^{222}Rn short-lived decay products can be determined from the filter-activity decay curve but not the ratio of $^{218}Po/^{214}Pb/^{214}Bi$. Assuming a ratio of 1:1:1, we can calculate the concentration of ^{214}Pb in the air from the decay curve of the alpha activity on the filter. Even under the assumption of very different naturally occurring ratios of these nuclides, the so-calculated ^{214}Pb concentration shows little variation (Märk, 1969). Therefore we chose the value of the ^{214}Pb concentration to characterize the content of ^{222}Rn decay products in the air investigated. Also the amount of alpha activity accumulated during inhalation is mainly determined by the ^{214}Pb content in the air.

RESULTS OF MEASUREMENTS

External Gamma Radiation

Our measurements showed that the gamma radiation fluctuated relatively strongly with sites indoors as well as outdoors, whereas the temporal fluctuations in the same site were not higher than ±10% (standard deviation). Frequency-distribution histograms for all indoor and outdoor measurements are given in Fig. 1.

Radon and Decay Products

The main problem lies in obtaining significant annual mean values of the air content of each radionuclide for a certain site, which is complicated by the large short- and long-term fluctuations due to meteorological and other parameters (Steinhäusler, 1975). An example of variations within a few days in one room with constant ventilation conditions is given in Fig. 2, and long-time variations are demonstrated in Fig. 3, which shows the fluctuations of the monthly mean radon content by day and night in another room. Figure 4 gives the corresponding values of the ^{214}Pb content in the air. To obtain significant mean values, we used the method mentioned previously; i.e., at the control stations we sampled once or twice a day and thus obtained long-term mean values for these places. At all other sites only grab samples were taken, usually four times a year at different seasons. The resulting measurements of these grab samples were then corrected according to the simultaneous deviation from

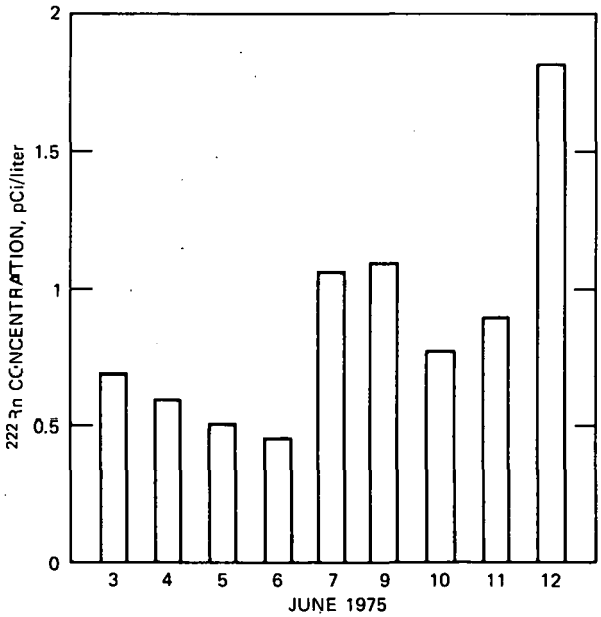


Fig. 2 Temporal variation of the ^{222}Rn concentration indoors at control station 3 with constant ventilation conditions.

the mean values at the control stations. In this way it was possible to obtain significant annual mean values for the radionuclides in the air at various places; these values were then taken as a basis for dose calculations. From these annual mean values we also calculated the frequency distributions for the ^{222}Rn content indoors and outdoors as shown in Fig. 5. It can be seen that, in more than 2.3% of the cases, the annual mean radon content of the room air is higher than 3 pCi/liter and in 16.4%, it is higher than 1 pCi/liter!

Indoors the mean ratio ^{214}Pb/^{222}Rn was found to be 0.62 ± 0.08. In some cases we also estimated the ratio ^{222}Rn/^{218}Po/^{214}Pb/^{214}Bi, the indoors mean value being 1:0.9:0.6:0.4. Lead-210 as well as ^{220}Rn and ^{212}Pb we determined only in the control stations, rooms that were unventilated with the exception of self-airing through the pores of the walls and the gaps around the closed windows and doors. In Table 1 the results only for ^{210}Pb and ^{212}Pb are given because ^{220}Rn—^{216}Po are practically negligible for dose calculations in a normal environment. Lead-212—polonium-212 is much more important for the radiation burden than ^{210}Pb—^{210}Po; therefore it was measured more frequently (1400 and

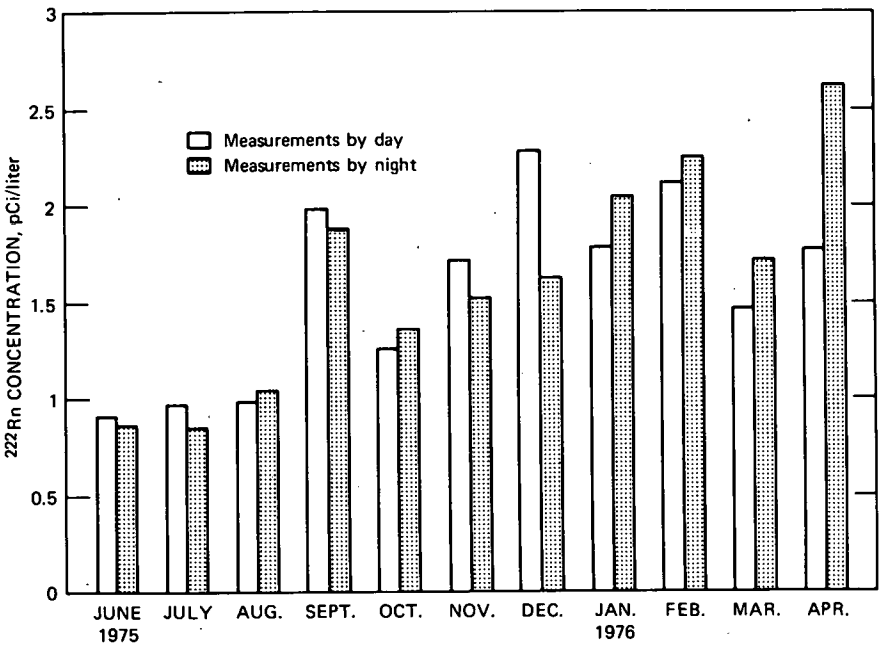


Fig. 3 Monthly mean ^{222}Rn concentrations indoors by day and by night at control station 4 from June 1975 to April 1976.

60 measurements, respectively). It can be seen from the table that the ratio ^{210}Pb/^{214}Pb varies only slightly from one site to the other. Furthermore, the concentration of ^{212}Pb increases with higher values of ^{210}Pb and consequently also of ^{222}Rn.

DOSE CALCULATIONS

The doses for the most important organs and tissues were calculated separately for each of the 729 test persons.

Organ Doses by External Radiation

External gamma radiation is absorbed by tissues and organs of the organism. To calculate the absorbed dose for a certain organ, we must not only convert the exposure dose (in roentgens) given by the dosimeter into the absorbed dose (in rads), but we also must take into account the shielding by the covering tissues. For the latter

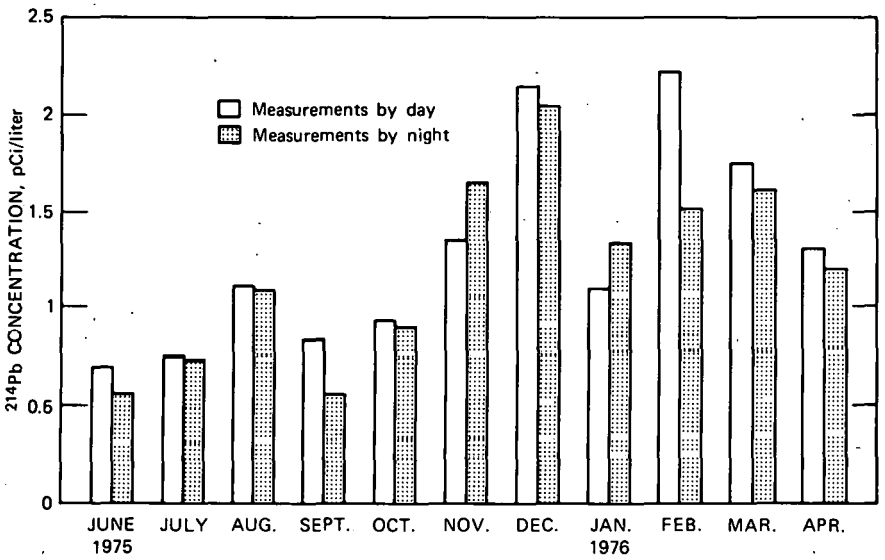


Fig. 4 Monthly mean ^{214}Pb (RaB) concentrations indoors by day and by night at control station 4 from June 1975 to April 1976.

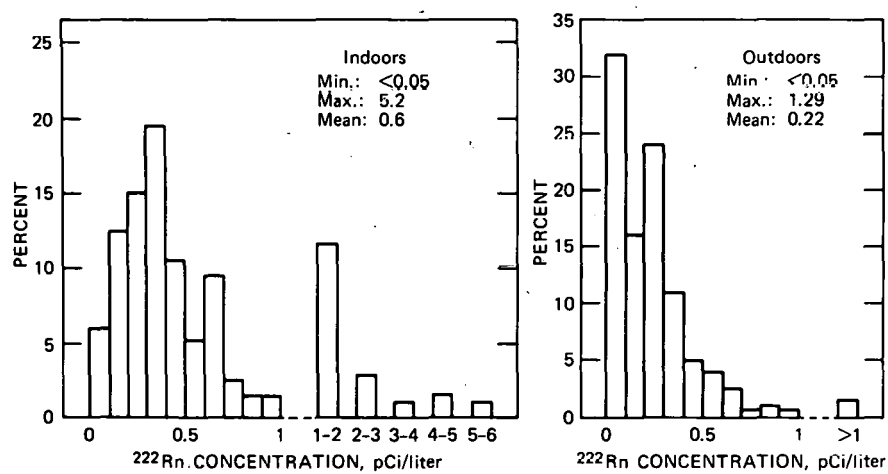


Fig. 5 Frequency distribution in percent of the mean annual ^{222}Rn concentration in picocuries per liter indoors and outdoors.

TABLE 1

Mean and Extreme Values of ^{210}Pb and ^{212}Pb in the Air of the Control Stations

Control station number	^{210}Pb, fCi/l			$^{210}Pb/^{214}Pb$ Mean	^{212}Pb, fCi/l		
	Minimum	Mean	Maximum		Minimum	Mean	Maximum
1	0.043	0.19	0.32	0.10×10^{-3}	17.0	56	930
2	0.013	0.039	0.088	0.12×10^{-3}	0.08	9.7	27
3	0.004	0.048	0.18	0.14×10^{-3}	<0.01	12.5	90
4	0.006	0.059	0.48	0.12×10^{-3}	0.06	27	502
5	0.013	0.11	0.30	0.10×10^{-3}	6.0	38	384

attenuation factors, F, for each organ have to be used which are also dependent on the radiation field geometry which is about 2π outdoors and 3π indoors. We used factors given in the literature (United Nations Scientific Committee on the Effects of Atomic Radiation, 1972; O'Brien and Sanna, 1976; Beninson et al., 1977) which are compiled in Table 2. Certainly these factors are also influenced by age, sex, and weight, but we did not find any data. For the mean annual dose due to cosmic radiation, we took 48 mrems for all organs corresponding to the altitude above sea level and the geomagnetic latitude of Salzburg (Oakley and Goldin, 1972).

The annual mean gamma doses for a certain organ have been calculated by this formula:

$$D_\gamma = 0.96 \, (F_b \sum D_{b,i} \, t_i + F_{out} \sum D_{out,i} \, t_i)$$

where $\Sigma \, t_i = 8760$ hr

D_γ = mean annual organ gamma dose, μrads

0.96 = converts the exposure rate in microroentgens per hour into the tissue absorbed dose in microrads per hour

F_b = gamma dose attenuation factor inside buildings for a certain organ (Table 2)

F_{out} = gamma dose attenuation factor outdoors for a certain organ (Table 2)

$D_{b,i}$ = exposure rate at site i inside buildings, μR/hr

$D_{out,i}$ = exposure rate at site i outdoors, μR/hr

t_i = time spent at site i, hr

TABLE 2

Gamma Dose Attenuation Factors for Various Organs in Adults

Organs	Irradiation indoors (F_b)		Irradiation outdoors (F_{out})	
	Male	Female	Male	Female
Bone marrow	0.64	0.64	0.73	0.73
Bones	0.69	0.69	0.78	0.78
Gonads	0.69	0.57	0.78	0.67
Bronchial epithelium and alveolar region	0.57		0.67	
Kidneys	0.57		0.67	
Liver	0.57		0.67	
Blood	0.64	0.64	0.73	0.73

Organ Doses by Inhalation

In another paper of this symposium (Hofmann, Steinhäusler, and Pohl, this volume), we gave details on our calculations of the doses due to inhalation of radon and daughters for various organs and tissues of the human organism. These calculations have been applied for each of our 729 test persons.

Organ Doses by Ingestion

Numerous investigations have already dealt with radiation doses caused by the incorporation of natural radionuclides in water and food. They have found only small differences for various populations living in normal environments. We therefore used values compiled by Muth (1974) and Kaul et al. (1974) as given in Table 3. The radioactivity of the drinking water at Salzburg town is small and contributes only negligibly to the annual doses. We measured the ^{222}Rn and ^{226}Ra content of numerous water samples taken from the water supplies in the houses. The mean and extreme values are given in Table 4.

FREQUENCY DISTRIBUTION OF MEAN ANNUAL ORGAN DOSES IN A POPULATION

For each test person the single components of the mean annual organ doses were determined according to the methods previously given and then summed up (with QF = 10 for alpha radiation). From

TABLE 3

Mean Annual Dose Equivalents Due to Incorporated Natural Radioactive Nuclides for a Population Living in a Normal Environment

Nuclide	Dose equivalent rate, mrems/year		
	Gonads	Bones	Bone marrow
Carbon-14	0.7	0.8	0.7
Potassium-40	19	15	15
Rubidium-87	0.3	0.6	0.6
Radium-226	0.02	0.6	0.1
Radium-228	0.03	0.8	0.1
Polonium-210	0.6	1.6	0.3
Uranium-238	0.03	0.3	0.06

TABLE 4

^{222}Rn and ^{226}Ra Concentration in Drinking Water of Salzburg (City), Austria

Nuclide	Number of measurements	Concentration, pCi/liter		
		Minimum	Mean	Maximum
Radon-222	156	<0.05	44 ± 4	188
Radium-226	138	<0.05	1.3 ± 0.2	7

these values organ-dose frequency distributions were computed, the results of which are given in histograms in Figs. 6 and 7. Mean* and extreme values can be taken from Table 5. It can be seen that those organ and tissue doses, which are remarkably influenced by the inhaled ^{222}Rn decay products, show wide ranges. The ratio of the maximum to the minimum is only 1.7 for the gonads and bone marrow, increases to about 5 for the kidneys, to 35 for the alveolar tissue, and even to 92 for the bronchial epithelium.

*In previous papers (Steinhäusler, Hofmann, and Pohl, 1975; Steinhäusler et al., 1976; Pohl et al., 1976), we published higher values for the basal cells of the bronchial epithelium because we used the dose estimation of Jacobi (1964). In the meantime our own dose estimation (Hofmann, this volume) showed that the most probable value is between that of Jacobi (1964) and that of Harley and Pasternack (1972); (see also Table 5). Furthermore, at that time we did not consider the age dependencies of the doses.

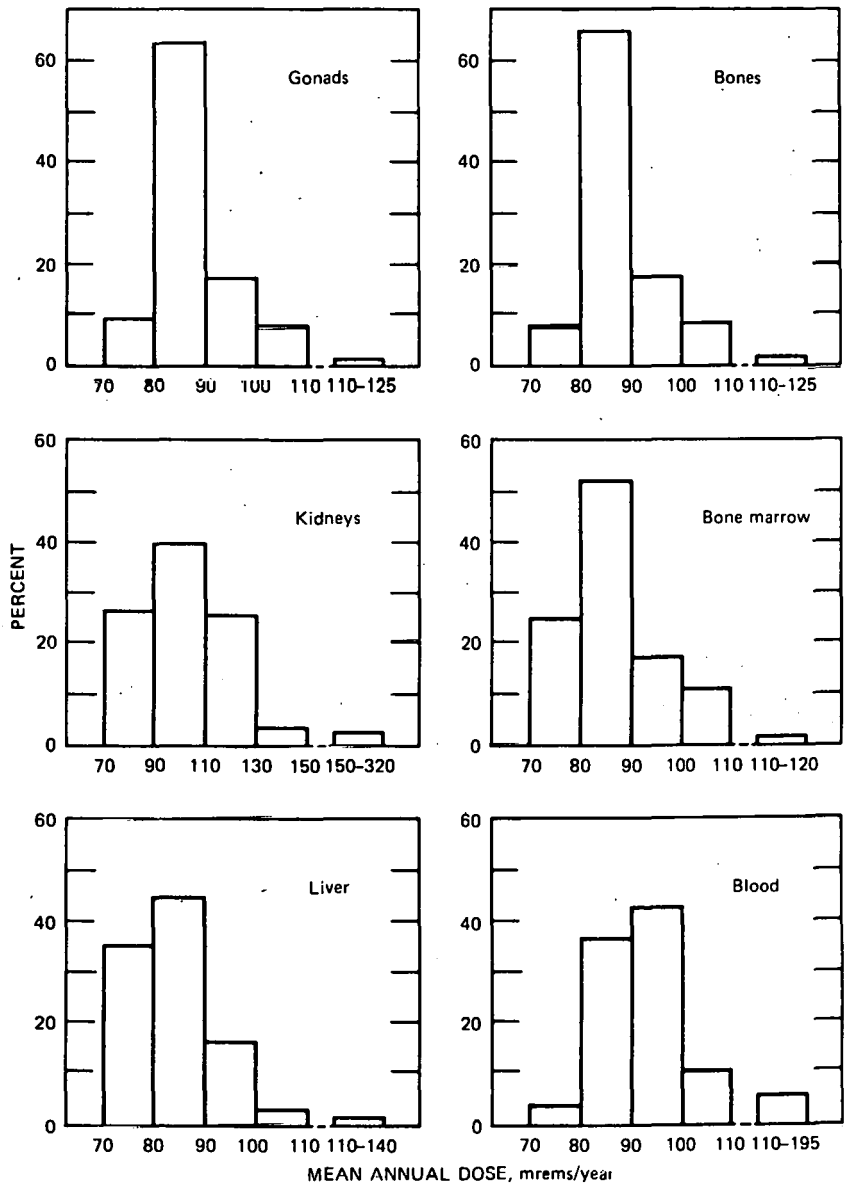


Fig. 6 Frequency distribution in percent of the mean annual dose in millirems per year from external and internal radiation for several organs.

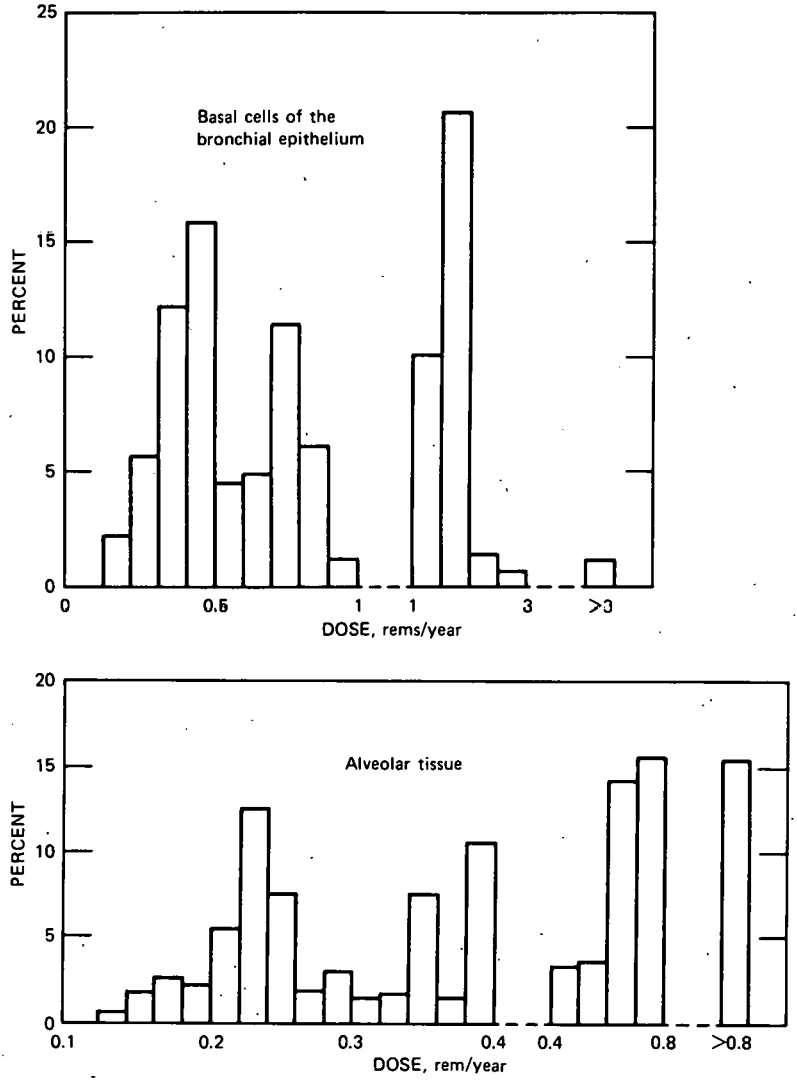


Fig. 7 Frequency distribution in percent of the mean annual dose in rems per year from external and internal radiation for the basal cells of the bronchial epithelium (segmental and subsegmental bronchi) and for the alveolar tissue.

TABLE 5

Mean and Extreme Values of Mean Annual Organ Dose Equivalents for 729 Test Persons Investigated

Organ or tissue	Dose equivalent rate, mrems/year		
	Minimum	Mean	Maximum
Liver	70	85	145
Bone marrow	71	85	123
Bones	73	87	126
Gonads	73	87	126
Blood	73	94	200
Kidneys	70	104	336
Alveolar tissue	110	448	3,885
Basal cells of the segmental and the subsegmental bronchi	117	980	10,700

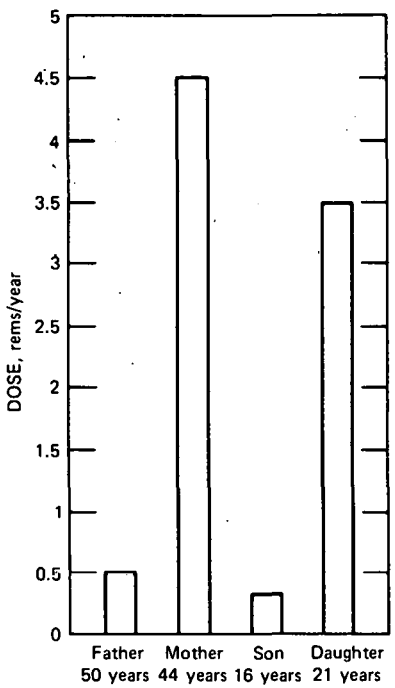


Fig. 8 Mean annual total dose equivalent to the bronchial epithelium in rems per year for four members of one family.

CONCLUSIONS

Our investigation shows that even in a normal environment high dose values can occur as a result of the inhalation of radon and decay products. The tissue with the highest natural radiation burden is the basal cell layer of the epithelium of the segmental and subsegmental bronchi (fourth to ninth generation in the lung model of Weibel). These cells are the critical ones for the induction of lung cancer. It is remarkable that about 64% of the population investigated by us receive more than 0.5 rem/year, 25% more than 1.5 rems/year and 1.3% more than 3 rems/year! It might be possible that these doses act synergistically in connection with other carcinogenic factors, especially cigarette smoking.

From our studies it can be seen, furthermore, that the estimation of mean values alone is not sufficient in considering all aspects of the radiation burden of a population. Individual differences even within one family living in the same flat could be rather high as shown in Fig. 8. The four members of this family receive very different lung doses because of their different workplaces.

We emphasize that none of our 729 test persons was handling radioactive material or other radiation sources. The different air activities of the living and working rooms are entirely caused by differences in building materials and in the construction of the houses. This is not only typical for the town of Salzburg but also for many other European cities, which are therefore supposed to exhibit similar results. In areas on subsoils with higher natural radioactivity, the dose values will even be higher.

ACKNOWLEDGMENTS

This work was supported under contract 928 of the Fonds zur Förderung der wissenschaftlichen Forschung, Austria, by International Atomic Energy Agency contract 1493, and by the Stiftungs- und Förderungsgesellschaft der Paris-Lodron-Universität Salzburg.

REFERENCES

Beninson, D. J., A. Bouville, B. J. O'Brien, and J. O. Snihs, 1977, Dosimetric Implications of the Exposure to the Natural Sources of Irradiation, in *International Symposium on Areas of High Natural Radioactivity*, Symposium Proceedings, Poços de Caldas, Brazil, June 16—20, 1975, T. L. Cullen and E. Penna-Franca (Eds.), pp. 75-106, CONF-750671, NTIS.

Harley, N. H., and B. S. Pasternack, 1972, Alpha Absorption Measurements Applied to Lung Dose from Radon Daughters, *Health Phys.*, 23: 771-782.

Jacobi, W., 1964, The Dose to the Human Respiratory Tract by Inhalation of Short-Lived ^{222}Rn- and ^{220}Rn-Decay Products, *Health Phys.*, 10: 1163-1174.

Kaul, A., E. Oberhausen, H. D. Roedler, and E. Werner, 1974, Interne Strahlenexposition durch ^{40}K, in *Die natürliche Strahlenexposition des Menschen*, Symposium Proceedings, Frankfurt/Main, Sept. 18, 1973, pp. 103-111, Georg Thieme Verlag, Stuttgart.

Kolb, W., and U. Lauterbach, 1972, A Scintillation Dose Rate Meter for Environmental Surveys, in *The Natural Radiation Environment II*, Vol. 1, Symposium Proceedings, Houston, Tex., Aug. 7—11, 1972, J. A. S. Adams, W. M. Lowder, and T. F. Gesell (Eds.), ERDA Report CONF-720805-P1, pp. 245-254, Rice University and the University of Texas, Houston, NTIS.

Märk, T., 1969, Eine Apparatur hoher Empfindlichkeit zur Messung der natürlichen Radioaktivität der Atmosphäre, *Ber. Med. Natw. Verein Innsbruck*, 57: 71-93.

Muth, H., 1974, Bilanz der externen und internen natürlichen Strahlenexposition, in *Die natürliche Strahlenexposition des Menschen*, Symposium Proceedings, Frankfurt/Main, Sept. 18, 1973, pp. 129-139, Georg Thieme Verlag, Stuttgart.

Oakley, P. T., and A. S. Goldin, 1972, Cosmic Ray Population Exposure, in *The Natural Radiation Environment II*, Vol. 1, Symposium Proceedings, Houston, Texas, Aug. 7—11, 1972, J. A. S. Adams, W. M. Lowder, and T. F. Gesell (Eds.), ERDA Report CONF-720805-P2, pp. 91-100, Rice University and the University of Texas, Houston, NTIS.

O'Brien, K., and R. Sanna, 1976, The Distribution of Absorbed Dose-Rates in Humans from Exposure to Environmental Gamma Rays, *Health Phys.*, 30: 71-78.

Pohl, E., 1962, Die Strahlenbelastung bei der Inhalation von Radium-Emanation, *Strahlentherapie*, 119: 77-96.

——, and J. Pohl-Rüling, 1976, Determination of Environmental or Occupational Rn 222 in Air and Water and Ra 226 in Water with Feasible and Rapid Methods of Sampling and Measurement, *Health Phys.*, 31: 343-348.

——, Steinhäusler, F., W. Hofmann, and J. Pohl-Rüling, 1976, Methodology of Measurement and Statistical Evaluation of Radiation Burden to Various Population Groups from All Internal and External Sources, in *Biological and Environmental Effects of Low-Level Radiation*, Symposium Proceedings, Chicago, Nov. 3—7, 1975, pp. 305-315, STI/PUB/409, International Atomic Energy Agency, Vienna.

Steinhäusler, F., 1975, Long-Term Measurements of Rn 222, Rn 220, Pb 214, and Pb 212 Concentrations in the Air of Private and Public Buildings and Their Dependence on Meteorological Parameters, *Health Phys.*, 29: 705-713.

——, W. Hofmann, and E. Pohl, 1975, Urban Natural Radioactivity in Salzburg, Austria, and Its Resulting Dose for Various Organs in Different Groups of Inhabitants, in *Third European Congress of the International Radiation Protection Association, Symposium Proceedings, Amsterdam, May 13—16, 1975*, International Radiation Protection Association, Amsterdam.

——, W. Hofmann, E. Pohl, and J. Pohl-Rüling, 1976, Natural Radioactivity in an Urban Environment and the Resulting Dose Frequency Distributions of the Population for the Most Important Organs, in *Tenth Midyear Topical Symposium of the Health Physics Society*, Symposium Proceedings, Saratoga

Springs, N. Y., Oct. 11—13, 1976, pp. 167-181, Rensselaer Polytechnic Institute, Troy, N. Y.

United Nations Scientific Committee on the Effects of Atomic Radiation (UNSCEAR), 1972, *Ionizing Radiation: Levels and Effects, Vol. I: Levels*, UN Sales No. E.72.IX.17., United Nations Publications, New York.

DISCUSSION

Wrenn: You measured a mean radon indoor-to-outdoor ratio of about 3. Would you speculate on whether the rates might be less in an area with different construction?

Steinhäusler: In Austria only very few buildings are built of wood, and single family dwellings as well as apartments generally have no air conditioning. It can be assumed that, in the mainly wooden houses in the United States and in buildings with air conditioning, this ratio could be somewhat lower.

Jonassen: Did your measurements of radon show an annual variation?

Steinhäusler: Measurements both of radon and decay products showed pronounced annual variations, in general with higher values during periods of increased atmospheric stability (e.g., inversion layers) and vice versa.

Jonassen: How did you ensure the same state of ventilation in summer and winter for a given room?

Steinhäusler: For the network of uninhabited control stations, ventilation conditions were defined since, during the course of the investigation, all openings (doors, windows) were closed, and indoor atmospheric temperature and humidity were monitored. At the other inhabited test sites selected, measurements were made several times at different seasons and under different ventilation conditions so as to account for the living habits of the inhabitants.

Cliff: In rooms stated to have constant ventilation conditions, were any ventilation-rate measurements made?

Steinhäusler: The rate of ventilation was monitored indirectly by continuous measurements of atmospheric temperature and relative humidity indoors as well as outdoors.

Participant (EPA): Were your alpha-dose equivalent estimates based on a quality factor of 10 or 20?

Steinhäusler: A quality factor of 10 was used for alpha-dose calculations.

Muth: May I give a more general but very personal comment or remark concerning the subject dealt with in the papers of this session? Within the Advisory Committee of the European Com-

munity for Radiation Protection, the group scientifically responsible for the Radiation Protection Directives that are obligatory for the nine member states of the community, we discussed several times during recent years the problem of indoor exposure of the population. However, my personal opinion is that up to now we still are far away from laying down directives with, for example, acceptable "concentration limits" for radionuclides in building materials. I think that this is a very complex problem which varies to a certain degree from country to country, and there will be a lot of further work to do to arrive at a final decision with respect to the protection of populations from these radiation sources. I should like to hear some opinions, if possible from the audience, concerning this problem.

Human Dose from Radiation of Terrestrial Origin

KERAN O'BRIEN
Environmental Measurements Laboratory, U. S. Department of Energy, New York, New York

ABSTRACT

The distribution of radiation doses in the organs and tissues of the U. S. population due to externally incident beta and gamma radiation have been calculated. The calculations were carried out using a Monte Carlo code based on the MIRD phantom. Tissue doses from gamma rays are typically in the neighborhood of 30 mrads/year. Beta-ray doses, except for the skin dose, are orders of magnitude less.

At 1 m above sea-level earth and at higher geomagnetic latitudes, the total ionization in air may amount to about 13 I.* This is due to the interaction of ionizing radiation with the constituents of the atmosphere and represents energy transfer to air from the rapidly moving charged particles.

Such ionization is readily measured and calculated and, since it is essentially proportional to radiation dose, is often used as an indicator of the radiation insult delivered by the natural radiations in the environment. However, the radiations whose ionization totals 13 I are quite different sorts and interact in different ways, from a biological point of view, with the massive, heterogeneous, geometrically complex, transpiring human body.

About 5 of the 13 I are due to airborne radon and thoron and their decay products (Ikebe, 1970). These materials produce their

*One I corresponds to 1 ion pair/sec per cubic centimeter of air at STP.

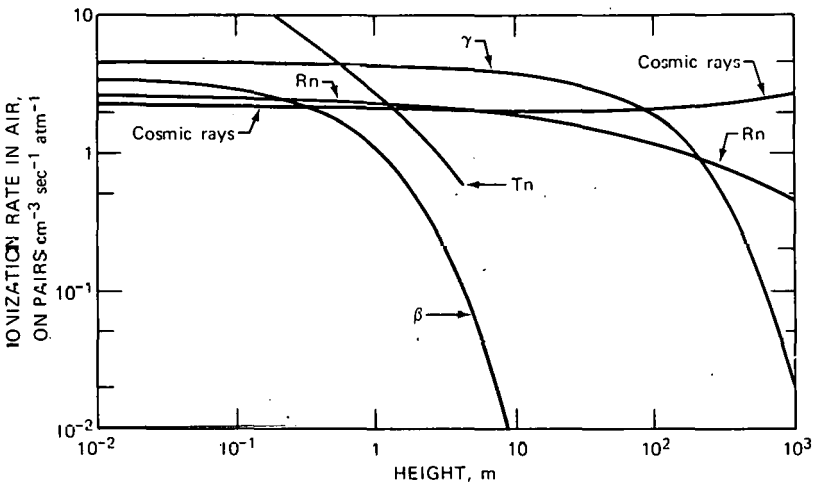


Fig. 1 Ionization as a function of altitude above soil. Radon and thoron data are from Ikebe (1970), gamma-radiation data are from Beck (1975), cosmic-ray data are from O'Brien (1975), and the beta-ray data are from this study.

most important effects by the alpha irradiation of lung tissue following inhalation. Another 2 I result from cosmic rays. At sea level these are mostly muons and their decay products, fast electrons and associated cascade showers. These radiations are very penetrating and behave just oppositely to the emanation gases, radon and thoron, irradiating the whole body uniformly, insensitive to its details.

The problems of evaluating the human dose from these two sources are very different and will not be touched on here. The remaining 6 I arise from beta and gamma radiation produced by terrestrial radioactive minerals. The interaction of these radiations with the human body is sensitive to the details of its architecture, and this paper addresses the calculation of the distribution of radiation dose in the human body from naturally occurring beta and gamma radiation.

The ionization profile as a function of altitude for the various contributors to atmospheric ionization is shown in Fig. 1. In temperate climates, people spend most of their time indoors. Because of the variety of types of housing and of housing materials and the paucity of research on the subject, no neat picture comparable to Fig. 1 can be drawn representative of normal human exposure to ionizing radiation indoors. Nonetheless, a reasonable attempt to account for this important influence will be made.

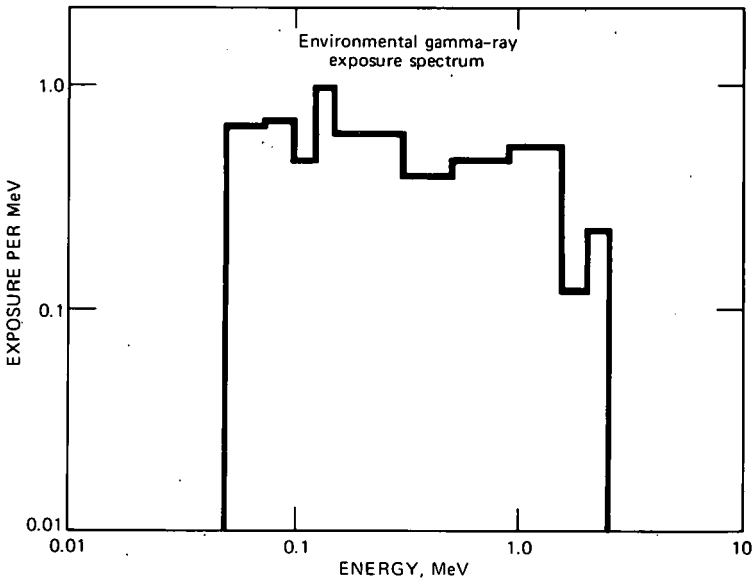


Fig. 2 Natural gamma-ray exposure as a function of energy. The area under the curve has been adjusted to be equal to unity. The data are from Beck (1975).

THE RADIATION SOURCE

Abstracting from a large number of measurements carried out by the former Health and Safety Laboratory* of the gamma-radiation background, Beck (1975) has described the sources that make up the typical radiation background field in the continental United States: 14 pCi of ^{40}K, 1.1 pCi of thorium and its decay products, and 1.8 pCi of uranium and its associated decay products per gram of soil, along with small amounts of fallout ^{137}Cs and $Zr—^{95}Nb$, as well as gamma radiation from airborne radon and its daughters, for a total of 4.5 I.

The gamma-ray ionization profile resulting from this source in a uniform section of earth is shown, as noted above, in Fig. 1. The exposure spectrum, normalized to unit dose, 1 m above the earth, is shown in Fig. 2. Both sets of data were taken from Beck (1975).

The beta-ray ionization was calculated by using a DP-1 polynomial approximation to the Boltzmann equation, according to the method of O'Brien et al. (1964). The cross sections were obtained

*Now the Environmental Measurements Laboratory of the U. S. Department of Energy.

TABLE 1

The Composition of the A Horizon of a New Jersey Sandy Loam

Material	Weight, %	Material	Weight, %
SiO_2	73.406	K_2O	0.575
TiO_2	0.397	Na_2O	0.068
Fe_2O_3	5.514	P_2O_3	0.101
Al_2O_3	2.605	SO_3	0.042
MnO	0.008	N	0.025
CaO	0.372	Organic $(C_{11}H_{15}O_5)$	1.734
MgO	0.152	H_2O	15.00

from O'Brien (1974). The source concentrations were the identical concentrations chosen by Beck. The decay series were assumed to be in secular equilibrium. The soil composition (see Table 1) is that of the A horizon (topsoil) of a New Jersey sandy loam. The water concentration corresponds to our own experience in the past few years in the northeastern United States. The ionization contributed per picocurie of uranium, thorium, and potassium per gram of soil at a height of 1 m above the surface is summarized in Tables 2 and 3.

A significant degree of disequilibrium usually exists in the uranium series. Radon-222, one of the decay products of radium, is a noble gas with a 3.8-day half-life. On the order of 20 to 30% (Beck, 1975) of the radon escapes the soil. A smaller amount of thoron also escapes, and these are the sources of the well-known radon and thoron concentrations in the atmosphere noted above.

Typical concentrations of radon, thoron, and ^{85}Kr are shown in Table 4 (from National Council on Radiation Protection and Measurements, 1975), along with the beta-ray ionization calculated for 1 m above the ground. A reduction by 25% of radon and daughters in the soil would reduce the air ionization by 0.06 I, about 5% of the total, and the ionization produced by airborne radon and thoron beta rays is about 0.14 I, raising the total ionization by 7%, from 1.13 to 1.21 I.

Beck calculates that the airborne radon contributes about 0.07 I on average to the gamma-ray dose rate at 1 m.

These concentrations of natural radioactive materials and the ionization spectra associated with them are chosen to be averages for the United States. The range of values about these averages is considerable, depending on local rock and soil geology (Beck, 1975;

TABLE 2

Ionization at 1 M above a Soil Surface from Natural Beta Emitters

Source	End-point energy, MeV	Ionization at 1 m, I
^{40}K (14 pCi/g)	1.31	0.707
Uranium series		
UX_2 (^{234}Pa)	2.29	0.135
RaB (^{214}Pb)	0.65	0.002
	0.71	0.002
	0.98	0.001
RaC (^{214}Bi)	1.00	0.005
	1.51	0.024
	3.26	0.047
RaE (^{210}Bi)	1.16	0.031
Total (0.769 pCi/g)		0.247
Thorium series		
MsTh II (^{228}Ac)	1.18	0.001
	1.75	0.014
	2.09	0.019
ThC (^{212}Bi)	1.55	0.004
	2.26	0.102
ThC'' (^{208}Tl)	1.28	0.005
	1.52	0.006
	1.80	0.022
Total (1.06 pCi/g)		0.173
Total (all sources)		1.128

TABLE 3

Ionization at 1 M above Soil from Beta and Gamma Radiation per Unit Source in I/(pCi/g)

Source	Gamma radiation	Beta radiation
^{40}K	0.103	0.051
Uranium series	1.05	0.322
Thorium series	1.63	0.164

TABLE 4

Beta-Ray Ionization from Airborne Beta Emitters

Source	End-point energy, MeV	Concentration, pCi/m^3	Ionization, I
^{85}Kr	0.67	0.5	7×10^{-5}
Uranium series			
RaC (^{214}Bi)	1.00	100	0.022
	1.51		0.034
	3.26		0.079
RaE (^{210}Bi)	1.16	20	0.005
Total			0.140
Thorium series			
ThC (^{212}Bi)	1.55	1	3.5×10^{-4}
	2.26		5.5×10^{-5}
ThC'' (^{208}Tl)	1.28	1	2.8×10^{-4}
	1.52		3.4×10^{-4}
	1.80		4.2×10^{-4}
Total			0.0014
Total (all sources)			0.141

Beninson et al., 1977). Variations with time at a given place also occur due to changes in soil moisture (which changes the density of beta- and gamma-ray sources in the ground), water cover on saturated soil, and snow cover (Burke, 1975).

These data will form the base for the calculation of human exposure to beta and gamma radiation. Modifications will be introduced to account for the effect of human radiation exposure indoors.

DOSE DISTRIBUTION IN HUMANS

The Human Irradiation Environment

People assume a variety of orientations both indoors and out. Indoors, the radiation source is distributed over the entire room. Outdoors, the source is distributed through a half-space and generates a radiation field that is approximately isotropic (Beck, 1975). The best simple model of radiation exposure would assume isotropic radiation incidence on some mathematical approximation to the human body.

TABLE 5

Composition and Mass of the Three Kinds of Tissue Making Up the MIRD Phantom as Incorporated in DISDOS

Element	Whole bone, %	Lung, %	Average bulk tissue, %
H	7.04	10.2	10.5
C	22.8	10.0	23.0
N	3.86	2.80	2.34
O	48.6	76.0	63.2
Mg	0.11	7.41×10^{-3}	1.51×10^{-2}
P	6.94	8.11×10^{-2}	0.24
S	0.17	0.23	0.22
Ca	9.91	7.01×10^{-3}	0
Cl	0.14	0.27	0.14
K	0.15	0.20	0.21
Na	0.32	0.19	0.13
Fe	8.03×10^{-3}	3.70×10^{-2}	6.30×10^{-3}
Zn	4.76×10^{-3}	1.10×10^{-3}	3.23×10^{-3}
Zr	0	0	7.96×10^{-4}
Sr	3.17×10^{-3}	5.91×10^{-6}	3.38×10^{-5}
Rb	0	3.70×10^{-4}	5.69×10^{-4}
Pb	1.09×10^{-3}	4.10×10^{-5}	1.62×10^{-5}
Total mass, g	10,116	1,000	59,091
Density, g/cm^3	1.49	0.296	0.987

The Mathematical Human Model

Snyder et al. (1969) have represented the human body and 32 organs and tissues by a set of equations known collectively as the MIRD phantom. This phantom (see Fig. 2), although somewhat idealized, is detailed and three-dimensional. It has been incorporated by Koblinger (1971 and undated) into the geometry routine of his Monte Carlo code DISDOS. The phantom is composed of three kinds of tissue: whole bone, lung, and average bulk tissue, each with its own composition and density. These are shown as they are incorporated in DISDOS in Table 5.

In the geometry routine of DISDOS, as in the MIRD phantom on which it is based, the testes were located with the internal organs at a depth of 6 cm in tissue. This is clearly too much shielding for a study

of the dose from externally incident radiation, so they were relocated to a point just behind the skin on the anterior surface of the phantom.

Other modifications and additions to the geometry routine of DISDOS were necessary. The dose to the marrow constituent of whole bone is calculated in DISDOS on the assumption that the marrow is uniformly distributed in the bone. The distinction between red, blood-forming, marrow and total marrow had not been incorporated into the MIRD model when DISDOS was written. If the fraction of the red marrow in each of the bones of the skeleton is known, however, then the red-marrow dose can be calculated in the same way.

The dose to the marrow is given by

$$D_m = \sum_{i=1}^{6} f_i D_i$$

where D_m is the dose to the marrow, D_i is the dose to the *ith* class of bones, and f_i is the fraction of the marrow mass in a given class of bone.

There are six classes of bone in the MIRD phantom as Fig. 3 (taken from Snyder et al., 1969) indicates: skull, arm bones, spine ribs, pelvis, and leg bones. The distribution and quantity of red marrow in the human is a function of age and health. However, numerical experimentation has shown that the dose to the red marrow is insensitive to the details of its distribution. The values of f_i used in this study are shown in Table 6 and are adapted from Ellis (1961) and Hashimoto and Yamada (1964). As Fig. 4 indicates, the MIRD phantom has a rather simplified skeleton, and it has been necessary to lump scapulae, clavicles, and the sternum in with the ribs. In addition, the red marrow occurs primarily in the heads and necks of the two humeri and femurs, but it was necessary to average it over the simplified skeletal structure.

The lens of the eye has also not been incorporated into the MIRD phantom or into DISDOS. However, Billings and Yucker (1974a, 1974b) have calculated isotropic chord-length distributions for a number of organs in a detailed 74-kg male phantom. The chord-length distributions for chords longer than about 3 g/cm^2 of the lens of the eye and of the skin are virtually identical. Hence the dose to the lens of the eye from the relatively penetrating environmental gamma radiation can be taken as identical to the skin dose.

The MIRD phantom is a 70-kg 174-cm hermaphrodite and is intended to represent both sexes. However, although this body size

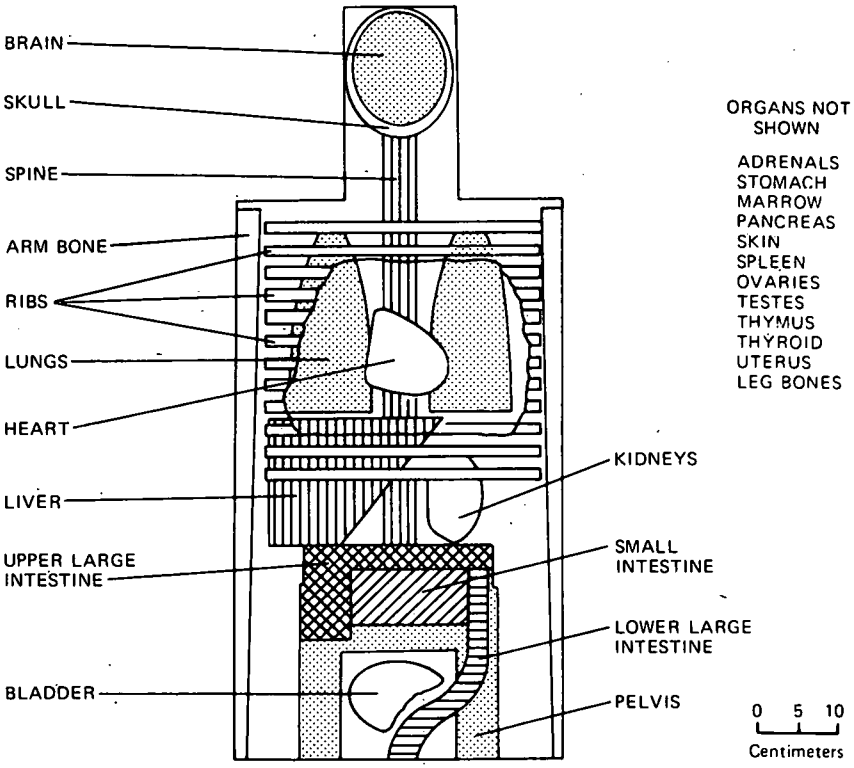


Fig. 3 Anterior view of the principal organs in the head and trunk of the MIRD phantom, taken from Snyder et al. (1969).

TABLE 6

Percent of Red Marrow in Various Bones

Site in phantom	Red marrow, %
Skull	10.3
Arm bones	2.8
Spine	39.15
Ribs	17.9
Pelvis	22.25
Leg bones	7.6

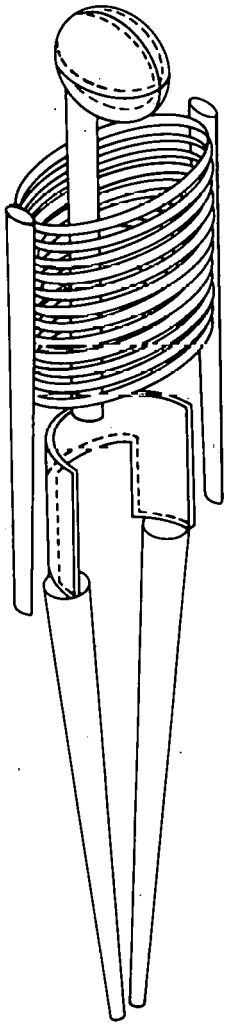


Fig. 4 The MIRD skeleton, taken from Snyder et al. (1969).

corresponds well with the ICRP reference male, the reference female weighs 57 kg and is 160 cm tall (International Commission on Radiological Protection, 1975). To represent the background dose to the population, gamma-ray doses to the male population were calculated with the unaltered DISDOS phantom, and doses to the female population were calculated with a smaller phantom scaled down to correspond more closely with the reference female of

ICRP-23 (International Commission on Radiological Protection, 1975).

Some of the properties of the scaled (female) and unaltered (male) phantoms used in this study are compared with the reference male and female of ICRP-23 in Table 7. Most of the organs and tissues of the scaled phantom used to represent the reference female are too large, but the reduction from the original sizes is clearly an improvement. Ovaries and uterus are an exception. In the unaltered MIRD phantom, they were smaller than reference female values by 27 and 18%, respectively; too small that is to begin with.

The Calculation

DISDOS uses the Monte Carlo technique to follow particles entering the phantom from collision site to collision site in the phantom until the particle escapes or is absorbed.

The incident isotropic flux is simulated by the following procedure. The phantom is covered by a rectangular starting surface (see Fig. 5). The starting electron or photon, as the case may be, can leave any point on the surface with equal probability. The particle direction is chosen so as to be isotropic in the inward direction. The relation between particle fluence and the number of histories is then

$$\Phi = \frac{N}{4C}$$

where Φ is the fluence, N is the number of histories, and C is the area of the starting surface in square centimeters.

Photoelectric and pair-production cross sections were obtained from Hubbell (1969). The Compton cross section was calculated from Hastings' approximation to the Klein—Nishina formula (Hastings, 1955).

The energy distribution of the beta rays was assumed to be given by the simple Coulomb-uncorrected allowed spectrum. As before, in the case of the polynomial calculation of beta-ray ionization above ground, the cross sections used were those described by O'Brien (1974).

A Note About Units

The dose absorbed in human organs and tissues from beta and gamma radiation in the environment will be expressed in this paper in rads. Since the environmental source is variable, doses will also be expressed per unit fluence and per unit of exposure. The unit of

TABLE 7

Comparison of Organs and Tissues of MIRD Phantom (DISDOS Version) with Those of Reference Male and Reference Female

Organs and tissues	Weight of organs and tissues, g					
	Scaled MIRD phantom, body height 163 cm	Reference female,* body height 160 cm	Percent deviation†	MIRD phantom, body height 174 cm	Reference male,* body height 170 cm	Percent deviation†
G. I. tract (and contents)	2,312	2,105	10	2,790	2,205	27
Kidney	239	275	−13	288	310	−7
Liver	1,519	1,400	8	1,833	1,800	2
Lungs	840	800	5	1,013	1,000	1
Ovaries	7	11	36			
Skeleton	8,428	6,800	24	10,183	10,000	2
Skin	2,148	1,790	20	2,593	2,600	0.3
Spleen	146	150	−3	176	180	−2
Testes				36	35	3
Thyroid	16	17	−6	19	20	−5
Uterus	55	80	31			
Total body	58,340	58,000	0.6	70,470	70,000	0.7

*Data are from ICRP-23 (International Commission on Radiological Protection, 1975).

†Percent deviation $= \left(\frac{\text{MIRD phantom organ weight} - \text{reference weight}}{\text{Reference weight}}\right) \times 100.$

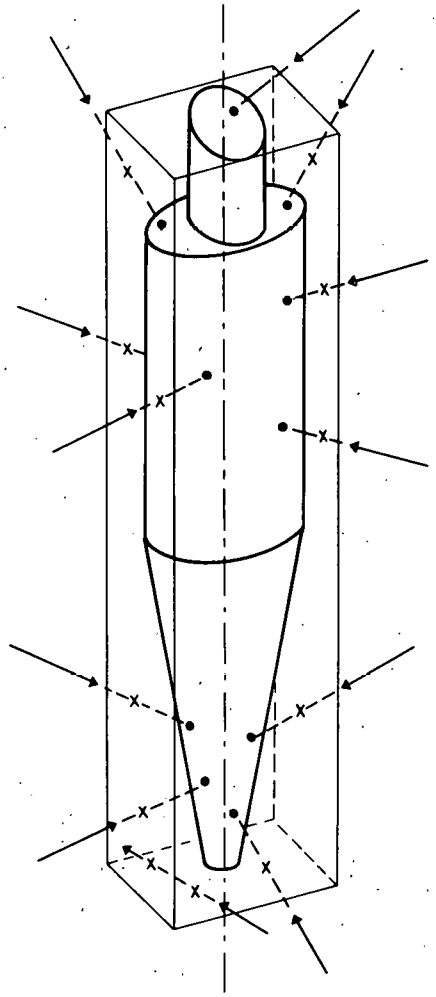


Fig. 5 Diagram of the particle starting surface of DISDOS, taken from Koblinger (1971).

exposure chosen is the roentgen, which for the purpose of this paper is defined by

$$X = Jet$$

where X = exposure, R
J = ionization density, I (ion pairs/sec per cubic centimeter of air at STP)

e = electronic charge (4.8032×10^{-10} esu)
t = exposure time, sec

The usual qualifications which hedge about the use of the roentgen (and which prevent its use outside the laboratory or hospital) have been erected to allow certain inferences to be drawn concerning the primary fluxes that set in motion the electrons registered as ionization. It is felt that the environmental field is well enough understood to make these cautions unnecessary. In fact, it is essentially no simpler to calculate air dose in free air in rads than to calculate exposure in roentgens. However, it is the ionization that is measured in most cases, not the air dose. Thus the qualifications being immaterial, they are dispensed with. The advantage accrues that a detector of known energy response, calibrated with a gamma-ray source under laboratory conditions, will yield exposure directly. In addition, a potential source of confusion is removed. Dose in rads in this paper is always the tissue dose, never the air dose or kerma.

RESULTS OF CALCULATIONS

The dose to 33 organs and tissues per unit fluence and per unit exposure [rads/(particle/cm^2) and rads/R] for 9 photon energies from 20 keV to 10 MeV has been calculated for men and women exposed to an isotropic gamma-ray field representing the energy composition of the natural gamma-ray background (Tables 8 and 9). Likewise, the results of the calculations from beta rays having 7 end-point energies ranging from 0.2 to 5 MeV are given in Table 10. The beta-ray dose calculations were carried out with only one phantom, the unaltered 70-kg MIRD phantom.

Whitton (1973) has shown that the old value of 7 mg/cm^2 generally used for the epidermal thickness is in error. As a result of her measurements, she concludes that the epidermis should be represented by three thicknesses, depending on body site, namely, 4, 8, and 40 mg/cm^2. Since the Monte Carlo phantom calculations give the dose to the whole skin, polynomial transport calculations of the dose to these layers of the skin have been made. And since nuclear beta rays are relatively soft, the assumption that the skin dose is equal to the dose to the lens of the eye is no longer valid. An estimate of this was also obtained by calculating the dose at a depth of 5 mm of tissue, which corresponds to the depth of the lens of the eye (International Commission on Radiological Protection, 1975). These results are shown in Table 11.

Finally, the dose to the skin from superficial contamination by beta emitters is given in Table 12. These values were obtained using the method of discrete ordinates (Abbott, Berger, and Sandmeier, 1968) with the same cross sections as before. Owing to the softness of the radiation, the energy deposition close to the source is quite high.

There is some recent evidence that the radiation dose to the female breast is of considerable importance (Gregg, 1977). Unfortunately, there is no simple way these calculations can be modified to yield this quantity. As an approximate estimate, under conditions of isotropic irradiation by gamma rays in the environment, a dose midway between the dose to the skin and the lungs may be used.

ENVIRONMENTAL DOSE RATES

The radiation profiles shown in Figs. 1 and 2 and in Table 4 are typical of the outdoor United States. However, most people spend most of their time, and hence get most of their exposure to radiation, indoors. Radiation exposures in a building are due to the radioactivity in the materials which comprise it and to any radiations that penetrate it from outside. Masonry has a higher concentration of radioactivity than wood, and, as one would suppose, gamma-radiation levels in houses of masonry tend to be higher than radiation levels in frame houses. Oakley (1972) developed a quantitative treatment to account for this important factor based on the following data:

1. Published data on gamma-radiation dose rates in houses of frame and masonry construction in terms of the radiation dose rates measured outside.
2. Census Bureau and Federal Housing Administration information on types and construction of dwellings.
3. Census Bureau data and other material in the literature on the living, working, and recreation habits of the population.

These data were applied to a formula which partitioned the population as to dwelling type, time spent indoors in each type of structure, and time spent outdoors. He applied the appropriate indoor dose rate in terms of the ratio of this radiation dose rate to the dose rate measured out-of-doors. This yielded a "housing factor" of 0.8; i.e., the effect of housing on human background radiation exposure in the United States is to reduce it to 20% below the mean outdoor value. Hence, as we have noted above, the mean outdoor gamma-ray exposure rate being 4.5 I, the mean annual exposure is 54 mR. The energy distribution of the exposure is given in Fig. 2.

(Text continues on page 1199.)

TABLE 8

Gamma-Ray Doses to the Organs and Tissues of the Reference Female

Organs and tissues	Dose					
	rads / photons/cm^2	rads / R	Standard deviation, %	rads / photons/cm^2	rads / R	Standard deviation, %
	20 keV			50 keV		
Adrenals	2.995 E − 12	1.591 E − 02	12.82	1.631 E − 11	4.352 E − 01	6.22
Bladder	2.928 E − 12	1.556 E − 02	2.71	1.517 E − 11	4.058 E − 01	1.53
Brain	1.241 E − 12	6.595 E − 03	2.59	1.565 E − 11	4.186 E − 01	1.00
G. I. tract	1.691 E − 12	8.982 E − 03	1.51	1.373 E − 11	3.673 E − 01	0.74
Stomach	1.982 E − 12	1.053 E − 02	3.63	1.513 E − 11	4.047 E − 01	1.67
Small intestine	1.185 E − 12	6.294 E − 03	2.22	1.282 E − 11	3.430 E − 01	0.97
Large intestine						
Upper	3.196 E − 12	1.698 E − 02	2.76	1.551 E − 11	4.150 E − 01	1.52
Lower	2.106 E − 12	1.119 E − 02	4.05	1.460 E − 11	3.905 E − 01	1.81
Heart	1.226 E − 12	6.515 E − 03	3.82	1.506 E − 11	4.029 E − 01	1.43
Kidneys	4.850 E − 12	2.577 E − 02	2.72	1.569 E − 11	4.197 E − 01	1.80
Liver	2.186 E − 12	1.162 E − 02	1.64	1.532 E − 11	4.098 E − 01	0.89
Lungs	3.254 E − 12	1.729 E − 02	1.74	1.768 E − 11	4.730 E − 01	0.89
Ovaries	7.080 E − 14	3.762 E − 04	58.33	1.373 E − 11	3.672 E − 01	8.68
Pancreas	1.972 E − 13	1.048 E − 03	22.96	1.321 E − 11	3.534 E − 01	3.58
Skeleton	7.039 E − 12	3.740 E − 02	0.35	3.381 E − 11	9.043 E − 01	0.28
Skull	1.012 E − 11	5.376 E − 02	0.86	3.746 E − 11	1.002 E 00	0.80
Arm bones	1.888 E − 11	1.003 E − 01	0.62	5.269 E − 11	1.409 E 00	0.65
Spine	5.672 E − 13	3.014 E − 03	1.91	2.403 E − 11	6.427 E − 01	0.92
Rib	2.321 E − 11	1.233 E − 01	0.59	4.782 E − 11	1.279 E 00	0.69

Pelvis	2.037 E − 12	1.082 E − 02	1.42	3.578 E − 11	9.570 E − 01	0.86
Leg bones	1.185 E − 12	6.294 E − 03	0.90	2.546 E − 11	6.809 E − 01	0.52
Red marrow	6.491 E − 12	3.449 E − 02	0.77	3.320 E − 11	8.879 E − 01	0.80
Marrow	6.110 E − 12	3.246 E − 02	0.35	3.255 E − 11	8.707 E − 01	0.28
Skin	7.846 E − 11	4.168 E − 01	0.22	2.558 E − 11	6.843 E − 01	0.40
Spleen	1.487 E − 12	7.898 E − 03	6.06	1.473 E − 11	3.939 E − 01	2.37
Thymus	2.123 E − 12	1.128 E − 02	12.67	1.784 E − 11	4.773 E − 01	4.96
Thyroid	1.216 E − 11	6.462 E − 02	6.23	2.052 E − 11	5.489 E − 01	5.44
Uterus	3.253 E − 13	1.728 E − 03	17.69	1.283 E − 11	3.432 E − 01	3.76
Head	1.832 E − 11	9.732 E − 02	0.36	2.455 E − 11	6.566 E − 01	0.50
Trunk	1.200 E − 11	6.375 E − 02	0.14	1.898 E − 11	5.077 E − 01	0.19
Legs	1.560 E − 11	8.286 E − 02	0.18	1.920 E − 11	5.136 E − 01	0.27
Total body	1.360 E − 11	7.224 E − 02	0.09	1.947 E − 11	5.208 E − 01	0.13
		100 keV			**200 keV**	
Adrenals	2.218 E − 11	5.148 E − 01	6.97	5.739 E − 11	5.813 E − 01	7.77
Bladder	2.297 E − 11	5.331 E − 01	1.51	4.698 E − 11	4.760 E − 01	1.64
Brain	2.307 E − 11	5.353 E − 01	1.00	5.202 E − 11	5.270 E − 01	1.03
G. I. tract	2.173 E − 11	5.042 E − 01	0.73	4.550 E − 11	4.610 E − 01	0.76
Stomach	2.201 E − 11	5.108 E − 01	1.70	4.700 E − 11	4.762 E − 01	1.82
Small intestine	2.097 E − 11	4.865 E − 01	0.93	4.373 E − 11	4.430 E − 01	0.97
Large intestine						
Upper	2.390 E − 11	5.545 E − 01	1.52	5.098 E − 11	5.164 E − 01	1.68
Lower	2.270 E − 11	5.268 E − 01	1.84	4.593 E − 11	4.653 E − 01	2.07
Heart	2.331 E − 11	5.410 E − 01	1.41	4.853 E − 11	4.916 E − 01	1.51
Kidneys	2.387 E − 11	5.540 E − 01	1.80	5.077 E − 11	5.143 E − 01	2.02
Liver	2.234 E − 11	5.183 E − 01	0.89	4.719 E − 11	4.781 E − 01	0.93
Lungs	2.362 E − 11	5.480 E − 01	0.94	4.985 E − 11	5.051 E − 01	1.06
Ovaries	1.921 E − 11	4.457 E − 01	9.95	4.627 E − 11	4.687 E − 01	10.85
Pancreas	2.048 E − 11	4.753 E − 01	3.70	4.103 E − 11	4.157 E − 01	4.39

(Table continues on the next page.)

TABLE 8 (Continued)

Organs and tissues	Dose					
	rads / photons/cm^2	rads / R	Standard deviation, %	rads / photons/cm^2	rads / R	Standard deviation, %
Skeleton	3.625 E − 11	8.411 E − 01	0.31	5.445 E − 11	5.516 E − 01	0.34
Skull	3.589 E − 11	8.328 E − 01	0.92	5.443 E − 11	5.514 E − 01	1.02
Arm bones	4.302 E − 11	9.983 E − 01	0.75	6.561 E − 11	6.646 E − 01	0.85
Spine	3.343 E − 11	7.758 E − 01	0.92	4.863 E − 11	4.926 E − 01	1.01
Rib	3.909 E − 11	9.071 E − 01	0.79	5.881 E − 11	5.958 E − 01	0.95
Pelvis	4.583 E − 11	1.063 E 00	0.88	6.801 E − 11	6.889 E − 01	0.97
Leg bones	3.216 E − 11	7.462 E − 01	0.56	4.847 E − 11	4.910 E − 01	0.60
Red marrow	3.763 E − 11	8.732 E − 01	0.88	5.582 E − 11	5.655 E − 01	0.97
Marrow	3.604 E − 11	8.362 E − 01	0.32	5.399 E − 11	5.470 E − 01	0.35
Skin	3.200 E − 11	7.427 E − 01	0.48	7.434 E − 11	7.532 E − 01	0.55
Spleen	2.210 E − 11	5.129 E − 01	2.41	4.592 E − 11	4.652 E − 01	2.69
Thymus	2.313 E − 11	5.368 E − 01	5.78	5.260 E − 11	5.329 E − 01	6.17
Thyroid	2.764 E − 11	6.414 E − 01	6.22	5.973 E − 11	6.051 E − 01	6.91
Uterus	2.247 E − 11	5.215 E − 01	3.51	4.233 E − 11	4.288 E − 01	4.25
Head	2.999 E − 11	6.959 E − 01	0.54	6.058 E − 11	6.137 E − 01	0.54
Trunk	2.519 E − 11	5.845 E − 01	0.21	5.214 E − 11	5.282 E − 01	0.20
Legs	2.552 E − 11	5.923 E − 01	0.29	5.273 E − 11	5.341 E − 01	0.29
Total body	2.566 E − 11	5.953 E − 01	0.15	5.296 E − 11	5.365 E − 01	0.15
	500 keV			1 MeV		
Adrenals	1.566 E − 10	5.746 E − 01	5.45	2.843 E − 10	5.553 E − 01	3.80
Bladder	1.401 E − 10	5.141 E − 01	1.05	2.921 E − 10	5.705 E − 01	1.25
Brain	1.566 E − 10	5.744 E − 01	0.63	3.153 E − 10	6.158 E − 01	0.75

G. I. tract	1.338 E − 10	4.911 E − 01	0.47	2.747 E − 10	5.365 E − 01	0.57
Stomach	1.362 E − 10	4.996 E − 01	1.19	2.756 E − 10	5.383 E − 01	1.44
Small intestine	1.283 E − 10	4.706 E − 01	0.61	2.658 E − 10	5.191 E − 01	0.73
Large intestine						
Upper	1.497 E − 10	5.494 E − 01	1.10	3.039 E − 10	5.936 E − 01	1.33
Lower	1.407 E − 10	5.161 E − 01	1.36	2.856 E − 10	5.579 E − 01	1.69
Heart	1.395 E − 10	5.118 E − 01	0.98	2.881 E − 10	5.627 E − 01	1.18
Kidneys	1.479 E − 10	5.427 E − 01	1.33	3.084 E − 10	6.023 E − 01	1.60
Liver	1.405 E − 10	5.154 E − 01	0.58	2.903 E − 10	5.670 E − 01	0.68
Lungs	1.455 E − 10	5.340 E − 01	0.71	3.028 E − 10	5.914 E − 01	0.86
Ovaries	1.201 E − 10	4.406 E − 01	8.18	2.401 E − 10	4.690 E − 01	9.95
Pancreas	1.266 E − 10	4.643 E − 01	2.98	2.542 E − 10	4.965 E − 01	3.66
Skeleton	1.484 E − 10	5.445 E − 01	0.23	3.003 E − 10	5.866 E − 01	0.27
Skull	1.519 E − 10	5.572 E − 01	0.66	2.994 E − 10	5.849 E − 01	0.79
Arm bones	1.892 E − 10	6.940 E − 01	0.55	3.801 E − 10	7.425 E − 01	0.67
Spine	1.289 E − 10	4.729 E − 01	0.66	2.629 E − 10	5.134 E − 01	0.81
Rib	1.685 E − 10	6.182 E − 01	0.65	3.376 E − 10	6.593 E − 01	0.80
Pelvis	1.763 E − 10	6.467 E − 01	0.67	3.556 E − 10	6.946 E − 01	0.82
Leg bones	1.286 E − 10	4.719 E − 01	0.39	2.638 E − 10	5.152 E − 01	0.46
Red marrow	1.506 E − 10	5.524 E − 01	0.65	3.040 E − 10	5.938 E − 01	0.79
Marrow	1.463 E − 10	5.368 E − 01	0.23	2.968 E − 10	5.796 E − 01	0.28
Skin	2.200 E − 10	8.073 E − 01	0.37	4.374 E − 10	8.544 E − 01	0.45
Spleen	1.375 E − 10	5.045 E − 01	1.77	2.794 E − 10	5.457 E − 01	2.15
Thymus	1.529 E − 10	5.608 E − 01	4.28	3.425 E − 10	6.689 E − 01	5.17
Thyroid	1.673 E − 10	6.137 E − 01	4.74	3.291 E − 10	6.428 E − 01	5.78
Uterus	1.295 E − 10	4.751 E − 01	2.83	2.586 E − 10	5.052 E − 01	3.51
Head	1.780 E − 10	6.531 E − 01	0.33	3.570 E − 10	6.972 E − 01	0.38
Trunk	1.533 E − 10	5.623 E − 01	0.12	3.126 E − 10	6.106 E − 01	0.14
Legs	1.538 E − 10	5.642 E − 01	0.17	3.106 E − 10	6.066 E − 01	0.20
Total body	1.553 E − 10	5.697 E − 01	0.09	3.155 E − 10	6.162 E − 01	0.10

(Table continues on the next page.)

TABLE 8 (Continued)

Organs and tissues	Dose					
	rads / photons/cm^2	rads / R	Standard deviation, %	rads / photons/cm^2	rads / R	Standard deviation, %
	2 MeV			5 MeV		
Adrenals	6.148 E − 10	7.134 E − 01	6.92	1.229 E − 09	7.670 E − 01	6.58
Bladder	5.409 E − 10	6.276 E − 01	1.31	1.095 E − 09	6.835 E − 01	1.27
Brain	5.585 E − 10	6.480 E − 01	0.79	1.097 E − 09	6.849 E − 01	0.76
G. I. tract	5.134 E − 10	5.956 E − 01	0.58	1.047 E − 09	6.533 E − 01	0.56
Stomach	5.173 E − 10	6.002 E − 01	1.50	1.070 E − 09	6.680 E − 01	1.43
Small intestine	5.020 E − 10	5.825 E − 01	0.75	1.015 E − 09	6.338 E − 01	0.72
Large intestine						
Upper	5.400 E − 10	6.265 E − 01	1.44	1.165 E − 09	7.271 E − 01	1.36
Lower	5.379 E − 10	6.241 E − 01	1.75	1.061 E − 09	6.620 E − 01	1.74
Heart	5.315 E − 10	6.167 E − 01	1.22	1.061 E − 09	6.620 E − 01	1.18
Kidneys	5.606 E − 10	6.504 E − 01	1.68	1.178 E − 09	7.353 E − 01	1.62
Liver	5.379 E − 10	6.241 E − 01	0.71	1.104 E − 09	6.888 E − 01	0.67
Lungs	5.426 E − 10	6.296 E − 01	0.92	1.090 E − 09	6.806 E − 01	0.89
Ovaries	5.391 E − 10	6.254 E − 01	9.99	9.925 E − 10	6.194 E − 01	10.00
Pancreas	4.704 E − 10	5.458 E − 01	3.89	9.233 E − 10	5.763 E − 01	3.88
Skeleton	5.502 E − 10	6.384 E − 01	0.29	1.143 E − 09	7.136 E − 01	0.28
Skull	5.470 E − 10	6.347 E − 01	0.83	1.113 E − 09	6.947 E − 01	0.80
Arm bones	6.889 E − 10	7.993 E − 01	0.70	1.386 E − 09	8.653 E − 01	0.67
Spine	4.920 E − 10	5.708 E − 01	0.84	1.028 E − 09	6.416 E − 01	0.80
Rib	6.171 E − 10	7.160 E − 01	0.85	1.282 E − 09	8.004 E − 01	0.81
Pelvis	6.638 E − 10	7.702 E − 01	0.86	1.432 E − 09	8.937 E − 01	0.81

Leg bones	4.846 E − 10	5.623 E − 01	0.48	1.009 E − 09	6.298 E − 01	0.46
Red marrow	5.632 E − 10	6.535 E − 01	0.83	1.181 E − 09	7.370 E − 01	0.80
Marrow	5.462 E − 10	6.338 E − 01	0.29	1.133 E − 09	7.070 E − 01	0.29
Skin	7.719 E − 10	8.956 E − 01	0.48	1.470 E − 09	9.175 E − 01	0.49
Spleen	5.188 E − 10	6.020 E − 01	2.26	1.061 E − 09	6.621 E − 01	2.18
Thymus	5.623 E − 10	6.524 E − 01	5.61	1.119 E − 09	6.985 E − 01	5.59
Thyroid	6.126 E − 10	7.108 E − 01	6.26	1.218 E − 09	7.604 E − 01	6.05
Uterus	4.833 E − 10	5.608 E − 01	3.66	9.718 E − 10	6.065 E − 01	3.70
Head	6.372 E − 10	7.393 E − 01	0.40	1.256 E − 09	7.840 E − 01	0.38
Trunk	5.731 E − 10	6.649 E − 01	0.14	1.150 E − 09	7.178 E − 01	0.14
Legs	5.619 E − 10	6.520 E − 01	0.21	1.120 E − 09	6.992 E − 01	0.19
Total body	5.746 E − 10	6.667 E − 01	0.10	1.148 E − 09	7.166 E − 01	0.11
		10 MeV				
Adrenals	2.134 E − 09	7.991 E − 01	6.58			
Bladder	2.021 E − 09	7.568 E − 01	1.21			
Brain	1.947 E − 09	7.291 E − 01	0.73			
G. I. tract	1.862 E − 09	6.975 E − 01	0.54			
Stomach	1.996 E − 09	7.474 E − 01	1.37			
Small intestine	1.800 E − 09	6.741 E − 01	0.70			
Large intestine						
Upper	1.973 E − 09	7.390 E − 01	1.34			
Lower	1.908 E − 09	7.146 E − 01	1.68			
Heart	1.910 E − 09	7.153 E − 01	1.14			
Kidneys	2.203 E − 09	8.249 E − 01	1.53			
Liver	1.946 E − 09	7.288 E − 01	0.65			
Lungs	1.958 E − 09	7.331 E − 01	0.86			
Ovaries	1.700 E − 09	6.366 E − 01	9.98			
Pancreas	1.932 E − 09	7.233 E − 01	3.51			

(Table continues on the next page.)

TABLE 8 (Continued)

Organs and tissues	Dose					
	rads / photons/cm^2	rads / R	Standard deviation, %	rads / photons/cm^2	rads / R	Standard deviation, %
Skeleton	2.148 E − 09	8.045 E − 01	0.26			
Skull	2.059 E − 09	7.710 E − 01	0.75			
Arm bones	2.616 E − 09	9.797 E − 01	0.63			
Spine	1.963 E − 09	7.350 E − 01	0.74			
Rib	2.436 E − 09	9.123 E − 01	0.76			
Pelvis	2.678 E − 09	1.003 E 00	0.77			
Leg bones	1.890 E − 09	7.077 E − 01	0.43			
Red marrow	2.229 E − 09	8.349 E − 01	0.75			
Marrow	2.137 E − 09	8.002 E − 01	0.26			
Skin	2.669 E − 09	9.994 E − 01	0.46			
Spleen	1.920 E − 09	7.189 E − 01	2.10			
Thymus	1.954 E − 09	7.317 E − 01	5.47			
Thyroid	2.168 E − 09	8.118 E − 01	5.87			
Uterus	1.773 E − 09	6.639 E − 01	3.54			
Head	2.232 E − 09	8.359 E − 01	0.36			
Trunk	2.079 E − 09	7.787 E − 01	0.13			
Legs	1.995 E − 09	7.470 E − 01	0.19			
Total body	2.069 E − 09	7.747 E − 01	0.10			

TABLE 9

Gamma-Ray Doses to the Organs and Tissues of the Reference Male

Organs and tissues	Dose					
	rads / photons/cm^2	rads / R	Standard deviation, %	rads / photons/cm^2	rads / R	Standard deviation, %
	20 keV			50 keV		
Adrenals	2.120 E − 12	1.126 E − 02	13.99	1.338 E − 11	3.579 E − 01	5.85
Bladder	1.802 E − 12	9.575 E − 03	3.15	1.354 E − 11	3.621 E − 01	1.41
Brain	5.725 E − 13	3.042 E − 03	3.44	1.397 E − 11	3.736 E − 01	0.92
G. I. tract	1.001 E − 12	5.319 E − 03	1.76	1.148 E − 11	3.071 E − 01	0.70
Stomach	1.247 E − 12	6.626 E − 03	4.21	1.297 E − 11	3.470 E − 01	1.56
Small intestine	6.795 E − 13	3.610 E − 03	2.62	1.045 E − 11	2.796 E − 01	0.91
Large intestine						
Upper	1.994 E − 12	1.059 E − 02	3.15	1.365 E − 11	3.652 E − 01	1.39
Lower	1.121 E − 12	5.956 E − 03	5.05	1.235 E − 11	3.304 E − 01	1.67
Heart	6.243 E − 13	3.317 E − 03	4.73	1.252 E − 11	3.349 E − 01	1.36
Kidneys	3.272 E − 12	1.738 E − 02	3.03	1.363 E − 11	3.647 E − 01	1.65
Liver	1.271 E − 12	6.755 E − 03	1.94	1.337 E − 11	3.577 E − 01	0.82
Lungs	1.887 E − 12	1.002 E − 02	2.07	1.546 E − 11	4.135 E − 01	0.80
Pancreas	1.046 E − 13	5.556 E − 04	36.10	1.042 E − 11	2.786 E − 01	3.33
Skeleton	5.059 E − 12	2.688 E − 02	0.36	2.889 E − 11	7.728 E − 01	0.25
Skull	7.221 E − 12	3.837 E − 02	0.90	3.308 E − 11	8.848 E − 01	0.71
Arm bones	1.380 E − 11	7.330 E − 02	0.65	4.773 E − 11	1.277 E 00	0.58
Spine	3.174 E − 13	1.686 E − 03	2.28	1.885 E − 11	5.042 E − 01	0.87
Rib	1.735 E − 11	9.217 E − 02	0.61	4.359 E − 11	1.166 E 00	0.61

(Table continues on the next page.)

TABLE 9 (Continued)

Organs and tissues	Dose					
	rads / photons/cm^2	rads / R	Standard deviation, %	rads / photons/cm^2	rads / R	Standard deviation, %
Pelvis	1.225 E − 12	6.506 E − 03	1.58	2.921 E − 11	7.814 E − 01	0.80
Leg bones	7.118 E − 13	3.782 E − 03	1.01	2.067 E − 11	5.529 E − 01	0.47
Red marrow	4.686 E − 12	2.490 E − 02	0.81	2.800 E − 11	7.489 E − 01	0.72
Marrow	4.385 E − 12	2.330 E − 02	0.36	2.757 E − 11	7.376 E − 01	0.25
Skin	7.507 E − 11	3.988 E − 01	0.20	2.479 E − 11	6.631 E − 01	0.34
Spleen	7.183 E − 13	3.817 E − 03	7.75	1.298 E − 11	3.472 E − 01	2.19
Testicles	1.979 E − 11	1.051 E − 01	3.56	2.109 E − 11	5.642 E − 01	3.52
Thymus	1.072 E − 12	5.693 E − 03	16.58	1.529 E − 11	4.091 E − 01	4.52
Thyroid	8.268 E − 12	4.393 E − 02	6.86	1.948 E − 11	5.211 E − 01	4.73
Head	1.546 E − 11	8.211 E − 02	0.36	2.236 E − 11	5.981 E − 01	0.45
Trunk	1.000 E − 11	5.313 E − 02	0.14	1.685 E − 11	4.508 E − 01	0.17
Legs	1.313 E − 11	6.974 E − 02	0.18	1.728 E − 11	4.522 E − 01	0.24
Total body	1.139 E − 11	6.049 E − 02	0.09	1.740 E − 11	4.655 E − 01	0.12
		100 keV			200 keV	
Adrenals	2.347 E − 11	5.447 E − 01	6.21	4.987 E − 11	5.052 E − 01	5.91
Bladder	2.133 E − 11	4.950 E − 01	1.48	4.412 E − 11	4.470 E − 01	1.27
Brain	2.207 E − 11	5.122 E − 01	0.98	4.933 E − 11	4.998 E − 01	0.80
G. I. tract	1.989 E − 11	4.616 E − 01	0.72	4.145 E − 11	4.200 E − 01	0.60
Stomach	2.049 E − 11	4.755 E − 01	1.64	4.340 E − 11	4.396 E − 01	1.42
Small intestine	1.910 E − 11	4.432 E − 01	0.92	3.974 E − 11	4.026 E − 01	0.76
Large intestine						
Upper	2.200 E − 11	5.105 E − 01	1.46	4.591 E − 11	4.651 E − 01	1.30
Lower	2.073 E − 11	4.811 E − 01	1.77	4.214 E − 11	4.269 E − 01	1.60

Heart	2.114 E − 11	4.905 E − 01	1.38	4.328 E − 11	4.385 E − 01	1.20
Kidneys	2.152 E − 11	4.994 E − 01	1.75	4.541 E − 11	4.601 E − 01	1.58
Liver	2.114 E − 11	4.905 E − 01	0.87	4.435 E − 11	4.493 E − 01	0.73
Lungs	2.255 E − 11	5.234 E − 01	0.89	4.697 E − 11	4.759 E − 01	0.82
Pancreas	1.899 E − 11	4.407 E − 01	3.55	3.747 E − 11	3.796 E − 01	3.34
Skeleton	3.399 E − 11	7.888 E − 01	0.30	5.147 E − 11	5.214 E − 01	0.27
Skull	3.484 E − 11	8.084 E − 01	0.88	5.169 E − 11	5.237 E − 01	0.79
Arm bones	4.157 E − 11	9.647 E − 01	0.72	6.365 E − 11	6.448 E − 01	0.65
Spine	3.030 E − 11	7.032 E − 01	0.90	4.644 E − 11	4.705 E − 01	0.78
Rib	3.806 E − 11	8.831 E − 01	0.74	5.699 E − 11	5.773 E − 01	0.72
Pelvis	4.173 E − 11	9.685 E − 01	0.85	6.308 E − 11	6.390 E − 01	0.76
Leg bones	2.963 E − 11	6.877 E − 01	0.54	4.496 E − 11	4.554 E − 01	0.47
Red marrow	3.497 E − 11	8.114 E − 01	0.84	5.294 E − 11	5.363 E − 01	0.75
Marrow	3.362 E − 11	7.802 E − 01	0.31	5.097 E − 11	5.164 E − 01	0.27
Skin	3.105 E − 11	7.204 E − 01	0.44	7.122 E − 11	7.215 E − 01	0.41
Spleen	2.043 E − 11	4.741 E − 01	2.32	4.359 E − 11	4.416 E − 01	2.06
Testicles	2.846 E − 11	6.605 E − 01	4.08	6.304 E − 11	6.386 E − 01	3.74
Thymus	2.376 E − 11	5.515 E − 01	5.11	4.583 E − 11	4.643 E − 01	4.92
Thyroid	2.721 E − 11	6.314 E − 01	5.53	5.565 E − 11	5.638 E − 01	5.27
Head	2.886 E − 11	6.697 E − 01	0.53	5.740 E − 11	5.815 E − 01	0.43
Trunk	2.371 E − 11	5.503 E − 01	0.20	4.880 E − 11	4.944 E − 01	0.16
Legs	2.401 E − 11	5.572 E − 01	0.29	4.956 E − 11	5.021 E − 01	0.23
Total body	2.419 E − 11	5.614 E − 01	0.15	4.968 E − 11	5.033 E − 01	0.11
		500 keV			**1 MeV**	
Adrenals	1.270 E − 10	4.661 E − 01	6.48	2.885 E − 10	5.635 E − 01	6.79
Bladder	1.288 E − 10	4.725 E − 01	1.22	2.638 E − 10	5.152 E − 01	1.29
Brain	1.473 E − 10	5.403 E − 01	0.74	3.005 E − 10	5.869 E − 01	0.76

(Table continues on the next page.)

TABLE 9 (Continued)

Organs and tissues	Dose					
	rads / photons/cm^2	rads / R	Standard deviation, %	rads / photons/cm^2	rads / R	Standard deviation, %
G. I. tract	1.198 E − 10	4.395 E − 01	0.56	2.523 E − 10	4.928 E − 01	0.58
Stomach	1.276 E − 10	4.682 E − 01	1.37	2.604 E − 10	5.086 E − 01	1.46
Small intestine	1.138 E − 10	4.175 E − 01	0.72	2.423 E − 10	4.733 E − 01	0.75
Large intestine						
Upper	1.340 E − 10	4.916 E − 01	1.29	2.807 E − 10	5.482 E − 01	1.36
Lower	1.239 E − 10	4.547 E − 01	1.60	2.601 E − 10	5.081 E − 01	1.70
Heart	1.268 E − 10	4.651 E − 01	1.15	2.627 E − 10	5.132 E − 01	1.20
Kidneys	1.354 E − 10	4.966 E − 01	1.56	2.802 E − 10	5.472 E − 01	1.65
Liver	1.280 E − 10	4.697 E − 01	0.68	2.630 E − 10	5.137 E − 01	0.70
Lungs	1.364 E − 10	5.003 E − 01	0.82	2.773 E − 10	5.416 E − 01	0.88
Pancreas	1.142 E − 10	4.189 E − 01	3.43	2.249 E − 10	4.394 E − 01	3.75
Skeleton	1.385 E − 10	5.081 E − 01	0.26	2.802 E − 10	5.472 E − 01	0.27
Skull	1.420 E − 10	5.209 E − 01	0.76	2.937 E − 10	5.737 E − 01	0.80
Arm bones	1.794 E − 10	6.580 E − 01	0.64	3.603 E − 10	7.037 E − 01	0.68
Spine	1.162 E − 10	4.262 E − 01	0.78	2.388 E − 10	4.665 E − 01	0.82
Rib	1.609 E − 10	5.903 E − 01	0.74	3.153 E − 10	6.158 E − 01	0.81
Pelvis	1.616 E − 10	5.929 E − 01	0.77	3.286 E − 10	6.417 E − 01	0.83
Leg bones	1.201 E − 10	4.405 E − 01	0.45	2.419 E − 10	4.725 E − 01	0.48
Red marrow	1.390 E − 10	5.100 E − 01	0.75	2.818 E − 10	5.504 E − 01	0.80
Marrow	1.363 E − 10	5.000 E − 01	0.26	2.752 E − 10	5.376 E − 01	0.28
Skin	2.110 E − 10	7.742 E − 01	0.42	4.212 E − 10	8.226 E − 01	0.45
Spleen	1.244 E − 10	4.565 E − 01	2.05	2.522 E − 10	4.926 E − 01	2.22
Testicles	1.831 E − 10	6.719 E − 01	3.74	3.665 E − 10	7.159 E − 01	4.06
Thymus	1.358 E − 10	4.983 E − 01	5.09	3.103 E − 10	6.062 E − 01	5.31

Thyroid	1.628 E − 10	5.972 E − 01	5.38	3.850 E − 10	7.520 E − 01	5.46
Head	1.678 E − 10	6.158 E − 01	0.38	3.405 E − 10	6.651 E − 01	0.39
Trunk	1.423 E − 10	5.220 E − 01	0.14	2.906 E − 10	5.676 E − 01	0.14
Legs	1.444 E − 10	5.298 E − 01	0.20	2.914 E − 10	5.691 E − 01	0.21
Total body	1.449 E − 10	5.315 E − 01	0.10	2.947 E − 10	5.757 E − 01	0.10
		2 MeV			**5 MeV**	
Adrenals	4.265 E − 10	4.949 E − 01	7.37	1.024 E − 09	6.394 E − 01	6.73
Bladder	4.919 E − 10	5.707 E − 01	1.28	1.018 E − 09	6.354 E − 01	1.22
Brain	5.464 E − 10	6.339 E − 01	0.75	1.081 E − 09	6.747 E − 01	0.72
G. I. tract	4.762 E − 10	5.525 E − 01	0.56	1.001 E − 09	6.250 E − 01	0.53
Stomach	4.762 E − 10	5.525 E − 01	1.46	1.052 E − 09	6.568 E − 01	1.35
Small intestine	4.629 E − 10	5.370 E − 01	0.73	9.755 E − 10	6.088 E − 01	0.69
Large intestine						
Upper	5.214 E − 10	6.049 E − 01	1.37	1.078 E − 09	6.727 E − 01	1.31
Lower	4.883 E − 10	5.665 E − 01	1.71	9.987 E − 10	6.233 E − 01	1.66
Heart	4.935 E − 10	5.726 E − 01	1.19	1.007 E − 09	6.287 E − 01	1.13
Kidneys	5.296 E − 10	6.145 E − 01	1.63	1.148 E − 09	7.165 E − 01	1.53
Liver	4.986 E − 10	5.785 E − 01	0.69	1.014 E − 09	6.326 E − 01	0.66
Lungs	5.167 E − 10	5.995 E − 01	0.88	1.037 E − 09	6.475 E − 01	0.85
Pancreas	4.499 E − 10	5.220 E − 01	3.72	8.938 E − 10	5.579 E − 01	3.65
Skeleton	5.185 E − 10	6.016 E − 01	0.28	1.088 E − 09	6.792 E − 01	0.26
Skull	5.280 E − 10	6.126 E − 01	0.80	1.058 E − 09	6.601 E − 01	0.76
Arm bones	6.517 E − 10	7.561 E − 01	0.68	1.341 E − 09	8.371 E − 01	0.64
Spine	4.469 E − 10	5.185 E − 01	0.82	9.686 E − 10	6.045 E − 01	0.76
Rib	5.853 E − 10	6.791 E − 01	0.81	1.209 E − 09	7.548 E − 01	0.77
Pelvis	6.287 E − 10	7.295 E − 01	0.83	1.341 E − 09	8.371 E − 01	0.78
Leg bones	4.550 E − 10	5.279 E − 01	0.46	9.631 E − 10	6.011 E − 01	0.44
Red marrow	5.268 E − 10	6.113 E − 01	0.80	1.114 E − 09	6.951 E − 01	0.76
Marrow	5.131 E − 10	5.953 E − 01	0.28	1.077 E − 09	6.722 E − 01	0.27

(Table continues on the next page.)

TABLE 9 (Continued)

Organs and tissues	Dose					
	rads / photons/cm^2	rads / R	Standard deviation, %	rads / photons/cm^2	racs / R	Standard deviation, %
Skin	7.451 E − 10	8.645 E − 01	0.46	1.443 E − 09	9.009 E − 01	0.46
Spleen	4.742 E − 10	5.501 E − 01	2.19	9.803 E − 10	6.118 E − 01	2.09
Testicles	6.572 E − 10	7.625 E − 01	4.11	1.396 E − 09	8.711 E − 01	3.86
Thymus	5.103 E − 10	5.920 E − 01	5.63	1.126 E − 09	7.027 E − 01	5.21
Thyroid	5.591 E − 10	6.487 E − 01	6.14	1.215 E − 09	7.580 E − 01	5.65
Head	6.091 E − 10	7.068 E − 01	0.39	1.210 E − 09	7.550 E − 01	0.36
Trunk	5.405 E − 10	6.272 E − 01	0.14	1.103 E − 09	6.885 E − 01	0.14
Legs	5.345 E − 10	6.201 E − 01	0.20	1.076 E − 09	6.717 E − 01	0.18
Total body	5.436 E − 10	6.307 E − 01	0.10	1.103 E − 09	6.882 E − 01	0.10
		10 MeV				
Adrenals	1.808 E − 09	6.769 E − 01	7.22			
Bladder	1.905 E − 09	7.132 E − 01	1.27			
Brain	1.900 E − 09	7.114 E − 01	0.76			
G. I. tract	1.773 E − 09	6.640 E − 01	0.56			
Stomach	1.821 E − 09	6.820 E − 01	1.45			
Small intestine	1.713 E − 09	6.415 E − 01	0.73			
Large intestine						
Upper	1.951 E − 09	7.307 E − 01	1.38			
Lower	1.816 E − 09	6.801 E − 01	1.74			
Heart	1.803 E − 09	6.751 E − 01	1.20			
Kidneys	2.092 E − 09	7.836 E − 01	1.61			
Liver	1.878 E − 09	7.031 E − 01	0.68			
Lungs	1.906 E − 09	7.137 E − 01	0.90			
Pancreas	1.831 E − 09	6.856 E − 01	3.67			

Skeleton	2.075 E − 09	7.771 E − 01	0.26
Skull	1.991 E − 09	7.454 E − 01	0.79
Arm bones	2.558 E − 09	9.579 E − 01	0.65
Spine	1.860 E − 09	6.967 E − 01	0.78
Rib	2.350 E − 09	8.802 E − 01	0.79
Pelvis	2.543 E − 09	9.523 E − 01	0.80
Leg bones	1.826 E − 09	6.838 E − 01	0.45
Red marrow	2.130 E − 09	7.978 E − 01	0.78
Marrow	2.058 E − 09	7.707 E − 01	0.27
Skin	2.607 E − 09	9.763 E − 01	0.48
Spleen	1.846 E − 09	6.912 E − 01	2.17
Testicles	2.493 E − 09	9.335 E − 01	4.08
Thymus	2.148 E − 09	8.043 E − 01	5.35
Thyroid	2.423 E − 09	9.073 E − 01	5.67
Head	2.187 E − 09	8.190 E − 01	0.37
Trunk	2.000 E − 09	7.491 E − 01	0.13
Legs	1.945 E − 09	7.284 E − 01	0.20
Total body	2.000 E − 09	7.491 E − 01	0.10

TABLE 10

Beta-Ray Doses to the Organs and Tissues of the Reference Man

Organs and tissues	Dose					
	rads / beta/cm^2	rads / R	Standard deviation, %	rads / beta/cm^2	rads / R	Standard deviation, %
	200 keV			500 keV		
Adrenals	2.479 E − 15	2.990 E − 08	12.35	2.768 E − 14	5 971 E − 07	13.24
Bladder	5.961 E − 15	7.189 E − 08	2.30	4.569 E − 14	9 856 E − 07	2.45
Brain	3.295 E − 17	3.974 E − 10	15.74	8.455 E − 16	1.824 E − 08	10.62
G. I. tract	4.263 E − 15	5.140 E − 08	1.71	3.298 E − 14	7.113 E − 07	1.69
Stomach	4.121 E − 15	4.970 E − 08	2.80	3.189 E − 14	6.880 E − 07	2.96
Small intestine	3.692 E − 15	4.452 E − 08	1.92	2.947 E − 14	6.356 E − 07	1.96
Large intestine						
Upper	6.058 E − 15	7.306 E − 08	2.35	4.365 E − 14	9.417 E − 07	2.51
Lower	5.265 E − 15	6.349 E − 08	2.72	3.999 E − 14	8.627 E − 07	2.94
Heart	2.001 E − 15	2.414 E − 08	3.22	2.181 E − 14	4.705 E − 07	3.15
Kidneys	5.406 E − 15	6.519 E − 08	2.70	4.006 E − 14	8.641 E − 07	3.12
Liver	3.588 E − 15	4.326 E − 08	1.91	3.044 E − 14	6.567 E − 07	1.90
Lungs	3.263 E − 14	3.935 E − 07	1.65	1.056 E − 13	2.278 E − 06	1.63
Ovaries	2.839 E − 15	3.424 E − 08	16.03	2.498 E − 14	5.388 E − 07	14.10
Pancreas	2.507 E − 15	3.024 E − 08	6.39	2.270 E − 14	4.396 E − 07	7.31
Skeleton	6.589 E − 14	7.946 E − 07	1.36	5.718 E − 13	1.249 E − 05	1.30
Skull	6.498 E − 14	7.836 E − 07	1.52	5.519 E − 13	1.215 E − 05	1.81
Arm bones	8.571 E − 14	1.034 E − 06	1.46	7.609 E − 13	1.705 E − 05	1.68
Spine	2.068 E − 14	2.493 E − 07	1.74	1.960 E − 13	4.228 E − 06	1.61
Rib	2.073 E − 13	2.500 E − 06	1.41	1.732 E − 12	3.772 E − 05	1.36
Pelvis	8.411 E − 14	1.014 E − 06	1.51	7.555 E − 13	1.630 E − 05	1.45

Leg bones	3.478 E − 14	4.194 E − 07	1.42	3.052 E − 13	6.590 E − 06	1.39
Red marrow	7.565 E − 14	9.123 E − 07	1.59	6.612 E − 13	1.438 E − 05	1.53
Marrow	6.389 E − 14	7.705 E − 07	1.36	5.430 E − 13	1.172 E − 05	1.32
Skin	1.425 E − 09	2.237 E − 02	0.06	4.910 E − 09	1.544 E − 01	0.05
Spleen	3.398 E − 15	4.098 E − 08	3.93	2.632 E − 14	5.677 E − 07	4.49
Testicles	1.241 E − 14	1.497 E − 07	4.25	1.738 E − 13	4.709 E − 06	24.97
Thymus	3.199 E − 15	3.858 E − 08	9.87	3.147 E − 14	6.789 E − 07	11.20
Thyroid	9.239 E − 15	1.114 E − 07	5.89	6.391 E − 14	1.379 E − 06	8.80
Uterus	3.979 E − 15	4.798 E − 08	5.39	3.280 E − 14	7.075 E − 07	6.00
Head	7.819 E − 11	1.228 E − 03	0.25	2.687 E − 10	8.443 E − 03	0.20
Trunk	4.645 E − 11	7.291 E − 04	0.10	1.603 E − 10	5.036 E − 03	0.08
Legs	5.643 E − 11	8.859 E − 04	0.13	1.948 E − 10	6.124 E − 03	0.11
Total body	5.195 E − 11	8.156 E − 04	0.06	1.792 E − 10	5.631 E − 03	0.05
		1 MeV			2 MeV	
Adrenals	1.229 E − 13	3.555 E − 06	19.19	6.218 E − 13	2.047 E − 05	15.18
Bladder	2.471 E − 13	7.149 E − 06	2.64	1.604 E − 12	5.939 E − 05	5.24
Brain	1.215 E − 14	3.515 E − 07	6.75	9.767 E − 13	4.576 E − 05	9.21
G. I. tract	1.740 E − 13	5.035 E − 06	1.75	9.100 E − 13	3.040 E − 05	2.10
Stomach	1.786 E − 13	5.167 E − 06	3.30	9.193 E − 13	3.027 E − 05	3.47
Small intestine	1.531 E − 13	4.430 E − 06	2.04	8.153 E − 13	2.750 E − 05	2.82
Large intestine						
Upper	2.394 E − 13	6.925 E − 06	2.81	1.167 E − 12	3.866 E − 05	3.20
Lower	1.973 E − 13	5.709 E − 06	3.51	1.087 E − 12	3.579 E − 05	3.89
Heart	1.325 E − 13	3.834 E − 06	3.12	7.699 E − 13	2.598 E − 05	3.94
Kidneys	1.988 E − 13	5.752 E − 06	3.47	1.206 E − 12	4.295 E − 05	9.74
Liver	1.627 E − 13	4.706 E − 06	2.01	8.831 E − 13	2.912 E − 05	2.14
Lungs	1.669 E − 13	4.829 E − 06	1.81	4.280 E − 13	1.679 E − 05	8.28
Ovaries	1.095 E − 13	3.169 E − 06	26.39	4.627 E − 13	1.523 E − 05	19.22
Pancreas	1.172 E − 13	3.390 E − 06	7.82	7.543 E − 13	2.483 E − 05	9.20

(Table continues on the next page.)

TABLE 10 (Continued)

Organs and tissues	Dose					
	rads / beta/cm^2	rads / R	Standard deviation, %	rads / beta/cm^2	rads / R	Standard deviation, %
Skeleton	1.023 E − 11	4.014 E − 04	0.70	1.364 E − 10	6.646 E − 03	0.35
Skull	1.239 E − 11	4.969 E − 04	1.75	1.894 E − 10	9.246 E − 03	0.89
Arm bones	3.053 E − 11	1.263 E − 03	1.06	4.391 E − 10	2.148 E − 02	0.54
Spine	1.043 E − 12	3.018 E − 05	1.58	1.232 E − 12	4.142 E − 05	2.50
Rib	3.174 E − 11	1.251 E − 03	1.16	4.741 E − 10	2.315 E − 02	0.58
Pelvis	3.757 E − 12	1.087 E − 04	1.45	5.295 E − 12	1.995 E − 04	2.62
Leg bones	1.629 E − 12	4.881 E − 05	1.60	4.362 E − 12	1.896 E − 04	2.57
Red marrow	1.210 E − 11	4.347 E − 04	14.22	1.753 E − 10	7.636 E − 03	13.69
Marrow	2.785 E − 12	8.224 E − 05	1.25	6.516 E − 12	2.605 E − 04	0.68
Skin	1.050 E − 08	4.515 E − 01	0.05	1.726 E − 08	8.494 E − 01	0.06
Spleen	1.548 E − 13	4.478 E − 06	4.88	8.274 E − 13	2.724 E − 05	5.20
Testicles	1.924 E − 11	8.208 E − 04	9.69	3.582 E − 10	1.760 E − 02	4.04
Thymus	1.384 E − 13	4.003 E − 06	12.51	1.094 E − 12	3.602 E − 05	11.78
Thyroid	3.259 E − 13	9.427 E − 06	9.61	1.770 E − 12	5.826 E − 05	11.02
Uterus	1.773 E − 13	5.130 E − 06	6.45	8.514 E − 13	2.803 E − 05	8.33
Head	6.110 E − 10	2.625 E − 02	0.20	1.366 E − 09	6.716 E − 02	0.19
Trunk	3.676 E − 10	1.579 E − 02	0.08	8.218 E − 10	4.040 E − 02	0.08
Legs	4.478 E − 10	1.924 E − 02	0.10	1.006 E − 09	4.947 E − 02	0.11
Total body	4.110 E − 10	1.766 E − 02	0.05	9.202 E − 10	4.526 E − 02	0.05
		3 MeV			4 MeV	
Adrenals	3.060 E − 12	1.174 E − 04	16.94	2.965 E − 11	1.380 E − 03	22.47
Bladder	1.171 E − 11	5.387 E − 04	6.16	5.157 E − 11	2.460 E − 03	3.88
Brain	1.806 E − 11	8.912 E − 04	3.09	7.875 E − 11	3.861 E − 03	1.90

G. I. tract	3.933 E − 12	1.609 E − 04	3.52	1.547 E − 11	6.990 E − 04	2.65
Stomach	3.552 E − 12	1.378 E − 04	7.37	1.540 E − 11	6.891 E − 04	6.36
Small intestine	3.985 E − 12	1.678 E − 04	4.71	1.338 E − 11	6.033 E − 04	3.43
Large intestine						
Upper	4.868 E − 12	1.982 E − 04	7.62	2.826 E − 11	1.309 E − 03	5.25
Lower	2.748 E − 12	9.517 E − 05	4.42	9.120 E − 12	3.785 E − 04	9.10
Heart	3.507 E − 12	1.409 E − 04	8.01	1.420 E − 11	6.407 E − 04	6.51
Kidneys	8.738 E − 12	3.937 E − 04	7.56	6.371 E − 11	3.059 E − 03	4.61
Liver	4.358 E − 12	1.806 E − 04	4.72	2.161 E − 11	9.988 E − 04	2.89
Lungs	7.115 E − 12	3.487 E − 04	5.37	3.909 E − 11	1.920 E − 03	3.02
Ovaries	1.500 E − 12	4.995 E − 05	23.40	2.482 E − 12	8.175 E − 05	25.17
Pancreas	1.770 E − 12	5.893 E − 05	8.85	3.633 E − 12	1.196 E − 04	10.33
Skeleton	4.052 E − 10	2.002 E − 02	0.27	7.622 E − 10	3.725 E − 02	0.24
Skull	5.900 E − 10	2.919 E − 02	0.65	1.092 E − 09	5.345 E − 02	0.58
Arm bones	1.282 E − 09	6.349 E − 02	0.42	2.379 E − 09	1.165 E − 01	0.38
Spine	3.815 E − 12	1.498 E − 04	4.05	1.507 E − 11	6.745 E − 04	3.21
Rib	1.373 E − 09	6.794 E − 02	0.44	2.512 E − 09	1.230 E − 01	0.39
Pelvis	3.040 E − 11	1.389 E − 03	2.51	1.036 E − 10	4.888 E − 03	1.79
Leg bones	1.869 E − 11	8.789 E − 04	1.73	5.546 E − 11	2.641 E − 03	1.20
Red marrow	5.219 E − 10	2.303 E − 02	7.22	9.819 E − 10	4.288 E − 02	5.08
Marrow	3.422 E − 10	1.690 E − 02	0.27	6.805 E − 11	3.055 E − 03	0.34
Skin	2.109 E − 08	1.051 E 00	0.07	2.376 E − 08	1.171 E 00	0.08
Spleen	2.648 E − 12	9.593 E − 05	8.53	7.196 E − 12	2.926 E − 04	15.30
Testicles	1.040 E − 09	5.178 E − 02	2.96	1.881 E − 09	9.262 E − 02	2.74
Thymus	2.839 E − 12	9.455 E − 05	12.94	1.660 E − 11	7.465 E − 04	29.58
Thyroid	1.075 E − 11	4.869 E − 04	14.47	1.416 E − 10	6.855 E − 03	10.42
Uterus	2.191 E − 12	7.297 E − 05	8.80	3.368 E − 12	1.109 E − 04	9.68
Head	2.150 E − 09	1.071 E − 01	0.19	2.940 E − 09	1.448 E − 01	0.19
Trunk	1.305 E − 09	6.496 E − 02	0.08	1.803 E − 09	8.878 E − 02	0.08
Legs	1.605 E − 09	7.995 E − 02	0.10	2.227 E − 09	1.097 E − 01	0.10
Total body	1.462 E − 09	7.279 E − 02	0.05	2.021 E − 09	9.954 E − 02	0.05

(Table continues on the next page.)

TABLE 10 (Continued)

Organs and tissues	Dose					
	rads / beta/cm^2	rads / R	Standard deviation, %	rads / beta/cm^2	rads / R	Standard deviation, %
	5 MeV					
Adrenals	1.050 E − 10	4.977 E − 03	12.00			
Bladder	1.124 E − 10	5.333 E − 03	3.01			
Brain	2.081 E − 10	1.006 E − 02	1.32			
G. I. tract	4.600 E − 11	2.132 E − 03	1.98			
Stomach	5.423 E − 11	2.522 E − 03	4.82			
Small intestine	3.662 E − 11	1.689 E − 03	2.68			
Large intestine						
Upper	8.128 E − 11	3.823 E − 03	3.68			
Lower	3.840 E − 11	1.742 E − 03	6.46			
Heart	4.030 E − 11	1.860 E − 03	4.40			
Kidneys	1.793 E − 10	8.579 E − 03	3.03			
Liver	6.707 E − 11	3.151 E − 03	1.98			
Lungs	1.142 E − 10	5.535 E − 03	2.01			
Ovaries	3.275 E − 12	1.062 E − 04	33.62			
Pancreas	5.141 E − 12	1.666 E − 04	10.64			
Skeleton	1.181 E − 09	5.678 E − 02	0.21			
Skull	1.746 E − 09	8.405 E − 02	0.51			
Arm bones	3.666 E − 09	1.765 E − 01	0.34			
Spine	4.266 E − 11	1.968 E − 03	2.31			
Rib	3.667 E − 09	1.767 E − 01	0.35			
Pelvis	2.174 E − 10	1.024 E − 02	1.42			
Leg bones	1.131 E − 10	5.347 E − 03	0.96			

Red marrow	1.502 E − 09	6.455 E − 02	3.94
Marrow	1.343 E − 10	6.033 E − 03	0.29
Skin	2.571 E − 08	1.248 E 00	0.08
Spleen	4.392 E − 11	2.025 E − 03	8.07
Testicles	2.922 E − 09	1.417 E − 01	2.39
Thymus	2.350 E − 11	1.018 E − 03	13.92
Thyroid	5.142 E − 10	2.482 E − 02	6.51
Uterus	5.952 E − 12	1.948 E − 04	9.28
Head	3.744 E − 09	1.815 E − 01	0.19
Trunk	2.309 E − 09	1.119 E − 01	0.07
Legs	2.826 E − 09	1.371 E − 01	0.10
Total body	2.578 E − 09	1.250 E − 01	0.05

TABLE 11

Beta-Ray Dose to the Skin and Eyes

End-point energy, MeV	Dose, rads/R				
	Skin surface	Depth of 4 mg/cm^2	Depth of 8 mg/cm^2	Depth of 40 mg/cm^2	Eyes
0.1	0.738	0.040	0.002	0	0
0.2	0.738	0.315	0.136	0	0
0.3	0.719	0.477	0.317	0.012	0
0.4	0.711	0.554	0.432	0.059	0
0.5	0.704	0.593	0.499	0.127	0
0.6	0.696	0.613	0.540	0.195	0
0.7	0.689	0.624	0.565	0.255	0
0.8	0.682	0.629	0.581	0.305	0
0.9	0.675	0.632	0.590	0.345	0
1.0	0.669	0.632	0.597	0.377	0.001
1.1	0.663	0.631	0.600	0.403	0.001
1.2	0.657	0.629	0.602	0.423	0.003
1.3	0.651	0.626	0.602	0.440	0.005
1.4	0.646	0.623	0.602	0.454	0.008
1.5	0.640	0.620	0.601	0.465	0.012
1.6	0.635	0.617	0.599	0.474	0.016
1.7	0.631	0.614	0.597	0.481	0.021
1.8	0.626	0.610	0.595	0.487	0.027
1.9	0.621	0.607	0.593	0.492	0.033
2.0	0.617	0.604	0.591	0.496	0.040
2.1	0.613	0.601	0.588	0.499	0.047
2.2	0.609	0.597	0.586	0.502	0.054
2.3	0.605	0.594	0.583	0.504	0.061
2.4	0.602	0.591	0.581	0.506	0.068
2.5	0.598	0.588	0.579	0.507	0.076
2.6	0.595	0.585	0.576	0.508	0.081
2.7	0.591	0.583	0.574	0.509	0.090
2.8	0.588	0.580	0.571	0.509	0.097
2.9	0.585	0.577	0.569	0.510	0.104
3.0	0.582	0.575	0.567	0.510	0.111
3.1	0.579	0.572	0.565	0.510	0.118
3.2	0.577	0.570	0.563	0.510	0.124
3.3	0.574	0.567	0.560	0.510	0.131
3.4	0.571	0.565	0.558	0.510	0.137
3.5	0.569	0.563	0.556	0.509	0.143
3.6	0.566	0.561	0.554	0.509	0.149
3.7	0.564	0.558	0.552	0.509	0.159
3.8	0.562	0.557	0.551	0.508	0.158
3.9	0.560	0.554	0.549	0.508	0.165
4.0	0.557	0.552	0.547	0.507	0.170
4.2	0.553	0.548	0.544	0.506	0.181
4.4	0.550	0.545	0.540	0.505	0.189
4.6	0.546	0.541	0.537	0.503	0.198
4.8	0.542	0.538	0.534	0.502	0.206
5.0	0.539	0.535	0.531	0.500	0.214

TABLE 12

Dose Rate to the Basal Layers of the Skin Uniformly Contaminated with a Beta-Emitting Isotope

End-point energy of beta emitter, MeV	Dose rate to skin, rads day^{-1} μCi^{-1} cm^{-2}		
	Depth of 4 mg/cm^2	Depth of 8 mg/cm^2	Depth of 40 mg/cm^2
0.1	22		
0.2	104	43	
0.3	136	80	3
0.4	148	99	10
0.5	155	110	20
0.6	161	117	29
0.8	171	128	44
1.0	178	137	54
1.5	187	155	72
2.0	192	167	84
2.5	196	176	95
3.0	200	182	105
3.5	203	188	114
4.0	205	191	123
4.5	208	196	130
5.0	210	199	137

Since the calculations of the preceding section show some energy dependence of the organ and tissue dose response, assurance is needed that the photon spectra indoors and out are similar. In Figs. 6 to 8, the differential photon spectra 1 m above the soil per picocurie per gram of radioactivity in the soil are compared with the photon spectra per picocurie per gram in the walls at the center of a room 4 m square and 2.8 m high. The walls are of masonry, 20 cm thick and uniformly radioactive. The outdoor calculations were multiplied by 2 to put them on the same footing with the 4 π indoor source. These calculations were carried out using Koblinger's (1976) REBEL-II code. The spectra are essentially identical. There is slightly more scattering in the outdoors case, due to the overarching infinite air reflector. This, of course, does not come close to exhausting all the possibilities, but it does indicate that there is no reason to expect large departures from the dose-to-exposure ratios calculated on the basis of Beck's (1975) spectrum shown in Fig. 2.

The beta-ray ionization attenuates rapidly with distance from the source (Fig. 1), amounting to 1.1 I at 1 m, or about one-fourth the

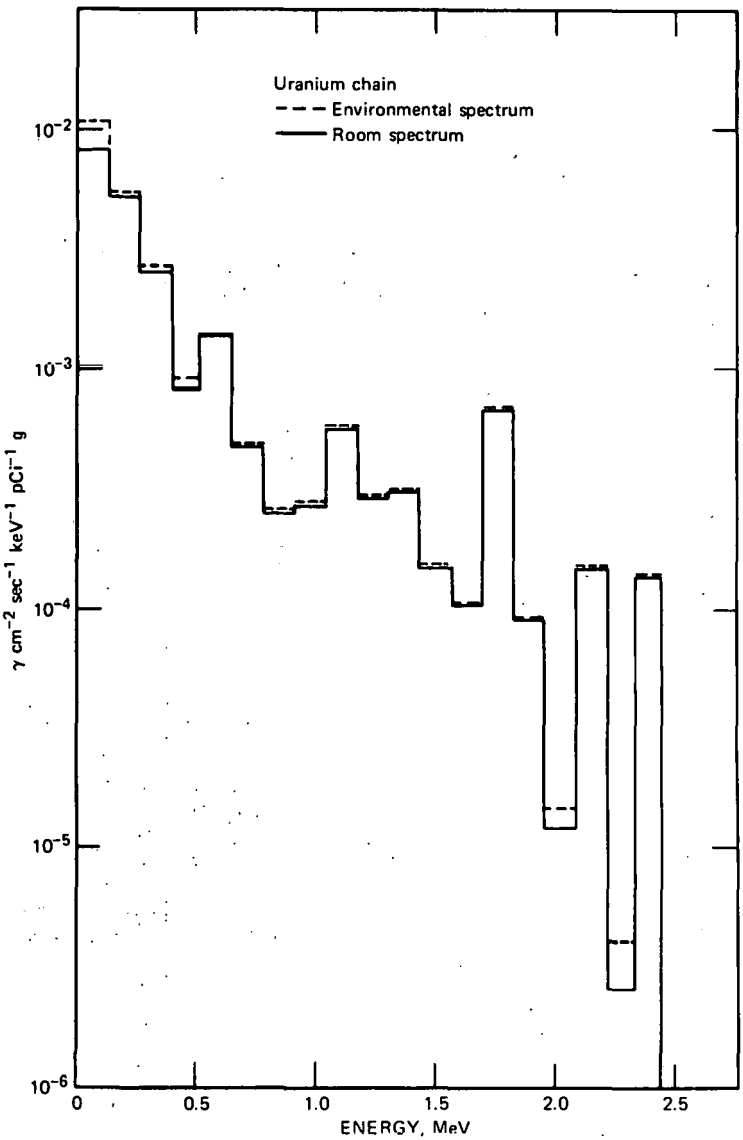


Fig. 6 Energy spectrum of environmental gamma radiation and gamma radiation in a room of masonry construction from the uranium chain.

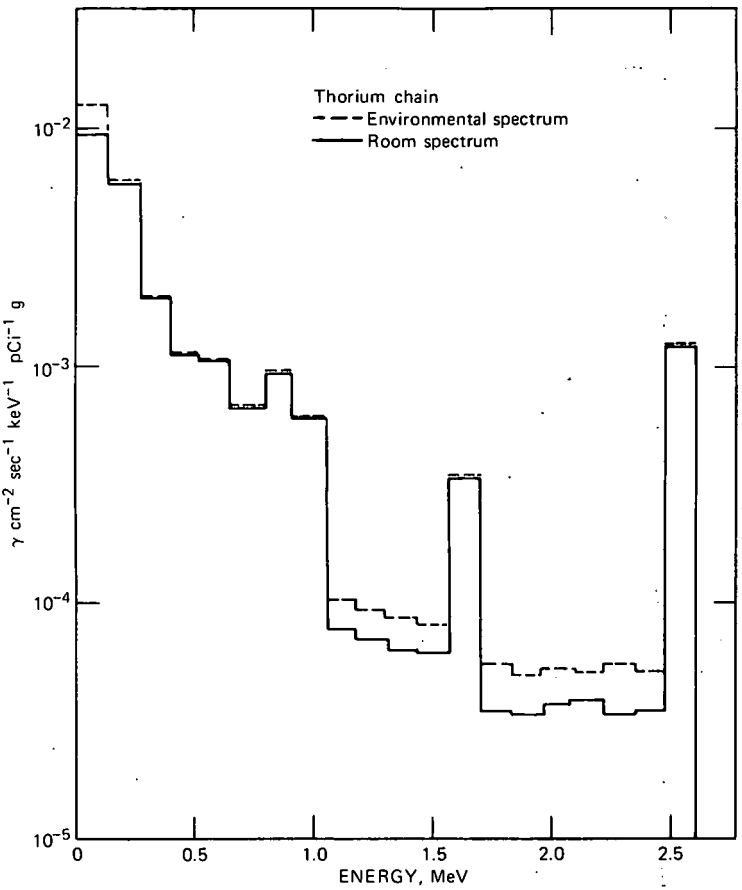


Fig. 7 Energy spectrum of environmental gamma radiation and gamma radiation in a room of masonry construction from the thorium chain.

gamma-ray ionization. It is nearly the same as the gamma-ray exposure at the source surface. It is uncertain what mean value should be assigned the beta-ray exposure. In this paper it will be arbitrarily assumed to be one-fourth the gamma-ray exposure, or 14 mR/year. The reduction will be assumed to represent attenuation due both to clothing and to some mean separation of the human body from the radioactive surfaces during the course of the year. The exposure will also be assumed to be uniform over the body for simplicity's sake and in the absence of quantitative human beta-ray exposure data.

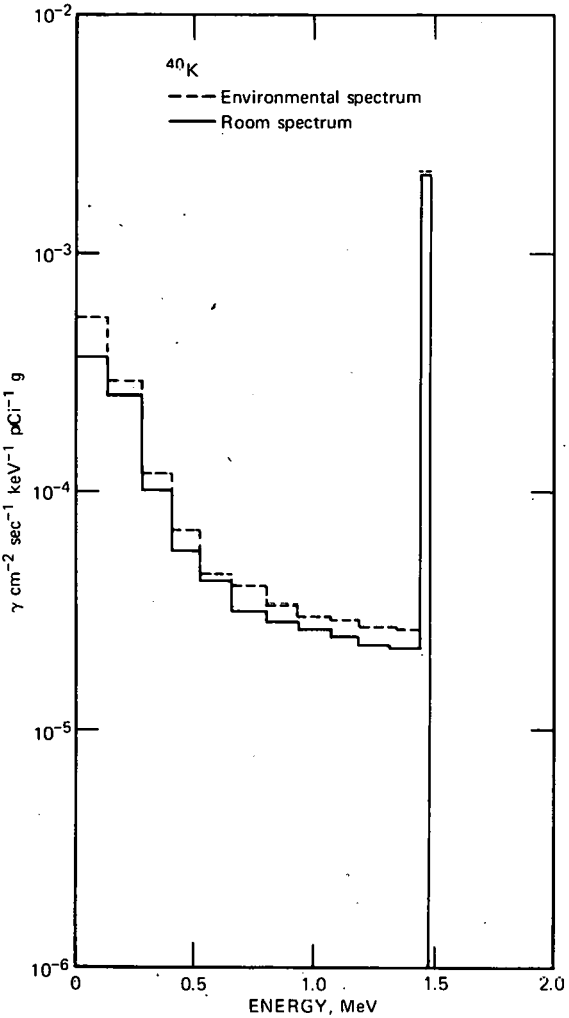


Fig. 8 Energy spectrum of environmental gamma radiation and gamma radiation in a room of masonry construction from ^{40}K.

HUMAN DOSE FROM THE RADIATION BACKGROUND

The gamma-ray doses of Tables 7 and 8 were convoluted with the exposure spectrum of Fig. 2 and multiplied by the mean annual exposure to yield mean doses per roentgen and the mean annual doses shown in Table 13. Similarly, the beta-ray doses of Table 9 were summed over the doses of Table 2 to yield the mean annual doses of Table 14.

Self-shielding results in gamma-ray doses that are about 60% of the exposure. Skin doses from beta irradiation are of the same order of magnitude, but the beta-ray doses to the deeper organs are orders of magnitude lower.

The uncertainty in the rads-per-roentgen ratios in Table 13 are estimated to be of the order of 10%. The uncertainty in the estimate of the mean annual exposure is much larger and may be as large as 50%, owing principally to uncertainties in the estimate of the mean annual exposure indoors as reflected in the housing factor.

The annual dose to the female breast, based on a conversion of 0.7 rad/R, should be about 40 mrads.

The rads-per-roentgen ratios in Table 14 have larger uncertainties than those in Table 13, particularly for the deeper organs. The energy response, as can be seen by examining Table 9, is not as flat. The dose response for the deeper organs may vary by a factor of 2 from contact with the source to a separation of 1.5 m per unit of exposure. And indeed it is quite difficult to account for the effect of clothing. This has only been done here to the extent of assuming a 1 m separation between source and body (in other words, an absorption layer of about 120 mg/cm^2). Since the mean exposure is hardly known, the mean annual doses can only be taken as order-of-magnitude estimates.

THE DOSE EQUIVALENT

In evaluating the somatic effect of sources of radiation exposure to the general population, recourse is often made to such concepts as "per capita dose" and "person rems" or "man rems." The dosimetry on which these concepts rely for quantitative expression is often extremely crude and inconsistent, and little consideration is given as to how doses to different regions of tissue or to different organs might be summed.

Recognizing these difficulties, Jacobi (1975) has formulated an effective somatic dose or dose equivalent. He assumed a linear dose—risk relation and the absence of interference among exposed organs and showed that these assumptions lead to a system of weighted doses to various human organs and tissues. The combined dose, D_{eff}, is the sum of the weighted organ doses yielding the same detriment as the total body dose of the same magnitude. The dose equivalent is

$$D_{eff} = \sum_i \beta_i D_i$$

TABLE 13

Doses Delivered to Human Organs and Tissues by Environmental Gamma Rays

Organs and tissues	Female			Male			Mean human dose		
	rad/R	mrads/year	% S.D.*	rad/R	mrads/year	% S.D.*	rad/R	mrads/year	% S.D.*
Adrenals	0.600	32	2.6	0.517	28	2.6	0.558	30	1.9
Bladder	0.560	30	0.5	0.510	28	0.5	0.535	29	0.4
Brain	0.599	32	0.3	0.572	31	0.3	0.586	32	0.3
G. I. tract	0.531	29	0.2	0.485	26	0.2	0.503	27	0.1
Stomach	0.537	29	0.5	0.500	27	0.6	0.513	28	0.4
Small intestine	0.514	28	0.3	0.466	25	0.3	0.490	26	0.2
Large intestine									
Upper	0.581	31	0.5	0.537	29	0.5	0.559	30	0.4
Lower	0.553	30	0.6	0.499	27	0.6	0.525	28	0.4
Heart	0.556	30	0.4	0.506	27	0.5	0.531	29	0.3
Kidneys	0.589	32	0.6	0.540	29	0.3	0.564	30	0.2
Lens of eye	0.836	45	0.2	0.803	43	0.2	0.820	44	0.1
Liver	0.558	30	0.3	0.511	28	0.3	0.534	29	0.2
Lungs	0.577	31	0.3	0.538	29	0.3	0.558	30	0.2
Ovaries	0.502	27	3.8				0.502	27	3.8
Pancreas	0.491	27	1.4	0.447	24	1.4	0.469	25	1.0

Skeleton	0.608	33	0.1	0.568	31	0.1	0.588	32	0.1
Skull	0.610	33	0.3	0.585	32	0.3	0.598	32	0.1
Arm bones	0.765	41	0.3	0.725	39	0.3	0.745	40	0.2
Spine	0.536	29	0.3	0.487	26	0.3	0.512	28	0.2
Rib	0.684	37	0.3	0.647	35	0.3	0.666	36	0.2
Pelvis	0.731	39	0.3	0.675	36	0.3	0.705	38	0.2
Leg bones	0.533	29	0.2	0.492	27	0.2	0.512	28	0.1
Red marrow	0.619	33	0.3	0.574	31	0.1	0.596	32	0.3
Total marrow	0.602	32	0.1	0.559	30	0.1	0.586	32	0.1
Skin	0.836	45	0.2	0.803	43	0.2	0.820	44	0.1
Spleen	0.540	29	0.8	0.491	27	0.8	0.516	29	0.6
Testes				0.705	38	1.5	0.705	38	1.5
Thymus	0.619	33	2.0	0.560	30	2.0	0.590	32	1.4
Thyroid	0.650	35	2.2	0.663	36	2.1	0.656	35	1.5
Uterus	0.504	27	1.0				0.504	27	1.0
Head	0.690	37	0.1	0.655	35	0.1	0.672	36	0.1
Trunk	0.604	33	0.1	0.563	30	0.1	0.584	32	0.1
Legs	0.600	32	0.1	0.564	30	0.1	0.582	31	0.1
Total body	0.609	33	0.04	0.570	31	0.04	0.590	32	0.03

*% S.D. = percent batch standard deviation of the Monte Carlo calculations.

TABLE 14

Dose Delivered to Human Organs and Tissues by Environmental Beta Rays

Organs and tissues	Dose	
	rads/R	mrads/year
Adrenals	3.00×10^{-5}	0.0004
Bladder	7.89×10^{-5}	0.0011
Brain	9.61×10^{-5}	0.0014
G. I. tract	3.21×10^{-5}	0.0004
Stomach	3.11×10^{-5}	0.0004
Small intestine	3.00×10^{-5}	0.0004
Large intestine		
Upper	4.39×10^{-5}	0.0006
Lower	2.90×10^{-5}	0.0004
Heart	2.79×10^{-5}	0.0004
Kidneys	6.82×10^{-5}	0.0010
Lens of eye	2.32×10^{-2}	0.325
Liver	3.51×10^{-5}	0.0005
Lungs	4.36×10^{-5}	0.0006
Ovaries	1.35×10^{-5}	0.0002
Pancreas	1.84×10^{-5}	0.0003
Skeleton	3.48×10^{-3}	0.0487
Skull	4.90×10^{-3}	0.0686
Arm bones	1.11×10^{-2}	0.155
Spine	4.82×10^{-5}	0.0007
Rib	1.19×10^{-2}	0.166
Pelvis	2.53×10^{-4}	0.0035
Leg bones	1.58×10^{-4}	0.0022
Red marrow	4.46×10^{-3}	0.0624
Total marrow	1.19×10^{-3}	0.0166
Skin	0.453	6.34
Surface	0.637	8.92
Depth of 4 mg/cm^2	0.616	8.62
Depth of 8 mg/cm^2	0.596	8.34
Depth of 40 mg/cm^2	0.459	6.42
Spleen	2.39×10^{-5}	0.0003
Testes	8.91×10^{-3}	0.125
Thymus	3.12×10^{-5}	0.0004
Thyroid	1.12×10^{-4}	0.0016
Uterus	2.18×10^{-5}	0.0003
Head	3.40×10^{-2}	0.484
Trunk	2.08×10^{-2}	0.292
Legs	2.55×10^{-2}	0.357
Total body	2.33×10^{-2}	0.327

TABLE 15

Weighting Factors for Evaluating Effective Somatic Dose

Organs and tissues	Weighting factor (β_i)
Red marrow, Lungs, G. I. tract	0.2
Skeleton, Kidney, Liver, Reproductive organs	0.06
Thyroid, Eye, Skin	0.02
Total for the rest of the body	0.1

where D_{eff} is the dose equivalent, D_i is the doses to the individual organs and tissues, and β_i is the weighting factors.

The values of the weighting factors are shown in Table 15.

Combining the values of β_i in Table 15 with the doses in Tables 7 to 9 yields D_{eff} for the natural beta and gamma radiation. These are listed in Tables 16 and 17. Since the dose equivalent, D_{eff}, contains the modifying factors β_i and since the rem, unlike the rad, allows for such modifying factors, D_{eff} is expressed in rems.

The mean annual effective somatic dose per capita in the United States is then 31 mrems of gamma radiation and about 0.5 mrem of beta radiation.

REFERENCES

Abbott, J. L., R. L. Berger, and H. A. Sandmeier, 1968, *Computed Neutron Flux at Coaltitude Ranges in Uniform Sea-Level Air*, U. S. Naval Weapons Evaluation Facility Report 1021.

Beck, H. L., 1975, The Physics of Environmental Gamma Radiation Fields, in *The Natural Radiation Environment II*, Vol. 1, Symposium Proceedings, Houston, Tex., Aug. 7—11, 1972, J. A. S. Adams, W. M. Lowder, and T. F. Gesell (Eds.), ERDA Report CONF-720805-P1, pp. 101-133, Rice University and the University of Texas, Houston, NTIS.

Beninson, D. J., A. Bouville, B. J. O'Brien, and J. O. Snihs, 1977, Dosimetric Implications of the Exposure to Natural Sources of Radiation, in *Interna-*

TABLE 16

Fluence to Dose Equivalent Factors and Exposure to Dose Equivalent Factors for Human Whole-Body Gamma-Ray Exposure

Photon energy, MeV	Male		Female		Mean human	
	prems/photon/cm^2	rem/R	prems/photon/cm^2	rem/R	prems/photon/cm^2	rem/R
0.02	4.27	0.0227	7.88	0.0419	6.08	0.0323
0.05	18.7	0.501	21.0	0.562	19.9	0.532
0.10	26.3	0.611	27.1	0.629	26.7	0.620
0.2	49.5	0.501	51.6	0.523	50.5	0.512
0.5	140	0.510	147	0.540	143	0.526
1.0	286	0.558	300	0.586	293	0.572
2	532	0.617	556	0.645	544	0.631
5	1110	0.691	1130	0.703	1120	0.697
10	2040	0.764	2050	0.766	2040	0.765
Environmental		0.561		0.588		0.575

TABLE 17

Exposure to Dose Equivalent Factors for Human Whole-Body Beta-Ray Exposure

Beta end-point energy, MeV	Exposure, rems/R		
	Male	Female	Mean human
0.2	9.77×10^{-4}	9.77×10^{-4}	9.77×10^{-4}
0.5	6.74×10^{-3}	6.74×10^{-3}	6.74×10^{-3}
1.0	2.00×10^{-2}	1.99×10^{-2}	2.00×10^{-2}
2.0	4.15×10^{-2}	4.04×10^{-2}	4.10×10^{-2}
3.0	5.84×10^{-2}	5.53×10^{-2}	5.68×10^{-2}
4.0	7.41×10^{-2}	6.85×10^{-2}	7.13×10^{-2}
5.0	9.00×10^{-2}	8.15×10^{-2}	8.57×10^{-2}
Environmental	3.28×10^{-2}	3.20×10^{-2}	3.24×10^{-2}

tional Symposium on Areas of High Natural Radioactivity, Academia Brasiliera de Ciencias, RJ-1977.

Billings, M. P., and W. R. Yucker, 1974a, Body Mass Distributions for Radiation Dose Analysis, *Trans. Am. Nucl. Soc.*, 19: 396.

——, and W. R. Yucker, 1974b, A Detailed Geometrical Model of the Human Anatomy, McDonnel-Douglas Report WD-2354.

Burke, G. de P., 1975, Thermoluminescent Dosimeter Measurements of the Natural Radiation Environment, in *The Natural Radiation Environment II*, Vol. 1, Symposium Proceedings, Houston, Tex., Aug. 7—11, 1972, J. A. S. Adams, W. M. Lowder, and T. F. Gesell (Eds.), ERDA Report CONF-720805-P1, pp. 305-315, Rice University and the University of Texas, Houston, NTIS.

Ellis, R. E., 1961, The Distribution of Active Bone Marrow in the Adult, *Phys. Med. Biol.*, 5: 255.

Gregg, E. C., 1977, Radiation Risks with Diagnostic X-Rays, *Radiology*, 123: 447.

Hashimoto, M., and K. Yamada, 1964, Distribution of Red Marrow and Its Weight, in *Annual Report of Scientific Research Grants*, 1963, Ministry of Education (Japan), as reported by T. Hashizume, Y. Kato, T. Maruyama, Y. Kumamoto, A. Shiragai, and A. Nishimura, Population Mean Marrow Dose and Lukaemia Significant Dose from Diagnostic Medical X-Ray Examinations in Japan, *Health Phys.*, 23: 845 (1972).

Hastings, C., Jr., 1955, *Approximations for Digital Computers*, Princeton University Press, Princeton, N. J.

Hubbell, J. H., 1969, *Photon Cross Sections, Attenuation Coefficients, and Absorption Coefficients from 10 keV to 100 GeV*, National Bureau of Standards Report NSRDS-NBS-29.

Ikebe, Y., 1970, Evaluation of the Total Ionization in the Lower Atmosphere, *J. Earth Sci.*, 18: 85.

International Commission on Radiological Protection, 1975, *Report of the Task Group on Reference Man*, ICRP Publication No. 23, Pergamon Press, Oxford.

Jacobi, W., 1975, The Concept of the Effective Dose—A Proposal for the Combination of Organ Doses, *Radiat. Environ. Biophys.*, 12: 101.

Koblinger, L., 1971, *Two Codes for Calculations of Dose Distribution in Human Phantoms Irradiated by External Photon Sources*, Report KFKI-71-12, Hungarian Academy of Sciences, Central Research Institute for Physics.

——, undated, *RSIC Computer Code Collection, DISDOS, Two Codes for Calculation of Dose Distribution in Human Phantoms Irradiated by External Photon Sources*, Report CCC-170, Radiation Shielding Information Center.

——, 1976, *REBEL-2: An Adjoint Monte Carlo Code for the Calculation of Radiation in Dwelling Rooms*, Report KFKI-76-65, Hungarian Academy of Sciences, Central Research Institute for Physics.

National Council on Radiation Protection and Measurements, 1975, Natural Background Radiation in the United States, NCRP Report No. 45.

Oakley, D. T., 1972, *Natural Radiation Exposure in the United States*, EPA Report ORP/SID 72-1.

O'Brien, K., S. Samson, R. Sanna, and J. E. McLaughlin, 1964, The Application of "One Group" Transport Theory to β-Ray Dosimetry, *Nucl. Sci. Eng.*, 18: 90.

——, 1974, The Subcutaneous Beta-Ray Dose Rate from Fission Products Deposited on the Skin, *Health Phys.*, 26: 122.

——, 1975, The Cosmic Ray Field at Ground Level, in *The Natural Radiation Environment II*, Vol. 1, Symposium Proceedings, Houston, Tex., Aug. 7—11, 1972, J. A. S. Adams, W. M. Lowder, and T. F. Gesell (Eds.), ERDA Report CONF-720805-P1, pp. 15-54, Rice University and the University of Texas, Houston, NTIS.

Snyder, W. S., M. R. Ford, G. G. Warner, and H. L. Fisher, Jr., 1969, MIRD Pamphlet No. 5, Estimates of Absorbed Fractions for Monoenergetic Photon Sources Uniformly Distributed in Various Organs of a Heterogeneous Phantom, *J. Nucl. Med.* (Suppl.), 10: 3.

Whitton, J. T., 1973, New Values for Epidermal Thickness and Their Importance, *Health Phys.*, 24: 1.

Exhalation of Radon-222 from Building Materials and Walls

NIELS JONASSEN and J. P. McLAUGHLIN*
Technical University of Denmark, Lyngby, Denmark, and University College, Dublin, Ireland

ABSTRACT

On the basis of a linear diffusion model, the porosity, length of diffusion, and radon production rate can be found for a given material by placing a sample of the material in a closed vessel and following the buildup of activity at various (constant) pressures. The model was tested on an alum-shale lightweight concrete (with a radium content of approximately 5 pg/g). The exhalation rate of radon from a series of building materials was determined by placing the materials in a closed vessel and measuring the equilibrium activity. The model predicts that the exhalation rate derived from the equilibrium activities will be lower than the values corresponding to exhalation into an infinite space. The difference depends upon the geometry of samples and vessels used, and the values may vary from a few up to maybe 20%. The model was finally used to determine the effective diffusion coefficient of radon in a concrete wall by measuring the radon concentration in the pore air at various depths.

When building materials with a high radium concentration are being used, the radon progeny in ordinary buildings may increase the radiation exposure of the public to unacceptable levels. In predicting these levels it is useful to know the radon exhalation properties of the building materials used. These properties can be studied by enclosing a sample of the material in a closed vessel and following the growth of activity in the vessel by analysis of air samples for radon content.

The procedure of placing materials in closed containers and studying the growth of activity with time somewhat resembles

*The work was done during a stay in Denmark.

methods for determining the exhalation of radon from soils whereby the usual procedure is to study the buildup of activity in a shallow can sealed onto the soil (Kraner, Schroeder, and Evans, 1964; Wilkening, 1974; Wilkening, Stanley, and Clements, 1975).

Because of the high porosity of most soils, the concentration of radon in such a can sealed onto the soil will in a matter of hours be comparable to the concentration in the pores of the soil. In this situation, owing to back diffusion of radon from the container into the soil, the net radon feed from the pores will progressively become smaller. This makes the rate of increase in activity in the can lower than should be expected from the simple law of radioactive growth from a constant source. Consequently growth times of less than 1 hr are normally used in such soil exhalation studies.

In materials such as concrete, bricks, etc., the exhalation rate will often be so small that growth times of several days are necessary to obtain activities in the container large enough to be measured with a reasonable accuracy. If, however, the low exhalation rate is primarily caused by a low porosity, then the concentration of radon in the container may still after several days be only a small fraction of the concentration in the pore air and the deviation from the constant feed growth may still be insignificant.

RADON DIFFUSION MODEL

To examine this problem let us consider a slab of material in a vessel with a dead space V_d (Fig. 1). The slab has a thickness 2L and a cross-sectional area S; it is assumed that the thickness is much smaller than the height or width, thus making the effective radon exhaling area equal to 2S.

The radon diffusion and exhalation are supposed to take place only perpendicular to the surface S and to be symmetrical with respect to a center plane in the material.

The following nomenclature is used:

C	Concentration of radon in the interstitial space of the material
f	Production rate of radon per unit volume of interstitial space
K_e^*	Effective diffusion coefficient of radon in the material
E	Exhalation rate of radon
λ	Decay constant of radon
ϵ	Porosity of material
x	Distance from center plane
V_d	Volume of dead space
V_b	Volume of material, equivalent to 2L x S
l	Diffusion length for radon in the material

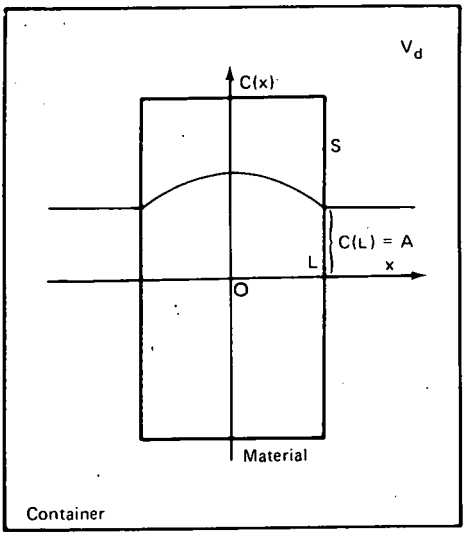


Fig. 1 Sample of radon-exhaling material in closed container at equilibrium conditions.

The diffusion of radon inside the material along the x-axis is governed by the equation

$$\frac{\partial C(x)}{\partial t} = K_e^* \frac{\partial^2 C(x)}{\partial x^2} - \lambda C(x) + f \tag{1}$$

The full time-dependent solution to this equation has been given by Krisiuk et al. (1971). In our study only steady-state situations, where $\partial C(x)/\partial t = 0$, are considered. Equation 1 can then be written as

$$K_e^* \frac{d^2 C(x)}{dx^2} - \lambda C(x) + f = 0 \tag{2}$$

The exhalation rate E is given by

$$-\epsilon K_e^* \frac{dC(x)}{dx}\bigg|_{x=L} = E \tag{3}$$

When the steady state is reached, the concentration in the whole dead space is C(L) and the exhalation equals the decay. This can be written as

$$-\epsilon K_e^* \frac{dC(x)}{dx}\bigg|_{x=L} 2S = C(L) V_d \lambda \tag{4}$$

When the diffusion length l is introduced,

$$l = \left(\frac{K_e^*}{\lambda}\right)^{1/2} \tag{5}$$

and the solution to Eq. 2 can be written as

$$C(x) = B \cosh \frac{x}{l} + C_0 \tag{6}$$

because of symmetry about x = 0.

From the boundary conditions we find

$$C_0 - \frac{f}{\lambda} \tag{7}$$

and

$$B = -\frac{f/\lambda}{\cosh \beta} \left\{\frac{1}{1 + [(\tanh \beta)/\alpha\beta]}\right\} \tag{8}$$

where $\alpha = V_d/\epsilon V_b$ and $\beta = L/l$.
The solution can thus be written as

$$C(x) = \frac{f}{\lambda} \left\{1 - \frac{\cosh (x/l)}{[\cosh \beta + (1/\alpha\beta)(\sinh \beta)]}\right\} \tag{9}$$

If $V_d \gg V_b$, which corresponds to an open vessel, then $\alpha \to \infty$ and the concentration of radon in the material will approach

$$C_0(x) = \frac{f}{\lambda}\left[1 - \frac{\cosh (x/l)}{\cosh \beta}\right] \tag{10}$$

The corresponding "free" exhalation will be

$$E = -\epsilon K_e^* \frac{dC_0(x)}{dx}\bigg|_{x=L} = \epsilon f l \tanh \beta \tag{11}$$

This exhalation value one must expect a material to show when it is used as a building material in a room that is not completely sealed.

We can assume, however, that, if the material is enclosed in a container with radon-free air, the initial exhalation will be equal to E given by Eq. 11 and, therefore, the initial growth rate of the activity in the container will be

$$r = \frac{E\ 2S}{V_d} \tag{12}$$

from which E can be determined. If the material is left in the container, the exhalation rate will slow down until an equilibrium concentration A in the container is reached, which can be found from Eq. 9 by setting x equal to L, as

$$A = \frac{f}{\lambda}\left\{1 - \frac{1}{1 + [(\tanh \beta)/\alpha\beta]}\right\} \tag{13}$$

The corresponding net exhalation rate E′ obtained from Eq. 9 is

$$E' = \frac{\lambda A V_d}{2S} = \left\{\frac{\epsilon l f (\tanh \beta)}{1 + [(\tanh \beta)/\alpha\beta]}\right\} \tag{14}$$

or

$$E' = E\left\{\frac{1}{1 + [(\tanh \beta)/\alpha\beta]}\right\} \tag{15}$$

Equations 11 to 13 yield

$$f = \frac{\lambda A r}{r - \lambda A} \tag{16}$$

and

$$\frac{\tanh \beta}{\alpha\beta} = \frac{r}{\lambda A} - 1 \tag{17}$$

or

$$\frac{2S\epsilon l \tanh (L/l)}{V_d} = \frac{r}{\lambda A} - 1 = \frac{\lambda A}{f - \lambda A} \tag{18}$$

A determination of r and A will thus give the free exhalation rate E as well as the production rate f. Also, some information of the porosity ϵ and diffusion length l is obtained in this manner, as appears from Eq. 18, but it is not possible to separate the two quantities. As now shown, however, a separate determination of ϵ and l can be obtained from a consideration of the dependence of diffusion on pressure.

Whereas the production rate f is assumed to be constant independently of the pressure p, the diffusion length l can be written

$$l = k\left[\frac{1}{(p)^{1/2}}\right] \tag{19}$$

where k is a constant.

Let us assume that the equilibrium activities A_1 and A_2 are measured at two (constant) pressures p_1 and p_2 and that f has also been determined, then

$$\epsilon\left[\frac{k}{(p_1)^{1/2}}\right]\tanh\left[\frac{L(p_1)^{1/2}}{k}\right]=\left(\frac{V_d}{2}\right)\left(\frac{\lambda A_1}{f-\lambda A_1}\right) \tag{20}$$

and

$$\epsilon\left[\frac{k}{(p_2)^{1/2}}\right]\tanh\left[\frac{L(p_2)^{1/2}}{k}\right]=\left(\frac{V_d}{2}\right)\left(\frac{\lambda A_2}{f-\lambda A_2}\right) \tag{21}$$

From Eqs. 20 and 21, ϵ and k (and thus l) can be found.

EXPERIMENTAL RESULTS

Two types of containers were used for the exhalation studies. One is a heavy cast-iron pressure chamber able to stand pressures from approximately zero to 2.5 atm. The internal volume is 200 liters. The other type is a simple sheet-metal barrel with an internal volume of approximately 120 liters.

For testing the formulas developed above, an experiment was made using 6 slabs of an alum-shale lightweight concrete. The dimensions of the slabs were 0.50 by 0.25 by 0.10 m, which yield a thickness (2L) of 0.10 m, a surface area (2S) of 1.5 m^2, and a volume of material (V_b) of 75 liters.

The slabs were placed in the pressure chamber with a V_d of 125 liters. The pressure chamber was left open for 10 days to allow the exhalation rate to reach its free value given by Eq. 11.

The chamber was then closed and the growth rate r_1 was measured at the approximate atmospheric pressure p_1. The radon measurements were performed by filling 100-cm^3 scintillation flasks and counting their activity in a standard manner (Jonassen and McLaughlin, 1976). Each sample was counted for 10 or 20 min. which usually involved 3000 to 5000 counts.

When equilibrium was reached, the concentration A_1 in the chamber was determined. The pressure was then changed to p_2, and the new equilibrium concentration A_2 was determined after several weeks.

This procedure was repeated at a pressure p_3 which yielded the concentration A_3. The following results were found:

—At p_1 = 745 mm Hg, A_1 = 692 pCi/liter ± 0.4% (31 measurements)

r_1 = 5.96 pCi $liter^{-1}$ hr^{-1} ± 1.5%

—At p_2 = 495 mm Hg, A_2 = 718 pCi/liter ± 1% (7 measurements)
—At p_3 = 1027 mm Hg, A_3 = 647 pCi/liter ± 1.2% (9 measurements)

By introducing A_1 and r_1 in Eq. 16, we obtain

$$f = 42.52 \text{ pCi liter}^{-1} \text{ hr}^{-1} = 2.08 \times 10^5 \text{ atoms m}^{-3} \text{ sec}^{-1}$$

From Eqs. 20 and 21, we find

$$k = 2.05 \text{ m} \times (\text{mm Hg})^{1/2} \tag{22}$$

and from Eq. 19

$$l = 7.51 \times 10^{-2} \text{ m at p} = 745 \text{ mm Hg}$$
$$(l = 7.44 \times 10^{-2} \text{ m at p} = 760 \text{ mm Hg})$$

A value for ϵ (the porosity) can now be obtained from Eq. 18

$$\epsilon = \left(\frac{r_1}{\lambda A_1} - 1\right)\left[\frac{V_d}{2Sl_1 \tanh (L/l_1)}\right] \tag{23}$$

From the experimental data the porosity is obtained as

$$\epsilon = 0.265 \tag{24}$$

The diffusion length l_3, corresponding to p_3 = 1027 mm Hg, is

$$l_3 = 6.40 \times 10^{-2} \text{ m} \tag{25}$$

If this is introduced in Eq. 13 with the values for ϵ and f determined above, the expected equilibrium concentration A_{3e} is found as

$$A_{3e} = 1.16 \times 10^{10} \text{ atoms/m}^3 = 661 \text{ pCi/liter} \tag{26}$$

whereas the measured value was 647 pCi/liter.

The effective diffusion coefficient K_e^* is found as $K_e^* = 1.16 \times 10^{-8}$ m^2/sec = 1.16×10^{-4} cm^2/sec for p = 760 mm Hg.

The free exhalation rate can be found from Eq. 11 to be

$$E = 2400 \text{ atoms m}^{-2} \text{ sec}^{-1} = 0.136 \text{ pCi m}^{-2} \text{ sec}^{-1} \tag{27}$$

It should be emphasized that this value is probably too high since the area of the edges is quite comparable to the area 2S of the sides of the slabs.

The net exhalation rate E′ is found from Eq. 15 as

$$E' \simeq 2100 \text{ atoms m}^{-2} \text{ sec}^{-1} = 0.119 \text{ pCi m}^{-2} \text{ sec}^{-1} \quad (28)$$

The relative difference between the two exhalation values can be written

$$\frac{\Delta E}{E} = \frac{E - E'}{E} = \frac{1}{1 + (\alpha\beta/\tanh \beta)} = \frac{1}{1 + (V_d\beta/V_b\epsilon \tanh \beta)} \quad (29)$$

Only in cases where this quantity is larger than the uncertainty of measurement is it possible to distinguish between the actual activity growth with a time-variable exhalation rate and the simple theoretical growth curve corresponding to a constant radon feed.

To show this, we placed four blocks of granitic concrete with a volume of 32 liters in the pressure chamber, which left a dead space V_d of 168 liters.

If the diffusion length l and porosity ϵ of this material have approximately the same values as the ones determined above, then with L = 10 cm, Eq. 29 gives

$$\frac{\Delta E}{E} = 3.6\% \quad (30)$$

In Fig. 2 are shown the activities as a function of time. Each corresponds to a counting time of usually 30 min., and the relative standard deviation on the points due to the counting statistics varies from 5 to 12%. The full line is given by

$$A = A_0[1 - \exp(-\lambda t)] \quad (31)$$

where the equilibrium concentration A_0 is taken as 28.4 pCi/liter or 5.0×10^5 atoms/liter.

This curve corresponds to a constant feed of radon during the whole growth period equal to

$$\lambda A_0 V_d = 176 \text{ atoms/sec}$$

It appears that the experimental points fall so close to the curve that it is not possible to detect a change in radon feed during the growth period, in accordance with the value of $\Delta E/E$ calculated in Eq. 30.

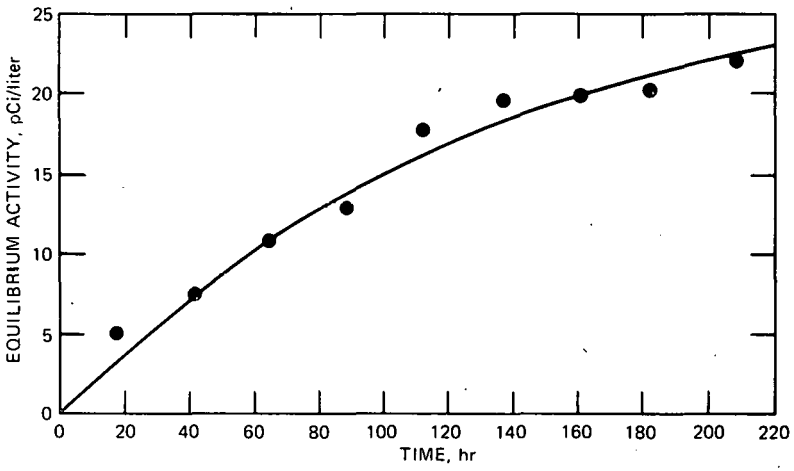


Fig. 2 Concentration of radon as a function of time in pressure chamber with concrete blocks.

If the ratio between dead-space volume and sample volume is large enough, the exhalation of a given material can thus be determined by enclosing the material in a container and following a part of the activity growth curve. From this curve the equilibrium concentration A_0 is calculated assuming a constant exhalation rate E which is then given by

$$E = \frac{\lambda A_0 V_d}{S_0} \tag{32}$$

where S_0 is the total exhaling surface of the sample.

The error on E as given by Eq. 32 is less than 10% if $V_d > 2 \rightarrow 3\, V_b$.

Such measurements were performed on the following materials: ordinary concrete, lightweight concrete, expanded clay concrete, bricks, chipboard, fiberboard, and gypsum board.

In Table 1 are shown the results of the measurements. For each material the volumes of the material and of the dead space are given. The exhalation rate is expressed in number of atoms per second relative to the surface area as well as to the volume and mass of the sample. Finally, the relative error of the exhalation rates is calculated from Eq. 29 under the assumption of $\epsilon \simeq 0.3$ and $\beta \approx 1$. The value of beta may vary by as much as a factor of from 0.5 to 2, which may change the error with a factor of from 1.2 to 0.6.

TABLE 1

Exhalation Rate of Various Building Materials

Material	V_b, liters	V_d, liters	Surface / Volume, m^{-1}	Exhalation rate (E) atoms / m^2 sec	atoms / kg sec	atoms / m^3 sec	$\frac{\Delta E}{E}$, %
1. Ordinary concrete, gravel and sand from the sea, Danish deposits	47.7	152.3	30	167	2.38	5,573	6.7
2. Ordinary concrete, gravel and sand from pits, Danish deposits	47.7	152.3	30	134	1.98	4,453	6.7
3. Ordinary concrete, composition unknown	37.1	163	34	156	2.22	5,319	4.9
4. Ordinary concrete, composition unknown	32.0	168	30	184	2.30	5,514	4.2
5. Lightweight concrete, Swedish origin, alum shale, old type	20.6	179.4	28	4089	210	113,744	2.6
6. Lightweight concrete, Swedish origin, alum shale, new type	75.0	125	32	1436	71.8	45,942	12.0
7. Lightweight concrete, Danish origin, clay based	67.0	133	33	32	1.42	1,066	10.3
8. Lightweight concrete, Danish origin, clay based	32.5	85.5	52	21	1.42	1,102	8.0
9. Expanded clay concrete, LECA	44.6	73.6	35	22	1.19	769	12.2
10. Bricks, solid type	109.8	90.2	67	2.3	0.08	155	21.7
11. Bricks, cavity type	11.4	106.8	161	0.97	0.08	156	2.4
12. Chipboard	63.9	54.1	175	0.34	0.09	60	21.3
13. Fiberboard	63.9	54.1	175	0.53	0.11	92	21.3
14. Gypsum board	71.5	46.5	178	0.61	0.11	108	26.0

It is not possible beforehand to predict which of the exhalation units is appropriate to use in scaling up the results obtained from samples to a room with walls made of the same material.

For two of the materials examined, lightweight concrete (samples 7 and 8) and bricks (samples 10 and 11), however, the exhalation rate was determined twice, using samples with different surface-to-volume ratio. This approach was adopted in an attempt to see how the three exhalation ratios depend on the geometrical configuration of the samples. For the lightweight concrete, this was achieved by slicing the normal-size slabs into smaller ones. For the bricks measurements were performed on two types made of the same material. One type was solid throughout, whereas the second type was of the cavity variety. Although the results are very limited, it seems for these materials and for the geometrical configurations used that the activity per unit mass or per unit volume rather than the activity per unit area remains constant. This behavior is probably closely related to the porosity of the materials and should be investigated more closely for each individual material.

The materials investigated fall into four groups insofar as their radon-exhaling power is concerned.

The two types of alum-shale lightweight concrete (samples 5 and 6) are by far the strongest exhalers, with 210 and 71.8 atoms kg^{-1} sec^{-1} or 4089 and 1436 atoms m^{-2} sec^{-1}, respectively.

The second group consists of the samples 1 to 4 of ordinary concrete with exhalation rates of approximately 2.0 to 2.4 atoms kg^{-1} sec^{-1} or 130 to 180 atoms m^{-2} sec^{-1}. The difference between the results for the samples made from sea deposits and those made from land deposits is hardly significant.

The two clay-based lighter types of concrete (samples 7 and 8) make up the third group and show exhalation rates of 1.2 to 1.4 atoms kg^{-1} sec^{-1} or 20 to 30 atoms m^{-2} sec^{-1}. In the fourth group of very weak exhalers (samples 9 to 14), we find ordinary bricks and the different types of composition board with exhalation rates of from 0.08 to 0.11 atoms kg^{-1} sec^{-1} or from 0.3 to 2.3 atoms m^{-2} sec^{-1}.

RADON MIGRATION THROUGH WALLS

Concretes are inhomogeneous matrices consisting mainly of solid aggregates, cement paste, and porous capillaries. The migration of radon through such media is considered to be best described by the use of an effective diffusion coefficient K_e^*. For a particular concrete, because of the lack of precise knowledge of its micro-

structure, attempts at a computation of K_e^* on a theoretical basis present great difficulties.

Realistic values of K_e^* for the walls in a given basement room can, however, be obtained from a knowledge of the radon concentrations in the pore air at various depths within the walls.

The thickness of the wall is 30 cm. Narrow-bore sampling pipes were carefully sealed with epoxy resin in holes drilled to various depths, ranging from 2 to 15 cm from the surface of the wall. The surface of the wall surrounding each sampling pipe was also sealed with epoxy resin. Pore-air samples were obtained by attaching 1-liter evacuated glass sampling flasks to these pipes. The resistance to such vacuum sucking of the concrete was so great that after a 24-hr period the pressure of air collected by a sampling flask would typically have risen only to approximately 300 mm Hg. This is equivalent to obtaining a sample of pore air at STP of about 400 cm^3. On the basis of leak tests on evacuated sampling flasks connected to solid rods sealed into the walls in the regular manner, we considered that the majority of air obtained in a normal sampling came from wall pores. The air in any sample, however, comes from an undefined volume of wall pores surrounding the inner end of the sampling tube used. It is therefore impossible to assign the radon content of an air sample to the pore air at a precisely known depth within the wall.

In Fig. 3 are shown the concentrations as a function of the distance x from the center of the wall. The full line represents Eq. 10 with $f/\lambda = 575$ pCi/liter and $l = 4 \times 10^{-2}$ m. This corresponds to a value of

$$K_e^* = 3.4 \times 10^{-5} \text{ cm}^2/\text{sec} \tag{33}$$

The production rate f is found as

$$f = 2.12 \times 10^4 \text{ atoms m}^{-3} \text{ sec}^{-1} \tag{34}$$

In a series of measurements reported in the paper following this (J. P. McLaughlin and N. Jonassen, this volume), the average exhalation rate for the walls in question was found to be

$$E = 379 \pm 107 \text{ atoms m}^{-2} \text{ sec}^{-1} \tag{35}$$

This value is taken to be the free exhalation value given by Eq. 11,

$$E = \epsilon f l \tanh \frac{L}{l} \tag{11}$$

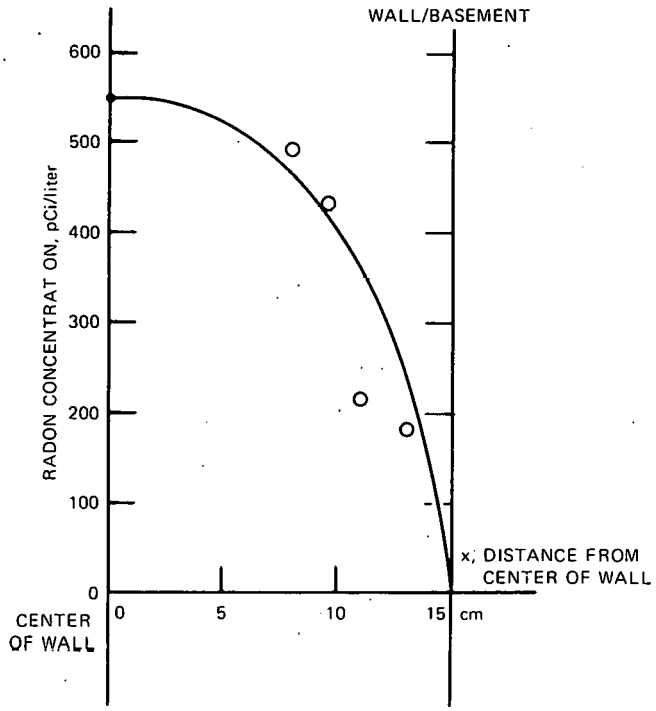


Fig. 3 Radon concentration profile inside concrete wall.

If the numerical values are introduced, we find

$$\epsilon = 0.45$$

with a minimum value of 0.32 and a maximum of 0.57.

The model used for obtaining these values assumes that the radon profile in the wall is symmetrical around the center plane and that the concentration is virtually zero in the air space on either side of the wall. Although this is true at the wall/basement interface, it should be mentioned that high radon concentrations (~600 pCi/liter) have been detected in the soil air at the wall/foundation interface, which may influence the shape of the radon profile in the wall and make the effective half thickness larger, which will increase l and decrease ϵ.

It should be emphasized that the experimental technique used for obtaining the pore-air samples is still rather crude and might involve large uncertainties in the derived values of l, K_e^*, and especially ϵ.

It is of interest, though, to note that the value of $K_e^* = 3.4 \times 10^{-5}$ cm^2/sec is comparable to the value of $K_e^* = 2.5 \times 10^{-5}$ cm^2/sec that Culot, Olson, and Schiager (1976) obtained for concrete by a different experimental approach.

ACKNOWLEDGMENTS

The authors thank Mr. Aa. R. Nielsen for doing the initial work on the diffusion model and for performing part of the experimental work.

This study was supported by grants from the Danish Natural Science Research Council and the Danish Council for Scientific and Industrial Research.

REFERENCES

Culot, M. V. J., H. G. Olson, and K. J. Schiager, 1976, Effective Diffusion Coefficient of Radon in Concrete: Theory and Method for Field Measurements, *Health Phys.*, 30: 263-270.

Jonassen, N., and J. P. McLaughlin, 1976, *Radon in Indoor Air I*, Research Report 6, Laboratory of Applied Physics I, Technical University of Denmark, Lyngby, Denmark.

Kraner, H. W., G. L. Schroeder, and R. D. Evans, 1964, Measurements of the Effects of Atmospheric Variables on Radon-222 Flux and Soil-Gas Concentrations, in *The Natural Radiation Environment*, J. A. S. Adams and W. M. Lowder (Eds.), p. 191, University of Chicago Press, Chicago.

Krisiuk, E. M., S. I. Tarasov, V. P. Shamov, N. I. Shalak, E. P. Lisachenko, and L. G. Gomelsky, 1971, *A Study of Radioactivity in Building Materials*, Research Institute for Radiation Hygiene, Leningrad.

McLaughlin, J. P., and N. Jonassen, 1978, The Effect of Pressure Drops on Radon Exhalation from Walls, this volume.

Wilkening, M. H., 1974, Radon-222 from the Island of Hawaii, *Science*, 183: 413-415.

——, D. Stanley, and W. E. Clements, 1975, Radon-222 Flux Measurements in Widely Separated Regions, in *The Natural Radiation Environment II*, Vol. 2, Symposium Proceedings, Houston, Tex., Aug. 7—11, 1972, J. A. S. Adams, W. M. Lowder, and T. F. Gesell (Eds.), ERDA Report CONF-780805-P2, pp. 717-730, Rice University and The University of Texas, Houston, NTIS.

The Effect of Pressure Drops on Radon Exhalation from Walls

J. P. McLAUGHLIN† and NIELS JONASSEN‡
†University College, Dublin, Ireland, and ‡Technical University of Denmark, Lyngby, Denmark

ABSTRACT

The exhalation of radon (^{222}Rn) from walls was measured in a concrete-walled basement room by studying the growth of activity in exhalation cans sealed to various portions of the walls. In a series of measurements, constant underpressures from 5 to 25 mm Hg were maintained in the exhalation cans during the build-up of activity. The exhalation rate appears to increase linearly with the underpressure.

In the theoretical considerations of pressure drops, it is assumed that the basement concrete walls in toto are capable of sustaining for many hours underpressure-enhanced exhalation values comparable to those experimentally measured at various places on the walls.

The fractional increase in room air activity is proportional to the total pressure drop and increases with the time it takes the pressure drop to establish. As an example, a pressure drop of 20 mm Hg will double the equilibrium activity in the room if its establishment takes place at a constant rate over a period of approximately 27 hr. This is in keeping with observations on the room air radon levels over a number of months.

In another paper in this symposium (Jonassen and McLaughlin, 1978), experiments on determinations of the exhalation of radon (^{222}Rn) from building materials placed in closed vessels are described.

To study the exhalation properties of actual walls, we performed a series of experiments in an underground basement room approximately 18 by 6 by 3 m. The complete structure (except for two walls that connect with other basements), the remaining walls, the

ceiling, and the floor are set into the surrounding soil and foundations. Circular "exhalation cans" were mounted at various places on the walls to measure radon emanating from the walls. The cans, which were made of steel, were screwed to the walls and sealed mainly with epoxy resin. The cans normally used were 0.60 m in diameter and 0.10 m in height.

The wall area S_c covered by each exhalation can was thus approximately 0.28 m^2. The cans were used for measuring radon exhalation rates both at atmospheric pressure and at pressures below atmospheric.

EXHALATION MEASUREMENTS AT ATMOSPHERIC PRESSURE

After an exhalation or flux can was sealed to the wall, it was flushed out with room air. A 1-liter sample of this filling air was then taken for radon measurement prior to closing the sampling tube of the can. This "zero-point" filling usually had a radon content of about 6 pCi/liter, which was typical of the air in the basement. At approximately 24-hr intervals, further 1-liter samples of air from the flux can were taken and processed. The growth of radon in the flux can could thus be easily followed over a period of many days.

If it is assumed that the exhalation rate E (in atoms m^{-2} sec^{-1}) is constant during the whole growth period, E can be determined from the equation

$$E = \frac{\lambda N_c}{S_c[1 - \exp(-\lambda t)]} \tag{1}$$

where S_c = area of wall covered by the flux can
λ = decay constant of radon
N_c = number of radon atoms
λN_c = radon activity in the can at any time t after the initial sealing

In an actual experiment, two minor corrections were usually required to use Eq. 1. The radon growth activity over any time t is equal to the measured value minus the contribution due to any undecayed fraction of the initial filling remaining in the can. An activity of 70 pCi/liter of radon in the can air after 10 days was typical, whereas an initial filling of, say, 6 pCi/liter would have decayed during this period to the relatively insignificant level of approximately 1 pCi/liter. Another small correction to the measured activities was

applied to take into account the slight dilution of the can air which occurred when a sample was taken.

The assumption of E being constant during the whole growth period is not strictly fulfilled. As the activity in the can grows, the net exhalation slows down due to back diffusion into the wall until an equilibrium value is reached.

For the wall in question, it can be shown (Jonassen and McLaughlin, 1978) that the equilibrium value of E may be considerably lower than the free exhalation rate corresponding to exhalation into a radon free space. The exhalation values measured in the present investigation, however, were determined as average extrapolated values corresponding to growth periods, which were, in many cases, considerably shorter than the time required to reach equilibrium. Thus the deviation from the free exhalation value will usually be insignificant compared to the uncertainties of the measurements. This was further substantiated by making exhalation measurements on the same part of the wall with cans ranging from 0.10 to 0.30 m in height. Within the uncertainties of the techniques involved, no differences in the exhalation values were found.

Since the total surface area of the room was 360 m^2 and the area of the exhalation cans was less than 0.3 m^2, it was unrealistic to attempt to measure exhalation values over the whole room.

To obtain an approximate mean exhalation value for the wall material, we performed a series of measurements at 11 different and widely spaced locations throughout the room. The mean of 53 such observations gave an exhalation value of

$$E = 379 \pm 107 \text{ atoms } m^{-2} \text{ sec}^{-1} \quad (2)$$

The magnitude of the spread in exhalation values is acceptable with regard to the limitations of the techniques involved and, more important, to the fact that variations in the porosity and radium content of the wall material can strongly influence the value of E.

In calculations of the equilibrium level of radon in the room air that an exhalation rate of E can support, the normal radon decay constant λ cannot be used, because the room, although not artificially ventilated, has a natural ventilation rate that influences the growth of radon in the room. This natural ventilation rate was determined by introducing N_2O gas into the room and measuring its rate of disappearance with a sensitive N_2O detector. Expressing the ventilation rate so determined as a decay constant λ_v, we found that the mean λ_v value for the room was 3.742×10^{-6} sec^{-1}. With such natural ventilation occurring, the makeup air

coming into the room from adjacent rooms also contains radon. Because of this, the effective radon ventilation constant λ_v^* will be less than the measured λ_v for N_2O. It can be shown that

$$\lambda_v^* = (1 - M)\lambda_v \tag{3}$$

where M is the ratio between the mean radon activity in adjacent rooms and that in the basement room being studied. Although M is not a constant, a value of M = 0.375 was found to be appropriate to typical conditions in the rooms, giving $\lambda_v^* = 2.339 \times 10^{-6}$ sec^{-1}. The total effective decay constant for radon in the basement room is thus

$$\lambda^* = \lambda + \lambda_v^* = 4.437 \times 10^{-6} \text{ sec}^{-1} \tag{4}$$

The mean radon concentration A_0 in the room will then be given by

$$A_0 = \frac{\lambda}{\lambda^*} \frac{S}{V} E \tag{5}$$

where S is the total exhaling area and V is the volume of the room.

Introduction of the values

$$\lambda = 2.098 \times 10^{-6} \text{ sec}^{-1}$$
$$\lambda^* = 4.437 \times 10^{-6} \text{ sec}^{-1}$$
$$S = 360 \text{ m}^2$$
$$V = 331 \text{ m}^3$$
$$E = 379 \pm 107 \text{ atoms m}^{-2} \text{ sec}^{-1}$$

results in

$$A_0 = (0.199 \pm 0.06) \text{ dps/liter} = (5.4 \pm 1.5) \text{ pCi/liter} \tag{6}$$

The mean of the measured activity in the room air over a period of 5 months was found to be 6.9 ± 1.7 pCi/liter. Although a reasonable agreement between the predicted and actual radon concentrations thus is shown, an exact verification of the correctness of the exhalation value on the basis of room air concentrations is not possible owing to the presence of the inevitable extra radon feeds that are induced from the walls by atmospheric pressure changes.

EXHALATION MEASUREMENTS AT REDUCED PRESSURE

Previous work at this laboratory in an unventilated basement has shown that the occurrence of a pressure front is accompanied by an inverse change in the ^{222}Rn and radon daughter levels in the air (Jonassen, 1975). Similar pressure-induced effects on outdoor radon exhalation from soils have been widely reported in the literature (Kovach, 1945; Wilkening, Stanley, and Clements, 1974). A decision was made to ascertain the dependence of radon exhalation from the walls of the basement under conditions of falling pressure by means of exhalation cans maintained at different pressures below atmospheric pressure (underpressures). It was felt that the results obtained would greatly help in setting up a workable model to predict variations in radon levels which might be expected inside real buildings during falling pressure.

The enhanced radon exhalation rates E at various underpressures were determined by taking samples of air from exhalation cans maintained below atmospheric pressure. The experimental setup is shown in Fig. 1. When the exhalation cans were operated at an

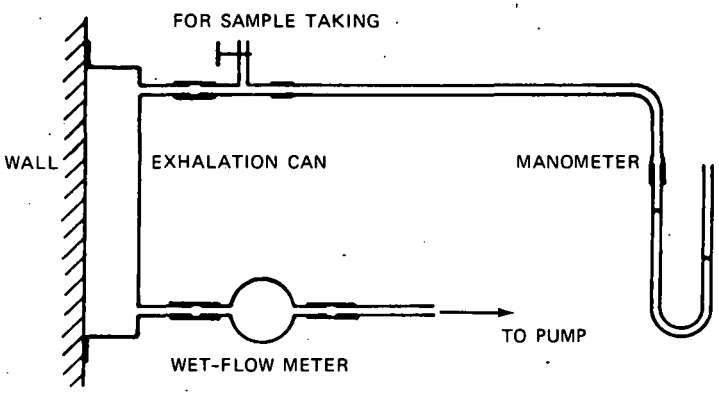


Fig. 1 Experimental arrangement to measure exhalation at reduced pressure.

underpressure, small amounts of air were continually removed from the cans. When the growth of radon within a can under these conditions is being dealt with, the appropriate decay constant that must be used is

$$\lambda' = \lambda + \frac{u}{V} \tag{7}$$

where u is the rate of removal of air from the can as measured with the wet-flow meter and V is the volume of the can. Typically, values of u were in the range 0.3 to 2 liters/hr, depending on the magnitude of the underpressure used.

The corresponding range in λ' values was 5.0 to 22×10^{-6} sec^{-1}. As for exhalation measurement at atmospheric pressure, the radon growth activity at any time is obtained from the measured activity by applying small corrections for any undecayed radon from the initial filling remaining in the can and also for the slight dilution of the radon content in the can which occurred every time a sample was taken. The cans were screwed to the wall and were very well sealed, with epoxy resin being the principal sealant both between the wall and the rim of the can and over the surrounding wall surface for a distance of approximately 0.30 m. However, it was impossible to determine what fraction of the air being removed at a flow rate u was coming from the radon-rich wall-pore air as distinct from any low radon content room air that might have leaked into a can. Because of this uncertainty, two distinct and extreme cases must be considered when measurements are being taken. In case 1, all the air removed from a can is considered as being replaced by wall-pore air; and, in case 2, it is considered as being replaced completely by room air. The reality of the situation probably lies between these two extremes, which are now treated individually.

Case 1

In this case the growth of radon in a can is given by

$$\frac{dN_c}{dt} = ES_c - \lambda' N_c \tag{8}$$

where N_c is the total number of radon atoms at any time t in a can covering a wall area S_c. If it is assumed that E is constant with time, Eq. 8 yields

$$E = \frac{\lambda N_c}{\frac{\lambda}{\lambda'}[(1 - \exp(-\lambda' t)]} S_c^{-1} \tag{9}$$

Case 2

In this case the appropriate equation governing radon growth in a can is

$$\frac{dN_c}{dt} = (ES_c + un) - \lambda' N_c \tag{10}$$

where n is the number of atoms of radon per unit volume of room air leaking into a can.

Values of n are obtained by taking samples of room air at the same time that a sample is taken from a can.

Equation 10 yields

$$E = \left\{ \frac{\lambda N_c}{\frac{\lambda}{\lambda'}\left[1 - \exp\left(-\lambda' t\right)\right]} - un \right\} S_c^{-1} \tag{11}$$

In all underpressure experiments, values of E were calculated for both case 1 and case 2 situations. The mean value of E from the two calculations was then assigned to each underpressure ΔP since, in most cases, the percentage difference between the two values of E obtained was found to be insignificant.

Because the atmospheric pressure at Copenhagen rarely falls below 735 mm Hg, it was decided to restrict the investigations of E values to underpressures only as low as 25 mm Hg below atmospheric pressure. The results obtained are summarized in Table 1. For purposes of comparison, the exhalation rate at atmospheric pressure is the first entry in the table. The value of E given represents the mean of usually three or four measurements made at the underpressure in question.

TABLE 1

Exhalation Rate at Various Underpressures

Underpressure (ΔP), mm Hg	Mean exhalation rate (E), atoms m^{-2} sec^{-1}
0	379
5	1130
7	630
8	1184
12	1425
13.5	1376
14	1875
19	2070
23	2705
24	2394

The general increase in E with the underpressure is obvious, but a closer interpretation of the relationship is undoubtedly very complex and must take into account such factors as the ability of radon to move both by diffusion and transport mechanisms through the micropores of the inhomogeneous wall concrete matrix. However, assuming as a first approximation that the lowering of the pressure across the interface between a concrete wall and the room air causes an expansion of the radon-rich pore air into the room, then a linear relationship between E and ΔP may not be unreasonable. The results given in Table 1 were analyzed by least-squares analysis, and the best straight-line fit in accordance with the equation

$$E = m(\Delta P) + C = \left[\frac{dE}{d(\Delta P)}\right] \Delta P + E_0 \tag{12}$$

yielded

$$m = \frac{dE}{d(\Delta P)} = 90.9 \text{ atoms } m^{-2} \text{ sec}^{-1}/\text{mm Hg}$$

and

$$E_0 = 376 \text{ atoms } m^{-2} \text{ sec}^{-1}$$

This straight line is plotted in Fig. 2 together with the experimental points.

If the $dE/d(\Delta P)$ value thus obtained can be validly applied to the total wall surface of the basement, then it is possible by means of the treatment given in the following section to predict the levels of radon in the room for pressure drops of given magnitudes and durations. The treatment is also general enough to be easily adapted to other situations where large air cavities exist within structures made of radon-producing materials. Radon levels in such widely different situations as the interior of normal living rooms and underground mines can thus in principle be dealt with in a similar manner.

EFFECT OF PRESSURE DROPS ON ROOM AIR ACTIVITY

If the pressure in the room drops at a constant rate $g = d(\Delta P)/dt$, then, according to Eq. 12, the value E at any time t is

$$E = E_0 + mgt \tag{13}$$

where $m = dE/d(\Delta P)$.

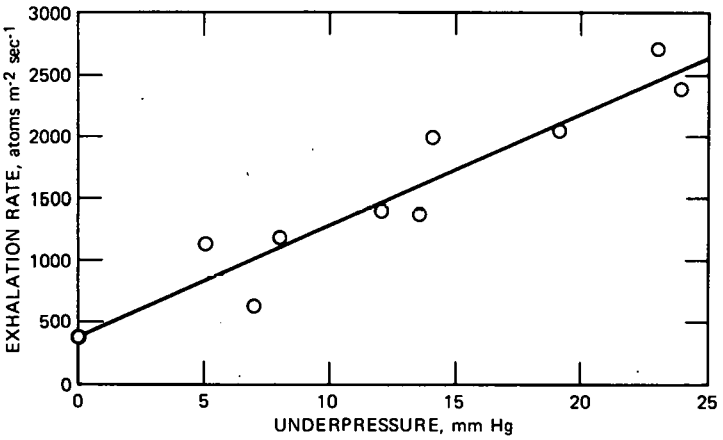


Fig. 2 Exhalation rate as a function of the underpressure.

During a time interval dt from t to t + dt, the extra number of atoms of radon fed into the room is

$$dN = Smgt\,dt \tag{14}$$

where S is the wall area of the room.

At a subsequent time t_s, these dN atoms will contribute an activity $(\lambda dN)_s$ given by

$$(\lambda dN)_s = \lambda dN \exp\left[-\lambda^*(t_s - t)\right] \tag{15}$$

where λ^* is defined by Eq. 4.

If the pressure drop continues at its steady rate g until a final time t_f, then the total extra activity in the room air at a time $t_s \leqslant t_f$ due to the pressure drop is given by

$$\begin{aligned}\Delta(\lambda N)_s &= \int_0^{t_s} \lambda Smgt \exp\left[-\lambda^*(t_s - t)\right] dt \\ &= \frac{\lambda S}{\lambda^*} mg\left[\frac{\lambda^* t_s - 1 + \exp(-\lambda^* t_s)}{\lambda^*}\right]\end{aligned} \tag{16}$$

If a total pressure drop ΔP takes place in the time t_f, then

$$g = \frac{d(\Delta P)}{dt} = \frac{\Delta P}{t_f}$$

Thus

$$\Delta(\lambda N)_s = \frac{\lambda}{\lambda^*} \frac{Sm(\Delta P)}{t_f} \left[\frac{\lambda^* t_s - 1 + \exp(-\lambda^* t_s)}{\lambda^*} \right] \quad (17)$$

If the room air is assumed to be initially at its equilibrium activity value of $\lambda N_0 = (\lambda/\lambda^*)\, SE_0$, then at $t = t_f$ the fractional increase in activity due to the pressure drop is

$$\frac{\Delta(\lambda N)_f}{\lambda N_0} = \frac{m(\Delta P)}{E_0} \left\{ 1 - \frac{[1 - \exp(-\lambda^* t_f)]}{\lambda^* t_f} \right\} \quad (18)$$

Equation 18 is now used to calculate $\Delta(\lambda N)_f/\lambda N_0$ values for the basement room air for situations where a pressure drop of total final magnitude $\Delta P = 20$ mm Hg takes place for t_f values ranging up to 36 hr. For each case, its value for $g = d(\Delta P)/dt$ is considered to be constant during the full pressure-drop establishment time t_f. It must be assumed that the radon budget within the walls of the room is such that the walls are capable of maintaining with little diminution enhanced pressure-drop-induced E values for many hours. For the room in question, the following values of m, E_0, and λ^* are used

$$m = 90.9 \text{ atoms m}^{-2} \text{ sec}^{-1}/\text{mm Hg}$$

$$E_0 = 379 \pm 107 \text{ atoms m}^{-2} \text{ sec}^{-1}$$

$$\lambda^* = 5 \times 10^{-6} \text{ sec}^{-1}$$

It should be noted that the value of λ^* used here is slightly greater than the value of 4.43×10^{-6} sec^{-1} previously used to allow for the fact that the M factor in Eq. 3 will decrease as the activity in the room increases.

The values of $\Delta(\lambda N)_f/\lambda N_0$ predicted at various t_f values according to Eq. 18 are presented graphically in Fig. 3. It appears from the figure that $\Delta(\lambda N)_f/\lambda N_0 = 1$ for $E_0 = 379$ atoms m^{-2} sec^{-1} if it takes approximately 27 hr for the full pressure drop to occur.

Since the equilibrium activity A_0 for $\lambda^* = 5 \times 10^{-6}$ sec^{-1} is, according to Eq. 5, equivalent to 4.77 pCi/liter, the activity will thus grow to 9.54 pCi/liter if the 20 mm Hg pressure drop is established at a constant rate over approximately 27 hr. During a series of measurements on the basement room air over many months, increases of this magnitude during pressure drops have in fact been observed. As the following argument shows, an exact correspondence

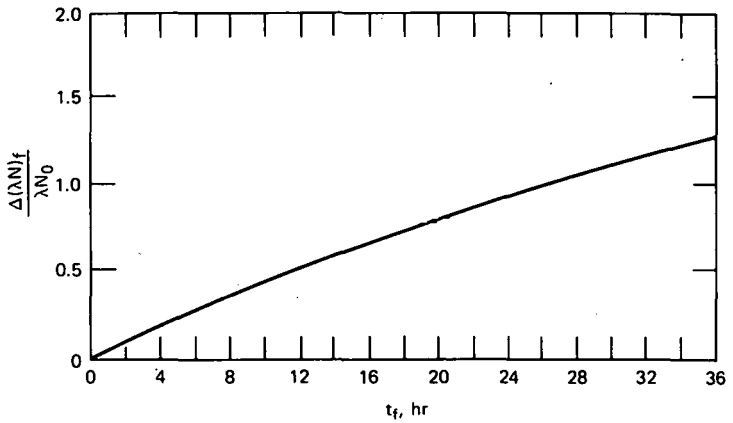


Fig. 3 Fractional increase in total room activity for a pressure drop of 20 mm Hg as a function of the pressure-drop establishment time, t_f.

between theoretical predictions and experimental measurements cannot, however, be reasonably expected. With real atmospheric pressure drops, the value of $g = d(\Delta P)/dt$ does not normally remain constant. It is also considered that small changes in λ^* may occur during a pressure change. In addition, in the treatment given above, it was assumed for simplicity that the room had been at steady atmospheric pressure for a considerable period before the pressure drop occurred. In reality, both positive and negative pressure changes are continually taking place. The radon activity in the room before any pressure drop is at a level determined chiefly by its preceding history of pressure and, possibly, temperature changes, although in the underground room in question temperature changes are negligible. Notwithstanding the above, the model presented here gives valuable insight into the type of changes in radon level which may be expected in such a room due to pressure drops. The less dramatic reduction of radon levels caused by rising pressure is not treated here, but in future investigations this phenomenon will also be studied.

ACKNOWLEDGMENT

This work was supported by grants from the Danish Natural Science Research Council and the Danish Council for Scientific and Industrial Research.

REFERENCES

Jonassen, N., 1975, On the Effect of Atmospheric Pressure Variations on the Radon-222 Concentration in Unventilated Rooms, *Health Phys.*, 29: 216-220.

——, and J. P. McLaughlin, 1978, Exhalation of Radon-222 from Building Materials and Walls, this volume.

Kovach, E. M., 1945, Meteorological Influences upon the Radon Content of Soil Gas, *Trans. Am. Geophys. Union*, 26: 241-248.

Wilkening, M. H., D. Stanley, and W. E. Clements, 1974, Radon-222 Flux Measurements in Widely Separated Regions, in *The Natural Radiation Environment II*, Vol. 2, Symposium Proceedings, Houston, Tex., Aug. 7—11, 1972, J. A. S. Adams, W. M. Lowder, and T. F. Gesell (Eds.), ERDA Report CONF-720805, pp. 717-730, Rice University and the University of Texas School of Public Health, NTIS.

Radon in Dwellings in Sweden

GUN ASTRI SWEDJEMARK
Environmental Laboratories, National Institute of Radiation Protection, Stockholm, Sweden

ABSTRACT

Studies on specific activities in building materials, gamma-radiation levels in dwellings, the concentrations of radon and daughters in the air indoors and the concentration of radon in tap water are in progress in Sweden. On basis of these investigations and of the investigation of Hultqvist from the beginning of the 1950s, an attempt has been made to show how the radiation doses in dwellings have changed or may be changed by human activities and what these changes imply in terms of collective dose.

The annual collective absorbed dose in the basal cells of the critical bronchial region have increased from 11×10^3 man-Gy for the occupants of dwellings existing in 1950 to 25×10^3 man-Gy for dwellings existing in 1975. If the building of houses continues as at present, it can be estimated that the annual collective dose will be between 25 and 31×10^3 man-Gy for dwellings in 1985.

Radon and its daughter products indoors present a serious problem in Sweden for several reasons. Since the energy crisis in 1973, major efforts have been made to save energy on a national level. Because of the cold climate in Sweden, about 20% of the total energy consumed is used for the heating of dwellings (Swedish Committee on Energy and Environment, 1977). Of this amount, it has been estimated that about 25% is lost with ventilation air. The energy-saving program is being supported by economic contributions from the government and by advice in newspapers and booklets on the practical aspects of saving energy. One of the easiest ways is to fit sealing strips around windows and doors and to close air inlets and also to decrease the speed of the fans or to stop them for part of the day. The building

regulations have been adapted to conform to the energy-saving program, and, in the 1975 Swedish Building Code, the lowest permissible ventilation rate was decreased to 0.5 air exchange per hour for houses with mechanical ventilation systems. At the same time, new requirements have been introduced on how well sealed dwelling houses should be.

The National Board of Urban Planning has been given directions by the government to investigate the feasibility of a further decrease in the lowest permissible air exchange rate. Most of the existing single-family houses have natural draft ventilation, and, when new houses are built more and more airtight and the airtightness of older houses is improved, the natural draft ventilation system does not work. These problems must be common to all countries with cold climates.

Aerated concrete based on alum shale was used in buildings in Sweden from 1930 until 2 years ago. Today, only about 10% of the existing houses are built of this material. Until the energy crisis the radon concentrations did not cause problems even in those houses, as was shown by Hultqvist (1956), because the ventilation rates were mostly good. Furthermore, it was not possible to build the old houses as airtight as the new houses built today.

Studies of specific activities in building materials, gamma-radiation levels in dwellings, the concentrations of radon and radon daughters in the air indoors, and the concentration of radon in the tap water are in progress in Sweden. On the basis of these investigations and of the investigation of Hultqvist from the early 1950s, an attempt has been made to show how the radiation doses in dwellings have changed or may be changed and what these changes imply in terms of collective dose.

EXPERIMENTAL RESULTS

Houses Built Before 1946

Hultqvist (1956) investigated the gamma-radiation levels in almost 1000 dwellings built before 1946 in 13 towns in central Sweden. In almost 300 of these dwellings in four towns he also determined the concentration of radon (Table 1). The houses measured were intended to constitute a representative selection of Swedish dwellings. However, for estimation of the average radiation level for the whole country, in this investigation the results have been weighted for the frequency of building materials in the dwellings existing in 1946. The specific activity of ^{226}Ra in local brick and in soil is an important factor in explaining the regional variations of the

TABLE 1

MEASUREMENTS OF RADON CONCENTRATION IN AIR IN FOUR TOWNS IN CENTRAL SWEDEN AT THE BEGINNING OF THE 1950s IN HOUSES BUILT BEFORE 1946 (Hultqvist, 1956)

	Radon concentration,* Bq/m^3		
	Unaired houses†	Aired houses‡	Weighted average
Wood	15.2	15.5	15.2
Brick	47.4	26.0	40.0
Aerated concrete based on alum shale	133	67.0	116

*1 $Bq/m^3 \approx 0.027$ pCi/liter.
†No thorough airing was carried out since the day before the measurement.
‡Dwellings were aired the morning before the sampling.

radon concentration for this period. These specific activities tend to be greater in central Sweden than the countrywide average.

Houses Built Around 1970

In a joint project the National Institute of Radiation Protection and the National Institute of Building Research have investigated the concentrations of radon and its daughter products, the ventilation rates, and the gamma-radiation levels in seven groups of houses built around 1970 in the town of Gävle in central Sweden (Table 2) (Erikson et al., 1976). Each group of houses consisted of nine dwellings and represented various types of houses, building materials, and ventilation systems.

The planning of the investigation in Gävle took into account both the continuous recording of radon levels in typical houses (Swedjemark, 1974) and the extensive measurements of radionuclides in building materials, which had previously been carried out.

The averages of the radon concentrations in the various types of dwellings in Gävle were 50 to 440 Bq/m^3 (1.4 to 12 pCi/liter). This is discussed in more detail in a later section. This radon originates mostly from building materials, in some degree from the soil, and by about 10 Bq/m^3 of air (0.3 pCi/liter of air) from tap water as an annual average. The concentration of radon in the tap water in Gävle was fairly small, about 20 Bq/liter (0.5 nCi/liter). The estimation of the concentration in air from the concentration in water has been based on a Finnish investigation (Castrén et al., 1977) and on an

TABLE 2

CONCENTRATIONS OF RADON AND DAUGHTER PRODUCTS IN 63 DWELLINGS IN THE TOWN GÄVLE (Erikson et al., 1976)

Group No.	Building materials in the walls and vent. system*	Air exchange per hour		Concentration,†‡ Bq/m^3			
				Radon		Radon daughters	
				I	II	I	II
	Multifamily Houses						
1	Concrete, F	0.3—0.6	Low	59	48	22	11
			Av.	170	140	70	52
			High	590	780	260	310
2	Concrete + sand-based aerated concrete, F	0.5—0.9	Low	37	26	13	9
			Av.	89	85	31	23
			High	150	140	48	41
3	Concrete + sand-based and alum shale based aerated concrete, F	0.4—0.8	Low	74	93	22	11
			Av.	180	160	52	44
			High	440	410	150	140
	Single-Family Houses						
4	Facade brick (sandstone), wood construction, F	0.4—0.7	Low	n§		8	
			Av.	56		22	
			High	140		38	
5	Wood, the cellar of alum shale based aerated concrete, F	0.4—0.7	Low	n		4	
			Av.	200		81	
			High	370		140	
	As above without cellar	0.8	Low	100		33	
			Av.	100		37	
			High	100		41	
6	Alum shale based aerated concrete, S	0.2—0.5	Low	150		67	
			Av.	270		120	
			High	410		190	
7	Facade brick (clay), wood construction, S	0.1—0.2	Low	220		82	
			Av.	410		170	
			High	560		310	

*F = mechanical exhaust ventilation system, S = natural draft ventilation system in the houses studied with fan over kitchen stove.

†I and II mean the first and second phases between which the ventilation systems were adjusted.

‡1 Bq/m^3 ≈ 0.027 pCi/liter.

§n ≤ minimum detectable value, 26 Bq/m^3 for radon.

estimation made in a report by the U. S. Environmental Protection Agency (1976).

The dwellings studied can be regarded as representative for dwellings built around 1970 not only in Gävle but also for the whole country. However, the relative frequency of various types of houses or of various building materials have varied with time and between different parts of the country.

CALCULATIONS

Building Materials

Up to about the 1940s, houses were built of wood or of brick. The floor structures consisted of wood and the foundations and the cellars of stone blocks. At the beginning of the 1930s, aerated concrete began to replace brick. The aerated concrete was based either on sand or on alum shale, with about the same production of each type up to the beginning of the 1970s. Since 1976, no aerated concrete based on alum shale has been produced.

With the exception of aerated concrete, which was widely distributed, local building materials have been used in most houses. The range of the specific activities in samples of clay brick from most of the brick factories in Sweden at the beginning of the 1950s was ±60% of the average (Hultqvist, 1956). The specific activity of ^{226}Ra in soil and stone varies considerably between different places in Sweden. For the calculations, the average of the radon concentration in houses of a certain building material in all Sweden has been assumed to be the same as the corresponding average for the dwellings studied in the four towns in central Sweden.

Several different structural systems with different dominant materials are used in modern houses. In the available statistics the materials in the outer walls have been used as the basis for the classification, but this is not always the most suitable classification from the radiation viewpoint. For example, apartment houses built of a structure of concrete with the outer walls of some wooden material are classified as wooden houses. Detached houses of wood are often faced with such materials as wood, brick, or limestone, and this can influence the radon concentration indoors. Many wooden houses have basements built of aerated concrete. If the rate of air exchange in the basement is poor, the radon concentration in the whole house can be as high as in a house built entirely of aerated concrete.

Nowadays most building materials are produced in a small number of factories that supply the whole country. Exceptions are

clay bricks and concrete which are often produced locally. A very minor part of the building materials is imported from other countries. Most of the concrete is mixed at the building site using ballast materials from local gravel pits. For apartment houses, prefabricated concrete components produced in a few factories are not unusual.

Cement forms about 20% of the finished concrete, and, because the specific activity in cement is at present low, it is mostly the ballast materials that determine the specific activity of ^{226}Ra in the finished concrete. Of the building materials in modern houses, it is therefore the specific activity of ^{226}Ra in the ballast material which can influence the regional variations of radon in buildings in the country. Further, particular building materials are used to greater or lesser degrees in various parts of the country.

Concrete is used to some extent in almost all modern dwellings. The specific activity of radionuclides in concrete is therefore very important both for the gamma-radiation level and for the radon concentration in the dwellings. The specific activity of ^{226}Ra in ballast material from Gävle (Hagberg and More, 1976) is not significantly higher than the countrywide average. Table 3 is an abstract from a countrywide investigation into the specific activity in natural ballast materials. According to the table, the results of the measurements of radon concentrations in Gävle would be reasonably representative for the whole country. This is confirmed by a comparison between the gamma levels measured during the investiga-

TABLE 3

SPECIFIC ACTIVITY OF BALLAST MATERIALS FROM THE TOWN OF GÄVLE AND OF BALLAST MATERIALS FROM ALL SWEDEN (in Bq/kg)*

	Gävle			Sweden		
	Average	Lowest	Highest	Average	Lowest	Highest
^{226}Ra	55	54	59	48	7	185
^{232}Th	81	65	113	70	3	480
^{40}K	730	680	770	810	150	1300
$\Sigma\gamma$Bq/kg†	440	400	540	405	41	2000

Note: The standard deviation due to counting statistics in each sample varies with the activity so that for 370 γBq/kg the standard deviation is 2%, and for γBq/kg it is about 10%.

*1 Bq/kg $\approx$ 0.027 pCi/g.

†$\Sigma\gamma\text{Bq/kg} = 2.2 \cdot C_{Ra} + 3.0 \cdot C_{Th} + 0.11 \cdot C_K$.

tion in Gävle and the preliminary values from the countrywide investigation with thermoluminescent detectors (Mjönes, 1978).

The specific activity of ^{226}Ra in aerated concrete based on alum shale depends mostly on the specific activity in the alum shale. This varies between different mining sites. Figure 1 shows how the specific activity of ^{226}Ra in aerated concrete based on alum shale, weighted for the production, has varied over a period of years. Corrections for this variation have been made when the average concentrations were being calculated.

Apartment houses are defined as dwelling houses with at least three apartments. Detached houses are defined as one- or two-family houses placed separately or built together and can be courtyard houses, linked houses, or bungalows.

Available statistics over the proportions of the dwellings built of various building materials are imperfect for our purpose. Our figures

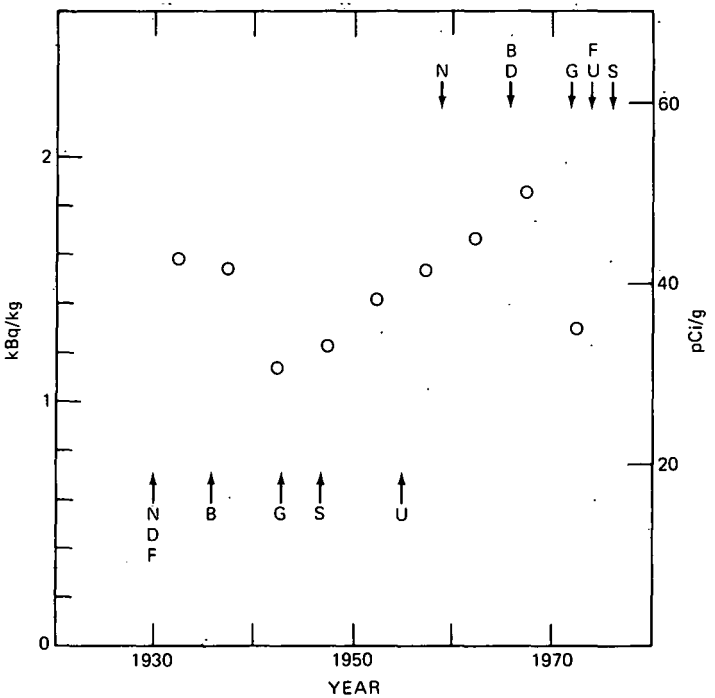


Fig. 1 The countrywide averages of the specific activity of ^{226}Ra weighted for the annual production of aerated concrete based on alum shale. The arrows directed upward show new factories starting production, and the arrows directed downward show when the production ceased.

are taken from official Swedish statistics (*Statistical Abstracts of Sweden*, 1976 and earlier) and information from factories and trade organizations (Svanholm, 1977; Svedisol, 1975; Vinberg, 1977). This information has been modified for the purpose of the problem presented by radon in dwellings.

For the calculations for the period up to 1950, three categories have been used to classify houses, wood, clay brick, and aerated concrete based on alum shale. For this period, "brick" implies a masoned load-bearing wall of clay brick.

For the period after 1950, separate classifications have been used for apartment houses and for detached houses. The apartment houses have been classified into two categories, "concrete" and "aerated concrete based on alum shale." The category "concrete" comprises houses built of concrete, often combined with other materials, such as wood or aerated concrete based on sand. In apartment houses, aerated concrete based on alum shale is almost always combined with concrete. For detached houses, a more detailed classification has been used. It is perhaps worth pointing out that "brick" for this period consists in most cases of facade brick of clay and only to a small extent of masoned load-bearing walls of clay brick.

For the estimation of radon concentrations for the next 10-year period, the number of categories has been reduced because aerated concrete based on alum shale has not been produced since 1975.

Ventilation

Natural draft ventilation (the S-system) was used in all dwellings up to the 1940s, when mechanical exhaust air systems (the F-system) began to be introduced in apartment houses. As illustrated in Fig. 2, this type of ventilation system was the most common system in dwellings built during 1970s. From 1976 the S-system is prohibited in new apartment houses. For detached houses the S-system was the only type of ventilation system up to about 1970, when mechanical ventilation systems for detached houses began to be available. The S-system is still allowed in detached houses.

As is seen in Table 4, the air exchange rates vary to a high degree between houses built during different periods (Swedish Energy Commission, 1977). For old houses, both the average rates and the deviations are relatively large. Better techniques and an effort to build houses more airtight have resulted in lower averages and smaller deviations for the air exchange rates in modern houses. Because of the lack of available statistics, the air exchange rates in the calculations have been assumed to be the same in houses with F-system ventilation as in houses with S-system ventilation. The air

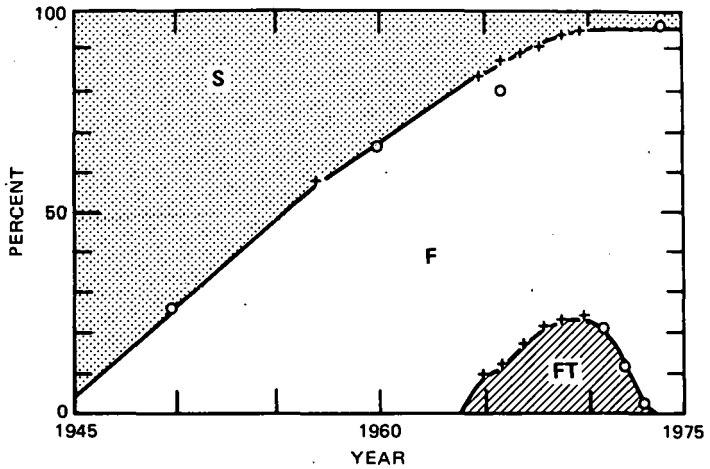


Fig. 2. Estimated relative frequencies of ventilation systems in newly built apartment houses (Swedish Committee on Energy and Environment, 1977). S, natural draft ventilation system; F, mechanical exhaust air systems; and FT, mechanical ventilation for both the incoming air and the exhaust air.

exchange rates have also been assumed to be the same in wooden houses as in the other categories of houses built during the same periods. The number of houses of the various types which has been demolished has not been taken into account.

Air Exchange Rates and the Radon Concentration

The radon concentration, C(t), in a room follows the equation

$$C(t) = C_\infty(1 - e^{-(l+\lambda)t}) + C_0 e^{-(l+\lambda)t} \quad (1)$$

where C_∞ = concentration of radon in equilibrium with a constant air exchange rate
C_0 = initial concentration of radon when the ventilation is changed
l = air exchange rate
λ = decay constant

When equilibrium with the air exchange rate has been reached, C_∞ is given by

$$C_\infty = \frac{lC_{in} + G/V}{l + \lambda} \quad (2)$$

where C_{in} = concentration of radon in the supply air
G = radon emanation rate
V = volume of the room

and G/V is assumed to be constant in a dwelling because variations of the air exchange rates have more effect on the radon concentration in a room than on variations in the emanation of radon.

An expression for the concentration of radon given by the air exchange rate l_2 calculated from an air exchange rate l_1 can be derived from Eqs. 1 and 2

$$C_2 = C_1\left(\frac{l_1}{l_2}\,rs + 1 - u\right) + C_{in}u\,\frac{l_2 - l_1}{l_2 + \lambda} - C_0\,\frac{l_1}{l_2}\,rse^{-(l_1+\lambda)t} \quad (3)$$

where $r = \dfrac{l_1 + \lambda}{l_2 + \lambda}\dfrac{l_2}{l_1}$

$$s = \frac{1 - e^{-(l_2+\lambda)t}}{1 - e^{-(l_1+\lambda)t}}$$

$$u = 1 - e^{-(l_2+\lambda)t}$$

For the conditions applying for most of the calculations,

$$t \approx 15 \text{ hr}$$

$$l_1 > 0.25/\text{hr}$$

$$l_2 \approx 0.5 \text{ or } 0.3/\text{hr}$$

The following approximations can be made:

$$rs \approx 1$$

$$u \approx 1$$

$$\frac{l_2 - l_1}{l_2 + \lambda} \approx \frac{l_2 - l_1}{l_2}$$

Consequently Eq. 3 can be simplified to

$$C_2 = C_1\,\frac{l_1}{l_2} + C_{in}\,\frac{l_2 - l_1}{l_2} \quad (4)$$

The error in C_2 will be $< 4\%$ for $l_2 = 0.5/\text{hr}$
$< 2\%$ for $l_2 = 0.3/\text{hr}$

TABLE 4

NUMBER OF DWELLINGS IN SWEDEN AND ESTIMATED AVERAGE AIR EXCHANGES IN EXISTING HOUSES BUILT DURING VARIOUS PERIODS

Building year	Number of dwellings in			Air exchange per hour	
	Apartment houses ($\times 10^3$)	Detached houses ($\times 10^3$)	Total ($\times 10^3$)	Apartment houses	Detached houses
Before 1900	89.5	232.9	316	0.8 ± 0.5	0.9 ± 0.5
1901—1920	115.5	150.5	266.0	0.8 ± 0.45	0.9 ± 0.45
1921—1930	89.2	124.1	213.3	0.8 ± 0.4	0.9 ± 0.4
1931—1940	189.5	166.7	356.2	0.8 ± 0.35	0.9 ± 0.33
1941—1950	277.2	147.4	424.6	0.8 ± 0.3	0.9 ± 0.3
1951—1960	427.1	167.5	594.6	0.6 ± 0.25	0.8 ± 0.25
1961—1965	284.9	120.0	404.9	0.5 ± 0.2	0.6 ± 0.2
1966—1970	341.8	146.9	488.7	0.5 ± 0.2	0.6 ± 0.2
1971—1975	251.0	202.8	453.8	0.3 ± 0.15	0.45 ± 0.45
Unknown	1.8	9.9	11.7	0.6	0.75
Total	2061.5	1468.7	3530.0	0.605	0.73

Note: The estimated standard deviations (1σ) are based on a limited material, but they are in basic agreement with other studies carried out up to now (Swedish Energy Commission, 1977).

Equation 4 has been used for the calculations for all groups of houses with the exception of group 7.

The daughter products are very seldom in equilibrium with the radon. The equilibrium factor for radon is defined as the ratio between the total potential alpha energy of the actual concentration of the radon daughters and the potential alpha energy of the radon daughters if they were in equilibrium with the radon. The equilibrium factor varies with the air exchange rate. At very low exchange rates, it may be as high as 0.7 to 0.8 but it decreases as the rate increases. However, at very high exchange rates it is the conditions outdoors which dominate the concentrations of radon and radon daughters, and in this case too the equilibrium factor may be high. For the present calculations the equilibrium factor has been taken as constant and equal to 0.5, which is the value used in a report by the United Nations Scientific Committee on the Effects of Atomic Radiation (UNSCEAR) (1977).

This approximation can result in significant errors in the results. Owing to a lack of sufficient information to attribute a probable

equilibrium factor when the ventilation rates are changed, no corrections have been made in this respect. However, some attempts have been made to estimate the magnitude of the errors.

For exchange rates between 0.5 and 1 per hour, the equilibrium factor may be lower than 0.5. At low air exchange rates, it may be greater than the value 0.5 used. The radiation doses, calculated for a decrease from the present exchange rate to the standard of new houses built today, may therefore have been underestimated by as much as 50%. A decrease in the air exchange rate to 0.5 per hour can also result in an underestimation of the calculated radiation doses, depending on how the equilibrium factor for radon varies with the exchange rate.

How well the radon concentration follows the above equations in practice is illustrated by the investigation in two single-family houses (Erikson et al., 1976) presented in Table 5. After an alteration of the

TABLE 5

VALIDITY IN PRACTICE OF EQ. 3 FOR ESTIMATION OF RADON CONCENTRATION FOR AN AIR EXCHANGE l_2 FROM A PREVIOUS AIR EXCHANGE OF l_1 AND DEVIATIONS DUE TO COUNTING STATISTICS

No.	Radon concentration, Bq/m^3 Measured C_1	Air exchange per hour l_1	l_2	Radon concentration,* Bq/m^3 Measured C_2	Calculated C_2	Calculated / Measured
Radon						
7 : 9	465 ± 27	0.15	0.23	413 ± 26	332 ± 19	0.80 ± 0.07
	465 ± 27	0.15	0.09	533 ± 27	635 ± 37	1.19 ± 0.09
7 : 10	710 ± 28	0.14	0.07	969 ± 28	1040 ± 41	1.07 ± 0.05

*1 Bq/m^3 ≈ 0.027 pCi/liter.

exchange rates from 0.15 first to 0.07 and then to 0.23 per hour, the difference between the calculated and the measured radon concentration was less than 20%. Equation 3 was used because the exchange rates were less than 0.25 per hour. The conditions assumed in this calculation are not fulfilled to the same degree as for the calculations of the countrywide averages, because the equilibrium with the ventilation rate is influenced to a greater extent at these low exchange rates than at higher rates. For example, if the doors and the windows of the rooms were kept closed during 24 hr instead of 15 hr, as has been assumed, the error might be as much as 15%.

Correction Factors

It is probable that most persons open the windows twice a day. For practical reasons it has been assumed that windows are opened a short time every 12 hr sufficiently effectively for the concentration of radon to decrease to the outdoor level. From Eq. 1 the concentration, $\overline{C}$, averaged during a 24-hr period is

$$\frac{1}{12}\int_0^{12} C(t)\,dt = \frac{1}{12}\int_0^{12} \{C_\infty [1 - e^{-(1+\lambda)t}] + C_0 e^{-(1+\lambda)t}\}\,dt \qquad (5)$$

This can be simplified to

$$\overline{C} = C_\infty \left[1 - \frac{1 - e^{-12(1+\lambda)}}{12(1+\lambda)}\right] + \frac{C_0}{12}\,\frac{1 - e^{-12(1+\lambda)}}{1+\lambda} \qquad (6)$$

where the last term can be neglected for the actual combinations of air exchange rates and radon concentrations. Equation 6 can then be written as

$$\overline{C} = C_M \left[1 - \frac{1 - e^{-12(1+\lambda)}}{12(1+\lambda)}\right] \frac{1}{C_M/C_\infty} \qquad (7)$$

where C_M is the measured radon concentration

$$\frac{C_M}{C_\infty} = 1 - e^{-t(1+\lambda)} \qquad (8)$$

$\overline{C}/C_M$ decreases from 0.9 to 0.68 when the air exchange rate decreases from 0.80 to 0.20 per hour.

From interviews with the persons living in the dwellings it has been found that about 30% normally sleep with the windows at least partly open during winter time and about 80% during summer time. These values are valid for the houses investigated in Gävle but because of lack of more relevant values for the whole country they have been used as the basis for correction factors regarding open windows. Some people have their windows at least partly open both day and night during summer time and a smaller number both day and night throughout the whole year. The latter group has been assumed to be negligible in the calculations of the correction factors to be applied for the whole country. It was found in earlier measurements (Swedjemark, 1974, 1978; Erikson et al., 1976) that the radon concentration decreases by about one-half when a window stands ajar. On a countrywide average, a reduction of the radon concentration by about 20% is found.

Exhaust air ducts in modern houses are mostly found only in kitchens and bathrooms. A bedroom has at best an outlet for air, for example, in the form of a chink in the upper part of the door. When a door to a bedroom is closed, the concentration of radon may increase if the specific activity of the building materials in the bedroom is the same or higher than the average for the whole dwelling (Swedjemark, 1974); otherwise it may become lower. If it is assumed that half of the population close their bedroom doors for the night and that the concentration of radon increases in 90% of the dwellings to an average value during the night which is 1.5 times the measured value in the whole dwelling, the average level during a 24-hr period may increase by about 20% as an average for the whole population.

Consequently for the average population these two bedroom ventilation factors—opening the window and closing the door—will cancel each other out.

Average Concentrations of Radon

The Swedish population, which is about 8 million, has been assumed to be constant. The number of persons living in each dwelling has been assumed to be the same in apartments and in detached houses.

The Period Before 1950

For the period up to 1950, the measurements of the radon concentrations made by Hultqvist (1956) in 293 dwellings built before 1946 have been used for the calculations of the countrywide averages.

Hultqvist's measurements in four towns in central Sweden did not include measurements of the air exchange rates. These have been assumed not to differ from the countrywide averages for dwellings built before 1950.

The investigation covered both dwellings that were aired in the morning before the measurement and dwellings that had not been aired. Equilibrium with the ventilation air can be assumed in the unaired dwellings. If the calculations are based on the values from these dwellings corrected for airing, the average values were, at the most, 3% higher than the corresponding average for all the investigated dwellings.

The Period 1951—1975

For the period after 1950, the measurements of radon and radon daughters and air exchange rates made at the beginning of 1970 have

been used (Erikson et al., 1976). The measured air exchanges have been used for calculating the radon concentrations for the air exchanges estimated for each building period. The occupants had been requested to keep the windows closed after 9:00 p.m. on the evening before the measurements. Corrections have been made for regular airing.

The Period 1976—1985

The 1975 Swedish Building Code requires that the average air exchange rates must not be below 0.5 per hour in newly built houses with mechanical ventilation. The requirements for airtightness which the Building Code also specifies, however, have led to average air exchange rates of 0.3 to 0.4 per hour for houses built during the last few years. For the coming 10-year period, therefore, two alternatives have been given. In the first alternative, A, it has been assumed that the average air exchange rate will follow the requirements of the 1975 Building Code of at least 0.5 exchange per hour. In the second alternative, B, it has been assumed that the houses will be built in the same way as today, that is, the air exchange rates would be about 0.3 per hour in apartment houses and 0.45 per hour in detached houses.

DISCUSSION

Radon Concentrations

The average radon concentrations in dwellings built during various periods and existing in 1975 are given in Table 6. For apartment houses and detached houses, the radon concentrations have increased with time. One reason is the increased use of aerated concrete based on alum shale between about 1930 and 1975. Another reason is the decreasing air exchange rates. For the averages the increase in the relative frequency of apartment houses, mostly built of stone materials, is also an important factor.

Estimates have also been made for houses built during the next 10 years for the two alternatives described above. In Table 6 the values for alternative B are not much higher than for alternative A, although the air exchange rates are lower. The explanation is that the assumptions made for regular airing imply that the airing results in a greater decrease of the radon concentration for 0.3 air exchange per hour than for 0.5 per hour.

In reality, it is probable that the values for alternative B are higher than the values given in Table 6 for two reasons. First, the equilibrium factor for radon is greater for low than for high air

TABLE 6

AVERAGE RADON CONCENTRATIONS IN DWELLINGS BUILT DURING VARIOUS PERIODS AND EXISTING IN 1975*

Period	Radon concentration,† Bq/m^3		
	Apartment houses	Detached houses	Averages
Before 1900	29	13	17
1901—1920	29	13	20
1921—1930	29	13	20
1931—1940	31	15	23
1941—1950	40	16	32
1951—1960	79	48	70
1961—1970	91	64	83
1971—1975	120	91	107
1976—1985 est.			
A‡	63	61	62
B§	65	66	65

*Weighted for the frequency of various types of houses and with an occupancy factor at 0.8. An estimate for the period 1975—1986 has been included.

†1 Bq/m^3 $\approx$ 0.027 pCi/liter.

‡In alternative A the newly built houses comply with the 1975 Swedish Building Code regarding the air exchange rates.

§In alternative B the newly built houses will be built as today regarding the air exchange rates.

exchange rates in the rate range concerned. Second, the regular airing is perhaps not as thorough as has been assumed in the calculations, and the influence of the airing is greater for low than for high air exchanges.

Table 7 gives the average concentrations for radon for dwellings existing in 1950, 1975, and 1985. Two alternatives have been given for the houses existing in 1985 based on the assumptions given for the houses built during the period 1976—1985 given in Table 6.

Radiation Doses

For calculation of the absorbed doses in the basal cell layer of the critical bronchial region, 1 rad per working level month (WLM) has been used in the 1977 UNSCEAR report. This value corresponds to 107 μGy per Bq year m^{-3} (45 μrads per pCi hr liter^{-1}) for the conditions indoors and outdoors, when correction has been made for the smaller breathing rate in the average population in comparison with miners during their work.

TABLE 7

AVERAGE RADON CONCENTRATIONS IN DWELLINGS EXISTING IN 1950, 1975, AND ESTIMATES FOR 1985*

Houses existing in	Radon concentration,† Bq/m^3		
	Apartment houses	Detached houses	Averages
1950	34	14	23
1975	71	38	57
1985 est.			
A‡	70	41	58
B§	70	42	58

*An occupancy factor of 0.8 has been assumed.

†1 Bq/m^3 $\approx$ 0.027 pCi/liter.

‡In alternative A the newly built houses comply with the 1975 Swedish Building Code regarding the air exchange rates.

§In alternative B the newly built houses will be built as today regarding the air exchange rates.

Table 8 gives the average absorbed doses in the basal cells of the critical bronchial region from radon and daughter products. Here only alternative A has been given because of the small difference between the alternatives A and B.

TABLE 8

ABSORBED DOSES IN BASAL CELLS OF THE TRACHEOBRONCHIAL REGION FROM RADON AND DAUGHTER PRODUCTS IN DWELLINGS EXISTING IN 1950, 1975, AND 1985*

Houses existing in	Absorbed dose,† mGy/year		
	Apartment houses	Detached houses	Averages
1950	1.8	0.7	1.3
1975	3.8	2.0	3.0
1985 alternative A‡	3.7	2.2	3.1

*The values refer to the average occupants of apartment houses, detached houses, and all types of houses in Sweden. It is assumed that the houses built during the period 1976—1985 will have air exchange rates conforming to the 1975 Swedish Building Code. An occupancy factor at 0.8 has been assumed.

†1 Gy = 100 rads.

‡Nothing is done to the houses existing in 1975.

The absorbed doses for the houses existing in 1975 are more than twice those for the houses of 1950 for both apartments and detached houses. Although aerated concrete based on alum shale has not been in production since 1975, the absorbed doses from houses built during the period 1976—1985 are estimated to be more than twice the dose for all the houses of 1950. This is due both to the more frequent use of stone materials even in detached houses and on changes in the building regulations regarding the ventilation rates and airtightness of the houses.

The anticipated absorbed doses from radon and daughter products for houses existing in 1985 do not differ very much from those for houses existing in 1975, in spite of the fact that aerated concrete based on alum shale has not been produced since 1975. There are two reasons for this. First, the absorbed doses in the houses built during the period 1976—1985 do not differ very much from the houses existing in 1975. Second, even if this difference had been greater, the total doses from the houses existing in 1985 would not have differed very much from the houses of 1975, because the additional dwellings will only form a small part of total number of dwellings.

In reality, however, the difference would be greater because the aim is to improve the airtightness of all houses to obtain 0.5 air exchange per hour. This aim is not quite realistic because it does not seem possible to make old houses so airtight that the air exchange is decreased by more than 0.2 to 0.3 air exchange per hour.

Table 9 gives the collective absorbed doses in the basal cells of the critical bronchial region in the Swedish population from radon and daughter products in dwellings existing in 1950, 1975, and 1985. The population has been assumed to be constant. For the 1985 estimate, three alternatives have been given. The first alternative, A, corresponds to the assumptions in Table 6. The second alternative, C, includes the additional doses resulting from reducing the air exchange rates in all houses to 0.5 per hour but not lower, as specified in the 1975 Swedish Building Code. The values for alternative C in Table 9 are higher than those for the houses existing in 1975. The third alternative, D, is the same as alternative C except that it has been assumed that the air exchange rates have not been reduced in houses built of aerated concrete based on alum shale.

It is also of interest to see to what extent the radiation doses would be expected to imply additional cases of lung cancer (Table 10). For this estimation the risk factor used is that given in 1977 by the International Commission on Radiological Protection (ICRP), 2×10^{-3} Sv^{-1} (1 Sv = 100 rems). For this risk factor the

TABLE 9

COLLECTIVE ABSORBED DOSES FOR THE SWEDISH POPULATION IN BASAL CELLS OF THE CRITICAL BRONCHIAL REGION FROM RADON AND DAUGHTER PRODUCTS IN DWELLINGS EXISTING IN 1950, 1975, AND 1985*

Houses existing in	Absorbed dose,† 10^3 man-Gy/year		
	Apartment houses	Detached houses	Total
1950	7	3	11
1975	18	7	25
1985			
A‡	17	8	25
C§	21	10	31
D¶	20	9	29

*An occupancy factor of 0.8 has been assumed.

†1 Gy = 100 rads.

‡In alternative A the ventilation rates in the houses existing in 1975 are unchanged.

§In alternative C the air exchange rates in the houses existing in 1975 are reduced to the lowest value, 0.5 per hour, as specified in the 1975 Swedish Building Code.

¶In alternative D the assumptions are the same as those in alternative C except that the air exchange rates are not reduced in houses built of aerated concrete based on alum shale.

dose equivalent refers to the average lung, for which the dose equivalent has been estimated to be one-fifth of the value for the basal cells of the critical bronchial region in the 1977 UNSCEAR report. For calculation of dose equivalent, the quality factor 20 given by the ICRP (1977) for alpha radiation has been used.

If, instead, the risk factor from the epidemiological investigations for miners, after correction for the lower breathing rates, is used for the whole population, it would be two to five times greater, according to the 1977 UNSCEAR report. However, there are several reasons why the risk factor found for miners should probably not be used for the whole population. One factor that may indicate a lower risk factor for the whole population than for the miners is the difference in the proportion of smokers.

CONCLUSIONS

The "normal" occurrence of lung cancers has increased in Sweden and is now about 2000 cases per year. The radon daughters

TABLE 10

ANTICIPATED LUNG CANCER CAUSED BY RADON AND DAUGHTER PRODUCTS IN DWELLINGS EXISTING IN 1950, 1975, AND 1985*

Houses existing in	Apartment houses calculated from		Detached houses calculated from		Total calculated from	
	ICRP	Miners	ICRP	Miners	ICRP	Miners
1950	56	140—310	26	65—150	82	205—460
1975	143	360—800	56	140—310	199	500—1100
1985						
A†	139	350—780	64	160—360	203	510—1140
C‡	173	430—970	76	190—430	250	620—1400
D§	162	405—910	74	185—410	236	590—1300

*Two sources have been used for the risk factor: ICRP (1977) and the risk factor extrapolated from miners given in the 1977 UNSCEAR report.

†In alternative A the ventilation rates in the houses existing in 1975 are unchanged.

‡In alternative C the air exchange rates in the houses existing in 1975 are reduced to the lowest value, 0.5 per hour, as specified in the 1975 Swedish Building Code.

§In alternative D the assumptions are the same as those in alternative C except that the air exchange rates are not reduced in houses built of aerated concrete based on alum shale.

in dwellings existing in 1950 may have caused about 80 to 450 of these cases of lung cancer.

The collective absorbed doses in the basal cells of the critical bronchial region has increased by 14×10^3 man-Gy/year (14×10^5 man-rads/year) from 1950 to 1975, implying about 100 to 600 additional cases of lung cancer per year in the Swedish population, the lower value is from the ICRP risk factor and the higher value is from the upper value for the miners. The corresponding values for a million persons are 1.7×10^3 man-Gy/year (1.7×10^5 man-rads/year).

The differences in the collective doses between houses existing in 1950 and those existing in 1975 are greater than would be expected from the decreased air exchanges. The reasons are several. More houses existing in 1975 were built of aerated concrete based on alum shale than in the houses existing in 1950. More people live in apartment houses now than in 1950, and more modern detached houses contain more stone materials than did houses that existed in 1950.

Consequently it is not enough to avoid decreasing the air exchange rate in order to return to the radiation doses for the houses existing in 1950.

Aerated concrete containing alum shale has not been produced since 1975. The collective dose from houses existing in 1985 is nevertheless estimated to be about the same or greater than that in the houses existing in 1975. This is because of the decreased air exchange rates and the large amounts of aerated concrete based on alum shale in the houses remaining from the period up to 1975. This material is mostly found in houses built during the 1950s and the 1960s, and these houses are naturally expected to be in use for many years. However, even in houses built of other materials, the decreased air exchange rates cause significantly higher radiation doses.

The increase of the radiation dose between 1950 and 1975 due to the decrease of the air exchange rates may be as much as 40%. Together with the plans to make old houses more airtight and to reduce the air exchange rates, the collective absorbed doses in the bronchial region could be enhanced by about 12×10^3 man-Gy/year (12×10^5 man-rads/year), implying an additional risk for lung cancer of perhaps 5 to 30% of the "normal" occurrence today.

In reality, the additional risk might be even greater because these calculations only take into account the doses from radon originating from the building materials and the ground. The appreciable contributions from radon in tap water to the radon concentrations in air for the population are being investigated.

Intensive efforts to develop new technical solutions for heating and ventilation systems of dwellings are in progress. Many of these efforts involve recirculation of the air with a minimal addition of fresh air. Some technical solutions under certain circumstances may give rise to substantially increased radon concentrations. This is now being investigated.

REFERENCES

Castrén, O., M. Asikainen, M. Annamäki, and K. Stenstrand, 1977, *High Natural Radioactivity of Bored Wells as a Radiation Hygienic Problem in Finland*, presented at the 4th International Congress of the International Radiation Protection Association, Paris, April 24—30.

Erikson, B. E., B. Löfstedt, G. A. Swedjemark, and B. Håkansson, 1976, *Ventilation Requirements in Single and Many Family Houses* (in Swedish), Report SIB 17:1976, National Institute of Building Research, Gävle, Sweden.

Hagberg, N., and H. Möre, 1976, *The Radioactive Content of Ballast Material for Production of Concrete in Sweden*, Report SSI:1978-029, National Institute of Radiation Protection, Stockholm, Sweden.

Hultqvist, B., 1956, *Studies on Naturally Occurring Ionizing Radiations, with Special Reference to Radiation Doses in Swedish Houses of Various Types*, Kungliga Svenska vetenskapsakademiens handlingar, fjärde serien, Band 6, nr 3, Stockholm.

International Commission on Radiological Protection, 1977, *Recommendations of the International Commission on Radiological Protection*, ICRP Publication 26, Annals of ICRP, Vol. 1, No. 3, Pergamon Press, Inc.

Mjönes, L., 1978, Measurements of Gamma Radiation in Swedish Houses by Means of Mailed $CaSO_4$/Dy Dosimeters, this volume.

Statistical Abstracts of Sweden, 1976 and earlier, published by the Central Bureau of Statistics, Stockholm.

Svanholm, G., 1977, Intong AB, Kumla, Sweden, personal communication.

Svedisol, 1975, It Is Profitable To Insulate More (in Swedish), Jönköping, Sweden.

Swedish Committee on Energy and Environment, 1977, *Energy, Health, and the Environment* (in Swedish), Report SOU 1977:67, The Ministry of Agriculture, Stockholm, Sweden.

Swedish Energy Commission, 1977, *A Report from the Expert Group for Energy Economy*, Stockholm.

Swedjemark, G. A., 1974, Radon in Dwellings, Some Preliminary Results of Continuous Recording (in Swedish), Report SSI:1974-020, National Institute of Radiation Protection, Stockholm, Sweden.

——, 1978, *Radon in Dwellings, Variations Because of Changes in the Ventilation Systems*, unpublished.

United Nations Scientific Committee on the Effects of Atomic Radiation (UNSCEAR), 1977, Sources and Effects of Ionizing Radiation, UNSCEAR, 32nd Session, Suppl. No. 40 (A/32/40), New York.

U. S. Environmental Protection Agency, 1976, *Radiological Quality of the Environment*, Report EPA-520/1-76-010, Washington, D. C.

Vinberg, H. A., 1977, The Changes of the Building Technology During 25 Years—A Study of Statistics of the Production (in Swedish), *Vaeg-Vattenbyggaren*, 11: 15-19.

DISCUSSION

Jonassen: How can you give the concentration of radon daughters as one figure?

Swedjemark: The measurements have been made by pumping air through a filter and measuring the total alpha. The concentration has then been calculated by Kuznet's method.

Nazaroff: You stated that an increase of 12×10^5 man-rads/year might lead to an increase of 5 to 30% in the incidence of lung cancer. Is this an increase in nonsmoking-caused lung cancers or an increase in the total incidence?

Swedjemark: It is an increase in the incidence of lung cancers caused by radon. No correction has been done because of the difference between the frequency of lung cancers in miners and in the population as a whole, partly because there are different opinions of the risk factors for nonsmokers.

Muth: In Germany, in contrast to other countries, we have had no problems up to now with uranium mining and milling, but, with respect to radon in dwellings, we have a situation similar to that in Sweden. In his paper Professor Wachsmann had summarized the results of a countrywide program of measuring indoor and outdoor gamma-ray dose rates. In addition, this year the Federal Ministry of the Interior, which is responsible for radiation protection, will begin a corresponding nationwide program of indoor and outdoor measurements of radon and its decay products. We (H. Muth, B. Global, and G. Keller) measured the emanation rate of different construction materials, including the "chemical gypsum," and found figures between 2×10^{-13} pCi sec m^{-2} (chemical gypsum) and 2×10^{-17} pCi sec m^{-2} (Dutch clinker). The radium content of chemical gypsum is about 20 pCi/g. For rooms with such materials in the walls and ceilings, the bronchi and trachea of the lungs receive estimated annual doses of up to 1 rem or more (a quality factor of 10 being used for alpha particles), if we use the measured data of the emanation rate and make special assumptions concerning the ventilation rate of the dwellings, percentage of the equilibrium between radon and its decay products, and other factors that cannot be given here in detail. These are preliminary results that can be corrected and amended later, according to the results of the indoor measurements of radon.

Measurements of Radon-222 Concentrations in Dwellings in Great Britain

K. D. CLIFF
National Radiological Protection Board, Harwell, Didcot, Oxon., England

ABSTRACT

The rate of emanation of ^{222}Rn from room surfaces into room air was assessed in living rooms of 87 dwellings in England and Scotland. The mean rate of emanation of ^{222}Rn found was 0.54 pCi liter^{-1} hr^{-1}, but for rooms in which there was some exposed stone the mean was 2.5 pCi liter^{-1} hr^{-1}. On the basis of a mean emanation rate of 0.54 pCi liter^{-1} hr^{-1}, it is concluded that the current population exposure rate to the short-lived daughters of ^{222}Rn for the population of Great Britain is 0.15 WLM/year. This exposure rate is dependent on the ventilation rates in dwellings and will increase as ventilation rates are reduced to conserve energy used for space heating.

In the sixteenth century Agricola (1556) wrote that miners in certain European communities were ". . . dying from the pestilential air they breath; sometimes their lungs rot away." Studies at the end of the nineteenth century and early twentieth century revealed that between 50 and 75% of deaths among working miners at Schneeberg, Germany, and Joachimstal, Czechoslovakia, was due to lung cancer (Harting and Hesse, 1879; Peller, 1939). Beginning in 1924 the noble gas ^{222}Rn was suspected of causing lung cancer in miners (Ludewig and Lorenser, 1924; Sikl, 1930; Saupe, 1933), but in 1951 Bale (unpublished memoranda quoted in Stewart and Simpson, 1963) demonstrated that 99% of the dose delivered to lung was due to the short-lived daughters of ^{222}Rn. These daughters are ^{218}Po (half-life, 3.05 min), ^{214}Pb (half-life, 26.8 min), ^{214}Bi (half-life, 19.7 min), and ^{214}Po (half-life, 1.6×10^{-4} sec). In view of the short half-life of ^{214}Po, it is invariably found in equilibrium with ^{214}Bi, and the alpha emission from ^{214}Po may be regarded as a prompt alpha

emission from ^{214}Bi. The hazards of exposure to the short-lived daughters of ^{222}Rn were confirmed by an intensive study of the mortality of uranium miners in the United States (Lundin, Wagoner, and Archer, 1971) which revealed a strong correlation between the excess incidence of lung cancer and exposure to high concentrations of radon daughter products.

Uranium occurs widely in the earth's crust and consequently occurs in many materials used by the building industry. The fifth daughter product of ^{238}U is ^{226}Ra and this nuclide is also found in building materials and acts as a source for its decay product ^{222}Rn, a gas which diffuses from soils and building materials into room air where it and its daughters are available for inhalation. The short-lived daughters attach to dust particles in the air and these, when deposited in the lung, may deliver a high dose to cells of the bronchial epithelium following the subsequent alpha decay of the attached ^{218}Po and ^{214}Po. Thus the population as a whole is also exposed to the short-lived daughters of radon. It is of interest to determine the current levels of this exposure in order to assess the implications of using waste materials that have a higher uranium concentration than traditional materials because of changes in building practice. One such material considered for use is gypsum, a by-product of the phosphate fertilizer industry. The effects of the use of by-product gypsum on the radon daughter concentrations in dwellings has been studied by O'Riordan et al. (1972), but at the time of this study no extensive survey of radon daughter concentrations in Great Britain had been made. To rectify this situation, Duggan and Bradford (1974) published the results of a preliminary survey of radon daughters in dwellings, and the work reported here is the result of an extension of the survey initiated by those authors.

METHOD OF MEASUREMENT

The radon concentration measured in both indoor and outdoor air is known to be subject to large temporal variation (Steinhausler, 1975). The concentrations of ^{222}Rn and its short-lived daughters within a room are predominantly determined by the rate of emanation of ^{222}Rn from room surfaces into the room air and the ventilation rate existing in the room. The emanation rate is mainly dependent on the radium content and porosity of the materials used in the construction of the building and of the ground beneath it. The effects of ventilation will be considered later. The measurements made during the survey reported here were designed to measure the rate at which ^{222}Rn was emanating from room

surfaces into room air in picocuries of ^{222}Rn per liter of room air per hour. The direct measurement of radon gas concentrations at environmental levels is not easily accomplished with readily transportable equipment, and it was found easier to measure the ^{218}Po concentration. Measurements of ^{218}Po activity concentrations were made with the Radon Daughter Monitor (James and Strong, 1973) and the method of calculation described by Cliff (1978b).

It can be shown (Cliff, 1978a) that the rate of emanation of ^{222}Rn can be found from

$$K = j\left(1 + \frac{j}{\lambda_A}\right)(C_A - C_A^1) \quad \text{pCi liter}^{-1}\ \text{hr}^{-1} \tag{1}$$

where j = ventilation rate in room changes per hour, hr^{-1}

C_A = activity concentration of ^{218}Po within the room, pCi $liter^{-1}$

C_A^1 = activity concentration of ^{218}Po in the outside air, pCi $liter^{-1}$

K = radon output of the room

and Eq. 1 is valid only if the air interchange occurs solely between the room and the outside air. To ensure that this was the case, rooms on the windward side of each dwelling were chosen for study. Equation 1 is also true only in the steady state, i.e., when the rate of the production of radon into the room is equal to the rate of loss resulting from radioactive decay and ventilation. The measurement of environmental concentrations of radon daughters is subject to statistical uncertainties that decrease as the concentrations increase. Thus, to reduce these uncertainties to a minimum, doors and windows were shut before measurements were made, and the concentrations of the nuclides within the room were allowed to increase. Some 2½ hr must elapse between the reduction in ventilation and making the measurements if it is to be assumed that conditions have sensibly reached the steady state (Cliff, 1978a).

ORGANIZATION OF THE SURVEY

Since the main aim of this survey was to estimate the population exposure to the short-lived daughters of radon, the dwellings chosen were situated mainly in such areas of large population density as London, Leeds, Birmingham, Glasgow, and Edinburgh. In addition, some dwellings were measured at rural locations and some in areas where the ^{222}Rn concentrations might be high because of the granitic subsoil and the use of granite as a building material; such

areas were Cornwall and Aberdeen. Where possible, dwellings were chosen which were typical of the housing stock for that area, although there was a higher proportion of dwellings of recent (post 1935) construction in the survey than in the total housing stock of Great Britain. Measurements were made in a total of 87 dwellings.

The main results of the measurements are summarized in the following sections. A more detailed description of the results has been published elsewhere (Cliff, 1978a).

RESULTS

The range of radon outputs measured was large (from 0.012 pCi liter^{-1} hr^{-1} to 5.5 pCi liter^{-1} hr^{-1}), and the distribution was unsymmetrical. For this reason the distribution is shown on a logarithmic scale in Fig. 1. The median value of all the results is 0.32 pCi liter^{-1} hr^{-1} with a geometric standard deviation of 3.1. The mean for all the measurements is 0.60 pCi liter^{-1} hr^{-1}, but the highest value recorded of 5.5 pCi liter^{-1} hr^{-1} (which is nearly twice the next highest value of 2.8 pCi liter^{-1} hr^{-1}) occurred in a dwelling situated in an area of low population density, and this dwelling was constructed from local granite known to contain an elevated radium concentration. Such dwellings form a very low proportion of the housing stock of Great Britain, and for the purposes of estimating population exposure this value was elimi-

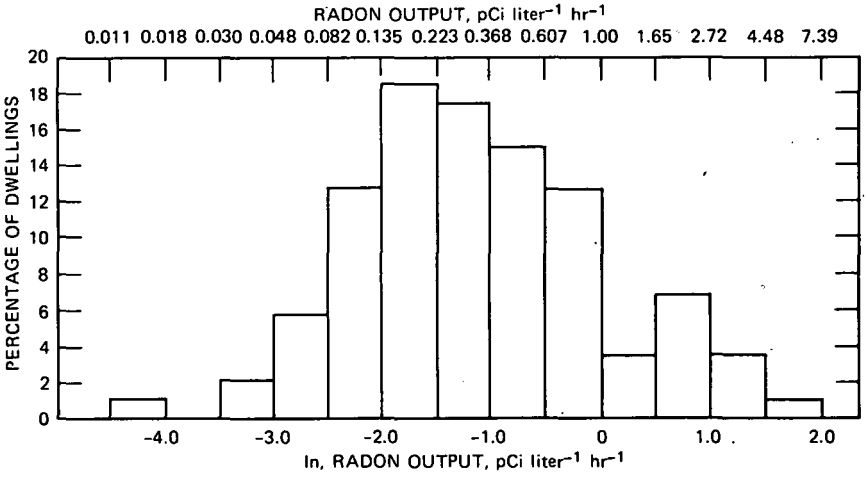


Fig. 1 Distribution of radon outputs.

nated. The removal of this one high value reduces the mean value to 0.54 pCi liter^{-1} hr^{-1}. When the dwellings surveyed are categorized by age or style (house, bungalow, or flat), there are no significant differences between the groups. As is to be expected, the factor most influencing the radon output of the room measured is the material used for the inner walls of the room. Those rooms having inner walls made of stone and plaster exhibit a higher radon output than those composed of other materials, such as brick and plaster, lathe and plaster, or plaster board. In particular, all rooms surveyed that had exposed stone within them had radon outputs which were elevated compared with rooms of similar construction without the exposed stone. The range of radon outputs found in rooms with some exposed stone surfaces is 0.80 pCi liter^{-1} hr^{-1} to 5.5 pCi liter^{-1} hr^{-1} with a mean of 2.5 pCi liter^{-1} hr^{-1}.

INTERPRETATION OF THE RESULTS

In a discussion of exposure to the short-lived daughters of radon, the usual unit of concentration for radon daughters is the working level (WL), which is defined as any combination of the short-lived daughters of radon (^{218}Po, ^{214}Pb, ^{214}Bi, and ^{214}Po) in 1 liter of air which will result in the ultimate emission of 1.3×10^5 MeV of alpha energy. Exposure is then measured in working level months (WLM) where the working month is taken as 170 hr. Thus exposure at 1 WL for 170 hr results in 1 WLM of exposure.

The mean radon output for dwellings in Great Britain is taken as 0.54 pCi liter^{-1} hr^{-1} on the basis of the survey results presented here, but the actual concentrations of the short-lived daughters of radon within a room with a given radon output is strongly dependent on the ventilation rate. Table 1 shows the activity concentrations of the short-lived daughters in a room with a radon output of 0.54 pCi liter^{-1} hr^{-1} when the incoming air has a radon concentration of 0.07 pCi/liter with activity ratios ^{222}Rn : ^{218}Po : ^{214}Pb : ^{214}Bi = 1 : 1 : 0.8 : 0.6. These conditions for incoming air are typical for outside air as measured during this survey and agree with values quoted in the literature (Davies and Forward, 1970; Harley, 1973). Changes in the equilibrium conditions existing in the incoming air have little effect on the daughter concentrations within the room when the ventilation rate is below 1.5 room changes per hour. Ventilation rates measured in closed living rooms were often below 0.7 room changes per hour, and these are probably typical values during the winter heating season. Warren (1975) has reported the results of measurements of whole-house ventilation rates in six

TABLE 1

Radon Daughter Concentrations Within a Room Emanating 0.54 pCi liter^{-1} hr^{-1} for Various Ventilation Rates

Ventilation rate, hr^{-1}	Concentration, pCi/liter			Working level, WL
	^{218}Po	^{214}Pb	^{214}Bi, ^{214}Po	
0.1	5.07	4.76	4.55	0.0471
0.2	2.64	2.35	2.15	0.0230
0.5	1.10	0.85	0.69	0.0081
1.0	0.57	0.37	0.26	0.0035
1.5	0.39	0.23	0.15	0.0022
2.0	0.31	0.17	0.11	0.0016

dwellings and found the range to be 0.3 to 1.35 air changes per hour. If we assume a mean ventilation rate of 1 room change per hour then assume that people spend 80% of their time within buildings (occupancy factor 0.8, UNSCEAR, 1977), the mean population cumulative exposure rate is 0.144 WLM/year from exposure within buildings. The total mean cumulative exposure rate, including that received while in the open air, is then 0.15 WLM/year. The interpretation of this exposure rate must be approached with caution. Jacobi (1976) reviewed the data for the increased incidence of lung cancer in uranium and other miners and has derived a risk factor for this group of 200 excess lung cancers per 10^6 persons per WLM. Reissland (1977) has applied this risk estimate to the population exposure derived from this survey and, on this basis, has predicted the incidence of lung cancer in women in Great Britain. As shown in Table 2, the predicted incidence exceeds the observed incidence for women of all ages below 40. This shows that the risk estimate derived from exposure of miners is unlikely to be applicable to the exposure of the population as a whole to radon daughters from building materials.

CONCLUSION

The mean population exposure to the short-lived daughters of ^{222}Rn derived from this survey is 0.15 WLM/year, based on the assumption of a mean ventilation rate in dwellings of 1 room change per hour over the year. With the inevitable rise in energy costs and the consequent reduction in ventilation rates to reduce the costs of heating dwellings, this exposure will increase.

TABLE 2

Predicted and Observed Incidence of Lung Cancer in Women in Great Britain*

Age, years	Number of lung cancers per 100,000 persons		
	Observed incidence	Predicted incidence†	
		1 WLM/year	0.15 WLM/year
20—24	0.1	2.4	0.36
25—29	0.3	6.4	0.96
30—34	1.0	10.4	1.6
35—39	1.9	14.4	2.2
40—44	6.4	18.2	2.7

*Data from J. A. Reissland, 1977.
†Based on 200 excess cancers per million persons per WLM.

REFERENCES

Agricola, G., 1556, *De re Metallica,* translated from the first Latin edition by H. C. Hoover and L. H. Hoover, Dover Publications, Inc., 1950, New York.

Cliff, K. D., 1978a, Assessment of Airborne Radon Daughter Concentrations in Dwellings in Great Britain, *Phys. Med. Biol.,* 23: 696-711.

——, 1978b, The Measurement of Low Concentrations of Radon-222 Daughters in Air, with Emphasis on RaA Assessment, *Phys. Med. Biol.,* 23: 55-65.

Davies, B. L., and J. Forward, 1970, Measurement of Atmospheric Radon in and out of Doors, *Health Phys.,* 19: 136.

Duggan, M. J., and G. F. Bradford, 1974, The Exposure of the General Population to Airborne Radon and Its Daughters, in *Radiation Protection Measurement: Philosophy and Implementation,* Selected Papers of the International Symposium, Aviemore, Scotland, June 2—6, 1974 (copies available from K. D. Cliff, National Radiological Protection Board).

Harley, J. H., 1973, Environmental Radon, in *Symposium on Noble Gases,* Las Vegas, Sept. 24—28, 1973, R. E. Stanley and A. A. Moghissi (Eds.), Report CONF-730915, pp. 109-114, Environmental Protection Agency's National Environmental Research Center, Las Vegas, and the University of Nevada, Las Vegas.

Harting, F. H., and W. Hesse, 1879, Der Lungenkrebs, die Bergkrankheit in den Schneeberger Gruben, *Vierteljahrsschr. gerichtl. off. Med.,* (N.F.) 30: 296-309; 31: 102-129.

Jacobi, W., 1976, Interpretation of Measurements in Uranium Mines: Dose Evaluation and Biomedical Aspects, in *Personal Dosimetry and Area Monitoring Suitable for Radon and Daughter Products,* Proceedings of the NEA Specialist Meeting, Elliot Lake, Canada, Oct. 4—8, 1976, Report CONF-761071, Nuclear Energy Agency, Organization for Economic Co-operation and Development, Paris, France.

James, A. C., and J. C. Strong, 1973, A Radon Daughter Monitor for Use in Mines, in *Proceedings of the Third International Congress of the International Radiation Protection Association,* Washington, D. C., Sept. 9—14,

1973, pp. 932-938, W. S. Snyder (Ed.), USAEC Report CONF-730907-P2, International Radiation Protection Association.

Ludewig, P., and E. Lorenser, 1924, Unterschung der Grubenluft in den Schneeberger Gruben auf den Gehalt an Radiumemanation, *Z. Phys.*, 22: 178-185.

Lundin, F. E., J. K. Wagoner, and V. E. Archer, 1971, *Radon Daughter Exposure and Respiratory Cancer, Quantitative and Temporal Effects*, National Institute of Occupational Safety and Health, and National Institute of Environmental Health Sciences, Joint Monograph No. 1, U. S. Department of Health, Education, and Welfare.

O'Riordan, M. C., M. J. Duggan, W. B. Rose, and G. F. Bradford, 1972, The Radiological Implications of Using By-Product Gypsum as a Building Material, National Radiological Protection Board Report R-7, Her Majesty's Stationery Office, London.

Peller, S., 1939, Lung Cancer Among Mine Workers in Joachimstal, *Hum. Biol.*, 11: 130-143.

Reissland, J. A., 1977, *The Interpretation of Radon-Daughter Measurements in Houses*, NRPB Memorandum Series M-38, National Radiological Protection Board, Harwell, Didcot, Oxon., England.

Saupe, E., 1933, Über die Beziehungen zwischen, Lungenkrebs und Staublungenerkrankung, *Z. Med.*, 54: 825-838.

Sikl, H., 1930, Über den Lungenkrebs der Bergleute in Joachimstal (Tschechoslowakia), *Z. Krebsforsch.*, 32: 609-613.

Steinhausler, F., 1975, Long Term Measurements of ^{222}Rn, ^{220}Rn, ^{214}Pb and ^{212}Pb and Their Dependence on Meteorological Parameters, *Health Phys.*, 29: 705-713.

Stewart, C. G., and S. D. Simpson, 1963, The Hazards of Inhaling Radon-222 and Its Short-Lived Daughters: Consideration of Proposed Maximum Permissible Concentration in Air, in *Radiological Health and Safety in Mining and Milling of Nuclear Materials*, Symposium Proceedings, Vienna, 1963, pp. 333-357, STI/PUB/78, Vol. 1, International Atomic Energy Agency, Vienna, 1964.

UNSCEAR, 1977, *Sources and Effects of Ionizing Radiation*, United Nations Scientific Committee on the Effects of Atomic Radiation, 1977, Report to the General Assembly, p. 73.

Warren, P. R., 1975, Natural Infiltration Routes and Their Magnitude in Houses, Part I: Preliminary Studies of Domestic Ventilation, in *Proceedings of the Conference on Controlled Ventilation—Its Contribution to Lower Energy Use and Improved Comfort, Sept. 24, 1975*, Aston University, Birmingham, England, published August 1976.

BIBLIOGRAPHY

Aprilesi, G., A. Loria, G. Magnoni, S. Marseguerra, S. Morelli, and M. R. Rivasi, 1978, Absolute Estimation of Radon Daughter Concentrations in Air by α-Spectrometry, *Nucl. Instrum. Methods*, 148: 187-194.

Auxier, J. A., 1976, Respiratory Exposure in Buildings Due to Radon Progeny, *Health Phys.*, 31: 119-125.

——, K. Becker, E. M. Robinson, D. R. Johnson, R. H. Boyett, and C. H. Abner, 1971, A New Radon Progeny Personnel Dosimeter, *Health Phys.*, 21: 126-128.

——, W. H. Shinpaugh, G. D. Kerr, and D. J. Christian, 1974, Preliminary Studies of the Effect of Sealants on Radon Emanation from Concrete, *Health Phys.*, 27: 390-392.

Barton, C. J., R. E. Moore, and P. S. Rohwer, 1973, *Contribution of Radon in Natural Gas to the Natural Radioactivity Dose in Homes*, USAEC Report ORNL-TM-4154, Oak Ridge National Laboratory, NTIS.

Becker, K., 1969, Alpha Particle Registration in Plastics and Its Application for Radon and Neutron Personnel Dosimetry, *Health Phys.*, 16: 113-123.

Caruthers, L. T., and A. W. Waltner, 1975, Need for Standards for Natural Airborne Radioactivity (Radon and Daughters) Concentrations in Modern Buildings, *Health Phys.*, 29: 814-817.

Chapuis, A., A. Lopez, J. Fontan, and G. J. Madelaine, 1973, Determination de la fraction d'activite existant sous form de RaA non attache dans l'atmosphere d'une mine d'uranium, *Health Phys.*, 25: 59-65.

Costa-Ribeiro, C., J. Thomas, R. T. Drew, McD. E. Wrenn, and M. Eisenbud, 1969, A Radon Detector Suitable for Personnel or Area Monitoring, *Health Phys.*, 17: 193-198.

Countess, R. J., 1976, ^{222}Rn Flux Measurements with a Charcoal Cannister, *Health Phys.*, 31: 455-456.

Culot, M. V. J., H. G. Olson, and K. J. Schiager, 1976, Effective Diffusion Coefficient of Radon in Concrete, Theory and Method for Field Measurements, *Health Phys.*, 30: 263-270.

Duggan, M. J., and D. M. Howell, 1968, A Method for Measuring the Concentration of the Short-Lived Daughter Products of Radon-222 in the Atmosphere, *Int. J. Appl. Radiat. Isot.*, 19: 865-870.

——, and D. M. Howell, 1969, The Measurement of the Unattached Fraction of Airborne RaA, *Health Phys.*, 17: 423-427.

——, and D. M. Howell, 1969, Relationship Between the Unattached Fraction of Airborne RaA and the Concentration of Condensation Nuclei, *Nature*, 224: 1190-1191.

Frank, A. L., and E. V. Benton, 1977, Radon Dosimetry Using Plastic Nuclear Track Detectors, *Nucl. Track Detect.*, 1: 149-179.

Gels, G. L., and P. H. Bedrosian, 1969, Leak Testing Sealed Sources of Radium-226 by Radon Photography, *Health Phys.*, 16: 497-501.

George, A. C., 1972, Indoor and Outdoor Measurements of Natural Radon and Radon Decay Products in New York City Air, in *The Natural Radiation Environment II*, Vol. 2, Symposium Proceedings, Houston, Tex., Aug. 7—11, 1972, J. A. S. Adams, W. M. Lowder, and T. F. Gesell (Eds.), ERDA Report CONF-720805, Pt. 2, pp. 741-750, Rice University, and the University of Texas, Houston, NTIS.

——, 1972, Measurement of the Uncombined Fraction of Radon Daughters with Wire Screens, *Health Phys.*, 23: 390-392.

Groer, P. G., R. D. Evans, and D. A. Gordon, 1973, An Instant Working Level Meter, *Health Phys.*, 24: 387-395.

Haque, A. K. M. M., A. J. L. Collinson, and C. O. S. Blythebrooke, 1965, Radon Concentration in Different Environments and the Factors Influencing It, *Phys. Med. Biol.*, 10: 505-514.

James, A. C., G. F. Bradford, and D. M. Howell, 1972, Collection of Unattached RaA Atoms Using a Wire Gauze, *Aerosol Sci.*, 3: 243-254.

Jonasson, N., 1975, On the Effect of Atmospheric Pressure on the Radon-222 Concentration in Unventilated Rooms, *Health Phys.*, 29: 216-220.

——, and W. E. Clements, 1974, Determination of Radon-222 Concentrations by an Integrated Count Method, *Health Phys.*, 27: 347-351.

——, and E. I. Hayes, 1974, The Measurement of Low Concentrations of Short-Lived Radon-222 Daughters in the Air by Alpha Spectrometry, *Health Phys.*, 26: 104-110.

——, and E. I. Hayes, 1974, A Correction When Measuring ^{222}Rn Daughter Concentrations by Alpha Spectroscopy of Filter Samples, *Health Phys.*, 27: 310-313.

——, and J. P. McLaughlin, 1976, The Effect of RaB Recoil Losses on Radon Daughter Measurements, *Health Phys.*, 30: 234-238.

——, and J. P. McLaughlin, 1976, *Radon in Indoor Air I*, Research Report 6, Laboratory of Applied Physics I, Technical University of Denmark.

——, and J. P. McLaughlin, 1977, *Radon in Indoor Air II*, Research Report 7, Laboratory of Applied Physics I, Technical University of Denmark.

Kriston, J., and I. Kobal, 1973, A Modified Scintillation Cell for the Determination of Radon in Uranium Mine Atmospheres, *Health Phys.*, 24: 103-104.

Kritidis, P., I. Uzunov, and L. Minev, 1977, Precision Alpha-Counting Methods for Determination of Radon Daughters in Air, *Nucl. Instrum. Methods*, 143: 299-305.

Mayya, Y. S., 1976, Revision of Raghavayya and Jones Data on the Radon Decay Products in Mine Air, *Health Phys.*, 31: 380-382.

McLaughlin, J. P., 1972, The Attachment of Radon Daughter Products to Condensation Nuclei, *Proc. R. Ir. Acad., Sect. A*, 72(4): 53-70.

Newstun, H., L. D. Cohen, and R. Krablin, 1971, An Automated Radon Sampling System, *Atmos. Environ.*, 5: 823-831.

Noguchi, M., and H. Wakita, 1977, A Method for Continuous Measurement of Radon in Groundwater for Earthquake Prediction, *J. Geophys. Res.*, 82: 1353-1357.

Ogden, T. L., 1974, A Method of Measuring the Working-Level Values of Mixed Radon and Thoron Daughters in Coal Mine Air, *Ann. Occup. Hyg.*, 17: 23-24.

——, 1977, Radon and Thoron Working-Levels from Ordinary Industrial Hygiene Dust Samples, *Ann. Occup. Hyg.*, 20: 49-53.

Parthasarathy, K. S., 1976, Decay Products of ^{222}Rn in the Living Environment, *Health Phys.*, 31: 187-188.

Pensko, J., 1975, Somatic and Genetic Risks for Population Due to the Natural Radiation and Type of Building Development in Poland, *Kerntechnik*, 17: 533-536.

Pohl, E., and J. Pohl-Ruling, 1976, Determination of Environmental or Occupational ^{222}Rn in Air and Water and ^{226}Ra in Water with Feasible and Rapid Methods of Sampling and Measurement, *Health Phys.*, 31: 343-348.

Prichard, H. M., and T. F. Gesell, 1977, Rapid Measurement of ^{222}Rn Concentrations in Water with a Commercial Liquid Scintillation Counter, *Health Phys.*, 33: 577-581.

Raghavayya, M., and J. H. Jones, 1974, A Wire Screen—Filter Combination for the Measurement of Fractions of Unattached Radon Daughters in Uranium Mines, *Health Phys.*, 26: 417-429.

Rangarajan, C., and S. Gopalakrishnan, 1973, The Estimation of the Relative Concentrations of Short-Lived Radon Daughters by Gamma Measurement, *Health Phys.*, 24: 433-436.

Roberts, P. B., and B. L. Davies, 1966, A Transistorized Radon Measuring Equipment, *J. Sci. Instrum.*, 43: 32-35.
Rolle, R., 1972, Rapid Working Level Monitoring, *Health Phys.*, 22: 233-238.
Schiager, K. J., 1977, The 3R-WL Working Level Survey Meter, *Health Phys.*, 33: 595-604.
Sill, C. W., 1969, An Integrating Air Sampler for Determination of ^{222}Rn, *Health Phys.*, 16: 379-381.
Strong, J. C., and M. J. Duggan, 1973, The Effect of the Presence of Thoron Daughters on the Measurement of Radon Daughter Concentrations, *Health Phys.*, 25. 299-300.
Thomas, J. W., 1972, Measurement of Radon Daughters in Air, *Health Phys.*, 23: 783-789.
——, and P. C. LeClare, 1970, A Study of the Two Filter Methods for Radon-222, *Health Phys.*, 18: 113-122.
Toth, A., 1972, Determining the Respiratory Dosage from RaA, RaB, and RaC Inhaled by the Population of Hungary, *Health Phys.*, 23: 281-289.
Wilkening, M. H., and D. E. Watkins, 1976, Air Exchange and ^{222}Rn Concentrations in the Carlsbad Caverns, *Health Phys.*, 31: 139-145.

DISCUSSION

Ellett: You have shown the fallacy of applying absolute risk estimates based on male to a female population. However, Jacobi also calculated a relative risk (100% increase per 100 WLM) based on early miner data. Have you calculated the increased relative risk to women based on female lung cancer mortality data?

Cliff: I have not calculated the relative risk for women because this concept is population dependent and using the relative risk derived from a male population and applying it to a female population is just as fallacious as using absolute risk.

Jonassen: Your average radon output of 0.54 pCi liter^{-1} hr^{-1} will with an 0.5 volume/surface ratio correspond to an exhalation rate of 1300 atoms m^{-2} s^{-1}, which is what we find for alum shale aerated concrete. Would you care to comment on that?

Cliff: If we consider that the only source of emanation is room surfaces, then I agree that 0.54 pCi liter^{-1} hr^{-1} is supported in a room of an 0.5 volume/surface ratio by an exhalation rate of 1300 atoms m^{-2} sec^{-1}. However, the model used to derive emanation rate does not assume this. All the model states is that within the room there is a source or sources which together result in the injection of 0.54 pCi of ^{222}Rn per liter of room air per hour. Most of the rooms investigated were situated on the ground (first) floor where a major source would be ingress through cracks in the floor from the subsoil. However, since rooms with exposed stone surfaces yielded generally higher radon emanation rates it would appear that exposed stone is a large contributory factor. The fact that exposed stone usually provided only a small proportion of room surface area

suggests that further investigation of the sources of radon in room air is required.

Wrenn: Does your calculation of efflux rate (pCi/hr^{-1}) depend on the assumption that the only mechanism of removal of RaA is by dilution ventilation? If so, how might this affect your results?

Cliff: My calculation does assume that the removal of RaA and other daughters is purely by ventilation and radioactive decay. Since ventilation rate was recorded at the time that measurements were made of RaA, RaB, and RaC, I have looked at 18 of the results and calculated the equilibrium factor on the basis of the ventilation rate measured and compared it with the equilibrium factor actually measured from the daughter concentrations actually found. The mean of the ratios of these two results was 0.95 for the 18 cases studied. In five of the cases, the equilibrium factor derived from the daughter concentrations measured was lower than that predicted with the ventilation rate used as the sole means of daughter removal. This indicates that convective diffusion of daughters to walls may be a method of removal. However, the statistical uncertainty in the ratio derived from the two equilibrium factors calculated was usually about 50%. Thus this work is inconclusive, and I intend to carry out further studies on the effects of plateout of daughters onto walls in dwellings.

Wrenn: (Comment) Some years ago we showed that radon daughters in enclosed spaces (mine areas actually) could decrease by moving air (i.e., convective diffusion of aerosols and daughters to walls). This was very dependent on the concentration of condensation nuclei, and the effectiveness of removal increased dramatically with decreasing condensation nuclei concentration.

Jonassen: Both radon- and decay-product measurements showed pronounced annual variations, in general, with higher values during periods of increased atmospheric stability (e.g., inversion layers) and vice versa.

For the network of uninhabited control stations ventilation conditions were defined since, during the course of the investigation, all openings (doors, windows) were closed and indoor atmospheric temperature and humidity were monitored. At the other selected inhabited test sites, measurements were carried out several times at different seasons and different ventilation conditions to account for the living habits of the inhabitants.

Cliff: The rate of ventilation was monitored indirectly via continuous measurements of atmospheric temperature and relative humidity indoors as well as outdoors.

Participant (EPA): A quality factor of 10 was used for alpha-dose calculations.

The Distribution of Ambient Radon and Radon Daughters in Residential Buildings in the New Jersey–New York Area

A. C. GEORGE and A. J. BRESLIN
Environmental Measurements Laboratory, U. S. Department of Energy,
New York, New York

ABSTRACT

The distribution of radon (^{222}Rn) and radon daughter concentrations in 21 New Jersey and New York residences was investigated over a 2-year period. Most of the residences were single-family, one- or two-story buildings of wood frame or brick construction. Typically, 1-week time-integrated measurements of radon concentration and working level were obtained simultaneously on several floors of a building, and these measurements were repeated periodically over the study period to yield estimates of annual mean concentrations.

For additional information with which to calculate lung dose, unattached fractions and particle size distributions of radon daughters were measured in a few of the residences. Also, the radium content of surrounding ground, radon exhalation from cellar floors, and radon concentration in water supplies were measured at most residences to evaluate sources of airborne radon.

Annual mean air concentrations varied 10-fold among the residences and correlated reasonably well with radon exhalation rates, although radon in water also was found to contribute to air radon. On the average, concentrations on first floors were one-half of the concentrations in cellars and about equal to concentrations on second floors. In all cases, indoor concentrations exceeded concentrations outside. The average fraction of unattached radon daughters was 0.07, and the average activity median diameter of attached daughters was 0.12 μm. The average annual bronchial dose calculated for occupants was 150 mrads and ranged from 42 to 420 mrads.

The United Nations Scientific Committee on the Effects of Atomic Radiation (UNSCEAR) (1977) attributes a substantial part of the public's natural radiation dose to the inhalation of radon daughters, the solid, short-lived decay products of radon gas. The annual per capita dose to the whole lung is 110 mrads, of which 30 mrads is from ^{222}Rn with daughters. Moreover, the alpha radiation from the

radon daughters is considered to have a higher relative biological effectiveness than the beta and gamma radiations, which cause more than 90% of the dose in other tissues.

Most of the exposure leading to this component of lung dose occurs indoors because the radon concentrations within buildings are usually higher than outside air. Therefore accurate information on concentrations of radon in buildings is vital for an accurate assessment of natural radiation dose. Several investigations have been made of indoor radon and radon daughter concentrations (Hultqvist, 1956; Steinhausler, 1975; Yeates, Goldin, and Moeller, 1972; Toth, 1972), but results are difficult to interpret with respect to public exposures. In some cases the data were obtained in artificial conditions intended to maximize concentrations or were based on few measurements of brief duration that may not reflect average concentrations. Collectively the reported concentrations cover an extremely wide range since they depend on many factors, including building size, construction materials, ventilation rate, and the radium content of the ground. From the published data, UNSCEAR assumes the average indoor radon concentration to be 1 pCi/liter, but the actual exposures of individuals or groups may vary by a large factor.

There is a relatively small margin between UNSCEAR's estimate of average indoor radon concentration and the limits prescribed for the general public by standards and regulatory organizations. For example, one-tenth of the limit set by the International Commission on Radiological Protection (ICRP) (1959) for occupational exposure would be 3 pCi/liter, and the Office of the U. S. Surgeon General (1970) recommended a 0.01 working level (WL),* which is roughly equivalent to 2 pCi/liter of radon at ordinary conditions, for the special circumstances in Grand Junction, Colo., where uranium ore tailings were used in building construction. Because of the small difference between prescribed limits and normal concentrations, inexact knowledge about normal concentrations can cause practical difficulties in applying the limits. One difficulty arises in determining a suitable background to subtract from the limits which, ordinarily, exclude "natural radiation." Another difficulty arises in connection with the "as low as practicable" principle: there is a risk of striving for an unattainably low concentration if natural background is assumed to be lower than its actual value. Therefore there are practical as well as scientific needs for reliable data.

*The working level is any combination of radon daughters in 1 liter of air which will ultimately release 1.3×10^5 MeV of alpha energy during decay to ^{210}Pb (RaD).

To provide accurate information on natural airborne radioactivity, we have been measuring radon and related variables in the metropolitan New York area for a number of years. The initial phase of our investigation was reported by George (1972) in *The Natural Radiation Environment II.* Detailed measurements were obtained on radon and radon daughter concentrations and on the physical characteristics of radon daughters for periods of a few days at each of several indoor and outdoor locations. The considerable time variation in concentrations observed in the study convinced us that time-averaging instrumentation would be needed for systematic monitoring of exposure. With the subsequent development of suitable instruments, measurements were begun and have continued for about 2 years in a small group of residences in New York and New Jersey. Although initiated primarily as a pilot study to test instruments and procedures, enough information has been acquired to estimate average exposures and to ascertain the magnitude of the possible sources of radon in these buildings.

LOCATION AND TYPES OF BUILDINGS

The 21 buildings in this study, residences of laboratory staff and acquaintances, were chosen for accessibility. They were about evenly divided between New Jersey and New York and were all within a radius of 35 miles from Manhattan, as shown in Fig. 1. Most of the buildings were single-family residences with full cellars. Two-thirds of the buildings were of wood-frame construction, and the remainder were of brick construction. One apartment building and two multifamily houses were included. Heating was by hot-air or hot-water systems, fueled either by gas or oil. All buildings were occupied normally during the study period.

MONITORING PROCEDURES

Annual mean concentrations of radon and of radon daughters (in terms of the WL) were determined in each building by periodic, week-long measurements, distributed over 1 to 2 years. Typically, radon concentration and WL measurements were obtained simultaneously on two or three floors (e.g., cellar, first floor, second floor); outside air also was measured in some cases.

The type and scope of measurements was broadened during the study as more instrumentation became available. Primary attention was initially focused on cellars, which were considered to be

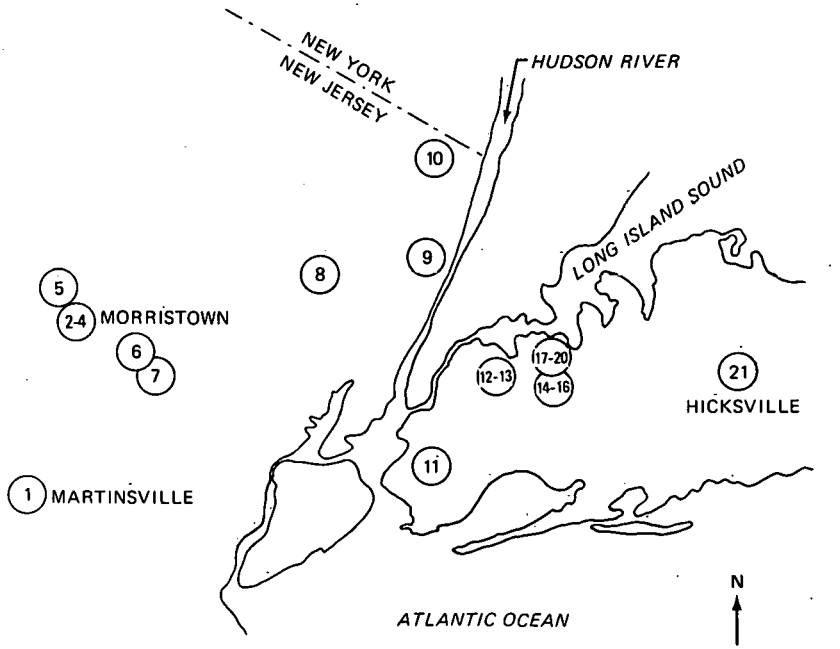


Fig. 1 Geographical distribution of residences.

indicative of source strengths; later, simultaneous measurements on other floors were begun. In addition, the initial dozen buildings were expanded gradually as more instruments were acquired. Time-integrating WL monitors (Breslin, 1976) were used from the beginning, and hence WL data are the most comprehensive. One type of time-integrating radon monitor was developed (George, Breslin, and Guggenheim, 1976) after the program was under way, but only a few of the monitors were constructed, and consequently WL measurements continued to dominate. Still later, a much simpler and less expensive radon monitor was developed (George and Breslin, 1977) and constructed in sufficient numbers to be used extensively in the program.

Diurnal variation was examined in a few houses by two methods. The first method consisted in measuring the radon concentration and the WL at 6-hr intervals throughout the day for several weekly periods by operating four pairs of monitors on timers. The other method used a continuous radon flask monitor (Countess and Thomas, 1977) which records radon concentration at 30-min intervals.

To acquire additional information with which to estimate doses, we made measurements of the uncombined fraction and the particle-size distribution of attached radon daughters in a few houses under representative conditions of occupancy. Uncombined fraction was measured by the wire screen method (George, 1972) and particle size was measured by means of high flow rate diffusion batteries (Sinclair, George, and Knutson, 1977).

At most of the buildings, radon exhalation from cellar floors, radium content of soil, and radon in water were measured to acquire information on sources. Radon exhalation was measured with charcoal canisters (Countess, 1976) which integrate flux over periods of 24 to 48 hr. In general, measurements were obtained at several locations in each building and repeated several times during several months.

Samples of soil were collected to a depth of 10 to 15 cm in the front and rear yards of each house and analyzed for radium by gamma spectrometry.

Samples of water were collected in modified Marinelli beakers and analyzed for radon by gamma spectrometry (Countess, 1978). Several samples were collected from each house at monthly or longer intervals.

RESULTS

All types of measurements, except particle size and uncombined fractions, are summarized in Table 1.

Air Concentrations

The radon concentrations and WL listed are arithmetic means of all measurements obtained at the respective locations. Because of the number and spacing of the week-long measurements in each case, the concentrations listed are considered to be representative of annual means. Standard errors of the means can be estimated from standard deviations and sample sizes. Except for a few single measurements, they vary from 5 to 60% and average 19% for radon concentrations, and they vary from 5 to 25% and average 13% for the WL.

Sample distributions exhibit both normal and lognormal forms, with more of the latter occurring at higher concentrations. But differences in arithmetic means calculated from the log parameters differ negligibly from the arithmetic averages of the untransformed measurements, therefore justifying the simple averaging procedure that was applied.

TABLE 1

Sources and Air Concentrations of Radon and Radon Daughters and Estimated Doses in Residential Buildings in New Jersey and New York

Location and type of residence	Location	Radium in soil, pCi/g	Radon flux on cellar floor, aCi cm^{-2} s^{-1}	Radon in water, pCi/liter	Air concentrations							Annual mean dose, mrads
					Radon, pCi/liter			Working level				
					Min.	Max.	Mean	Min.	Max.	Mean	WLR	
New Jersey												
1. Martinsville												
Wood frame,	Cellar	1.1	8.3	1400	2.2	5.0	3.6	0.0080	0.039	0.024	0.54	350
one story,	First floor				2.1	3.1	2.6	0.0063	0.022	0.012	0.63	
cellar	Outdoors				0.19	0.22	0.20			0.0018	0.89	
2. Morristown												
Wood frame,	Cellar	0.85	18.0	15	2.1	7.4	4.4	0.010	0.067	0.026	0.56	200
two story,	First floor				0.60	2.9	1.3	0.0032	0.012	0.0072	0.76	
cellar	Second floor				0.50	2.9	1.3	0.0039	0.014	0.0074	0.65	
	Outdoors							0.0015	0.0029	0.0024		
3. Morristown												
Wood frame,	Cellar	0.88		10	2.2	6.6	4.1	0.0064	0.019	0.013	0.37	310
raised ranch,	First floor				1.3	2.7	2.0	0.0042	0.018	0.011	0.80	
cellar (finished)	Outdoors				0.31	0.36	0.34	0.0017	0.0034	0.0026	0.87	
4. Morristown.												
Wood frame,	Cellar	0.82	10.0	300	1.1	6.0	3.4	0.0042	0.036	0.016	0.56	420
raised ranch,	First floor				1.2	5.9	3.1	0.0040	0.029	0.013	0.62	
cellar (finished)	Outdoors				0.08	0.40	0.25	0.0020	0.0046	0.0029	0.89	
5. Denville												
Wood frame,	Cellar		13.0	410	1.4	3.0	2.2	0.0034	0.0068	0.0055	0.26	160
two story,	First floor				1.0	1.7	1.3	0.0033	0.0054	0.0044	0.33	
cellar (⅔ finished)	Second floor				1.1	1.9	1.5	0.0035	0.0066	0.0047	0.31	
	Outdoors				0.16	0.18	0.17	0.0011	0.0018	0.0014	0.82	
6. Madison												
Wood frame,	Cellar		2.6	260	0.87	1.6	1.2	0.0037	0.016	0.0093	0.60	130*
one-story,	First floor							0.0015	0.0073	0.0040		
cellar	Outdoors							0.0015	0.0026	0.0022		
7. Chatham												
Wood frame,	Cellar	1.0	4.0	330	0.72	2.1	1.4	0.0035	0.016	0.0078	0.57	160
two story,	First floor				0.90	1.2	1.0	0.0023	0.010	0.0048	0.77	
cellar (finished)												

(Table continues on the next page.)

TABLE 1 (Continued)

Location and type of residence	Location	Radium in soil, pCi/g	Radon flux on cellar floor, aCi cm^{-2} s^{-1}	Radon in water, pCi/liter	Air concentrations: Radon, pCi/liter Min.	Max.	Mean	Working level Min.	Max.	Mean	WLR	Annual mean dose, mrads
8. Passaic												
Wood frame, one story, cellar	Cellar	1.1		<10	1.7	2.5	2.1	0.0054	0.012	0.0088	0.49	120
	First floor				0.60	1.3	1.0	0.0035	0.0052	0.0040	0.49	
9. Teaneck												
Wood frame, two story, cellar (½ finished)	Cellar	0.82	11.0	30	1.6	4.0	2.3	0.0080	0.018	0.012	0.50	150
	First floor				0.40	0.69	0.52	0.0018	0.0037	0.0029	0.65	
	Second floor				0.50	0.60	0.57	0.0020	0.0052	0.0034	0.57	
10. Rivervale												
Wood frame, one story, cellar (finished)	Cellar	0.88	11.0	330			2.8	0.017	0.021	0.020		230
	First floor						1.1	0.0045	0.0060	0.0050		
New York												
11. Bensonhurst												
Brick apartment house	3rd floor apt.	0.98	1.0	<10	0.23	0.28	0.26	0.0037	0.0021	0.0013	0.65	42
12. Jackson Heights												
Brick, two family, no cellar	2nd floor bedroom	1.1	0.8	<10	0.20	0.34	0.27	0.0010	0.0038	0.0022	0.79	61
	2nd floor living room				0.26	0.30	0.28	0.0015	0.0025	0.0022	0.82	
13. Jackson Heights												
Brick, three family, cellar (½ finished)	Cellar storage	0.91	2.5	<10	0.63	1.2	0.95	0.0053	0.010	0.0074	0.76	
	Cellar apt.				0.61	1.0	0.81	0.0024	0.0053	0.0036	0.55	190
	First floor				0.20	0.34	0.25	0.0012	0.0020	0.0017	0.69	50
14. Flushing												
Wood frame, two story, cellar	Cellar	0.86	11.0	<10	0.80	2.9	1.5	0.0045	0.0083	0.0064	0.47	110
	First floor				0.20	1.0	0.60	0.0012	0.0062	0.0031	0.61	
	Second floor						1.0	0.0012	0.0080	0.0033		

TABLE 1 (Continued)

Location and type of residence	Location	Radium in soil, pCi/g	Radon flux on cellar floor, aCi cm^{-2} s^{-1}	Radon in water, pCi/liter	Air concentrations							Annual mean dose, mrads
					Radon, pCi/liter			Working level				
					Min.	Max.	Mean	Min.	Max.	Mean	WLR	
15. Flushing												
Brick,	Cellar	1.5		<10	1.9	4.6	2.7	0.0070	0.020	0.010	0.41	190
two story,	First floor				0.90	1.2	1.0	0.0033	0.0065	0.0050	0.60	
cellar (finished)	Second floor				0.80	1.0	0.90	0.0042	0.010	0.0066	0.77	
	Outdoors				0.15	0.15	0.15	0.0009	0.0020	0.0013	0.70	
16. Flushing												
Wood frame,	Cellar	1.1	5.2	<10	0.42	1.4	0.73	0.0012	0.0048	0.0032	0.47	78
two family,	First floor				0.25	0.80	0.52	0.0007	0.0048	0.0022	0.48	
cellar	Second floor						0.45	0.0007	0.0044	0.0027		
17. Bayside												
Brick,	Cellar	0.83	4.6	<10	0.60	2.3	1.1	0.0033	0.016	0.0077	0.67	130
one story,	First floor				0.20	0.70	0.43	0.0010	0.0065	0.0029	0.64	
cellar (finished)	Outdoors				0.10	0.25	0.18	0.0007	0.0027	0.0014	0.77	
18. Bayside												
Brick,	Cellar	0.90	3.8	<10	0.60	1.4	0.90	0.0030	0.0050	0.0039	0.49	92
two story,	First floor				0.50	0.60	0.50	0.0016	0.0039	0.0030	0.62	
cellar (finished)	Second floor							0.0018	0.0039	0.0026		
19. Bayside												
Wood frame,	Cellar	1.1	2.6	<10	0.20	0.65	0.39	0.0009	0.0028	0.0017	0.48	59
two story,	First floor				0.23	0.60	0.41	0.0016	0.0026	0.0019	0.48	
cellar (finished)	Second floor							0.0009	0.0038	0.0016		
	Outdoors				0.08	0.13	0.11	0.0007	0.0010	0.0009	0.82	
20. Bayside												
Brick,	Cellar	0.96	6.2	<10	0.60	1.7	0.96	0.0024	0.0087	0.0057	0.61	
two family,	First floor				0.30	0.60	0.39	0.0010	0.0043	0.0025	0.53	89
cellar (finished)	Second floor				0.40	0.80	0.57	0.0014	0.0080	0.0039	0.80	110
21. Hicksville												
Wood frame,	First floor	1.1	0.9	200	0.42	1.2	0.77	0.0012	0.0067	0.0038	0.67	110
two story,	Second floor				0.36	1.4	0.83	0.0009	0.0060	0.0032	0.56	
no cellar	Outdoors				0.15	0.17	0.16	0.0009	0.001	0.0009	0.57	

*The radon concentration on the first floor is assumed to be 50% of that in the cellar.

Distributions of the mean radon concentration in the cellars, first floors, and outside the study buildings are shown in Fig. 2. At the midpoint of the distributions, the first-floor radon concentration is one-half of the cellar radon concentration, and the outside radon concentration is one-fifth of the first-floor concentration. The average ratio of individual paired values is 0.53 ± 0.22 for the first floor/cellar and 0.17 ± 0.06 for the outside/first floor. The average ratio of second-floor/first-floor radon concentration for the individual buildings is 1.01 ± 0.28.

Distributions of the mean WL in the cellars, first floors, and outside are shown in Fig. 3. At the midpoint of the distributions, the first-floor WL is one-half of the cellar WL, and the outside WL is four-tenths of the first-floor WL. The average ratio of individual paired values is 0.56 ± 0.30 for the first floor/cellar and 0.33 ± 0.12 for the outside/first floor. The average ratio of second-floor to first-floor WL for individual buildings is 1.06 ± 0.29.

The WL ratios (WLR)* in Table 1 are averages calculated from simultaneous weekly measurements of the radon concentration and the WL. Overall averages for cellars, first floors, second floors, and outside are 0.50 ± 10, 0.61 ± 0.12, 0.66 ± 0.18, and 0.78 ± 0.12, respectively.

Considerable variation in concentrations occurred over 24-hr periods in the measurements that were made to study diurnal variation, but no consistent pattern emerged, possibly because of an insufficient number of observations. In any case, we have no basis for adjusting exposures for different times of the day spent indoors. A typical trace of radon concentration vs. time is shown in Fig. 4.

Similarly, weekly average concentrations of radon and radon daughters varied markedly in all locations, as indicated by the ranges in Table 1, but no consistent seasonal variation could be identified.

Sources of Radon

Soil radium values listed in Table 1 are averages of two samples each. The overall mean is 1.0 pCi/g, the value usually assumed to be normal background. For the most part, differences in locations are within 20% of the mean.

Radon exhalation values are averages of all measurements obtained at a site, the number varying from 2 to 50 and averaging 13. Wide variations were observed among simultaneous measurements and between successive sets of measurements in any given building.

*Working level ratio = $\frac{100 \times \text{working level}}{\text{radon concentration (pCi/liter)}}$

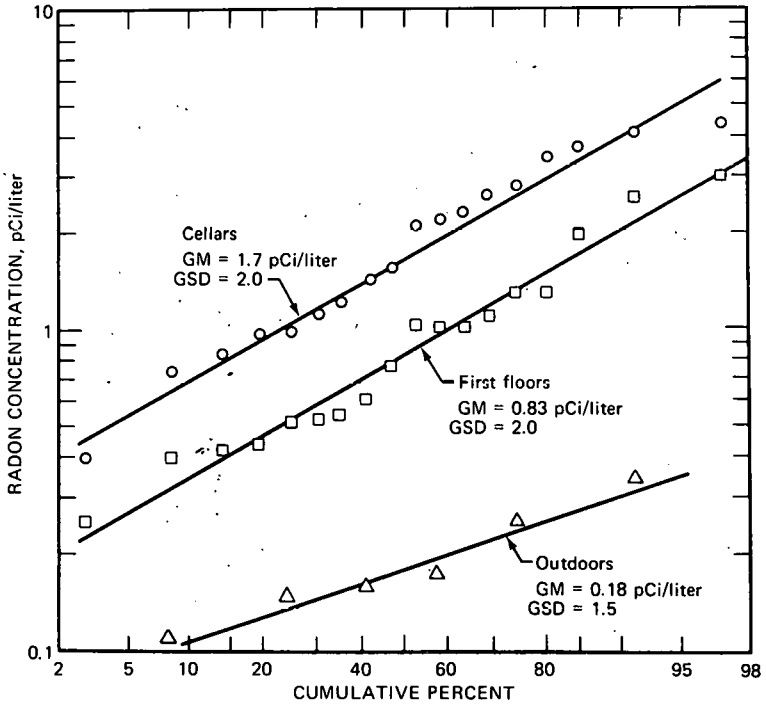


Fig. 2 Distribution of annual mean radon concentrations. GM = geometric mean; GSD = geometric standard deviation.

Part of the variation may be related to the small surface area ($\sim$80 cm^2) represented by each measurement. The marked range of mean exhalation values implies a correspondingly large range of radon input rates.

Concentrations of radon in water are averages of all measurements obtained, which numbered from two to eight per building. These values were much more consistent with time than the exhalation values.

The source data account reasonably well for the observed indoor air concentrations. To begin with, radon concentrations in cellars correlate closely with average exhalation rates ($r = 0.82$, $p < 0.001$). The relationship is shown in Fig. 5. Moreover, most of the scatter around the regression line in Fig. 5 can be explained at least qualitatively by noting that (1) the values above the regression line tend to be associated either with houses in which significant concentrations of radon were found in water supplies or houses where the WLR exceeded the average (implying lower-than-average

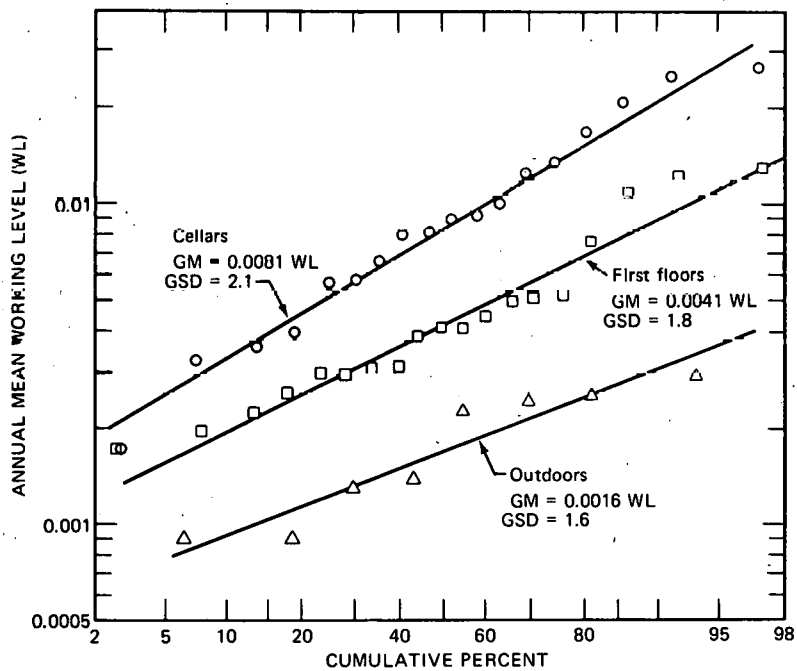


Fig. 3 Distributions of annual mean WLs.

ventilation rates) and (2) values below the regression line tend to be associated with houses in which no radon was detected in water supplies or where the WLR was lower than the average. These observations support the reasonable conclusion that indoor radon concentrations in the investigated dwellings depend mainly on radon exhalation rates and secondarily on ventilation rate and radon in water. On the basis of our measurements of radon flux, a typical daily input of radon to a house from cellar floors is on the order of 5×10^5 pCi. This quantity is nearly matched by the radon in 1000 liters of water at a concentration of 300 pCi/liter, which approximates the concentration found in several houses of the study group. The amount of radon in water that actually escapes into the air within a house has not been determined (except for specific modes of use such as showers), but it appears plausible that this source can be significant (see papers by Castren and by Gesell and Pritchard, this volume).

The large variation among exhalation rates has not yet been explained. Given the uniform soil radium concentrations and local

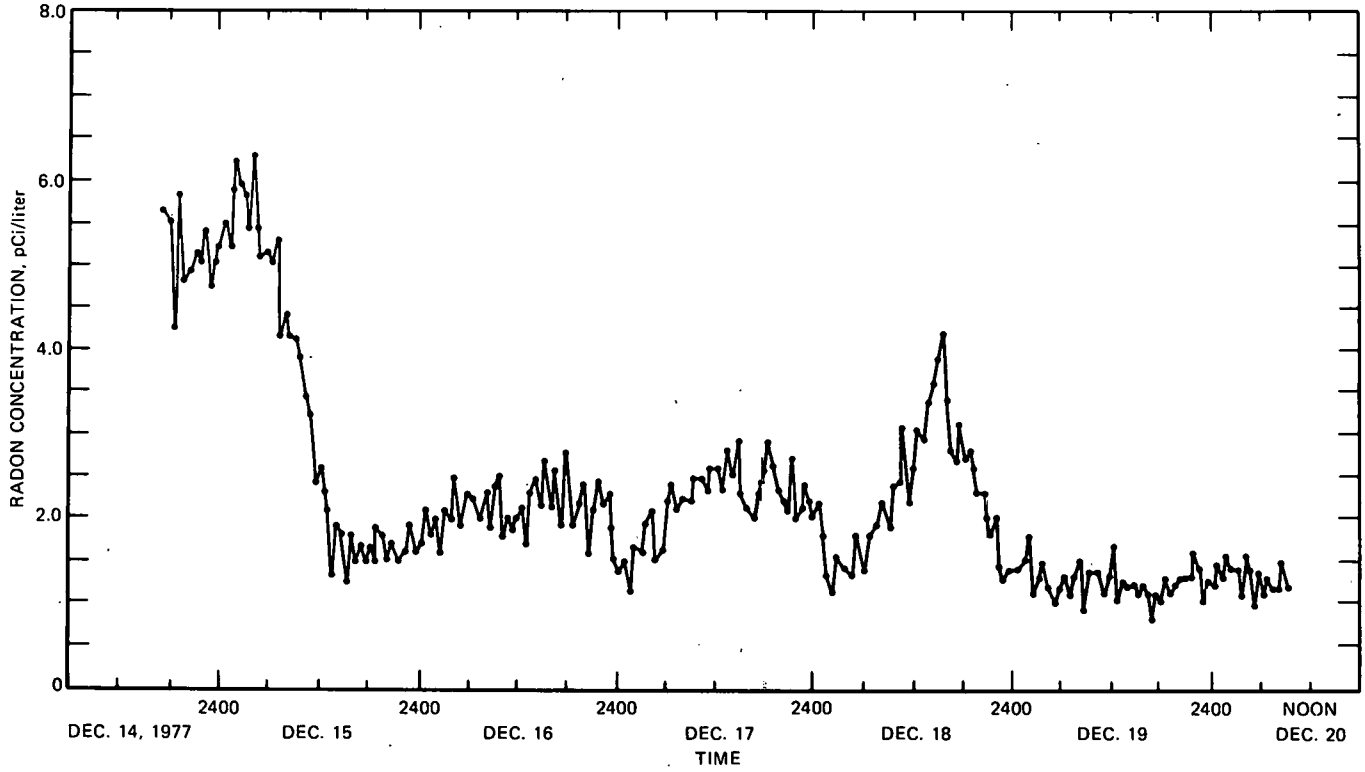


Fig. 4 Radon variation with time.

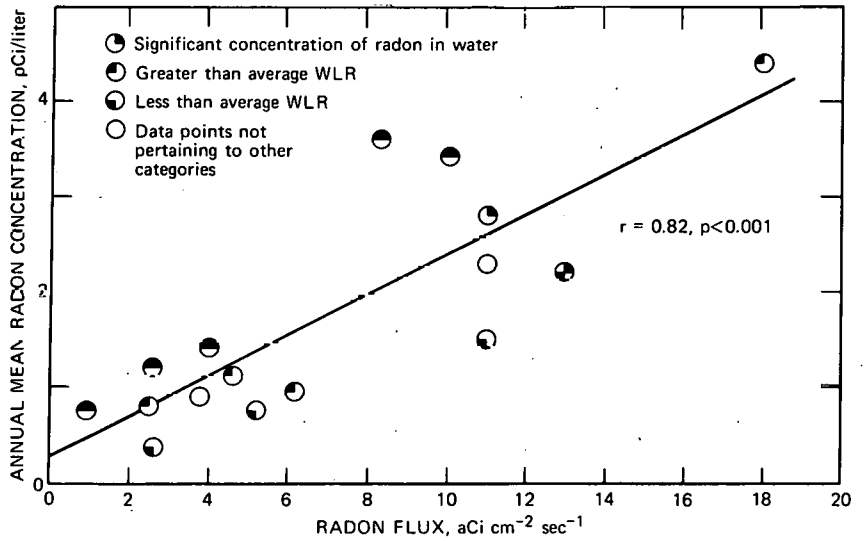


Fig. 5 Mean radon concentration in lowest level of house vs. mean radon flux.

building codes that call for 4-in. concrete floors, variation among exhalation rates should be less pronounced. Possible reasons are differences in "emanating power" of soil radium, departures in actual floor thickness from legal requirements, and differences in the density of radium content of concrete mixtures (Scott, this volume).

Particle Size and Uncombined Fraction

From measurements of particle size in four of the residences, the average activity median diameter and average unattached fraction were 0.125 and 0.07 μm, respectively. Figure 6 shows three typical bimodal size distributions. The particles in the small mode are thought to be unattached radon daughters. The magnitudes of unattached fractions obtained by diffusion batteries were confirmed by the independent measurements with wire screens.

Exposures

Since most concentrations indoors are substantially in excess of those outdoors, average exposures are governed primarily by the division of occupants' time among different parts of their houses and by the respective average concentrations in each part. However,

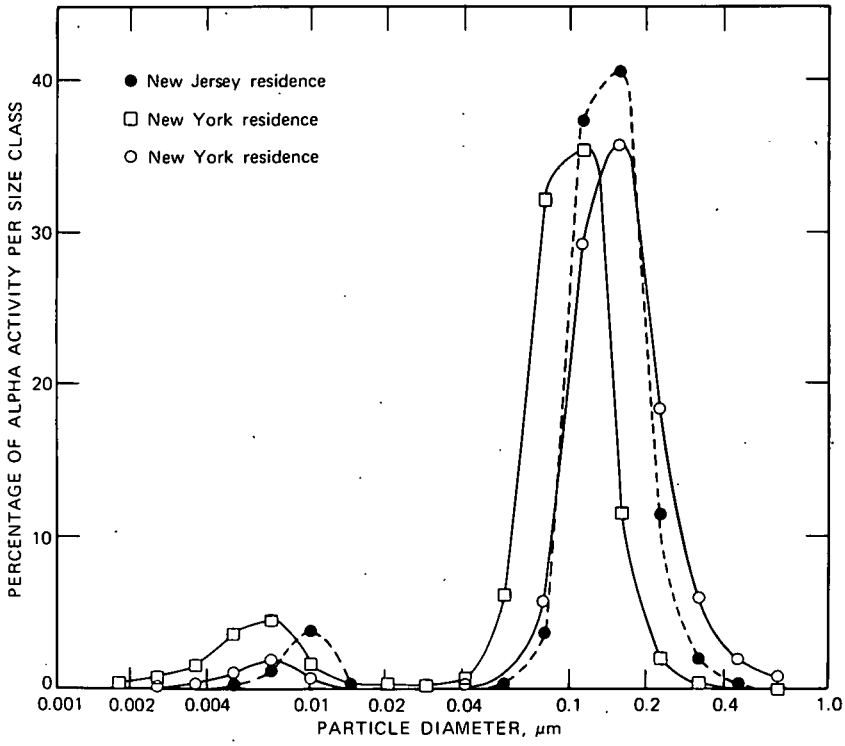


Fig. 6 Histograms of radon daughter size distribution.

reasonable estimates of exposure can be made without specific time-study information by applying certain observations and assumptions.

Cellar concentrations tend to exceed first-floor concentrations, but time spent in unfinished cellars is usually incidental and, for exposure estimates, will thus be ignored. There are two basic types of finished cellars, which need to be treated differently. The first type is associated with conventional one-story (ranch-style) or two-story houses. Concentrations in these cellars exceed concentrations on first floors by a factor of 2, on the average, and some allocation of time is necessary. The actual time spent depends on the functions of the finished rooms, i.e., bedroom, den, playroom, but 4 hr/day is taken as a reasonable compromise. The second type of finished cellar is associated with the "raised ranch" style of house. This style consists of two stories, the finished basement comprising the lower story and being an integral part of the living space. The first and second stories

are connected by a wide, open staircase, which facilitates the free circulation of air between the levels, and, in fact, first-floor concentrations average 90% of cellar concentrations. Therefore the first-floor concentrations are reasonable approximations of total indoor exposure.

A convenient simplification in conventional two-story houses is the virtual equivalence of first- and second-floor concentrations, making unnecessary any time allocation between the floors.

For allocating exposures, 20% of the time is assumed to be spent outdoors (UNSCEAR, 1977).

Dose Calculation

Several authors have calculated the lung dose from inhaled radon daughters, each using different anatomical models and different reference atmospheres. Hamrick and Walsh (1974) reviewed the published dose calculations from 1940 through 1972 and found that the results had differed mainly because of the choice of critical tissue. The calculations of Altshuler, Nelson, and Kuschner (1964), Jacobi (1964), Haque and Collinson (1967), and Harley and Pasternack (1972) refer to the average dose to the bronchial epithelium of the tracheobronchial tree. The other reasons for variation in the dose are related to the assumptions of the radon daughter characteristics. The essential characteristics for accurate dose calculations are the concentrations of the short-lived radon daughters, the fraction of daughters that are unattached to aerosols, and the particle size distribution of the aerosols onto which the radon daughters become attached.

In this investigation, estimates of dose are from the work of Harley and Pasternack (1972), who based their calculation on the lung model of Weibel (1963). They determined the absorbed dose to the shallow lying basal cells 20 μm from the surface of the bronchial epithelium at Weibel generation 4, or about the level of the segmental bronchi. This is the region where the greater number of cancers are found in uranium miners.

The assumptions used for dose estimates, however, differ from the work of Harley and Pasternack in the following respects (Harley, 1978).

1. The particle size of the attached fraction of radon daughters is 0.1 μm in diameter. There is little change in the dose for particle sizes from 0.1 to 0.15 μm in diameter.

2. Aerosol deposition is based on breathing rates of 10 liters/min for 12 hr and 15 liters/min for 12 hr, and the total amount of air inhaled per day (24 hr) is 18 m^3.

3. Deposition in the bronchial tree for 0.1-μm particles is assumed to be due to diffusion and is calculated using the Gormley and Kennedy (1949) expressions and the Martin and Jacobi (1972) empirical factors to correct for turbulent deposition in the first five generations of the bronchial tree.

If it is assumed that the fraction of unattached radon daughters is 0.07 and the activity median diameter of attached daughters is 0.1 μm, approximating the average median diameter of 0.125 μm found in this study, and using the dosimetric input data of Harley (1978), the approximate annual mean absorbed dose to the basal cells in millirads can be calculated from the following equation:

$$\text{Annual dose (mrads)} = 42\ C_{Rn} + 25{,}000\ \text{WL}$$

where C_{Rn} is the annual mean concentration of radon (in pCi/liter) and WL is the annual mean working level. The first term of the expression gives the dose due to unattached ^{218}Po (RaA), assuming that the unattached RaA is 0.07 of the radon concentration. This expression is an approximation and cannot be used in cases of severe daughter disequilibrium.

Annual mean doses are listed in the last column of Table 1.

DISCUSSION

Generalities from this study are limited by the similarity of most of the residences and the nonrandomized manner of selection. The reported doses are mainly for residents of single family houses of wood frame or brick construction. Even so, the spread of doses is 10-fold, as shown by the distribution in Fig. 7. The lower limit of exposure is represented by the outdoor air concentration, a value that is approached in a few cases. In the area covered by this study, that limit is on the order of 0.001 WL, yielding an annual dose of 30 mrads. Certainly exposures higher than the maximum reported here are possible. Therefore reliable estimates of the dose to the general population from radon daughters must reflect a much wider range of conditions than we have presented and, of course, must be weighted by demographic factors.

On the average, exposures in New Jersey residences exceed exposures in New York residences by a factor of 2.5. Also, all three houses in which the WL in the living area exceeds 0.01 are in New Jersey. Differences in the two geographical groups are readily seen in Fig. 8, giving the separate distributions of the annual mean WL in

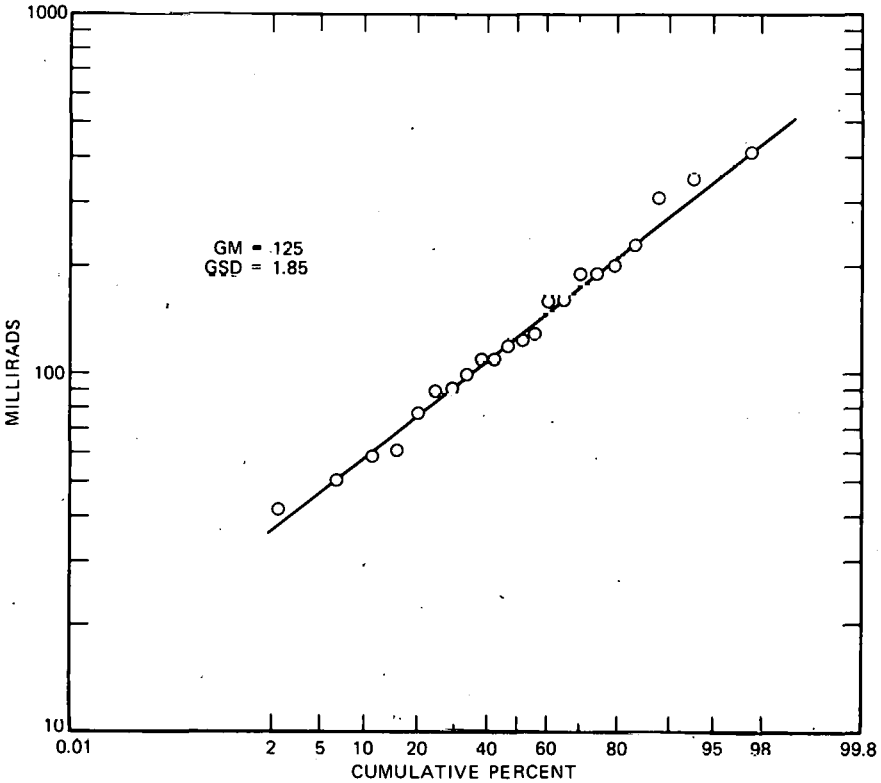


Fig. 7 Distributions of annual mean doses to occupants of New Jersey—New York residences.

cellars and on first floors. We are aware of no reason why concentrations should differ, and it is entirely possible that the imbalance is accidental, but the observation seemed worthy of brief mention.

The distribution of average concentrations obtained in this study is remarkably similar to distributions from other investigations in which the annual mean WL was measured with time-integrating monitors. Two such investigations from which detailed data are available were conducted by the Colorado Department of Health in Grand Junction (Barnes, 1975) and the Florida Department of Health and Rehabilitative Services (1978) in Polk and Hillsborough counties. The purpose of both investigations was to monitor radon daughter concentrations in buildings affected by abnormal amounts of radium in soil or construction materials, but the investigations included buildings in normal background areas to serve as controls.

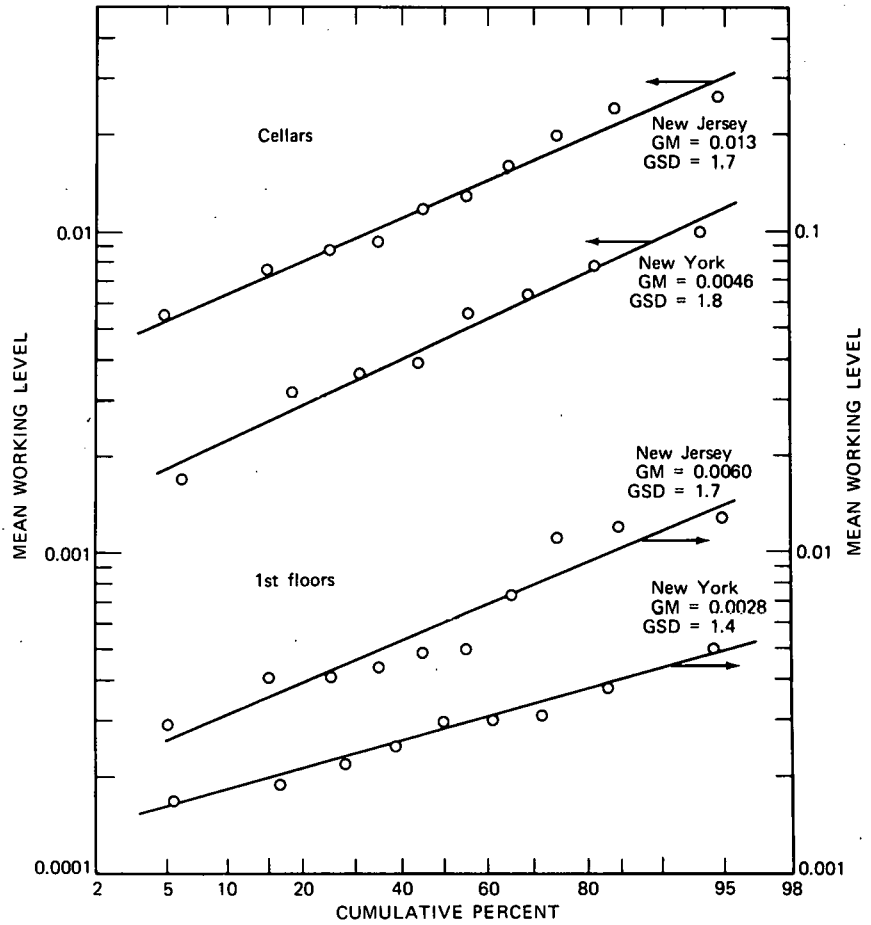


Fig. 8 Comparison of WL distributions in New Jersey and New York houses.

There are about 60 control buildings in the Grand Junction group, but for comparison we selected the 29 which were residential and for which first-floor measurements were obtained. Since the average concentration of radium in Grand Junction soil is 1.5 pCi/g, we divided the reported annual mean WLs by 1.5.

There are 28 control buildings in the Florida group, all single family residences and all without basements. The concentration of radium in background soil was not reported, and hence the annual mean WLs were not adjusted.

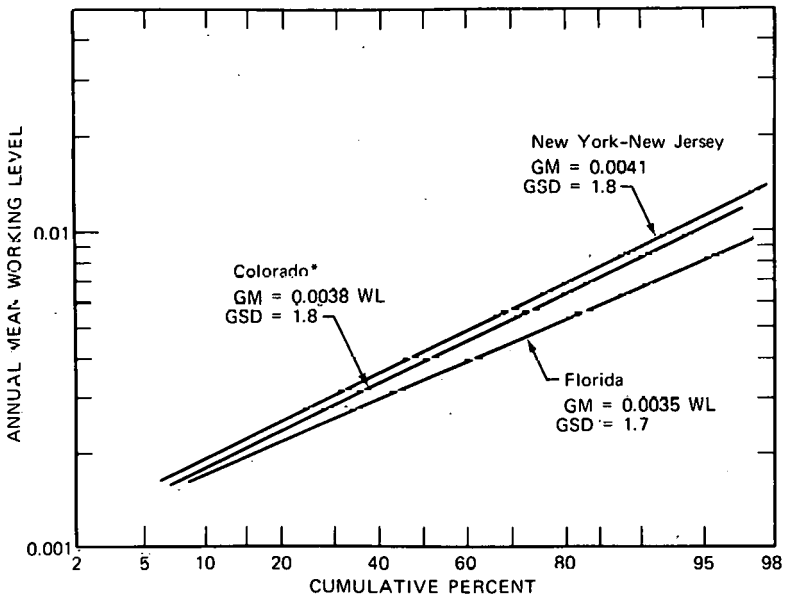


Fig. 9 Distributions of annual mean WLs in houses in New Jersey—New York, Colorado, and Florida.

Distributions for the New Jersey—New York, the Colorado, and the Florida houses are shown in Fig. 9.

Ventilation rates can be calculated from rates of radon input, based on flux measurements, and average radon concentrations. In cellars, where flux and air concentration would be expected to be most closely related, the calculated ventilation rates average about 0.1/hr. The ventilation rate can also be inferred from the WLR, an index of the degree of equilibrium between radon and radon daughters. A WLR of 0.5, the average value found for cellars, is equivalent to an air change rate of 1/hr, calculated with the usual assumptions of instantaneous, uniform mixing, and no loss of radon daughters by surface deposition. We lack a definite explanation for the large difference in the two results, but either estimate could be in error for one or more reasons. For example, the ventilation rate based on flux and air concentration would be low if the radon input rate is underestimated or the ventilation rate based on the WLR would be high if the radon daughter deposition is significant. At present, we tend to favor the lower rate, 0.1/hr, because it is more nearly in agreement with preliminary measurements of the ventilation rate that we have made using tracer gas techniques.

ACKNOWLEDGMENTS

The authors are grateful to Dr. Naomi Harley for her contribution to the lung dose calculations and to Dr. Earl O. Knutson for his calculations of particle size distributions. We offer special thanks to our many colleagues in the laboratory who made their homes available for measurements during the course of this study.

REFERENCES

Altshuler, B., B. Nelson, and M. Kuschner, 1964, Estimation of Lung Tissue Dose from the Inhalation of Radon and Daughters, *Health Phys.*, 10: 1137.

Barnes, W. J., 1975, Colorado Department of Health, personal communication.

Breslin, A. J., 1976, Two Area Monitors with Potential Application in Uranium Mines, in *Proceedings of NEA Specialist Meeting on Personal Dosimetry and Area Monitoring Suitable for Radon and Daughter Products,* Elliot Lake, Canada, October 4—8.

Countess, R. J., 1976, ^{222}Rn Flux Measurement with a Charcoal Canister, *Health Phys.*, 31: 456.

——, 1978, Measurement of ^{222}Rn in Water, *Health Phys.*, 34: 390.

——, and J. W. Thomas, 1977, *Radon Flask Monitor,* ERDA Report HASL-330, Health and Safety Laboratory, NTIS.

Florida Department of Health and Rehabilitative Services, 1978, *Study of Radon Daughter Concentrations in Structures in Polk and Hillsborough Counties,* January.

George, A. C., 1972, Indoor and Outdoor Measurements of Natural Radon and Radon Decay Products in New York City Air, in *The Natural Radiation Environment II,* Vol. 2, Symposium Proceedings, Houston, Tex., Aug. 7—11, 1972, J. A. S. Adams, W. M. Lowder, and T. F. Gesell (Eds.), ERDA Report CONF-720805-P2, pp. 741-750, Rice University and the University of Texas School of Public Health, NTIS.

——, and A. J. Breslin, 1977, *Measurements of Environmental Radon with Integrating Instruments,* Workshop on Methods for Measuring Radiation in and Around Uranium Mills, Atomic Industrial Forum, Vol. 3, August.

——, A. J. Breslin, and S. F. Guggenheim, 1976, A Cumulative Environmental Radon Monitor, in *Proceedings of the Ninth Midyear Health Physics Symposium,* Denver, Colo.

Gormley, P. G., and M. Kennedy, 1949, Diffusion from a Stream Flowing Through Cylindrical Tube, *Proc. Irish Acad.*, 52A: 163.

Hamrick, P. E., and P. J. Walsh, 1974, Environmental Radiation and the Lung, *Environ. Health Perspect.*, 9: 33.

Haque, A. K., and A. J. Collinson, 1967, Radiation Dose to the Respiratory System Due to Radon and Its Daughter Products, *Health Phys.*, 13: 431.

Harley, N. H., 1978, New York University Medical Center, personal communication.

——, and B. S. Pasternack, 1972, Alpha Absorption Measurements Applied to Lung Dose from Radon Daughters, *Health Phys.*, 23: 771.

Hultqvist, B., 1956, Studies of Naturally Occurring Ionization Radiations with Special Reference to Radiation Doses in Swedish Houses of Various Types, *Kungl. Svenska Vetenskapsakad. Handlingar*, Ser. 4, 6.

International Commission on Radiological Protection, 1959, *Report of Committee II on Permissible Dose for Internal Radiation*, ICRP Publication No. 2, Pergamon Press, Inc., Oxford.

Jacobi, W., 1964, The Dose to the Human Respiratory Tract by Inhalation of Short-Lived ^{222}Rn and ^{220}Rn Decay Products, *Health Phys.*, 10: 1163.

Martin, D., and W. Jacobi, 1972, Diffusion Deposition of Small-Sized Particles in the Bronchial Tree, *Health Phys.*, 23: 23.

Office of the U. S. Surgeon General, Department of Health, Education, and Welfare, July 27, 1970.

Sinclair, D., A. C. George, and E. O. Knutson, 1977, *Application of Diffusion Batteries to Measurements of Submicron Aerosols*, presented at the American Nuclear Society Winter Meeting, San Francisco, Nov. 27—Dec. 2.

Steinhausler, F., 1975, Long Term Measurements of ^{222}Rn, ^{220}Rn, ^{214}Pb and ^{212}Pb Concentrations in the Air of Private and Public Buildings and Their Dependence on Meteorological Parameters, *Health Phys.*, 29: 705.

Toth, A., 1972, Determining the Respiratory Dosage from RaA, RaB and RaC Inhaled by the Population in Hungary, *Health Phys.*, 23: 281.

United Nations Scientific Committee on the Effects of Atomic Radiation, 1977 Report, Annex B, paragraphs 152-204.

Weibel, E. R. 1963, *Morphometry of the Human Lung*, Academic Press, Inc., New York.

Yeates, D. B., A. S. Goldin, and D. W. Moeller, 1972, Natural Radiation in the Urban Environment, *Nucl. Safety*, 13(4): 275 (July—August 1972).

DISCUSSION

Wrenn: Did you calculate the doses assuming occupancy during average conditions? Radon indoors correlated with occupancy in many cases.

George: The doses were calculated by dividing the occupant's time among different parts of the house and by using the respective average concentration in each part.

Steinhausler: It was interesting to see that, despite the different types of construction of the U. S. houses investigated in your study, the indoor levels are increased by about the same amount as we found in European houses, which are mainly brick and stone buildings. Can you comment?

George: I think that the houses in the study area are basically similar in terms of insulation, ventilation, and habitation, and one would expect higher indoor concentrations irrespective of construction material.

Jonassen: Have you tried to correlate the radon peaks with pressure changes?

George: We did not measure meteorological parameters at the time.

Methods for a Continuous Registration of Radon, Thoron, and Their Decay Products Indoors and Outdoors*

J. PORSTENDÖRFER, A. WICKE, and A. SCHRAUB
Institut für Biophysik, Strahlenzentrum der Justus-Liebig Universität
Federal Republic of Germany

ABSTRACT

The devices and methods used to determine concentrations of radon (^{222}Rn), thoron (^{220}Rn), and their daughters and the ventilation rate and the average exhalation rate inside buildings are discussed. Radon and thoron concentrations are detected continuously by collecting the positively charged RaA (^{218}Po) and ThA (^{216}Po) atoms on a surface-barrier detector with the use of electric field precipitation. The determination of radon and thoron decay-product concentrations is made by collecting the aerosols on a membrane filter and simultaneously counting the activities by alpha spectroscopy. The decrease of a tracer-gas concentration (CO_2) is used to determine the ventilation rate of a room.

The internal exposure due to the decay products of radon (^{222}Rn) or thoron (^{220}Rn) is not confined to underground miners in uranium industries but is, at a lower level, a general problem. Uranium and thorium are widely distributed in the earth's crust, in soils, and in most common materials used by the building industry. Many studies show that there is not only a significant external irradiation (UNSCEAR, 1977; Ohlsen, 1969; Kolb and Schmier, 1975; Storruste et al., 1965; Pensko, Mamont, and Wardaszko, 1969; Hultqvist, 1956; Mjönes and Swedjemark, 1976; Spiers, 1960; Lindeken, Jones, and McMillen, 1973; Lowder and Condon, 1965; Bundesministerium des Innern, 1976) from the members of the

*This study is a part of the Ph.D. thesis of A. Wicke, Justus-Liebig Universität, Federal Republic of Germany.

uranium and thorium chain but also an internal irradiation by inhalation of the radium and thorium daughters radon and thoron and their decay products (UNSCEAR, 1977; Tóth, 1972; Pensko, Mamont, and Wardaszko, 1969; Hultqvist, 1956; Haque, Collinson, and Blyth Brooke, 1965; George, 1972; Yeates, Goldin, and Moeller, 1972). Inside buildings, especially, radon, thoron, and their decay products accumulate owing to the diffusion of the radioactive gases out of the building materials. The inhalation of radon and thoron presents little hazard compared with their daughters which, if inhaled either as free ions or attached to atmospheric aerosol, result in a significant dose to the lung, where the radioactive aerosols are deposited (UNSCEAR, 1977; Harley and Pasternak, 1972; Jacobi, 1972; Lundin, Wagoner, and Archer, 1971; Altshuler, Nelson, and Kuschner, 1964; Haque and Collinson, 1967; International Commission on Radiological Protection, 1966).

To estimate the level of exposure of the population, we must know some further details about the mechanism of radon and thoron accumulation in dwellings and about the factors influencing the concentration of each daughter. Applying our experience and that of numerous authors (Tóth, 1972; Steinhäusler, 1975; Haque, Collinson, and Blyth Brooke, 1965; George, 1972; Hultqvist, 1956) to an appropriate model (Porstendörfer, Wicke, and Schraub, 1978), we found that the actual amount of radon and thoron indoors mainly depends on the exhalation of the construction material, the geometry of the room, the ventilation rate, and the outdoor concentrations.

A few of these parameters are influenced by meteorological variables (Steinhäusler, 1975; Gabrysh and Davies, 1954; Jonassen, 1975). To study this problem experimentally, we combined different devices to a complex data acquisition system that permits us to register the following parameters continuously and simultaneously: (1) radon and thoron concentration indoors and outdoors, (2) radon and thoron daughter concentration indoors and outdoors, and (3) the ventilation rate of a room. In addition, a method to determine the average exhalation rate in a room is proposed.

RADON AND THORON MEASUREMENT

Several attempts have been made not only to measure environmental concentrations of radon by spot checks but also to register diurnal variations of radon concentration by a continuous method. Generally such a device consists of a flow type of ionization chamber or a large-volume scintillation chamber (Evans, 1935; Damon and

Hyde, 1952; Van Dilla and Taysum, 1955; Lucas, 1957). However, their limits of detection generally lie about the environmental level ($\sim 10^{-13}$ Ci/liter). Further, the two-filter technique can be used (Jacobi, 1963; Thomas and LeClare, 1970; Fontan, 1964). The first filter preceding the decay volume collects the decay products of radon. The radon daughters produced inside the chamber are collected on the second filter, and its activity can be registered by an alpha detector. This method is rather simple, and the sensitivity is very high (detection limit $\sim 10^{-14}$ Ci/liter). The only disadvantage is the requirement of high flow rates and huge chambers. Jacobi (1963, 1964) investigated the electroprecipitation of the positively charged RaA (^{218}Po) ions on an aluminized plastic foil facing an alpha detector. Like him, other authors (Albrecht and Kaul, 1969; Reiter, 1967; Haider and Jacobi, 1972; Dalu and Dalu, 1971) did not favor this method, because the deposition rate was too low, not constant, and sensitive to water vapor. Only Wrenn, Spitz, and Cohen (1975) reported that their monitor, used in dwellings, appeared to be unaffected by normal fluctuations of relative humidity.

For our purposes the principle of electric-field precipitation seemed to be most effective, and we tried to design an improved type with a spherical volume (14.2 liters) and a higher electrostatic field (applied voltage, maximum, 20 kV) (Fig. 1). The positively charged radon and thoron decay products are directly deposited on a silicon surface barrier detector (active area, 300 mm^2). Their disintegrations are directly detected by alpha spectroscopy. With an energy resolution of about 80 keV, the complete separation of the energies of RaA (^{218}Po)/ThC (^{212}Bi), ThA (^{216}Po), RaC′ (^{214}Po), and ThC′ (^{212}Po) was possible (Fig. 2). The counts due to RaA and RaC′ are proportional to the radon concentration. The determination of radon concentration by means of RaA activity measurement serves for a good time resolution, but in the presence of detectable amounts of thoron the fraction of ThC at the same energy (6.0 MeV) must be subtracted (ThC′ at 8.76 MeV as reference). The collection efficiency for RaA was checked with a calibrated radon source as a function of the applied high voltage (Fig. 3). For this type of chamber there is saturation above 16 keV. At this level the collection efficiency for RaA was about 74% at a flow rate of $\leqslant$100 liters/hr. Since the surface barrier detector detects only half of the disintegrations, the sensitivity of the system (14.2 liters by volume) is about 12 cpm/(pCi/liter). At a mean background of 5 cph, the monitor can detect as little as 1×10^{-14} Ci/liter with a 1-hr count. The air to be detected must be carefully dried ($CaCl_2$) because the sensitivity drops drastically with increasing relative humidity (Fig. 4). For radon the sensitivity is relatively independent of small flow rate variations,

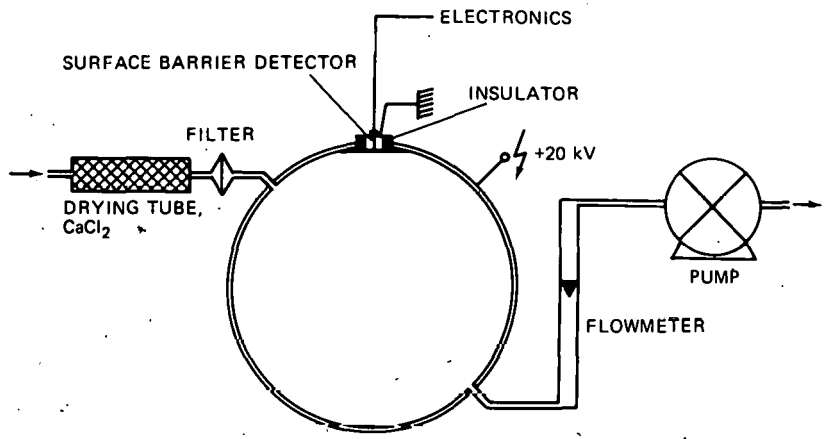


Fig. 1 Electrostatic collection chamber system for radon and thoron measurements.

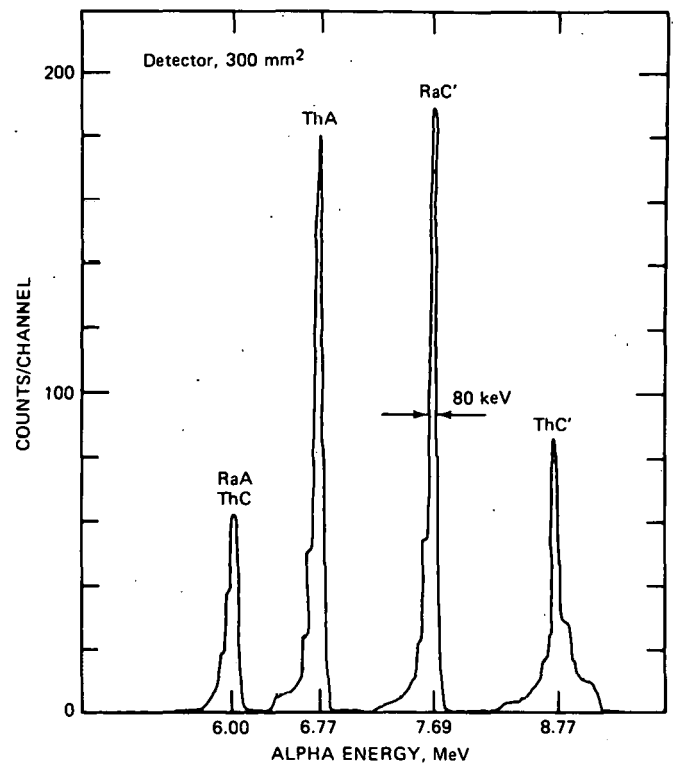


Fig. 2 A typical alpha spectrum of the precipitated decay products to determine natural radon and thoron concentrations.

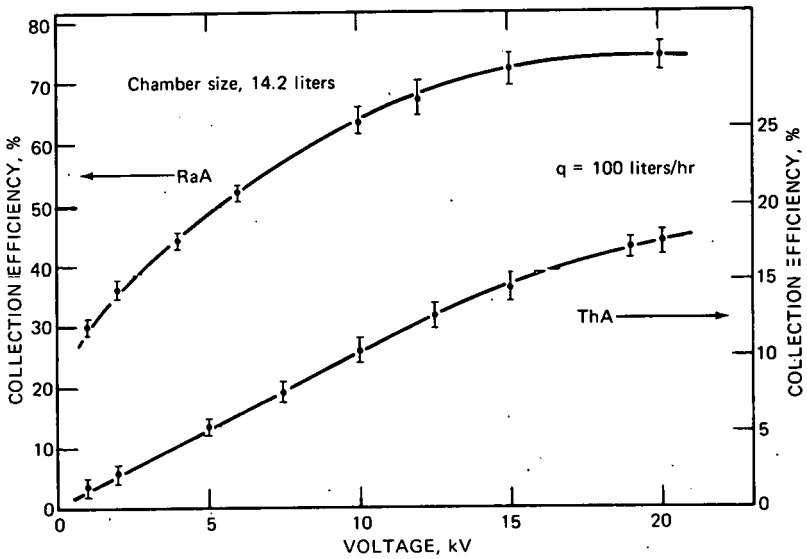


Fig. 3 Collection efficiencies for RaA and ThA as a function of the potential of the chamber (q = flow rate).

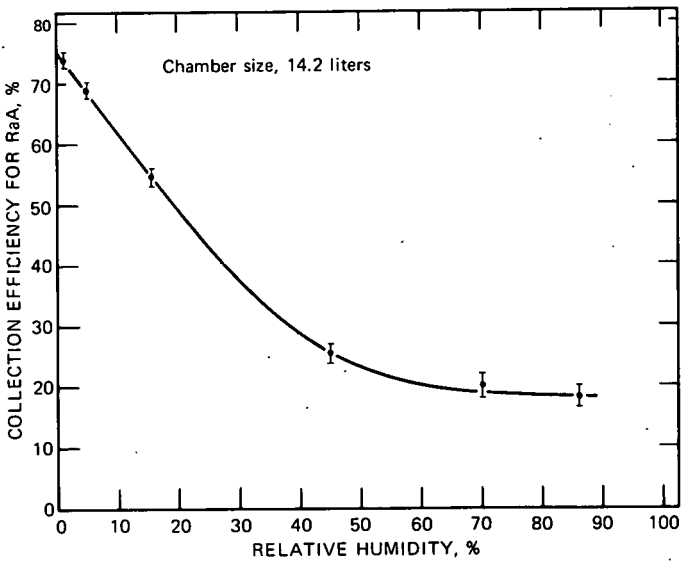


Fig. 4 Collection efficiency for RaA as a function of relative humidity.

and for long-term measurements only a small pump may be used according to the time resolution.

The excellent energy resolution of the alpha spectrometer enables us also to determine the thoron concentration continuously by counting the alpha decays of ThA (Fig. 2). The collection efficiency for ThA did not show saturation at 20 kV because of the short half-life of ThA (0.16 sec) (Fig. 3). The maximum value for ThA collection was only 18.5% at a flow rate of 100 liters/hr. This led to a sensitivity of about 0.4 cpm/(pCi/liter) for thoron. At a background of 5 cph, the monitor is able to detect concentrations as low as 7×10^{-14} Ci/liter.

MEASUREMENT OF RADON AND THORON DECAY PRODUCTS

Methods that use the alpha counts from RaA and RaC′ to determine radon daughter concentrations and implicitly the working level (WL) have been in use for a long time (Tsivoglou, Ayer, and Holaday, 1953; Thomas, 1970; Martz et al., 1969; James and Strong, 1973; Raabe and Wrenn, 1969; Duggan and Howell, 1968). The now classic method of Tsivoglou, Ayer, and Holaday (1953) used alpha activity measurements at three different decay times after the end of sampling to assess the radon daughter concentration. Thomas (1970) observed that the precision of such a method could be improved by recording the total alpha counts during three time intervals of varying length, and Martz et al. (1969) found that increased precision and convenience would result from a spectroscopic separation of RaA and RaC′ alpha counts. Neither these methods nor the commercially available Instant Working Level Meter (Groer et al., 1973) are able to register long-term variations of daughter product concentration. Especially in the case of measurements in buildings, attention should also be directed to thoron daughters (ThC and ThC′) which can be separated from radon daughters by alpha spectroscopy. Wachsmann and David (1973) proposed such an instrument for continuous and long-term measurements of radon WL.

Our aim was to improve this instrument in such a way that we could use a multichannel analyzer instead of a single-channel analyzer in order to use all alpha pulses to determine each daughter concentration during sampling. A surface barrier detector was used (active area, 300 mm^2), protected with a thin plastic foil (3 μm) against damaging and contamination. To improve energy resolution, we used a collimator (Fig. 5). This reduces the overall counting efficiency from 15% to 12%. The detector faces the membrane filter

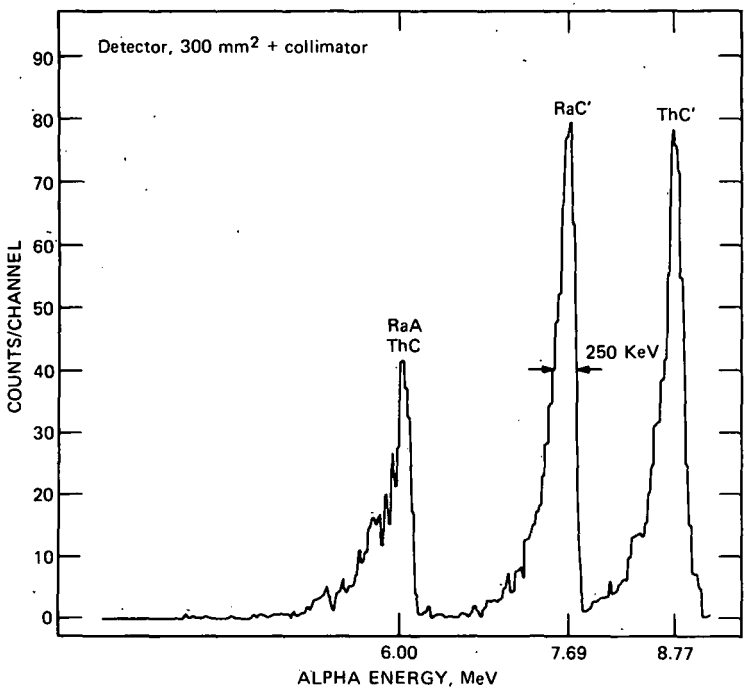


Fig. 5 A typical alpha spectrum of natural radon and thoron decay products collected on a membrane filter.

directly, at a distance of 4.5 mm from the detector surface. The sampling unit was combined with a charge-sensitive preamplifier and a voltage supply within a double AEC—NIM bin (Fig. 6). The pulses from the preamplifier were fed via a main amplifier into a multichannel analyzer.

A detailed description of the basic relations for buildup and decay of radon and thoron daughters on a filter is given by Raabe and Wrenn (1969). For a continuous measuring device, the equations must be integrated for the time interval of interest. For a continuous determination of the working level by alpha spectroscopy, two assumptions about radon and thoron daughter equilibrium must be made: RaB/RaC and ThB/ThC. For a correct WL measurement, these ratios can be determined separately with a spot test described by Duggan and Howell (1968).

The system has been calibrated with a ThB/C test filter, obtained by sampling the decay products of an emanated ^{228}Th source which were attached to atmospheric aerosols. The activity of the sample was determined by gamma spectrometry and compared with the

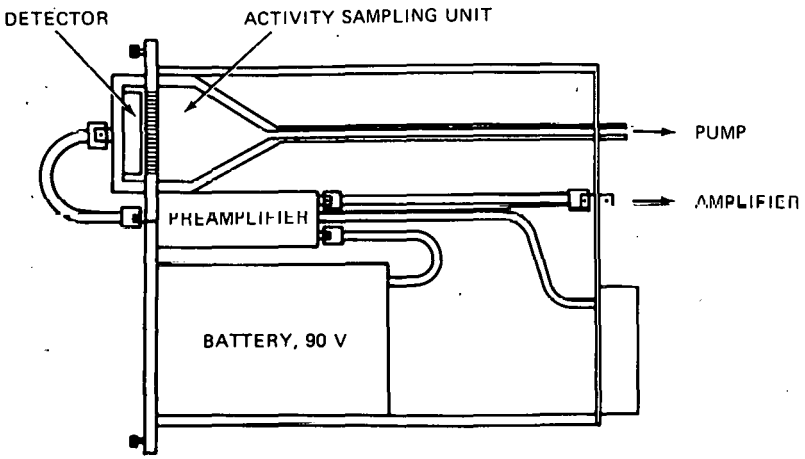


Fig. 6 Sampling unit for collection and detection of radon and thoron decay products.

counts registered by the alpha detector. The results of the calibration were used to calculate the sensitivity for RaA and ThC′ under steady-state conditions of the filter activity. Their absolute values are 36 cpm/(pCi/liter) and 5220 cpm/(pCi/liter), respectively, at a detector efficiency of 15% and at a flow rate of 1500 liters/hr. For a background of 5 cph, the limits of detection are 1×10^{-14} Ci/liter for RaA and 5×10^{-17} Ci/liter for ThB/C at a 1-hr count.

For our measurements in buildings, the continuous radon and thoron instrument and the filter device are combined in one arrangement. We also use a parallel system outdoors to register the outdoor reference data. The signals from the different detectors are analyzed and controlled by a multichannel analyzer (4 by 256 channels). A punch unit is connected to bring the data in a computer compatible form.

DETERMINATION OF THE VENTILATION RATE

Handley and Barton (1973) published a literature survey of home ventilation rates, taking into account that this parameter has an important effect on doses to home occupants from airborne radionuclides. The available data suggest that the average annual ventilation rate (v) of most occupied houses in the United States fall in the range of 0.5 to 1.5 air changes per hour. Other publications from Germany (Dick and Thomas, 1951; Georgii, 1954; Wolpert,

1899; Ilzhöfer, 1931) show ventilation rates between 0.1 and 1.5 hr^{-1}.

For our study we adopted a CO_2 method used by Georgii (1954). For the experimental determination the test space is filled up to about 1% with CO_2. The concentration of CO_2 is measured and registered by an infrared absorption instrument in connection with a plotter. If the air-exchange rate is constant and there is a complete mixing in the room air, the concentration of the tracer (CO_2) will decrease exponentially. A semilogarithmic scale is used to calculate the ventilation rate from the linear decrease of the CO_2 concentration. For an automatic operation of this device, the valve of the CO_2 supply is electromagnetically opened at a low concentration level and then closed at a high level.

EXHALATION RATE OF A ROOM

Figure 7 shows the increase of radon concentration just after thoroughly ventilating the room and closing doors and windows. The ventilation rate, v, was checked as 0.3 hr^{-1} by the method described in the preceding paragraph. From the increase of radon concentration, we can calculate the mean exhalation rate (e) of the room. The differential equation for the radon accumulation in a room can be written as (Porstendörfer, Wicke, and Schraub, 1978)

$$\frac{dc}{dt} = e\,\frac{F}{V} - c\lambda - (c - c_0)\,v \qquad (1)$$

c_0 and c are the radon concentration outdoors and indoors, λ is the radon decay constant, and F/V is the ratio of the surface (F) and volume (V) of a room. The solution of Eq. 1 is given by

$$c(t) = \frac{e(F/V) + v\,c_0}{v + \lambda}\,[1 - e^{-(v+\lambda)t}] + c_0 \times e^{-(\lambda+v)t} \qquad (2)$$

For ventilation rates between 0.1 to 3 hr^{-1}, we can assume $\lambda \ll v$ and Eq. 2 becomes

$$c(t) = \frac{eF}{vV}\,(1 - e^{-vt}) + c_0 \qquad (3)$$

In the case of $t < 1/v$, Eq. 3 can be simplified and the exhalation rate can be determined by means of equation

$$e = \frac{V}{F}\,\frac{c(t) - c_0}{t} \qquad (4)$$

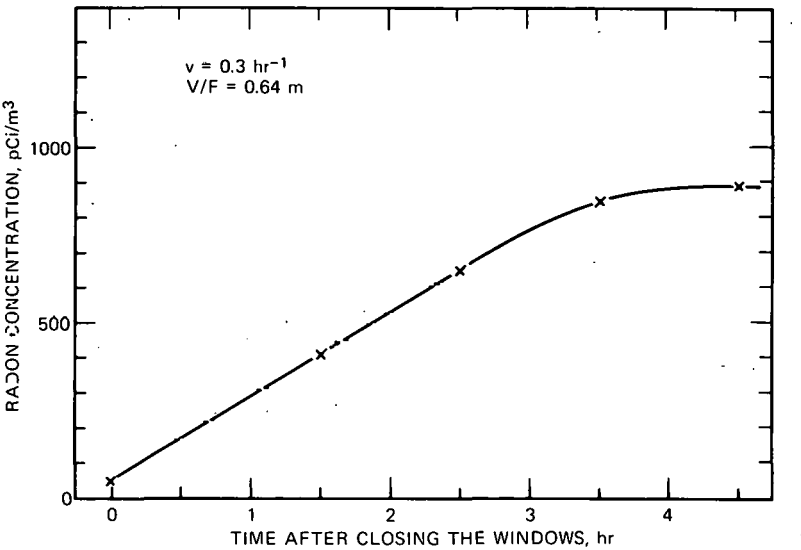


Fig. 7 The increase of radon concentration in a room after closing the window (v = ventilation rate, F = surface, and V = volume of a room).

For example, the experimental data from Fig. 7 give an average value for $e = 154$ pCi m^{-2} hr^{-1}, close to the result of direct measurements ($e = 110$ pCi m^{-2} hr^{-1}) (Scheibel, 1977). After 5 hr of radon accumulation, we got a relatively constant concentration $c(\infty)$. From this value we can also estimate the actual ventilation rate of a room derived from Eq. 3 for steady state and by means of Eq. 4:

$$v = \frac{eF}{V[c(\infty) - c_0]} = \frac{1}{t}\,\frac{c(t) - c_0}{c(\infty) - c_0} \tag{5}$$

If we use the experimental data from Fig. 7, we get a value of $v = 0.28$ hr^{-1} in agreement with the direct determination ($v = 0.3$ hr^{-1}).

RESULTS (EXAMPLE)

The diurnal variation of the concentrations of radon, thoron, and their decay products indoors and outdoors of a typical room is plotted in Fig. 8 to demonstrate the operation of the continuous device.

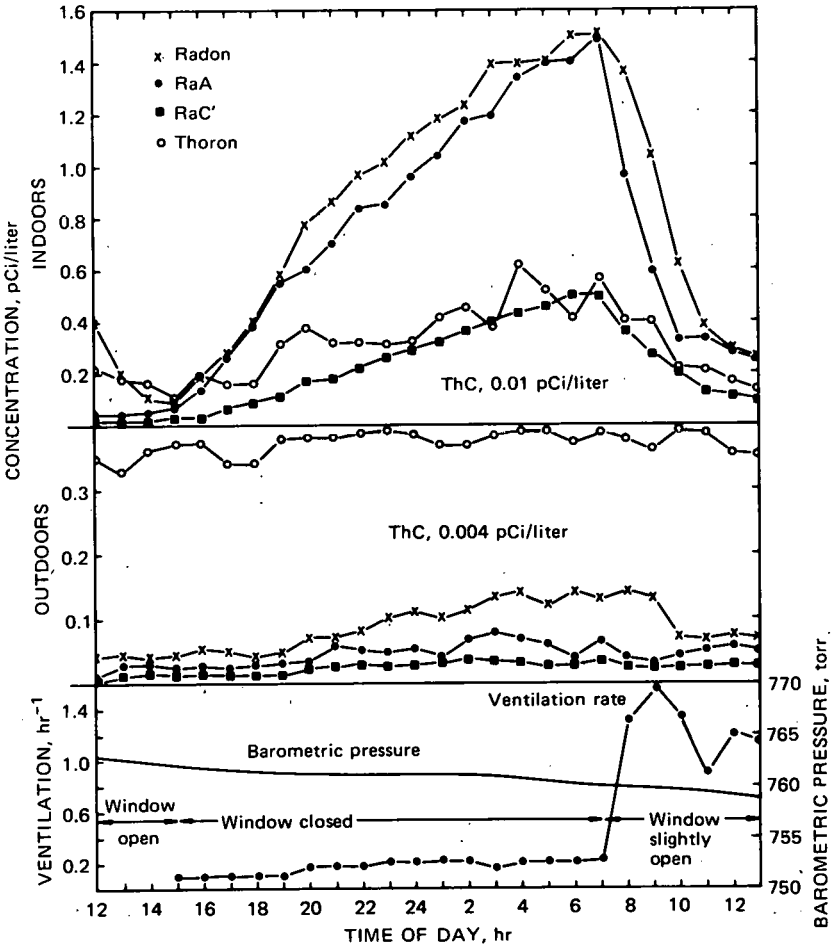


Fig. 8 Diurnal variation of concentrations of radon, thoron, and their decay products indoors and outdoors of a typical dwelling.

ACKNOWLEDGMENT

This research project is supported by the Federal Ministry of the Interior, Federal Republic of Germany, under contract St. Sch. 603.

REFERENCES

Albrecht, E., and A. Kaul, 1969, Eine Methode zur Bestimmung des zeitlichen Verlaufs von Radon-222-Konzentrationen, Tagungsbericht, *Strahlenschutz-*

probleme bei der Freisetzung und Inkorporation radioaktiver Stoffe, Berlin, pp. 174-183.

Altshuler, B., N. Nelson, and M. Kuschner, 1964, Estimation of Lung Tissue Dose from the Inhalation of Radon and Daughters, *Health Phys.*, 10: 1137-1161.

Bundesministerium des Innern, 1976, *Umweltradioaktivität und Strahlenbelastung*, Jahresbericht, 1974, Bonn, Deutschland.

Dalu, G., and G. A. Dalu, 1971, An Automatic Counter for Direct Measurements of Radon Concentration, *Aerosol Sci.*, 2: 247-255.

Damon, P., and H. Hyde, 1952, Scintillation Tube for the Measurement of Radioactive Gases, *Rev. Sci. Instrum.*, 23: 766.

Dick, J. B., and D. A. Thomas, 1951, Ventilation Research in Occupied Houses, *Vent. Eng.*, 19: 279-305.

Duggan, M. J., and D. M. Howell, 1968, Method for Measuring the Concentrations of the Short-Lived Daughter Products of Rn-222 in the Atmosphere, *Int. J. Appl. Radiat. Isot.*, 19: 865-870.

Evans, R. D., 1935, Apparatus for the Determination of Minute Quantities of Radium, Radon, and Thoron in Solids, Liquids and Gases, *Rev. Sci. Instrum.*, 6: 99-112.

Fontan, J., 1964, *The Quantitative Determination of Gaseous Radioelements Which Yield Radioactive Daughter Products*, Dissertation, Université Toulouse.

George, A. C., 1972, Indoor and Outdoor Measurements of Natural Radon and Radon Daughter Decay Products in New York City Air, in *The Natural Radiation Environment II*, Vol. 2, Symposium Proceedings, Houston, Tex., Aug. 7—11, 1972, J. A. S. Adams, W. M. Lowder, and T. F. Gesell (Eds.), ERDA Report CONF-720805-P2, pp. 741-750, Rice University and the University of Texas, Houston, NTIS.

Gabrysh, A. F., and F. J. Davies, 1954, Radon Released from Concrete in Radiant Heating, *Nucleonics*, 13: 50.

Georgii, H. W., 1954, Untersuchungen über den Luftaustausch zwischen Wohnräumen und Außenluft, *Arch. Meteorol. Geophys. Bioklimatol., Ser. B*, 5: 191-214.

Groer, P. G., D. J. Keefe, W. P. McDowell, and R. F. Selman, 1973, An Instant Working Level Meter with Automatic Individual Radon Daughter Readout for Uranium Mines, in *Proceedings of the Third International Congress of the International Radiation Protection Association*, Washington, D.C., Sept. 9—14, 1973, pp. 950-956, W. S. Snyder (Ed.), USAEC Report CONF-730907-P2, NTIS.

Haider, B., and W. Jacobi, 1972, *Entwicklung von Verfahren und Geräten zur langzeitigen Radonüberwachung in Bergbau*, Forschungsbericht K72-14, Bundesministerium für Bildung und Wissenschaft.

Handley, T. H., and C. J. Barton, 1973, *Home Ventilation Rates: A Literature Study*, USAEC Report ORNL-TM-4318, Oak Ridge National Laboratory, NTIS.

Haque, A. K. M., and A. J. L. Collinson, 1967, Radiation Dose to the Respiratory System Due to Radon and Its Daughter Products, *Health Phys.*, 13: 431-443.

——, A. J. L. Collinson, and S. O. S. Blyth Brooke, 1965, Radon Concentration in Different Environments and the Factors Influencing It, *Phys. Med. Biol.*, 10: 505-514.

Harley, N. H., and B. S. Pasternak, 1972, Alpha Absorption Measurements Applied to Lung Dose from Radon Daughters, *Health Phys.*, 23: 771-782.

Hultqvist, B., 1956, Studies on Naturally Occurring Ionizing Radiations, *K. Svenska VentenskAkad. Handl.*, Fjärde Serien, 6: Nr. 3.

Ilzhöfer, H., 1931, Untersuchungen über natürliche und künstliche Lüftung von Wohnräumen, *Arch. Hyg.*, 105: 322.

International Commission on Radiological Protection, 1966, Task Group on Lung Dynamics, Deposition and Retention Models for the Internal Dosimetry of the Human Respiratory Tract, *Health Phys.*, 12: 173-207.

Jacobi, W., 1963, A New Method to Measure Radon and Thoron in Flowing Gases and Its Use to Determine the Thoron Content of Atmospheric Air, Paper of Colloque international sur la pollution radioactive des milieux gazeux, Saclay, France.

——, 1964, A Double-Filter Device to Measure Radon and Thoron in the Breath, in *Assessment of Radioactivity in Man*, Symposium Proceedings, Heidelberg, 1964, pp. 275-289, STI/PUB/84, Vol. 1, International Atomic Energy Agency, Vienna.

——, 1972, Relations Between the Inhaled Potential Alpha Energy and Rn-222 and Rn-220-Daughters and the Absorbed Alpha Energy in the Bronchial and Pulmonary Region, *Health Phys.*, 23: 3-11.

James, A. C., and J. C. Strong, 1973, A Radon Daughter Monitor for Use in Mines, in *Proceedings of the Third International Congress of the International Radiation Protection Association*, Washington, D.C., Sept. 9—14, 1973, pp. 932-938, W. S. Snyder (Ed.), USAEC Report CONF-730907-P2, International Radiation Protection Association.

Jonassen, N., 1975, On the Effect of Atmospheric Pressure Variations on the Radon-222 Concentration in Unventilated Rooms, *Health Phys.*, 29: 216-220.

Kolb, W., and H. Schmier, 1975, Building Material Induced Radiation Exposure of the Population, presented at *The Third European Congress of the International Radiation Protection Association*, Amsterdam, May 13—16, 1975, Municipal Congress Bureau, O. Z. Acklerburgwal 199, Amsterdam, The Netherlands.

Lindeken, C. L., D. E. Jones, and R. E. McMillen, 1973, Environmental Radiation Background Variations Between Residences, *Health Phys.*, 24: 81-86.

Lowder, W. M., and W. J. Condon, 1965, Measurement of the Exposure of Human Population to Environmental Radiation, *Nature*, 206: 658-662.

Lucas, H. F., 1957, Improved Low-Level Alpha-Scintillation Counter for Radon, *Rev. Sci. Instrum.*, 28: 680.

Lundin, F. E., Jr., J. K. Wagoner, and V. E. Archer, 1971, *Radon Daughter and Respiratory Cancer, Quantitative and Temporal Aspects*, Joint Monograph No. 1, U. S. Department of Health, Education, and Welfare.

Martz, D. E., D. F. Holleman, D. E. McCurdy, and K. Schiager, 1969, Analysis of Atmospheric Concentrations of RaA, RaB and RaC by Alpha Spectroscopy, *Health Phys.*, 17: 131-138.

Mjönes, L., and G. A. Swedjemark, 1976, *Investigation of Gamma Radiation in Swedish Dwellings, Preliminary Results from Seven Countries*, National Institute of Radiation Protection Report, 1976-09-01, Stockholm.

Ohlsen, H., 1969, *Determination of the Mean Population Burden from Natural External Radiation in the Soviet Zone of Germany*, USAEC Report AEC-tr-7216, NTIS.

Pensko, J., K. Mamont, and T. Wardaszko, 1969, Measurements of Ionizing Radiation Inside Blocks of Flats in Poland, *Nucleonics*, 14: 415-424.

Porstendörfer, J., A. Wicke, and A. Schraub, 1978, The Influence of Exhalation, Ventilation and Deposition Processes upon the Concentration of Radon (Rn-222), Thoron (Rn-220) and Their Decay Products in Room Air, *Health Phys.*, 34: 465-473.

Raabe, O. G., and McD. E. Wrenn, 1969, Analysis of the Activity of Radon Daughter Samples by Weighted Least Squares, *Health Phys.*, 17: 593.

Reiter, R., 1967, Geräte und Maßnahmen zum Schutz gegen Radon und seine Folgeprodukte in Grubenwettern, *Nucleonics*, 9: 359-367.

Scheibel, H. G., 1977, *Meßverfahren zur Bestimmung kleinster Radon-Konzentrationen*, Diplomarbeit, Justus-Liebig-Universität Gießen, Germany.

Spiers, F. W., 1960, Gamma Dose-Rate to Human Tissues from Natural External Sources in Great Britain, in *The Hazards to Man of Nuclear and Allied Radiation, A Second Report to the Medical Research Council, London*, pp. 66-72.

Steinhäusler, F., 1975, Long Term Measurements of Rn-222, Rn-220, Pb-214 and Pb-212 Concentrations in the Air of Private and Public Buildings and Their Dependence on Meteorological Parameters, *Health Phys.*, 29: 705-713.

Storruste, A., A. Reistad, T. Rudjord, A. Dahler, and I. Liestöl, 1965, Measurement of Environmental Gamma Radiations in Norwegian Houses, *Health Phys.*, 11: 261-269.

Thomas, J. W., 1970, Modification of the Tsivoglou Method for Radon Daughters in Air, *Health Phys.*, 19: 691.

——, and P. C. LeClare, 1970, A Study of the Two-Filter-Method for Radon-222, *Health Phys.*, 18: 113-122.

Tóth, A., 1972, Determining the Respiratory Dosage from RaA, RaB and RaC Inhaled by the Population in Hungary, *Health Phys.*, 23: 281-289.

Tsivoglou, E. C., H. E. Ayer, and D. A. Holaday, 1953, Occurrence of Nonequilibrium Atmospheric Mixtures of Radon and Its Daughters, *Nucleonics*, 11: 40.

UNSCEAR, 1977, Sources and Effects of Ionizing Radiation, United Nations Scientific Committee on the Effects of Atomic Radiation, 1977 Report, with Annexes, to the General Assembly, United Nations, New York.

Van Dilla, M. A., and D. H. Taysum, 1955, Scintillation Counter for Assay of Radon Gas, *Nucleonics*, 13: 2.

Wachsmann, F., and J. David, 1973, Monitoring Radon Concentrations in Respirable Air, in *Symposium on Noble Gases*, Sept. 24—28, 1973, R. E. Stanley and A. A. Moghissi (Eds.), Report CONF-730915, pp. 131-133, Environmental Protection Agency's National Environmental Research Center, Las Vegas, and the University of Nevada, Las Vegas.

Wolpert, H., 1899, Über die Größe des Selbstlüftungskoeffizienten kleiner Wohnräume, *Arch. Hyg.*, 36: 220.

Wrenn, McD. E., H. Spitz, and N. Cohen, 1975, Design of a Continuous Digital Output Environmental Radon Monitor, *IEEE Trans. Nucl. Sci.*, NS-22: 645.

Yeates, D. B., A. S. Goldin, and D. W. Moeller, 1972, Natural Radiation in the Urban Environment, *Nucl. Safety*, 13(4): 275-286.

DISCUSSION

Porstendörfer: With your membrane filter collection system for radon daughters, what is your sampling time?

Nazaroff: We sample and count continuously and simultaneously. Every hour (count-time) there is a printout of the count for RaA, RaC′, and ThC′.

Jackson: Do you have a problem of the loss of your conducting surface on your surface barrier diodes from the electrostatic field?

Porstendörfer: We had not seen any loss of the conducting surface on our surface barrier detectors. We always use the ruggedized diodes.

Adams: Is the ^{210}Po, for example, deposited on the gold or on a protecting foil over the silicon detector? Do you change the protective foil often?

Porstendörfer: The deposition probability of ^{210}Po on the foil is very low, and if there is contamination (we can see it on the alpha spectrum), we change the foil.

Jonassen: Will the background counts not increase because of deposition of long-lived daughter products of radon and thoron?

Porstendörfer: We have no background problems because we record alpha spectra, and we can separate the different alpha counts of the short- and long-lived decay products.

McLaughlin: Have you taken full account in your experiments of the possible alpha counting losses associated with, for example, the approximately 110-KeV recoil of RaB when it is produced by the alpha decay of RaA?

Porstendörfer: The recoil atoms are positively charged and return to the detector surface at once.

Diurnal Variation of Radon Measured Indoors and Outdoors in Grand Junction, Colorado, and Teaneck, New Jersey, and the Influence That Ventilation Has on the Buildup of Radon Indoors

HENRY B. SPITZ,* McDONALD E. WRENN, and NORMAN COHEN
New York University Medical Center, Institute of Environmental Medicine, New York, New York

ABSTRACT

Continuous measurements of ^{222}Rn were performed indoors and outdoors in two localities that differ primarily in the amount of radon source material within, under, and around building foundations. Grand Junction, Colo., represents an area where uranium mill tailings have been incorporated into several residential and commercial structures. There is also a uranium mill tailings pile within the boundary of the city.

The radon concentration measured in the basement of a residential structure in Grand Junction known to have no uranium mill tailings within or around the foundation (i.e., a "control" house) was 0.9 ± 0.2 pCi/liter [mean ± 1 standard deviation (SD) of the mean]. Results of continuous measurements of radon in other structures in Grand Junction indicate that the presence of uranium mill tailings increased the average indoor radon concentration by at least a factor of 10 compared to the structure without tailings. The outdoor radon concentration averaged 0.7 pCi/liter with a range of 0.3 to 1.6 pCi/liter.

Continuous radon measurements were made in a two-story, wood-frame residential structure in Teaneck, N. J., which represents a locality where the ^{226}Ra content of soil and building materials is not artificially enhanced. The daily average radon content of the basement (February 1977) was 0.9 ± 0.2 pCi/liter (mean ± 1 SD) of the mean) which is the same as the concentration measured in the control house in Grand Junction.

Diurnal-like fluctuations were observed in the radon concentration in Grand Junction and Teaneck. These fluctuations were primarily a result of ventilation

*Present address: Battelle, Pacific Northwest Laboratories, Richland, Wash.

changes made by the occupants of the homes, such as periodically opening windows and doors. In a vacant house the temperature difference between indoor and outdoor air governed the rate at which air was exchanged and also determined the periodicity of the variation.

An algebraic equation was developed relating the equilibrium indoor and outdoor radon concentrations, the ventilation rate, and the radon flux from the ^{226}Ra in the soil beneath the structure and in the fabrication materials of the foundation floor and walls. This relationship was used to calculate the basement ventilation rate of the house in New Jersey. The radon flux measured 3.1×10^4 pCi/hr, the average indoor and outdoor radon concentrations were 0.83 and 0.13 pCi/liter, respectively, so that the calculated ventilation rate for the basement was 0.28 hr^{-1}. It is also shown that the ratio of the concentration of radon daughters [working level (WL)] to radon (pCi/liter) in the air of the basement is less sensitive to changes in ventilation than is the radon concentration.

The general population is exposed to naturally occurring radionuclides that deliver an internal radiation dose as the source of the activity is inhaled or ingested. For inhalation, radon is the most important naturally occurring radionuclide because, together with its short-lived alpha-emitting decay products (^{218}Po, ^{214}Bi, ^{214}Pb, and ^{214}Po), it is the primary source of radiation dose to the lung (Oakley, 1971; Klement et al., 1972; Bale and Shapiro, 1956; Harley, 1953). The natural outdoor atmospheric concentration of radon ranges from 0.01 pCi/liter to 1.0 pCi/liter for continental areas with higher concentrations occurring where uranium-bearing geologic structures are located.

Results of radon measurements within residential structures show that the airborne concentrations of radon are, approximately, three times greater than average values measured outdoors (Dawson, 1952). Spitz (1977) has shown that the ratio of the concentration of radon indoors to that outdoors was 6.4 and 1.0, respectively, for the basement and first floor of a typical residential structure in northern New Jersey. This ratio is significantly larger than the difference between the natural indoor and outdoor terrestrial gamma radiation (UNSCEAR, 1978; Hultquist, 1956). In Sweden, Hultquist was able to show that the indoor radon concentration was dependent to an extent on the materials from which a home was constructed. UNSCEAR (1978) reports indoor airborne radon measurements of 0.13 and 0.05 pCi/liter for New York and Boston, respectively.

An unfortunate situation developed in Grand Junction, Colo., where approximately 4800 residential structures were found to have uranium mill tailings material placed under or near the house (Larson, 1971). The radon, which emanates from the ^{226}Ra in the tailing sands, tends to accumulate within the house and achieve concentrations ranging from 1 to over 100 pCi/liter depending upon

the quantity of tailings and the ventilation status of the house (Spitz and Wrenn, 1974).

Inhalation exposure to radon and radon daughters by residents of a house constructed with uranium mill tailings is partially dependent on the amount of time spent indoors. Family members spending at least 8 hr per day at home could accrue a significant exposure to radon in comparison to the same family living in a house constructed without tailings. The highest exposure presumably would be to mothers and young children who remain indoors longer than other members of the family.

To quantitate the radon exposure received by residents of a particular house, it is important that we measure and characterize the range of the concentration when the family is occupying the structure as well as the mean radon concentration over a diurnal cycle. Because of the well-documented diurnal concentration pattern of radon in outdoor air (Wilkening, 1952; Cotton, 1955; Gale and Peaple, 1958; Pearson and Moses, 1965; Newstein, Cohen, and Krablin, 1971), it might be expected that the indoor atmosphere would show a similar radon diurnal cycle with only, perhaps, a difference in absolute magnitude (Gemesi, Szy, and Tóth, 1975).

RESEARCH PROGRAM

Continuous radon measurements were performed in Grand Junction, Colo., and in an eastern metropolitan area (Teaneck, N. J.) to assess what significance the presence of naturally occurring or artificially enhanced amounts of radon source material might have upon the buildup of radon indoors and outdoors. Several continuous, environmental, digital-readout, radon measuring instruments, developed at the New York University Medical Center, Institute of Environmental Medicine (Wrenn, Spitz, and Cohen, 1975; Spitz and Wrenn, 1974) were used in the monitoring program.

Figure 1 shows the sensitive region of the radon measuring instrument and illustrates the collection and detection mechanism for the short-lived, alpha-emitting radon daughters which result exclusively from ^{222}Rn which has diffused through the porous foam filter. The detector is sensitive to only ^{222}Rn in the air since the particulate radon daughters cannot diffuse through the foam filter.

Several residential structures in Grand Junction were selected for measurement of radon indoors. The detectors were usually installed in locations where the radon concentration was expected to be maximum for the structure. For example, ground floor or basement

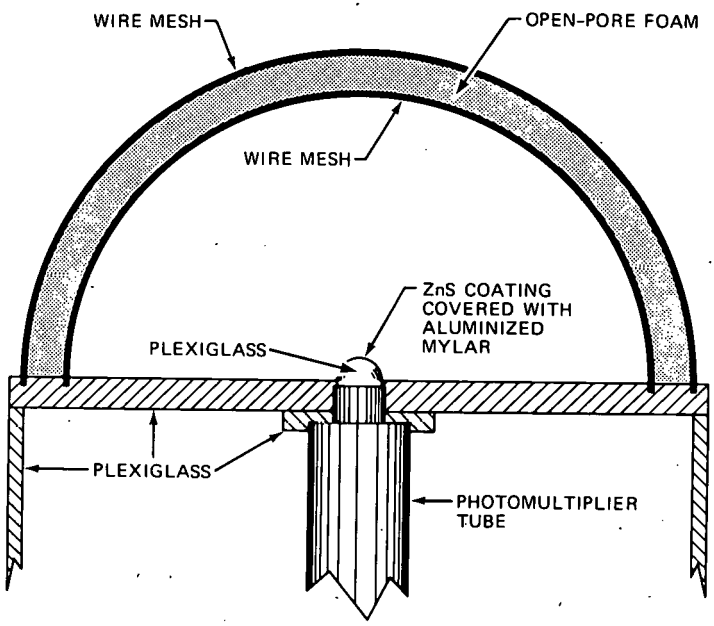


Fig. 1 Cross-sectional diagram of the sensitive region of the detector.

bedrooms were chosen because of the close proximity to the radon source material within or under the foundation. Also, rooms with poor ventilation were selected for measurement since radon could accumulate in the enclosed area. Radon measurements were made for at least 24 hr in order to observe whether or not any diurnal-like pattern of the concentration would occur. Most sites were measured for several days.

Continuous radon measurements were performed in Teaneck, N. J., to represent an area where the amount of radon source material is not artificially enhanced. With the use of continuous radon instruments located in the basement, simultaneous measurements were made indoors and outdoors: first floor, second floor, and outside of a two-story wood-frame residential structure. The detector positioned outdoors was shielded from direct exposure to the weather.

Rather than perform radon measurements in several different structures in the New York metropolitan area, we decided to concentrate on a single dwelling and collect data for many weeks in order to adequately characterize the diurnal-like variation in the

airborne radon content. The spatially distributed detectors provide data showing how radon varies with location in the house.

RESULTS OF RADON MEASUREMENTS IN GRAND JUNCTION

The ambient outdoor ^{222}Rn content in Grand Junction was measured continuously with a radon instrument for slightly more than 3 days in September 1975 (Fig. 2). The radon concentration values were calculated from sequential 4-hr periods of integration. The average radon concentration was 0.73 pCi/liter with a range from 0.25 to 1.59 pCi/liter. The concentration of radon in the atmosphere displayed a diurnal-like cycle with a maximum appearing after midnight and a minimum in the late afternoon.

Shearer and Sill (1969) measured 0.8 pCi ^{222}Rn/liter in the air of Grand Junction. They determined that the uranium mill tailings distributed throughout the community did not significantly raise the environmental levels of radon. In addition, they found that the atmospheric radon concentration was unaffected by radon emanation from the nearby uranium mill-tailings pile at a distance greater than ½ mile from the pile.

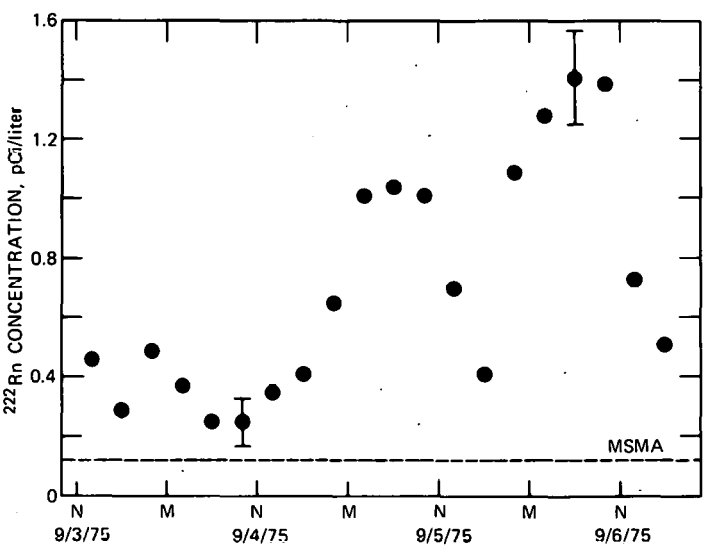


Fig. 2 Continuous radon measurements performed outdoors in Grand Junction, Colo., Sept. 3—6, 1975, 4-m cumulative observations. ^{222}Rn concentration, pCi/liter: minimum, 0.25; maximum, 1.59; mean, 0.73.

Radon was measured inside a structure in Grand Junction known to be void of any radon source material other than that normally found in trace amounts within materials of construction. No uranium mill tailings were known to be within, under, or around this structure. Continuous radon measurements were made for 6 days in the basement of this control home during the summer (June 13—18, 1974). The results, based on 40-min counts (Fig. 3), display a prominent diurnal-like pattern that was generated primarily by the type and nature of the ventilation used by the residents to cool the house during the afternoon. The evaporative cooling technique involves exchanging large amounts of air with the outdoors and restricts the build up of radon indoors while the cooling unit is in operation. The average radon concentration in the basement of the control home was 0.92 pCi/liter with a range, based upon 80-min counts, from < 0.4 to 2.3 pCi/liter.

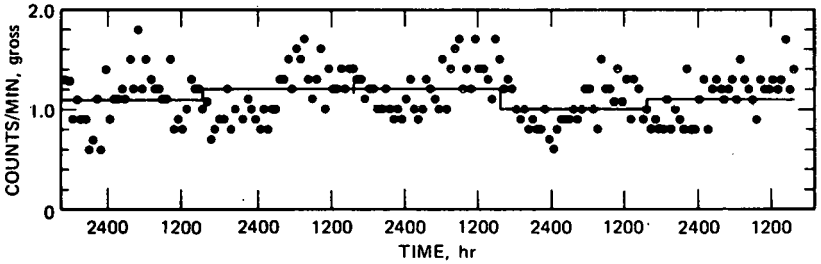


Fig 3 Continuous radon measurements performed in a home in Grand Junction, Colo., where the origin of radon source material is due to environmental conditions, June 13—18, 1974. Mean, ^{222}Rn = 0.9 pCi/liter.

We believe intuitively that the mean radon content would be greater than 0.9 pCi/liter if evaporative cooling was not used to condition the air of the house. A characteristic feature of an occupied structure is that the radon concentration varies over a greater range than that measured in an unoccupied structure. The increased variation is due, at least in part, to the large changes in ventilation produced by normal routine traffic entering and leaving the house as well as the demands of the air-treatment system. The unoccupied house presents an enclosed structure into which radon can build up without the variation produced by man-made changes in ventilation.

Figures 4 and 5 show the radon variations in vacant houses that have substantial amounts of uranium mill tailings beneath their

foundations. The range of the radon measurements shown in Fig. 4 varies over two orders of magnitude (namely, from 49.3 to 129.0 pCi/liter with a mean of 86.2 pCi/liter). The variation in the radon content of the unoccupied house is produced by the exchange of warm indoor air, heated slowly during the day by the sun, with the cooler outdoor air in the evening. Thus radon can build up inside the house during the daytime but will be exhausted during the evening as the warm air inside diffuses into the cooler evening atmosphere carrying radon outdoors.

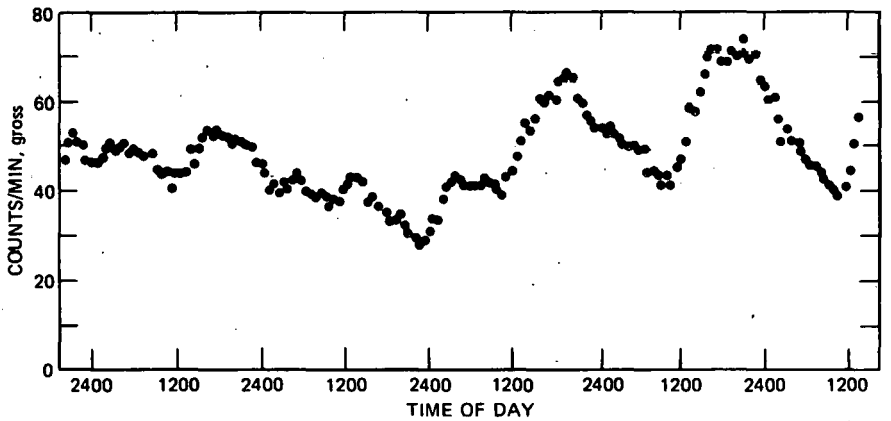


Fig. 4 Continuous measurements of ^{222}Rn in a vacant house in Grand Junction, Colo., Aug. 30 to Sept. 4, 1973. Radon concentration: average, 86.2 pCi/liter; maximum, 129.0 pCi/liter; minimum, 49.3 pCi/liter.

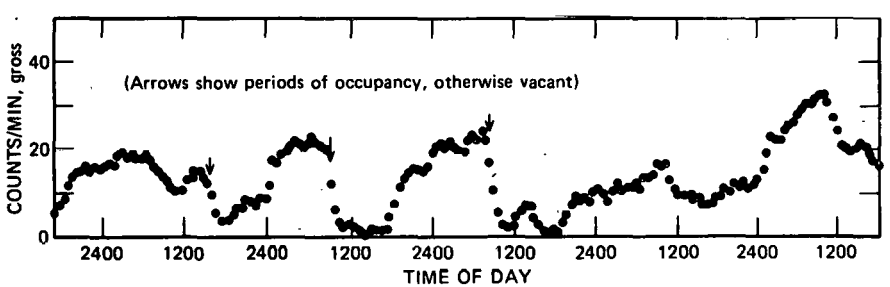


Fig. 5 Continuous measurements of ^{222}Rn in a house, vacant except for three periods, annotated by arrows, in Grand Junction, Colo., Sept. 12—19, 1973. Radon concentration: average, 29.9 pCi/liter; maximum, 72.4 pCi/liter; minimum, 0.1 pCi/liter.

The ventilation status of another vacant house (Fig. 5) was significantly disturbed three times for several hours, as indicated in Fig. 5 by arrows, producing a decrease in the indoor concentration. The average measured radon content was 29.9 pCi/liter with a range from 0.1 to 72.4 pCi/liter. During the third period of occupancy, the radon concentration decreased by three orders of magnitude. Assuming that the house remained vacant without disturbance, the minimum radon concentration probably would not have been observed and the range would encompass only two orders of magnitude.

Radon measurements were performed in the basement of an occupied house during October 1973 (Fig. 6). The frequency of maximums and minimums was controlled by the air-treatment system that was activated around midday when the air temperature indoors became uncomfortable. This system enhanced the indoor/outdoor air-exchange rate. The range of the radon concentration encompasses three orders of magnitude owing to the ventilation of the house which periodically replaces the air indoors with outdoor, relatively radon-free air.

The preceding examples demonstrate the significance that ventilation has on the ultimate buildup of radon indoors. The high radon content from the uranium mill tailings within the foundation of these structures magnifies the effect that any ventilation change will have upon radon buildup.

Continuous radon measurements described here show that the average radon concentration for a structure may not be a valid indicator of the radon exposure incurred by residents of a house. The radon concentration tends to be at maximum when the house is vacant. The minimum radon concentration occurs during periods of

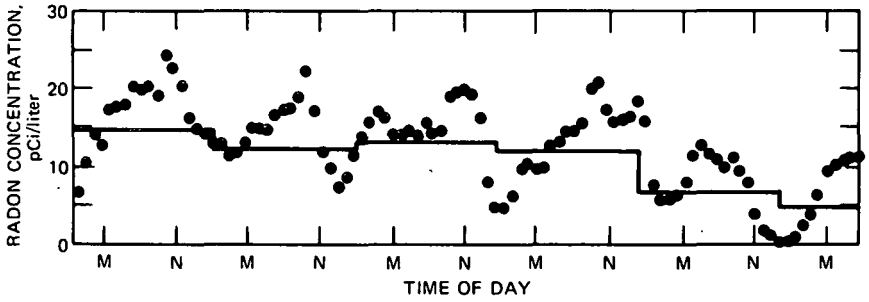


Fig. 6 Continuous measurements of ^{222}Rn in an occupied house in Grand Junction, Colo., Oct. 9—15, 1973. Minimum < MSMA, 0.24 pCi/liter; maximum, 22.3 pCi/liter; mean, 10.6 pCi/liter.

occupancy and, therefore, the exposure to the residents is actually less than would be calculated from an average concentration value.

This fact is demonstrated by the results of radon monitoring shown in Fig. 7. The average radon content of this house, during the 13-day observation period, was 56.8 pCi/liter with a range from 236.8 to 16.4 pCi/liter. The fluctuations are consistent with the fact that the house was closed and vacant during the day so that radon could build up inside the "sealed" structure. Radon diminished when the occupants returned and opened doors and windows and started the air-cooling unit. Any estimate of cumulative exposure to radon for the occupants of this house would be in error if based only on the mean concentration. It would be more appropriate to use estimates of exposure determined from radon measurements made only when the house was occupied. Table 1 lists the cited radon measurements performed in Grand Junction.

RESULTS OF LONG-TERM RADON MONITORING IN NEW JERSEY

A long-term measurement program was performed to examine the fluctuation of radon inside a typical wood-frame residential structure in an eastern metropolitan area, approximately 15 miles west of Manhattan (Teaneck, N. J.). Unlike other investigations where several locations were surveyed on a short-term "grab sample" basis (Hultquist, 1956; Dawson, 1952; Steinhausler, 1975), this monitoring concentrated on a single dwelling and measured radon simultaneously in the basement, a second floor room, and outdoors. The house has two stories above a full basement which is completely below the grade level. During the measurements the house was occupied, and the hot-air heating system maintained the ambient indoor temperature at 21°C.

The first phase of the monitoring was initiated in January and extended for a total of 48 days through the month of February 1976. Table 2 lists the results of the measurements. The continuous radon measurements provided the opportunity to examine the indoor fluctuations in a unique manner. With simultaneous measurements made in the basement and the second floor of the house, the spatial characteristics and diurnal variability of indoor radon were investigated. An 80-min integration period was used, thereby producing 18 radon measurements each day. Figure 8 shows a portion of the results and shows each consecutive measurement along with 24-hr mean values.

The results of the radon measurements show that the magnitude of radon in the basement is 60% larger than that on the second floor.

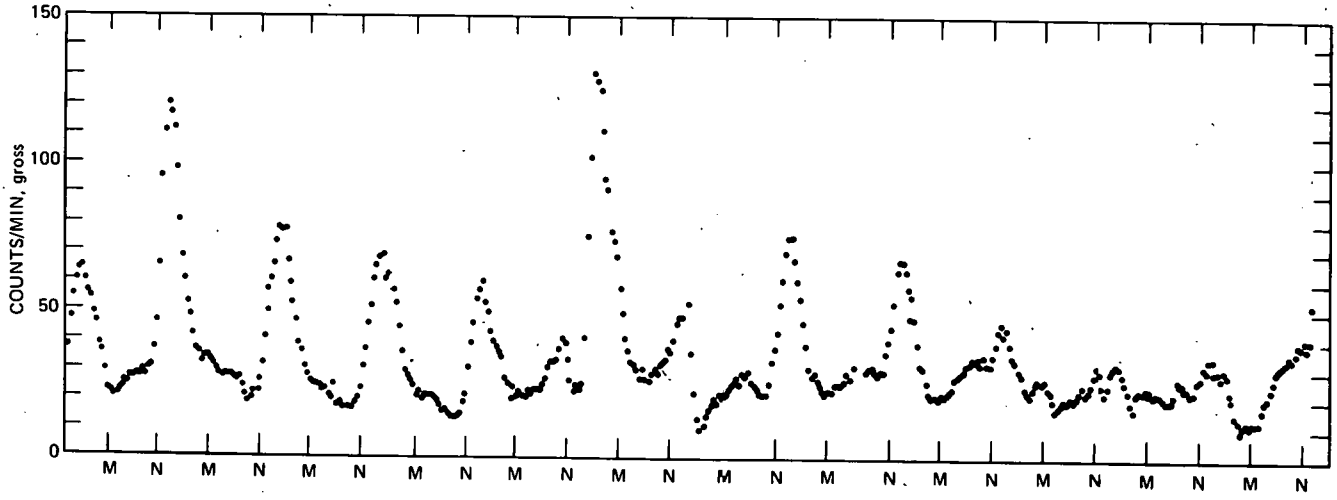


Fig. 7 Continuous measurements of ^{222}Rn in an occupied house in Grand Junction, Colo., performed for 13 days in the basement of the structure. Average radon concentration, 56.8 pCi/liter; maximum, 236.8 pCi/liter; minimum, 16.4 pCi/liter.

TABLE 1

Summary of Continuous Radon Measurements Performed in Grand Junction, Colo.

Site	Mean, pCi/liter	Range, pCi/liter
Outdoor	0.73	0.25—1.59
Indoor (control, occupied)	0.92	<0.4—2.3
Indoor (No. 1112, vacant)	86.2	49.3—129.0
Indoor (No. 1109, vacant)	29.9	0.1—72.4
Indoor (No. 1110, occupied)	56.8	16.4—236.8
Indoor (No. 1111, occupied)	10.6	<0.2—22.3

TABLE 2

Summary of Indoor Radon Measurements in Teaneck, N. J.

Site	24-hr mean ± 1 SD,* pCi/liter	Range, pCi/liter
	Jan. 11—Feb. 28, 1976	
	n = 48 days	n = 864 meas.
Basement	1.14 ± 0.25	1.84—0.69
Second floor	0.42 ± 0.10	0.61—0.21
	June 26—July 3, 1976	
	n = 8 days	n = 144 meas.
Basement	0.33 ± 0.05	0.81—0.15

*Error represents 1 SD of the mean.

This is expected because the basement of the structure provides a volume into which the radon can diffuse directly from the walls and floor and build up with time. The location of the second-floor room does not afford a direct pathway to the radon source material so that the radon concentration will not be as high as in the basement.

Although the radon concentration upstairs is less than that measured for the basement, the temporal fluctuations are very similar. A factor that might account for the measured variation is the change in the ventilation of the structure caused by the air-treatment system.

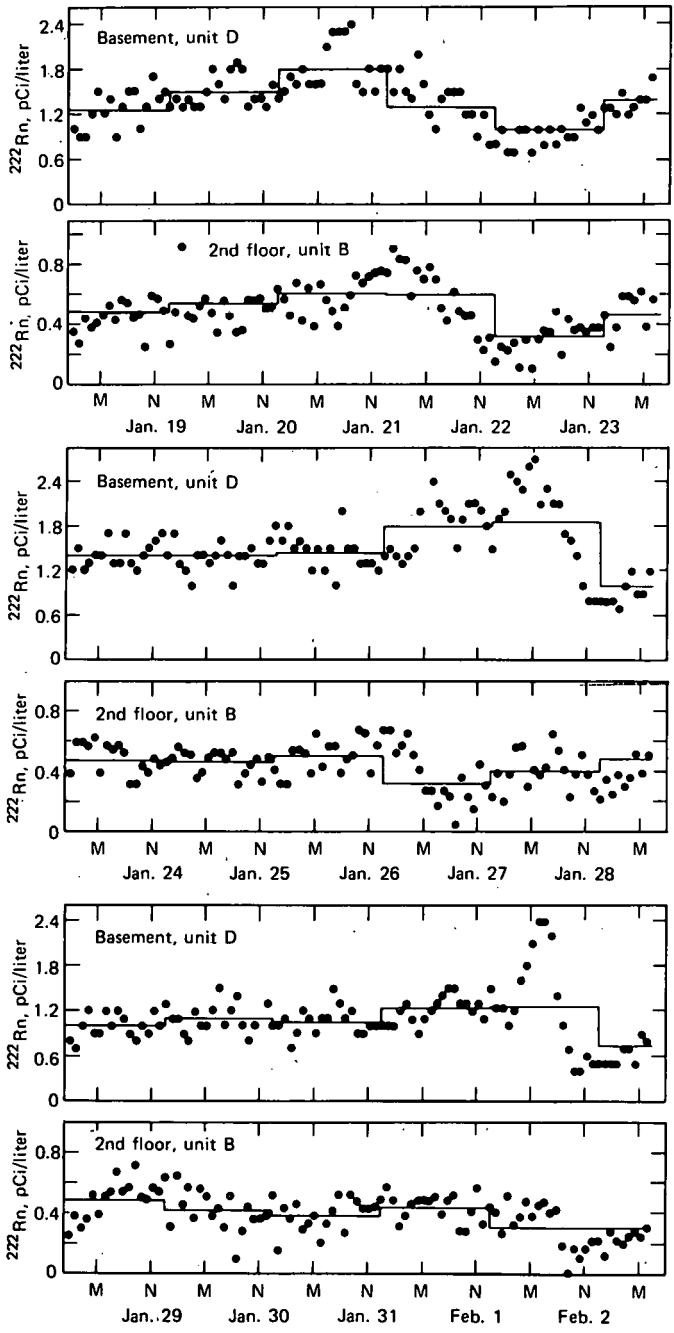


Fig. 8 Continuous radon measurements performed simultaneously in the basement and on the second floor of a wood-frame house in Teaneck, N. J.

By virtue of the continuous nature in which radon measurements are made by this instrument, the fluctuations of the indoor radon content are easily investigated. One of the unique results that developed from the long-term monitoring was a description of the radon diurnal variation measured in the basement and on the second floor of the residential structure in New Jersey. For the diurnal pattern of the indoor radon concentration to be determined, a mean value was calculated from identical 80-min periods each day for the duration of the monitoring program. For example, Fig. 9 shows the diurnal radon pattern for the basement and second floor of the house as measured from Feb. 11—28, 1976. The mean value and one standard deviation for each period of the day is plotted to show the diurnal pattern.

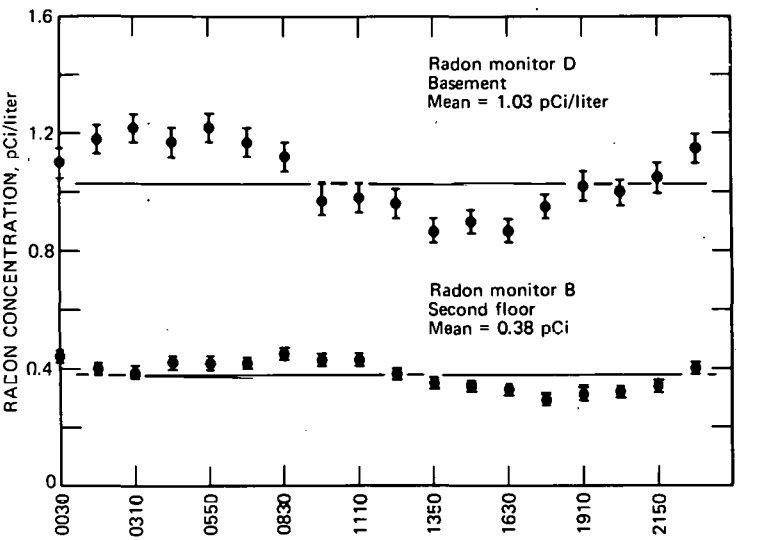


Fig. 9 Diurnal variation in the radon concentration measured in the basement and on the second floor of a wood-frame house in Teaneck, N. J., for 18 days during the winter, Feb. 11—28, 1976.

The radon concentration in the basement (1.03 pCi/liter) was greater than the mean value on the second floor (0.38 pCi/liter). Also, the fluctuations in the basement were much greater in magnitude than on the second floor. The maximum radon content occurs in the early morning hours, and the minimum appears in the late afternoon. It is most interesting to note that the occurrence of

minimums and maximums measured indoors is similar to that measured outdoors by Moses, Stehney, and Lucas (1960), Li (1974), Wilkening (1952), Dike (1906), Cotton (1955), and Israël (1951).

The radon monitoring was repeated for a short duration in the summer months to assess what change might occur in the radon content of the air due to seasonally altered ventilation conditions. A radon measuring instrument was installed in the basement for only 6 days from June 26 to July 1, 1976. The average radon concentration (0.31 pCi/liter) was approximately 30% lower for the basement in the summer than for the winter. However, the diurnal pattern measured in the summer was the same as that measured in the winter since the maximum and minimum occurred at the same time regardless of the season (Fig. 10).

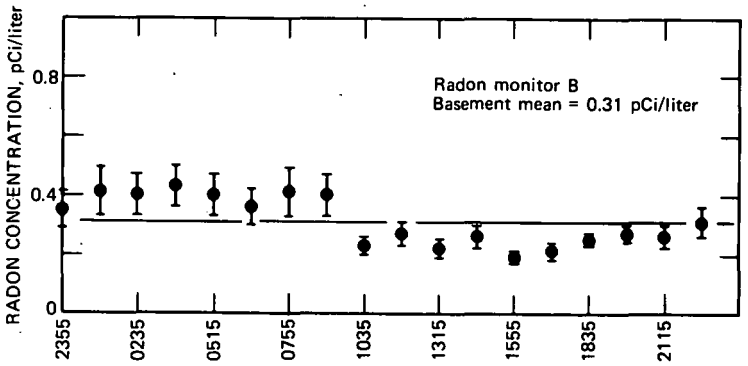


Fig. 10 Diurnal variation in the radon concentration measured only in the basement in a wood-frame house in Teaneck, N. J., during the summer, June 26—July 1, 1976.

The second phase of the radon monitoring program started in January 1977 and included three detectors: one in the basement, one on the first floor, and one outdoors. The results of a selected portion of the measurements are shown in Fig. 11. Sequential 24-hr mean values are also shown on the figure. The radon concentration (mean ± 1 SD of the mean) for the basement, first floor, and outdoors was 0.89 ± 0.17 pCi/liter, 0.14 ± 0.05 pCi/liter, and 0.09 ± 0.02 pCi/liter, respectively. Table 3 lists the average radon concentrations measured during the total observation period between Jan. 15 and Mar. 11, 1977.

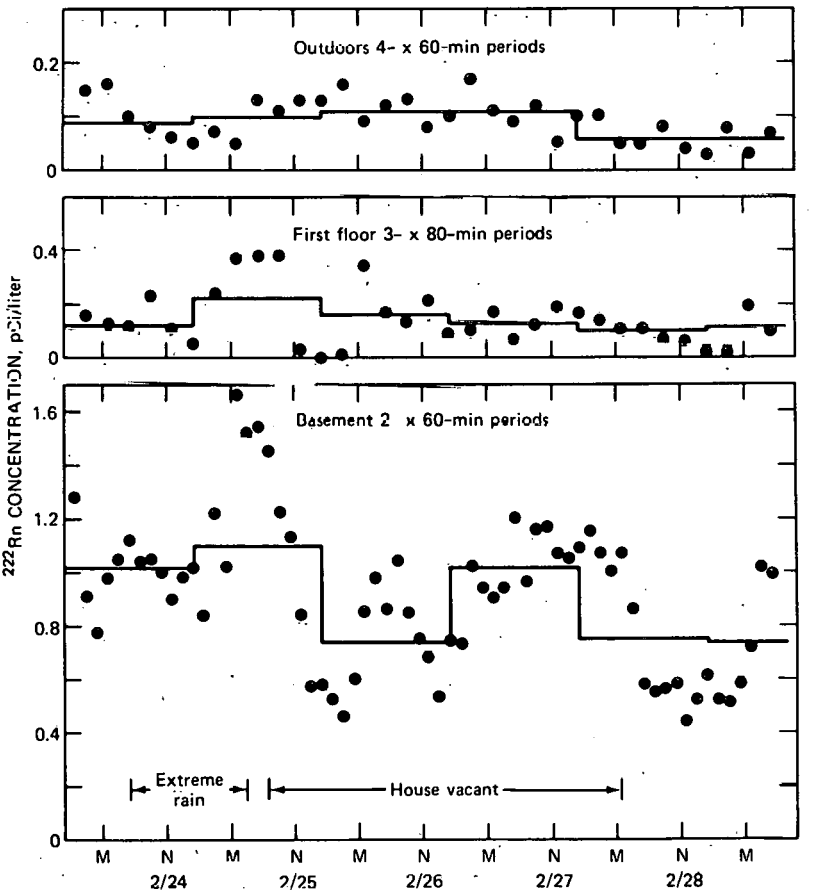


Fig. 11 Simultaneous measurements of ^{222}Rn performed indoors (basement and first floor) and outdoors in a wood-frame house in Teaneck, N. J.

TABLE 3

Continuous Radon Measurements Teaneck, N. J., 1/15/77–3/11/77 (54 Days)

Location	Radon conc., pCi/liter, mean ± 1 SD
Basement	0.79 ± 0.15
First floor*	0.15 ± 0.06
Outside	0.08 ± 0.03

*1/31/77–3/4/77 (32 days).

INFLUENCE OF VENTILATION ON CONCENTRATION OF RADON INDOORS

A mathematical expression based on fundamental principles has been developed to relate the radon concentration indoors and outdoors, the ventilation rate of a structure, and the radon flux into the structure from ^{226}Ra in the foundation walls and floor and the subsoil and backfill. The rate of change of ^{222}Rn in an enclosed structure or room can be described by the following differential equation:

$$\frac{d}{dt}(\text{radon}) = \text{influx} - \text{removal} - \text{decay} \tag{1}$$

and

$$\frac{d}{dt}(\text{radon content}) = \bar{S}A - \lambda_r C_i V - \lambda_v C_i V + \lambda_v C_o V \tag{2}$$

where C_i = ^{222}Rn concentration indoors, pCi/liter
C_o = ^{222}Rn concentration outdoors, pCi/liter
$\bar{S}A$ = radon flux, pCi/hr
λ_v = ventilation rate, hr^{-1}
λ_r = radioactivity decay constant for ^{222}Rn, hr^{-1}
V = volume of site, liters

If $\lambda_r \ll \lambda_v$, $C_i > C_o$, and assuming that a steady-state condition exists with respect to the radon concentration, i.e., $d/dt\ C_i = 0$, then

$$\frac{\bar{S}A}{\lambda_v V} = C_i - C_o \tag{3}$$

Therefore, under steady-state conditions, the radon concentration indoors can be described in terms of the parameters of Eq. 3.

We calculated the ventilation rate for the basement of the structure in New Jersey using Eq. 3 and measurements of the simultaneous radon concentrations indoors and outdoors and a measure of the radon flux through the floor and walls of the basement foundation. Figure 12 shows the variation in the radon concentration measured during the time in which radon flux measurements were made in the basement. Table 4 lists the results of the measurement and shows that the ventilation rate of the basement was 0.28 hr^{-1}.

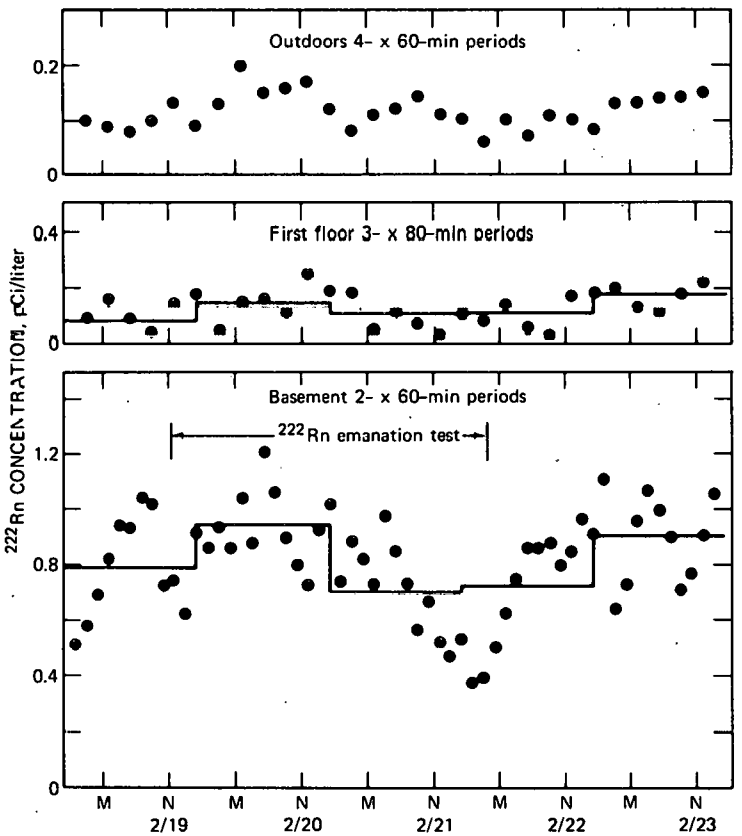


Fig. 12 Simultaneous measurements of ^{222}Rn performed indoors (basement and first floor) and outdoors in Teaneck, N. J., concurrently with radon flux measurements in the basement.

TABLE 4

Ventilation Rate Calculation

Flux,* pCi/hr	Radon conc., pCi/liter		Ventilation rate, hr^{-1}
	Indoor	Outdoor	
3.1×10^4	0.83	0.13	0.28

*Measured with charcoal canisters [Environmental Measurements Laboratory, formerly Health and Safety Laboratory (USAEC).]

The ventilation rate calculation from Eq. 3 requires a steady-state radon concentration. Figure 12 shows that the radon concentration decreased during the flux measurements so that conditions established for derivation of Eq. 3 may not have been rigorously met.

The flux measurements were performed with 16 charcoal canisters attached to structurally intact locations on the floor and walls of the basement foundation (Countess, 1976). (The Environmental Measurements Laboratory of the Department of Energy supplied the charcoal canisters and performed the spectrometric analysis to determine the radon flux.) Radon emanation through cracks in the foundation was ignored for this calculation. The average radon flux for the floor and walls, measured between Feb. 19 and Feb. 21 of 1977, was 5 and 2 pCi m^{-2} hr^{-1}, respectively.

The addition of a ventilation term to the radon buildup and decay equations as described by Hultquist (1956) provides a relationship between radon, radon daughters in the air, and the ventilation rate of the enclosed structure under conditions where the *only* removal mechanism is dilution ventilation. Obviously other mechanisms for daughter product removal exist also such as electrostatic and convective diffusion to surfaces. Figure 13 shows the effect that ventilation has on the equilibrium between radon and its various daughter products taking only ventilation into account for removal. We can see from the figure that the ratio of the concentration of radon daughters (WL) to radon (100 pCi/liter) approaches unity as the rate of ventilation decreases. In addition, Table 5 shows that the upper limit ratio of the concentration of radon daughters to radon is less sensitive to changes in the ventilation of a room than to the radon content. Thus, with a knowledge of the concentration of ^{222}Rn in a structure and with estimates of the ventilation rate, conservative upper limit values for the ratio of the concentration of radon daughters to radon can be determined from Fig. 13. Since this ratio is relatively insensitive to changes in ventilation, it can be a useful indicator of the equilibrium between radon and its short-lived daughter products.

By using the previous argument, we can translate very simply into radon concentrations the exposure limits declared in units of the working level. Since radon is easier to measure than its short-lived decay products and since radon has been shown to be related to an upper limit of the radon daughter concentrations, exposure estimates can be made directly from measures of the radon concentration whenever the ratio of the short-lived daughters to radon will not vary too greatly.

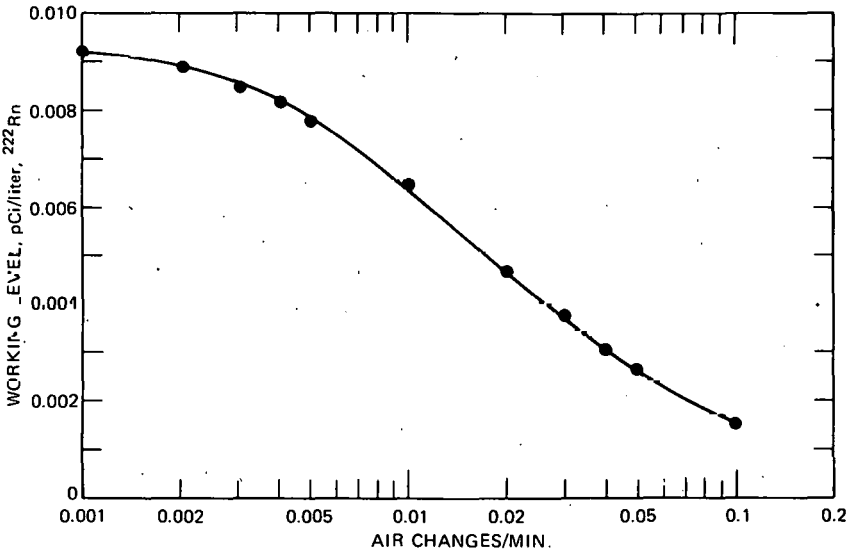


Fig. 13 Calculated upper limit of ratio of working level to radon concentration as a function of the ventilation rate.

TABLE 5

Evaluation of Radon Balance Equation

λ_v, hr^{-1}	^{222}Rn concentration, pCi/liter	WL/^{222}Rn	WL
0.06 (0.001 min^{-1})	3.3	0.009	0.030
0.3 (0.005 min^{-1})	1	0.008	0.008
—	—	—	—
—	—	—	—
—	—	—	—
1 (0.017 min^{-1})	0.2	0.004	0.008
Range 16	~20	~2	

SUMMARY AND CONCLUSIONS

Several conclusions have been developed as a result of long-term, continuous measurements of radon in two widely separated localities

that differ essentially only in the amount of radon source material, from natural and man-made origins, found in the environment. The conclusions are:

1. There is a direct relationship between the airborne radon content indoors or outdoors and the amount of radon source material found in the environment. For example, the presence of uranium mill tailings in or under the foundation of a structure will increase the radon content of the air indoors above that for a similar structure without tailings.

2. Ventilation of a structure, either by an air-treatment system or as a result of living habits, is the most significant influence on the levels of radon established indoors.

3. The indoor radon concentration exhibits a pronounced cyclic pattern with a period of approximately 24 hr.

4. Enclosed spaces (e.g., basements) in contact with, or a short pathway from, source material in or under the foundation exhibit a higher radon content than other rooms in the structure which have direct access, via windows and doors, to the outside air.

The importance that the radon source term has on the ultimate buildup of radon in the air of a closed structure was demonstrated from extensive field monitoring conducted indoors and outdoors in two localities that differ primarily in the amount of source material from nature and man-made origins. The mean radon content of outdoor air measured in Grand Junction, Colo., where uranium mill tailings had been accidentally incorporated in building materials and distributed around the locality, was 0.73 pCi/liter. In New Jersey, where radon source material is derived from natural conditions, the mean outdoor radon concentration measured 0.13 pCi/liter. Unlike "grab" samples, these outdoor concentrations represent mean values measured over several diurnal cycles. The mean (range) indoor radon content measured during the summer in the basements of a control location (no tailings) in Grand Junction and a structure in New Jersey was 0.92 pCi/liter (0.18 to 2.32 pCi/liter) and 0.33 pCi/liter (0.15 to 0.81 pCi/liter), respectively.

The range of the concentration is cited along with the mean value since indoor radon displays a cyclic variation with a period of approximately 24 hr as determined from the continuous radon measurements. The diurnal variation has a maximum in the early morning before sunrise and a minimum in the late afternoon. Ventilation of a house appears to be the factor that determines the appearance of a diurnal variation. For an occupied structure, the cyclic behavior of the radon content is strongly influenced by the occupance pattern of the family. The range of the radon diurnal

variation in Grand Junction was greater in magnitude than that measured at the site in New Jersey which demonstrates the significant contribution that radon source material in the tailings has on the ultimate build up of radon indoors. At one location in Grand Junction the mean (range) radon content indoors was 56.8 pCi/liter (16.4 pCi/liter to 236.8 pCi/liter), which was 60 times that measured at the control site where no uranium mill tailings were present.

From fundamental principles describing the rate of change of the concentration of ^{222}Rn indoors, a mathematical relationship may be developed between the ^{222}Rn concentration indoors and outdoors, the ventilation rate of the structure, and the radon flux through the foundation walls and floor. Using measurements of the radon flux and the indoor and outdoor radon concentrations, a calculation of the ventilation rate of the basement of the structure in New Jersey was made.

ACKNOWLEDGMENTS

We thank Frank McGinley, in the Grand Junction Office of the Department of Energy, for his assistance with the logistical arrangements in Grand Junction; Al Breslin and Richard Countess of the Department of Energy's Environmental Measurements Laboratory for their help with the radon emanation measurements; and the Albert Spitzs for sharing their home with several radon measuring instruments for over 14 months.

This research is supported by the U. S. Department of Energy and is part of center programs supported by Grant No. ES 00260, from the National Institute of Environmental Health Sciences, and Grant No. CA 13343, from the National Cancer Institute.

REFERENCES

Bale, W. F., and J. V. Shapiro, 1956, Radiation Dosage to Lungs from Radon and Its Daughter Products, in *Proceedings of the International Conference on the Peaceful Uses of Atomic Energy, Geneva, 1955*, Vol. 13, p. 233, United Nations, New York.

Cotton, E. S., 1955, Diurnal Variations in Natural Atmospheric Radioactivity, *J. Atmos. Terr. Phys.*, 7: 90.

Countess, R. J., 1976, ^{222}Rn Flux Measurements with a Charcoal Canister, *Health Phys.*, 31: 455.

Dawson, K. B., 1952, Radioactive Material in the Atmosphere, *Br. J. Cancer*, 6: 22.

Dike, P. H., 1906, The Diurnal Variation of the Amount of Radioactive Emanation in the Atmosphere, *J. Geophys. Res.*, 11(3): 125.

Gale, H. J., and L. H. J. Peaple, 1958, A Study of the Radon Content of Ground Level Air at Harwell, *Int. J. Air Pollut.*, 1: 103.

Gemesi, J., D. Szy, and A. Tóth, 1975, Radon-222 Content in the Internal Atmosphere of Hungarian Residential Buildings, in *The Natural Radiation Environment II*, Vol. 2, Symposium Proceedings, Houston, Tex., Aug. 7—11, 1972, J. A. S. Adams, W. M. Lowder, and T. F. Gesell (Eds.), ERDA Report CONF-720805-P2, pp. 751-756, Rice University and the University of Texas, Houston.

Harley, J. H., 1953, Sampling and Measurement of Airborne Daughter Products of Radon, *Nucleonics*, 11: 12.

Hultquist, B., 1956, Studies on Naturally Occurring Ionizing Radiations, *K. svenska VetenskAkad. Handl.*, Fjarde Sevien, Band 6, Nr. 3.

Israël, H., 1951, Radioactivity of the Atmosphere, *Compendium of Meteorology*, p. 155, American Meteorological Society, Boston.

Klement, A. W., C. R. Miller, R. P. Minx, and B. Schleien, 1972, *Estimates of Ionizing Radiation Doses in the United States: 1960—2000*, EPA Report ORP/CSD-72-1, Environmental Protection Agency.

Larson, C., 1971, USAEC Commissioner, Statement Before the Subcommittee on Raw Materials, Joint Committee on Atomic Energy.

Li, T. Y., 1974, Diurnal Variations of Radon and Meteorological Variables near the Ground, *Boundary-Layer Meteorol.*, 7: 185.

Moses, H., A. F. Stehney, and H. F. Lucas, 1960, The Effect of Meteorological Variables upon the Vertical and Temporal Distributions of Atmospheric Radon, *J. Geophys. Res.*, 64(4): 1223.

Newstein, H., L. D. Cohen, and R. Krablin, 1971, An Automated Atmospheric Radon Sampling System, *Atmos. Environ.*, 15: 823.

Oakley, D. T., 1971, *Natural Radiation Exposure in the United States*, Doctoral Dissertation, Harvard School of Public Health.

Pearson, J. E., and H. Moses, 1965, Atmospheric Radon-222 Concentration Variation with Height and Time, *J. Appl. Meteorol.*, 5: 175.

Shearer, S. D., and C. W. Sill, 1969, Evaluation of Atmospheric Radon in the Vicinity of Uranium Mill Tailings, *Health Phys.*, 17: 77.

Steinhausler, F., 1975, Longterm Measurements of ^{222}Rn, ^{220}Rn, ^{214}Pb, and ^{212}Pb Concentrations in the Air of Private and Public Buildings and Their Dependence upon Meteorological Parameters, *Health Phys.*, 29: 705.

Spitz, H., 1977, *Design and Utilization of a Continuous, Digital-Output, Environmental Radon Measuring Instrument*, Doctoral Thesis, New York University, Graduate School of Arts and Science.

——, and M. E. Wrenn, 1974, *The Diurnal Variation of the Radon-222 Concentration in Residential Structures in Grand Junction, Colorado*, Second Workshop on the Natural Radiation Environment, USAEC Report HASL-287, pp. 100-117, Health and Safety Laboratory, NTIS.

United Nations Scientific Committee on Effects of Atomic Radiation, 1977, *Sources and Effects of Ionizing Radiation*, 1977 Report to the General Assembly, United Nations Publication No. E.77.1X.1.

Wilkening, M. H., 1952, A Monitor for Natural Atmospheric Radioactivity, *Nucleonics*, 10(6): 36.

Wrenn, M. E., H. B. Spitz, and N. Cohen, 1975, Design of a Continuous Digital-Output Environmental Radon Monitor, *IEEE Trans. Nucl. Sci.*, NS-22(1): 645.

DISCUSSION

Swedjemark: Have you thought of the wall effect when you looked at the equilibrium factor for radon?

Spitz: The relationship we describe provides an upper-limit estimate for the ratio of working level to ^{222}Rn. The measurements we make of ^{222}Rn, of course, are unaffected by mechanisms that cause the radon daughters to plate out onto the walls of the structure.

Radiation Exposure from Building Materials

G. G. EICHHOLZ, F. J. CLARKE, and B. KAHN
Georgia Institute of Technology, Atlanta, Georgia

ABSTRACT

A survey procedure was developed to find buildings in which the radiation exposure from gamma rays is relatively high. For modern structures NaI(Tl) survey meters are used to identify building materials with higher radionuclide content. Samples of these materials are analyzed by gamma-ray spectroscopy for ^{226}Ra daughters, ^{232}Th daughters, and ^{40}K. The exposure rate in a building is computed from these concentrations on the basis of the geometrical configuration of building materials, acting both as radiation sources and as shield against terrestrial radiation, and also on the basis of the outside radiation exposure rate at the building site. The procedure may also be applied to surveys of building material constituents and to materials in place in older structures. The methodology was tested in subdivisions under construction in the Atlanta metropolitan area. Brick, concrete block, and poured concrete were found to be the sources of radiation exposure in these one-family homes. It was feasible to survey the local main suppliers of these materials and to relate count-rate ranges obtained with the survey meters to low, medium, and high radiation exposure potential for the material. A calculational model was developed to predict radiation exposure rates within the houses; these rates then were checked by comparing computed with measured values obtained with a pressurized ionization chamber. Concentrations of ^{226}Ra daughters, ^{232}Th daughters, and ^{40}K in the surveyed building materials and their constituents are given in the paper as well as exposure rates in newly constructed houses.

The attention currently focused on radiation dose equivalents of a few millirems per year to the maximally exposed person from the nuclear fuel cycle suggests the significance of variations of the same magnitude in the natural radiation background. The background consists of cosmic rays, radionuclides produced by cosmic rays, and terrestrial radionuclides of which the main components are ^{238}U and

its radioactive progeny (including ^{226}Ra), ^{232}Th and its radioactive progeny, and ^{40}K. Concentrations of these terrestrial radionuclides are known to differ among materials (National Council on Radiation Protection, 1975) to the extent that even local selection of site and construction materials for a building affects the occupants' annual dose equivalent by several millirems and, in some cases, by well above 25 mrems. This paper reports one aspect of a study concerned with determining the contribution to population radiation exposures by these terrestrial radionuclides in building materials.

The magnitude of the incremental radiation dose equivalent delivered to population groups as a result of gamma rays from building materials has been computed by Moeller and Underhill (1976), Beninson et al. (1977), Oakley (1972), and Krisiuk et al. (1971a). They have utilized measurements of the radionuclide content of building materials throughout the world (Hamilton, 1972; Krisiuk et al., 1971b; Kolb, 1974a) as well as direct measurements of the radiation exposure from gamma rays within buildings (Solon et al., 1960; Lowder and Condon, 1965; Yeates, Goldin, and Moeller, 1972; Lindeken et al., 1973; Kolb, 1974b). Moeller and Underhill (1976) estimated that the effect of building materials both as radiation source and as shield reduces the terrestrial exposure rate within frame homes by 30% and increases it by 30% within masonry homes built with indigenous materials. These investigators then calculated population dose equivalents by combining the derived exposure rate values with information on the number of buildings of each type, building materials used, occupancy by persons of workplaces, schools, and homes, and the fraction of time spent in areas within these buildings. Although the other authors arrived at somewhat different values of outside-to-inside ratios, all conclusions are remarkably similar despite the wide range of observations.

Surveys to find building materials with relatively high radiation levels are needed to ensure that exposure limits are not exceeded; these surveys should include incremental dose equivalents from all types of sources in the consideration of possible control measures. As the above-cited studies indicate, such surveys can use three approaches, depending on the situation: (1) knowledge that certain constituents of building materials have relatively high radionuclide contents, (2) measurements that identify those construction materials with highest radionuclide contents, and (3) direct measurements in buildings to find highest radiation exposure rates due to construction practices. The first approach has identified groups exposed to higher levels of terrestrial radionuclides in buildings constructed with or on uranium and phosphate tailings (Duncan and

Eadie, 1974; Guimond and Windham, 1975; Fitzgerald and Sensintaffar, 1978).

For a systematic program a computational model is needed to relate the three types of information to each other and to exposure rates in the structures of interest. It should be possible to develop such a relation by combining the two previously applied calculations, one for exposure rates inside buildings from measured concentrations of uranium, thorium, and potassium in materials and the other for inside exposure rates from measured outside values. The existing relations also need to be expanded from their present limited concepts to include source terms other than infinitely thick walls that totally surround the point of exposure, and building materials that have various radionuclide levels.

Presented here are initial observations from surveys in the Atlanta metropolitan area of the radionuclide content of brick, concrete, and concrete block and of external exposure rates in one-family homes built with these materials. The study began with one-family homes of brick and concrete, which were predicted to yield the highest population dose equivalents in Atlanta based on the values used by Moeller and Underhill (1976). By a survey of houses under construction, it was possible to identify the major contributors of gamma-ray radiation exposures and to test the calculation of exposure rates from radionuclide concentrations. Other construction materials and other types of buildings will be included in a continuing study.

PROCEDURE

Two factors were considered in selecting building sites for measurement: the styles of homes being built in the seven-county Atlanta metropolitan area and the types of building materials in common use for each type of construction. This information was obtained through the local branch of the National Association of Home Builders. Representative groups of homes were selected in each price range where materials in general use were being assembled. Measurements were made on site before the foundation was poured, later when foundation walls were erected, and finally when the shell was closed in, and indicated that clay brick, concrete block, and concrete slabs were the principal radionuclide-containing media.

The three groups of materials—clay bricks, concrete block, and ready-mix concrete—were then traced back to determine their origin and marketing patterns. At supply yards the materials were examined for radionuclides that emit gamma rays with a survey

meter, which consisted of a cylindrical 5- by 5-cm NaI(Tl) detector with count-rate meter, adjusted to measure gamma rays above 90 keV. The detector was placed on piles of bricks, concrete blocks, and concrete constituents for brief count-rate measurements to indicate whether the material was in an exposure-rate category considered medium (similar to ambient levels) or in a significantly higher or lower category. Representative samples of commonly used material at ambient levels and samples of all materials at the higher or lower levels were collected for radionuclide analysis. Samples of concrete were obtained at the building sites in the surveyed subdivisions (see below).

The samples, in cylindrical 500-cc containers, were weighed and then analyzed for photon-emitting radionuclides with a heavily shielded Ge(Li) detector and a 4000-channel spectrometer. The laboratory counting period was usually 10,000 sec. The following radionuclides were measured by the indicated gamma rays, with the percent gamma ray per disintegration given in parentheses:

^{226}Ra	186 keV (3.7%)
^{214}Pb	295 keV (17.9%); 352 keV (35.0%)
^{214}Bi	609 keV (43.0%); 1120 keV (14.2%); 1764 keV (15.6%)
^{228}Ac	338 keV (11.0%); 911 keV (29.0%)
^{208}Tl	583 keV (30.5%); 2615 keV (35.9%)
^{40}K	1461 keV (10.7%)

The disintegration rates of the two ^{214}Pb and three ^{214}Bi gamma rays were used to determine the activity of these two radionuclides, which emit all the gamma rays among the short-lived ^{226}Ra progeny and contribute most of the exposure rate due to gamma rays from the ^{238}U chain. The measurement at 186 keV includes a gamma ray from ^{235}U (54%); if ^{238}U is in equilibrium with ^{226}Ra and is at its natural isotopic ratio, then ^{235}U contributes 2.5% per disintegration, for a total of 6.2%. Hence this measurement can be used if the ratio of ^{226}Ra to ^{235}U is known. The disintegration rates of the two ^{228}Ac and ^{208}Tl gamma rays represent the activity of the ^{232}Th progeny if the two radionuclides are found to be equal.

The detector system had been calibrated for counting efficiency with National Bureau of Standards (NBS) radioactivity solution standards. Small correction factors for gamma-ray attenuation within the sample were applied when sample densities were between 1.0 and 1.8 g/cc. The samples were counted in the form obtained, except that bricks, blocks, and poured concrete were broken into smaller pieces.

Three subdivisions under construction were selected for measuring the exposure rate in detached one-family houses. The houses at locations A, B, and C had approximately 130, 170, and 250 m^2 of floor space, respectively. Exposure rates were also measured in one larger new house (D) and a group of older houses (E).

Radiation exposure rates outside and inside these homes were measured 1 m above ground with a pressurized ionization chamber (PIC). The PIC had been calibrated in terms of microroentgens per hour (μR/hr) with a ^{226}Ra standard checked by NBS before use. At least 20 consecutive readings were averaged at each location to obtain standard deviations between 0.3 and 0.8 μR/hr. Outside levels were determined around the house at sufficient distance to minimize radiation exposure from house walls. Inside the house the PIC was placed at the center of rooms as well as next to potential radiation sources such as walls, floors, and fireplaces so as to identify the major contributors to the radiation exposure.

The exposure rate index, $\dot{X}_{ERI}$, of construction materials was selected as the value equivalent to the radiation exposure at 1 m from naturally occurring radionuclides in an infinitely extended and thick slab (or from an infinite hemisphere). This index, in microroentgens per hour, was computed from the analyzed radionuclide concentration C in picocuries per gram (pCi/g) on the basis of the factors given by Beck (1972),

$$\dot{X}_{ERI} = 1.82\, C_{Ra\ daughters} + 2.82\, C_{Th\ daughters} + 0.179\, C_K \quad (1)$$

The ERI value was used to represent the radiation exposure in buildings from construction materials and to compare the exposure potential of these materials with their constituents. The ERI values were also used to calibrate approximately the NaI(Tl) survey meter, which was usually placed on piles of building materials so that the radiation exposure rate was approximately 80% of the value from an infinite hemisphere.

CALCULATIONAL MODEL

The calculational model developed for obtaining the exposure rate within a building utilized this exposure rate index. The exposure rate within the house was considered to be the sum of the exposure rates from attenuated cosmic rays, from radionuclides in soil as attenuated by house walls (but not windows) and floor, and from

radionuclides in the walls and floor. In the model the radiation exposure rate from terrestrial radiation is the measured outside value multiplied by the fraction of the total in the solid angle from the vertical subtended at the test point by wall or floor and also multiplied by the fraction transmitted by wall or floor. The radiation exposure rates from walls and floor are the ERI values multiplied by the fraction of the exposure rate from the angle subtended by walls and floor and the fraction from the actual thickness of material. The fractional exposure rate as a function of angle was read from a figure given by Beck (1972) and was averaged for the geometrical configuration of walls and floor relative to the exposure point. Thus,

$\dot{X}_i$ = attenuated cosmic ray exposure

+ attenuated terrestrial exposure

+ exposure from wall and floor materials (2)

$$\dot{X}_i = c\dot{X}_c + (\dot{X}_a - \dot{X}_c)\,[a_f b_f + (1 - k)(1 - a_f) + k(1 - a_f)b_w]$$

$$+ a_f(1 - b_f)\dot{X}_{ERI(f)} + ka_w(1 - b_w)\dot{X}_{ERI(w)}$$

where $\dot{X}_i$ = exposure rate in house, μR/hr
$\dot{X}_c$ = cosmic-ray exposure rate, μR/hr
$\dot{X}_a$ = outside exposure rate, μR/hr
a = fraction of exposure rate in angle subtended relative to exposure rate from infinite medium
b = fractional transmission of gamma rays by building materials
c = fractional transmission of cosmic rays by building materials
k = fraction of wall surface not windows
f = floor
w = walls

For the sample calculation, surface densities of 4, 17, and 23 g/cm^2 were used for wood-frame wall, brick veneer wall, and concrete slab construction, respectively. No consideration was given to radiation sources and attenuation within the building; 90% transmission (c = 0.9) of cosmic rays by roofing was assumed (National Council on Radiation Protection, 1975). The building was considered to be a one-floor plan, 9.0 by 17.6 by 2.4 m, with windows occupying 15% of the wall space (k = 0.85). The point of exposure was taken to be on the long centerline, 3 m from one end

wall, and 1 m above the floor. The term exp ($-\mu x$) was used for the fractional transmission, b, where μ is the mass attenuation coefficient and x is the material thickness (ρx). An attenuation coefficient for 1.0-MeV gamma rays of 0.064 cm^2/g was applied.

RESULTS AND DISCUSSION

The production of ready-mix concrete and the manufacture of concrete blocks are concentrated in the Atlanta area. Two major producers and one smaller company provide the bulk of the concrete used locally. The concrete varies in strength but is generally the lightweight type, in contrast to the heavier types used as recently as 10 years ago. Samples were obtained from all three sources.

Concrete blocks and ready-mixed concrete are produced from a mixture of cement, fine aggregate, and coarse aggregate, conventionally in the ratio 1 : 2 : 4, with water. As the demand for stronger and lighter concretes has been rising, producers have been experimenting with other ratios and with various substitutes for the traditional materials. For example, grindings or rock dust may be used as part of the fine aggregate, and as much as 20% of the cement material may be fuel ash rather than portland cement. Large-size aggregate is usually granite but dolomite is also used locally. Expanded shales and exploded clays are increasing in use as coarse aggregate, resulting in lower weight. Of these constituents gravel and rock dust are obtained nearby, sand is from Georgia and nearby Alabama and South Carolina, and ash and cement can be of either local or distant origin.

Clay bricks are commonly used in the Atlanta area as veneer on homes and commercial buildings in conjunction with wood frame, masonry, or concrete blocks. Samples were obtained from six of seven brick companies operating in Georgia. In addition, samples of bricks from adjacent states but stocked for use in Atlanta were obtained. Included were bricks from South Carolina, North Carolina, Virginia, Tennessee, and one lot from Ohio. Georgia bricks were from clay at Atlanta, Augusta, Macon, and Columbus. In most cases the user orders bricks by color and type, and delivery is made directly by the producer. Popular styles and colors are stocked in Atlanta and were available for sampling and analysis.

The survey of construction materials with a NaI(Tl) detector at the suppliers' yards suggested the five exposure rate categories given in Table 1. Count rates ranged from 2,000 to 10,000 counts/min in the environment and up to 12,000 counts/min over building material. The categories were in clearly differentiated narrow count-rate ranges, except for two types of brick that were borderline between

TABLE 1

Radionuclide Content of Exterior Wall Construction Materials

Exposure rate category	Number of samples	Radionuclide, pCi/g: ^{226}Ra daughters* Mean	^{226}Ra daughters* Range	^{232}Th daughters† Mean	^{232}Th daughters† Range	^{40}K Mean	^{40}K Range	Exposure rate index, μR/hr Mean	Exposure rate index, μR/hr Range
Brick									
Very low	2	0.2	0.1—0.3	0.08	0.04—0.1	0.3	0.2—0.4	0.7	0.6—0.7
Low	5	0.6	0.6—0.7	0.9	0.8—1.0	12.0	11—13	5.8	5.3—6.4
Medium	24	1.8	1.0—3.4	1.9	1.1—3.0	17.0	10—28	12.0	9.4—16
High	6	3.5	2.8—4.8	2.9	2.4—3.9	27.0	21—32	20.0	17—22
Concrete									
Low	3	0.7	0.5—1.1	0.5	0.4—0.6	8.0	7.1—9.8	4.1	3.3—5.4
Medium	3	1.3	1.0—1.6	1.6	1.3—1.9	26.0	18—31	12.0	8.7—13
High	1	2.4		3.2		27.0		18.0	
Concrete Block									
Medium	8	1.3	1.1—1.6	1.7	1.2—2.2	26.0	24—31	12.0	10—14
Very high	2	21.0		1.0		8.6	7.7—9.4	43.0	42—43

*Concentrations of individual samples were computed for ^{226}Ra daughters by averaging five gamma-ray values for ^{214}Pb and ^{214}Bi.

†Concentrations of individual samples were computed for ^{232}Th daughters by averaging four gamma-ray values for ^{228}Ac and ^{208}Tl.

medium and high. The medium category had count rates near the upper end of the range of the natural background and is by far the most common for brick, concrete, and concrete block. The bricks in the high category were mostly of local origin; those in the low category were mostly from South Carolina. The bricks that yielded very low count rates are used only for special decorative purposes; one type was made of lime and sand, the other of marble chips. The two concrete blocks that showed a high reading are not in current use but were obtained from older buildings.

The content of ^{226}Ra daughters and ^{232}Th daughters in the medium-category bricks was approximately 1 to 3 pCi/g each, and that of ^{40}K was 10 to 30 pCi/g. In the medium-category concrete and concrete blocks, the concentrations of ^{226}Ra and ^{232}Th daughters were at the lower end of this range, whereas the concentration of ^{40}K was at the upper end. These concentrations are of the same magnitude as reported for materials elsewhere by Hamilton (1972), Krisiuk et al., (1971b), and Kolb (1974a). Measured values of the ^{228}Ac and ^{208}Tl concentrations were identical within the uncertainty of measurement, which suggests that the radioactive decay series beginning with ^{228}Ra was in equilibrium. The concentrations of ^{214}Pb and ^{214}Bi also were equal and averaged 92 ± 11% of the equilibrium value relative to the concentration of ^{226}Ra, on the basis of the summed 186-keV gamma rays of ^{226}Ra and ^{235}U.

The exposure rate indices (see Table 1) computed from radionuclide concentrations were consistent with the categories used in surveying the construction materials. The medium category for each of the three materials showed an average index of 12 μR/hr, which is just above the high end of the range of terrestrial radiation background (see below). The index, therefore, appears to fulfill its main function, i.e., to describe the combined radiation exposure rate from three radionuclides of variable concentrations. Because the index is the exposure rate from an infinite hemisphere, it can be reasonably applied for surveying large piles of construction materials. This index is slightly less than one-half of such descriptors used by Krisiuk et al. (1971a) and Beninson et al. (1977), which are for exposure rates in an infinite medium with regard to gamma rays. The possibility of radionuclides in the chain from ^{238}U to ^{226}Ra not being in equilibrium with their daughters does not significantly affect the index because the gamma-ray exposure rate from these radionuclides is relatively small.

Most samples of the constituents of concrete—granite, gravel and rock dust, clay and shale, and fuel ash—have similar medium

exposure rate indices as the materials in which they are used, as indicated in Table 2. Summed algebraically, however, the radionuclide content and the exposure rate index of the concrete constituents are less than those of the medium-category concrete, which suggests the need for a more-detailed comparison of radionuclides in concrete and its constituents. Of particular interest is the currently unknown* source of radium in the high-level concrete block. The sand, cement, and dolomite-gravel samples contain much less radioactivity than the other constituents, whereas some ash samples contain more.

The radiation exposure rate in the Atlanta area out of doors was observed to range from 6 to 14 μR/hr. The terrestrial component is lower by the amount contributed by cosmic rays, which at the 300-m elevation of Atlanta was estimated to be 3.8 μR/hr. This value was calculated from a curve of dose rate in air vs. elevation (National Council on Radiation Protection, 1975) and was also used by Lindeken et al. (1972). Average exposure rates differed significantly among locations (Table 3) but were usually within the standard deviation range at a particular location. Measurements repeated at specific locations after intervals of several months were in some cases identical, but in others they differed by as much as 2 μR/hr. Seasonal variations by approximately 10% have been observed by Lindeken et al. (1972). Such changes are attributed to the accumulation and release of ^{222}Rn and its daughters near the surface of the ground in response to changes in ground-moisture and atmospheric pressure.

The observed exposure rates within homes in Atlanta (Table 3) have the same qualitative relation to outside rates as in the houses for which data have been reported earlier, e.g., inside exposure rates are lower in the wood-frame house than those outside and are either the same or higher in homes built with concrete and brick. Frame-house construction materials attenuate the gamma radiation from the soil outside and contribute essentially no radiation, whereas concrete and brick act as both radiation source and shield. The source effect was especially noticeable at location B where concrete with a higher radiation exposure index used in three of eight homes led to higher exposure rates. Within multistory concrete-slab houses, the highest exposure rates were measured consistently in the "family room" located usually at the lowest level, and directly on the slab; the lowest exposure rates were on the upper floors, away from brick walls. Exposure rates as much as 1 μR/hr higher than those recorded

*Note added in proof: Subsequent work has identified the source of this activity to be phosphate slag.

TABLE 2

Radionuclide Content of Concrete Components

Building material constituents	Exposure rate category	No. of samples	Radionuclide, pCi/g: ^{226}Ra daughters Mean	^{226}Ra daughters Range	^{232}Th daughters Mean	^{232}Th daughters Range	^{40}K Mean	^{40}K Range	Exposure rate index, μR/hr Mean	Exposure rate index, μR/hr Range
Coarse Aggregate										
Gravel	Very low	1	0.4		0.06		1.5		1.2	
	Medium	5	0.9	0.6—1.5	1.2	1.0—1.7	22.0	15—30	9.1	6.6—13
Expanded shale and clay	Medium	6	1.2	0.9—1.6	1.6	1.3—2.1	23.0	16—34	11.0	8.8—12
	High	4	2.1	1.9—2.3	3.4	2.9—4.0	25.0	22—29	18.0	16—19
Fine Aggregate										
Sand	Low	5	0.3	0.1—0.6	0.4	0.2—0.6	3.2	1.1—5.6	2.4	1.4—3.0
Rock dust	Low	1	0.4		0.4		8.8		3.4	
	Medium	3	1.2	0.7—1.9	1.3	0.8—2.0	21.0	14—33	9.6	6.0—15
Cement										
Cement	Low	6	1.0	0.5—1.4	0.3	0.2—0.6	2.1	0.7—2.9	3.3	1.6—5.9
Fly ash	Medium	2	3.4	3.3—3.5	2.4	2.0—2.8	8.2	3.3—13	14.0	14—15
	High	14	5.3	3.5—8.3	3.1	2.2—4.3	19.0	4—28	22.0	16—29

TABLE 3

Exposure Rates in New Homes

House type	No. of houses	Exposure rate, μR/hr					
		Outside		Inside, low		Inside, high	
		Mean	Range	Mean	Range	Mean	Range
Location A							
1-floor partial brick veneer, concrete wall base	1	8.6	7.4–9.7	8.4		9.9	
1-floor partial brick veneer, concrete slab	4			10.3	9.6–11.6	12.1	10.8–12.9
Split-level frame, concrete slab at lowest level	2			8.6	8.1–9.1	15.8	15.6–16.0
Location B							
1-floor frame, concrete slab	2	6.8	6.3–7.6	7.0	6.7–7.2	7.2	6.8–7.6
Split-level frame, concrete slab at lowest level	3			6.8	6.7–6.9	7.9	7.5–8.1
	1			8.3		14.7	
2-story frame, concrete slab and block-wall basement	2			8.8	8.6–8.4	15.3	14.3–16.4
Location C							
2-story brick veneer, concrete slab and block-wall basement	6	10.6	10.2–11.2	8.6	8.0–10.2	13.9	10.6–15.0
Location D							
3-story brick veneer, concrete slab and block-wall basement	1	12.3		11.9		16.4	
Location E							
1-floor wood frame, pillar foundation (old house)	1	9.7		8.0		8.8	

in Table 3 were measured when the PIC was moved next to obvious sources of radiation, i.e., concrete floors, brick or concrete block walls, and brick fireplaces. Source materials were readily identified by this technique. No other construction materials showed elevated radiation exposure readings.

Use of inside-to-outside ratios of 0.70 relative to the terrestrial background for frame houses and 1.3 for masonry houses, which was recommended by Moeller and Underhill (1976), predicts the median inside non-cosmic-ray exposure rate (i.e., the measured value minus 0.9×3.8 μR/hr) reasonably well for these homes. Frame houses with concrete slabs must be considered in the masonry category for this purpose. The generally higher values in basements and lower exposure rates in upper stories are also consistent with the factor of 1.3 for basements relative to the outside and the additional factor of 0.85 for upper stories, which was used by Moeller and Underhill. The obvious exception is in the case of the relatively high level of radiation in concrete slabs used at location B.

The influence of various levels of radioactivity in building materials is taken into account by the calculational model in terms of the exposure rate index. The sample calculations based on Eq. 2 result in the following equations for a one-floor house:

For wood frame,

$$\dot{X}_i = 0.9\,\dot{X}_c + 0.8\,(\dot{X}_a - \dot{X}_c) \tag{3a}$$

For frame with concrete slab,

$$\dot{X}_i = 0.9\,\dot{X}_c + 0.4\,(\dot{X}_a - \dot{X}_c) + 0.6\,\dot{X}_{ERI(f)} \tag{3b}$$

For brick veneer with concrete slab,

$$\dot{X}_i = 0.9\,\dot{X}_c + 0.3\,(\dot{X}_a - \dot{X}_c) + 0.6\,\dot{X}_{ERI(f)} + 0.2\,\dot{X}_{ERI(w)} \tag{3c}$$

Accordingly, the non-cosmic-ray exposure rate is 80% of the outside value in a frame house; if the radiation exposure index of building materials is the same as the terrestrial exposure, then the non-cosmic-ray exposure rate would be the same inside and outside a frame house with concrete slab and 10% higher within a house with concrete slab and brick veneer.

The values computed with these equations are within the range of the measurements. The inside exposure rate in the frame house with wooden walls at location E is computed to be 8.1 μR/hr and the concrete-slab houses at location A, 12.5 μR/hr if the concrete has a

radiation exposure index of 12 μR/hr. At location B the computed radiation exposure rate in a concrete-slab house is 7.1 μR/hr if the concrete index is 4.1 μR/hr, and 11.8 μR/hr if the index is 12 μR/hr. If both the concrete slab and the brick walls have an index of 12 μR/hr, then the exposure rate is 13.9 μR/hr.

Predicted exposure rates within a house would be expected to vary appreciably because the coefficients in Eq. 2 are strongly dependent on the angles subtended at the measurement point by the walls and floor, which are functions of the location of the point within the house and of the shape and size of the house. Because the subtended angle is smaller, for example, exposure rates are less in upper floors than they are directly on the concrete slab. Exposure rates are also affected by the following factors: the thickness, density, and type of wall material; the amounts of each radionuclide in the mixture; the source effects and shielding effects by materials outside and within the house; and the fraction of radon and its daughters remaining in brick or concrete.

A computational program is being written for relating the radionuclide content and radiation shielding properties of materials to the radiation exposure rate for a variety of building styles and for any location within the building. Predicted exposure rates will then be compared with available measured values on a more-detailed basis to check the model. The survey approach will also be expanded to include other building materials, the influence of radon, and the possibility of using survey measurements in existing buildings to infer exposure rates in other building styles.

SUMMARY AND CONCLUSION

A methodology is proposed for surveys to determine significantly elevated radiation exposure rates from photon-emitting radionuclides in building materials. One approach is to monitor the radiation level of construction materials and to predict in buildings the exposure rates due to the most radioactive materials. This was tested for selected one-family houses being built in the Atlanta metropolitan area with brick, concrete block, poured concrete, and wood. Materials with high, medium, and low radiation exposure potentials were categorized with portable NaI(Tl) survey meters and analyzed with gamma-ray spectrometers for ^{232}Th daughters, ^{226}Ra daughters, and ^{40}K. A computational model was used to predict exposure rates in a building from its walls and floor and the ground outside in terms of an exposure rate index related to the radionuclide content of building materials and the measured "outside" radiation

exposure rates. The calculational results were compared with exposure rate measurements obtained with pressurized ionization chambers in one-family homes under construction. On the basis of these tests, calculation of exposure rates in buildings appears to be feasible if appropriate contributions are considered from cosmic rays, from terrestrial radionuclides in the ground and building materials, and from shielding by building walls and floor. The surveys of materials readily identified sources of elevated radiation exposure rates, and no other significant sources were observed in the one-family houses.

Surveys can also attempt to identify the constituents of building materials that are known to have high radionuclide contents or to determine radiation exposures in buildings for which high levels are suspected. A radiation exposure index was used to relate the exposure potential in building material to that of its constituents on the one hand and the actual exposure rate in buildings on the other. Radionuclide concentrations in the constituents of concrete were found to be comparable with those of prepared concrete slabs and blocks, but some differences need still to be resolved. Measurements of radiation exposure rates within houses have shown that the one or two materials which frequently are major sources of radiation are readily identified.

ACKNOWLEDGMENTS

We gratefully acknowledge the participation of M. D. Matheny, A. Aissi, B. A. Byrne, and C. Hodgson, who made many of the field measurements. We also thank J. Gasper for radioanalytical determinations.

This work was supported by the Office of Radiation Programs, U. S. Environmental Protection Agency, under EPA contract #68-01-4601.

REFERENCES

Beck, H. L., 1972, The Physics of Environmental Gamma Radiation Fields, in *The Natural Radiation Environment II*, Vol. 1, Symposium Proceedings, Houston, Tex., Aug. 7—11, 1972, J. A. S. Adams, W. M. Lowder, and T. F. Gesell (Eds.), ERDA Report CONF-720805-P1, pp. 101-133, Rice University and the University of Texas, Houston, NTIS.

Beninson, D. J., A. Bouville, B. J. O'Brien, and J. O. Snies, 1977, Dosimetric Implications of the Exposure to the Natural Sources of Irradiation, in *International Symposium on Areas of High Natural Radioactivity*, Symposium Proceedings, Poços de Caldas, Brazil, June 16—20, 1975, T. L. Cullen and E. Penna Franca (Eds.), CONF-750671, NTIS.

Duncan, D. L., and G. G. Eadie, 1974, *Environmental Surveys of the Uranium Mill Tailings Pile and Surrounding Areas—Salt Lake City, Utah*, USEPA Report EPA-520/6-74-006, Environmental Protection Agency, NTIS.

Fitzgerald, J. E., and E. L. Sensintaffar, 1978, Radiation Exposure from Construction Materials Utilizing By-Product Gypsum from Phosphate Mining, in *Radioactivity in Consumer Products*, Report NUREG/CP-0001, U. S. Nuclear Regulatory Commission, NTIS.

Guimond, R. J., and S. T. Windham, 1975, *Radioactivity Distribution in Phosphate Products, By-Products, Effluents, and Wastes*, USEPA Report ORP/CSD-75-3, Environmental Protection Agency, NTIS.

Hamilton, E. I., 1972, Relative Radioactivity of Building Materials, *Am. Ind. Hyg. Assoc. J.*, 32: 398.

Kolb, W., 1974a, Influence of Building Materials on the Radiation Dose to the Population, *Kernenergie und Öffentlichkeit*, 4: 18.

——, 1974b, Die Strahlenbelastung der Beölkerung in Wohnhäusern—Zwischenbericht über ein BML-Vorhaben, paper presented at Annual Convention of the Radiation Protection Association, Helgoland, F. R. Germany, September 1974 [cited by Moeller and Underhill (1976)].

Krisiuk, E. M., S. I. Tarasov, V. P. Shamov, N. I. Shalak, E. P. Lisachenko, and Y. Gomelsky, 1971a, Exposure from Radiation Sources of Natural Origin, in *Proceedings of the Third International Congress of the International Radiation Protection Association*, Sept. 9—14, 1973, Washington, D. C., International Radiation Protection Association, Washington, D. C.

——, E. P. Lisachenko, S. I. Tarasov, V. P. Shamov, and N. I. Shalak, 1971b, A Study on Radioactivity of Building Materials, Leningrad Research Institute for Radiation Hygiene, Ministry of Public Health of the U.S.S.R., Leningrad [cited by Moeller and Underhill (1976)].

Lindeken, C. L., K. R. Peterson, D. E. Jones, and R. E. McMillen, 1972, Geographical Variations in Environmental Radiation Background in the United States, in *The Natural Radiation Environment II*, Vol. 1, in Symposium Proceedings, Houston, Tex., Aug. 7—11, 1972, J. A. S. Adams, W. M. Lowder, and T. F. Gesell (Eds.), ERDA Report CONF-720805-P1, pp. 317-332, Rice University and the University of Texas, Houston, NTIS.

——, D. E. Jones, and R. E. McMillen, 1973, Environmental Radiation Background Variations Between Residences, *Health Phys.*, 24: 81.

Lowder, W. M., and W. J. Condon, 1965, Measurement of the Exposure of Human Populations to Environmental Radiation, *Nature*, 206: 658.

Moeller, D. W., and D. W. Underhill, 1976, *Study of the Effects of Building Materials on Population Dose Equivalents*, Harvard School of Public Health, Boston, Mass.

National Council on Radiation Protection, 1975, *Natural Background Radiation in the United States*, NCRP Report 45, National Council on Radiation Protection and Measurements, Washington, D. C.

Oakley, D. T., 1972, *Natural Radiation Exposure in the United States*, USEPA Report ORP/SID 72-1, Environmental Protection Agency, NTIS.

Solon, L. R., W. M. Lowder, A. Shamban, and H. Blatz, 1960, Investigations of Natural Environmental Radiation, *Science*, 131: 903.

Yeates, D. B., A. S. Goldin, and D. W. Moeller, 1972, Natural Radiation in the Urban Environment, *Nucl. Saf.*, 13: 275.

The Contribution of Radon in Tap Water to Indoor Radon Concentrations

THOMAS F. GESELL and HOWARD M. PRICHARD
The University of Texas, Health Science Center at Houston,
School of Public Health, Houston, Texas

ABSTRACT

The contribution of radon (^{222}Rn) in domestic water supplies to the concentration of ^{222}Rn in indoor atmospheres has been investigated and found to be significant for concentrations over a few thousand picocuries per liter in the water supply. A model predicting average indoor increments due to this source is presented and supported by a series of measurements made in the laboratory and in private homes in the vicinity of Houston, Tex. The efficiency with which radon is transferred from water to air was experimentally determined for the more important domestic uses of water, and these efficiencies were combined with estimates of average indoor water use to produce a source term proportional to the concentration of ^{222}Rn in the tap water. The importance of the dwelling volume and the air change rate is discussed, and a method by which the air change rate may be estimated from the record of a continuous radon monitor is described.

The growing concern about radon* and radon progeny in indoor environments (Auxier, 1976; Gemesi, Szy, and Toth, 1975; Jonassen and McLaughlin, 1976; Parthasarathy and Unnikrishnan, 1977) has led us to examine the role played by the domestic use of groundwater as a source of indoor radon. It was estimated in 1975 that, in a 200 m^3 dwelling with one air change per hour, an indoor radon concentration increment of 1 pCi/liter could be expected for every 10,000 pCi/liter in the water used (Gesell and Prichard, 1975).

*In this paper the term "radon" refers to ^{222}Rn unless otherwise stated.

Although few U. S. public water supplies have been analyzed for radon content, the data currently available indicate that concentrations on the order of 10,000 pCi/liter or more may not be particularly uncommon. A recent review of published and unpublished data on the radon content of groundwaters (Duncan, Gesell, and Johnson, 1976) showed that, of 438 wells and springs analyzed in the United States (excluding New England), 26% contained at least 2000 pCi of radon per liter and 5% at least 10,000 pCi/liter. Data from 76 dug wells in the state of Maine showed a pattern similar to that seen in the rest of the United States, but the radon content of 128 drilled wells in Maine was an order of magnitude higher than that seen in the other sample tests. As was noted in the review, the data were not necessarily representative of groundwaters used as public water supplies. However, it does seem evident that numerous sources of drinking water contain high concentrations of radon.

A general model for the average incremental indoor radon concentration attributable to water use can be expressed as

$$C_a = \frac{C_w}{24RV} \sum_{i=1}^{n} e_i w_i$$

where C_a and C_w are the concentrations (pCi/liter) of radon in air and water, respectively, R is the air change rate of the dwelling (hr^{-1}), V is the dwelling volume (liters), the set of w_i's represents the average amount of water used daily for various domestic applications (liters), and the set of e_i's denotes the transfer efficiency, or fraction of radon released to the air for each application.

TRANSFER OF RADON FROM WATER TO AIR

The factors e_i were experimentally determined by a series of measurements using a liquid scintillation technique (Prichard and Gesell, 1977) which permitted the rapid analysis of a large number of water samples. Determinations of the loss rate of radon from water were made in the laboratory to guide later field work. A number of 10-ml samples were withdrawn at intervals from the center of a beaker containing 750 ml of water as the water was held at constant temperature. The contact surface between the water and the air was 81 cm^2, and water agitation was kept to a minimum.

Figure 1 shows the data for 80°C, 50°C, and 22°C. As might be expected, the data are consistent with a temperature-dependent

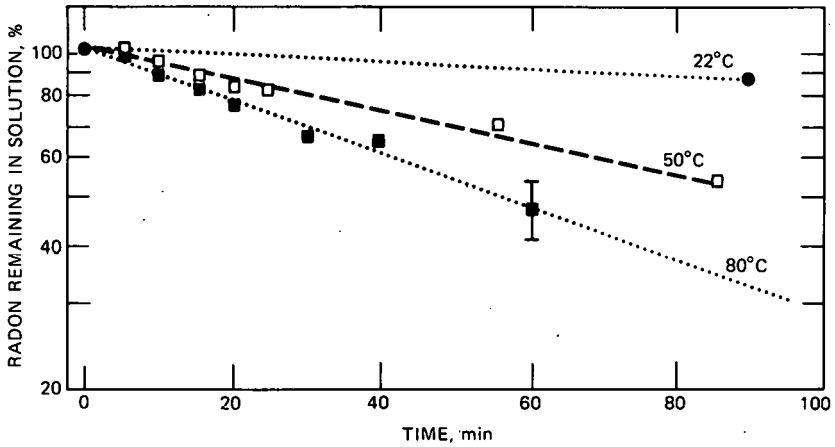


Fig. 1 Loss of radon from 750-ml water sample at three constant temperatures.

exponential loss rate. Note, however, the slow loss of radon from the unagitated beaker held at 22°C, or room temperature. Even when 750 ml of water at room temperature was agitated for 15 min with a high-speed magnetic stirrer, only 40% of the initial radon content was lost. The implication is that substantial amounts of radon will be retained by the water even when limited contact with the atmosphere occurs in the home or in the distribution system. On the other hand, a few seconds of vigorous boiling was sufficient to remove virtually all the radon from a 750-ml water sample, as is shown in Fig. 2.

The amount of radon transferred to the atmosphere during actual domestic use was investigated in a similar fashion. It was assumed that the radon liberated during a given process must be equal to the volume of water used times the difference in radon concentrations at the beginning and the end of the process. The transfer efficiencies were therefore determined by measuring the radon content of the water entering a use cycle and the radon content of the water leaving the dwelling through the drain. These measurements were performed in a number of different homes. The general results are shown in Table 1, which also includes water use data (i.e., the set of w_i's in our model) for an average American family of four (Bond, Straub, and Prober, 1973). These measurements were consistent with the laboratory work: applications involving unagitated cool water, such as the storage of water in a commode tank, released little radon to the air, even after several hours.

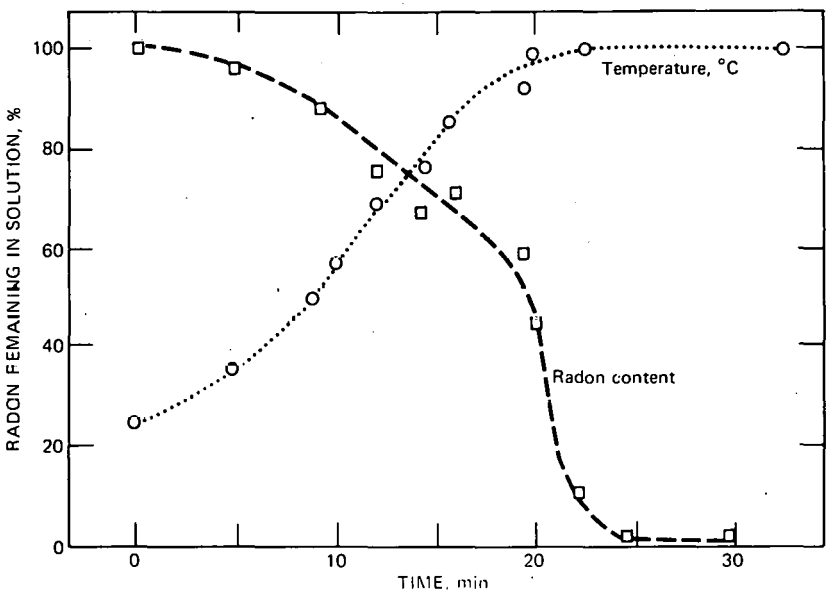


Fig. 2 Loss of radon as water is heated and boiled.

TABLE 1

Radon Liberated in the Course of Domestic Water Use per 1000 pCi/liter of Radon in the Water Supply

Use	Daily consumption, liters	Transfer efficiency, %	Radon liberated, pCi
Showers	150	63	94,500
Tub baths	150	47	70,500
Toilet	365	30	109,500
Laundry	130	90	117,000
Dishwasher	55	90	49,500
Drinking and kitchen	30	30	9,000
Cleaning	10	90	9,000
Total	890		459,000

Table 1 also shows the amount of radon released daily by the "normal" use of water containing 1000 pCi/liter of radon. The influence that this radon source has on indoor radon concentrations is affected by the dwelling volume and air change rate, as previously defined. Table 2 shows the predicted effect of the source term given

in Table 1 for a number of common dwelling types. Note that the predicted concentration increments range over a factor of 50, depending on dwelling type. It is to be emphasized that these increments refer only to the average over the entire dwelling and the entire day; actual increments will, of course, be higher during times of heavy water use and in rooms in which the water is used most.

TABLE 2

The Increment in Atmospheric Radon per 1000 pCi/liter in Water Supply*

Dwelling type	Floor area, ft^2	Volume, liters	Air change rate, hr^{-1}	Average radon increment, pCi/liter
Small apartment	680	150,000	0.25	0.51
New brick house	1,500	340,000	0.50	0.11
Old frame house	1,500	340,000	1.00	0.05
Large older structure	3,000	680,000	2.00	0.01

*Assuming occupancy by four people and radon liberation as in Table 1.

TECHNIQUES USED TO MEASURE RADON IN AIR

A series of measurements of radon concentrations in private dwellings was made to test the predictions of the model described above. Grab samples were taken with several types of scintillation flasks, including the Lucas Cell (Lucas, 1957), the 500-ml flow-through flask described by George (1975), and a 20-ml flask of our design that could be counted automatically on a liquid scintillation counting system. These 20-ml flasks (or ZnS vials) are inexpensive, easily constructed, and highly portable. Ordinary glass scintillation vials were coated on the interior surface with ZnS:Ag phosphor by applying a light coating of silicone grease, then shaking about 1 ml of powdered phosphor around inside the vial until a uniform coating was achieved. Excess phosphor was then emptied into the next vial to be coated. Calibration was effected by multiple air exchange in a glove box containing a known radon concentration. The vials are set aside for at least 3 hr after filling to allow for the ingrowth of radon progeny, then counted on an ordinary liquid scintillation counter. Table 3 presents summary statistics for a batch of 30 ZnS vials compared with parameters for a typical Lucas Cell. The chief disadvantage of the ZnS vial is that its small volume and correspondingly small calibration factor imposes a $(5)^{1/2}$ penalty in counting statistics compared to a standard Lucas Cell. However, for many

TABLE 3

Summary Statistics for ZnS Vials and Lucas Cells

	ZnS scintillation vials	Typical Lucas Cell
Radon concentration in sampled air	281 ± 8* pCi/liter	
Mean cell background	0.12 ± 0.19 cpm	0.1 cpm
Absolute efficiency	4.0 ± 0.5 (cpm)/pCi	5.0 (cpm)/pCi
Relative efficiency	0.60 ± 0.08 $\frac{\text{counts}}{\text{alpha particle}}$	0.8 counts/alpha particle
Calibration factor	0.100 ± 0.013 (cpm)/(pCi/liter)	0.5 (cpm)/(pCi/liter)

*All errors are ±1.96 sigma.

applications in which atmospheric radon concentrations are at least a few picocuries per liter, this disadvantage is outweighed by the low cost, high portability, and automatic sample counting made possible by this approach.

The bulk of the routine measurements of radon in air were made with continuous readout, electrostatic precipitation devices based on the design by Wrenn et al. (1975). These precipitators were calibrated in a 200-liter chamber into which an electric fan and an electronic relative humidity gauge had been installed, along with feed-through connectors for the instrument cables. Radon was introduced into the chamber by a small pump connected by plastic tubing to a 200-liter drum containing approximately 50 kg of uranium mill tailings. Radon concentrations inside the calibration chamber were determined by grab samples taken with scintillation flasks through sample ports leading into the interior of the chamber.

Concern has been expressed that the response of the precipitator is to some extent dependent on relative humidity (Watnick, Negro, and Graveson, 1976). Calibration was therefore carried out at room temperature at several relative humidity values, as determined by the relative humidity meter installed in the calibration chamber. The resulting instrument response (cpm per pCi/liter) vs. relative humidity (percent) is shown in Fig. 3. Although there is marked humidity dependence below 30% relative humidity, the response is relatively flat above that level. This was not considered to be an especially serious problem in the relatively humid study area.

The response of the precipitator lags behind the variations in the actual radon field because of the time required for radon to diffuse through the foam hemisphere surrounding the sensitive volume and because of the length of time between the decay of a radon atom in the sensitive volume and the pulse ultimately produced by the alpha decay of ^{218}Po or ^{214}Po on the detector surface. Consequently a

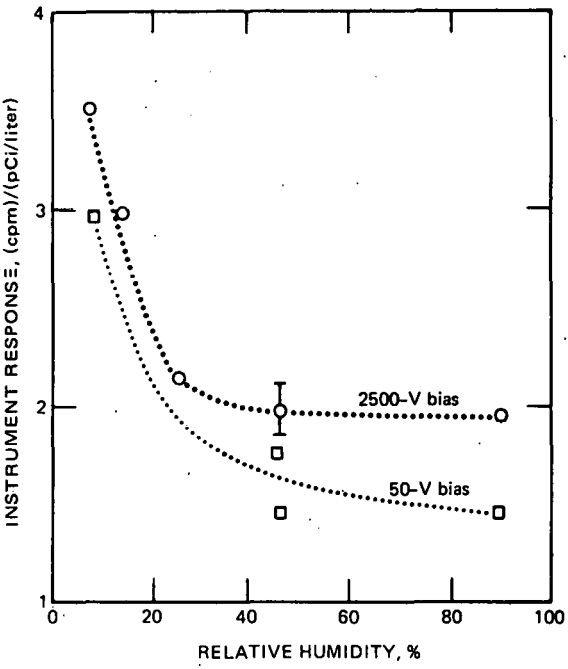


Fig. 3 Precipitator response vs. relative humidity at 20°C for two precipitation field biases.

"feature" or rapid variation in the ambient radon concentration is broadened in the precipitator record. We assumed that, to a first approximation, all the factors affecting the response time could be described by a single term that effectively added a constant amount to the half-life of an exponentially decreasing feature. Figure 4 shows four records taken to test this assumption. Two curves show the response after the radon concentration in the calibration chamber was abruptly lowered, and the other two show the effect of removing the electrostatic precipitation field while the instruments remained in a high radon concentration. In the former case the decline in the count rate is initially slowed by the retention of radon inside the still-functioning field, but all four curves have essentially the same ultimate slope that indicates a "half-life" of about 45 min. The precipitator record can therefore be used as an estimator of the air change rate in a structure, provided that prominent features can be found which can be assumed to be undergoing simple exponential decay and which have a "true" half-life appreciably greater than 45 min.

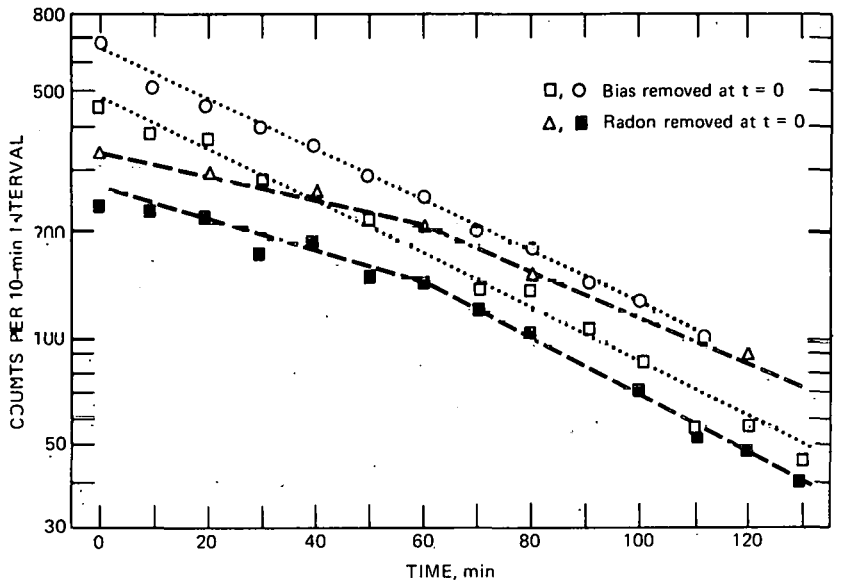


Fig. 4 Response of precipitator to sudden removal of electrostatic precipitation field or ambient radon.

EXPERIMENTAL CORROBORATION OF GENERAL MODEL

Field tests were performed in a 17,000-liter trailer supplied with water containing 6000 pCi/liter of radon. Simultaneous air measurements were made by a radon precipitator and by scintillation flask grab samples. The air change rates indicated by the precipitator record are compared to rates measured by grab samples for two experiments made on Dec. 9 and 10, 1976. The air change rate in the trailer was so high (about $3\ hr^{-1}$) that the greater part of the indicated half-life of the feature was due to the precipitator's lag time, as is shown in Fig. 5. The precipitator is therefore functioning near the limit of its capacity to indicate air change rates. Nevertheless, the agreement with the air change rates indicated by periodic grab sample as shown in Fig. 6 is close enough to be of some value at the level of one significant figure. (The air change rate of a structure is itself a variable and highly dependent on meteorological factors.)

Measured radon concentrations were compared to concentrations predicted from the size of the trailer, the air change rate, and the rate of radon release from the shower. The latter was determined by measuring the flow rate of the shower and taking frequent samples of the water emerging from the shower head and leaving via the drain.

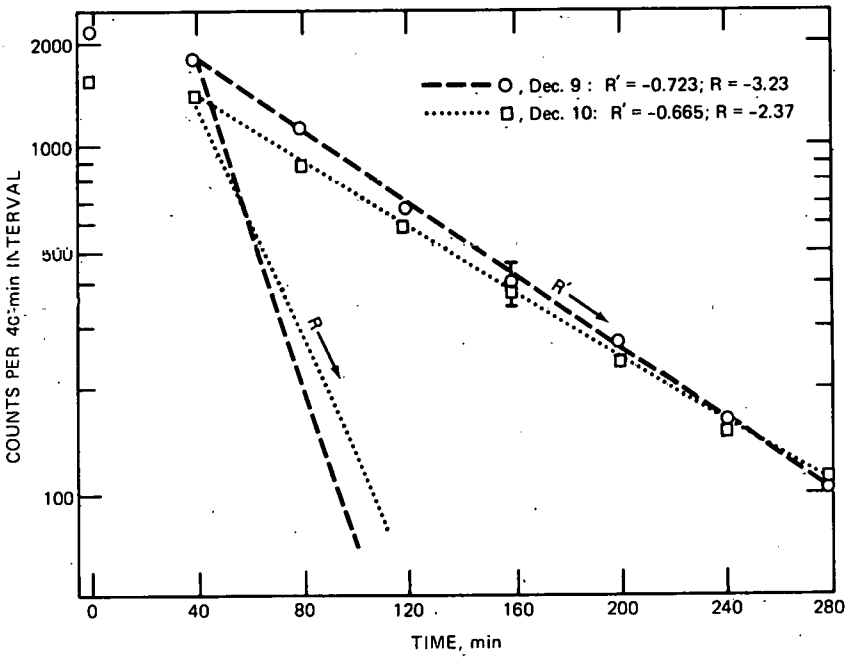


Fig. 5 Estimation of air change rate in trailer from precipitator data.

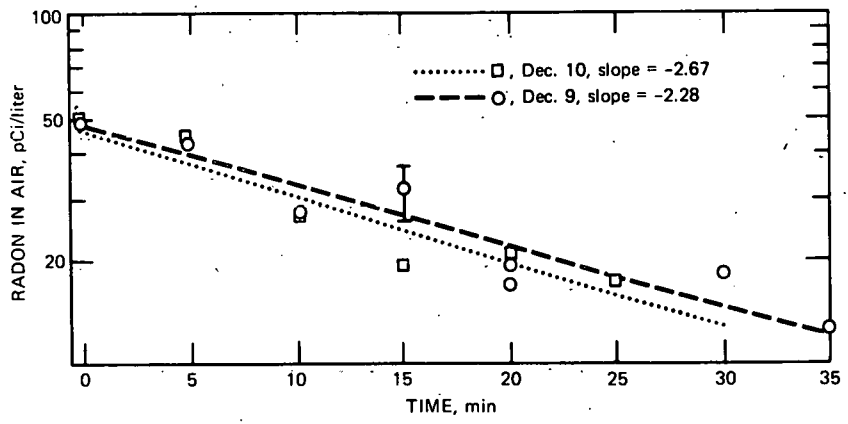


Fig. 6 Determination of air change rate in trailer from grab sample data.

The results are shown in Table 4, in which the term Q is the experimentally determined radon source term and, for a 24-hr interval, corresponds to the factor $C_w \Sigma e_i w_i$ in the general model stated previously. Radon concentration is expressed in terms of the integrated exposure (pCi · hr/liter) or the product of the average

TABLE 4

Integrated Radon Exposures by Three Methods

Date	Q,* pCi	R,† hr^{-1}	V,‡ liters	Integrated exposure, pCi · hr/liter		
				Theoretical	Grab sample	Precipitator
12-9-76	2×10^6	2.28	17,000	51.6	44.0	50.4
12-10-76	1.4×10^6	2.67	17,000	30.8	36.0	60.0

*Q is the experimentally determined radon source term.
†R is the air change rate.
‡V is the dwelling volume.

radon concentration and the exposure interval. Good agreement is seen between the predicted integrated radon exposure and the value obtained by integrating under a curve determined by the grab sample measurements. This agreement between predicted and measured concentrations is again shown in Fig. 7, which depicts the grab sample data from December 9 and the concentrations predicted by

$$C_a = \frac{q}{RV}(1 - e^{-Rt})$$

while the shower was running and by

$$C_a = C_{a,t'}\, e^{-Rt}$$

after the shower had been turned off. Here, q is the measured rate of radon release from the shower in picocuries per hour, t is time in hours, and $C_{a,t'}$, is the concentration of radon in the air at the moment, t′, when the shower is turned off. (This model assumes complete and instantaneous mixing of the air inside the trailer, so the inflection point at t′ is unrealistically sharp.)

Integrated exposures were deduced from the precipitator record under the assumption that the steady-state calibration factor (2 cpm per pCi/liter) could be extended to mean that, for every minute of exposure to an ambient concentration of 1 pCi/liter, an average of

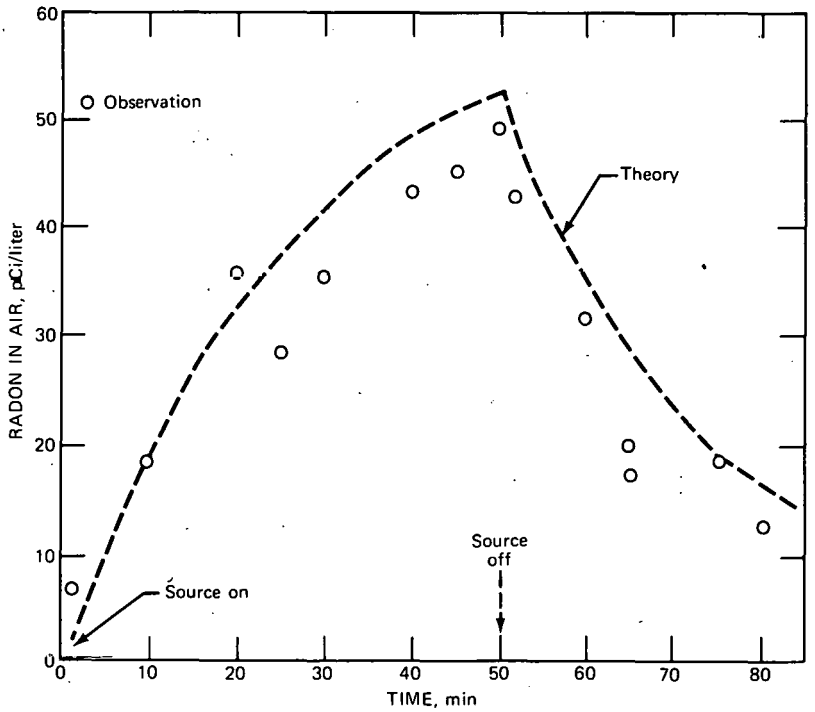


Fig. 7 Predicted and observed radon concentrations in trailer vs. time.

two counts would be expected at some time during the next hour or so. Then, no matter how fast the external radon concentration varied, the integrated exposure could be obtained by dividing the total number of counts observed in an appropriately defined interval by the calibration factor. The agreement between the precipitator estimate and the theoretical and grab sample estimates in Table 4 is only fair, indicating that the variation in radon concentration in the trailer is high enough to strain that assumption. A subsequent determination made under more favorable (and realistic) circumstances produced better agreement between theoretical and precipitator-derived estimates. A 250-liter bathtub was filled from the shower head in an empty apartment having a volume of 1.75×10^5 liters. The net amount of radon liberated was computed in the manner described above to be 3.8×10^5 pCi. The air change rate had been previously determined to be about 0.2 air change per hour, which is not considered uncommonly low for a newly constructed apartment of that type. Precipitator measurements were

taken inside and outside the apartment as the shower was run and for several hours thereafter. The apartment was left closed and unoccupied as soon as the water source was turned off. Figure 8 shows the record of the inside precipitator and the baseline used to estimate the net counts due to the radon liberated by the shower. The nonconstant baseline was required because the outside precipitator

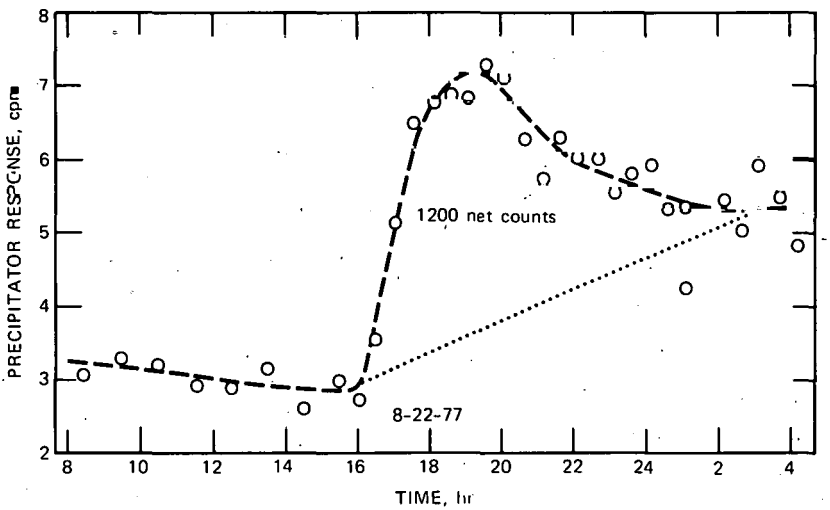


Fig. 8 Determination of integrated radon exposure in an apartment following the use of 250 liters of water in a shower.

recorded a marked increase in the outside radon concentrations commencing at 2000, which is believed to be reflected in the higher background observed indoors after 2400. The merging of the baseline with the presumed new background occurs 10 hr after the beginning of the feature, which at 0.2 air change per hour corresponds to two e-folding intervals. The predicted integrated radon exposure is

$$C_a(t_2 - t_1) = \frac{3.8 \times 10^5 \text{ pCi}}{0.2 \text{ hr}^{-1} \times 1.75 \times 10^5 \text{ liters}} = 10.9 \text{ pCi} \cdot \text{hr/liter}$$

The measured count rate indicates an integrated exposure of

$$\frac{1200 \text{ net counts}}{(60 \text{ m/hr} \times 2 \text{ pCi/liter per cpm})} = 10 \text{ pCi} \cdot \text{hr/liter}$$

MEASUREMENTS IN PRIVATE DWELLINGS

Additional measurements of radon concentrations were made in a number of dwellings in the Houston area. Figure 9 shows a portion of a precipitator record taken at an apartment occupied by a four-member family and served by water containing 1500 to 2000 pCi/liter of radon. The apartment was unoccupied for 1 week prior to the time indicated in Fig. 9 while the family was on vacation. Radon concentrations for that period did not differ

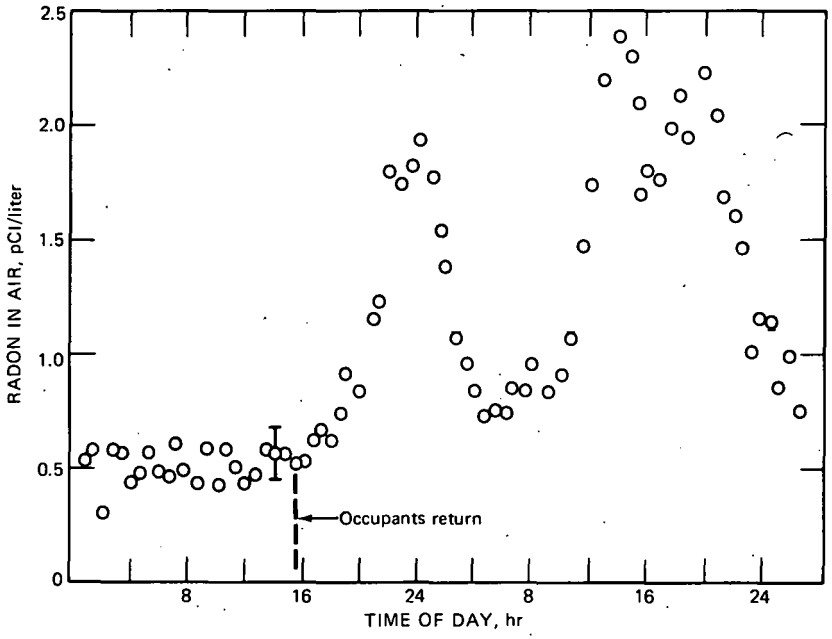


Fig. 9 Atmospheric radon levels in an apartment using water containing 1500 to 2000 pCi/liter of radon.

appreciably from those indicated in the left half of the figure. When the family returned, the radon concentrations increased considerably. Since the apartment was all-electric, and radon concentrations due to building materials would be expected to decrease when occupancy was resumed, the pattern observed is considered to strongly implicate domestic water use as the source of the radon.

The pattern apparent in the diurnal averages of radon concentrations measured in private homes was seen as indicative, although not conclusive, evidence of the influence of the water supply on indoor radon concentrations. Figure 10 shows a 28-day composite of

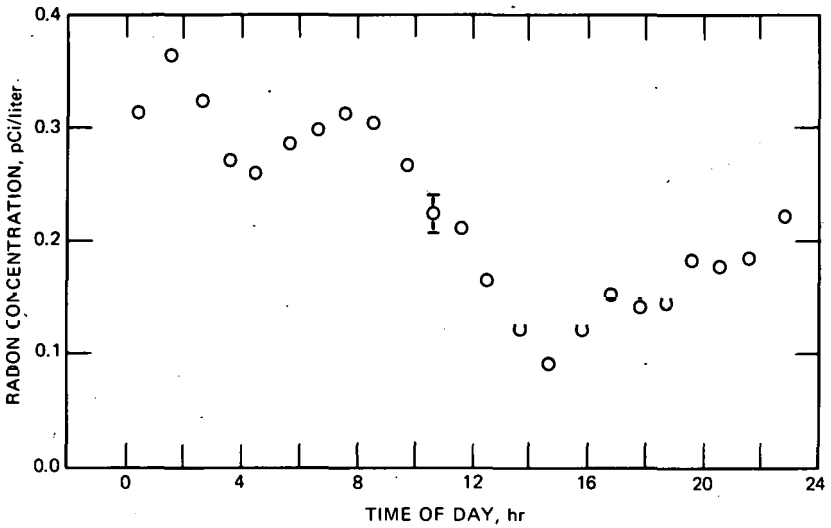


Fig. 10 A 28-day composite of concentrations of radon in outdoor air.

precipitator data taken outdoors or in highly ventilated structures. As expected, outdoor radon levels are highest in the early hours of the morning and then decline as the breakup of the inversion layer produces greater vertical mixing. The indoor records shown in Fig. 11 display a different pattern—the maximums occur in the middle of the day. This pattern is consistent with heavy water use in the early morning, followed by additional use for laundry, cleaning, etc., in the late morning. Although residents were asked to indicate their major water use patterns, the notes taken during these measurements were not sufficient to exclude the alternate hypothesis that the houses shown in Fig. 11 were simply left closed and empty during the day, thus allowing radon from the ground and building materials to accumulate.

Interesting results were obtained, however, when calculations were made on the assumption that the midday and early evening features were due to radon from the water supply. Table 5 compares predicted and measured radon concentration increments for four Houston area dwellings. The predicted values were obtained by the use of the model stated earlier. The measured values were obtained by assuming that the radon levels seen from midnight to 0800 constituted the natural background in the dwelling and by subtracting that average concentration from the average concentration observed for the entire 24 hr. Since the natural background is at its highest from midnight to 0800, and some radon due to water use is also

TABLE 5

Measured and Predicted Radon Increments in Four Houston Dwellings

Dwelling	Date	Radon in water, pCi/liter	Occupants	V,* liters	R,* day^{-1}	Q,* pCi	Radon increment, pCi/liter	
							Predicted	Measured‡
Apartment 1	1-77	1,750	4	175,000	6	803,000	0.77	0.35
House 1	5-77	700	4	340,000†	24†	410,000	0.04	0.04
House 2	5-77	2,000	3	340,000†	12	702,000	0.17	0.18
House 3	7-77	2,000	5	500,000†	24†	1,170,000	0.10	−0.10

*Symbols are defined in Table 4.

†Values for the air change rate and the volume are assumed or estimated.

‡The measured value is considered to be the minimum probable value, since the data from 2400 to 0800 are used as the dwelling's own background. Some activity due to water use can be expected in that interval, and ambient background is usually highest at that time.

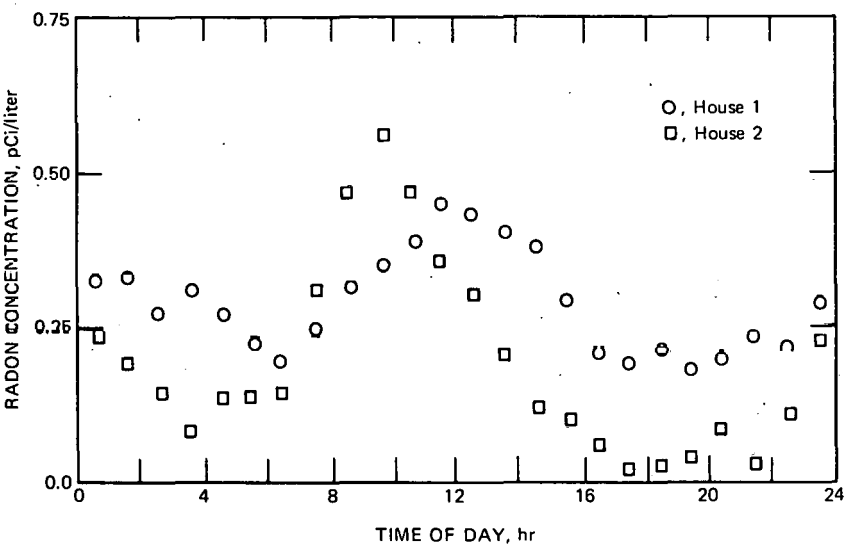


Fig. 11 Diurnal averages of radon concentrations inside house 1 (11 days) and house 2 (6 days).

present at this time, the values so computed were regarded as the minimum probable increments. In three of the four dwellings the agreement is good, considering the inherent error of the background assumption estimate. House 3, which deviates from this pattern, was constructed of rock and was undergoing extensive renovation at the time the measurements were made.

In summary, both experimental and theoretical methods indicate that groundwaters containing levels of ^{222}Rn near or above 1000 pCi/liter can be a significant source of indoor radon. The magnitude of the increment is strongly dependent on climatic and architectural factors, but community-wide population exposures may be more readily calculated for this mechanism than for many other radon exposure mechanisms under current consideration.

REFERENCES

Auxier, J. A., 1976, Respiratory Exposures in Buildings Due to Radon Progeny, *Health Phys.*, 31: 119-125.

Bond, R. G., C. P. Straub, and R. Prober, 1973, *Handbook of Environmental Control*, Vol. III: Water Supply and Treatment, Chemical Rubber Co. Press, Cleveland, Ohio.

Duncan, D. L., T. F. Gesell, and R. H. Johnson, 1976, Radon-222 in Potable Water, in *Proceedings of the Tenth Midyear Topical Symposium of the Health Physics Society*, Saratoga Springs, N. Y., pp. 340-357.

Gemesi, J., D. Szy, and A. Toth, 1975, Radon-222 Content in the Internal Atmosphere of Hungarian Residential Buildings, in *The Natural Radiation Environment II*, Vol. 2, Symposium Proceedings, Houston, Tex., Aug. 7—11, 1972, J. A. S. Adams, W. M. Lowder, and T. F. Gesell (Eds.), ERDA Report CONF-720805-P2, pp. 751-756, Rice University and the University of Texas, Houston, NTIS.

George, A. C., 1975, Scintillation Flasks for the Determination of Low Level Concentrations of Radon, in *Proceedings of the Ninth Midyear Topical Symposium of the Health Physics Society*, Denver, Colo., pp. 112-115.

Gesell, T. F., and H. M. Prichard, 1975, The Technologically Enhanced Natural Radiation Environment, *Health Phys.*, 28: 361-366.

Jonassen, N., and J. P. McLaughlin, 1976, *Radon in Indoor Air I*, Research Report 6, Laboratory of Applied Physics, the Technical University of Denmark.

Lucas, H. F., 1957, Improved Low Level Alpha Scintillation Counter for Radon, *Rev. Sci. Instrum.*, 28: 680-683.

Parthasarathy, K. S., and K. Unnikrishnan, 1977, Bronchial Dose Due to Decay Products of Radon-222 in the Living Environment, *Chemosphere*, 5: 279-284.

Prichard, H. M., and T. F. Gesell, 1977, Rapid Measurements of Radon Concentrations in Water with a Commercial Liquid Scintillation Counter, *Health Phys.*, 33: 577-581.

Watnick, S., V. C. Negro, and R. T. Graveson, 1976, *Environmental Radon Monitor Varies with Relative Humidity*, Technical Memorandum 76-14, ERDA Health and Safety Laboratory.

Wrenn, M. E., H. Spitz, and N. Cohen, 1975, Design of a Continuous Digital Output Environmental Radon Monitor, *IEEE Trans. Nucl. Sci., NS-22:* 645-647.

DISCUSSION

Cathey: Have you considered the fact that, in about half the hours of water use, there is always a person closely coupled to the released radon cloud, and thus the lung exposures will be much higher than the averaged figures you derive by spreading the radon uniformly over the house?

Prichard: An excellent point. This afternoon I was emphasizing the concentrations in the general indoor environment since this makes our work relate more directly to the other papers presented. The daily average exposure underestimates the effective exposure in two ways: First, as you stated, people are exposed to high local concentrations of freshly liberated radon in the course of a number of activities. However, the freshly liberated radon is far from equilibrium, and dosimetry is therefore complicated or at least controversial. Second, the high points in the diurnal profile would occur when persons are present and using water, and the lowest points would occur when the occupants are away.

The Contribution of Bored Wells to Respiratory Radon Daughter Exposure in Finland

O. CASTRÉN
Institute of Radiation Protection, Helsinki, Finland

ABSTRACT

Results of radon measurements in the water of bored wells in Finland are reviewed. The distribution of radon concentration in the breathing air of the users is constructed on the basis of the distribution in the water and a transfer model presented earlier.

For about 8.5% of the users, the annual respiratory radon daughter exposure may exceed 2 working level months (WLM). The annual collective exposure from bored wells is estimated to be less than 10% of that from other radon sources in Finland. Without remedial measures, individual exposures up to 20 WLM/year are possible.

The number of radon-related lung cancers calculated on the basis of the risk estimates for miners, reduced to one-half, is one order of magnitude lower than the actual annual number of new cases.

Until recently the high concentrations of natural radionuclides in the water of some wells bored in rock (Kahlos, 1969; Kahlos and Asikainen, 1973) were regarded as an insignificant anomaly from the point of view of collective radiation dose to the population. When it was found that the tap water from these wells acts as an important radon source to the indoor air of dwellings, a model was developed for the transfer of radon from the tap water to the breathing air of the residents (Castrén et al., 1977). In this paper an estimate is made on the collective radon daughter exposure from the bored wells in Finland. This estimate is compared with the corresponding estimate for other radon sources. The role of radon in the incidence of lung cancer in Finland is discussed.

RADON FROM BORED WELLS

Because the thickness of the earth layer above the bedrock in Finland seldom exceeds 10 m, the quality or quantity of ordinary groundwater is often insufficient. During the last 20 years, wells bored in rock have become a popular alternative. Bored wells are typically used by single families or small groups of people on outlying farms or on the outskirts of population centers where no municipal distribution net exists. It has been estimated that water in the bedrock forms the major part of groundwater supplies in Finland (Niini, 1977). It is therefore likely that the use of bored wells will increase in the future.

The highest radon concentration, 1200 nCi/liter (45 kBq/liter), was measured in the well of an elementary school in a country village. It was originally found by the prospectors of the Geological Survey of Finland who recommended the residents to get in touch with the Institute of Radiation Protection. About 16 persons, members of teacher families and personnel of the school kitchen, were exposed. An elevated level of chromosome aberrations has been found in the peripheral blood lymphocytes of the exposed persons (Castrén et al., 1977). In the beginning of 1977, the construction of an aerator was completed which reduced the radon concentration to between 5 and 15 nCi/liter, depending on consumption.

The situation in the whole country can be described by the cumulative distribution of Fig. 1, which is based on measurements up to the beginning of April 1977. Later measurements have not changed the distribution significantly (Asikainen and Kahlos, 1977). The water—air transfer model (Castrén et al., 1977) was applied to the distribution of Fig. 1. The resulting distribution of average radon concentration in breathing air of the residents is presented in Fig. 2. The left-hand ordinate scale refers to the daily average concentration. The right-hand scale gives the corresponding number of annual working level months (WLM), under assumption that the equilibrium factor is 0.5.

From the diagram of Fig. 2, it can be calculated that about 8.5% of the users receive more than 2 WLM annually. According to our present estimates on the number of users, this would correspond to more than 10,000 persons. Although these people may be at risk to receive more than 100 WLM in 50 years, it is not probable that 100 WLM is often exceeded, because living in the same dwelling for half a century is not very common.

At the bottom of Fig. 2, the mean concentrations calculated from the distributions are given. In the region of Helsinki, this

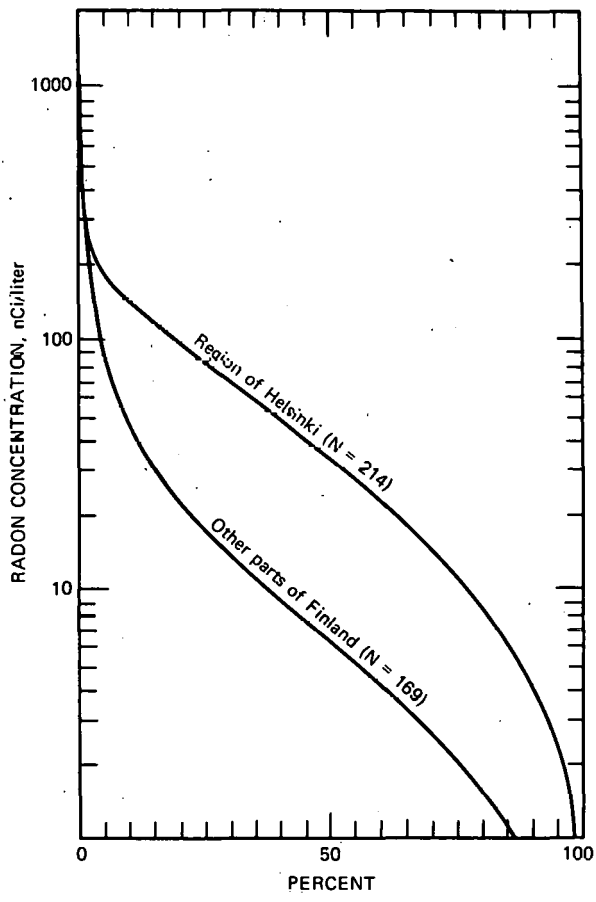


Fig. 1 Cumulative distribution of ^{222}Rn concentration in the water of bored wells. Mine waters and measurements before 1975 are included. N = number of samples.

corresponds to 1.4 WLM/year, and in the other parts of the country, 0.5 WLM/year. Assuming that the number of users is 20,000 in the region of Helsinki and 100,000 in the other parts of the country, it can be calculated that the collective annual exposure from bored wells in Finland might amount to about 75,000 WLM. Neither the exact number of users nor that of the wells is yet known. The representativeness of the water—air transfer model also needs further checking.

The influence of the use of water to the radon concentration in air is demonstrated in Figs. 3 and 4, in which registrations of a

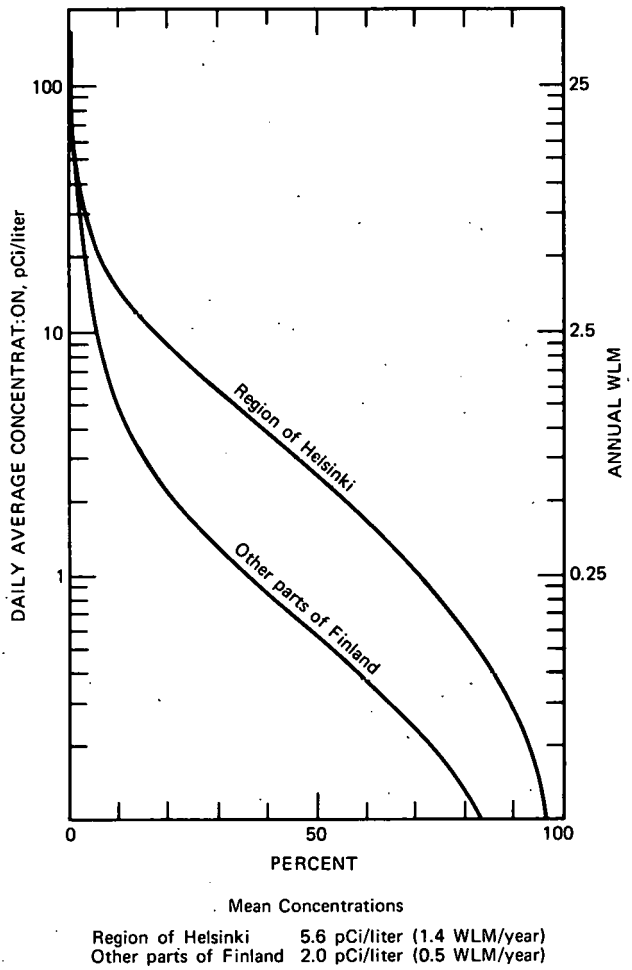


Fig. 2 Cumulative distribution of daily average ^{222}Rn concentration in breathing air of the users of bored wells (according to water measurements and the water—air transfer model).

continuous radon monitor are graphically presented. If radon originates from building materials, the highest concentrations are measured early in the morning. In Fig. 3 a high peak appears in the evening after people have washed themselves before going to bed. The air movements in the dwelling also may have a strong effect. In the latter part of the time presented in Fig. 4, the bathroom door was held well closed and further attention was paid to the proper ventilation.

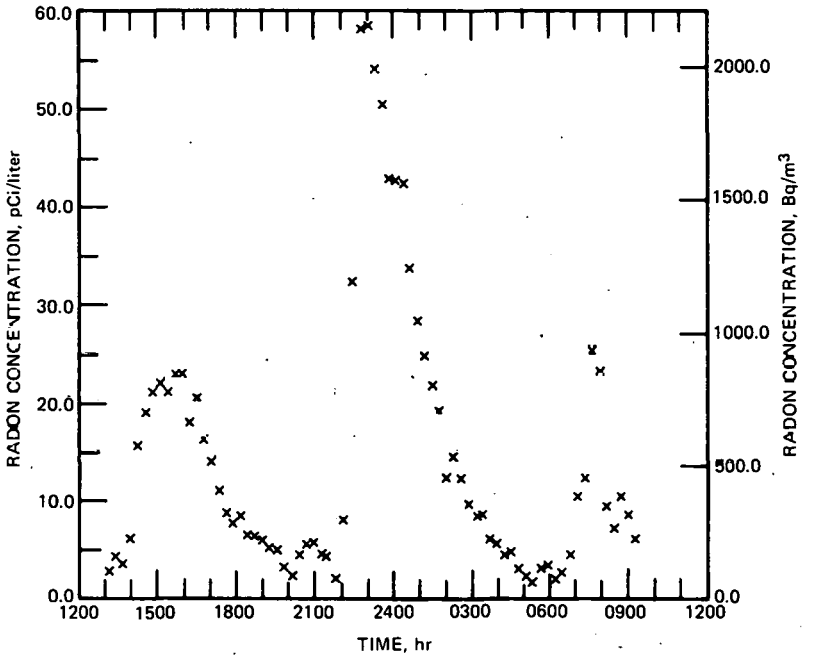


Fig. 3 Typical daily variation of radon in air when radon-rich tap water is used. Concentration in water: 200 nCi/liter (7.4 kBq/liter).

RADON FROM OTHER SOURCES

A really representative survey on radon in indoor air has not yet been performed. According to the measurements performed thus far by the Institute of Radiation Protection, it seems probable that the average level is in the range of 1.0 to 1.2 pCi/liter. This might correspond to 0.20 to 0.25 WLM/year, and the collective exposure for a 4.5-million population would thus be 900,000 to 1,100,000 WLM/year. The contribution of bored wells to collective radon daughter exposure in Finland thus seems to be less than 10%. Instead, the highest individual exposures are caused by the radon originating from bored wells.

LUNG CANCER IN FINLAND

The incidence of lung cancer in Finland is one of the highest in the world. The mean annual age-adjusted incidence rate in

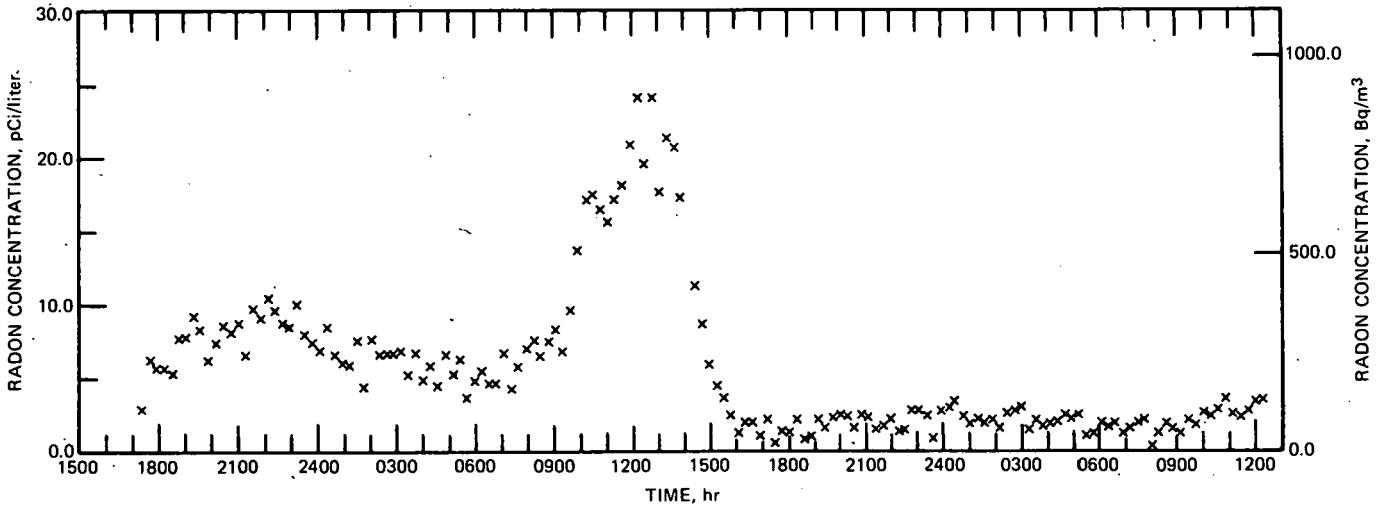


Fig. 4 Radon in living-room air during normal living (before 3 p.m.) and during attempts to keep the concentration low (after 3 p.m.).

1966—1970 was 765 per million in males and 47 per million in females. The annual number of new cases in 1970 was about 2000 (Teppo et al., 1975). Smoking is usually regarded as the main culprit. The high incidence in males is often explained by smoking habits and the fact that cigarette-smoking became popular in Finland earlier than in many other countries.

According to the United Nations Scientific Committee on the Effects of Atomic Radiation (1977), the lung cancer risk for miners is 200 to 450 per million per WLM. If the lower breathing rate is taken into account by reducing the risk estimate to one-half, the collective exposure estimates presented above would correspond to 90 to 240 new cases annually, of which 8 to 17 are caused by radon from bored wells. The risk calculations thus do not support the hypothesis that exposure to radon daughters would have caused the high lung cancer incidence in Finland.

REFERENCES

Asikainen, M., and H. Kahlos, 1977, *Pohja- ja pintavesien luonnollinen radioaktiivisuus Suomessa*, Report STL-A24, Säteilyturvallisuuslaitos, Helsinki.

Castrén, O., M. Asikainen, M. Annanmäki, and K. Stenstrand, 1977, High Natural Radioactivity of Bored Wells as a Radiation Hygienic Problem in Finland, p. 1033, in the Fourth International Congress of the International Radiation Protection Association.

Kahlos, H., 1969, *Radon-222 Concentration of Some Water Samples Determined with Gammaspectrometric Measurements*, Report SFL-A14, Säteilyfysiikan laitos, Helsinki.

——, and M. Asikainen, 1973, *Natural Radioactivity of Ground Water in the Helsinki Area*, Report SFL-A19, Säteilyfysiikan laitos, Helsinki.

Niini, H., 1977, Kallioperässä oleva pohjavesi, *Vesitalous*, No. 6, p. 22 (in Finnish).

Teppo, L., M. Hakama, T. Hakulinen, M. Lehtonen, and E. Saxén, 1975, Cancer in Finland 1953—1970: Incidence, Mortality, Prevalence, *Acta Pathol. Microbiol. Scand., Sect. A*, Suppl. 252.

United Nations Scientific Committee on the Effects of Atomic Radiation, 1977, *Sources and Effects of Ionizing Radiation.*

Radon- and Thoron-Produced Radiation in National Park Service Caves

KEITH A. YARBOROUGH
National Park Service, Southwest Regional Office, Santa Fe, New Mexico

ABSTRACT

This paper describes the findings of the National Park Service Cave Radiation Research and Monitoring Program which has been carried on since August 1975. Two working hypotheses have been established and verified: (1) For all caves having minimal man-made disturbances to natural airflow patterns, the airborne alpha radioactivity increases in the summer and decreases in the winter in caves in which the primary cause of airflow is produced by temperature-induced density gradients. (2) Two general types of physical cave configurations have been identified to relate natural cave airflows and resulting airborne alpha-radioactivity levels; "up-side-down" (USD) caves go "up into" a hillside or mountain and "right-side-up" (RSU) caves go "down into" the earth.

In most natural caves investigated (both RSU and USD), the temperature gradients were found to produce the primary force type by creating density differences between the inside and the outside of the caves. Air then moves either into (incast flow) or out of (outcast flow) under the action of gravity. Pressure affects the air density as well as producing gradients which can cause airflows that may augment or resist the main temperature-produced airflow.

Radioactivity levels which show the upper bounds of data obtained to date are given. A number of long-term plots of the radiation levels at various National Park Service (NPS) caves are given to show the seasonal fluctuations in both RSU and USD caves and the effects of management actions. Short-term plots of USD caves show the cyclic "breathing" nature of the airflows in these caves, again using the airborne alpha radiation as an indicator. The average results of special measurements: individual radon daughter concentrations, unattached (free ion) fraction concentrations, and radon-gas concentrations are tabulated. The annual radiation exposure accumulations for personnel in various NPS caves are also given.

Among the many hazards involved in entering caves for both the casual visitor to a "developed" cave and the sport caver or ardent

speleologist who enters "wild" caves are rock falls; slips and falls; O_2 deficient air; deep water pools and flowing streams; and the danger of contracting rabics, histoplasmosis, and other diseases. In a series of articles in a caving newsletter from 1962 to 1963 (see Bibliography), Verne Reckmeyer and others described their measurements of radon (^{222}Rn), thoron (^{220}Rn), and actinon (^{219}Rn) gases in several caves in Alabama. This is the first reference to such work in U. S. caves, except for a single cave measurement of radon gas made by Saul Harris in New York State in 1954. In late 1968, Richard Breisch gave a detailed description of this possible "new" hazard to U. S. cavers: natural radiation. Subsequently, in 1974 to 1975, Jo Bob Trout, Marvin Wilkening, and David Watkins measured radon gas concentrations in caves of southern New Mexico, including Carlsbad Caverns. Their results suggested a possible health hazard for National Park Service (NPS) cave employees from radon gas and daughter products.

In late fall of 1975, the NPS initiated a program of research and monitoring to study levels of airborne alpha radiation resulting from radon and thoron in all NPS administered caves in which tours for visitors are regularly conducted. The NPS research has the dual but complementary objectives: (1) to safeguard health at the NPS administered caves and (2) to develop data on alpha-radiation levels and on natural airflows in NPS caves. The results reported here for NPS caves describe findings for both of these objectives. The data are being considered by various agencies to clarify health standards for exposures to airborne alpha-radiation levels in cave environments. The investigation's results show daily and seasonal radon trends and the influence of natural ventilation for each cave investigated, as this air movement is affected by meteorological conditions in the vicinity of the various caves.

Checks of many NPS administered caves made since early 1976 revealed radiation levels of sufficiently high magnitude to continue the program of research and monitoring for some years into the future. As part of this program NPS purchased the necessary equipment in the fall of 1976 and trained selected people from each cave area (which is regularly toured by visitors) in its use. The radiation levels and personnel exposure amounts at these caves have been measured continuously since early 1977.

All through this work NPS has consulted with other agencies having expertise in radiation: Environmental Protection Agency (EPA), Occupational Safety & Health Administration (OSHA), National Institute for Occupational Safety & Health (NIOSH), and U. S. Bureau of Mines (USBM). Especially helpful has been the assistance of the Radiation Group of Mining Safety & Health Administration (MSHA) Denver Technical Support Center. Repre-

sentatives from the several agencies concerned with this type of radiation health problem conferred in early November 1976 about health standards to be applied to NPS caves. The consensus was that until more adequate research data became available, the health standards for uranium miners' exposure to this type of radiation were to be used. However, adequate data had become available by January 1978 so that interim standards for NPS cave management purposes could be drafted. These are now being reviewed by the various sectors of the caving community. Table 1 summarizes NPS and concessioner alpha-radiation exposure in working level months (WLM) at several caves.

Two working hypotheses were developed based on preliminary data. These have been verified by subsequent work and somewhat modified by the additional data into the following form:

1. For all caves having minimal man-made disturbances to natural airflow patterns, the airborne alpha radiation increases in the summer and decreases in the winter in those caves in which the primary cause of airflow is produced by temperature-induced density gradients. These set up gravity airflows.

2. For all undisturbed caves in which the primary cause of airflow is temperature/density gradients, two general types of physical cave configurations have been identified to relate natural cave airflows and resulting airborne alpha-radiation levels: Type I: "upside-down" (USD) caves that go "up into" the earth (as up into a hillside or mountain); Type II: "right-side-up" (RSU) caves that go "down into" the earth.

These two hypotheses (and two types of unique cave alpha radiation/airflow exceptions which have been observed) are based on data from the field investigations; generalized and organized using Newton's Second Law for the Conservation of Linear Momentum (written here per unit volume of fluid flowing):

$$\sum \mathbf{F} = \frac{d(\rho \mathbf{V})}{dt} = \rho \mathbf{a} \qquad (1)$$

where ρ = density of the air (i.e., mass per unit volume of air). Both pressure and temperature affect the density of the air by the gas laws.

$\mathbf{a}$ = acceleration induced in the fluid mass by the vector sum of the forces acting upon it. (The product, $\rho\mathbf{a}$, is the "inertial force" of the fluid which reacts to the sum of the acting forces.)

TABLE 1

Annual Exposures of National Park Service Personnel to Cave Airborne Alpha Radiation

Cave area	Year and dates	Annual personnel exposures, WLM						Remarks
		Visitor services			Maintenance			
		Max.	Min.	Av. (No.)	Max.	Min.	Av. (No.)	
Carlsbad Caverns, N. Mex.	Sept.—Dec. 1975	0.86 0.81 Concessioner	0.06 0.12 Concessioner	0.511 (19) 0.569 (12) Concessioner	0.74	0.02	0.278 (17)	Open all year
	Jan.—Dec. 1976	2.17	0.22	1.287 (18)	1.79	0.04	0.574 (16)	Tours are not guided
	Jan.—Dec. 1977	2.09	0.41	1.23 (18)	1.70	0.02	0.548 (17)	All data are for permanent personnel only
Lehman Cave, Nev.	Jan.—Dec. 1977, permanent personnel	0.54	0.04	0.243 (6)	0.15	0.03	0.083 (3)	Open all year
	Mar.—Dec. 1977, seasonal personnel	1.36	0.13	0.849 (10)	0.08	0.02	0.053 (2)	Tours are guided
	Construction work on lighting system, May—Dec. 1977				0.73	0.005	0.436 (6)	
Mammoth Cave, Ky.	May 1, 1976—April 30, 1977	3.06	0.03	1.237 (85)	3.45	0.37	2.077 (15)	Data are for all personnel; open
	Jan. 1, 1977—Dec. 31, 1977	2.87 3.98 Concessioner	0.04 0.002 Concessioner	1.202 (84) 0.427 (49) Concessioner	3.82	0.006	1.474 (17)	all year; tours guided only in fall, winter, and spring
Round Spring Cave (Ozark), Mo.	Jan. 1, 1977—Nov. 22, 1977	1.13	0.10	0.518 (8)				Open only in summer
Crystal Cave (Sequoia), Calif.	April—Sept. 1978	0.985 (Apr.—Dec. 1977)	0.03	0.264 (7)	(Included in "Visitor Services")			Open only in summer
	June—Sept. 1977	0 29	0.05	0.140 (17)				

$[d(\rho V)]/dt$ = time rate of change of the fluid momentum, ρV. [In fluid mechanics this derivative is expanded into the "substantial" or total acceleration which is composed of the local (temporal) and the convective (spatial) acceleration, the latter being velocity changes in space regardless of time and the former being velocity changes in time regardless of space. These subdivisions are considered here since it is important to describe both the local and spatial parts of the total acceleration of the air in the analysis.]

In Eq. 1, ΣF represents the vector sum of the major force types which act on the fluid flowing:

1. The pressure force (P) which is produced by atmospheric pressure gradients between the inside and the outside of the cave.

2. The gravity force (G) which is produced by the body force effect on the fluid due to its mass interacting with the earth's gravitational field. Because the force depends on the fluid's density (i.e., mass per unit volume), it varies with both pressure and temperature.

3. The total drag force (D) which is made up of both form drag (D_f) and viscous drag (D_v). Both D_f and D_v are small in resisting cave airflows, though some of these flows may be laminar or only slightly turbulent. Thus D is small because of usually low airflows, densities, and velocities (and hence low Reynolds numbers). Therefore D has been neglected here for a first approximation:

$$\sum F = P + G \tag{2}$$

Thus the two force types interact to produce the net airflow (with negligible D effects incorporated in the net forces and accelerations),

$$P + G = \rho a \tag{3}$$

In most natural caves investigated (both RSU and USD), the temperature gradients produce the primary force type by creating density differences between the inside and the outside of the caves. Air then moves either in (incast flow) or out (outcast flow) under the action of gravity. Pressure affects the air density as well as the gradients produced by air density which can cause airflows that may augment or resist the main temperature-produced airflow, but to a lesser extent in most natural caves.

Exceptions are Wind Cave and Jewel Cave in South Dakota. Here the primary force is atmospheric pressure. Although this force type

also acts at all other caves, it is secondary to the gravity force. However, at Wind and Jewel, airflows are induced primarily by alternating high- and low-pressure systems which pass through the area, as well as the location of the caves and the overall position of the Black Hills in which they are located with respect to the overall winter and summer meteorological patterns and atmospheric wave systems. Flows produced by temperature/density gradients and gravity do act, but here they are secondary to the atmospheric pressure effects. The pressure can also affect air density. Mainly, however, the passage of a high-pressure system seems to "charge" the caves with higher pressure, incast air. It also decreases emanations of radon gas within the caves. This air is then released when a low-pressure system enters the area following the high. The pressure gradient produces outcast airflows. Also, the reduced pressure that subsequently occurs in the caves enhances the emanation of the radon gas from the rocks and formations of the cave. Hence neither of these RSU caves shows a definite seasonal trend. They mainly respond to the external pressure changes in a scientifically interesting way.

Another less significant exception is Timpanogos Cave which has a "straight through" configuration. Its alpha-radiation levels are low (less than 0.10 WL), in general, with a slight increase during the summer over those of the winter. It is a small cave system situated high on a canyon wall with its main passage parallel to the canyon's axis. Both up and down canyon winds flush the cave regularly throughout the year. Doors at each end of the tour route do not preclude this air movement since there are other larger natural openings for continuous venting. This venting keeps the radiation in the cave low.

Another exception that has been observed is New Cave near Carlsbad Caverns. The radioactivity levels there remain about constant (at 0.20 to 0.25 WL) throughout the year, with only minor fluctuations seasonally. The reason is not fully clear in terms of interrelated airflows, but there seems to be an effect of wind as at Timpanogos Cave, although more subtle. New Cave is an RSU type of configuration but may have other openings for venting. No strong air movements have been observed near its main natural entrance.

Therefore, except for these anomalies, when unaffected by man-made alterations of airflows, both of the two general configurations experience airborne alpha increases in the summer compared to the winter but for opposite reasons. NPS has the most extensive radioactivity data on its two largest cave systems. Figure 1 summarizes 2 years of radiation monitoring at Carlsbad Caverns and shows the long-term trends of radiation level parameters and seasonal

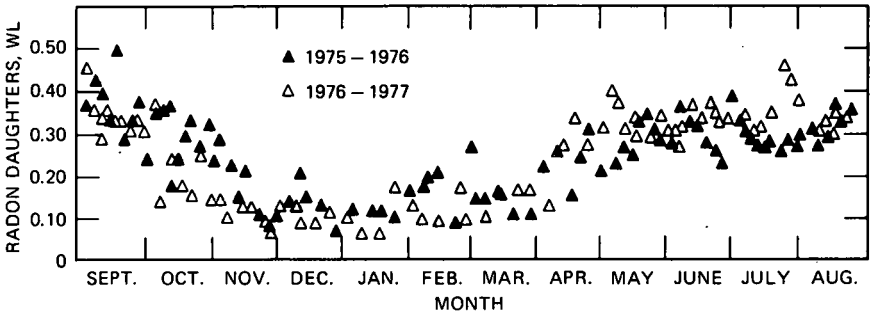


Fig. 1 Seasonal variations of alpha radiation at Carlsbad Caverns, N. Mex.

variations vs. chronological time. The 2 years show a definite similarity. The NPS-administered cave area which consistently has exhibited the highest airborne alpha radioactivity is Mammoth Cave in Kentucky.

Figures 2 to 7 show the long-term (seasonal) variation of radioactivity levels (in WL) at several NPS caves where monitoring is being conducted.

The effects of man's management actions also can be seen here. The natural airflow patterns have not been appreciably altered by tour development at Carlsbad Caverns (RSU), Lehman Cave (USD), or Crystal Cave in Sequoia (USD). However, airflows have been altered by gates and covers over the major natural entrances of Round Spring Cave in Ozark (USD), Oregon Cave (USD), and Mammoth Cave (USD). A heavy iron door has sealed Round Spring Cave for several years. This was replaced by a grille work gate in November 1977. It is expected that this will enhance the airflows. Thus incast winter air should further decrease the already low winter radioactivity levels, but outcast airflows in summer should increase. This is expected to further increase the already high radioactivity levels of summer. Oregon Cave has a man-made exit tunnel which permits greater airflows than naturally existed. This decreases the radioactivity levels in both summer and winter. In spring and fall there are short periods of little airflow or oscillatory (in and out) airflow at which times the radiation increases. This also happens at Mammoth Cave.

Mammoth Cave has a large natural entrance and gate on which covers are placed each fall through spring to preclude strong flows of incast, cold air. These are removed for the warm and hot seasons so that the cave air flows out of this essentially USD cave system (185

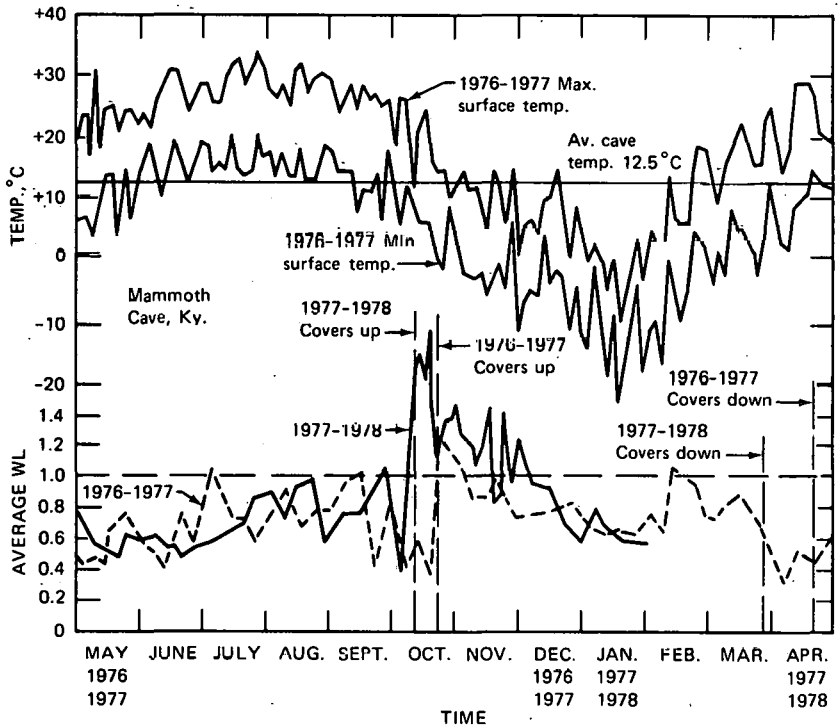


Fig. 2 Seasonal variations of alpha radiation at Mammoth Cave, Ky., 1976—1977.

miles long). This prevents the winter radioactivity levels from being depressed but does permit the summer values to rise to naturally high levels. Therefore the overall result is to cause the winter levels to be artificially elevated to magnitudes equal to or exceeding the summer values. Table 2 summarizes the first full year's data for Mammoth Cave, all tour routes, showing ranges and averages. Table 3 summarizes an experiment performed on the cave's entrance from Oct. 10 to Nov. 23, 1977, when the covers were alternately installed and removed. The data show that when the air is incast the covers increase the radiation levels when put up. When the air is outcast there is little difference, however. This is exactly what would be expected because the incast air can dilute the radiation concentrations in the areas near the natural entrance (i.e., Historic Tour Route) when not excluded by the covers being up. However, when airflows are outcast, the levels are about the same because the air has mobilized radiation materials from deeper within the cave. Although

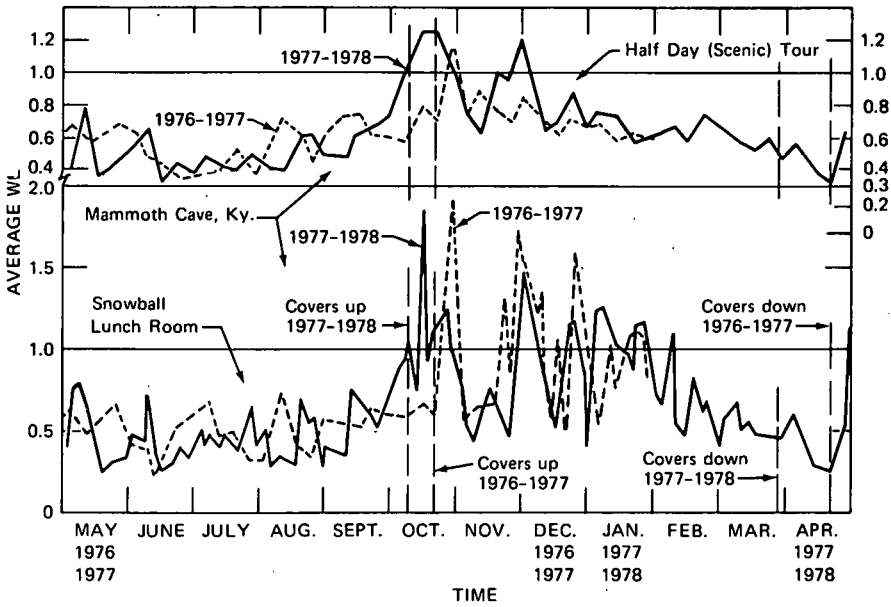


Fig. 3 Seasonal variations of alpha radiation at Mammoth Cave, Ky., 1977—1978.

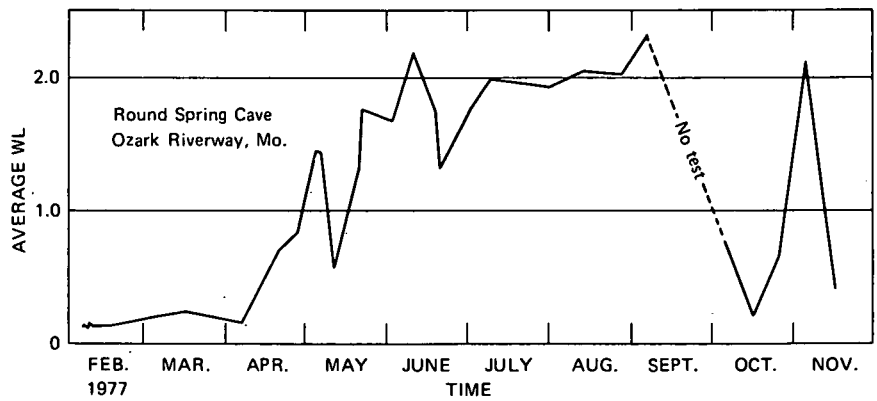


Fig. 4 Seasonal variations of alpha radiation at Round Spring Cave, Mo.

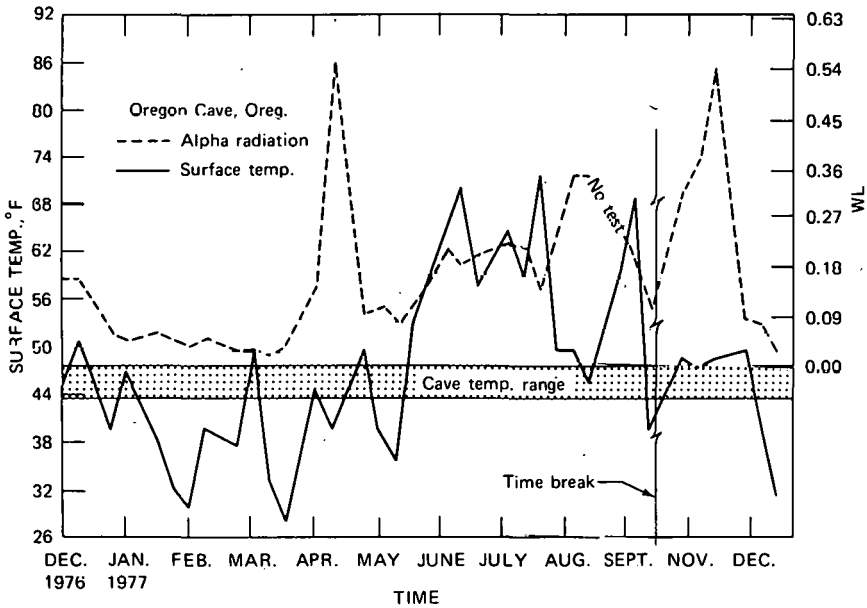


Fig. 5 Seasonal variations of alpha radiation at Oregon Cave, Oreg.

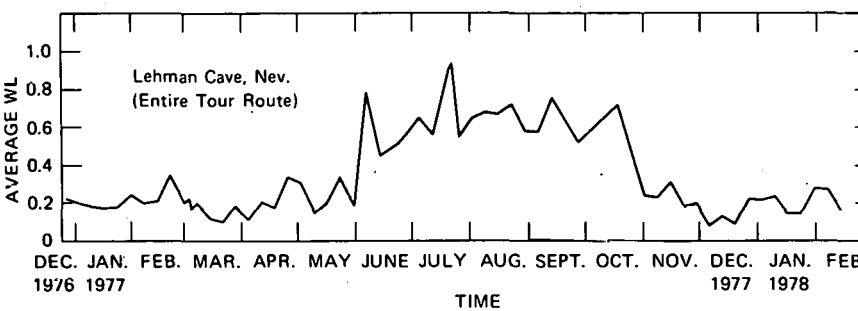


Fig. 6 Seasonal variations of alpha radiation at Lehman Cave, Nev.

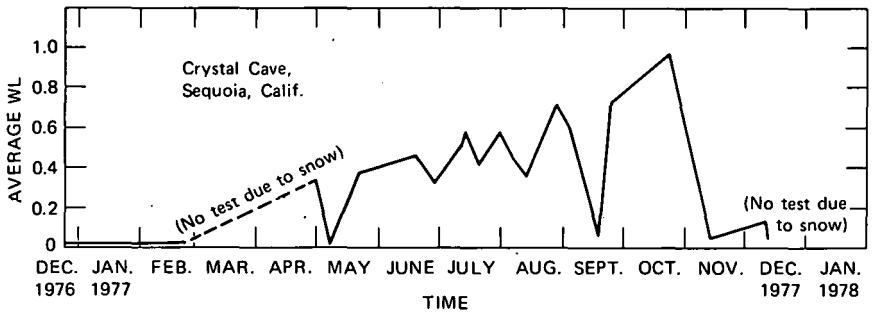


Fig. 7 Seasonal variations of alpha radiation at Crystal Cave, Calif.

the covers reduce airflow *out* of the entrance to some extent, the radioactivity is not greatly reduced since the outcast flows at this time of year are considerably less than the incast flows. The comparison of the walking sample locations closest to and farthest from the entrance shows this same effect but also shows the attenuation of incast air, due to distance. Table 4 shows a summary of sample sets having one or more values exceeding 1.00 WL, for various NPS caves. This indicates the upper bound of the radioactivity levels for these caves, in particular, Mammoth.

The natural airflow in this immense cave system has been modified by one elevator shaft, several constructed access portals, and certain operational practices. The most important of these latter is the placement of sheet-metal covers over the gateway at the large natural, "Historic" entrance to the cave. This is done in mid to late October each year. These are removed in mid to late March, annually. This is an interruption of the natural airflow regime for Mammoth which is generally a USD type cave system: strongly outcast airflows during the summer with some cyclic, diurnal variations and concomitant alpha radioactivity fluctuations which reverse in winter to have strongly incast airflows at the Historic entrance. (Mammoth's stable temperature is about 54°F.) General evaluation of overall flow patterns has been made for the major seasonal temperature gradient situations: (1) when the outside average air temperature exceeded that of the cave's 54°F and (2) when the outside average air temperature was less than 54°F. This evaluation shows a general *outflow* for temperature gradient situation 1 and a general *incast flow* for temperature gradient situation 2. However, the placement of the covers each fall causes the radiation levels to surge upward immediately. A peak is reached in about a day with a lowering of general radiation following that,

TABLE 2

Summary of Monthly Alpha Radiation Levels (in WL) for Mammoth Cave

Tour route	May 1976		June 1976		July 1976		Aug. 1976		Sept. 1976		Oct. 1976*	
	Range	Av.	Range	Av.	Range	Av.	Range	Av.	Range	Av.	Range	Av.
Scenic (half day)	0.58—0.68	0.64	0.37—0.61	0.48	0.38—0.51	0.43	0.45—0.70	0.59	0.60—0.74	0.67	0.59—1.12	0.80
Frozen Niagara	0.28—0.61	0.50	0.28—0.51	0.38	0.32—0.55	0.40	0.33—0.43	0.39	0.38—0.70	0.50	0.38—0.92	0.60
Wild Cave	0.25—0.62	0.44	0.34—0.40	0.36	0.38—0.50	0.44	0.33—0.55	0.44	0.50—0.71	0.59	0.62—0.92	0.74
Lantern	0.64—0.99	0.85	0.70—0.89	0.82	0.75—0.91	0.82	1.09—0.90	0.99	0.56—1.03	0.80	0.12—1.13	0.65
Echo River						0.42					1.51—2.02	1.77
Historic	0.45—0.75	0.57	0.48—0.73	0.58	0.60—1.08	0.80	0.68—0.88	0.78	0.42—1.00	0.79	0.37—1.29	0.65
Snowball Room	0.48—0.68	0.59	0.26—0.52	0.40	0.34—0.68	0.49	0.35—0.73	0.52	0.53—0.62	0.58	0.59—1.89	0.94
Great Onyx Cave			0.63—0.84	0.71	0.68—0.94	0.80	0.64—0.95	0.81				1.12

Tour route	Nov. 1976		Dec. 1976		Jan. 1977		Feb. 1977		Mar. 1977†		April 1977		Annual averages	
	Range	Av.	Range	Av.	Range	Av.	Range	Av.	Range	Av.	Range	Av.	Range Av.	Overall Av.
Scenic (half day)	0.70—0.87	0.78	0.61—0.70	0.66	0.58—0.75	0.66	0.58—0.72	0.65	0.47—0.64	0.56	0.32—0.63	0.47	0.52—0.72	0.62
Frozen Niagara	0.47—0.68	0.61	0.46—0.71	0.54	0.49—0.69	0.55	0.59—0.67	0.63	0.36—0.56	0.46	0.29—0.68	0.44	0.39—0.64	0.50
Wild Cave	0.65—0.76	0.70	0.58—0.62	0.59	0.53—0.64	0.59	0.51—0.58	0.54	0.34—0.77	0.58	0.30—0.47	0.36	0.44—0.63	0.53
Lantern		0.99				0.84				0.66	0.25—0.71	0.47	0.64—0.92	0.79
Echo River	0.82—1.13	0.97	0.81—0.96	0.89	0.52—0.77	0.67	0.68—1.00	0.80	0.40—0.88	0.70	0.16—0.97	0.48	0.67—1.02	0.84
Historic	0.72—1.07	0.90	0.76—0.81	0.79	0.62—0.66	0.64	0.64—1.03	0.84	0.53—0.87	0.73	0.31—0.59	0.46	0.55—0.89	0.71
Snowball Room	0.48—1.47	0.77	0.42—1.16	0.79	0.89—1.25	1.10	0.48—1.10	0.70	0.41—0.68	0.53	0.27—1.09	0.56	0.46—0.99	0.66
Great Onyx Cave						0.67		0.76		1.22		0.74	0.81—0.91	0.85

*Natural entrance gate covers put up in late October 1976.
†Natural entrance gate covers taken down on March 27, 1977.

TABLE 3

Effects of Management Activities at Natural Entrance of Mammoth Cave on Airborne Alpha Radiation Levels (Oct. 10—Nov. 22, 1977)

Cave area sampled	Average radon daughter, WL	Gate cover configuration	Airflow direction	For some airflow direction, % change when covers put up	Remarks
Historic Tour Route	1.46	Up	Incast	+54%	Average is for entire tour route
	0.67	Down (off)	Incast		
Historic Tour Route	1.33	Up	Outcast	—5%	Average is for entire tour route
	1.40	Down	Outcast		
Natural entrance to Methodist Church	1.21	Up	Incast	+65%	Average is for that part of the Historic Tour Route nearest the entrance. This is the most changeable sample (walking).
	0.42	Down	Incast		
	1.38	Up	Outcast	—9%	
	1.51	Down	Outcast		Difference: up/in vs. up/out = —0.17 WL
					Difference: down/in vs. down/out = —1.09 WL
Stairway before Fat Man's Misery to River Hall	1.54	Up	Incast	+16%	Average is for that part of the Historic Tour Route farthest from the entrance. This is the least changeable sample (walking).
	1.29	Down	Incast		
	1.22	Up	Outcast	—9%	
	1.34	Down	Outcast		Difference: up/in vs. up/out = +0.32 WL
					Difference: down/in vs. down/out = —0.05 WL

TABLE 4

Summary of Representative Cave Radon Daughter WL Values at Selected Caves Having High Radioactivity

Cave area	Weighted average of all tour route sampling sets with one or more values ⩾ 1.00 WL (No.)				Weighted average of all sample values ⩾ 1.00 WL in each sampling set (No.)			
LECA (Lehman Cave, Nev.)	0.68 (115) (Based on 13 sample sets)				1.12 (22)			
CRCA (Crystal Cave, Sequoia, Calif.)	0.79 (82) (Based on 21 sample sets)				1.37 (24)			
CUGA Indian Cave (Cumberland Gap, Ky.)	1.01 (17) (Based on 5 sample sets)				1.18 (10)			
ROSP (Round Spring Cave, Ozark, Mo.)	1. Overall Cave: 1.50 (146) (Based on 19 sample sets)				1.93 (98)			
	2. North Passage: 1.00 (52) (Based on 14 sample sets)				1.35 (22)			
	3. South Passage: 1.86 (70) (Based on 19 sample sets)				2.04 (64)			
	1976—1977		1977—1978		1976—1977		1977—1978	
	Covers up	Covers down	Covers up	Covers down	Covers up	Covers down	Covers up	Covers down
MACA (Mammoth Cave, Ky.)	0.89 (246)	0.91 (152)	1.07 (454)	1.03 (263)	1.20 (87)	1.10 (67)	1.35 (252)	1.21 (148)
Other caves at Mammoth Cave National Park, Ky.:								
Crystal Cave of Floyd Collins	1.13 (12)	1.17 (25)	0.81 (7)	1.07 (14)	1.18 (10)	1.32 (10)	1.02 (3)	1.42 (8)
White's Cave	None	1.03 (12)	None	1.59 (20)	None	1.25 (7)	None	1.63 (19)
Great Onyx Cave	1.00 (8)	1.03 (8)	0.81 (8)	1.26 (10)	1.09 (4)	1.13 (4)	1.25 (4)	1.26 (10)
New Discovery Entrance Area	0.86 (7)	1.00 (16)	None	1.02 (5)	1.09 (4)	1.06 (10)	None	1.15 (4)

probably due to equilibration of the cave system to this interruption of the natural airflow and the establishment of incast flows of lesser extent through other, though less effective, portals.

Because the overall, man-affected situation at Mammoth Cave produces a buildup of radiation levels during the winter compared to the summer when the levels are somewhat lower, the covers will not be put up again after the 1978 winter period. It can be speculated that, without the interruption of the natural airflows and the

seasonal variations in them, this huge USD cave system probably would respond to temperature/density gradient (gravity) airflows in an overall way similar to smaller USD caves such as Lehman in eastern Nevada and Crystal in Sequoia, Calif. This will be observed starting in the fall of 1978. Oregon Cave, also of the USD type, has the man-made exit tunnel which has greatly modified the natural airflow patterns and serves to depress the radiation levels, especially in the summer, below what otherwise might occur. *We therefore must be very careful in our management practices in caves.* Although desirable decreases in airborne alpha radioactivity may occur, great and undesirable alteration of cave microclimate can also take place. Table 5 compares some summer 1976 and 1977 data—time of year when basically unaltered "airflow" is occurring at Mammoth Cave and when other USD caves, having little alteration in natural airflow patterns, experience high radioactivity levels. Table 6 indicates that on occasion the thoron (^{220}Rn) daughter levels exceed 0.10 WL and must be accounted for in the calculation of employee alpha-radiation exposure amounts. No other NPS caves investigated have ever had more than a few hundredths WL, never exceeding 0.10 WL, except Mammoth and Round Spring in Ozark Riverway, Mo.

Due to careful management efforts at Mammoth by which personnel were shifted from work in the cave to surface activities, none exceeded 4.0 WLM exposure during the first year's monitoring from May 1976 to April 1977 (see Table 1). The maximum exposure for this 12-month period for all of the tour guide personnel was 3.06 WLM. This individual also had carried out the monitoring measurements on an interim basis for 4 months during the summer of 1976. The maximum annual exposure among maintenance workers was 3.45 WLM. These exposures were achieved by rotating personnel to surface activities during the year.

Table 6 shows the shift in general radiation level which occurs (from first week of May 1977 data) when the thoron (^{220}Rn) daughter level exceeds 0.10 WL and a correction must be made.

Thoron (^{220}Rn) produced alpha radiation is much more hazardous per unit concentration than that from radon. At radioactive equilibrium 100 pCi/liter of radon produces 1.0 WL radiation, but only 8 pCi/liter of thoron is needed to give 1.0 WL.

In USD caves the radiation levels increase in summer because the airflow does occur in a strong way, while in RSU caves the radiation levels also increase in summer, but because the air tends to stagnate (except for weather front passages which may induce some airflows). This seeming paradox may be explained by considering the temporal and convective accelerations—of how the air tends to flow in each general cave configuration type: USD vs. RSU (i.e., with

TABLE 5

Comparison of Summer Radioactivity Levels at Mammoth Cave ("Unaltered" Airflows)

Tour	No. of samples	Average WL, July 1977	Average WL, July 1976	% change	Average WL, Sept. 1977	Average WL, Sept. 1976	% change
Historic	33	0.68	0.80	−15.0	0.88	0.79	+10.0
Scenic (half day)	44	0.44	0.43	+2.3	0.59	0.67	−12.0
Lantern	35	0.93	0.82	+12.0	0.96	0.80	+17.0
Wild Cave	28	0.46	0.44	+4.3	0.50	0.59	−15.0
White's Cave	7	1.63	1.23	+24.5			
Snowball Room	6	0.49	0.49	0.0	0.53	0.58	−9.0
Great Onyx	12	0.72	0.80	−10.0			
Frozen Niagara	6	0.36	0.40	−10.0	0.45	0.50	−10.0

TABLE 6

Effect of Thoron-Daughter Radiation on Overall Alpha Radiation Levels at Mammoth Cave

Tour route	Average level without T-D's, WL	Average level with T-D's, WL
Historic	0.39	0.82
Scenic (half day)	0.73	0.83
Wild Cave	0.57	0.68
Lantern	0.43	0.53

respect to both time and space). In the USD type the airflow process is cyclic and unsteady in general (except as perturbated by weather systems inducing pressure changes and thus pressure-produced airflows superimposed on the cave's general gravity airflows). The airflow increases from morning to afternoon but dies away at night. However, in winter these cyclic flows are of short duration and occur only near the cave's portal(s). In winter, although air may sink into USD caves upslope, it takes it a long time, i.e., perhaps several days of cyclic actions (which may be interrupted by cloudy weather), to carry this air to the portal(s). Thus the airflows mobilize small total amounts of radioactivity per unit of time in winter and move these to the toured areas where the measurements are made. Therefore, even if in radioactive equilibrium, the concentrations are less. However, in summer, air moves from the cave extremities more quickly, moving greater total quantities of radioactivity (per unit time) in shorter time periods to the toured area. Hence the concentrations measured there are higher in the summer than in the winter because of high air velocities. Figures 8 to 10 compare those cyclic variations at selected locations in three USD caves: Oregon Cave, Crystal Cave in Sequoia, and Lehman Cave. Oregon has considerable man-caused airflow alteration but Crystal and Lehman have very little. Although Lehman has both an entry and an exit tunnel, these are well sealed so that the natural airflows are little affected. These three figures show the cave "breathing."

At Oregon Cave the entrance and exit had been covered in January 1976. These covers were removed in the spring of 1976 and not replaced. Figure 8 shows the interesting result of this management practice with summer 1977 higher than winter 1977 as would

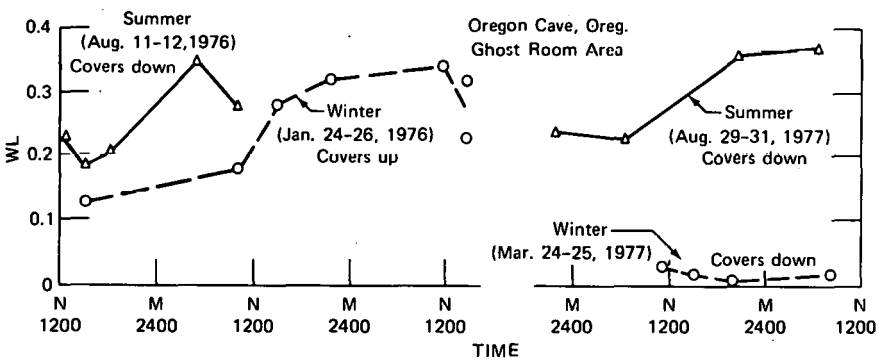


Fig. 8 Daily alpha-radiation changes under different ventilation control regimes at Oregon Cave, Oreg., by seasons.

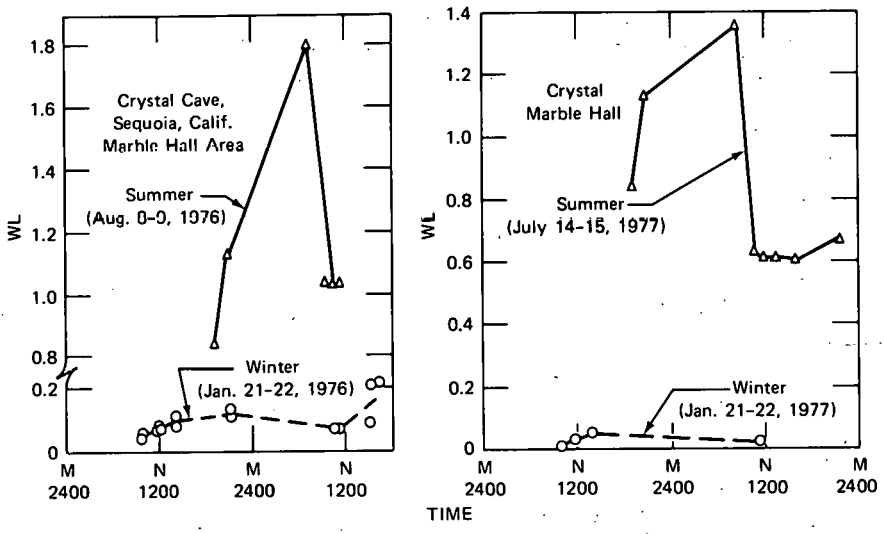


Fig. 9 Daily alpha-radiation changes due to natural ventilation variations at Crystal Cave, Calif., by seasons.

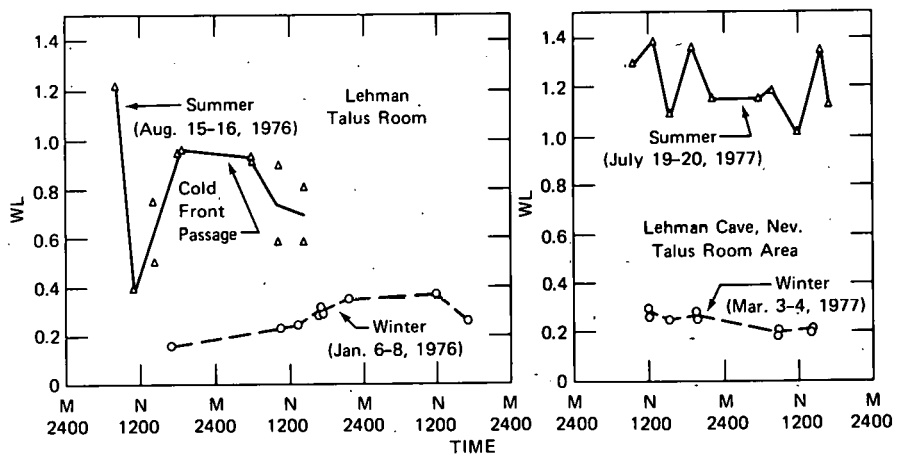


Fig. 10 Daily alpha-radiation changes due to natural ventilation variations at Lehman Cave, Nev., by seasons.

be expected for a USD cave, even one with altered airflows such as Oregon is. The cyclic "breathing" is more pronounced and sustained in summer. The airflow increases from morning through afternoon and flushes out the radiation. As the airflows (produced by temperature/density gradients which increase during the day) die away in the evening, the radiation levels increase at night. This is most pronounced at Crystal and Lehman, while the artificial tunnel at Oregon modifies the sharpness of the cyclic breathing.

On the other hand, the RSU cave types have more sustained and steadier airflows in winter because then the colder, more dense outside air sinks into the cave, displacing its comparatively warmer, less dense air and flushing out the radioactivity. This process continues in a long-term fashion so that the winter radiation levels are lower than in summer. Indeed, the winter airflow in RSU caves can be greater at night than in the daytime since the outside air temperature is lower at night. In summer, the reverse of this process occurs, and the cave air, being comparatively colder and denser than the outside air, tends to stagnate. Hence the radioactivity levels can build up and become higher in winter. Of course, as in the USD caves, the effects of passing weather fronts can perturbate an RSU cave and produce airflows in summer which overcome the stagnation to some extent. In winter these can augment the gravity flows and depress the radiation levels further. Indeed, it can be speculated that the fluctuation on long-term plots might be the superposition of pressure-produced airflow/radioactivity level oscillations on the long-term gravity airflow/radioactivity situation.

Obviously, an RSU cave seen from below appears to be USD, and vice versa. Therefore it is not unreasonable to expect some caves in both general types of cave configurations to be double-ended. A situation of this kind has been found to exist in Cumberland Gap Historic Park. Jim Quinlan (of Mammoth Cave National Park) has shown that Cudjo's Cave (the main portals of which lie on one side of a ridge line at an elevation of about 1550 ft MSL) is connected by water flow passages with Indian Cave, which lies on the other side of and up the ridge line with a portal elevation of about 1850 ft MSL. Airflows can also pass between the cave systems. (It also appears that the three other caves, Skylight, Big, and Little Saltpeter, which also lie across and up the ridge from Cudjo's Cave with portal elevations of about 1820, 1970, and 1800 ft MSL, respectively, connect with Cudjo's.)

Table 7 presents data which suggest that in summer air can sink down into the RSU caves, Skylight and Indian, and flow out of the USD cave, Cudjo's. The radioactivity levels are low in the RSU caves

TABLE 7

Seasonal Comparison of Airflows and Radiation Levels at Cudjo's Cave and Indian Cave

Date	Radioactivity, WL		Airflow	
	Cudjo's	Indian	Cudjo's	Indian
8-02-77	0.38	0.12	Outcast	Somewhat incast
6-24-77	0.44	0.54	Slightly outcast	Slightly incast to none
3-25-77	0.05	1.31	Very slightly outcast	Very slightly incast to none
1-22-77	0.03	1.01	Very slightly incast	None to very slightly outcast

and higher in the USD cave. A transition with almost equivalent radiation levels occurs during the spring when little airflow develops at either end of this cave system. In the winter the modest reversal of airflow produces a reversal of radiation levels.

Indian Cave has a small entrance with an overhanging lip that causes a very interesting and unique situation which I have seen in only one other cave—nearby Skylight. This lip greatly modifies the possibility of airflows in or out of Indian and produces a very sharp transition from outside air conditions to true cave air of constant temperature and humidity. This occurs within 15 to 20 ft at most. During the bitter winter weather of January 1977, cave radioactivity monitors entering Indian Cave went from sub-zero cold to the stable cave temperature of about 53°F in this short distance.

Skylight has a lip located about 100 ft in from its portal. This cave has a very large mouth similar to a shelter overhang and another "skylight" opening above the main portal. Hence it is well ventilated. In the spring and summer the radiation levels both in front of and behind the lip are low and about the same, but in winter a startling difference occurs. In all seasons the "sealing" lip tends to create a true cave air situation behind it, whereas the outer area of the open cave is very nearly like surface air. Table 8 shows comparative data.

The importance of the effects of natural airflows on cave radiation must always be emphasized along with radiation measurements because the basic rule of thumb is that increased radiation occurs when cave air stagnates but decreased radiation occurs in the immediate vicinity of noticeably moving cave air, in general. It seems generally true that airflow decreases airborne radioactivity while stagnation increases it. Any seeming paradoxes result from *how the*

TABLE 8

Seasonal Comparison of Radioactivity Levels on Each Side of Sealing Lip at Skylight Cave

Date	Outside lip, WL	Behind lip, WL	Portal, WL	Portal airflow
8-02-77	0.011	0.010	0.005	Incast at ceiling, outcast along floor
6-25-77	0.002	0.002	0.002	Incast at ceiling, outcast along floor
5-08-77	0.005	0.038	0.005	None
3-26-77		0.58		None
3-27-77	0.01	0.72		None
1-23-77	0.034	0.176	0.031	None

air moves through a cave system with respect to time and space. Airflows are controlled by the interaction of atmospheric pressure gradients and temperature-induced density (gravity) gradients as the major forces.

Thus of particular importance to the personnel radiation exposure rates in natural caves are the natural ventilation patterns. These airflows are the only means by which the radiation is dissipated or concentrated. In mines, forced air ventilation is used to minimize the airborne alpha radiation in order to meet the health standards. In caves, although the potential alpha radioactivity could usually be lessened, it is not possible to use artificial ventilation because of the adverse effects on the microclimates of the caves. John McLean of the U. S. Geological Survey has shown this by his studies of cave microclimates at Carlsbad Caverns.

The measurement of radon daughter radioactivity levels serves as a useful means to describe airflow patterns, in addition to employing the methods of fluid mechanics. Indeed, radiation is a "tracer" for airflow and indicates its general tendencies. This has already been seen in Figs. 8 to 10 which show the caves' breathing. The presence of considerable levels of alpha radioactivity can be used to indicate the existence of extensive, although as yet unknown, additional cave system networks so long as the natural airflow patterns have not been distributed. Thus, at Round Spring Cave in Ozark Riverway, Mo., I predicted that the "left-hand" passage that leads off to the southwest from the tee-shaped entry passage and "Junction Room"

should connect with a more extensive system, at least by airflow passageways. This was confirmed subsequently by a very knowledgeable local caver. He indicated that another large cave system does adjoin the southwest passage of Round Spring through which only air can move, but people can shout between. Therefore I predict that Lehman Cave is much more extensive, as Crystal Cave in Sequoia, Calif., should be also.

Very little alpha radioactivity has ever been found in lava tube caves or volcanic areas. These results agree with those of other investigators. Nor has much alpha radioactivity been found in thermally active areas that are open to free surface air movements; e.g., Lassen, Yellowstone, Hot Springs, Ark. However, at Hot Springs the radiation levels are high in enclosed, unventilated water collection reservoirs. Also, at Yellowstone's Mammoth Hot Springs, old, inactive fissures, which may interconnect over a considerable distance in the sort of RSU (at higher elevations) USD (at lower elevations) configuration described above for Cudjo's Cave and Indian Cave at Cumberland Gap, have significant alpha radioactivity levels, especially in the summer.

The thoron (^{220}Rn) daughter levels were usually varied from trace to very low values in almost all NPS caves investigated. Hence this source of alpha radioactivity is no problem except at Mammoth Cave, Ky., and Round Spring Cave, Mo., on a few occasions.

ACKNOWLEDGMENTS

I would like to thank the following persons for their support and contributions to this work.

Ted Sudia, Chief Scientist and Associate Director for Science and Technology, National Park Service, Washington, D. C., who provided the initial funds to begin this research program after recognizing the need for this work.

Gary Ahlstrand, Research Ecologist for Carlsbad Caverns and Guadalupe Mountains National Park, who did the important initial 2 years' work at Carlsbad Caverns.

Robert Rock (now deceased), Robert Beckman, and their colleagues of the Radiation Branch, Denver Technical Support Center, MSHA, for continuous advice, assistance, and equipment loans.

Robert Droullard, Chief, Special Studies Group, Denver Mining Research Center, USBM, for lab analysis and equipment loans.

Tom Aley and Wm. Austin of the National Caves Association for consultation on cave management *vis a viz* the potential cave radiation health problem.

All the NPS cave monitors, many of whom were "volunteered" for this work and most of whom have done an excellent job, in particular, Gary Ahlstrand and Patty Fry at Carlsbad Caverns and Joe McGown, Danny Close, and Bobby Carson at Mammoth Cave, guided by Jay Cable and Superintendent Amos Hawkins there. They all deserve great credit for their efforts on this project.

BIBLIOGRAPHY

Ahlstrand, Gary, and Patty Fry, 1976, *Alpha Radiation Monitoring at Carlsbad Caverns*, Paper No. 180, presented at Proceedings of First Conference on Scientific Research in the National Parks.

Ahlstrand, Gary, and Patty Fry, 1977, *Alpha Radiation Project at Carlsbad Caverns: Two Years and Still Counting*, paper presented at Proceedings of National Cave Management Symposium.

Beckman, Robert T., 1975, *Calibration Procedures for Radon and Radon-Daughter Measurement Equipment*, MESA-IR1005, 47 pp.

Breisch, Richard L., 1968, Natural Radiation in Caves, *Southwestern Caver*, VII(5): 81-110.

Mining Enforcement and Safety Administration (MESA), *Radiation Monitoring*, 1976 ed., 88 pp., Radiation Group, Denver Technical Support Center.

Reckmeyer, Verne, et al., 1962—1963, Radioactivity in Alabama Caves, *Huntsville Grotto Newsletter*.

Rock, Robert L., 1975, *Sampling Mine Atmospheres for Potential Alpha Energy Due to the Presence of Radon-220 (Thoron) Daughters*, MESA-IR1015, 15 pp.

Trout, Jo Bob, 1975, An Investigation of Radon Levels and Air Exchange Characteristics in Cottonwood and Jurnigan Caves, *Southwestern Caver*, XIII(3): 1-27.

Wilkening, Marvin H., and David E. Watkins, 1976, Air Exchange and 222 Rn Concentrations in the Carlsbad Caverns, *Health Phys.*, 31: 139-145. (First communicated in draft form in June 1975.)

Yarborough, Keith A., et al., 1976, *Investigation of Radiation Produced by Radon and Thoron in Natural Caves Administered by the National Park Service*, Proceedings of First Conference on Scientific Research in the National Parks.

Yarborough, Keith A., 1977, *Measurements of Seasonal and Daily Radon Daughter Concentration Fluctuations in National Park*

Service Caves, Proceedings of Radon Workshop at Health and Safety Laboratory.

Yarborough, Keith A., 1977, *Airborne Alpha Radiation in Natural Caves Administered by National Park Service*, Proceedings of National Cave Management Symposium.

DISCUSSION

Wilkening: I wish to compliment Keith Yarborough and the National Park Service on all the data they have accumulated on radiation in caves in a relatively short time. Has radon versus radon daughter information been obtained for caves other than for Carlsbad Caverns?

Yarborough: Yes, radon daughter and radon data are presently being collected at Mammoth Cave (the Snowball Room) in Kentucky. Also, inside and outside barometric pressure temperature, relative humidity, and evaporation rates are being observed and recorded. The radon-gas monitor is a continuous recording device specially prepared by the U. S. Bureau of Mines, Special Studies Group, Denver Mining Research Center (Mr. Robert Droullard). The radon daughters are measured by Kusnetz grab sampling and occasional Tsivoglov measurements too.

Distribution of Natural Radioactive Isotope Concentrations and Emanation Factors Measured on Concrete and Brick Samples Produced in Hungary

Á. TÓTH,* I. FEHÉR,† S. NOVOTNY LAKATOS,* L. KOSZORUS,‡ and B. KESZTHELYI¶
*Ore Mining Co. of Mecsek, Medical Center, Pécs; †Central Research Institute for Physics, Budapest; ‡Medical University, Biophysical Institute, Pécs; ¶Spa Hospital, Harkány

ABSTRACT

Natural radioactive isotope concentrations and emanation factors were measured on concrete and brick samples produced in different parts of Hungary. The natural activity parameters measured on samples produced in a given factory within a period of 1 to 2 years show normal distribution at a confidence level of 0.05 in 95% of the cases. Samples received at different times from all the building factories under investigation (mixed distributions) showed about half normal and half lognormal distributions of natural activity parameters at a confidence level of 0.05.

Calculating with the arithmetical means obtained for each of the natural activities substituted into simple models, it was found that the radon and thoron activity is expected to increase by about 25% and the exposure from external radiation to decrease by a factor of 2.3 in the new prefabricated apartments made of concrete as compared with the conventional apartments with brick walls and concrete ceilings. The data obtained from the measurements were used to establish reference levels for the radiological grading of concrete and brick produced in Hungary.

A considerable contribution to the natural radiation exposure of the population is due to radiation from building materials. For this reason it is important to know the concentration and frequency distribution of natural radioelements in building materials. If the type and parameters of the activity distribution are known, the building material can be radiologically graded before use and an increase in the exposure of the population to natural radiation can be avoided.

The frequency distribution of radioelements in rocks is, in general, of the lognormal type (Ahrens, 1965). The type of distribution appropriate for building materials has not yet been published.

For a reliable analysis, a possibly homogeneous group of samples has to be found to establish the mean value and the standard deviation that are the characteristics of a homogeneous group of samples. Homogeneous samples are obtained if samples are taken from the same producer for a long period or if they are taken from different producers over the same period (Waite and Bramson, 1976).

Concrete and brick are the most frequently used building materials in Hungary. Concrete and brick samples collected from different parts of Hungary were studied to establish the ^{232}Th, ^{226}Ra, emanating (or effective) ^{226}Ra, and ^{40}K activity concentrations, as well as the emanation factor K_{Rn} for radon and the types and parameters of the frequency distributions of these data.

The obtained results have been used not only to estimate the gamma dose rate and the air activity to be expected in apartments built of brick and/or concrete but also to estimate the expected exposure to gonads and respiratory organs—thus a radiological grading of building materials could be made before their use.

METHODS

The radon gas emanation from concrete and brick samples (i.e., the so-called "effective" radium content) was assessed on the original form of the building material by scintillation counter (Tóth and Fehér, 1976a). The ^{232}Th, ^{226}Ra, and ^{40}K activities were determined from pulverized samples by gamma spectrometry (Tóth, Beleznay, and Pauka, 1975; Tóth and Fehér, 1976b), which differed from the previously reported measurements in that the evaluation covered not three but the following five ranges of energy:

0.82 to 1.06 MeV, ^{228}Ac, characteristic of ^{228}Ra
2.48 to 2.76 MeV, ^{208}Tl, characteristic of ^{228}Th
1.06 to 1.32 MeV, ^{214}Bi, characteristic of ^{226}Ra
1.34 to 1.58 MeV, ^{40}K
1.64 to 1.88 MeV, ^{214}Bi, characteristic of ^{226}Ra

The values of the concentration ratio ^{228}Ra/^{228}Th in different samples and their standard deviations are shown in Table 1. The data in Table 1 shows that secular equilibrium has been established between the elements of the thorium series so that the arithmetic

TABLE 1

The $^{228}Ra/^{228}Th$ Activity Ratios in Concrete and Brick Samples

Building material	Number of samples, n	$^{228}Ra/^{228}Th$ ratios		
		Arithmetical mean	Standard deviation, s	Deviation of the arithmetical mean, $s/(n)^{1/2}$
Concrete	106	1.02	0.15	0.01
Brick	208	0.99	0.05	0.004

means of the ^{228}Ra and ^{228}Th concentrations can be taken to be equivalent to the ^{232}Th concentration. A similarly good agreement was found between the ^{226}Ra concentrations measured in the two ranges of energy.

INSTRUMENTS

Radon measurements were made previously with 500-cm^3 ionization chambers and vibrating-reed electrometers. Recently 1000-cm^3 volume scintillation counters have been used (Tóth and Fehér, 1976a). The pulverized samples were measured by an 8- by 4-in. NaI/Tl crystal and a 512 channel pulse height analyzer and with the low background shielding of the HY 3.2 whole body counter. Details of the measurement have been already reported (Tóth, Beleznay, and Pauka, 1975; Tóth and Fehér, 1976b).

ERRORS

The error due to counting statistics of radon measurement was calculated by using the correction suggested by Lucas and Woodward (1964). Accordingly, the error due to counting statistics, evaluated in the usual way, had to be multiplied by 1.22 or 1.28 under the given experimental conditions. The radon emanation from each building material was measured at least twice (thus under different atmospheric pressures) to reduce the error due to the atmospheric pressure dependence of radon emanation. The arithmetical mean of the thus measured two radon activities was taken to be the radon activity of the given sample. The average of the statistical errors of the two measurements was taken to be the statistical error of the measured radon activity. The error due to counting statistics of the

radon measurements was 18% at the maximum and 5% on the average. The statistical error of the measured gamma spectrum was calculated in the same way as previously described (Tóth, Beleznay, and Pauka, 1975) in both the high and the low energy range. For a given element the mean value of the two statistical errors was taken to be the net statistical error. The net statistical errors of the ^{232}Th, ^{226}Ra, and ^{40}K measurements by gamma spectrometry were not more than 6%, 9%, and 3%, respectively, even for the concretes of lowest activity.

NORMALITY TEST

The normality of the relative frequency distributions of the data (concentration, emanation factor) obtained on building material was checked by use of the Kolmogorov—Smirnov test as modified by Lilliefors (1967), taking the critical values $D_{0.05}$ given for different numbers of samples and for the significance level $\alpha = 0.05$.

RESULTS

Figure 1 shows the territorial distribution of the building-material factories from which samples were systematically obtained for analysis over a year. Each of the 28 building-material factories sent in at least four samples. Each sample was analyzed to determine the ^{232}Th, ^{226}Ra, ^{40}K, and ^{226}Ra concentrations and the K_{Rn} emanation factor. Thus $28 \times 5 = 140$ minor distributions that were obtained, and the normality of each was established by use of the previously mentioned test.

The shape of the distribution was found to be normal in 133 cases ($n = 992$). Three distributions ($n = 14$, 9, and 10) were found to be lognormal, while four distributions ($n = 10$, 5, 4, and 4) were neither normal nor lognormal at the given confidence level.

The radioisotope concentrations and emanation factor distributions measured on the concrete and brick samples are shown in Figs. 2 and 3. The parameters characterizing the distributions are summarized in Table 2.

The thorium and potassium concentrations in concrete and the radium and effective radium concentrations and the emanation factor in bricks showed distributions that can be divided into two types. Samples showing higher than normal concentrations were, in every case, of a small number between 4 and 18. The types of distributions obtained in these cases are shown in Table 2. The effective radium content as evaluated from the emanation factor

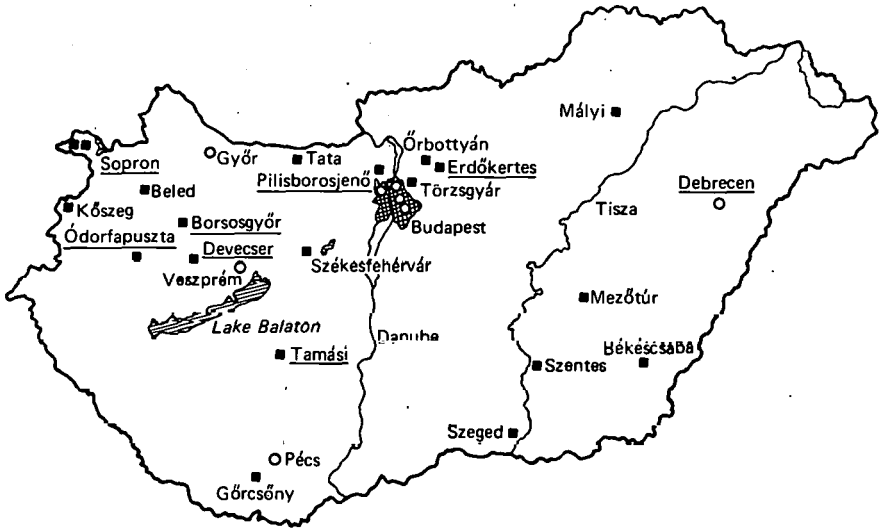


Fig. 1 Map of Hungary showing locations of the building-material factories. ○, concrete; ■, brick. Underscored names are for factories whose samples contained at least 20% more of either thorium, radium, or potassium than the already established national average.

cannot be correctly assessed because the latter could have been influenced by a change in atmospheric pressure. The thorium and potassium concentrations measured on concrete ($n = 4, 8$) which were found to exceed the average values by about 45% were obtained on samples sent in from one particular factory. The 18 radium values that proved to be significantly higher than the national average assessed to date on bricks were obtained on samples sent in from the brick factories in the western part of the country.

CONCLUSIONS

The concentrations of natural radioisotopes and the emanation coefficients show normal distributions at a confidence level of 0.05 in specimens produced within 1 to 2 years in any given building-material factory. The normal distribution can be attributed to the probably similar geological origin of the samples during the period of 1 to 2 years covered by the investigation.

The concrete and brick samples received from 28 building-material factories show partly lognormal and partly (and unexpectedly) normal distributions of the natural activity concentrations and of the emanation factors. In some cases, both types of

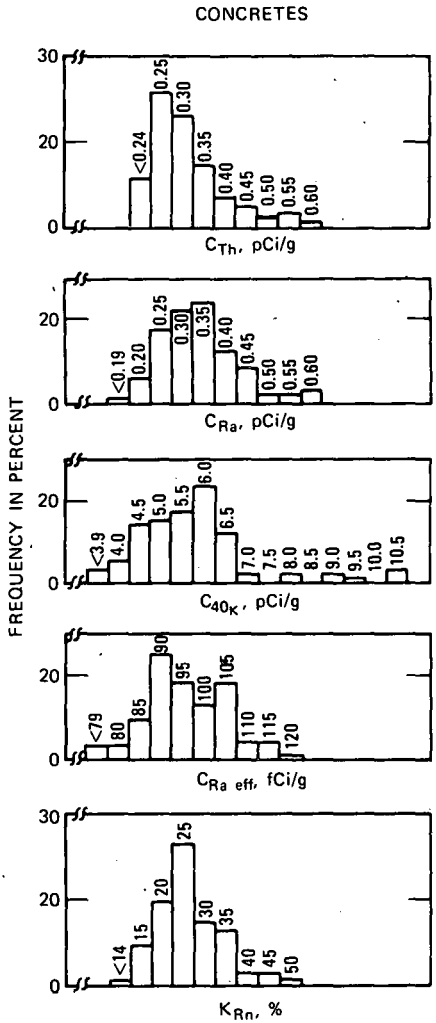


Fig. 2 Frequency distributions of natural radioactivity parameters in concrete samples.

distributions can be identified. We can attribute this to the fact that the geological provenances of the basic raw materials for building materials show natural activity concentration distributions of a similarity such that the normal distributions obtained for individual factories seem to hold for the whole country. This assumption is supported by the observation that the readily identifiable second type of distribution found in some cases in the range of higher than

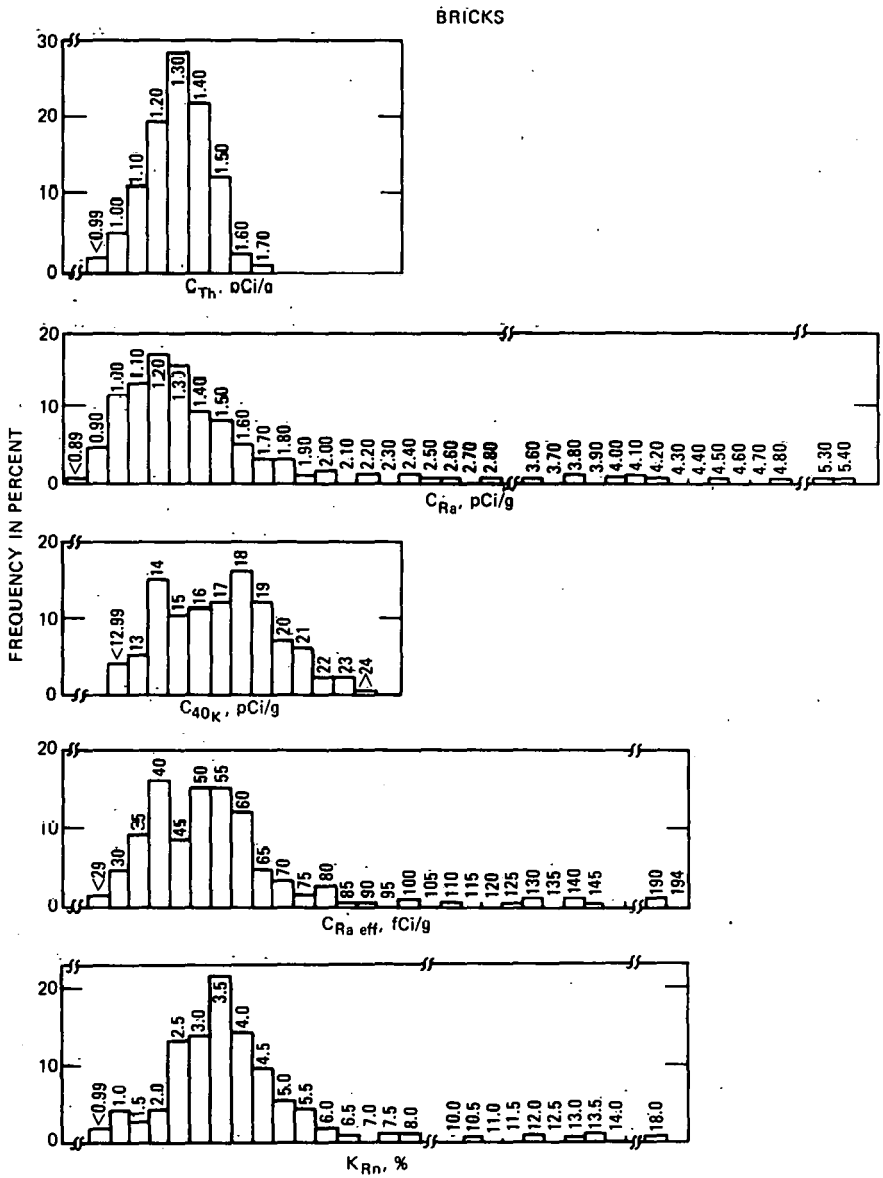


Fig. 3 Frequency distributions of natural radioactivity parameters in bricks.

TABLE 2

Natural Activities Measured on Concrete and Brick Samples

Parameter, x	Unit	Number of samples, n	Extreme values		Average, normal or lognormal, x	Standard deviation, %, δ	Type of distribution at 0.05 significance level
			$x_{min.}$	$x_{max.}$			
Building Material, Concrete							
^{232}Th conc.	pCi/g	91	0.2	0.6	0.3	21	Lognormal
		4	0.6	0.64	0.6	5	Normal
^{226}Ra conc.	pCi/g	95	0.2	0.6	0.4	27	Lognormal
^{40}K conc.	pCi/g	87	4	8	6	15	Normal
		8	8	11	10	11	Normal
$^{226}_{eff}$Ra conc.	fCi/g	116	70	130	100	10	Normal
Emanation coeff.	%	94	15	60	30	27	Lognormal
Building Material, Brick							
^{232}Th conc.	pCi/g	176	0.9	1.8	1.3	11	Normal
^{226}Ra conc.	pCi/g	158	0.8	2.2	1.3	19	Lognormal
		18	2.2	5.4	3.6	29	Normal
^{40}K conc.	pCi/g	176	12	25	18	16	Lognormal
$^{226}_{eff}$Ra conc.	fCi/g	182	30	120	50	26	Lognormal
		8	120	190	150	24	Lognormal
Emanation coeff.	%	165	1	8	4	33	Normal
		11	8	18	12	29	Normal

usual activity concentrations was always normal and that the samples originated from given factories or regions.

The products of the investigated factories provide two-thirds of the country's building materials and can be regarded more or less as representative. In Table 3 the average of concentrations and emana-

TABLE 3

Average Values of Natural Activity Concentrations and Emanation Factors of Concrete and Brick as Weighted by the Relative Production Factors and Upper Limits Suggested for Grading Before Use

		Concrete		Brick	
Isotopes	Units	Weighted average	Upper limit	Weighted average	Upper limit
^{232}Th	pCi/g	0.30	0.50	1.3	1.6
^{226}Ra	pCi/g	0.36	0.60	1.5	4.0
^{40}K	pCi/g	5.5	10	15	22
$^{226}_{eff}Ra$	fCi/g	100	110	50	110
K_{Rn}	%	28	40	3.6	8

tion factors, as weighted by the yearly production factor, are given for the total distribution. The weighted averages agree with the mean value within the error, even in the case of lognormal distributions. By use of these averages, the radon and thoron concentrations and the dose rates in air to be expected in apartments were calculated from simple models (Tóth, 1977a; 1977b) as *equilibrium radon content*

$$C^e_{Rn} \approx 2.47 \times C_{Ra} \times K_{Rn} \times k^{-1} \frac{pCi}{liter}$$

equilibrium thoron content

$$C^e_{Tn} \approx 5.15 \times C_{Th} \times K_{Tn} \frac{pCi}{liter}$$

and *exposure rate*

$$D\dot{e} \approx 20\,(1 - K_{Rn})C_{Ra} + 32\,(1 - K_{Th})C_{Tn} + 2.4\,C_K \text{ mR/year}$$

where C_{Ra}, C_{Th}, and C_K are the ^{226}Ra, ^{232}Th, and ^{40}K concentrations, respectively, given in picocuries per gram units; k is

the air exchange rate in $hour^{-1}$, and K_{Rn} and K_{Tn} are the emanation coefficients.

Using the assumptions of the models and the arithmetical means of Table 3, we calculated the radon and thoron contents and the exposure rate for the old (brick and concrete) and for the new (only concrete) types of apartments.* These data and the ratios of old to new are listed for some parameters in Table 4.

Table 4 shows that, in the new prefabricated apartments made of concrete, the average radon—thoron concentration is expected to be higher by about 25%, whereas the dose rate from external radiation should be lower by a factor of 2.3 as compared with the conventional (brick and concrete) apartments, if all other conditions are equal.

TABLE 4

Activity Parameters of Individual Apartments and Brick and Concrete to Concrete Parameter Ratios

Parameter	Unit	Brick and concrete, old type	Concrete, new type	Brick and concrete / Concrete
Radon-equilibrium concentration	pCi/liter	1.6	2.0	0.80
Thoron-equilibrium concentration	pCi/liter	0.35	0.43	0.81
Exposure rate in air	mR/year	58	25	2.3

There has of late been an increase in the amount of concrete used to build apartments. The percentage of use has changed from 8.1% (concrete) in 1970 to 15% in 1977. Thus, in our country, the exposure of the population to natural ionizing radiation is expected to decrease if the fraction of apartments made of concrete increases.

Building material should be chosen to prevent an increase in the natural radiation exposure of the population unless the increase is strongly supported by a risk—benefit analysis. Therefore the natural

*The conventionally built room situated on the first floor is built with 14.9 tons of bricks and 21.1 tons of concrete. The air exchange rate of $k = 0.127\ h^{-1}$, $K_{Rn} = K_{Tn}$, etc. For the apartment built from prefabricated concrete, the same equations were used as for the conventionally built room.

activity concentration of the building material to be used should not exceed the present average value (given in Table 3). To facilitate the radiological grading of building materials, we think it expedient to establish an upper limit. It is suggested that this upper limit could be the concentrations and emanation factor, below which 95% of the present values lie. The values for concrete and brick in Hungary are given in Table 3. The values of the suggested upper limit are only approximate and further measurements on more samples with a more accurate determination of the distributions are expected to give more precise values for the upper limit.

REFERENCES

Ahrens, L. H., 1965, *Distribution of the Elements in Our Planet*, p. 74, McGraw-Hill Book Co., New York.

Lilliefors, H. W., 1967, On the Kolmogorov—Smirnov Test for Normality with Mean and Variance Unknown, *J. Am. Stat. Assoc.*, 62: 399-402.

Lucas, H. F., and D. A. Woodward, 1964, Effect of Long Decay Chains on the Counting Statistics in the Analysis of Radium^{224} and Radon^{222}, *J. Appl. Phys.*, 35(2): 452-456.

Tóth, Á., 1977a, Calculations of the Radon and Thoron Concentrations in the Air of Dwelling Rooms and Comparisons with Measured Data (in Hungarian), *Magy. Fiz. Foly.*, 25(2): 95-103.

——, 1977b, Estimation of the Gamma Dose Rate in Dwelling Rooms and Comparisons Between the Calculated and Measured Data (in Hungarian), *Magy. Fiz. Foly.*, 25(2): 105-111.

——, E. Beleznay, and I. Pauka, 1975, Gamma-Spectrometric Study of Natural Radioactivity of Power Station Fly Ashes and Ash-Cement Mixtures (in Hungarian), *Izotóptechnika* (Budapest), 18: 397-409.

——, and I. Fehér, 1976a, *Effective ^{226}Ra Content of Some Hungarian Building Materials*, Report KFKI-76-8, Hungarian Academy of Sciences, Central Research Institute for Physics, Budapest.

——, and I. Fehér, 1976b, *Gamma Spectrometric Method for Measuring Natural Radioactivity of Building Materials*, Report KFKI-76-80.

Waite, D. A., and P. E. Bramson, 1976, Interpretation of Near-Background Environmental Surveillance Data by Distribution Analysis, in *Biological and Environmental Effects of Low-Level Radiation*, Symposium Proceedings, Chicago, 1975, pp. 291-302, STI/PUB/409, International Atomic Energy Agency, Vienna.

Emanating Power of Radon-222 Measured in Building Materials

J. PEŃSKO, Z. STPICZYŃSKA, and K. BLATON-ALBICKA
Radiation Protection Department, Institute of Nuclear Research,
Swierk-Otwock, Poland

ABSTRACT

It is estimated that the application of a great amount of industrial wastes in dwelling-house technology could create a considerable hazard to the Polish population due to lung cancer. Therefore great attention has been paid to the problem of radon emanation from various commonly used building materials. The principle and development of a method of radon-222 (^{222}Rn) emanation coefficient measurements are described. The results obtained for traditional building materials as well as for the modern ones containing considerable amounts of industrial wastes are presented.

The emanation power of fly ash and slag is very low (average, 0.62%) and nearly identical for both materials. However, because of the relatively high concentrations of radium-226 (^{226}Ra) in these materials, the ^{222}Rn concentration in the atmospheres of dwelling houses can achieve a value more than one order of magnitude higher in comparison with out-of-door concentrations.

The emanation power of by-product gypsum is very high for phosphorite rocks used as raw material (more than 21%). This property together with the high concentration of ^{226}Ra can create a relatively high hazard for a population living in a great number of dwelling houses constructed from this material.

Natural radioactive elements occurring in building materials, the traditional ones as well as the modern materials containing industrial wastes, create a considerable health hazard. In addition to other trace elements, these materials contain uranium and thorium with their daughter products as well as potassium-40, all of which are main sources of gamma exposure. Materials containing radium-226 create an alpha-radiation hazard for the human respiratory system because of the airborne progeny of its daughter radon-222.

Ionizing radiation levels indoors are at present determined much less accurately than those out of doors. The results obtained earlier (Peńsko and Bysiek, 1963) and in the course of this work have shown that some of the building materials commonly used in Poland, such as boiler and blast-furnace slags, fly ash, and by-product gypsum, contain appreciable amounts of natural radioactive isotopes. These waste materials are produced in great quantities by power plants and the chemical and metallurgical industry. Table 1 presents the ranges of radioactivity concentration measured for some building materials

TABLE 1

Concentration of ^{40}K, ^{226}Ra, and ^{228}Th in Typical Building Materials Used in Poland

Material	Number of samples	Range of concentration, pCi/g		
		^{40}K	^{226}Ra	^{228}Th
Fly ash	106	10.4—48.0	1.7—16.5	0.9—8.7
Slag	42	6.1—60.2	0.5—12.4	0.6—16.0
By-product gypsum	4	0.3—3.2	0.7—19.9	0.3—1.2
Red brick	3	19.1—25.5	0.5—0.6	0.6—1.2
Silicon brick	3	3.5—7.5	0.2—0.4	<0.1—0.2
Cement	4	5.1—8.2	0.2—0.7	0.3—1.8
Soil	5	0.8—7.6	0.1—0.5	<0.1—0.4

commonly used in our country. Similar data obtained for typical soil samples are included in the table for comparison.

Theoretically it is possible to compute the gamma-radiation level as well as the radon concentration in the air inside any building on the basis of various known environmental factors and radionuclide concentrations. However, the parameters that should be taken into account are frequently only roughly estimated and such calculations do not lead to accurate results. Therefore the need for direct measurements of ionizing radiation levels has been recognized; extensive measurements have been performed in several countries and are still continuing. Representative data obtained up to now were recently published in a UN report (United Nations Scientific Committee on the Effects of Atomic Radiation, 1977). Such measurements, however, are still not numerous enough. Even fewer data are available on the concentration of radon and its progeny in the atmospheres of dwelling houses.

The gamma-radiation dose rate and the concentration of ^{222}Rn were measured in the atmospheres of 97 rooms in new blocks of flats constructed in Poland of concrete, slag concrete, light silica concrete, gravel concrete, aglophorith ballast, and bricks (Pensko, Mamont, and Wardaszko, 1969). This study indicated that ^{222}Rn concentrations in the atmospheres of unventilated rooms are always higher than those out of doors and depend mainly on the kind of building material used. The highest ^{222}Rn concentrations were found inside buildings made of slag concrete.

Recently some investigations were undertaken in Poland which served as a basis for the evaluation of the additional annual doses of natural gamma radiation received indoors by the Polish population. These doses are of the order of 40 mrads as indicated in Table 2 (Pensko and Geisler, 1978). Similarly, in Table 3 are presented the

TABLE 2

Mean Values of Additional Indoor Gamma-Ray Doses in the Air and to Important Body Organs

Building material	Dose rate, mrads/year			
	Air	Soft tissue	Bone marrow	Gonads
Concrete	20	19	14	16
Brick	38	36	27	31
Prefabricated	41	39	29	34

TABLE 3

Mean Values of ^{222}Rn Concentrations in the Air Measured Outdoors and Inside Unventilated Dwelling Houses in Poland and Corresponding Yearly Doses to the Critical Tissue of the Respiratory System

Building material	Number of measurements	Average concentration, pCi/m^3		Average dose rate, mrems/year
		Indoors*	Outdoors	
Concrete	136	323	100	681
Brick	6	85	100	178
Prefabricated	20	418	100	879

*Additional indoor concentration obtained after subtracting 100 pCi/m^3, i.e., average outdoor concentration.

results of ^{222}Rn concentration measurements in the atmospheres of unventilated dwelling rooms as well as the results of evaluation of additional annual alpha-radiation doses to the critical tissues of the respiratory system (basal cells of the bronchial epithelium). As shown in Table 3, these doses are found to be in general not greater than 880 mrems.

On the basis of the above dosimetric data as well as of the demographic and forecasting data, the numbers of severe genetic effects and cancer deaths caused by additional radiation doses inside houses were assessed for the population of Poland for the period 1951—2010 (Pensko and Geisler, 1978). It is estimated that, owing to the increasing contribution from buildings constructed of materials containing industrial wastes to the entire building development, the additional somatic effects in six consecutive decades will amount to approximately 31,222 cases of cancer death (of that number about 26,294 deaths will be caused by lung cancer).

Severe genetic effects caused by additional doses of ionizing radiation absorbed by parents indoors will be manifest in about 260 cases in the first generation of their offspring and by about 7500 cases in following generations. Such a number of cases is not alarming in our opinion. However, the relatively great number of lung carcinomata is self-evident. Therefore we decided to pay more attention in our further investigations to the problem of radon diffusion from various commonly used building materials.

SAMPLE PREPARATION AND LABORATORY TECHNIQUE

The samples of typical building materials were supplied by the Institute of Building Technology in Warsaw. The samples of by-product gypsum, fly ash, and slag were supplied by chemical and power industries, producers of these waste products. Soil samples were taken in the surroundings of Warsaw.

All ash samples were taken from each funnel of electro-filters six times daily during the optimal load of an electric generator. Slag samples were taken similarly from the slag tank. The measurements were performed separately for averaged samples taken from three areas of fly-ash fall at 10 large coal-fueled power plants. For the purpose of comparing results under similar conditions, all samples were granulated and dried at 105°C.

Each sample of the material investigated was placed in an airtight glass container 22 cm in diameter and 6000 cm^3 in volume (Fig. 1) and allowed to de-emanate for a minimum of 4 days. Radon diffusing from the sample into the air inside the container became

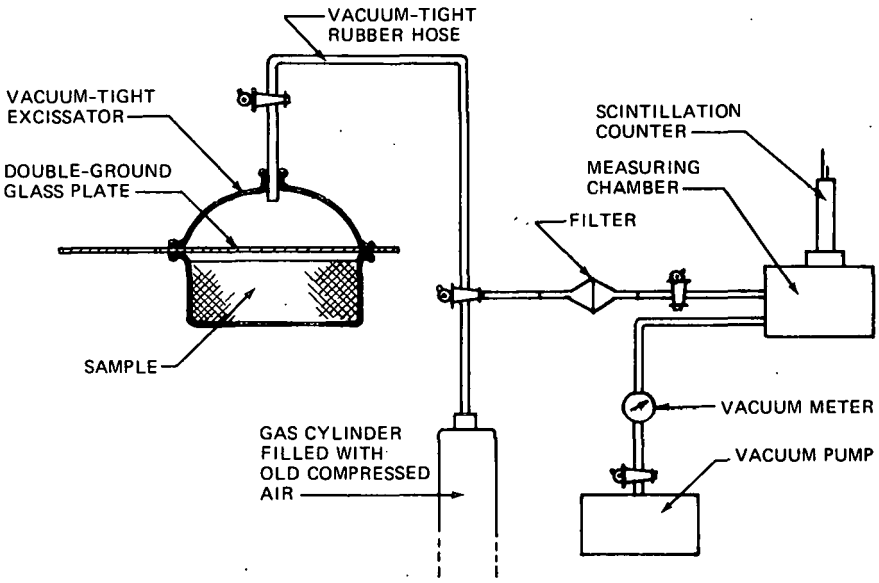


Fig. 1 General schematic of measuring equipment.

uniformly distributed in the air volume through the gap in the double-ground glass plate that divided the container into two parts. Using this plate made it possible to separate the air radon from the sample radon while transferring the air sample into the measuring chamber by a vacuum technique.

Radon was measured in an electrostatically operated cylindrical 3-liter steel chamber, fitted with a collecting electrode, which simultaneously served as an alpha-radiation detector of suitable geometry (Wardaszko, 1966). The alpha-ray scintillations of ^{222}Rn daughter products were counted. The sensitivity of our typical measuring system was better than 50 pCi/m^3, i.e., about two orders of magnitude lower than for typical measurements. The sensitivity could be improved if necessary.

The countings were registered for 2 hr and began 2 hr after transferring radon into the chamber when equilibrium between ^{222}Rn and its short-lived daughters was achieved. The total efficiency of the method, determined by measuring the radon from a standard solution of ^{226}Ra, was found to be 1.8×10^{-2} cps/pCi.

All samples were analyzed for ^{40}K, ^{226}Ra, and ^{228}Th by gamma-ray spectrometry as described in an earlier paper (Pełnsko and Stpiczyńska, 1977).

RESULTS

The emanation coefficients of building material and soil samples were determined for thick samples, the reasonable thickness of which was found to be approximately 9 cm. This was assessed by measuring the diffusion factor, which for the fly ash amounted to 8.5×10^{-6} cm^2/sec.

The theoretical description of radon migration across a porous medium has been extensively discussed in the literature (e.g., Tanner, 1964; Sjerdjukowa and Kapitanow, 1975). We used the simplest model according to which a radioactive gas of decay constant λ, of concentration C at a distance Z from a plane source in which the concentration is C_0, diffuses in the Z direction through an infinite, porous half-space of diffusion coefficient D according to the following equation:

$$C = C_0 \exp\left[-Z\left(\frac{\lambda}{D}\right)^{1/2}\right]$$

For the condition $C/C_0 \leqslant 0.01$, $Z_{max} = 4.6(D/\lambda)^{1/2}$. Estimated values of D and Z_{max} (approximately 9 cm) for fly ash turned out to be very small compared with those for soil, i.e., 5×10^{-2} cm^2/sec and 160 cm, respectively (Tanner, 1964). Radium-226 concentrations and emanation coefficients estimated for several building materials commonly used in Poland are presented in Table 4.

CONCLUSIONS

These preliminary results make it possible to formulate the following conclusions:

1. The emanation power of fly ash and of slag is very low and nearly identical for both materials. The emanation coefficients do not exceed 1.6%. However, because of the relatively high concentrations of ^{226}Ra in these materials, the ^{222}Rn concentration (with decay products) in the atmospheres of dwelling houses can achieve the range of 2000 to 4000 pCi/m^3, i.e., values more than one order of magnitude higher in comparison with out-of-door concentrations.

2. The emanation power of by-product gypsum for some samples (phosphorites) is very high. The emanation coefficient in this instance exceeds 21%. The high concentration of ^{226}Ra in this by-product as well as the high emanation power of ^{222}Rn can create a relatively high hazard for a population living in great numbers of dwellings constructed from this material.

3. The ^{226}Ra concentration and emanation power of other building materials depend mainly on the amount of fly ash and slag admixtures used as aggregates in the production of cement, brick, and prefabricated materials.

TABLE 4

Emanation Coefficients of Building Materials

Building material	Number of samples	^{226}Ra concentration, pCi/g		Emanation coefficient, %		Specification
		Range	Mean	Range	Mean	
Fly ash	33	1.7—3.9	2.6	0.20—1.16	0.54	From 10 power plants
Slag	11	1.0—3.6	1.8	0.24—1.53	0.70	From 10 power plants
By-product gypsum			0.7		3.5	Kola (apatite)
			18.9		12.9	Florida (phosphorite)
	4	0.7—20	19.9	3.5—21.3	21.3	Morocco (phosphorite)
			15.8		19.7	Togo (phosphorite)
Red brick			0.5		2.2	Old brick (1928)
	3	0.5	0.5	2.2—5.1	2.3	
			0.5		5.1	
Silicon brick			0.2		16.3	
	3	<0.2—0.4	0.2	0.8—16.3	3.2	
			0.4		0.8	
Cement			<0.25		>5	Warszawa "350"
			0.65		4.1	Górażdże "350"
	4	<0.25—0.7	0.7	0.8—8.5	0.8	Chełm
			0.5		8.5	Małogoszcz
Soil	5	0.1—0.5	0.3	12.1—50.1	28.9	Sandy soil

REFERENCES

Pensko, J., and M. Bysiek, 1963, *The Gamma Radioactivity of Building Materials for the Construction of Low Background Laboratories*, Report CLOR-20, Central Laboratory for Radiological Protection, Warsaw.

——, and J. Geisler, 1978, *Analysis of Potential Hazard of Population in Poland Due to Ionizing Radiation in Dwelling Houses*, Report of Medical Physics Committee to the Polish Academy of Sciences, Warsaw, in press.

——, K. Mamont, and T. Wardaszko, 1969, Measurements of Ionizing Radiation Inside Blocks of Flats in Poland, USAEC-tr-7027/4, UC-34, TT 69-50012/4, translated from *Nukleonika*, 14(4): 415-424, NTIS.

——, and Z. Stpiczyńska, 1977, The Method and Preliminary Results of Measurements of the Natural Radioactivity in Power-Station Fly-Ash and Slags, *Nukleonika*, 22: 459-472.

Sjerdjukowa, A. S., and J. T. Kapitanow, 1975, *Izotopy Radona*, 2nd ed., Atomizdat, Moscow.

Tanner, A. B., 1964, Radon Migration in the Ground, in *The Natural Radiation Environment*, J. A. S. Adams and W. M. Lowder (Eds.), pp. 161-190, The University of Chicago Press, Chicago.

United Nations Scientific Committee on the Effects of Atomic Radiation, 1977, *Sources and Effects of Ionizing Radiation*, Report to the General Assembly with Annexes, United Nations, New York.

Wardaszko, T., 1966, *Measurement of ^{222}Rn Concentration in Air by Means of Electrostatic Precipitation of Its Daughter Products*, Report CLOR-47/D, Central Laboratory for Radiological Protection, Warsaw.

Outdoor and Indoor Radon Concentrations in Air in the Territory of Slovenia, Yugoslavia

I. KOBAL, M. ŠKOFLJANEC, and J. KRISTAN
J. Stefan Institute, University of Ljubljana, Ljubljana, Yugoslavia

ABSTRACT

In connection with the investment in uranium mining and milling facilities at Žirovski vrh (northwestern part of Slovenia), some time ago field measurements of radon concentrations in air in Slovenia were started. Emphasis was given to the uranium deposit area, but some other reference sites were also selected. Radon determinations were accompanied by measurement of the meteorological parameters, i.e., wind speed and direction, humidity, temperature, and atmospheric pressure. At representative sites, diurnal variations in concentration were followed. Radon concentrations were usually found to be below 1 pCi/liter (or 37 Bq/m^3), but in the vicinity of mine tailings and in houses built of stone from Žirovski vrh, this level was exceeded and concentrations up to 20 pCi/liter were found.

This paper presents the results of measurements of ambient outdoor and indoor concentrations of radon (^{222}Rn) for 43 locations throughout this region of low-grade uranium ore deposits and its wider surroundings.

Prospective mining in this region started some years ago and milling facilities are in preparation. Rising concern for the environment demands measurements as accurate as possible of the present status of the air with regard to radioactive contamination, both particulate and gaseous. To be able to evaluate the environmental impact of the mine, we need a better definition of background levels and more thorough evaluations.

In the vicinity of the explorative uranium mine at Žirovski vrh, there are a few sources of radon (apart from natural emanation from the ground) such as the mine exhaust air and deposits of the

excavated material. However, at the present stage the contamination of air by radon may be considered to be of a local character. Thus the results in this report, except those in Fig. 1, represent natural background concentrations.

The region, not densely populated, bears all the characteristics of wooded subalpine areas, with steep hills and scattered farms. The geological pattern changes from alluvial sediments in the valleys to covered Permian sandstone and conglomerate on the slopes. Older houses are built mostly of stone from the environment, so we may assume an increased radon concentration in such dwellings (Eadie, 1975; Toth and Feher, 1976).

MEASUREMENTS

The low radon concentrations in air were measured by the alpha-scintillation method, which is described elsewhere (Kobal, Kristan, and Škofljanec, 1978). In Fig. 2 the geographical positions of coded sampling places are given. The results of measurements are given in Table 1, with accompanying meteorological data. Sampling was done between 0900 and 1600 at a height of 25 cm above the ground. (Exceptions only at J. Stefan Institute.)

On the deposits of mined material, about 200 m from the main mine entrance, the diurnal variation of radon concentration was followed and is presented in Fig. 1. Air was sampled at two different heights, namely 10 and 500 cm above the ground. For a reference the same measurements were performed in the park at the J. Stefan Institute; the results are charted in Fig. 3.

For indoor measurements several old houses made of stone from the uranium deposit area were selected. Radon concentrations in the house and outdoors were always determined simultaneously (1 hour's difference). Results are shown in Table 2.

RESULTS AND CONCLUSIONS

It is obvious from Table 1 that ambient outdoor radon concentrations found at some selected locations in the uranium deposits area at Žirovski vrh are relatively low when compared with values for other uranium ore regions (Eadie et al., 1976). They are not so increased when compared with values obtained in Ljubljana in the park at the J. Stefan Institute. We may consider them as natural background. Thus we still have time to screen background radon concentrations in this region before the beginning of uranium milling

(Text continues on page 1420.)

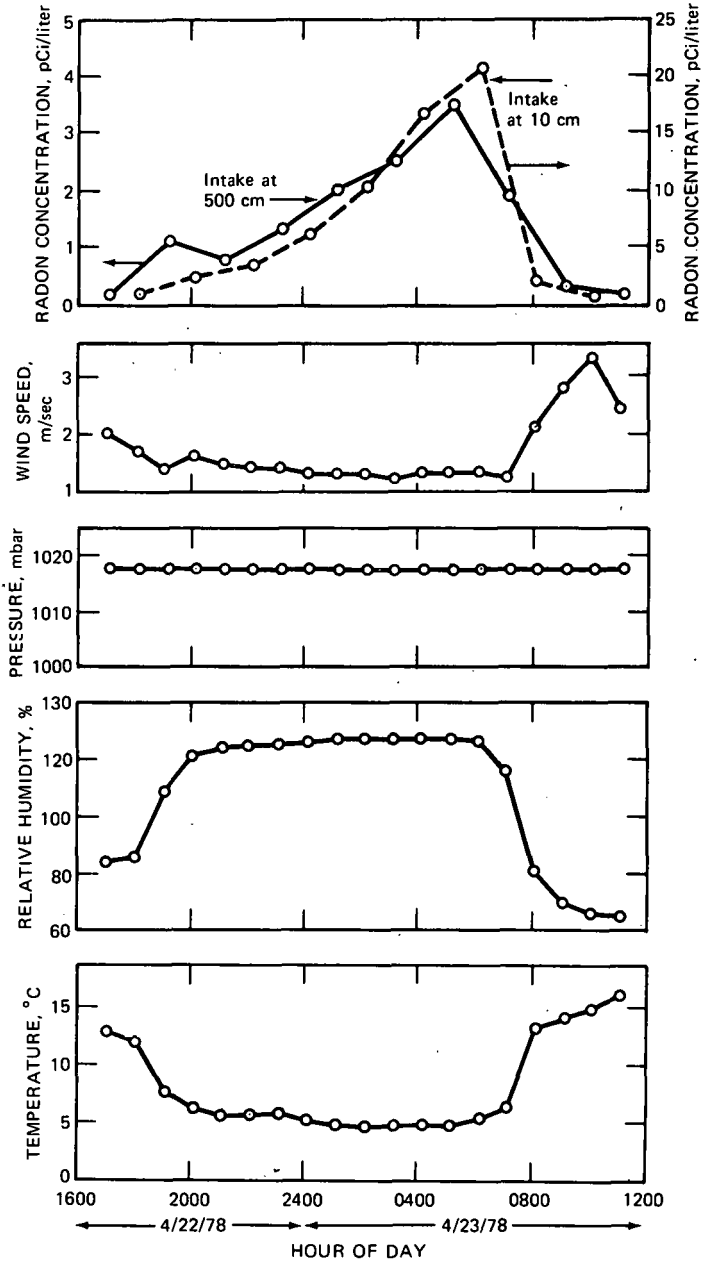


Fig. 1 Diurnal variation in radon concentration and concurrent meteorological parameters at the mined material deposit.

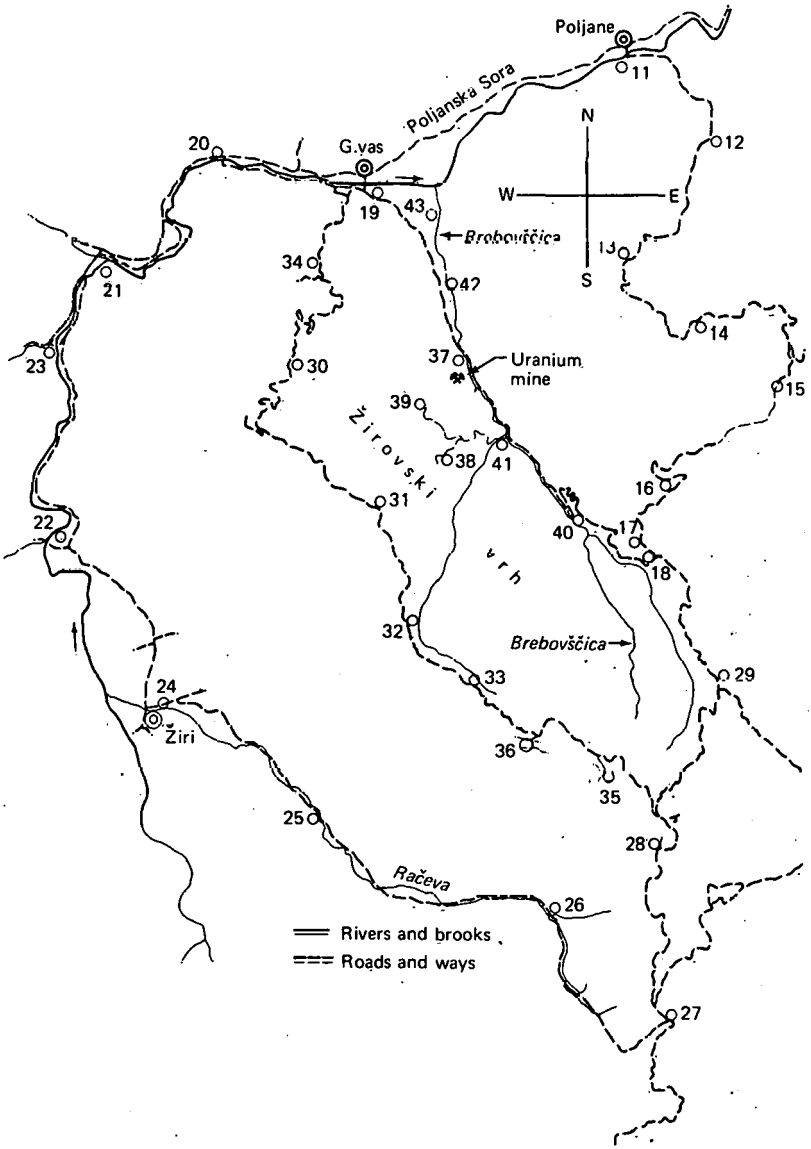


Fig. 2 Geographical positions of coded sampling places.

TABLE 1

Radon Concentrations and Meteorological Parameters in Air over the Mining District

Coded sampling station number	Radon concentration, pCi/liter	Temperature, °C	Pressure, mbar	Relative humidity, %	Average wind speed, m/sec	Date of sampling	Time of sampling, hr
11	0.09	18	1008	45	1.9	3/30/78	1300
11	0.08	14	1004	61	1.1	4/01/78	0900
12	0.06	17	1000	44	0.9	3/30/78	1400
13	0.13	16	989	47	0.8	3/31/78	0900
14	0.08	15	978	44	1.9	3/31/78	1000
15	0.08	13	966	46	1.9	3/31/78	1200
16	0.10	17	978	46	1.6	3/31/78	1300
17	0.10	18	981	46	2.5	3/31/78	1400
18	0.08	18	983	46	1.0	3/31/78	1500
19	0.06	15	1002	63	1.8	4/01/78	1000
19	0.09	7	1002	69	2.4	4/08/78	0900
19	0.06	15	1011	50	1.7	4/22/78	1500
20	0.02	17	1001	57	1.3	4/01/78	1100
21	0.08	18	999	55	1.3	4/01/78	1200
22	0.07	19	995	46	0.8	4/01/78	1300
24	0.16	15	991	63	0.3	4/02/78	1000
25	0.05	16	988	56	0.3	4/02/78	1100
26	0.08	14	981	56	0.7	4/02/78	1200
27	0.09	13	971	67	1.6	4/02/78	1300
27	0.12	10	977	76	3.0	4/09/78	1000
28	0.10	16	964	61	1.3	4/02/78	1400
28	0.10	8	969	66	1.6	4/09/78	1000
29	0.20	13	973	61	1.5	4/02/78	1500
29	0.16	13	978	60	2.1	4/09/78	1300
30	0.10	3	966	74	1.1	4/08/78	1000
31	0.10	3	960	80	2.2	4/08/78	1100
32	0.09	7	967	72	1.6	4/08/78	1200
33	0.07	6	962	69	1.3	4/08/78	1300
34	0.09	13	996	61	2.5	4/08/78	1400
35	1.10	7	958	65	2.6	4/09/78	1100
36	0.10	11	958	62	1.4	4/09/78	1200
37	0.09	11	1009	33		4/18/78	1000
37	0.03	18	1010	42		4/22/78	1300
38	0.18	10	993	28		4/18/78	1100
39	0.17	12	990	23		4/18/78	1500
40	0.09	16	1004	40	0.9	4/22/78	1100
41	0.08	14	1009	50	0.4	4/22/78	1200
42	0.07	18	1011	33	1.1	4/22/78	1400
43	0.07	4	1000	50	0.9	4/22/78	1600

(Table continues on next page.)

TABLE 1 (Continued)

Coded sampling station number	Radon concentration, pCi/liter	Temperature, °C	Pressure, mbar	Relative humidity, %	Average wind speed, m/sec	Date of sampling	Time of sampling, hr
IJS*	0.25	21	974	74	0.5	8/02/77	1800
IJS	0.44	13	975	100	0.1	8/02/77	2400
IJS	0.91	10	975	100	0.1	8/03/77	0500
IJS	0.11	24	975	54	0.9	8/03/77	1200
IJS	0.13	15	1015	62	0.2	4/10/78	1200
IJS	0.16	6	1007	68	0.8	4/15/78	1000
IJS	0.07	6	1007	85	0.7	4/15/78	1200
IJS	0.07	5	1007	95	0.8	4/15/78	1400
IJS	0.12	8	1013	60	0.4	4/16/78	0900
IJS	0.08	13	1013	45	0.5	4/16/78	1200
IJS	0.08	16	1013	45	0.5	4/16/78	1300
IJS	0.09	7	1014	74	0.2	4/16/78	1800

*In the park at J. Stefan Institute.

facilities which are expected to be a substantial artificial source of radon contamination.

As expected, the highest value was obtained on the deposits of excavated material, which do not yet contain mill tailings.

It is well known that the diurnal variation in radon concentration can be very high, as much as an order of magnitude (Israelsson, Knudsen, and Ungethum, 1972; Nakatani, 1975; Toth, 1976). This was found in our experiments as presented in Figs. 1 and 3. That means that values in Tables 1 and 2 must be interpreted very carefully, with possible changes, mainly due to wind, taken into account. Having made all measurements between 0900 and 1000, we can expect the radon concentration in Tables 1 and 2 to be much higher during the night, especially at about 0400, when the atmosphere appears to be the most calm (Israelsson, Knudsen, and Ungethum, 1972; Nakatani, 1975). Still, the values can be considered as natural background with no "hot point" with markedly increased value.

It is evident from Table 2, as expected (Eadie, 1975), that air radon concentrations in houses built of stone from the uranium ore area are higher than those in new houses built of bricks, and much higher than outdoor values.

The measurements will be continued in the future so as to obtain a more definite picture of the real status. The emphasis will be given to concentration variations due to different meteorological parame-

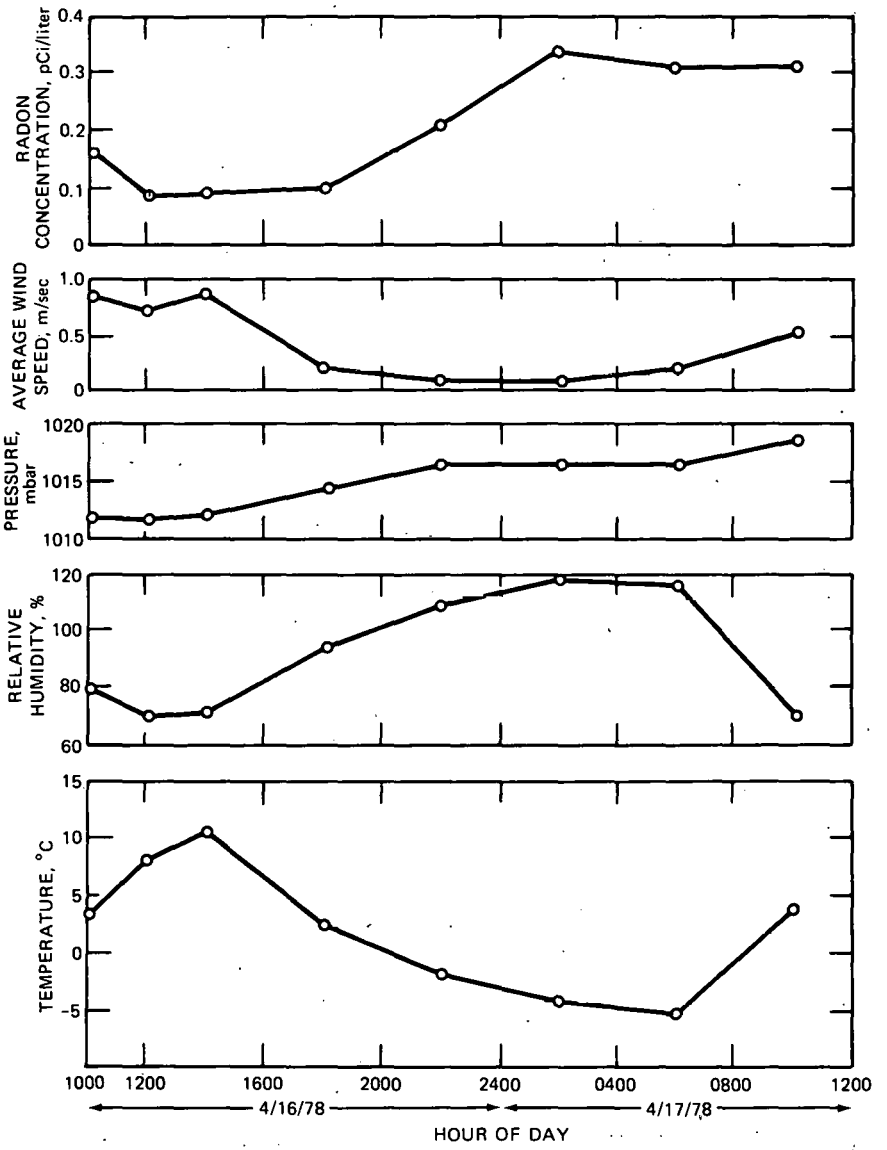


Fig. 3 Diurnal variation in radon concentration and concurrent meteorological parameters in the park at the J. Stefan Institute.

TABLE 2

Air Radon Concentrations and Meteorological Parameters in Dwellings in the Mining District

Village and test site	Radon concentration, pCi/liter	Temperature, °C	Pressure, mbar	Relative humidity, %	Time of sampling, hr
		April 18, 1978			
Todraž 1					
In the courtyard (outdoors)	0.09	12	1009	33	1000
Inside the old house	2.2	15	1009	60	1100
Žirovski vrh nad Zalo 6					
In the courtyard (outdoors)	0.18	10	993	28	1200
Inside the old house (stone)	3.2	7	993	50	1300
Inside the new house (brick)	1.3	11	993	59	1400
Žirovski vrh nad Zalo 3					
In the courtyard (outdoors)	0.17	12	990	23	1500
Inside the old house	1.1	13	990	57	1400
		April 19, 1978			
Jančje Brdo					
In the courtyard (outdoors)	0.14	13	983	26	1100
Inside the old church	1.9	6	983	45	1200
Inside the old house	0.8	19	983	43	1300

ters (Megumi and Mamuro, 1971), especially in winter when temperature inversions are quite often encountered in that region.

ACKNOWLEDGMENTS

We are grateful to the Research Community of Slovenia for the financial support of this work. We also appreciate the technical assistance of Mr. J. Šubelj.

REFERENCES

Eadie, G. G., 1975, Radioactivity in Construction Materials: A Literature Review and Bibliography, Technical Note, USEPA Report ORP/LV-75-1, Environmental Protection Agency, NTIS.

——, R. F. Kaufmann, D. J. Markley, and R. Williams, 1976, *Report of Ambient Outdoor Radon and Indoor Radon Progeny Concentrations During November 1975 at Selected Locations in the Grants Mineral Belt, New Mexico,* Technical Note, USEPA Report ORP/LV-76-4, Environmental Protection Agency, NTIS.

Israelsson, S., E. Knudsen, and E. Ungethum, 1972, *Radon and Thoron in the Air Near the Ground,* Report No. 28, Marsta Observatory, Uppsala, Sweden.

Kobal, I., J. Kristan, and M. Škofljanec, 1978, Alpha-Scintillation Method for Measuring Low Radon Concentrations in Air, in *Monitoring of Radioactive Effluents from Nuclear Facilities,* Symposium Proceedings, Portorož, Yugoslavia, Sept. 9—13, 1977, pp. 173-180, STI/PUB/466, International Atomic Energy Agency, Vienna.

Megumi, K., and T. Mamuro, 1971, Radon and Thoron Exhalation from the Ground, *Annu. Rep. Radiat. Center Osaka Prefect.*, 12: 18-21.

Nakatani, S., 1975, *Characteristics of Natural Radioactivity Appearing in Its Diurnal Variation,* Researches of the Electrochemical Laboratory, No. 755, Agency of Industrial Sciences and Technology, Tokyo, Japan.

Toth, A., 1976, Natural Population Load from the Radioactivity of Building Materials. 1. Estimation of Radon—Thoron Dose, *Izot. (Budapest),* 19: 148-160.

——, and I. Feher, 1976, *Effective ^{226}Ra Content of Some Hungarian Building Materials,* Report KFKI-76-8, Hungarian Academy of Sciences, Budapest.

Population Dose Equivalent from Naturally Occurring Radionuclides in Building Materials

DADE W. MOELLER, DWIGHT W. UNDERHILL, and GARY V. GULEZIAN*
Harvard School of Public Health, Boston, Massachusetts

ABSTRACT

Naturally occurring radionuclides in building materials are a source of external and internal radiation exposure to the U. S. population. Under certain conditions exposure rates are sufficiently high that control measures, either on a voluntary or mandatory (legislative) basis, should be considered. Such measures include (1) material substitution, (2) improved manufacturing standards, (3) changes in basic building designs, (4) application of surface sealants, and (5) increased ventilation accompanied by processes for the adsorption and/or filtration of airborne radionuclides. Analyses show that several of these measures appear to be well justified in terms of the $1000 per person-rem cost-effectiveness guideline used for commercial nuclear power plants by the U. S. Nuclear Regulatory Commission.

Although the U. S. population receives radiation exposure from a variety of sources, the greatest contribution to the dose equivalent (D.E.) rate today is from natural background. A significant part of this contribution is from naturally occurring radionuclides in building materials. Estimates are that the average annual contribution from such radionuclides to the external whole-body D.E. rates in brick, masonry, and concrete houses is 10 to 20 mrems. For some population groups in certain types of housing, the contribution from this source may range up to 100 mrems/year or more (Hultqvist, 1956); D.E. rates to the lungs can be even higher.

The investigation reported here is part of an ongoing research effort at the Harvard School of Public Health to quantify radiation

*Present address: U. S. Environmental Protection Agency, Region V Office, Chicago, Ill.

exposure rates within buildings and to evaluate the effectiveness and feasibility of control technologies. This paper, which represents a status report on the work to date, consists of two major sections: (1) summary information on a computer program developed to provide estimates of D.E. rates within buildings, and (2) a review of the advantages, disadvantages, and relative cost-effectiveness of several approaches available for the control of such exposures.

COMPUTER PROGRAM FOR DOSE ESTIMATES

The dose equivalent rate within a given building is a complex function of the geometric distribution of radionuclides within the structure, the shielding characteristics of the building materials, the air-exchange rate, and the time-utilization factor for each room (Fig. 1). With these factors taken into account, a flexible computerized model has been developed for determining the contribution of construction materials and building design factors to the external exposure from gamma radiation and the internal exposure from inhaled radon (and thoron) daughter products within specified areas of a home. This model can also be used to assess the relative effectiveness of a variety of radiation control techniques.

The computer program, written in Fortran IV, is for descriptive purposes divided into two parts: (1) the calculation of the whole-body gamma D.E. rate caused by uranium, thorium, and potassium in construction materials, and (2) the calculation of the internal D.E. rate to the bronchial epithelium from radon and thoron daughters that arise from the diffusion of radon and thoron from the walls and floor of a room.

The program for calculating the external gamma D.E. rates requires the following input data:

1. Dimensional data: room height, width, length, thickness of walls (and of interior plaster if present), and placement of windows and doors.

2. Diffusional data: the diffusion coefficient for radon in the building materials and the influence of impervious coatings (e.g., waterproofing or surface sealants).

3. The uranium, thorium, and potassium contents of the building materials.

Some useful equations derived for these calculations are given in the Appendix to this paper.

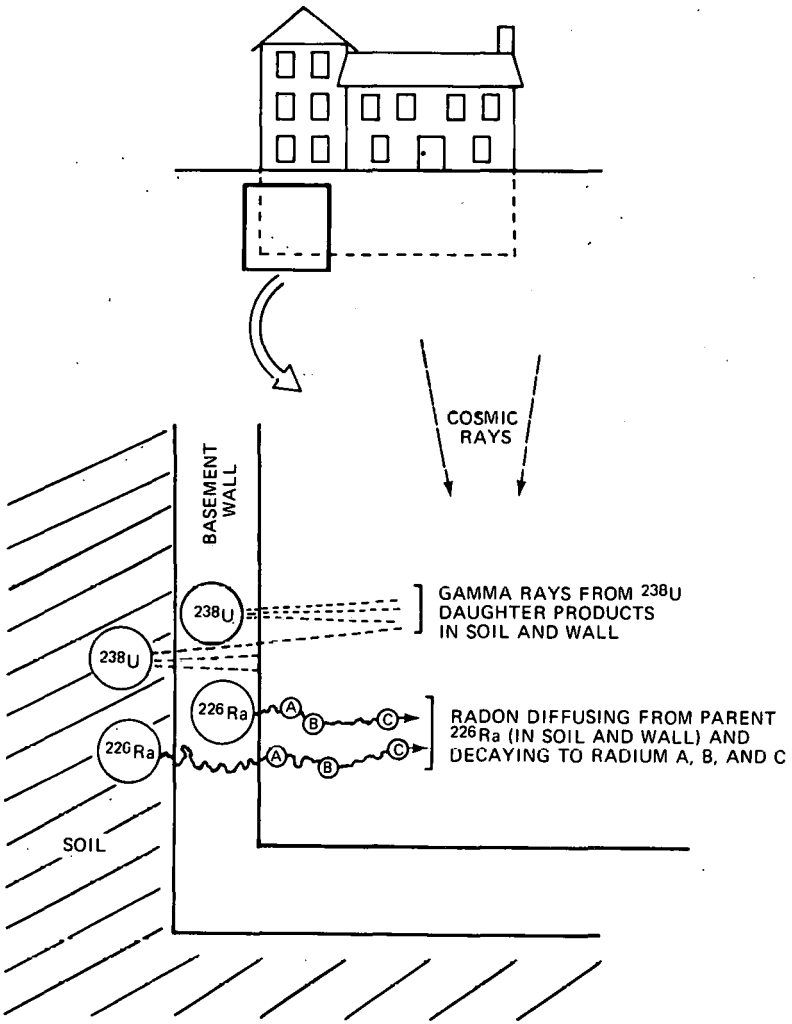


Fig. 1 Major sources of natural radiation exposure in basements.

Subroutines of the program can be used to compute the gamma-ray flux from the ^{238}U—^{226}Ra, ^{222}Rn—^{206}Pb, ^{232}Th—^{208}Pb, and the ^{40}K decay series, taking into account self-absorption in the construction materials. Because of the diffusion of radon from building materials, ^{238}U and ^{222}Rn may not be in equilibrium and, therefore, the decay products from these two radionuclides are considered separately. The approach used in the

program was first to divide the walls in each room into 100 sections and then sum the radiation exposure from each section, starting at the floor and passing by decades from left to right. Areas with windows and doors were included in the input data so that their lesser contribution to the radiation flux could be taken into account.

The advantage of this type of calculation for this particular case is its very high degree of flexibility. In the calculation of the theoretical gamma-ray flux in a room, the program can, for example, be used to account for the presence of windows and doors, the diffusion of radon daughters, and the presence of multiple layers of material, all of which factors are present in real buildings.

The program for calculating the internal D.E. rates from radon and radon daughters requires the following input data:

1. Building material factors: wall and floor thickness, wall and floor area, concentration of radium in building material, presence of multiple layers of wall or floor material, presence of paint and its permeability, and permeability of the construction materials to radon.
2. Ventilation rates for the rooms.
3. Radon concentration in the soil.
4. Radon concentration in the ambient atmosphere.

The basic equations used in calculating indoor radon concentrations are reviewed below. The emanation of radon from the adjacent soil through the building material was calculated as

$$F_s = PAC_s (\lambda D)^{1/2} \operatorname{csch} \left[L \left(\frac{\lambda}{D} \right)^{1/2} \right] \quad (1)$$

where F_s = emanation of radon through the wall, pCi/sec
P = fractional wall volume consisting of interparticle pore volume
C_s = concentration of radon in the air in the soil, pCi/cm^3
A = wall or floor area, cm^2
D = diffusion coefficient for radon in the building material, cm^2/sec
λ = decay coefficient for radon, sec^{-1}
L = wall thickness, cm

Separate calculations are made for the diffusion of radon through the walls and floors.

As would be expected, it may be necessary to use more complex equations if (1) more than one building material is present in the wall or floor, (2) appreciable transfer of radon into the room takes place

through small wall fractures, (3) the concentration of radon within the room air is not at least an order of magnitude lower than the radon concentration in the air within the adjacent soil, and/or (4) the diffusion coefficient for radon in the soil is not considerably greater than the diffusion coefficient for radon in the building material. Through the use of more complex equations, the computer program can be made sufficiently general to account for these factors. However, Eq. 1 should be applicable for most cases under consideration, and the more complex equations need be applied only when their use is clearly indicated.

The emanation of radon from a building material into a living space can be calculated as follows:

$$F_B = AC_B\,(\lambda D)^{1/2} \tanh\left[\frac{L}{2}\left(\frac{\lambda}{D}\right)^{1/2}\right] \qquad (2)$$

where F_B is the emanation of radon into a room from the building material in picocuries per second and C_B is the concentration of ^{226}Ra in the building material in picocuries per cubic centimeter. A, L, D, and λ are as defined for Eq. 1. Separate calculations must be conducted for the diffusion of radon through the walls and the floor.

CONTROL MEASURES

Control measures that have been evaluated in this study for the reduction of external and internal D.E. rates within buildings include: (1) material substitution, (2) manufacturing standards, (3) changes in basic building designs, (4) increased ventilation, (5) adsorption, filtration, and/or chemical reactions, and (6) surface sealants.

To establish the economic feasibility of the more promising control measures, we have made estimates of their cost-effectiveness relative to the dose reduction they can accomplish. Since the highest concentrations of airborne radon and radon daughter products are generally present in the basement, specific attention has been directed to cost—benefit assessments of reducing exposures in this portion of the home.

Construction Material Substitution

One technique for reducing the D.E. rate within buildings is to replace construction materials of high radionuclide content with those of reduced radionuclide content. A prime advantage of this approach is that it is a passive method; once the home is built, the

effectiveness of this radiation control methodology is not dependent on any action or compliance on the part of the inhabitants. Although the direct costs of material substitution are difficult to quantify, most changes would result in cost increases. This is due to the fact that the home-construction industry is highly competitive and current building practices have been developed on the basis of maintaining costs at a minimum. An example of material substitution is the use of wood (a material of relatively low radionuclide content) in place of concrete, concrete block, and/or brick (materials of relatively high radionuclide content). Field surveys have shown that external D.E. rates are generally lower by 30% or more in wooden buildings than in brick, concrete, or masonry structures (Oakley, 1972; National Council on Radiation Protection, 1975; Stranden, 1977).

Many additional factors must be considered in assessing the cost-effectiveness of material substitution. Construction materials vary in strength, durability, maintenance requirements, thermal-insulation properties, safety aspects, and aesthetic characteristics. As a result the trade-offs involved in substituting one construction material for another are not always straightforward. For example, it would seem reasonable to assume that the use of wood, instead of brick, would increase the risk of fire. Experience has shown, however, that this is not true. The fire hazard of a home is primarily governed by the combustibility of its furnishings (J. A. Sharry, National Fire Protection Association, personal communication, 1976).

Improved Manufacturing Standards

Another method of control would be to establish concentration limits for naturally occurring radionuclides in materials approved for use in home construction. This approach would then require manufacturers to determine the radionuclide content of the raw materials used in construction products. Examples of materials that would be tested include the sand, cement, and aggregate used in concrete, the clay used in brick, and the gypsum used in wallboard and plaster. If this approach were adopted, some manufacturers and building suppliers would incur additional costs because of problems in the procurement of acceptable raw materials, added freight expenses through the necessity of shipping acceptable materials from more distant locations, and additional costs associated with quality control and monitoring procedures. These costs and any added expenses associated with the rejection of raw material lots would eventually be passed on to the consumer.

In some cases the removal of naturally occurring radionuclides from building materials may be necessary. This need not result, however, in increased costs in every instance. Various processes developed for the removal of uranium from the gypsum produced as a by-product of the phosphate industry may be cited as technologically feasible procedures that could result in reductions in the radionuclide content of building materials (Nadig and Burnet, 1962; Boontje, 1973). This is an area where additional research would be helpful.

Changes in Basic Building Designs

A number of studies have shown that the D.E. rates, from both internal and external sources, are significantly higher in the basement than in other areas of a home (Yeates, Goldin, and Moeller, 1972). On this basis one could possibly conclude that one approach for reducing exposures in homes would be to eliminate basements. The social, economic, and psychological effects of such a design change, however, would undoubtedly be large. Although economically the purchase price of a home without a basement would be lower, should a buyer desire a basement, there would be psychic and behavioral changes involved in foregoing that option. In addition, a basement within a home often satisfies special needs. For example, children are frequently encouraged to use underdeveloped basement areas for recreation because of the basement's ability to withstand abuse. Shifting this function to the first or second floor could increase both space requirements and maintenance costs.

Another design approach would be to protect building occupants from external gamma exposure through the addition of shielding to the inside walls and floors. Evaluations show that the amount of shielding required to reduce the D.E. rate 50% in most cases would be about 5 g/cm^2. This could probably be most economically provided through the use of materials such as natural gypsum or low-activity concrete or plaster. The costs of such an approach, however, would probably be high.

Increased Ventilation

Several studies (Caruthers and Waltner, 1973; Spencer et al., 1968) have documented the effectiveness of increased ventilation in reducing the concentrations of radon and its daughter products within buildings. Ventilation systems can reduce airborne radionuclide concentrations by diluting the contaminated air with fresh air, passing the air through a filtration or adsorption system, or by a combination of these approaches.

The costs associated with increased ventilation include added energy usage due to more frequent blower operation plus added maintenance costs for the air-circulation system. In homes without forced air heating, the costs may include capital investments in ventilation equipment.

The major drawback to the use of increased ventilation for the control of airborne radionuclide concentrations is the loss of heat energy associated with the rapid air turnover. If fresh outside air is brought into the home during either cold or hot weather, heating or cooling costs may increase substantially. For example, Snell, Achenbach, and Peterson (1976) have estimated that the energy to provide heating of makeup air under winter conditions may account for one-third to one-half the total heating costs of a normal residence. In a single-family home, these costs can range from $200 to $300/year. One possible way to overcome the heat loss would be through use of heat exchangers. The technical details of this approach, however, are yet to be developed. As a result definitive cost data are not yet available.

Adsorption, Filtration, and/or Chemical Reactions

Air circulation within a home, in combination with some method of filtration and/or adsorption, can accomplish much of the desired radionuclide removal without the accompanying heat loss. Filtration, for example, has proven to be a very effective mechanism for removing radon daughter products. One problem associated with this approach, however, is the short time (~3 min) required for radium A to come into equilibrium with radon. Thus, if it were desired to reduce the concentration of radium A by a factor of 10, a filtration system—either electronic or mechanical—would require a throughput equal to twice the volume of the room each minute. Fortunately, the radionuclides of primary importance from a radiation-dose point of view are radium B and radium C. Since these nuclides have half-lives of the order of one half hour, a flow-through filtration system in which the recirculation time is less than one half hour can provide significant reductions in their airborne concentrations. Because home air-circulation systems normally have filters for dust control, the cost-effectiveness of such systems should be reasonably high.

The application of charcoal adsorbers and chemical reactants is under development for use in the removal of airborne contaminants in mines. A cyclic adsorption—desorption system to remove radon from ambient air has been patented (Thomas, 1974). In this system radon is removed from air by sorption on a charcoal bed at room

temperature. When the bed becomes saturated, it is heated, the radon desorbed, and the bed cooled and reused. Continuous cleansing of the air is assured by the use of two adsorption beds in alternation. The advantage of a system of this type is that it permits both radon and radon daughters to be removed. Such a system requires a lower throughput than a radon-daughter filtration system to accomplish the same dose reduction. Preliminary calculations indicate that as little as 100 lb of activated charcoal, operated on a cyclic basis, would be adequate for removing airborne radon within the basement of a home. One potential problem is that other contaminants within the air in the home (such as cooking vapors) would poison the charcoal bed and shorten its useful operating cycle. However, the poisoned adsorbent can be returned to the manufacturer for reactivation. Recoveries of between 90 and 95% by weight of the original material are common, and the material recovered in this manner is said to have an adsorption coefficient very nearly equal to that of the original charcoal. In time such systems may be developed commercially for use in residences. The main costs would be initial installation plus the operational expenses associated with recharging the bed on, roughly, an hourly basis. Although it is too early to perform definitive cost analyses, the installation and operating costs of such a system, once developed commercially, would be intermediate between a simple filtration system and a home air-conditioning system.

Another control procedure that could be both inexpensive and effective is space charging. It is known that, if an excess quantity of ions of one charge is added to a space containing an aerosol, mutual repulsion of the particles will lead to their removal. The physics of space charging is well known, and articles on the application of this technique to home atmospheres have been published (Yaglou, 1961).

Chemical reaction of radon to form fixed compounds is also, at least in theory, a possible removal procedure (Stein, 1973). At this time, however, the substances used, metallic fluorides, require that the input air be absolutely dry. Another negative factor is that such a system may release fluoride compounds. If these problems can be solved, this approach will be worthy of further exploration for home use.

Application of Surface Sealants

Another approach that has been considered is to coat the interior surfaces of the walls and floor of a home with a sealant which is impervious to radon and would therefore preclude or retard seepage of radon into the air. This approach is highly flexible. It can be used

to retrofit existing homes as well as to provide a relatively inexpensive method for the control of airborne concentrations of naturally occurring radionuclides within newly constructed homes. Other advantages of this control technique include the absence of behavioral-change requirements, few if any architectural complications, and no negative aesthetic effects.

One disadvantage of this method is that it is often difficult to effectively seal a given surface. Small cracks can permit significant fractions of the radon emissions to be released. Another disadvantage is that an effective sealant will lead to an increase in the external gamma exposure rate caused by the build-up of radon daughter products beneath the sealant surface (Culot, Shiager, and Olson, 1976). The computer model described earlier has been used to investigate this effect in detail. Computer plots of the gamma flux from radon daughters in concrete of medium, low, and high permeability to radon under a variety of wall-sealant conditions are presented in Figs. 2 to 4. As would be expected, the highest gamma flux is from a wall with an impervious coating on both the inside and outside, and the lowest flux is from an uncoated wall. In the case of a concrete wall of medium permeability to radon (Fig. 2), it can be seen that a wall 20 cm thick which is sealed on both sides will yield a gamma flux rate from radon daughters more than four times greater than that of an unsealed wall of equal thickness. Figures 3 and 4 also illustrate the strong effect on gamma-ray flux brought about by the permeability of a construction material and the consequent need to know this factor before calculating the gamma flux rate from the walls of a building.

The increased external gamma exposure rate resulting from the use of a surface sealant must, of course, be evaluated in comparison with the reduction in the internal exposure rate. In general, however, the D.E. rate reduction to the lungs brought about by this control measure will exceed the increase in the whole-body external gamma exposure rate.

The cost-effectiveness of surface sealants, in relatively high exposure situations such as basements, can be expressed in terms of the dollar cost per person-rem reduction in the lung dose equivalent. For purposes of these calculations, the following assumptions were made: (1) The average number of people per home is three (U. S. Department of Housing and Urban Development, 1974). (2) The average time spent in the basement area for typical occupants is about 30 min/day (2% of their time); for basement-apartment dwellers, this could range up to 75% of their time. (3) The average concentration of ^{218}Po in the basement of a home is 0.4 pCi/liter (Yeates, Goldin, and Moeller, 1972). On this basis the annual D.E.

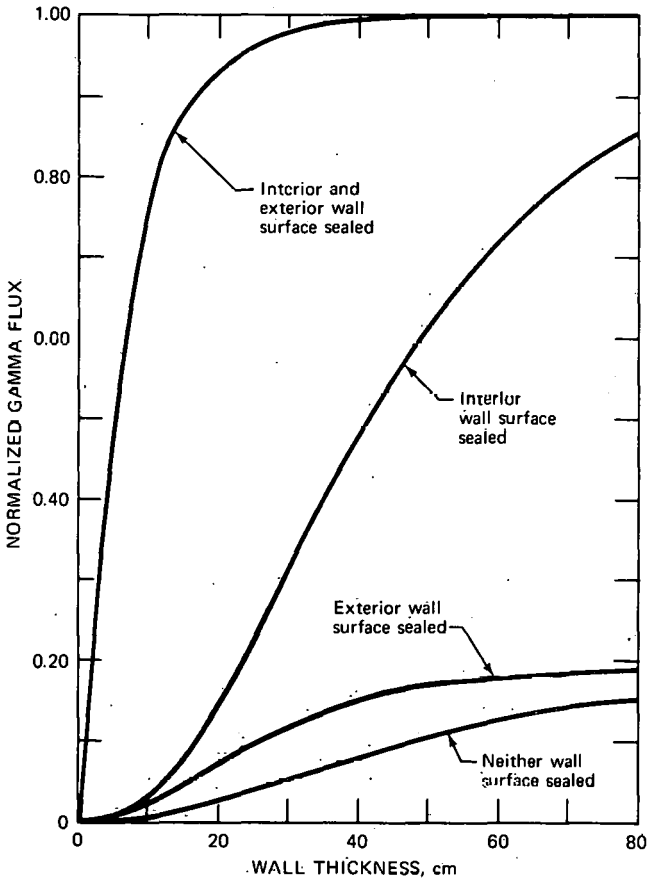


Fig. 2 Gamma flux from radon daughters in concrete of medium permeability to radon.

rate to the segmental bronchioles of the lung (National Council on Radiation Protection, 1975) resulting from airborne naturally occurring radionuclides in the basement of a typical home would be about 2.7 person-rems/year (if three people at 75% occupancy is assumed) and 0.072 person-rem/year (three people at 2% occupancy).

For purposes of evaluating the cost-effectiveness of surface sealants, it appears reasonable also to assume that applying such sealants to the surfaces of the walls and floor of a basement room would result in a 90% reduction in the airborne radionuclide concentrations of radon and its daughter products (Auxier et al., 1974; Culot, Olson, and Schiager, 1973; Franklin, Nuzum, and Hill,

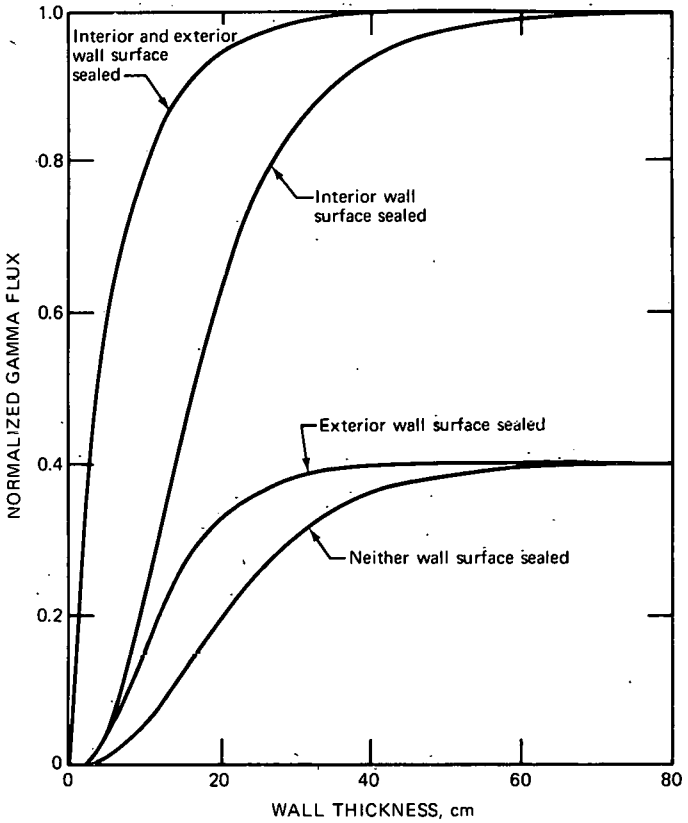


Fig. 3 Gamma flux from radon daughters in concrete of low permeability to radon.

1975). On this basis the application of sealants in the basement of the home described above would reduce the 2.7 person-rems/year lung D.E. rate (for 75% occupancy) by about 2.4 person-rems/year; for a 2% occupancy, the corresponding 0.072 person-rem/year D.E. rate would be reduced by about 0.065 person-rem/year. If the sealants are assumed to remain effective, the benefits of these reductions would accrue over the lifetime of the sealant, which has been estimated to be 20 to 30 years (G. Young, Dow Chemical Company, Freeport, Texas, personal communication, 1976).

Estimates of the costs of sealing a wall with epoxy-based paint range from \$2.70 to \$5.40/m^2. Since the basement in a typical U. S. home measures approximately 7.5 by 12 m (by 2.5 m high), its total

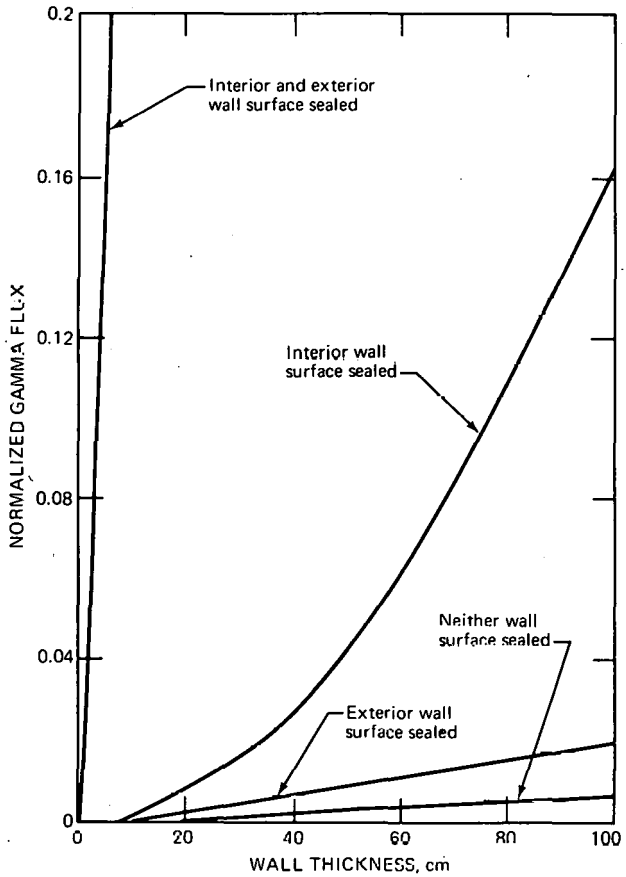


Fig. 4 Gamma flux from radon daughters in concrete of high permeability to radon.

surface area (walls and floor) is about 1·87 m^2. Thus the estimated cost for sealing these surfaces will range from a minimum of about \$500 (at \$2.70/m^2) to a maximum of about \$1000 (at \$5.40/m^2).

If this expenditure is allocated over a 20-year period, the average annual cost including principal and interest will range from \$46.50 to \$93.00. If the expenditure is allocated over a 5-year period, the corresponding costs range from \$117.50 to \$235.00. These data and estimates for other periods of time as well as for a range of occupancy factors are summarized in Table 1. From these data, it can be seen that the annual cost per person-rem reduction in lung dose, if 75% occupancy is assumed, ranges from about \$19 to \$48 (at

TABLE 1

Cost-Effectiveness of Control Methodology via Surface Sealants for Home Basement Area*

Amortization of home loan		Occupancy, %	Reduction in lung dose, person-rems/year	Application cost-effectiveness			
				At $\$2.70/m^2$		At $\$5.40/m^2$	
Number of years	Annual rate, %			Annual cost	Cost/person-rem reduction	Annual cost	Cost/person-rem reduction
5	23.5	2	0.065	$117.50	$1808	$235.00	$3616
		10	0.32	117.50	367	235.00	734
		75	2.43	117.50	48	235.00	97
10	13.9	2	0.065	69.50	1069	139.00	2138
		10	0.32	69.50	217	139.00	434
		75	2.43	69.50	29	139.00	58
20	9.3	2	0.065	46.50	715	93.00	1430
		10	0.32	46.50	145	93.00	290
		75	2.43	46.50	19	93.00	38

*Assumptions: The home has three occupants.
The basement size is 7.5 by 12 m with 187 m^2 of surface to be sealed.
The annual interest rate on home loans is 7%.
The average ^{218}Po concentration is 0.4 pCi/liter, with a $^{218}Po/^{214}Pb/^{214}Po$ ratio of 1 : 0.7 : 0.6.
Brick glazing or surface sealants will reduce the airborne concentrations (and accompanying lung D.E. rate) by 90%.

an application cost of $\$2.70/m^2$) to \$38 to \$97 per person-rem reduction (at $\$5.40/m^2$). At an occupancy factor of 2%, the cost-effectiveness of this approach would range from \$715 to \$1808 (at $\$2.70/m^2$) to \$1430 to \$3616 (at $\$5.40/m^2$) per person-rem reduction in lung dose. At an occupancy factor of 10%, the figures would be somewhere in between these values.

In the data as presented it must be noted that the estimates are based on the assumption that the entire cost of painting the surfaces is attributable to control of the radon and radon daughter products. In the case of the new home where the prospective owner wanted the basement surfaces painted, this task could be performed during construction and the true cost of sealing the surfaces would be only the marginal (differential) cost between painting the surfaces with regular paint vs. an epoxy sealant. This marginal cost would be, at most, only about $\$0.54/m^2$ or about 10% of the estimate given above.

Another method for the control of radon emanation from basement wall surfaces, in the case where the walls are constructed of precast block or brick, would be to seal the exposed surfaces during manufacture of the product. Cost figures provided by the Brick Institute of America (P. Harrington, Brick Institute of America, personal communication, 1976) indicate that the application of glaze sealing to the exposed surface of a brick would increase its cost by about 50%. With a wholesale cost of \$0.01/brick, sealing the exposed surface would increase the price by about \$0.005/brick, which on the basis of the final wall surface amounts to an added cost of about $\$0.43/m^2$. Although it is not clear what effect the five nonsealed sides of each brick, or the mortar between them, would have, the cost of the added glaze would appear to be cost-effective. If all six sides of each brick were sealed during manufacture, the cost would be comparable to that required for the application of epoxy surface sealants.

COMMENTARY

As has been noted, there is a variety of approaches or techniques that could be used to control the population D.E. rates arising through naturally occurring radionuclides in building materials. These techniques and their advantages and disadvantages are listed in Table 2.

If one accepts the premise that control should be sought, there appear to be two strategies which might be used. One would be to approach the problem by seeking to bring about appropriate changes

TABLE 2

Comparison of Control Measures

Control measure	Advantages	Disadvantages
Material substitution	Can control both external and internal exposure Passive control Only marginal costs incurred when applied to new structures	Impractical for existing structures Potentially high cost
Manufacturing standards	Preventive measure Passive control	Not applicable to existing structures Potentially high cost
Building design changes	Areas of highest exposure can be eliminated	Life-style/behavioral changes may be required Not applicable to existing structures
Increased ventilation	Retrofit possible Relatively low cost	Does not reduce external gamma exposure rate Increases heating and cooling costs
Adsorption, filtration, and/or chemical reactions	Retrofit possible Potentially high effectiveness for reducing internal dose equivalent	Technologies not yet fully developed Cost estimates are uncertain Does not reduce external gamma exposure rate
Surface sealants	Retrofit possible Passive control Can provide aesthetic improvements Relatively low cost	May cause increase in external gamma exposure rate

in the behavioral or living patterns of people; the other would be to seek reductions through appropriate changes in the design, construction, and functioning of buildings.

Effecting the necessary corrections through changes in behavioral patterns would be an extremely difficult task. It would involve education, persuasion, and many other factors and is beyond the scope of this paper. The second strategy, although possible, would involve economic, political, and attitudinal problems. Its successful accomplishment also would again involve education and persuasion, as well as perhaps financial incentives and regulatory procedures (Snell, Achenbach, and Peterson, 1976). This would be particularly true if the suggested changes resulted in significantly increased

building costs. However, if one accepts the basic public health principle that all unnecessary radiation exposure should be avoided, then it should be possible to justify action, especially in those cases where given practices are clearly resulting in population D.E. rates well above the national average.

One possible mechanism for controlling unusual situations would be to effect the necessary action through legislation. The simplest approach would appear to be to set limits on permissible concentrations for specific naturally occurring radionuclides in building materials. This could be directed initially to the elimination of products incorporating, for example, materials such as uranium tailings or high-activity phosphate products and by-products. If it were deemed wise at a later date to establish legislation to prevent additional unusual radiation-exposure situations in buildings, the basic approach should probably be to mandate that a specified D.E. rate should not be exceeded. Such legislation might be implemented along the lines of the "as low as reasonably achievable" criterion of the U. S. Nuclear Regulatory Commission (1975).

With regard to the Nuclear Regulatory Commission (NRC), it may be noted that this agency currently uses values of $1000 per person-rem and $1000 per person-thyroid-rem as guides for determining whether additional reductions in population dose are necessary for routine radionuclide releases from commercial nuclear power plants. On the basis of estimates given in this paper for the control of radiation exposure in the basement of a home, the use of surface sealants would appear to have a cost—benefit ratio one to two orders of magnitude better than this, if 75% occupancy by 3 to 4 persons per household is assumed. In fact, control methodology based on the use of surface sealants yields cost—benefit ratios that equal or exceed the NRC guide so long as the occupancy factor is greater than 5%, even for amortization periods as short as 5 years.

ACKNOWLEDGMENT

This study was supported in part by the Office of Radiation Programs, U. S. Environmental Protection Agency, under contract No. EPA 68-01-3292.

APPENDIX: Calculation of the Gamma-Ray Flux from Radon Daughters Remaining in Walls and Floors

More than half of the gamma radiation from radionuclides in the ^{238}U decay series has its origin in ^{222}Rn and its daughter products.

Therefore, building materials in which natural uranium is present can have a significant reduction in their flux of external gamma radiation as a result of the loss of radon by diffusion. This loss is usually greatest near the surface of a building material, which is also the region where emitted photons have the greatest opportunity to reach the inhabited space within a room.

In the calculations that follow, the self-absorption coefficients are determined as a function of the

Gamma-ray absorption coefficient
Radon diffusion coefficient
Wall thickness
Presence of a radon-impervious coating

The distribution of radon in a wall where there is no surface coating to impede diffusion is given by

$$C = \frac{C_0}{\lambda}\left\{1 - \frac{\cosh\left[(\lambda/D)^{1/2}x\right]}{\cosh\left[(\lambda/D)^{1/2}L\right]}\right\} \tag{1}$$

where C = concentration of radon, atoms/cm^3
λ = decay coefficient for radon, sec^{-1}
C_0 = production of radon, atoms/sec-cm^3
D = diffusion coefficient for radon in the building material, cm^2/sec
L = half-thickness of the building material, cm
x = distance from the center of the wall, cm

If there were no diffusion of radon in the building material, the concentration of radon would be: $C = C_0/\lambda$. However, in most building materials there is an appreciable loss of radon by diffusion, and the number of curies of both radon and its daughter nuclides in equilibrium, as a function of distance from the center of the wall, is given by Eq. 1. If both the exterior and interior surfaces are permeable to radon, the gamma-ray emission coefficient, S_1, is equal to

$$S_1 = \frac{e^{-\alpha L}}{2L}\int_{-L}^{+L}\left\{1 - \frac{\cosh\left[(\lambda/D)^{1/2}x\right]}{\cosh\left[(\lambda/D)^{1/2}L\right]}\right\}e^{-\alpha x}\,dx$$

$$= \frac{1}{2L[\alpha^2 - (\lambda/D)]}\left\{\left(\frac{\lambda}{D}\right)^{1/2}(1 + e^{-2\alpha L})\tanh\left[\left(\frac{\lambda}{D}\right)^{1/2}L\right]\right.$$

$$\left. - \frac{\lambda}{\alpha D}(1 - e^{-2\alpha L})\right\} \tag{2}$$

where L, D, and λ are as defined in Eq. 1 and α is the linear absorption coefficient for the gamma radiation under consideration.

If the surface of the wall facing the interior of the room has been coated with a radon-impervious paint, then the emission coefficient is

$$S_2 = \int_0^L \left\{1 - \frac{\cosh\left[(\lambda/D)^{1/2}\, x\right]}{\cosh\left[(\lambda/D)^{1/2}\, L\right]}\right\} e^{-\alpha x}\, \frac{dx}{L}$$

$$= \frac{1}{\alpha L} + \frac{\lambda\, e^{-\alpha L}}{\alpha D[\alpha^2 - (\lambda/D)]\, L} - \frac{1}{[\alpha^2 - (\lambda/D)]\, L}$$

$$\times \left\{\left(\frac{\lambda}{D}\right)^{1/2} \tanh\left[\left(\frac{\lambda}{D}\right)^{1/2} L\right] e^{-\alpha L} - \alpha \operatorname{sech}\left[\left(\frac{\lambda}{D}\right)^{1/2} L\right]\right\} \qquad (3)$$

where L is now the thickness of the wall in centimeters.

The final case to be considered, that of a wall where there is an impervious backing, leads directly to the following equation:

$$S_3 = e^{-\alpha L} \int_{-L}^{0} \left\{1 - \frac{\cosh\left[(\lambda/D)^{1/2} x\right]}{\cosh\left[(\lambda/D)^{1/2} L\right]}\right\} e^{-\alpha x}\, \frac{dx}{L}$$

$$= \frac{\lambda}{\alpha L(\lambda - D\alpha^2)} - \frac{e^{-\alpha L}}{L\alpha} + \frac{1}{L[\alpha^2 - (\lambda/D)]}$$

$$\times \left\{\alpha e^{-\alpha L} \operatorname{sech}\left[\left(\frac{\lambda}{D}\right)^{1/2} L\right] + \left(\frac{\lambda}{D}\right)^{1/2} \tanh\left[\left(\frac{\lambda}{D}\right)^{1/2} L\right]\right\} \qquad (4)$$

REFERENCES

Auxier, J. A., W. H. Shinpaugh, G. D. Kerr, and D. J. Christian, 1974, Preliminary Studies of the Effects of Sealants on Radon Emanation from Concrete, *Health Phys.*, 27: 390-392.

Boontje, J. T., 1973, *Verfahren zur Reiningung von Abfallcalciumsulfat*, German Patent 2,320,654.

Caruthers, L. T., and A. W. Waltner, 1973, Need for Standards for Natural Airborne Radioactivity (Radon and Daughters) Concentrations in Modern Buildings, *Health Phys.*, 29: 814-817.

Culot, M. V., H. G. Olson, and K. J. Schiager, 1973, *Radon Progeny Control in Buildings*, M.S. Thesis, Colorado State University, Boulder, USAEC Report COO-2273-1, NTIS.

——, K. J. Schiager, and H. G. Olson, 1976, Prediction of Increased Gamma Fields After Application of a Radon Barrier on Concrete Surfaces, *Health Phys.*, 30: 471-478.

Franklin, J. C., L. T. Nuzum, and A. L. Hill, 1975, *Polymeric Materials for Sealing Radon Gas into the Walls of Uranium Mines*, BM-RI-8036, Bureau of Mines, U. S. Department of the Interior.

Hultqvist, B., 1956, Studies on Naturally Occurring Ionizing Radiation, with Special Reference to Radiation Doses in Swedish Houses of Various Types, *Kgl. Svenska Vetenskaps. Handl.*, Ser. 4, 6(3).

Nadig, E. W., and G. Burnet, 1962, Recovery of Uranium in Wet Process Phosphoric Acid, in *Nuclear Engineering*, Chemical Engineering Progress Symposium Series, No. 58, pp. 104-107, American Institute of Chemical Engineers, New York.

National Council on Radiation Protection and Measurements, 1975, *Natural Background Radiation in the United States*, Report No. 45, NCRP Publications, Washington, D. C.

Oakley, D. T., 1972, *Natural Radiation Exposure in the United States*, USEPA Report ORP/SID 72-1, Environmental Protection Agency, NTIS.

Snell, J. E., P. R. Achenbach, and S. R. Peterson, 1976, Energy Conservation in New Housing Design, *Science*, 192: 1305-1311.

Spencer, N., L. Spittel, T. Towles, and G. Lady, 1968, *Control of Radiation Exposure in Uranium Mines: A Cost and Economic Analysis*, RMC Report UR-42, Report prepared for the Federal Radiation Council, Resource Management Corporation, Bethesda, Md.

Stein, L., 1973, Chemical Methods for Removing Xenon and Radon from Contaminated Atmospheres, in *Noble Gases*, Symposium Proceedings, Las Vegas, Nevada, Sept. 24—28, 1973, R. E. Stanley and A. A. Moghissi (Eds.), USERDA Report CONF-730915, Environmental Protection Agency, Washington, D. C.

Stranden, E., 1977, Population Doses from Environmental Gamma Radiation in Norway, *Health Phys.*, 33: 319-323.

Thomas, J., 1974, United States Patent Application No. 443,262.

U. S. Department of Housing and Urban Development, 1974, *1973 HUD Statistical Yearbook*, Washington, D. C.

U. S. Nuclear Regulatory Commission, 1975, *Numerical Guides for Design Objectives and Limiting Conditions for Operation to Meet the Criterion "As Low As Practicable" for Radioactive Material in Light-Water-Cooled Nuclear Power Reactor Effluents*, Rulemaking Hearing Docket RM-50-2, Report NRCI-75/4, Nuclear Regulatory Commission Issuances, NTIS.

Yaglou, C. P., 1961, Are Air Ions a Neglected Biological Factor? in *The Air We Breathe*, S. Farber and H. Wilson (Eds.), Charles C Thomas Company, Inc., Springfield, Ill.

Yeates, D. B., A. S. Goldin, and D. W. Moeller, 1972, Natural Radiation in the Urban Environment, *Nucl. Safety*, 13: 275-286.

Summary of an Informal Meeting on Radon in Buildings

ABSTRACT

An informal meeting of persons interested in the general topic of radon in buildings was held during the afternoon of April 26, 1978. Subjects discussed were technologically enhanced and natural radon sources, the routes by which radon entered structures, the radon/radon daughter concentrations expected from entry rates, and actions that could modify these concentrations.

Most attention in the United States and Europe was being paid to technologically enhanced sources, such as radioactive building materials and the reclaimed phosphate mining areas in Florida. Most measurements on materials had been of total radium content by gamma spectroscopy, but measurements of radon release rates were becoming more common. The natural source that had received most attention was well water containing high levels of dissolved radon. Since radon levels up to 50 pCi/liter were found in Canadian homes constructed in areas of apparently normal radioactivity, it appeared that more work would be required before potential problem areas could be identified. Measurements of the exhalation rate of radon from the ground, as done in Florida, seemed a promising approach.

The routes by which radon entered the house had not been examined in great detail because they were either believed to be obvious, as in the case of water and building materials, or assumed to diffuse through concrete from external sources. Studies at one Canadian location showed that neither water, building materials, nor diffusion could account for the high and variable radon levels measured in houses. The cause at that location was the entry of soil gas containing radon through open joints and connections in the basement.

Radon daughter concentrations in excess of a working level (WL) of 0.02 (5 pCi/liter) were measured in a few percent of houses tested in Canada, Europe, and the United States. The expected effect on these levels of decreased ventilation rates resulting from greater energy conservation was discussed. There was no general agreement as to what the acceptable annual average WL should be for homes. In several countries the question was under discussion, but no decisions were made. An upper limit of 0.02 WL averaged over the year was in use in Canada for those houses where remedial work had been carried out to reduce the WL, but this did not apply to the country as a whole.

Experience with remedial measures to date has been largely confined to cases of massive contamination with mill or refinery wastes, and the techniques developed for those difficult cases may be overelaborate or impracticable in other areas of technologically enhanced or natural radon sources. For example, source removal may not be practicable. Preliminary work in a naturally radioactive area in Canada suggests that properly constructed Canadian basements will not allow the entry of significant amounts of radon, and thus only higher quality control rather than new building techniques may be required for new construction. Whether the same is true for other countries is not yet known. Radon concentrations in existing houses in that area have been successfully reduced by closing open joints with a variety of commercial materials and putting water traps on sump connections. Elaborate sealing was not necessary.

Population Doses from Natural Radionuclides Due to Certain Aspects of Human Activity

L. A. ILYIN, V. A. KNIZHNIKOV, R. M. BARKHUDAROV,
R. M. ALEXAKHIN, B. K. BORISOV, and N. Ja. NOVIKOVA
Institute of Biophysics of the Ministry of Health of the USSR, Moscow, USSR

ABSTRACT

Radiation exposures and resulting population doses due to a number of nonnuclear technical and economic activities in the USSR are estimated and compared to exposures and doses due to natural background radiation and to nuclear technology. Local and nationwide population dose commitments to the whole body and to specific organs are calculated for a new coal-fired power station and for a nuclear power plant of similar capacity. The coal-fired power station was found to produce a larger population dose in all organs considered except the thyroid. Similar computations were made for exposures due to the use of agricultural fertilizers, with consideration given the biological mobilities of the several naturally radioactive elements involved. The use of building materials high in naturally radioactive isotopes is also examined, with particular attention to the resulting enhanced indoor radon concentrations.

The study of radiation dose burdens obtained from the exposure of either the whole population or its separate parts to natural radionuclides has recently acquired a particular importance. This is primarily because the irradiation due to the natural radiation background not only makes the main contribution to the population doses but also is constantly increased as a result of human economic activity, this increase being greater than that from artificial radionuclides. The interest in hygienic aspects of natural radioactivity was also aroused by the investigation of new approaches to the problem of normalizing radiation exposures (International Commission on Radiological Protection, 1976). According to these approaches the recommended dose limits, as low as they are, do not provide complete safety. A competent decision on the value of

permissible radiation dose due to a certain type of human activity can be made on the basis of using the benefit—risk criterion, i.e., the principle of "optimization."

The natural radiation background, as previously mentioned, now makes the greatest contribution to the population dose. For a long time the dose value of human exposure to natural radionuclides changed slowly and not significantly. However, with the industrial development and quick growth of cities and power production, the situation changed. With the new approaches to radiation exposure normalization, it is quite possible that in the near future there will be a need to restrict certain types of economic activities which result in additional radiation exposure of population, e.g., restriction on the operation of some reactor types or on the use (in house building) of materials with a high content of natural radionuclides.

The first step toward the optimization and regulation of population dose burdens is, probably, to study population dose burdens existing at the present time. In this paper we have considered the radiation exposure of population due to the burning of organic fuel (mainly coal) and also due to such economic activities as the use of fertilizers in agriculture and mineral substances in buildings. A comparative estimate of radiation exposure from these types of human activity and from other radiation sources was also made.

BURNING OF COAL AT FOSSIL-FUEL STATIONS

One of the main sources of environmental contamination is now (and probably will remain in the near future) the production of electric and thermal energy. The satisfaction of growing energy requirements will lead to increased contamination of the environment. Recently great attention has been paid to the releases of natural radioactive elements (NRE) and to the resulting radiation doses from the operation of fossil-fuel stations. However, the published data (Martin et al., 1971; Jawarowsky et al., 1974) usually include only some isotopes and do not give complete characteristics of the value of population radiation exposure due to fossil-fuel stations.

We have tried to estimate possible population doses from radiation exposures due to the releases from fossil-fuel and nuclear power stations and to calculate the risk for each of these releases. In estimating radiation exposure of the whole population, we assumed that releases from these stations were uniformly distributed over territory occupied by agricultural crops (5.42×10^6 km^2). In

TABLE 1

Radionuclide Content in Coal and Fly Ash, pCi/g

Nuclides	Coal, Donetsk and Kuznetsk	Ash of Donetsk coal	Coal, Poland*
^{226}Ra	0.5—2.9	5.0	0.4—2.4
^{228}Ra		3.3	
^{232}Th		2.3—8.7	
^{40}K		16—60	
^{222}Rn	0.3—8.0		
^{210}Pb	0.3—14	12	

*Jawarowsky et al., 1974.

TABLE 2

Radionuclide Content in Coal from Five Deposits in the Ukraine Region, pCi/g

Name of coal samples	^{226}Ra	^{232}Th	^{40}K
Donbass	2.4		9.3
Pavlograd	0.39	4.2	9.6
Voroshilovgrad	2.9		4.6
Dnepropetrovsk	3.2		7.4
Donetsk	0.5	3.6	14.7

estimating the radiation exposure of separate population groups, we considered the area within 1000 km^2 around power stations. For comparison, we took two modern power stations: the 1200-MW(e) Zaporozhje fossil-fuel station, and the 1400-MW(e) Novo-Voronezh nuclear station. It was assumed that these stations had been in operation for 20 years with constant power.

The Zaporozhje station burns 3.4×10^6 tons of coal and releases 1.3×10^5 tons of ash to the atmosphere annually. Data on the most important NRE in the coal that is widely used in the country are given in Table 1. Table 2 presents data that characterize the NRE content of the coal obtained in one region of the country, i.e., some deposits in the Ukrainian Soviet Socialist Republic. This table shows that even within one coal basin and with a limited number of determinations, the NRE content of the coal varies by several times—a fact that can be of a significant practical value.

Table 3 gives data on the estimated releases of radionuclides from the Zaporozhje fossil-fuel station and on their accumulation in the soil for 20 years of operation.

TABLE 3

Releases and Accumulations in the Soil and Atmosphere near the Zaporozhje Fossil-Fuel Power Station*

Parameters	^{226}Ra	^{228}Ra	^{210}Po	^{210}Pb*	^{232}Th	^{40}K
Annual release, Ci	0.53	0.3	2.0	2.2	0.53	5.3
Integral accumulation in soil, Ci	10.5	2.5	19	31		105
Fallout, Ci/km^2	0.53	0.3	2.0	2.2		5.3
Contamination of land, mCi/km^2	10.5	2.5	19	31		105
Content in the atmosphere, 10^{-18} Ci/liter	1.7	1.1	3.9	4.0	1.7	

*Normalized for 10^3 MW(e).

†For estimation of ^{210}Pb production, it was assumed that ^{222}Rn is released into the atmosphere.

The NRE in the fallout infiltrates biological chains and enters the human body with food products, inhaled air, and drinking water. The solubility of coal ash, which determines the biological acceptability of its radionuclide content, reaches 40% in 1N HCl solution (Jawarowsky et al., 1974). In our calculations we took the maximum value, 100%. In estimating NRE concentrations in the air, we assumed that all released ash precipitates uniformly over the territory surveyed, the constant rate of precipitation being 0.01 m/sec.

Natural ^{40}K always accompanies stable potassium whose accumulation is controlled by homeostatic mechanisms. Therefore an intake of ^{40}K is also limited by physiological requirements of the body, and this radionuclide can be considered only as a source of external irradiation. An intake of ^{232}Th through the food chain is also not taken into account because of its extremely low absorption from the gastrointestinal tract. The calculations of absorbed doses are made by conventional models. When internal organs are irradiated by external sources, the shielding factor is assumed to be 0.8. From Table 4, which presents the calculated results, it is seen that the main contribution to the irradiation of the bone marrow and the bone tissue is made by ^{210}Po, whereas that to the lungs is made by ^{232}Th.

The influence of releases from the normally operating nuclear power station on the radiation environment cannot be detected against the background of fallout from nuclear explosions and natural

TABLE 4

Average Individual Radiation Doses for the Population Near a Fossil-Fuel Power Station, mrems/year per 1000 MW(e)

Irradiated organ	^{226}Ra	^{228}Ra	^{210}Pb	^{210}Po	^{232}Th	^{40}K	Total
Bone tissue	0.74	1.7×10^{-3}	19.3	93		0.45	114
Bone marrow	0.05	5.3×10^{-4}	1.9	12		0.45	14.5
Lungs	0.71	0.1	1.44	0.88	38	0.45	42
Whole body						0.53	0.53

radiation, even in the vicinity of the station. The average gamma dose rate around the Novo-Voronezh nuclear station is about 10 μR/hr, which corresponds to the natural background (Atomizdat, 1974). Measurements of ^{131}I and ^{137}Cs in the bodies of persons living 3 to 4 km from a nuclear station show that the influence of the station is not detected. Comparative data on the irradiation of the population living near a fossil-fuel power station and a nuclear power station and data on the irradiation of the whole population of the USSR are given in Table 5.

Estimates of radiation risk are made by calculating the possible number of additional deaths from malignant neoplasms induced by radiation exposure. The quantitative data on the dose—effect dependence (Table 6) show that the risk due to radiation exposure to the operating stations of both types is quite negligible.

The main cause of radiation carcinogenesis in the region of a fossil-fuel station is lung irradiation by radionuclides in the ash. The risk of leucosis due to irradiation of the bone marrow is also relatively high. External irradiation is the main cause of carcinogenesis for the regions where nuclear stations are located. Thus our data show that the radiation risk from the atomic station is significantly lower than that from the fossil-fuel station. However, it should be noted that in the estimation of radiation doses from nuclear power stations neither additional dose burdens due to the complete operation of the nuclear fuel cycle, fuel transport and waste disposal, nor radiation exposure due to accidental releases were considered.

Risk estimates from fossil-fuel stations are also not quite complete since releases from these stations contain such carcinogenic agents as polycyclic hydrocarbons, arsenic, nickel, chrome, and beryllium. In addition, it is well known that human health is affected by such released components as dust, sulfur anhydrite, and nitrogen

TABLE 5

Population Doses Due to Releases from USSR Fossil-Fuel and Nuclear Power Stations
[Doses per 10^3 MWt(e)]

Irradiated organ	Individual doses near power stations, mrems/year		Whole population doses			
			From fossil-fuel station		From nuclear power station	
	Fossil fuel	Nuclear	Individual dose, mrems	Pop. dose, man-rems/year	Individual dose, mrems	Pop. dose, man-rems/year
Bone tissue	114	48×10^{-2}	21×10^{-3}	5250	11.7×10^{-5}	29
Bone marrow	15	9.6×10^{-2}	2.8×10^{-3}	700	4.7×10^{-5}	3.8
Thyroid		7.8×10^{-2}			4.3×10^{-5}	3.4
Lungs	42	7.6×10^{-2}	7.8×10^{-3}	1950	4.2×10^{-5}	3.4
Whole body	0.53	13.5×10^{-2}	9.8×10^{-5}	15	6.0×10^{-5}	4.8

TABLE 6

Predicted Number of Additional Deaths from Malignant Neoplasms, Cases/year per 10^3 MW(e)

Cause of death	From fossil-fuel power station		From nuclear power station	
	Near station, per 10^6 persons	Whole population	Near station, per 10^6 persons	Whole population
Leucoses	0.6	2.1×10^{-2}	2.9×10^{-3}	3.5×10^{-4}
Bone tumors	0.1	5.2×10^{-3}	1.8×10^{-4}	2.9×10^{-5}
Thyroid tumors			4.8×10^{-4}	1×10^{-4}
Lung tumors	1.7	7.8×10^{-2}	3.0×10^{-3}	4.2×10^{-4}
Various types of tumors due to whole-body irradiation	0.1	4.9×10^{-3}	2.7×10^{-3}	3.0×10^{-3}
All above causes	2.4	10.9×10^{-2}	3.4×10^{-2}	3.9×10^{-3}

oxides. Therefore complete estimates of the comparative risk from operating fossil-fuel and nuclear power stations require a more detailed analysis of possible consequences. Nevertheless, the data obtained allow us to conclude that nuclear power stations are less harmful for human health than fossil-fuel stations under normal operating circumstances.

THE USE OF MINERAL FERTILIZERS

It is known that phosphate-rich minerals often contain increased amounts of radionuclides of the uranium and thorium series. Part of the available phosphate-containing minerals is used as a raw material for obtaining uranium. The production and use of phosphate fertilizers is constantly increasing and in some countries reaches several hundred kilograms per hectare of agricultural land annually. About 100 kg of phosphate fertilizers of approximately 10 types are used annually in the USSR. The mean ^{228}Th content of fertilizers is practically equal to its content in arable land in the USSR, i.e., 0.8 pCi/g, whereas the mean content of ^{226}Ra in fertilizers (about 4.0 pCi/g) is about 10 times more than its content in the soil (0.76 pCi/g) (Drichko et al., 1977).

The great variety of physical and chemical characteristics of the heavy natural radionuclides (with a mass of more than 200) produces a very wide range of differences in their transfer patterns in the biological and food chains. Biological absorption coefficients of

heavy NRE during transfer from the soil to plants of the same species range over two orders of magnitude, with a maximum ($n \cdot 10$ to $n \cdot 10^2$) for ^{226}Ra and a minimum for thorium radioisotopes (less than 1.0). The relative biogenic mobility of heavy natural radionuclides in the "soil—plant system" is described by Ra > U > Th.

The different chemical mobilities of these radionuclides determine geographical differences in their mobility and content (in the soil) in various regions of the USSR. The usual content of these radionuclides in the soils of the country can vary by 10 or more times, and, natural radioactive anomalies being considered, these variations can reach 1000 or more times. The ^{238}U content in the natural waters of the USSR increases from $n \cdot 10^{-7}$ to $n \cdot 10^{-5}$ g/liter from the northwest to the southeast. The mobility of the main heavy NRE in the water is described by U > Ra > Th, i.e., this sequence differs somewhat from the soil—plant system.

Our studies of the "rocks—water—soil—plants" system show that those radionuclides which are "fresher," i.e., which are daughter products, are characterized by greater mobility than those which stayed in the soil for longer periods. Thus analyses of isotopic spectrums in the soil—plant system shows that ^{224}Ra is more mobile than ^{226}Ra, ^{234}U is more intensively absorbed by plants than ^{239}U, and such radionuclides as ^{238}Th and ^{230}Th are more mobile on transfer to the plants than ^{232}Th. Similar differences in isotopic ratios are also found between liquid and solid phases in the soil—water system.

These data are of double interest: on the one hand, they confirm the dependence of heavy NRE absorption on their chemical form, and on the other hand they show that in the transfer of heavy NRE from the technological cycles to the biosphere (for example, the wastes from uranium ore processing) they can be more mobile than their more stable analogs. Various mobilities of different radionuclides of the same elements naturally present in the soil in situ and introduced by man were shown experimentally.

The transfer of NRE of the uranium and thorium series from the soil to the food chains determines internal whole-body irradiation of man (average dose of 35 mrems/year in the USSR). The calculations show that, regardless of the use of fertilizers, the mean individual doses of internal whole-body irradiation remained for the last 10 years within 0.1 mrem/year. Long (by the order of tens and hundreds of years) use of fertilizer with the highest content of NRE of the uranium and thorium series can lead to significant (1.5 to 2.0 times or more) increase of the population dose as a result of internal irradiation by natural radionuclides.

BUILDING MATERIALS OF MINERAL ORIGIN

Radiation inside buildings is one of the most important and interesting types of human exposure to NRE. The importance of this problem is determined by the comparatively large radiation doses that can be received in buildings built of mineral materials. Part of the dose is caused by external gamma radiation, but the main source of the dose is probably the inhalation of the alpha-emitting exhalation products of radium and thorium. The concentrations of ^{222}Rn and other decay products of ^{226}Ra inside the buildings often exceed their concentration in the open air by tens and hundreds of times. The highest content of NRE is found in the building materials obtained from rocks (some types of gravels or slags added to concrete, building stone blocks, etc.) (Krisyuk et al., 1974).

It should be noted that the increase in the lung cancer mortality rate observed throughout the world (especially in urban populations) over the last several decades parallels an increase in the number of people living in stone buildings. In rural regions of our country people usually live in wooden houses, and this may be the main factor responsible for a lower death rate from lung cancer in rural population.

The dose rate inside the brick and concrete buildings is on an annual average about 12 μrads/hr; the dose rate inside the wooden houses is about 6 μrads/hr. Consideration being given to the sizes of the urban and rural populations in the USSR, these values predict an average dose of about 60 mrems/year to the whole body from external irradiation (Vorobyev et al., 1977). The mean radiation dose to the lungs from inhalation of decay products of radium and thorium is about 400 mrems/year. The radiation exposure of the bronchial epithelium can be five times more, i.e., 2 rems/year. The radiation doses to the gonads and the bone marrow are only 2 to 4 mrems/year.

About 10% of all deaths from lung cancer in the country probably are due to exposure to radionuclides that enter the air of the dwelling houses from the building materials of mineral origin. In those cities where gravels, slags, and other building materials with increased content of ^{226}Ra are used, this value is much higher.

COMPARATIVE CONTRIBUTION OF NATURAL RADIONUCLIDES TO THE POPULATION DOSE

Mean individual radiation doses to the population of the USSR for 1976 to 1977 are given in Table 7. The continuous injection of

TABLE 7

Average Individual (Population) Radiation Doses in the USSR from the Main Artificial and Natural Radiation Sources

Radiation sources	Level of dose, mrems/year to the whole body
Natural background	110
Medical X-diagnostic	72
Building materials	60
Worldwide fallout	2
Luminescent watch	1
Air transport	<0.5
Television	<0.2
Fossil-fuel power station releases*	3.6×10^{-3}
Nuclear power station releases	$<1.0 \times 10^{-3}$
Mineral fertilizers	<0.1
Total	246

*Dose due to only external irradiation from the ash deposited on the ground.

natural radionuclides into the biosphere has already resulted in a significant increase in the population dose. Today, irradiation due to "migration" of large numbers of people to stone buildings has led to a greater increase in the population dose than the corresponding development of nuclear electric power or other types of atomic energy. This process will obviously retain its significance in the near future. There is also no doubt that irradiation due to the use of atomic energy will constantly increase as well. Therefore measures for possible reduction of the population dose by regulating radiation exposures due to NRE contained in the building materials, fertilizers, and coal seem very important.

REFERENCES

Atomizdat, 1974, *Twenty Years of Atomic Energy*, Moscow.

Drichko, V. F., E. M. Krisyuk, I. G. Travnikova, E. P. Lissachenko, and M. A. Dubinskaya, 1977, Frequency Distribution of ^{226}Ra, ^{228}Th, ^{40}K Concentrations in Arable Soils, *Pochwovedenije*, No. 9: 75-78.

International Commission on Radiological Protection, 1976, Publication No. 26.

Jawarowsky, Z., J. Bilkiewicz, E. Dobosz, D. Grzybowska, L. Kownacka, and Z. Wrónski, 1974, Radiation Hazards to the Population Resulting from Conventional and Nuclear Electric Power Production, in *Environmental Surveillance Around Nuclear Installations*, Symposium Proceedings, Warsaw,

1973, pp. 403-412, International Atomic Energy Agency, Vienna (STI/PUB/353), Vol. 1.

Knizhnikov, V. A., and R. M. Barkhudarov, 1977, Comparative Estimation of Radiation Safety for Population from Releases of Fossil-Fuel and Atomic Power Stations, *Atomn. Energ.*, 43(3): 191-196.

Krisyuk, E. M., S. I. Tarasov, V. P. Shamov, N. I. Shalak, and E. P. Lissachenko, 1974, *The Study and Normalization of Radioactivity in Building Materials*, Atomizdat, Moscow.

Martin, J. E., E. D. Harward, D. T. Oakley, J. M. Smith, and P. H. Bedrosian, 1971, Radioactivity from Fossil-Fuel and Nuclear Power Plants, in *Environmental Aspects of Nuclear Power Stations*, Symposium Proceedings, 1970, pp. 325-337, International Atomic Energy Agency, Vienna (STI/PUB/261).

Vorobyev, E. I., L. A. Ilyin, V. A. Knizhnikov, D. I. Gusev, and R. M. Barkhudarov, 1977, The Atomic Energy and Environment, *Atomn. Energ.*, 43(5): 374-384.

DISCUSSION

Bouville: The local doses arising from discharges from coal-fueled power plants seem to me to be very high, especially the bone doses from ^{210}Po. I would like to know whether those doses were calculated from measured concentrations in diet or if they are completely theoretical. If they are theoretical, what were the assumptions used?

Barkhudarov: All values (fallout, soil contamination, concentration in diet, body burdens) represented in our paper have been calculated only theoretically. The most extreme conditions have been used: (1) all radon contained in the coal is released into atmosphere; (2) the radionuclides contained in the coal ash are fully accessible for vegetation; and (3) all ash is found in the surface layer of soil (20 cm). Contamination of diet and food stuffs was calculated by liner model: $C_d(f) = P_f F_f(f) + P_s F_s(f)$, where P_f (fallout coefficient) is about 10 times higher than P_s (soil coefficient). The maintenance of radionuclides in the human body was calculated by exponential model. For ^{210}Po, taken into account was its accumulation in the bone due to radioactive decay of ^{210}Pb. The ratio ^{210}Po/^{210}Pb in the bone was 0.7. Obtained data of absorption doses can be several times higher than realistic ones.

Tanner: In the USA the long-term hazard from nuclear power stations is likely to be from disposal of waste. Does the USSR have a plan for permanent disposal of waste?

Knizhnikov: The USSR has a plan for long-term disposal of waste. However, I would like to note that this is an economical and technological problem. It is known that the main factor of the formation of dose burden is the content of radionuclides in atmospheric releases.

Radiological Evaluation of Structures Constructed on Phosphate-Related Land

RICHARD J. GUIMOND and SAMUEL T. WINDHAM
Office of Radiation Programs, U.S. Environmental Protection Agency

ABSTRACT

A study of the radiological impact of living in structures built on reclaimed phosphate-mine land was conducted in Central Florida. The study concluded that areas which contain radium-bearing soil associated with phosphate materials generally have greater gamma exposure and indoor radon-decay-product concentrations than normal background areas in Florida. Average indoor radon-decay-product levels of up to 0.20 working level (WL) were measured. Various soil and structure characteristics are represented in the study. These characteristics were examined to evaluate their significance on the indoor radiation levels.

In June 1975 the U.S. Environmental Protection Agency (EPA), in conjunction with the Florida Department of Health and Rehabilitative Services (DHRS) and the Polk County Health Department, initiated a pilot study to examine the radiological impact of living in structures built on reclaimed phosphate mine land. The study was a part of a comprehensive investigation conducted by EPA covering all impacts from releases of radiation and radioactive materials directly or indirectly due to the phosphate industry.

The study area was the Bone Valley Phosphate Region of Central Florida which is shown in Fig. 1 along with the other phosphate mineralized regions of Florida. In 1975 about 93% of the U. S. phosphate mine rock production came from Florida with the remainder coming from Tennessee and several western states (Stowasser, 1975). About 174 million tons of phosphate mine rock was extracted in 1975. Over the 80 years that phosphate has been mined in Florida, a total of about 2 billion tons of phosphate mine rock has

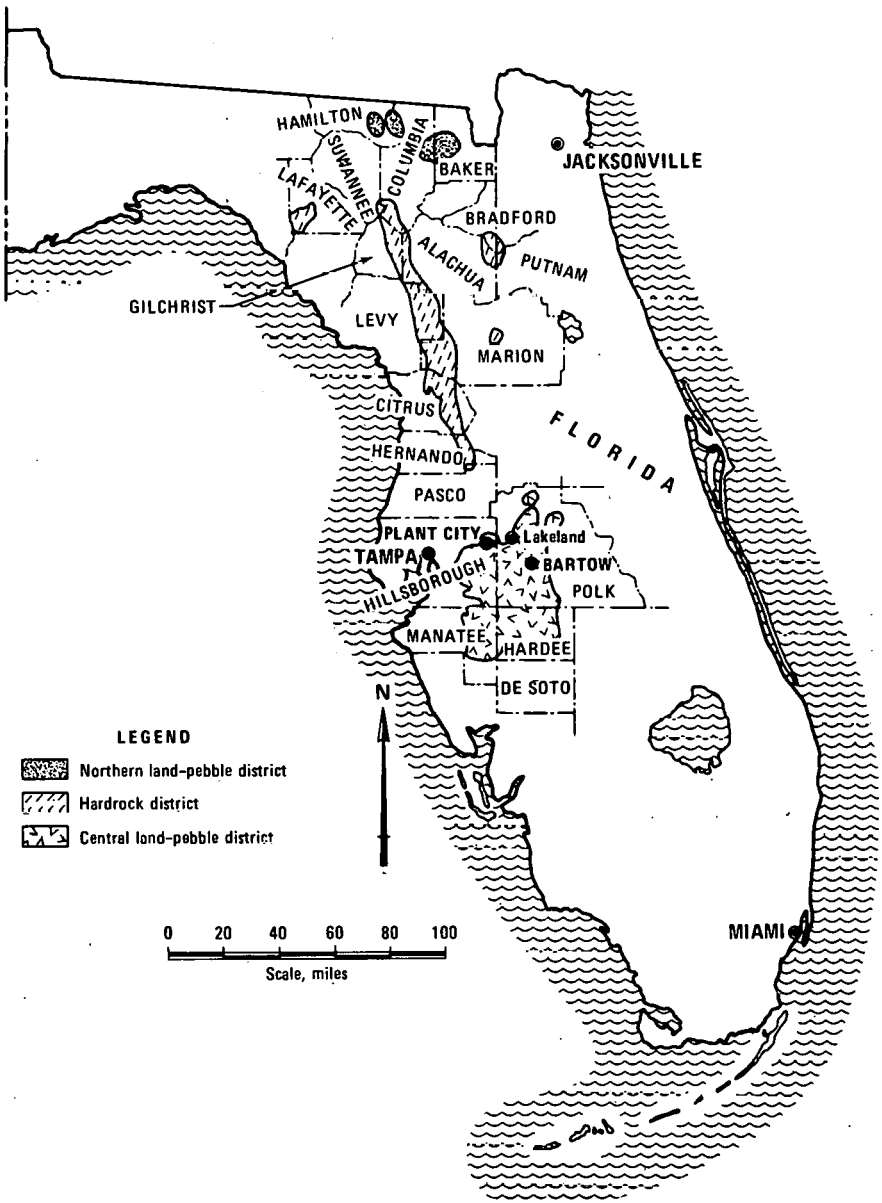


Fig. 1 Phosphate deposits in Florida. [From Bureau of Mines Circular 8653, *Economic Significances of the Florida Phosphate Industry.*]

been extracted through the strip mining of approximately 150,000 acres of land (Cathcart and Gulbrandsen, 1973; Wang, 1974).

Uranium is present in the phosphate matrix at varying concentrations which are usually 100 to 150 ppm (35 to 55 pCi/g). The uranium is generally in equilibrium with its decay products at least through ^{226}Ra (Guimond and Windham, 1975). Radioactivity is also present in parts of the overburden. Figure 2 shows the general

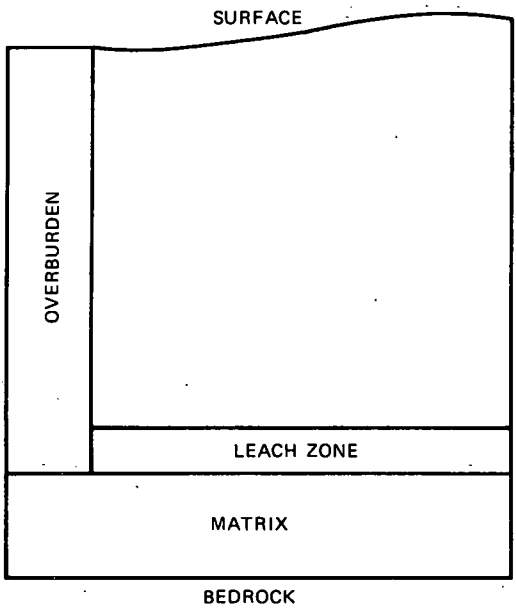


Fig. 2 General economic geology of Florida land-pebble deposits.

geological structure found throughout much of the Florida land-pebble district. A "leach zone," which is about 5 ft thick and covers much of the pebble deposits, contains radium in concentrations comparable to that of the matrix. In some areas other portions of the overburden also contain elevated radioactivity, although not in such high concentrations (Cathcart, 1966).

Unmined, reclaimed, and disturbed phosphate land can be composed of widely varying concentrations of ^{226}Ra depending on the relative thickness and presence of low activity overburdened soil and sand tailings to higher activity matrix, slimes, or leach zone material.

RADON TRANSPORT INTO STRUCTURES

Radon-222 is produced in the soil through the decay of ^{226}Ra. It is transported through the soil through various mechanisms and enters structures built on the ground through the foundation. The balance of ^{222}Rn in a structure can be simply characterized by the following equation: at equilibrium $Rn_{in} = Rn_{out}$. The rate of ^{222}Rn leaving the structure is

$$Rn_{out} = C_I\lambda_v V + C_I\lambda_R V \quad (1)$$

where C_I = Rn-222 concentration in the structure, pCi/m^3
V = volume of the structure, m^3
λ_v = effective ventilation rate, sec^{-1}
λ_R = radiological decay constant, 2.1×10^{-6} sec^{-1}

Therefore

$$Rn_{in} = C_I V(\lambda_v + \lambda_R)$$

and

$$C_I = \frac{Rn_{in}}{V(\lambda_v + \lambda_R)}$$

Ventilation rates in structures usually range between 0.5 to 5 air changes per hour; therefore λ_v ranges from 1.4×10^{-4} sec^{-1} to 1.4×10^{-3} sec^{-1}. Since $\lambda_v \gg \lambda_R$, $\lambda_v + \lambda_R \simeq \lambda_v$ and

$$C_I = \frac{Rn_{in}}{V\lambda_v} \quad (2)$$

As noted by Eq. 2, within a structure, the principal variables in determining the indoor radon concentration are the entrance rate and the effective ventilation rate.

STUDY DESIGN: TECHNIQUES AND PROCEDURES

Structures were selected in Polk County that were constructed on phosphate mineralized land, nonmineralized land, and reclaimed land. Gamma radiation exposure was determined inside and outside each structure with portable scintillometers calibrated with a pressurized ion chamber relative to a slab source (phosphate

materials). The average indoor and outdoor gamma exposures were estimated by determining the mean of several measurements inside and outside the structures, respectively.

Several techniques were used for measuring the radon-decay-product levels within structures. These were: radon progeny integrating sampling units (RPISU), track etch badges, an instant working level meter (IWLM), and alpha spectrometry.

A total of 133 structures had WL measurements made for a period of 1 year using the RPISU devices. A total of 153 structures had WL measurements made for a period of about 1 year using track etch badges. Some structures had both track etch badges installed as well as RPISUs whereas others had only one of the dosimetry systems. At each location data were collected according to classification (residence, business, etc.), construction type (basement, slab, crawl space, etc.), number of levels, material (masonry, nonmasonry), and whether it was air conditioned.

At one location detailed measurements were made regarding selected parameters over an extended time period. This is discussed in more detail later in the paper.

CALIBRATION OF TRACK ETCH FILMS

The calibration of the track etch films used in the study was accomplished by randomly selecting 22 structures and installing track etch films and air sampler (RPISU) devices in each of them. A total of two or three films were used in each structure. In the structures one film was deployed for a period of about 1 year and the other two films were deployed for consecutive 6-month intervals coincident with the film in place for a year. The RPISU devices were operated for approximately a 1-week period for 4 to 7 weeks during the year, with at least 1 week in each of the four seasons.

The data set for statistical analysis was comprised of 40 points from 22 locations. Two types of film measurements were included. The first was the set of films exposed for the entire year. The second was constructed by summing results of two films exposed to consecutive 6-month periods at the same location. These two types of measurements did not differ significantly. Corresponding air-sampler measurements (RPISU) for indoor working levels are averages of from four to seven measurements taken during the study period at each of the 22 locations. The data were analyzed with the air-sampler data as the independent variable and the track etch film data as the dependent variable.

The equation that best describes the relationship between track density on the films and air pump measurements is

$$W = T/0.06978 \quad (3)$$

where W is the exposure measured in WL hours and T is the track density measured in tr/mm^2.

The 95% confidence interval for predicted W from a measured T is

$$\frac{T}{0.06875} \pm 250\left(0.9852 + \frac{T^2}{19{,}967}\right)^{1/2} \quad (4)$$

It should be noted that the formula for the confidence interval is not in a standard form but has been rearranged for easy computing. It is noted that Eq. 3 passes through the origin. This situation is suggested by theory, but various factors could make it intercept the y-axis at another point. A correlation developed for measurements made in Grand Junction, Colo., did not pass through the origin. The formulas given here are valid for exposure times of approximately 1 year. Results from analyses of 6-month exposures suggest some seasonal variation, and therefore conversions from track density to radon exposure based on short-term data should not be done using these formulas. Figure 3 is a plot of the formula with the 95% intervals identified. As the origin is approached, the percentage of error rapidly increases. For example, at 60 tr/mm^2, the 95% interval is about ±30%, whereas at 20 tr/mm^2 it is about ±100%.

By the use of the exposure period and measured track density data for each structure and the calibration formula, average indoor radon decay product levels were calculated for each test structure where a track etch film was in place for about 1 year.

TOTAL BACKGROUND EXTERNAL RADIATION LEVELS

Measurements of the total normal background in Central Florida were made by EPA in several locations with various types of detection equipment. The average outdoor gamma exposure level measured with portable scintillation instruments at 26 structures built on unmined nonmineralized land was 45 mrems/year (5 μrems/hr). For these same structures, indoor gamma exposure levels averaged 43 mrems/year (4.9 μrems/hr). In Dundee, Lake Wales, and Polk City, Fla., which are outside the phosphate area, thermoluminescent dosimeters (TLDs) were placed and left for an extended time period. The average of these measurements was 41 mrems/year

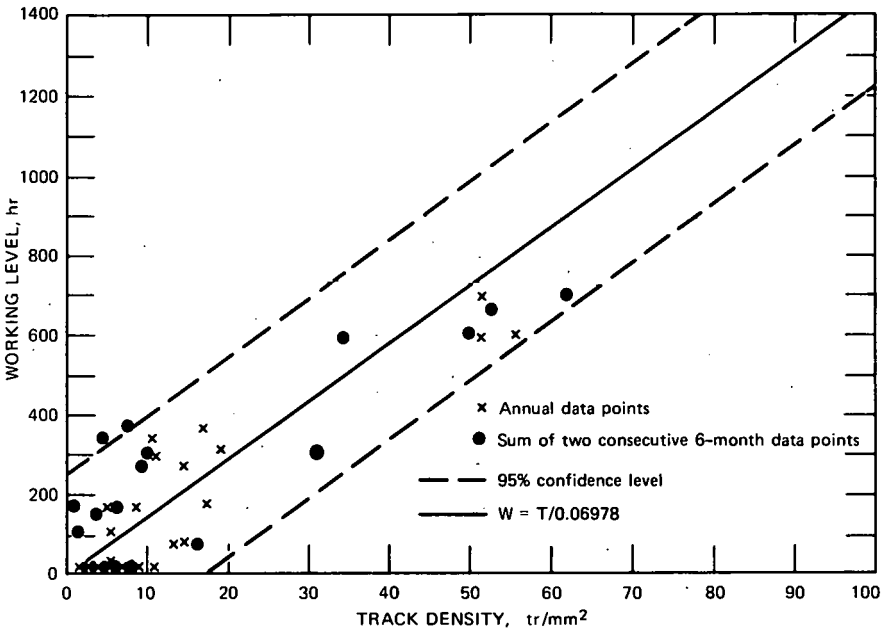


Fig. 3 Calibration formula at 95% confidence level.

(4.7 μrems/hr). Pressurized ion chamber measurements were made at nine locations outside the phosphate region. The average of these measurements was 51 mrems/year (5.8 μrems/hr). It should be noted that the measurements by portable scintillation instruments and TLDs will not reflect cosmic-ray exposure as accurately as the pressurized ion chamber.

NORMAL RADON-DECAY PRODUCT LEVELS

Radon in the atmosphere primarily originates from the decay of radium in soil and rocks. The outdoor radon concentration at ground level depends on the rate of radon emanation from the ground and its dispersal rate in the atmosphere. Inside structures the concentration of ^{222}Rn and its decay products is generally considerably higher than corresponding outdoor concentrations because of poorer indoor dispersion characteristics. Measurements using the RPISU system in 26 structures on nonmineralized land in Central Florida showed an indoor average of about 0.004 WL (0.0007—0.014 WL) over a 1-year period.

DATA ASSESSMENT

Evaluation of Radon Progeny Levels in Structures with RPISU

The RPISU draws air through a particulate filter, measuring the radon progeny radiation with a TLD. These air-sampling units were rotated to the subject structures on a periodic basis to ensure several measurements at each structure which would reflect any seasonal and diurnal variations in radon-decay-product concentrations.

TABLE 1

EPA and DHRS Annual Average Indoor Radon-Decay-Product Levels Distribution (RPISU)

Level, WL gross	EPA	DHRS	Composite
Greater than 0.05	5	3	8
0.03 to 0.05	3	9	12
0.01 to 0.03	4	22	26
Less than 0.01	10	77	87
Total	N = 22	N = 111	N = 133

Of the 133 locations sampled with these devices, 22 structures were from the original pilot study initiated by EPA, with the remainder selected later as a part of the population group chosen by the Florida Department of Health and Rehabilitative Services (DHRS). The TLDs from the group chosen by the DHRS were read out either by EPA or DHRS. The TLDs from the original pilot group were read out only by EPA. The distribution of the two samples vary to a large degree, although this would be expected owing to the smaller pilot study sample size and the practical aspects of selecting the structures. In the selection of the EPA pilot group, the agency picked houses known to be on reclaimed land. This was confirmed by external gamma measurements made on site. The DHRS study group was selected from reviewing land records showing reclaimed and other types of land. Consequently the DHRS group has a greater percentage of its reclaimed land structures exhibiting lower external gamma and indoor radon-decay-product levels than the EPA pilot group. The distributions of each group are shown in Table 1.

From information collected in the survey, the land on which the structures were constructed was classified according to four categories: nonmineralized (no deposits), mineralized (deposits present, but unmined), reclaimed, and other (primarily missing or lack of

information). Of the 133 structures, the annual average indoor radon-decay-product concentration for each category is shown in Table 2. The land categories are abbreviated as ND, M, R, and O, respectively. This distribution indicates that mineralized land may have as much radiological impact as reclaimed land. However, the most elevated levels are on reclaimed land. The highest annual average indoor concentration observed with the RPISU system was 0.10 WL.

TABLE 2

Distribution of Indoor Radon-Decay-Product Levels According to Land Classification (RPISU)

Level, WL gross	M	ND	R	O
Greater than 0.05	0	0	8	0
0.03 to 0.05	1	0	11	0
0.01 to 0.03	4	1	19	2
Less than 0.01	4	28	55	0
Total	N = 9	N = 29	N = 93	N = 2
Average level	0.015	0.003	0.016	0.018

To delineate the influence of structure design (particularly foundation design) on radon transport into the structure, we evaluated the average annual WL measured in various types of structures. Four typical structure types found in Central Florida are basements, slabs on grade, crawl spaces, and trailers. The distribution of annual average indoor radon-decay-product concentrations for each category is shown in Table 3. The structure categories are abbreviated as B, S, C, and T, respectively. Although sample size for these categories may influence the distribution, the indication is that crawl space and trailer design allow less radon transport and buildup than typical basement or slab on grade constructions. Some levels in crawl space and trailer design houses are elevated because of contiguous additions to the structures which are of slab on grade design or enclosure of the crawl space under the structure.

Ventilation has been identified as a determining factor on the degree of buildup of radon-decay products. The use of air conditioning in the study structures was of interest because it was initially believed that maintaining a lower indoor temperature at a reasonable cost entails reducing the degree of infiltration of ventilation from the outside air. It was anticipated that houses without air conditioning would have more natural ventilation and therefore lower average

TABLE 3

Distribution of Indoor Radon-Decay-Product Levels According to Structure Type (RPISU)

Level, WL gross	B	S	C	T
Greater than 0.05	0	7	1	0
0.03 to 0.05	2	9	0	1
0.01 to 0.03	0	21	3	2
Less than 0.01	2	65	9	11
Total	N = 4	N = 102	N = 13	N = 14
Average level	0.02	0.015	0.01	0.008

radon-decay-product levels. However, studies by EPA show that operation of a central air-conditioning system does tend to significantly reduce the indoor radon-decay-product levels when compared to no air flow (Windham, Savage, and Phillips). This is discussed in more detail later in the paper. This reduction is attributed to plate out of decay products in the ventilation system as well as increased influx of outside air due to pressure difference brought about by the operation of the ventilation system. Data collected for the 133 structures show that the annual average working level for structures with and without conditioning is 0.012 and 0.016 WL, respectively. This implies that any short-term differences caused by operation of the air-conditioning system or opening of windows for natural ventilation are minimized when considering the average indoor levels over extended periods.

Evaluation of Radon Progeny Levels in Structures with Track Etch Films

Films were placed in a structure for at least a year, after which a representative portion of the etches were counted to determine alpha energy deposition. This was translated into an estimate of the indoor radon-decay-product levels through the use of calibration curves as previously discussed. The distribution of average annual indoor radon-decay-product levels according to land category is shown in Table 4. The highest annual average indoor radon-decay-product concentration observed track etch film was 0.14 WL.

Evaluation of Gamma Exposure Levels

Gamma exposure rate measurements were made at 1101 sites by both EPA and DHRS. The gamma surveys were performed with a

TABLE 4

Distribution of Indoor Radon-Decay-Product Levels According to Land Classification, Track Etch

Level, WL gross	M	ND	R	O
Greater than 0.05	3	0	26	0
0.03 to 0.05	0	1	13	0
0.01 to 0.03	4	11	41	2
Less than 0.01	1	15	32	4
Total	N = 8	N = 27	N = 112	N = 6

standard portable scintillometer held about 1 m from the floor or ground level for indoor and outdoor measurements, respectively. Average indoor and outdoor external gamma exposure rates were estimated from several indoor and outdoor measurements.

The distribution is summarized in Table 5 for outdoor external gamma exposure rates according to three primary land categories: reclaimed nonmineralized, mineralized, and reclaimed. The highest outdoor external gamma exposure rate observed was 42 μR/hr.

The influence of structural design, especially the degree of foundation shielding, was evaluated for the four structure types considered in this study. The average ratio of indoor gamma levels to corresponding outdoor gamma levels was calculated and found to be fairly similar for all structure types (about 0.9). However, a percent distribution plot of the indoor gamma exposure rate by structure type for reclaimed land shows 12 and 18% of crawl space structures and trailers having gamma rates in excess of 20 μR/hr. In contrast, both basement and slab on grade structures showed no measured values in excess of this level. This observation correlates with the

TABLE 5

Distribution of Outdoor External Gamma Exposure Rates

Level, R/hr	Reclaimed	Mineralized	Nonmineralized
Greater than 20	49	1	0
11—20	175	4	8
Less than 11	447	97	292
Total	N = 671	N = 102	N = 300
Percent of total structures	61%	9%	27%
Average gamma exposure	11 R/hr	7 R/hr	6 R/hr

degree of floor shielding present in these structures with the latter two having concrete bases and the former just wood or thin metal.

INTENSIVE STUDY OF ONE STRUCTURE

An extensive study was conducted at a single structure built on reclaimed land to determine the effects of typical home ventilating systems on indoor radon and radon-decay-product concentrations. The home was a single family unit, which had a single floor, with masonry construction, and was a slab on grade. It was typical of houses in the area. The house, which was approximately 187 m^2, was heated and cooled by a central recirculating air system. The air conditioning/heating unit was located in the attic space with all air delivery ducts in the ceiling of each room. No make-up or fresh air was intentionally introduced into the system. The house was unoccupied at the time of the study which covered a 17-day period.

In the course of the study, many parameters were measured in and around the study house. These included radon and radon-decay-product concentrations, working level, condensation nuclei, temperature, relative humidity, and outside meteorological conditions.

Measurements of radon concentration in the house were made using 125-cm^3 volume scintillation cells. An air sample to be counted for radon was drawn into an evacuated cell through a drying column and filter to remove water vapor and radon daughters. The sample was counted after an appropriate time for radon daughter ingrowth was allowed.

Measurements of radon-decay-product concentrations were performed in several ways. In one method, depending on the decay-product levels expected, 50 to 300 liters of air were drawn through an 0.8-μm pore size filter which was then counted on an alpha spectroscopy system using a surface barrier detector. Data were accumulated in a 1024 channel analyzer and computer-reduced to determine the working level and radon-decay-product values. Methods of data reduction described by Harley and Pasternack were also used in some cases to obtain immediate results at the study site.

Measurements of working level and radon-decay products were also made with a prototype instant working level meter (IWLM) developed by Argonne National Laboratory (Groer and Keefe, 1974). This instrument draws approximately 20 liters of air through a 1.2-μm pore size filter then counts the filter for 3 min. Both alpha and beta detectors are used. Data are reduced in the instrument, and the working level and individual decay-product concentrations are

displayed digitally in only 6 min. This ability to sample and obtain data rapidly was very useful in the ventilation experiments performed in the house. Comparisons of data were made between those produced by the alpha spectroscopy methods described previously and by the IWLM. Comparison of these two measurement techniques showed that the data produced agreed satisfactorily. The radon-decay-product concentrations used to estimate ventilation rates and equilibrium ratios were determined by the alpha spectroscopy method.

Concentrations of airborne submicron particles were determined with a condensation nuclei monitor which recorded the real-time concentration of nuclei. The instrument detects particles with diameters of 0.0025 μm and larger in concentrations from 50 particles per cubic centimeter up to 10^6 particles per cubic centimeter of air. Outdoor meteorological data were obtained from a National Weather Service facility located approximately 9.7 km from the house. Air velocities through windows or through the ducts and grills of the central heating/cooling system were measured with a thermoanemometer.

At the beginning of the study, the house had been unoccupied and closed for 10 days. The central heating and air-conditioning system had been off for this period and all windows had been closed. The only air exchange with outside air was due to leakage around or through window and door cracks, flaws in the weather stripping, etc. It was believed that the radon-decay-product level in the house at this time would be at a maximum for the particular set of environmental parameters which affect radon influx into the structure. Several measurements of the WL for the closed structure ranged from 0.17 to 0.20. Outside ambient levels, 0.5 to 1.5 pCi/liter radon, 0.003 to 0.005 WL, determined before experiments were sufficiently lower than unventilated levels found in the house to preclude interference from diurnal variation. Measurements showed the relative radon-decay-product equilibrium (WL x 100/Rn) to range from 0.41 to 0.44 for this set of conditions. On the basis of the relative concentrations of RaB (^{214}Pb) and RaC (^{214}Bi) measured in the house during the closed condition, it was estimated that the house had an inherent ventilation or infiltration rate of approximately 0.4 to 0.6 air changes per hour. This is consistent with commonly accepted values of 0.5 to 1.5 air changes per hour for occupied homes. An unoccupied home such as this would be expected to have a slightly lower ventilation rate.

Previous unpublished work by EPA and others indicated that operation of a central heating or air-conditioning system would

reduce the radon- and decay-product concentrations inside a home. This was reported even in houses equipped with a system which did not introduce "fresh or make-up" air into the central system. A study was conducted in the house to quantitatively determine the reduction of radon and WL caused by operation of the central air-conditioning system. The house had been closed and the air-conditioning system off for at least 12 hr before the beginning of the study. Measurements of radon and radon-decay products were made before and at selected intervals for approximately 700 min after the air-conditioning system was turned on.

TABLE 6

Air-Conditioning Experiment Data

	Radon, pCi/liter	WL	Equilibrium, WL X 100/radon	Condensation nuclei per cm^3	Ventilation rate, air changes per hr
Baseline	34	0.11	0.35	6×10^3	0.50
Steady state	7	0.01	0.10	3×10^3	2.5

Data presented in Table 6 are an average of two separate but duplicate experiments. After approximately 180 min of continuous running, the radon-decay-product concentrations had been reduced by a factor of approximately 10. Radon levels were reduced by a factor of approximately 5. At the time the air conditioner was turned on, the indoor temperature was 30°C. The system thermostat was set at 24°C, and the system ran continuously for approximately 180 min to lower the temperature sufficiently for the unit to cycle. After reaching this point, the unit continued to cycle as might be expected in a typical occupied home.

Since no makeup air was intentionally introduced into the system, it is assumed the increased ventilation rate resulted from leaks in the duct system and alteration of the relative indoor/outdoor pressures.

It was believed that the reductions in radon- and decay-product levels as measured during the air-conditioning experiment resulted from the movement of air and not as a result of cooling the air. If this were the case, then the central heating system or simply the operation of the central fan or blower would have the same effect. Accordingly, measurements of radon and radon-decay-product con-

centrations were made before and at selected intervals for 600 min after the central blower was started.

Data presented in Table 7 are an average of two separate but duplicate experiments. After approximately 180 min of operation, the WL had been reduced by a factor of 9. Radon levels had been reduced by a factor of 6. The central fan system ran continuously during the experiment with no cycling. Air flow in the duct system was the same as in the air-conditioning experiment.

All reductions in radon and radon-decay-product concentrations, changes in equilibrium, increases in ventilation rate, and condensa-

TABLE 7

Central Fan Experiment Data

	Radon, pCi/liter	WL	Equilibrium, WL X 100/radon	Condensation nuclei per cm^3	Ventilation rate, air changes per hr
Baseline	25	0.09	0.33	5×10^3	0.57
Steady state	5	0.01	0.15	3×10^3	2.1

tion nuclei concentrations were consistent with those measured in the air-conditioning experiment. This indicates that the reduction in radon and daughters was principally the result of increased ventilation rate due to air movement in the central duct system, not the cooling of air.

Another ventilation condition commonly encountered in most homes is when windows are opened and outside air is purposefully allowed to circulate through the house. The outside air at the time of this study had radon concentrations between 0.5 and 1.5 pCi/liter and working levels between 0.003 and 0.005. Although both the radon and radon-decay-product values may be slightly high for normal outside air, it is believed that the large amount of radon entering the atmosphere from nearby phosphate land tracts may cause somewhat elevated levels in this area. It was expected that these levels would quickly dilute the indoor levels when ventilation was initiated.

For an accurate measurement of the quantity of outside air entering through the open windows to be obtained, a window fan was used to exhaust a measured amount of inside air. Measurements showed that the influx rate of outside air equaled the exhaust rate of

the fan. A fan was installed in a window and used to exhaust indoor air from this location. Windows in the other rooms of the house were opened different amounts to assure approximately equal air flow through each room. The fan exhausted 0.68 m^3/sec which represents an air turnover rate of 5.4 changes per hour. The condition established by operation of the window fan is typical of what might be seen if windows remained open on a typical day with light winds. All measurements of radon and WL in the house were made in the central hall to avoid sampling in a direct flow of incoming outside air. Measurements of radon and its decay products were made before and at selected intervals for 160 min after the windows were opened and the window fan started.

TABLE 8

Outside Air Ventilation Data

	Radon, pCi/liter	WL	Equilibrium, WL X 100/radon	Condensation nuclei per cm^3	Ventilation rate, air changes per hr
Baseline	25	0.11	0.30	1.7×10^3	0.50
Steady state	1.5	0.01	0.08	$20–36 \times 10^3$	5.4

Data given in Table 8 are an average of two separate but duplicate experiments. Radon-decay-product values dropped from 0.11 to outdoor concentrations in 20 min. Radon concentrations also fell in 20 min from 25 pCi/liter to 1.5 pCi/liter. On the basis of the volume of air being moved by the fan, this reduction occurred after 1.8 air changes in the house.

From the work done in this structure, we found that other structures which differ appreciably in natural infiltration or ventilation rate would produce depletion rates different from those described above. In an old or poorly built new structure in which the natural leakage rate was high, the radon-decay-product buildup would not be as great for the same radon influx. In addition, the operation of a central air-movement system would produce a more rapid reduction in radon and decay-product concentrations. In a newly built house that incorporated extensive measures toward being an energy efficient structure, the natural infiltration or leakage would be low, and thus depletions would occur less rapidly for a given radon influx. Therefore, in conducting surveys of homes in

which the WL is to be measured, it may be necessary in some cases to determine the natural leakage rate.

In addition to the effects of the leakage rates, the living habits of the occupants have a great influence on the WL that may be measured. For example, a home which has several children who frequently exit and enter the house will have a greater turnover rate than a home which has no children and the adult occupants work during the day. The preference of the occupants for running the air-conditioning system vs. that for fresh air and opening windows must also be taken into account. Seasonal changes in the natural climatic conditions will also have an influence on the extent to which the occupant depends on outside air or the air-conditioning/heating system.

As a result of the factors discussed, it follows that a "grab sample" or short duration measurement of WL will generally not represent the average or typical condition for a structure. It was shown that, for a given radon input rate for a particular house, the WL as measured at any one period in time would be dependent on where the heating or cooling system was in its operating cycle or the number of windows and/or doors open and may vary by a factor of 10. For this reason, we believe that a single measurement of WL with no regard for these other factors could be very misleading in estimating an average value. To circumvent these problems, it would be necessary either to account for these variables at the time of measurement or take an integrated measurement over a sufficient time period to find the average WL.

CONCLUSIONS

Radium-226 associated with phosphate ores and reclaimed land can be a significant source of radon and its short-lived decay products within structures built on or with the materials. Reclaimed land appears to present the greatest potential for increased exposure to radon-decay products, although unmined land containing phosphate minerals can also present a hazard from this source if a structure is built on it.

Structures built using slab on grade construction techniques appear to be the most significant type of construction presenting a hazard from radon-decay products. This is because of the high prevalence of this type of design in Florida and the physical characteristics which make this type of structure design contiguous with the soil. Basements also appear to be of concern because they can allow considerable influx of radon. However, this design style is

used very infrequently in Central Florida. Structures built with open crawl space and trailers present the least hazard from radon originating in the soil. However, enclosure of the crawl space and/or construction of additions using a slab on grade design can greatly increase the indoor radon-decay-product levels.

Effective ventilation rate is a principal factor in determining the indoor radon and radon-decay-product concentrations. In structures where the underlying soil contained considerable ^{226}Ra concentrations, indoor radon-decay-product levels could be minimized if a concerted effort was made to assure high ventilation rates. Under normal conditions in Florida, effective annual ventilation rates in structures with air conditioning or no air conditioning do not appear to be markedly different.

Clearly, anyone considering the construction of structures on reclaimed phosphate land or land underlined by phosphate ores must recognize the possibility of indoor radon-decay-product levels up to 50 times normal concentrations unless adequate measures are taken during the structure design, site selection, and site preparation steps.

Additional investigation is necessary to develop guidelines for site and design evaluation. Methods are also needed for rapid screening of structures during a short time period to determine whether or not the annual average indoor radon-decay-product levels are undesirable.

REFERENCES

Cathcart, J. B., 1966, *Economic Geology of the Fort Meade Quadrangle, Polk and Hardee Counties, Florida*, Geological Survey Bulletin 1207.

——, and R. A. Gulbrandsen, 1973, *Phosphate Deposits, United States Mineral Resources*, Bobst and Pratt (Eds.), Geological Survey Professional Paper 820, U.S. Department of the Interior.

Florida Department of Health and Rehabilitative Services, 1978, Study of Radon Daughter Concentrations in Structures in Polk and Hillsborough Counties.

Groer, P. G., and D. Keefe, 1974, Argonne National Laboratory, Report P7334C.

Guimond, R. J., and S. T. Windham, 1975, *Radioactivity Distribution in Phosphate Products, By-Products, Effluents, and Wastes*, Technical Note ORP/CSD-75-3, Office of Radiation Programs, U.S. Environmental Protection Agency.

Stowasser, W. F., Phosphate Rock, *1975 Mineral Yearbook*, Bureau of Mines, Department of the Interior.

Wang, K. L., 1974, *Economic Significances of the Florida Phosphate Industry*, Information Circular 8653, Bureau of Mines, Department of the Interior.

Windham, S. T., E. D. Savage, and C. R. Phillips, *The Effect of Home Ventilation on Indoor Radon—Radon Daughter Level*, Report EPA-520/5-77-011, U. S. Environmental Protection Agency.

DISCUSSION

Naaroff: Could you say a few words about how you measured ventilation rates?

Windham: Ventilation *estimates* were made on the basis of the relative concentrations of radium B to radium C.

Silker: We found that the air-conditioning system effectively reduced fission-product concentrations in a reactor containment vessel's atmosphere, the concentrations being removed in the air-conditioner condensate. It didn't appear that this was the case for radon daughters presented by your data.

Windham: Yes, radon daughters were removed. In fact, the WL was reduced by a factor of 10. However, the operation of the central fan also reduced the WL, so it wasn't a function of cooling the air.

Tanner: Do you have information indicating whether or not the sand used in constructing the slabs used for houses over reclaimed land was the very purest sand normally found at the surface or sand recovered from phosphate tailings? It would make a substantial difference. Overlying the phosphate is a leached zone that is very clayey and impermeable, as a result of which the groundwater in the overlying sand is, according to my experience, less radioactive than we might otherwise expect. Do you have data on radon in well waters in the reclaimed land?

Windham: We have found no evidence to indicate that sand used in construction came from the phosphate industry, at least in the structures we surveyed in detail.

Regarding your second question, yes, we have a limited quantity of radon in water data for the Central Florida area.

Scott: Do you have any idea how the radon actually enters the houses from the soil?

Windham: Yes, some radon enters through the slab of the structure. However, we have found that a large portion of the indoor radon enters through cracks, voids, etc., in the slab.

The Effect of Mining and Land Reclamation on the Radiological Characteristics of the Terrestrial Environment of Florida's Phosphate Regions

C. E. ROESSLER, R. KAUTZ, W. E. BOLCH, JR.,
and J. A. WETHINGTON, JR.
College of Engineering, University of Florida, Gainesville, Florida

ABSTRACT

Studies were performed to evaluate the extent and nature of the redistribution of uranium-series radioactivity in phosphate mining, reclamation, and land development. Radium-226 was measured in waste materials that enter into land reclamation. Radium-226 surface soil concentrations and depth profile, soil surface radon flux, and gamma radiation above the surface were reported for unmined and mined, reclaimed, and otherwise altered lands. Mining, land reclamation, and construction site preparation can increase the near-surface soil radium and related characteristics. There is a general pattern with land type. The impact was evaluated in terms of effect on actual and potential indoor radon progeny concentrations in structures. It was concluded that debris lands, resulting from a former mining practice, represent the greatest impact on existing structures. However, a fraction of the lands produced by current practices may exceed criteria for unrestricted use if such criteria are based on limiting predicted indoor radon progeny concentrations in future structures to the lower limit of the Surgeon General's guidelines. Procedural modifications were identified for producing lands likely to meet criteria for unrestricted use.

Uranium and its decay series are associated with phosphate deposits. Recently, considerable attention has been focused on this naturally occurring radioactivity and the possible environmental effects of phosphate mining and processing, land reclamation and development, and product, by-product, and waste-product distribution, use, or disposal. In 1975 the U. S. Environmental Protection Agency (EPA) reported that the data from preliminary sampling suggested elevated levels of airborne radon progeny and a possible increased risk of lung cancer to residents in structures built on reclaimed Florida phosphate

land (U. S. Environmental Protection Agency, 1975). Other impacts, including possible effects on radioactivity in ambient air, the food chain, and surface and ground water, have been raised in the press and in private discussions. The purpose of this study was to develop basic data for (1) assessing the radiological impact on the environment of mining, beneficiation, and land reclamation and (2) devising recommendations for modification of procedures to minimize such impact if indicated.

DESCRIPTION OF PHOSPHATE LANDS AND MINING

Location and Nature of Florida Phosphate Deposits

Present-day phosphate mining in Florida is carried out in the two districts shown in Fig. 1, the North Florida land-pebble district of

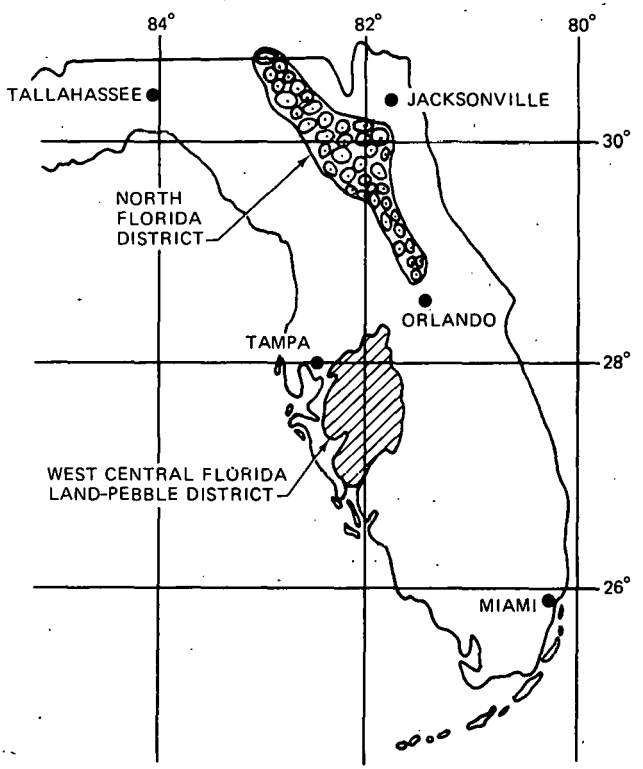


Fig. 1 Map of Florida showing location of phosphate districts (adapted from Cathcart, 1970).

Columbia and Hamilton counties and the Central Florida land-pebble district of Polk, Hillsborough, Manatee, Hardee, and De Soto counties (also referred to as West Central Florida and as the Bone Valley formation). The commercially recovered calcium phosphate-bearing ore or matrix ranges from <1 to 15 m thick and averages 4 m; it lies under a sand and clay overburden that varies from ~1 to 20 m thick. Much of the Central Florida matrix and some of the North Florida matrix is overlain by an irregular aluminum phosphate leached zone which may be as thick as 15 m but which is typically <1 to 5 m thick. Uranium is reported to be concentrated in the lower portion of the leached zone (Altschuler, Cathcart, and Young, 1964; Cathcart, 1970).

Phosphate Mining and Beneficiation

The flow of the major solid materials in phosphate mining and rock beneficiation is shown in Fig. 2. The overburden is removed and cast aside so as to expose and remove the matrix. The leached zone, when present, may be designated as part of the overburden or as part

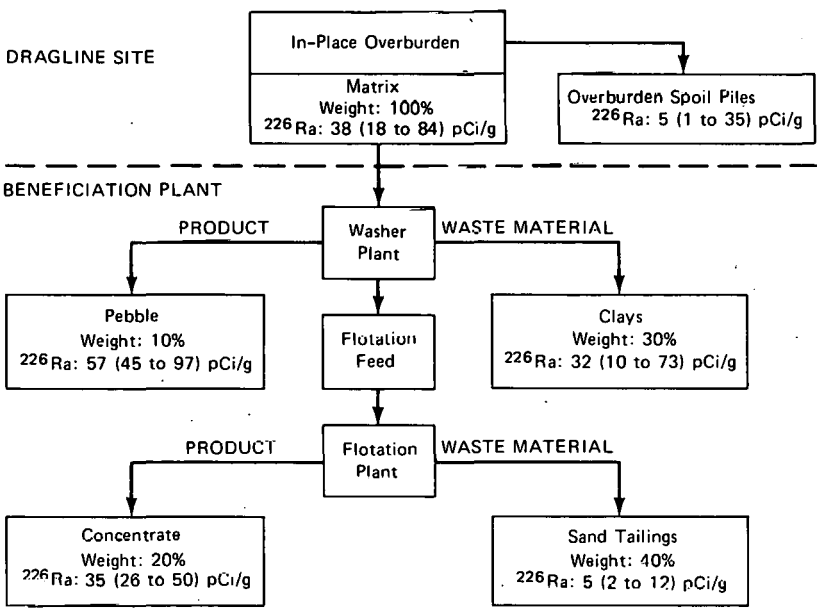


Fig. 2 Flow diagram for major products and mineral waste products of phosphate rock mining and beneficiation. Geometric means and ranges of ^{226}Ra are shown for Central Florida materials.

of the matrix, depending upon the practice of the mining company; in actuality it is probably distributed between the two. In subsequent steps the matrix is slurried with water and pumped to the beneficiation plant where it undergoes washing, screening, flotation, and other sizing and separation processes. Two phosphate rock products, a coarse "pebble" fraction and a fine "rock concentrate," then become input for other steps in phosphate processing such as drying, grinding, phosphorus production, phosphoric acid manufacture, and production of fertilizer ingredients and other products, either nearby or at a remote location.

Typically, the matrix contains about ⅓ recoverable phosphate rock, about ⅓ sand, and about ⅓ nonrecoverable fine (—0.1 mm) material referred to as "clays." The sand tailings fraction is usually pumped onto the land where it rapidly dewaters. The clay suspension, often called "slimes," traditionally has been pumped to impoundments where dewatering takes place slowly. Since this conventional method of clay dewatering ties up considerable quantities of water and withholds substantial acreages of land from reclamation and productive use for many years, the industry is striving to develop alternative methods of clay dewatering and disposal. Methods under development include various schemes of mixing with sand tailings.

Prior to the 1940s, technology was not available to recover the fine phosphatic fraction (—1 mm) from the sand and, accordingly, this fraction (with its phosphate and radioactivity) also was left behind in so-called debris.

Land Reclamation

Overburden, sand tailings, dewatered clays, and debris are returned to the land in various mixes and combinations of layering. Types of land resulting are summarized in Table 1; they are grouped into major categories according to the material judged to be most significant in determining radiological characteristics at the surface.

Very old mined lands are likely to contain overburden and debris. Reclaimed lands mined between 1940 and 1970 are likely to contain overburden spoil banks and tailings piles which have been submitted to some degree of leveling and may include dewatered clay settling areas which have been capped with overburden and/or tailings. Recently mined and reclaimed lands are likely to contain various combinations of sand tailings and overburden, with a deliberate attempt at contouring to simulate natural features of rolling terrain and lakes. In the future reclaimed lands will likely continue to have these features and increasing quantities of clays.

TABLE 1

Definition of Land Types as Used in This Study

Land type	Description
Unaltered land	Unmined land either inside or outside of the phosphate district which has not received radioactive fill or cover.
Land with radioactive fill	Unmined land that has received fill or cover containing debris, leached-zone overburden, matrix-bearing material, or other materials of enhanced radioactivity.
Tailings reclaimed	Lands where sand tailings only were used in reclamation and no cap of overburden materials is present.
Overburden lands	
Overburden reclaimed land	Land reclaimed only by redistribution of overburden materials; frequently includes lakes in former mine cuts (also referred to as "land and lakes" reclamation).
Sand-fill reclamation	Sand tailings are pumped into old mine cuts to near original grade and are then capped with 1 or 2 ft of overburden from adjacent spoil piles.
Clays lands	
Reclaimed clays settling area	Former clays settling area in which the crust has been allowed to dry; may or may not be capped with overburden or tailings.
Sand-spray clays reclamation	Clays are pumped into an old mine cut and allowed to settle after which sand tailings are sprayed over the clays and intermixing occurs; the settling and spraying processes are repeated until the mixture fills the cut to near original grade. The mixture is allowed to dewator and is capped with overburden from surrounding spoil piles.
Sand–clays mix	Clays and tailings are pumped into a mine cut simultaneously until grade is reached; then the mixture is capped with overburden. This technique has largely been abandoned because of the failure of the clays and tailings to mix, but a few experimental parcels do exist.
Debris land	Lands upon which the fine- (<1 mm) sized fraction of the matrix was deposited. These lands originated prior to the widespread use of the flotation process to separate the 0.1- to 1-mm-sized phosphate fraction from the sand (prior to the 1940s). This material is high in phosphate and uranium-series nuclides.

METHODS

Approximately 100 sites, both unmined and mined, were studied in Polk County in the Central Florida phosphate mining region. In addition, a small number of unmined and reclaimed land sites were studied in the North Florida mining region.

Three principal radiological characteristics were measured: soil and other mineral radioactivity, gamma-radiation exposure rate above the surface, and land-surface radon exhalation rate or flux.

Radioactivity Sampling and Analysis

Four types of samples were collected for radioactivity analysis. Samples to determine depth profile were collected at 13 mining and five reclaimed-land sites. These samples were collected either by drilling 6 m or more or by removing samples from the face of mine cuts. Shallow 1.8-m cores were collected with a hand auger in 0.3-m increments at the remaining sites. In addition, composite surface samples were collected at a number of sites. The first 10- to 15-cm depth was removed with a shovel; grass, roots, and twigs were discarded and several portions of soil from the vicinity were mixed to constitute a composite for the site. Finally, process materials were collected at beneficiation plants.

All samples were analyzed by high-resolution gamma-ray spectroscopy (Bolch et al., 1976).

In the analysis of the soil data, two particular depth increments were emphasized: the surface soil layer and the average layer over a 1.8-m depth. The surface soil represents the medium in which crops are grown and the zone whose radon has the greatest probability of reaching the surface. The 1.8-m layer represents the major contributor to surface radon flux (80% of the total from a typical uniform medium).

Gamma-Radiation Levels

Gamma radiation was measured with scintillation survey meters held 1 m above the ground. These meters were intercalibrated in extended natural radiation fields with a pressurized ionization chamber. A number of readings were recorded for each site, and site means were calculated.

Radon Flux

Radon exhalation rate, or flux, at the soil surface was measured by the flux can technique (Breslin, 1977) or by the charcoal cannister technique (Countess, 1976). Radon flux values for indi-

vidual parcels of land were based on the average of from one to three replicate measurements per sampling and from one to seven samplings (at different times) per site. During the course of this study, it was determined that radon flux measurements are characterized by substantial variation in time and space and thus considerable replication is necessary to predict a site's long-term average radon flux with an acceptable degree of confidence. For detecting anomalous values and for measuring long-term average flux within a factor of two at the 95% confidence level with the techniques employed, at least three collectors should be deployed at a time and the measurement should be repeated six to eight times.

RESULTS

Radioactivity Profile of Unmined Lands

The radioactivity profile with depth in unmined lands indicates the baseline situation prior to mining and provides an insight as to the origin, distribution, and magnitude of the source of radioactivity potentially appearing in mined and reclaimed lands. Individual profiles of radioactivity with depth at a number of unmined sites were presented previously by Roessler, Bolch, and Groome (1976). Although considerable variation is observed from site to site, there is a general pattern of radioactivity with depth. Figure 3 shows a normalized general profile of radium concentration from the surface to the top of the matrix in unmined lands; the shaded portion of the figure represents the range of values that might be expected at any

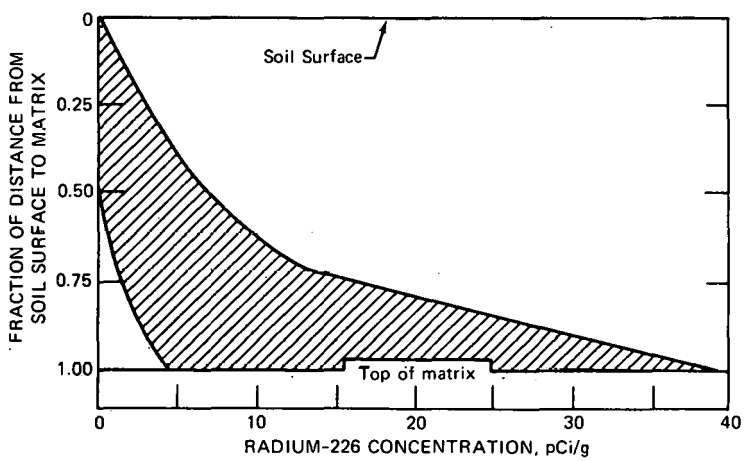


Fig. 3 Normalized radium profile for unmined phosphate lands.

fractional depth from the surface. In general, radioactivity is low at the surface, increases with depth, and is most concentrated in or just above the matrix.

Inputs to Altered Land Radioactivity

Table 2 indicates the mean* and range of soil radium concentrations that were found in various layers from mining. The ranges of values for individual samples are also presented to indicate the variation that might be associated with a collection of small, discrete random samples, rather than mixing, compositing, or weighting proportionally with depth throughout the indicated layer.

The values for the upper overburden layer (0 to 1.8 m) indicate that, except where the matrix is very near the surface, mixed upper layer overburden will have relatively low radioactivity if selectively removed and placed. The other two overburden layers indicate the increased level of radioactivity likely to result from thorough mixing of the entire overburden (1) down to the leached zone and (2) down to the matrix, respectively. In practice disturbed overburden may include matrix since stripping with a dragline bucket does not achieve perfect separation at the interface. The radioactivity concentrations in the leached zone and in the matrix listed in the table indicate localized soil radium concentrations that might result from indiscriminate or adventitious placement of either of these two materials at the surface.

By-products from beneficiation represent the remaining major source of materials found in mined lands and in mining-derived fill. Table 3 summarizes the results of sampling inputs, products, and waste products of phosphate rock beneficiation. The waste-product sand tailings have lower radioactivity than the matrix but have higher concentrations than the original surface soil. Settled clays, on the other hand, represent radium concentrations similar to those of the original matrix. The majority of the radioactivity appears in the phosphate rock products which have concentrations exceeding that of the input matrix. These products are not land-reclamation materials in present-day practice; however, the material now represented by the rock concentrate was originally returned to the land without separation from the sand fraction in the debris of the preflotation mining era. If surplus or wasted phosphate rock were to be present near the land surface, this also would cause a considerable localized radiation and radioactivity enhancement.

*The various measurements tended to be log normally distributed; hence, the geometric mean was chosen as the most representative parameter for averaging in data summaries.

TABLE 2

Radium-226 Concentrations in Topsoil, Overburden, Leached Zone, and Matrix of Mining Lands

Material type	^{226}Ra concentration, pCi/g	
	North Florida	Central Florida
Surface soil (depth, 0 to 30 cm)		
Average*	0.4	0.5
Range of site means	0.2 to 0.8	0.2 to 3.8
Range of individual samples	0.2 to 0.8	0.2 to 3.8
Number of sites	3	5
Upper layer overburden (depth, 0 to 1.8 m)		
Average*	1.3	0.6
Range of site means	0.6 to 4.4	0.3 to 2.1
Range of individual samples	0.6 to 10.6	0.2 to 3.8
Number of sites	3	6
Overburden (surface to top of leached zone)		
Average*	†	1.6
Range of site means		0.5 to 7.2
Range of individual samples		0.2 to 7.2
Number of sites		7
Leached zone		
Average*	†	9.4
Range of site means		2.0 to 45.6
Range of individual samples		1.2 to 45.6
Number of sites		7
Overburden (surface to matrix)		
Average*	2.5	2.5
Range of site means	1.5 to 5.3	0.5 to 7.2
Range of individual samples	0.6 to 10.6	0.2 to 30.6
Number of sites	3	8
Matrix		
Average‡	10.9	25.9
Range of site means	5.1 to 31.6	13.2 to 84.2
Range of individual samples	2.6 to 58.8	6.0 to 136.5
Number of sites	6	13

*Average is the geometric mean of the site means.

†Leached zone is not present in typical North Florida profile.

‡Site means are calculated from mixed matrix samples and from depth-weighted average of cores.

TABLE 3

Radium-226 Concentration* of Materials in Phosphate Rock Beneficiation

Material	^{226}Ra concentration,* pCi/g					
	North Florida			Central Florida		
	N†	Mean	Range	N†	Mean	Range
Input						
Matrix	4	8.6	5.1—13.3	6	37.6	18.1—84.2
Phosphate rock products						
Pebble	1	25.8		13	57.4	44.5—96.6
Rock concentrate	4	16.6	16.1—16.9	12	34.9	26.0—50.4
Waste products						
Sand tailings	4	2.7	2.0—3.3	24	5.2	1.7—12.2
Clays	Not sampled			10	32.4	9.8—72.6‡

*All concentrations reported on a dry-weight basis.

†N denotes number of samples in summary.

‡Based on pooling University of Florida data and data from Guimond and Windham (1975).

Radiological Characteristics by Land Type

The results of actually measuring soil radium, gamma radiation, and soil-surface radon flux on various land types in the Central Florida mining region are summarized in Table 4 and Fig. 4. These data indicate that

(1) Mining and reclamation can cause an increase in radiation and radioactivity levels.

(2) The characteristics have a wide range of values within land types, and, thus, there is an overlap between land types. (Much of what appears to be a high site-to-site radon flux variation within land types can be attributed to inadequate replication.)

(3) A general ranking is based on radiological characteristics: unaltered land < tailings ≤ overburden < debris.

(4) Settled clays have a high radium content, but, since the data represent a composite of a few samples from each of a variety of different practices, it is difficult to draw conclusions.

(5) The greatest radiation and radioactivity values are associated with debris lands and thus not with present or future mining practices.

(6) The indiscriminate choice of fill materials also can result in increases in the radiological parameters measured.

TABLE 4

Summary of Radiological Characteristics of Various Land Types

Land type	^{226}Ra content, pCi/g						Gamma level, μR/hr			Radon flux, pCi m^{-2} sec^{-1}		
	Surface soil (0—0.3 m)			Soil core (0—1.8 m)								
	N*	Mean†	Range	N*	Mean†	Range	N*	Mean†	Range	N*	Mean†	Range
Unaltered land	20	0.6	0.1—3.8	18	0.4	0.2—3.1	9	5	4—7	17	0.2	<0.1—1.7
Unmined radioactive fill	2	3.2	2.5—4.1	2	2.2	1.1—4.4	1	9		2	1.3	0.6—2.8
Tailings	20	3.2	0.4—9.2	16	3.1	0.5—8.7	11	11	6—16	19	0.7	<0.1—2.7
All overburden‡	28	5.0	0.8—35 3	24	5.3	1.0—23.1	16	13	7—33	27	1.5	<0.1—12.8
Capped and mixed clays§	6	6.8	3.3—14 6	6	7.4	2.8—18.3	6	17	11—24	6	1.6	0.3—7.2
Debris	18	9.5	3.4—23 3	18	7.3	3.1—24.7	8	22	11—54	15	4.2	1.7—13.7

*N denotes number of sites in summary.

†Means are geometric means of average values for N sites of indicated land type.

‡Overburden category includes (1) reclaimed overburden piles and (2) sand-fill reclamations capped with overburden.

§Clays category includes (1) settled clays areas capped with overburden and/or tailings and (2) clays—sand mixtures capped with overburden.

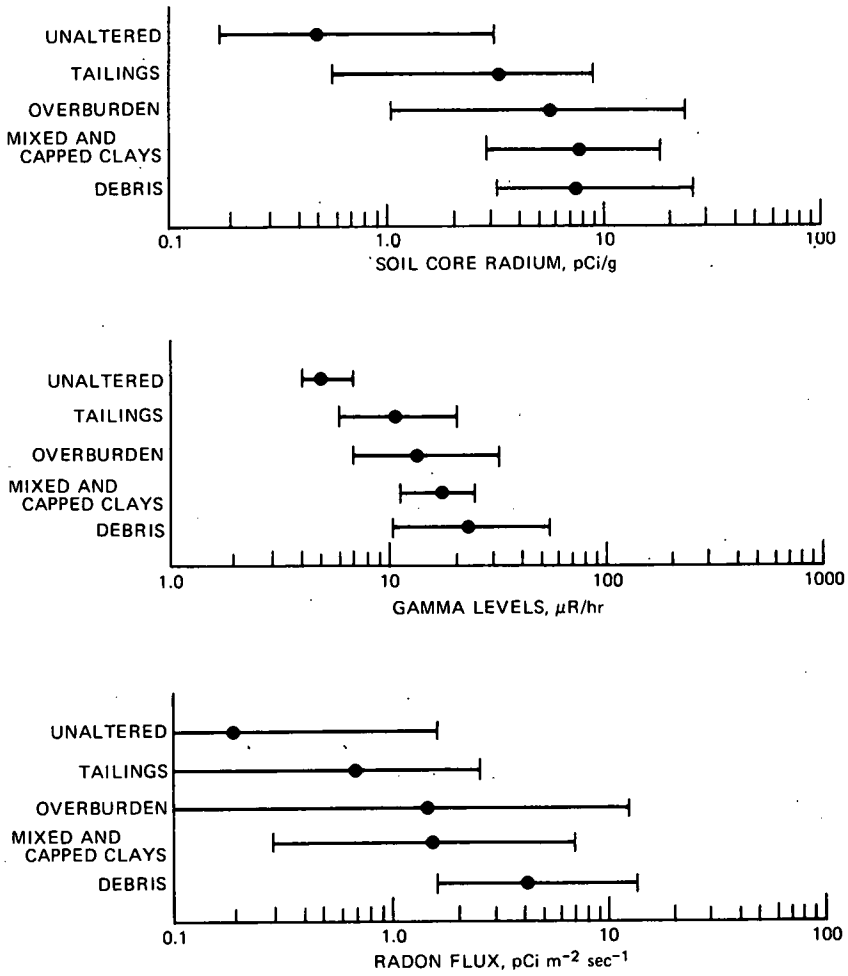


Fig. 4 Radiological characteristics of Polk County lands. Geometric means and ranges are shown by land type.

Samples at nine unaltered land sites in North Florida indicated surface soil radium concentrations and gamma-radiation levels essentially the same as those reported in Table 4. The average 1.8-m soil-core radium concentration, 1.0 pCi/g, and the radon flux value, 0.7 pCi m^{-2} sec^{-1}, were slightly higher than the unaltered-land values in Table 4; thus a thinner overburden is reflected at the North Florida sampling sites. Sampling one parcel each of tailings and overburden reclaimed land in the North Florida mining region gave respective soil radium concentrations of 4.8 and 8.1 pCi/g, gamma-

radiation levels of 9.8 and 7.9 μR/hr, and radon flux values of 1.2 and 3.0 pCi m^{-2} sec^{-1}. These values fall about midrange in the data for similar land types in Table 4. This very limited sampling suggests that radiological characteristics of mined lands in the North Florida mining region do not differ greatly from those reported for the Central Florida mining region.

DISCUSSION

The impact of the redistribution of natural radioactivity by phosphate mining and land reclamation can be assessed in terms of radiation exposure routes through the environment to man. Such potential routes encompass exposure to direct gamma-radiation and radionuclide transfer routes, including those involving (1) airborne radon and progeny in structures, (2) radionuclide uptake by plants and transfer through the food chain, (3) radionuclides in surface and ground water, and (4) ambient airborne radioactivity.

It is not the intent of this paper to relate a detailed environmental impact analysis. However, the scope of some of the potential impacts can be defined rather easily without elaborate analysis.

Direct Gamma Radiation

For persons continuously present with no attenuation from structures or vehicles, the observed average increments of gamma-radiation exposure above the average unaltered-lands background represent annual whole-body dose equivalents of 50, 70, 100, and 150 mrems for tailings, overburden, clays, and debris lands, respectively. These values are all less than 170 mrems/annum, the guideline recommended by the Federal Radiation Council (1960) for average exposure to a population group.

The maximum gamma-radiation exposure rates represent increments above background of about 100, 250, 150, and 425 mrems/annum for tailings, overburden, clays, and debris lands, respectively. These values are all less than the Federal Radiation Council guideline of 500 mrems/annum above background for any individual of the general population.

Structures built over these lands are likely to attenuate these radiation levels. If adjustments were made for the effects of time spent indoors and of time spent away from these lands, then both the average and the maximum doses would be less than those cited, and the number of individuals receiving the maximum would be small.

Impact via Indoor Radon Progeny

Although all the radionuclide transfer routes previously cited should be considered, the greatest efforts to date have been directed toward studying indoor radon progeny concentrations and their interrelationships with Florida phosphate lands. Assessment of impact via this route is limited by the facts that a consensus has not yet emerged on appropriate standards for indoor radon progeny concentrations, satisfactory models relating characteristics of Florida lands to human exposure by various routes are lacking, and there are insufficient predictive standards for application to undeveloped lands.

One point of reference on which to base evaluation criteria is the guidance issued by the Surgeon General for use in the state of Colorado for assessing dwellings constructed over uranium mill tailings (Surgeon General, 1970). According to these guidelines, no remedial action is indicated for structures where indoor airborne radon progeny levels are less than 0.01 WL above background, remedial action is indicated for concentrations exceeding 0.05 WL above background, and remedial action may be indicated for concentrations between these two values.*

Impact on Existing Structures

After reviewing the available data, the Florida Department of Health and Rehabilitative Services (HRS) in 1978 adopted a control level of 0.029 WL (0.025 WL above an average indoor background of 0.004 WL) for existing structures in Florida. The HRS has estimated that, of the approximately 4000 structures on reclaimed land in the Central Florida mining region, 6 to 10% will require some kind of corrective action to achieve the control level of 0.029 WL.

Analysis of the HRS findings and of additional University of Florida data leads to the conclusion that most of the structures exceeding the HRS control level were on debris lands. Furthermore, for lands with more than about 10 pCi/g of radium-226, indoor radon progeny levels in conventional slab-on-grade buildings constructed without incorporation of land cover or other remedial measures are likely to exceed the HRS control level. On the other

*WL represents "working level," a unit defined for expressing concentrations of short-lived radon progeny in air. One WL is any combination of radon progeny in 1 liter of air whose ultimate decay through polonium-214 will deliver 1.3×10^5 MeV of alpha-particle energy. This is the same quantity of energy as that delivered by the alpha particles from the complete decay of the radon progeny in secular equilibrium with 100 pCi of radon-222 in 1 liter of air.

hand, tailings lands and overburden lands without leached-zone material or adventitious matrix are not likely to have this level of soil radium, and relatively few structures on such lands are likely to have indoor radon progeny levels exceeding the HRS control level. No slab-on-grade structures currently exist on clays.

Impact on Future Structures

Of particular importance is the impact with respect to future structures on currently undeveloped lands and on lands mined and reclaimed in the future. When the lower range of the Surgeon General's guidelines (0.01 WL above background) is used as a basis for discussion and when the HRS estimate of 0.004 WL is adopted as the average indoor background, 0.014 WL becomes the reference indoor radon progeny concentration upon which to base lands criteria for unrestricted construction.

Modeling work still in progress indicates that, for limiting indoor radon progeny levels in conventionally constructed slab-on-grade structures to no more than 0.014 WL without remedial action measures, the appropriate lands criteria are approximately 10 μR/hr of gamma radiation, 4 pCi/g of soil radium, or 3 pCi m^{-2} sec^{-1} of radon flux. From the data presented in Table 4 and Fig. 4, it is concluded that, in addition to the lands cited above, about one-half the tailings and overburden lands reclaimed according to current practices would exceed these criteria.

Soil radium can also be expected to exceed 4 pCi/g in future clays reclamations. Preliminary information suggests that radon exhalation from clays lands will be comparable to that from other soils of similar radium content, but at present there is insufficient information on radon emanating and transport properties of such mixtures.

Measures to Moderate the Impact of Radioactivity in Phosphate Lands

The major impacts demonstrated to date from the redistribution of natural radioactivity in the course of phosphate mining, reclamation, and land development have been the existing and the projected contributions to airborne radon progeny in structures. Fortunately, in many cases land and materials management techniques can be used to obviate the need for imposing land-use restrictions or requiring the incorporation of remedial measures into new structures.

Three areas in which to apply such techniques are

1. Site preparation and building construction avoiding the use of fill materials containing radium-226 in concentrations greater than several picocuries per gram.

2. Utilization of existing lands where possible, covering or replacing high-radioactivity or high-radon-flux land with a sufficient depth of low-radioactivity material.

3. Future mining and land reclamation with simulation of the natural situation by selectively placing higher radioactivity material under a lower radioactivity cover.

The high-radioactivity materials to avoid as fill and upper-layer materials include debris, lower-layer overburden containing leached-zone material and adventitious matrix, waste phosphate rock, and sand tailings. The data in Table 2 and Fig. 3 indicate that, with the possible exception of locations with thin overburden, sufficient low-radioactivity overburden should be available for use as fill or cover.

Suggested modifications in mining and land-reclamation procedures include placing clays, lower-layer overburden, and sand tailings in the bottom of empty cuts and covering these materials with the lower-activity upper-layer overburden from another cut. Engineering methods, based on radon-flux prediction, are currently being developed for use in designing and evaluating specific materials placement strategies.

CONCLUSIONS

In the natural state the uranium-series radioactivity associated with phosphate deposits is buried under sufficient low-radioactivity cover (Fig. 3) to substantially moderate any effects at the land surface. In the process of mining and land reclamation, this naturally occurring radioactivity is redistributed with a likely increase of near-surface soil radium and a resultant increase in soil surface radon flux and above-surface gamma-radiation levels. Although there are wide ranges of values within and considerable overlapping between land types, there is a general pattern of radiological characteristics with land type as shown in Fig. 4.

This redistribution of radioactivity has a significant impact in that several hundred structures were reported to exceed the Florida Department of Health and Rehabilitative Services 0.029 WL control level for existing structures. Interestingly, these structures are believed to be primarily on debris lands; such lands are the result of pre-1940s mining techniques and are not produced by present mining practices. If lands criteria traceable to the lower-level Surgeon General's guideline of 0.01 WL above background are applied for lands to be used for new construction, it is concluded that some of the overburden and tailings reclaimed lands produced by current and

proposed mining and reclamation techniques would exceed criteria for construction of slab-on-grade structures without remedial action.

The impact on future construction, however, can be substantially moderated by avoiding the use of materials of designated high radium content for fill, by covering or replacing soil of high radioactivity in the development of existing lands, and by modifying mining and land-reclamation techniques to selectively place designated high-radioactivity materials under a cover of materials selected for low radioactivity.

The indoor airborne radon progeny pathway is probably the most significant exposure route associated with this radioactivity source; however, other routes through the environment to man should be evaluated as well.

ACKNOWLEDGMENTS

This work was supported by the Florida Phosphate Council and by the Industrial and Engineering Experiment Station of the University of Florida.

The contribution to this work by phosphate mining companies in providing drill cores, assistance in land sampling, and information on mining technology and land-reclamation methods is gratefully acknowledged. Appreciation is also expressed for the assistance of a number of undergraduate and graduate students who participated in field studies, laboratory analyses, and data tabulation and analysis.

REFERENCES

Altschuler, Z. S., J. B. Cathcart, and E. J. Young, 1964, Geology and Geochemistry of the Bone Valley Formation and Its Phosphate Deposits, West Central Florida, in *Geological Society of America Field Trip Guidebook*, Miami Geological Society, Miami.

Bolch, W. E., E. D. Whitney, R. M. Chhatre, and C. E. Roessler, 1976, Uranium and Radium Concentrations in Florida Phosphate, in *Natural Radioactivity in Man's Environment*, Health Physics Society Tenth Midyear Symposium, Saratoga Springs, N. Y., Oct. 11—13, 1976, pp. 407-4. 1, Rensselaer Polytechnic Institute, Troy, N. Y.

Breslin, A. J., 1977, Methods Used by HASL for Ambient Radon Studies, in *Radon Workshop—February 1977*, ERDA Report HASL-325, pp. 9-16, Health and Safety Laboratory, NTIS.

Cathcart, J. B., 1970, Phosphate Deposits in Florida, in *Methods Used and Adopted by the Association of Florida Phosphate Chemists*, 5th ed., pp. 6-14, Association of Florida Phosphate Chemists, Bartow, Fla.

Countess, R. J., 1976, ^{222}Rn Flux Measurement with a Charcoal Cannister, *Health Phys.*, 31: 455-456.

Federal Radiation Council, 1960, *Background Material for the Development of Radiation Protection Standards*, FRC Report No. 1, GPO.

Florida Department of Health and Rehabilitative Services, 1978, *Study of Radon Daughter Concentrations in Structures in Polk and Hillsborough Counties*, Tallahassee, Fla.

Guimond, R. J., and S. T. Windham, 1975, *Radioactivity Distribution in Phosphate Products, By-Products, Effluents, and Wastes*, Technical Note ORP/CSD-75-3, U. S. Environmental Protection Agency, Office of Radiation Programs, Washington, D. C.

Roessler, C. E., W. E. Bolch, Jr., and C. D. Groome, 1977, Uranium and Radium-226 in the Litho-Environment of Florida's Phosphate Regions, in *Natural Radioactivity in Man's Environment*, Health Physics Society Tenth Midyear Symposium, Saratoga Springs, N. Y., Oct. 11—13, 1976, pp. 29-42, Rensselaer Polytechnic Institute, Troy, N. Y.

Surgeon General, Public Health Service, 1970, Recommendations of Action for Radiation Exposure Levels in Dwellings Constructed on or with Uranium Mill Tailings, in *Use of Uranium Mill Tailings for Construction Purposes*, Hearings Before the Subcommittee on Raw Materials of the Joint Committee on Atomic Energy, Congress of the United States, Oct. 28—29, 1971, pp. 52-54, Superintendent of Documents, Government Printing Office, Washington, D. C.

U. S. Environmental Protection Agency, 1975, *Preliminary Findings: Radon Daughter Levels in Structures Constructed on Reclaimed Florida Phosphate Lands*, Technical Note ORP/CSD-75-4, Office of Radiation Programs, U. S. Environmental Protection Agency, Washington, D. C.

DISCUSSION

Tanner: Were you able to discriminate between radon and thoron in your measurements of flux in northern Florida? An aeroradiometric survey in 1954 by the U. S. Geological Service of potential phosphate areas in Florida yielded a weak, factor-of-2 anomaly that I studied subsequently by measuring soil-gas samples and then by drilling and measuring the radon in shallow groundwater. The anomaly was related primarily to thoron. The water samples did not support the idea of upward movement of radon.

Roessler: We did not attempt to distinguish ^{220}Rn from ^{222}Rn or to quantitate ^{220}Rn flux. We are aware of the heavy mineral deposits to the east of the area identified in Fig. 1 as North Florida Phosphate Region. My initial reaction is that the thoron you observed was related to similar deposits. I do not think a significant amount of thoron was involved in our measurements. We would like to have a copy of your report so we can follow through on this.

Modification of the Natural Radionuclide Distribution by Some Human Activities in Canada

G. B. KNIGHT and C. E. MAKEPEACE
Atomic Energy Control Board, Ottawa, Canada

ABSTRACT

Examples are presented of three types of human activity that have resulted in elevated natural radiation levels. Investigations carried out by a Federal–Provincial Task Force are described. The distributions of grab sample measurements of radon and radon daughter concentrations are compared for the Bancroft area, Cobourg, Deloro, Elliot Lake, and Port Hope in Ontario, and Uranium City in Saskatchewan; it is concluded that the major point of difference between the communities that were investigated and the reference community of Cobourg is the departure from a symmetrical lognormal distribution at the higher concentrations.

In Canada, responsibility for the control and supervision of the development, application and use of atomic energy is assigned to the Atomic Energy Control Board (AECB). The AECB receives its authority from the Atomic Energy Control Act, which was promulgated in 1946 and empowers the AECB to write regulations and to administer a comprehensive system of licences for nuclear facilities and prescribed substances. Further information on the AECB is given in its annual reports.

During 1975 a number of investigations were initiated by the AECB which were concerned with radioactive contamination that may have resulted from past operations and disposal practices. By early 1976 the increasing number and magnitude of the investigations led to a Federal Cabinet decision to form a Federal–Provincial Task Force under the leadership of the AECB to expedite the investigation across Canada and to coordinate the use of Federal and

Provincial resources. The investigation has followed a similar pattern in each area; following a preliminary radiation survey by the appropriate member agencies of the Federal–Provincial Task Force, the normal approach has been to hire a consultant to act as Program Manager in each area. The Program Manager carries out a more comprehensive radiation survey and determines the appropriate remedial measures for those homes where the radiation levels exceed the criteria (AECB, 1977) that have been adopted by the Task Force and, in consultation with the AECB and the homeowner, carries out the remedial measures. After completion of the remedial work, the AECB and other regulatory bodies make protracted measurements to test whether or not the average radiation levels are below the criteria.

This paper describes the preliminary radiation surveys conducted in several areas across Canada and discusses the results of these surveys.

PRELIMINARY RADIATION SURVEYS

Purpose

The purpose of the preliminary radiation survey in each selected area was specifically to determine if a problem existed. If the answer was affirmative, the survey provided information on the magnitude of the radiation levels and the approximate number of homes and buildings involved.

Organization

The radiation surveys have been conducted at various times over a 2-year period in several different communities; consequently the approach to team organization and type of survey has changed. At first it was thought that a gamma radiation survey of the streets would provide a rapid guide to the "worst" areas, but it was soon found that the correlation was poor between gamma exposure rates outdoors and the radon or daughter concentrations inside houses in the vicinity. This type of survey was quickly replaced by an "on-demand" program that responded to those homeowners who requested a survey. It was soon evident from the random nature of the "discoveries" that a complete survey of the whole community would be necessary to provide assurance that significant cases of contamination had not been overlooked and, incidentally, to give a balanced view of the extent of the problem.

The decision to survey the whole community in each case has allowed a more efficient organization to evolve. Emphasis has been

placed on measurement of the radon daughter concentration in the basement and in a representative living area in each house; radon concentrations and gamma exposure rates have been measured only in those homes where a significant daughter concentration was found. The surveys have been carried out by teams of two people; one person fills out the information sheet and the other collects the samples. After visiting four or five homes, the team returns the samples to a central point for counting and then continues visiting more homes. An information office has been set up in each community to provide a working base for the survey teams and a communication point for local residents. The staff members manning the information office schedule the homes to be sampled each day and have usually followed a street-by-street plan. Homeowners have been warned ahead of time either by announcements in the local newspaper or by telephone. It is usually necessary to repeat coverage of an area two or three times and to make visits during the evening in order to find the majority of residents at home. This approach has resulted in a relatively small percentage of homes being missed in each community. These missed homes are checked subsequently by the Program Manager.

Experienced survey teams have been provided by Health and Welfare Canada, the Department of Labor in Saskatchewan, and the Ministry of Labor in Ontario, which replaces the Ministry of Health in this role by a recent provincial reorganization. This experienced core has been considerably augmented by AECB-trained teams made up of members of the Nuclear Accident Support Teams from the Department of National Defense and university students hired for the summer.

Instruments and Procedures

A variety of instruments and techniques has been used in the different surveys to measure the concentration of radon in picocuries per liter of air, the concentration of radon daughters in working levels (WL), and the gamma radiation exposure rates in milliroentgens or microroentgens per hour.

Radon. Measurements made by the Ontario Ministry of Labor are based on work of Cowper and Simpson (1953) with modifications introduced by Tai-Pow (1978). Briefly a sample of room air is collected by opening an evacuated 2-liter glass bottle; the sample bottle is then sealed and returned to the laboratory where the sampled air is transferred to a counting flask that has a thin aluminum collection foil in contact with a Lucite window coated with zinc sulfide. The air sample is left for 4 hr for the radon

daughters to come to equilibrium, and the alpha activity is then counted for 2 to 16 hr. The system is calibrated with a standard radium solution obtained from the U. S. National Bureau of Standards.

Measurements made by Health and Welfare Canada followed the Lucas chamber method (Lucas, 1957) using commercially available cells and a portable counting unit. The cells were calibrated using standard radium solutions obtained from the U. S. National Bureau of Standards.

Radon Daughters. Measurements made by Health and Welfare Canada depended on the modified Kusnetz method (Kusnetz, 1956). Air samples were taken using a portable air pump and a 25-mm-diameter filter; samples were taken at a flow rate of 10 liters/min for 5 min. The same commercially available portable counting units that are used for radon measurements were modified to hold the filter papers in contact with a disk coated with zinc sulfide.

Measurements made by the AECB followed the same general procedure as that just described except that in one community (Elliot Lake) a different procedure was adopted that depended on counting the beta radiation from the decay of the RaB and RaC daughters (Horwood, 1978). Briefly an air sample is drawn through a Whatman 41 coarse filter at a flow rate of 850 liters/min for 5 min. The filter is then folded and placed between two pancake Geiger detectors, and the beta activity is counted for 5 min. The system is calibrated by comparison with the modified Kusnetz method that includes a correction for the age of the filter.

Gamma Radiation. Measurements of the gamma-ray exposure rate were intended to give an indication of the presence of excessive concentrations of gamma-emitting sources like radium and thorium. Commercially available survey meters employing Geiger detectors were used to make measurements at 1 meter above the ground and in contact with the ground. All meters were calibrated using a radium source.

Data Analysis. The distribution of radon daughter concentrations was analyzed in each community (except one, Port Hope, where the radon concentration was analyzed) in order to determine the best fit for the data, the mean, and the upper limit as defined by the mean plus three times the standard deviation; the cumulative frequency of the concentration distribution was also examined. These analyses were in addition to the simple distributions made according to arbitrary concentration intervals that have been reported previously (Aitken et al., 1977; Taniguchi, 1977). No special statistical analysis was made of the gamma exposure rates.

AREAS SURVEYED

The areas selected for investigation were those where radioactive contamination was already suspected, and, in the first instance, the selection was based on a knowledge of the past operations in each area.

The first area selected for investigation was the community in which a radium—uranium refinery had operated for several decades; investigation of this community led to investigation of other communities in which nonnuclear metallurgical operations had made use of the refinery residues, and, finally, following the "trail" in reverse, it was speculated that there could be a contamination problem in the uranium mining communities. Each of these potential problem areas is considered below with a brief review of the human activities that may have affected the human exposures to radiation.

Operation of a Radium–Uranium Refinery in Port Hope

Port Hope is a community located on the north shore of Lake Ontario about 100 km east of Toronto in the Province of Ontario; the population today is about 9000.

A refinery has been operating in Port Hope since 1932. Initially radium was recovered from ores mined in Port Radium, Northwest Territories; the location of the refinery was chosen on economic grounds since it was less costly to ship each ton of pitchblende concentrates than to ship the 7 tons of chemicals required for treatment. During the 1940s and early 1950s, the refinery operation was converted to the recovery of uranium, although some radium refining continued until 1953 when it ceased altogether. Since the mid-1950s, the refinery has obtained feed material in the form of uranium concentrates from mines in northern Ontario and northern Saskatchewan and from various mines in the United States. During this entire period the refinery has produced residues that have been more or less radioactive according to the treatment of the concentrates prior to shipment from the mine; in the early years the concentrates received little or no treatment. The first residues were placed on the refinery property; later residues were deposited in areas close to the refinery. In the following years the residues were reprocessed and redeposited, and some were sold for the recovery of other important metals. There were several periods during which there was an active building program at the refinery when old buildings were demolished to make way for new construction. Consequently contamination of the town of Port Hope could have resulted from any of the following causes:

1. Spillage of residue during loading for shipment by road or rail.
2. Contamination as a result of temporary storage of residues in various locations in the town while awaiting reprocessing.
3. Distribution of contaminated fill, building rubble, and reclaimed building materials that originated from the refinery property.
4. The existence of past residue disposal areas within the present built-up area of the town.

Further details of the historical background of the Port Hope situation are given by Knight (1976).

The preliminary survey began in Port Hope early in 1976 and has extended over a period of 2 years to complete measurements in each of the approximately 3000 homes, schools, and business premises.

Since the Radiation Protection Laboratory of the Ontario Ministry of Health was located in nearby Toronto and possessed an excellent capability for measuring radon concentrations, it was decided to perform this analysis on the air samples taken in Port Hope.

Nonnuclear Metallurgical Operations

Another type of operation that is more difficult to recognize is that of a nonnuclear operation, usually metallurgical, where the use of radioactive material is quite incidental to the end product and hence may not be recognized by the operator or by the regulatory agency. The particular concern in such situations is with the waste-disposal practices used by the processor which do not take account of the radioactive aspect of their waste. Two examples are given below to illustrate this particular problem.

1. *An Abandoned Cobalt Smelter.* Deloro is a small village of about 70 houses situated in Hastings County in Ontario about 65 km east of Peterborough. A custom smelter specializing in handling arsenical ores operated in Deloro from 1907 to 1961. The smelter also specialized in the extraction of cobalt using feed materials from northern Ontario, Morocco, Rhodesia, and, of particular significance in this discussion, from the radium—uranium refinery in Port Hope. The smelter was abandoned in 1961, leaving a major problem of handling large volumes of arsenic-contaminated waste. In 1975, following preliminary investigations in Port Hope, the AECB became aware of radioactive contamination of the waste at Deloro resulting from the sale of residues to the smelting company for the extraction of cobalt. Measurements of the gamma exposure rates on the abandoned smelter property made in the fall of 1975 showed a widespread, low-level radioactive contamination of slag and other

waste that had been deposited on the property. Radon measurements were made in those houses which were closest to the abandoned property, and one family whose home was only a meter from the property boundary was evacuated by the Provincial Ministry of Health when it was found that the father had lung cancer. A complete survey of the community was made in 1977.

2. *Ferrocolumbium Alloy Production.* Gloucester Township adjoins the Federal capital of Ottawa. In 1976, three locations were found to be radioactively contaminated in the Township; there were two abandoned sites where ferrocolumbium alloys were produced from pyrochlore concentrates and one operating site which contained thorium and radium. The feed materials originated from Brazil and eastern Canada. After the thorium is processed, it remains with the slag, which had been buried on the two abandoned sites and which is currently under company control at the operating site. A complicating factor from a jurisdictional point of view has been the additional presence of chemically toxic contaminants. As abandoned sites, the first two did not present a serious problem, since access to them could have been restricted, but plans for building development at both sites led to both areas being cleaned up in order to avoid possible elevated radon levels inside any homes built there.

Elevated Radiation Levels in Uranium Mining Communities

Acting on the experience at Grand Junction, Colo. (Aspinall, 1971), and Port Hope, Ontario, it was suspected that a radioactive contamination problem could exist in uranium mining communities resulting from the use of waste rock from the mines being used on driveways or as backfill or from the siting of houses on or close to natural occurrences.

Consequently preliminary radiation surveys have been conducted in all the major uranium mining communities in Canada. In each case the survey has stressed the measurement of radon daughter concentrations in working levels as being most meaningful to the mining population, but measurements of radon concentrations and gamma exposure rates have been made in those locations where the radon daughter concentrations were found to be significant.

There are three long-established, major uranium mining communities in Canada: Uranium City in Saskatchewan and Elliot Lake and the Bancroft area in Ontario. Recently opened uranium mines in Saskatchewan do not have local communities.

1. *Uranium City, Saskatchewan.* Uranium City is located in northern Saskatchewan near the north shore of Lake Athabaska. The town was first laid out in 1953 and currently has a population of

about 2200 living in about 500 homes. Radiation surveys of the community were undertaken by Health and Welfare Canada and the Provincial Department of Labor from February to June 1976 and was completed in the fall of that year (Taniguchi, 1977).

2. *Elliot Lake, Ontario.* Elliot Lake is located about 20 km north of the northern shore of Lake Huron and about 135 km west of Sudbury. The town was first laid out in 1955 and has a present-day population of about 9000, which is rapidly increasing as a result of an expansion in the mining activity; there are about 2000 homes and other buildings. Radiation surveys of the community were undertaken by AECB-trained teams made up of students and Canadian Forces personnel, with assistance from the staff of Health and Welfare Canada.

3. *Bancroft area, Ontario.* The village of Bancroft is situated in central Ontario and is surrounded by many smaller communities that have some association with uranium mining in the area. Currently, only one of the four mines in the area is operating. Central Ontario is a vacation area, and many of the homes predate the establishment of the uranium mines in 1953; there are about 1200 homes in the uranium mining area. Radiation surveys of the area were undertaken in the summer of 1977 by teams of students working under the guidance of experienced staff from AECB, Health and Welfare Canada, and the Provincial Ministry of Labor.

RESULTS

The distribution of the maximum measured radon concentrations found in each of 2961 homes in Port Hope is shown in Fig. 1; it is noted that this maximum concentration was usually found in the basement. For comparison, Figs. 2a and 2b show the distribution in Cobourg, Ontario. Cobourg is located on the north shore of Lake Ontario about 10 km east of Port Hope and, having no suspected contamination problem, was used as a convenient reference for evaluating the measurements obtained in Port Hope. Measurements were made by the Ontario Ministry of Health in the spring and fall of 1976 (Aitken et al., 1977). The distribution of the maximum measured radon daughter concentrations found in homes in Uranium City, Elliot Lake, and the Bancroft area are shown in Figs. 3, 4, and 5, respectively. Attempts were made to fit the data to the normal and Poisson distributions without success; finally it was found that the lognormal distribution when fitted to the logarithms to base 10 of the data gave an acceptable value for the chi-square statistic in each case. The significant statistics calculated were the mean and

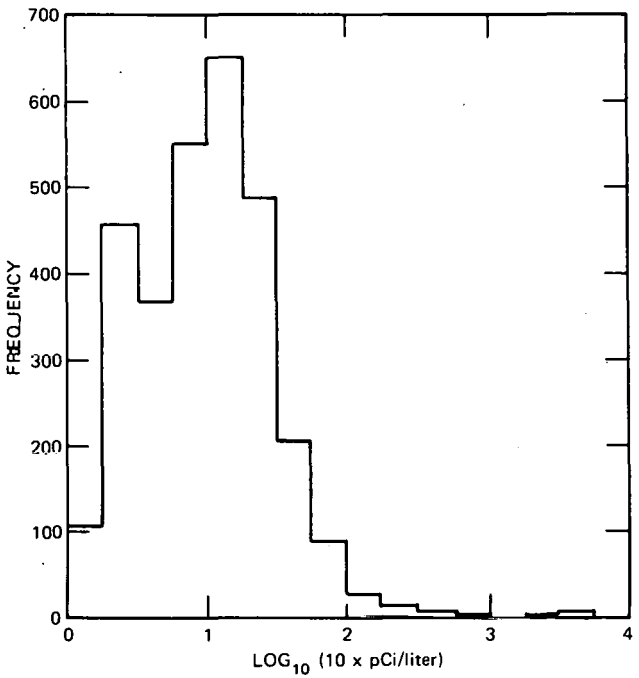


Fig. 1 Distribution of the log of radon concentrations inside homes in Port Hope.

standard deviation of the lognormal distribution and the upper 99% confidence level; for comparison with other studies, the percentage of observations greater than 0.02 WL was also calculated since this is the primary criterion for remedial work.

The antilog of the lognormal statistics for the air samples is listed in Table 1 for each of the communities where these measurements were made; included for comparison are the same statistics for Cobourg. The values for the radon daughter concentrations in Table 1 for Port Hope and Cobourg were calculated from the radon figures using an equilibrium factor of 30% to convert to working levels. The statistics for Deloro are also listed, but, with only 68 homes sampled, a graph showing the distribution was not thought to be worthwhile.

The cumulative frequency plots for Port Hope, Cobourg, Uranium City, Elliot Lake, and the Bancroft area are shown in Figs. 6, 7, 8, 9, and 10, respectively.

A summary of the soil sample analysis from the locations in Gloucester Township is given in Table 2. The gamma exposure rates

(Text continues on page 1509.)

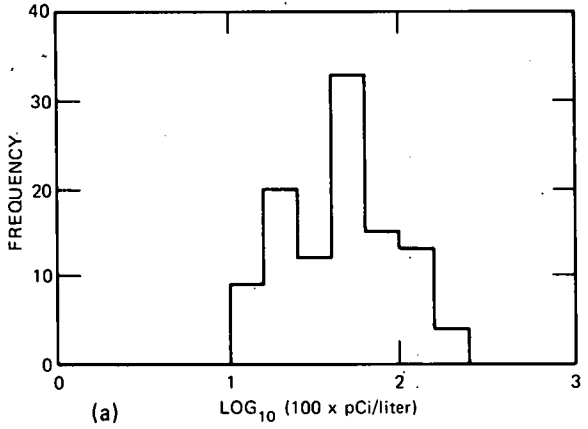


Fig. 2a Distribution of the log of radon concentrations inside homes in Cobourg in the spring of 1976.

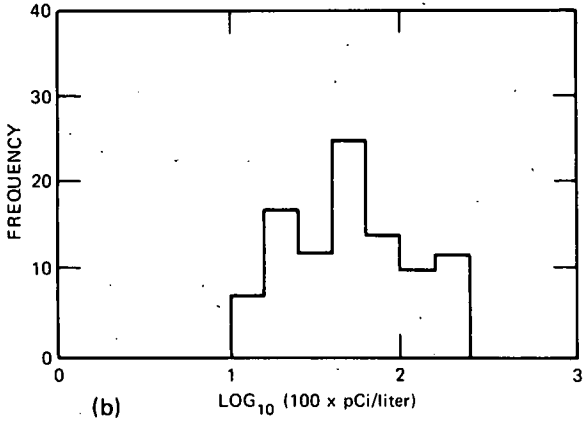


Fig. 2b Distribution of the log of radon concentrations inside homes in Cobourg in the fall of 1976.

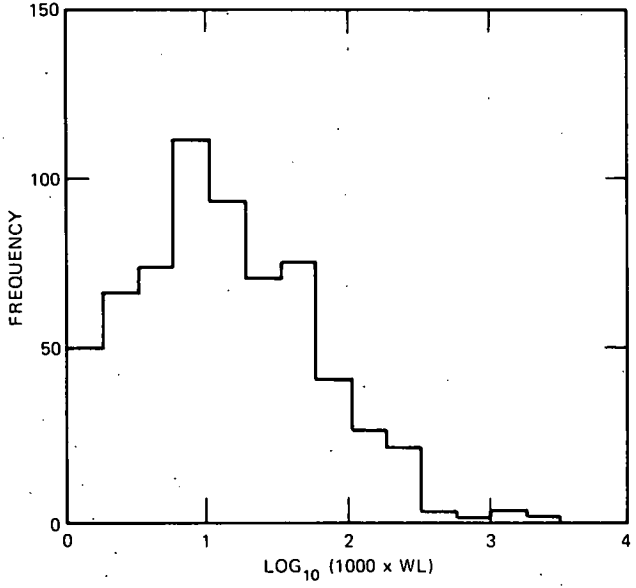


Fig. 3 Distribution of the log of radon daughters concentrations inside homes in Uranium City.

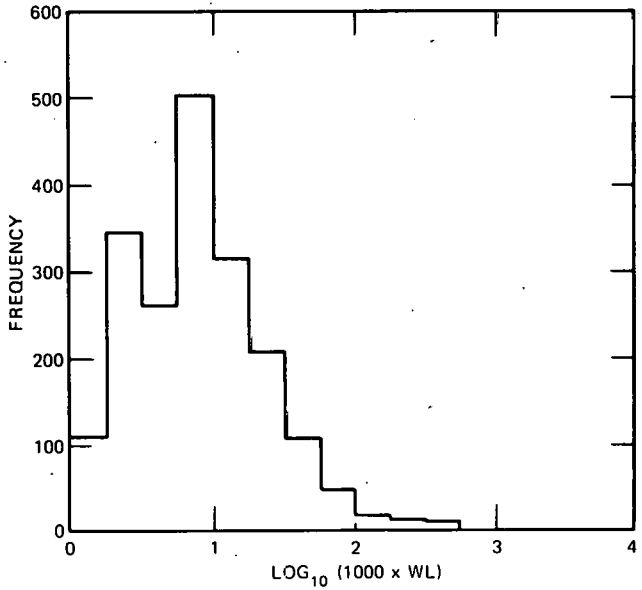


Fig. 4 Distribution of the log of radon daughters concentrations inside homes in Elliot Lake.

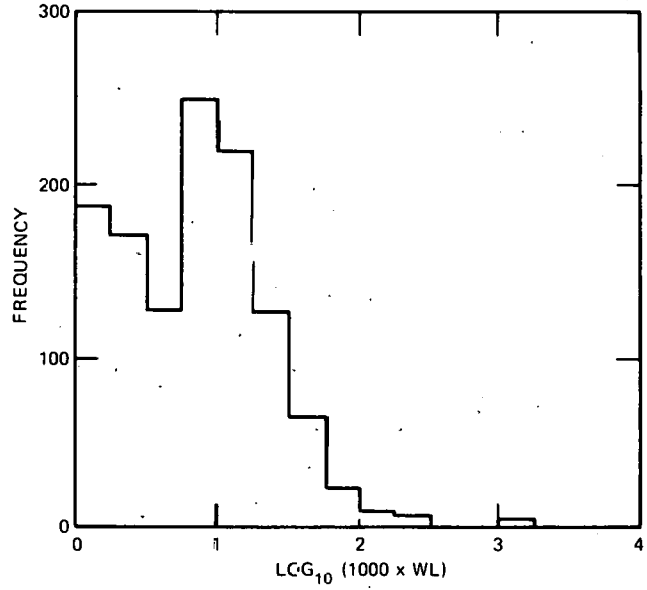


Fig. 5 Distribution of the log of radon daughters concentrations inside homes in the Bancroft area.

TABLE 1

Statistical Data on Air Samples

Location	Variable	Units	Mean	Standard deviation	Upper 99% conf. level	Highest observation	Percentage >0.02 WL	No. of homes sampled
Port Hope	Radon	pCi/liter	0.98	0.3	25.9	532		2961
	Daughters*	WL	0.0029	0.0009	0.0777	1.596	3	
Cobourg (spring of 1976)	Radon	pCi/liter	0.45	0.02	4.1	2.15		106
	Daughters*	WL	0.0014	0.0001	0.0123	0.0065	0	
Cobourg (fall of 1976)	Radon	pCi/liter	0.50	0.02	7.21	6.7		97
	Daughters*	WL	0.0015	0.0001	0.0216	0.0201	0	
Uranium City	Daughters	WL	0.013	0.0041	0.891	2.48	15	632
Elliot Lake	Daughters	WL	0.008	0.0029	0.195	0.397	16	1921
Bancroft area	Daughters	WL	0.007	0.0031	0.204	1.95	17	1162
Deloro	Daughters	WL	0.006	0.0033	0.236	0.088	13	68

*Radon daughter concentrations for Port Hope and Cobourg are calculated from the radon concentrations using an equilibrium factor of 0.3.

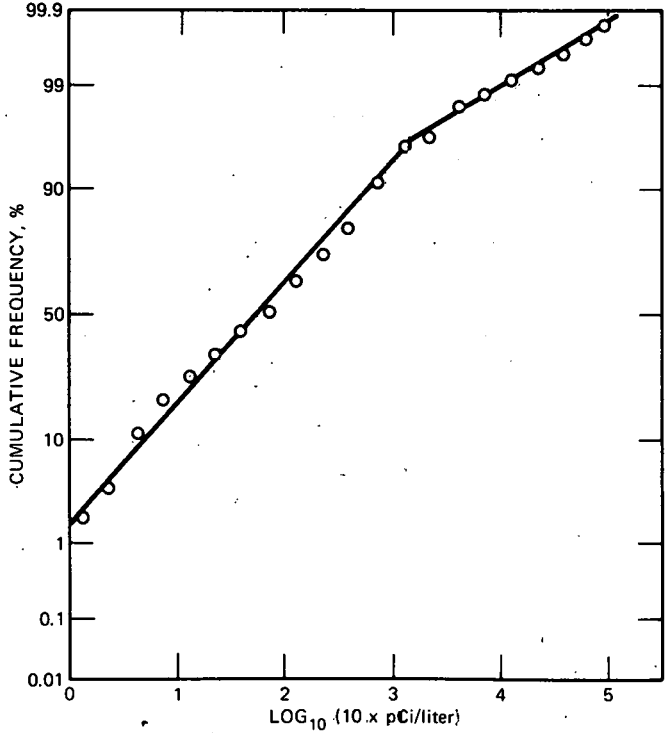


Fig. 6 Cumulative frequency plot of the logarithm of radon concentrations inside homes in Port Hope.

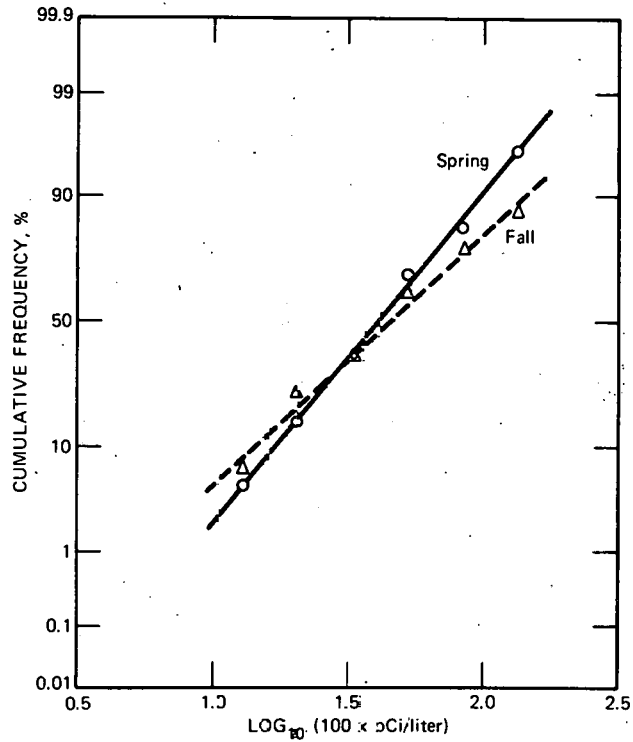


Fig. 7 Cumulative frequency plot of the logarithm of radon concentrations inside homes in Cobourg during the spring and fall of 1976.

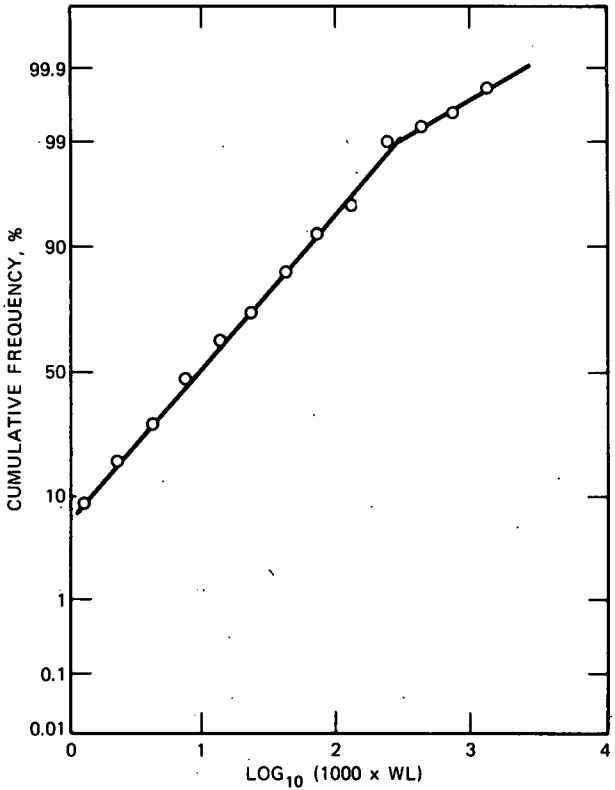


Fig. 8 Cumulative frequency plot of the logarithm of radon daughters concentrations inside homes in Uranium City.

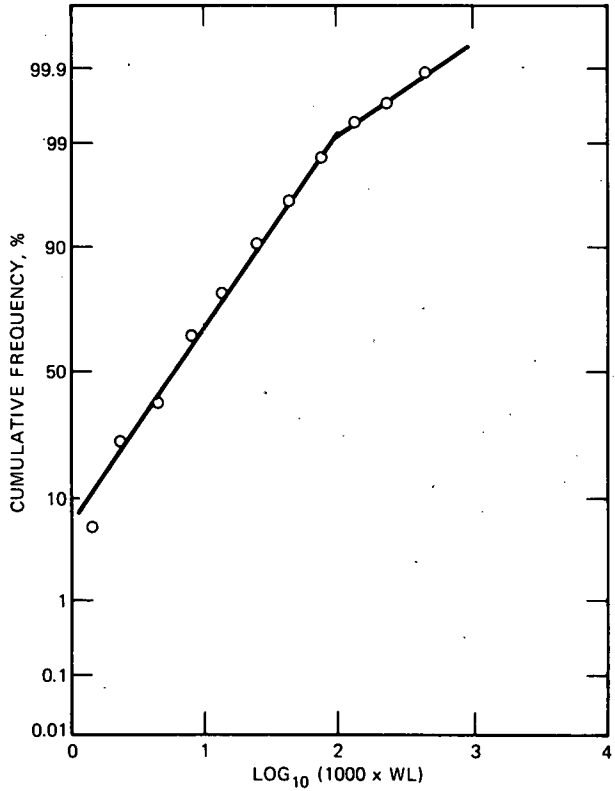


Fig. 9 Cumulative frequency plot of the logarithm of radon daughters concentrations inside homes in Elliot Lake.

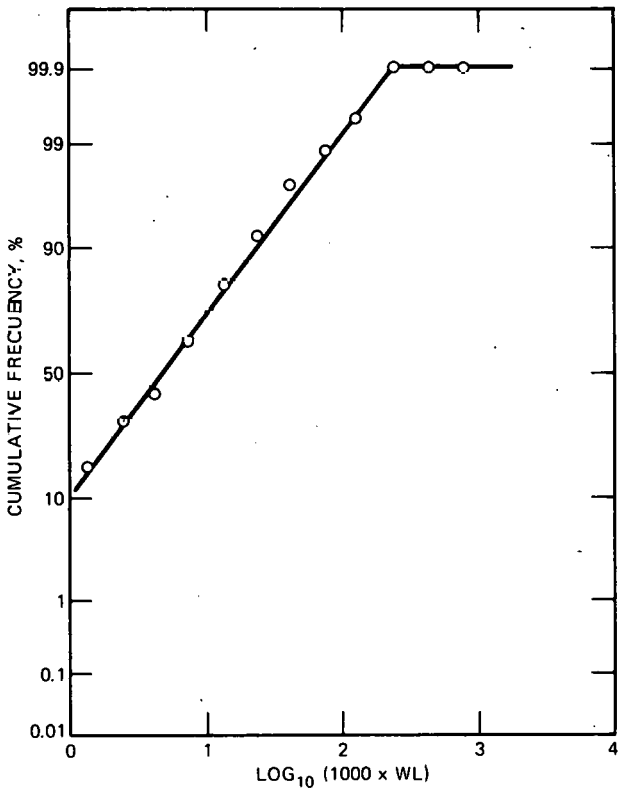


Fig. 10 Cumulative frequency plot of the logarithm of radon daughters concentrations inside homes in the Bancroft area.

TABLE 2

Analyses of Slag Samples Taken from Gloucester Township Sites

Sample No.	Location	^{226}Ra, pCi/g	U, μg/g	^{232}Th, pCi/g	^{230}Th, pCi/g	^{228}Th, pCi/g
1	Doncaster Road	3.1	<10	<5	<5	<5
2	Doncaster Road	190	110	8	14	8
3	Rideau Road	170	190	20	12	22
4	Rideau Road	9.3	<10	7	6	11
5	Albion Road	22	55	140	110	140
6	Albion Road	27	90	60	120	90
7	Albion Road	355	900	160	280	190
8	Albion Road	546	1120	1500	620	1600

measured in contact with the ground at the site of each sample ranged from 0.2 to 5.0 mR/hr, but the correlation between these field measurements and the laboratory analyses of the principal radionuclides was poor. Generally the estimated errors for the laboratory analyses are better than a few percent, but the presence of low-energy radiation plus the energy-dependence characteristics of the field-survey instrument introduce relative large errors and thus a poor correlation is not surprising. The analyses were performed by the Radiation Protection Laboratory of the Ontario Ministry of Labor.

DISCUSSION OF RESULTS

Before drawing any conclusions, it is necessary to establish the value of the data to be discussed. With respect to the radon and radon daughter measurements, the surveys were very broad in that virtually every house in the community was sampled. However, the sample times were of very short duration (a matter of minutes), and the whole survey in a single community extended over a relatively long time and, in some cases, over several seasons. It is well known that the radon and daughter concentrations vary considerably according to ventilation and meteorological conditions. Hence the one-time measurement recorded for a single house has little meaning, but the total distribution provides a useful qualitative picture for each community, and comparisons will be made on a community basis.

A comparison of the lognormal distributions shown in Figs. 1 to 5 shows that only the "normal" community of Cobourg has a symmetrical distribution and that all the others exhibit a marked asymmetry by having a significant number of homes with higher concentrations.

A comparison of the cumulative frequency plots in Figs. 6 to 10 shows the same departure from a symmetrical distribution for the investigated communities, as was noted in Figs. 1 to 5.

Using Bartlett's method (Bartlett, 1937) for testing the homogeneity of the variances of the seven lognormal distributions listed in Table 1, it is concluded that at the 95% confidence level:

1. There is no significant difference between the spring and fall distributions for Cobourg.

2. There are three mutually exclusive populations, i.e., Cobourg, Port Hope, and the remaining communities, which correspond to a normal, uncontaminated community in southern Ontario; a com-

munity in the same area contaminated by human activities; and a group of communities sited in or near uranium mining areas.

It will be interesting to compare these results with those of the survey conducted by Health and Welfare Canada during the summer of 1977, which are to be published shortly (Letourneau, Taniguchi, and Vasudev, 1978).

The analyses listed in Table 2 have no particular significance other than to demonstrate the concentrations found in areas where uncontrolled disposals have taken place.

Finally it is noted that two types of mechanism have been introduced in the communities under discussion which have modified the distribution of the natural radionuclides concerned. At Port Hope, Deloro, and Gloucester Township, radioactive material was brought from other places for processing purposes and subsequently resulted in the contamination of local communities, with possible unanticipated exposure of the local populations. In the uranium mining communities, the mechanism is slightly different in that the local population has been deliberately introduced to the area where the concentrations of the natural radionuclides are higher than elsewhere in order to mine them.

FUTURE WORK

Program managers have been appointed for Port Hope, Uranium City, Elliot Lake, and the Bancroft area. In each case they have carried out a much more detailed investigation, and further interesting data can be expected in the future.

A particular shortcoming of the preliminary investigation has already been noted, i.e., the inability of the grab sampling technique to allow for variations in the air concentration. To deal with this problem, G. Cowper at the Chalk River Nuclear Laboratories of Atomic Energy of Canada Limited has developed an instrument for integrating the exposure to radon in air; it is planned to use many of these instruments in making compliance inspections at those sites where remedial work has been completed.

ACKNOWLEDGMENT

The gathering and analysis of the large body of data discussed here have involved a large number of people from the member agencies of the Federal—Provincial Task Force on Radioactivity and their help and assistance are gratefully acknowledged.

An Assessment of Natural Radionuclides in the Coal Fuel Cycle

CLARENCE E. STYRON
Mound Facility,* Miamisburg, Ohio

ABSTRACT

An assessment of naturally occurring radionuclides in the coal fuel cycle is necessitated by the increasingly important role that coal is expected to play in meeting national energy needs and by the attendant potential for enhancement of concentrations of radionuclides in the environment. This paper describes a preliminary study designed to broadly survey pathways of radionuclides in the coal fuel cycle and to identify critical questions and provide direction for subsequent definitive studies. The scope of the project was limited to western coal because of its prominence in the National Energy Plan. Concentrations of radionuclides in western coal from 19 seams varied widely as do other trace constituents, but on the average these concentrations are comparable to eastern coal. Environmental deposition of radionuclides from stack emissions at a modern power plant burning western coal is estimated by atmospheric dispersion modeling to be 0.1 to 1.0% of background. The major portion of radionuclides in feed coal was associated with bottom ash and fly ash. The emanation of ^{222}Rn (radon) and the leaching of other radionuclides from disposal sites of ash and flue gas desulfurization sludge are recommended for further study.

Coal is expected to play an increasingly important role in meeting energy needs of the United States (Starr, 1976; Rall, 1978), and the attendant potential for enhancement of concentrations of radionuclides in the environment necessitates an assessment both of the naturally occurring radionuclides in the coal fuel cycle and of the environmental control technology needed to minimize this potential

*Mound Facility is operated by Monsanto Research Corporation for the U. S. Department of Energy under contract No. DE-AC04-76-DP00053.

enhancement. In addition to trace elements and other minor constituents, coal contains uranium and its decay products (Barber and Giorgio, 1977; Vine, 1962; Guimond and Fitzgerald, 1976). Although 0.6 pCi/g (1.8 ppm) may be a reasonable national average for ^{238}U in coal, some deposits with concentrations as high as 15 pCi/g (before cleaning) are being used by electric power utilities in the United States (Swanson et al., 1976). Coal deposits with atypically high concentrations of uranium if burned at all would likely be used with dual resource recovery in mind. The process of coal combustion releases trace elements to the atmosphere as vapors and particles, and these particles have relatively greater concentrations of certain trace elements than the feed coal (Kaakinen et al., 1975; Natusch, Wallace, and Evans, 1974). Enrichment in lead of soil and vegetation has been reported at the Four Corners Plant in New Mexico (Cannon and Anderson, 1972), and enrichment of soil in ^{226}Ra (radium) and thorium has been reported in industrialized areas of Poland (Jaworowski and Grzybowska, 1977). Although the environmental impact of these residuals on ecosystems is not certain, conventional wisdom suggests that control of these residuals is a reasonable goal within acceptable cost limits.

The U. S. Environmental Protection Agency (EPA) and the Department of Energy which encompasses the former Energy Research and Development Administration and the former Federal Energy Administration jointly initiated a project with Monsanto Research Corporation at Mound Facility (formerly Mound Laboratory) to assess the fate of radionuclides in coal and their associated health and environmental effects. A preliminary phase was included in the experimental design to broadly survey pathways of radionuclides in the coal fuel cycle and to identify critical questions and provide guidance for subsequent definitive studies of technological enhancement of natural radiation. [The term "technological enhancement of natural radiation" was suggested by Gesell (1976).] The scope of this preliminary phase of the study was limited to only one coal province, and western coal was selected for its prominence in the National Energy Plan. The specific objectives were (1) to investigate the fate of radionuclides in the coal fuel cycle and, where possible, to delineate the scope of the potential environmental and human health problem associated with radioactivity in coal; (2) to compile and evaluate data for ^{238}U, ^{234}U, ^{210}Pb, ^{210}Po, and ^{230}Th found in western coal; (3) to study the release, fate, and accumulation of radionuclides from a power plant burning western coal; and (4) to assess the possible need for additional control technology or standards.

MATERIALS AND METHODS

Samples of coal were collected from 18 western mines representing 19 coal seams. Samples of coal, ash, stack effluents, airborne particulates, soil, and vegetation were collected from a power plant using coal from one of the previously sampled mines. All samples were prepared and analyzed by alpha pulse height spectroscopy. The data were used in calculating a radionuclide balance for the power plant and in atmospheric dispersion modeling to estimate environmental deposition of radionuclides and doses to populations. Details of sampling and analytical procedures are given by Styron et al. (1979).

RESULTS AND DISCUSSION

Western mines sampled in this study included those producing $\geq$0.5 million tons per year of lignite or subbituminous coal. Coal from these mines contained ^{238}U and ^{234}U ranging from 0.04 to 1.2 pCi/g. (For ^{238}U, 1 pCi/g = 3.0 ppm; for ^{234}U, 1 pCi/g = 0.16 ppb.) Analyses specific for ^{238}U and ^{234}U were used since (1) data (unpublished) from a joint project by Mound and EPA-Las Vegas investigating ^{238}U and ^{234}U in soil indicated that $^{234}U/^{238}U$ ratios frequently are significantly different from unity, i.e., on the order of 1.5, and (2) disequilibria in isotopes of the ^{238}U decay chain would have important consequences for estimating the total radionuclide content of coal. For the coal samples, however, ratios of $^{234}U/^{238}U$ were not significantly different from unity, which indicates that these two isotopes are in secular equilibrium. Combining data from all mines studied gave a mean (±95% confidence limit) concentration for ^{238}U of 0.30 (±0.10) pCi/g and ^{234}U of 0.31 (±0.10) pCi/g. These data for ^{238}U and ^{234}U are within the range reported by Swanson et al. (1976) for western coal, slightly below the national average (0.6 pCi/g) reported in their study, and roughly comparable to eastern coal (Bedrosian, Easterly, and Cummings, 1970; Martin, Harward, and Oakley, 1971; Strong, 1977).

Coal samples from the mines were also analyzed for ^{210}Po, the final radionuclide in the ^{238}U decay series. These analyses were somewhat problematic, however, largely because of the absence of a satisfactory standard for ^{210}Po in coal. Samples of coal from the mines evinced concentrations of ^{210}Po ranging from 0.03 to 0.58 pCi/g, with a mean (±95% confidence limit) concentration for

all mines of 0.23 (±0.05) pCi/g. Standards for ^{210}Po in coal are under development.

Pathways of radionuclides in a coal-fired steam electric generating plant (Fig. 1) were investigated by sampling coal, bottom ash, fly ash, stack effluents, airborne particulates, soil, and vegetation. The subject power plant used > 0.5 million tons of coal per year from one of the mines sampled in Wyoming. The power plant is located 17.7 km south of Sioux City, Iowa, and consists of three units with a combined generating capacity of 1020 MWe. Unit 2 (330-MWe capacity) was sampled in this study and operated at 32 to 33% efficiency. The feed coal typically contained 0.61% sulfur, 11.91% ash, 9000 Btu/lb, ^{238}U at 0.48 pCi/g, ^{234}U at 0.51 pCi/g, ^{230}Th at 0.52 pCi/g, ^{210}Pb at 0.84 pCi/g, and ^{210}Po at 1.10 pCi/g. Samples of bottom ash typically contained ^{238}U at 2.54 pCi/g, ^{234}U at 2.72 pCi/g, ^{230}Th at 3.30 pCi/g, ^{210}Pb at 5.63 pCi/g, and ^{210}Po at 5.05 pCi/g. Fly ash contained ^{238}U at 4.23 pCi/g, ^{234}U at 4.36 pCi/g, ^{230}Th at 3.95 pCi/g, ^{210}Pb at 5.76 pCi/g, and ^{210}Po at 5.31 pCi/g. Stack effluents at the output of the electrostatic precipitator contained on the average ^{238}U at 7.56 pCi/m^3, ^{234}U at 7.48 pCi/m^3, ^{222}Rn at 290 pCi/m^3, ^{210}Pb at 14.6 pCi/m^3, and ^{210}Po at 9.17 pCi/m^3.

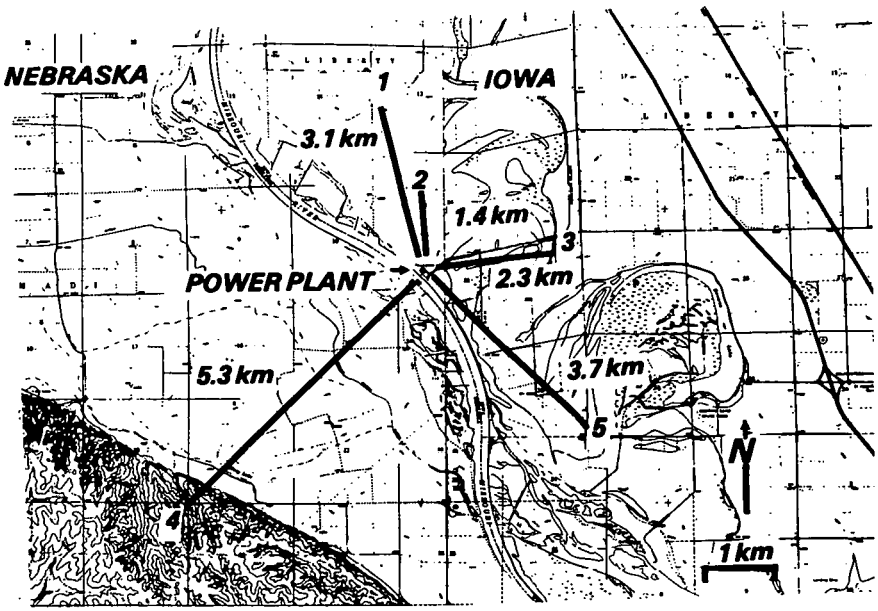


Fig. 1 Map of the study area showing the power plant and five air-quality monitoring stations.

Bottom ash and fly ash contained higher concentrations of all radionuclides than did the feed coal, largely as a result of carbon depletion. The radionuclide balance as calculated for unit 2 indicated that the greatest fraction of radionuclides was retained in fly ash: 79% of ^{238}U and ^{234}U, 72% of ^{210}Pb, and 77% of ^{210}Po. Bottom ash contained an additional 7% of ^{238}U, 8% of ^{234}U, and 10% of ^{210}Pb and ^{210}Po. Whereas some fraction of radionuclides apparently bypassed the electrostatic precipitator as vapors or in association with very fine particles as do other trace constituents of coal (Natusch, Wallace, and Evans, 1974), the beneficial effects of the electrostatic precipitator in retaining the greatest part ($\geqslant$72%) of radionuclides is clear. It should be noted that during the sampling period the electrostatic precipitators were apparently operating at less than design efficiency (99%), and it is suspected that normally the precipitators remove a great deal more than 72% of radionuclides associated with fly ash.

Samples of airborne particulates were collected at five air-quality monitoring stations near the power plant (Fig. 1) and at one station 16 km NNW of the plant. Radionuclide concentration of airborne particulates collected at the five monitoring stations averaged 44 aCi/m^3 for ^{238}U, 41 aCi/m^3 for ^{234}U, 14,000 aCi/m^3 for ^{210}Pb, and 1300 aCi/m^3 for ^{210}Po. These concentrations were not significantly different from those for the station 16 km NNW of the plant. Furthermore, there was no discernable pattern in distribution of radionuclides in airborne particulates relative to the power plant.

Samples of soil from the five monitoring stations contained on the average ^{238}U at 0.77 pCi/g, ^{234}U at 0.74 pCi/g, ^{230}Th at 1.12 pCi/g, ^{210}Pb at 1.74 pCi/g, and ^{210}Po at 1.82 pCi/g. Concentrations of radionuclides in soil from a park and a cornfield 40 and 96 km, respectively, south of the power plant were not significantly different from concentrations at the five monitoring stations. Vegetation (corn and *Bromus* sp. grass) at the monitoring stations contained ^{238}U and ^{234}U at 0.011 pCi/g, ^{210}Pb at 1.31 pCi/g, and ^{210}Po at 0.23 pCi/g. Vegetation collected at locations 40 and 96 km south of the plant did not contain radionuclides at significantly different concentrations from vegetation at the monitoring stations.

Atmospheric-dispersion calculations were made from data on stack effluents to estimate concentrations of radionuclides in air, to estimate ground deposition of radionuclides, and to estimate inhalation doses around the power plant. The results of dispersion modeling indicated that none of the radionuclides released from the plant stack produced significant inhalation doses or ground depositions. The calculated maximum depositions over a 20-year operation

were 0.1 to 1.0% of measured background concentrations. These levels are of no dosimetric significance.

Another type of analysis frequently applied to test soil for enrichment in trace elements by a power plant involves comparing concentrations in upper vs. lower soil strata. Presumably the upper stratum of undisturbed soil would have a higher concentration than a lower stratum if deposition were the predominating mechanism for enrichment. In this study concentrations of radionuclides in the 0- to 5-cm stratum were compared to concentrations in the 5- to 30-cm stratum. For all sites there was no significant difference in ratios (ratios, $\simeq 1$) for ^{238}U, ^{234}U, and ^{230}Th, either for one isotope in the upper vs. lower strata or for pairs of isotopes in a single stratum.

Ratios for ^{210}Pb and ^{210}Po were significantly different [$P \leqslant 0.05$ (probability of no significant difference is $\leqslant 5\%$)] from unity, as would be expected from characteristics of the ^{222}Rn decay scheme (Eisenbud, 1973). Radon-222 diffuses upward through soil to the atmosphere and decays to ^{210}Pb which deposits on soil and vegetation. Subsequently, ^{210}Pb decays to ^{210}Po (via ^{210}Bi), with the $^{210}Po/^{210}Pb$ ratio depending on the length of time ^{210}Pb and its matrix coexist and whether the ^{210}Po is selectively removed by geochemical mechanisms. The ratios of concentrations of ^{210}Pb in upper vs. lower soil strata and similar ratios for ^{210}Po do, however, provide useful information on the possible existence of a centralized source. Should the power plant be releasing discernable quantities of ^{210}Pb (or of its parents, ^{226}Ra and ^{222}Rn), one could expect the ratios of ^{210}Pb in upper vs. lower soil strata to decline with increased distance from the power plant. Ratios of concentrations of ^{210}Pb in upper vs. lower soil layers and similar ratios for ^{210}Po were regressed (first order, least squares) on distance from the power plant. Neither the regression coefficient for ^{210}Pb (—0.0251) nor that for ^{210}Po (—0.0087) were significantly different from zero. The r^2 (coefficient of determination) for the ^{210}Po slope was 0.59, and an r^2 for ^{210}Pb could not be calculated, since there were too few observations. Thus the regression analysis indicated that there was neither a significant decrease in concentration of ^{210}Pb in upper soil strata nor a significant decrease in concentration of ^{210}Po in upper soil strata with increasing distance from the power plant. Clearly, the power plant is not making a discernable contribution to the concentration of these naturally occurring radionuclides.

Accumulation of radionuclides in ash ponds and subsequent emanation of ^{222}Rn from these disposal sites have been suggested (Lee et al., 1977) as potential problem areas. The accumulation of

radionuclides in the ash pond is related to radionuclide concentration of feed coal, amount of coal burned, efficiency of emission controls, and partitioning of radionuclides to bottom ash, fly ash, and stack gases. If it is assumed that ^{226}Ra is in secular equilibrium with and follows ^{238}U during combustion, a total of 17.4 Ci of ^{226}Ra would accumulate in the ash pond over a 30-year period. This quantity of ^{226}Ra could result in the emanation of 3 Ci/day of ^{222}Rn if all ^{222}Rn growing in from ^{226}Ra escaped to the atmosphere. A more realistic assumption of 5% for the ^{222}Rn emanation coefficient (Lee et al., 1977) would suggest that 0.15 Ci/day of ^{222}Rn could be released to the atmosphere. Even though it is not probable that all the ^{222}Rn formed within the ash pond is released to the atmosphere, the determination of emanation coefficients for various ash and flue gas desulfurization sludge disposal sites warrants further attention. Similarly, effort is required in assessing emanation coefficients for ^{222}Rn from concrete blocks and wallboard which incorporate coal ash and flue gas desulfurization sludge as raw materials.

ACKNOWLEDGMENTS

The author gratefully acknowledges the assistance of Dr. Al Shapiro, University of Cincinnati, in the radionuclide balance exercise and the atmospheric dispersion modeling; Mr. Vern Swanson, U. S. Geological Survey, Denver, for help in locating western mines sampled in this study; and Mr. L. Oleson and other members of Iowa Public Service Company for their excellent cooperation and help in collecting samples at the power plant and air-quality monitoring stations.

Appreciation is also expressed to the staff of Environmental Assessment and Planning, Mound Facility, for their efforts in collecting and analyzing samples.

This assessment was supported by the U. S. Environmental Protection Agency (EPA) and the Federal Energy Administration under Interagency Agreement EPA/IAG-P5-E681, and the EPA and the U. S. Department of Energy under Interagency Agreement EPA/IAG-D7-H1161.

REFERENCES

Barber, D. E., and H. R. Giorgio, 1977, Gamma-Ray Activity in Bituminous, Subbituminous and Lignite Coals, *Health Phys.*, 32(2): 83-88.

Bedrosian, P. H., D. G. Easterly, and S. L. Cummings, 1970, *Radiological Survey Around Power Plants Using Fossil Fuel*, EPA Report EERL71-3, U. S. Environmental Protection Agency, Washington, D. C.

Cannon, H. L., and B. M. Anderson, 1972, *Trace Element Content of the Soils and Vegetation in the Vicinity of the Four Corners Plant,* in Part III of Appendix J of the Southwest Energy Study Report of the Coal Resources Work Group, U. S. Geological Survey, Washington, D. C.

Eisenbud, M., 1973, *Environmental Radioactivity,* 2nd ed., Academic Press, New York.

Gesell, Thomas F., 1976, Technologically Altered Natural Radiation Environments, in *Natural Radioactivity in Man's Environment,* Proceedings of the Health Physics Society Tenth Midyear Symposium, Sarasota Springs, N. Y., Oct. 11—13, 1976, pp. 6-12, Rensselaer Polytechnic Institute, Troy, N. Y.

Guimond, Richard J., and Joseph E. Fitzgerald, 1976, The Radiological Implications of Increased Coal Utilization, in *Natural Radioactivity in Man's Environment,* Proceedings of the Health Physics Society Tenth Midyear Symposium, Sarasota Springs, N. Y., Oct. 10—13, 1976, pp. 43-57, Rensselaer Polytechnic Institute, Troy, N. Y.

Jaworowski, Z., and D. Grzybowska, 1977, Natural Radionuclides in Industrial and Rural Soils, *Sci. Total Environ.,* 7: 45-52.

Kaakinen, J. W., R. M. Jorden, M. H. Lawasani, and R. E. West, 1975, Trace Element Behavior in Coal-Fired Power Plant, *Environ. Sci. Technol.,* 9(9): 862-868.

Lee, H., T. O. Peyton, R. V. Steele, and R. K. White, 1977, *Potential Radioactive Pollutants Resulting from Expanded Energy Programs,* Report SRI-EGU-4869, Stanford Research Institute, Menlo Park, Calif.

Martin, J. E., E. D. Harward, and D. T. Oakley, 1971, Radiation Doses from Fossil Fuel and Nuclear Power Plants, in *Power Generation and Environmental Change,* D. A. Berkowitz and A. M. Squires (Eds.), pp. 107-125, American Association for the Advancement of Science, Washington, D. C.

Natusch, D. R. S., J. R. Wallace, and C. A. Evans, Jr., 1974, Toxic Trace Elements: Preferential Concentration in Respirable Particles, *Science,* 183(4121): 202-204.

Rall, David P., 1978, Report of the Committee on Health and Ecological Effects of Increased Coal Utilization, *Fed. Regis., (Wash., D. C.),* 43(10): 2229-2240.

Starr, C., 1976, The Year 2000: Energy Enough, *EPRI (Electr. Power Res. Inst.), J.,* 5.

Strong, A. B., 1977, Power Plant Samples for Thorium and Uranium, from Monitoring and Analytical Services Branch to Herman L. Krieger, Radiochemistry and Nuclear Engineering Branch, Office of Radiation Programs, U. S. Environmental Protection Agency (August 24, 1977).

Styron, C. E., et al., 1979, *Assessment of the Radiological Impact of Coal Utilization. 1. Preliminary Studies on Western Coal,* Report MLM-2514, Monsanto Research Corporation, Miamisburg, Ohio.

Swanson, Vernon E., et al., 1976, *Collection, Chemical Analysis, and Evaluation of Coal Samples in 1975,* Open File Report No. 76-468, U. S. Geological Survey.

Vine, J. D., 1962, *Geology of Uranium in Coaly Carbonaceous Rocks,* Professional Paper 356-D, U. S. Geological Survey.

DISCUSSION

Bland: We have measured activities in fly ash from thermal plants in Alberta. In particular, activities due to thorium are evident and in

the case of ^{230}Th might indicate a nonequilibrium with ^{226}Ra. Have you data for thorium for the locations reported?

Styron: Yes. Our data on ^{230}Th suggest an equilibrium with ^{238}U in coal, bottom ash, and fly ash.

Landa: How long was the power plant in operation?

Styron: The power plant began generating electricity in 1969.

Landa: Recent work presented in the journal *Plant Physiology* by Browne and Fang suggests that stomatal entry of elemental-mercury vapor from coal combustion may be a significant source of vegetation contamination with mercury. You have attributed elevated levels of ^{210}Pb in vegetation to ^{222}Rn exhalation from soils and subsequent deposition of ^{210}Pb on vegetation surfaces. Have you any experimental data or do you know of any literature which addresses the question of the possible entry of ^{222}Rn into the interior of vegetative structures and the subsequent in situ formation of ^{210}Pb?

Styron: Our data do not speak to this very interesting problem, and I am unaware of any literature on the question of possible entry of ^{222}Rn into the interior of plants and the subsequent in situ formation of ^{210}Pb.

Matsunami: Can you mention the concentration of uranium in coal in parts per million?

Styron: For ^{238}U, 1 pCi/g = 3.0 ppm; for ^{234}U, 1 pCi/g = 0.16 ppb; for ^{210}Po, 1 pCi/g = 0.22×10^{-6} ppb. Therefore, 0.3 pCi/g of ^{238}U is equivalent to 0.9 ppm of ^{238}U.

Boeri: Which is the cause of high concentration in vegetables? Airborne effluents deposition?

Styron: Elevated concentration of ^{210}Pb on vegetation is most likely to have occurred from exhalation of ^{222}Rn from soil, decay of atmospheric ^{222}Rn to ^{210}Pb, and subsequent return of ^{210}Pb to the earth's surface where broadleafed plants present a convenient surface for deposition (Eisenbud, 1973). Environmental concentrations of ^{210}Pb predicted by atmospheric diffusion modeling of stack effluents are 0.1 to 1% of measured concentrations in the environment. This suggests that the power-plant stack is not a significant source of environmental radionuclides.

Boeri: What deposition velocity was used in your atmospheric dispersion model?

Styron: The deposition velocity for the atmospheric diffusion model was assumed to be 0.01 m/sec.

Holtzman: Did you obtain data from control areas on corn? The level in the kernel seems to be quite high relative to other values I have seen by factors of 4 or 5.

Styron: Our control areas were 40 and 96 km, respectively, south of the power plant. Concentration of radionuclides in vegetation from the control areas was not significantly different from that in vegetation near the power plant. We did not, however, have control areas in other states.

Holtzman: Why does your data base not contain data on ^{210}Pb, since it appears to produce the greatest dose?

Styron: Coal and other samples associated with the power plant were also analyzed for ^{210}Pb. Coal from the mines was analyzed for ^{210}Po, and, since an equilibrium for radionuclides of the uranium series is suggested, the ^{210}Pb should also be in equilibrium with ^{238}U.

Holtzman (Comment): The distribution of ^{210}Pb and stable lead in soil is similar to that which you observed, i.e., high at the surface and decreasing with depth. This is not necessarily related to fallout.

Perturbations on the Natural Radiation Environment Due to the Utilization of Coal as an Energy Source

HAROLD L. BECK, CARL V. GOGOLAK, KEVIN M. MILLER, and WAYNE M. LOWDER
Environmental Measurements Laboratory, U. S. Department of Energy, New York, New York

ABSTRACT

The radionuclide content of coal, ash, and released fly ash from coal-fired power plants is examined, and previous estimates of environmental effects and radiation exposures of the population are reviewed and modified. New measurements of deposited radioactivity in the environs of a large power plant are presented. Releases from coal fuel-cycle wastes are discussed, and the relative radiological hazards of coal-fired and nuclear power plants are reviewed.

Coal, like most materials found in nature, contains trace quantities of the naturally occurring radionuclides, ^{238}U, ^{232}Th, and ^{40}K as well as their associated daughter products. Utilities in the United States burned 3.6×10^{11} kg of coal in 1974 and may burn as much as 8×10^{11} kg per year by 1984 (Ray and Parker, 1977). Present U. S. coal resources are estimated to be 4×10^{15} kg (Averitt, 1975). The direct combustion of this coal, or its conversion to other fuels, results in the concentration of the noncombustible mineral matter, including most of the radionuclides, in the ash or gaseous residues. The release of some of these residues to the environment, either directly through stack releases or indirectly from waste storage areas, results in a redistribution of this natural activity from deep in the earth to locations where it can modify ambient radiation fields and population radiation exposure. Whether or not this redistribution constitutes a potential health problem has become a matter of some public and scientific concern.

The purpose of this paper is to review and analyze, in some detail, the data available in the literature pertaining to the sources and releases of radionuclides from the coal fuel cycle, to present some new data, to examine the potential environmental and population exposures resulting from these releases, to compare the relative impacts of coal-fired vs. nuclear power, and to discuss and assess problem areas where further research is desirable.

RADIOACTIVITY IN COAL

Inorganic mineral matter is incorporated into coal because of its presence in the original peat beds or in layers of interspersed inorganic material, or as a result of intrusion during or after coalification by leaching from surrounding rocks and soils (Ray and Parker, 1977; Abernethy and Gibson, 1963; Magee, Hall, and Varga, 1973).

In general, the concentrations of trace elements in coal, including the primordial radionuclides ^{238}U, ^{232}Th, and ^{40}K, are less than their respective average concentrations in the earth's mantle (Gluskoter et al., 1977; Ruch, Gluskoter, and Shimp, 1974; Swanson et al., 1976). Occasionally, however, usually as a result of leaching from abnormally radioactive overburdens of volcanic origin, unusually high concentrations of some radionuclides, in particular uranium, can be found in various coal deposits in up-to-ore-grade concentrations (> 0.1%) (Abernethy and Gibson, 1963; Vine, 1955, 1962; Denson, 1959; Lee et al., 1977; Guimond and Fitzgerald, 1977). These uraniferous coals are the exception and occur almost invariably in such low-grade coal deposits as lignite, subbituminous, and carbonaceous shale (Vine, 1955, 1962; Denson, 1959; Abernethy and Gibson, 1963). Most of these deposits are in the western United States, although small pockets of uraniferous coal have also been found in other parts of the country. The largest deposits are in the lignites of the Northern Great Plains and in some deposits in Wyoming (Vine, 1955; Denson, 1959). These uraniferous coals constitute only a small fraction, perhaps 0.1%, of the U. S. Western coal reserves, and because of their low rank (BTU value) are not presently mined or contemplated for mining (Lee et al., 1977; Vine, 1955; Denson, 1959; Guimond and Fitzgerald, 1977). Unfortunately the existence of these deposits has led to some published reports which incorrectly give the impression that Western coals are, in general, more radioactive than other coals and that the vast reserves of low-sulfur Western coal may thus contain unusually high uranium contents (Federal Register, 1978; Environmental Protection

Agency (EPA), 1977; Farmer et al., 1977; Guimond and Fitzgerald, 1977). Actually, Western coals taken as a whole, contain lesser quantities of all types of trace elements, including radionuclides, than other coals (Gluskoter et al., 1977; Swanson et al., 1976).

Data on radionuclide contents in coal actually being mined, or available for mining, are shown in Table 1. Listed are the uranium, thorium, and potassium contents measured in almost 1000 samples obtained directly from mines providing most of the coal used in the United States today, as well as much of our proven reserves. Note that the Northern Great Plains lignites, excluding the pockets of uraniferous coal, are lower in activity than coal from other regions. The data of Farmer et al. (1977) are particularly significant since they were obtained from mines in the western United States which produced 65% of the total coal mined in 1974 in the states of Arizona, Colorado, North Dakota, New Mexico, Wyoming, and Montana. The frequency distributions of uranium, thorium, and potassium for all coals, with the distributions for Western coals shown separately, are given in Fig. 1.

We believe the data in Table 1 and Fig. 1 present a reasonable summary of the mean and range of concentrations of uranium, thorium, and potassium likely to be encountered in coal. The geometric means have been given in Table 1 as well as the arithmetic mean (average) since, as shown in Fig. 1, these are better estimates of the most probable values, i.e., the values that would probably be obtained by analyzing a single sample or a small number of samples. The mean values for all coals sampled, 1.7 μg/g for natural uranium, 4.5 μg/g for natural thorium, and 1700 μg/g for total potassium, correspond to activities for ^{238}U, ^{232}Th, and ^{40}K of 0.6, 0.5, and 1.4 pCi/g, respectively. For comparison, we have also listed in Table 1 typical values and ranges for these nuclides in soils and rocks.

The actual radionuclide activities in coal as delivered to power plants may differ slightly from the coal as mined since about 50% of the coal mined in the United States is washed before delivery to remove a portion of the heavier interspersed mineral matter and thus reduce the ash and sulfur content (Wewerka et al., 1976). The washability of various elements from coal mine samples appears to vary significantly, depending on their mode of incorporation into the coal and subsequent major identification with either its organic or inorganic fractions (Ruch et al., 1974; Gluskoter et al., 1977). Although uranium tends to associate more with the organic fraction, whereas potassium and thorium tend to concentrate in the inorganic fractions, none of these nuclides appear to be sufficiently washable to be significantly reduced in coal delivered to power plants (Gluskoter et al., 1977). To verify this, we have attempted to

TABLE 1

Uranium, Thorium, and Potassium Concentrations in Coal as Mined
(Fraction of Dry Weight)

Region, type	No. of samples	U, μg/g			Th, μg/g			K, g/100 g			Investigator
		Range	Geo. mean	Mean	Range	Geo. mean	Mean	Range	Geo. mean	Mean	
Pennsylvania, anthracite	53	0.3—25.2	1.2	1.5	2.8—14.4	4.7	5.4	0.019—1.5	0.13	0.24	Swanson et al., 1976
Appalachian*	331	<0.2—10.5	1.0	1.4	2.2—47.8	2.8	4.9	0.008—2.4	0.13	0.23	Swanson et al., 1976
Midwest*	143	0.2—43	1.4	3.3	<3—79	1.6	5.2	0.011—0.53	0.11	0.16	Swanson et al., 1976
Northern Great Plains†*	93	<0.2—2.9	0.7	0.9	<2—8.0	2.4	2.7	0.006—0.37	0.03	0.04	Swanson et al., 1976
Gulf Coast, lignite	34	0.5—16.7	2.4	3.2	<3—28.4	3.0	8.3	0.012—1.3	0.15	0.30	Swanson et al., 1976
Rocky Mountains*†	134	<0.2—23.8	0.8	1.6	<3—34.8	2.0	3.6	0.003—1.7	0.03	0.08	Swanson et al., 1976
Alaska†	18	0.4—5.2	1.0	1.2	<3—18	3.1	4.4	0.016—0.37	0.08	0.12	Swanson et al., 1976
Illinois Basin	56(113 K)	0.31—4.6	1.3	1.5	0.71—5.1	1.9	2.1	0.04—0.56	0.16	0.17	Gluskoter et al., 1977
Appalachian	14(23 K)	0.4—2.9	1.3	1.5	1.8—9.0	4.0	4.5	0.06—0.68	0.23	0.25	Gluskoter et al., 1977
Western	22(29 K)	0.3—2.5	1.0	1.2	0.62—5.7	1.8	2.3	0.01—0.32	0.05	0.05	Gluskoter et al., 1977
Western	19	0.11—3.5	0.85	0.9							Farmer et al., 1977
All samples	910(983 K)		1.04	1.74		2.40	4.47		0.13	0.17	
		Typical range		Avg.	Typical range		Avg.	Typical range		Avg.	
Soil		0.9—4.0		1.8	2—12		6	0.12—2.5		1.3	UNSCEAR, 1977; NCRP, 1975
Rocks		0.5—5		2.7	1.6—20		9.6	0.8—5		2.1	NCRP, 1975; Swanson et al., 1976

*Bituminous.
†Subbituminous.

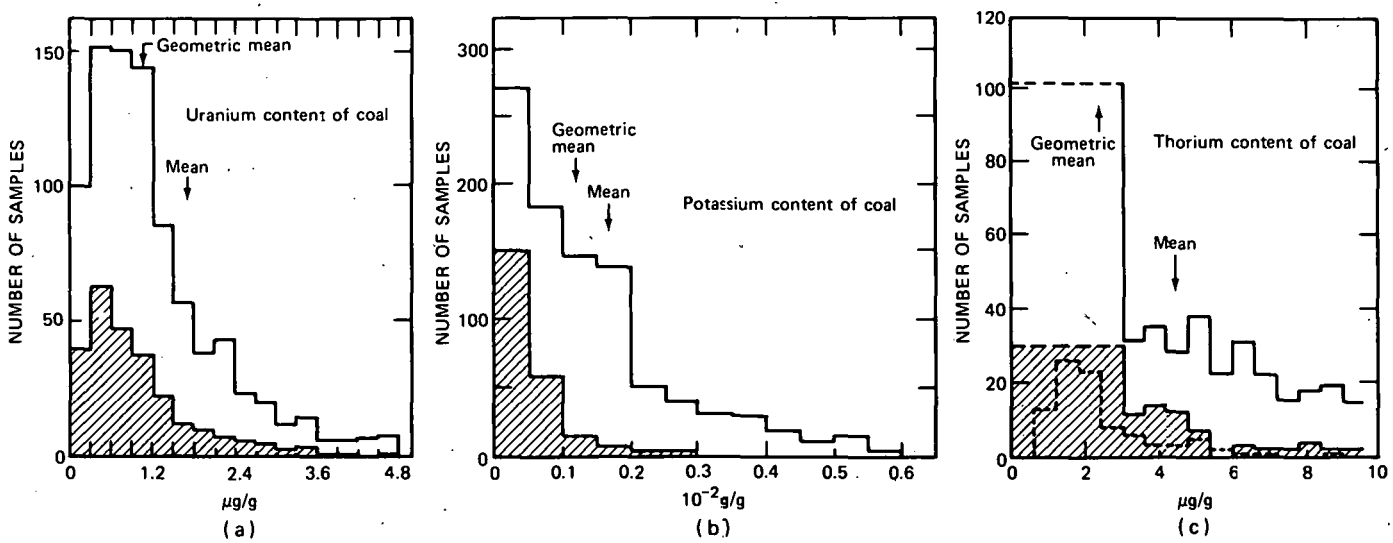


Fig. 1 Frequency distributions of measured uranium, thorium, and potassium contents in coal samples from mines. Solid histograms include all samples from Table 1, hatched histograms are Western coals analyzed by Swanson et al. (1976) and Farmer et al. (1977). Because the minimum detectable level for most of the Swanson et al. thorium analyses was 3 μg/g, all data below 3 μg/g were grouped and the data for the 92 samples of Gluskoter et al. (1977) are shown separately by the dotted histogram to show the low concentration frequencies. Also shown are the mean and geometric mean for each distribution.

evaluate available data on analyses of coal samples obtained directly from power plants. Data available in the literature, as well as our own measurements, are listed in Table 2. Only analyses of U. S. coals are listed, and the limited data available are not sufficient either in number or variety to warrant a direct statistical comparison with the extensive data in Table 1. They do show, however, that the values from Table 1 are, in fact, typical of actual coals burned in operating power plants. The data in Table 2, in contrast to the concentration values of natural uranium, thorium, and potassium measured in the mine samples, are in most cases direct measurements of radioactivity for the major radionuclides and in some cases their decay products. In the table we have assumed that ^{238}U and ^{234}U are in secular equilibrium. The few simultaneous measurements of both indicate that this is usually true (Farmer et al., 1977).

The actual activity of the coal burned in a single power plant can vary widely within the ranges of values given in Table 1. Many power plants, particularly those not in mining areas, obtain fuel from a number of different mines. In addition, the activity in the coal obtained from a single mine, in fact a single seam, has been found to vary by as much as an order of magnitude. Data obtained by Gluskoter et al. (1977) on the range of concentrations with depth in five different seams of coal mined in Illinois showed variations of 0.4 to 28 $\mu g/g$ of uranium, 0.1 to 3.3 $\mu g/g$ of thorium, and 100 to 4200 $\mu g/g$ of potassium. Similar results have been documented for coal mined in the Powder River Basin of Wyoming where uranium, thorium, and potassium concentrations in a single coal seam varied over the ranges 0.2 to 1.7 $\mu g/g$, 1 to 3 $\mu g/g$, and 150 to 520 $\mu g/g$, respectively (Lee et al., 1977; U. S. Department of the Interior, 1974; Ray and Parker, 1977). The highest uranium concentrations were usually found at the top of the seams, whereas the highest thorium and potassium values were found both at the top and bottom, indicating the effect of leaching and intrusion of trace elements from higher activity overburdens and underburdens.

Further substantiation of the probable large variations in activity in coal burned in a single plant, even over a short period of time, is shown by the range of activities in coal reported by Bedrosian, Easterly, and Cummings (1970), which were all obtained from a single plant in Alabama. The three Illinois and two Western coal samples were analyzed by us and were all obtained from a single Midwestern utility (see Table 2). However, with these large variations in fuel activity, we would expect that over the long lifetime of most power plants these variations in activity would average out and the average activity of all the coal burned would tend toward the arithmetic mean for the majority of coal resources. We can thus

TABLE 2

Radioactivity in Coal Samples Collected from U. S. Power Plants*

Origin	No. of samples	Picocuries per gram							Reference
		$^{238}U(^{234}U)$	^{226}Ra	^{210}Pb	^{210}Po	^{232}Th	^{228}Ra	^{40}K	
West		0.24	0.21	0.26		0.17	0.17	0.73	Coles, Ragaini, and Ondov, 1978
West		0.85	0.64	0.68		0.56	0.55	1.4	Coles, Ragaini, and Ondov, 1978
Illinois, Kentucky		0.74				0.23		1.2	Klein et al., 1975b
Wyoming			0.014	0.28					Kaakinen et al., 1975
West Kentucky			0.4			0.58		1.1	Bedrosian, Easterly, and Cummings, 1970
East Tennessee			0.06			0.51		2.8	Bedrosian, Easterly, and Cummings, 1970
North Alabama			0.26			0.43		5.6	Bedrosian, Easterly, and Cummings, 1970
Widows Creek Power Plant	4		0.23(0.16—0.31)			1.4(0.19—2.3)		3.8(1.9—4.7)	Bedrosian, Easterly, and Cummings, 1970
Wyoming	4	0.42(0.36—0.54)		0.86(0.5—1.2)	1.2(0.9—1.7)				Farmer et al., 1977
Pennsylvania bituminous		0.51	0.45			0.40		4.1	This volume
Montana		<0.1	0.16			<0.1		<1.0	This study
Wyoming		0.14	0.13			<0.1		<1.0	This study
Illinois	3	0.61(0.43—0.83)	0.62(0.42—0.72)			0.15(0.11—0.21)		1.5(<1—2.4)	This study
Appalachian		0.80	0.57			0.43		4.8	This study
Range: all measurements (equivalent natural element)		<0.3—2.5 μg/g (ppm uranium)	<0.03—2.1 μg/g (ppm equivalent uranium)			<1—21 μg/g (ppm tnorium)		0.13—0.7 g/100g (% potassium)	

*All values are for whole air-dried coal. Where more than a single value was reported, the mean, range, and number of samples are shown. Most of the other values reported also represent the mean of composite or duplicate analyses. For comparison with the data in Table 1, 1 ppm of thorium = 0.11 pCi/g ^{232}Th, 1 ppm of uranium = 0.34 pCi/g ^{238}U, and 1% of potassium = 8 pCi/g ^{40}K. Our measurements for ^{232}Th are inferred from gamma-ray spectrometric analyses of ^{228}Ac and ^{208}Tl lines assuming equilibrium.

justifiably choose to calculate long-term releases from these means even though short-term releases may vary significantly.

The data in Table 2 show secular equilibrium can be assumed in coal among members of the ^{238}U and ^{232}Th decay series. Considering the probable great age of most coal deposits, this might be expected. The only significant reported departures from equilibrium were by Farmer et al. (1977) and Kaakinen et al. (1975), both of whom reported apparent enhanced ^{210}Pb and ^{210}Po levels in some Western coals. The data of Coles, Ragaini, and Ondov (1978), however, indicate ^{210}Pb to be in equilibrium with ^{226}Ra in other samples of Western coal. Unfortunately Farmer et al. (1977) did not analyze for ^{226}Ra, and thus it is not clear whether their data represent enhanced lead and polonium or a deficiency in uranium, and the Kaakinen analyses were apparently only for a limited number of samples from a single mine. We can, however, conceive of a realistic potential mechanism for enhanced ^{210}Pb and ^{210}Po activities in coal. This might occur where large quantities of the gaseous ^{222}Rn diffuse from adjacent uraniferous rocks into a lower activity coal seam with subsequent trapping of the particulate decay products in the coal. High activity overburdens and protrusions of shale and clays containing up to 50 $\mu g/g$ of uranium were measured by Gluskoter et al. (1977) in samples from an Illinois mine. We would not expect such elevated ^{210}Pb and ^{210}Po levels to be typical of most coals. More data on these nuclides in coal are needed, and we are in the process of analyzing samples for this purpose.

Lacking conclusive evidence to the contrary, we will assume that all the daughters of ^{238}U and ^{232}Th are in equilibrium in coal and the activities of the daughters can be estimated from the measurements of natural uranium and thorium concentrations. For all further calculations in this paper, we will assume, using the data in Table 1, that the mean activities in coal are 0.6 pCi/g of ^{238}U, 0.5 pCi/g of ^{232}Th, and 1.4 pCi/g of ^{40}K.

RADIOACTIVITY IN COAL PLANT EFFLUENTS

In the production of electric power, coal is burned in furnaces operating at temperatures of up to 1700°C. Most of the mineral matter in the coal is fused into a vitrified glass-like ash. The amount of inorganic solid residue remaining after high-temperature combustion is usually termed the ash content of the coal. A portion of the heavier ash, along with incompletely burned organic matter, drops to the bottom of the furnace as bottom ash or slag. The fly ash, however, is carried through the boiler along with the hot flue gases

and any volatilized mineral compounds to the stack where, depending on the efficiency of emission control devices, some fraction is released to the atmosphere. The amount of fly ash produced and its physical and chemical characteristics depend on the type of combustion system as well as the mineral content and fusion temperature of the coal being burned. The furnaces commonly used in the United States today burn pulverized coal converting 60 to 85% of the ash content of the coal into fly ash (Ray and Parker, 1977; Meikle, 1975). Ash contents of coals vary widely, as shown in Table 3, with the mean value being about 13 to 14% of dry weight. Table 3 shows that the heat content (BTUs/lb) and moisture content of coal are also highly variable. The total amount of ash generated by a typical plant will thus depend on the type and amount of coal burned. A 1000-MW(e) power plant operating 80% of the time will consume about 2.7×10^9 kg/year of coal, assuming 35% thermal efficiency and an average heat content of 11,180 BTU/lb (see Table 3). Other estimates range from 2.1×10^9 to 3.7×10^9 kg/year depending on the type of coal used (Lee et al., 1977; McBride et al., 1977; Eisenbud and Petrow, 1964). The lower the coal rank (BTU value), the greater the amount of coal which must be burned to produce a given amount of electricity.

The radionuclides included in the noncombustible mineral matter will be partitioned between the bottom ash and fly ash, except for the gases and volatilized minerals that will be incorporated directly into the flue gases. A number of recent studies at operating power plants have indicated that certain more volatile trace elements partition unequally between bottom ash and fly ash. They become concentrated on the smaller fly ash particles because of their larger surface-to-volume ratios as the hot flue gases cool down on their way to the stack (Klein et al., 1975a, 1975b; Kaakinen et al., 1975; Natusch, Wallace, and Evans, 1974; Linton, Loh, and Natusch, 1976; Ray and Parker, 1977). This process results in the depletion of certain elements in bottom ash and their consequent enrichment in fly ash, an effect which increases as the size of the fly-ash particles decreases (Coles, Ragaini, and Ondov, 1978; Natusch, Wallace, and Evans, 1974; Linton, Loh, and Natusch, 1976). These smaller particles are less efficiently collected by emission-control devices, such as electrostatic precipitators and scrubbers (Linton, Loh, and Natusch, 1976; Coles, Ragaini, and Ondov, 1978) and thus preferentially escape from the plant. Among the radionuclides shown in Table 4, lead and polonium seem to exhibit the greatest enrichment on released fly ash. Unfortunately the amount of available data is limited. Uranium exhibits a modest enrichment, while thorium and potassium exhibit no significant enrichment. The isotope ^{226}Ra

TABLE 3

Ash, Moisture, and Heat Content of Coal*

Origin	Ash, % Mean (range)	Moisture, % Mean (range)	Heat content, BTU/lb Mean (range)	Reference
Pennsylvania anthracite	12.6(5.2—45.1)	1.4(0.5—3.9)	12,780(6,730—14,360)	Swanson et al., 1976
Appalachian†	11.0(2.4—45.2)	2.8(0.7—15.1)	12,890(6,700—15,000)	Swanson et al., 1976
Interior†	12.6(1.7—36.7)	7.2(1.3—18.6)	11,580(6,670—14,770)	Swanson et al., 1976
Gulf lignite	16.0(2.8—41.1)	46.9(36.5—52.5)	4,170(2,050—5,290)	Swanson et al., 1976
Northern Great Plains,‡ lignite	8.3(4.2—21.9)	24.5(17.8—36.9)	8,480(6,330—9,900)	Swanson et al., 1976
Rocky Mountains†‡	9.1(2.1—32.2)	12.9(1.6—35.0)	10,480(4,660—13,370)	Swanson et al., 1976
799 U. S. coals	11.3 13.5(dry weight)	10.0	11,180	Swanson et al., 1976
165 U. S. coals	11(4—20)(dry weight)	9.9(0.5—37)	12,545(dry weight)	Gluskoter et al., 1977
Average U. S. coals	13.4			FPC, 1975
Average U. S. coals	11			Rohrman, 1971
Ohio Basin	13(11.5—23)			Rohrman, 1971

*For whole coal as mined except as noted.
†Bituminous.
‡Subbituminous.

TABLE 4

Measured Enrichment Ratios in Escaping Fly Ash*

Investigator	Fly ash released, %	Enrichment ratio					
		U	^{226}Ra	^{228}Ra	Th	^{210}Pb	^{210}Po
Coles, Ragaini, and Ondov, 1978	<3	1—3	1—2	~1	~1	1—5	
Klein et al., 1975a,b	0.47		1.7†	1.7†	1.4	11§	
	3.5					~1	
Kaakinen et al., 1975	4.8		~1			~5	~5
Bayliss and Whaite, 1966	7.5		2				
Natusch et al., 1974	‡					6—10§	

*Range for various size fractions, maximum enrichment was for particles with mean diameter of 2.4 μm.

†Our estimate from measurement of barium.

‡Range of composite samples of different size fractions from eight power plants; maximum enrichment for particles of 1—2 μm diameter.

§Measurements for stable lead.

does exhibit a slight enrichment in contrast to ^{228}Ra, perhaps due to its association with the more volatile uranium compounds in the organic fraction of the coal (Coles, Ragaini, and Ondov, 1978). Since the maximum enrichment occurs on the smallest particles, we would expect the net enrichment to increase as the total amount of fly ash escaping decreases and the smaller particles become a larger fraction of escaping mass. This is shown by the lead enrichment factors in Table 4 which range from ~1 to 11 for different fly-ash emission-control efficiencies. This enrichment mechanism should, therefore, only be important for estimating radionuclide releases from well-controlled plants.

Using the data in Tables 1 and 4, we can estimate the activity expected in both collected and released fly ash. Assuming an average ash content for dry coal of 13.4%, our mean ^{238}U, ^{232}Th, and ^{40}K activities in coal would result in unenriched fly ash activities of 4.5, 3.7, and 10 pCi/g, respectively. The actual activities in collected fly ash and escaping fly ash will be larger as discussed in the preceding paragraphs. Except for this enrichment, the daughter products of ^{238}U and ^{232}Th would be expected to be present in the ash with the same activity as their longer lived ancestors except perhaps for the short-lived antecedents of the gases ^{222}Rn and ^{220}Rn. These estimates are compared to actual measurements on ash samples

TABLE 5

Radioactivity in Ash Samples Collected from Power Plants in the United States*

Origin	No. of samples	Sample	Picocuries per gram							Reference
			$^{238}U(^{234}U)$	^{226}Ra	^{210}Pb	^{210}Po	$^{232}Th(^{228}Th)$	^{228}Ra	^{40}K	
Western United States	8	FA	2.3(1.4—2.8)				4.7(2.4—6.7)		6.1(1.2—16.2)	Furr et al., 1977
Appalachian and Midwest	14		2.2(1.7—6.5)				4.9(1.4—7.5)		16.6(9.4—27.8)	Furr et al., 1977
Appalachian	6	FA		3.8(2.1—5.0)			2.6(2.1—3.3)	2.4(1.8—3.1)		Eisenbud and Petrow, 1964
Western United States		FA	1.9	2.3	1.4		1.7	1.7	8.1	Coles, Ragaini, and Ondov, 1978
Western United States		BA	1.5	1.9	0.6		1.5	1.5	6.8	Coles, Ragaini, and Ondov, 1978
Western United States		FA	3.5	2.9	2.2		2.4	2.4	6.3	Coles, Ragaini, and Ondov, 1978
Western United States		BA	2.8	2.5	0.8		2.2	2.1	6.2	Coles, Ragaini, and Ondov, 1978
Western United States		FA	3.6	3.0	2.8		2.5	2.5	6.2	Coles, Ragaini, and Ondov, 1978
Western United States	4	SA	5.4—12	3.3—5.9	4.3—17		2.8—3.3	2.7—4.2	7.0—7.4	Coles, Ragaini, and Ondov, 1978
Appalachian	6	FA		1.9(1.0—3.3)			1.4(0.4—2.0)		21.4(16.5—28.6)	Bedrosian, Easterly, and Cummings, 1970

Wyoming	FA	4.3		5.8	5.3				Farmer et al., 1977
Wyoming	BA	2.6		5.6	5.0				Farmer et al., 1977
Wyoming	FA		0.8	10.5					Kaakinen et al., 1975
Wyoming	BA		0.6	1.0					Kaakinen et al., 1975
Appalachian	FA		2.8			1.2	1.2	10.7	Goldstein, Sun, and Gonzales, 1971
Illinois, Kentucky	FA	3.4				2.2		16	Klein et al., 1975b
Pennsylvania bituminous	FA	2.3	2.3			2.1		18.9	This study
Pennsylvania bituminous	BA	1.8	1.6			1.4		12.6	This study
Appalachian	FA	2.6	2.5			2.4		13.3	This study
	Soil	0.7	0.7	$\geq$0.7	$\geq$0.7	0.7	0.7	10	UNSCEAR, 1977

*Where more than one value was reported, the mean, range, and number of samples are shown. Most of the other values shown also represent the mean of composite or duplicate analyses. FA, collected fly ash; SA, escaping fly ash; and BA, bottom ash. The SA values from Coles, Ragaini, and Ondov (1978) are the range for four different size fractions. The average activities of typical soil are also shown for comparison.

collected from power plants in Table 5. The highest activities measured were for ^{210}Pb and ^{210}Po on escaping fly ash (stack samples), as expected. The measured activities of ^{238}U, ^{232}Th, and ^{40}K and their daughters agree fairly well with our predictions considering the limited number and variety of ash samples analyzed. The most extensive measurements reported were by Furr et al. (1977) who measured trace metals, including uranium and thorium, in samples of fly ash collected from 22 different power plants in the United States. We have divided their data into two groups representing plants burning coal from Western mines and those burning Midwest and Appalachian coals to again show that Western coals are no more radioactive than other coals.

Whereas the activity in coal is usually less than in typical soil, the typical ash activity becomes several times that for typical soil because of concentration in the ash after combustion.

Using the activities of fly ash calculated from the coal, as substantiated by the measurements reported in Table 5 and the enrichment data from Table 4, we can now estimate the expected radionuclide releases for typical 1000-MW(e) power plants. Table 6 shows these estimates for two model plants, along with similar estimates of releases made by other investigators. Our estimates labeled "modern" are for a plant whose total ash release is limited by EPA clean air standards which all plants must eventually meet (Federal Register, 1971). These regulations require particulate releases to be less than 0.1 lb per 10^6 BTU of fuel burned. Basing the emissions on this standard, rather than on a particular control efficiency, removes the variations in emissions that would occur due to burning varying amounts of coal with different heat and ash contents. Our second set of estimates, labeled "1972 reference," is designed to represent an older, more poorly controlled plant typical of the average U. S. plant in 1972, which, according to Federal Power Commission (1975) data, released ~8% of the total ash content of coal burned. For our model modern plant, we estimated uranium to be enriched in escaping fly ash by a factor of 2, ^{226}Ra by a factor of 1.5, and ^{210}Pb and ^{210}Po each by a factor of 5. All other nuclides were assumed to be unenriched. For the 1972 reference plant, we assumed only ^{210}Pb and ^{210}Po to be enriched and only by a factor of 2 each. The only other studies, listed in Table 6, to include the enrichment effect were UNSCEAR (1977) who assumed factors of 5 for uranium and 10 for lead and polonium, and Lee et al. (1977) who assumed only lead and polonium nuclides to be enriched by a factor of 5 each.

Although some of the short-lived daughters of ^{222}Rn and ^{220}Rn will also be released, we have neglected these nuclides because their

TABLE 6

Estimates of Radionuclide Releases from Coal-Fired Power Plants*

Investigator	Fraction of fly ash released, %	Total fly ash released, kg/year	Activity released, mCi/year										
			^{238}U	^{234}U	^{230}Th	^{226}Ra	^{232}Th	^{228}Th	^{228}Ra	^{210}Pb	^{210}Po	^{40}K	^{222}Rn
Eisenbud and Petrow, 1964	~3	4.5×10^6				17.2			10.8				
Martin et al., 1970	~3	4.5×10^6	7.2	7.2	7.2	7.2	8.1	8.1	8.1				
McBride et al., 1977†	1–2	$\sim 3 \times 10^6$	8	8	8	8	5	5	5	8	8		800
NCRP, 1977	30	9.5×10^7	133	133	152	152	171	171	171				
Lee et al., 1977‡	0.5	$1.1–4.9 \times 10^6$	4–11	4–11	4–11	4–11	3–10	3–10	3–10	18–54	18–54	18–54	800–2600
UNSCEAR, 1977	~3–5	1.0×10^7	50	50	10	10	10	10	10	100	100	150	1000
This study, modern plant§	~1–2	3.1×10^6	28	28	15	21	11	11	11	70	70	31	1000–2000
This study, 1972 reference plant¶	~10	2.8×10^7	126	126	126	126	104	104	104	252	252	280	1000–2000

*All values are per year per 1000-MW(e) plant.

†Calculated on basis of 1% of all activity in 2.3×10^9 kg of coal released.

‡Range of releases reported for plants burning different types of coal.

§Ash released based on just meeting EPA standard of 0.1 lb/10^6 BTU, assuming 80% utilization factor, 35% thermal efficiency.

¶Ash released based on average releases from all U. S. plants in 1972, assuming typical 1000-MW(e) plant burns 2.7×10^9 kg of coal per year.

contribution to background perturbations and population exposure is relatively minor. As did most of the other investigators, we have conservatively assumed that essentially all the ^{222}Rn gas in the coal is released upon combustion and escapes from the plant. Anderson, Mayneord, and Turner (1974) have estimated that only ~80% of the radon actually escapes. The ^{220}Rn releases were neglected due to the short half-life.

Since, according to the National Council on Radiation Protection and Measurements (1977), hereafter referred to as NCRP, over one-half the power plants now operating in the United States release less than 2.5% of their fly ash, our two model plants should bracket the range of expected annual releases for most plants operating today. For a given year the actual releases might be more or less than those estimated, depending on the amount and activity of coal burned. The estimated releases should, however, be quite appropriate for use in estimating the long-term average releases and resulting perturbations on the natural radiation environment.

RADIOACTIVITY IN WASTES

Wastes containing small quantities of natural radionuclides are produced during mining and pretreatment of coal, as well as from its combustion. Caldwell, Crosby, and Lockard (1970) reported detecting high alpha activity in rivers in coal basins which they traced to acid runoff from coal mines. Some rivers exhibited alpha activity levels exceeding the MPCs (maximum permissible concentrations) for drinking water. These results are consistent with other reports that large numbers of streams and rivers in Appalachia have been contaminated with acid runoff from mines and mine refuse piles (Wewerka et al., 1976). Caldwell, Crosby, and Lockard hypothesized that the increased activity was due to leaching of uranium from coal and its shale overburden, which is exposed to weathering and groundwater during and after mining, with subsequent runoff into the watershed.

Another source of radionuclide-containing wastes is the residue from coal cleaning processes. This cleaning or "washing" reduces the original weight of the coal as mined by about 23% (Lee et al., 1977). The current U. S. rate of waste production from this activity is about 10^{11} kg/year, and about 3×10^{12} kg of carbonaceous mineral wastes have accumulated in the United States so far (Wewerka et al., 1976). The fraction of coal undergoing this process can be expected to increase in an effort to reduce sulfur and ash contents to meet emission standards. Very little has been reported on the radionuclide

content of these wastes or their potential for redistribution by leaching or other mechanisms. A related waste source for which little information is available is the "blackwater" or silt-loaded water used to wash or separate out the various specific gravity fractions of the mined coal.

The other major source of wastes is, of course, the power plant. Using our estimated 2.7×10^9 kg of coal burned per GW(e) year with 13% ash content, a typical plant will generate about 3.5×10^8 kg of ash per gigawatt (electric) year [GW(e) year]. About 3×10^{10} kg of ash was produced in the United States in 1970 (Meikle, 1975). Most of this ash is sluiced to holding ponds, although about 20% is currently sold for use as landfill or in building materials (Meikle, 1975). The use of scrubbers to reduce sulfur emissions results in an additional source of waste whose radiological properties have been little studied.

PERTURBATIONS OF THE NATURAL RADIATION ENVIRONMENT

The redistribution of the radionuclides in coal from relatively isolated underground coal deposits to the external environs of power plants may result in small perturbations in local ambient natural radiation levels in air and soil. Because the released nuclides are identical to those naturally present, unlike releases from nuclear power plants, the detection and quantification of these small perturbations are often quite difficult. Since the average escaping fly ash has a specific activity only a few times greater than that of the typical soil, and well within the range of activities typically found in soils (see Table 1), the result of deposition of fly ash onto the ground may not alter the specific activity of the soil to any measurable extent and in fact could even lower it. The extent to which power-plant releases will increase ambient air concentrations of natural nuclides will also depend on the local soil activity, the mean dust (assumed to be resuspended soil) loading of the area, and the local rate of ^{210}Pb and ^{210}Po natural fallout.

There have been only a few attempts to measure perturbations of natural radiation levels in the vicinity of coal-fired plants. One of the earliest U. S. studies was by Bedrosian, Easterly, and Cummings (1970) who in 1969 detected increased levels of ^{226}Ra, ^{232}Th, and natural uranium in ground-level air of up to 1.3 fCi/m^3, 0.3 fCi/m^3, and 2.7 fCi/m^3, respectively, downwind from the 1960-MW(e) Widows Creek Power Plant in Alabama. In an earlier study, Martin et al. (NCRP, 1977) had measured several fCi/m^3 of uranium

downwind from a 1400-MW(e) plant. Bedrosian, Easterly, and Cummings (1970) were unable to detect any increased levels of radionuclides in soil or plants even though the plant was one of the older and more poorly controlled operating plants in the United States, releasing over 30% of its fly ash.

Farmer et al. (1977) have recently reported preliminary results of a study at a 330-MW(e) plant in Iowa burning Western coal. More recent data from this study are presented by Styron (this volume). They were unable to definitely document increased levels of natural radionuclides due to power-plant emissions either in air samples or soil samples, even though this plant also appeared to be relatively poorly controlled.

Jaworowski et al. (1971, 1974, 1975) have reported on a number of studies of radionuclides in glacial snow, fossils, and soils which indicate a buildup in ^{226}Ra in ground-level air has occurred over the past few centuries. They attribute this buildup to the release of ^{226}Ra from power plants and other industrial sources.

We have made our own measurements in the environs of three large coal-fired power plants in an attempt to detect increases in ambient natural radionuclide soil concentrations as a function of distance and direction from the stacks. Samples of both surface (~1 to 2 cm) and deep soil (> 2 cm) were collected at each plant. We also made ionizing radiation exposure rate measurements using sensitive high-pressure ionization chambers, and we obtained in situ gamma ray spectra using a large Ge(Li) detector. The only plant where we obtained positive results was the Widows Creek Plant in Alabama studied by Bedrosian, Easterly, and Cummings, the oldest of the three plants surveyed and the most poorly controlled. It is located in a region where the winds blow toward the north some 20% of the time, thus providing a well-defined direction in which to search for preferential deposition of fly-ash activity. The results of the analyses of the soil samples obtained near this plant are shown in Table 7. The excess activity in the surface soil shows a definite pattern, peaking at about 1.5 to 2 km toward the north for all nuclides measured. Using their data, we estimated the total depositions of ^{226}Ra, ^{232}Th, and ^{40}K, shown in Table 7. Because of the limited number of soil samples, the small incremental increases in specific soil activity for surface as compared to deep samples, and the large uncertainties in the depth of the actual surface sample, we estimate the depositions given in Table 7 to have associated uncertainties of at least ±100%. Nevertheless, a definite increase is shown. The in situ field spectrometer and ionization data chamber by themselves were insufficiently precise to verify the soil-sample results, but they do qualitatively substantiate the increased activities at 1 to 2 km. As a

TABLE 7

Activity of ^{226}Ra, ^{232}Th, and ^{40}K in Soil Samples Collected Around Widows Creek Power Plant. Total Deposition Inferred from Measured (Meas.) Excess Activity in Surface Soil Compared to Deposition Calculated (Calc.) with Plume Dispersion Model

Distance, km, and direction	^{226}Ra				^{232}Th				^{40}K			
	Soil activity, pCi/g		Deposition, mCi/km^2		Soil activity, pCi/g		Deposition, mCi/km^2		Soil activity, pCi/g		Deposition, mCi/km^2	
	Surface	Deep	Meas.	Calc.	Surface	Deep	Meas.	Calc.	Surface	Deep	Meas.	Calc.
0.9 SW	1.72	1.43	10	2.8	1.60	1.50	5	2.3	12.1	9.0	12	6
1.5 NNW	1.36	1.09	8	6.6	1.32	1.30	1	5.4	3.9	2.7	30	15
2.0 N	1.41	0.94	13	6.6	1.02	0.69	7	5.4	5.5	1.7	90	15
2.8 NNE	1.0	0.90	3	4.6	0.66	0.64	<1	3.8	3.5	2.8	18	10
4.0 WSW	0.86	0.81	1	0.9	0.89	0.88	<1	0.7	1.8	1.5	7	2

further check, however, we attempted to calculate the expected deposition from the Widows Creek Plant over its lifetime. The plant releases effluents through six 52-m stacks servicing 853 MW(e) of capacity in operation since 1952 and two 152-m stacks servicing 1125 MW(e) of capacity in operation since 1961. Using our mean activities in coal and ash, we made estimates of total coal burned on the basis of actual 1971 usage and a value for fly-ash control efficiency of ~70% (Bedrosian, Easterly, and Cummings, 1970). We estimated an average activity release rate of ~600 mCi/year of ^{226}Ra, ~500 mCi/year of ^{232}Th, and ~1600 mCi/year of ^{40}K. The total deposition over the life of the plant up to the time of our measurements in 1973 was calculated using our own version of the standard sector-averaged Gaussian plume dispersion model (Slade, 1968) and using average meteorological data for the Widows Creek area obtained from U. S. Weather Bureau records. To account for both wet and dry deposition, we applied a deposition velocity of 1 cm/sec for each. [The use of a deposition velocity of about 1 cm/sec to account for wet deposition has been shown to provide reasonable average results over long time periods (Crawford, 1978).] The calculated depositions (see Table 7) are in reasonable agreement with the measured depositions considering the large uncertainties in both. The calculated values peak at 1 to 2 km, further substantiating our attribution of the excess soil activities to releases from the plant.

The soil samples obtained at the Widows Creek area were also analyzed for ^{210}Pb. The highest ratio of surface ^{210}Pb to deep soil ^{226}Ra activity found was 4.6, 2 km from the plant. The ratios obtained at the other sites ranged from 1.7 to 2.6. Because the first 1 to 2 cm of surface soil is already enriched in ^{210}Pb by about a factor of 3 due to natural fallout (Moore and Poet, 1976; NCRP, 1975), our apparently enhanced ^{210}Pb measurement at 2 km cannot be definitively attributed to plant releases.

Our plume dispersion code was also used to calculate the expected air concentrations of various nuclides. Under neutral stability conditions, with a wind speed of 5 m/sec, the calculated ^{226}Ra activities ranged from 0.7 to 2.2 fCi/m^3 for distances of 2 to 7 km, in reasonable agreement with the range of 0.3 to 1.3 fCi/m^3 for 2.6 to 8.2 km, measured by Bedrosian, Easterly, and Cummings (1970). For this calculation we used actual source and release data given by Bedrosian, Easterly, and Cummings (1970).

The fact that we were able to detect increased levels of radionuclides in soils at Widows Creek is due in part to the low height of release from the older boilers. The local air concentrations and resultant depositions are very dependent on the height of release, and thus most modern plants release from tall stacks in order to

more easily meet ambient air standards for nonradioactive pollutants. This results in diffusing all pollutants over a greater area and greatly reducing the chance of any significant local increase in ambient-air radionuclide activity or of any significant deposition near the plant.

To conservatively estimate the impact of our model plants described in Table 6, we have used the Widows Creek plant meteorology and plume rise characteristics (providing an extra measure of conservatism of about a factor of 3 due to the peaked wind pattern) along with the source terms from Table 6 to calculate the expected mean annual concentrations of each nuclide in ground-level air at the distance and direction of maximum annual exposures for both short and tall stacks. The expected annual deposition was also calculated, again using a total deposition velocity of 2 cm/sec. Plume depletion in the first 50 km was calculated to be negligible, indicating the majority of the fly ash is dispersed long distances from the source. The results of these calculations are given in Table 8. Also shown for comparison are some estimated mean background levels in air based on typical soil activity levels and a mean dust loading of 100 $\mu g/m^3$ (NCRP, 1975). The ^{210}Pb and ^{210}Po values are based on actual measurements (NCRP, 1975). These background estimates can be expected to vary considerably from site to site and are presented only to provide some perspective. For the short stacks the maximum concentrations and depositions occur at about 2 km and for the tall stacks at about 6 km. The maximum air activities calculated for the 1972 reference plant with short stacks are several times the background levels for radium and thorium nuclides. However, the number of people exposed at this distance would be quite small. For the tall stacks the activities are fractions of background even for the 1972 reference plant. Even though ^{210}Pb and ^{210}Po may be enriched in the fly ash, because the background activities of these nuclides are on the average much higher than for the other naturally occurring nuclides, the relative increases in ambient ^{210}Pb and ^{210}Po levels will usually be much smaller than for the other nuclides.

We have not listed the expected increases in ^{222}Rn air concentrations. The releases are about the same for all plants and will result in maximum increases in ground-level air activity of less than 10 fCi/m^3 which are trivial compared to typical natural background levels on the order of 100 pCi/m^3 (NCRP, 1975; Harley, 1975). In fact, we can calculate on the basis of a soil exhalation rate of 50 aCi/cm^2-sec (Harley, 1975; NCRP, 1975) that the ^{222}Rn released from a typical 1000-MW(e) power plant is roughly equivalent to the radon released from ~ 0.1 km^2 of typical soil.

TABLE 8

Calculated Ground-Level Air Activity and Deposition from Model Power-Plant Emissions*

Type plant	Stack height	Ash, $\mu g/m^3$	Activity, fCi/m^3									
			^{238}U	^{234}U	^{230}Th	^{226}Ra	^{232}Th	^{228}Th	^{228}Ra	^{210}Pb	^{210}Po	^{40}K
Modern	52 m	7.8	0.070	0.070	0.035	0.052	0.029	0.029	0.029	0.18	0.18	0.078
Modern	152 m	0.67	0.0060	0.0060	0.0030	0.0045	0.0025	0.0025	0.0025	0.015	0.015	0.0067
1972 reference	52 m	69.4	0.31	0.31	0.31	0.31	0.25	0.25	0.25	0.62	0.62	0.69
	152 m	6.0	0.027	0.027	0.027	0.027	0.022	0.022	0.022	0.054	0.054	0.060
Natural background		100	0.07	0.07	0.07	0.07	0.07	0.07	0.07	10—20	1—2	1.0
			Deposition, mCi/km^2-year									
Modern	52 m	4,992†	0.045	0.045	0.023	0.034	0.018	0.018	0.018	0.11	0.11	0.050
Modern	152 m	429†	0.0038	0.0038	0.0019	0.0028	0.0016	0.0016	0.0016	0.010	0.010	0.0043
1972 reference	52 m	44,416†	0.20	0.20	0.20	0.20	0.16	0.16	0.16	0.40	0.40	0.44
	152 m	3,817†	0.017	0.017	0.017	0.017	0.014	0.014	0.014	0.034	0.034	0.038

*All estimates are maximum annual averages which occur at ~2 km from plant for short stacks and ~6 km from plant for tall stacks.

†kg/km^2-year.

The total deposition of each nuclide over an assumed 50-year plant life can be calculated from the average yearly deposition rates given in Table 8. For example, the ^{226}Ra deposition from our model plant with short stacks would be about 10 mCi/km^2. This amount of activity, if contained in the upper 2 cm of soil, would increase the activity by about 0.3 pCi/g, or by about 40% over the assumed 0.7 pCi/g background activity. If the soil were mixed down to a depth of about 30 cm, as might occur if the land were plowed for farming, the increase in soil activity would only be about 0.02 pCi/g, or less than a 3% increase. The increases for ^{40}K, ^{210}Pb, and ^{210}Po would be even less due to smaller differences in specific activities between fly ash and soil.

The perturbations of the natural radiation environment due to leaching of radionuclides from mines or coal-cleaning wastes have not been adequately studied and, therefore, cannot be assessed at this time. The impacts of the stored ash at the power-plant site can be estimated, however. Lee et al. (1977) suggest that 2 to 6 Ci/year of ^{222}Rn might be released to the atmosphere for each GW(e) year of power production, assuming the exhalation rate of ^{222}Rn from ash piles per unit ^{226}Ra activity is similar to that measured for uranium mill tailings.

If this estimate is correct, the eventual ^{222}Rn production from the uranium and radium in the cumulative wastes built up after many years of operation could significantly perturb local levels and the contributions from all the world's power plants could eventually become a not insignificant fraction of the total exhaled to the atmosphere from natural sources. Lee's assumption is probably not correct, however. The radon emanation (ratio of escape to production rate) for uranium mill tailings has been measured at ~20% (Swift, Hardin, and Calley, 1976). Table 9 shows the results of radon emanation measurements made by us on samples of ash and coal obtained from three different power plants. Various measurements on soils are also shown for comparison. In all cases the ^{222}Rn escaping from the vitrified glassy fly-ash particles was less than 1% of the production rate, compared to ~15% for coal and up to 70% for soils. Data presented by Pensko, Stpiczyńska, and Blaton-Albica, (this volume) substantiate our results. They report measurements of emanation from 33 fly-ash samples averaged 0.6%, and emanation from 11 slag samples averaged 0.7%. It thus appears that little ^{222}Rn will be released from ash-disposal ponds even if the liquid in the ponds is allowed to evaporate and the ponds dry up. Should this occur, however, resuspension and redistribution of fine ash particles by the wind might be a factor in perturbing the local radiation environment. The possibility also exists that the water used to sluice

ash to the holding ponds will leach radionuclides from the ash which will eventually reach public water supplies. However, measurements (Rohrman, 1971) in a number of sluice ponds indicated little dissolved activity in the water, although suspended fine-particle alpha activities ranged as high as 160 pCi/liter. This indicates that the fly ash is highly insoluble, so the impact on the natural radiation environment from those wastes is probably insignificant.

TABLE 9

Measurements of ^{222}Rn Emanation from Various Materials

Sample	^{226}Ra activity, pCi/g	Emanation, %
Ash	3.0	<1
Fly ash	2.5	<1
Fly ash	2.3	<1
Bottom ash	1.6	<1
Coal	0.5	14
Coal	0.5	13
Soils, five samples	0.8—1.4	14
Soils		
NCRP, 1975, typical and range		~20, 10—70
UNSCEAR, 1977, typical		~15

The 20% of the ash now being sold by utilities is being used in a variety of applications, the largest of which is the manufacturing of cement and concrete, where up to 30% of the cementing medium is composed of fly ash (Meikle, 1975). Other major uses described by Meikle are as road-base stabilizers, lightweight aggregate, road fill, and in asphalt mix. The only radiologically related concern with respect to these utilizations of ash is the possibility of increased radiation exposures to people occupying structures built with ash-containing materials. The extent of this impact will depend on the ash activity relative to the activity in other types of building materials, the percentage of ash used in the various building materials, and the relative amount of ^{222}Rn released to room air by the materials. A recent literature survey (Eadie, 1975) found a lack of meaningful data available in the literature on radioactivity in building materials used in the United States.

RADIATION EXPOSURE TO THE POPULATION

The perturbations on the natural radiation environment described in the preceding paragraphs can lead to increases in the dose some persons receive from environmental radioactivity. The potential pathways for this increased exposure are inhalation of air containing fly ash, ingestion of locally grown food with enhanced radionuclide content, and exposure to higher external penetrating radiation fields from deposited radionuclides.

The extent to which airborne fly ash will produce increased radiation doses depends on the duration of exposure, whether or not the particles are in the respirable size range, and whether or not the particles are soluble or insoluble in body fluids. The fly-ash particles from a well-controlled modern power plant can be considered to be mostly in the respirable range (< 1-μ diameter) since this is just the size range where present effluent control devices are least efficient (Linton, Loh, and Natusch, 1976; Coles, Ragaini, and Ondov, 1978). Even though a considerably larger mass of ash is released from older, more poorly controlled plants, much of this material will not be in the respirable range, and thus the dose due to inhalation will not increase in proportion to the released fly-ash mass.

The solubility of fly ash has not been extensively investigated. Bedrosian, Easterly, and Cummings (1970) found fly ash to be quite insoluble in distilled water, as did an Environmental Protection Agency analysis of ash from 12 power plants (Rohrman, 1971) which indicated only 4 to 7% solubility. Theis and Wirth (1977) studied the solubility of fly ash and concluded that the trace elements inside the glass matrix would be released only through the action of long-term weathering processes, but the enhanced surface activity, described earlier, would be chemically more active. They found the release of surface trace elements increased as the solute became more acidic, with 40% of the lead surface concentration being released at a *p*H of 3. Even in neutral solutions, ~10% of the surface contamination was soluble. Linton, Loh, and Natusch (1976) suggested that the smaller fly-ash particles could be thought of as consisting of a highly insoluble alumina—silicate glass matrix with an extractable surface concentration capable of interacting with body fluid. Rohrman (1971) concluded that the components of the vitrified ash and slag were not easily dissolved or dispersed, as evidenced by the small amounts of dissolved alpha activity found in ash-disposal sluice ponds.

From these studies we conclude that most of the radioactivity in the respirable particles escaping the plant will be insoluble in body

fluids and thus would either remain in the lung or be cleared from the body, with little transfer from the lung to other body organs. However, a fraction of the enhanced uranium, ^{226}Ra, ^{210}Pb, and ^{210}Po on the surface of the particles might be dissolved. We conclude that the critical organ with respect to potential dose is the lung and that estimates of doses to other organs, assuming complete solubility (as is customary), will be considerably too high.

We have estimated the dose equivalent to the lung of the maximum exposed individual resulting from inhalation of the fly ash released from our two model power plants. We used the same air concentration to dose-equivalent conversion factors used by the NCRP (1977) supplemented by factors for ^{210}Pb and ^{210}Po from an earlier NCRP (1975) report. We assumed all the airborne fly ash was respirable. These results are shown in Table 10. These estimates

TABLE 10

Estimated Dose Equivalents to Lung of Maximum Exposed Individuals from Model Power-Plant Releases

Nuclide	Dose equivalent, mrem/year	
	Modern plant	1972 reference plant
^{238}U–^{234}U	0.009	0.46
^{230}Th	0.015	1.55
^{226}Ra	0.003	0.23
^{210}Pb	0.005	0.22
^{210}Po	0.075	3.10
^{232}Th	0.009	0.93
^{228}Th	0.018	1.85
^{228}Ra	0.004	0.38
Total	0.14	8.7

can be compared to the typical dose equivalent of about 100 mrems/year from inhaled naturally occurring radionuclides (NCRP, 1975). About 90% of this dose equivalent from natural background radioactivity is due to short-lived daughters of ^{222}Rn (NCRP, 1975; UNSCEAR, 1977) whereas, as shown in Table 10, the majority of the power-plant contribution is due to ^{210}Po and ^{228}Th. We have not attempted to estimate doses to other organs from inhaled nuclides. To the extent a dose to other organs does occur, the corresponding lung doses given in Table 10 would be reduced. The

NCRP (1975) estimated that, if the particles were completely soluble, the maximum dose equivalent to bone for their source term (see Table 6) would be ~7 mrems/year. We have also assumed ^{40}K does not contribute significantly to dose since potassium is homeostatically controlled in the body and thus unlikely to build up in body organs. The potassium retained in the lung on insoluble particles would be much less effective dosimetrically due to the lower relative biological effectiveness (RBE) of its beta–gamma radiations compared to the high RBE alpha particles emitted by most of the other nuclides.

Other estimates given in the literature of the maximum dose equivalents from inhaled fly ash range from 0.7 to 3.8 mrems/year to the lung and 0.3 to 7 mrems/year to the bone surfaces (Martin et al., 1970; NCRP, 1977; McBride et al., 1977). These wide ranges are due to varying assumptions with respect to sources (see Table 6) and maximum annual average ground-level air concentrations, as well as to differences in assumed air concentration to dose conversion factors.

As far as the ingestion-dose pathway is concerned, the uptake by plants of radionuclides in deposited insoluble fly ash is likely to be relatively much smaller than the uptake of radionuclides normally present in the soil. Since the amount of deposited activity is very small (see Table 8), the expected increases in soil activity will be insignificant, particularly if the fly-ash particles eventually penetrate to any depth. In addition, only a small fraction of an individual's food supply is likely to come from contaminated land, in particular from the small region of maximum deposition. Finally, intake of contaminated foods must continue over long periods of time to build up increased body burdens. It is thus highly unlikely that any significant increase in man's radiation dose would occur via this pathway, even if the radionuclides in fly ash were readily available for uptake by plants. The radionuclides present in the largest quantities on the more soluble surface layers of fly ash are ^{210}Pb and ^{210}Po, and the surface soil is already enriched in these nuclides.

McBride et al. (1977) did estimate upper limits for the dose equivalent to the maximum exposed individuals living near a model power plant as a result of ingesting contaminated foods. We feel their estimates, which ranged up to 19 mrems/year to bone, are far too high since they result from a number of unlikely and very conservative assumptions. These included completely soluble particles, a very high deposition close to the plant, no dilution of deposited activity in the soil or correction for activity already present, and 100% of diet obtained from food grown at the point of

maximum deposition. We conclude, as did the NCRP (1977), that ingestion can be neglected as a potential pathway for increased population doses from coal-fired power production.

The maximum population dose to individuals from the direct external radiation pathway can be estimated from the data we obtained at the Widows Creek plant which was given in Table 7. We have calculated the increase in exposure rate for the depositions inferred from our soil-sample analyses, assuming very conservatively that the excess activity constitutes an additional infinite plane source on the soil surface. The resulting increases in exposure rate in free air are 1.8, 3.2, and 2.3 mrads/year from ^{40}K and the gamma-ray emitting daughters of ^{226}Ra and ^{232}Th, respectively. The expected exposure rate increases resulting from our model plants can be estimated from the relative depositions given in Tables 7 and 8. These will be much less than the preceding rate increases, even after many years of operation, due to the smaller source terms. These predicted increases in exposure rate apply only to individuals continually exposed at the point of maximum deposition and only after the deposition has built up to this level. They can be compared to the typical ambient external exposure rate of about 80 mrads/year and are even smaller than the temporal and geographical variations in this ambient rate (NCRP, 1975). We thus conclude that this pathway can also be neglected as a source of significant dose to the population.

A number of estimates have been published of the additional population dose commitments resulting from coal-fired power-plant radioactivity releases (UNSCEAR, 1977; McBride et al., 1977; Lee et al., 1977; NCRP, 1977). These estimates range from less than a man rem up to 1000 man rems. Here the differences are due not only to the differing source terms and dose models but also to differences in the number of people assumed to be exposed. Even the largest estimates are minute fractions (<1%) of the dose commitments received by the same population from ambient natural activity.

Finally, very little has been published on the increase in individual doses from natural radionuclides released from mine and cleaning-waste acid drainage, scrubber sludge, ash pond leaching or resuspension, or the utilization of fly ash in building materials. We estimate these to be relatively minor, although all warrant further study. For the latter, the low ^{222}Rn emanation from fly ash might actually result in decreases in population exposure due to reduced levels of ^{222}Rn in dwellings made from fly ash containing materials, particularly if the total ^{226}Ra activity and gamma-ray emission of the fly ash containing materials is not significantly greater than the material usually used in construction.

COMPARISON OF NUCLEAR AND COAL FUEL CYCLES

In recent years there have appeared in the literature, and also in the news media, a number of claims that coal-fired power plants release greater amounts of radioactivity than nuclear-powered plants, or constitute a greater radiological hazard to the public (Eisenbud and Petrow, 1964; Ray, 1976; Hull, 1971; Devaney, 1976; Eggermont and Devaney, 1977). A direct comparison is complicated by the fact that the two types of plants emit different radionuclides, with different half-lives, radiations, dose pathways, and transport properties. Coal plants redistribute very small quantities of very long-lived natural alpha emitters, and nuclear power plants release newly created radionuclides including thousands of curies per year of short-lived beta–gamma emitting noble gases, small quantities of volatile iodines, and very small quantities of the low-energy beta-ray emitters ^{14}C and ^{85}Kr (McBride et al., 1977). Complicating the picture still further is the fact that most of the potentially significant emissions from nuclear power, from a radiological hazard standpoint, occur not from the power plant but from other parts of the fuel cycle, particularly from mining, mill-tailings piles, reprocessing, and radioactive waste disposal. It is thus inappropriate to compare only the estimated health hazards from power-plant emissions. The entire fuel cycles must be considered. Some of the most publicized comparisons suffer in that they do not present a balanced view in this respect.

We do not intend to present our own comparison here since we believe the data presented in the preceding sections show the radiological hazard from coal-fired plants to be insignificant. However, we will discuss some of the other published assessments.

One of the first comparisons was made by Eisenbud and Petrow (1964) who estimated the relative radiological hazards by comparing the biological effects of the uranium and thorium series releases from coal plants to the ^{85}Kr and ^{131}I releases from a typical pressurized-water reactor (PWR) based on the MPCs recommended by the ICRP. They concluded that the emissions from coal plants were more hazardous than those from nuclear plants. Their analysis was updated but confirmed by Hull (1971) who calculated the relative amounts of air necessary to dilute the two types of stack gases to meet the MPCs. The Eisenbud and Petrow study is often quoted. Had Eisenbud and Petrow chosen to include the contribution from short-lived noble gases and ^{14}C releases and picked a boiling-water reactor (BWR) rather than a PWR, or had they chosen to include the entire fuel cycle necessary to support the nuclear plant in their analysis, their conclusion would probably have been just the

opposite. Furthermore, as discussed in the preceding section, the dose to humans depends on a large number of factors and the implication that increased radionuclide levels in stack releases will result in proportionately increased population doses is overly simplistic.

A number of more recent evaluations present a clearer picture of the relative hazards. Martin et al. (1970) compared the expected radiological impacts from modern coal-fired and nuclear plants on the basis of 1968 data and concluded that, neglecting the rest of the fuel cycle, the impact of the coal-fired plant was ~400 times that of a PWR but 180 times less than that of a BWR, although all estimated radiation doses were tiny fractions of the ICRP recommended maximum permissible limits. They concluded that nuclear energy produced a greater hazard than coal if both long- and short-term effects were considered. Martin (1974) later published a more comprehensive and up-to-date comparison that included the effects for the entire fuel cycle. This comparison was made on the basis of expected health effects committed per GW(e) year for a period of 100 years following release, assuming 30 years of operation of each cycle. For the coal cycle, Martin estimated 0.002 effects from released fly ash and 0.005 effects from ^{222}Rn releases from ash tailings. Note that our emanation data indicate the latter effects probably will not occur. They estimate these 0.007 effects are reduced by 0.2 effects to −0.19, however, by the Suess effect, i.e., the released carbon from the coal cycle would dilute the ^{14}C already present in the biosphere as a result of cosmic-ray production and man's activities. In comparison, Martin estimated 0.03 effects from the total nuclear cycle except for ^{85}Kr, ^{3}H, ^{14}C, and ^{222}Rn releases, which is a factor of 10 greater than that for the coal-fired plant alone. Tritium, if uncontrolled, would add another 0.05 effects, ^{14}C another 0.8, and ^{85}Kr another 0.15. The largest impact would be from the ^{222}Rn released from unstabilized mill-tailings piles which could contribute almost half the total effects from the nuclear fuel cycle. Martin's analysis indicates that, even if the nuclear fuel cycle uses the most modern cost-effective controls, making the health effects insignificant on an absolute scale, it will still have a much larger radiological impact than the coal cycle on the population.

The estimated impact from mill tailings is interesting since ^{222}Rn is the one common nuclide released in both cycles. Mill tailings have often been cited as one of the most significant sources of population exposure from nuclear power (Lee et al., 1977; Eggermont and Devaney, 1977; Environmental Protection Agency, 1973, 1977). The ^{222}Rn exhalation rate from unstabilized tailings

has been estimated to be ~640 pCi/m^2-sec (Swift, Hardin, and Calley, 1976) in good agreement with actual measured values (Bernhardt, Johns, and Kaufmann, 1975; Swift, Hardin, and Calley, 1976). This results in the release of some 225 Ci/year of ^{222}Rn for each GW(e) year of power production, assuming ~11,000 m^2 of land are needed for storage of the resulting 10^8 kg of tailings (Environmental Protection Agency, 1973; Swift, Hardin, and Calley, 1976). Since, as shown earlier, the emanation rate from ash is apparently < 1% compared to ~20% for tailings, we estimate the ^{222}Rn release from ash per GW(e) year power production to be less than 0.1 Ci/year, which is less than the ^{222}Rn which would have been released from the underlying soil. Conversely, about 15 km^2 of soil is needed to produce the same amount of ^{222}Rn as 1 GW(e) year worth of uranium mill tailings.

Another comparison of nuclear vs. coal radiological impact was made by McBride et al. (1977). They compared a modern well-controlled coal-fired plant, releasing only 1% of the total radionuclide inventory in the coal (see Table 6), with modern nuclear power plants. The comparison was only for the direct plant releases and not the entire fuel cycles. McBride concluded that the maximum individual dose commitments to individuals from coal-plant effluents would be less than that from BWR effluents for all organs except bone and only slightly greater than that for PWR effluents. If, as discussed in the preceding section, the McBride et al. ingestion doses are too high and the ingestion pathway can be neglected, the resultant revisions in their dose-equivalent estimates would result in the coal-fired plant having a smaller impact than either the BWR or PWR.

Lee et al. (1977) and UNSCEAR (1977) also concluded that the radiological hazard from the coal fuel cycle is far less than that from the nuclear fuel cycle. Some perspective on the radiological hazards of coal combustion and nuclear power compared to other human activities is provided in Table 11, which summarizes the estimates made by UNSCEAR of the additional exposure to typical natural-background radiation levels necessary to cause the same dose commitment as exposure to various man-made sources. For the same level of power production, the impact of the nuclear fuel cycle is ~400 times that for coal, but both are small fractions of the natural-background impact and also small compared to other radiological impacts.

A number of investigators have called attention to the fact that the long-lived ^{230}Th and ^{226}Ra in tailings piles will continue to produce ^{222}Rn for many tens of thousands of years (Eggermont and Devaney, 1977; Pohl, 1976). The total dose commitment becomes

TABLE 11

Comparative Dose Commitments for Various Types of Radiation Exposure (UNSCEAR, 1977)

Source of exposure	Duration of exposure to natural background to cause equivalent population dose commitment, days
One year of natural background	365
One year of commercial air travel	0.4
Utilization of 1 year's production of phosphate fertilizer at present annual rate	0.04
One year's global production of electricity from coal at present world capacity of 10^6 MW(e)	0.02
One year's exposure to radiation-emitting consumer products	3
One year's global production of nuclear power at present world capacity of 8×10^4 MW(e)	0.6
One year's use of radiation in medical diagnosis	70

more imposing numerically when the integration is made over such long time periods. It is important to remember, however, that man will continue to be exposed to natural-background radiation for the same time period and the relative increase in effects will still be the same. The population dose commitment from all the natural activity present now, if integrated over the same time period, would be a very large number indeed. The type of comparison shown in Table 11 provides a far more reasonable indication of the relative long- and short-term hazards of both coal and nuclear power production.

Finally, the conclusion reached here that the radiological impacts of coal combustion are small compared to the radiological impact of nuclear power is not at all meant to suggest that coal combustion has a smaller overall impact on the environment or public health. In fact, most studies of comparative risks have concluded just the opposite (Lave and Freeburg, 1973; Hull, 1971; Gotchy, 1977; Hub and Schlenker, 1974; and Terrill et al., 1967).

SUMMARY AND CONCLUSIONS

The average concentrations in coal are typically about 1.7 μg/g of uranium, 4.5 μg/g of thorium, and 1700 μg/g of potassium, although

actual concentrations vary over a wide range even for coal samples from a single seam. Contrary to some published assertions, Western coals, with the exception of the small percentage of uraniferous deposits, are not more radioactive than coals from other sections of the United States.

Perturbations of the natural radiation environment have been seen around an older, poorly controlled coal-fired plant, but these were small compared to ambient background levels. Estimated radionuclide releases from a 1972 reference 1000-MW(e) model power plant releasing ~10% of its fly ash may result in increases in average annual ambient air concentrations several times the background levels for some nuclides at sites close to the plant, whereas the increases expected from a modern plant, meeting EPA particulate emission standards and releasing from tall stacks, will be only small fractions of ambient levels.

The critical pathway for population exposure is via inhalation of highly insoluble ash particles, and the critical organ is the lung. Ingestion of contaminated crops does not seem to be a potential concern. The maximum dose equivalents likely to be incurred by individuals and the total population dose commitment expected from the long-term operation of even the most poorly controlled plant are small fractions of the contributions from ambient natural-background radiation.

The possibility of a gradual increase in atmospheric ^{222}Rn levels due to the buildup of ^{238}U and its daughters in waste ash-disposal ponds seems small since it appears that the emanation of radon from ash is considerably lower than from other materials, such as soil or uranium mill tailings.

The radiological impact of the coal-fired fuel cycle is, in general, far less than for the nuclear fuel cycle when the best present technology is assumed for both. The impacts from both types of energy production are miniscule compared to the radiological impacts of other sources of radiation exposure.

Although there still remain some areas where data are sparse and further information is desirable, there would seem to be few really serious areas of concern with respect to radiological hazards from coal-fired power plants. The utilization of uraniferous coal for short periods of time in a well-controlled plant would have a negligible impact on the nearby environment owing to the long time period required to build up significant deposited activity in the soil or to inhale a sufficient quantity of activity to build up a significant lung burden. The acid leaching of uranium and other alpha emitters from coal mines and coal-cleaning wastes would appear to be the most significant potential radiological health problem connected with the

use of coal, particularly considering the projected increase in mining, cleaning, and utilization projected in the national energy plan.

In conclusion, we reemphasize that the radiological hazards are only a small and probably relatively insignificant fraction of the total environmental, health, and safety problems associated with the utilization of coal as an energy source. Further studies of the radiological aspects of coal utilization, including those related to coal conversion processes as well as direct combustion, should be made in conjunction with ongoing studies of other pollutants and at an effort level commensurate with the likely relative impacts on the environment and public health.

ACKNOWLEDGMENTS

We thank Norman Frigerio of the Argonne National Laboratory for providing some of the coal samples analyzed for this study. We also thank Merrill Heit and Isabel Fisenne of the Environmental Measurements Laboratory for their assistance in obtaining and analyzing samples.

REFERENCES

Abernethy, R. R., and F. H. Gibson, 1963, *Rare Elements in Coal*, Bureau of Mines Report I. C. 8163, pp. 60-69, U. S. Department of the Interior, Washington, D. C.

Anderson, W., W. V. Mayneord, and R. C. Turner, 1974, The Radon Content of the Atmosphere, *Nature*, 174: 424.

Averitt, P., 1975, *Coal Resources of the United States, January 1, 1974*, Bulletin 1412, U. S. Geological Survey, Washington, D. C.

Bayliss, R. J., and H. M. Whaite, 1966, A Study of the Radium Alpha-Activity of Coal, Ash and Particulate Emission at a Sydney Power Station, *Int. J. Air Water Pollut.*, 10: 813.

Bedrosian, P. H., D. G. Easterly, and S. L. Cummings, 1970, *Radiological Survey Around Power Plants Using Fossil Fuel*, Report EERL-71-3, U. S. Environmental Protection Agency, Rockville, Md.

Bernhardt, D. E., F. B. Johns, and R. F. Kaufmann, 1975, *Radon Exhalation from Uranium Mill Tailings Piles*, EPA Technical Note ORP/LV-75-7(A), Office of Radiation Programs, Las Vegas Facility, U. S. Environmental Protection Agency, Las Vegas, Nev.

Caldwell, R. P., R. F. Crosby, and M. P. Lockard, 1970, Radioactivity in Coal Mine Drainage, in *Environmental Surveillance in the Vicinity of Nuclear Facilities*, W. C. Reinig (Ed.), Chap. 48, Charles C Thomas, Springfield, Ill.

Coles, D. G., R. C. Ragaini, and J. M. Ondov, 1978, The Behavior of the Natural Radionuclides in Western Coal-Fired Power Plants, *Environ. Sci. Technol.*, 12: 442.

Crawford, T. V., 1978, Atmospheric Transport of Radionuclides, in *Proceedings of the Workshop on the Evaluation of Models Used for the Environmental*

Assessment of Radionuclide Releases, Sept. 6—9, 1977, Gatlinburg, Tenn., F. O. Hoffman, T. V. Crawford, F. F. Gloyra, J. K. Soldat, I. L. Ophel, and P. S. Rohwer (Eds.), DOE Report CONF-770901.

Denson, N. M., 1959, *Uranium in Coal in the Western United States,* Bulletin 1055, U. S. Geological Survey, Washington, D. C.

Devaney, J. D., 1976, Letter to the Editor, *Phys. Today,* June 1976.

Eadie, G. G., 1975, *Radioactivity in Construction Materials: A Literature Review and Bibliography,* Office of Radiation Programs Report ORP/LV-75-13, U. S. Environmental Protection Agency, Las Vegas, Nev.

Eggermont, G., and J. D. Devaney, 1977, More on Coal vs. Fission and Reply, Letter to the Editor, *Phys. Today,* April 1977.

Eisenbud, M., and H. G. Petrow, 1964, Radioactivity in the Atmospheric Effluents of Power Plants That Use Fossil Fuels, *Science,* 144: 288.

Environmental Protection Agency, 1973, *Environmental Analysis of the Uranium Fuel Cycle, Part 1, Fuel Supply,* Report No. EPA-520/9-73-003-B, Office of Radiation Programs, Washington, D. C.

——, 1977, *Radiological Quality of the Environment in the United States, 1977,* Report No. EPA-520/1-77-009, Office of Radiation Programs, Washington, D. C.

Farmer, B. M., C. E. Styron, C. A. Phillips, B. Robinson, and W. H. Westendorf, 1977, *The Assessment of the Radiological Impact of Western Coal Utilization, Phase 1,* Monsanto Research Corp., Mound Laboratory Report, Miamisburg, Ohio, Jan. 5, 1977.

Federal Power Commission, 1975, *Steam—Electric Plant Air and Water Control Data for the Year Ending December 31, 1972,* Report FPC-S-246, Washington, D. C.

Fed. Regist., 1971, 31: 247.

——, 1978, 43: 10.

Furr, A. K., et al., 1977, National Survey of Elements and Radioactivity in Fly Ashes, *Environ. Sci. Technol.,* 11: 1194.

Gluskoter, H. J., R. R. Ruch, W. G. Miller, R. A. Cahill, G. B. Dreher, and J. K. Kuhn, 1977, *Trace Elements in Coal: Occurrence and Distribution,* Illinois State Geological Survey Circular 499, Urbana, Ill.

Goldstein, N. P., K. H. Sun, and J. L. Gonzales, 1971, Radioactivity in Fly Ash from a Coal Burning Power Plant, *Trans. Am. Nucl. Soc.,* 14: 66.

Gotchy, R. L., 1977, *Health Effects Attributable to Coal and Nuclear Fuel Cycle Alternatives,* Draft NRC Report NUREG-0332, U. S. Nuclear Regulatory Commission, Washington, D. C.

Guimond, R. J., and J. E. Fitzgerald, 1977, The Radiological Implications of Increased Coal Utilization, in *Proceedings of the 10th Midyear Topical Symposium of the Health Physics Society,* Saratoga Springs, N. Y., Oct. 11—13, 1976, pp. 43-57, Rensselaer Polytechnic Institute, Troy, N. Y.

Harley, J. H., 1975, Environmental Radon, in *The Noble Gases,* A. A. Moghissi and R. E. Stanley (Eds.), GPO, Washington, D. C.

Hub, K. A., and R. A. Schlenker, 1974, Health Effects of Alternative Means of Electrical Generation, in *Population Dose Evaluation and Standards for Man and His Environment,* Symposium Proceedings, Portoroz, 1974, pp. 463-482, STI/PUB/375, International Atomic Energy Agency, Vienna.

Hull, A. P., 1971, Radiation in Perspective: Some Comparisons of the Environmental Risks from Nuclear and Fossil-Fueled Power Plants, *Nucl. Safety,* 12: 185.

Jaworowski, Z., J. Bilkiewicz, and E. Zylica, 1971, Radium-226 in Contemporary and Fossil Snow, *Health Phys.,* 20: 449.

——, J. Bilkiewicz, L. Kownacka, and S. Wlodek, 1975, Artificial Sources of Natural Nuclides in the Environment, in *The Natural Radiation Environment*, Vol. II, Symposium Proceedings, Houston, Tex., Aug. 7—11, 1972, J. A. S. Adams, W. M. Lowder, and T. F. Gesell (Eds.), ERDA Report CONF-720805-P2, pp. 809-818, Rice University and the University of Texas, Houston, NTIS.

——, J. Bilkiewicz, E. Dobosz, D. Grzybowska, L. Kownacka, and Z. Wroński, 1974, Radiation Hazards to the Population Resulting from Conventional and Nuclear Electric Power Production, in *Environmental Surveillance Around Nuclear Installations*, Symposium Proceedings, Warsaw, 1973, pp. 403-412, STI/PUB/353(Vol. 1), International Atomic Energy Agency, Vienna.

Kaakinen, J. W., R. M. Jorden, M. H. Lawasani, and R. E. West, 1975, Trace Element Behavior in Coal-Fired Power Plants, *Environ. Sci. Technol.*, 9: 862.

Klein, D. H., A. W. Andren, and N. E. Bolton, 1975a, Trace Element Discharges from Coal Combustion for Power Production, *Water, Air, Soil Pollut.*, 5: 71.

——, et al., 1975b, Pathways of Thirty-Seven Trace Elements Through Coal-Fired Power Plants, *Environ. Sci. Technol.*, 9: 973.

Lave, L. B., and L. C. Freeburg, 1973, Health Effects of Electricity Generation from Coal, Oil, and Nuclear Fuel, *Nucl. Safety*, 14(5): 409.

Lee, H., T. O. Peyton, R. V. Steele, and R. K. White, 1977, *Potential Radioactive Pollutants Resulting from Expanded Energy Programs*, Report EPA-600/7-77-082, Environmental Monitoring and Support Laboratory, U. S. Environmental Protection Agency, Las Vegas, Nev.

Linton, R. W., A. Loh, and D. F. S. Natusch, 1976, Surface Predominance of Trace Elements in Airborne Particles, *Science*, 191: 852.

Magee, E. M., H. J. Hall, and G. M. Varga, Jr., 1973, Potential Pollutants in Fossil Fuels, Report No. EPA-R2-73-249, Office of Research and Monitoring, U. S. Environmental Protection Agency, Washington, D. C.

Martin, J. E., 1974, Comparative Population Dose Commitments of Nuclear and Fossil-Fuel Electric Power Cycles, in *Proceedings of the Eighth Midyear Topical Symposium of the Health Physics Society*, Knoxville, Tennessee, October 21—24, 1974, Report CONF-741018, pp. 317-326.

——, E. D. Harward, D. T. Oakley, J. M. Smith, and P. H. Bedrosian, 1970, Radioactivity from Fossil-Fuel and Nuclear Power Plants, in *Environmental Aspects of Nuclear Power Stations*, Symposium Proceedings, New York, 1970, pp. 025-027, STI/PUB/261, International Atomic Energy Agency, Vienna.

McBride, J. P., R. E. Moore, J. P. Witherspoon, and R. E. Blanco, 1977, *Radiological Impact of Airborne Effluents of Coal-Fired and Nuclear Power Plants*, ERDA Report ORNL-5315, Oak Ridge National Laboratory, NTIS.

Meikle, P. G., 1975, Fly Ash, *Solid Waste*, Chap. V.7, C. L. Mantell (Ed.), John Wiley & Sons, New York.

Moore, H. E., and S. E. Poet, 1976, ^{210}Pb Fluxes Determined from ^{210}Pb and ^{226}Ra Soil Profiles, *J. Geophys. Res.*, 81: 1056.

National Council on Radiation Protection and Measurements (NCRP), 1975, *Natural Background Radiation in the United States*, NCRP Report No. 45, Washington, D. C.

——, 1977, *Radiation Exposure from Consumer Products and Miscellaneous Sources*, NCRP Report No. 56, Washington, D. C.

Natusch, D. F. S., J. R. Wallace, and C. A. Evans, Jr., 1974, Toxic Trace Elements: Preferential Concentration in Respirable Particles, *Science*, 183: 202.

Pohl, R. O., 1976, Health Effects of Radon-222 from Uranium Mining, *Search*, 7: 345.

Ray, J. H., 1976, Letter to the Editor, *Phys. Today*, June 1976.

Ray, S. S., and F. G. Parker, 1977, *Characterization of Ash from Coal-Fired Power Plants*, Report EPA-600/7-77-010, Office of Energy, Minerals and Industry, U. S. Environmental Protection Agency, Washington, D. C.

Rohrman, F. A., 1971, Analyzing the Effect of Fly Ash on Water Pollution, *Power*, August 1971.

Ruch, R. R., H. J. Gluskoter, and N. F. Shimp, 1974, *Occurrence and Distribution of Potentially Volatile Trace Elements in Coal*, Illinois State Geological Survey Environmental Geology Note 72, Urbana, Ill.

Slade, D. H. (Ed.), 1968, *Meteorology and Atomic Energy—1968*, USAEC Report TID-24190, NTIS.

Swanson, V. E., J. H. Medlin, J. R. Hatch, J. L. Coleman, G. H. Wood, S. D. Woodruff, and R. T. Hildebrand, 1976, *Collection, Analysis, and Evaluation of Coal Samples in 1975*, Open File Report 76-468, U. S. Geological Survey, Washington, D. C.

Swift, J. J., J. M. Hardin, and H. W. Calley, 1976, *Potential Radiological Impact of Airborne Releases and Direct Gamma Radiation to Individuals Living Near Inactive Uranium Mill Tailings Piles*, Report EPA-520/1-76-001, U. S. Environmental Protection Agency, Office of Radiation Programs, Washington, D. C.

Terrill, J. C., Jr., E. D. Harward, and I. P. Leggett, Jr., 1967, Environmental Aspects of Nuclear and Conventional Power Plants, *Ind. Med. Surg.*, 36: 412.

Theis, T. L., and J. L. Wirth, 1977, Sorptive Behavior of Trace Metals on Fly Ash in Aqueous Systems, *Environ. Sci. Technol.*, 11: 1096.

UNSCEAR, 1977, *Sources and Effects of Ionizing Radiation*, Report of the United Nations Scientific Committee on the Effects of Ionizing Radiation, United Nations, New York.

U. S. Department of the Interior, 1974, *Bureau of Land Management, Final Environmental Impact Statement*, Eastern Powder River Coal Basin of Wyoming, Vols. III and IV, Washington, D. C.

Vine, J. D., 1955, *Uranium Bearing Coal in the United States*, U. S. Geological Survey, Professional Paper No. United Nations P/55 prepared for the Proceedings of the International Conference on Peaceful Uses of Atomic Energy, Geneva, 1955, United Nations, New York.

——, 1962, *Geology of Uranium in Coaly Carbonaceous Rocks*, Bulletin 356D, U. S. Geological Survey, Washington, D. C.

Wewerka, E. M., J. M. Williams, P. L. Wanek, and J. O. Olsen, 1976, *Environmental Contamination from Trace Elements in Coal Preparation Wastes*, Report EPA-600/7-76-007, U. S. Environmental Protection Agency, Office of Research and Development, Washington, D. C.

DISCUSSION

Adams: Much of the coal ash is glassy, resulting in low ^{222}Rn emanation wastes and low leachability of such nuclides as ^{210}Pb.

Beck: Yes, I agree.

Jaworowski: (Comment) Substantial amounts of coal industrially burned in the world, for many years to come, will be emitting natural

radionuclides into the atmosphere at rates much greater than your 1972 rates. Coal spent for household uses emits these nuclides at still greater rates, as no dust-removal systems are used at the consumer level. This last source of emission in some countries may be greater than industrial sources.

Uranium Mill Tailings Piles as Sources of Atmospheric Radon-222

WILLIAM E. CLEMENTS, SUMNER BARR, and M. LYNN MARPLE
Los Alamos Scientific Laboratory, Los Alamos, New Mexico

ABSTRACT

Uranium mill tailings piles are anomalous local area sources of radon (^{222}Rn) to the atmosphere as a result of their high ^{226}Ra content. Measured values of the radon flux from tailings piles obtained by us and by other investigators show a range of 2 to 2820 atoms $cm^{-2} \cdot sec^{-1}$ compared with about 1 atom cm^{-2} sec^{-1} for background soils. This wide range reflects the variation in radium content of tailings material and in the meteorological and substrate conditions under which measurements are made. Similarly, concentrations of ^{222}Rn in the air near the ground are reported from 0.8 to 282 pCi/liter on tailings piles, whereas measurements within 1 km of the piles show values from near background up to 42 pCi/liter. In general, the lack of detailed meteorological and substrate data makes both these radon flux and air concentration measurements difficult to interpret. Although tailings piles represent high local sources of radon, it is estimated that all the uranium mill tailings that will exist in the U. S. by the year 2000 will at most increase the mean atmospheric radon content by 0.2%. Results obtained by a simple two-layer diffusion model, which yields an analytical solution for the surface radon flux from a tailings pile, agree reasonably well with measured values. A molecular diffusion coefficient of 0.004 cm^2/sec was inferred from this model and from actual flux measurements for a particular location on an inactive tailings pile. The model is also used to evaluate the attenuating effects of overburdens on the escape of radon from tailings piles. Simple atmospheric dispersion techniques for treating area sources produce results that are in general agreement with measured radon concentrations on and near isolated piles, whereas other methods work well in regions of spatially varying wind fields containing several such sources.

Uranium mining and milling operations can result in anomalous local releases of ^{222}Rn to the atmosphere as a result of the omnipresent

high concentrations of ^{226}Ra in uranium ore. Radon* ($T_{1/2}$ = 3.8 days) is produced directly by the decay of the radium* ($T_{1/2} \cong 1600$ years), and, being an inert gas, it can participate in transport and diffusion processes in porous media. Depending on the condition of the material containing the radium, some fraction of the radon produced can escape to the atmosphere where it is dispersed by meteorological processes.

In a uranium mining region, several mines and mills may operate in relatively close proximity to each other. Among the man-made radon sources associated with these operations are open-pit mine areas, forced-air vents from underground mines, ore piles, milling operations, and mill tailings piles. Also, it is possible in such an area to have high radium-bearing geological formations on or near the earth's surface which could also present locally high natural radon sources. In such a situation the interpretation of ambient atmospheric radon concentrations is complicated by the existence of these various interacting sources superimposed on the natural background radon flux from the earth's surface. The natural background flux is known to vary widely with location and meteorological conditions (Wilkening, Clements, and Stanley, 1974).

In this paper we will discuss only uranium mill tailings piles as sources of atmospheric radon. Our purpose is to give a general review of what is known about these sources and to present some simple analytical techniques that can be used in predicting their effects. We hope this will aid in understanding the general problem of atmospheric radon in regions of uranium mining and milling activities.

URANIUM MILL TAILINGS PILES

In the nuclear fuel cycle, the milling of mined uranium ore produces waste products consisting of the bulk of the ore, spent solvents, and process water. These materials are stored in mill tailings ponds, parts or all of which eventually dry up to form mill tailings piles. Established piles are normally several meters deep and range in area from a few tenths to one or two square kilometers. On the basis of past U_3O_8 production data (New Mexico Energy Institute, 1976), it is estimated that as of 1975 there existed in the United States about 10^{11} kg of uranium mill tailings, which covered an estimated area of 10 km^2. Future predictions (New Mexico Energy Institute, 1976) suggest that by the year 2000 there will be some 2×10^{12} kg of tailings in the U. S. requiring some 200 km^2 for storage.

*Radon and radium will hereafter refer to ^{222}Rn and ^{226}Ra, respectively.

Compared with the earth's total land area, this latter figure represents around 1.5 ppm.

The milling process is very selective for uranium; hence almost all the radium in the original ore remains in the tailings. Reported values of radium concentrations in uranium mill tailings range from a few hundred to a few thousand picocuries per gram (Swift, Hardin, and Calley, 1976; Ford, Bacon, and Davis Utah Inc., 1976; 1977a—1977i; Haywood et al., 1977; Marple and Clements, 1977). These average about 1000 times the radium concentration found in background soils (Wilkening, Clements, and Stanley, 1974). Some of the radon produced by this radium will escape to the atmosphere. The fraction escaping depends upon a number of factors, including the radon emanating power of the tailings (i.e., the ratio of radium that produces radon which is free to migrate in the interstitial space to the total radium present), porosity, permeability and moisture content of the tailings, and meteorological conditions. Discussions of radon migration in the soil and what is known about some of these parameters can be found in papers by Tanner (1964; this volume); Wilkening (this volume); Wilkening, Clements, and Stanley (1974); Clements and Wilkening (1974); Clements (1974); Kraner, Schroeder, and Evans (1964); and others. Measured values of radon flux from tailings piles, which will be discussed subsequently, vary from one to three orders of magnitude above background; hence these piles represent high local area sources of radon to the atmosphere. To what extent the escaped radon and its daughters represent an environmental problem depends upon how they are dispersed in the atmosphere and how various sources interact.

RADON FLUX MEASUREMENTS

Radon flux has been measured from numerous mill tailings piles in eight western states either by the accumulation method (Wilkening, Clements, and Stanley, 1974) or by the charcoal canister technique (Countess, 1976). A condensed summary of these measurements is given in Table 1. Extremely low values obtained under unusual conditions, such as ice cover, have been omitted from this tabulation. The reported values range from a low of 2 to a high of 2820 atoms cm^{-2} sec^{-1}.* For comparison, background soils emanate radon at about 1 atom cm^{-2} sec^{-1} (Wilkening, Clements, and Stanley, 1974). The large variation in the radon flux measure-

*1 atom cm^{-2} sec^{-1} = 0.57 pCi m^{-2} sec^{-1}.

ments from tailings piles reflects the wide range in radium content, emanating power, and other physical characteristics of different tailings material and the varied meteorological and soil conditions under which measurements are made.

For the same reasons stated previously, temporal and spatial variations in the radon flux from a particular tailings pile are expected. We have measured the flux from an inactive tailings pile over a period of more than 1 year. The pile covers 0.4 km^2 and varies in depth from 1 to 10 m. Radium concentrations measured at various locations on this pile range from 175 to 1700 pCi/g. The radon flux measurements were made by the accumulation method at various locations and times and under different atmospheric and substrate conditions. The results obtained ranged from 202 to 1843 atoms cm^{-2} sec^{-1}, excluding extremely wet areas. One measurement made at a location with standing water gave 30 atoms cm^{-2} sec^{-1}, and one from water-saturated tailings yielded 300 atoms cm^{-2} sec^{-1}.

To investigate the temporal variations in the flux, we made 23 measurements between May 1976 and July 1977 at a single location on the pile. A permanent accumulator ring (Wilkening, Clements, and Stanley, 1974) was installed at a location where the tailings were 2.5 m deep, and the surface radium concentration was determined to be 1230 pCi/g. This made it possible to make repeated measurements at precisely the same location without disturbing the surface. Table 2 gives the results of these measurements and the general meteorological conditions for each. The values range from 288 to 1744 with a mean of 970 ± 290 atoms cm^{-2} sec^{-1}. Multiple entries for the same

TABLE 1

Measured Radon Flux (atoms cm^{-2} sec^{-1}) from Tailings Piles

Type of study	Method	Reference	Range of results
Several measurements at several piles	Accumulator	Bernhardt, Johns, and Kaufmann, 1975	20 to 387
Intensive study over one year at one pile	Canister	Countess, 1977	29 to 323
Intensive study at one pile and occasional measurements at two others	Accumulator	Marple and Clements, 1977	65 to 1843
Few measurements at numerous inactive piles	Canister	Ford, Bacon, and Davis Utah Inc., 1976; 1977a–1977i	2 to 2820

TABLE 2

Temporal Variation of Radon Flux from a Single Location on a Tailings Pile

Date	Mountain standard time	Conditions*	Radon flux, atoms cm^{-2} sec^{-1}
May 18, 1976	1300	W	1154 ± 14†
			1169 ± 14
July 15, 1976	0600		1005 ± 16
Sept. 15, 1976	0730		897 ± 18
Sept. 28, 1976	1300		971 ± 22
Oct. 14, 1976	1130	W	1158 ± 29
Nov. 3, 1976	1600	W	1380 ± 34
			1210 ± 30
Nov. 5, 1976	0730		588 ± 16
			596 ± 19
Dec. 22, 1976	1000	S	1744 ± 27
Jan. 12, 1977	1130	S	288 ± 7
Mar. 10, 1977	1200	W, G	766 ± 19
Apr. 7, 1977	0930		889 ± 21
			795 ± 21
			896 ± 22
May 11, 1977	1200	C, W	914 ± 15
			845 ± 14
June 16, 1977	1300		1114 ± 22
June 21, 1977	1100	C	1029 ± 24
July 7, 1977	1000		934 ± 23
July 11, 1977	1000	C, W	825 ± 26
			1099 ± 29

*C, cloudy; W, windy; G, ground wet; S, snow cover; no indication, relatively calm and clear with dry ground.

†Standard deviation due to random counting errors and other experimental uncertainties.

time were taken within 10 min of each other and demonstrate the reproducibility of the accumulation method.

It is interesting that the extreme values of the flux for this one location were both measured during periods when the tailings were covered with snow. The highest flux (Dec. 22, 1976) was measured when 5 to 8 cm of granular snow covered the pile, whereas the lowest value (Jan. 12, 1977) was obtained through 15 cm of powdery snow. Details of the moisture conditions in the surface layer of the tailings are not known. Both measurements were made at about the same time of day, and other observed meteorological

conditions were similar. Countess (1977) reports a factor of 10 decrease in the flux from tailings after a 3-cm rain and a 2 to 3 order of magnitude reduction by ice cover. It is not our intention to discuss the effect of moisture; however, this emphasizes that more than cursory observational data are required to predict its effect.

The measurements presented in this section show a great variation in the radon flux from pile to pile, at different locations on the same pile, and with time at a single location. Hence, in attempts to document tailings piles as sources of atmospheric radon, adequate temporal and spatial measurements must be made. Furthermore, because of different physical characteristics, all tailings piles cannot be expected to respond exactly the same to meteorological processes, and extrapolation of empirical studies should be done with caution.

ATMOSPHERIC RADON MEASUREMENTS

Because of the potential health hazard from the inhalation of high levels of radon daughters, numerous investigations of atmospheric radon have been made in and around uranium mines, mills, and tailings piles. A condensed summary of radon concentrations measured on or near mill tailings piles is given in Table 3. The range of values reflects different distances from the source and the

TABLE 3

Ambient Radon Levels (pCi/liter) near Uranium Tailings Piles

Type of study	Reference	Range of results*	
		On pile	Within 1 km
Several measurements at four piles	Shearer and Sill, 1969	1 to 34	0.5 to 3.4
Intensive study at one pile for a year	Duncan et al., 1977	8 to 66	0.8 to 7.2
Several samples at two piles in one month	Snelling, 1971	3.2 to 8.4	0.4 to 14
	Snelling, 1970	0.8	0.1 to 0.5
Few measurements at numerous inactive piles over a few days	Ford, Bacon, and Davis Utah Inc., 1976; 1977a—1977i	12 to 282	0.2 to 42
Several samples at one pile over a one-month period	Duncan and Eadie, 1974	4.5 to 7.7	1.7 to 7.8

*The range of results presented for multiple pile studies are from measurements made at different piles as opposed to a range for any particular pile.

meteorological conditions under which the measurements were made. Reported radon concentrations measured directly on tailings piles range from 0.8 to 282 pCi/liter, whereas measurements away from piles drop to background levels in a few kilometers downwind, depending on meteorological conditions. Some diurnal trends of atmospheric radon on or near tailings piles have been measured (Ford, Bacon, and Davis Utah Inc., 1976; 1977a—1977i) and show an order of magnitude variation, with the higher levels found at night as would be expected. Often interpretation of measurements is complicated by the existence of other nearby sources of radon and a lack of detailed meteorological information. Eadie et al. (1976) measured ambient radon in an area containing several uranium mining and milling operations and found levels of 1.9 to 3.6 pCi/liter compared with 0.1 to 1.2 pCi/liter in nearby background locations.

Many of the details of the time and space variations of atmospheric radon concentrations are amenable to estimation by existing modeling techniques of the type described in subsequent sections of this paper. If modeling concepts are applied in the design of an experiment or monitoring program, all the requisite measurements can be included in the design to be able to apply the models diagnostically.

CONTRIBUTION TO TOTAL ATMOSPHERIC RADON BUDGET

As stated above, the present area covered by tailings piles in the U. S. is 10 km^2, and that is projected to increase to 200 km^2 by the year 2000. Assuming an upper limit for the value of the mean radon flux to be 1000 atoms cm^{-2} sec^{-1}, the total radon source to the atmosphere from uranium mill tailings is estimated to be 0.0057 Ci/sec at present and to be 0.11 Ci/sec by the year 2000. On the basis of a total worldwide radon exhalation rate of 60 Ci/sec (Wilkening, Clements, and Stanley, 1974; Styra, 1968), tailings piles currently represent about 0.01% of the total radon input to the atmosphere. This will increase to 0.2% by the year 2000.

If the only sink for this radon is radioactive decay, then the percent of change in the mean atmospheric radon concentration due to tailings piles will be the same as the percent of the total exhalation given above. Hence the storage of uranium mill tailings on the surface of the earth appears to present only a very minor perturbation to the total atmospheric radon budget. These estimates were made for bare tailings piles, and no consideration has been given to the reduction of radon escape by overburdens that may be used in rehabilitation efforts. When this and the value of the mean flux used are considered, the values given here probably represent upper limits.

TABLE 4

Attenuation by Shallow Soil Overburden

Date	Radon flux, atoms cm^{-2} sec^{-1}		Attenuation, %
	Control	Soil*	
July 15, 1976	1005	718	29
Sept. 15, 1976	897	551	39
Nov. 5, 1976	592	419	29
Apr. 7, 1977	860	556	35
June 21, 1977	1029	768	25
July 7, 1977	934	736	21

*30 to 40 cm of clay-textured soil.

MEASURED EFFECTS OF OVERBURDENS

Various estimates have been made of the attenuation of radon flux by overburdens of radium-poor soil and other materials in evaluating overburdens as a method of tailings stabilization. Some measurements have been made on tailings piles stabilized with shallow soil covers, and a wide range of flux results are reported (Bernhardt, Johns, and Kaufmann, 1975; Ford, Bacon, and Davis Utah Inc., 1976, 1977c, 1977f—1977i; Marple and Clements, 1977). Relatively few measurements have been made on overburdens where the flux was previously measured from the bare tailings.

A series of measurements at an inactive tailings pile in New Mexico were made both on bare tailings and on an adjacent area covered by 30 to 40 cm of clay-textured soil. Prior to the placement of the soil cover, the measured flux from the two areas agreed to within 10%. Table 4 gives the results obtained under comparable calm and dry conditions. Although large fluctuations were observed under windy and moist conditions, they have been omitted from this analysis because of the uncertainty in the response of the two different surfaces to such variables. The average measured attenuation is 30%, which is about what is expected from this type of overburden as will be discussed in the following section.

Occasional measurements were made at two other tailings areas with similar soil covers, and the attenuation was approximately 40 to 50%. Preliminary results on overburdens 1 m deep on other sites show an attenuation of about 75%. The lack of detailed information on the diffusion properties of these overburdens prevents further interpretation of the results. These measurements do, however,

indicate that several meters of this type of soil would be required to completely prevent radon escape to the atmosphere.

RADON FLUX MODEL

In the absence of transport mechanisms, Fickian diffusion is normally used to describe radon migration in the ground (Tanner, 1964; Kraner, Schroeder, and Evans, 1964; Wilkening and Hand, 1960). A transport component can be incorporated in the theory to account for meteorologically induced soil gas movement (Clements and Wilkening, 1974; Bulashevich and Khayritdinov, 1959; and Grammakov, 1936). However, meteorological effects tend to average to zero over the long term, and hence pure diffusion theory should represent average conditions. Culot, Olson, and Schiager (1973) used a numerical solution of a three-layer diffusion model to study the effects of uranium mill tailings used as landfill under buildings. Schiager (1974) gives a method of estimating the radon flux from tailings on the basis of the radium content and assumed diffusion properties. Haywood et al. (1977) also present an equation for the radon flux from a bare tailings pile. Radon diffusion equations in the literature sometimes differ in appearance because of the way that certain parameters, such as the diffusion coefficient, are defined, and care should be taken in comparing them.

Our purpose here is to present a simplified model of a uranium mill tailings pile that yields an analytical solution for the surface radon flux. This result should prove useful and convenient in addressing uranium mill tailings piles as well as similar problems involving radon escape from porous media.

The Model

A simple two-layer one-dimensional diffusion model is employed which consists of an upper layer (1) of depth ℓ and a lower layer (2) of infinite extent as shown in Fig. 1. The parameters for each layer are the porosity ϵ (ratio of void to bulk volume), the bulk density ρ, the bulk radon diffusion coefficient D, the total radium concentration R, and the emanating power E. The emanating power is defined as the ratio of the "effective radium" (Wilkening, 1974) to the total radium in the material and is a measure of the fraction of the total radium that supplies radon to the interstitial gas. Subscripts refer to the layer and the z-axis is chosen perpendicular to the surface as shown.

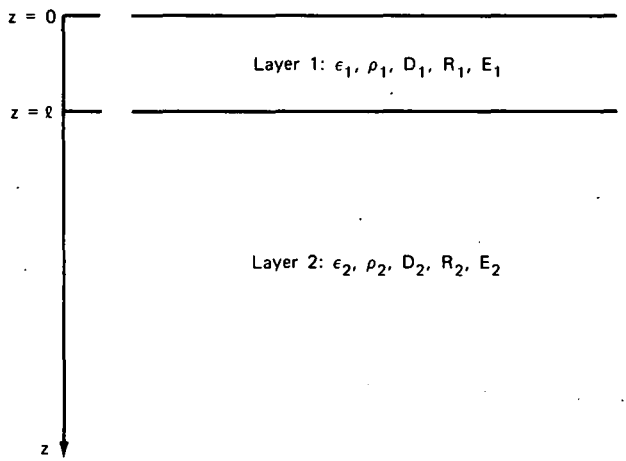


Fig. 1 Simplified diagram of the two-layer model indicating the required parameters in each layer.

In this development the following assumptions are made:

1. The upper layer is sufficiently large in horizontal extent that edge effects can be neglected and that it can be approximated by a semi-infinite slab.

2. Each layer consists of a homogeneous isothermal porous medium that is free of moisture.

3. Molecular diffusion is the only transport mechanism for radon in the interstitial space, and it is governed by the local concentration gradient through Fick's law.

4. The radon concentration at the interface of the upper layer and the atmosphere is negligible in comparison with that deep in the layers.

With these assumptions the results obtained must be considered average values that do not reflect diurnal or seasonal variations caused by meteorological conditions. The parameters used in the model must also be average values which best represent each layer which, in reality, are usually not homogeneous.

Under the above assumptions the steady-state governing equation for radon diffusion in the *ith* layer can be written after Clements and Wilkening (1974) as

$$\frac{\partial^2 C_i}{\partial z^2} - (\epsilon_i \lambda / D_i) C_i + (\epsilon_i / D_i) \phi_i = 0 \qquad (1)$$

where C is radon concentration (number of radon atoms per unit volume of the interstitial space), λ is the decay constant for radon, and ϕ is the radon production rate (the number of radon atoms produced per unit time per unit volume of pore space which are free to migrate). The ϕ is defined by

$$\phi = ER' \rho/\epsilon \tag{2}$$

where R' is the total radium concentration R expressed as disintegrations per unit time per unit mass of the medium.

The boundary conditions are

$$C_1 \ (z = 0) = 0 \tag{3}$$

$$C_2 \ (z \to \infty) = \phi_2/\lambda \tag{4}$$

$$C_1 \ (z = \ell) = C_2 \ (z = \ell) \tag{5}$$

$$D_1 \ (\partial C_1/\partial z)_{z=\ell} = D_2 \ (\partial C_2/\partial z)_{z=\ell} \tag{6}$$

The radon current density (flux) j at any point is given by Fick's law as

$$j = -D(\partial C/\partial z) \tag{7}$$

With this expression and the boundary conditions (Eqs. 3 to 6) the set of equations (Eqs. 1 and 2) can be solved for the radon flux J at the surface (z = 0) of the upper layer. This solution yields

$$J = J_\infty \left[\frac{(1+\eta)\exp(\ell/\beta) - (1-\mu)}{\sinh(\ell/\beta) + \eta \cosh(\ell/\beta)} - 1 \right] \tag{8}$$

where $J_\infty = \phi_1 (\epsilon_1 D_1/\lambda)^{1/2}$, the surface flux for $\ell \to \infty$

$\mu = \phi_2/\phi_1$, a measure of the relative radon production rates in the layers

$\eta = (\epsilon_1 D_1/\epsilon_2 D_2)^{1/2}$, a measure of the relative radon diffusion in the two layers

$\beta = (D_1/\epsilon_1 \lambda)^{1/2}$, the relaxation length for radon diffusion in the upper layer

Applications

Figure 2 shows J/J_∞ as a function of ℓ/β as predicted by the model for $\eta = 1$ and $\mu = 0.0025$. Also shown are measured values

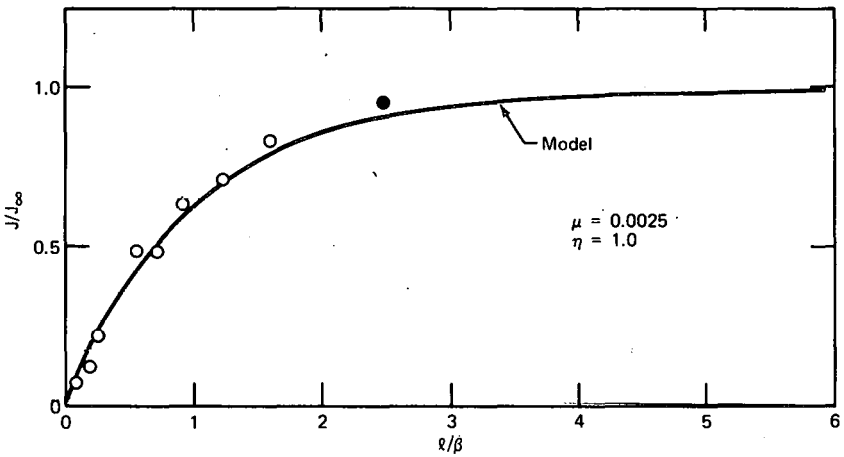


Fig. 2 Comparison of model prediction with some measured values of J/J_∞ as a function of ℓ/β. ○, data from Macbeth et al. (1978). ●, data from Marple and Clements (1977).

obtained by Macbeth et al. (1978) on fine tailings with a mean radium content of 400 pCi/g and a single measurement by Marple and Clements (1977) on tailings with a radium content of 1230 pCi/g. The model calculations shown here assume that the diffusion properties of the tailings and the underlying soil are the same ($\eta = 1$), the radium content of the soil is 1 pCi/g, and the radon production rate ϕ is proportional to the total radium ($\mu = 1/400 = 0.0025$). Since J/J_∞ does not vary much with μ for $\mu < 0.1$, the model calculations are appropriate for both radium levels. The agreement between model and observed values is good and indicates that this model works well for the prediction of J/J_∞ as a function of depth.

The actual surface flux depends on the values of ϵ, ρ, D, $\bar{R}$, and E in each layer. The deeper the upper layer, the less dependent the surface flux is on the characteristics of the lower layer. This is particularly true for cases where $\mu < 1$. We are not aware of radon flux measurements on tailings piles where all these parameters have been determined. In particular, the radon diffusion coefficient in tailings is poorly understood and experimental measurements of this quantity are needed. Therefore, rather than try to guess the value of D in tailings in an attempt to further verify this model, we will see which diffusion coefficient gives reasonable results for a set of measurements and then compare this with some published values.

Between May 1976 and July 1977, 23 radon flux measurements (Table 2) were made by the accumulation method (Wilkening, Clements, and Stanley, 1974) on an inactive uranium mill tailings pile in New Mexico. The mean radon flux determined for these measurements is 970 ± 290 atoms cm^{-2} sec^{-1}. At the location of these investigations, the tailings are 2.5 m deep and nine determinations of the total radium concentration near the surface yielded 1230 ± 207 pCi/g. The underlying soil is a typical desertic soil. The other required parameters at this location were not measured but are estimated in Table 5 from the best available information that is thought appropriate. The values of ϵ, ρ, and E for the tailings are estimated from values measured by Culot, Olson, and Schiager (1973) on Colorado tailings, whereas all the parameters for the underlying soil are taken to be similar to those used by Clements and Wilkening (1974) for a desertic soil.

Figure 3 shows the value of J from Eq. 8 as a function of D_1 for $\ell = 2.5$ m and the parameters in Table 5. As shown, the radon flux of 970 atoms cm^{-2} sec^{-1} from our measurements yields a diffusion coefficient of 0.004 cm^2/sec. Published diffusion coefficients for radon in various media are labeled for comparison. Where necessary the published values have been multiplied by an assumed porosity of 0.4 to make them consistent with the definition of the diffusion coefficient used here. On the basis of this determination, the value of D for these tailings is closer to that of a varved clay or loam than to that of a sand or desertic soil.

Using 0.004 cm^2/sec for the diffusion coefficient of this location yields a maximum flux, $J_\infty = 1005$ atoms cm^{-2} sec^{-1}, and a relaxation length, $\beta = 0.7$ m. Hence these tailings are producing 97% of the possible flux for a depth equal to 3.6β. This is consistent with the results of Fig. 2 which show 96% of the maximum flux obtained for $\ell/\beta = 4$. Therefore, as expected, the radon flux from tailings piles will not change much for depths greater than three to four times β.

Equation 8 can also be used to evaluate the attenuating effects of radium-poor overburdens on the radon escape from tailings piles. For this evaluation the lower layer is given the properties of the tailings in Table 5 and the determined diffusion coefficient of 0.004 cm^2/sec. Three types of overburden material are examined as the upper layer. These are a desertic soil, a clay, and concrete. The properties of these materials used in this analysis are given in Table 6. The radium content and the emanating power of the overburdens in each case are taken to be the same as those of the soil described in Table 5. Because the other properties of the clay for which a diffusion coefficient could be found are not known, they are

TABLE 5

Parameters Used in Model Calculation Shown in Figure 3

Parameter (units)	Tailings	Soil*
ϵ (unitless)	0.4†	0.5
ρ, g/cm^3	1.6†	1.5
D, cm^2/sec		0.00
R, pCi/g	1230‡	1.5
E (unitless)	0.2†	0.08

*All soil parameters from Clements and Wilkening (1974).

†Culot, Olson, and Schiager (1973).

‡Measured by the authors.

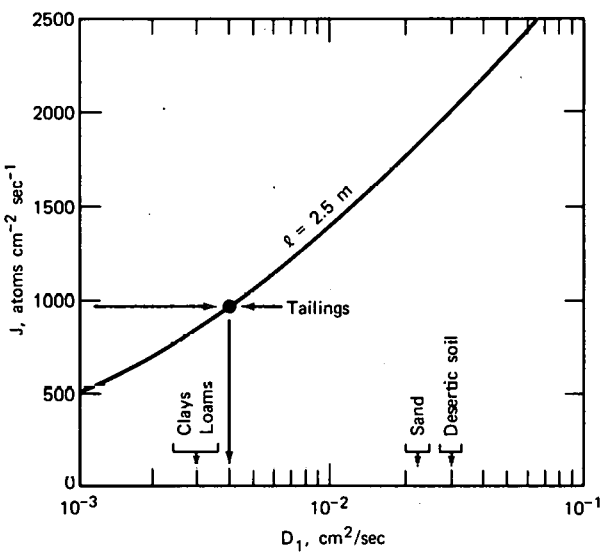


Fig. 3 Model prediction of J as a function of D_1 for ℓ = 2.5 m and the parameters given in Table 5. Our measurements of radon flux from a single tailings site indicates D_1 = 0.004 cm^2/sec. Published diffusion coefficients for radon in other media are indicated for reference.

estimated to be the same as those of the desertic soil. For comparison purposes this introduces little error.

Figure 4 is a semilog plot of the attenuation of each of these overburdens as a function of their depth (log scale) as determined from Eq. 8. Total attenuation is accomplished with 30 cm of

TABLE 6

Parameters Used in Attenuation Calculations Shown in Figure 4

Parameter (units)	Soil*	Clay	Concrete†
ρ, g/cm^3	1.5	1.5	2.65
ϵ (unitless)	0.5	0.5	0.25
D, cm^2/sec	0.03	0.003‡	3.1×10^{-5}

*Clements and Wilkening (1974).
†Culot, Olson, and Schiager (1973, 1976).
‡Tanner (1964) multiplied by $\epsilon = 0.5$.

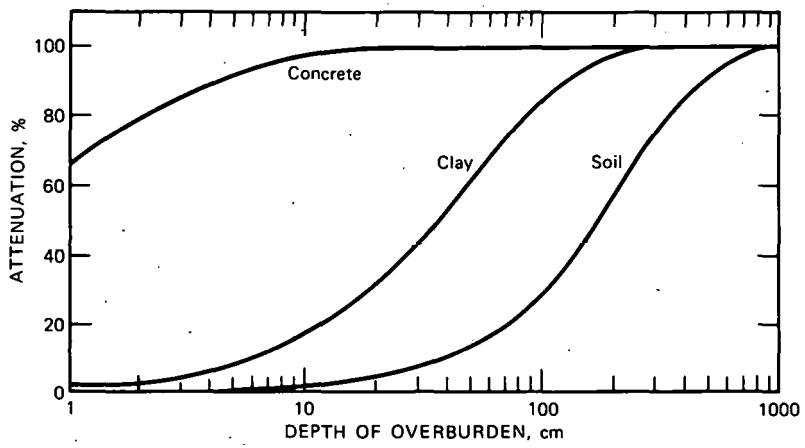


Fig. 4 Model prediction of radon flux attenuation by three overburden materials.

concrete, whereas the clay and desertic soil require 4 and 10 m, respectively, for the same result. For a depth range of 30 to 40 cm, the attenuation from the clay overburden is between 44 and 53%. This is in good agreement with the 30 to 50% measured attenuation for clay-textured soils given in the earlier section "Measured Effects of Overburdens" and in the results of Ford, Bacon, and Davis Utah Inc. (1976).

Fairly large depths of soil material are needed to stop radon escape, whereas materials with a diffusion coefficient similar to that of concrete can accomplish this with a more reasonable depth. In the consideration of overburden material, we must take into account other factors such as cost and long-term stability which are beyond the scope of this paper. In addition, serious thought must be given to

what are acceptable levels of radon escape from tailings piles to the atmosphere. This latter question involves consideration of atmospheric dispersion and subsequent exposure to man. In the next section some simple methods of estimating atmospheric dispersion and the handling of area and multiple sources will be discussed; however, we will not discuss health effects.

ATMOSPHERIC DISPERSION MODEL

The transport and diffusion of tailings pile effluents through the atmosphere to potential receptor sites can be estimated by means of atmospheric dispersion models. Algorithms are available which address a variety of source configurations and meteorological conditions. The concepts behind many of the practical assessment models were described by Gifford (1968).

Near-Field Concentration

Tailings piles tend to occupy significant areas of ground surface, and this source configuration should be taken into account in estimating air concentrations close to the tailings piles. Several investigators (Culkowski and Patterson, 1976; Haywood et al., 1977; Ford, Bacon, and Davis Utah Inc., 1977c) have used area source models of varying complexity. We have observed that the simplest operational modeling techniques for area sources characterize the important elements of the concentration field within four source diameters of a tailings pile.

Figure 5 shows centerline downwind concentration profiles for a hypothetical source 600 x 600 m with a radon flux of 10^3 atoms cm^{-2} sec^{-1}. Two estimation methods were employed, primarily for their simplicity of application and their rather graphic interpretability. Data from two tailings piles (Ford, Bacon, and Davis Utah Inc., 1977c; Shearer and Sill, 1969) with similar dimensions and emanation rates are plotted on the figure for comparison although no effort was made to fit the calculations to the data.

Conceptually, an area source is constructed as an integral of point sources. In the familiar Gaussian plume context,

$$C(x,y,z) = \int_{-a}^{a}\int_{-b}^{b} \frac{q}{(2\pi)^{1/2}\, u\sigma_y(x-x')\,\sigma_z(x-x')} \times \exp -\left[\frac{(y-y')^2}{2\sigma_y^2(x-x')} + \frac{z^2}{2\sigma_z^2(x-x')}\right] dx'dy' \qquad (9)$$

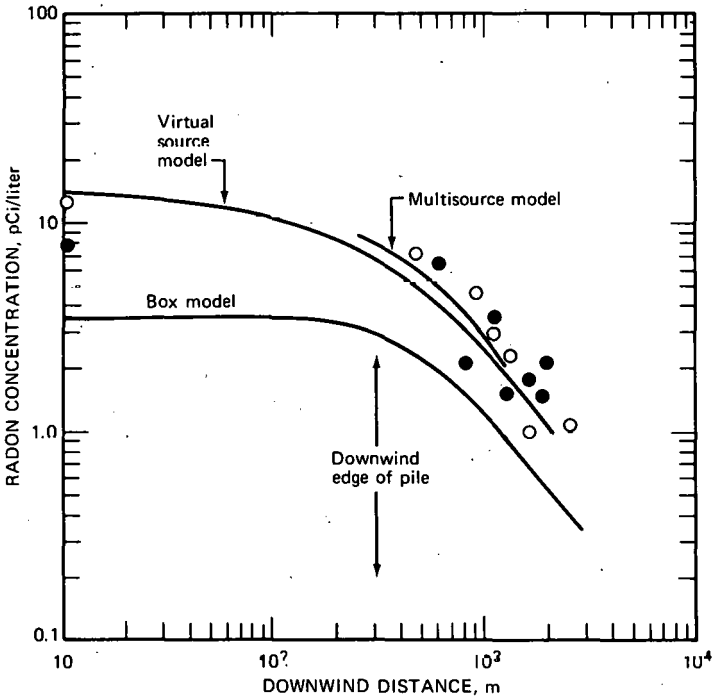


Fig. 5 Comparison of three simple dispersion models with some measured values of ground-level atmospheric radon on and near uranium mill tailings piles. ○, measurements made by Ford, Bacon, and Davis Utah Inc. (1977c). ●, measurements made by Shearer and Sill (1969).

where C = the air concentration (Ci length^{-3})
q = the source strength (Ci time^{-1} length^{-2})
u = mean wind speed (length time^{-1})
a, b = source dimensions (length)

Also, $\sigma_y(x - x')$ and $\sigma_z(x - x')$ are diffusion parameters reflecting downwind plume expansion obtained, for example, from nomograms presented by Gifford (1968).

In practice Eq. 9 is very difficult to evaluate and more convenient techniques are applied. The most frequently used method is the virtual point source (Cramer et al., 1964). The area source is considered to be equivalent to the dispersed material from a hypothetical point source located far enough upstream that its plume dimension equals the dimension of the area source. Hans (1977) uses a Gaussian plume model with a virtual source parameter to estimate

source strength from measured close-in air concentrations and obtains results that are quite consistent with other methods.

The curve labeled "box model" in Fig. 5 is based on the simplest assumptions possible; i.e., that effluent from the area source is uniformly distributed through a specified volume. The lateral dimensions of the plume volume are the width of the area source plus downwind expansion given by the Pasquill—Gifford (P—G) σ_y curves (Gifford, 1968). The vertical dimension is the Pasquill—Gifford σ_z parameter initiated at the upwind edge of the source.

The C stability category was selected for all three model displays in Fig. 5 as a reasonable intermediate value since the data points reflect samples collected over a range of stabilities. At a site in New Mexico with similar altitude and topography, C stability is the median and 75% of the hours are within one stability class step. The box model estimates fall below the Gaussian plume axial values by about a factor of 2. This is a direct result of the method of calculation and is explained by the observation that the ratio of the peak of a Gaussian function to the average over four standard deviations centered on the peak is 1.9.

The third technique used for comparison was a dense array of point sources in a multisource Gaussian plume model. The nonuniformity introduced by this method of simulating a uniform area source is smoothed out within a few grid points from the source array, and the method produces concentration estimates that are consistent with the virtual source method.

Far-Field Concentration

Areas of uranium mining and milling activity tend to have a number of sources of atmospheric radon. Often the radon emanations enter a complex field of wind and turbulence associated with topographically dominated meteorology. For an understanding of the interaction of a variety of sources in the airflow of a valley or basin, some additional analytical techniques and data must be introduced. A sufficient network of wind observations to describe the path of radon between the sources and possible receptors is a fundamental data requirement not generally available. Given the variable wind field or some method of estimating it, there are several available techniques for tracking pollutant plumes. Wendell (1973) describes a Gaussian puff technique in which sequences of instantaneous point sources are released into a wind field and allowed to grow as they travel. Quasi-continuous sources are built up by the sequence of puffs. Lange (1973) presents a particle-in-cell computational model that operates with a time and space variable wind field.

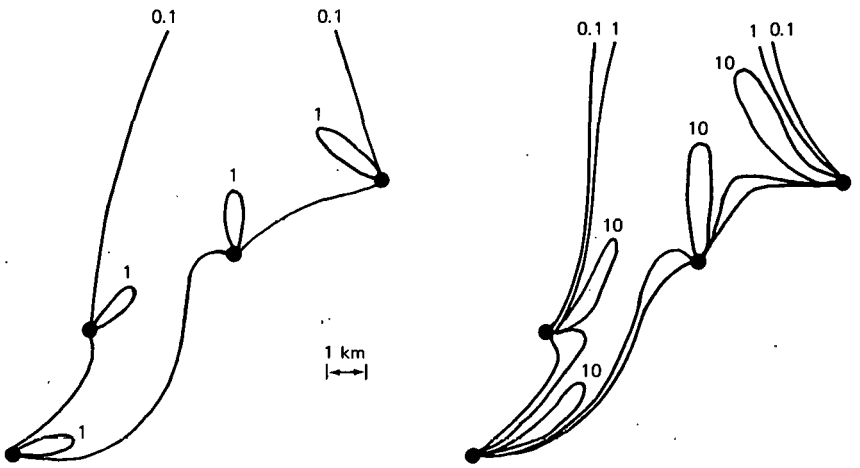


Fig. 6 Ground-level atmospheric radon concentration isopleths (pCi/liter) from four hypothetical continuous point sources of 10^8 pCi/liter in a spatially varying wind field for both unstable and stable atmospheric conditions. The wind enters from both sides, turns gradually, and exits at the top of each figure.

Thompson (1971) and Watson and Barr (1976), among others, have adapted Monte Carlo computational methods to this problem. In this case the pollutant cloud is represented as an ensemble of particles, each of which travels according to a prescription of velocities including mean and turbulent components. We have adapted a simple multisource Gaussian plume model used earlier by Wiedersum and Barr (1973) to a variable wind field. This code has been run on several different computers and has extremely modest machine-time requirements. Figure 6 shows sample calculations for a convergent flow field which might represent drainage winds in a broad valley. Winds come in from both sides, turn gradually, and finally exit at the top of the grid. Four sources of equal strength (10^8 pCi/sec) are distributed arbitrarily in the wind field. Isopleths of air concentration are drawn for unstable (P—G = B) and stable (P—G = E) meteorological conditions. The total area covered by the ensemble plume is not very different in the two stability classes, although the concentrations on the axis of the flow are about 20 times as great in the stable case as in the unstable case. The range of values produced

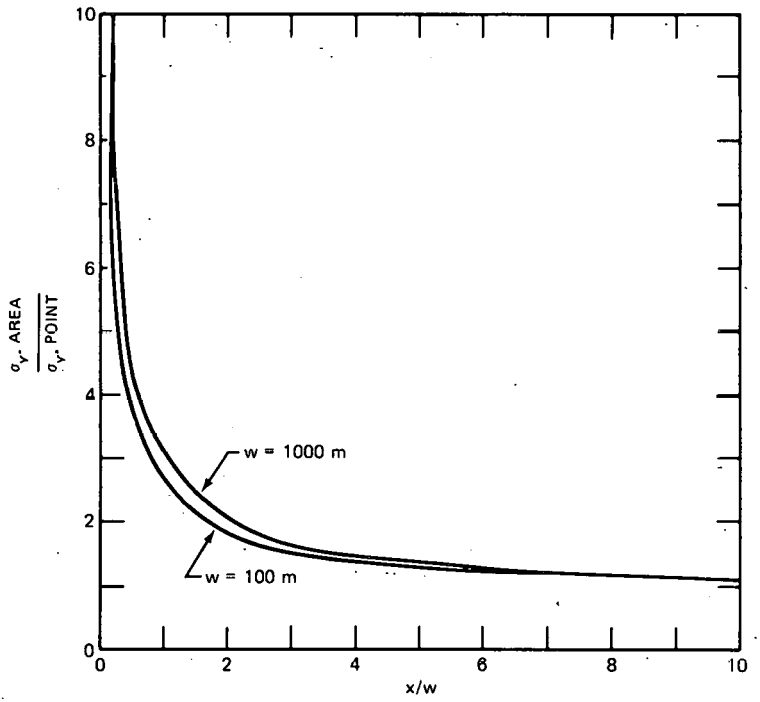


Fig. 7 Ratio of area source and point source diffusion coefficients as a function of dimensions of the area source (w) and downwind distance (x) from the center of a pile.

by the simple model is 0.1 to 10 pCi/liter, the same range observed in ambient radon measurements in areas of uranium mining and milling activity as stated earlier (Eadie et al., 1976).

The far-field calculations are based on isolated point sources, whereas we showed the need for consideration of the areal extent of the source in the near field. We should consider the transition from one to the other. Figure 7 shows the ratio of the lateral diffusion coefficients, σ_y, for the area and point sources as a function of the width of an area source, w, and the travel distance from the center of the source. The function is very weakly dependent on w and rapidly approaches unity in the first few source dimensions downstream. It gets within 10% of unity by x/w = 20. For points within about five source dimensions from an area source, it is recommended to explicitly account for the source configuration, whereas beyond 10 to 20 source dimensions the error introduced by a point source assumption will be a minor part of the total error.

SUMMARY

Radon escape from uranium mill tailings piles in the U. S. has been measured at rates that range from 1 to 3 orders of magnitude above that of background soils. Large temporal and spatial variation in the radon flux from individual piles has also been reported. The wide range of results is due to differences in radium content, emanating power, and diffusion properties of tailings piles and in meteorological and substrate conditions under which measurements are made. In general, the lack of detailed information about these governing variables makes comparisons of reported results difficult.

These relatively high sources of radon can produce locally elevated concentrations of atmospheric radon. However, estimates based on projected U_3O_8 production in the U. S. indicated that all the tailings piles which may exist by the year 2000 will not cause a major perturbation on the total atmospheric radon budget.

A two-layer diffusion model of a tailings pile has been used, and it yields results that agree reasonably well with measured values of the radon flux and with observed attenuation effects of overburdens. The model is useful in the assessment of radon flux from tailings piles if the necessary model parameters are available.

In treating the atmospheric dispersion of radon from tailings piles, the source configuration is important for calculations within about five source dimensions. At further distances simple point source methods yield reasonable results. In either case adequate meteorological data must be available to ensure confidence in the predictions. This is especially true in regions of multiple sources, complex terrain, and varying wind fields.

In future investigations of tailings piles, care should be taken to ensure that adequate measurements are made to describe the radon exhalation. Attempts to quantify the source strength of a pile from a few measurements should be approached with caution. Furthermore, modeling considerations should be incorporated in the design of experimental studies to ensure that necessary parameters are available so that meaningful comparisons can be made. Finally, tailings piles are but one of the man-made sources at atmospheric radon in regions of uranium mining and milling activities, and all these sources, man made and natural, must be incorporated when assessing the effects on the natural radiation environment.

ACKNOWLEDGMENTS

We thank Dr. Marvin H. Wilkening for the use of the radon accumulators used in this study and Harold M. Ide for the use of

sampling and analysis equipment. Our appreciation goes to John Archuleta for the preparation of the illustrations and to him, J. W. Booth, and N. E. Kelley for assistance with the field measurements. This work was performed under the auspices of the U. S. Department of Energy.

REFERENCES

Bernhardt, D. E., F. B. Johns, and R. F. Kaufmann, 1975, *Radon Exhalation from Uranium Mill Tailings Piles,* EPA Technical Note ORP-LV-75-7 (A), Environmental Protection Agency, Washington, D. C.

Bulashevich, Yu. P., and R. K. Khayritdinov, 1959, K teorii diffuzii emanatsii v poristykh sredakh (On the theory of diffusion of emanation in porous media), translated by Irving Emin from *Akad. Nauk SSSR Izv., Ser. Geofiz.*, 12: 1787-1792.

Clements, W. E., 1974, The Effect of Atmospheric Pressure Variation on the Transport of ^{222}Rn from the Soil to the Atmosphere, Ph.D. Dissertation, New Mexico Institute of Mining and Technology, Socorro, N. M.

——, and M. H. Wilkening, 1974, Atmospheric Pressure Effects on ^{222}Rn Transport Across the Earth—Air Interface, *J. Geophys. Res.*, 79: 5025-5029.

Countess, R. J., 1976, ^{222}Rn Flux Measurement with a Charcoal Canister, *Health Phys.*, 31: 455-456.

——, 1977, Measurements of ^{222}Rn Flux with Charcoal Canisters, in *Workshop on Methods of Measuring Radiation in and Around Uranium Mills,* Program Report, Albuquerque, N. M., May 23—26, 1977, Atomic Industrial Forum, Inc., Washington, D. C.

Cramer, H. E., G. M. DeSanto, K. R. Dumbauld, P. Morgenstern, and R. N. Swanson, 1964, *Meteorological Prediction Techniques and Data System,* Technical Report No. 64-3-G, Geophysics Corporation of America, Bedford, Mass.

Culkowski, W. M., and M. R. Patterson, 1976, *A Comprehensive Atmospheric Transport and Diffusion Model,* USAEC Report ORNL/NSF/EATC-17, Oak Ridge National Laboratory, NTIS.

Culot, M. V. J., H. G. Olson, and K. J. Schiager, 1973, *Radon Progeny Control in Buildings,* USAEC Report COO-2273-1, Colorado State University, NTIS.

——, H. G. Olson, and K. J. Schiager, 1976, Effective Diffusion Coefficient of Radon in Concrete. Theory and Method of Field Measurements, *Health Phys.*, 30: 263-270.

Duncan, D. L., G. A. Boysen, L. Grossman, and G. A. Franz, 1977, *Outdoor Radon Study (1974—1975): An Evaluation of Ambient Radon-222 Concentrations in Grand Junction, Colorado,* EPA Technical Note ORP/LV-77-1, Environmental Protection Agency, Washington, D. C.

——, and G. G. Eadie, 1974, *Environmental Surveys of the Uranium Mill Tailings Pile and Surrounding Areas, Salt Lake City, Utah,* Report EPA-520/6-76-066, Environmental Protection Agency, Washington, D. C.

Eadie, G. G., R. F. Kaufmann, D. J. Markley, and R. Williams, 1976, *Report on Ambient Outdoor Radon Progeny Concentrations During November 1975 at Selected Locations in the Grants Mineral Belt, New Mexico,* EPA Technical Report ORP/LV-76-4, Environmental Protection Agency, Las Vegas.

Ford, Bacon, and Davis Utah Inc., 1976, *Phase II—Title I Engineering Assessment of Inactive Uranium Mill Tailings, Vitro Site, Salt Lake City, Utah*, Ford, Bacon, and Davis Utah Inc., Salt Lake City, Utah.

——, 1977a, *Phase II—Title I Engineering Assessment of Inactive Uranium Mill Tailings, Mexican Hat Site, Mexican Hat, Utah*, Ford, Bacon, and Davis Utah Inc., Salt Lake City, Utah.

——, 1977b, *Phase II—Title I Engineering Assessment of Inactive Uranium Mill Tailings, Monument Valley Site, Monument Valley, Arizona*, Ford, Bacon, and Davis Utah Inc., Salt Lake City, Utah.

——, 1977c, *Phase II—Title I Engineering Assessment of Inactive Uranium Mill Tailings, Shiprock Site, Shiprock, New Mexico*, Ford, Bacon, and Davis Utah Inc., Salt Lake City, Utah.

——, 1977d, *Phase II—Title I Engineering Assessment of Inactive Uranium Mill Tailings, Tuba City Site, Tuba City, Arizona*, Ford, Bacon, and Davis Utah Inc., Salt Lake City, Utah.

——, 1977e, *Phase II—Title I Engineering Assessment of Inactive Uranium Mill Tailings, Phillips/United Nuclear Site, Ambrosia Lake, New Mexico*, Ford, Bacon, and Davis Utah Inc., Salt Lake City, Utah.

——, 1977f, *Phase II—Title I Engineering Assessment of Inactive Uranium Mill Tailings, Grand Junction Site, Grand Junction, Colorado*, Ford, Bacon, and Davis Utah Inc., Salt Lake City, Utah.

——, 1977g, *Phase II—Title I Engineering Assessment of Inactive Uranium Mill Tailings, Maybell Site, Maybell, Colorado*, Ford, Bacon, and Davis Utah Inc., Salt Lake City, Utah.

——, 1977h, *Phase II—Title I Engineering Assessment of Inactive Uranium Mill Tailings, Slick Rock Site, Slick Rock, Colorado*, Ford, Bacon, and Davis Utah Inc., Salt Lake City, Utah.

——, 1977i, *Phase II—Title I Engineering Assessment of Inactive Uranium Mill Tailings, New and Old Rifle Sites, Rifle, Colorado*, Ford, Bacon, and Davis Utah Inc., Salt Lake City, Utah.

Gifford, F. A., 1968, An Outline of Theories of Diffusion in the Lower Layers of the Atmosphere, in *Meteorology and Atomic Energy 1968*, D. H. Slade (Ed.), TID-24190, pp. 65-116, Air Resources Laboratories, NTIS.

Grammakov, A. G., 1936, O vliyanii nekotorykh faktorov na rasprostraneniye radioaktivnykh emanatsiy v prirodnykh usloviyakh (On the influence of some factors in the spreading of radioactive emanations under natural conditions), *Zhur. Geofiziki*, 6: 123-148.

Hans, J. M., Jr., 1977, Techniques for the Estimation of Radon-222 Source Tailings Piles, in *Workshop on Methods for Measuring Radiation in and Around Uranium Mills*, Symposium Proceedings, Albuquerque, New Mexico, May 23—26, 1977, Atomic Industrial Forum, Inc., Washington, D. C.

Haywood, F. F., W. A. Goldsmith, P. T. Perdue, W. F. Fox, and W. H. Shinpaugh, 1977, *Assessment of Radiological Impact of the Inactive Uranium Mill Tailings Pile at Salt Lake City, Utah*, USDOE Report ORNL/TM-5251, Oak Ridge National Laboratory, NTIS.

Kraner, H. W., G. L. Schroeder, and R. D. Evans, 1964, Measurements of the Effects of Atmospheric Variables on Radon-222 Flux and Soil-Gas Concentrations, in *The Natural Radiation Environment*, J. A. Adams and W. M. Lowder (Eds.), pp. 191-215, University of Chicago Press, Chicago.

Lange, R., 1973, *ADPIC—A Three-Dimensional Computer Code for the Study of Pollutant Dispersal and Deposition Under Complex Conditions*, USAEC Report UCRL-51462, Lawrence Livermore Laboratory, NTIS.

Macbeth, P. J., C. M. Jensen, V. C. Rogers, and R. F. Overmyer, 1978, *Laboratory Research on Tailings Stabilization Methods and Their Effectiveness in Radiation Containment*, Report GJT-21, Ford, Bacon, and Davis Utah, Inc., Salt Lake City, Utah.

Marple, M. L., and W. E. Clements, 1977, *Measurement of Radon-222 Flux from Inactive Uranium Mill Tailings Piles*, ERDA Report LA-6898-PR, Los Alamos Scientific Laboratory, NTIS.

New Mexico Energy Institute, 1976, *Uranium in New Mexico*, Report NMU-76-100B, Energy Resources Board, University of New Mexico, Albuquerque, N. M.

Schiager, K. J., 1974, Analysis of Radiation Exposures on or near Uranium Mill Tailings Piles, *Radiat. Data Rep.*, 15: 411-425.

Shearer, S. D., and C. W. Sill, 1969, Evaluation of Atmospheric Radon in the Vicinity of Uranium Mill Tailings, *Health Phys.*, 17: 77-88.

Snelling, R. N., 1970, Environmental Survey of Uranium Mill Tailings Pile, Monument Valley, Arizona, *Radiol. Health Data Rep.*, 11: 511-517.

——, 1971, Environmental Survey of Uranium Mill Tailings Pile, Mexican Hat, Utah, *Radiol. Health Data Rep.*, 12: 17-27.

Styra, B. I., 1968, *Selfpurging of the Atmosphere of Radioactive Contamination*, pp. 11-21, Hydrometeorological Publication, Leningrad (English translation by M. Lang).

Swift, J. J., J. M. Hardin, and H. W. Calley, 1976, *Potential Radiological Impact of Airborne Releases and Direct Gamma Radiation to Individuals Living near Inactive Uranium Mill Tailings Piles*, Report EPA-520/1-76-001, Environmental Protection Agency, Washington, D. C.

Tanner, A. B., 1964, Radon Migration in the Ground: A Review, in *The Natural Radiation Environment*, J. A. S. Adams and W. M. Lowder (Eds.), pp. 161-217, The University of Chicago Press, Chicago.

Thompson, R., 1971, Numeric Calculation of Turbulent Diffusion, *Q. J. R. Meteorol. Soc.*, 97: 93-98.

Watson, C. W., and S. Barr, 1976, *Monte Carlo Simulation of the Turbulent Transport of Airborne Contaminants*, DOE Report LA-6103, Los Alamos Scientific Laboratory, NTIS.

Wendell, L. L., 1973, Some Influences of Regional Boundary Layer Flow on Atmospheric Transport and Dispersion, in *Second Joint Conference on Sensing of Environmental Pollutants*, Conference Proceedings, Washington, D. C., Dec. 10—12, 1973, pp. 271-278, Instrument Society of America, Pittsburgh, Penna.

Wiedersum, George C., and S. Barr, 1973, The Effect of Power Plant Stack Emissions on the Ground Level SO_2 Concentrations in an Urban Area, Abstract No. 73-123, 66th Annual Meeting, June 24—28, 1973, Air Pollution Control Association, Chicago.

Wilkening, M. H., 1974, Radon-222 from the Island of Hawaii: Deep Soils Are More Important Than Lava Fields or Volcanoes, *Science*, 183: 413-415.

——, W. E. Clements, and D. Stanley, 1974, Radon-222 Flux in Widely Separated Regions, in *The Natural Radiation Environment II*, Vol. 2, Symposium Proceedings, Houston, Tex., Aug. 7- 11, 1972, J. A. S. Adams, W. M. Lowder, and T. F. Gesell (Eds.), ERDA Report CONF-720805-P2, pp. 717-730, Rice University and the University of Texas, Houston, NTIS.

——, and J. E. Hand, 1960, Radon Flux at the Earth—Air Interface, *J. Geophys. Res.*, 65: 3367-3370.

DISCUSSION

Cheng: Your data show large variation on radon fluxes from tailings—from 2 to nearly 3000 atoms/cm^2/sec. Have you ever attempted to correlate the radium content of the tailings with the radon emanation rates? We believe the radium in the tailings is one of the major factors on changing flux rate.

Clements: We did not make the correlation in our study. Although it would be convenient to find a universal relationship between the radium content and the radon flux, the effect of other parameters such as emanating power, diffusion properties, and widely varying meteorological conditions suggests that this is not feasible.

Bernhardt: Have you considered the effect of the moisture content and its variation in the vertical profile on the radon diffusion coefficient? The piles are not homogeneous, but are, rather, layers of sand and slimes of varying moisture content, which fact probably explains what appears to be an unusual diffusion coefficient.

Clements: In our model we assumed a dry homogeneous medium, which, I agree, is very seldom the case in nature. Future modeling efforts should include the effects you mention, but we will have to learn more about the effect of moisture before we can incorporate that into an operational model. The diffusion coefficient we estimated for a particular site is not really that unusual, especially in light of the fact that presently we don't have a lot of experimental data on diffusion coefficients in tailings material.

Jensen: We have verified lower diffusion coefficients of tailings and soil, depending on the size distribution or the clay content of the soil. Did you measure the size distribution of tailings for which you determined the diffusion coefficients?

Transport of Radon Which Diffuses from Uranium Mill Tailings

W. A. GOLDSMITH,* F. F. HAYWOOD, and R. W. LEGGETT
Health and Safety Research Division, Oak Ridge National Laboratory,
Oak Ridge, Tennessee

ABSTRACT

Considerable attention has been given recently to potential hazards of radon exposure in the vicinity of large piles of uranium mill tailings. A procedure has been developed, using the results of numerous independent investigations, to describe the average annual behavior of radon that escapes from a tailings pile. The radon source term is developed from known profiles of ^{226}Ra in soil and is treated as an area source. Dispersion is calculated by using local meteorological data in a Gaussian diffusion model. A comparison has been made between calculated annual average radon concentrations attributable to the tailings pile in Salt Lake City, Utah, and a series of radon measurements which were made in the vicinity of the tailings pile over a period of 1 year. Population exposures were estimated and compared to those associated with exposure to background concentrations of ^{222}Rn. It was found that annual exposures to ^{222}Rn of tailings-pile origin are about 10% of those associated with background ^{222}Rn in the Salt Lake City metropolitan area.

Milling processes remove about 90% of the uranium but only a few percent at most of the other radionuclides in uranium ore. Daughters of ^{238}U contribute about 95% of tailings activity; the daughters of ^{235}U contribute about 5%. Differences in geochemical properties of uranium and thorium suggest that ^{232}Th will not be concentrated in postmagmatic minerals containing uranium (Gera, 1975). Ores commonly mined in the United States contain only thorium isotopes

*Current address: Union Carbide Nuclear Division, Office of Waste Isolation, Oak Ridge, Tennessee.

attributable to uranium decay (U. S. Environmental Protection Agency, 1973). Tailings that resulted from processing ores older than a few hundred thousand years may contain activities of chain members approaching equilibrium with the original parent uranium activity.

There are currently 23 inactive uranium-milling sites in the western United States. These sites contain almost 350 ha covered by tailings averaging about 600 pCi/g of ^{226}Ra (Goldsmith, 1976).

Several generic radiological assessments have been made for these inactive uranium-mill sites (Sears et al., 1975). These generic assessments have usually shown that ^{222}Rn diffusion constitutes the most significant pathway to human exposure because of inhalation of radon progeny (Swift, Hardin, and Calley, 1976).

This paper presents techniques developed for estimating potential health effects attributable to exposure to ^{222}Rn and progeny which could possibly be of tailings-pile origin. An example application is shown for Salt Lake City, Utah, site of an inactive tailings pile within a metropolitan area (Haywood et al., 1977).

THEORETICAL ASPECTS

The first step in the radon diffusion pathway is the migration of this inert gas to the surface of the tailings pile. Migration consists of two stages: (1) diffusion of ^{222}Rn from its point of origin into the intergranular capillary network and (2) migration through the capillaries to the pile surface.

Only those ^{222}Rn atoms formed by the decay of ^{226}Ra at or very near the surface of a particle are likely to escape from the particle. The fraction of radon which escapes from a particle is called the "emanation factor" or "emanating power." Culot, Olson, and Schiager (1973) gave an average value for this factor of about 23% for uranium mill tailings. This figure is in good agreement with the experimental results obtained for various sandy soils by Sisigina (1972) of 14 to 29% and by Megumi and Mamuro (1974) of 25%.

Radon released to the interstitial pores migrates toward the surface of the pile. It behaves in this manner due to molecular diffusion whereby ^{222}Rn moves from a volume of air at a high concentration (pore air) to a volume whose concentration is lower (atmosphere). The movement of the pore air itself may either enhance or retard the diffusion process. The instantaneous flux of radon across a unit area of the pile surface may be influenced by factors affecting the movement of pore air, for example, atmospheric pressure, temperature differential between atmosphere and tailings,

moisture, wind speed, atmospheric stability, and presence or absence of freezing conditions (Clements and Wilkening, 1974; Guedalia et al., 1970; Kramer, Schroeder, and Evans, 1964; Cox, Blanchard, and Kahn, 1970). The movement of pore air has little effect on long-term average flux because of the cyclical nature of the short-term variations.

The application of Fickian diffusion equations to describe the migration of ^{222}Rn through tailings material has been developed by Culot, Olson, and Schiager (1973) who considered a layer of tailings material sandwiched between a concrete cover and an earthen base. A similar approach can be used to derive an equation describing the ^{222}Rn flux diffusing from a bare tailings pile:

$$J = \frac{K_1 q_1 R E \rho}{p_1}\left(\frac{K_2 q_2 \cosh q_1 t + K_1 q_1 \sinh q_1 t - K_2 q_2}{K_1 q_1 \cosh q_1 t + K_2 q_2 \sinh q_1 t}\right) \times 10^4 \qquad (1)$$

where

$$q_i = \left(\frac{\lambda p_i}{K_i}\right)^{1/2} \qquad (2)$$

and J = ^{222}Rn flux from the pile surface, pCi m^{-2} sec^{-1}
K = bulk diffusion coefficient, cm^2/sec
λ = decay constant of ^{222}Rn (2.10×10^{-6} sec^{-1})
p = porosity of the medium, fraction
E = emanation factor
R = ^{226}Ra content of the tailings, pCi/g
ρ = bulk density of the tailings, g/cm^3
t = depth of the tailings pile, cm
subscript 1 refers to tailings, subscript 2 refers to soil below tailings

The inverse of q is called the "relaxation length"—the thickness of source-free material required to reduce the radon flux to 37% [(1/e) x 100%] of its original value. The diffusion coefficient K represents the effect of the properties of the medium on the diffusion process.

Baver (1965) presents evidence which shows that the diffusion coefficient of a porous medium varies inversely with the tortuosity of the medium. The porosity, p, which represents the ratio of the cross-sectional area of pores compared to the total cross section of the bulk medium, directly affects the value of the diffusion coefficient (Culot, Olson, and Schiager, 1973; Kramer, Schroeder, and Evans, 1964; Tanner, 1964; Schroeder, Kramer, and Evans, 1965). The effect of moisture in the medium is shown in Fig. 1

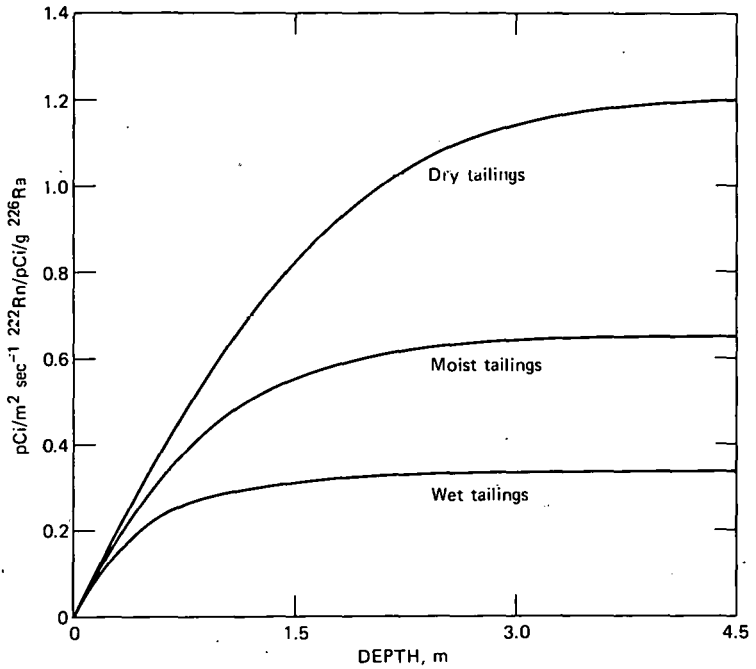


Fig. 1 Graphic representation of radon emanation from wet, moist, and dry tailings as a function of ^{226}Ra concentration and depth of tailings.

where Tanner's (1964) data for sand are used to solve Eq. 1. These data are in general agreement with the trends observed by Guedalia et al. (1970).

In the application of Eq. 1, it is assumed that the porosity of the medium does not vary with depth; for example, there is no compaction of the medium at lower depths. Furthermore, the properties of the medium represented in Eq. 1 are assumed to be isotropic. If the terms representing the soil below the tailings are omitted from Eq. 1, it can be shown that this equation is identical with that proposed by Schiager (1977).

The average ^{222}Rn flux attributable to diffusion can be estimated by applying Eq. 1 to data obtained from on-site physical measurements. The atmospheric dispersion of the ^{222}Rn from the tailings pile may then be used to estimate the annual average human exposure attributable to this source. Atmospheric dispersion may be calculated by representing the tailings pile as an area or strip source and using local meteorological data in a Gaussian diffusion model.

We chose the differential area source model developed by Culkowski and Patterson (1976).

Results of short-term (~1 week) atmospheric sampling of ^{222}Rn on and near tailings piles have been reported by Snelling (1970, 1971) and Snelling and Shearer (1969). However, results reported by Shearer and Sill (1969) show that using results of a short-term sampling program to represent the annual average can lead to serious errors. Their (Shearer and Sill, 1969) 57 sampling stations were operated for 48-hr periods at 3-week intervals for a 1-year period or about 10% of the time. The results reported for each sampling station showed ranges of about an order of magnitude because the short-term ^{222}Rn emanation rate from the pile is affected by pore air movements and atmospheric dilution, and dispersion of the emanated radon is affected by the meteorological conditions prevailing at the time of sampling. Thus extrapolation of short-term measurements to represent annual average human exposures can lead to serious errors.

Human exposure attributable to ^{222}Rn emitted by a tailings pile may be estimated conservatively by making the following assumptions:

1. During transport from pile to receptor, no ^{222}Rn is lost by decay, dry deposition, or rainout.

2. The outdoor airborne radon concentration at a height of 3 m is the same as the ground-level concentration calculated by the dispersion model.

3. The airborne radon concentration within a habitable structure due to the tailings pile is the same as the outdoor radon concentration attributable to the tailings pile.

4. The individual resides continuously in the structure.

Maximum exposure to ^{222}Rn progeny will occur in poorly ventilated structures. For purposes of these calculations, we assume one air exchange per hour (Handley and Barton, 1973) and that the rate of molecular diffusion of radon from outside air into a structure is insignificant compared to that from ventilation. Radon in the outside air arising from the tailings pile is assumed to enter a structure at the rate of $C_0\lambda_V$ (pCi liter^{-1} sec^{-1}), where C_0 is the outside radon concentration and λ_V is the ventilation rate. Radon inside the structure is removed by ventilation and decay, so that the concentration is decreased at a rate of $C_i(\lambda_V + \lambda_R)$ (pCi liter^{-1} sec^{-1}), where λ_R is the radiological decay rate and C_i is the concentration of radon inside the structure. Over a long period of time, equilibrium will be established such that

$$C_0 \lambda_v = C_i(\lambda_v + \lambda_R) \tag{4}$$

and since $\lambda_v \gg \lambda_R$,

$$C_0 \approx C_i \tag{5}$$

Thus the indoor concentration of ^{222}Rn attributable to the tailings pile will approach the annual average outdoor ^{222}Rn concentration resulting from atmospheric dispersion.

The conversion of an indoor ^{222}Rn concentration to a dose equivalent is dependent on an extensive knowledge of exposure environment and lung dosimetry conditions. At present an adequate definition of these conditions is not available for nonmining situations. Epidemiological studies of lung-cancer incidence in uranium miners have used exposures estimated in terms of working-level months* (WLM) (Federal Radiation Council, 1967). The conversion of the WLM unit to rems can be done only with major uncertainties (Parker, 1969).

We can, however, develop a rough correlation between two measurable factors: cumulative exposure in WLM and the number of lung cancers. Even these two factors are difficult to quantify in real-life situations of population exposures. Concentrations of airborne ^{222}Rn progeny can be calculated with formulas relating these values to ventilation rate (Haque and Collinson, 1967). For a ventilation rate of 1 hr^{-1}, an indoor concentration of 1 pCi/liter of ^{222}Rn will produce 0.005 WL of progeny and continuous exposure will result in an annual exposure of 0.25 WLM. Therefore we will assume that an outdoor concentration of 1 pCi/liter ^{222}Rn attributable to the tailings pile will result in an annual exposure of 0.25 WLM inside a structure.

Health effects attributable to these ^{222}Rn progeny exposures may be estimated using data provided in the BEIR Report (BEIR, 1972a, 1972b). An absolute risk estimator for death due to lung cancer was derived on the basis of a life-time duration of risk. The footnote of Table 3-2 of the BEIR Report (1972b) shows that lung cancer accounts for 26% of the absolute risk of "5 deaths/10^6/year/rem" for those over age 9 in the population. It was assumed that this ratio of 0.26 was also valid for individuals aged 0 to 9 years. Table 3-1 of the BEIR Report shows that all cancers

*One working level (1 WL) is any combination of short-lived radon daughters in 1 liter of air that has a potential alpha energy of 1.3×10^5 MeV; one working level month (1 WLM) is exposure at a level of 1 WL for a duration of 170 hr.

account for 1410 deaths among persons in a population of 198×10^6 exposed to 0.1 rem/year at all times after birth. Deaths from in utero exposure were not included in our estimate because the short half-lives of ^{222}Rn progeny, the low penetrating power of alpha particles, and the exposure route of inhalation preclude any significant in utero exposure to airborne ^{222}Rn progeny. Lung cancer death risk is estimated as $(0.26 \times 1410)/(197.9 \times 0.1)$, or 18.6 deaths/year in a population of 10^6 exposed to 1 rem/year postpartum.

The authors of the BEIR Report considered inherent inadequacies in estimating absorbed dose in rads from a given exposure in WLM and made the following statement (p. 148):

> On the basis of the present evidence, 1 rad/WLM is probably close to the upper limit for a reasonably uniform dose to the basal cell layer of the epithelium of the larger bronchi on a probabilistic basis. In the presence of existing chronic bronchitis, the dose factor may well be substantially lower, owing to increased thickness of the mucous layer as well as of the epithelium, and thus a figure of 0.5 rad/WLM has been adopted for this report. It should be emphasized that uncertainties in this value are probably greater than for the working level measurements themselves in determining risks per rad for the mining populations.

On the basis of this discussion, we estimated that an exposure of 1 WLM/year could be considered, in a very conservative manner, to result in a lung dose (bronchial epithelium) of 10 rems/year to members of the general population. Thus continuous exposure to 1 WLM/year will result in approximately 185 deaths per year per 10^6 persons exposed under these conditions. The reader should realize that the absolute risk estimator was obtained from epidemiological studies of uranium and other mineral miners, many of whom were cigarette smokers. Thus the risk estimator is not precise and should not be regarded as an absolute number.

EXAMPLE: SALT LAKE CITY, UTAH

The inactive uranium mill in Salt Lake City, Utah, was formerly operated by the Vitro Corporation. At this mill site is a tailings pile that contains an inventory of ~1400 Ci of ^{226}Ra and its daughters spread over an area of $\sim 5 \times 10^5$ m^2 (50 ha). The metropolitan area of Salt Lake City and its 400,000 inhabitants are within 11 km of the site. An aerial photo of the present setting of this site is shown in Fig. 2.

The average ^{226}Ra concentration in the tailings was determined from gamma logs and gamma spectroscopy for each of 24 test holes

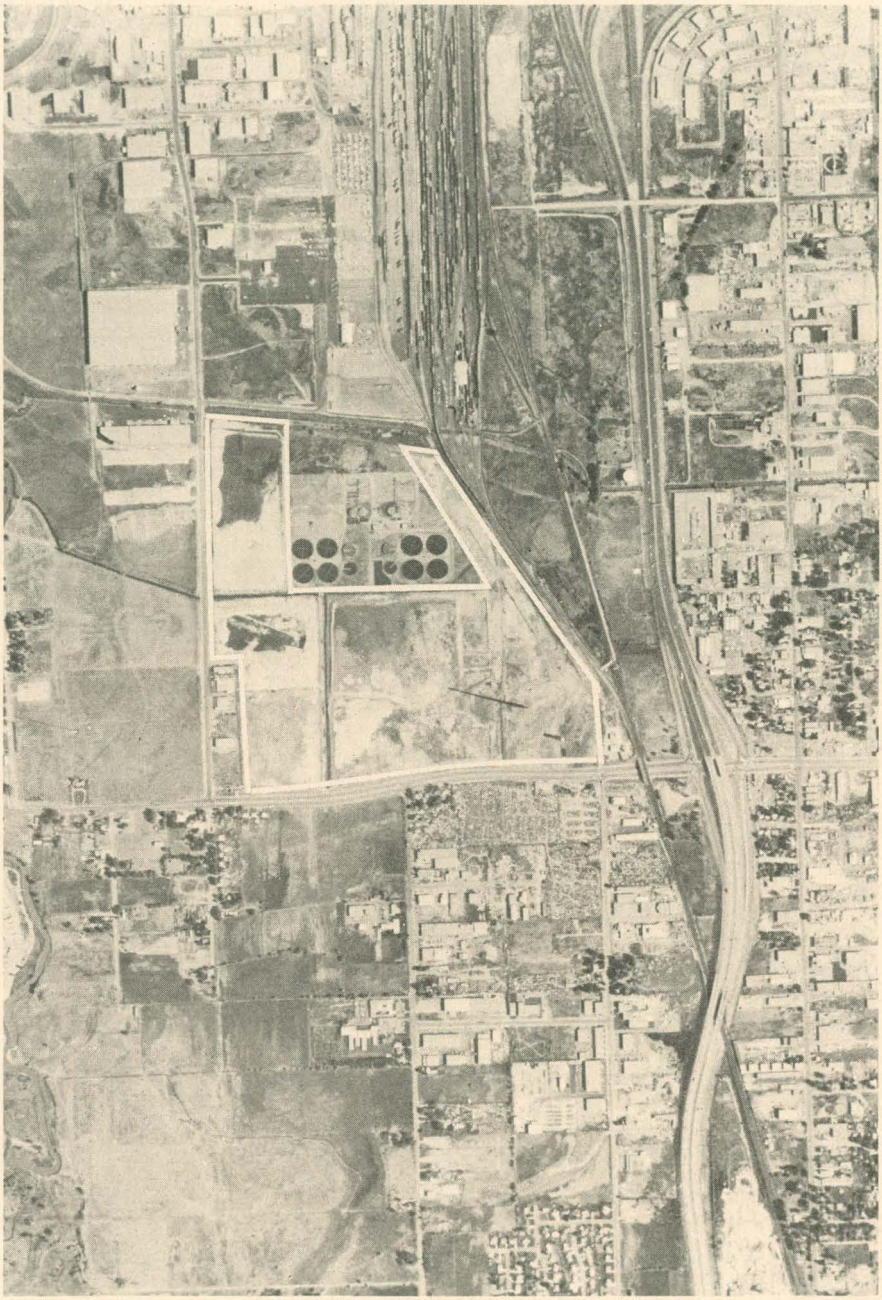


Fig. 2 Aerial view of Vitro mill site, tailings pile, and surrounding area.

bored into the pile. The estimated overall average ^{226}Ra content of the pile is 460 pCi/g. The average depth of contamination is estimated to be 4 m. The contaminated area, including mill site and ore storage area, is estimated as approximately 4.7×10^5 m^2 (47 ha). Assuming that the specific gravity of the tailings material is 1.6 g/cm^3, the total ^{226}Ra inventory may be calculated as 1384 Ci, which compares favorably with the estimate of 1380 Ci based on the assays of ore processed by the Vitro Corporation mill (Environmental Protection Agency and USAEC, 1974).

The estimated mass of contaminated material, 3×10^9 kg, is almost twice the amount of uranium ore processed by the mill, 1.54×10^9 kg (Environmental Protection Agency and USAEC, 1974). The additional mass includes an undetermined volume of low-activity vanadium tailings mixed with and piled upon the uranium tailings, the contaminated soil beneath the tailings piles and the ore storage area, and a large quantity of sewage sludge.

Emanation of ^{222}Rn from the surface of the Vitro tailings pile was estimated by use of Eq. 1. Porosity was assumed to be 0.4, specific gravity 1.6 g/cm^3, bulk diffusion coefficient 0.028 cm^2/sec [equivalent to that observed for sand with nearly 0% moisture (Tanner, 1964)], and emanation fraction 0.2. Diffusion properties of the subsoil were assumed to be similar to those for water-saturated clay described by Tanner (1964). These assumptions, coupled with an average ^{226}Ra content of 460 pCi/g and an average depth of 4 m, yielded a ^{222}Rn emanation rate of 550 pCi m^{-2} sec^{-1}.

Radon emanation rates have been measured at various locations on the Vitro tailings pile (Bernhardt, Johns, and Kaufman, 1975). The average of these short-term measurements was 320 pCi m^{-2} sec^{-1}. This measured value is only about 60% of the calculated value. However, the physical descriptions of the measured sites imply that the radon emanation rate from the ore storage area was not measured. This is the area containing the highest concentration of ^{226}Ra contamination. Furthermore, all assumptions related to the calculated emanation rate were made to maximize computed results. Thus the calculated emanation rate of 550 pCi m^{-2} sec^{-1} should be a conservative estimate of the annual average.

The area source model of Culkowski and Patterson (1976) was used in conjunction with the most recent wind profile and stability data for Salt Lake City to estimate the outdoor ^{222}Rn concentrations attributable to the tailings pile. Results of dispersion calculations for an area source with an equivalent point source strength of 2.6×10^8 pCi/sec are shown in Table 1. The two horizontal lines in Table 1 correspond to distances at which the ^{222}Rn concentration

TABLE 1

Radon-222 Concentration, pCi/liter, Resulting from the Vitro Tailing Pile

Distance from edge of pile, km	Compass direction															
	N	NNE	NE	ENE	E	ESE	SE	SSE	S	SSW	SW	WSW	W	WNW	NW	NNW
0	4.1	3.1	2.3	1.5	1.7	1.8	2.4	2.4	2.3	2.1	1.7	1.2	1.7	2.6	4.1	4.5
0.4	1.2	0.72	0.34	0.36	0.42	0.47	0.45	0.64	0.72	0.58	0.31	0.21	0.27	0.57	1.1	1.4
0.8	0.68	0.27	0.17	0.16	0.21	0.23	0.22	0.28	0.40	0.27	0.15	0.09	0.13	0.25	0.54	0.70
1.2	*0.46	0.12	0.10	0.10	0.13	0.13	0.13	0.15	0.28	0.14	0.09	0.05	0.08	0.13	0.33	0.42
2.8	0.15	0.04	0.03	0.03	0.04	0.04	0.04	0.05	0.09	0.04	0.02	0.01	0.02	0.04	0.10	0.13
4.4	0.08	0.02	0.02	0.01	0.02	0.02	0.02	0.02	0.05	0.02	0.01	0.007	0.01	0.02	0.05	0.07
6.0	0.05	0.01	0.01	0.009	0.01	0.01	0.01	0.01	0.03	0.001	0.009	0.004	0.007	0.01	0.03	0.04
7.6	0.03	0.008	0.008	0.006	0.009	0.009	0.01	0.009	0.02	0.009	0.006	0.003	0.005	0.009	0.02	0.03
9.2	0.03	0.006	0.005	0.005	0.007	0.007	0.007	0.007	0.02	0.007	0.005	0.002	0.004	0.006	0.02	0.02
10.8	†0.02	0.005	0.004	0.004	0.005	0.006	0.005	0.006	0.01	0.006	0.004	0.002	0.003	0.005	0.01	0.02

*———, pile contribution ≃ background.

†– – – –, pile contribution ≃ 10% of background.

TABLE 2

Comparison of Calculated and Measured ^{222}Rn Concentrations in Salt Lake City

Station number	Measured,* pCi/liter	Calculated,† pCi/liter
83	0.43 + 0.31‡	0.5 ± 0.0
84	0.39 ± 0.24	0.46 ± 0.14
85	0.68 ± 0.30	0.71 ± 0.15
86	0.28 ± 0.14	0.38 ± 0.14
91	0.44 ± 0.30	0.40 + 0.14
92	0.42 ± 0.24	0.38 ± 0.14
93	0.24 + 0.12	0.35 ± 0.14
94	0.44 ± 0.26	0.40 ± 0.14

*Shearer and Sill (1969).

†This value represents the calculated concentration plus the background of 0.25 ± 0.14 pCi/liter obtained from data of Shearer and Sill (1969) for two stations approximately 3 km northeast of the tailings pile.

‡This error is an estimate of the 68% confidence interval.

attributable to the tailings pile is approximately equal to the annual average background [0.25 pCi/liter determined from data collected by Shearer and Sill (1969)] and 10% of background, respectively. As may be seen from Table 1, radon attributable to the tailings pile is about 10% of background at a distance of about 3 km from the tailings pile in all but four sectors. Radon concentration decreases to 10% of background in all directions at about 9 km from the pile.

A comparison of calculated and measured annual ^{222}Rn concentrations is shown in Table 2. Good agreement was obtained at all points except Shearer and Sill's (1969) station 83. The sampling location map given by Shearer and Sill (1969) shows that this station was located on 3300 South across the street approximately 100 m from the tailings pile. It is expected that, for individual points this close to a tailings pile, assumptions concerning uniformity of radon emanation from the pile could lead to large errors in the estimate of the average annual radon concentration. Furthermore, the samples taken by Shearer and Sill (1969) covered only 10% of an annual meteorological cycle.

Atmospheric dispersion of ^{222}Rn attributable to the tailings pile was calculated for a distance of 11 km from the center of the pile in 16 compass directions. The area included in this 11-km radius is

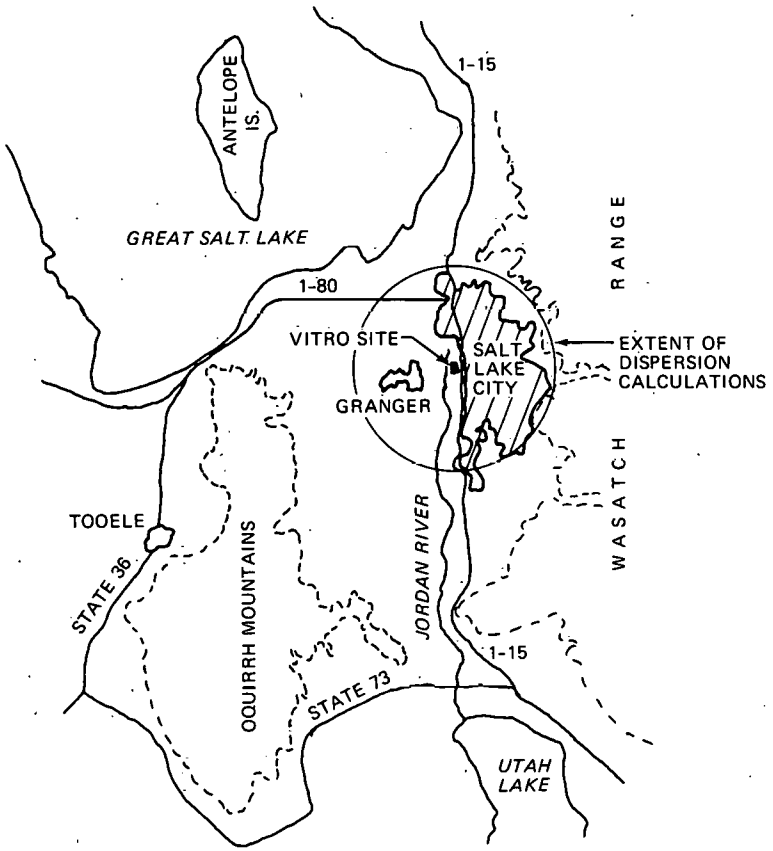


Fig. 3 Map of Salt Lake Valley showing area included in calculations of radon dispersion.

shown in Fig. 3. Extrapolations beyond this distance involve concentrations approaching 1% of background and would affect only a small percentage of the metropolitan population. Furthermore, the presence of mountain ranges at distances beyond 11 km would invalidate the turbulent diffusion model used to perform the calculations.

It was assumed that no ^{222}Rn was lost between the source and the receptor by decay, rainout, or dry deposition. Thus the concentrations shown in Table 1 are conservative estimates of annual averages.

Annual average ^{222}Rn progeny exposures may be calculated at each point listed in Table 1 by multiplying the values in this table by 0.25. Thus maximum exposure of 1.1 WLM/year would occur inside

TABLE 3

Summary of Estimated ^{222}Rn Exposures Attributable to Vitro Tailings Pile

Sector km*	Annual average ^{222}Rn concentration, pCi/liter	Annual average exposure, WLM/year	Population	Population exposure, person—WLM/year
0—1.6	0.61 ± 0.35	0.15 ± 0.09	1,518	228 ± 137
1.6—3.2	0.10 ± 0.07	0.025 ± 0.018	19,792	495 ± 356
3.2—4.8	0.039 ± 0.029	0.0098 ± 0.0072	60,047	588 ± 432
4.8—6.4	0.024 ± 0.016	0.0056 ± 0.0041	72,585	406 ± 298
6.4—8.0	0.015 ± 0.011	0.0037 ± 0.0027	97,366	360 ± 263
8.0—9.6	0.011 ± 0.008	0.0027 ± 0.0019	102,613	277 ± 195
9.6—11.2	0.0084 ± 0.006	0.0021 ± 0.0015	44,592	94 ± 67
0—11	0.025 ± 0.017	0.0061 ± 0.0044	398,513	2431 ± 730
Background	0.25 ± 0.14	0.063 ± 0.035	400,000	25,000 ± 14,000

*Measured from center of tailings pile. Sector refers here to the area between two concentric circles.

a structure at the north-northwest edge of the tailings pile. For comparison, the lower limit of the Surgeon General's Action Guide,* 0.01 WL, using the continuous occupancy assumptions, would result in an annual exposure of 0.5 WLM. Furthermore, an annual outdoor exposure at this point would be about 0.1 WLM. This value is based on average wind speed in the north-northwest direction, distance from the center of the pile, time of transport from source to receptor, and rate of growth of radon-decay products during transport. The resulting value of 0.1 WLM is for continuous outdoor exposure to a radon daughter level concentration of 0.002 WL.

A summary of estimated indoor exposures to ^{222}Rn progeny attributable to the Vitro tailings pile is given in Table 3. Population exposures were calculated for each of the 16 compass directions within each radial sector and summed to provide the estimate for that radial sector. Thus total population exposure of about 2500 person-WLM/year represents the best estimate obtainable. It is only in the first sector (up to 1.2 km from the *edge* of the pile) that annual average exposure exceeds the *error* associated with exposure due to background ^{222}Rn levels.

Exposure summaries for two separate population projections are shown in Table 4. These exposures considered a maximum, uniform population distribution for medium (31,000 persons/km^2) and high

*10 CFR 712.

(~51,000 persons/km^2) density urban growth. In these two exposure projections, as well as exposure estimates for the current population, it was assumed that prohibition of public access to the tailings area was the only method for controlling population exposures.

Health effects that we postulate as attributable to ^{222}Rn diffusion from the Vitro tailings pile are given in Table 5. These were calculated from exposures given in Tables 3 and 4. Health effects that may be attributable to background ^{222}Rn progeny levels are shown in Table 5 for comparison. It may be noted that, in every case, effects due to the tailings pile are about 10% of the effects due to background radon.

TABLE 4

Extrapolated ^{222}Rn Exposures Attributable to Vitro Tailings Pile for Medium and High-Density Population Projections

Exposure source	Population	Population exposure, person-WLM/year
Tailings	1,850,000	15,500
Background*	1,850,000	116,000 ± 65,000
Tailings	3,000,000	24,400
Background*	3,000,000	188,000 ± 105,000

*0.25 ± 0.14 pCi/liter.

TABLE 5

A Comparison of Potential Health Effects Attributable to ^{222}Rn Progeny Exposure from the Vitro Tailings Pile and from Background for the Population Residing Continuously Within 11 km of the Vitro Tailings Pile

Population	Lung-cancer deaths* per year in the population attributable to:	
	Vitro tailings pile	Background, 0.25 ± 0.14 pCi/liter
Present, 400,000	0.4	5 ± 3
Extrapolated, 1,850,000	3	21 ± 12
Extrapolated, 3,000,000	4	34 ± 19

*Based on a lifetime duration of risk.

SUMMARY AND CONCLUSIONS

One of the principal concerns over uranium mill-tailings piles, whether active or inactive, is the potential for radiation exposure to the surrounding population. It has been shown that, in many cases, the diffusion and dispersion of radon from these piles constitutes the principal exposure pathway. Therefore, to assess potential radiological hazards, we must calculate the radon concentration at points where people reside. A methodology has been developed which predicts the concentration of radon as a function of distance and direction from tailings and may be used for any pile provided certain input data are available. The pertinent features of this methodology include (1) a comprehensive description of the profile of ^{226}Ra as a function of depth in tailings, (2) the application of Fickian diffusion equations to describe the migration of ^{222}Rn through bare tailings residing on an earthen base, (3) the use of area source geometry resulting in an estimate of the emanation of ^{222}Rn per unit area, (4) the use of Culkowski and Patterson's Gaussian diffusion model for the dispersion of radon, and (5) the assumption that over a long period (i.e., 1 year), the indoor radon concentration attributable to the tailings pile will approach the annual average outdoor radon concentration resulting from atmospheric dispersion.

An assessment was made of the radiological hazards associated with ^{222}Rn diffusion from the inactive uranium tailings pile in Salt Lake City, Utah. This tailings pile represents a large, steady-state source of radon at 2.6×10^8 pCi/sec. Estimates of radon dispersion showed that radon concentrations, based on a methodology described here, had decreased to $< 10\%$ of background in all directions at about 9 km from the pile. Calculations were carried out to a distance of 11 km from the center of the pile. Beyond this distance, concentrations of radon were less than 1% of natural background and the additional population represented only a small fraction of the total within 11 km. Also, concentration estimates provided with the area source diffusion model used to make these calculations lose validity when air masses reach the mountain range to the east. Comparisons were made of calculated values of radon concentration as a function of distance from the pile with measurements of radon at several places in the vicinity of the Vitro site. Except for one station, the averages of the calculated and measured values were well within the stated limits of error for both sets of data. It was estimated that the annual incidence of lung cancer due to continuous exposure to the pile in its current condition is 0.4 cases per year in the present Salt Lake City population. It should be emphasized that

these effects represent less than 10% of those which might be attributed to exposure of the same population to background ^{222}Rn.

ACKNOWLEDGMENT

Research sponsored by the Division of Environmental Control Technology, U. S. Department of Energy, under contract W-7405-eng-26 with the Union Carbide Corporation.

REFERENCES

Baver, L. D., 1965, *Soil Physics*, 3rd ed., p. 214, John Wiley & Sons, New York.

BEIR, 1972a, *The Effects on Populations of Exposure to Low Levels of Ionizing Radiation*, pp. 145-156, National Academy of Science—National Research Council Report.

——, 1972b, *ibid*, pp. 167-173.

Bernhardt, D. E., F. B. Johns, and R. F. Kaufman, 1975, *Radon Exhalation from Uranium Mill Tailings Piles*, Environmental Protection Agency Technical Note ORP/LV-75-7(a).

Clements, W. E., and M. H. Wilkening, 1974, Atmospheric Pressure Effects on ^{222}Rn Transport Across the Earth—Air Interface, *J. Geophys. Res.*, 79: 5025-5029.

Cox, W. M., R. L. Blanchard, and B. Kahn, 1970, Relation of Radon Concentration in the Atmosphere to Total Moisture Retention in Soil and Atmospheric Thermal Stability, in *Radionuclides in the Environment*, pp. 436-446, American Chemical Society, Washington, D. C.

Culkowski, W. M., and M. R. Patterson, 1976, *A Comprehensive Atmospheric Transport and Diffusion Model*, ERDA Report ORNL-NSF-EATC-17, Oak Ridge National Laboratory, NTIS.

Culot, M. V. J., H. G. Olson, and K. J. Schiager, 1973, *Radon Progeny Control in Buildings*, USAEC Report COO-2273-1, Colorado State University, NTIS.

Federal Radiation Council (U. S.), 1967, *Guidance for the Control of Radiation Hazards in Uranium Mining*, Staff Report No. 8, revised.

Gera, F., 1975, *Geochemical Behavior of Long-Lived Radioactive Wastes*, ERDA Report ORNL-TM-4481, Oak Ridge National Laboratory, NTIS.

Goldsmith, W. A., 1976, Radiological Aspects of Inactive Uranium-Milling Sites: An Overview, *Nucl. Safety*, 17(6): 722-732.

Guedalia, D., J. I. Laurent, J. Fontan, D. Blanc, and A. Druilhet, 1970, A Study on Radon-220 Emanation from Soils, *J. Geophys. Res.*, 75: 357-369.

Handley, T. H., and C. J. Barton, 1973, *Home Ventilation Rates: A Literature Survey*, USAEC Report ORNL-TM-4318, Oak Ridge National Laboratory, NTIS.

Haque, A. K. M. M., and A. J. L. Collinson, 1967, Radiation Dose to the Respiratory System Due to Radon and Its Daughter Products, *Health Phys.*, 13: 431-443.

Haywood, F. F., W. A. Goldsmith, P. T. Perdue, W. F. Fox, and W. H. Shinpaugh, 1977, *Assessment of Radiological Impact of the Inactive*

Uranium-Mill Tailings Pile at Salt Lake City, Utah, ERDA Report ORNL/TM-5251, Oak Ridge National Laboratory, NTIS.

Kramer, H. W., G. L. Schroeder, and R. D. Evans, 1964, Measurement of the Effects of Atmospheric Variables on Radon-222 Flux and Soil—Gas Concentrations, in *Natural Radiation Environment*, J. A. S. Adams and W. M. Lowder (Eds.), pp. 191-215, University of Chicago Press, Chicago.

Megumi, K., and T. Mamuro, 1974, Emanation of Radon and Thoron Gases from Soil, *J. Geophys. Res.*, 79: 5025-5029.

Parker, H. M., 1969, The Dilemma of Lung Dosimetry, *Health Phys.*, 10: 553-561.

Schiager, K. J., 1977, Radwaste Radium—Radon Risk, in *A Workshop on Policy and Technical Issues Pertinent to the Development of Environmental Protection Criteria for Radioactive Wastes*, Workshop Proceedings, pp. 2-45 to 2-81, Report ORP/CSD-77-2.

Schroeder, G. L., H. W. Kramer, and R. D. Evans, 1965, Diffusion of Radon in Several Naturally Occurring Soil Types, *J. Geophys. Res.*, 70: 471-474.

Sears, M. B., R. E. Blanco, R. C. Dahlman, G. S. Hill, A. D. Ryon, and J. P. Witherspoon, 1975, *Correlation of Radioactive Waste Treatment Costs and the Environmental Impact of Waste Effluents in the Nuclear Fuel Cycle for Use in Establishing "As-Low-as-Practicable" Guides: Milling of Uranium Ores*, ERDA Report ORNL-TM-4903(Vol. 1), Oak Ridge National Laboratory, NTIS.

Shearer, S. D., Jr., and C. W. Sill, 1969, Evaluation of Atmospheric Radon in the Vicinity of Uranium Mill Tailings, *Health Phys.*, 17: 77-88.

Sisigina, T. I., 1972, Assessment of Radon Emanation from the Surface of Extensive Territories, in *Nuclear Meteorology*, Gidrometeoizdat, Moscow, USAEC Report TT-74-50011, pp. 239-244, NTIS.

Snelling, R. N., 1970, Environmental Survey of Uranium Mill-Tailings Pile, Monument Valley, Arizona, *Radiol. Health Data Rep.*, 11: 511-517.

——, 1971, Environmental Survey of Uranium Mill-Tailings Pile, Mexican Hat, Utah, *Radiol. Health Data Rep.*, 12: 17-28.

——, and S. D. Shearer, Jr., 1969, Environmental Survey of Uranium Mill-Tailings Pile, Tuba City, Arizona, *Radiol. Health Data Rep.*, 10: 475-487.

Swift, J. J., J. M. Hardin, and H. M. Calley, 1976, *Potential Radiological Impact of Airborne Releases and Direct Gamma Radiation to Individuals Living Near Inactive Uranium Mill-Tailings Piles*, Report EPA-52011-76-001, Environmental Protection Agency, NTIS.

Tanner, A. B., 1964, Radon Migration in the Ground: A Review, in *The Natural Radiation Environment*, pp. 161-190, J. A. S. Adams and W. M. Lowder (Eds.), University of Chicago Press, Chicago.

U. S. Environmental Protection Agency, 1973, *Environmental Analysis of the Uranium Fuel Cycle, Part I. Fuel Supply*, Report PB-235804, Environmental Protection Agency, NTIS.

——, and USAEC, 1974, *Summary Report, Phase I. Studies of Inactive Uranium Mill Sites and Tailings Piles*, Environmental Protection Agency—USAEC Joint Report. Available from the Department of Energy, Office, Grand Junction, Colo.

DISCUSSION

Bland: What is the justification for using a steady-state equation for radon diffusion in the presence of marked diurnal variations?

Goldsmith: These short-term variations may be caused by changes in such factors as wind speed, atmospheric pressure, temperature differential between tailing and atmosphere, and atmospheric stability and rainfall. These variations are quite important in making determinations of instantaneous flux rates. However, these variations have a cyclical nature. Thus, over a long period of time, such as the annual cycle, these short-term variations are insignificant when compared to diffusion. I recall that Dr. Wilkening addressed this point in his paper at this symposium.

Clements: Since the effect of moisture on emanating power and radon exhalation is poorly understood, how did you make your calculations concerning these effects? Did you consider the effect on the emanating power?

Goldsmith: These calculations, shown graphically in Fig. 1, were based on effects of moisture on the diffusion coefficient as given by Tanner (1964). The effect on emanating power was not considered. However, as may be noted from Equation 1, any change in the emanating power would change the estimated flux in the same proportion.

The Uranium District of the Texas Gulf Coastal Plain

LEWIS M. COOK
Texas Department of Health, Austin, Texas

ABSTRACT

The uranium in Texas is derived from Miocene age volcanic ash deposits. Uranium is leached from tuffs and precipitates in sandstones. Mining of the deposits results in increased gamma-ray exposures and exposes groundwater high in radium to the surface. Radon in groundwaters is released to the atmosphere by uranium in situ mines and water wells, but few data are available on resulting concentrations in the atmosphere. A catalog of uranium deposits is presented, and an announcement of the discovery of high levels of radon daughters in oil field processing equipment is included.

The uranium district of the Texas Gulf Coastal Plain is an area extending northeast from the southern border of Texas into east Texas near Houston. The geological formations in which the uranium occurs extend into Mexico on the south and into Louisiana on the east.

The original discovery of uranium occurred accidentally using airborne scintillation detectors. Now the typical method of finding ore (based first on geological reconnaissance) is to drill wells and log them with gamma-ray instruments to detect the uranium daughters. Frequently an area being explored will be drilled to a depth of 200 m or deeper, using a rectangular grid pattern with about 30-m spacing between wells. After analysis of the data, those areas where substantial uranium has been found are examined more closely using holes drilled 15 m apart or closer to determine the exact location of the uranium deposit, its grade, depth, and thickness.

Locations where exploration drilling and development drilling were reported for 1976 and 1977 by Dubois (1977, 1978) are shown in Fig. 1.

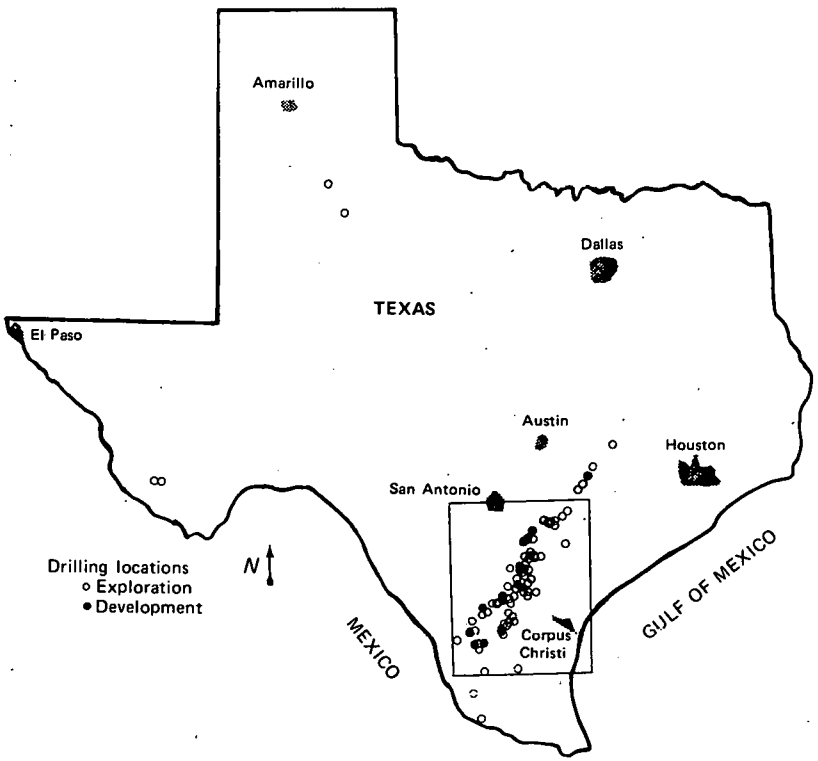


Fig. 1 Locations of exploration and development drilling during 1976 and 1977. The rectangle indicates the boundaries of the map in Fig. 2.

Two methods of mining are used in South Texas, the open-pit method and in situ, also called solution mining. In the open-pit method, the sediments overlying the deposit are removed by conventional earthmoving equipment and piled near the mine. Next the ore is removed and stockpiled at the edge of the pit until it is taken to the mill.

To mine a deposit using the solution mining method in Texas, wells are drilled in patterns, with a rectangular grid system preferred. The spacing between wells is usually 15 m but may be varied by the operator. In the center of each pattern another well is placed to withdraw solutions injected in the other wells. A slightly alkaline (pH 7 to 9) carbonate leach is used.

The Texas Department of Health is the radiation control agency for the state and administers a program for licensing and inspecting

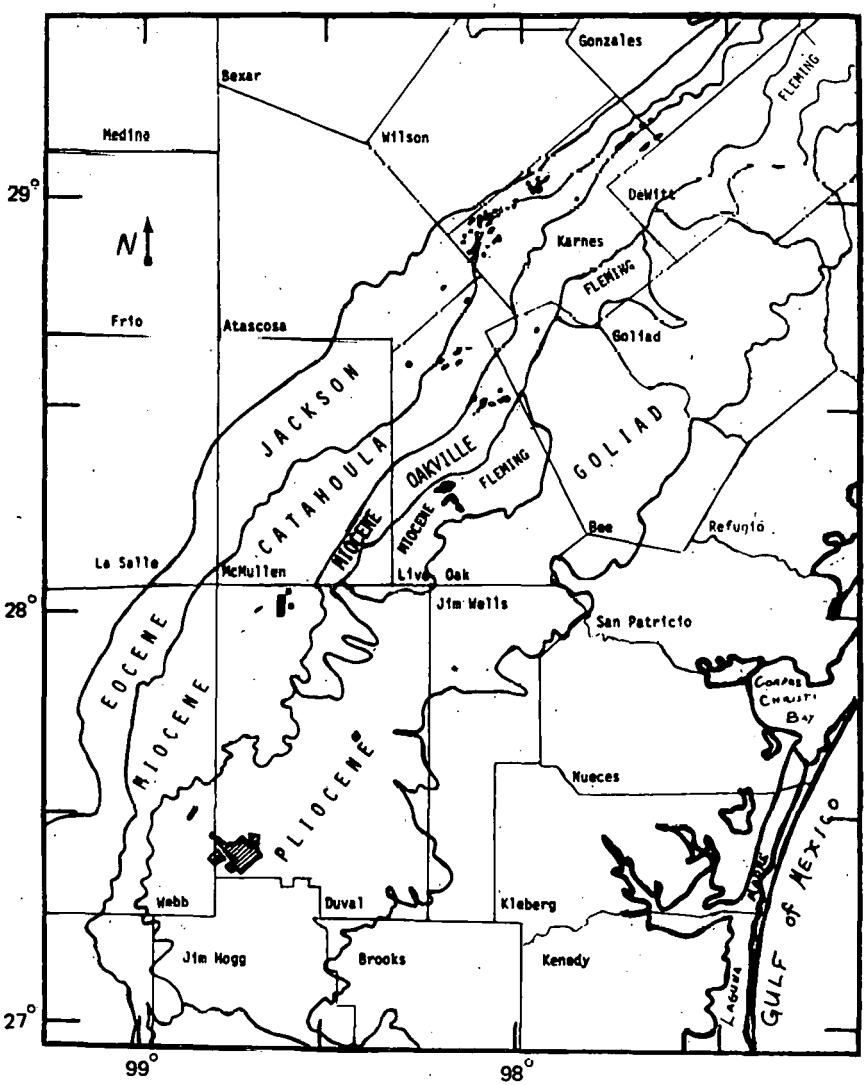


Fig. 2 Uranium deposits in South Texas counties (solid spots) or in situ permit areas (shaded areas). Surface outcrops of major sediments are shown.

users of radioactive material in the state under a 1963 agreement signed with the U. S. Atomic Energy Commission (now with the U. S. Nuclear Regulatory Commission). Since then, numerous investigations have been conducted into the uranium district and the levels of radioactivity to be found there. High levels of activity have been found to be due both to natural conditions and to man's intervention.

HISTORY

The search for oil and gas deposits using airborne gamma-ray scintillation detectors intended to detect theorized radon "halos" around the periphery of the petroleum deposits proved to be a failure, but it did result in the discovery of commercial-grade uranium deposits in Texas in 1954.

Radiation anomalies near Tordillo hill in Karnes County proved to be due to oxidized uranium deposits lying on the surface. Because of the comparatively high rainfall and other geochemical factors, uranium had been thought to be unlikely to be found in the Texas Gulf Coastal Plain. Soon after the discovery, prospecting using trenching methods had proven the potential of the area, and by 1959 mining had begun in the vicinity. The open-pit method was used.

A mill using the acid leach process was built near the abandoned town of Deweesville in 1961, and the ore stockpiled on the nearby Korzekwa ranch was milled. In 1963, unoxidized ore was found about 3 km southeast of the Deweesville deposits. This discovery of unoxidized ore at a depth of about 30 m was made after one exploration geologist rejected the informal guideline of the area that uranium was not to be found below the "blue shale" and drilled deeper. In the area the color of the rock in the oxidized zone is tan to buff, whereas a blue-gray color is observed in the unoxidized layers. Since the initial discovery of unoxidized ore in the Galen mine, most of the ores discovered have been in unoxidized deposits.

In 1968 another mill was opened near Ray Point in Live Oak County, about 35 km south of the Karnes County deposits. This mill used carbonate leaching chemistry since it was designed to mill ores from the Felder and nearby deposits. The Felder deposit, adjacent to Sulfur Creek, was found after a radiation anomaly in the creek at the Oakville fault was investigated. There are other mines in the area which are associated with faults, including the McLean No. 1 on the Oakville fault.

About the same time as the Ray Point mill was opened, development studies were being conducted at the Palangana Salt

Dome deposit in Duval County and the Burns deposit in the southwest corner of Live Oak County. A shaft was sunk at the Palangana deposit, but little ore was removed because conditions were unsuitable for underground mining. Instead, both at the salt dome and at the Burns deposit, methods of solution mining were being investigated.

By 1972 a third conventional mill had been constructed and was operating, milling ores from the Karnes County area. This mill, also using the acid leach process, is located 3 km east of the first mill at Deweesville. In the meantime the area affected by surface mining was increasing steadily as the mills' requirements for ores grew. Deposits of ore grade minerals were found to extend southward from the Galen deposit for 6 km, and another group was developed to the southwest of this long chain.

Deposits to the east were also being developed. By 1978 a fourth mill (acid leach) was under construction 21 km east of the original Deweesville site, which was beginning to mine a deposit of ore 7 km long in the vicinity of the mill. South and west of these areas, solution mining was being conducted on a commercial scale from southern Duval and Webb counties, at the Palangana Salt Dome, at several deposits near the town of George West, including the Burns deposit, which will be examined in more detail later. Other solution mining operations were being conducted near the Felder deposit and near the small town of Pawnee.

In 1972, both of the first mills to operate closed down. The tailings pond at the Ray Point mill was sprayed with an asphalt coating to reduce wind erosion of the tailings, and some of six tailings areas at Deweesville were required to be covered with at least 0.6 m of dirt. By 1978, no activity had occurred at the Ray Point mill, but a heap leach test to remove uranium from the tailings pond at Deweesville was in progress.

GEOLOGY

The deposits being mined in South Texas occur in Eocene and younger rocks (Fig. 2). In Table 1 the major sediments are listed. These host rocks are gently dipping sediments whose outcrop on the surface (and strike of the beds) roughly parallels the modern-day coastline. The beds typically thicken toward the coast.

The rocks believed to be the source rock for much of the uranium are the sediments comprising the Catahoula tuff.

Volcanic ash from west Texas and northern Mexico volcanoes during Miocene times was deposited by winds and stream runoff into

TABLE 1

Stratigraphic Column, South Texas Uranium District

System	Series	Group	Geologic unit	Member	Description
Quaternary	Recent and Pleistocene		Flood plain alluvium and terraces		Gravel, sand, silt, clay
	Pleistocene		Lissie Fm.		Gravel, sand, silt, clay
Tertiary	Pliocene		Goliad sand*		Sandstone, clay
	Pliocene or Miocene		Lagarto clay		Clay and sand
	Miocene		Oakville sandstone*		Clay and reworked sand
	Miocene or Oligocene		Catahoula tuff*		Tuff, clay, sand
	Oligocene		Frio clay*		Marine clay
	Eocene	Jackson	Whitsett formation	Fashing clay	(Marine)
				Tordillo sandstone*	Fine sand
				Dubose	Sand, clay, lignite
				Deweesville sandstone*	Sand, clay (carbonaceous)
				Conquista clay	Clay (carbonaceous)
				Dilworth sandstone	Fine sand
				Manning clay	Clay and tuff
			Wellborn sandstone		Fine sand
			Caddell formation		Clay and silt (carbonaceous)
		Claiborne	Yegua formation		Medium to fine sand, silt, clay
			Laredo formation		Marine clay, fine sand

*Indicates uranium host rock.

the ancestral Gulf of Mexico. According to Eargle, Hinds, and Weeks (1971), the deposits include a fluvial-delta system; a barrier-island, lagoonal and marsh system; and other marine beach sandstones. Often these sandstones are unconsolidated and require little grinding in the mill.

After deposition, the geological lifting of the area and subsequent retreat southeastward of the Gulf shoreline left the sediments on the

surface. These rocks were subjected to dry-climate weathering that dissolved the uranium. Then in solution in the groundwater, the uranium circulated until stratigraphic traps and reducing conditions were encountered, such as hydrogen sulfide, lignite deposits, methane gas, or carbonaceous matter. There the uranium precipitated. It has been suggested (Updegraff, 1969) that microorganisms may also contribute. Faults may be important factors in this process, providing a barrier to circulation and allowing gases to seep up from deeper sediments.

As more oxygenated water circulated through the deposit, the uranium slowly redissolved and would then reprecipitate downdip. This slow process of dissolution and reprecipitation continues today. A modification of it is used by the solution mining ventures. The deposits formed in this manner are termed roll front deposits and display a crescentic cross section (Eargle and Weeks, 1973, and Eargle, Dickson, and Davis, 1975). Radiometric and chemical studies of the deposits have shown differing assays on the order of 30% each way, with the radiometric assay of uranium in the downdip portion of the deposit indicating less uranium than proven by chemical assay. In the updip portion of the deposit, the radiometric assay usually indicates more uranium than the chemical assay shows is present. Since uranium is mobilized easier than its daughters, this lack of equilibrium indicates the dynamic nature of the ore deposit.

Oxidized ore deposits have also been mined. They are believed to be the remnants of old unoxidized deposits left above the water table due to lifting and a lowering of the level of the groundwater. Slow dry weathering oxidized the uranium again, and erosion caused the land surface to approach the deposits. The relatively dry climate in earlier times permitted the formation of a caliche cap that protected the deposits from further leaching by rainwater under the present climatic conditions, classified as semiarid to subhumid.

It was the occurrence of these oxidized deposits that had been exposed by erosion that led to their discovery. The deposits were the first ones mined and are noted in Table 2.

RADIATION LEVELS AND MEASUREMENTS

Numerous measurements have been made in the uranium district to determine radiation levels and radioactivity content of waters and soils. In many instances, however, background levels unaffected by technology have been impossible to measure since the need to take these did not arise until it was suspected that problems had developed.

The initial radiation levels on the surface near the first mines must have been high, since the deposits were on the surface. Radiation levels on the surface on unmined ground adjacent to the Korzekwa No. 1 mine exceed 200 μR/hr today. Other areas on the outcrop of the Deweesville sandstone near the Luckett mine are somewhat elevated also with readings of 20 to 30 μR/hr common. In 1972, Ward (1974) measured a background level of 20 μR/hr also on the Deweesville sandstone.

Measurements between the Conquista Mill and the Sickenius mine show levels of around 20 to 30 μR/hr which are quite similar to those at the southern edge of the Lauw mine. Both of these sites are on the Tordillo sandstone.

Using aerial radioactivity measurements, Moxham and Eargle (1961) determined the average uranium content of the Jackson sediments (of which both the Tordillo and Deweesville sandstones are members) to be 20 to 30 ppm in the area, which generally agrees with these findings.

Recently we reported results of radiation surveys of several mines (Cook, Caskey, and Wukasch, 1977). As practiced in South Texas, uranium mining increases the gamma-ray dose rate over parts of the property mined due to the deliberately incomplete removal of mineralized rock. The economics of open-pit mining require that a lower limit for milling uranium ore be established. Currently this limit is about 0.03% U_3O_8 (300 ppm). Material of lower concentration is placed in the overburden piles or not removed from the pit. With the industry rejecting sands with up to 300 ppm of U_3O_8, radiation levels on piles of this material could be expected to be over 150 μR/hr. In fact, this was found to be the case on 3% of the area surveyed.

Using the 0.5 rem/year limit to individual members of the public as a guide, we examined the open-pit uranium mine data we had collected. We found on older mines when the mill cutoff limit was higher and when no reclamation for returning the land to productive (agricultural) use was done that radiation levels over 24% of the land exceeded 0.5 rem/year. Partial land reclamation coupled with a lower milling cutoff resulted in only 2% of the land having this high exposure rate.

Because of the recentness of the mining and the unaesthetic nature of the land, no one now lives on mined land, although residences are often within a few hundred meters of the pits. Reclamation restores some of the beauty of the land and may encourage home building.

Radon exhalation from piles of mine overburden, uranium mill tailings, and mineralized ground in the area has not been measured,

(Text continues on page 1617.)

TABLE 2

South Texas Uranium Mine Catalog

Name	County	Longitude, W	Latitude, N	Pit depth, m	Radiation levels, μR/hr	Comments
Banduch-Cochran	Karnes	97°43′18″	29°06′50″	34	NS	24-ha pit, 1981—1985
Bargmann (Superior)	Karnes	98 08 20	28 52 37	6	NS	Oxidized deposit, no overburden, surface deposit; abandoned in 1960
Beiker	Karnes	98 06 25	28 53 20	25	5—35	Abandoned; 8/76 ^{226}Ra 1.2 pCi/liter
Boots	Live Oak	98 13 00	28 17 00	NP	NS	In situ 1978
Brelum 106-200	Duval	98 38 00	28 00 00	NP	NS	In situ planned
Brelum 199	Duval	98 37 00	28 01 30	NP	NS	In situ planned
Brown	Karnes	98 03 13	28 54 03	35	7—20	Abandoned; overburden sloped, covered, seeded; 7/76 ^{226}Ra 13.7 pCi/liter
Bruni	Webb	98 51 56	27 31 50	NP	NS	In situ operating 1978
Brysch	Karnes	97 57 50	28 58 54	25	NS	Oxidized deposit; abandoned in 1968
I. M. Brysch	Karnes	98 04 30	28 54 40	U	NS	Abandoned in 1974
Burns	Live Oak	98 12 05	28 14 27	NP	NS	In situ operating 1978
Butler	Karnes	98 07 00	28 52 00	35	10—300	Large mine, abandoned in 1972
Chapman	Live Oak	98 13 54	28 36 07	16	NS	Mined 1977, 3-ha pit
Clay West	Live Oak	98 14 00	28 14 11	NP	NS	In situ operating 1978
Cochran	Karnes	97 43 52	29 06 30	31	NS	8-ha pit, 1980—1983
DCRC	Duval	98 46 45	27 59 10	32	NS	24-ha pit, 1979—1982

Dickson—Pawelek	Karnes	98 03 30	28 53 55	44	NS	6-ha pit, mined in 1978
Dobie	Live Oak	98 12 35	28 36 15	60	NS	10-ha pit, 1978—1982
Dziuk	Karnes	98 06 20	28 49 30	54	NS	8-ha pit, 1978—1980
Dziuk—Lyssy	Karnes	98 05 45	28 49 35	70	NS	13-ha pit, 1982—1984
Esse	Live Oak	98 08	28 44	30	5—250	Abandoned; 5/76 ^{226}Ra 4.0 pCi/liter
Felder 1, 2, 3	Live Oak	98 04 38	28 29 40	40	8—550	Large deposit (2000 metric tons of U_3O_8) adjacent to McLean No. 2 reworking 1978
Ft. Worth National Bank	Karnes	97 56 47	28 58 47	36	NS	4-ha pit, mined in 1976
Franklin—Swierc	Karnes	98 03 34	28 54 20	51	NS	12-ha pit, 1978—1981
Galen	Karnes	98 06 40	28 52 11	30	10—170	First unoxidized deposit mined; abandoned; 9/76 ^{226}Ra 2.0 pCi/liter
Garcia	Karnes	98 04 08	28 53 02	81	NS	17-ha pit, 1980—1983
Gembler—Lyssy	Karnes	98 07 42	28 54 04	13	11—63	Holds mill tailings, covered with weekly mineralized overburden, oxidized deposit
Griffin	Gonzales—Karnes	97 39 25	29 09 13	27	NS	8-ha pit, 1979—1981
Haase	Karnes	97 42 37	29 07 21	30	2—125	Abandoned; between Wiatrek—Haase and Haase—Moy
Haase—Moy	Karnes	97 42 14	29 07 29	30	6—20	Abandoned; adjacent to Haase
Hackney	Karnes	98 08 16	28 52 32	7	NS	Abandoned; used for chemical waste disposal, mined about 1960, oxidized deposit

TABLE 2 (Continued)

Name	County	Longitude, W	Latitude, N	Pit depth, m	Radiation levels, μR/hr	Comments
Hackney (Boso)	Karnes	98 08 52	28 51 58	5	15—240	Abandoned, no overburden; at base of Tordillo Hill; used as chemical waste-disposal pit, oxidized deposit, mined in early 1960s
Holiday—El Mesquite	Duval	98 43 00	27 25 00	NP	NS	In situ operating 1978
House	Live Oak	98 10 40	28 36 45	NP	NS	28-ha pit, 1978—1985
House—Seale—Taylor	Live Oak	98 15 45	28 38 00	48	NS	17-ha pit, operating in 1978
Hurt	Atascosa	98 11 43	28 46 22	25	NS	Mined in 1978
Kellner	Karnes	98 07 40	28 50	35	6—140	Southern end of Butler, abandoned; 1/76 ^{226}Ra in water 1.5 pCi/liter
Knispel—Vaughn—Taylor	Live Oak	98 09 30	28 38 00	60	NS	23-ha pit, 1977—1987
Kopecki	Karnes	97 56 12	28 58 40	62	NS	8-ha pit, 1982—1986
Kopplin	Live Oak	98 03 52	28 31 00	30	5—260	Abandoned before 1970; fault visible in pit, 5/76 ^{226}Ra 2.1 pCi/liter
Korth—Hartman—Finch—Otton	Karnes	97 39 30	29 06 40	64	NS	21-ha pit, 1978—1983
Korzekwa No. 1	Karnes	98 07 42	28 53 29	3	16—1000	Shallow pit, no overburden, abandoned in 1960, oxidized deposit on surface, no water in pit

Korzekwa No. 2	Karnes	98 07 30	28 53 36	15	10—110	Overburden used for covering tailings, 1974; abandoned in 1964
Korzekwa No. 3—Nieschwietz	Karnes	98 09 00	28 54 10	31	NS	42-ha pit, 1977—1982
Kotzur	Karnes	97 54 15	28 59 45	15	6—60	Mined in 1976, 7/76 ^{226}Ra 1.4 pCi/liter; 2-ha pit
Labus—Hoffman	Karnes	98 00 20	28 56 20	48	NS	10-ha pit, mining 1977—1980
Lamprecht	Live Oak	98 02 15	28 30 15	NP	NS	In situ operating 1978
Lauw	Karnes	98 07 15	28 52 36	25	7—1600	Abandoned; no water in pit in 1977
Luckett	Karnes	98 06 55	28 54 34	15(?)	5—75	Filled with tailings, covered with overburden, oxidized deposit; mined 1961
Lyssy	Karnes	98 07 44	28 53 50	12	29—130	Filled with tailings, covered with weakly mineralized overburden; part unfilled, holds mill acid; mined in 1960, oxidized deposit
Mabel New	Live Oak	98 17 18	28 33 30	5(?)	NS	Deposit in old stream (Eargle and Weeks, 1973) oxidized deposit
Manka	Karnes	98 01 47	28 56 03	35	7—140	Abandoned in 1976
McGrady	Karnes	98 07 04	28 49 38	30	3—65	Connected to Weddington South deposit and Wright; abandoned in 1976
McLean No. 1	Live Oak	98 05 12	28 29 10	20	8—3000	Abandoned prior to 1970; on Oakville fault; 6/76 ^{226}Ra 11.3 pCi/liter; molybdenum present

TABLE 2 (Continued)

Name	County	Longitude, W	Latitude, N	Pit depth, m	Radiation levels, μR/hr	Comments
McLean No. 2	Live Oak	98 04 52	28 29 25	20	20—160	Adjacent to Felder, abandoned; selenium present
McLean No. 5	Live Oak	98 05 38	28 28 48	25	12—210	Abandoned 1974; 6/76 ^{226}Ra 10.3 pCi/liter
Moczygemba	Karnes	98 02 14	28 56 03	22	NS	Mined in 1976
Moser	Live Oak	98 13 17	28 14 27	NP	NS	In situ operating 1978; water 1/76 ^{222}Rn 167,000 pCi/liter, ^{226}Ra 473 pCi/liter
Nieschwietz No. 1	Karnes	98 04 57	28 54 23	19	NS	6-ha pit, 1981—1984
Nieschwietz No. 2	Karnes	98 04 20	28 54 40	24	NS	2-ha pit, 1981—1984
Nieschwietz No. 3	Karnes	98 04 35	28 53 50	32	NS	2-ha pit, 1981—1984
O'Hearn	Webb—Duval	98 48 00	27 23 30	NP	NS	In situ operating 1978
Palangana	Duval	98 24 55	27 41 00	NP	NS	In situ operating 1978; Goliad Sand deposit
Panna Maria	Karnes	97 56 00	28 58 00	35	NS	Mining, 1978—1985
Pawelek	Karnes	98 06 55	28 52 32	25	6—300	Uraniferous lignite and sandstone, second working 1977
Pawelek—Lyssy—Butler	Karnes	98 06 50	28 52 45	31	NS	Mined in 1977, 10-ha pit
Pawnee	Bee	97 57 55	28 39 40	NP	NS	In situ working 1978
Pfeil	Karnes—Atascosa	98 07 32	28 48 47	35	4—50	Southern end of Weddington South deposit; 6/76 ^{226}Ra 1.3 pCi/liter
Piedre Lumbre East	Duval	98 36 00	27 59 55	NP	NS	Planned in situ

Piedre Lumbre North	Duval	98 36 45	28 00 10	NP	NS	Planned in situ
Piedre Lumbre West	Duval	98 37 30	27 57 00	NP	NS	Planned in situ
Rosenbrock—Carmody	Karnes	98 05 18	28 50 16	85	NS	17-ha pit; deepest open-pit mine, operating 1978
Ryan	Live Oak	98 14 03	28 36 00	10	10—80	Abandoned; near surface adjacent to Chapman; 8/76 ^{226}Ra 3.3 pCi/liter
Searcy	Karnes	98 06 57	28 54 10	25	12—70	Abandoned; 8/76 ^{226}Ra 2.0 pCi/liter
Sickenius	Karnes	98 06 00	28 53 05	15	6—180	Complex, mined several times; uraniferous lignite in part of pit
Smith	Gonzales	97 33 16	29 09 46	25	NS	6-ha pit, 1979—1981
Smith	Live Oak	98 02 14	28 30 20	30	4—250	Abandoned; 5/76 ^{226}Ra 14.2 pCi/liter
Steinman—Latta—Swanson	Karnes	97 41 30	29 07 50	24	NS	57-ha pit, 1981—1988
Stoeltje	Karnes	98 01 12	28 54 26	40	6—115	Abandoned; three pits; 7/76 ^{226}Ra, north pit, 8.7 pCi/liter; middle pit, 21.6 pCi/liter; south pit, 21.2 pCi/liter
Thomas—Knandel—Dybowski	Karnes—Gonzales	97 37 45	29 07 29	41	NS	40-ha pit, mined 1978
Turner	Karnes	98 06 40	28 52 02	35	20	Part of Butler roll front deposit
Weddington	Karnes	98 07 20	28 51	38	6—280	Part of Butler deposit; 9/76 ^{226}Ra 1.1 pCi/liter
Weddington South	Karnes	98 06 52	28 49 53	35	4—12	Roll front parallel to Butler front; 8/76 ^{226}Ra 2 pCi/liter

TABLE 2 (Continued)

Name	County	Longitude, W	Latitude, N	Pit depth, m	Radiation levels, μR/hr	Comments
Weinrich	Karnes	97 50 09	28 58 05	35	NS	4-ha pit mined 1978
Wiatrek—Haase	Karnes	97 52 41	29 07 14	30	5—35	Abandoned; adjacent to Haase
Wright	Karnes	98 07 12	28 49 16	35	2—10	Connected to McGrady and Pfeil; 6/76 ^{226}Ra 1.5 pCi/liter
Zamzow	Karnes	98 06 11	28 52 45	23	NS	7-ha pit working 1978
Zamzow	Live Oak	98 03 50	28 29 30	NP	NS	In situ near Felder deposit working 1978

Notes: NS = no survey, NP = no pit, U = unknown.

and relatively few data are available. During one 24-hr period in the fall of 1976, one study was done by Ford, Bacon and Davis Utah, Inc. (1977) to measure the impact of the mill tailings pile at the Deweesville abandoned mill. Owing to the complexity of determining the source term (six tailings piles, some covered, mineralized uranium mine overburden, and naturally high concentrations of uranium in the surface rock), interpretation of the data is difficult, but it does indicate relatively high radon levels in the air. A 24-hr average of the radon concentration ranged from 0.8 to 1.9 pCi/liter in outside air, whereas indoor levels ranged from 0.9 to 6.0 pCi/liter. The reason for the relatively high value in one home has not yet been determined. In a separate study we measured air concentrations of radon daughters in the vicinity of the Conquista mill at Deweesville. Maximum values of 1.5 pCi/liter of radon daughters were obtained just before sunrise. Atmospheric mixing later in the day reduced these levels to 0.4 pCi/liter.

Another source of radon in the atmosphere is the aeration of groundwater from uranium operations and water wells. That radon-bearing groundwater used for domestic purposes can lead to radon daughter exposures to household occupants is becoming a recognized exposure pathway. Less widely recognized is the possibility that water wells and uranium in situ mining plants can be important point sources of radon in the atmosphere, just as underground mine ventilation systems are.

The radon concentrations in some South Texas well waters were reported at a Brazil symposium (Gesell and Cook, 1977). We found maximum radon concentrations over 9000 pCi/liter in the municipal water supply in Flatonia, Tex. (Fayette County). This supply produces between 35 and 50 million liters of water per month. Using an average value for radon, the net production of radon is on the order of 0.1 to 0.2 Ci of ^{222}Rn each month. Although no aeration system is included in this supply, much of the radon would be lost to the atmosphere through use in homes, businesses, or the sewage treatment plant.

A sample of water from the production steam at the uranium in situ plant on the Clay West deposit had a ^{222}Rn content of 167,000 pCi/liter. This implies that very high levels of radon in air can be expected above the level of the water in tanks. As of this writing, there has been considerable interest in measuring radon levels in homes when domestic supplies have elevated radon concentrations in the water supply, but little study of radon levels in the air at large industrial users of water or at the treatment plants themselves seems to have been done.

Studies of the occurrence of high levels of ^{226}Ra in well water have also been done (Wukasch and Cook, 1972, 1974; Moore and Cook, 1975; Gesell and Cook, 1977). In every case where radium levels have been found to exceed 10 pCi/liter, uranium mineralization has been known to be present in the rock in the vicinity of the well, either before or after the sample was taken.

As part of documentation to support in situ permit applications, uranium mining operators submit preoperational data on the chemical and radiometric character of the waters associated with the ore deposit to be mined. It is evident from Fig. 3 that both the spacial variation and ranges of radium in the ore zone are extreme. Because of the magnitude of these variations and the spotty occurrences of even small uranium deposits, each well used for drinking in the area should be analyzed to verify that the radium content is sufficiently low to drink.

In the second Natural Radiation Environment symposium, we reported (Wukasch and Cook, 1972) that rainfall runoff from ore stockpiles carried with it high dissolved radioactivity levels. Spalding and Sackett (1972) have also done measurements in water flowing into the Gulf of Mexico. Sediment can also be transported. In the cleanup of the old AEC ore-buying station, the path of rainfall runoff from the 8-ha area can be traced by the high gamma-ray levels from the sediment washed from the ore storage area (Ward, 1974). Similar results can be found at the old Deweesville mill, where radiation levels in the adjacent pasture are as high as 1200 μR/hr. Because uranium often occurs as a salt coating on sand grains in the deposits, it follows that the smallest grains, having a higher surface area/volume ratio, would have a higher than average uranium content. Since these small particles are the ones most easily transported by runoff, the result is a radiation level higher than that which would have existed on the pile of ore itself.

The same principles apply to windborne deposition, so tailings blown from the mills present a somewhat greater hazard than the tailings themselves seem to present. The study by Ford, Bacon and Davis Utah (1977) for the U. S. Department of Energy has indicated windborne tailings from the old Deweesville mill up to $\frac{1}{2}$ km away which will require some cleanup.

Open-pit uranium mines themselves offer unique opportunities for study. In the case of unoxidized deposits, for example, the McLean No. 1 mine, we have seen the ^{226}Ra levels decrease from 63 pCi/liter in April 1971 (Wukasch and Cook, 1972) to 11 pCi/liter in 1976. This decrease is presumably due to precipitation of the radium through aeration and biological activity. In his study of several mines, Itin (1975) found relatively little biological activity.

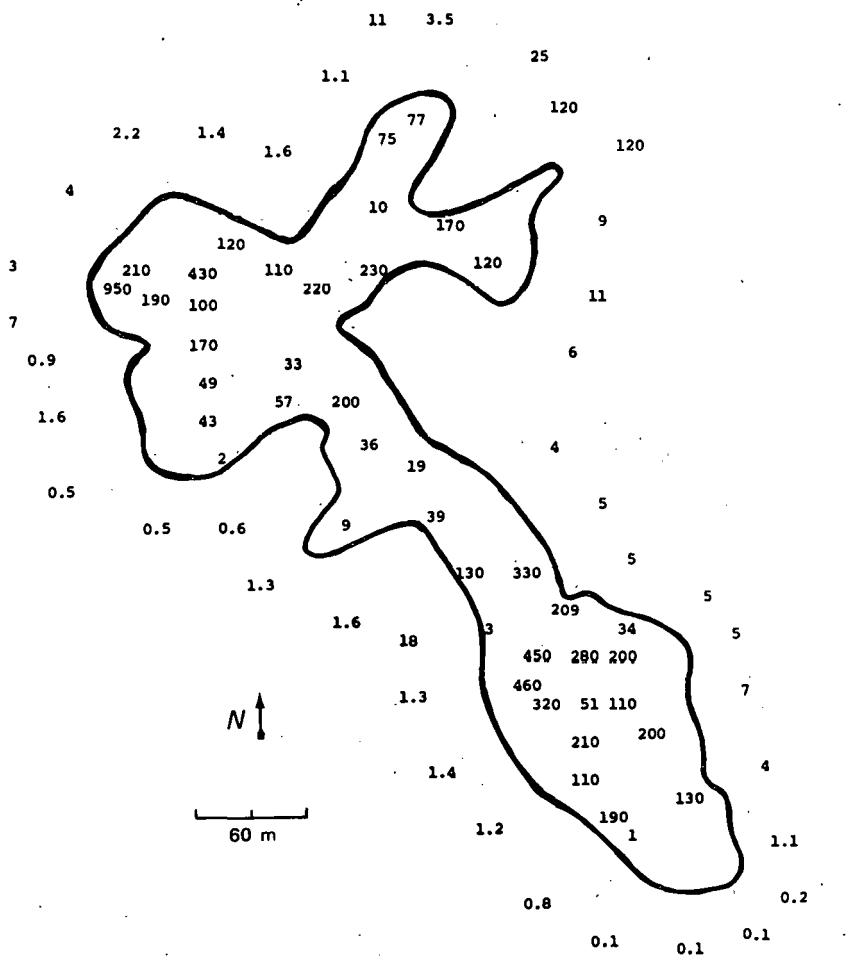


Fig. 3 Radium-226 concentrations (pCi/liter) in water in the Burns Deposit (source: U. S. Steel permit application).

During the preoperational radiation survey for the Panna Maria mill, an anomalous area reading of 30 μR/hr was discovered. We investigated further and found that a disconnected gas—oil—water separator (called a heater treater) had deposits of an iron—sulfide scale which resulted in radiation levels exceeding 3000 μR/hr in contact with the unit. The brine from the oil field there contained 317 pCi/liter of radium and an unknown quantity of radon. It is hypothesized that ^{210}Pb coprecipitated with the iron sulfide as ^{210}Pb sulfide. Approximately 30% of the other heater-treater units in nearby oil fields had elevated levels of radiation, although none so

high as the initial discovery. Eargle and Weeks (1962) reported levels of ^{226}Ra of 106 pCi/liter, and ^{222}Rn of 10,700 pCi/liter had been found in oil field brines in the area by Tanner.

Other oil fields have also been reported to contain elevated radium and radon (Reid, 1977). We have made measurements at natural gas processing plants and have found levels of over 30 μR/hr on the ground. Subsequent analyses of soil samples indicated that the exposure was due predominantly to ^{238}U daughters.

SUMMARY

We continue to find high levels of radiation at uranium operations of in situ and surface mines, at processing plants, at private and municipal water wells, and in oil field brines.

The use of land reclamation coupled with regulatory control of mines to be abandoned results in a reduction of radiation levels and some reduction, as yet unmeasured, of radon emanation. The occurrence of ^{222}Rn levels in groundwaters at oil and water wells and uranium in situ plants causes concern for the area immediately around these sources. A need to determine occupational and general public exposures exists. Since these are situations where extreme disequilibrium between radon and its daughters can exist, great care must be taken in estimating doses.

The practice of piling uranium mill tailings in diked ponds on the surface and covering them with earth is one of questionable wisdom as a long-term disposal technique. The long half-life (78,000 years) of ^{230}Th, the parent of ^{226}Ra, means that the tailings will be potentially hazardous for long periods of time. Although some piles in the South Texas area where the original mines were on or very near the surface mimic the natural conditions, other piles containing tailings generated from deeper deposits result in an additional hazard to that which existed in nature. As a regulatory agency, we are encouraging below ground-level disposal of tailings to minimize these problems.

The uranium industry in Texas has expanded considerably since the second Natural Radiation Environment symposium and will continue to expand in the next several years.

ACKNOWLEDGMENTS

The writer wishes to express his appreciation to Bradley Caskey for his assistance in performing mine surveys; to the late Martin

Wukasch, Director of the Division of Occupational Health and Radiation Control, for his encouragement and support; and to Joi Lucas for her assistance in preparing the manuscript.

REFERENCES

Cook, L. M., B. W. Caskey, and M. C. Wukasch, 1977, The Effects of Uranium Mining on Environmental Gamma Ray Exposures, in *Proceedings IRPA IV International Congress*, Paris, Apr. 24—30, 1977, pp. 1029-1032, International Radiation Protection Association, Fontenay-aux-Roses, France.

Dubois, Deane, 1977, *South Texas Uranium Monthly Letter*, January, D. Dubois, Corpus Christi, Tex.

——, 1978, *South Texas Uranium Monthly Letter*, January, D. Dubois, Corpus Christi, Tex.

Eargle, D. H., and A. D. Weeks, 1962, *Possible Generation of Uranium from High Sulfide-Hydrocarbons*, Professional Paper 424-D, pp. D7-D9, U. S. Geological Survey, Washington.

——, G. W. Hinds, and A. M. D. Weeks, 1971, *Uranium Geology and Mines*, Guidebook No. 12, Bureau of Economic Geology, University of Texas, Austin.

——, and A. M. D. Weeks, 1973, Geologic Relations Among Uranium Deposits, South Texas, Coastal Plain Region, USA, in *Ores in Sediments*, International Union Geology Science, pp. 101-113, G. C. Amstatz and A. J. Bernard (Eds.), Springer-Verlag, Berlin.

——, K. A. Dickson, and B. O. Davis, 1975, South Texas Uranium Deposits, *Am. Assoc. Pet. Geol. Bull.*, 59(5): 766-779.

Ford, Bacon and Davis Utah, 1977, *Phase II—Title I Engineering Assessment of Inactive Uranium Mill Tailings, Falls City Site, Falls City, Texas.*

Gesell, T. F., and L. M. Cook, 1977, Environmental Radioactivity in the South Texas, USA Uranium District, in *International Symposium on Areas of High Natural Radioactivity*, Poços de Caldas, Brazil, June 16—20, 1975, Thomas L. Cullen and Eduardo Penna Franca (Eds.), Report CONF-750671, pp. 167-179, Academia Brasileira de Ciências, NTIS, 1977.

Itin, S. C., 1975, *The Public Health Significance of Abandoned Open Pit Uranium Mines in South Texas* (Masters Thesis), unpublished, University of Texas at Houston, School of Public Health, Houston.

Moore, W. S., and L. M. Cook, 1975, Radium Removal from Drinking Water, *Nature*, 253: 262-263.

Moxham, R. M., and D. H. Eargle, 1961, Airborne Radioactivity and Geologic Map of the Coastal Plain Area, Southeast Texas, Geophysical Investigations Map GP-198, U. S. Geological Survey, Washington.

Reid, D., 1977, U. S. Naval Oceanographic Research Office, Biloxi, Miss., telephone communication.

Spalding, R. F., and W. M. Sackett, 1972, Uranium in Runoff from the Gulf of Mexico Distributive Province: Anomalous Concentrations, *Science*, 175: 629-631.

Updegraff, D. M., 1969, *The Relationship of Microorganisms to Uranium Deposits*, Denver Research Institute—University of Denver, Denver.

Ward, D. L., 1974, *Uranium Ore Stockpile Site Decontamination*, Falls City, Tex., Lucius Pitkin, Inc., Grand Junction.

Wukasch, M. C., and L. M. Cook, 1972, Environmental Surveillance in South Texas, in *The Natural Radiation Environment II*, Vol. 2, Symposium Proceedings, Houston, Tex., Aug. 7—11, 1972, J. A. S. Adams, W. M. Lowder, and T. F. Gesell (Eds.), ERDA Report CONF-720806-P2, pp. 845-862, Rice University and the University of Texas, Houston, NTIS.

——, and L. M. Cook, 1974, High Radioactivity in Drinking Water and Ground Water in South Texas, in *Proceedings of the Third International Congress of the International Radiation Protection Association*, Vol. 1, Washington, D. C., Sept. 9—14, 1973, W. S. Snyder (Ed.), USAEC Report CONF-730907-P1, pp. 272-278, NTIS.

DISCUSSION

Tanner: We have found that numerous oil-field brines contain a substantial part of the mobile radium of the field. Perhaps it also collects in the separators. Much of the South Texas area was surveyed by aeroradiometry. With respect to external radiation, it should provide some baseline information.

Cook: Yes, we have recently discussed this matter with David Reid of the Navy Oceanographic Office. He has found radium over 50 pCi/liter and, I recall, possibly over 500 pCi/liter. We have also found contamination of natural gas equipment cleaning and disposal areas. This is a problem that we may have been overlooking. We have tried to use the aeroradiometry maps, but their coarseness versus the fine detail and extreme variation that we find on the ground present formidable problems. To match the two is very difficult without much, much more data.

Radon and Radon Daughters Due to Natural Uranium Occurrences in a Rural Ontario Community

H. TANIGUCHI and P. VASUDEV
Radiation Protection Bureau, Department of National Health and Welfare, Ottawa, Ontario, Canada

ABSTRACT

The results of a survey of ^{222}Rn and its short-lived radon daughters in 343 homes in the rural community of March Township, near Ottawa, Canada, are reported. Aerial gamma-ray spectrometry carried out over the 90-km^2 area showed the presence of up to 5 ppm uranium.

The arithmetic average value of the radon daughters in the basement of these homes was 0.014 ± 0.026 WL (working level). Thirteen percent of the homes had radon daughter concentrations exceeding an arbitrary reference value of 0.02 WL and the highest was 0.19 WL. The most frequently observed radon gas values for the homes in this category were in the 5 to 10 pCi/liter interval. From these measurements the equilibrium factor between radon and its daughters was shown to be 0.38 ± 0.19.

A number of thorough investigations of elevated radon and radon daughter levels in Canadian homes in communities associated with uranium mining and refining have been carried out in recent years (Aitken et al., 1977; Knight and Makepeace, 1978; Taniguchi, 1977a). The results of the radiation survey of Port Hope, Ontario, showed that the elevated levels of gamma radiation and radon which were found there were attributable to radioactive contamination resulting from industrial activities. Surveys of the uranium mining and milling communities of Bancroft and Elliot Lake, Ontario, and Uranium City, Saskatchewan, however, strongly suggested that uranium present in its natural undisturbed state was contributing to the observed levels in addition to technologically enhanced natural radiation.

In an attempt to evaluate the relative importance of the two sources, it was of interest to carry out measurements of radon and

radon daughters in areas of higher than average natural background which were not associated in any way with uranium mining. March Township (75°57'W, 45°22'N), a rural community of about 90 km^2 conveniently located 15 km west of Ottawa, Canada, had been identified as being suitable for such an investigation.

Using the techniques of airborne gamma-ray spectrometry, the Geological Survey of Canada reported an unexpected uranium anomaly over the Paleozoic rocks in this township (Grasty, Charbonneau, and Steacy, 1973). Ground surveys and subsequent mineralogical studies identified up to 0.05% U_3O_8 as discrete radioactive grains associated with amorphous hydrocarbon materials (Jonasson, Charbonneau, and Ford, 1977). The location of the study area and the concentrations of uranium in parts per million as determined by the aerial survey are shown in Fig. 1. The contour map was adapted from detailed, large-scale maps prepared by Charbonneau et al. (1975).

A detailed survey of radon and radon daughters in all of the homes in March Township was undertaken from September to mid-October 1977. In addition to determining the significance to public health of the radiation levels present, an important purpose was to evaluate the extent to which aerial gamma-ray spectrometry could be used to identify areas in which uranium occurs in concentrations high enough to lead to readily detectable levels of radon in homes. The conduct of future surveys could be greatly simplified if a quantitative correlation could be established. This paper describes the survey and discusses the results obtained.

INSTRUMENTATION AND PROCEDURE

Radon Daughters

The concentrations of short-lived radon daughters were measured by the Kusnetz field method (Kusnetz, 1956) modified by replacing the counting ratemeter with a scaler—timer. In this study the air to be sampled was drawn through a 25-mm-diameter membrane-type filter with a pore size of 0.8 μm. A flow rate of 20 liters/min for 3 min was obtained from a rotary-vane pump operated from the household electricity supply. The flow rate was set with a rotameter-type flowmeter, calibrated against a wet-test meter.

After the collected radon daughters were allowed to decay for a known period of 40 to 90 min after sampling, the alpha disintegration rate was determined by using a zinc sulfide alpha scintillation detector. The detector was calibrated by using a source of ^{241}Am in the same geometry, prepared from an aliquot of a standardized

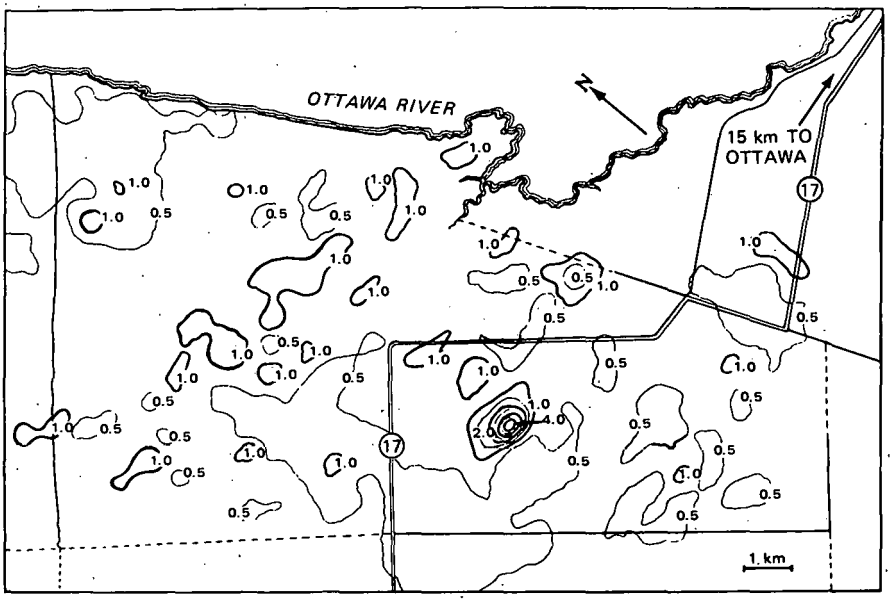


Fig. 1 Contour map of March Township showing uranium occurrences in parts per million. Adapted from Charbonneau et al. (1975).

solution. The radon daughter concentration in working levels (WL's) was calculated from the disintegration rate per liter by using the conversion factors given by Kusnetz.

Radon Gas

Samples of radon gas in air were taken simultaneously with the collection of radon daughters. These were collected directly into radon detectors similar to the Lucas design (Lucas, 1957) in which zinc sulfide is used. To avoid the need of maintaining a vacuum before sampling, the cell design was modified for flow-through operation by providing an inlet port and an outlet port. These ports consisted of quick-connecting couplings that contain a valve in the normally closed position. To fill the cell, a matching connector fitted with a hose nipple was inserted into the inlet port, automatically opening the valve. The filter used to collect radon daughters was attached to this connector. The outlet was connected to the sampling pump with a similar coupling. Thus, while radon daughters were being collected, the radon cell was being continuously flushed with the air being sampled.

The cells were calibrated by filling them with known concentrations of radon and measuring the counting rate of the scintillations after ingrowth of the short-lived daughters. The concentration of radon in the air used to fill the cells was determined by sampling an aliquot with conventional Lucas cells. These cells had been calibrated by de-emanating known amounts of radon from standard solutions of ^{226}Ra obtained from the U. S. National Bureau of Standards. Both the radon daughters and the radon cells were counted on portable detectors having a 2.54-cm photomultiplier tube, a high-voltage supply, a timer, and a scaler in a compact unit. The equipment used has been described more fully elsewhere (Taniguchi, 1977b).

Survey Procedure

The survey was undertaken by systematically calling on every household in the Township, covering an area of about 90 km^2. Locating all of the rural homes was greatly aided by having a large-scale map showing the owner of every property.

On the basis of previous experience (Taniguchi, 1977a) which showed that radon daughter concentrations were generally higher in the basement than on the main floor, sampling was carried out in the basement. The samples were taken to a centrally located mobile laboratory for counting under controlled conditions in preference to counting in the field.

For each house a survey form was completed giving information on physical parameters, such as the type of house, construction material, heating system, ventilation, the presence of basement windows, type of basement floor and walls, the nature of the excavation, and geological environs. Data were obtained concerning occupancy factors, including the extent of use of the basement, the number of years living in the house, and the household size. The householder was also asked if smokers lived in the house.

The main part of the survey was conducted from early September to mid-October 1977. The climate during this period was such that doors and windows were normally closed. Temperatures were not low enough in general to require the operation of furnaces.

RESULTS AND DISCUSSION

The distribution of the radon daughter concentrations measured in 343 homes is shown in Table 1. The WL ranges chosen in Table 1 are arbitrary. Values below 0.01 WL are generally considered to be within the normal background range. A total of 258 homes (75%)

TABLE 1

Distribution of Radon Daughter Levels in March Township

Range of WL	No. of homes	Percent of total
0.000—0.010	258	75
0.011—0.020	40	12
0.021—0.030	17	5
0.031—0.040	7	2
0.041—0.050	3	0.9
0.051—0.100	9	2.6
0.101—0.150	5	1.4
0.151—0.190	4	1.1
Total	343	100.0

were found to be in this category. At the upper level, 4 homes exceeded 0.15 WL, a level that is one-half of the occupational WL in some countries. The arithmetic mean of all the results was 0.014 WL with a standard deviation of 0.026 WL.

In Fig. 2 the number of homes having radon daughter concentrations in a given WL range is plotted as a histogram to show the distribution. Over 90% of the homes showed radon daughter levels below 0.03 WL. The distribution is skewed, however, with WL values extending to a maximum of 0.19 WL.

A test was carried out to determine the fit of the data to a lognormal distribution. In Fig. 3 the radon daughter concentrations have been plotted on a logarithmic scale against the percent cumulative frequency. The relatively good fit of the plotted points to a straight line confirms that the distribution is lognormal.

The sampling procedure followed in this survey allowed the simultaneous collection of radon in air samples and radon daughter samples. To avoid the long counting times required to achieve acceptable statistical errors at low counting rates, however, only those samples collected in homes which had radon daughter levels over 0.02 WL were counted. For the 45 homes in this category, the distribution of the number of homes in selected intervals of radon gas levels is shown in Fig. 4. The levels found most frequently were in the 5 to 10 pCi/liter interval. The maximum observed was 58 pCi/liter.

After the concentrations of radon and radon daughters were measured simultaneously, the apparent equilibrium values for conditions existing at the time of sampling could be calculated. In a survey

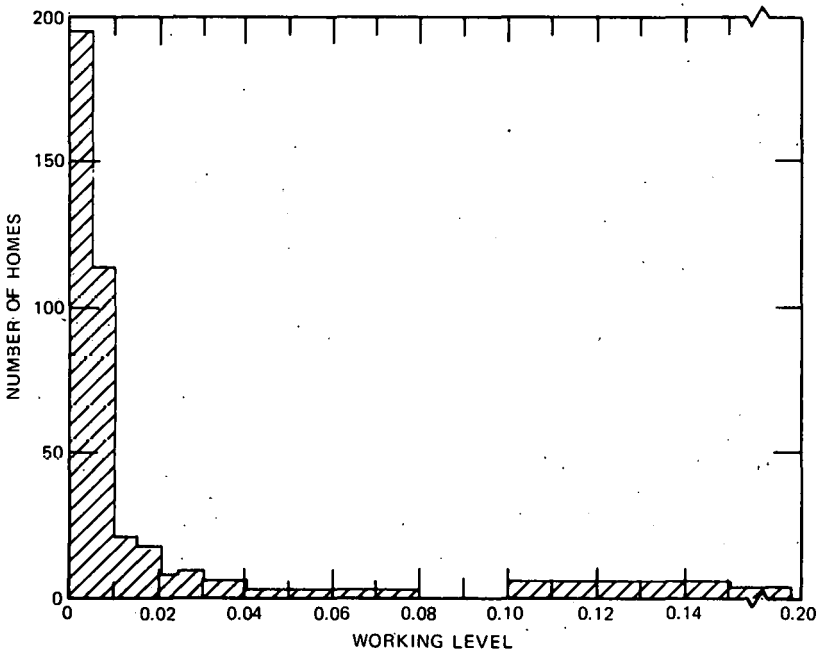


Fig. 2 Distribution of radon daughter levels.

such as the present one which included a variety of types of houses with differing occupancy and use patterns, it is not likely that any two houses would have the same conditions affecting the state of equilibrium. Nevertheless, it is not unreasonable to expect that a majority of the homes would have equilibrium factors within a finite range.

In Fig. 5 the measured WL is plotted against the radon gas concentration to determine this range. A linear regression analysis gave an equilibrium value of 0.38 ± 0.19, with a correlation coefficient of 0.77. For the wide range of parameters encountered, the range is reasonably narrow. Not uncommonly, selected reference values are expressed in WL units, whereas measuring methods give results in terms of radon concentration. The equilibrium ratio determined in this work provides a conversion factor which may be applied to future measurements taken under similar conditions.

When the locations of houses with elevated radon daughter levels were compared with the known uranium occurrences and abundances, no correlation was apparent. Radon daughter levels over 0.02 WL were found in houses built in areas showing only 0.5 ppm on the contour map. In contrast, homes in the vicinity of the highest

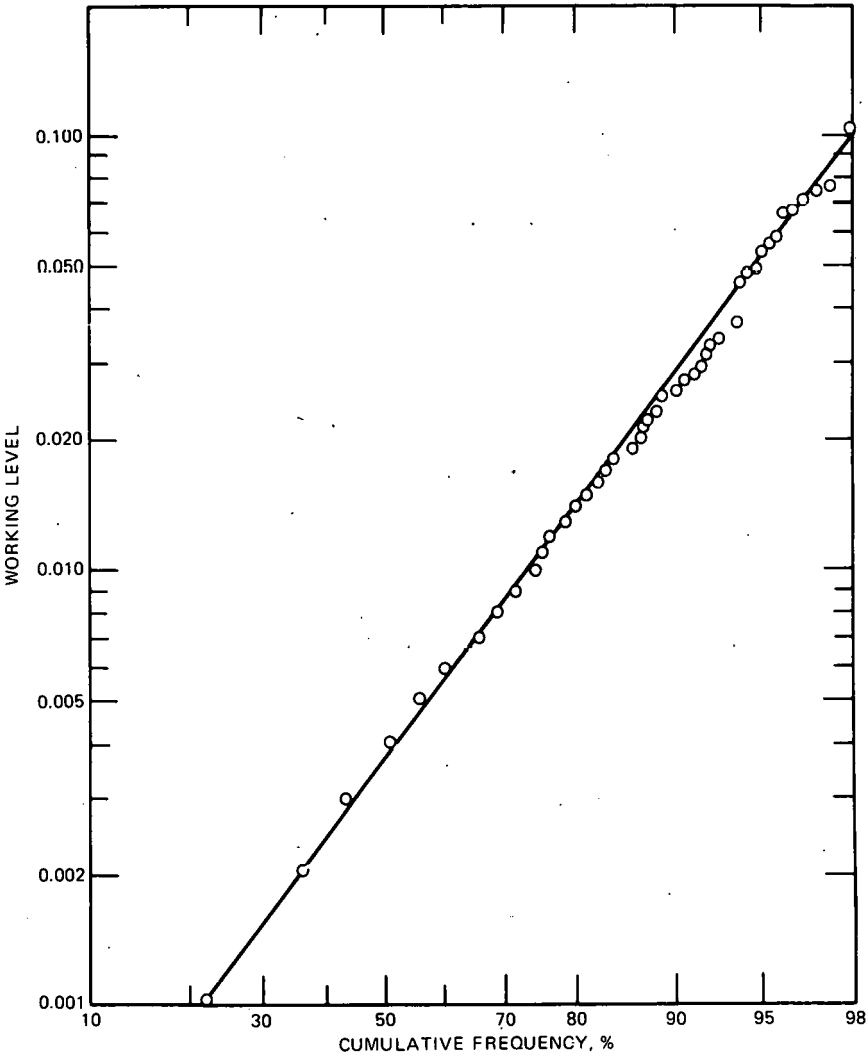


Fig. 3 Lognormal distribution of radon daughter levels.

anomaly of over 4 ppm did not necessarily contain high levels. It is clear that the origin of the radon and the pathway by which it finds its way into selected homes must be elucidated. Because of the rapidity with which large areas may be surveyed by aerial gamma-ray spectrometry, it is important to verify the absence of extraordinary mechanisms of radon transport which may be perturbing any correlation in the area surveyed.

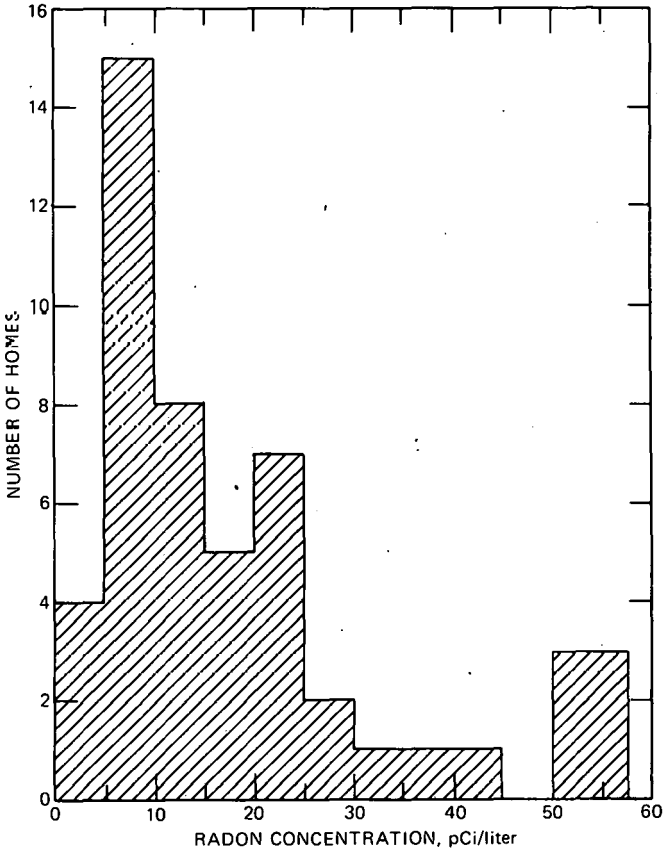


Fig. 4 Distribution of radon gas levels in homes with radon daughter levels over 0.02 WL.

SUMMARY

A survey of radon and radon daughter concentrations was conducted in 343 homes in the rural Ontario community of March Township. The number of homes with radon daughter levels below an arbitrary reference level of 0.02 WL was 298 (87%). The distribution of WL's was lognormal, with 4 of the homes exceeding 0.15 WL. The equilibrium factor for radon daughters relative to radon was found to be 0.38 ± 0.19.

There did not appear to be a useful correlation between radon levels in homes and known U—Ra occurrences in the range 0.5 to 5 ppm.

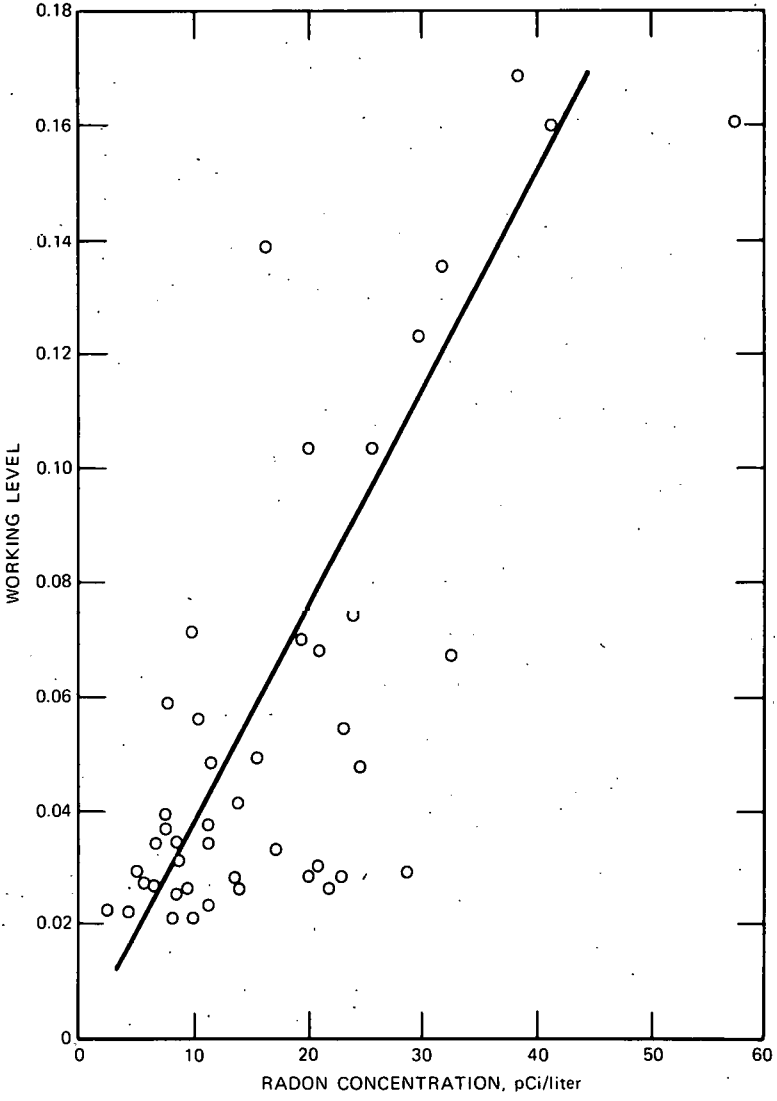


Fig. 5 Observed equilibrium ratios between radon and its daughters.

ACKNOWLEDGMENTS

The assistance and cooperation of the Reeve and officials of the Township of March are gratefully acknowledged. The measurements were carried out by J. Delaney, J. M. Fenning, L. A. Gourgon, W. B. Walker, and W. A. Wilson. Without their diligent work, the survey could not have been completed successfully.

REFERENCES

Aitken, J. H., E. G. Baker, R. M. Chatterjee, R. Kusiak, and J. Tai-Pow, 1977, Radon Concentrations in Contaminated and Uncontaminated Premises in Two Ontario Towns, in *Radon Workshop, February 1977,* ERDA Report HASL-325, pp. 129-131, Health and Safety Laboratory.

Charbonneau, B. W., I. R. Jonasson, P. B. Holman, and K. L. Ford, 1975, *Ground and Airborne Gamma-Ray Spectrometry, Stream Sediment and Soil Geochemistry Investigations of Paleozoic Uranium—Copper Mineralization in the Ottawa-Arnprior Area,* Geological Survey of Canada, Open File No. 264.

Grasty, R. L., B. W. Charbonneau, and H. R. Steacy, 1973, A Uranium Occurrence in Paleozoic Rocks West of Ottawa, in *Report of Activities,* GSC Paper 73-1 (Part A), pp. 286-289, Geological Survey of Canada.

Jonasson, I. R., B. W. Charbonneau, and K. L. Ford, 1977, On the Nature and Formation of Radioactive Hydrocarbons from the Ordovician Rocks of the Ottawa Area, in *Report of Activities,* GSC Paper 77-1 (Part B), pp. 109-111, Geological Survey of Canada.

Knight, G. B., and C. E. Makepeace, 1978, *Modification of the Natural Radionuclide Distribution by Some Human Activities in Canada,* this volume.

Kusnetz, H. L., 1956, Radon Daughters in Mine Atmospheres: A Field Method for Determining Concentrations, *Am. Ind. Hyg. Assoc. J.,* 17: 85-88.

Lucas, H. F., 1957, Improved Low-Level Alpha-Scintillation Counter for Radon, *Rev. Sci. Instrum.,* 28: 680-683.

Taniguchi, H., 1977a, Radon-222 and Its Daughters in Buildings at Uranium City, Saskatchewan, in *Radon Workshop, February 1977,* ERDA Report HASL-325, pp. 141-147, Health and Safety Laboratory.

——, 1977b, Present Practices of the Department of National Health and Welfare for the Area Monitoring of Radon and Daughter Products, in *Personal Dosimetry and Area Monitoring Suitable for Radon and Daughter Products,* Proceedings of the Specialist Meeting, Elliot Lake, Canada, Oct. 4—8, 1976, pp. 251-254, Nuclear Energy Agency, Organization for Economic Co-operation and Development, Paris.

DISCUSSION

Wrenn: Over what time period were the WL measurements taken?

Taniguchi: The measurements were carried out during a period of uniform weather from mid-September to mid-October 1977.

Radium-228 and Radium-226 Levels in a River Environment and Its Modification by Human Activities

A. C. PAUL, V. S. LONDHE, and K. C. PILLAI
Health Physics Division, Bhabha Atomic Research Center, Bombay, India

ABSTRACT

The Periyar River is of prime importance in the economy of Kerala because of the manifold utility of its waters. Consistently high background levels of ^{228}Ra in the river water, which amount to 10% of the maximum permissible concentration in water [$(MPC)_w$] during the peak and lean flow periods suggest geochemical transport from the drainage areas. Industrial discharges enhance radium levels by an order of magnitude in downstream locations. Monazite and rock phosphate processes, predominantly contributing ^{228}Ra and ^{226}Ra, respectively, change the nuclide ratio in the river environment due to differential inputs. Contribution of ^{226}Ra through liquid effluents to the river from either process is of the same order of magnitude, which together account for only 5% of the process output; the remaining 95%, held in the fertilizer sludges of $CaCO_3/CaSO_4$, disposed of on land is a potential source of this activity in the environment. Riverbed sediments carrying the bulk of the radium get displaced to backwaters where partial solubilization takes place because of monsoon flushes. The uptake of radium by fish in industrial and downstream locations in the river was evident. The analysis of paddy indicates higher uptake by soil and hay due to irrigation by river water drawn from downstream and marginal increase of activity in the fertilizer field.

Periyar, the longest river in Kerala, South India, in addition to being exploited for hydroelectric projects, is extensively used for agricultural, industrial, and domestic consumption. The river along with its tributaries provides drainage for about 10,000 km^2 of land area in Kerala. At the tether end of its 300-km stretch before joining the Arabian Sea, the river branches into two streams, one of which flows through the industrial area at Eloor before joining the backwaters. Of the industrial units located on the banks of the river, a monazite processing factory and an adjoining fertilizer complex processing

rock phosphate have been in operation for the last 25 years. The industrial units in the area use the river for discharge of their chemical effluents.

Paul and Pillai (1978) reported on the pollution status of the river. Some preliminary results on the radium levels in the river have been reported earlier (Murthy et al., 1962; Murthy and Nambiar 1964; Paul and Nambiar, 1973). Studies on the impact of monazite processing (Paul and Pillai, 1976), as in the case of other nuclear fuel-cycle operations (Pillai and Ganguly, 1976), have also been made. However, no work on the contribution of environmental activity from fertilizer processing has been reported in India. This paper deals with the investigations made on the background levels of the naturally occurring radionuclides ^{228}Ra and ^{226}Ra in the Periyar River environment and their modified levels in the river as a result of industrial operations, identifies the various inputs, and discusses their implications in respect to radiation exposure.

AREA OF STUDY

The investigation carried out in the river was limited to the stretch extending 28-km upstream from the industrial outfall area and 14-km downstream extending to the backwater (estuarine) area (Fig. 1). The proximity of the backwaters (5 km) introduces salinity in the river, especially during the lean flow period of summer. The effect of tidal influx has been observed in the 20-km stretch of the river from the backwaters. The net river flow is highly influenced by the monsoon in the area, which is of the order of 3000 mm/year, and is estimated to vary between 4×10^7 and 2×10^9 m^3/month (Paul and Pillai, 1976).

The water for domestic consumption in the industrial township at Eloor is drawn from the river stretch upstream; however, river water downstream is used for agriculture, especially for paddy cultivation. The estuarine area that supports paddy and coconut farms is used for fishing. In the river, both upstream and downstream, sand dredging and clay mining operations take place to a limited extent. The sand and clay thus recovered are used as building materials.

RADIUM LEVELS IN THE RIVER ENVIRONMENT

Location, Sampling, and Methods

For the purpose of the present investigations, the 42-km stretch of the river (Fig. 1) has been divided into the following three zones.

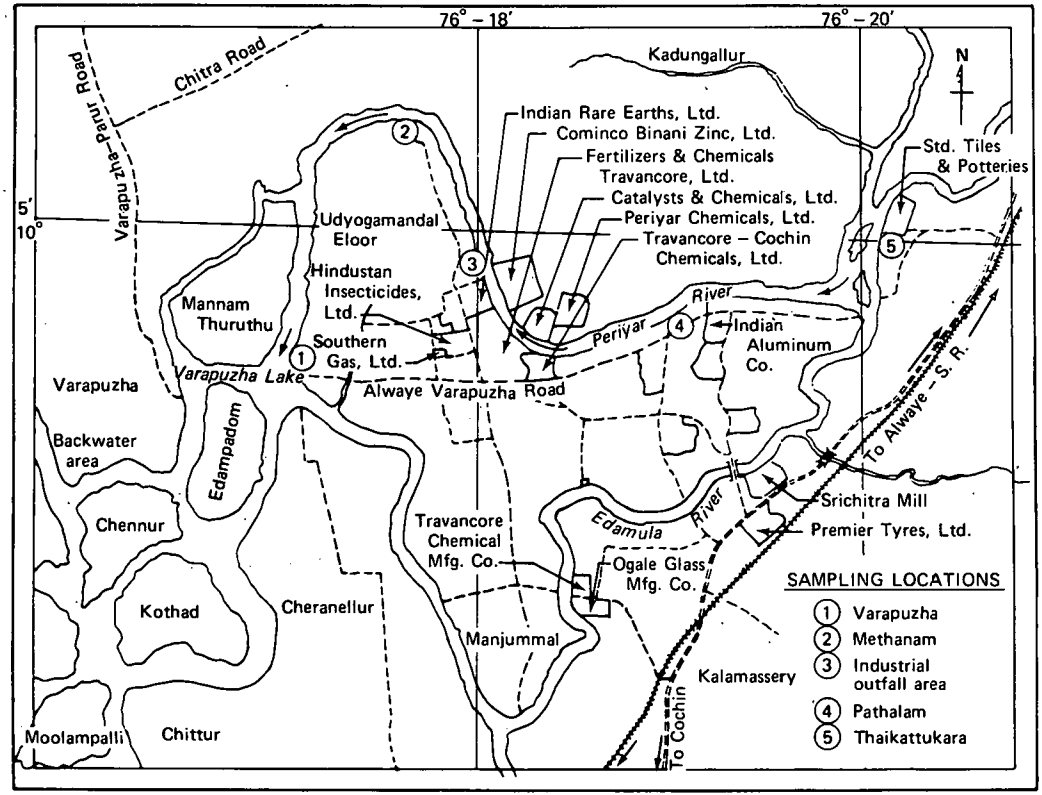


Fig. 1 Section of Periyar River indicating industrial units and sampling locations.

1. The stretch upstream of Alwaye up to Kalady where no contributions of radionuclides to the river is expected from industrial discharges, treated as a background area extending 19 km.

2. The stretch between Alwaye and Varapuzha where the major industries are located, treated as an industrial area extending 14 km.

3. The estuarine area from Varapuzha to Moolampalli, extending 9 km.

The study was initiated in 1974 and continued through 1977. Both river water and sediments were obtained from 15 fixed locations in the river. A motor boat was used for sampling, which was carried out during both pre- and postmonsoon seasons. Surface samples of water were collected in polythene containers. Sediments obtained were grab surface samples. Filtered water samples were assayed for ^{228}Ra and ^{226}Ra by radiochemical separation and counting. Gross beta activity of the sediments was obtained by direct counting of 100 mg of dried sediments in a low background beta counter. The sediments, after destroying the organic matter, were leached with dilute acid, and the leachings were analyzed for ^{228}Ra and ^{226}Ra.

Background Concentrations

The radium levels in water from upstream locations are given in Table 1. Radium-228 varies from < 0.4 to 3.6 pCi/liter in premonsoon seasons and 1.0 to 2.7 pCi/liter in postmonsoon seasons. The levels are nearly the same for both seasons in spite of the heavy discharges into the river from surface runoff. The ^{228}Ra levels confirm an earlier finding regarding the high background levels in the river which amount to 10% of the maximum permissible concentration in drinking water [$(MPC)_w$] applicable for general population.

Radium-226 levels vary from 0.7 to 3.3 pCi/liter in premonsoon and 0.05 to 0.06 pCi/liter in postmonsoon samples, indicating dilution by the excess river flow in monsoon.

The ratio of ^{228}Ra to ^{226}Ra in water varies from 0.1 to 3.0 in the premonsoon samples and 18 to 54 in the postmonsoon samples, indicating higher ^{228}Ra input to the river from monsoon flows mainly contributed by runoff from the drainage areas. This is also evident from the more or less similar levels of ^{228}Ra in both the seasons in spite of the higher river flow during monsoon. The higher background levels of ^{228}Ra observed in the river might be a result of higher background levels in the drainage areas and subsequent geochemical transport. More investigations in the drainage areas on the nuclide ratios will be of interest in this context.

The concentrations of gross beta, ^{228}Ra, and ^{226}Ra in riverbed sediments are given in Table 2. Radium-228 and gross beta average values are lower in the sediments during the postmonsoon period; however, slightly higher levels are observed in the case of ^{226}Ra. The dynamic nature of activity distribution in the sediments is obvious from the varying ratios of the nuclides in different seasons.

Concentrations in the Industrial Area

Radium levels in water in the stretch of river between Alwaye and Varapuzha are given in Table 3. Levels of ^{228}Ra are much higher than background in the premonsoon period. Radium-226 levels do not show significant change. In the postmonsoon period, significantly higher values were observed only for the industrial outfall area and downstream. During monsoon, because of the higher river flow amounting to almost 50 times the lean flow, radium levels in all locations above the outfall area can be considered as background levels in the river. Postmonsoon activity levels in downstream locations as compared to premonsoon are lower by factors of 5 to 30 at different locations owing to the larger volumes of water available for dilution.

Fluctuations in the activity levels in areas close to industrial outfalls are due to sporadic discharges from industrial operations. Large variations in concentrations of ^{228}Ra and ^{226}Ra and their ratios in samples from different locations indicate contribution of these nuclides from different sources. These nuclides being chemically identical are expected to maintain a constant ratio in the samples if they originate from sources having fixed isotopic composition. Ratios around 9 in the industrial outfall areas are indicative of effluent discharges from monazite processing, whereas lower ratios represent conditions when ^{226}Ra discharges from the fertilizer process predominate. These ratios bear no resemblance to the upstream background conditions reported earlier (see Table 1). The situation in the river stretch in the industrial area is further complicated by the varying pH conditions ranging from 3 to 11 which influence the dissolution and precipitation of radium in water. This aspect is discussed later.

Table 4 gives the gross beta, ^{228}Ra, and ^{226}Ra levels in riverbed sediments. The sediment activity levels in areas just above the industrial outfall areas are higher than the background levels observed for premonsoon period (see Table 2). However, the levels are lowered in the postmonsoon seasons. This clearly indicates bottom sediment transport during monsoon. This is also evident from the shift of sediments having high specific activity from

TABLE 1

Radium in River Water from Upstream Locations

Location	Distance from industrial outfall area (upstream), km	Concentration, pCi/liter					
		Premonsoon			Postmonsoon		
		^{228}Ra	^{226}Ra	$\frac{^{228}Ra}{^{226}Ra}$	^{228}Ra	^{226}Ra	$\frac{^{228}Ra}{^{226}Ra}$
Kalady	28.0	2.0 ± 0.2	0.7 ± 0.1	2.9	2.7 ± 0.41	0.05 ± 0.02	54.0
Vazhakulam	16.0	3.2 ± 0.3	3.3 ± 0.3	1.0	1.2 ± 0.16	0.03 ± 0.02	20.0
Chowara	13.0	<0.4	3.1 ± 0.3	<0.1	1.1 ± 0.16	0.03 ± 0.02	18.3
Alwaye	9.0	3.6 ± 0.3	2.7 ± 0.3	1.3	1.0 ± 0.15	0.05 ± 0.02	20.0

TABLE 2

Gross Beta and Radium in River Sediments from Upstream Locations

Location	Concentration, pCi/g							
	Premonsoon				Postmonsoon			
	^{228}Ra	^{226}Ra	$\frac{^{228}Ra}{^{226}Ra}$	Gross beta	^{228}Ra	^{226}Ra	$\frac{^{228}Ra}{^{226}Ra}$	Gross beta
Kalady	2.4 ± 0.3	0.05 ± 0.01	48.0	63.0 ± 5.7	0.5 ± 0.1	0.10 ± 0.02	5.0	32.1 ± 3.3
Vazhakulam	2.0 ± 0.4	0.03 ± 0.01	66.7	62.0 ± 5.5	2.1 ± 0.2	0.16 ± 0.02	13.1	45.5 ± 4.2
Chowara	2.6 ± 0.4	0.05 ± 0.02	52.0		1.2 ± 0.2	0.12 ± 0.02	10.0	40.2 ± 3.4
Alwaye	5.0 ± 0.5	0.06 ± 0.02	83.3	135.0 ± 6.5	1.5 ± 0.3	0.06 ± 0.02	25.0	37.3 ± 3.5

TABLE 3

Radium in River Water from Industrial Area

Location	Distance from industrial outfall area, km	Concentration, pCi/liter					
		Premonsoon			Postmonsoon		
		^{228}Ra	^{226}Ra	$\frac{^{228}Ra}{^{226}Ra}$	^{228}Ra	^{226}Ra	$\frac{^{228}Ra}{^{226}Ra}$
Thaikkattukara (upstream)	3.5				0.9 ± 0.1	0.16 ± 0.03	5.6
Pathalam (upstream)	2.0	8.6 ± 0.7	1.7 ± 0.2	5.1	0.4 ± 0.04	0.06 ± 0.02	6.7
Ferry (upstream)	1.3	12.3 ± 1.2*	1.7 ± 0.2*	7.2	1.1 ± 0.1	0.12 ± 0.02	9.2
Industrial outfall area	0.0	20.5 ± 1.5*	3.9 ± 0.3*	5.3	4.1 ± 0.4	1.20 ± 0.20	3.4
Ferry (downstream)	0.3	15.8 ± 1.5*	1.7 ± 0.2*	9.3	3.4 ± 0.3	0.26 ± 0.03	13.1
Methanam (downstream)	1.8	17.5 ± 1.8	1.9 ± 0.2	9.2	0.9 ± 0.1	0.06 ± 0.01	15.0

*Composite sample (100 samples taken during 5 months).

TABLE 4

Gross Beta and Radium in River Sediments from Industrial Area

Location	Concentration, pCi/g							
	Premonsoon				Postmonsoon			
	^{228}Ra	^{226}Ra	$\frac{^{228}Ra}{^{226}Ra}$	Gross beta	^{228}Ra	^{226}Ra	$\frac{^{228}Ra}{^{226}Ra}$	Gross beta
Thaikkattukara	1.1 ± 0.2	0.03 ± 0.01	36.7	113.0 ± 3.5	3.2 ± 0.40	0.18 ± 0.02	17.8	54.3 ± 5.1
Pathalam	1.6 ± 0.2	0.06 ± 0.02	26.7	126.0 ± 6.3	1.6 ± 0.25	0.16 ± 0.02	10.0	70.8 ± 6.4
Ferry (upstream)	3.2 ± 0.3	1.1 ± 0.10	2.9	153.0 ± 7.8	2.4 ± 0.40	0.10 ± 0.01	24.0	54.3 ± 5.1
Industrial outfall area	320.0 ± 25.0	40.6 ± 3.50	7.9	1603.0 ± 81.0	11.4 ± 0.50	2.20 ± 0.15	5.2	655.5 ± 32.0
Ferry (downstream)	26.4 ± 2.1	3.5 ± 0.30	7.5	340.0 ± 16.5	6.0 ± 0.40	2.80 ± 0.20	2.1	273.1 ± 11.3
Methanam	4.6 ± 0.5	0.4 ± 0.03	11.5	200.0 ± 11.2	6.6 ± 0.60	1.50 ± 0.10	4.4	263.5 ± 10.8

industrial outfall areas to downstream locations. Higher levels of activity in sediment in upstream locations for the premonsoon season reflect the higher levels of activity in upstream waters due to the tidal influx and consequent activity transport.

Concentrations in the Estuarine Area

The river meets the estuarine (backwater) complex at Varapuzha. The area surveyed extends to about 15 km^2 in a network of water bodies embedded with several isolated land masses. Results of the pre- and postmonsoon samples obtained are given in Tables 5 and 6. Levels of ^{228}Ra in water during premonsoon ranged from 0.36 to 1.7 pCi/liter. However, the levels were higher in postmonsoon, which ranged from 3.0 to 4.8 pCi/liter. There was also an increase in ^{226}Ra levels during this period, in contrast to the lowering of its levels in upstream locations (see Tables 1 and 3). The enhanced levels of radium in backwaters in postmonsoon cannot be fully explained on the basis of inputs from the industrial area since only comparable concentrations prevail here, and river flows provide additional dilution. The higher levels in the estuarine waters can be explained on the basis of transport of contaminated riverbed sediments during monsoon, subsequent resuspension of the sediments, and partial solubilization of radium from sediments as a result of large volumes of fresh water available during the season. The cycle is repeated as the salinity increases in the backwaters in summer and radium dissolution from sediments is inhibited, resulting in lower concentrations of radium.

Table 6, which provides the sediment activity, indicates higher levels for the postmonsoon samples. The increases generally ranged from 1 to 7 for gross beta, 1 to 4 for ^{228}Ra, and 1 to 10 for ^{226}Ra. This confirms the earlier observation regarding sediment shift from the river into the downstream locations during monsoon. Activity ratios in water and sediments bear similarity with each other in respective seasons, indicating an exchange situation.

INDUSTRIAL OPERATIONS

The sources of radioactivity discharges into the river were examined.

Monazite Processing

Monazite obtained from beach sands of Kerala are processed by Indian Rare Earths, Ltd., to yield thorium concentrates, rare-earth

TABLE 5

Radium in Estuarine Waters

Location	Distance from industrial outfall area (downstream), km	Concentration, pCi/liter					
		Premonsoon			Postmonsoon		
		^{228}Ra	^{226}Ra	$\frac{^{228}Ra}{^{226}Ra}$	^{228}Ra	^{226}Ra	$\frac{^{228}Ra}{^{226}Ra}$
Varapuzha	5	0.36 ± 0.03	0.29 ± 0.03	1.2	4.6 ± 0.4	0.43 ± 0.04	10.7
Chettibagam	6	0.40 ± 0.03	0.26 ± 0.03	1.5	3.6 ± 0.3	0.37 ± 0.03	9.7
Korampadam	9	0.42 ± 0.04	0.14 ± 0.02	3.0	3.0 ± 0.3	0.78 ± 0.06	3.9
Cheranalloor (Chenur)	11	0.37 ± 0.03	0.23 ± 0.02	1.6	4.8 ± 0.4	0.50 ± 0.05	9.6
Moolampalli	14	1.70 ± 0.20	0.23 ± 0.02	7.4	4.6 ± 0.4	0.37 ± 0.03	12.4

TABLE 6

Gross Beta and Radium in Estuarine Sediments

Location	Concentration, pCi/g							
	Premonsoon				Postmonsoon			
	^{228}Ra	^{226}Ra	$\frac{^{228}Ra}{^{226}Ra}$	Gross beta	^{228}Ra	^{226}Ra	$\frac{^{228}Ra}{^{226}Ra}$	Gross beta
Varapuzha	2.0 ± 0.2	0.6 ± 0.03	3.3	20.0 ± 2.5	9.3 ± 0.8	0.8 ± 0.03	11.6	136.0 ± 12.5
Chettibagam	2.1 ± 0.1			63.0 ± 5.5	2.0 ± 0.2	0.4 ± 0.03	5.0	64.0 ± 5.6
Korampadam	1.5 ± 0.2	0.1 ± 0.02	15.0	32.0 ± 3.0	3.5 ± 0.3	1.0 ± 0.10	3.5	100.0 ± 9.1
Cheranalloor (Chenur)	1.1 ± 0.3	0.3 ± 0.02	3.7	39.0 ± 3.5	1.2 ± 0.2	0.2 ± 0.02	6.0	40.0 ± 3.5
Moolampalli	0.9 ± 0.3	0.3 ± 0.02	3.0	14.0 ± 1.2	3.1 ± 0.3	0.6 ± 0.05	5.2	42.0 ± 4.0

salts, and trisodium phosphate. The liquid effluents generated in the plant contain ^{228}Ra and ^{226}Ra activity in the ratio of 9 : 1 and are led into the river after preliminary treatment. Radioactive solid wastes obtained in the process are properly contained.

Rock Phosphate Processing

The fertilizer complex (Fertilizers and Chemicals Travancore, Ltd.) processes rock phosphate obtained mainly from Middle East countries and the rest from indigenous sources mostly mined from Rajasthan. Super phosphate, ammonium phosphate, and ammonium sulfate are the main marketable fertilizers produced here; phosphoric acid is produced as an intermediate product. At the time of this study, rock phosphate from Morocco was being used in the process.

The study of the inventory of radioactivity in rock phosphate processing covered 1 month of the operation during May and June 1977. Raw material, products, and effluents, both solid and liquid, were collected weekly, composited after completing four batches of sampling, and analyzed for radionuclides.

Systemic analysis of the raw material and products of the fertilizer process indicated that gross beta, ^{226}Ra, uranium, and thorium activities of the rock phosphate appear in such products as super phosphate and ammonium phosphate (Table 7). Pfister, Phillipp, and Pauly (1976) and Mills, Guimond, and Windham (1977) reported on the equilibrium status of uranium and ^{226}Ra in rock and super phosphates. A situation analogous to this is expected in the case of thorium and its daughter ^{228}Ra. The use of process water drawn by the fertilizer unit from the river, which is laden with such nuclides as thorium and ^{228}Ra from the monazite process, distorts

TABLE 7

Activity in Rock Phosphate and Fertilizer Products

Material	Activity, pCi/g			
	Gross beta	^{226}Ra	U	Th
Rock phosphate	169.4 ± 5.6	30.0 ± 2.0		5.8 ± 0.9
Super phosphate	84.9 ± 6.0	15.9 ± 0.6	12.2 ± 1.1	2.6 ± 0.6
Phosphoric acid (intermediate)	38.0 ± 5.5		5.3 ± 0.5	0.4 ± 0.1
Ammonium phosphate	40.1 ± 4.5	1.1 ± 0.1	5.8 ± 0.8	2.7 ± 0.4
Ammonium sulfate	5.5 ± 1.4	0.11 ± 0.03	0.05 ± 0.02	3.2 ± 0.9

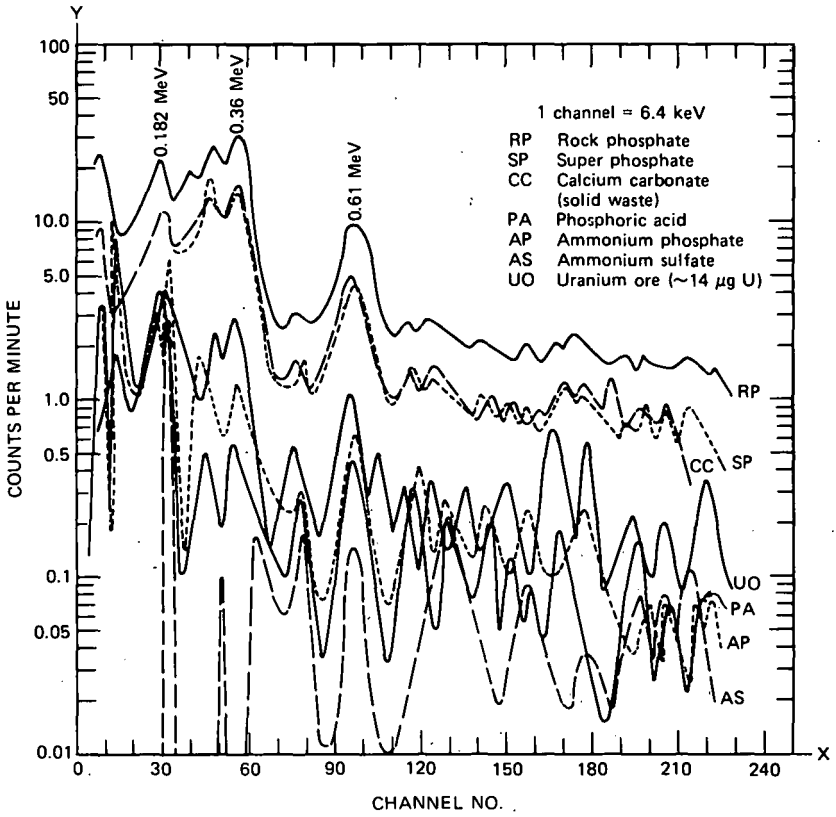


Fig. 2 Gamma spectrums of rock phosphate fertilizer products and solid waste.

the inventory picture of these nuclides in the fertilizer products. Figure 2 gives the gamma spectrums of rock phosphate and fertilizer products, including the calcium carbonate waste sludge. A spectrum of the Jaduguda uranium ore is superimposed on the figure to demonstrate the similarity of the uranium-based activities in the rock phosphate, products, and process waste.

Rock phosphate processing gives rise to significant levels of ^{226}Ra in the waste effluents. Higher levels of activity appear in the solid sludges of $CaCO_3$ and $CaSO_4$, which explains the reason for the higher fraction of activity carried by the suspended solids of liquid effluents laden with these materials (Table 8). Liquid effluent originating from the phosphoric acid plant is found to contain the maximum activity of 100 pCi/liter, 97% of which is accounted by the suspended solids even though the effluent pH was as low as 2.6.

TABLE 8

^{226}Ra in the Effluents of the Rock Phosphate Process

	^{226}Ra, pCi/liter	
	Dissolved	Suspended
Liquid effluents		
Super phosphate plant	1.2 ± 0.1	5.8 ± 0.5
Ammonium phosphate plant	2.6 ± 0.2	4.5 ± 0.4
Ammonium sulfate plant	1.9 ± 0.2	81.1 ± 7.5
Phosphoric acid plant	2.9 ± 0.3	97.1 ± 8.5
Solid effluents		
Calcium carbonate	29.5 ± 2.5 pCi/g*	Total
Calcium sulfate	15.0 ± 1.5 pCi/g*	Total

*Uranium = 3.0 ± 0.6 pCi/g; thorium = 2.5 ± 0.4 pCi/g.

Calcium sulfate generated from phosphoric acid production is partly used for making ammonium sulfate by the Mersberg process:

$$CaSO_4 + (NH_4)_2CO_3 \rightarrow (NH_4)_2SO_4 + CaCO_3$$

Radium present in the calcium sulfate is retained in $CaCO_3$ because $RaCO_3$ is insoluble.

The ^{226}Ra inventory in the rock phosphate process was estimated from the rated production data and is given in Table 9, which indicates that approximately 70% of the input of ^{226}Ra goes to the waste sludge fraction, the bulk of which is present in the $CaCO_3$. Liquid effluents account for only 1.4% of the total ^{226}Ra activity; the rest of the activity is distributed in products mainly in super phosphate and to a lesser extent in ammonium phosphate.

Contribution of Activity from Industrial Processes

Disposal of liquid waste from the monazite and rock phosphate processes contributes to activity in the river (Table 10). Although ^{228}Ra discharges from the monazite industry dominate activity-wise, ^{226}Ra discharges, even though lower by an order of magnitude, assume equal significance in terms of radiological hazard. The input of ^{226}Ra to a similar extent from the fertilizer process adds to its significance. Solid waste disposal on land by the fertilizer industry has a high potential of radium release into the environment through leaching since the solid waste holds 95% of the total ^{226}Ra inventory of the wastes.

TABLE 9

Estimated ^{226}Ra Inventory of the Rock Phosphate Process

Material	Total activity, mCi/day
Raw material	
Rock phosphate	18.0 ± 1.20
Products	
Super phosphate	2.40 ± 0.10
Ammonium phosphate	0.61 ± 0.06
Ammonium sulfate	0.06 ± 0.02
Effluents	
Calcium carbonate (solid)	11.04 ± 1.90
Calcium sulfate (solid)	1.50 ± 0.16
Liquid	0.25 ± 0.03

TABLE 10

Input of Radium to the River Environment from Waste Disposal of Industrial Operations

Operation	Total activity, mCi/day	
	^{226}Ra	^{228}Ra
Monazite process		
Liquid	0.36 ± 0.03	3.1 ± 0.2
Rock phosphate process		
Liquid	0.25 ± 0.03	
Solid	12.54 ± 1.30	

Table 11 indicates the leaching characteristics of $CaCO_3$ sludge. The values represented are averages of five experiments carried out in a solution-to-sludge ratio of 100 : 1 by a single agitation and settling of the fresh sludge. Distilled water leaches out 52.7 pCi/liter of ^{226}Ra from the cake at a pH of 5.5. Experiments carried out with rainwater and river water also indicated significant leaching of ^{226}Ra. Low pH greatly enhanced the radium release in all cases; however, the river water had a higher salinity and inhibited the release. The situation prevailing in the estuarine area regarding radium dissolution from sediments in the fresh water mediums during monsoon support the observation (see Table 5).

The bulk of the $CaCO_3/CaSO_4$ sludge produced over the years is disposed of in a low lying area where monsoon rains and low pH

TABLE 11

Leaching of ^{226}Ra from the $CaCO_3$ Sludge of Rock Phosphate Process

Leaching agent	Initial pH of leaching agent	Final pH of solution	^{226}Ra in leachate, pCi/liter
Distilled water	6.5	8.0	22.0 ± 2.1
Distilled water	6.5	5.5*	52.7 ± 4.5
Rainwater	6.1	8.0	15.5 ± 1.5
Rainwater	4.1	8.0	17.7 ± 1.7
Rainwater	4.1	5.3*	30.1 ± 3.0
River water	3.5	7.8	0.7 ± 0.07
River water	3.5	5.2*	11.5 ± 1.5

*The pH was adjusted with dilute H_2SO_4.

plant effluents leach out substantial quantities of ^{226}Ra into the environment. Part of the leachates directly enter the estuarine area by a canal, and the remainder seeps into the neighboring fields.

Fractionation of Radium in River Water

The influence of pH on radium fractionation in the river water at the outfall area was studied. Wide variations of pH in the range 3 to 11 are observed here, and the radium present in the water is distributed into soluble and insoluble fractions according to prevailing pH conditions, as shown in Fig. 3. At pH 6 the distribution of radium is equal in either fraction above which it goes gradually into the suspended fraction and below which it is predominantly in the solubles. Since most of the sedimentation of discharged radionuclides take place at the outfall area (Paul and Nambiar, 1973), acidic effluent released from the plants greatly enhances radium levels in water.

RADIUM TRANSFER FROM RIVER WATER AND FERTILIZER APPLICATION

Uptake by Fish

The most common of fishes found in the river, mainly from the industrial area, were sampled and analyzed for ^{228}Ra and ^{226}Ra in the flesh and bone. A sample collected from upstream served to compare the results obtained, as given in Table 12. Radium-228

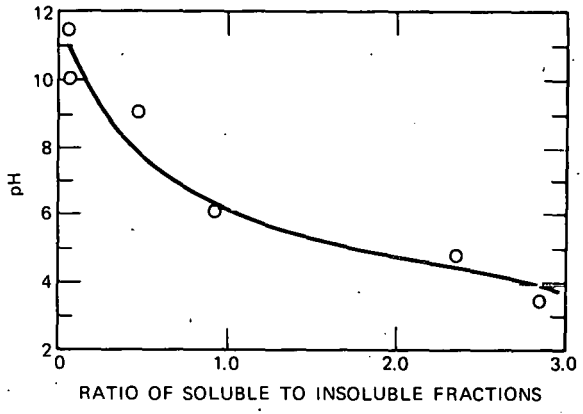


Fig. 3 pH vs. solubility of radium in river water at the outfall area.

TABLE 12

Radium Levels in Fish

Species	Location	Sample	Concentration, pCi/kg	
			^{228}Ra	^{226}Ra
Clupea Longicents	Industrial area and downstream	Flesh	<10	10.0 ± 2.0
		Bone	1940.0 ± 388.0	24.0 ± 4.0
Etroplus	Industrial area and downstream	Flesh	590.0 ± 31.0	6.5 ± 1.1
		Bone	757.0 ± 126.0	115.3 ± 14.4
Etroplus	Industrial area and downstream	Flesh	46.3 ± 12.0	4.1 ± 0.8
		Bone	1420.0 ± 92.0	231.0 ± 22.5
Chana (Ophicephalus Gachua)	Upstream (Vazhakulam)	Flesh	12.3 ± 3.5	<2
		Bone	<10	19.0 ± 6.2

concentration was found to vary significantly in flesh from < 10 to 590 pCi/kg. The upstream fish indicated an activity of 12.3 pCi/kg of ^{228}Ra in flesh, which compared with the lowest figure obtained since the detectable limit in this case was 10 pCi/kg. Radium-226 levels in flesh showed less variation between samples; the concentrations ranged from 4.1 to 10.0 pCi/kg, whereas this could not be detected in the upstream specimen, the limit being 2 pCi/kg.

Radium-228 levels in bone varied from 757 to 1940 pCi/kg compared to < 10 pCi/kg for the upstream fish. Radium-226 levels varied from 24 to 231 pCi/kg in bone, and the upstream sample

showed an activity of 19.0 pCi/kg, which was comparable with the lowest result obtained.

The foregoing data suggest higher levels of uptake of radium by fish in the industrial area of the river, where the ambient levels are higher by an order of magnitude due to the effluent release from plants. The species analyzed are premonsoon samples confined mostly to the particular stretches in the river from where they are caught since the river has rather well-defined zones of varying salinity levels during this season. Apart from indicating the influence of higher radium levels in water to the aquatic life, the limited number of analyses carried out are inadequate to assess nuclide ratios, species effect, concentration factors, seasonal variations, and the extent of population exposure by this mode of intake. More work is in progress on these lines.

Uptake in Paddy

River Water Irrigation

The river water drawn from downstream locations is used to irrigate the paddy field in the Eloor—Methanam stretch. Only a single crop is raised here in the postmonsoon period since the area comes under brackish waters thereafter. Rice, hay, and soil collected from this paddy field indicated significant levels of ^{228}Ra (Table 13). The field soil showed an activity of 5811 pCi/kg, compared to 8720

TABLE 13

Radium Levels in Paddy

Location	Sample	Activity, pCi/kg	
		^{228}Ra	^{226}Ra
Field irrigated by water drawn from downstream	Rice	280.0 ± 25.0	27.0 ± 9.0
	Hay	8720.0 ± 750.0	77.1 ± 13.0
	Field soil	5811.0 ± 450.0	310.0 ± 23.7
Field subject to experimental application of phosphatic fertilizers (mainly ammonium phosphate) and irrigated by water drawn from upstream	Rice	240.0 ± 24.0	4.8 ± 1.5
	Hay	1350.0 ± 160.0	36.6 ± 9.0
	Field soil	1300.0 ± 200.0	360.0 ± 30.0
Field having no history of phosphatic chemical fertilizer application (control)	Rice	787.0 ± 98.4	
	Hay	1290.0 ± 180.0	54.5 ± 10.9
	Field soil	1110.0 ± 150.0	130.0 ± 20.0

pCi/kg of the harvested hay, suggesting high intake. Assuming that the water requirement per hectare is in the range of 200 m^3/day and the water is supplied at this rate for 180 days in a year and the whole ^{228}Ra fraction is retained in the soil in the upper 10 cm layer, then after 10 years of irrigation the field soil will show an activity of 6600 pCi/kg, if the feed water has an activity of 30 pCi/liter, which is nearly 1 $(MPC)_w$. The observed value of 5800 pCi/kg is more or less in agreement with the calculated value irrespective of decay and leaching of ^{228}Ra from soil, suggesting higher activity transfer from feed water (see Table 3). This may be due to suspended solids that contribute to higher radium inputs. The ^{228}Ra level in rice was only 280 pCi/kg, indicating a low transfer ratio. The ^{226}Ra level in the field soil was 310 pCi/kg; however, it showed only 77.1 pCi/kg in hay and 27.0 pCi/kg in rice, indicating low transfer ratios.

Fertilizer Application

Rice, hay, and soil from an experimental paddy field subjected to ammonium phosphate fertilizer application have indicated nuclide distributions similar to those obtained earlier (see the preceding heading) even though the ^{228}Ra levels were much lower (Table 13). Water to irrigate this paddy is drawn from an upstream location, which explains the lower levels; however, ^{226}Ra levels were of the same order of magnitude as the earlier samples. Probably the lower levels in the irrigation water are offset by the addition of fertilizer containing a higher level of ^{226}Ra.

Samples from a field far removed from the locality having no recent history of phosphatic chemical fertilizer application indicated levels of ^{228}Ra in the field soil and hay comparable to the fertilized field.

The hay-to-soil activity ratios in all three samples varied from 1.0 to 1.5. However, a higher intake of ^{228}Ra to the rice in the control field, possibly due to radium being present in more available form, was observed. Available calcium levels may also influence radium uptake. A similar possibility may explain the higher ^{226}Ra transfer ratio to hay of 0.42 in the control field, which is higher than 0.1 obtained for the fertilized field and 0.25 for the river water irrigated field. All three samples suggest comparatively higher uptake of ^{228}Ra than ^{226}Ra by paddy.

The chemical form of the nutrient and the soil conditions determine the uptake by plants. This may also vary from species to species. The transfer ratios of radium from soil to the plant body need detailed investigations.

^{226}Ra Contribution from Super Phosphate

The application of super phosphate is likely to increase the soil ^{226}Ra levels significantly. Addition at the rate of 2.5 tons year^{-1} ha^{-1} may increase the activity by 20 pCi/kg of soil every year if the radium is retained in the upper 10-cm layer. Radium-226 present in the super phosphate is found to be leachable (Table 14).

TABLE 14

Leaching of ^{226}Ra from Super Phosphate

Leaching agent	Initial pH of leaching agent	Final pH of solution	^{226}Ra in leachate, pCi/liter
Distilled water	6.5	2.7	32.5 ± 2.5
Rainwater	4.1	2.5	30.0 ± 3.0
River water	3.5	2.5	23.2 ± 2.3

The leaching tests were carried out in a solution to sludge ratio of 10 : 1. Rainwater leachates were found to carry 30 pCi/liter of ^{226}Ra. Similar results were also obtained using distilled water and river water. All leachates indicated low pH, a condition that might result in increased mobility of radium through soil. Actual field measurements where super phosphates are applied must be carried out to assess the possible enhancement of radium levels in soils and uptake by this mode of application.

SUMMARY AND CONCLUSIONS

The background levels of ^{220}Ra in the Periyar River during the period of study varied from 0.4 to 3.6 pCi/liter, and the background levels of ^{226}Ra varied from 0.05 to 3.3 pCi/liter. Monsoon contributes to large outflows from the river, and the flow in the peak period is 50 times that in lean seasons. The higher background levels of ^{228}Ra amounting to 10% of $(MPC)_w$ values seen during monsoon are possibly due to the geochemical transport from the large drainage areas of the river. The river waters flowing through the industrial area have shown activity levels due to industrial discharges. Tidal influx from backwaters causes transport of this activity to upstream locations. Riverbed sediments get displaced during monsoon and result in the accumulation and release of radium in backwaters during monsoon. The backwaters serve as an intermediate sink for discharged activity, which is ultimately carried into the Arabian Sea.

The variation of ^{228}Ra and ^{226}Ra ratios in the river demonstrates the different sources of inputs. Although the monazite processing causes inputs of ^{228}Ra and ^{226}Ra in the ratio of 9 : 1, the input from rock phosphates processing is mainly ^{226}Ra. Direct discharge of liquid effluents contributes only a small fraction of the activity from this source. Estimates made of ^{226}Ra discharges into the river by liquid effluents show that the quantities involved from the above sources are of the same order. However, leaching of ^{226}Ra by rainwater from calcium carbonate/sulfate sludges disposed on land and possible direct disposal of these sludges into river water having wide pH fluctuations result in further ^{226}Ra inputs into the river. The fractionation of radionuclides from rock phosphates to different products was influenced by the radionuclides present in process water drawn from the river.

Few fish specimens obtained from the river near industrial units have shown ^{228}Ra and ^{226}Ra in flesh and bones above the levels found in specimens from upstream locations. Further studies on the species effect, age, seasonal variations, fish catch in the area, etc., are required to assess the possible radiation exposure through this pathway.

River water from downstream locations used to irrigate paddy fields has resulted in significant uptake in hay and in field soils, although the uptake by rice was not significant. The application of ammonium phosphate in paddy fields did not indicate any enhanced uptake by paddy, although there was marginal increase in the soil activity. Laboratory studies have indicated that ^{226}Ra in super phosphate is leachable.

Further studies will be directed toward extensive investigations on transfer ratios of radium to different agricultural products from irrigation water and from other fertilizer products. In addition, the radiation exposure arising from human consumption will be evaluated, and the enhanced external radiation exposure that might result from the accumulation of radionuclides from the use of fertilizers and irrigation water on agricultural lands will be assessed.

ACKNOWLEDGMENTS

The authors are grateful to Dr. A. K. Ganguly, Director, Chemical Group, Bhabha Atomic Research Center, for encouragement to pursue the work. Thanks are due Shri S. D. Soman, Head, Health Physics Division, for keen interest in the problem. We are indebted to Shri B. P. Nair, Manager, Rare Earths Division, Indian Rare Earths, Ltd., for making available all local facilities to carry out this work.

Dr. P. K. Narayanaswamy, Chairman and Managing Director, Fertilizers and Chemicals Travancore, Ltd., and Udyogamandal and his staff extended necessary help for investigation in the fertilizer plant, which is gratefully acknowledged.

REFERENCES

Murthy, S. V., K. S. Somayaji, K. C. Pillai, and M. M. Malhotra, 1962, *Health Physics Survey of Alwaye Plant of Indian Rare Earths, Ltd.*, Special Survey Report No. 66, Atomic Energy Establishment, Trombay.

—, and P. P. V. J. Nambiar, 1964, Operational Experience in the Health Physics Management of Thorium Industry in India, in *Radiological Health and Safety in Mining and Milling of Nuclear Materials*, Symposium Proceedings, Vienna, 1963, Vol. 1, p. 169, STI/PUB/78, International Atomic Energy Agency, Vienna.

Mills, W. A., R. J. Guimond, and S. T. Windham, 1977, Radiation Exposures in the Florida Phosphate Industry, Fourth International Congress of the International Radiation Protection Association, Paris, Apr. 24—30, available from Gilbert Bresson, Centre de Études Nucleaires de Fontenay-aux-Roses, BP. No. 33, F-92260, Fontenay-aux-Roses, France.

Paul, A. C., and P. P. V. J. Nambiar, 1973, *Health Physics Experience in the Alwaye Plant of Indian Rare Earths, Ltd.* (1963—1972), Indian Report BARC/I-281, Bhabha Atomic Research Center, Trombay.

——, and K. C. Pillai, 1976, *Studies on Pollution Aspects of Periyar River*, Indian Report BARC/I-419, Bhabha Atomic Research Center, Trombay.

——, and K. C. Pillai, 1978, Pollution Profile of a River, *Water, Air and Soil Pollut.*, 10: 133-146.

Pfister, H., G. Phillipp, and H. Pauly, 1976, Population Dose from Natural Radionuclides in Phosphate Fertilizers, *Radiat. Environ. Biophys.*, 13: 247-261.

Pillai, K. C., and A. K. Ganguly, 1976, Methodology for Assessment of Radioactive and Nonradioactive Discharges into Aquatic Environment—Indian Experience, *Technical Meeting on the Methodology for Assessment of Radioactive, Nonradioactive, and Thermal Discharges and Disposals on a Regional and Global Basis*, Cadarache, France, Sept. 7—10. Reprints are available from Bhabha Atomic Research Center, Trombay, Bombay, India.

Distribution of Radium and Chemical Toxins in the Environment of a Uranium Complex

P. M. MARKOSE, K. P. EAPPEN, S. VENKATARAMAN, and P. R. KAMATH
Bhabha Atomic Research Center, Health Physics Division, Jaduguda, India

ABSTRACT

The chemical and radiological impact of uranium mining and milling on the local aquatic environment has been investigated at the Uranium Complex in Bihar, India. Concentrations of radium and manganese, as well as other elements and compounds of concern, were measured at various stages along the effluent course. The uptake of these elements in aquatic life, the deposition in silts, and the dispersal into groundwaters in the vicinity are discussed. Although concentrations measured in the public domain have in general been considered acceptable, continued surveillance is indicated due to the possibility of changed conditions at the tailings pond and other important points in the complex. Methods for the removal of radium and manganese from the effluent stream are discussed.

The discharge of waste effluents from the mining and milling of uranium ore introduces radioactive pollutants and chemical toxins into the aquatic environment. The radioactive element of primary concern is radium and the nonradioactive pollutants are manganese, chlorides, sulfates, and water hardness. In the Uranium Complex at Bihar, India, the low grade ore is mined and processed for recovery of uranium. The waste slurries from the process are neutralized and discharged into the tailings pond where the solids settle and the effluents flow out into a natural stream, Juria nala (Fig. 1). The tailings pond effluent mixes with mine water and floor washings from the mill and flows into the Subarnarekha River. This study was conducted to assess the total pollution from the liquid discharges in the environment and the impact of discharges on water quality. The

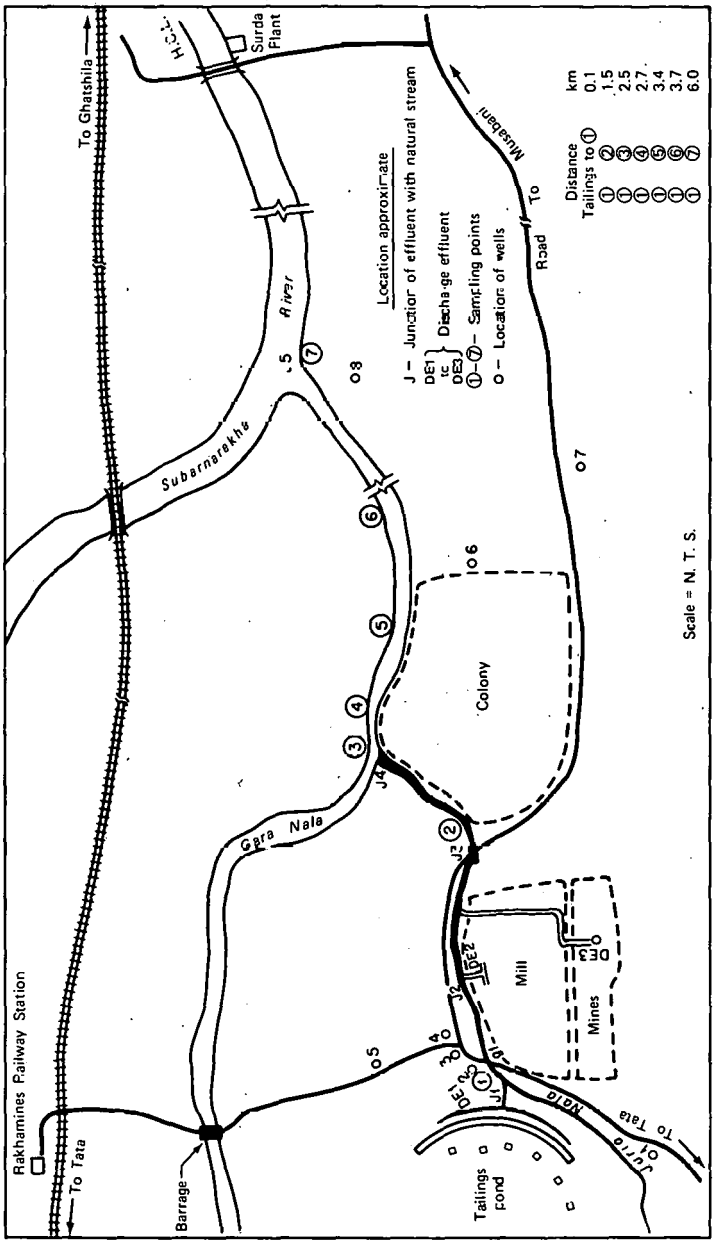


Fig. 1 Aquatic environment at the Uranium Complex site.

study of the movement of pollutants in the biosphere and laboratory investigations on containment are presented.

DESCRIPTION OF PROCESS AND SITE

The mill adopts the sulfuric acid leach process (Merritt, 1971) for uranium extraction. The waste slurry consists of the spent ore powder mixed with effluents from the ion-exchange units. The waste slurry is neutralized with lime to pH 10, and coarse and fines are separated with hydrocyclones. The coarse portion is sent back to the mine. The fines are slurried with effluents and piped into the farther end of the tailings pond. The solids settle in the pond, and the liquid effluents flow through the decantation wells and drains into a small natural canal, Juria nala. Water pumped out of the mine is led into the canals. Small volumes of locally originated effluents join the canal downstream releasing into it floor washings and miscellaneous water effluents. The Gara nala, consisting mainly of waters from the barrage (dam), flows into the canal 4 km downstream. The diluted stream finally meets the river 6 km away from the tailings pond. The dilution of waste concentrations in the stream depends on the volume of water available for dilution from natural flow in the canal and the Gara nala. The water availability in Juria nala depends on rains and is virtually negligible in summer. The total volume of discharges per day from the tailings pond (2.5×10^6 liters), plant drains (1.5×10^6 liters), and mines (0.5×10^6 liters) was 4.5×10^6 liters.

RELEASE OF RADIUM AND CHEMICAL TOXINS

Radium

An analysis of the effluents has shown that only about 0.5 to 1.5% of the total radium inventory is dissolved during leaching of the ore with sulfuric acid. This value is in agreement with that reported by Tsivoglou and Connel (1964). The determination of dissolved radium in the waste slurry discharged to the tailings pond was carried out by analyzing filtered effluent samples composited over 15 days. These composites, collected for 200 days, have shown dissolved radium content in the discharge ranging from 100 to 200 pCi/liter, with an average of about 160 pCi/liter ± 56 pCi/liter. The concentration of radium in the effluents from the tailings pond itself has shown wide variations, depending on seasonal conditions. Radium in the tailings pond effluent was found to range from 2 to 235 pCi/liter, with a median value of 43.0 pCi/liter. The contribution of radium to

TABLE 1
Manganese in Discharged Effluents as a Function of pH

pH	Dissolved manganese, ppm
11.4	<0.02
10.4	<0.02
9.8	0.17
9.5	0.22
9.0	1.30

the environment through the mill drain and mine water has been estimated and found to vary from 14 to 54 pCi/liter, with a median value of 23.5, in the mill drain and 7 to 80 pCi/liter, with a median value of 25.3 pCi/liter, in mine water.

Manganese

Pyrolusite (MnO_2) is used in the acid leaching of uranium from the ore. Divalent manganese comes into the effluent as a result. When the waste slurry is treated with lime for discharge, dissolved manganese is precipitated as $Mn(OH)_2$. At pH 10 and above, almost all the manganese is precipitated. Manganese hydroxide is sensitive to changes in the pH and may go in solution partially with a slight lowering of the pH (Table 1).

It is necessary to oxidize manganese to the higher valency (manganic) to prevent redissolution of the precipitated manganese. Subsequent to the discharge of neutralized waste from the mill in the tailings pond, various chemical and biological reactions (Duncan and Bruynesteyn, 1971) set in, and the pH of the tailings is lowered. Even when the tailings are discharged at a pH of 10 and above, the overflow from the pond has a pH around 7. A part of the precipitated manganese gets redissolved and appears in the effluent. The tailings mound (15 m high) has accumulated waste solids over the years from which manganese may leak into the effluents by weathering and degradation.

Sulfate, Chloride, and Hardness

The addition of such reagents as sulfuric acid, common salt, and lime at various stages of the processing introduces sulfate, chloride, and permanent hardness into the effluents. Typical concentrations of

these ions in the tailings pond effluents are sulfates, 1800 to 2000 ppm; chloride, 500 to 600 ppm; and hardness, 1500 to 1800 ppm.

DISTRIBUTION OF TOXINS IN THE AQUATIC SYSTEM

Water

Table 2 gives the radium and manganese concentrations in different waste streams joining the Juria nala and in mixed effluents flowing into the canal. Table 3 gives the concentration of nonactive dissolved matter containing chloride, sulfate, and hardness in the canal waters. The tabulated results show that at 4 km from the tailings pond the sulfate content is above the limits specified for water quality even though the radium and manganese contents are below permissible limits. At the junction (J_1) the tailings pond effluent flows into the canal, and the water contains the highest

TABLE 2

Movement and Dilution of Tailings Pond Effluents

Location	Distance from tailings pond, km	Radium, pCi/liter		Manganese, ppm	
		Median	σ_g	Median	σ_g
Juria nala stream	Upstream	0.3	1.5	0.04	0.02
Tailings pond effluent J_1		43.0	2.7	6.2	3.0
Mill effluents from the main drain J_2		23.5	1.9	5.2	3.9
Mines water J_3		25.3	1.9	3.4	0.9
Stream 1 (tailings pond effluent mixed with Juria nala)	0.05	42.5	2.9	4.6	2.7
Stream 1 (tailings pond effluent mixed with Juria nala) + mine water and mill washings	1.5	22.5	3.9	2.7	2.4
Stream 2 (Gara nala junction with Juria nala), J_4	2.5	9.2	2.5	1.0	2.7
Stream 2 (5)	3.2	2.9	3.3	0.8	3.0
Stream 2 (6)	4.0	1.1	2.1	0.1	2.1
River (at the point of mixing with Stream 2), J_5	6.0	0.6	1.7	0.04	2.9

TABLE 3

Dissolved Solids in the Effluent Stream

Location	Distance from tailings pond, km	Sulfate, ppm	Chloride, ppm	Hardness, ppm
Juria nala stream	Upstream	4.5	5.3	94.5
Tailings pond effluent		1900.0	550.0	1600.0
Stream 1 (tailings pond effluent mixed with Juria nala)	0.05	1775.8	378.0	1178.9
Stream 1 (tailings pond effluent mixed with Juria nala) + mine water and mill washings	1.5	498.8	153.8	693.0
Stream 2 (Gara nala junction with Juria nala)	2.5	401.9	90.7	336.5
Stream 2 (Gara nala junction with Juria nala)	3.2	420.3	82.9	242.2
Stream 2 (Gara nala junction with Juria nala)	4.0	375.6	120.8	223.6
River (at the point of mixing with Gara nala)	6.0	110.6	23.1	130.4

concentration of pollutants in its traverse from the tailings pond to the river (Fig. 1). Low concentrations are seen only during the monsoon when there is a good flow of water in the Juria nala. During winter and summer the natural flow of water in the Juria nala practically dries up and the tailings pond effluents constitute in itself the main source of water in Stream 1. The water of this stream is not used in any way by the public, until it is joined by the Gara nala water, which is mainly the release from a drinking water barrage. Water also is not available in the Gara nala during all seasons. Stream 2 consists of the water flow in the canal after the Gara nala joins the Juria nala and mixes with Stream 1. During lean seasons the concentration of contaminants in Stream 2 was similar to or only slightly less than that in Stream 1. The water from Stream 2 traverses in the canal for a further distance of 4 km before flowing into the Subarnarekha River, the only large river in the locality freely used by the general population (Table 2).

Bottom Sediments

The particles present in the effluents settle along the course of the canal. These particles adsorb radium and manganese and thus

TABLE 4

Radium and Manganese in Bottom Sediments

Location	Radium, pCi/g	Concentration factor for radium, $\frac{\text{pCi/g}}{\text{pCi/ml}}$	Manganese, mg/g	Concentration factor for manganese, $\frac{\text{mg/g}}{\text{mg/ml}}$
Sediment in the tailings pond drains	210.0	2.9×10^3	3.30	0.7×10^3
Stream 1, random samples along the stream up to 1.5 km	268.5	11.9×10^3	2.93	1.0×10^3
Stream at 2.5 km	55.1	6.7×10^3	1.30	1.3×10^3
Stream 2, random samples from 2.5 to 3.0 km	21.2	7.3×10^3	0.60	0.6×10^3
River bed, downstream	3.2	5.4×10^3	<0.02	

contribute to a decrease in the concentration of pollutants in water along the length of this stream.

At the same time the contamination of the streambed is increased by the deposition of fines. It has been found that the specific activity of radium associated with the fines is more than that associated with the coarse fraction of the tailings. As a result, the sediment holds a large amount of radium and manganese that may be released through leaching and biodegradation. Table 4 gives the analysis of bottom sediments for radium and manganese and concentration factors for the pollutants in the sediment.

Manganese in sediments constitutes a source of contamination when it is solubilized. Radium and manganese have been found in algae and tissues of fish living in the canal.

Well Water Samples

Subsoil water carries dissolved salts into well waters in the surrounding region. Sulfate and chloride present in the effluents move out faster than trace metals and radionuclides. Wiklander (1965) has reported that chloride and sulfate ions are not bound to many soils at pH 7 or above. Nevertheless, the increase of sulfate and chloride concentrations in well water samples is an indication of chemical ingress. To assess the quality of well water that is used for drinking and domestic use, water samples were obtained from the surrounding region and examined. The results of the analysis of well water samples are presented in Table 5. The dissolved matter in two

TABLE 5

Analysis of Well Water Samples

Location	Radium, pCi/liter	Manganese, ppm	Sulfate, ppm	Chloride, ppm	Hardness, ppm
Well No. 1, 50 m from tailings pond	0.48	1.89	816.0	312.5	1232.2
Well No. 2, 500 m from tailings pond	0.42	0.34	775.5	279.5	1471.6
Well No. 3, 600 m from tailings pond	0.38	0.02	104.4	91.2	385.4
Well No. 4, 750 m from tailings pond	0.18	0.21	12.5	56.0	220.5
Well No. 5, 1.0 km from tailings pond	0.35	0.05	9.2	13.4	148.6
Well No. 6, 2.5 km from tailings pond	0.44	0.02	1.3	105.8	238.8
Well No. 7, 3 km from tailings pond	0.16	0.04	3.8	11.3	152.8
Well No. 8, 6 km from tailings pond	0.65	0.02	29.4	33.4	221.7

TABLE 6

Nonradioactive Pollutants in Well No. 2 Water Samples (in ppm)

	1970	1972	1974	1977
Sulfate	125.0	970.7	509.3	1158.0
Chloride	189.1	319.9	304.9	384.7
Hardness	790.5	1180.5	853.6	1380.0
Manganese	0.14	0.33	0.36	0.74

well waters near the tailings pond has shown contamination of ground waters with manganese and inactive ions. Table 6 gives the results of the analyses of hardness, sulfate, chloride, and manganese in the samples of well No. 2 from 1970 to 1977. The concentration of pollutants in other well waters is well below maximum permissible concentration (MPC) limits.

Concentration in Aquatic Products

The hazard to man exists from the uptake of pollutants by aquatic organisms. Radium and manganese are also found in agricultural produce. Radium has been found to be concentrated

1000 to 2000 times in algae growing in the stream. Fish living in the contaminated stream concentrate radium. Paddy (rice) grown in the area where effluent seepages occurred has shown an increase in the radium activity compared to local background samples. Table 7 gives the results of the analysis of aquatic and land produce and observed concentration factors.

TABLE 7

Analysis of Aquatic Products

Type of sample	Radium, pCi/g	Concentration factor	Manganese, mg/g	Concentration factor
Algae; background sample	0.03	0.04×10^3	ND*	
Algae from drain carrying mine water	46	1.8×10^3	ND	
Algae from tailings pond drains	120	2.8×10^3	0.02	0.003×10^3
Fish from drains carrying mine water				
Bone	1.4	0.05×10^3	0.008	0.0023×10^3
Flesh	0.08	0.003×10^3	0.003	0.0008×10^3
Fish from drains carrying mine water				
Bone	0.98	0.039×10^3	0.018	0.0054×10^3
Flesh	0.16	0.006×10^3	0.004	0.0009×10^3
Fish from drains carrying mine water				
Bone	0.01	0.04×10^3	0.008	0.0023×10^3
Flesh	0.20	0.008×10^3	0.003	0.0008×10^3
Rice from a noncontaminated paddy field	0.002		0.023	
Rice from a contaminated paddy field	0.027		0.038	

*ND = not determined.

CONTAINMENT TRIALS FOR RADIUM AND MANGANESE IN EFFLUENTS

The containment of manganese and radium present in process effluents before discharge was investigated in the laboratory. Initial experiments were planned to raise the manganese to a higher valence during neutralization and to remove radium by coprecipitation with barium sulfate by adding a barium carrier. Although the system worked in the laboratory trials, the treatment process was not found

to be successful when the treated slurry was discharged to experimental ponds.

The tailings pond contains a large reserve of $Mn(OH)_2$, which leaks into the effluents by weathering. It appeared more practicable to treat the tailings pond effluents for the control of total pollutants in the effluents.

For this purpose the effluents were passed through pyrolusite pebbles and a bed of barytes. A 25- by 1-cm column of pyrolusite pebbles ranging from 3.3 to 1.6 mm was prepared and thoroughly washed in running water to remove any fine powder adhering to it. The column was then quickly washed with a solution of 0.01*M* HCl followed by water. The effluent was passed through the column at the rate of 5 ml/min. It was found that both manganese and radium from the effluent were adsorbed on the pyrolusite pebbles. Experiments were carried out at different pH conditions of the effluent. Maximum efficiency could be obtained under the following conditions:

1. The pH of the effluent should not be less than 8.
2. The effluent should be filtered free of any silt before it is passed through the column.

At lower effluent pH (pH 7 to 4), the efficiency was found to come down; and, at a pH below 4, the manganese deposited on the pebbles was found to be redissolved. The effluent from the pyrolusite bed was passed through a bed of barytes for radium removal. The pyrolusite bed was found to be effective in removing manganese from the effluent. More experiments are required to increase the efficiency of the barytes bed to meet water quality requirements.

DISCUSSION

Tables 2 and 3 give the pollutants in the canal waters at various distances from tailings pond down to the river. Canal waters are not used by the public up to 4 km. Beyond 4 km from the discharge point, the concentrations of radium and manganese in the canal waters are below the permissible levels for drinking water recommended by the World Health Organization (1963). If we apply to the canal water beyond 4 km the rule of mixtures, recommended by the International Commission on Radiological Protection (1959) when more than two pollutants are present in the water, the total hazard from the two pollutants would not be significantly different (Mn 0.1/0.1 ± Ra 1.1/10 = 1.11 MPC). This evaluation does not take into account any synergistic effect, if present. There is no evidence in the environment of synergistic damage at this level. The important

consideration in this assessment is the quality of water after the canal water mixes with the river. Fishing in the canal between 4 and 6 km is insignificant compared to quantities of fish caught in the river and fish harvested in private fish ponds. The hazard through concentration of activity in fish is not significant to the public since the quantity of fish produced in canal water is small. As the canal water mixes with the river, the concentration of pollutants at the junction is 2 to 5 times below the limit considered to be acceptable for use by the general population. It is expected that the levels will be further reduced by progressive dilution in the large water body. The nearest large consumers of river water are located 5 km downstream.

Table 4 gives the concentration factors in suspended silt that settles as sediment in the canal. The concentration factors of 10^3 for manganese and 10^3 to 10^4 for radium in the sediments demonstrate the self-cleaning properties of the stream. It is not in evidence that the contaminated silt from the canal has moved into the river. The pollutant content in the river sediment in the junction area (J_5) is close to background. The concentration of sulfate, chloride, and hardness in well waters (Table 5) is high up to 1 km from the tailings pond. Seepage of effluents to the wells around the tailings pond has resulted in a slow increase in the concentration of these ingredients over the years in the well waters, and two of the wells have reached unacceptable levels with respect to the contaminants (Table 6). These wells are not in use for domestic purposes, and the waters are used for irrigation and gardening. The sulfate, chloride, and hardness therefore serve as advance indicators of underground seepage.

The hazards from radium and manganese in the environment are controlled by two contributory factors, namely, chemical precipitation of $Mn(OH)_2$ as a function of pH and carry-over of radium in the presence of excess $(SO_4)^{-}$ with calcium sulfate. Quantitative elimination is not achieved because of fluctuation of pH on weathering, absorption of CO_2, etc., and chemical interactions. Calcium sulfate is a poor coprecipitant for radium. However, the pollutants are brought under permissible concentration limits by dilution with nonactive streams before the canal waters come into the public domain.

Aquatic organisms are good indicators for a number of nutrient elements, particularly zinc. The study revealed (Table 7) that algae is a useful indicator of radium. Algae has been reported to accumulate uranium in an earlier study in the environment (Iyengar and Markose, 1971). Uranium concentrations in the canal waters are not high (less than 10 μg/liter within 4 km).

It is important, however, that a watch be continually kept because of the following conditions:

1. Weathering and biodegradation of the accumulated material in the tailings pond.
2. Spillovers from tailings pond by breaches and flooding.
3. Reduction in dilution availability in the canal during dry seasons.
4. Unforeseen discharge from processing.
5. Use of canal waters by cattle and passersby and for domestic purposes in hutments.

ACKNOWLEDGMENTS

We are grateful for the support and encouragement received from our colleagues in the Health Physics Unit. Thanks are due Shri S. D. Soman, Head of the Health Physics Division, and Dr. A. K. Ganguly, Director of the Chemical Group, for the use of facilities and for permission to participate in the symposium. We are also grateful to Dr. A. K. Rakshit, Chief Medical Officer, Uranium Corporation of India, Ltd., for his helpful discussions. Finally, we wish to convey our thanks to the sponsoring authority in the United States for facilitating oral presentation of this paper.

REFERENCES

Duncan, D. W., and A. Bruynesteyn, 1971, Microbiological Leaching of Uranium, in *Selected Papers from the 1970 Uranium Symposium at Socorro, N. Mex.*, May 6—8, 1970, New Mexico State Bureau of Mines, Circular 118.

International Commission on Radiological Protection, 1959, *Recommendations of the International Commission on Radiological Protection*, Report of Committee II.

Iyengar, M. A. R., and P. M. Markose, 1971, Monitoring of Aquatic Environment in the Neighborhood of Uranium Mill at Jaduguda, Bihar, in *Proceedings of the National Symposium on Radiation Physics*, Bombay, India, Nov. 24—27, 1970, Bhabha Atomic Research Center.

Merritt, R. C., 1971, *Extractive Metallurgy of Uranium.*

Tsivoglou, E. C., and R. L. O. Connel, 1964, Nature, Volume, and Activity of Uranium Mill, *Radiological Health and Safety in Mining and Milling of Nuclear Materials*, Symposium Proceedings, Vienna, Vol. 2, pp. 101-122, STI/PUB/78, International Atomic Energy Agency, Vienna.

Wiklander, Lambert, 1965, *Chemistry of the Soil*, Firman E. Beor (Ed.), American Chemical Society, Monograph Series No. 160, 2nd ed., Reinhold Publishing Corp., New York.

World Health Organization, 1963, *International Standards for Drinking Water.*

Accumulation of Radium-226 from Phosphate Fertilizers in Cultivated Soils and Transfer to Crops

R. KIRCHMANN,* M. DARCHEVILLE,† and G. KOCH*
*Belgian Nuclear Centre, Mol, Belgium, and †Ministry of Agriculture, Belgian Agricultural Research Centre, Gembloux, Belgium

ABSTRACT

Actual values of the ^{226}Ra content of soils sampled in various experimental plots with well-known fertilization histories and the ^{226}Ra levels in crops produced are given. The statistical analysis led to the conclusion that there is no significant difference in the ^{226}Ra content of straw ($0.975 < p < 0.99$) or grain ($0.995 < p < 0.999$) of the winter wheat harvested in the plots fertilized, respectively, at low level (343 kg/ha) or at highest level (1356 kg/ha) of P_2O_5 applied in 11 years (1967—1977). The ^{226}Ra contamination due to the application of phosphate fertilizer represents only 0.25 and 1.08%, respectively, of the activity of ^{226}Ra observed in the upper layer (0 to 20 cm) of soil (870 ± 60 pCi/kg of dry soil). The ^{226}Ra ingested annually by man from cereals and milk is estimated.

Our laboratory has been involved since 1961 in the study of transfer in the environment of ^{226}Ra released in liquid effluents from industrial installations located in the northern part of Belgium. The description of the radioecological program, the results obtained, and the conclusions at the scientific, health, practical and executive levels have been published (Kirchmann et al., 1973). Special attention was devoted these last years to the naturally occurring radionuclides in mineral phosphates and in manufactured fertilizers; the transfer of ^{226}Ra in the food chain and the dose to man from internal exposure of ingested ^{226}Ra have been evaluated recently (Kirchmann et al., 1977).

The aim of this paper is to report investigations of the relation between the levels of application of the phosphate fertilizer and the

^{226}Ra content of some crops grown on soils with a well-known fertilization history; these plots are located in the experimental fields of the Belgian Agricultural Research Centre in Gembloux.

EXPERIMENTAL METHOD

Plots and Fertilization

Analyses have been performed on samples collected in two blocks of plots; these two blocks (A and D) are different because of rotation of cultures. Each block is divided into 18 plots of 250 m^2 each (three types of fertilizers times three levels, two replications). The type of soil is loamy, and the pH is neutral. The treatment applied to each plot analyzed is shown in Table 1. About 40 samples of mineral phosphates and phosphate fertilizers from various origins were analyzed for their ^{226}Ra content. The mean contents are 25.2 pCi ^{226}Ra/g, 18.7 pCi ^{226}Ra/g, and 0.52 pCi ^{226}Ra/g, respectively, in supersimple, superdouble, and scories (Kirchmann et al., 1977). On this basis, the activity brought by the application of phosphate fertilizers of various types has been computed, and the result is given in Table 2.

TABLE 1

Fertilizers Applied (kg/ha) During the Whole Period (1967–1977)

Block	Plot	Replication	N	P_2O_5	K_2O
A	17	I	505	358	591
	21	I	832.5	358	1322
	15	I	1150	358	591
	32	II	1150	358	591
	19	I	1150	358	2066
	53	II	1150	358	2066
	18	I	832.5	1356	1322
	42	II	1150	1356	2066
D	14	I	427.5	343	548
	38	II	427.5	343	548
	24	I	768.7	343	548
	26	I	768.7	343	2176
	36	II	1110	343	548
	25	I	1110	343	2176
	53	II	768.7	1346	1412
	19	I	1110	1346	2176
	40	II	1110	1346	2176

TABLE 2

Estimation of ^{226}Ra Contamination Due to the Phosphate Fertilizers Applied During the Whole Period (1967—1977)

Type of phosphate	Block A		Block D	
	Amount P_2O_5 (kg/ha)	^{226}Ra (nCi/ha)	Amount P_2O_5 (kg/ha)	^{226}Ra (nCi/ha)
	Plots: 17, 21, 15, 32, 19, 53		Plots: 14, 38, 24, 26, 36, 25	
Supersimple	142	3578	137	3452
Superdouble	33	617	36	673
Scories	183	95	170	88
Total	358	4290	343	4213
	Plots: 18, 42		Plots: 53, 19, 40	
Supersimple	142	3578	137	3452
Superdouble	808	15110	829	15502
Scories	406	211	380	198
Total	1356	18999	1346	19152

Sampling

Soils: Several cores per plot were sampled at different depths (0 to 20, 20 to 35, and 35 to 50 cm). The samples from the same layer were mixed, air-dried, and finely ground.

Plants: The whole crop of each plot was harvested, and some representative samples of each part of the plants were taken for analysis. The samples were dried in an oven at 110°C until constant weight; the dry matter was then finely divided.

Measurements

Soil: The ^{226}Ra in these samples was measured by gamma spectrometry. To avoid a nonequilibrium state at the ^{222}Rn level, which is gaseous and diffuses outside the sample, we used a sealed vial; furthermore we added a certain amount of charcoal. The activity of the 610-keV gamma peak of ^{214}Bi was measured with a NaI(Tl) crystal after a delay of 20 days (97% of equilibrium was reached at this time).

Plant material: The dried sample was ashed (500 to 550°C), and the ashes were dissolved in diluted HNO_3. The solution was stored during about 4 days, then the ^{222}Rn was extracted and transferred to a detector which was connected to a photomultiplier tube and a scaler.

TABLE 3

^{226}Ra Contents in Soils and Crops Sampled in the Experimental Fields (1977)

Block	Plot	Organ	^{226}Ra content in plants: pCi ^{226}Ra/g ash	^{226}Ra content in plants: pCi ^{226}Ra/100 g DW*	^{226}Ra content in soils (0—20 cm), pCi ^{226}Ra/100 g DW*
			Wheat (Winter Variety)		
A	17				80 ± 10†
	21	Straw	0.491 ± 0.009	3.49 ± 0.045†	
		Grain	0.217 ± 0.008	0.44 ± 0.01	
	15	Straw	0.60 ± 0.01	6.35 ± 0.11	
		Grain	0.216 ± 0.007	0.38 ± 0.01	
	32	Grain	0.182 ± 0.007	0.32 ± 0.01	
	19	Straw	0.51 ± 0.01	3.80 ± 0.07	
		Grain	0.228 ± 0.007	0.40 ± 0.01	
	53	Straw	0.383 ± 0.008	2.94 ± 0.06	
		Grain	0.335 ± 0.008	0.64 ± 0.02	
	18	Straw	0.454 ± 0.008	3.09 ± 0.05	
		Grain	0.245 ± 0.006	0.46 ± 0.01	
	42	Straw	0.522 ± 0.009	4.49 ± 0.08	90 ± 10
		Grain	0.240 ± 0.007	0.45 ± 0.01	
			Sugar Beets		
D	14	Root	0.41 ± 0.02	1.04 ± 0.05	
	38				93 ± 10
	24	Foliage	0.181 ± 0.006	3.35 ± 0.11	
		Root	0.80 ± 0.02	3.11 ± 0.08	
	26	Foliage	0.36 ± 0.01	5.54 ± 0.15	
		Root	0.53 ± 0.02	1.08 ± 0.04	
	36	Foliage	0.105 ± 0.006	1.81 ± 0.10	
		Root	0.34 ± 0.01	0.92 ± 0.03	
	25	Foliage	0.400 ± 0.009	7.74 ± 0.17	
		Root	0.620 ± 0.002	1.45 ± 0.05	
	53	Foliage	0.191 ± 0.006	3.80 ± 0.12	
		Root	0.88 ± 0.02	2.16 ± 0.05	
	40				87 ± 10

*DW = dry weight.
†Quadratic error.

RESULTS AND DISCUSSION

The ^{226}Ra contents in soils and plant organs collected in the various plots are listed in Table 3.

The statistical analysis (t test of two means) led to the conclusion that there is no significant difference in the ^{226}Ra content of straw

($0.975 < p < 0.99$) or grain ($0.995 < p < 0.999$) of the winter wheat harvested in the plots fertilized at low or high levels of P_2O_5. This conclusion is not surprising if we consider that the ^{226}Ra contamination due to the application of phosphate fertilizer represents only 0.25 and 1.08%, respectively, of the activity of ^{226}Ra observed in the upper layer (0 to 20 cm) of the experimental soil. It is interesting to note that the ^{226}Ra contents measured in our soil samples are in agreement with the values cited by Jaworowski and Grzybowska (1977). The data in Table 3 show also that the ^{226}Ra content in grain is 5 to 16 times lower than in the straw, an observation in accordance with our previous results (Kirchmann, Boulenger, and Lafontaine, 1968); the finding that the root of the sugar beet has a lower ^{226}Ra content than the foliage is also in agreement with the previously mentioned results. However, the concentration factors observed in the present study are also in accordance with the values computed from experiments performed in laboratory conditions (Kirchmann, Boulenger, and Lafontaine, 1968) on a soil of the same type contaminated with a known amount of $^{226}RaCl_2$.

If we consider that the leaves of the sugar beet are used as forage for lactating cows during the winter period, the milk produced will contain 0.02 pCi ^{226}Ra/liter if this source of feed is the only one; indeed the mean ^{226}Ra content of leaves is 4.45 pCi/100 g of dry matter, the calcium level is 73 mg/100 g of dry matter, and the observed ratio (i.e., the ratio of picocuries of ^{226}Ra per gram of calcium in milk to picocuries of ^{226}Ra per gram of calcium in forage) has a value of 0.01 (Kirchmann, Van den Hoek, and Van Puymbroeck, 1968). Nevertheless, in practice, the ratio will include other feeds in order to be equilibrated. Finally, considering an individual ingestion of ^{131}I milk/year, the annual intake will be 2.6 pCi ^{226}Ra; ingestion of 81 kg of wheat grain per year will contribute for about 36 pCi ^{226}Ra of the yearly ingested ^{226}Ra. These values represent 0.2 and 3.3%, respectively, of the annual ingestion of ^{226}Ra estimated by Michelson (1961) for the total diet of four cities in the United States. In conclusion, the application of phosphate fertilizers, even at high level, did not increase significantly the ^{226}Ra content of the crops under study; the contribution of the wheat grain and the milk to the ^{226}Ra ingestion by individual is very low (a few percent).

ACKNOWLEDGMENTS

We gratefully acknowledge the valuable technical assistance of E. Bonnijns-Van Gelder and J. Baton. Thanks are due to E. Blok and P. Vermeire for gamma-spectrometric analyses.

REFERENCES

Jaworowski, Z., and D. Grzybowska, 1977, Natural Radionuclides in Industrial and Rural Soils, *Sci. Total Environ.*, 7: 45-52.

Kirchmann, R., R. Boulenger, and A. Lafontaine, 1968, Absorption du ^{226}Ra par les plantes cultivées, in the Symposium Proceedings of the First International Congress of Radiation Protection, Roma, Italy, September 5—10, 1966, pp. 1045-1051, Pergamon Press-Oxford-New York.

——, R. Boulenger, J. Colard, and A. Lafontaine, 1977, Evaluation de la dose à l'homme résultant de la présence de radionuclides naturels dans les engrais phosphatés d'origine minérale, p. 1045, in the Proceedings of IVth International Congress of IRPA, Paris, 24—30 April.

——, J. Van den Hoek, and S. Van Puymbroeck, 1968, Rapport observé, en conditions naturelles, entre les teneurs de l'herbage et du lait en radiostrontium et en radium, in Actes du Congrès International sur la Radioprotection du Milieu devant le développement des utilisations pacifiques de l'Energie Nucléaire, Toulouse, France, 14—16 mars, 1967, pp. 357-367, Societé Française Radioprotection, 26 rue d'Ulm, Paris.

——, A. Lafontaine, G. Cantillon, and R. Boulenger, 1973, Etude du cycle biologique parcouru par la radioactivité, Report BLG 477, Centre d'Etude de l'Energie Nucléaire, Bruxelles (Belgium).

Michelson, I., 1961, Radium-226 in the Total Diet, *Health Phys.*, 5: 229.

Determinants of Radon Flux from Complex Media: Virgin and Reclaimed Lands in Florida Phosphate Region

W. EMMETT BOLCH, NAYAN DESAI, CHARLES E. ROESSLER, and RANDY S. KAUTZ
University of Florida, Gainesville, Florida

ABSTRACT

Mathematical models for the transport of radon through two strata media are described. The bilayer model reduces to a transport equation for a single layer of finite depth when the upper layer does not exist. The finite model approaches a simpler expression, an infinite model, when depths exceed several meters.

The models use a number of media parameters that can be measured independently or estimated from media characteristics. Summarized are the media parameters for several land types found in the West Central Florida phosphate region. Measured flux values by land type are compared to predicted flux values for the respective land type.

The bilayer model is used to demonstrate reclamation management to reduce radon flux at the soil surface.

Historically, most of the inventories of the world's uranium resources mention the Florida phosphate ores as a potential source. The concentrations are significant but not to the point of encouraging direct mining. The deposits are located some 10 to 20 ft below the surface, and in the undisturbed state radionuclides associated with the uranium pose little hazard to man. In recent times, however, large-scale mining, significant reclamation, and subsequent development of these lands have altered the potential hazard. Of considerable interest is the enhanced radon flux from the surface of reclaimed lands and radon transport to the interior of occupied structures. The major concern is a potential for increased lung cancer due to exposure to ^{222}Rn daughters over a long period of time. Radon flux is expected to be a major parameter in classifying reclaimed lands for development purposes.

Virgin areas of Central Florida have shown a characteristic ^{226}Ra profile: the surface concentration is low, and the level increases nearly exponential until the top of the phosphate matrix is reached. These profiles suggest the separation of the overburden into two strata based on relative ^{226}Ra concentrations: a low and a high activity portion. Mining tends to reverse the concentrations with the high activity portion at or near the surface. Beneficiation of the ore produces two waste functions—sand and clay. Reclamation practices and proposals usually consider combinations of the waste fractions and overburden. The result is again often a two-phase system. The use of waste fractions or any of the high activity materials as fill material on virgin lands yields a multistrata source. These facts led to the development of a bilayer model for predicting the radon flux.

DEFINITION OF VARIABLES

Table 1 summarizes the parameters important to the model, their units, and the method of measurement or prediction. Roessler et al. (1978) have shown that if the Central Florida phosphate district lands are classified into unaltered lands, tailings (sand waste fraction remaining after phosphate beneficiation), overburden reclaimed lands, mixed and capped clay areas (fine waste fractions remaining after flotation), and debris lands (debris was a class of waste before the flotation process was widely used), then each will have a distinct range and geometric mean of radon flux and radium concentration.

The other measured parameters were also grouped by this classification scheme. Table 2 summarizes these parameters by land type.

MATHEMATICAL MODELS

Bilayer Model

The bilayer model will describe the transport of radon through a two-layer system. The bottom layer is considered to be bounded on the underside by a layer nearly impervious to radon. The water table would be an effective lower boundary. The second or top layer is bounded by the lower media and the atmosphere. Each layer is considered to be homogeneous within itself but may have different properties. Both layers contain ^{226}Ra and have both production and decay terms. The boundary conditions however dictate an upward flux, and thus the relationship of the lower layer parameters to the upper layer parameters must reflect this condition. The model is greatly simplified if the concentration of ^{222}Rn above the surface is

TABLE 1

List of Model Parameters

Description	Symbol	Units	Method of determining value
Radon flux at the soil—air interface	J	pCi m^{-2} sec^{-1}	Field collection of ^{222}Rn accumulated in either an inverted drum or charcoal canisters
Radium-226 concentration in the dry soil	C_{Ra}	pCi/g	High-resolution gamma spectroscopy on sealed, equilibrated samples of the media
Bulk density, volume per unit of dry weight	ρ	g/cm^3	Laboratory determination of dry weight in a known volume
Porosity, void space fraction in a bulk volume	p		Literature values (i.e., soil mechanics and foundation design references) based on media description
Emanating power, amount of ^{222}Rn released to void per unit of radium (or radon)	E	pCi/pCi	Observed difference in ^{222}Rn daughters in sample: after aged-air deemanation vs. sealed for equilibrium
Decay constant for ^{222}Rn	λ	sec^{-1}	Known constant = 2.1×10^{-6} sec^{-1}
Media diffusion coefficient radon in dry air within the media	D_0	cm^2/sec	The Fick's Law coefficient modified by the media; taken as 5.0×10^{-2}
Media diffusion coefficient radon in moist air within the media	D	cm^2/sec	Assumed to follow the expression $D = D_0 e^{-0.1M}$
Moisture content of the soil	M	%	Differences in oven dry weight vs. field wet weight
Depth of media	d	cm	Layer thickness or distance from surface to barrier
Conversion constant	10^4	cm^2/m^2	Basic equation yields flux in pCi cm^{-2} sec^{-1}; convenient unit for flux is pCi m^{-2} sec^{-1}
Subscripts			1 denotes lower layer; 2 denotes upper layer; no subscript denotes single layer models

TABLE 2

Values of Model Parameters by Land Type

Land type	Geometric mean (range) of measured values				Estimated values	
	C_{Ra}	ρ	E*	M	p†	D‡
Unaltered	0.45 (0.2—3.1)	1.60 (1.4—1.9)	0.07 (0.01—0.11)	11 (7—18)	0.40	1.7×10^{-2}
Tailings	3.1 (0.5—8.7)	1.4 (1.0—1.8)	0.10 (0.09—0.11)	10 (5—15)	0.35	1.8×10^{-2}
Overburden	5.3 (1.0—23)	1.3 (1.0—1.5)	0.16 (0.02—0.39)	15 (8—20)	0.40	1.1×10^{-2}
Mixed and capped clays	7.4 (2.8—18)	0.9 (0.6—1.2)	0.19 (0.17—0.20)	33 (5—130)	0.50	5×10^{-3} §
Debris	7.3 (3.1—25)	1.4 (1.2—1.6)	0.16 (0.13—0.19)	10 (8—14)	0.35	1.8×10^{-2}

*Arithmetic mean due to small number of samples.
†Assigned by physical description of media.
‡$D = D_0 \exp(-0.1M)$.
§Lower limit of D.

considered negligible. It was determined that ground-level concentrations of ^{222}Rn would have to exceed 8000 pCi/m^3 before any changes in the flux would be noted. This assumption may not be valid for capped surfaces, such as home foundations and flux measurements.

The final equation becomes

$$J_2 = -10^4 m_2 D_2 (2Ae^w + k_2) \qquad (1)$$

where

$$A = \frac{D_2 k_2 e^{w-z} + D_1 (\tanh z)\,[k_2 e^{w-z} - (k_2 - k_1)]}{D_1 (\tanh z)\,(e^z - e^{2w-z}) - D_2 (e^z + e^{2w-z})}$$

and

$$z = m_1 d_1 \qquad w = m_2 (d_1 + d_2)$$

$$m_1 = \left(\frac{\lambda p_1}{D_1}\right)^{1/2} \qquad m_2 = \left(\frac{\lambda p_2}{D_2}\right)^{1/2}$$

$$k_1 = \frac{C_{Ra_1} \rho_1 E_1}{p_1} \qquad k_2 = \frac{C_{Ra_2} \rho_2 E_2}{p_2}$$

Monolayer Model

In the absence of the upper layer, Eq. 1 reduces to

$$J_1 = 10^4 \, k_1 m_1 D_1 \tanh z \qquad (2)$$

or

$$J_1 = 10^4 \, C_{Ra} \rho E (\lambda D/p)^{1/2} \tanh [d(\lambda p/D)^{1/2}] \qquad (3)$$

Equation 3 models a single layer of material homogeneous within itself and bounded by the air and a lower barrier for radon. This model can also be derived directly from basic production, decay, and transport considerations. Since tanh z approaches unity at values of z in excess of 2, increasing depths (d) rapidly begin to have a decreasing effect on the surface flux. If $(D/\lambda p)^{1/2}$ is defined as a relaxation length (L_R), the $1L_R$ will contribute some 76% of the surface flux, and depths equivalent to $2L_R$ will contribute 96% of the surface flux. For the field parameters given in Table 2, L_R values by land type are as follows:

Land type	L_R, cm
Unaltered	140
Tailings	160
Overburden	110
Clays	70
Debris	160

Cores taken in the disturbed lands of West Central Florida suggest that the condition of homogeneous layers extending to depths of $2L_R$ is common.

Infinite Layer Model

If the hyperbolic tangent term is set equal to unity or for the case that the depth exceeds $2L_R$, Eq. 3 becomes

$$J_\infty = 10^4 \, C_{Ra} \rho E \, (\lambda D/p)^{1/2} \qquad (4)$$

This expression models a homogeneous layer of infinite depth. If all factors except the radium concentration are grouped into a "constant" for a given land type or for other specific cases, then Eq. 4 rearranges to

$$J_\infty = [10^4 \rho E \, (\lambda D/p)^{1/2}] \, C_{Ra} \qquad (5)$$

Predicted or measured values of the J_∞ / C_{Ra} ratio would provide a valuable rule-of-thumb for classifying lands, especially reclaimed areas.

EXAMPLE CALCULATIONS

Table 3 illustrates calculations with the three models. When example 1 is compared to example 2, it can be seen that the cover material attenuates the radon from the debris. If the upper layer contains one-fourth as much radium, as in example 3, the attenuation is only increased by 15%. Examples 2, 4, and 5 illustrate the concept of an infinite depth and suggest that the infinite model is a useful approximation when the depth of the media is suspected to be on the order of 6 to 10 ft or more.

TABLE 3

Use of the Flux Models with Specific Parameters

	Media characteristics	
Variable	Debris	Low activity overburden
C_{Ra}, pCi/g	10	2
ρ, g/cm^3	1.4	1.3
E	0.16	0.16
p	0.35	0.40
M, %	10	15
D, cm^2/sec	1.8×10^{-2}	1.1×10^{-2}

Example 1. Six feet of debris overlain with 2 ft of low activity overburden.
Bilayer model: $J_2 = 3.4$ pCi m^{-2} sec^{-1}
Example 2. Six feet of debris with no cover.
Monolayer model: $J_1 = 6.1$ pCi m^{-2} sec^{-1}
Example 3. Same as example 1 except the low activity overburden is 0.5 pCi/g of ^{226}Ra.
Bilayer model: $J_2 = 2.9$ pCi m^{-2} sec^{-1}
Example 4. Eight feet of debris with no cover.
Monolayer model: $J_1 = 6.8$ pCi m^{-2} sec^{-1}
Example 5. Debris of unknown depth exceeding 8 ft.
Infinite model: $J_\infty = 7.4$ pCi m^{-2} sec^{-1}

RESULTS

In a preliminary evaluation, use of the infinite model with measured values of C_{Ra}, assigned values for E, ρ, and M based on

selective measurements and values of p inferred from soil descriptions predicted the field measured radon flux with a range of ±50% approximately 70% of the time. Considering the error bounds on each measurement, the agreement encouraged a more detailed analysis.

Categorization by land type was considered a necessary step to attempt to reduce the variation. The data in Table 2 can be used to predict the radon flux and the result compared to the geometric mean of all the field flux measurements made on known land types. Table 4 summarizes these data. It is clear that the model is a

TABLE 4

Comparison of Predicted and Measured Radon Flux by Land Type

Land type	Predicted radon flux		Measured radon flux			
	Equation 5	Flux	Equation 5	Flux	(Range)	No.
Unaltered	$J_\infty = 0.33\ C_{Ra}$	0.15	$J = 0.44\ C_{Ra}$	0.2	(<0.1—1.7)	17
Tailings	$J_\infty = 0.45\ C_{Ra}$	1.4	$J = 0.23\ C_{Ra}$	0.7	(<0.1—2.7)	19
Overburden	$J_\infty = 0.49\ C_{Ra}$	2.6	$J = 0.28\ C_{Ra}$	1.5	(<0.1—12.8)	27
Mixed and capped clays	$J_\infty = 0.24\ C_{Ra}$	1.8	$J = 0.22\ C_{Ra}$	1.6	(0.3—7.2)	6
Debris	$J_\infty = 0.73\ C_{Ra}$	5.3	$J = 0.57\ C_{Ra}$	4.2	(1.7—13.7)	15

reasonable rule-of-thumb for land types, and the parameters can be expressed as a coefficient, as in Eq. 5. If any of the model parameters are known for a particular application, the coefficient can be corrected by simple ratios.

The theoretical infinite model appears to overpredict the flux. The coefficients, either predicted or measured for all land categories, except debris land, may not be statistically different. Since debris lands are no longer produced, a conservative rule-of-thumb that could be applied to any other West Central Florida land type is the expression

$$J = \tfrac{1}{3}\ C_{Ra} \tag{6}$$

Boudreau (1978) has carried out a simulation experiment for the monolayer model in which seven 61-cm-diameter vertical columns between 61 and 368 cm high were filled with high activity overburden.

Column-to-column differences in parameters, environmental conditions such as rainfall, and continued settling during the 104 days of the experiment obscured the exact shape of the height function. However, the flux values followed a $(1 - e^{-m_1 d_1})$ increase with the highest column, 366 cm, producing 85% of the estimated J_∞. The 366-cm columns produced an average J_1/C_{Ra} ratio of 1.0 on the 104th day of the experiment, with preliminary indication that the flux has decreased between 20 and 50% during the succeeding 100 days. Studies on the settling effect are continuing.

Column studies with bilayer media are planned within the year. Field investigations of bilayer media as indicated by core samples have not proved conclusive.

RECLAMATION MANAGEMENT

If Eq. 1 is divided by Eq. 2, it can be shown that J_0/J_1 is a function of C_{Ra_2}/C_{Ra_1}. This relationship is used to construct design curves for attenuation of high flux areas by lower activity fill. Figure 1 represents one set of curves for low activity overburden as fill over debris land for a range of values for C_{Ra_2}/C_{Ra_1}. The use of attenuation curves is demonstrated in example 6 (Table 5).

TABLE 5

Use of Models in Reclamation Management

Example 6
Six feet of debris at 10 pCi/g
J_1 = 6.1 pCi m^{-2} sec^{-1} from example 2
Design fill required to yield J_2 = 2.4 pCi m^{-2} sec^{-1}
J_2/J_1 = 0.39 to enter Fig. 1
Read 4 ft of cover at R = 0.2 (C_{Ra_2} = 2 pCi/g) or
Read 3 ft of cover at R = 0.1 (C_{Ra_2} = 1 pCi/g)

CONCLUSION

The mathematical models are useful tools in interpreting field data and in assisting the investigations of parameters shown to be sensitive in producing radon flux. The variable with the greatest range and lack of specificity to land type appears to be emanating power, E. Until this parameter can be easily independently measured or estimated from other observations, the mathematical models provide only rule-of-thumb estimates.

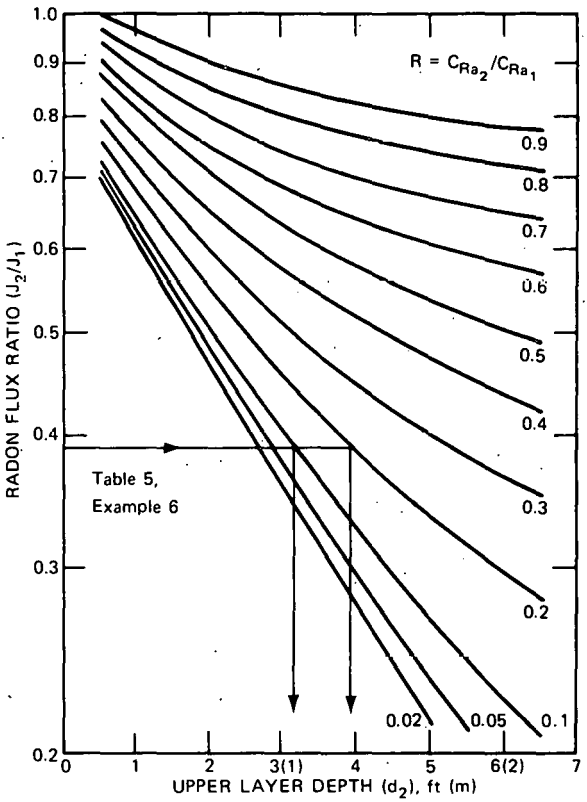


Fig. 1 Typical design curve for attenuation of radon flux from 6 ft of debris land.

ACKNOWLEDGMENTS

This work was supported by the Florida Phosphate Council and the University of Florida Engineering and Industrial Experiment Station. Mark Lang and Zachary Smith participated in the data analyses and tabulations. Bruce Butler made the emanating power measurements under the supervision of J. A. Wethington, Jr.

REFERENCES

Boudreau, Harold, 1978, *Development and Verification of Test Models Predicting Radon-222 Flux Emanation from Soils,* Master's Thesis, University of Florida.

Roessler, C. E., R. Kautz, W. E. Bolch, Jr., and J. A. Wethington, Jr., 1978, *The Effect of Mining and Land Reclamation on the Radiological Characteristics of the Terrestrial Environment of Florida's Phosphate Regions,* this volume.

Ecological Considerations of Natural and Depleted Uranium

WAYNE C. HANSON*
Environmental Science Group H-12, Los Alamos Scientific Laboratory, Los Alamos, New Mexico

ABSTRACT

Depleted ^{238}U is a major by-product of the nuclear fuel cycle for which increasing use is being made in counterweights, radiation shielding, and ordnance applications. The potential for releases of substantial amounts of depleted uranium to the environment is, therefore, a consideration that requires careful evaluation of the ecological consequences of such releases (UPI, 1977). This paper (1) summarizes the pertinent literature on natural and depleted uranium in the environment, (2) integrates results of a series of ecological studies conducted at Los Alamos Scientific Laboratory (LASL) in New Mexico where 70,000 kg of depleted and natural uranium has been expended to the environment over the past 34 years, and (3) synthesizes the information into an assessment of the ecological consequences of natural and depleted uranium released to the environment by various means.

Experimental data to be discussed were developed at a LASL dynamic testing site where soil uranium concentrations were 20 to 3500 times background and were 50 times greater than background at 20- to 30-cm depths, indicating significant penetration into soil horizons. Results of studies of soil, plant, and animal communities exposed to this radiation and chemical environment over a third of a century provide a means of evaluating the behavior and effects of uranium in many contexts.

Differences in the properties of natural uranium and depleted uranium, of the same purity and chemical form, are insignificant and depend only on their differences in atomic weight (238 vs. 235) (NMAB, 1971). Few environmental studies of natural uranium have

*Current address: Ecological Sciences Department, Battelle Pacific Northwest Laboratories, Richland, Washington.

been pursued in depth, and fewer still have been conducted on depleted uranium because of the limited opportunities for such studies. Chemical explosive testing areas at the Los Alamos Scientific Laboratory (LASL) in north-central New Mexico offered the opportunity to study ecological aspects of an estimated 75,000 to 100,000 kg of uranium dispersed over a relatively small area during approximately 22 years of testing.

This paper summarizes much of the pertinent literature on natural and depleted uranium in the environment and synthesizes the information into an evaluation of the ecological consequences of uranium released to the environment. In the current world political situation where conventional arms are emphasized, various scenarios are possible where appreciable amounts of depleted uranium munitions might be expended. Extrapolating the available information on uranium to such a situation is possibly complicated by the alloy nature of the ordnance applications (NMAB, 1971), which should be less subject to corrosion and less available to biotic constituents of ecosystems. However, initial results from our studies of aged deposits of natural and depleted uranium debris suggest that uranium is much more mobile in the environment than earlier literature would indicate.

SOURCE-TERM CONSIDERATIONS

Most uranium ores contain 0.1 to 2% uranium expressed as U_3O_8 and average about 0.25%. Uranium-238 constitutes about 99% and ^{235}U about 1% of the total uranium in most ores. Milling the ore removes more than 90% of the total uranium and about 2% of the ^{226}Ra, which is one of the major radioactive contaminants in the tailings (Tsivoglou and O'Connell, 1964). The refined uranium is then treated by an enrichment process at the U. S. Department of Energy gaseous diffusion complex. The treatment increases the concentration of ^{235}U in a product stream of UF_6 gas. The depleted-uranium waste from the process contains about 0.2 wt.% ^{235}U, and the remainder is composed of ^{238}U. The milling process removes most of the ^{238}U decay chain products that are of principal concern. The extremely long physical half-life of ^{238}U (4.5×10^9 years) precludes appreciable buildup of ^{226}Ra in depleted uranium during the time frame of consideration.

Most of the uranium-mill waste environmental studies have emphasized ^{226}Ra because of its radiation hazard to human health, and information about ^{238}U has been secondary (Tsivoglou, 1964).

This is perhaps because of a general feeling that uranium is an integral part of our environment.

Several investigations were made at naturally radioactive areas of terrestrial ecosystems, where elevated concentrations of Th and U minerals in local soils provided opportunities to study the translocation of heavy radionuclides from soil to man through food chains. Other investigations showed radiation effects of natural radioactivity on native biota and man. Most of these studies involved aged geological deposits of radioactive elements, in contrast to our main consideration of a contemporary, more concentrated, and perhaps more insoluble form of uranium.

A typical ordnance projectile of the type being tested by the U. S. Air Force is 30 mm in diameter and contains about 300 g, or 100 μCi, of depleted uranium, which emits predominantly 4.20-MeV (75%) and 4.12-MeV (25%) alpha particles. These have very low penetrability (< 6 μm in uranium, ~ 33 μm in water, and 2.6 cm in air) which is contained by a nylon or other coating in storage. Fired projectiles presumably lose the nylon cover. Those projectiles which impact on targets will release a variety of depleted-uranium particles that will behave similarly to natural uranium within the biogeochemical cycles.

CHARACTERISTICS AND CONSEQUENCES OF URANIUM IN TERRESTRIAL ECOSYSTEMS

Plants growing on U—V deposits of the Colorado Plateau were reported to respond to the chemical environment in three ways (Cannon, 1952). First, controlled experiments with uranium nitrate (Stoklasa and Penkava, 1928) showed that plant metabolism was affected by unusual amounts of available uranium, producing anomalous growth habits. Growth was stimulated by additions of 2 ppm uranium; poisoning symptoms were noted at 47.6 ppm; acute toxicity symptoms appeared at 476 ppm; and complete toxicity to germination of seeds occurred at 10,000 ppm. Other studies (Acqua, 1912, 1913; Bambacioni-Mezzeti, 1934) showed that 50 ppm uranium in nutrient solutions caused root injury in higher plants.

The second response is uranium absorption and translocation, where the highest concentrations are usually found in seeds and roots rather than leaves. Absorption is probably influenced by the clay content, organic matter content, soil acidity, and combination of available elements. The uranium content of any species growing in nonmineralized soil is rarely greater than 1 ppm, compared to 2 to 100 ppm in plants rooted in soil derived from uranium-bearing rock.

Most of the soluble uranium in the roots can penetrate the epidermis and then be precipitated or bonded to cellular structures within the root near the point of uptake, which may explain the localization of uranium in plant roots.

The third response of plants in high uranium areas is the development of a particular flora, or indicator species, in areas where the uranium ore body is located as much as 15 m underground. This must be viewed as a long-term response of plant communities to an environmental gradient, whose most important aspect is the chemical properties of uranium. An important consideration in all plant responses is the influence of uranium on soil microorganisms, where there was a stimulant effect at low concentrations and a toxic effect at 100 ppm. Generally, the detrimental effects of uranium on soil bacteria are expected to be less than the effects on plant cells (Luchetti, 1932).

Concentration factors (CF's) for plants growing in uraniferous soils vary considerably. Cannon (1952) reported that a wide spectrum of plants growing in mineralized soils of the Colorado Plateau contained 0.09 to 0.9 times the uranium content of shale and 0.007 to 0.01 times the uranium content of sandstone. Plants rooted in non-mineralized sandstone contained 1.25 to 1.5 times the uranium content of their substrate, although the soils contained 20 to 100 times less uranium than the mineralized types. Values of concentration factors between these two ranges were reported in Russia (Kovalsky, Vorotnitskaya, and Lekarev, 1967), where samples of soils, plants, and domestic sheep from a very broad range of environments yielded the following uranium concentration factors:

	Control area		Uranium-rich area	
Component	U (ppm, dry weight)	CF	U (ppm, dry weight)	CF
Soils	0.5		3.3	
Plants	0.013	0.026	0.78	0.24
Grasses	0.017	0.034	0.27	0.082
Sheep	0.003	0.22	0.02	0.038

Assuming that the daily intake of a sheep is about 2 kg of dry matter (Bustad and Terry, 1956), the estimated daily intake of natural uranium from the control area would be 0.06% of the amount required to produce a slight malaise in sheep, and from the uranium-rich area, the intake would be 0.1 to 0.3% of the effective level of about 50 mg (Garner, 1963). From the human radiological

health standpoint, it is estimated that sheep and cows must ingest daily 1 and 7 g of natural uranium, respectively, for mutton or beef to achieve maximum permissible concentrations. Similarly, to give the maximum permissible concentration in milk to be consumed by a child (0.6 mg/liter), the daily intake of a cow would have to be approximately 4 g of natural uranium (Garner, 1965). Although sheep inhabiting the Russian uranium-rich areas accumulated five to eight times as much uranium as the animals in the control areas, no somatic changes were noted; detrimental effects on humans would not be anticipated from the above estimates.

Experimental evidence has shown that exposure to natural U—Th terrestrial gamma radiation can be genetically and ecologically important to highly radiosensitive plant populations, such as *Tradescantia* (Mericle and Mericle, 1965). Demonstrable differences were reported in degree of morphological variability, the incidence of gross abnormalities and the rate of floral abortion in potted plants exposed to 0.25 mR/hr compared to similar plants exposed to 0.10 mR/hr external radiation from U—Th deposits. The Russian work (Kovalsky, Vorotnitskaya, and Lekareva, 1967) reported that 10 to 25% of the total number of a plant species showed morphological variability such as double flowering, leaf splitting, and corolla color variation in five plant species growing in an area where soils contained increased uranium.

Experimental study areas established at LASL in north-central New Mexico have provided unique opportunities to study the ecological behavior of aged deposits of natural and depleted uranium. Approximately 70,000 kg of uranium was expended as a part of dynamic tests conducted at the main study site during 1943 to 1972 (Hanson and Miera, 1977). This material was distributed over the landscape in a pattern (Fig. 1) that yielded uranium concentrations in surface (0- to 2.5-cm depth) soils that ranged from 30 to 5300 μg U/g soil within a distance of 140 m from the detonation point (Hanson and Miera, 1978). Background concentrations of uranium in this area ranged from 0.6 to 2.7 μg U/g. During 3 years of study of the ecosystem components of this area where uranium concentrations in surface soils are 20 to 3500 times background, we have concluded that the uranium in soil column increments to 30-cm depths has significantly penetrated into the soil horizons (Fig. 2). At 50 m from the detonation point, the concentration at 20- to 30-cm depth was about 50 times background. Plants growing in those soils exhibited uranium concentration factors of 0.05 to 0.08, or about the middle of the range of values for "uranium indicator" plants of the Colorado Plateau reported by Cannon (1952). However, much of

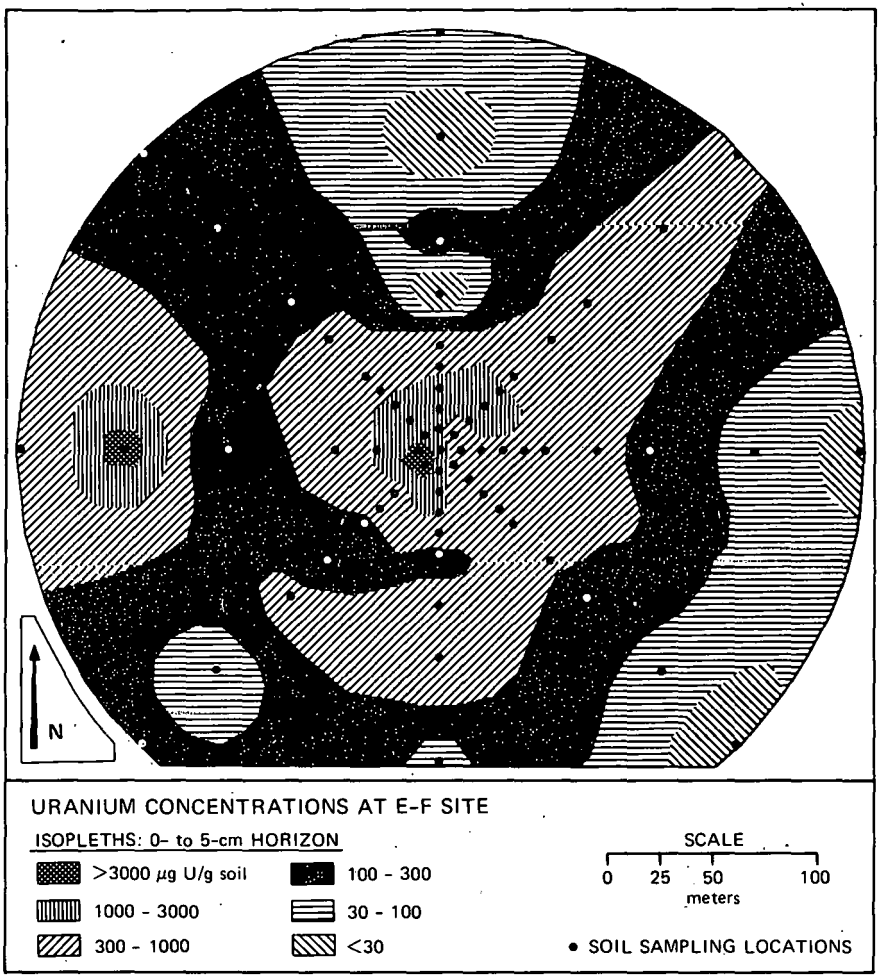


Fig. 1 Areal distribution of uranium concentrations in surface (0- to 5-cm depth) soils determined by a polar coordinate sampling method at the Los Alamos Scientific Laboratory E-F study site.

the uranium was probably due to adhering particles of uranium or uranium-contaminated soil of $< 100\ \mu m$ in diameter, as shown by collection of substantial amounts of wind redistributed uranium particulates that were moved by the phenomena of surface creep, saltation, and suspension (Hanson and Miera, 1978). We attempted to determine whether plant distribution, as reflected by species diversity, canopy coverage, frequency, and density, was affected by

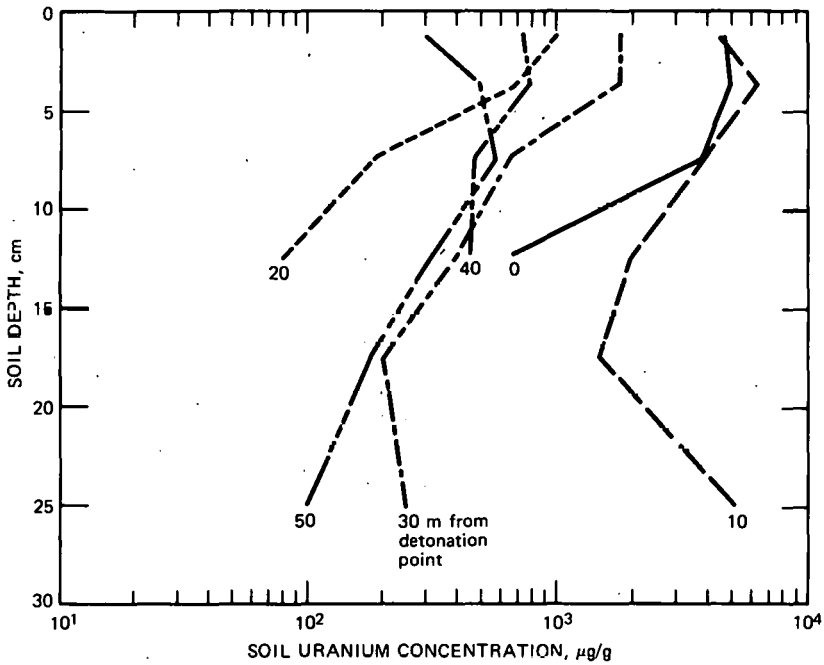


Fig. 2 Vertical distribution of uranium concentrations in soil core increments at various distances from the E-F study site detonation point.

long-term uranium deposition and to establish the possible presence of uranium indicator plants. Companion studies were conducted to evaluate possible differences in soil invertebrate populations in areas of high soil uranium compared to control areas. The data from 2 years of study of vegetation community analyses and of the soil and litter macrofauna indicated that environmental gradients other than the uranium concentrations in surface soils were responsible for natural population variations that masked any community responses to the chemical toxicity of uranium.

Uranium concentrations in tissues of deer mice (*Peromyscus maniculatus*) and pocket gophers (*Thomomys bottae*) collected from the area of elevated soil uranium concentrations were highly variable, and the concentration distributions were often positively skewed. However, there were significant differences between the several tissue types examined. Deer mice, which are surface-active animals, generally contained greater uranium concentrations in their tissues than did the pocket gophers, which burrow and are subterranean in habit. Highest uranium concentrations were in gastrointestinal tract

contents, and slightly lower values occurred in pelts. Kidneys and livers contained 5 to 10% of pelt concentrations, whereas lung and carcass samples contained amounts that were slightly above background. Food habits of these small mammals vary appreciably; the pocket gopher is a vegetarian heavily dependent on plant roots and other vegetative plant parts, whereas the deer mouse diet shifts from a preponderance (94%) of seeds, fruits, and roots during winter to mostly animal foods (76% large insects and other invertebrates) during spring, and then to mostly (68%) plant foods during summer (Martin, Zim, and Nelson, 1951). The food habits would presumably influence the concentrations of uranium in internal organs, although appreciable amounts of soil and uranium are ingested by these animals during their normal grooming habits. The relatively low fraction (10^{-4}) of uranium transferred from the gastrointestinal tract to blood (ICRP, 1959) presumably accounts for the modest concentrations found in carcass and lung samples and mitigates the consequences of ingestion of uranium from whatever source. The data in general support the conclusion that the greater bioavailability of uranium in the top few millimeters of soil at the study site resulted in greater contamination of the deer mice than of the sympatric pocket gopher population.

NATURAL URANIUM IN FRESHWATER ENVIRONMENTS

The natural-uranium content of fresh water depends on several factors, such as the geological formations in which groundwater occurs and the size and diversity of aquifer watersheds. An average value for river water in the United States may be 0.5 μg U/liter for rivers in environments of igneous rocks and clays, whereas higher values may be expected in waters leaching carbonate rocks (Koczy, 1963). Maximum uranium values are often near 200 μg/liter, which indicates a wide variance of values. The importance of this range of values can be characterized by the report that, within the United States during 1960 to 1961 "water year," the total uranium-solute load of the Nezinscot River (Maine) was about 45 kg, compared to 284,000 kg carried by the Mississippi River. The calculated total uranium-solute load of all of the U. S. rivers sampled was used to calculate that an estimated 900,000 kg of uranium was carried in solution from the continental United States to the oceans during the 1960 to 1961 "water year" (Mallory, Johnson, and Scott, 1969). In south-central Russia the inland Aral Sea was estimated to receive 176 kg/year in dissolved form and 117 kg/year as suspended material from two rivers (Kochenov and Baturin, 1967). The high uranium

concentrations in midwest U. S. rivers, relative to other rivers of the world, may be explained by solubilization of soil uranium by phosphate fertilizers applied to the land surface (Sackett and Cook, 1969; Sackett et al., 1973). The concentration of dissolved uranium in several Indian rivers ranged from 0.01 to 7.0 μg/liter, depending on the terrain through which the river flowed (Bhat and Krishnaswamy, 1969). The total annual transport of uranium by rivers to oceans and seas was estimated to be about 18 to 20 million kg in dissolved form and an equal amount as suspended material (Baturin and Kochenov, 1969; Sackett et al., 1973).

The importance of uranium solubility in surface waters as an agent in the redistribution of uranium from the Los Alamos study site was evaluated by determining uranium concentrations in intermittent stream channel sediments and by sampling storm runoff water. Alluvium samples were collected along the drainage pathway from the detonation point into the adjacent canyon and downstream to a distance of 9000 m. Water and suspended sediments that resulted from thunderstorms were collected at the study site on two occasions following rainfalls of 3.5 cm over several hours (1975) and 1 cm during a span of about 30 min (1976) (Hanson and Miera, 1977). Surface (0 to 2.5 cm) alluvium samples at a distance of 250 m from the detonation area contained 300 μg U/g, or about 10% of the uranium concentration measured in surface soils at the detonation point. Alluvium samples at 2800 m downstream contained twice the background levels (0.6 to 1.2 μg U/g). Concentrations within the alluvium at distances up to 200 m from the detonation point were highly variable to depths of 15 cm, but concentrations were homogeneous to depths of at least 20 cm throughout the 350- to 5000-m segment of the canyon stream bed downstream from the study site. We estimated that there was 58 kg of natural and depleted uranium in the top 15 cm of alluvium in the canyon below the study site, 76% being within 300 m of the source and the remainder was distributed down the canyon to 9000 m. The 58 kg is < 0.1% of the estimated total uranium expended at the detonation point and 1 to 2% of the estimated uranium inventory in the 0- to 5-cm surface soil horizon within a 12.6 ha circle centered on the detonation point (Fig. 1).

Concentrations of uranium in standing and runoff waters following the thunderstorms (Table 1) were much greater than had been expected. Standing water at the detonation point crater contained 87 mg/liter in 1975 and 280 mg/liter in 1976, with nearly all the uranium in solution. The higher uranium values in 1976 probably resulted from the more intense rainfall that contained

TABLE 1

Uranium Concentrations in Duplicate Samples of Standing Water and Runoff from E-F Site on Sept. 5, 1975, and Sept. 17, 1976

Sample	Date	Uranium in water, μg U/liter	Uranium in suspended sediments, μg U/liter	Total uranium, μg U/liter	Uranium in solution (<0.45 μm), %
Standing water at detonation point	1975	86,000 ± 2,000	590 ± 30	87,000	99
	1976	235,000 ± 5,000	47,000 ± 4,000	282,000	83
Standing water 20 m SW of detonation area	1975	63 ± 6	1,250 ± 200	1,300	5
	1976	240 ± 20	890 ± 30	1,100	21
Runoff 100 m SW of detonation point (mesa top drainage)	1975	52 ± 5	100 ± 8	152	34
	1976				
Runoff 250 m SW of detonation point (canyon stream channel)	1975	37 ± 2	54 ± 5	91	41
	1976	125 ± 9	410 ± 20	535	23

higher uranium concentrations, as seen in Table 1, carried as sediment. Concentration in the suspended sediments during the 1975 runoff event was 3900 μg U/g, or nearly comparable to average surface soil uranium concentrations within 30 m of the detonation point. These results implicated storm runoff as an important vector in transporting uranium from areas of concentration and indicate that solubility, and hence movement, of uranium through the ecosystem may be greater than anticipated (Hanson, 1974).

NATURAL URANIUM IN MARINE ENVIRONMENTS

After release into the oceans and seas, the residence time of uranium in the marine waters varies from tens of years to hundreds of thousands of years, depending on the depth.

Uranium is soluble so long as the water has a high redox potential, where it exists in the hexavalent state as a uranyl complex. In a reducing environment, uranium is reduced to tetravalent uranium, in which form it has a high affinity for organic material. Organic muds, black shales, and decaying organic material in marine environments contain uranium concentrations up to 350 μ/g. Conversely, uranium can be easily held in solution as complex uranium tetracarbonate in high carbonate waters, such as well-aerated bodies of water. These oxidizing conditions, such as found in upper layers of open oceans, often contain the low uranium

concentrations representing the soluble, long-lived portion of the uranium budget. Increases of uranium occur most spectacularly in the reducing environments of the oceans (Koczy, 1963). Uranium is present in seawater at concentrations of a few parts per billion (Stewart and Bentley, 1954). However, it is mostly associated with the sediments and has a high affinity for the organic matter in sediments. Lowest uranium values of 1 to 5 μg/g were reported in sand and silty ooze along coastal areas of the inland Aral Sea and at the junction of fresh and salt waters (Kochenov and Baturin, 1967). Values increased to 10 μg/g in sediments of the central areas of the oceanic basin. Uranium content of water around river mouths was mostly 30 to 35 μg/liter, compared to 50 to 60 μg/liter in the central area of the sea. In the large Black and Mediterranean Seas, average uranium concentrations of 2.0 μg/liter were reported in seawater (Nikolaev et al., 1960); it was generalized that such elements as molybdenum, cobalt, nickel, and vanadium might be distributed in the same way as uranium in organic matter. In the Black Sea a correlation with organic matter was more obvious for uranium and molybdenum, whereas in the Mediterranean Sea, the distribution of the metals was quite similar. A poor correlation between organic matter and metals other than uranium in the surface layer of silts was explained by redistribution or recombination processes (Baturin, Kochenov, and Shimkus, 1967). The enrichment of uranium in sediments of the Baltic and Black Seas by a factor of 8 over the amounts in seawater was attributed to appreciable amounts of hydrogen sulfide in those waters (Baturin, 1966). By comparison, sediments from the central Caspian Sea, which was low in H_2S, contained 0.1 to 1.0 as much uranium as the Baltic and Black Sea sediments.

The concentration of uranium in the sediments compartment of the aquatic ecosystems is indicative of low uranium inventories in biological systems. In humid regions of eastern Siberia, plants growing in moist soils had a range of CF's of 10^{-4} to 10^{-1}, with maxima in mosses (Lopatkina et al., 1970). This ranking suggests that plants growing in wet environments, having extensive surface areas, provide more accumulation sites for uranium rather than an active uptake of the element. Aquatic food webs of Lake Issyk-Kul in southeastern Russia, which had a relatively high uranium concentration in water (30 μg/liter), showed a regular decrease along the route algae $\rightarrow$ benthic and planktonic animals $\rightarrow$ fish. Least amounts of uranium were concentrated by predatory fish, whereas greatest amounts were concentrated by plant-feeding species (Kovalsky and Vorotnitskaya, 1966; Kovalsky, Vorotnitskaya, and Lekarev, 1967).

TOXICITY OF URANIUM IN AQUATIC ENVIRONMENTS

The relative toxicity of uranium compounds is reported as follows (Tannenbaum and Silverstone, 1951):

UO_2, U_3O_8, UF_4	Relatively nontoxic, even in large doses
UO_3, UCl_4	Toxic in large doses
$UO_2(NO_3)_2$, UO_4, $Na_2U_2O_7$	Toxic in moderate doses
UO_2F_2	Toxic, even in relatively small doses, probably due to F toxicity

Thus, when uranyl nitrate $UO_2(NO_3)_2$ was added to a freshwater reservoir at a uranium concentration of 1.0 mg/liter, the growth of microflora was inhibited and decomposition processes were hindered. At a concentration of 100 mg/liter, a bactericidal effect was noted. The same level of ^{239}Pu radioactivity in water did not affect the growth and development of microorganisms, bacteria, or algae; therefore it was concluded that the toxicity of the uranium resulted from its chemical action (Gus'kova, Gurfein, and Tikhonova, 1966). Similarly, Gross and Koczy (1946) concluded from experiments that soluble uranium at concentrations greater than 100 μg U/liter severely decreased diatom survival.

ANTICIPATED CONSEQUENCES OF DEPLETED URANIUM IN AQUATIC ECOSYSTEMS

Depleted uranium released to aquatic systems is expected to consist of the relatively nontoxic uranium compounds, which will possibly be less soluble in water than natural uranium because of its alloy properties. The slow corrosion behavior of depleted uranium, the extremely low CF's for biota expected on the basis of data obtained from the more soluble natural uranium, and the appreciable natural-uranium load of the major water areas of the world indicate that most, if not all, of the anticipated additions of depleted uranium will have little or no impact on major water bodies.

Depleted-uranium deposits in small water bodies probably will involve conditions of slow dissolution of the depleted uranium but will promote its mobility and widely distribute it by natural means, particularly in carbonate waters. A greater proportion of the uranium will be in the soluble form under such conditions, and it may be physically translocated or be biologically concentrated in small amounts. Uranium concentrated in lake sediments might inhibit decomposition and thus perturb normal nutrient cycles.

A similar release to marine environments will free the depleted uranium in a much shorter time because of the corrosive nature of seawater; however, the release of depleted uranium, under the expected conditions, will not be noticed in the normal uranium background of seawater.

SUMMARY AND CONCLUSIONS

Depleted uranium in various ecosystems will behave as natural uranium, but with lower solubility if in an alloy form and without the serious consequences of ^{226}Ra that normally accompanies unrefined uranium. These characteristics provide conservative measures for comparing depleted uranium with most of the reported studies of occurrence, behavior, and effects of natural uranium in ecosystems. The principal concern will be its chemical toxicity rather than its radioactive properties.

Depleted uranium released to aquatic environments is expected to have a minor impact because of low solubility, except in the case of carbonate waters, and because of the appreciable amount of natural uranium normally transported by rivers from the continental landscape. This soluble and suspended solids load of uranium has been estimated to be 1000 tons/year from the United States and 40,000 tons from all world land areas. Marsh environments may contain aquatic plants that concentrate uranium in water by factors of 10^{-4} to 10^{-1}; however, such concentrations are expected to occur in limited components. Uranium is decreasingly concentrated along the aquatic food webs, with least amounts in those food chains terminating in predatory fish, such as salmon or trout. These are the major human food sources of interest and should be minimally affected from released depleted uranium.

Consequences of depleted uranium released to terrestrial ecosystems are of major importance because of the chemical toxicity of uranium, its demonstrated solubility, and mobility into soil profiles. Based on plant communities that colonize natural-uranium ore bodies and on controlled experiments, toxicity may occur at soil concentrations near 50 μg U/g, and acute toxicity symptoms may be expected in higher plants at about 10 times that concentration. Field studies at LASL have not shown detrimental responses of plant communities, soil and litter macrofauna, and small mammal populations to elevated levels of uranium in soils; however, other environmental gradients may have masked such responses. Therefore those lower values of 50 to 500 μg U/g should be considered as realistic guidelines until further evaluations can be made of the

ecological consequences of depleted uranium exposed to environmental weathering for long periods.

ACKNOWLEDGMENTS

The assistance of F. R. Miera, Jr., K. V. Bostick, J. L. Martinez, G. Trujillo, E. Gladney, P. Jose, and J. Owens in these studies is gratefully acknowledged. Financial support was provided by the U. S. Air Force Armament Laboratory at Eglin Air Force Base, Florida, and by U. S. Department of Energy contract W-7405-ENG-26.

REFERENCES

Acqua, C., 1912, The Action of Uranium on the Vegetable Cell, *Arch. Farmacd. Sper.*, 14: 81-84.

——, 1913, Nuclear Degeneration Produced by Uranium in the Plant Cell, *R. Accadi Lincei e Sci., Rendus*, 22: 390-392.

Bambacioni-Mezzeti, V., 1934, Action of Uranium Chloride and of Gamma Rays on the Geotropical Sensibility of Roots, *Soc. Ital. Progr. Sci.*, 22: 56-57 (in Italian).

Baturin, G. N., 1966, Uranium Content in Caspian Sea Sediments, *At. Energ. (USSR)*, 21: 516-517 (in Russian).

——, and A. V. Kochenov, 1969, Migration of Uranium in Rivers and the Duration of Its Presence in Waters of the World's Oceans, Seas, and Lakes, *Geokhimiya*, 6: 715-723 (in Russian).

——, A. V. Kochenov, and K. M. Shimkus, 1967, Uranium and Minor Metals in Columns of Bottom Sediments of the Black and Mediterranean Seas, *Geokhimiya*, 1: 41-50 (in Russian).

Bhat, S. G., and S. Krishnaswamy, 1969, Isotopes of Uranium and Radium in Indian Rivers, *Proc. Indian Acad. Sci., Sect. A*, 1: 1-17.

Bustad, L. K., and J. L. Terry, 1956, *Basic Anatomical, Dietary, and Physiological Data for Radiological Calculations*, USAEC Report HW-41638, General Electric Co., Richland, Wash.

Cannon, H. L., 1952, The Effect of Uranium—Vanadium Deposits on the Vegetation of the Colorado Plateau, *Am. J. Sci.*, 250: 735-770.

Garner, R. J., 1963, Environmental Contamination and Grazing Animals, *Health Phys.*, 9: 597-605.

——, 1965, Natural Uranium and Grazing Animals, *Health Phys.*, 11: 323.

Gross, F., and F. F. Koczy, 1946, Photometric Measurements of the Growth of Phytoplankton Cultures, *Medd. Oceanogr. Inst.*, No. 10.

Gus'kova, V. N., L. N. Gurfein, and A. I. Tikhonova, 1966, Uranium Action in a Reservoir, *Gidrobiol. Zh.*, 2: 53-57 (in Russian).

Hanson, W. C., 1974, *Ecological Considerations of Depleted Uranium Munitions*, Report LA-5559, Los Alamos Scientific Laboratory.

——, and F. R. Miera, Jr., 1977, *Continued Studies of Long-Term Ecological Effects of Exposure to Uranium*, Report LA-6742 (AFATL-TR-77-35), Los Alamos Scientific Laboratory.

——, and F. R. Miera, Jr., 1978, *Further Studies of Long-Term Ecological Effects of Exposure to Uranium*, Report LA-7162 (AFATL-TR-78-8), Los Alamos Scientific Laboratory.

International Commission on Radiological Protection (ICRP), 1959, *Report of Committee II on Permissible Dose for Internal Radiation*, ICRP Publication 2, p. 225, Pergamon Press, New York.

Kochenov, A. V., and G. N. Baturin, 1967, The Distribution of Uranium in the Bottom Sediments of the Aral Sea, *Okeanologiya*, 7: 623-627 (in Russian).

Koczy, F. F., 1963, The Natural Radioactive Series in Organic Material, in *Radioecology*, V. Schultz and A. W. Klement, Jr. (Eds.), pp. 611-613, Reinhold Publishing Corporation, New York.

Kovalsky, V. V., and I. E. Vorotnitskaya, 1966, Regularities in the Biogenic Migration of Uranium, *Ukr. Biokhim. Zh.*, 38: 419-442 (in Russian).

——, I. E. Vorotnitskaya, and V. S. Lekarev, 1967, Biogeochemical Food Chains of Uranium in Aquatic and Terraneous Organisms, in *Radioecological Concentration Processes*, B. Aberg and F. P. Hungate (Eds.), pp. 329-332, Pergamon Press, Oxford.

Lopatkina, A. P., V. S. Komarov, A. N. Sergeyev, and A. G. Andreyev, 1970, Brief Communications on Concentration of Uranium by Living and Dead Peat-Forming Plants, English translation, *Geochem. Int.*, 7: 277-282.

Luchetti, G., 1932, The Action of Uranium Salts on Soil Microorganisms and on Their Functions, *Boll. Inst. Super. Agrar. Pisa*, 8: 471-491.

Mallory, E. C., Jr., J. O. Johnson, and R. C. Scott, 1969, Water Load of Uranium, Radium, and Gross Beta Activity at Selected Gaging Stations, Water Year 1960—1961, USGS Report WP-1535-0.

Martin, A. C., H. S. Zim, and A. L. Nelson, 1951, *American Wildlife and Plants*, pp. 261-262, McGraw-Hill Book Co., New York (Dover reprint).

Mericle, L. W., and R. P. Mericle, 1965, Reassessing the Biological Role of Background Terrestrial Radiation as a Constituent of the Natural Environment, *Health Phys.*, 11: 1607-1620.

National Materials Advisory Board (NMAB), 1971, Trends in the Use of Depleted Uranium, Report NMAB-275, National Academy of Sciences—National Academy of Engineering, Washington.

Nikolaev, D. C., O. P. Koron, K. F. Lazarev, L. B. Kolyadin, Yu. V. Kunznetsov, and S. M. Grashehenko, 1960, The Concentration of Uranium in the Waters of the Black Sea, *Dokl. Akad. Nauk SSSR*, 132: 1411-1412 (in Russian).

Sackett, W. M., and G. Cook, 1969, Uranium Geochemistry of the Gulf of Mexico, *Trans. Gulf Coast Assoc. Geol. Soc.*, 19: 233-238.

——, T. Mo, R. S. Spalding, and M. E. Exner, 1973, A Revaluation of the Marine Geochemistry of Uranium, in *Radioactive Contamination of the Marine Environment*, pp. 757-769, STI/PUB/313, International Atomic Energy Agency, Vienna.

Stewart, D. C., and W. C. Bentley, 1954, Analysis of Uranium in Sea Water, *Science*, 120: 50-51.

Stoklasa, J., and J. Penkava, 1928, Biology of Uranium, *Biochem. Z.*, 194: 15-77.

Tannenbaum, A., and H. Silverstone, 1951, Factors Affecting Uranium Poisoning, in *Toxicology of Uranium*, A. Tannenbaum (Ed.), pp. 11-15, McGraw-Hill Book Co., New York.

Tsivoglou, E. C., 1964, Environmental Monitoring in the Vicinity of Uranium Mills, in *Radiological Health and Safety in Mining and Milling of Nuclear*

Materials, pp. 231-245, STI/PUB/78, International Atomic Energy Agency, Vienna.

——, and R. L. O'Connell, 1964, Nature, Volume and Activity of Uranium Mill Wastes, in *Radiological Health and Safety in Mining and Milling of Nuclear Materials*, pp. 101-121, STI/PUB/78, International Atomic Energy Agency, Vienna.

United Press International (UPI), 1977, Uranium Debris Harmless, news item, *Playground Daily News*, page 2B, Fort Walton Beach, Fla.

Intercomparison Experiment at NRE III

CARL V. GOGOLAK* and THOMAS F. GESELL†
*U. S. Department of Energy, Environmental Measurements Laboratory;
†University of Texas, School of Public Health

ABSTRACT

As part of the third international symposium on the natural radiation environment, an informal instrument intercomparison experiment was held near Burnet, Tex. Thirteen groups representing 11 laboratories from 5 countries participated. Measurements of air concentrations of ^{222}Rn and its short-lived daughters and of the external exposure rate due to gamma and cosmic radiation were made. The results at each of three sites especially chosen for each type of measurement are reported. References to the methods and techniques used by the various groups are given.

On Apr. 29, 1978, the day after the close of the symposium, an informal intercomparison of environmental radiation measurements was held near Burnet, Tex. Thirteen groups representing 11 laboratories from 5 countries brought instruments, and a number of symposium attendees participated as observers. Two sections were organized, one to accommodate those whose primary interest was in the measurement of air concentrations of radon and its short-lived decay products and the other for those whose primary interest was the measurement of external gamma and cosmic radiation levels. Several groups participated in both sections. The measurements made and techniques used, by each group, are listed in Tables 1 and 2. Where appropriate, references to literature describing instruments and methods are also given. Some groups used this opportunity to field test prototype or partially calibrated instruments for the first time, while others used well-established techniques. The participating laboratories are listed in Table 3.

TABLE 1

Radon and Radon Progeny Concentration Measurement Techniques

Group	Measurement	Sample	Analysis technique	References
A	^{222}Rn	125 ml of air	Alpha counting of scintillation (Lucas) cell	Lucas, 1957
C	Working level	Air filter	Kusnetz	Kusnetz, 1956
D	^{222}Rn	153 ml of air	Alpha counting of scintillation (Lucas) cell	Lucas, 1957
	Working level	0.8 μ Millipore air filters Glass fiber air filters	Modified Kusnetz	IAEA, 1976
F	^{222}Rn	Air	Prototype ionization chamber alpha count rate, first field use	
	^{218}Po, ^{214}Pb, ^{214}Bi, working level	Air filter	Prototype instrument, alpha and beta counting, first field use	Groer et al., 1974
G	^{218}Po, ^{214}Pb, ^{214}Bi, working level	Glass fiber air filter	Least squares fit to alpha decay curve	Raabe and Patterson, 1964
H	^{222}Rn	515 ml of air	Alpha counting of scintillation cell	George, 1976
	^{218}Po, ^{214}Po, ^{214}Bi, working level	Glass fiber air filter	Modified Tsivoglou (3 alpha counts)	Thomas, 1972
I	^{222}Rn	1 liter of air	Alpha counting, pulse ionization chamber	Harley, 1972
K	^{218}Po, working level	Air filter	2 alpha counts	James and Strong, 1973
	^{218}Po, ^{214}Po, ^{214}Bi, working level	Air filter	3 alpha counts	Cliff, 1978
M	^{218}Po, ^{214}Po, ^{214}Bi, working level	Air filter	Modified Tsivoglou (3 alpha counts)	Thomas, 1972

TABLE 2

External Exposure Rate Measurement Techniques

Group	Measurement	Instrumentation	Technique	References
A	Gamma	1 in. by 1 in. NaI(Tl) (Eberline PRM-7)	Count rate, ^{226}Ra calibration	
		1 in. by 1 in. NaI(Tl) (Ludlum 19)	Count rate, ^{226}Ra calibration	
B	Gamma and cosmic	1.5 in. by 1.5 in. ZnS coated organic scintillator (Automess Corp. Szintomat 6134)	Direct PM current, factory calibration	Kolb and Lauterbach, 1974
C	Gamma and cosmic	High pressure argon ionization chamber (Reuter—Stokes RS 111)	Direct current, factory calibration	
D	Gamma	1 in. by 1 in. NaI(Tl) (Eberline PRM-7)	Count rate	
E	Gamma	3 in. by 3 in. NaI(Tl)	Count rate	Wollenberg and Smith, 1964
	^{238}U, ^{232}Th, ^{40}K	8 in. by 4 in. NaI(Tl) spectrometer	Spectral analysis	Wollenberg and Smith, 1964
F	Gamma and cosmic	High pressure argon ionization chamber (Reuter—Stokes RS 111)	Direct current	
G	Gamma and cosmic	High pressure argon ionization chamber	Direct current	DeCampo, Beck, and Raft, 1972
	Cosmic	Calculated		O'Brien, 1978
	^{238}U, ^{232}Th, ^{40}K	Ge(Li) spectrometer	In situ spectrum	Beck, DeCampo, and Gogolak, 1972
	Concentration			Gogolak and Miller, 1978
J	Gamma and cosmic	3-in. diameter spherical NaI(Tl)	In situ spectrum	Okano, Izumo, and Kumagai, this volume
L	Gamma and cosmic	3 in. by 3 in. ZnS coated organic scintillator (Halle Corp. H 7201B)	Direct PM current	Kolb and Lauterbach, 1974a; 1974b

In the following discussion, averages refer to the simple arithmetic mean of the final values reported by each group, omitting those specifically indicated as the result from a prototype or partially calibrated instrument. The errors shown are those reported by each participant and usually indicate one standard deviation counting statistics.

TABLE 3

Participating Laboratories

Radon section
- National Radiological Protection Board, Harwell, Didcot, Oxon, United Kingdom
- Naval Surface Weapons Center, White Oak, Md., U.S.A.
- U. S. Department of Energy, Environmental Measurements Laboratory, Analytical Chemistry Division and Aerosol Studies Division, New York, N. Y., U.S.A.

External exposure rate section
- Institut fur Strahlenschutz, Gesellshaft fur Strahlen und Umweltforschung MBH, Munchen—Neuherberg, Federal Republic of Germany
- Institute of Physical and Chemical Research, Wako—Shi, Saitama, Japan
- Physikalisch—Technische Bundesanstalt, Braunschweig, Federal Republic of Germany
- University of California, Lawrence Berkeley Laboratory, Health Physics Division, Berkeley, Calif., U.S.A.

Both sections
- Dilworth, Secord, Meagher, and Associates in consultation with Acres Consulting Services Limited (DSMA/ACRES), Elliot Lake, Ontario, Canada
- University of Texas, School of Public Health, Houston, Tex., U.S.A.
- U. S. Department of Energy, Environmental Measurements Laboratory, Radiation Physics Division, New York, N. Y., U.S.A.
- U. S. Environmental Protection Agency, Eastern Environmental Radiation Facility, Montgomery, Ala., U.S.A.
- U. S. Environmental Protection Agency, Office of Radiation Programs, Las Vegas, Nev., U.S.A.

RADON AND RADON DAUGHTER CONCENTRATIONS

The Radon Section made measurements at two underground caverns and outdoors over a lawn. These sites were chosen to provide a range of anticipated ^{222}Rn concentrations from greater than 100 pCi/liter to less than 1 pCi/liter. The results at each of these locations are given in Tables 4, 5, and 6.

Cavern A

The ^{222}Rn concentration measurements at this site ranged from 110 to 122 pCi/liter, with the exception of the prototype instrument used by group F. There was more scatter in the radon daughter and working level measurements (0.442 to 0.756 WL). With a large number of people working in a relatively confined area, the radon daughter air concentrations would be expected to be disturbed more than that of the radon gas, especially with several pumps operating to draw air samples. To what extent this may have affected the results is uncertain.

A comparison of the average ^{222}Rn concentration (116 pCi/liter) with the average working level determination (0.62 WL) indicates a relatively high degree of disequilibrium between radon and its daughters.

Cavern B

In this cavern the ^{222}Rn concentration measurements ranged from 5.3 to 7.0 pCi/liter, and the working level determinations ranged from 0.034 to 0.056 WL. The average ^{222}Rn concentration (6.2 pCi/liter) and the average working level determination (0.048 WL) indicate that radon and its decay products were nearer to secular equilibrium at this location than in cavern A. The results from group K show the concentrations may have been changing significantly with time.

Outdoor Site

Few of the groups brought instrumentation sensitive enough for the measurement of outdoor ambient levels of radon and its daughters. The results show ^{222}Rn concentrations of 0.15 to 0.3 pCi/liter and daughter concentrations of 0.0007 to 0.0008 WL.

EXTERNAL PENETRATING RADIATION

External gamma- and cosmic-ray exposure rate measurements were made primarily at three sites, over a limestone outcrop, over a granite outcrop, and over a lake. In addition, several groups made

TABLE 4

Cavern A, Georgetown and Edwards Limestones of the Lower Cretaceous System*

Group	Time, CST	Concentration, pCi/liter ^{222}Rn	^{218}Po	^{214}Pb	^{214}Bi	Working level	Notes
A	1710—1725	122 ± 15					Six measurements, range 101—142
C						0.581 ± 0.017	
D	1706—1719	110 ± 17					Four measurements, range 84—117
	1705—1723					0.64 ± 0.06	Four measurements, range 0.59—0.64; negligible thoron daughters equilibrium fraction = 58%
F	1703 —1745	60	63.5	47.5	36.5	0.442	Average of two measurements
H	1742	115 ± 3					
	1742	117 ± 3					
	1707—1717		78.5 ± 6.1	81.4 ± 1.2	79.4 ± 1.6	0.756 ± 0.005	
I	1730	120 ± 2					
	1727	115 ± 2					
K	1705—1715		48.4 ± 2.2			0.490 ± 0.003	
	1705—1715		49.2 ± 3.8	52.6 ± 2.8	49.6 ± 1.1	0.512 ± 0.010	
M			135	96	22	0.72	Count times not optimal

Group	Exposure rate, μR/hr Total	Cosmic ray	Terrestrial gamma
B	8—11		
E	10		
J	9.7 ± 0.2	0.29 ± 0.03	9.4 ± 0.2
L	10—15		

*Elevation: 244 m (MSL at surface). Latitude: 30°36′37″N (geographic), 40°39′00″N (geomagnetic). Longitude: 97°41′16″W (geographic), 33°01′48″W (geomagnetic).

TABLE 5

Cavern B, Upper Massive Limestone Member of the Gorman Formation of the Ellenberger Group in the Lower Ordovician System*

Group	Time, CST	Concentrations, pCi/liter				Working level	Notes
		^{222}Rn	^{218}Po	^{214}Pb	^{214}Bi		
A	0900	6.8 ± 0.5					Three measurements, range 6.4—7.3
C						0.051 ± 0.005	
D	0928	6.0 ± 1.5					
	0927—0932					0.043 ± 0.004	70% equilibrium fraction
F	0917—1020		3.7	3.8	3.2	0.035	Average of three measurements
H	1008	5.3 ± 0.3					
	1013	5.3 ± 0.3					
	0927—0937		3.4	5.7	6.1	0.056	Count times not optimal
I	0946	7.0 ± 0.1					
	0953	6.1 ± 0.1					
K	0925—0935		3.8 ± 0.6			0.035 ± 0.001	
	1010—1020		4.5 ± 0.6			0.046 ± 0.001	
	0925—0935		3.5 ± 1.0	3.3 ± 0.7	3.6 ± 0.6	0.034 ± 0.002	
	1010—1020		4.6 ± 1.1	5.3 ± 0.8	4.5 ± 0.7	0.049 ± 0.003	

*Elevation: 415 m (MSL at surface). Latitude: 30°41′02″N (geographic), 40°39′00″N (geomagnetic). Longitude: 98°20′57″W (geographic), 33°46′48″W (geomagnetic).

TABLE 6

Outdoor Site*

Group	Time, CST	Concentrations, pCi/liter				Working level	Notes
		^{222}Rn	^{218}Po	^{214}Pb	^{214}Bi		
A	1445	0.3 ± 0.2					Six measurements, range 0.19—0.52
D	1445					0.0007 ± 0.0001	
	1514					0.0007 ± 0.0001	
G	1511—1526		0.13 ± 0.02	0.09 ± 0.01	0.06 ± 0.01	0.0008 ± 0.0001	
	1536—1551		0.09 ± 0.03	0.08 ± 0.03	0.08 ± 0.01	0.0008 ± 0.0001	
I	1530	0.15 ± 0.02					
	1535	0.15 ± 0.02					
H	1536	<0.2					
	1551	<0.2					

Group	Time, CST	Exposure rates, μR/hr		
		Total	Cosmic ray	Terrestrial gamma
E	1530			3.8
G	~1600	8.0	4.2	3.8
J	1520	8.5 ± 0.2	4.1 ± 0.1	4.4 ± 0.2

*Elevation 402 m (MSL). Latitude: 30°45′24″N (geographic), 40°44′24″N (geomagnetic). Longitude: 98°13′53″W (geographic), 33°39′36″W (geomagnetic).

measurements at cavern A and at the outdoor radon site. These sites were chosen to provide a range of exposure rates over undisturbed areas. The results for the three primary locations are given in Tables 7, 8, and 9.

The instruments used by groups A and B had not been fully calibrated at the time of the intercomparison. Group A had noted that previously instruments of the type they used required a 0.5 correction factor to their ^{226}Ra calibration in order to infer the correct terrestrial gamma-ray exposure. The same is true for their newer instruments.

In the following, it should be noted that NaI(Tl) scintillometers usually have an internal background and a small cosmic-ray response. Unless these are specifically accounted for, measurements taken with these instruments tend to be slightly high, which is especially apparent when the terrestrial gamma-ray exposure rates are low.

Limestone Outcrop

With the exceptions noted previously, the total exposure rate measurements at this site were closely grouped near a mean of ~5.7 μR/hr. The terrestrial gamma exposure rates inferred from spectral data by groups E and G (0.8 and 1.0 μR/hr) appear low compared to that determined by other means (1.4—2 μR/hr). The spectral analyses of groups G and E assume a uniform source in converting in situ primary gamma-ray flux and radionuclide concentrations, respectively, to exposure rate. However, the surrounding soil was higher in activity than the limestone (see the spectral data of group E). Scattered radiation from this source appears to have added ~0.5 μR/hr to the exposure rate which would be obtained over a semi-infinite slab of the limestone.

Granite Outcrop

The majority of the total exposure rate measurements were in the narrow range of 24.7 to 27.5 μR/hr, with an average of approximately 25.7 μR/hr. Estimates from spectral data of the terrestrial gamma-ray component alone ranged from 20.6 to 23.6 μR/hr. The cosmic-ray contribution to the total exposure rate was ~4.0 μR/hr.

It should be noted that an in situ spectrometer, with the detector positioned 1 m above the ground, sees an effective sample area approximately 10 m in diameter. Caution must be exercised when comparing sample analyses with in situ spectrums, since samples are not always representative of as large an area (for example, see the results of Group E for three different samples). In addition,

TABLE 7

Limestone Outcrop, Upper Massive Limestone Member of the Gorman Formation of the Ellenberger Group in the Lower Ordovician System*

Exposure rate, μR/hr			Concentrations			
Group	Total	Terrestrial gamma	^{238}U, ppm	^{232}Th, ppm	^{40}K, %	Notes
A		5.5				Calibrated for ^{226}Ra only
		5.7				Calibrated for ^{226}Ra only
B	2.2—3.6					Not fully calibrated
C	5.8					Measurement not concurrent with others
D		2—3				
E		1.9				
		0.8	0.52 ± 0.01	0.36 ± 0.02	0.210 ± 0.002	Limestone rock sample; little ^{222}Rn emanation
			1.52 ± 0.01	5.20 ± 0.04	0.518 ± 0.003	Sample of surrounding soil; ~12% ^{222}Rn emanation
G	5.7	1.5				4.2 μR/hr cosmic calculated
	5.2	1.0	0.75 ± 0.05	0.48 ± 0.10	0.21 ± 0.01	4.2 μR/hr cosmic calculated
J	5.4 ± 0.1	1.45 ± 0.05				4.1 ± 0.1 μR/hr cosmic measured
L	5.5—6.5					

*Elevation: 414 m (MSL). Latitude: 30°41′02″N (geographic), 40°39′00″N (geomagnetic). Longitude: 98°20′57″W (geographic), 33°46′48″W (geomagnetic).

TABLE 8

Granite Outcrop, Precambrian Pink Quartz—Feldspar Gneiss (Valley Spring Gneiss)*

Group	Exposure rate, μR/hr		Concentrations			Notes
	Total	Terrestrial gamma	^{238}U, ppm	^{232}Th, ppm	^{40}K, %	
A		45				Calibrated for ^{226}Ra only
		46				Calibrated for ^{226}Ra only
B	17—19					Not fully calibrated
C	25.2					Measurement not concurrent with others
D		25				
E		27.5				
		20.6	6.06 ± 0.13	34.2 ± 0.5	4.05 ± 0.03	Fine grained rock sample; no ^{222}Rn emanation
			2.63 ± 0.06	13.6 ± 0.2	5.80 ± 0.02	Coarse grained rock sample; no ^{222}Rn emanation
			5.44 ± 0.06	24.6 ± 0.2	4.18 ± 0.01	Sample of surrounding soil; ~17% ^{222}Rn emanation
F	25.5					
G	24.7	20.6				4.1 μR/hr cosmic calculated
	25.2	21.1	8.71 ± 0.18	31.0 ± 0.6	3.82 ± 0.05	4.1 μR/hr cosmic calculated
J	27.5 ± 0.7	23.6 ± 0.6				3.9 ± 0.1 μR/hr cosmic measured
L	26					

*Elevation: 305 m (MSL). Latitude: 30°45′01″N (geographic), 40°43′12″N (geomagnetic). Longitude: 98°21′19″W (geographic), 33°48′00″W (geomagnetic).

TABLE 9

Lake*

Group	Exposure rate, μR/hr				Notes
	Lake		Shore		
	Total	Terrestrial gamma	Total	Terrestrial gamma	
A		3		26	Calibrated for ^{226}Ra only
		2		29	Calibrated for ^{226}Ra only
B	2.8—4.0		12—14		Not fully calibrated
C	4.5				Measurements not concurrent with others
D		0.5—1.0		14—15	
E		0.6			
G	4.3	0.2			4.1 μR/hr cosmic calculated
J	4.4 ± 0.1	0.26 ± 0.02	19.4 ± 0.1	15.3 ± 0.9	4.1 ± 0.1 μR/hr cosmic measured
L	4.2—4.8		15—19		

*Elevation: 309.4 m (MSL). Latitude: 30°44′30″N (geographic), 40°42′00″N (geomagnetic). Longitude: 98°25′30″W (geographic), 33°52′48″W (geomagnetic).

sample results are usually quoted for dry soil, with ^{226}Ra in equilibrium with its daughters. Group E's results show little or no ^{222}Rn exhalation from the granite outcrop, and there was very little moisture in the rock. They considered the fine grained rock to be the most representative of the area. Figures 1 and 2 show in situ NaI(Tl) and Ge(Li) spectrums taken at this site by Group J and Group G, respectively.

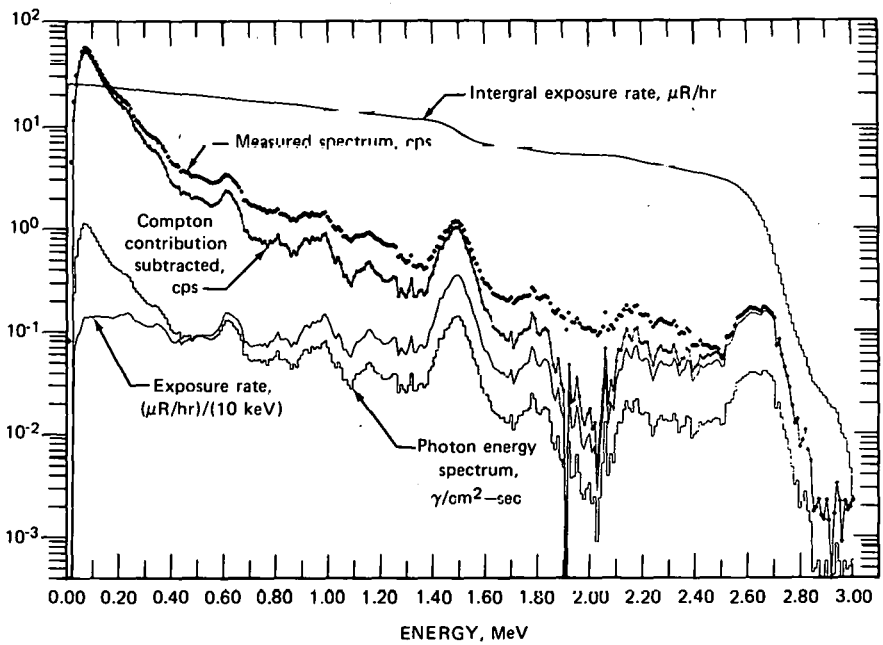


Fig. 1 A 1500-sec in situ spectrum taken with a 3-in. diameter spherical NaI(Tl) detector at the granite outcrop by Group J.

Lake

Measurements were made over a large lake to compare the cosmic-ray response of the various instruments used. The mean exposure rate measured was ~4.4 μR/hr. Two independent determinations of the cosmic-ray component gave 4.1 μR/hr (theoretical calculation by Group G and inferred from the NaI(Tl) spectrum from 3 to 8 MeV by Group J). This indicates ~0.3 μR/hr was due to terrestrial sources, most probably radon daughters in the air and ^{40}K in the experimenters.

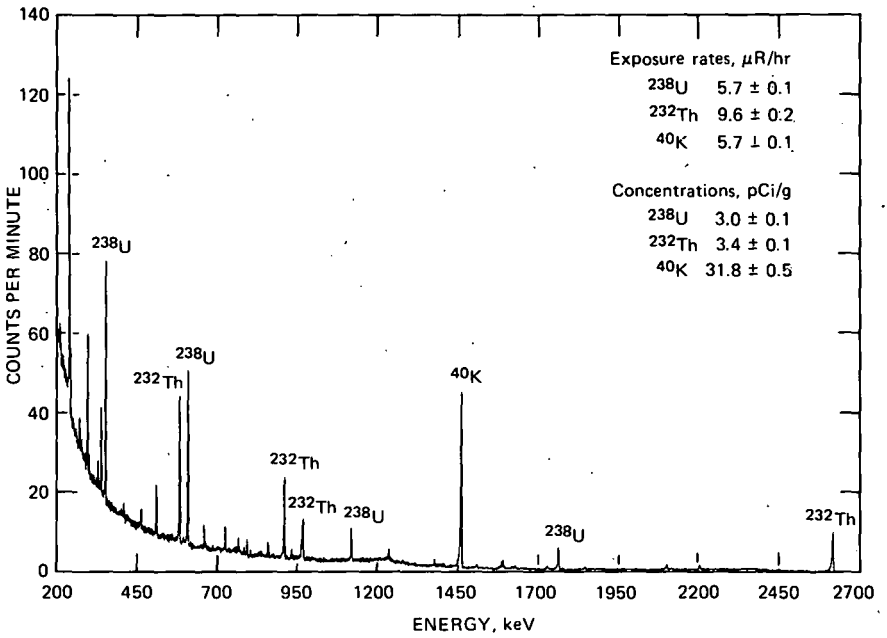


Fig. 2 A 2000-sec in situ spectrum taken with a 130 cm^3 Ge(Li) detector at the granite outcrop by Group G (peaks used in calculating the exposure rates from the ^{238}U and ^{232}Th series, assuming equilibrium, and ^{40}K are indicated).

CONCLUSIONS

As the data indicate, the agreement among the various groups participating in the experiment was generally quite good, especially considering the sometimes difficult circumstances under which the measurements were performed. Of course, some of these difficulties are an unavoidable part of field investigations. It is important to intercompare methods and techniques in the circumstances under which they are actually used. However, some of the variance in the results is unquestionably the result of having a large number of people attempting simultaneous measurements, particularly of radon daughters in the confined areas of the caverns.

The intercomparison was attended by representatives of laboratories throughout the world who used many different measurement techniques. Thus the consistency of the results obtained provides a degree of confidence in the data published by these groups. In addition, there are other important reasons for conducting periodic informal intercomparison experiments. They provide an opportunity

for new instruments and new techniques to be compared with the older more established ones, and this should aid in their development and use. Subtle differences in technique are sometimes revealed and ideas can be exchanged in ways that are not usually possible on the floor of the conference hall. Some of these less tangible results are often the most rewarding.

ACKNOWLEDGMENTS

This intercomparison could not have been carried out without the cooperation of Lewis Cook and Brad Caskey of the Texas State Department of Health, the staff of the Texas State Department of Parks, the owners and managers of the underground caverns, and the students and staff of the University of Texas School of Public Health.

REFERENCES

Beck, H. L., J. DeCampo, and C. Gogolak, 1972, *In Situ Ge(Li) and NaI(Tl) Gamma-Ray Spectrometry*, USAEC Report HASL-258, Health and Safety Laboratory, NTIS.

Cliff, K. D., 1978, The Measurement of Low Concentrations of Radon-222 Daughters in Air with Emphasis on RaA Assessment, *Phys. Med. Biol.*, 27: 55.

DeCampo, J. A., H. L. Beck, and P. D. Raft, 1972, *High Pressure Argon Ionization Chamber Systems for the Measurement of Environmental Radiation Exposure Rates*, USAEC Report HASL-260, Health and Safety Laboratory, NTIS.

George, A. C., 1976, Scintillation Flasks for the Determination of Low Level Concentrations of Radon, in *Proceedings of the 9th Midyear Topical Symposium of the Health Physics Society: Operational Health Physics*, Feb. 9—12, 1976, Denver, Colo., P. L. Carson, W. R. Hendee, and D. C. Hunt (Eds.), pp. 112-115.

Gogolak, C. V., and K. M. Miller, 1977, New Developments in Field Gamma Ray Spectrometry, USDOE Report EML-332.

Groer, P. G., D. J. Keefe, W. P. McDowell, and R. F. Selmon, 1974, An Instant Working Level Meter with Automatic Individual Radon-Daughter Readout for Uranium Mines, in *Proceedings of the Third International Congress of the International Radiation Protection Association*, Sept. 9—14, 1973, Washington, D. C., USAEC Report CONF-730907-P2, pp. 950-956, NTIS.

Harley, J. H. (Ed.), 1972, *HASL Procedures Manual*, USAEC Report HASL-300, pp. E-Rn-01-01—E-Rn-01-08, NTIS.

International Atomic Energy Agency, 1976, *Manual on Radiological Safety in Uranium and Thorium Mines and Mills*, Safety Series No. 43, STI/PUB/449, Vienna.

James, A. C., and J. C. Strong, 1974, A Radon Daughter Monitor for Use in Mines, in *Proceedings of the Third International Congress of the Interna-*

tional Radiation Protection Association, Sept. 9—14, 1973, Washington, D. C., USAEC Report CONF-730907-P1, p. 32, NTIS.

Kolb, W., and U. Lauterbach, 1974a, A Scintillation Exposure Rate Meter for Environmental Surveys, in *The Natural Radiation Environment II, Vol. 1*, Aug. 7—11, 1972, J. A. S. Adams, W. M. Lowder, and T. F. Gesell (Eds.), ERDA Report CONF-720805-P1, pp. 245-254, Rice University and the University of Texas, Houston, NTIS.

——, and U. Lauterbach, 1974b, *Das Szintillationsdosimeter PTB7201 in verbesserer Ausfuhrung*, Jahrestagung des Fachverbandes fur Strahlenschutz e.v., Helgoland, 1974, S. 662.

Kusnetz, H. L., 1956, Radon Daughters in Mine Atmospheres: A Field Method for Determining Concentrations, *Ind. Hyg. Quart.*, 17: 85-88.

Lucas, H. F., 1957, Improved Low-Level Alpha Scintillation Counter for Radon, *Rev. Sci. Instrum.*, 28: 680.

O'Brien, K., 1978, Environmental Measurements Laboratory, personal communication.

Raabe, O. G., and F. S. Patterson, 1964, *A Method of Analysis of Air Sampling Data for Particulate Alpha Emitters in a Radon—Thoron Daughter Atmosphere*, USAEC Report UR-658, New York University Atomic Energy Project.

Thomas, J. W., 1972, Measurement of Radon Daughters in Air, *Health Phys.*, 23: 783-789.

Wollenberg, H. A., and A. R. Smith, 1964, Studies in Terrestrial γ Radiation, in *The Natural Radiation Environment*, J. A. S. Adams and W. M. Lowder (Eds.), pp. 513-566, The University of Chicago Press, Chicago.

LIST OF ATTENDEES*

ABE, Siro
National Institute of Radiological Sciences
9-1, Anagawa-4
Chiba, 280 Japan

ADAMS, J. A. S.
Department of Geology
Rice University
Houston, Tex. 77001

AUSTIN, Bruce T.
Wright State University
Dayton, Ohio 45435

BACON, Michael P.
Woods Hole Oceanographic Institution
Woods Hole, Mass. 02543

BARD, Stephen T.
Radiation Source Analysis Branch
U. S. Environmental Protection Agency (AW-459)
Washington, D. C. 20460

BASTON, V. F. (Woody)
Energy, Incorporated
P. O. Box 736
Idaho Falls, Idaho 83401

BECK, Harold L.
U. S. Department of Energy
376 Hudson Street
New York, N. Y. 10014

BERK, James V.
Lawrence Berkeley Laboratory
University of California
Building 90, Room 3026-C
Berkeley, Calif. 94720

BERNHARDT, David E.
Environmental Protection Agency
P. O. Box 15027
Las Vegas, Nev. 89114

BINNEY, Stephen E.
Department of Nuclear Engineering
Oregon State University
Corvallis, Oreg. 97331

BLAND, C. John
Physics Department
University of Calgary
2920 24th Avenue, NW
Calgary, Alberta Canada T2N1N4

BOECK, William L.
Niagara University
3890 Carlock Drive
Boulder, Colo. 80303

BOERI, Gian Carlo
CNEN–DISP–Viale Regina Marguerita R5
00198 Rome, Italy

*Addresses given are those provided by the attendee during registration for the conference. In some cases the personal address may be given rather than the address of the affiliation cited.

BOHLINGER, L. Hall
Louisiana Department of Natural Resources
P. O. Box 14690
Baton Rouge, La. 70808

BONKA, Hans
Akademie Oberrat, Lehrstuhl fur Reaktortechnik der RWTH Aachen
Eilfschornsteinstrasse 18
D-5100 Aachen, West Germany

BORISOV, Boris
USSR Ministry of Health
Guest of National Institutes of Health
Building 31, Room 2C-05
Bethesda, Md. 20014

BØTTER-JENSEN, Lars
Risø National Laboratories
4000 Roskilde
Risø, Denmark

BOUVILLE, André C. M. J.
Commissariat á l'Energie Atomique
CEN–FAR BP n° 6
F 92260 Fontenay aux Roses, France

CARSON, Steven R.
Lamont–Doherty Geological Observatory
Columbia University
Palisades, N. Y. 10964

CASTREN, Olli I.
Institute of Radiation Protection
P. O. Box 268
00101 Helsinki 10, Finland

CATHEY, LeConte
University of South Carolina
Columbia, S. C. 29208

CAWLEY, Charles N.
The University of Texas at Dallas
215 Bradley
Denton, Tex. 76201

CHENG, Ku-Chuan
Elliot Lake Mining Research Laboratory
CANMET
Department of E.M.R., Box 100
Elliot Lake, Ontario, Canada P5A2J6

CLEMENTS, William E.
Los Alamos Scientific Laboratories
P. O. Box 1663
Los Alamos, N. Mex. 87545

CLIFF, Keith David
National Radiological Protection Board
Harwell, Didcot, Oxon,
OX11 ORQ, United Kingdom

CLIFFORD, Charles
Radiation Research Associates
3550 Hulen Street
Fort Worth, Tex. 76107

COHEN, Norman
New York University Medical Center
Institute of Environmental Medicine
Long Meadow Road
Tuxedo, N. Y. 10987

COMES, Roger A.
Philip Morris USA
P. O. Box 26583
Richmond, Va. 23261

COOK, Lewis M.
Texas Department of Health
1100 West 49
Austin, Tex. 78756

CZARNECKI, Robert
Bendix Field Engineering Corporation
P. O. Box 1569
Grand Junction, Colo. 81501

DALEBROUX, Marc A.
Commission of the European Communities
INRA-B.V. 1540
21034 Dijon Cedex, France

DE HAZAS, Raquel Herrera
Subsecretaria de Mejoramiento del Ambiente
Av. Canal de Miramontes 2377
Mexico 21, D.F. Mexico

DELPOUX, Marcel Rene
Université Paul Sabatier
39 Allées Jules-Guesde
31077 Toulouse Cedex, France

DENHAM, Geoffrey M.
CJM, SEG, EAEG, PDA
6380 Viscount Road
Mississauga, Ontario, Canada L4V1H3

DE RAS, Eugene M. M.
Communaute Européene de l'Energie Atomique
Bureau General de Measures Nucleares
Steenweg naar Retie
Geel, Belgium

DODD, Philip H.
U. S. Department of Energy
NURE Project Office
P. O. Box 2567
Grand Junction, Colo. 81501

ELLETT, William H.
Office of Radiation Programs
U. S. Environmental Protection Agency (AW-460)
Washington, D. C. 20460

EVANS, Hilton B.
Bendix Field Engineering Corporation
P. O. Box 1569
Grand Junction, Colo. 81501

FENYVES, Ervin J.
The University of Texas at Dallas
P. O. Box 688
Richardson, Tex. 75234

FINCK, Robert R.
National Defence Research Institute
FOA 480, Box 5607
S-114 87 Stockholm, Sweden

FITZGERALD, Joseph E., Jr.
U. S. Environmental Protection Agency (AW-460)
401 M Street, S. W.
Washington, D. C. 20460

GARBER, Wayne
EG&G Ortec
100 Midland Road
Oak Ridge, Tenn. 37830

GASTON, Gary W.
U. S. Army Environmental Hygiene Agency
Laser Microwave Division
Aberdeen Proving Grounds, Md. 21010

GEORGE, Andreas C.
U. S. Department of Energy
376 Hudson Street
New York, N. Y. 10014

GERHARD, Haury
Heppenheimer Street
6800 Mannheim, West Germany

GESELL, Thomas F.
The University of Texas School of Public Health
P. O. Box 20186
Houston, Tex. 77025

GILCHRIST, Roger L.
Battelle-Northwest Laboratories
P. O. Box 999
Richland, Wash. 99352

GINGRICH, Jim
Terradex Corporation
1900 Olympic Boulevard
Walnut Creek, Calif. 94596

GOGOLAK, Carl V.
U. S. Department of Energy
376 Hudson Street
New York, N. Y. 10014

GOLDSMITH, William A.
Union Carbide Nuclear Division
Oak Ridge, Tenn. 37830

GOMEZ, Leo S.
Sandia Laboratories
Division 5413
P. O. Box 5800
Albuquerque, N. Mex. 87185

GUEDALIA, Daniel
Université Paul Sabatier
118, route de Narbonne
Toulouse, France

GUINASSO, Norman L., Jr.
Department of Oceanography
Texas A&M University
College Station, Tex. 77843

HALL, Dennis
Reuter Stokes, Inc.
18530 South Mills Parkway
Cleveland, Ohio 44128

HAYWOOD, Fred F.
Oak Ridge National Laboratory
P. O. Box X
Oak Ridge, Tenn. 37830

HESS, Charles Thomas
Physics Department
University of Maine
Orono, Maine 04473

HIGGO, J. J. W.
University of Cape Town
Physics Department
Rondebosch, C. P. 7700,
South Africa

HOLM, Elis G. G.
Department of Radiation Physics
University of Lund
Lasarettet, S-22185
Lund, Sweden

HOLTZMAN, Richard B.
Argonne National Laboratory
9700 South Cass Avenue, Building 203
Argonne, Ill. 60439

HORTON, Thomas R.
U. S. Environmental Protection Agency
P. O. Box 3009
Montgomery, Ala. 36109

HOUSTON, James R.
Battelle-Northwest Laboratories
P. O. Box 999
Richland, Wash. 99352

HUEBNER, Leo G.
Nalco E.S.
1418 Walters Avenue
Northbrook, Ill. 60062

ISRAELSSON, Sven S. O.
Department of Meteorology
Box 516
S-75120 Uppsala, Sweden

JACKSON, P. O.
Battelle-Northwest Laboratories
Richland, Wash. 99351

JAWOROWSKI, Zbigniew
Central Laboratory for Radiological
Protection
Konwaliowa 7
Warsaw 03-134, Poland

JENSEN, Craig M.
Ford, Bacon and Davis Utah
P. O. Box 8009
Salt Lake City, Utah 84108

JOBST, Joel Edward
EG&G
P. O. Box 1912
Las Vegas, Nev. 89101

JOHN, George
Air Force Institute of Technology
Dayton, Ohio 45400

JOHNSON, James E.
Department of Radiation Biology
Colorado State University
Fort Collins, Colo. 80523

JOHNSON, John W.
Department of Oceanography
Texas A&M University
College Station, Tex. 77843

JOHNSON, Raymond H.
U. S. Environmental Protection Agency
Office of Radiation Programs (AW-461)
401 M Street, S.W.
Washington, D. C. 20460

JONASSEN, Niels
Laboratory of Applied Physics I
Technical University of Denmark
2800 Lyngby, Denmark

JONES, Mary Feild
The University of Texas School of
Public Health
P. O. Box 20186
Houston, Tex. 77025

KAHN, Bernd, Director
Environmental Resources Center
Georgia Institute of Technology
Atlanta, Ga. 30332

KEEFER, Douglas H.
U. S. Environmental Protection Agency
7306 Foxworth Drive
Dallas, Tex. 75248

KEY, Robert M.
Department of Oceanography
Texas A&M University
College Station, Tex. 77843

KHADEMI, Badri
School of Public Health
Tehran University
P. O. Box 1310
Tehran, Iran

KIMURA, Shigehiko
National Research Institute of Agricultural Engineering
Ministry of Agriculture and Forestry
300-21, Kannon-dai 2-1-2
Yatabe, Tsukuba, Ibaragi, Japan

KING, Chi-Yu
U. S. Geological Survey
345 Middlefield Road
Menlo Park, Calif. 94025

KNIGHT, Geoffrey B.
Atomic Energy Control Board
P. O. Box 1046
Ottawa, Canada K1P5S9

KNIZHNIKOV, Viktor
USSR Ministry of Health
Guest of National Institutes of Health
Building 31, Room 2C-05
Bethesda, Md. 20014

KODAIRA, Kiyoshi K.
Ashikaga Institute of Technology
Ohmae-cho, Ashikaga-shi
Tochigi-ken, 326 Japan

KODAMA, Masahiro
Institute of Physical and Chemical Research
7-13, Kaga-1, Itabashi-ku
Tokyo, 173 Japan

KOPERSKI, Jerzy
Instytut Fizyki Jadrowej
ul. Radzikowskiego 152
31-342 Krakow, Poland

LANDA, Edward R.
U. S. Geological Survey
National Center, MS432
Reston, Va. 22092

LARSON, Reginald E.
U. S. Naval Research Laboratory
Code 8326, Atmospheric Physics Branch
Washington, D. C. 20275

LEGGETT, Richard W.
Oak Ridge National Laboratory
P. O. Box X
Oak Ridge, Tenn. 37830

LOWDER, Wayne M.
U. S. Department of Energy
376 Hudson Street
New York, N. Y. 10014

LOWE, Leo M.
James F. MacLaren Limited
435 McNicoll Avenue
Willowdale, Ontario, Canada M3H2R8

LUCAS, Henry F.
Argonne National Laboratory
9700 South Cass Avenue
Argonne, Ill. 60439

MARKOSE, P. M
Bhabha Atomic Research Centre
UC16, Po, Jadugida Mines
District Singhbhum Bihar, India

MARPLE, M. Lynn
Los Alamos Scientific Laboratory
P. O. Box 1663, MS-522 H-12
Los Alamos, N. Mex. 87545

MASTINU, Giovanni
CNEN
CSN Casaccia CNEN
Rome, Italy

MATSUNAMI, Tadao T. M.
Radiation Center of Osaka Prefecture
Health Physics Department
Shinke-Cho, Sakai
Osaka, 593 Japan

McCORMICK, Dan J.
Reuter Stokes, Inc.
18530 South Mills Parkway
Cleveland, Ohio 44128

McLAUGHLIN, James E.
U. S. Department of Energy
376 Hudson Street
New York, N. Y. 10014

McLAUGHLIN, James P.
University College
Physics Department
Belfield, Dublin 4, Ireland

McLEAN, Richard I.
Power Plant Siting Program, Energy and Coastal Zone Administration
Box 2355
Baltimore, Md. 21203

MECHAM, Harvey D.
Utah State Division of Health
Star Route
Heber, Utah 84032

METCALF, James H.
Sandia Laboratories
P. O. Box 5800
Albuquerque, N. Mex. 87185

MEYER, Charles R.
The University of Texas School of Public Health
P. O. Box 20186
Houston, Tex. 77025

MILLER, Mark L.
Battelle-Northwest Laboratories
P. O. Box 999/OSB
Richland, Wash. 99352

MJÖNES, Lars H.
National Institute of Radiation Protection
Fack, S-10401
Stockholm, Sweden

MOCHIZUKI, Sadamu S. M.
Department of Physical Sciences
University of Tokyo
1-3 Kagurazaka, Shinjuku-ku
Tokyo, 162 Japan

MOED, Barbara
Department of Geology
Rice University
Houston, Tex. 77001

MOELLER, Dade W.
Harvard University
27 Wildwood Drive
Bedford, Mass. 01730

MOGRO-CAMPERO, Antonio
General Electric Research and Development Center
P. O. Box 8
Schenectady, N. Y. 12301

MOORE, Howard E.
Department of Physical Sciences
Florida International University
Tamiami Campus
Miami, Fla. 33199

MORSE, Robert H.
EDA Instruments, Inc.
1 Thorncliffe Park Drive
Toronto, Canada M4H1G9

MURRAY, Andrew S.
Research Laboratory for Archaeology
6 Keble Road
Oxford, United Kingdom

MUTH, Hermann K.
Institut für Biophysik der Universität des Saarlandes
Boris Rajewsky Institut
D-6650 Homburg (Saar), West Germany

NAKATANI, Sigeru S. N.
Electrotechnical Laboratory
5-4-1 Mukodai-Machi
Tanashi-shi, Tokyo, Japan

NAZAROFF, William W.
Lawrence Berkeley Laboratory
University of California
Building 90, Room 3026-C
Berkeley, Calif. 94720

NELSON, Neal S.
U. S. Environmental Protection Agency
Office of Radiation Programs (AW-460)
401 M Street, S.W.
Washington, D. C. 20460

NENOT, Jean-Claude
Electricité de France
Comité de Radioprotection
71, rue de Miromesnil
75008 Paris, France

NEVISSI, Ahmad
Laboratory of Radiation Ecology (WH-10)
College of Fisheries
University of Washington
Seattle, Wash. 98195

O'DELL, Austin A.
Lawrence Livermore Laboratory
Box 808
Livermore, Calif. 94550

OKANO, Masaharu
Institute of Physical and Chemical Research
Hirosawa 2-1 Wako-shi,
Saitama, 351 Japan

OVERHOFF, Mario W.
Overhoff and Associates
P. O. Box 8091
Cincinnati, Ohio 45208

PACER, John
Bendix Field Engineering Corporation
P. O. Box 1569
Grand Junction, Colo. 81501

PENNA-FRANCA, Eduardo
Institute of Biophysics UFRJ
Centro de Ciencias da Saude
Bloco G, Ciudade Universitaria
Rio de Janeiro 20000, Brazil

PERDUE, Phillip T.
Oak Ridge National Laboratory
P. O. Box X
Oak Ridge, Tenn. 37830

PEREIRA, Enio Bueno
Department of Geology
Rice University
P. O. Box 1892
Houston, Tex. 77001

PERSSON, Bertil R. R.
Radiation Physics Department
Lasarettet S-22185
Lund, Sweden

PHILIPPOT, Jean-Claude
French Atomic Energy Commission
Laboratoire 501
Orsay F91400, France

PHILLIPS, Colin R.
Department of Chemical Engineering
and Applied Chemistry
University of Toronto
Toronto, Canada M5S1A4

PIERCE, Stephen P.
Department of Fisheries and
Environment
351 St. Joseph Boulevard
Hull, Quebec, Canada

PIESCH, Ernst K. A.
Karlsruhe Nuclear Research Center
Postfach 3640
7500 Karlsruhe, West Germany

POHL, Egon
Director of Institute of Physics
University of Salzburg
Akademiestrasse 26
A-5020 Salzburg, Austria

POHL-RÜLING, Johanna
Research Institute Gastein of the
Austrian Academy of Science
Akademiestrasse 26
A-5020 Salzburg, Austria

POMANSKY, Alexander A.
Institute for Nuclear Research USSR
117312 Moscow, Profsojuzhaja 7a
USSR

PORSTENDORFER, Justin
Institut für Biophysik
der Universität in Giessen
6300 Giessen, West Germany

POWERS, Robert P.
Tennessee Valley Authority
Radiological Hygiene Branch
River Oaks Building
Muscle Shoals, Ala. 35630

PRICE, Keith R.
Battelle-Northwest Laboratories
P. O. Box 999
Richland, Wash. 99352

PRICHARD, Howard M.
The University of Texas School of
Public Health
P. O. Box 20186
Houston, Tex. 77025

QUINN, Michael J.
Atomic Energy Control Board
P. O. Box 1046
Ottawa, Ontario, Canada K1P5S9

RATHBUN, Lyle
Petrotomics
Box 2509
Shirley Basin, Wyo. 82615

RICHARDSON, Keith A.
Geological Survey of Canada
601 Booth Street
Ottawa, Canada K1A0E8

RIEL, Gordon K.
Naval Surface Weapons Center
R-41
White Oak, Md. 20910

ROBERTS, Eugene H.
Bendix Field Engineering Corporation
P. O. Box 1569
450 West Scenic Drive
Grand Junction, Colo. 81501

ROBERTS, Joan
U. S. Department of Energy
Technical Information Center
P. O. Box 62
Oak Ridge, Tenn. 37830

ROESSLER, Charles E.
Department of Environmental Engineering Sciences
University of Florida
114 Black Hall
Gainesville, Fla. 32611

RUBIN, Richard
Radiation Research Associates
3550 Hulen Street
Fort Worth, Tex. 76107

SALMONSON, Bradley J.
Exxon Minerals Company, USA
Room 1380, Dresser Tower
P. O. Box 2180
Houston, Tex. 77001

SANNI, Adeyinka O.
Physics Department
University of Ibadan
Ibadan, Nigeria

SARUHASHI, Katsuko
Meteorological Research Institute
Koenji Kita 4-35-8, Suginami
Tokyo 166, Japan

SAVIGNAC, Noel F.
United Nuclear Corporation
P. O. Box 3951
Albuquerque, N. Mex. 87110

SCHIAGER, Keith J.
University of Pittsburgh
A512 Crabtree Hall
Pittsburgh, Pa. 15261

SCHINK, David R.
Department of Oceanography
Texas A&M University
College Station, Tex. 77843

SCHRIBER, Gerhard J. A.
Physics Institut, Abt. LLC
University of Berne
Sidlerstrasse 5
CH-3012 Berne, Switzerland

SCHUTTELKOPF, Heinz
Karlsruhe Nuclear Research Center
Postfach 3640
7500 Karlsruhe, West Germany

SCOTT, Arthur G.
DSMA/ACRES
2846 Hollington Crescent
Mississauga, Ontario, Canada L5K1E9

SHAPIRO, Mark H.
Department of Physics
California State University, Fullerton
Fullerton, Calif. 92634

SILKER, Wyatt B.
Battelle-Northwest Laboratories
P. O. Box 999
Richland, Wash. 99352

SINGH, Narayani P.
Institute of Environmental Medicine
New York University Medical Center
Long Meadow Road
Tuxedo, N. Y. 10987

SMITH, Alan R.
Lawrence Berkeley Laboratory
University of California
Berkeley, Calif. 94720

SPITZ, Henry B.
New York University Medical Center
A. J. Lanza Research Laboratory
Tuxedo, N. Y. 10987

SPITZBERG, D. Blair
The University of Texas at Dallas
P. O. Box 688, B.E. 22
Richardson, Tex. 75080

STEINHAUSLER, Fritz
Institute of Environmental Medicine
New York University Medical Center
Long Meadow Road
Tuxedo, N. Y. 10987

STYRON, Clarence E.
Monsanto Research Corporation
P. O. Box 32
Miamisburg, Ohio 45342

SUGIMURA, Yukio Y. S.
Meteorological Research Institute
Koenji-kita 4-35-8, Suginami
Tokyo 166, Japan

SWEDJEMARK, Gunastri
National Institute of Radiation Protection
Fack, S-10401
Stockholm, Sweden

TANIGUCHI, Harry
Radiation Protection Bureau
Health and Welfare Department
Brookfield Road
Ottawa, Ontario, Canada K1A1C1

TANNER, Allan B.
U. S. Geological Survey
990 National Center
Reston, Va. 22092

TAPPEN, Jeffrey J.
Dames and Moore
20 Haarlem Avenue
White Plains, N. Y. 10603

THOMAS, C. W.
Battelle-Northwest Laboratories
P. O. Box 999
Richland, Wash. 99352

THUMA, William R.
EDA Instruments, Inc.
1 Thorncliffe Park Drive
Toronto, Ontario, Canada M4H1G9

TOWNSEND, Michael G.
E.M.R.
555 Booth Street
Ottawa, Ontario, Canada

TUCKER, Allen B.
Physics Department
San Jose State University
San Jose, Calif. 95192

UZZAN, Guy
Commissariat á l'Energie Atomique
DPr/Euratom
BP n° 6, 92 260
Fontenay aux Roses, France

VAN MIDDLESWORTH, Lester
Department of Physiology and Biophysics
University of Tennessee
800 Madison Avenue
Memphis, Tenn. 38163

VAVASSEUR, Camille
Commissariat á l'Energie Atomique
Stepam, Cen/Saclay
BP n° 2
91190 Gif sur Yvette, France

VIGNES, Suzanne S.
Electricité de France
Comité de Radioprotection
71, rue de Miromesnil
75008 Paris, France

VOHRA, Krishan Gopal
Division of Radiological Protection
Dhabha Atomic Research Centre
Bombay-400 085, India

VOLD, Erik L.
California Department of Health
Radiological Health Section, Room 1455
555 Capital Mall
Sacramento, Calif. 95814

WACHSMANN, Felix Kurt
Professor Dr. ing
1 Ingolstaedter Landstrasse
D 8042 Neuherberg
Oberschleissheim, West Germany

WADDLE, Ted C.
Western Systems, Incorporated
P. O. Box 2133
Evergreen, Colo. 80439

WETHINGTON, John A., Jr.
Department of Nuclear Engineering
University of Florida
202 Nuclear Sciences Center
Gainesville, Fla.

WHITE, Joel H.
Lawrence Livermore Laboratory
P. O. Box 808
Livermore, Calif. 94550

WILKENING, Marvin H.
New Mexico Tech
Socorro, N. Mex. 87801

WINDHAM, Sam T.
U. S. Environmental Protection Agency
P. O. Box 3009
Montgomery, Ala. 36109

WORDEN, Alfred E.
Texas Department of Health
Radiation Control
6607 Auburndale Lane
Austin, Tex. 78723

WRENN, McDonald E.
Department of Environmental
Medicine
New York University Medical Center
Long Meadow Road
Tuxedo, N. Y. 10987

YARBOROUGH, Keith A.
National Park Service
Southwest Regional Office
P. O. Box 728
Santa Fe, N. Mex. 87501

AUTHOR INDEX

Abe, M., 430
Abe, S., 430, 1034
Adams, J. A. S., 1
Aitken, M. J., 927
Alemi, A. A., 600
Alexakhin, R. M., 724, 738, 1446
Alter, H. W., 84
Ardouin, B., 445

Bacon, M. P., 473
Barkhudarov, R. M., 1446
Barr, S., 1559
Beasley, T. M., 502
Beck, H. L., 259, 1521
Bell, J., 514
Bland, C. J., 600, 633
Blaton-Albicka, K., 1407
Boeck, W. L., 201
Bolch, W. E., Jr., 1476, 1673
Borisov, B. K., 1446
Bøtter-Jensen, L., 912
Bouville, A., 1059
Bowman, S. G. E., 927
Bramson, P. E., 826
Breslin, A. J., 1272
Bressan, D. J., 308
Brewer, P. G., 473
Broecker, W. S., 514
Brutsaert, W. F., 529
Bysiek, M., 383

Carson, S., 514
Casparius, R. E., 529
Castrén, O., 1364
Cherry, R. D., 502
Christiansen, B. M., 912
Clarke, F. J., 1331
Clements, W. E., 1559
Cliff, K. D., 1260
Cohen, N., 783, 1308
Cook, L. M., 1602
Copping, N. A., 137
Cowart, J. B., 711

Dalebroux, M., 1072
Darcheville, M., 1667
Davie, E., 514
Delpoux, M., 1072
de Planque, G., 987
Desai, N., 1673
Druilhet, A., 226, 242
Dulieu, H., 1072

Eapen, C. D., 327
Eappen, K. P., 1655
Ebisawa, R., 611
Eichholz, G. G., 1331

Fabries, M., 1072
Faure, F., 1072
Fehér, I., 1396
Fenyves, E. J., 839
Finck, R. R., 357
Fix, J. J., 826
Fleischer, R. L., 57, 72
Fontan, J., 226, 242
Fowler, S. W., 502
Fujimoto, K., 1034
Fujitaka, K., 1034

Ganapathy, S., 1090
George, A. C., 1272
Gesell, T. F., 1347, 1698
Gladney, E. S., 681
Gogolak, C. V., 259, 1521, 1698
Goldsmith, W. A., 1584
Guedalia, D., 226, 242
Guczcngar, J. -M., 1059
Guimond, R. J., 1457
Gulezian, G. V., 1424

Haghi, M. A., 124
Hamada, T., 896
Hanson, W. C., 681, 1682
Haywood, F. F., 347, 1584
Hess, C. T., 529
Hewitt, J. E., 854
Heyraud, M., 502
Higgo, J. J. W., 502
Hofmann, W., 1116, 1145
Holm, E., 560
Holtzman, R. B., 755
Hughes, L., 854

Ibrahim, S. A., 783
Ilyin, L. A., 1446
Imai, T., 882
Israelsson, S., 210
Iyengar, M. A. R., 1090
Izumo, K., 896

Jaworowski, Z., 383
Jonassen, N., 1211, 1225
Jose, P., 681

Kahn, B., 1331
Kamath, P. R., 1090, 1655
Kanazawa, T., 547
Kanipe, L. G., 640
Kato, M., 611
Katou, T., 896
Katsuragi, Y., 547
Kautz, R. S., 1476, 1673
Kawamura, A., 611
Kawasaki, S., 882
Keefer, D. H., 839
Keszthelyi, B., 1396
Khademi, B., 600
Kimura, S., 581
King, C.-Y., 175
Kirchmann, R., 1667
Knight, G. B., 1494
Knizhnikov, V. A., 1446
Kobal, I., 1415
Kobayashi, H., 1004
Koch, G., 1667
Kodaira, K., 611
Kodama, M., 882, 896
Komae, T., 581
Komamura, M., 611
Komura, K., 611
Koperski, J., 1049
Koszorus, L., 1396
Kovalchuk, E. L., 661, 673
Kownacka, L., 383
Kristan, J., 1415
Kumagai, H., 896
Kuzminov, V. V., 673

Lakatos, S. Novotny, 1396
Lalit, B. Y., 800
Lambert, G., 445
Larson, R. E., 308
Leggett, R. W., 347, 1584
Leonard, A., 1072
Li, Y.-H., 514
Lindeken, C. L., 950
Londhe, V. S., 1633
Løvborg, L., 912
Lowder, W. M., 1521

Madelmont, C., 1059
Makepeace, C. E., 1494
Markose, P. M., 1655
Marple, M. L., 1559
Martell, E. A., 415
Maslov, V. I., 724, 738
Maslova, K. I., 738
Mastinu, G. G., 700, 800
McCaslin, J. B., 854
McLaughlin, J. P., 1211, 1225
Melvin, J. D., 137
Mercer, T. T., 281
Miera, F. R., Jr., 681
Miller, K. M., 1521
Miller, M. L., 826
Minato, S., 370
Mishra, U. C., 327
Miyake, Y., 458, 547
Mjönes, L., 1077
Mochizuki, S., 105
Moeller, D. W., 1424
Mogro-Campero, A., 57, 72
Moore, H. E., 415
Morrison, G., 514
Mosier, D. F., 154
Murray, A. S., 927

Nakatani, S., 294
Nasseri, A., 600
Nevissi, A., 405
Nielsen, B. L., 912
Niewiadomski, T., 1049
Nishida, M., 896
Norton, S. A., 529
Novikova, N. Y., 1446
N'Tsila, A., 242

O'Brien, K., 1163
Okano, M., 896
Osmond, J. K., 711

Paul, A. C., 1633
Pońsko, J., 1407
Perdue, P. T., 347
Percira, E. B., 117
Persson, B. R. R., 357, 560
Pillai, K. C., 1633
Poet, S. E., 415
Pohl, E., 1116, 1145
Pohl-Rüling, J., 1145
Pomansky, A. A., 661, 673
Popova, O. N., 440
Porstendörfer, J., 281, 1293
Powers, R. P., 640
Prichard, H. M., 1347

Rajan, M. P., 1090
Ramachandran, T. V., 800
Rangarajan, C., 327
Rao, P. V., 124
Regulla, D. F., 1022
Roessler, C. E., 1476, 1673
Ryba, E., 1049

Saccomanno, G., 783
Sakanoue, M., 611
Sanak, J., 445
Santaroni, G. P., 810
Santschi, P. H., 514
Saruhashi, K., 458, 547
Sasaki, A., 1004
Savani, N. K., 124
Scacco, F., 1107
Schell, W. R., 405
Schraub, A., 1293
Sciocchetti, G., 1107
Sekikawa, T., 105
Shapiro, M. H., 137, 256
Singh, N. P., 783
Škofljance, M., 1415
Smith, A. R., 154, 854
Smolnikov, A. A., 661
Spencer, D. W., 473
Spitz, H. B., 1308
Steinhäusler, F., 1116, 1145
Stephens, L. D., 854
Stpiczyńska, Z., 1407
Styron, C. E., 1511
Sugimura, Y., 458, 547
Sunbeck, C. W., 950
Swedjemark, G. A., 1237
Syvertson, C. A., 854

Takahashi, K., 882
Taniguchi, H., 1623
Tanner, A. B., 5
Taskaev, A. I., 440, 724
Temmoev, E. L., 661
Thomas, R. H., 854
Titaeva, N. A., 724
Tombrello, T. A., 137
Tóth, Á., 1396
Tsukuda, M., 1004
Tucker, A. B., 854
Turnage, N. E., 640

Uemura, H., 547
Underhill, D. W., 1424

Van Middlesworth, L. V., 832
Vasudev, P., 1623
Venkataraman, S., 1655
Vohra, K. G., 184
Vold, E., 965

Wachsmann, F., 1022
Wada, M., 882
Wethington, J. A., Jr., 124, 1476
Whitcomb, J. H., 137
White, J. H., 950
Wicke, A., 1293
Wilkening, M., 90
Windham, S. T., 1457
Wollenberg, H. A., 154
Wrenn, M. E., 783, 1308

Yamomoto, A., 611
Yarborough, K. A., 1371

SUBJECT INDEX

Actinides
  isotopic ratios as indicators of migration, 724
  in lichen—reindeer food chain, 560
  pathways of, for human exposure, 560
  radioanalytic techniques for measurement of, 560
  in seawater and sediments, 560
Aerosol, atmospheric
  lead-212, attachment rates, 281
  over oceans, 308
  origin, size distribution, and residence times for ^{210}Pb, ^{210}Bi, and ^{210}Po, 430
  particle size vs. humidity, 281
  radon daughters
    interaction, 281
    size distribution, 294
Alpha spectrometry, application to radon daughter measurement, 347
Animals, effects on radionuclide redistribution in soil, 738
Atmosphere
  alpha activity in, variations of, 210
  beryllium-7 concentration in, seasonal variations of, 327
  beta activity in, variations of, 210
  deposition of radon daughters in, 357, 405
  injection of uranium, ^{226}Ra, and ^{210}Pb in, sources and rates, 383
  radon and radon daughter concentrations in (*see* Radon daughters, Radon-220, and Radon-222)
  stability
    determination by radon and sodar measurements, 242
    effect on radon daughter concentrations, 259
  vertical diffusion, model test using radon daughter activity ratios, 256
  vertical exchange, dependence on temperature and wind velocity gradients, 226
Atmospheric dust (*see* Dust)
Atmospheric electricity (*see* Electricity)
Atmospheric ionization (*see* Ionization)
Atmospheric particulates (*see* Aerosol and Dust)

Beryllium-7, air concentrations, seasonal variations in, 327
Beta radiation
  effective dose equivalent, background, 1163
  external, doses to human organs, 1163
Bismuth-210 (radium E), air concentrations, specific activity, and particle sizes, 415
Bismuth-214 (radium C)
  See also Radon daughters
  particle size, attached, 294

Building materials
contribution to indoor radon levels, 1396, 1407, 1424
effect on indoor gamma levels, 1022, 1049, 1331, 1396, 1407, 1424
natural radionuclide contents, 1237, 1331, 1396, 1407
radon emanation from, 1396, 1407
radon exhalation from
measurements, 1211
model, 1211, 1272
use, effect on population dose, 1446

Cesium-137
in the atmosphere, compared with ^{210}Pb, 405
deposition from the atmosphere, 611
in glacier ice, 383
in soil, 611
Coal
ash distribution, effect on exposure, 1521
fly ash
natural radionuclides in, 1407, 1446, 1511, 1521
radon emanation from, 1407, 1521
natural radionuclides in, 1446, 1511, 1521
radon emanation from, 1521
slag
natural radionuclides in, 1407, 1446, 1521
radon emanation from, 1407
Cosmic radiation
at aircraft altitudes, 854
flux measurement with NaI(Tl) spectrometer, 896
intensity profiles, altitude and latitude, 854
intercomparison experiments, 1698
ionizing component, doses and fluxes, 854
neutrons
attenuation near ground, 882
doses, fluxes, and energy spectra, 854
response of TLD's to, 965

Dust, atmospheric
in glacier ice, vs. depth, 383
injection to atmosphere, sources and rates, 383
lead-210, specific activity, 611
radionuclides in, 383

Earth sciences, role of natural radiation in, 184
Earthquake prediction
from radon and daughter measurements, 5, 137, 154, 175
role of natural radionuclides in, 154
Electricity, atmospheric
effects of radiation-induced ionization on, 184, 201, 210
theory, review of, 201

Food
actinides in lichen—reindeer food chain, 560
diet
radium, ^{210}Pb, and ^{210}Po in, 755
uranium and thorium in, 560, 800
natural radionuclides in, in India, 1090
radium-226 in, 810, 839, 1090
radium-226 in flour, in France, 1059
radium-226, ^{40}K, and ^{228}Th in, 800

Gamma radiation
from airborne and deposited radon daughters, 357
background
effective dose equivalent, 1163
time variations, measurements, and model, 987
dose in ground, TLD and scintillator comparison, 927
exposure rates
in Canadian communities, 1494
effect of building materials on, 1022, 1331
on Greenland plateau, 912
indoor, northeast United States, 1331
indoor and outdoor
in Bavaria, Federal Republic of Germany, 1022
in Florida, USA, 1457
outdoor, Japan, 1034
space and time variations, 987, 1049

in Swedish houses, 1077
time variations, altitude profile, 1059
external, doses to human organs, 1163
flux density, variations during rainfall, 370
flux and dose measurement with NaI(Tl) spectrometer, 896
indoor, effect of building materials, 1049, 1077, 1331, 1424
intercomparison experiments, 1698
measurement
with NaI(Tl) spectrometer, 896
TLD error analysis, 950
TLD response and energy dependence, 965
TLD tandem systems, 965
with TLD's and ionization chamber, 1049
Gamma spectrometry
determinations of exposure rate and radionuclide concentration, 912
Ge(Li), measurement of radon daughters, 357
NaI(Tl), spherical, for gamma- and cosmic-ray measurement, 896
Glacier ice, concentrations vs. depth of uranium, ^{226}Ra, ^{210}Pb, and ^{137}Cs, 383

Human body
lung doses from radon daughters, indoors, 1272
organ doses
from external beta and gamma radiation, 1163
from inhaled radon and daughters, 1116
in Salzburg, Austria, 1145
skeletal burden of ^{210}Pb and ^{210}Po in spa workers, in Italy, 1107
thorium in tissues of, 783

Inhalation, dose distribution patterns, natural radionuclides, 1116
Intercomparison experiments
gamma and cosmic radiation, 1698
radon-222 and daughters in caverns and outdoors, 1698
Ionization, atmospheric
altitude profile, from terrestrial sources and cosmic radiation, 184, 201
effects
on atmospheric electricity, 184, 201, 210
on atmospheric nucleus formation, 184
latitude variations, radiation induced, 201
Ionization chambers
air, normal pressure, for absolute environmental radiation measurements, 1004
alpha contamination, measurement of, 1004
application to gamma radiation survey, 1034

Lead in soil, 611
Lead-210 (radium D)
air concentrations
indoor, 1142
over land and sea, 327, 405, 415, 430, 445
seasonal variations, 405
vertical distribution, 445
in coal ash, 1446, 1511, 1521
contamination of soil and plants, 440
deposition
from atmosphere, 405, 440, 547, 611
during precipitation, 547
in food
dietary intake and ingestion dose, 755
in India, 1090
in glacier ice, 383
injection in atmosphere, sources and rate, 383
in lichen—reindeer food chain, 560
marine geochemistry, review of, 473
in marine organisms, concentration factors, 1090
in oceans, migration and distribution, 473
particle size and specific activity in soil and air, 415
in rainwater, 547

skeletal burden of spa workers, in Italy, 1107
in soil and phosphate rocks, 611
specific activity in metal and dust, 611
transport with air masses, large scale, 405
Lead-212 (thorium B)
diffusion coefficients and attachment rates, 281
in indoor air, 1145
in outdoor air
altitude profile, 226
over land and sea, seasonal variations in, 327
for vertical exchange measurement, 226
Lead-214 (radium B)
See also Radon daughters
air concentrations
diurnal and seasonal variations in, 327
in gold mines, 327
indoor, 1145
over land and sea, 327
particle size, attached, 294
Low-activity materials
determination of, 661
use in low-background chamber, 661
Lung
dose (*see* Human body)
models for dose calculations, 1116

Measurement methods
See also Alpha spectrometry, Gamma spectrometry, Ionization chambers, Nuclear track detectors, Scintillation detectors, and Thermoluminescence dosimeters
error analysis for TLD gamma measurements, 950
for gamma radiation surveys, 1022, 1049
ionization chambers, alpha contamination, 1004
lognormal analysis for radionuclide concentrations, 826
neutrons in cosmic radiation, 854
radioanalytic, for low-level alpha activity, 560
radium in water, using impregnated fibers, 633
radium-226 in soil and water, 640
radon and daughters, monitoring techniques, 1293, 1308
radon daughters in air, 256, 347, 1457
radon in water, 529
radon-222 in air and water, scintillator-deemanation technique, 700
spectrometry (*see* Alpha spectrometry and Gamma spectrometry)
TLD—scintillator comparison for gamma dose determination, 927
TLD tandem system for gamma measurement, 965
TLD's for environmental gamma-ray measurement, 965, 987

Natural Radiation Environment symposiums
key issues at, 1
origin and history, 1
Natural radionuclides and radioactivity
See also Actinides and specific radionuclides
alpha activity of materials, 673
in building materials, 1237, 1331, 1396, 1407
in coal and coal ash, 1407, 1446, 1511, 1521
content on Greenland plateau, 912
gamma activity of common materials, 661
isotopic ratios
as indicators of migration, 724
in rock—soil—water—plant system, 724
low-activity materials, 661
migration through rock—soil—water—plant system, 724
in phosphate materials and products, 1407, 1446, 1476, 1633
releases from coal-fired power plants, 1446, 1511, 1521
role in earthquake prediction, 154
use as tracers
in atmospheric studies, 184
in bay water for trace metals, 514

Neutrons
cosmic ray
attenuation near ground, 882
doses, fluxes, and energy spectra, 854
detectors, for cosmic-ray measurement, 854
Nuclear track detectors for radon measurement, 57, 84, 175, 1457

Oceans
lead-210 distribution, 473
polonium-210 distribution, 473
radium-226, concentration and distribution, 458, 473
radon-222
concentration and distribution, 458
residence time in mixed layer, 458
vertical eddy diffusion, 458
vertical transport of alpha emitters in, 502

Particulates, atmospheric (*see* Aerosol and Dust)
Phosphate materials and products
gypsum
natural radionuclides in, 1407
radon emanation from, 1407
land, industrial and reclaimed
characteristics, 1476
model for radon exhalation, 1673
radon in houses, 1457
phosphate fertilizers
effect on ^{226}Ra in soil and crops, 1667
use, effect on population dose, 1446
phosphate rocks, products and waste
^{226}Ra activity, 1476, 1633
^{228}Ra activity, 1633
Plants
effects on radionuclide redistribution in soil, 738
genetic effects, radiation induced, 1072
lead-210 and ^{210}Po contamination, 440
uptake and accumulation of natural radionuclides, 724, 738
uranium in aquatic and terrestrial, 1682
Plutonium-239 and plutonium-240
See also Actinides
in lichen—reindeer food chain, 560
in oceans, vertical transport, 502
Polonium-210 (radium F)
in air
concentration, 430
concentration, specific activity, and particle size, 415
in bay water, concentration and seasonal variations in, 514
chemical state in airborne dusts, 430
in coal ash, 1446, 1511, 1521
contamination of soil and plants, 440
deposition from atmosphere, 405, 440
in food
dietary intake and ingestion dose, 755
in India, 1090
in lichen—reindeer food chain, 560
in marine organisms, concentration factors, 1090
in oceans
migration and distribution, 473
vertical transport, 502
skeletal burden of spa workers, in Italy, 1107
sources, natural and artificial, 430
Polonium-218 (radium A), particle size, attached, 294
Population dose
comparison, nuclear and coal-fired power plants, 1446, 1521
effect of building materials on, 1048, 1424, 1446
gamma exposure, measurement methods, 1049
from the main natural and artificial sources, 1446
natural radiation, distribution and sources, in Salzburg, Austria, 1145
from radon daughters, in Finland, 1364
from radon and radon daughters, in Italian mines and spas, 1107
reduction and control measures in building construction, 1424

from use of phosphate fertilizers, 1446
Potassium-40
in building materials, 1237, 1331, 1396, 1407
in coal and coal ash, 1407, 1446, 1521
in food, dietary intake, 800
in gypsum, 1407
in soils and vegetation, Hanford, Wash., 826
Power plants, coal fired
natural radionuclides and doses from, 1446, 1511, 1521
radiological impact, comparison with nuclear, 1446, 1521

Radiation (*see* Beta radiation, Cosmic radiation, and Gamma radiation)
Radium-223
elevated levels in contaminated areas, 347
in water, detection near uranium mine tailings, 633
Radium-224, concentrations in Hanford, Wash., soils, 826
Radium-226
analysis for, in soil and water samples, 640
in building materials, 1237, 1331, 1396, 1407
in cattle thyroids, elevated levels, 832
in coal and coal ash, 1407, 1446, 1521
dose, internal, from ingestion, 755
in drinking water
dietary intake, 810
in India, 1087
in Oklahoma, USA, 839
in Salzburg, Austria, 1145
effect of industry and irrigation on soil concentrations, 1633
in flour, in France, 1058
in food, dietary intake, 755, 800, 810, 839
in glacier ice, 383
injection in atmosphere, sources and rate, 383
in land produce and seafoods, in India, 1090
in liquid effluents from uranium complex, 1655
in marine organisms, concentration factors, 1090
in oceans, concentrations and distribution, 458, 473
in phosphate materials and products, 1407, 1446, 1476, 1633
in plants and soil, in Iran, 600
in river water, sediments, and fish, in India, 1633, 1655
in soil, 611, 738, 836
in soil and plant organs, effect of phosphate fertilizers, 1667
specific activity in soil particles, 415
in water
in South Texas (USA) uranium district, 1602
use of impregnated fibers for, 633
Radium-228
in coal and coal ash, 1446, 1521
in drinking water
in India, 1090
in Oklahoma, USA, 839
effect of industry and irrigation on soil concentrations, 1633
in food
dietary intake and ingestion dose, 755
in India, 1087
in marine organisms, concentration factors, 1090
in phosphate materials and products, 1633
in river water, sediments, and fish, in India, 1633
Radon daughters
See also individual nuclides
activity ratios
as diffusion model test, 256
effect of atmospheric mixing, 259, 415
in gold mines, 327
in lower atmosphere, 256, 259, 327, 415
measurement by gamma spectrometry, 256
in caves, in United States, 1371
deposition during precipitation, 357
exposure
monitoring techniques, 1308

uranium mill tailings, 1584
users of well water, in Finland, 1364
gamma radiation from airborne and deposited, 357, 370
in gold mines, 327
indoor
in British dwellings, 1260
in Canadian communities, 1494, 1623
control measures, 1424
effect of ventilation and air conditioning, 1457
in Swedish dwellings, concentrations and doses, 1237
in U. S. dwellings
concentrations and doses, 1272, 1457
variations, 1293
inhaled, dose calculations for standard exposures, 1116
interaction with atmospheric aerosol, 281
intercomparison experiments, 1698
long lived
activity ratios and residence times, 415
air concentrations, specific activity, and particle sizes, 415
lung cancer risk, 1237, 1260, 1364
measurement techniques, 347, 1308
in mines and spas, in Italy, 1107
in outdoor air, diurnal variations of, 1293
particle size distributions, 294, 415, 1272
short lived, concentrations in lower atmosphere, 259, 327
Radon-219 (actinon), detection in contaminated buildings, 347
Radon-220 (thoron)
in air
application to vertical exchange measurement, 226
diurnal variations, 1293
monitoring techniques, 1293
exhalation rate, variations in, 210
measurement, for earthquake prediction, 137
migration in the ground, 5
in soil gas, 210
Radon-222
in air and water, in South Texas (USA) uranium district, 1602
balance in indoor air, 1225, 1272
in breath of well-water users, in Finland, 1364
diffusion and exhalation, 5, 90
distribution and transport in ground, anomalous, 5, 57, 72, 137
in drinking water
in Salzburg, Austria, 1145
in United States, 1272, 1347
emanation
from building materials, 1396, 1407
from coal and coal ash, 1521
processes and measurements, 5, 117
exhalation
from building materials
effect of pressure drop, 1225
measurements, 1211, 1260, 1272, 1293
model, 1211
from ground
in Florida phosphate region, 1476
model, 1673
variations in, 105, 124, 242, 259, 1476
flow in ground channels, caves, 90
in groundwater
as indicator of water circulation, 581
measurements, 154, 529, 1347
sources, 154, 529
indoor
in Canadian communities, 1494, 1623
control measures, 1424
in France, 1059
in Slovenia, Yugoslavia, 1415
in Swedish dwellings, 1237
in U. S. dwellings, 1272, 1308
variations, 1145, 1237, 1293, 1308, 1457
from water usage, 529, 1347, 1364
intercomparison experiments, 1698
measurement
in air and water, scintillator-deemanation technique, 700

for earthquake prediction, 137, 154, 175
monitoring techniques, 1293, 1308
with nuclear track detectors, 57, 84
in water, 529
migration
effect on gamma radiation field, 5
in ground, 5, 57, 90
in mines and spas, in Italy, 1104
in oceans, concentrations and distribution, 458
in outdoor air
altitude profile, 226
application to vertical exchange and stability measurement, 226, 242
latitude distribution, 445
over oceans, 308, 445
in Salzburg, Austria, 1145
variations in, 210, 226, 242, 1293, 1308, 1415
pathways from water to human environment, 529, 1347
population exposure, in Salzburg, Austria, 1145
in rainwater, 547
release
from coal combustion and wastes, 1521
from uranium mill tailings, 1559, 1584
in soil gas, 5, 57, 105, 175, 210, 547
tracer of air masses over oceans, 308
volcanic source, 90
in well water, in Finland, 1364
Rainfall
effect on gamma radiation intensity, 357, 370
radioactivity in, 370, 547
radon daughter deposition by, 357
Rocks
geology, effect on gamma radiation levels, 1034
radon emanation from, 117

Scintillation detectors
NaI(Tl), spherical, for gamma- and cosmic-ray measurement, 896
ZnS, for ^{222}Rn measurement, 700
Sodar, use in measurement of inversion layer thickness, 242
Soil
lead-210 and ^{210}Po contamination, 440
lead-210 in, relative to ^{90}Sr, ^{137}Cs, lead, ^{226}Ra, and ^{238}U, 611
moisture, effect on environmental gamma radiation, 987
natural radionuclide activity ratios in, 724
radionuclide concentrations, lognormal analysis, 820
radium-226 activity, Florida phosphate region, 1476
radon emanation from, 1407
radon migration in, 5, 57, 72
uranium mobility in, 681, 1682
uranium, thorium, and potassium in, 738
Soil gas, radon in, 5, 57, 105
Strontium-90
on atmospheric particulates, percent vs. size, 415
deposition from atmosphere, 611
in soil, 611
Surveys, radiation and radioactivity
in Florida phosphate region, 1476
gamma exposure rates
in France, 1059
indoor, model and measurements, 1331
indoor and outdoor
in Bavaria, Federal Republic of Germany, 1022
in Florida, USA, 1457, 1476
in Poland, 1059
outdoor, in Japan, 1033
in Swedish houses, 1077
gamma radiation and radon
in Canadian communities, 1494, 1623
in South Texas (USA) uranium district, 1602
on Greenland plateau, 912
in low-monazite area, in India, 1090
natural radiation exposure, in Salzburg, Austria, 1145
radium-226
in flour, in France, 1059
in plants and soil, in Ramsar, Iran, 600

in water and food, in Italy, 810
radon and daughters
in dwellings
in Sweden, 1237
in United Kingdom, 1260
in United States, 1272, 1308, 1457
in mines and spas, in Italy, 1107
radon-220
in dwellings, in France, 1059
radon-222
in groundwater, in Maine, USA, 529
in water from bored wells, in Finland, 1364

Thermoluminescence dosimeters (TLD's)
applications
archaeological dating, 927
environmental gamma-ray measurement, 965, 987
gamma radiation surveys, 1022, 1049, 1059, 1077
population dose assessment, 1049
$CaSO_4$/Dy, energy dependence and fading, 1077
comparison with scintillator for gamma dose measurement, 927
energy dependence and response calibrations for environmental radiation, 965
error analysis for environmental measurements, 950
tandem systems for field measurements, 965
transit dose estimation, 1077
Thorium-228
in bay water, concentration and seasonal variations, 514
in building materials, 1407
in cattle thyroids, elevated levels, 832
in coal ash, 1407, 1521
in food, dietary intake, 800
in gypsum, 1407
in human tissues, 783
in phosphate fertilizer, 1446
Thorium-230
in coal and coal ash, 1511, 1521
in human tissues, 783
in phosphate materials and products, 1633
Thorium-232
See also Actinides
in building materials, 1237, 1331, 1396
in coal and coal ash, 1446, 1521
in food, dietary intake, 800
in human tissues, 783
in lichen—reindeer food chain, 560
in oceans, vertical transport, 502
in phosphate materials and products, 1633
in soil, 738
Thoron (*see* Radon-220)
Thyroid, cattle, elevated radium and thorium levels in, 822
Trace metals
in aquatic systems, pathways and removal rates, 514
manganese in river system near uranium complex, 1655
natural radionuclides as tracers for, in bay water, 514

Uranium-234, in coal and coal ash, 1511, 1521
Uranium-238
See also Actinides
in aquifers, concentrations and isotopic activity ratios in, 711
in coal and coal ash, 1511, 1521
near coal-fired power plants, 1511
concentration factors in plants and animal tissues, 681, 1682
effect on plants and animals of high soil concentrations and intake, 1682
in glacier ice, 383
injection in atmosphere, sources and rate, 383
isotope geochemistry in ground water, 711
in lichen—reindeer food chain, 560
mobility
in soil, 681, 1682
in water, soil, and plants, 1682
in oceans, vertical transport, 502

in phosphate materials and products, 1633
in soil, 611, 738
in soils and vegetation, in Hanford, Wash., 826
superficial abundance, 84
Uranium mill tailings, radon-222, release, transport, and air concentrations and health effects, 1559, 1584

Ventilation
effect on radon and daughter concentrations in indoor air, 1237, 1260, 1308, 1457
measurement of, using CO_2, 1293
rate calculation from radon measurements, 1272

Water
See also Oceans and Rainfall
actinide concentrations in, 560
for drinking
^{226}Ra content, 810, 839, 1090, 1145
^{228}Ra content, 839, 1090
^{222}Rn content, 1272, 1347
radium distribution in river system, 1633
radium measurement using impregnated fibers, 633
radium-226 and ^{222}Rn in, South Texas (USA) uranium district, 1602
radon-222
in ground water
applications to water circulation, 560
correlation with geology, 529
in well water, in Finland, 1364
rainwater
radioactivity in, 370
^{222}Rn and ^{210}Pb contents, 547
uranium concentrations and isotopic ratios in aquifers, 711
uranium mobility in, 1682
usage, as indoor radon source, 529, 1347

Zooplankton, role in vertical oceanic transport of alpha emitters, 502

DISCLAIMER

This book was prepared as an account of work sponsored by an agency of the United States Government. Neither the United States Government nor any agency thereof, nor any of their employees, makes any warranty, express or implied, or assumes any legal liability or responsibility for the accuracy, completeness, or usefulness of any information, apparatus, product, or process disclosed, or represents that its use would not infringe privately owned rights. Reference herein to any specific commercial product, process, or service by trade name, trademark, manufacturer, or otherwise, does not necessarily constitute or imply its endorsement, recommendation, or favoring by the United States Government or any agency thereof. The views and opinions of authors expressed herein do not necessarily state or reflect those of the United States Government or any agency thereof.

PRECIPITATION SCAVENGING (1974)

Proceedings of a symposium held at
Champaign, Illinois
October 14—18, 1974

Sponsored by Illinois State Water Survey
and
U. S. Atomic Energy Commission

Coordinators
Richard G. Semonin, Illinois State Water Survey
Robert W. Beadle, U. S. Atomic Energy Commission

Published by the Technical Information Center,
Energy Research and Development Administration
1977. 856 pages, 6 by 9 inches, paper binding
Library of Congress Catalog Card No. 76-53788 (CIP)

In a world becoming ever more aware of the need to guard against the pollution of its essential resources, there is an increasing need to understand the role of precipitation in removing from the atmosphere the waste products of man's many and varied activities. The effects of overloading the atmosphere will be felt by all segments of society and will reach across national boundaries. Among the most obvious problems will be the effects on visibility and on man's health and welfare and the damage to property. But not to be ignored are the more subtle effects on local weather, the impact of atmospheric removal processes on water quality, and, on a longer time scale, the serious implications regarding the result on incoming solar radiation and consequent large-scale climatic changes. Thus it is extremely important to understand the behavior of particulate and gaseous materials in the atmosphere, the mechanisms by which they are removed, and the pattern of deposition to be expected.

The 48 papers in *Precipitation Scavenging (1974)* include research in six countries and cut across the fields of chemistry, biology, geology, meteorology, and oceanography. Subjects discussed are problems, approximate solutions, and suggestions for future research; scavenging ratios; SO_2 scavenging research; microphysics—laboratory and theoretical; mesoscale field studies; regional studies; scavenging modeling; and proposed terminology. Also included is a supplemental bibliography of relevant publications published by the authors after the conference (compiled in August 1976).

Available as CONF-741003 for $10.50 from

National Technical Information Service
U.S. Department of Commerce
Springfield, VA 22161

Transuranic Elements in the Environment: A Summary of Environmental Research on Transuranium Radionuclides Funded by the U. S. Department of Energy Through Calendar Year 1979, Wayne C. Hanson (Ed.), Pacific Northwest Laboratory, 1980 (746 pages, 7 by 10 inches, hard binding). Describes the behavior of transuranic elements in the environment after their release from a variety of source terms, their translocation by physical and biological transport phenomena, and the interpretation of the consequences of such concentrations as might be found in biological components of various ecosystems. Following a comprehensive synthesis of the research literature, six major topics are addressed: source terms, inventory and distribution, experimental and field studies in terrestrial ecosystems of transuranic elements, models, freshwater and marine studies, and biological and ecological effects. Available as DOE/TIC-22800 for $18.50 from the National Technical Information Service, U. S. Department of Commerce, Springfield, Va. 22161.

Handbook on Aerosols, Richard Dennis (Ed.), GCA/Technology Division, 1976 (148 pages, 84 illus., 8½ by 11 inches, paper binding). Discusses key aspects of particulate behavior in the context of their many applications in field and laboratory activities. These applications include ambient atmosphere and stack monitoring, assessment of size-related biological effects, development of high-efficiency control systems for waste-gas emissions, meteorological transport and dispersion of particulates, forecasting of pollution levels and visibility, commercial handling and production of fine particles, and compliance with the emission standards set by regulatory agencies. Available as TID-26608 for $6.00 from the National Technical Information Service, U. S. Department of Commerce, Springfield, Va. 22161.

Atmospheric Transport Processes. Part 4: Radioactive Tracers, Elmar R. Reiter, Colorado State University, 1978 (620 pages, 278 illus., 7 by 9¾ inches, paper binding). Summarizes some of the aspects of nuclear decay and of various transport and removal processes operating in the atmosphere. Radon and its daughter products, cosmogenetic radionuclides, and fission products of anthropogenic origin are discussed in detail. Special attention is given to the theoretical modeling of atmospheric transport processes and to the removal of pollutants from the atmosphere. Available as TID-27114 for $12.50 from the National Technical Information Service, U. S. Department of Commerce, Springfield, Va. 22161.

*U.S. GOVERNMENT PRINTING OFFICE: 1980 648-997 1-3

Selected publications from the

U. S. DEPARTMENT OF ENERGY SYMPOSIUM SERIES

Available from National Technical Information Service, U. S. Department of Commerce, Springfield, Virginia 22161. Purchasers outside the United States, Canada, and Mexico should write NTIS for prices.

Radioactive Fallout from Nuclear Weapons Tests (CONF-765), 1965, $6.00
Radioactive Pharmaceuticals (CONF-651111), 1966, $6.00
Luminescence Dosimetry (CONF-650637), 1967, $6.00
Thorium Fuel Cycle (CONF-660524), 1968, $6.00
Radioisotopes in Medicine: In Vitro Studies (CONF-671111), 1968, $6.00
Biological Implications of the Nuclear Age (CONF-690303), 1969, $6.00
Radiation Biology of the Fetal and Juvenile Mammal (CONF-690501), 1969, $10.00
Inhalation Carcinogenesis (CONF-691001), 1970, $6.00
Myeloproliferative Disorders of Animals and Man (CONF-680529), 1970, $9.00
Medical Radionuclides: Radiation Dose and Effects (CONF-691212), 1970, $6.00
Morphology of Experimental Respiratory Carcinogenesis (CONF-700501), 1970, $6.00
Precipitation Scavenging (1970) (CONF-700601), 1970, $6.00
Neutron Standards and Flux Normalization (CONF-701002), 1971, $6.00
Survival of Food Crops and Livestock in the Event of Nuclear War (CONF-700909), 1971, $9.00
Biomedical Implications of Radiostrontium Exposure (CONF-710201), 1972, $6.00
Radiation-Induced Voids in Metals (CONF-710601), 1972, $9.00
Clinical Uses of Radionuclides: Critical Comparison with Other Techniques (CONF-711101), 1972, $13.60
Interactive Bibliographic Systems (CONF-711010), 1973, $7.60
Radionuclide Carcinogenesis (CONF-720505), 1973, $13.60
Carbon and the Biosphere (CONF-720510), 1973, $10.60
Thermal Ecology (CONF-730505), 1974, $13.60
The Cell Cycle in Malignancy and Immunity (CONF-731005), 1975, $13.60
Mammalian Cells: Probes and Problems (CONF-731007), 1975, $7.60
Cooling Tower Environment—1974 (CONF-740302), 1975, $13.60
Mineral Cycling in Southeastern Ecosystems (CONF-740513), 1975, $13.60
Radiation and the Lymphatic System (CONF-740930), 1976, $9.00
Atmosphere—Surface Exchange of Particulate and Gaseous Pollutants (1974) (CONF-740921), 1976, $13.60
Impact of Energy Production on Human Health: An Evaluation of Means for Assessment (CONF-751022), 1976, $6.75
Thermal Ecology II (CONF-750425), 1976, $11.00
Precipitation Scavenging (1974) (CONF-741003), 1977, $10.50
Biological Implications of Metals in the Environment (CONF-750929), 1977, $10.50
Pulmonary Macrophage and Epithelial Cells (CONF-760927), 1977, $12.50
Evaluation of Current Developments in Municipal Waste Treatment (CONF-770108), 1977, $4.75
Environmental Chemistry and Cycling Processes (CONF-760429), 1978, $15.00
Scientific Problems of Coal Utilization (CONF-770509), 1978, $9.00
Developmental Toxicology of Energy-Related Pollutants (CONF-771017), 1978, $12.50
Energy and Environmental Stress in Aquatic Systems (CONF-771114), 1978, $15.00
Computers in Activation Analysis and Gamma-Ray Spectroscopy (CONF-780421), 1979, $15.00
Biological Effects of Extremely Low Frequency Electromagnetic Fields (CONF-781016), 1979, $10.50
Natural Radiation Environment III [CONF-780422 (Vols. 1 and 2)], 1980, $39.50

(Listing current as of April 1980)